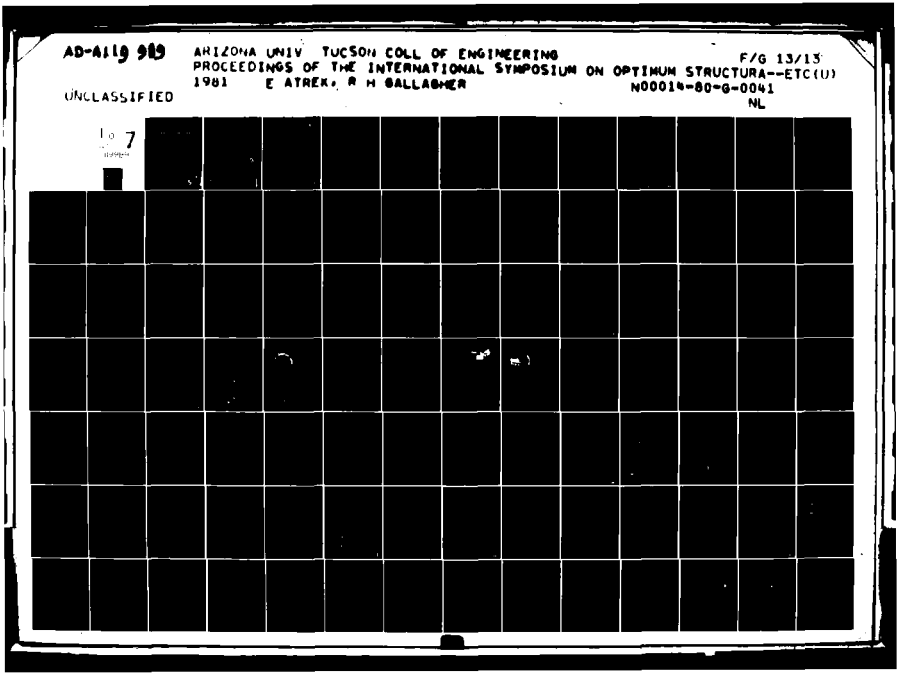
AD-A119 919 ARIZONA UNIV TUCSON COLL OF ENGINEERING F/G 13/13
PROCEEDINGS OF THE INTERNATIONAL SYMPOSIUM ON OPTIMUM STRUCTURA--ETC(U)
1981 E ATREK, R H GALLAGHER N00014-80-G-0041
UNCLASSIFIED NL



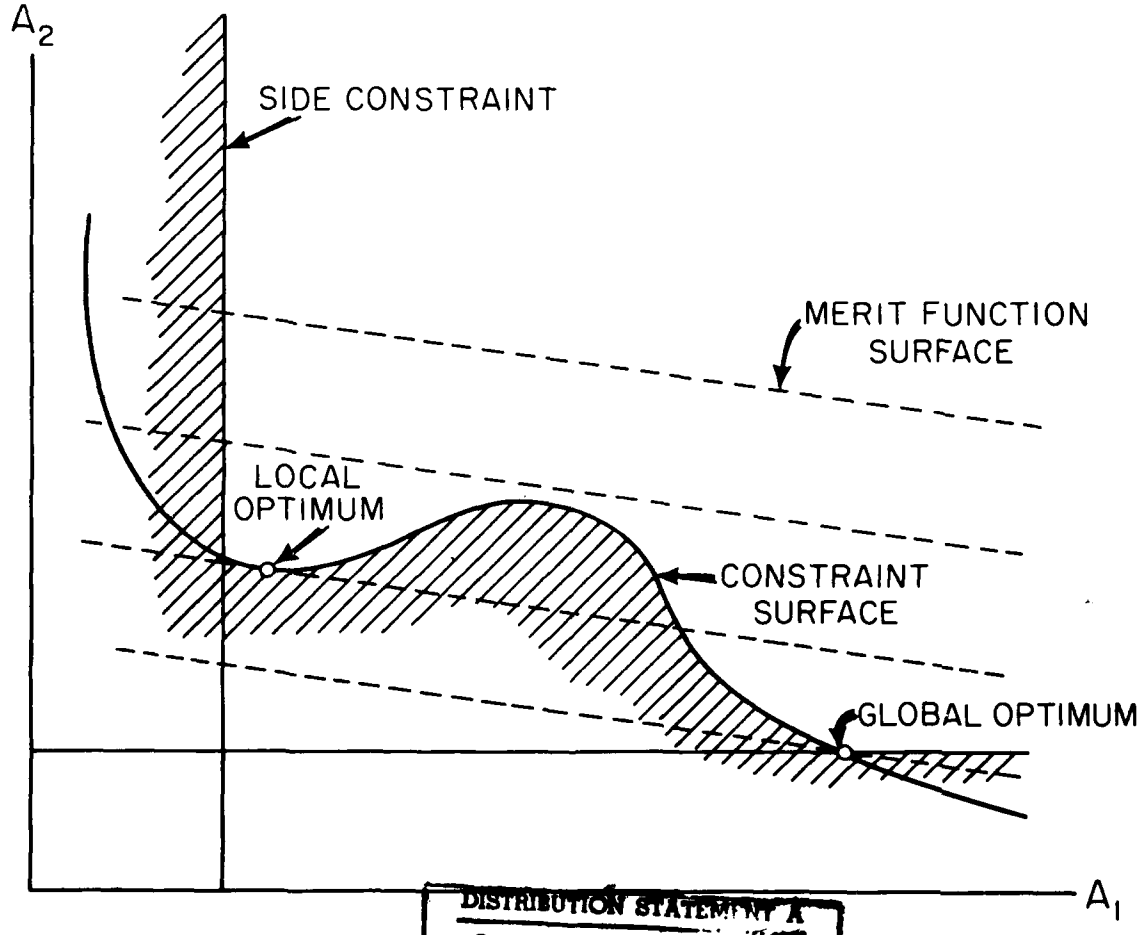
AD A119989

PROCEEDINGS

INTERNATIONAL SYMPOSIUM ON

OPTIMUM STRUCTURAL DESIGN

The 11th ONR Naval Structural Mechanics Symposium



DISTRIBUTION STATEMENT A
Approved for public release;
Distribution Unlimited

OCTOBER 19–22, 1981
UNIVERSITY OF ARIZONA
TUCSON, ARIZONA

DTIC FILE COPY

DTIC ELECTE OCT 1 1982 H

82 10 01 038

UNCLASSIFIED

SECURITY CLASSIFICATION OF THIS PAGE (When Data Entered)

REPORT DOCUMENTATION PAGE	READ INSTRUCTIONS BEFORE COMPLETING FORM
1. REPORT NUMBER	2. GOVT ACCESSION NO. AD-A119989	3. RECIPIENT'S CATALOG NUMBER
4. TITLE (and Subtitle) Proceedings of the International Symposium on Optimum Structural Design	5. TYPE OF REPORT & PERIOD COVERED 6. PERFORMING ORG. REPORT NUMBER
7. AUTHOR(s) E. Atrek and R. Gallagher	8. CONTRACT OR GRANT NUMBER(s) N00014-80-G-0041
9. PERFORMING ORGANIZATION NAME AND ADDRESS University of Arizona College of Engineering Tucson, Arizona 85721	10. PROGRAM ELEMENT, PROJECT, TASK AREA & WORK UNIT NUMBERS NR 064-649
11. CONTROLLING OFFICE NAME AND ADDRESS Office of Naval Research Mechanics Division Arlington, Virginia 22217	12. REPORT DATE 1981 13. NUMBER OF PAGES
14. MONITORING AGENCY NAME & ADDRESS(if different from Controlling Office)	15. SECURITY CLASS. (of this report) unclassified 15a. DECLASSIFICATION/DOWNGRADING SCHEDULE

16. DISTRIBUTION STATEMENT (of this Report)

APPROVED FOR PUBLIC RELEASE; DISTRIBUTION UNLIMITED

17. DISTRIBUTION STATEMENT (of the abstract entered in Block 20, if different from Report)

DTIC ELECTE OCT 1 1982 D H

18. SUPPLEMENTARY NOTES

19. KEY WORDS (Continue on reverse side if necessary and identify by block number)

structural design
structures
optimal design
materials
fabrication
stress
mechanics

20. ABSTRACT (Continue on reverse side if necessary and identify by block number)

Structural optimization is a field with many distinct avenues of investigation. Among those which are covered in this endeavor are optimality criteria methods and fully stressed design; reliability based design; optimal control methods; shape optimization; local vs. global optima; linearization and condensation methods; mathematical programming methods; practical applications (e.g., steel and concrete design); multi-objective optimization; and optimization software. Including a spectrum of papers covering these areas, an International Symposium

DTIC FILE COPY

DD FORM 1 JAN 73 1473 EDITION OF 1 NOV 65 IS OBSOLETE
S/N 0102-LF-014-6601

UNCLASSIFIED
SECURITY CLASSIFICATION OF THIS PAGE (When Data Entered)

on Optimum Structural Design was held 19-22 October 1981 on the campus of the University of Arizona, Tucson, and this associated proceedings prepared as a result.

International Symposium On

OPTIMUM STRUCTURAL DESIGN

October 19-22, 1981
Tucson, Arizona

ORGANIZING COMMITTEE

Dr. R. H. Gallagher
University of Arizona
(Symposium Chairman)

Dr. E. Atrek
Istanbul Technical University, Turkey
(Symposium Secretary)

Dr. A. J. Morris
Royal Aircraft Establishment, United Kingdom

Prof. O. C. Zienkiewicz
University of Wales, United Kingdom

Dr. N. Perrone
Office of Naval Research, D.C.

Prof. K. M. Ragsdell
Purdue University, Indiana

Prof. J. L. Armand
Institut de Recherches de la Construction Navale, France

Prof. G. Vanderplaats
U. S. Naval Postgraduate School, California

Prof. D. Shanno
University of Arizona

THE 11TH ONR NAVAL STRUCTURAL MECHANICS SYMPOSIUM

Sponsored by:

U. S. Office of Naval Research
and
University of Arizona
College of Engineering

TABLE OF CONTENTS

Preface vii

OPENING LECTURE

Structural Optimization, Some Key Ideas and Insights 1
L. A. Schmit, Jr.

SESSION #1, OPTIMALITY CRITERIA METHODS AND FULLY STRESSED DESIGN

Achievements in Structural Optimization Using Optimality Criteria Methods. 1-1
N. S. Khot and L. Berke

Optimal Design of a Structure for System Stability for a Specified Eigenvalue Distribution 1-3
N. S. Khot

Optimal Design of Inelastic Cable Structures 1-11
C. Cinquini and R. Contro

Minimum Weight Design Within a Bound on Eigenvalues. 1-19
N. Kikuchi and J. E. Taylor

Two Applications of Optimum Structural Design in the Field of Nuclear Technique. 1-23
J. F. Stelzer

Optimality Criteria Design and Stress Constraint Processing. 1-31
R. Levy

SESSION #2, DYNAMICS AND RELIABILITY BASED DESIGN

Optimum Structural Designs in Dynamic Response 2-1
H. Yamakawa

Interactive Optimal Design of Dynamically Loaded Structures Using the OPTNSR Software System 2-9
R. Balling, V. Ciampi, K. S. Pister, and M. A. Bhatti (PUBLISHED IN SESSION 12)

Structural Optimization on Geometrical Configuration and Element Sizing With Statical and Dynamical Constraints. 2-11
J. H. Lin, W. Y. Che, and Y. S. Yu

Optimum Distribution of Additive Damping for Vibrating Beam Structures 2-21
R. Lunden and B. Akesson

An Iterative Eigenvector Technique for Optimization Analysis 2-27
P. S. Jensen

Optimum Structural Design Under Dynamic Forces With Uncertainties. 2-33
K. Matsui, K. Yamamoto, Y. Kikuta, and Y. Niinobe

Lifetime Cost Earthquake Resistant Design: An Algorithm for Automation. 2-41
N. D. Walker, Jr.

A Comparison of Reliability Based Optimum Designs and AISC Code Based Designs. 2-49
K. B. Rojiani and G. L. Bailey

SESSION #3, OPTIMAL CONTROL METHODS

Existence of Solutions of the Plate Optimization Problem 3-1
J.-L. Armand, K. A. Lurie, and A. V. Cherkaev

Stability Implications and the Equivalence of Stability and Optimality Conditions in the Optimal Design of Uniform Shallow Arches. 3-3
W. Stadler

Hybrid Optimization of Truss Structures With Strength and Buckling Constraints 3-11
P. Hajela and H. Ashley

Stochastic Control in Structural Design. 3-19
D. G. Carmichael

Application of Perturbation Method to Optimal Design of Structures 3-23
N. V. Banichuk

SESSION #4, SHAPE OPTIMIZATION I

Shape Optimal Design of Elastic Structures 4-1
E. J. Haug, K. K. Choi, J. W. Hou, and Y. M. Yoo

SESSION #4, SHAPE OPTIMIZATION I (cont'd)

Maxwell's Theorem for Frames 4-5
O. E. Lev

Developments in Michell Theory 4-9
J.-M. Lagache

Hencky-Prandtl Nets and Constrained Michell Trusses. 4-17
G. Strang and R. V. Kohn

Optimum Geometry of Stepped-Taper Beams. 4-23
L. Spunt

Pattern Transformation Method for Shape Optimization and Its Application to Spoked Rotary Disks 4-29
J. Oda and K. Yamazaki

A General Theory of Optimal Structural Layouts 4-37
G. I. N. Rozvany

An Optimized Configuration of an Enclosure Structure for Safe Containment of Internal Blasts 4-47
A. D. Gupta and H. L. Wisniewski

Optimum Column Buckling Under an Axial Load and Its Own Weight 4-53
S. M. Makky

SESSION #5, SHAPE OPTIMIZATION II

Shape Determination of Structures Based on the Inverse Variational Principle/The Finite Element Approach 5-1
Y. Tada and Y. Seguchi

Optimal Shape Design of Turbine and Compressor Blades. 5-9
J. P. Queau and P. Trompette

Application of Optimization to Aircraft Engine Disk Synthesis. 5-15
J. O. Song and R. E. Lee

Optimal Shape Design to Minimize Stress Concentration Factors in Pressure Vessel Components. 5-23
J. Middleton

Numerical Methods for Shape Optimization/An Assessment of the State of the Art 5-31
G. N. Vanderplaats

Multilevel Optimization of Arrays of Protective Structures 5-33
S. Ginsburg and U. Kirsch

SESSION #6, LOCAL AND GLOBAL OPTIMA

Rigorous Simplification and Bounding of Optimization Models with Obscured Monotonicity 6-1
D. J. Wilde and M. Human

On Local and Global Minima in Structural Optimization. 6-3
K. Svanberg

A Self Contained Theory for Optimum Design of Skeletal Structures and the Global Optimum 6-11
E. Atrek

A Study of Global Buckling Effects on Optimum Riser Design 6-19
M. M. Bernitsas and P. Papalambros

Connectedness Criterion and the Unique Optimum of the Izo-Static Trusses 6-27
M. Bayer

SESSION #7, LINEARIZATION AND CONDENSATION METHODS

Parameterization in Finite Element Analysis. 7-1
B. P. Wang and W. D. Pilkey

Application of Linear Constraint Approximations to Frame Structures. 7-9
J. A. Bennett

Approximate Behavior Models for Optimum Structural Design. 7-17
U. Kirsch and B. Hofman

Weight Optimization of Membrane Structures 7-27
B. Esping

About Determination Optimal--Weight Statically Indeterminate Bar Structures of Complex Stress by Using Explicit Forms of the Conditions 7-37
E. Halmos

SESSION #8, MATHEMATICAL PROGRAMMING I

The Utility of Nonlinear Programming Methods for Engineering Design. 8-1
K. M. Ragsdell

Application of a Reduced Quadratic Programming Technique to Optimal Structural Design. 8-5
N.-H. Chao, S. J. Fenves, and A. W. Westerberg

Modified SUMT for Structural Synthesis 8-13
M. P. Kamat and P. Ruangsilasingha

An Algorithm for Optimum Structural Design Without Line Search 8-23
J. S. Arora and S. V. Belsare

A Barrier Form of the Method of Multipliers. 8-35
R. R. Root and K. M. Ragsdell

Geometric Programming for Continuous Design Problems 8-43
A. Diaz, P. Papalambros, and J. Taylor

Associated Solutions in Optimization Applications to Structural Mechanics. 8-49
P. Brousse

SESSION #10, MATHEMATICAL PROGRAMMING II

Multiobjective Optimization in Structural Design: The Model Choice Problem. 10-1
L. Duckstein

A Method for Nonlinear Optimum Design of Large Structures, and Applications to Naval Ship Design. 10-5
O. Hughes

Optimum Configuration of Transmission Line Towers in Dynamic Response Regime 10-13
M. P. Kapoor and K. Kumarasamy

Optimization of Multiple Safety Factors in Structural Designs. 10-21
E. D. Eason, J. M. Thomas, and P. M. Besuner

Multicriterion Optimization in Structural Design 10-29
J. Koski

An Approach to Multicriterion Optimization for Structural Design 10-37
A. Osyczka

SESSION #9, STEEL AND CONCRETE DESIGN

Rigid-Plastic Minimum Weight Plane Frame Design Using Hot Rolled Shapes. 9-1
R. C. Johnson

Light Gage Steel Design Via the Method of Multipliers. 9-7
N. Sarigul and R. Gallagher

Optimum Design of Grillages Including Warping. 9-13
M. P. Saka

Optimum Cost Design of Precast Concrete Buildings. 9-21
J. Knapton and K. A. Andam

Reinforced Concrete Members Optimizing Relationships 9-31
L. M. Laushey

SESSION #11, OPTIMIZATION SOFTWARE I

Access Computer Program for the Synthesis of Large Structural Systems. 11-1
C. Fleury, R. K. Ramanathan, M. Salama, and L. A. Schmit, Jr.

A Programming System for Research and Applications in Structural Optimization. 11-9
J. Sobieszczanski-Sobieski and J. L. Rogers, Jr.

Large Scale Structural Optimization by Finite Elements 11-23
C. Fleury

SESSION #12, OPTIMIZATION SOFTWARE II

An Interactive Software System for Optimal Design of Statically and Dynamically Loaded Structures with Nonlinear Response 12-1
M. A. Bhatti, V. Ciampi, K. S. Pister, and E. Polak

Interactive Optimal Design of Dynamically Loaded Structures Using the OPTNSR Software System 12-9
R. Balling, M. A. Bhatti, V. Ciampi, and K. S. Pister

SESSION #12, OPTIMIZATION SOFTWARE II (cont'd)

Sway Frames Optimization by Means of Mini Computers 12-19
P. Stojanovski

Efficient Optimal Design of Structures--Program DDDU. 12-27
L. Qian, W. Zhong, Y. Sui, and J. Zhang

A Computer Program System for Design of Power Transmission Towers 12-37
L. Hanssen

Current Research on Shear Buckling and Thermal Loads with PASCO: Panel Analysis and Sizing Code. 12-47
W. J. Stroud, W. H. Greene, and M. S. Anderson

PANDA--Interactive Computer Program for Preliminary Minimum Weight Design of Composite or Elastic-Plastic, Stiffened Cylindrical Panels and Shells Under Combined In-Plane Loads. 12-59
D. Bushnell

Interactive Optimum Design System 12-73
T. Altuzarra, C. Knopf-Lenoir, C. Sayettat, and G. Touzot

SESSION #13, NEW METHODS AND SPECIAL APPLICATIONS

Optimal Principles for Design of Indeterminate Trusses. 13-1
L. M. Laushey

A New Method for Optimal Design of Structures 13-7
R. Xia, P. T. Hsu, and M. M. Chen

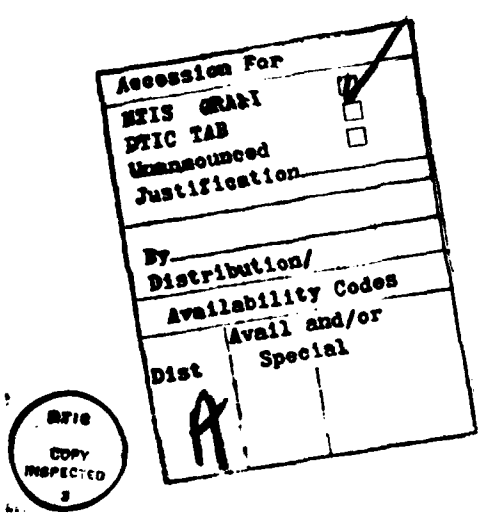
Optimal Finite Element Discretization--A Dynamic Programming Approach 13-13
Y. Seguchi, M. Tanaka, and Y. Tomita

Optimization Procedure for Material Composition of Composite Material Structures. 13-21
J. Oda

Some Smear-Out Models for Integrally Stiffened Plates With Applications to Optimal Design 13-29
M. P. Bendsøe

Elastic Synthesis for Large Displacements 13-35
J. A. Teixeira de Freitas and J. P. B. Moitinho de Almeida

Derivation and Convergence of Power Series in Structural Design 13-43
J. Whitesell



PREFACE

The topic of optimum structural design has intrinsic importance on account of the motivation of all designers to evolve the "best" product in terms of cost, weight, aesthetics, reliability, or a combination of these. The topic is taking on new and additional importance, however, because of resource scarcity and escalating costs of material and fabrication. In ships, for example, the reduction of structural weight directly influences the cost of fuel required to power them. The same is true of automobiles, aircraft, and other vehicles. Another reason for heightened interest in optimum structural design is that the great strides in computer hardware are placing the formidable computational requirements of this topic within reach.

It can be said that the modern era of optimum structural design began about twenty years ago when the potentiality of the newly-developed mathematical programming techniques for this purpose was identified. In succeeding years many such techniques were adapted to optimum structural design problems. These accomplishments opened the eyes of many to the possibility of practical optimum design exercises and brought about a re-examination and further development of more traditional methods. It should be noted the mathematical programming methods were often computationally expensive and the development of the traditional methods were made in the hopes of circumventing this difficulty.

In 1972, in an attempt to bring together the accomplishments of the prior decade, a Symposium on Optimum Structural Design was held at the University of Wales, Swansea. Nearly a decade has passed since the organizational efforts leading to that Symposium. The techniques that were described there have advanced considerably. Some important new techniques have appeared and significant applications have been reported. Thus, it is timely to convene a Symposium on this topic. Fortunately, this objective is shared by the Office of Naval Research. For over twenty years that Office has sponsored symposia in diverse fields of structural mechanics. It had not previously sponsored a program in structural optimization, although activities in that area are within the purview of modern developments in structural mechanics. It has, therefore, given its support to this program, which is designated The Eleventh Naval Structural Mechanics Symposium.

Structural optimization is a field with many distinct avenues of investigation. Among those which are covered in this endeavor are the following:

1. Optimality Criteria Methods and Fully Stressed Design
2. Reliability Based Design
3. Optimal Control Methods
4. Shape Optimization
5. Local vs. Global Optima
6. Linearization and Condensation Methods
7. Mathematical Programming Methods
8. Practical Applications (e.g. steel and concrete design)
9. Multi-Objective Optimization
10. Optimization Software

The International Symposium on Optimum Structural Design was therefore held on October 19-22, 1981 on the campus of the University of Arizona, Tucson. Planning of the Symposium was coordinated by the Organizing Committee listed on the cover page of these proceedings.

This volume contains all contributed papers received in time for inclusion prior to the press date for publication as well as summaries of the invited lectures. Approximately 15 of the contributed papers listed in the program announcement were not received in time for publication. It should be noted that it is planned that full versions of the invited lectures, plus extended versions of certain contributed papers which are felt to be of more general interest, will subsequently appear in a book in the J. Wiley Book Co. series "Numerical Methods in Engineering".

The editors wish to take this opportunity to thank all of those who have contributed to these proceedings and to the success of the Symposium. Foremost in this regard are the authors themselves. We also wish to acknowledge the helpful advice and guidance of Dr. N. J. Perrone of the Office of Naval Research. Arrangements for the symposium were in the hands of the Office of Special Professional Education and we are especially indebted to Dr. Charles Hausenbauer, Director, and to Miss Nina Albert of that office. Mrs. Janice Jones and Mrs. Sharon Thomas of the Department of Civil Engineering were most helpful in numerous typing chores.

Erdal Atrek

Richard Gallagher

OPENING LECTURE

COMPONENT PART NOTICE

THIS PAPER IS A COMPONENT PART OF THE FOLLOWING COMPILATION REPORT:

(TITLE): International Symposium on Optimum Structural Design.

(SOURCE): Arizona Univ., Tucson. Coll. of Engineering.

TO ORDER THE COMPLETE COMPILATION REPORT USE AD-A119 989.

THE COMPONENT PART IS PROVIDED HERE TO ALLOW USERS ACCESS TO INDIVIDUALLY AUTHORED SECTIONS OF PROCEEDINGS, ANNALS, SYMPOSIA, ETC. HOWEVER, THE COMPONENT SHOULD BE CONSIDERED WITHIN THE CONTEXT OF THE OVERALL COMPILATION REPORT AND NOT AS A STAND-ALONE TECHNICAL REPORT.

THE FOLLOWING COMPONENT PART NUMBERS COMPRISE THE COMPILATION REPORT:

AD#:	TITLE:
AD-P000 026	Structural Optimization, Some Key Ideas and Insights.
AD-P000 027	Optimal Design of a Structure for System Stability for a Specified Eigenvalue Distribution.
AD-P000 028	Optimal Design of Inelastic Cable Structures.
AD-P000 029	Minimum Weight Design Within a Bound on Eigenvalues.
AD-P000 030	Two Applications of Optimum Structural Design in the Field of Nuclear Technique.
AD-P000 031	Optimality Criteria Design and Stress Constraint Processing.
AD-P000 032	Optimum Structural Designs in Dynamic Response.
AD-P000 033	Structural Optimization on Geometrical Configuration and Element Sizing With Statical and Dynamical Constraints.
AD-P000 034	Optimum Distribution of Additive Damping for Vibrating Beam Strcutures.
AD-P000 035	An Iterative Eigenvector Technique for Optimization Analysis.
AD-P000 036	Optimum Structural Design Under Forces With Uncertainties.
AD-P000 037	Lifetime Cost Earthquake Resistant Design: An Algorithm for Automation.
AD-P000 038	A Comparison of Reliability Based Optimum Designs and AISC Code Based Designs.
AD-P000 039	Stability Implications and the Equivalence of Stability and Optimality Conditions in the Optimal Design of Uniform Shallow Arches.
AD-P000 040	Hybrid Optimization of Truss Structures With Strength and Buckling Constraints.
AD-P000 041	Stochastic Control in Structural Design.
AD-P000 042	Application of Perturbation Method to Optimal Design of Structures.

This document has been approved for public release and sale; its distribution is unlimited.

Availability Codes

Dist	Avail and/or Special
A	

COMPONENT PART NOTICE (CON'T)

AD#:	TITLE:
AD-P000 043	Shape Optimal Design of Elastic Structures.
AD-P000 044	Maxwell's Theorem for Frames.
AD-P000 045	Developments in Michell Theory.
AD-P000 046	Hencky-Prandtl Nets and Constrained Michell Trusses.
AD-P000 047	Optimum Geometry of Stepped-Taper Beams.
AD-P000 048	Pattern Transformation Method for Shape Optimization and Its Application to Spoked Rotary Disks.
AD-P000 049	A General Theory of Optimal Structural Layouts.
AD-P000 050	An Optimized Configuration of an Enclosure Structure for Safe Containment of Internal Blasts.
AD-P000 051	Optimum Column Buckling Under an Axial Load and Its Own Weight
AD-P000 052	Shape Determination of Structures Based on the Inverse Variational Principle/The Finite Element Approach.
AD-P000 053	Optimal Shape Design of Turbine and Compressor Blades.
AD-P000 054	Application of Optimization to Aircraft Engine Disk Synthesis.
AD-P000 055	Optimal Shape Design to Minimize Stress Concentration Factors in Pressure Vessel Components.
AD-P000 056	Multilevel Optimization of Arrays of Protective Structures.
AD-P000 057	On Local and Global Minima in Structural Optimization.
AD-P000 058	A Self Contained Theory for Optimum Design of Skeletal Structures and the Global Optimum.
AD-P000 059	A Study of Global Buckling Effects on Optimum Riser Design.
AD-P000 060	Connectedness Criterion and the Unique Optima of the Izo-Static Trusses.
AD-P000 061	Parmeterization in Finite Element Analysis.
AD-P000 062	Application of Linear Constraint Approximations to Frame Structures.
AD-P000 063	Approximate Behavior Models for Optimum Structural Design.
AD-P000 064	Weight Optimization of Membrane Structures.
AD-P000 065	About Determination Optimal--Weight Statically Indeterminate Bar Structures of Complex Stress by Using Explicit Forms of the Conditions.
AD-P000 066	The Utility of Nonlinear Programming Methods for Engineering Design.
AD-P000 067	Application of a Reduced Quadratic Programming Technique to Optimal Structural Design.
AD-P000 068	Modified SUMT for Structural Synthesis.
AD-P000 069	An Algorithm for Optimum Structural Design Without Line Search.
AD-P000 070	A Barrier Form of the Method of Multipliers.
AD-P000 071	Geometric Programming for Continuous Design Problems.
AD-P000 072	Associated Solutions in Optimization Applications to Structural Mechanics.
AD-P000 073	Multiobjective Optimization in Structural Design: The Model Choice Problem.

COMPONENT PART NOTICE (CON'T)

AD#:	TITLE:
AD-P000 074	A Method for Nonlinear Optimum Design of Large Structures, and Application to Naval Ship Design.
AD-P000 075	Optimum Configuration of Transmission Line Towers in Dynamic Response Regime.
AD-P000 076	Optimization of Multiple Safety Factors in Structural Designs.
AD-P000 077	Multicriterion Optimization in Structural Design.
AD-P000 078	An Approach to Multicriterion Optimization for Structural Design.
AD-P000 079	Rigid-Plastic Minimum Weight Plane Frame Design Using Hot Rolled Shapes.
AD-P000 080	Light Cage Steel Design Via the Method of Multipliers.
AD-P000 081	Optimum Design of Grillages Including Warping.
AD-P000 082	Optimum Cost Design of Precast Concrete Buildings.
AD-P000 083	Reinforced Concrete Members Optimizing Relationships.
AD-P000 084	Access Computer Program for the Synthesis of Large Structural Systems.
AD-P000 085	A Programming System for Research and Applications in Structural Optimization.
AD-P000 086	Large Scale Structural Optimization by Finite Elements.
AD-P000 087	An Interactive Software System for Optimal Design of Statically and Dynamically Loaded Structures with Nonlinear Response.
AD-P000 088	Interactive Optimal Design of Dynamically Loaded Structures Using the OPTNSR Software System.
AD-P000 089	Sway Frames Optimization by Means of Mini Computers.
AD-P000 090	Efficient Optimal Design of Structures--Program DDDU.
AD-P000 091	A Computer Program System for Design of Power Transmission Towers.
AD-P000 092	Current Research on Shear Buckling and Thermal Loads with PASCO: Panel Analysis and Sizing Code.
AD-P000 093	PANDA--Interactive Computer Program for Preliminary Minimum Weight Design of Composite or Elastic-Plastic, Stiffened Cylindrical Panels and Shells Under Combined In-Plane Loads.
AD-P000 094	Interactive Optimum Design System
AD-P000 095	Optimal Principles for Design of Indeterminate Trusses.
AD-P000 096	A New Mehtod for Optimal Design of Structures.
AD-P000 097	Optimal Finite Element Discretization--A Dynamic Programming Approach.
AD-P000 098	Optimization Procedure for Material Composition of Composite Material Structures.
AD-P000 099	Some Smear-Out Models for Integrally Stiffened Plates With Applications to Optimal Design.
AD-P000 100	Elastic Synthesis for Large Displacements.
AD-P000 101	Derivation and Convergence of Power Series in Structural Design.

AD-P000 026

Opening Lecture

STRUCTURAL OPTIMIZATION, SOME KEY IDEAS AND INSIGHTS

Lucien A. Schmit
University of California, Los Angeles, California

Extended Abstract

The central purpose of structural analysis is to predict the behavior of trial designs. The results of structural analyses are used to assess the adequacy and relative merits of alternative trial designs with respect to established design criteria. The existence of general and reliable structural analysis capabilities coupled with the continuing growth of digital computing power, at ever lower cost per operation, has led rather naturally to a marked increased in structural optimization research, development, and applications activity. It will be assumed in the sequel that we know how to predict the behavior of a significant class of structural systems well enough to undertake structural optimization.

Historically, the desire to reduce structural weight without unduly compromising structural integrity, particularly in aerospace applications, has been a strong driving force behind the development of structural optimization methods. Today the need for energy conservation in transportation systems via weight reduction provides further motivation for the application of structural optimization methods. The growing use of fiber composite materials in structures is likely to increase demand for modern analytical tools that will make it possible to fully exploit the design potential offered by tailoring of these new materials. Looking further ahead the possibility of building large structures in space may place a new and challenging set of demands on our ability to analyze and design structural systems.

The development of rational automatable structural design procedures, aimed at finding the best possible design, is attractive and intellectually stimulating in its own right as an abstract concept. However, the broad applicability of such methods to structural systems that play a central role in civil, mechanical, and aerospace engineering, as well as naval-architecture, underscores the importance of gaining a deeper understanding and increasing the use of structural optimization methods in practice.

The main body of this lecture will be focused on a selected set of key ideas that have, in my opinion, played an important role in the development of structural optimization. At the outset it will be useful to recognize that complete specification of a structural system involves a *hierarchy of descriptors* as follows: (1) type of structure; (2) general arrangement (topology); (3) material; (4) geometric layout of elements (configuration); (5) sizing of elements; and (6) joints, attachments and fastener details. Much of the structural optimization literature deals with minimum weight sizing of structural systems under static loading. However, some progress has also been made on the more difficult problems associated with configuration and topology type descriptors.

Prior to introducing the design space concept the following terms will be defined: (1) preassigned parameters; (2) design variables; (3) load condition(s); (4) failure mode(s); and (5) objective function. The *design space concept*, a graphical interpretation of the inequality constrained minimization problem, is then illustrated using two simple examples involving explicit inequality constraints. Since each of these example problems involves only two independent design variables, the optimum designs are easily found by simply scanning the design space plots. Examining the characteristics of these optimum designs clearly reveals that, *in general it cannot be anticipated how many or which inequality constraints will become critical (i.e. become equality constraints) at the optimum design*. Because of this the use of inequality constraints is essential to the proper statement of the structural design optimization problem.

Three of the main prevailing ideas in structural optimization prior to 1958 are represented by works dealing with: (1) least weight layout of highly idealized frameworks; (2) optimum design of structural components (columns, wide columns, stiffened panels, etc) based on weight strength analysis or structural index methods; and (3) minimum weight optimum design of simple structural systems (e.g. planar trusses and frames) based on the plastic collapse or limit analysis design philosophy.

The basic theory for optimal layout seeks an arrangement of uniaxial members that produces a minimum weight structure for specified loads and materials. Maxwell-Michell theory provides a basis for optimal layout of minimum weight trusses under a single load condition and subject to stress constraints only. The resulting structures are statically determinate and potentially unstable if alternative loads are applied. However, *Michell structures can provide useful guidance for the layout of structural systems, particularly when a single load condition is dominant and stress constraints are of primary concern.*

Minimum weight optimum design of basic aircraft structural components, such as columns and stiffened panels subject to compressive loads, was initially developed during World Work II. The basic approach followed can be characterized as the "*simultaneous failure mode design optimization method*," wherein a structural component is proportioned so that several preselected failure modes

become critical simultaneously. Setting the number of simultaneously critical failure modes equal to the number of independent design variables *converted* the design optimization problem from an *inequality constrained weight minimization problem* to a set of *nonlinear simultaneous equations*. From a design space point of view, the solutions obtained by the simultaneous failure mode approach correspond to a *preselected vertex point*. By and large the success of these methods depended on: (1) sound intuition and good physical insight for an inspired choice of the "correct set" of critical constraints; and (2) the fact that even when the true optimum was not at a vertex the error in the optimum weight was often small.

For structural components such as columns and stiffened panels subject to a single loading condition, the simultaneous failure mode approach led to a set of constraint *equations* that could often be solved explicitly for the design variable values at the preselected vertex point. These values frequently corresponded to the minimum weight optimum design, and they were commonly expressed as functions of some appropriate measure of loading intensity, which was referred to as a "structural or loading index." *The significance of the "structural index" idea resides in the fact that it is selected to be a measure of loading intensity for which stress distributions will be identical in all geometrically similar elements.* Thus, in addition to providing explicit and frequently exact optimum design solutions, the simultaneous failure mode-structural index approach provides results that are applicable to an entire class of components. The "structural index" concept provides a valuable tool for comparing the weight efficiency of alternative materials and component design configurations. *It is important to recognize that the structural index concept is independent of the method used to obtain the optimum design data.* Therefore, results generated by the simultaneous failure mode approach, experimental measurement, as well as mathematical programming methods can all be presented in summary form via plots of mass index versus loading index.

Prior to 1958 application of mathematical programming algorithms to structural systems were limited to truss and planar frame type problems that could be formulated within the context of the plastic collapse design philosophy. Briefly stated this design philosophy seeks to minimize weight while precluding plastic collapse of the structure when it is subjected to one or more overload conditions obtained by scaling up service load conditions. *Within the plastic collapse design philosophy, a significant class of structural optimization problems could be formulated as linear programming problems.* The fact that these linear programming problems had minimum weight optimum design solutions corresponding to vertex points in the design space was probably reassuring to users of the simultaneous failure mode approach.

It is interesting to note that it was first recognized in 1955 that a more general class of structural optimization problems could be viewed as nonlinear mathematical programming problems. Although the *importance of nonlinear inequality constraints in properly stating these more general problems was appreciated, the influence of this key idea was initially limited* by the fact that example problems were solved by using *classical lagrange multiplier and slack variable concepts to transform the inequality constrained weight minimization problem into a set of nonlinear simultaneous equations*. The resulting large number of equations and unknowns, as well as the apparent need to exhaustively sort through all of the solutions, was a grim prospect when larger, more realistic design optimization problems were contemplated.

It is also interesting to observe that in 1958 in the course of continuing work on minimum weight design of truss and frame structures, within the plastic collapse design philosophy, an innovative solution method emerged which was a precursor of three key ideas that would subsequently play important roles in the development of structural optimization methods. Briefly stated these ideas were: (1) the *integrated approach to structural analysis and design optimization* where these two activities are carried out simultaneously rather than sequentially; (2) the *conversion* of an inequality constrained minimization problem *to one or more equivalent unconstrained minimizations*; and (3) *reducing the dimensionality of the space* in which the bulk of the numerical calculations are to be made via imaginative changes of variable.

By 1960 it was known that a rather general class of structural design optimization problems could be stated in standard form as follows: given the *preassigned parameters* and *load conditions*, find the vector of *design variables* $\vec{D}$ such that

$$g_q(\vec{D}) \geq 0 \quad ; \quad q \in Q \tag{1}$$

and the *objective function*

$$M(\vec{D}) \rightarrow \text{Min} \tag{2}$$

where the set of inequality constaints represented by Eq. (1) usually contains one behavior constraint for each *failure mode* in each *load condition* as well as side constraints that reflect fabrication and analysis limitations as well as other design guidelines. Although the validity of this problem statement has not been seriously challenged, the last two decades have seen a great deal of controversy over how to solve it efficiently for practical structures.

Structural design is fundamentally a multilevel design problem involving more detailed design descriptors at the component level than at the system level. Before turning attention to some of the successes and difficulties encountered during early applications of the nonlinear mathematical programming approach, it will be useful to *distinguish between system level and component level structural design*. At the system level gross proportioning, usually based on finite element analysis, is carried out subject to strength, deflection, system buckling, natural frequency, aeroelastic, and other constraints. On the other hand, detailed design of structural components

is often carried out one component at a time, using special purpose detailed analyses which consider constraints such as strength, component buckling, local buckling, and crack growth limitations.

During the decade 1960-1970 progress was made along two main lines. The first category includes component type problems of a fundamental and recurring nature. The second category involved the development of first generation system level structural optimization programs based on combining finite element and nonlinear mathematical programming algorithms.

The component type problems were characterized by: (1) relatively small numbers of design variables; (2) a wide variety of increasingly complex failure modes and loading environments; and in some instances (3) consideration of objective functions other than weight. A structural optimization capability that was representative of the state of the art in 1968 dealt with the minimum weight design of stiffened cylindrical shells. This particular component type optimum design capability will be briefly elaborated on because of the influence it was to have on future developments. The mathematical programming statement of the design optimization task was transformed into a sequence of unconstrained minimizations using the Fiacco-McCormick interior penalty function formulation; that is, find $\vec{D}$ such that

$$\phi(\vec{D},r_p) \rightarrow \text{Min} \qquad (3)$$

where

$$\phi(\vec{D},r_p) = M(\vec{D}) + r_p \sum_{q} \frac{1}{g_q(\vec{D})} \qquad (4)$$

and

$$r_{p+1} \leftarrow C\, r_p \; ; \; C < 1 \qquad (5)$$

The constraint repulsion characteristic of this interior penalty formulation causes successive designs obtained at the end of each unconstrained minimization stage p to stay away from the constraints. This led to the *idea that approximate analyses could be used during major portions of the design optimization process*, with good expectation that the sequence of designs generated would remain in the feasible region of the design space. Indeed, by using approximate buckling analyses within each unconstrained minimization stage, cylindrical shell buckling analysis run times were reduced by a factor of 75, while still generating a sequence of noncritical feasible designs which formed a trajectory that "funneled down the middle" of the feasible region in design space. In a philosophical sense, this approximate analysis feature was a precursor of the approximation concepts approach to system level structural optimization which was to emerge during the next decade (1970-1980).

During the 1960-1970 time frame two first generation system level structural optimization programs were developed by combining finite element analysis methods and mathematical programming algorithms. The most general and sophisticated system level structural optimization program available at the end of the 1960-1970 decade was based on an efficient finite element displacement method module and a sound implementation of the feasible directions algorithm. A form of design variable linking was included so that the number of design variables was independent of the number of finite elements employed in the structural analysis model. The importance of reducing the number of structural analyses and the number of partial derivative calculations was recognized and several devices aimed at improving overall efficiency of the design optimization procedure were introduced. Nevertheless, by 1970 it had become apparent that the then available system level structural optimization capabilities based on combining finite element analysis with mathematical programming techniques required inordinately long run times to solve structural design problems of only modest practical size.

Most of the ideas to be discussed subsequently have emerged in response to the difficult and challenging task posed by large system level structural optimization problems. Therefore, in the sequel, attention will be focused on this class of problem. When dealing with system level structural optimization problems, it is particularly important to distinguish between the *analysis model* and the *design model*. Generating a structural analysis model usually involves idealization and discretization. In the context of the finite element method *idealization* refers to selecting the kinds of elements (e.g. truss, beam, membrane, plate, shell, etc) and *discretization* refers to deciding on the number and distribution of finite elements and displacement degrees of freedom. Once the idealization and discretization judgment decisions have been made, the structural analysis problem has a definite mathematical form. Establishing the design model involves: (1) deciding on the kind, number, and distribution of design variables; (2) identifying the load conditions and constraints to be considered during the optimization; and (3) selecting the objective function. Making these judgments yields a structural design optimization problem with definite mathematical form. This process may be viewed as somewhat analogous to making the judgments that lead to an idealized and discretized structural analysis model. It is important to recognize that in many structural design optimization problems the number of finite elements needed in the analysis model, to adequately predict the behavior, is much larger than the number of design variables required to describe the practical design problem of interest. In some design optimization problems it may even be necessary to dynamically update the analysis model as the design evolves. In any event, *it should be recognized that analysis modeling and design modeling involve two distinct but interrelated sets of judgment decisions.*

As previously indicated, a rather general class of system level structural design optimization problems can be properly stated as multi-inequality constrained minimization problems (see Eqs. 1 and 2), independent of whether or not the use of mathematical programming algorithms is envisioned. Before turning attention to various approaches taken

in the quest for efficient optimum design procedures, it is appropriate to *enumerate the characteristics of the system level structural optimization problem that make it difficult and challenging*:
(1) in general it cannot be anticipated *how many or which inequality constraints will become critical* equality constraints at the optimum design; (2) many of the *behavioral constraints are often computationally burdensome implicit functions* of the design variables; (3) practical problems frequently involve *large numbers of inequality constraints* because it is necessary to guard against various failure modes under each of several load conditions; (4) the *number of independent design variables* required to describe a complex structural system *can be large*, particularly as attention shifts from preliminary design toward final design. Because of the foregoing characteristics, a direct attack on the general system level design optimization problem is difficult and development efforts that have followed this course have produced structural optimization capabilities that are computationally inefficient. It is important to recognize that *successful approaches to large system level structural optimization problems have generally been based on approximation concepts of one sort or another*. It will be useful to classify the various optimum design procedures into *three main categories* as follows: (1) *intuitive techniques*; (2) methods based on *optimality criteria*; and (3) methods that make use of *mathematical programming algorithms*. In examining representative design procedures from each of these catagories attention will be focused on the approximations involved.

The simplest intuitive redesign method consists of *scaling of sizing type design variables. Here the result is approximate because the scaling assumes that the design already has the proper proportions* and only the magnitude of the design vector needs to be modified. *Fully stressed design (FSD) techniques* are predicated on the assumption that, for stress limited structures subject to multiple load conditions, a design for which each member is fully stressed in at least one load condition corresponds to the minimum weight design. *The FSD method is approximate because it forces the final design to reside at a constraint vertex point in design space.* However, since the stress constraints for indeterminate structures are nonlinear functions of the design variables, the minimum weight optimum design is not necessarily at a vertex point. Note that the FSD method is essentially the same as the previously discussed simultaneous failure mode approach employed at the structural component design level. The commonly employed *stress ratio methods of redesign seek an FSD design neglecting the influcnce of force redistribution during each iteration*. Since the force redistribution in many indeterminate structures is relatively insensitive to modest changes in the design, the stress ratio method often converges in only a few cycles.

Conventional optimality criteria methods for structural optimization involve: (1) *the derivation of a set of necessary conditions* that must be satisfied at the optimum design; and (2) the *development of an iterative redesign procedure* that drives the initial trial design toward a design which satisfies the previously estabilished set of necessary conditions. Optimum design procedures based on *optimality criteria methods usually involve two distinct types of approximations*: (1) those associated with *identifying in advance the critical constraints and the active (free)*[†] *design variables* at the optimum; and (2) those *associated with the development of simple recursive redesign rules*.

The basic ideas involved in establishing optimality criteria are initially introduced in the context of problems involving a single dominant constraint where all the design variables are assumed to be active (free). The optimum design task is, therefore, simplified to a multivariable minimization problem subject to a single equality constraint. Using the classical Lagrange multiplier method one writes

$$L(\vec{D},\lambda) = M(\vec{D}) - \lambda g(\vec{D}) \tag{6}$$

and then the necessary conditions that must be satisfied at the optimum design are

$$\frac{\partial L}{\partial D_i} = \frac{\partial M}{\partial D_i} - \lambda \frac{\partial g}{\partial D_i} = 0;\ i = 1,2,\ldots I \tag{7}$$

and

$$\frac{\partial L}{\partial \lambda} = -g(\vec{D}) = 0 \tag{8}$$

Rewriting Eq. 7 in the form

$$\left[\frac{\partial g}{\partial D_i} \Big/ \frac{\partial M}{\partial D_i}\right] = \frac{1}{\lambda};\ i = 1,2,\ldots I \tag{9}$$

shows that *the optimality criterion for problems involving a single critical constraint can be stated as follows*. At the optimum design, the rate of change of the constraint function with respect to each design variable D_i divided by the rate of change of the objective function with respect to that design variable is the same for each independent design variable. If total volume is taken as the objective function $M(\vec{D})$ to be minimized and it is assumed that element weight and stiffness are both linear functions of the design variables, *then for various specific types of single equality constraints* $g(\vec{D})$ *the optimum design is characterized by an invariant energy density distribution*.

Using the single constraint case, it will be shown that various redesign rules are implied by assuming the objective function $M(\vec{D})$ and the constraint $g(\vec{D})$ to be approximated by certain specialized functional forms. *A particularly interesting and important case arises when* $M(\vec{D})$ *is linear in the* D_i *and* $g(\vec{D})$ *is linear in the* $\left(\frac{1}{D_i}\right)$ *reciprocal variables*. This case corresponds to the minimum weight structural sizing problem subject to a single compliance constraint that has been approximated by a first order Taylor series expansion in terms of reciprocal $\left(\frac{1}{D_i}\right)$ variables. When this class of problems was first addressed via the optimality criteria approach, *the*

[†]A design variable is said to be *active* or *free* when it *does not* take on its upper or lower limit value at the optimum design.

approximate form of the compliance constraints were found by using the virtual load method with the assumption of constant internal forces, which is equivalent to using first order Taylor series expansions in terms of the $\frac{1}{D_i}$ *reciprocal variables.*

For problems involving multiple equality constraints the previous Lagrange multiplier approach can be generalized to yield the following necessary conditions

$$\frac{\partial M}{\partial D_i} - \sum_{q \in Q_{cr}} \lambda_q \frac{\partial g_q}{\partial D_i} = 0; \quad i \in \tilde{I} \tag{10}$$

and

$$g_q(\vec{D}) = 0 \quad ; \quad q \in Q_{cr} \tag{11}$$

assuming the set of critical constraints Q_{cr} and the set of active design variables $\tilde{I}$ can somehow be determined. Equations 10 and 11 represent a set of nonlinear simultaneous equations in the D_i ; $i \in \tilde{I}$ and the λ_q ; $q \in Q_{cr}$. When the $M(\vec{D})$ and $g_q(\vec{D})$ are replaced by explicit approximations, Eqs. 10 and 11 take on specific algebraic form and efficient iterative methods of solution can often be devised. However, the *essential difficulty involved in applying conventional optimality criteria methods to the general class of structural optimization problems posed in Eqs. 1 and 2 is that of finding the correct set of critical constraints and the associated set of active (free) design variables.* It is important to note that recent applications of dual methods of mathematical programming have led to design procedures (that can be viewed as generalized optimality criteria techniques) which conclusively overcome these obstacles for a significant class of structural optimization problems.

Continuing interest in the development of efficient system level structural optimization procedures for structures represented by finite element analysis models stimulated work on *design oriented structural analysis* (DOSA) during the 1965-1975 time frame. This area of investigation reflected a growing realization that structural analysis for design optimization is a task with special characteristics. It was recognized that design optimization required behavior prediction for many structures of somewhat similar form. New attention was given to *the idea that, in the design context, the objective of structural analysis should be to generate, with minimum effort, an estimate of the critical and potentially critical response quantities adequate to guide the design modification process.* Developments in design oriented structural analysis fall into three categories: (1) methods for obtaining rates of change of response quantities with respect to design variables, i.e. *behavior sensitivity analysis;* (2) techniques for constructing approximate analysis solutions using a few well chosen basis vectors, i.e. *reduced basis methods;* and (3) *re-examination of how finite element analysis methods are organized,* focusing on how to improve their organization so that they are better matched to the special characteristics of the design optimization task. It is interesting to observe that the common practice in dynamic analysis of using a small set of generalized coordinates and normal mode basis vectors is a special case of the general reduced basis idea.

Prior to 1970 the main obstacles to the development of efficient system level structural optimization capabilities, based on the use of mathematical programming algorithms, were associated with the fact that the general formulation (see Eqs. 1 and 2) involved: (1) large numbers of design variables; (2) large numbers of inequality constraints; and (3) many inequality constraints that are computationally burdensome implicit functions of the design variables. During the past decade, *these obstacles have been overcome by replacing the basic problem statement* (see Eqs. 1 and 2) *with a sequence of relatively small, explicit, approximate problems that preserve the essential features of the original design optimization problem.* This has been accomplished through the coordinated use of approximation concepts which include: (1) reduction of the number of independent design variables by *linking and/or basis reduction;* (2) reduction of the number of constraints considered at each stage *by temporary deletion of inactive and redundant constraints;* and (3) *construction of high quality explicit approximations for retained constraint functions.*

In its simplest form *design variable linking* fixes the relative size of some preselected group of finite elements. *The reduced basis concept in design space* further reduces the number of independent design variables by expressing the vector of I design variables $\vec{D}$ *as a linear combination of prelinked basis vectors* $\vec{T}_b$, that is let

$$\vec{D} = \sum_{b=1}^{B} \vec{T}_b \delta_b = [T]\vec{\delta} \tag{12}$$

where the δ_b are generalized design variables. It is interesting to observe that this *reduced basis concept in design space may be viewed as a designers Ritz method.* As in the Ritz method of structural analysis success depends on the quality of the basis vectors selected and the results obtained are in general upper bound estimates of the optimum design. In the case where only design variable linking is employed, the matrix [T] contains only one nonzero entry per row and it can be replaced by a pointer vector. It will be argued that design variable linking may be viewed: (1) as a sharpening of the original problem statement (e.g. when it imposes symmetry, fabrication, or cost control considerations); or (2) as a special type of basis reduction based upon the designer's insight and prior experience.

A general multi-stage strategy for reducing the number of constraints and employing approximate analysis techniques may be outlined as follows. Each stage consists of the following steps: (1) carry out a complete structural analysis; (2) identify the critical and potentially critical constraints and temporarily delete the rest; (3) construct explicit approximations for the inequality constraints retained; (4) carry out a sequence of design improvements considering only the constraints retained in step (2). *Regionalization and truncation represent two techniques for temporarily reducing the number of inequality constraints retained.* They are

nothing more than the systematic implementation of conventional design practice. The regionalization idea can be simply explained in terms of static stress constraints as follows. Let the finite element model of a structure be divided up into several regions (e.g. regions corresponding to the design variable linking scheme). Then execute a complete structural analysis for each of K loading conditions and retain only the most critical stress constraint in each region in each load condition. The regionalization idea works well provided the design changes made during a stage are small enough so that they do not result in a shift of the critical constraint location within a region. The truncation idea simply involves temporary deletion of constraints for which the ratio of the response quantity to its allowable value is so low that the constraint will clearly be inactive during the stage. It should be noted that in the case of linear constraints it is often possible to identify strictly redundant constraints that can be permanently deleted.

In order to reduce the number of detailed finite element structural analyses needed to obtain an optimum design it is appropriate to *construct explicit approximations for the constraints retained during the pth stage of the design optimization process.* These explicit approximations of the constraints retained are used in place of the finite element analysis during the pth stage. In seeking high quality explicit approximations for constraint functions it is *important to appreciate the flexibility offered by the use of Taylor series expansions in terms of intermediate design variables.* It should be clearly recognized that the direct application of the Taylor series expansion technique to constraint functions $g_q(\vec{D})$ does not necessarily yield high quality approximations. It may sometimes be desirable to try and preserve the explicit nonlinearities that are apparent when the constraint functions are viewed as functions of the response quantities. Furthermore, the use of physical insight in selecting intermediate design variables is often worthwhile. In the context of system structural optimization *first order, second order diagonal, and full second order approximations have been used with success.* Depending upon the kind of constraint being approximated *direct* (D_i), *reciprocal* ($\beta_i = \frac{1}{D_i}$) *and mixed design variables have been used.*

Once the original problem has been replaced by a sequence of relatively small explicit problems various mathematical programming algorithms can be successfully applied to the system level structural optimization task. These include feasible direction methods, SUMT (Sequence of Unconstrained Minimizations Technique) methods based on interior and exterior penalty functions, and SLP (Sequence of Linear Programs) methods. It should be also noted that posynomial[7] approxmations can be constructed. When both the objective function M(D) and the constraint functions $g_q(D)$ are or can be approximated by posynomials geometric programming algorithms can be brought to bear on the structural optimization problem.

It is now well known that *a significant class of minimum weight structural sizing problems subject to static stress, deflection, and minimum member size constraints can be treated efficiently by solving a sequence of approximate problems each of which has the following form in terms of linked reciprocal design variables* $\alpha_b = \frac{1}{\delta_b}$:

$$W(\vec{\alpha}) = \sum_{b \in B} \frac{w_b}{\alpha_b} \rightarrow \text{Min} \qquad (13)$$

subject to behavior constraints

$$\tilde{h}_q(\vec{\alpha}) = \bar{h}_q - h_q(\vec{\alpha}) \geq 0 \; ; \; q \in Q_R \qquad (14)$$

and side constraints

$$\alpha_b^{(L)} \leq \alpha_b \leq \alpha_b^{(U)} \; ; \; q \in Q_R \qquad (15)$$

where

$$h_q(\vec{\alpha}) = \sum_{b \in B} C_{bq} \alpha_b \; ; \; q \in Q_R \qquad (16)$$

and Q_R denotes the set of retained constraints. The w_b are positive constants corresponding to the weight of the set of finite elements in the bth linking group when $\alpha_b = 1$. The set of independent design variables after linking is denoted by B and Eqs. 14 and 16 represent the current linear approximations of the behavior constraints. The $\alpha_b^{(L)}$ and $\alpha_b^{(U)}$ respectively denote the lower and upper limits on the independent reciprocal design variables α_b.

Each approximate primal problem of the form given by Eqs. 13-16 can be shown to correspond to an explicit dual problem of the following form:
Find $\vec{\alpha}$ such that the explicit dual function

$$\ell(\vec{\lambda}) = \sum_{b \in B} \frac{w_b}{\alpha_b} + \sum_{q \in Q_R} \lambda_q [h_q(\vec{\alpha}) - \bar{h}_q] \rightarrow \text{Max} \qquad (17)$$

subject to non-negativity constraints

$$\lambda_q \geq 0 \; ; \; q \in Q_R \qquad (18)$$

where $h_q(\vec{\alpha})$ is given by Eq. 16 and the primal variables α_b are given explicitly in terms of the dual variables λ_q by

$$\alpha_b = \begin{cases} \alpha_b^{(L)} & \text{if } \left[\alpha_b^{(L)}\right]^2 \geq \tilde{\alpha}_b^2 \\ \tilde{\alpha}_b & \text{if } \left[\alpha_b^{(L)}\right]^2 < \tilde{\alpha}_b^2 < \left[\alpha_b^{(U)}\right]^2 \\ \tilde{\alpha}_b^{(U)} & \text{if } \tilde{\alpha}_b^2 \geq \left[\alpha_b^{(U)}\right]^2 \end{cases} \qquad (19)$$

where

$$\tilde{\alpha}_b^2 = w_b / \sum_{q \in Q_R} \lambda_q C_{bq} \qquad (20)$$

[7] A posynomial is defined to be a generalized polynomial having positive coefficients and variables but arbitrary real exponents

The first derivatives of $\ell(\vec{\alpha})$ are readily available since it can be shown that they correspond to the primal constraints, that is

$$\frac{\partial \ell}{\partial \lambda_q}(\vec{\lambda}) = \sum_{b \in B} c_{bq} a_b - \bar{h}_q \qquad (21)$$

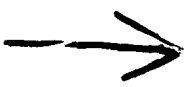
Dual methods exploit the special algebraic structure of the approximate primal problems. Since the approximate primal problem given by Eqs. 13-16 is convex, separable, and algebraically simple *is it possible to construct an explicit dual function* (see Eqs. 17-20). As a consequence, most the computational effort involved in optimization is expended on finding the maximum of the explicit dual function $\ell(\vec{\alpha})$, subject only to simple non-negativity constraints (Eq. 18). *The dimensionality of the dual space Q_R is relatively small for many problems of practical interest Furthermore special maximization algorithms have been devised which seek the maximum of $\ell(\vec{\alpha})$ by operating in a sequence of dual subspaces with gradually increasing dimension, such that the dimensionality of the maximization problem never exceeds the number of strictly critical constraints by more than one.*

Joining approximation concepts and dual methods of mathematical programming has led to a very efficient method of structural optimization that can be viewed as a generalized optimality criteria method. In this design optimization procedure finding the correct set of critical constraints and active (free) design variables is an intrinsic part of the special mathematical programming algorithm used to locate the maximum of the dual function $\ell(\vec{\alpha})$, subject to simple inequality constraints given by Eq. 18. Thus it is seen that for a significant class of minimum weight sizing problems the generalized optimality criteria and mathematical programming approaches have coalesced to the same method.

Sensitivity analysis plays an important role in structural analysis and optimization. In the analysis context rates of change of predicted response quantities (e.g. displacements, stresses, natural frequencies, normal modes, etc.) with respect to changes in design variables (e.g. cross sectional areas, thicknesses, nodal positions, etc.) are sought. These partial derivatives provide valuable information that can be used to guide the design process even when formal structural optimization is not contemplated. *The key to obtaining analysis sensitivity information usually involves implicit differentiation of the pertinent analysis equations with respect to the independent design variables selected. The option to call for such analysis sensitivity information should be available as an integral part of any modern finite element analysis program* because: (1) it provides valuable quantitative information that can help guide design via man-machine interaction, and (2) it provides a basis for constructing explicit approximations of response quantities in terms of design variables.

Optimum design sensitivity analysis is an important idea that has only recently (within the last two years) been brought to the attention of the structural optimization community. *Optimum design sensitivity analysis seeks rates of change of predicted optimum design variable values and Lagrange multiplier values with respect to changes in problem preassigned parameters* (e.g. allowable displacements, allowable stresses, allowable frequencies, load condition data, etc.). In other words, having obtained a base optimum design sensitivity derivatives are sought that can be used to estimate the revised optimum design, associated with specified perturbations of selected problem parameters, without recourse to reoptimization. The optimum design sensitivity derivatives provide valuable information that can be used to guide trade-off studies. It is also envisioned that optimum design sensitivity information, particularly with respect to applied loads, will be useful in multi-level design optimization because it may make it possible to replace many subsystem optimizations with a simple update, based on sensitivity analysis of a previously determined optimum design for the subsystem. *The key to obtaining optimum design sensitivity information usually involves implicit differentiation of the necessary conditions characterizing the base optimum design with respect to the independent preassigned parameters selected for perturbation. It is suggested that the option to call for optimum design sensitivity information should, in the future, be available as an integral part of advanced structural optimization capabilities.*

The broad scope of the structural optimization field is such that there are, unfortunately, many important topics and associated key ideas that I have not touched on in the main body of this lecture. These include the following problem areas: (1) optimum design of structural systems with coupled bending-membrane action; (2) optimum design of structural systems with discrete design variables or mixed continuous-discrete design variables; (3) extended space formulations and decomposition methods (formal and heurestic) for large structural systems; (4) reliability based optimum design methodology; (5) shape and/or configuration optimization of structural components and systems; (6) optimum design considering topological changes and/or materials selection; (7) optimum design considering both elastic (service load) and plastic collapse (overload) constraints; (8) optimum design in the dynamic response regime including consideration of active control devices; (9) optimum design considering complex failure modes such as elastic stability, aeroelastic behavior, and crack growth limitations; (10) nonconvexity, relative minima, and disjoint feasible regions; (11) consideration of objective functions other than weight minimizations (e.g. cost, performance, reliability); (12) optimum design of structural systems for global damage tolerance (e.g. battle damage); and (14) development of efficient, easy to use, well documented programs for structural optimization. Fortunately, many of these topics will be addressed in depth by sessions scheduled for presentation during this symposium.



SESSION #1

OPTIMALITY CRITERIA METHODS AND FULLY STRESSED DESIGN

ACHIEVEMENTS IN STRUCTURAL OPTIMIZATION USING OPTIMALITY CRITERIA METHODS

N. S. Khot
Structures and Dynamics Division
Flight Dynamics Laboratory
Wright-Patterson Air Force Base, Ohio 45433

and

L. Berke
NASA Lewis Research Center
Cleveland, Ohio 44135

Abstract

The essential idea in the development of optimality criteria methods was to take advantage of the special nature of structural optimization problems. Principally such concepts as statically determinate or indeterminate structures and certain variational principles of structural mechanics have been utilized to develop efficient algorithms for the optimum sizing of structures subject to stiffness related constraints. The theoretical foundation of the approach have been layed down by Prager and co-workers in a number of elegant papers dealing with simple continuum problems leading to differential equations as optimality criteria. The solutions to the differential equations, the Euler equations of the variational formulation stating the optimization problem, defined the optimum shape of the structures. The shape of a minimum volume column to carry a given compressive load is a typical example. The approach was viewed as theoretically powerful, but impractical due to inability of application to structures of general shape. Most practical structures are analyzed by Finite Element methods and, therefore, it became desirable to find an approach based on optimality criteria for discretized rather than continuum mathematical models. This also meant that the optimization problem is again reduced to finding solutions to optimality criteria equations which are algebraic rather than differential equations. However, due to the nonlinearity of the overall problem an iterative approach is necessary to solve the equations.

In optimality criteria methods the optimization procedure during each iteration can be divided into two phases. In the first phase a structure is analyzed to find the response of the structure to the applied loads. And in the second phase the design variables are modified so that the current design moves towards a design satisfying the applicable optimality criteria. The design satisfying the optimality criteria is then guaranteed to be at least a local optimum. In this sense the optimality criteria methods are indirect methods of optimization. For a discretized structure the analysis is performed by using a finite element method. The design variables are changed by using a recurrence relation derived from the optimality criteria. In the case of a single constraint or a single dominant constraint the recurrence relation actually becomes a formula for the sizing of the members of the structure. If the internal forces are independent of the member sizes, as in the case of statically determinate structures, or nearly independent, then a single or a very few sizing iterations will result in an optimum or near optimum structure. However, for strongly competing constraints, or for structures with member forces sensitive to member sizes, more number of iterations might be necessary even for a structure with small number of members. The potential strength of the method in practical applications is that the number of structural members has only a minor effect on the number of iterations needed to converge to an optimum design. This latter property makes these methods well suited for optimum sizing of large practical structures for stiffness type constraints.

The general structural optimization problem when the member "cost" (weight) is a linear function of the design variables can be stated as:

Minimize

$$W=\sum_{i=1}^{n} \rho_i A_i \ell_i \tag{1}$$

Subject to

$$g_j=C_j-\bar{C}_j\leq 0 \qquad j=1,\ldots,m \tag{2}$$

where

W = total structural "cost" (weight)

A_i = the design variable

ℓ_i = volume parameter for $A_i = 1$

ρ_i = "cost" (weight) per unit volume of the ith element

g_j = the jth constraint

C_j = actual value of the jth constraint

$\bar{C}_j$ = desired or limiting value of the jth constraint

n = number of design variables

m = number of constraints

The constraints imposed on the structure can be maximum allowable displacement at a node point, maximum allowable stress in an element, system stability, frequency constraint, minimum or maximum size of a design variable etc.

Using Eqs. 1 and 2 the Lagrangian can be written as

$$L(A,\lambda)=\sum_{i=1}^{n} \rho_i A_i \ell_i+\sum_{j=1}^{m} \lambda_j (C_j-\bar{C}_j) \tag{3}$$

where λ_j are the Lagrange multipliers. Differentiating Eq. 3 with respect to the design variables A_i and setting the resulting equations to zero gives

$$\rho_i \ell_i+\sum_{j=1}^{m} \lambda_j \frac{\partial C_j}{\partial A_i}=0 \qquad i=1,\ldots,n \tag{4}$$

or

$$\sum_{j=1}^{m} \frac{1}{\rho_i \ell_i} \lambda_j \frac{\partial C_j}{\partial A_i} = -1 \qquad i=1,\ldots,n \tag{5}$$

where

$$\lambda_j \geq 0 \tag{6}$$

$$\lambda_j g_j = 0 \tag{7}$$

Eq. 5 contains n algebraic equations associated with n design variables. These equations and Eqs. 6 and 7 are the optimality conditions or Kuhn-Tucker conditions in the formal sense of nonlinear mathematical programming. Depending on the nature of the constraints imposed on the structure suitable optimality criteria can be obtained by using Eq. 5. The 'n' optimality conditions and 'm' constraint equations form a set of (m+n) simultaneous equations for the solution of n unknowns A_i and m unknown λ_j.

The optimum design must satisfy the optimality criteria. Deriving the criteria is usually the easy part of the overall procedure. The difficult task is to develop an algorithm to solve these equations. Since the equations are generally nonlinear due to the nature of the problem they have to be solved by an iterative method. In the last decade a number of algorithms have been developed with various degrees of approximations to solve these equations. The commonalities, differences and relative merits will be discussed in the text of the paper. Application of various algorithms will be illustrated by designing four structures, 1) a 14-bar determinate truss, 2) a 17-bar indeterminate truss, 3) a 10-bar truss, and 4) a 49-bar portal truss, with different constraint requirements.

AD P000 027

OPTIMAL DESIGN OF A STRUCTURE FOR SYSTEM STABILITY FOR A SPECIFIED EIGENVALUE DISTRIBUTION

N. S. Khot
Structures and Dynamics Division
Flight Dynamics Laboratory
Wright-Patterson Air Force Base, Ohio 45433

Summary

A method based on the optimality criterion approach is presented to design a minimum weight structure with constraints on system stability. The stability constraints are stated with the requirement that the critical eigenvalues be separated by a specified interval and the critical buckling mode be the preselected one. The use of the method is illustrated by solving sample problems.

I. Introduction

The objective in structural optimization is generally to minimize the weight of the structure and satisfy all imposed constraints. The loads applied to the structure and the geometry of the structure are specified, and the unknowns are the individual sizes of the members. The constraints imposed on the structure may include maximum allowable stress, displacement limits at the nodal points, frequency constraints, local and system stability, minimum and maximum gauge constraints, etc. In a lightweight structure with a large number of elements, system stability can become the most critical constraint.

The algorithm based on an optimality criterion (Refs. 1, 2) uses a recurrence relation to modify the design variables. The optimality criterion is derived by differentiating the Lagrangian with respect to the design variables. The design satisfying the optimality criterion is a minimum weight design. This design may be a local minimum or a global minimum depending on the nature of the problem and the constraints imposed on the structure.

Initial attempts to optimize structures subjected to stability constraints were made in relation to columns (Refs. 3-7). The objective was to maximize the buckling load for a given weight of the column. In all the above references the model considered was one dimensional with one design variable. The use of a mathematical programming approach with a finite element idealization was presented in Ref. 8. In Ref. 9 a recurrence relation based on an optimality criterion was used to design a column subjected to a distributed load. An exponential recurrence relation based on an optimality criterion, using only one critical buckling mode, was proposed in Refs. 10 and 11 to design portal frames and truss structures. The design of columns and portal frames with two simultaneous critical modes was considered in Ref. 12. The optimality criterion approach was used in Ref. 13 to design columns and portal frames for stability under multiple loading conditions.

In the present paper, finite element analysis is used to predict the behavior of the structure. Three different recurrence relations based on an optimality criterion are derived and their use is illustrated by designing a truss tower structure with different requirements on the critical buckling loads and associated buckling modes.

II. Basic Equations of Analysis

The linear stability of a structure is defined by the eigenvalue problem

$$\{[K]-\mu_j[K_G]\}\{\eta_j\}=0 \tag{1}$$

where $[K]$ is the linear total stiffness matrix of the structure, $[K_G]$ is the geometric stiffness matrix of the structure, and $\{\eta_j\}$ is the eigenvector associated with the jth eigenvalue μ_j. The critical eigenvalue is the first eigenvalue μ_1, if the eigenvalues are arranged in ascending order. The linear buckling load of a structure is given by the product of μ_1 and the applied load vector, $\{P\}$. The geometric stiffness matrix $[K_G]$ is a function of the internal force distribution due to the applied load, $\{P\}$. Multiplying Eq. 1 by $\{\eta_j\}^t$ gives

$$\{\eta_j\}^t[K]\{\eta_j\}-\mu_j\{\eta_j\}^t[K_G]\{\eta_j\}=0 \tag{2}$$

Thus the eigenvalue μ_j can be written as

$$\mu_j=\frac{\{\eta_j\}^t[K]\{\eta_j\}}{\{\eta_j\}^t[K_G]\{\eta_j\}} \tag{3}$$

which is the Rayleigh quotient. The gradient of the eigenvalue μ_j can be obtained by differentiating Eq. 3 with respect to the design variable A_i (See Ref. 10). This gives

$$\frac{\partial\mu_j}{\partial A_i}=\frac{1}{A_i}\frac{\{\eta_j\}_i^t[k]_i\{\eta_j\}_i}{\{\eta_j\}^t[K_G]\{\eta_j\}} \tag{4}$$

where $[k]_i$ is the stiffness matrix and $\{\eta_j\}_i$ is the component of the buckling mode associated with the ith element.

In Eq. 3, the denominator $\{\eta_j\}^t[K_G]\{\eta_j\}=W_j$ represents the work done by the applied load during the transition from the unbuckled to the buckled state. If the buckled modes are normalized so that the denominator in Eq. 3 is equal to unity, then Eqs. 3 and 4 can be written as

$$\mu_j=\{\bar{\eta}_j\}^t[K]\{\bar{\eta}_j\} \tag{5}$$

and

$$\frac{\partial\mu_j}{\partial A_i}=\frac{1}{A_i}\{\bar{\eta}_j\}_i^t\{k\}_i\{\eta_j\}_i \tag{6}$$

where

$$\{\bar{\eta}_j\}=\frac{1}{\sqrt{W_j}}\{\eta_j\} \tag{7}$$

Eqs. 5 and 6 can also be written as

$$\mu_j = \sum_{i=1}^{n} \frac{B_{ij}}{A_i} \tag{8}$$

and

$$\frac{\partial \mu_j}{\partial A_i} = \frac{B_{ij}}{A_i^2} \tag{9}$$

where

$$B_{ij} = A_i \{\bar{\eta}_j\}_i^t [k]_i \{\bar{\eta}_j\}_i \tag{10}$$

In Eq. 8 n is the number of elements in the structure.

III. Optimality Criterion

The optimal design problem can be defined as:

minimize the weight

$$W = \sum_{i=1}^{n} \rho_i A_i \ell_i \tag{11}$$

subjected to

$$g_j = \mu_j - \alpha_j \bar{\mu} \geq 0 \qquad j=1,\ldots,m \tag{12}$$

where ρ_i is the density, A_i is the design variable, and ℓ_i is a fixed quantity associated with the ith element. For a bar structure A_i is the cross-sectional area, and ℓ_i is the length of the bar. For other types of elements A_i and ℓ_i have a different interpretation. In Eq. 12, g_j represents a constraint, and μ_j is the actual value of the eigenvalue associated with the jth eigenmode. The product $\alpha_j \bar{\mu}$ is the desired value of the jth eigenvalue. The parameter $\bar{\mu}$ is the lowest eigenvalue, and α_j represents the factor by which the eigenvalues are to be separated. If the eigenvalues are arranged in ascending order, then $\bar{\mu}$ is equal to μ_1, and α_1 is equal to unity.

Using Eqs. 11 and 12, the Lagrangian can be written as

$$L(A,\lambda) = \sum_{i=1}^{n} \rho_i A_i \ell_i - \sum_{j=1}^{m} \lambda_j (\mu_j - \alpha_j \bar{\mu}) \tag{13}$$

where λ_j are the Lagrange multipliers. Differentiating this equation with respect to the design variable A_i and setting the corresponding equations to zero gives

$$\rho_i \ell_i - \sum_{j=1}^{m} \lambda_j \frac{\partial \mu_j}{\partial A_i} = 0 \qquad i=1,\ldots,n \tag{14}$$

or

$$1 = \sum_{j=1}^{m} \frac{\lambda_j}{\rho_i \ell_i} \frac{\partial \mu_j}{\partial A_i} \qquad i=1,\ldots,n \tag{15}$$

Substituting Eq. 9 in Eq. 15 gives

$$1 = \sum_{j=1}^{m} \lambda_j \frac{B_{ij}}{A_i^2 \rho_i \ell_i} \tag{16}$$

or

$$1 = \sum_{j=1}^{m} \lambda_j \frac{b_{ij}}{\rho_i} \tag{17}$$

where $b_{ij} = \frac{B_{ij}}{A_i^2 \ell_i}$ is the strain energy density in the ith element due to the jth normalized buckling mode. In Eq. 16 the Lagrange multipliers λ_j associated with the critical buckling modes are positive and zero for other modes. All Lagrange multipliers satisfy the condition

$$\lambda_j (\mu_j - \alpha_j \bar{\mu}) = 0 \tag{18}$$

Eq. 16 or Eq. 17 together with Eq. 18 define the optimality criteion. All the elements in a structure must satisfy Eq. 16, except those whose sizes are fixed by some other requirement.

If $\alpha_j = 1$ for all the buckling modes, then the design satisfying the optimality criterion is a simultaneous mode design. The design, where the buckling load associated with all the critical buckling modes is the same, is known to be sensitive to geometric imperfections. The sensitivity of a structure to imperfections can be reduced by selecting $\alpha_j (j \geq 2)$ greater than unity. In this case the optimum design will have only one critical buckling mode associated with the design load.

IV. Design Algorithm

A. Recurrence Relations

The recurrence relations required to modify the design variables can be obtained from the optimality criterion (Eq. 16). In the design space the recurrence relations are used to modify the design variables so that the initial design moves towards a design satisfying the optimality criterion. Multiplying both sides of Eq. 16 by A_i^r and taking the rth root gives

$$A_i^{\nu+1} = A_i^{\nu} \left(\sum_{j=1}^{m} \lambda_j \frac{B_{ij}}{A_i^2 \rho_i \ell_i} \right)_{\nu}^{1/r} \tag{19}$$

where $\nu+1$ and ν are introduced to denote the iteration numbers, and r is the step size parameter. Eq. 19 is the exponential recurrence relation. The quantity within the parenthesis is equal to unity at the optimum. Thus once the optimality criterion is satisfied, the design variables will remain unchanged with any additional iterations.

A linear recurrence relation can be obtained from Eq. 19 by writing this equation as

$$A_i^{\nu+1} = A_i^{\nu} \left(1 + \left(\sum_{j=1}^{m} \lambda_j \frac{B_{ij}}{A_i^2 \rho_i \ell_i} - 1 \right) \right)_{\nu}^{1/r} \tag{20}$$

and expanding it using the binomial theorem. Retaining only the linear terms gives

$$A_i^{\nu+1}=A_i^{\nu}\left(1+\frac{1}{r}\left(\sum_{j=1}^{m}\lambda_j\frac{B_{ij}}{A_i^2\rho_i\ell_i}-1\right)\right)_{\nu} \tag{21}$$

This equation can also be written as

$$A_i^{\nu+1}=\frac{A_i^{\nu}}{\left(1+\frac{1}{r}\left(\sum_{j=1}^{m}\lambda_j\frac{B_{ij}}{A_i^2\rho_i\ell_i}-1\right)\right)_{\nu}^{-1}} \tag{22}$$

Now, if the denominator is expanded by using the binomial theorem and only the linear terms are retained, one obtains

$$A_i^{\nu+1}=\frac{A_i^{\nu}}{\left(1-\frac{1}{r}\left(\sum_{j=1}^{m}\lambda_j\frac{B_{ij}}{A_i^2\rho_i\ell_i}-1\right)\right)_{\nu}} \tag{23}$$

or

$$A_i^{\nu+1}=A_i^{\nu}\left(1-\frac{1}{r}\left(\sum_{j=1}^{m}\lambda_j\frac{B_{ij}}{A_i^2\rho_i\ell_i}-1\right)\right)_{\nu}^{-1} \tag{24}$$

Eq. 21 can be obtained from Eq. 24 by expanding it using the binomial theorem and retaining the linear terms. The essential difference in using the three recurrence relations (Eqs. 19, 21 and 24) is the rate at which the design variables are modified with each iteration for the same step size parameter r. The rate of change in the design variables decreases as one uses Eq. 21 instead of Eq. 19 and Eq. 24 instead of Eq. 21. Eqs. 23 and 24 are equivalent to the linear recurrence relation for a problem defined in terms of the reciprocal design variables.

The recurrence relations contain two unknowns B_{ij} and λ_j in addition to the step size parameter r. The coefficient B_{ij} for the desired buckled mode can be determined by using Eq. 10. The relations required to estimate the Lagrange multipliers can be derived by using various conditions which should be satisfied when the design variables are modified. We have chosen the condition that the constraint relations should be satisfied when the design variables are modified from one iteration to the next.

B. Equations to Determine Lagrange Multipliers

A change in the jth constraint due to a change in the design variable A_i can be written as

$$\Delta g_j=g_j(A+\Delta A)-g_j(A) \tag{25}$$

$$=\sum_{j=1}^{m}\frac{\partial g_j}{\partial A_i}(A_i^{\nu+1}-A_i^{\nu}) \tag{26}$$

Now, if we impose the condition that the change A_i^{ν} to $A_i^{\nu+1}$ should satisfy the constraint relation i.e. $g(A+\Delta A)=0$, then using Eqs. 9, 12 and 21, Eq. 26 can be written as

$$\sum_{k=1}^{m}\lambda_k^{\nu+1}\left(\sum_{i=1}^{n}\frac{B_{ij}B_{ik}}{\rho_i\ell_iA_i^3}\right)_{\nu}=r(\alpha_j\bar{\mu}-\mu_j^{\nu})+\sum_{i=1}^{n}\left(\frac{B_{ij}}{A_i}\right)_{\nu} \tag{27}$$

$$=r(\alpha_j\bar{\mu}-\mu_j^{\nu})+\mu_j^{\nu} \tag{28}$$

In deriving this relation we have assumed that all the design variables will satisfy the optimality criterion and are modified by using the recurrence relation. Those elements satisfying the optimality criterion are called active elements. However, if there are some elements whose sizes are governed by some other design criterion, then those elements are called passive elements, and Eq. 27 must be modified. The modified equation is

$$\sum_{k=1}^{m}\lambda_k^{\nu+1}\left(\sum_{i=1}^{n_1}\frac{B_{ij}B_{ik}}{\rho_i\ell_iA_i^2}\right)_{\nu}$$

$$=r(\alpha_j\bar{\mu}-\mu_j^{\nu})+\sum_{i=1}^{n_1}\left(\frac{B_{ij}}{A_i}\right)_{\nu}$$

$$+\sum_{i=n_1+1}^{n}\left(\frac{B_{ij}}{A_i^2}\right)_{\nu}(A_i^*-A_i^{\nu}) \tag{29}$$

where n_1 is the number of active elements and A_i^* is the size of the ith passive element. The passive elements may be the minimum size elements or the elements whose sizes are governed by maximum allowable stress. The size of a passive element is increased or decreased to satisfy the specific requirements.

C. Scaling of the Design

In most design problems the load applied to the structure is specified, and it is required that the structure have the capability to carry that load. The buckling load of a structure is given by the product $\bar{\mu}\{P\}$. Thus, in order to have the buckling load equal to the applied load, it is necessary to scale the design so that for the scaled design $\bar{\mu}$ is equal to unity. The relation between the scaled ($\tilde{A}_i$) and the unscaled (A_i) values of the design variables can be written as

$$\tilde{A}_i=\Lambda A_i \tag{30}$$

where Λ is the scaling parameter. Substituting this relation in Eq. 1, it can be shown that for

$$\Lambda=\frac{1}{\bar{\mu}} \tag{31}$$

the buckling load of a structure with areas equal to $\tilde{A}_i$ is equal to the applied load vector $\{P\}$. (See Ref. 10).

D. Relationship Between Lagrange Multipliers and Optimum Weight

A relationship can be derived between the Lagrange multipliers associated with the active constraints and the weight of the structure. The weight of the structure expressed in terms of the Lagrange multipliers is

called a dual weight. At the optimum the dual weight is equal to the optimum weight. In the iterative algorithm the dual weight is a lower bound, and the actual weight of the structure is the upper bound. The difference between the dual weight and the actual weight can be used to track the convergence of the algorithm.

The weight of a structure can be written as

$$W = \sum_{i=1}^{n_1} \rho_i A_i \ell_i + W^* \tag{32}$$

where $W^* = \sum_{i=n_1+1}^{n} \rho_i A_i \ell_i$ is the contribution of the passive elements to the total weight of the structure. If it is assumed that the constraint relations are satisfied as equality constraints, then Eq. 12 can be written as

$$g_j = 0 = \sum_{i=1}^{n_1} \frac{B_{ij}}{A_i} - \alpha_j \bar{\mu} + \sum_{i=n_1+1}^{n} \frac{B_{ij}}{A_i} \tag{33}$$

$$= \sum_{i=1}^{n_1} \frac{B_{ij}}{A_i} - \alpha_j \bar{\mu} + \mu_j^* \tag{34}$$

where μ_j^* is the contribution of the passive elements to the eigenvalue. Using the optimality criterion relation (Eq. 16), we can write

$$A_i = \sum_{j=1}^{m} \lambda_j \frac{B_{ij}}{A_i \rho_i \ell_i} \tag{35}$$

Substituting Eq. 35 in Eq. 32 and using Eq. 34 we can write

$$W(d) = \sum_{j=1}^{m} \lambda_j (\alpha_j \bar{\mu} + \mu_j^*) + W^* \tag{36}$$

where W(d) is the dual weight. If there are no passive elements, then Eq. 36 reduces to

$$W(d) = \sum_{j=1}^{m} \lambda_j \alpha_j \bar{\mu} \tag{37}$$

In the problems solved in the next section the dual weight is used to track the convergence of the algorithm.

V. Application and Conclusion

A computer program based on the relations derived in the previous section was written to design a minimum weight structure idealized with bar elements. The truss tower shown in Fig. 1 was designed to satisfy different stability constraint requirements. The structure was subjected to two axial loads of magnitude 500 lbs. applied in the vertical direction at nodes 1 and 2.

The tower was first designed to satisfy the condition $\alpha_1 = 1$. This constraint condition requires that the optimum design must have equal buckling loads associated with all critical active buckling modes. This is a simultaneous mode design. The structure was designed by using the three recurrence relations (Eqs. 19, 21, 24). The step size parameter r for all the recurrence relations was 2. The solution obtained by using the exponential recurrence relation (Eq. 19) diverged after the first iteration. This behavior was due to the large changes made in the design variables for the step size parameter r=2. Increasing the value of r would have reduced the step size and improved the convergence. The iteration history for the recurrence relations (Eqs. 21 and 24) is given in Tables 1 and 2 respectively. The tables contain the Lagrange multipliers associated with the active buckling modes and the dual weight. Only two buckling modes were found to be active at the optimum. The buckling modes are shown in Fig. 2. The first mode (Fig. 2(a)) was dominant at the beginning and end of the iterations. The second mode (Fig. 2(b)) was dominant at the middle of the iterations. Comparing the results in Tables 1 and 2, one sees that convergence with Eq. 24 was slightly slower than with Eq. 21. The final results for both recurrence relations were identical. The dual and actual weight were identical at the optimum, however the dual weight approached the optimum weight from the bottom and the actual weight approached the optimum weight from the top. The cross-sectional areas of the members for the minimum weight design are given in Table 8.

As discussed above the simultaneous failure mode, i.e. $\alpha_i = 1$, has two critical modes, Mode 1 (Fig. 2(a)) and Mode 2 (Fig. 2(b)). The tower can be designed so that at the optimum the critical buckling mode is only one of these two modes, and the buckling loads associated with the two modes are separated by a specified ratio. Two cases were considered. In Case I, the critical buckling mode was Mode 1 and α_2 was set equal to 1.1, 1.2, 1.3, 1.4 and 1.5 respectively. In Case II, the critical buckling mode was Mode 2 and the values of α_2 were the same as for Case I. For both cases α_1 would be equal to unity, however in Case I α_1 would be associated with Mode 1 and in Case II α_1 would be associated with Mode 2. The iteration history for both cases using Eqs. 21 and 24 is given in Tables 3 through 6 for α_2 equal to 1.1. The tables contain the Lagrange multipliers associated with the active buckling modes and the dual weight at each iteration. At the optimum the dual weight and the minimum weight were equal. The Lagrange multipliers and the optimum weights for all values of α_2 for both cases are given in Table 7. It is seen that the minimum weight for $\alpha_2 = 1$ is lower than for all other values of α_2. For the same value of α_2 the weight of the optimum design for Case II is higher than for Case I. The areas of the members for the optimum design for the two cases are given in Tables 8 and 9. For the two cases the distribution of the areas for the different elements is found to be substantially different.

The success of designing a structure to have a specific critical buckling mode depends on the flexibility of the structure to buckle in that mode. The flexibility depends on the stiffness of each element, the geometry of the structure and the boundary conditions. The algorithm discussed in the paper modifies the stiffness of the elements by changing the areas while keeping the geometry unchanged. For certain structures, changing the stiffness of each element may not be enough to achieve a specific buckling mode. In the truss tower this would occur if horizontal members are added to connect nodes 3-4, 5-6 etc. For this modified structure it was found that the critical buckling mode is Mode 1 (Fig. 2(a)). This structure cannot be designed to buckle in Mode 2. The algorithm reduces all horizontal members to the minimum size requirement. The optimum weight for this structure was found to be 465.28 lbs.

References

1. Khot, N. S., Venkayya, V. B. and Berke, L., "Comparison of Optimality Criteria Algorithms for Minimum Weight Design of Structures," AIAA J. 17, pp. 182-190, 1979.

2. Khot, N. S., "Algorithms Based on Optimality Criteria to Design Minimum Weight Structures," Engineering Optimization, Vol. 5, pp. 73-90, 1981.

3. Keller, J. B., "The Shape of the Strongest Column," Arch. Rati. Mech. Analysis, Vol. 5, pp. 275-285, 1960.

4. Tadjbakhsh, I. and Keller, J. B., "Strongest Columns and Isoperimetric Inequalities for Eigenvalues," J. Appl. Mech., Vol. 29, pp. 159-164, 1962.

5. Keller, J. B. and Niordson, F. I., "The Tallest Column," J. Math. Mech., Vol. 16, pp. 433-446, 1966.

6. Taylor, J. E., "The Strongest Column: An Energy Approach," J. App. Mech., Vol. 34, pp. 486-487, 1967.

7. Taylor, J. E. and Liu, C. Y., "Optimal Design of Columns," AIAA J., Vol. 6, pp. 1497-1502, 1968.

8. Zarghamee, M. S., "Minimum Weight Design with Stability Constraint," J. of the Structural Division, ASCE, Vol. 96, pp. 1697-1710, 1970.

9. Simitses, G. J., Kamat, M. P. and Smith Jr., C. V., "The Strongest Column by the Finite Element Displacement Method," AIAA J., Vol. 11, pp. 1231-1232, 1973.

10. Khot, N. S., Venkayya, V. B. and Berke, L., "Optimization of Structures for Strength and Stability Requirements," AFFDL-TR-73-98, Air Force Flight Dynamics Laboratory, Wright-Patterson Air Force Base, Ohio.

11. Khot, N. S., Venkayya, V. B. and Berke, L., "Optimum Structural Design with Stability Constraints," Int. J. Num. Met. Engg., Vol. 10, pp. 1097-1114, 1976.

12. Kiusalaas, J., "Optimal Design of Structures with Buckling Constraints," Int. J. Solids Struct., Vol. 9, pp. 863-878, 1973.

13. Turner, H. K. and Plaut, R. H., "Optimal Design for Stability Under Multiple Loads," J. of the Engg. Mech. Division, ASCE, Vol. 12, pp. 1365-1382, 1980.

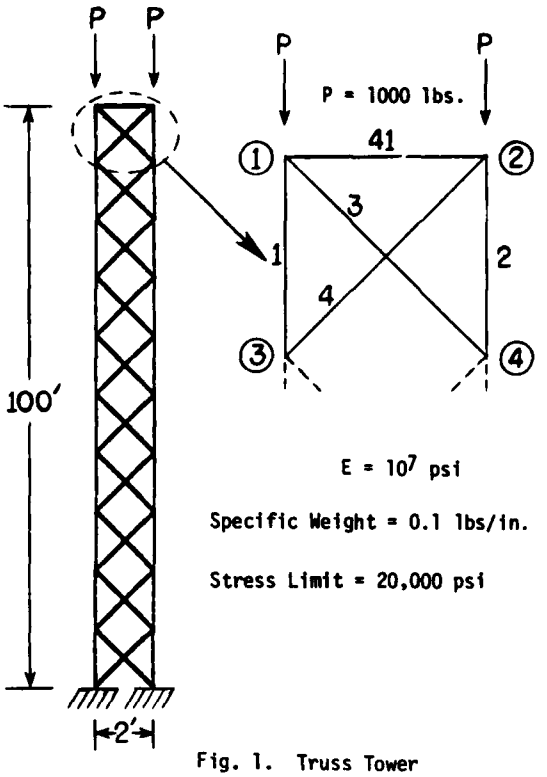


Fig. 1. Truss Tower

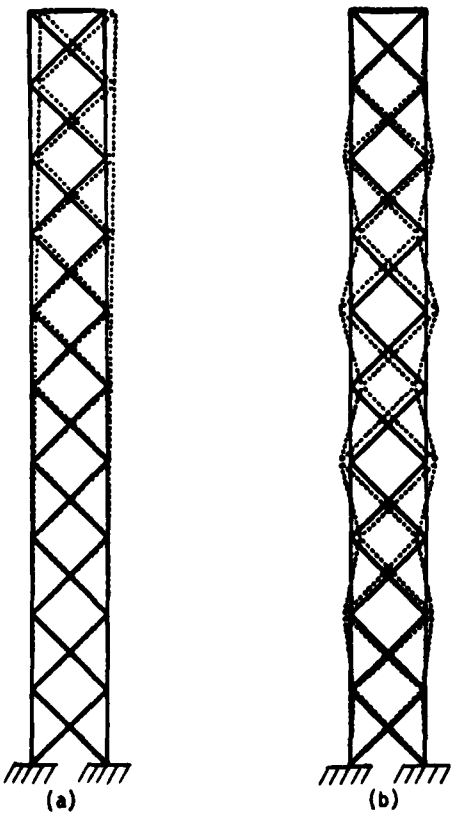


Fig. 2. Buckling Modes

TABLE 1. Iteration History of the Truss Tower (Eq. 21)
α_i=1

ITERATION NO.	μ_1	μ_2	λ_1	λ_2	WEIGHT (DUAL)	WEIGHT
1	1.0000(1)*	1.9776(2)*	329.36	0.0	329.36	989.82
2	1.0000(1)	1.2375(2)	363.13	106.94	470.07	689.17
3	1.0000(2)	1.0183(1)	208.12	348.42	556.54	606.26
4	1.0000(2)	1.0009(1)	219.98	355.29	575.27	591.23
5	1.0000(1)	1.0002(2)	363.99	221.00	585.00	585.65
6	1.0000(1)	1.0003(2)	364.40	220.92	585.32	585.52
7	1.0000(1)	1.0000(2)	364.41	221.04	585.45	585.45

TABLE 2. Iteration History of the Truss Tower (Eq. 24)
α_i=1

ITERATION NO.	μ_1	μ_2	λ_1	λ_2	WEIGHT (DUAL)	WEIGHT
1	1.0000(1)*	1.9776(2)*	329.36	0.0	329.36	989.82
2	1.0000(1)	1.4945(2)	369.67	27.76	397.44	775.22
3	1.0000(1)	1.1125(2)	362.77	145.56	508.33	652.16
4	1.0000(1)	1.0121(2)	361.25	201.24	562.49	605.46
5	1.0000(2)	1.0004(1)	216.81	360.79	577.61	591.93
6	1.0000(2)	1.0001(1)	220.44	362.04	582.48	587.50
7	1.0000(1)	1.0000(2)	363.50	220.96	584.47	585.94
8	1.0000(1)	1.0000(2)	364.30	221.00	585.30	585.51
9	1.0000(1)	1.0000(2)	364.41	221.04	585.45	585.45

TABLE 3. Iteration History of the Truss Tower for Case I (Eq. 21)
α_1=1.0 α_2=1.1

ITERATION NO.	μ_1	μ_2	λ_1	λ_2	WEIGHT (DUAL)	WEIGHT
1	1.0000(1)*	1.9776(2)*	329.36	0.0	329.36	989.82
2	1.0000(1)	1.2375(2)	349.67	152.64	517.56	689.18
3	1.0000(1)	1.0814(2)	347.53	232.47	603.24	616.14
4	1.0000(1)	1.0927(2)	348.24	236.86	608.78	608.56
5	1.0000(1)	1.1006(2)	350.14	234.01	607.55	608.54
6	1.0000(1)	1.1003(2)	350.48	234.17	608.07	608.31
7	1.0000(1)	1.1000(2)	350.49	234.30	608.23	608.23

*(1) Buckling Mode 1 - Fig. 2(a)
(2) Buckling Mode 2 - Fig. 2(b)

TABLE 4. Iteration History of the Truss Tower for Case I (Eq. 24)
α_1=1.0 α_2=1.1

ITERATION NO.	μ_1	μ_2	λ_1	λ_2	WEIGHT (DUAL)	WEIGHT
1	1.0000(1)*	1.9776(2)*	329.36	0.0	329.36	989.82
2	1.0000(1)	1.4945(2)	353.28	71.17	431.16	775.22
3	1.0000(1)	1.1844(2)	349.61	176.01	543.22	664.36
4	1.0000(1)	1.1051(2)	347.43	220.67	590.17	625.00
5	1.0000(1)	1.0996(2)	347.17	231.53	601.86	613.89
6	1.0000(1)	1.0999(2)	348.19	234.02	605.62	610.12
7	1.0000(1)	1.1000(2)	349.60	234.23	607.25	608.72
8	1.0000(1)	1.1000(2)	350.38	234.26	608.07	608.29
9	1.0000(1)	1.1000(2)	350.49	234.30	608.23	608.23

TABLE 5. Iteration History of the Truss Tower for Case II (Eq. 21)
α_1=1.0 α_2=1.1

ITERATION NO.	μ_1	μ_2	λ_1	λ_2	WEIGHT (DUAL)	WEIGHT
1	1.0000(1)*	1.9776(2)*	329.36	0.0	329.36	989.82
2	1.0000(1)	1.2374(2)	375.37	65.3	434.82	689.17
3	1.0000(2)	1.1277(1)	191.35	354.92	581.76	650.76
4	1.0000(2)	1.1114(1)	206.78	363.95	607.13	631.02
5	1.0000(2)	1.1007(1)	208.51	375.38	621.43	623.02
6	1.0000(2)	1.0997(2)	208.59	375.50	621.64	622.41
7	1.0000(1)	1.1000(1)	208.56	376.31	622.52	622.52

TABLE 6. Iteration History of the Truss Tower for Case II (Eq. 24)
α_1=1.0 α_2=1.1

ITERATION NO.	μ_1	μ_2	λ_1	λ_2	WEIGHT (DUAL)	WEIGHT
1	1.0000(1)*	1.1977(2)*	329.36	0.0	329.36	989.82
2	1.0000(1)	1.4945(2)	380.15	0.0	380.15	775.23
3	1.0000(1)	1.0902(2)	374.02	112.15	475.97	645.22
4	1.0000(2)	1.0698(1)	190.18	393.92	623.49	631.62
5	1.0000(2)	1.1101(1)	203.33	371.86	612.34	630.30
6	1.0000(2)	1.1001(1)	207.61	374.08	619.09	624.73
7	1.0000(2)	1.1000(1)	208.44	375.52	621.56	622.99
8	1.0000(2)	1.0999(1)	208.54	376.25	622.41	622.55
9	1.0000(2)	1.0999(1)	208.58	376.32	622.52	622.51
10	1.0000(2)	1.1000(1)	208.57	376.32	622.52	622.52

TABLE 7. Minimum Weights and Lagrange Multipliers for Case I and II

	$\mu_1(\alpha_1)$	$\mu_2(\alpha_2)$	λ_1	λ_2	WEIGHT
CASE I	1.000	1.0	364.41	221.04	585.45
	1.000	1.1	350.49	234.30	608.23
	1.000	1.2	335.60	247.25	632.31
	1.000	1.3	319.69	259.98	657.67
	1.000	1.4	302.73	272.55	684.30
	1.000	1.5	284.74	284.95	712.18
CASE II	1.000	1.1	208.56	376.33	622.52
	1.000	1.2	197.74	385.75	660.64
	1.000	1.3	188.17	393.41	699.61
	1.000	1.4	179.56	399.79	739.28
	1.000	1.5	171.71	405.22	779.54

TABLE 8. Minimum Weight Design for Case I

	Values of α_2 (α_1 = 1.0)					
Members	1.0	1.1	1.2	1.3	1.4	1.5
1, 2	0.8988	1.0068	1.1178	1.2328	1.3506	1.4713
3, 4	0.9161	1.0262	1.1394	1.2565	1.3768	1.4996
5, 6	0.9947	1.0669	1.1453	1.2301	1.3202	1.4153
7, 8	0.8157	0.9146	1.0167	1.1228	1.2320	1.3441
9, 10	1.1677	1.1916	1.2207	1.2559	1.2968	1.3434
11, 12	0.6294	0.7055	0.7847	0.8680	0.9545	1.0440
13, 14	1.3919	1.3774	1.3635	1.3507	1.3392	1.3293
15, 16	0.3733	0.4145	0.4585	0.5068	0.5580	0.6125
17, 18	1.6587	1.6274	1.5934	1.5564	1.5162	1.4725
19, 20	0.1484	0.1472	0.1460	0.1453	0.1454	0.1465
21, 22	1.9366	1.9077	1.8767	1.8429	1.8063	1.7667
23, 24	0.3215	0.3573	0.3943	0.4306	0.4671	0.5037
25, 26	2.1841	2.1669	2.1502	2.1334	2.1170	2.1011
27, 28	0.5850	0.6609	0.7393	0.8188	0.9001	0.9831
29, 30	2.3820	2.3778	2.3767	2.3785	2.3836	2.3925
31, 32	0.7927	0.8985	1.0080	1.1202	1.2356	1.3539
33, 34	2.5195	2.5257	2.5368	2.5528	2.5743	2.6018
35, 36	0.9355	1.0614	1.1919	1.3261	1.4644	1.6065
37, 38	2.5891	2.6008	2.6185	2.6420	2.6721	2.7092
39, 40	1.0062	1.1422	1.2833	1.4285	1.5784	1.7325
41	0.1795	0.2024	0.2258	0.2499	0.2744	0.2995

TABLE 9. Minimum Weight Design for Case II

	Values of α_2 (α_1 = 1.0)				
Members	1.1	1.2	1.3	1.4	1.5
1, 2	0.8854	0.8758	0.8695	0.8658	0.8643
3, 4	0.9024	0.8927	0.8862	0.8824	0.8808
5, 6	1.0296	1.0710	1.1174	1.1679	1.2218
7, 8	0.8031	0.7944	0.7890	0.7863	0.7857
9, 10	1.2662	1.3688	1.4745	1.5823	1.6917
11, 12	0.6210	0.6166	0.6152	0.6164	0.6196
13, 14	1.5462	1.7008	1.8557	2.0107	2.1657
15, 16	0.3741	0.3784	0.3854	0.3947	0.4048
17, 18	1.8535	2.0465	2.2385	2.4295	2.6199
19, 20	0.1646	0.1809	0.1972	0.2136	0.2300
21, 22	2.1570	2.3761	2.5944	2.8121	3.0293
23, 24	0.3171	0.3128	0.3089	0.3056	0.3031
25, 26	2.4198	2.6557	2.8920	3.1286	3.3657
27, 28	0.5683	0.5523	0.5368	0.5220	0.5078
29, 30	2.6266	2.8732	3.1212	3.3707	3.6211
31, 32	0.7681	0.7453	0.7237	0.7031	0.6833
33, 34	2.7692	3.0220	3.2774	3.5347	3.7936
35, 36	0.9061	0.8791	0.8538	0.8299	0.8071
37, 38	2.8412	3.0971	3.3559	3.6171	3.8801
39, 40	0.9742	0.9450	0.9175	0.8923	0.8680
41	0.1753	0.1717	0.1686	0.1658	0.1633

AD-P000 028

OPTIMAL DESIGN OF INELASTIC CABLE STRUCTURES

Carlo Cinquini* and Roberto Contro**

*Department of Structural Mechanics, University of Pavia, Pavia, Italy

**Department of Structural Mechanics, Technical University (Politecnico) of Milan, Milan, Italy

Summary

A nonlinear behaviour modelling of prestressed cable structures is firstly recalled, as dealt with in a previous paper and peculiar features of such structures are discussed. So, the important role played by pretension state is emphasized. Accordingly, optimum design problem is formulated assuming a cost function of pretension forces only. Optimality criterion is found by means of Langrangian multiplier method.

1. Main Features of the Plane Cable Structure Behaviour

An abundant literature deals with mechanical aspects and relevant solution methods of special structures made of individual cable members and stiffened by means of initial pre-tension state.
Such structures are susceptible to behave nonlinearily for both large displacements and cable responses. Generally speaking these causes of nonlinearity are not allowed for simultaneously (or do not occur). That depends on the strucural layouts, prestress states and load conditions which are considered. Moreover the analysis and design point of view often leads to different assumptions and approximations in order to yield methods fairly simple and efficient at the same time. The mostly considered nonlinearity concerns the geometric response. Large or moderately large displacements (depending on prestress level) make nonlinear the governing equations and hence appropriate techniques are needful. Webster, in a recent work [1], comprehensively outlines available methods for static analysis of geometrical nonlinear structures. Particularly he focuses essential characteristics as accuracy, stability, convergence and starting solution requirements. Each method enjoys of same aforementioned properties but all ones need a nonsingular initial stiffness matrix except for energy methods and dynamic relaxation (this last one discouraging for involved difficulties). Therefore just in the case of cable structures the energy methods attraction appears increased. In fact an appreciated peculiarity of such structures, designed to large size roofs, is their lightness, so that they are considered weightless in unloaded conditions. So usual structural layouts are mechanisms in absence of pre-tension forces. Even if the initial singularity can be overcome by adjusting in some way starting situation, it can appears again throughout the loading history because of loosening of some cable members. This sort of inelastic behaviour, typical of cables, seems play an important role in a deformability investigation, as it will be shown in the following.
For the above reasons the energy approach formulated in Ref.2, allowing for cable inelasticity, deserves, attention and it has given rise to fundamental ideas of this paper.
Finally, we agree with the unquestionable opinion expressed by the author of Ref.1, that optimum design problems, as those to which we are going, can be efficiently and elegantly solved by mathematical programming. Therefore these techniques, which are natural tools for energy methods, are direct translation of optimum design problems too. Concepts clarified an experiences performed in the first field can be an useful base to develop the second one.
In the following section 2. essential ideas stated in Ref.2, relating to the cable loosening model and to the energy approach will be concisely recalled. On the basis of such notions and principles, optimal design problems will be formulated in section 4, according to suggestions inspirated by numerical experiments illustrated in section 3.

2. Loosening Cable Model and Energy Analysis Formulation

As it can be drawn from Ref.3, strands and ropes exhibit a wide linear elastic behaviour in tension and a sharp deviation from linearity occurring when axial force vanishes and cable member loosenes. Therefore, if plastic deformations in tension can be neglected as usually it happens in design problems, a simple cable model is represented by bilinear force-elongation diagram of fig.1a (heavy line).

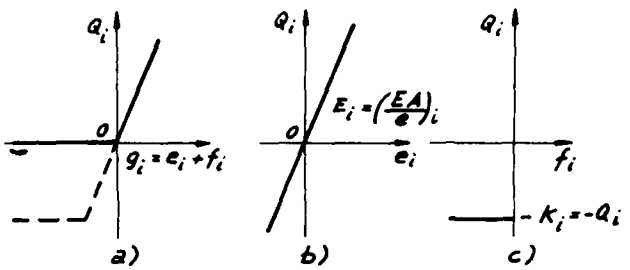


Fig.1 - Inelastic cable behaviour allowing for loosening.

When the i-th member is prestressed by a force K_i the constitutive model is similar to the previous one except for the horizontal branch which results translated (heavy line in the first quadrant plus dashed lines in the third quadrant). This model, which is nonlinear and reversible (holonomic) according to the real nature of loosening, is also represented by fig.s 1b, 1c where elongation q_i has been split into a linear elastic e_i and a nonlinear part f_i, i.e. $q_i = e_i + f_i$. Analytical depiction of the above idealized cable behaviour consists of the following relationships:

$$q_i = E_i^{-1} Q_i - \lambda_i \tag{2.1}$$

$$\phi_i = -Q_i - K_i \tag{2.2}$$

$$\lambda_i \geq 0 \tag{2.3}$$

$$\phi_i \leq 0 \tag{2.4}$$

$$\phi_i \lambda_i = 0 \tag{2.5}$$

where $\lambda_i = -f_i$ denotes loosening measure.
For a system of m cable members there will be a set of previous relations, which are in matrix form

$$\{q\} = [E]^{-1} \{Q\} - \{\lambda\} \tag{2.6}$$

$$\{\phi\} = -\{Q\} - \{K\} \tag{2.7}$$

$$\{\lambda\} \geq \{0\} \tag{2.8}$$

$$\{\phi\} \leq \{0\} \tag{2.9}$$

$$\{\phi\}^T \{\lambda\} = 0 \tag{2.10}$$

where $\{Q\}$, $\{q\}$, $\{\lambda\}$, $\{\phi\}$, $\{K\}$ are the column vectors of all Q_i, q_i, λ_i, ϕ_i, K_i for i=1...m and $[E]$ is the diagonal matrix of all $E_i = (EA/l)i$.
Let a prestressed cable structure (pin-jointed assembly) be considered in a known equilibrium configuration defined by nodal coordinates, nodal loads $\{\bar{P}\}$ and internal forces $\{\bar{Q}\}$. $\{\bar{P}\}$ is a n-vector, being n the nodal degree of freedom number; $\{\bar{Q}\}$ is the m-vector of cable forces.
In the quoted paper [2] it has been stated a theorem according to which vectors $\{u\}$, $\{\lambda\}$ solving the problem:

$$\inf_{\substack{\{u\}\\ \{\lambda\}\geq\{0\}}} \omega = \tfrac{1}{2}\{g\}^T[E]\{g\} + \tfrac{1}{2}\{\lambda\}^T[E]\{\lambda\} + \{\lambda\}^T[E]\{g\} + (\{\bar{Q}\}-[E]\{D\})^T\{g\} - (\{\bar{P}\}+\{P\})^T\{u\} + \{K\}^T\{\lambda\} - \{D\}^T[E]\{\lambda\} \qquad (2.11)$$

with total elongations

$$\{g\} = \{g(u)\} = \{q\} + \{D\} \qquad (2.12)$$

nonlinear functions of nodal displacements {u}, determine a change leading the structure to a new equilibrium configuration under added loads {P} and imposed member dislocations {D}.
Thus, this formulation, by means of a nonlinear programming algorithm, permits to find the structure response with possible cable loosening and large geometry changes. For further details on mechanical meaning and various specializations of the above statement it should be to refer to Ref.2. It is worth noting only that the briefly recalled method can describe the nonlinear behaviour of cable systems even if they are affected by a singular stiffness matrix. The encountered main difficulty is numerical and it concerns algorithm efficiency and mostly variable number. This last handicap generally does not appear in the case of plane cable structures, which are dealt with in this paper.

3. Significant Design Parameters

Some remarks can be made on optimum design procedures classified in Ref.4. Approximate methods (reanalysis) seem promise applications able to solve large size problems and iterative methods are fairly efficient, but often burdensome and meeting with some convergence difficulties. On the other hand, attraction of direct methods is faded by elaborate formulations, sometimes by too drastic idealizations and by the small size of solvable problems. Such desheartening peculiarities appear evident from Ref.s 5 and 6. In Ref.5 elastic and plastic structures are proposed to be optimized under behavioural constraints and Lagrangian multipliers techniques are employed. In Ref.6 optimum design of plastic structures under displacement constraints is carried out, using constitutive relationships similar to ones referenced in section 2. Linear expression of strength (and possibly of ductility) parameters are assumed as cost function and appropriate mathematical programming formulations are widely discussed. Reading two cited papers definitively shows chances and limits of direct methods which, in spite of their intrinsic complexity, are worth developing, mostly when design parameters particularly significant with respect to structure to be optimized, can be identified. A noticeable effort in this direction has been made by authors of Ref.7, just with regard to plane cable structures, the global minimum volume of which is shown to be approached by fully stressed solutions, thus representing a good starting point to the structural optimization under behavioural constraints.
In this paper new optimum design problems will be formulated, assuming some design parameters suggested by nonlinear behaviour of cable structures. So, referring to concepts seen in previous section 2 will appear justified. Particularly, taking into account cable loosening reveals worrying loss of local stiffness, dangerous, for instance, to the roof deck integrity. In order to obtain the aim previously declared, by means of described loosening cable model and energy method, the cable structure depicted in fig.2 has been analyzed. Firstly, note that cross sections have been chosen so that individual cable members preserve their linear elastic behaviour in tension.
Only loads conditions thought interesting design ends will be reported in the following. The structure has been subjected to three load cases indicated in table 1A: LC1, LC1*, symmetric loads (vertical downward forces P=58.86 kN on each node); LC2, LC2*, non symmetric loads (vertical downward forces of the same previous intensity); LC3, LC3* symmetric loads simulating wind effects (vertical upward forces P=39.24 kN). For each condition two cases are considered: corresponding to two assumptions on roofing location, LC1 LC2, LC3 differ from similar starred situations LC1*, LC2*, LC3* because in the first cases hogging cable nodes are loaded (nodes 15 and 23 instead of nodes 2 and 12). In table 1A, for several horizontal pre-tension components, representative kinematic parameters are depicted, i.e. maximum values of displacements u of loosening λ and of shortening g^- (obviously always affecting the same cable member). In all tested cases common aspects can be underlined: (a) remarkable elongations g due to loosening λ which are of the same order, for low pre-tension; (b) vanishing of previous phenomena at certain level of pre-tension force; (c) a rather linear response beyond the said level with a fairly constant global stiffness; (d) displacements moderately large in both elastic and inelastic range. What preceded is moreover emphasized by plots of fig.s 3, 4 and 5 relating to load conditions LC1, LC2 and LC3*. In these figures several quantities are drawn versus horizontal pre-tension force. The swift decrease of maximum shortening g^- and its subsequent stability at low values, after inelastic range (i.e. as cable loosening disappears), confirm a remarkable structural sensitiveness to pre-tension level. Such a property regards local deformability (here measured as change of distance between two adjacent nodes) much more than global stiffness. In fact diagrams of maximum displacements u are very smooth. Analogous behaviour is shown by plots of maximum lengthening g^+ and of maximum stress σ. g^+ is very small in both inelastic and elastic phases throughout which it approaches g^- values. σ stays under the elastic limit, according to the made assumption. Plot of the objective function ω evidences a transition from nonlinear to nearly linear behaviour, corresponding to the above observed pre-tension level. Among tabled load cases, not casually LC1, LC2 and LC3* have been selected to be illustrated, because maximum shortening relates cables supporting roof decks, which cannot undergo the deformations allowed by small pre-tensions. Thus prestress state appears as an important design parameter not only because of what said but also for the influence on cable foundations and on external supporting struts. On the contrary, within certain limits, the influence of cable cross section areas on local and global deformability seems to be negligible. This impression emerges from a comparison between third row of table 1A and results of table 1B, obtained by choosing the same stiffness EA=408MN for both cables. Finally, from analyzed examples a nonlinear behaviour much more physical than geometric has been shown. Hence design methods taking into account cable loosening seem fully justified.

4. General Formulation of Design Problem

Starting from natural stressless state of a cable structure, a first stage will be considered, in which pre-tensions only are applied. Let r denote the number of independent scalar parameters T_i (components of an r-vector {T}), that define such initial tensions.
If the absence of cable members loosening is supposed in this stage, the strain state of structure is completely defined by the m-vector {t} of member elongations ({t} is new notation of {g} for initial stage only governed by {T}). Each component of {t} can be seen as depending on nodal displacements, by means of compatibility relationships.
Let the r-vector {w} represent the nodal displacements that are referred to the applied initial tensions. The other nodal displacements are represented by the n-vector{v}.
On the basis of minimum theorem recalled in the foregoing, the equilibrium condition for pre-tension stage can be achieved by solving the following minimum problem

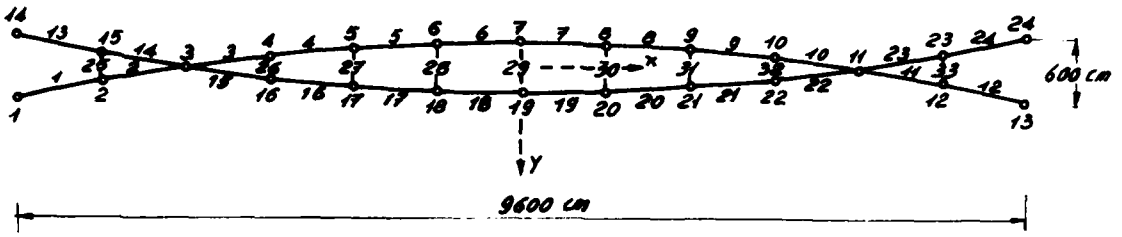


Fig. 2 - Layout of tested plane cable structure (Elastic stiffness EA: sagging cable 408 MN, hogging cable 275 MN, struts 245 MN).

TABLE 1

A

H/9.81 (kN)		LOAD CONDITIONS					
		LC1	LC2	LC3	LC1*	LC2*	LC3*
10	u(cm)	97.8	99.0	93.8	97.8	99.0	93.8
	λ(cm)	7.1	9.8	11.0	11.1	12.5	6.7
	g(cm)	7.4	10.1	11.2	11.4	12.8	7.2
20	. . .	93.4	91.6	85.9	93.4	91.6	85.9
	. . .	5.8	7.5	6.4	8.8	9.2	5.6
	. . .	6.4	8.1	6.8	7.1	9.8	6.0
30	. . .	89.0	84.[illegible]	77.9	89.0	84.0	77.9
	. . .	4.4	5.2	5.5	6.4	5.1	4.3
	. . .	5.3	6.1	6.1	6.9	6.[illegible]	4.
40	. . .	84.4	76.3	69.9	84.4	76.3	69.9
	. . .	3.0	1.5	4.1	4.0	1.5	2.9
	. . .	4.2	2.7	4.9	5.2	2.7	3.7
50	. . .	79.9	70.2	61.7	79.9	70.2	61.7
	. . .	1.6	0.0	1.8	1.7	0.0	1.5
	. . .	3.1	1.3	2.7	3.1	1.3	2.5
55	. . .	77.5	67.8	57.7	77.5	67.8	57.7
	. . .	0.5	0.0	0.6	0.5	0.0	0.6
	. . .	2.1	1.3	1.7	2.1	1.3	1.7
60	. . .	76.0	65.6	55.3	76.0	65.6	55.3
	. . .	0.0	0.0	0.0	0.0	0.0	0.0
	. . .	1.7	1.3	1.1	1.7	1.3	1.1
100	. . .	69.8	53.0	49.9	69.8	53.0	49.9
	. . .	0.0	0.0	0.0	0.0	0.0	0.0
	. . .	1.7	1.4	1.1	1.7	1.4	1.1

B

30	u(cm)	87.6	83.8	57.3	87.6	83.8	57.3
	λ(cm)	5.1	5.6	3.8	7.8	6.1	2.6
	g(cm)	5.7	6.2	4.4	8.4	6.7	3.2

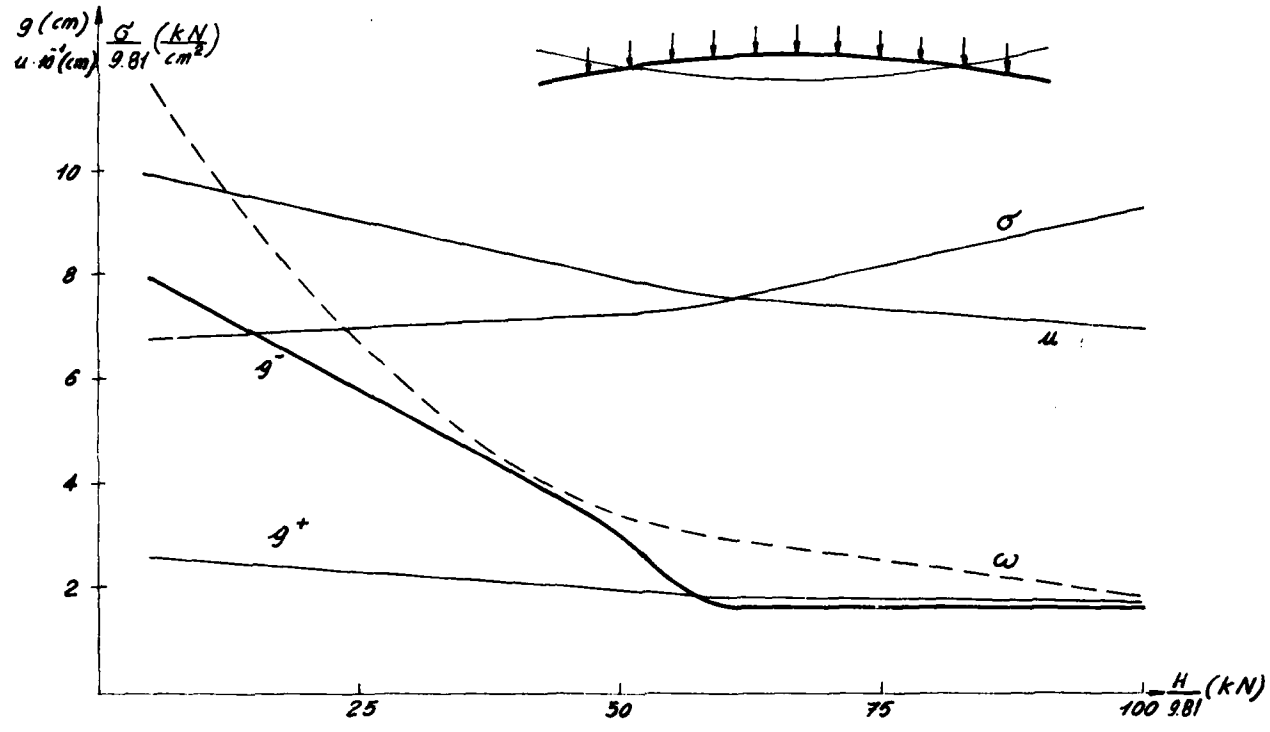


Fig. 3 - Load condition LC1. Plots of the objective function ω and of the maximum value of g^- (shortening), g^+ (lengthening), u (displacement vertical component), σ (cable stress) versus horizontal pre-tension component H. (member 1, 12 for g^-, member 13,24 for g^+ and σ , node 7 for u)

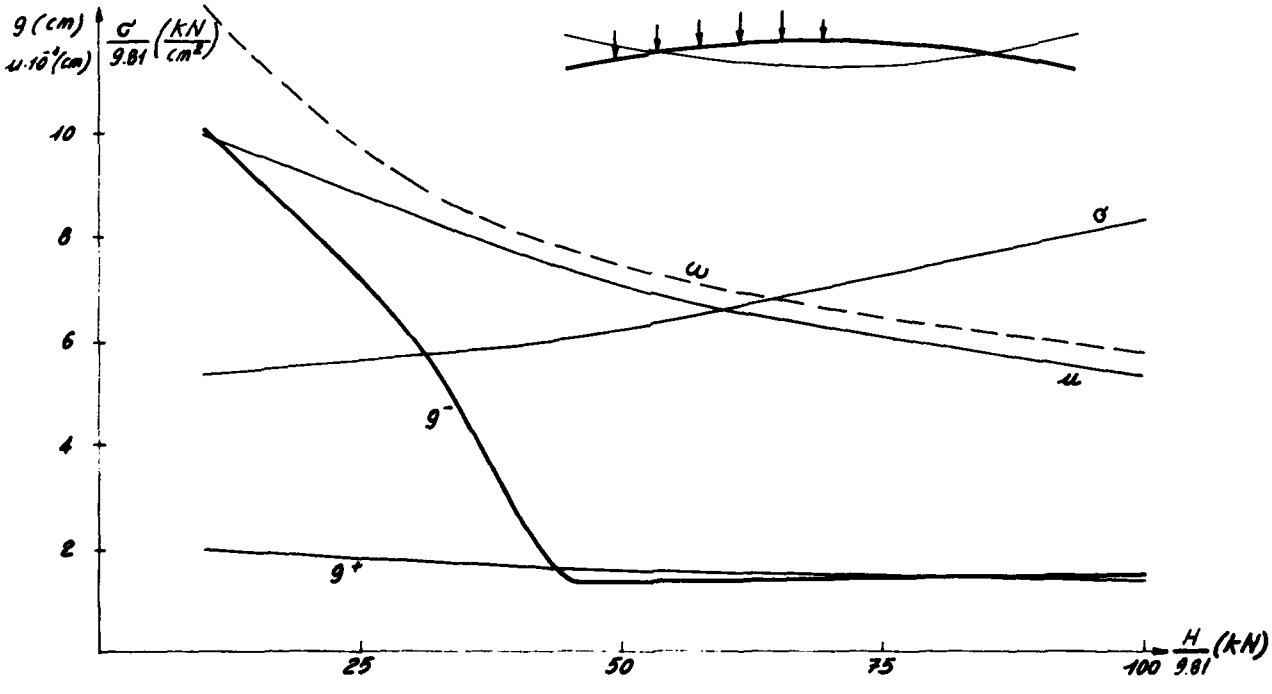


Fig. 4 - Load condition LC2. Plots of the objective function ω and of the maximum value of g^- (shortening), g^+ (lengthening), u (displacement vertical component), σ(cable stress) versus horizontal pre-tension component H. (member 1 for g^-, member 13 for g^+ and σ , node 17 for u)

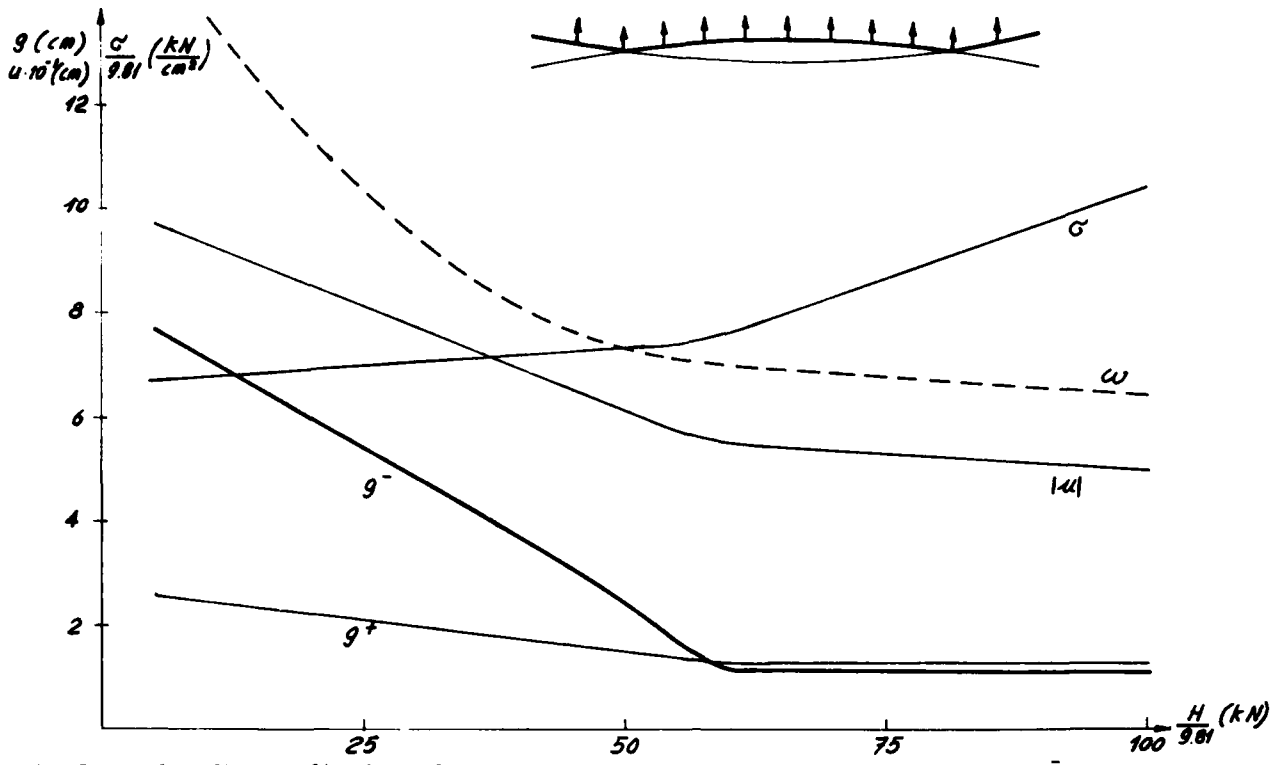


Fig. 5 - Load condition LC3*. Plots of the objective function ω and of the maximum value of g^-(shortening), g^+(lengthening), u (displacement vertical component), σ (cable stress) versus horizontal pre-tension component H. (Members 13,24 for g^-,members 1,12 for g^+ and σ , node 7 for u)

$$\inf_{\{w\},\{v\}} \tfrac{1}{2}\{t\}^T[E]\{t\} - \{T\}^T\{w\} \tag{4.1}$$

Accordingly, equilibrium conditions can be given as

$$[t,_w][E]\{t\} - \{T\} = \{0\} \tag{4.2}$$

$$[t,_v][E]\{t\} = \{0\} \tag{4.3}$$

where the (r x m) matrix $[t,_w]$ and the (n x m) matrix $[t,_v]$are defined as follows

$$[t,_w] = \begin{bmatrix} \frac{\partial t_1}{\partial w_1} & \cdots & \frac{\partial t_m}{\partial w_1} \\ \vdots & & \vdots \\ \frac{\partial t_1}{\partial w_r} & \cdots & \frac{\partial t_m}{\partial w_r} \end{bmatrix} \tag{4.4}$$

$$[t,_v] = \begin{bmatrix} \frac{\partial t_1}{\partial v_1} & \cdots & \frac{\partial t_m}{\partial v_1} \\ \vdots & & \vdots \\ \frac{\partial t_1}{\partial v_n} & \cdots & \frac{\partial t_m}{\partial v_n} \end{bmatrix} \tag{4.5}$$

The subsequent loading stage is now considered. Member elongations, nodal displacements and nodal loads will be indicated by the m-vector{p}, the n-vector {u} and the n-vector {P} , respectively. In particular, the final strain state of structure is defined by adding parameters {p} and {u} to {t} and {v} respectively. Then, functional ω defined in section 2 reads

$$\omega = \tfrac{1}{2}\{p\}^T[E]\{p\} + \tfrac{1}{2}\{\lambda\}^T[E]\{\lambda\} + \{\lambda\}^T[E]\{p\} + \{t\}^T[E]\{p\} + \{t\}^T[E]\{\lambda\} - \{P\}^T\{u\} \tag{4.6}$$

where each component of {p} depends on displacement parameters {u}.
If the initial tensions are known, structural analysis is carried out by solving the following minimum problem

$$\inf_{\substack{\{u\} \\ \{\lambda \geq 0\}}} \omega \tag{4.7}$$

so

$$[p,_u][E](\{p\}+\{\lambda\}+\{t\})-\{P\} = \{0\} \tag{4.8}$$

$$[E](\{\lambda\}+\{p\}+\{t\}) \geq \{0\} \tag{4.9}$$

$$[\lambda][E](\{\lambda\}+\{p\}+\{t\}) = \{0\} \tag{4.10}$$

In Rel.4.8 the (n x m) matrix $[p,_u]$is defined as

$$[p,_u] = \begin{bmatrix} \frac{\partial p_1}{\partial u_1} & \cdots & \frac{\partial p_m}{\partial u_1} \\ \vdots & & \vdots \\ \frac{\partial p_1}{\partial u_n} & \cdots & \frac{\partial p_m}{\partial u_n} \end{bmatrix} \tag{4.11}$$

In Rel.4.10 the (m x n) diagonal matrix $[\lambda]$ is assumed in such a way that

$$\{\lambda\} = \{\text{diag } [\lambda]\} \tag{4.12}$$

Absence of cable loosening in service conditions is firstly considered as behavioural constraint of optimization problem. So, from Rel.s 4.9 an 4.10 one has

$$[E](\{p\}+\{t\}) \geq \{0\} \tag{4.13}$$

and from Rel.4.8

$$[p,_u][E](\{p\}+\{t\})-\{P\}=\{0\} \tag{4.14}$$

Stiffness of whole structure is characterized by absolute values of nodal displacements and local stiffness by mutual nodal displacements. By suitably assuming an s-vector $\{\hat{u}\}$ and an (s x n) matrix $[C]$, behavioural constraints that are set on nodal displacements can be symbolized in a general form

$$[C]\{u\} \leq \{\hat{u}\} \tag{4.15}$$

If an upper bound for cable stresses is prescribed, a further behavioural constraint can be introduced

By assuming a cost function z linearly depending on pre-tensions only, one has

$$z = \{c\}^T \{T\} \tag{4.17}$$

The optimal design problem for cable structures is now formulated as the search for the minimum of the cost function z, subject to the constraints (4.2), (4.3), (4.13), (4.14), (4.15) and (4.16).
Applying the vectors $\{\eta\}$, $\{\alpha\}$ and $\{\beta\}$ of Lagrangian multipliers to the equality constraints (4.14), (4.2) and (4.3) respectively, and the nonnegative vectors $\{\theta\}$, $\{\mu\}$ and $\{\nu\}$ to the inequality constraints (4.13), (4.15) and (4.16) respectively, the following functional can be obtained

$$\begin{aligned} L_1 = {} & \{c\}^T\{T\}+\{\eta\}^T([p,_u][E](\{p\}+\{t\})-\{P\}) \\ & -\{\theta\}^T[E](\{p\}+\{t\})+\{\mu\}^T([C]\{u\}-\{\hat{u}\}) \\ & +\{\nu\}^T([E](\{p\}+\{t\})-\{\hat{Q}\}) +\{\alpha\}^T([t,_w][E]\{t\}-\{T\}) \\ & +\{\beta\}^T([t,_v][E]\{t\}) \end{aligned} \tag{4.18}$$

The stationarity conditions of L_1 are necessary conditions for the optimality of design [5],[8],[9].
In particular, from the stationarity conditions with respect to Lagrangian multipliers, the constraints set on design are obtained and the orthogonality constraints too:

$$[\theta][E](\{p\}+\{t\}) = \{0\} \tag{4.19}$$

$$[\mu](\{C\}\{u\}-\{\hat{u}\}) = \{0\} \tag{4.20}$$

$$[\nu](\{E\}(\{p\}+\{t\})-\{\hat{Q}\}) = \{0\} \tag{4.21}$$

From the stationarity conditions with respect to initial tensions $\{T\}$, the optimality criterion is found

$$\{c\}-\{\alpha\} \geq \{0\} \tag{4.22}$$

$$[T](\{c\}-\{\alpha\}) = \{0\} \tag{4.23}$$

The diagonal matrices $[\theta]$, $[\mu]$, $[\nu]$ and $[T]$ are defined in such a way that the following relations are fulfilled

$$\{\theta\} = \{\text{diag } [\theta]\} \tag{4.24}$$

$$\{\mu\} = \{\text{diag } [\mu]\} \tag{4.25}$$

$$\{\nu\} = \{\text{diag } [\nu]\} \tag{4.26}$$

$$\{T\} = \{\text{diag}[T]\} \tag{4.27}$$

The stationarity conditions of L_1 with respect to vectors $\{u\}$, $\{v\}$ and $\{w\}$ provide respectively

$$\begin{aligned} & ([p,_u][E][p,_u]^T + [[p,_{uu}]][E](\{p\}+\{t\}))\{\eta\} \\ & -[p,_u][E]\{\theta\}+[C]^T\{\mu\}+[p,_u][E]\{\nu\} = \{0\} \end{aligned} \tag{4.28}$$

$$\begin{aligned} & [t,_v][E][p,_u]^T\{\eta\}-[t,_v][E]\{\theta\}+[t,_v][E]\{\nu\} \\ & +([t,_v][E][t,_w]^T+[[t,_{wv}]][E]\{t\})\{\alpha\} \\ & +([t,_v][E][t,_v]^T+[[t,_{vv}]][E]\{t\})\{\beta\} = \{0\} \end{aligned} \tag{4.29}$$

$$\begin{aligned} & [t,_w][E][p,_u]^T\{\eta\} - [t,_w][E]\{\theta\}+[t,_w][E]\{\nu\} \\ & +([t,_w][E][t,_w]^T+[[t,_{ww}]][E]\{t\})\{\alpha\} \\ & +([t,_w][E][t,_v]^T+[[t,_{vw}]][E]\{t\})\{\beta\} = \{0\} \end{aligned} \tag{4.30}$$

Differentiating with respect to $\{u\}$ the matrix $[p,_u]$, defined in Rel.4.11 results on a three-index matrix $[[p,_{uu}]]$. This matrix is defined in such a way that the form $[[p,_{uu}]][E](\{p\}+\{t\})$ represents a (nxn) matrix (see appendix). The matrices $[[t,_{wv}]]$, $[[t,_{vv}]]$, $[[t,_{ww}]]$, $[[t,_{vw}]]$ are analogously assumed.
Analytical form of Euler-Lagrange equations is very complex because of the non-linearity of compatibility relationships between member elongations and nodal displacements. So phisical meaning of Lagrangian multipliers does not immediately appear and special features of the optimal design are very hard to be investigated.
It appears worth emphasizing that it can be interesting, from a practical point of view, to consider also a system of dislocations $\{D\}$ in the first stage, in such a way to represent turnbuckle operations. In this case a term depending on $\{D\}$ is to be included in cost function (4.17).
Form of relations of optimization problem is to be modified, in consequence of vector $\{D\}$, that appears in Rel.s 4.2 and 4.3. In particular, optimality criterion is completed by adding to Rel.s 4.22, 4.23 stationarity conditions with respect to $\{D\}$.

5. Optimization Problem with Global Constraint on Deformability

In order to investigate for more simplified approaches, some types of cable-structures can be studied neglecting loosening problems, because all the members are in tension under service loads. In several practical cases, also constraints on cable stresses can be desregarded. Such approximations do not involve a very simplified form of general problem seen in sect.4. On the contrary, some advantages are obtained if a global constraint on a suitably defined energetic functional is considered as behavioural constraint on deformability instead of Rel.4.15. In fact, such a problem is directly related to analysis formulations, if physical meaning of functional ω defined in sect.2 is taken into account.
Let the following functional be considered

$$\begin{aligned} L_2 = {} & \{c\}^T\{T\} - \mu(\tfrac{1}{2}\{p\}^T[E]\{p\}+\tfrac{1}{2}\{\lambda\}^T[E]\{\lambda\}+\{\lambda\}^T[E]\{p\} \\ & + \{t\}^T[E]\{p\}+\{t\}^T[E]\{\lambda\}-\{P\}^T\{u\}+\Omega) \\ & +\{\alpha\}^T([t,_w][E]\{t\}-\{T\})+\{\beta\}^T([t,_v][E]\{t\}) \end{aligned} \tag{5.1}$$

A saddle point of L_2 is looked for, i.e.

$$\begin{array}{llll} \inf & \sup & L_2 & \\ \{T\} & \mu\geq 0 & & \\ \{u\} & \{\alpha\} & & \\ \{\lambda\}\geq 0 & \{\beta\} & & \end{array} \tag{5.2}$$

The stationarity condition of L_2 with respect to μ results on an upper bound Ω on the absolute value of the functional ω; so a global constraint on deformability is set. From the stationarity conditions with respect to the n-vector $\{u\}$ and the nonnegative m-vector $\{\lambda\}$ Rel.s 4.8, 4.9 and 4.10 are found. The optimality criterion in the form of Rel.s 4.22 and 4.23 is provided by the stationarity condition with respect to $\{T\}$.
From the stationarity conditions with respect to the r-vector $\{w\}$ and the n-vector $\{v\}$, one obtaines equations analogous to Rel.s 3.29 and 3.30 respectively, which are here omitted for the sake of simplicity.

In order to investigate for numerical solutions, it is to be noticed that the optimization problem discussed in this section is strictly related to analysis problems, even if the above mentioned stationarity conditions with respect to $\{w\}$ and $\{v\}$ may involve some considerable difficulties. Nevertheless, by means of appropriate numerical expedients, solving numerical tools may be conceived, that are similar to the ones of the analysis problems.
Note that a more simplified formulation of design problems is found if only one stage is considered, so that both pre-tensions and loads are applied at the same time. In this way results less well reflecting practical construction procedures are obtained. A similar approache can seem to be useful in order to find less refined numerical tools.

6. Approximated linear model

If the relationships between elongations $\{p\}$ (or $\{t\}$) and nodal displacements $\{u\}$ ($\{v\}$ and $\{w\}$) can be modified to obtaine a linear homogeneous form (small displacements), the analytical formulations shown in the foregoing are very simplified.
In particular, matrices $[p,_u]$, $[t,_v]$ and $[t,_w]$ are depending only on undeformed structural geometry and they are not affected by further derivative operators (note

that $[p,_u]=[t,_u]$).
The stationarity conditions of functional L_1, defined in Rel.4.18, with respect to vectors $\{u\}$, $\{v\}$ and $\{w\}$ are modified respectively as follows

$$[p,_u][E][p,_u]^T\{\eta\}-[p,_u][E]\{\theta\}+[c]^T\{\mu\}+[p,_u][E]\{v\}=\{0\} \quad (6.1)$$

$$[t,_v][E][p,_u]^T\{\eta\}-[t,_v][E]\{\theta\}+[t,_v][E]\{v\} +[t,_v][E][t,_w]^T\{\alpha\}+[t,_v][E][t,_v]^T\{\beta\}=\{0\} \quad (6.2)$$

$$[t,_w][E][p,_u]^T\{\eta\}-[t,_w][E]\{\theta\}+[t,_w][E]\{v\} +[t,_w][E][t,_w]^T\{\alpha\}+[t,_w][E][t,_v]^T\{\beta\}=\{0\} \quad (6.3)$$

A physical meaning of the optimality criterion (4.25), (4.26) is allowed to be found by the virtue of the simple form of Rel.s 6.1, 6.2 and 6.3, and a dual problem can be defined.
Two subsequent stages can be conceived as contributing to such dual problem, as consequence of two stages of the primal one.
Firstly, a distorsion vector $\{D^*\}$ may be thought

$$\{D^*\} = \{\theta\} - \{v\} \quad (6.4)$$

Starting from the imposed distorsions $\{D^*\}$, the structure is subjected to a load

$$\{p^*\} = -[c]^T \{\mu\} \quad (6.5)$$

with zero-values prescribed to the r degrees of freedom corresponding to the components of pre-tension vector in the primal problem. Displacements and elongations are given by

$$\{u^*\} = \{\eta\} \quad (6.6)$$

$$\{p^*\} = [p,_u]^T\{\eta\} \quad (6.7)$$

So, the equilibrium equation referred to the first stage is provided by Eq.6.1, that reads

$$[p,_u][E](\{p^*\}-\{D^*\})-\{P^*\}=\{0\} \quad (6.8)$$

In the subsequent stage, loads $\{P^*\}$ are removed and displacements $\{w^*\}$ are allowed to be different from zero. In particular, displacements and elongations are given by

$$\{w^*\}=\{\alpha\} \quad (6.9)$$

$$\{v^*\}=\{\beta\} \quad (6.10)$$

$$\{t^*\} = [t,_w]^T\{\alpha\}+[t,_v]^T\{\beta\} \quad (6.11)$$

Equilibrium equations are given by Rel.s 6.2 and 6.3, that read respectively

$$[t,_v][E](\{p^*\}+\{t^*\}-\{D^*\}) = \{0\} \quad (6.12)$$

$$[t,_w][E](\{p^*\}+\{t^*\}-\{D^*\}) = \{0\} \quad (6.13)$$

Now, the optimality criterion of Rel.s 4.25 and 4.26 can be clarified: for each non-zero component of vector $\{T\}$, a known value, depending on the coefficients of the cost function, is prescribed for the corresponding element of $\{\alpha\}$, that represents nodal displacements (where $\{T\}$ are applied) in the second stage of dual problem.
The approximated model seen in this section permits discussions about properties of optimal design problems. The actual behaviour of cable structures can suggest fields of application and degree of approximation of such approaches. Nevertheless, in order to conceive numerical methods based on optimality criterion, an approximated form could be suggested by the formulation shown in this section.

Conclusions

Prestress state is checked to exert outstanding influence on the nonlinear response of cable structures. Particularly, loosening can reduce to such a point distance between nodes that this sort of local deformability could become incompatible with roofing, so susceptible of damages.
In addition, for some usual structural layout, subjected to prescribed service loads, it seems to exist a pre-tension level beyond wich all the cable members are in tension and relevant elongations are very small. Displacements, although moderately large reinforce the positive opinion on satisfactory degree of achieved stiffness. On the other hand pre-tension values, too higer than previous indentified ones, unnecessarly penalize cable stress state and mostly cable foundations and supporting struts.
Therefore pre-tension forces are considered in order to define optimum design problem formulated in a general form, i.e. allowing for both loosening and geometric nonlinearity under some behavioural constraints. Moreover two stages, pre-tensioning and subsequent loading, of which construction procedure usually consists, are taken into account. For such an optimization problem the optimality criterion is found by means of Lagrangian multiplier method. Finally, general form of design problem firstly formulated is suitably specialized and/or simplified in order to yield more handle methods. It is to be remarked that multiple load conditions not explicitly examined in optimum design problem, would involve immediate extensions. From the computational standpoint it is worth noting that, generally speaking, objective functions as ones defined in preceding sections, notwithstanding their formal complexity are rather easy to be cast into computer codes. On the contrary, variable number of problems to be solved and algorithm efficiency, mostly because of mathematical constraints nonlinearity and non convexity, imply actual difficulties.

Acknowledgements

Financial support of this work by National (Italian) Research Council (CNR) is gratefully acknowledged. The authors are also indebted to L.Omodeo Zorini for his coworking in preparating numerical examples.

References

(1) Webster, R.L., On the Static Analysis of Structures with Strong Geometric Nonlinearity. Comp. & Struct. Vol.11, 137-145, 1980.

(2) Maier, G. and Contro, R., Energy Approach to Inelastic Cable-Structure Analysis. J. of the Eng.Mech. Div. ASCE, 531-548, 1975.

(3) Gabriel, K., Ebene Seiltragwerke. Merkblatt Sthahl, 496, 1-31, 1980.

(4) Kirsch, U., Approximate Structural Reanalysis Based on Series Expansion. Comp.Meth.s Appl.Mech.Eng., 26, 205-223, 1981.

(5) Cinquini, C. and Sacchi, G., Problems of Optimal Design for Elastic and Plastic Structures. J.Méc. Appl., Vol.4, 1, 31-59, 1980.

(6) Kaneko, I. and Maier, G., Optimum Design of Plastic Structures under Displacement Constraints. Comp. Meth.s Appl.Mech.Eng., 27, 707, 1-23, 1981.

(7) Selleri, F. and Spadaccini, O., Optimal Design of Prestressed Plane Cable Structures. J.Struct.Mech., 5(2), 179-205, 1977.

(8) Sawczuk, A. and Mroz, Z., Ed.s, Optimization in Structural Design, Springer Verlag, New York, 1975

(9) Haug, E.J. and Cea J., Ed.s, Optimization of Distributed Parameter Structures, Sijthoff & Nordhoff, Netherlands, 1981.

Appendix: Matrix Differential Notations

Let the following scalar form be considered

$$A = \tfrac{1}{2}\{p\}[E]\{p\} \quad (A.1)$$

where each component of the m-vector $\{p\}$ depends on an n-vector $\{u\}$.
Once differentiating with respect to $\{u\}$ provides

$$\left\{\frac{\partial A}{\partial\{u\}}\right\} = [p,_u][E]\{p\} \qquad (A.2)$$

where the (n x m) matrix $[p,_u]$ is defined as follows

$$[p,_u] = \begin{bmatrix} \frac{\partial p_1}{\partial u_1} & \cdots & \frac{\partial p_m}{\partial u_1} \\ \vdots & & \vdots \\ \frac{\partial p_1}{\partial u_n} & \cdots & \frac{\partial p_m}{\partial u_n} \end{bmatrix} \qquad (A.3)$$

Now, a new scalar form B is considered, which appears in functional L_1 of Rel.4.18

$$B = \{\eta\}^T[p,_u][E]\{p\} \qquad (A.4)$$

In order to calculate the derivative vector of B with respect to $\{u\}$, a first part is immediately provided by

$$\{d_1\} = [p,_u][E][p,_u]^T\{\eta\} \qquad (A.5)$$

Note that $\{d_1\}$ represents actual derivative vector if $[p,_u]$ does not depend on $\{u\}$.
A second part may be calculated by representing matrix $[p,_u]$ as an m-row vector of n column vectors. So Rel.A.4 reads

$$B = \{\eta\}^T \left\langle \begin{pmatrix} \frac{\partial p_1}{\partial u_1} \\ \vdots \\ \frac{\partial p_1}{\partial u_n} \end{pmatrix} \cdots \begin{pmatrix} \frac{\partial p_m}{\partial u_1} \\ \vdots \\ \frac{\partial p_m}{\partial u_n} \end{pmatrix} \right\rangle [E]\{p\} \qquad (A.6)$$

or by assuming

$$\{a\} = [E]\{p\} \qquad (A.7)$$

$$B = \{\eta\}^T \left(a_1 \begin{pmatrix} \frac{\partial p_1}{\partial u_1} \\ \vdots \\ \frac{\partial p_1}{\partial u_n} \end{pmatrix} + \cdots + a_n \begin{pmatrix} \frac{\partial p_m}{\partial u_1} \\ \vdots \\ \frac{\partial p_m}{\partial u_n} \end{pmatrix} \right) \qquad (A.8)$$

Alternatively

$$B = \left(\left\{ \frac{\partial p_1}{\partial u_1} \cdots \frac{\partial p_1}{\partial u_n} \right\} a_1 + \cdots + \left\{ \frac{\partial p_m}{\partial u_1} \cdots \frac{\partial p_m}{\partial u_n} \right\} a_n \right)\{\eta\} \qquad (A.9)$$

Then

$$\frac{\partial B}{\partial\{u\}} = \{d_1\} + \{d_2\} \qquad (A.10)$$

where

$$\{d_2\} = (\,[b_1]\,a_1 + \cdots + [b_m]\,a_n)\{\eta\} \qquad (A.11)$$

if each (n x n) matrix b_i (i=1...m) represents the derivative of the i-th row vector

$$\frac{\partial p_i}{\partial u_1} \cdots \frac{\partial p_i}{\partial u_n}$$

In this way, the form of three-index matrix $[\![\, p,_{uu} \,]\!]$ introduced in sect.4 is pointed out. Analogous forms can be considered for three-index matrices $[\![\, t,_{wv} \,]\!]$ $[\![\, t,_{vv} \,]\!]$, $[\![t,_{ww}]\!]$ and $[\![\, t,_{vw}]\!]$

AD-P000 029

MINIMUM WEIGHT DESIGN WITHIN A BOUND ON EIGENVALUES

by

N. Kikuchi and J. E. Taylor
University of Michigan
Ann Arbor, Michigan 48109

Introduction

For the optimally designed Euler column with clamped-ends and where stiffness is proportional to the square of cross-sectional area, the lowest eigenvalue is a double root. The first-published solution to this problem is incorrect. Olhoff and Rasmussen (1) uncovered the error, and in 1977 they provided a correct interpretation for the problem. The clamped-column case provides an example from among such design problems, where the prediction of optimal design requires consideration of nonunique or multimodal measures of response. Issues that may arise in the treatment of problems in this category have been addressed in several studies reported since 1977, (e.g., (2-6)).

The problem statement given in (1) for the column problem corresponds to: maximize (relative to design) a given eigenvalue, within the constraint that the difference between the values of a second eigenvalue and the given one should be nonnegative. In the case of optimal design associated with bimodality, the values are equal so the constraint is active. For the formulation presented in this paper (also stated for the column), the design objective is expressed in terms of a lower bound, say λ_L, to eigenvalues λ_i. The problem statement has the form: maximize (λ_L) within the constraints $(\lambda_i \geq \lambda_L)$.† Multi-modality of arbitrary degree may be accommodated via this somewhat generalized form.

Governing equations (necessary conditions) for the optimal design problem are stated through applications of formal results) and interpretations are given for unique and multimodal solutions.

Design Problem Formulation

The design problem is stated in the form of an 'add-only' optimum remodeling (7) problem. This has the advantage that the results are broader than those obtained from the more usual (unconstrained) optimal design problem statement. At the same time, the solution for the more usual problem is available as the solution of a 'limit-case' optimal remodel problem. Also, with the restriction that the initial design should nowhere have zero stiffness, the set of trial functions for displacement are defined simply in terms of the usual admissibility requirement, i.e., continuous slope.

In the optimal remodel problem, remodeled design D(x) is expressed in terms of modification $D_+(x)$ and (specified) initial design $D_o(x)$, i.e., $D = D_o + D_+$. The design problem is stated in isoperimetric form by specifying an upper bound, say V_+, to the amount of material available for modification:

$$\int_o^\ell D_+ dx \leq V_+ .$$

For eigenvalues λ_i bounded from below by λ_L, the design problem is stated:

$$\max_{D_+} \lambda_L \quad \text{within} \quad \begin{cases} \lambda_i - \lambda_L \geq 0 \\ V_+ - \int D_+ dx \geq 0 \end{cases}$$

Necessary conditions for the solution to this problem may be identified with stationarity of the functional [$\min_{D_+}(-\lambda_L)$ replaces $\max_{\lambda_L}(\lambda_L)$] :

$$J = -\lambda_L - E(V_+ - \int_o^L D_+ dx) - \int_o^L c\, D_+ dx$$

$$- \sum_{i=1}^{M} [b_i(\mu_i - \lambda_L) + a_i \int_o^L (I(D_+)v_i''^2 - \mu_i v_i'^2)\, dx] .$$

The set of the first M solutions to the eigenvalue problem is associated with a minimum on admissible v_i of the sum of potential energies (the problem is expressed very nearly this way in (8)). The third term in the expression for J reflects the requirement $D_+ \geq 0$.

Conditions for stationarity are:

$$\text{(N1)} \quad -1 + \sum_{i=1}^{M} b_i = 0$$

$$\text{(N2)} \quad E - c - \sum_{i=1}^{M} a_i \frac{\partial I}{\partial D_+} v_i''^2 = 0$$

$$\text{(N3)} \quad \int_o^L D_+ dx - V_+ = 0$$

$$\text{(N4)} \quad (I v_i'')'' + \mu_i v_i'' = 0 \text{ and assoc. Bdy Conds.}$$

$$i = 1, 2, \ldots, M$$

† For both problem statements the design is constrained for a specified amount of material.

$$(N5)\quad a_i \int_o^L v_i'^2\,dx - b_i = 0, \qquad i=1,2,\ldots,M$$

$$(N6)\quad b_i(\mu_i - \lambda_L) = 0, \quad b_i \geq 0 \quad (\mu_i - \lambda_L) \geq 0, \qquad i=1,2,\ldots,M$$

$$(N7)\quad a_i\left[\int (Iv_i''^2 - \mu_i v_i'^2)dx\right] = 0 \quad a_i \geq 0 \qquad \int (Iv_i''^2 - \mu_i v_i'^2)dx \geq 0$$

$$(N8)\quad c(x)D_+(x) = 0 \quad c(x) \geq 0 \quad D_+(x) \geq 0$$

By equations N2 and N8, the optimality condition is reduced to either:

$$\left.\begin{array}{l} c=0 \text{ with } D_+ > 0; \quad E = \sum_i a_i \dfrac{\partial I}{\partial D_+} v_i''^2 \\ \text{or:} \\ c > 0 \text{ with } D_+ = 0; \quad E - c = \sum_i a_i \dfrac{\partial I}{\partial D_+} v_i''^2 \end{array}\right\} x \in (0, L)$$

Thus the length of the column is covered by intervals of modification where $D_+ > 0$, or sections where the design remains unchanged. For juncture points $D_+ = 0$ and $c = 0$.

The multipliers a_i are set equal to unity; this amounts to the imposition of a (nonsingular) normalization on the v_i, which is

$$\int_o^L v_i'^2 dx - b_i = 0 \qquad (i=1,2,\ldots,M)$$

from the fourth equation. According to the first condition, there must be at least one among the $\{b_i\}$ with nonzero value. By the fourth of the necessary conditions, the equation of (N7) is satisfied by

$$\int (Iv_i''^2 - \mu_i v_i'^2)dx \Big|_{(\lambda_i, u_i)} = 0,$$

where λ_i and $u_i(x)$ are introduced to represent the eigensolutions.

If for the complete solution there is only one nonzero b_i, say b_1, then:

$b_1 = 1$ and from (N6), $\lambda_1 = \lambda_L$.

The optimality condition becomes

$$\frac{\partial I}{\partial D_+} v_1''^2 = E - c$$

and from (N5), $\int v_1'^2 dx = 1$, whereby

$$\lambda_L = \lambda_1 = \int_o^L I u_1''^2 dx.$$

This summarizes the optimal design problem for the 'single mode' case, i.e., problems where the design is governed by the (unique) first mode.

If, on the other hand,

$$b_i > 0; \quad \lambda_i = \lambda_L \qquad i = 1,2,\ldots,N < M$$

$$b_i = 0; \quad \lambda_i > \lambda_L \qquad i = N+1,\ldots,M$$

at the solution point, the solution is N-modal. In this case dependence of the optimal design on response function v_i is reflected in the optimality condition:

$$\sum_{i=1}^N \frac{\partial I}{\partial D_+} v_i''^2 = E - c.$$

The results evaluated for N=2 are equivalent to the Olhoff-Rasmussen (1) formulation for bimodal optimal design.

With the designation $a_i \equiv 1$, the coefficients b_i conveniently measure the fraction of total strain energy (in the N-modal buckled column) associated with the function $u_i(x)$. This is easily verified; from (N5), (N7) and $\lambda_i = \lambda_L$,

$$\lambda_L b_i = \int_o^L I u_i''^2 dx.$$

Summing these equations provides (with (N1)):

$$\lambda_L \sum b_i = \lambda_L = \sum_{i=1}^M \left(\int_o^L I u_i''^2 dx\right),$$

whereby

$$b_i = \int I u_i''^2 dx \Big/ \sum_{i=1}^M \left(\int_o^L I u_i''^2 dx\right).$$

References

(1) Olhoff, N. and S. H. Rasmussen, "On Single and Bimodal Optimum Buckling Loads of Clamped Columns," Intntl. J. Solids and Structs., vol. 13, 1977, pp. 605-614.

(2) Masur, E. F. and Z. Mroz, "On Non-stationarity Optimality Conditions in Structural Design," Intnt'l. J. Solids and Structs., vol. 15, 1979, pp. 503-512.

(3) Masur, E. F., "Singular Problems of Optimal Design," Lect. No. 2.5, Proc. NATO-NSF ASI, Iowa City, 1980 (Sithiof-Noordhoff, Holland, 1981).

(4) Haug, E. J. and Kyung K. Choi, "Optimization of Structures with Repeated Eigenvalues," Lecture No. 2.7, ibid.

(5) Kirmser, Ph. G. and K. K. Hu, "Remarks on the Optimal Shape of the Fixed-Fixed Column," paper B.1, ibid.

(6) Haug, E. J. and B. Rousselet, "Design Sensitivity Analysis in Structural Mechanics II: Eigenvalue Variations," J. Struct. Mech. (to appear).

(7) Olhoff, N. and J. E. Taylor, "On Optimal Structural Remodeling," J. Opt. Th. and Applics., vol. 27, 1979, pp. 571-582.

(8) Courant, R. and D. Hilbert, Methods of Mathematical Physics, Interscience Publishers, New York, 1953, p. 459.

AD-P000 030

TWO APPLICATIONS OF OPTIMUM STRUCTURAL DESIGN IN THE FIELD OF NUCLEAR TECHNIQUE

J.F.Stelzer
Kernforschungsanlage
D-5170 Jülich
West Germany

The paper reports firstly the optimization of large magnetic coils for a fusion machine of the Tokamak type. The optimization was executed with object to minimum shear stresses within the insulating glass epoxy layers which are located between the layers of the copper coil. The optimization at first followed the fully stressed design but the results did not satisfy. An examination of the influences of different mechanical details, however, led to cognitions how the feared shear stresses considerably could be reduced.

The second topic introduces one problem occuring in the context with a neutron spallation source. One part of the target station is a flat containment holding pressurized water. For an improved stiffness the lid and the bottom of this containment had to be connected by rods. Sought for was the number, thickness and locations of these traverses with object to minimum deformations and stresses in the containment walls. The problem could be solved in a very agreeable way by the application of the fully stressed design.

Optimization of a Magnetic Coil

1. Introduction to the coil problem

The coils of fusion machines of the Tokamak type which produce the magnetic main field, the toroidal field, are mechanically highly charged structures. The load mainly is generated by the magnetic field which is because of its pulsed character quickly swelling and vanishing. This load is superimposed by thermal stresses stemming from the Joule's heating of the coils.

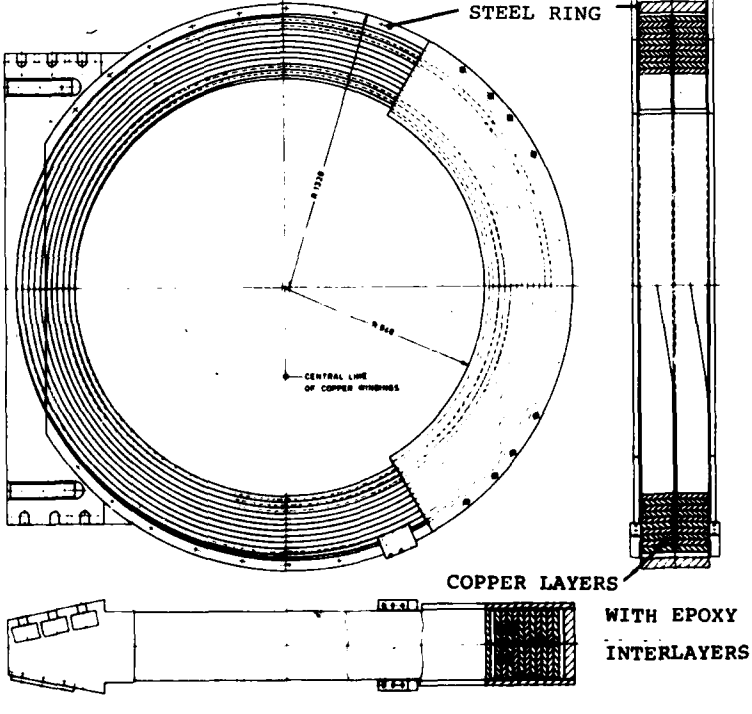


Fig.1 Design of the large magnetic coil of TEXTOR. Outer diameter 1320 mm

In our case we had to deal with circular coils, see fig.1. They consist of two parallel rolled up copper bands which are insulated against each other by epoxy layers reinforced with glass. Dependent on the formation of the glass fibres these layers tolerate only low shear stresses. If the tolerable limit is exceeded then the epoxy crumbles away. The coil stiffness, of course, decreases. Accordingly, the deformations increase which may lead to an accelerating of coil destruction. Therefore, we tried to optimize the coil design with respect to minimum shear stresses in the epoxy. On the other hand, the outer steel ring had to remain sufficiently rigid.

2. Additional Information to the Coil Design

The steel ring surrounding the copper, see again fig.1, possesses a wedge-shaped protrusion on that side which faces the torus centre. The 16 coils of the fusion machine fit together with these wedges like keystones in a vault. Therefore we speak of the coil wedges briefly as of the vault. The steel ring is fixed to the copper also by an epoxy layer.

3. The Calculation Model

All influences on the coil were examined using a finite element model, see fig.2 and 3. The half coil model consists of 144 elements of cylindrical shape. The 10 copper layers of the real design were comprised to two in the model. All epoxy layers were united to only one, situated between the copper outside and the steel ring inside, which got a thickness like the sum of the real single layers. In this position the highest shear stresses were to be expected, because the magnetic and thermal loads are induced and act within the copper. They try to move the copper relatively to the stiff steel which remains unchanged with its temperature. It is important to regard in the model the extremely non-isotropic character of the epoxy. Concerning the orthotropy of this stuff some pre-work (1) had been necessary, basing on publications of Hsu (2), Lekhnitskii (3), Hearmon (4), Nowinski (5) and Barker (6). The orthotropic properties we introduced are listed in fig.4. The vault was modelled by rods of appropriate stiffnesses, fig.3. This may seem a little poor but has some advantages for the optimization procedure. During the calculation it appeared that an additional supporting rod would be of some value, see fig.3.

4. Loads and Stresses

When distributing the magnetically caused radial forces we get a display as shown in fig.5. The inner copper layer suffers a considerably higher load, whereas the outer copper layer is somewhat pressed inwards in the region of smaller angles (right hand side, the angle counts anticlockwise). If we row the force vectors in a series we get relations as shown in fig.6. The resultant force has one centripetal component which pres-

ses the coil into the vault, and a vertical one. Our calculations also took regard of the axial forces occuring in the context with a plasma collapse. They are likewise rather small and may be neglected in this paper. The thermal loads result from an uniform upheating of the copper by 20 K.

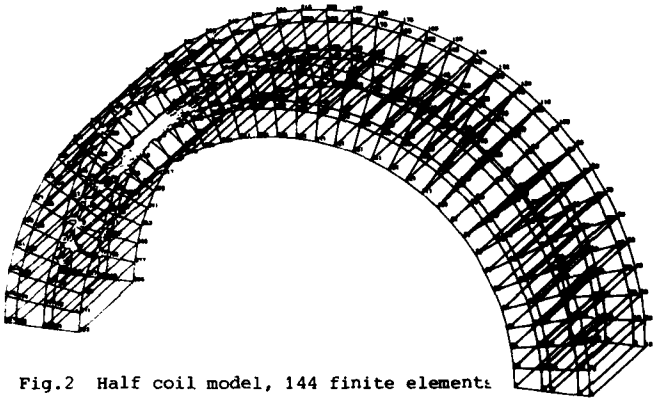


Fig.2 Half coil model, 144 finite elements

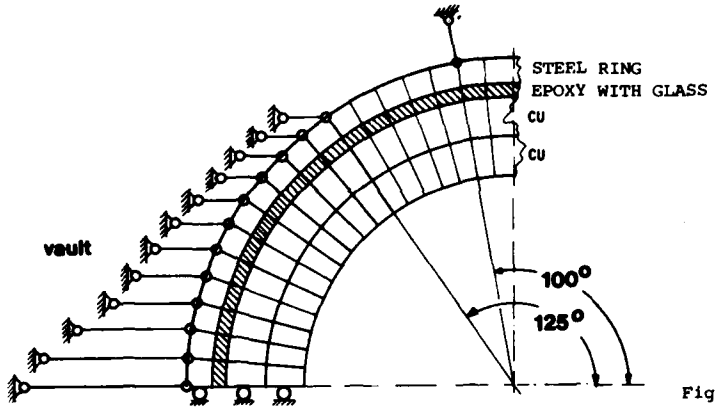


Fig.3 Boundary conditions of the model

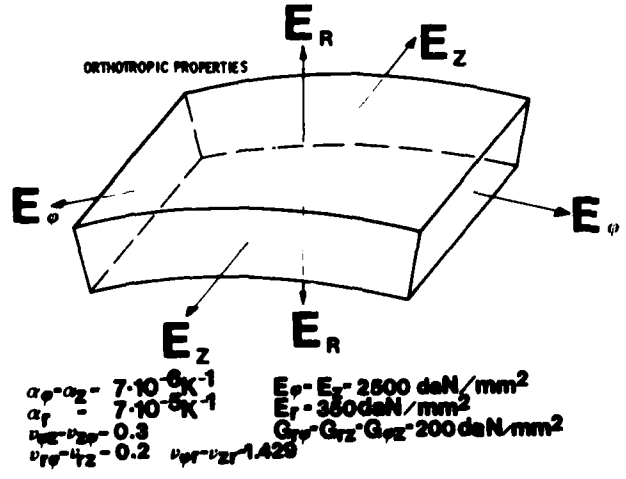
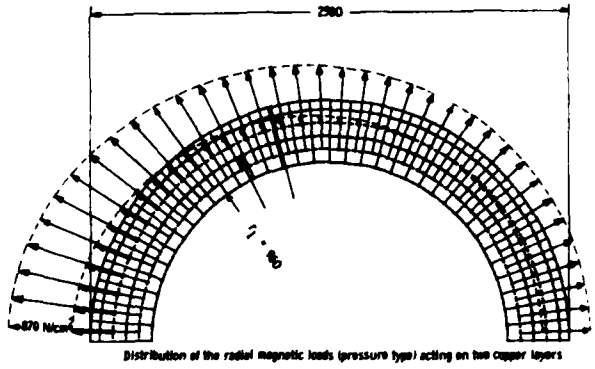


Fig.4 Orthotropic properties of the epoxy with glass



Distribution of the radial magnetic loads (pressure type) acting on two copper layers

Fig.5

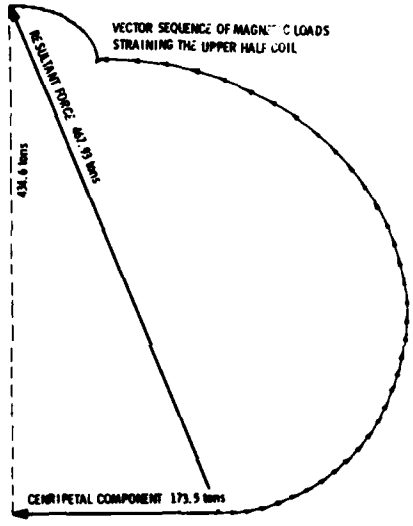


Fig.6 Vector diagram of the acting forces

The loads cause *tangential stresses* as exhibited in fig.7, the maximum of which in the steel is about 90 N/mm². This may possibly afflict the ring. It is valid for a steel ring thickness of 50 mm. The stresses in the copper and epoxy are not critical. In the stress pattern the influence of the vault is reflected, because the vault begins at an angle of 125 degree.

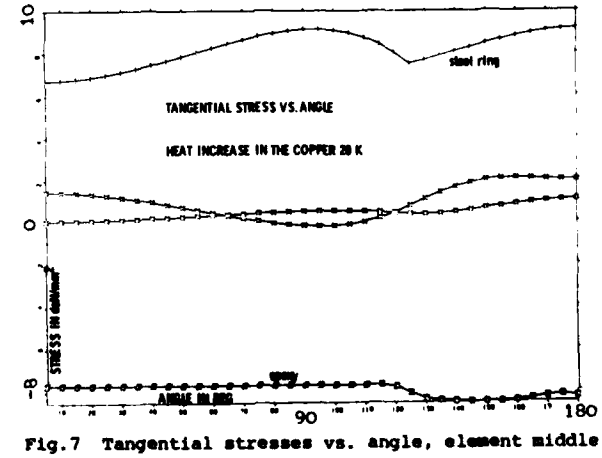


Fig.7 Tangential stresses vs. angle, element middle points

The thick curve in fig.11 shows the *shear stress* distribution in the epoxy the maximum value of which is -3.4 N/mm^2. Its location is at the vault begin, too.

5. Coil Deformations

Fig.8 shows the *radial* deformations of the steel ring. The maximum value with the hot copper occurs at 95 deg. It does not coincide with the force resultant which is at 112 deg which depends on the vault influence. In fig.9 the *tangential* deformations are displayed. The clockwise displacements are drawn circle-inwards.

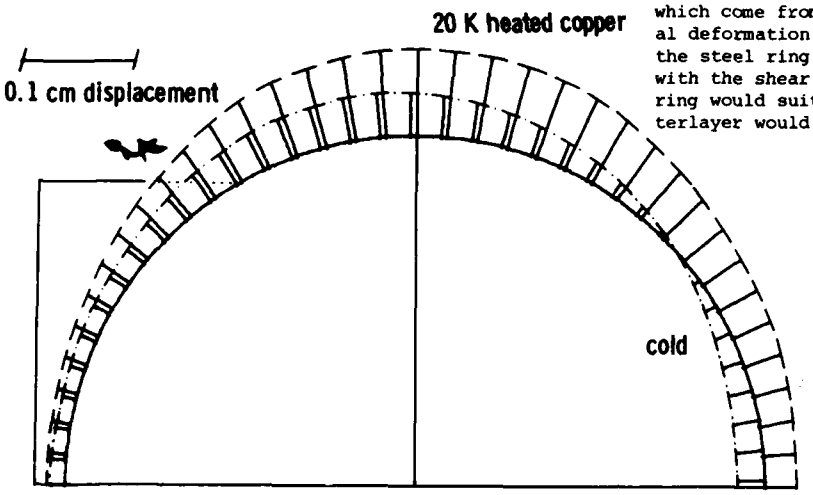


Fig.8 RADIAL DEFORMATIONS OF THE INNER EDGE OF THE STEEL RING, COLD CASE (INNER CONTOUR) AND UPHEATED CASE

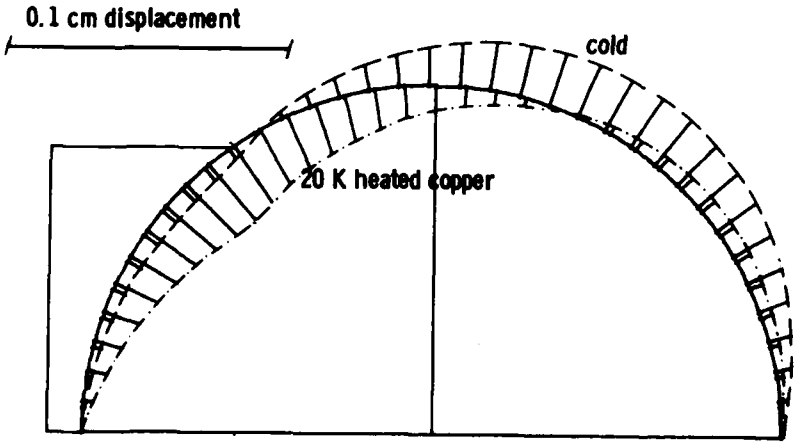


Fig.9 TANGENTIAL DEFORMATIONS OF THE INNER EDGE OF THE STEEL RING COLD AND UPHEATED CASE

The clockwise deformations are mainly due to the thermal load, as can be learned by comparing the cold and the upheated state. The anti-clockwise deformations are caused by the magnetic load. Displacement differences between the layers are responsible for the dangerous r-ϕ- (radial-tangential-) shear stresses in the epoxy.

6. Measures Dealing with the Shear Stress Reduction

By a systematic variation of the influences we tried to diminish the epoxy shear stresses. The following parameters could be changed:

i) the *steel ring*, here the parameters thickness and shape

ii) applying of an *additional supporting rod*

iii) variations of the *height* and *stiffness* of the *vault*

The copper coil must remain unchanged. In the following the influences of the appropriate parameters are examined. At first we may turn towards the *steel ring*.

Changes of the steel ring. If the steel ring is very rigid, it will oppose vigorously all deformation attempts which come from the forces in the copper. The tangential deformation differences between the copper coils and the steel ring would be large. The same would occur with the shear stresses in the epoxy. A very weak outer ring would suit all copper deformations. The epoxy interlayer would remain almost shear stress free. But the copper coils would then show intolerable deformations and the force transfer to the vault would be problematic.

Looking at the circumferential pattern of the tangential stresses in the steel ring, fig.7, an unevenness can be observed. It suggests itself to try to suit the steel ring to the local loads by an appropriate local thinning or thickening. This can be managed by a Fully Stressed Design (FSD) on behalf of the tangential stresses (7). Straight forward we should have executed it by an iterative change of the cross section A according to

$$A_i^{k+1} = \frac{\sigma_i^k}{\sigma_{id}} A_i^k \qquad (1)$$

σ the stress, σ_{id} the ideal and throughout wanted stress, i index of a certain element, k the iteration counter. However, we preferred to iterate on behalf of a fictitious Young's modulus which at the convergence of the iteration routine was converted into appropriate cross sections according to the stiffnesses. This gave the advantage of working during the iterative procedure with always the same geometrical mesh. Fig.10 reports the results. The relationships are valid for a σ_{id}=20 N/mm^2. As is to see in fig.11, the FSD succeeded in a rather large region, for the shear stress in the epoxy is now zero from zero degree to 110 degree. But, unfortunately, in the area of the vault the stress slopes suddenly down to a value of -4 N/mm^2 which is even worse than with the non-optimized coil. Because of the influence of the vault the FSD becomes inefficient.

FSD plus an additional supporting rod. Observing the context between the largest *radial* deformation and the appropriate *tangential* displacements suggests the claim for a suppression of the oval deformation, perhaps rather from the outside by a support which counteracts the resultant of the magnetic forces. We repeated then the FSD prodedure the results of which are shown in figs. 12 and 13. However, as fig. 13 reveals, the FSD is also here inadequate. With every iteration step the shear stress in the epoxy is increased.

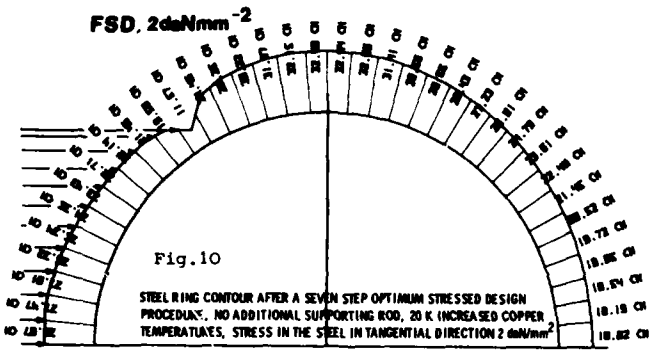


Fig.10

STEEL RING CONTOUR AFTER A SEVEN STEP OPTIMUM STRESSED DESIGN PROCEDURE. NO ADDITIONAL SUPPORTING ROD, 20 K INCREASED COPPER TEMPERATURES, STRESS IN THE STEEL IN TANGENTIAL DIRECTION 2 daN/mm²

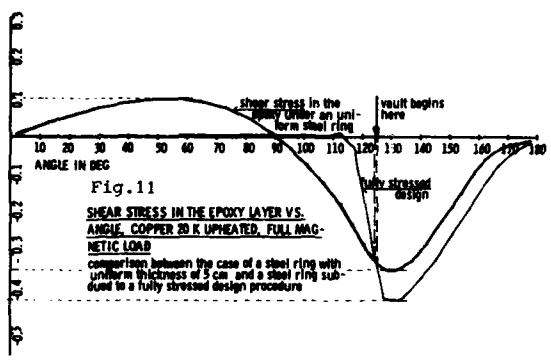


Fig.11

SHEAR STRESS IN THE EPOXY LAYER VS. ANGLE, COPPER 20 K UPHEATED, FULL MAGNETIC LOAD

comparison between the case of a steel ring with uniform thickness of 5 cm and a steel ring subdued to a fully stressed design procedure

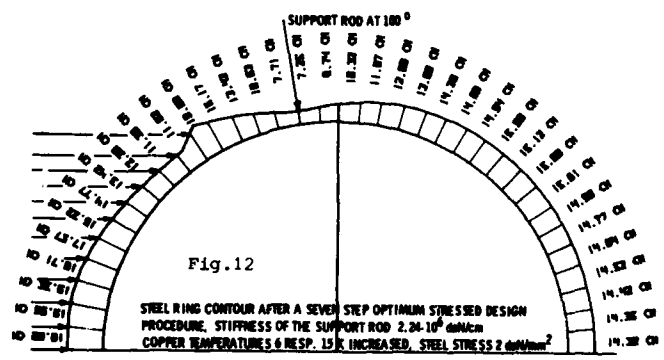


Fig.12

STEEL RING CONTOUR AFTER A SEVEN STEP OPTIMUM STRESSED DESIGN PROCEDURE. STIFFNESS OF THE SUPPORT ROD 2.24·10⁶ daN/cm COPPER TEMPERATURES 6 RESP. 15 K INCREASED, STEEL STRESS 2 daN/mm²

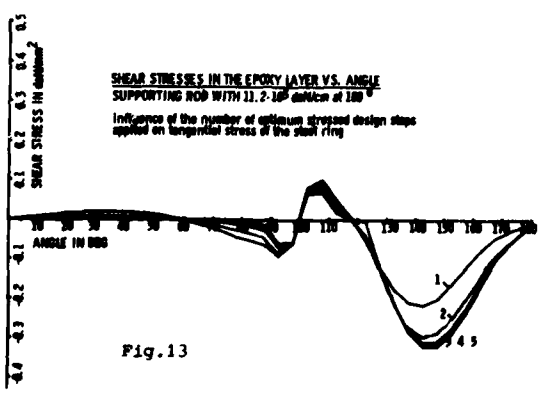
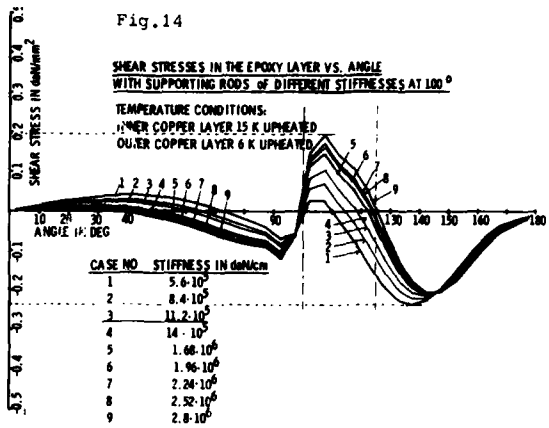


Fig.13

Variations of the stiffness of the supporting rod. Examinations on the influence of the rod stiffness resulted in the relationships as exhibited in fig. 14. A weak rod, curve no.1, causes a low shear stress maximum but a considerable minimum.

Fig.14



CASE NO	STIFFNESS IN daN/cm
1	$5.6 \cdot 10^5$
2	$8.4 \cdot 10^5$
3	$11.2 \cdot 10^5$
4	$14 \cdot 10^5$
5	$1.68 \cdot 10^6$
6	$1.96 \cdot 10^6$
7	$2.24 \cdot 10^6$
8	$2.52 \cdot 10^6$
9	$2.8 \cdot 10^6$

A stiff rod increases the shear stress maximum without a considerable minimum decrease. A reasonable compromise seems to be the case no.3. But this variation does not bring very much.

Variations of the vault. We saw that the vault has an important influence. There was the suspicion as though the vault height had a major importance

Vault height. It was supposed that a smaller, less high vault would bring some relief. However, the calculation test showed, see fig.15, pattern no.1, that with a vault not beginning before 155 deg the case is worsened. A trial in the other direction, to larger vaults, was not reasonable because of a lack of space.

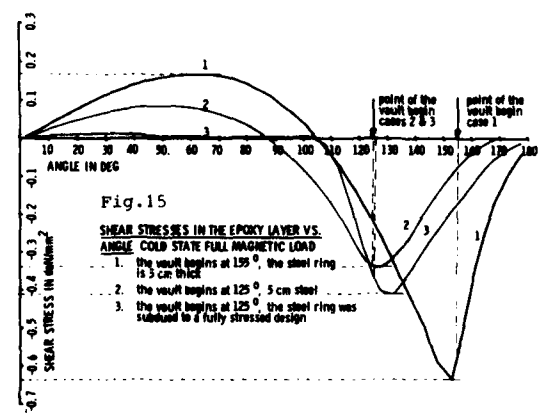


Fig.15

SHEAR STRESSES IN THE EPOXY LAYER VS. ANGLE COLD STATE FULL MAGNETIC LOAD

1. the vault begins at 155°, the steel ring is 5 cm thick
2. the vault begins at 125°, 5 cm steel
3. the vault begins at 125°, the steel ring was subdued to a fully stressed design

Vault stiffness. The vault stiffness variations were executed by changing the rod cross sections of the rods representing the vault, fig.3. This measure leads to a reduction of the epoxy shear stresses, as fig.16 displays, when the vault is weakened. However, the decrease of the vault stiffness has a practical limit at about 50 % of the original stiffness with respect to the load of the steel ring. The steel ring has to compensate the less support coming from the vault, as can be seen in fig.17.

By trying the different possibilities and choosing the suited improvements we succeeded in a shear stress re-

duction concerning the absolute maximum value from 3.4 N/mm^2 to 1.9 N/mm^2.

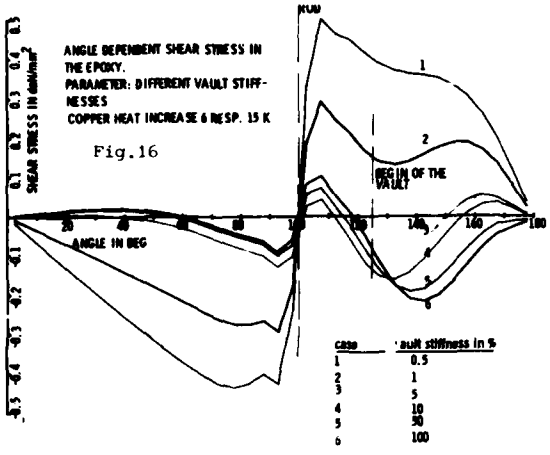


Fig.16

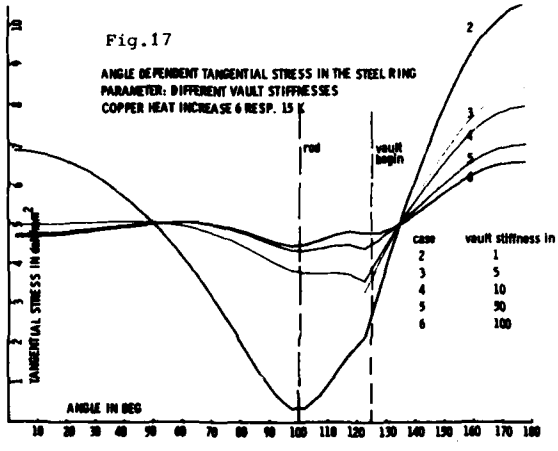


Fig.17

Optimization in the Context with a Mechanical Problem Occuring in the Target Station of a Spallation Neutron Source

7. Introduction to the Problem

The potential with respect to the neutron fluxes of the classical neutron source type, the fission reactors, is practically exhausted. The neutron source with higher fluxes and other new and promising properties, e. g. without the Plutonium problem will work with the nuclear spallation (8). This effect takes place when a highly accelerated proton penetrates the atomic nucleus of a heavy element like lead or Bismuth. Then the charged energy is balanced by the emmitance of nucleons. Hence, a spallation device consists of a proton accelerator and a target station where the nucleons are set free. In the planned spallation neutron source in Juelich, called DIANE, a proton energy of 1100 MeV and an averaged proton flux of 5 mA is anticipated. In the target station a maximum heat deposition of 120 kW/cm^3 (in the peak of a pulse) is to expect, or an averaged value of 12 kW/cm^3. For keeping the target material on a tolerable temperature level, a rotating target was proposed, according to the example of rotating anodes, see fig.18. The target material is lead. There are about 9000 lead filled, AlMg3-canned cylindrical rods of 24 mm outer diameter and 100 mm length sitting in a flow of water coolant.

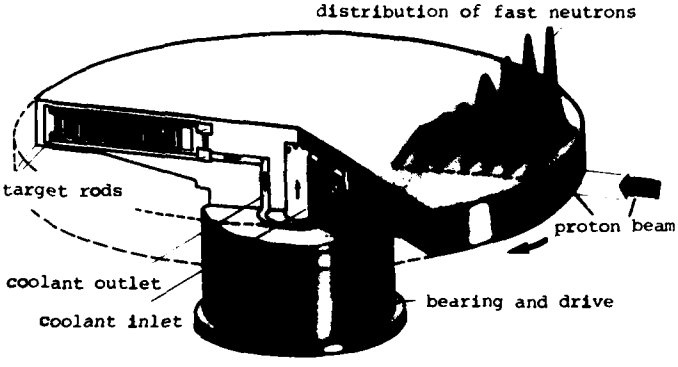


Fig.18 Rotating target wheel for a high-neutron-flux spallation source (Bauer's principle)

Because of the flow resistances the coolant must be under pressure. From this the sheet housing of the target wheel is stressed and deformed. There are still additional but smaller loads resulting from the weight of the lead rods, the centrifugal forces of the water (neglectable, rotation speed 0.5 revolutions per second) and stagnation pressure at the outside wall. The housing material is AlMg3. Most of the lead rods sit in the housing as fig.19 displays.

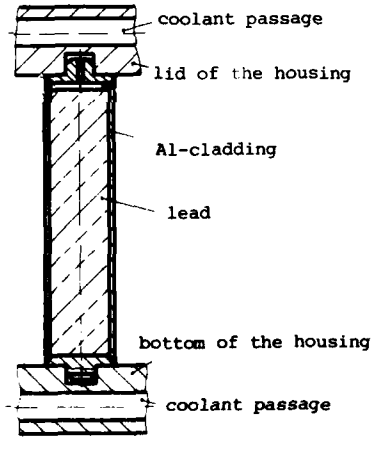


Fig.19 A single target rod. With the plugs at the ends it sits in the wheel structure. It can expand independently of the ambient rods

Because of the material and the geometry the housing is not very rigid and its deformations become intolerable if all rods are fixed according to fig.19.

8. Task

For an increase of the stiffness traverses between the housing lid and bottom should be provided for. From the aspect of manufacturing their number should be small. As traverses or through bolts target rods should be used with differently shaped ends by which they are firmly connected with the lid and the bottom. The optimization task was to determine the number and the locations of the throughbolts with regard to a minimum deformation of the housing and a tolerable stress in the connecting rods. With respect to the poor tensile properties of lead only the cross section of the Al cladding is considered.

9. The Calculation Model

In fig.20 the calculation model is displayed. It consists of 324 elements with 672 nodal points. Fig.21 gives some dimensions and the pressure distribution.

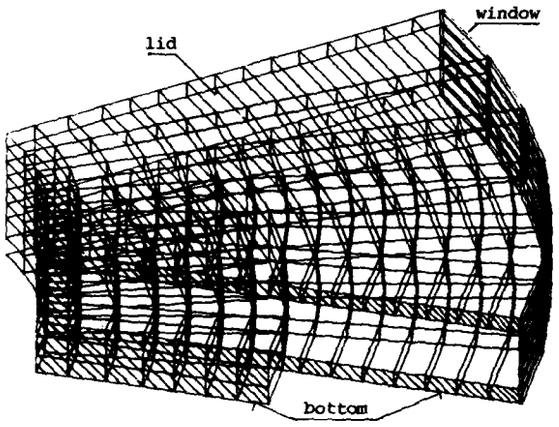


Fig.20 Projected view of the calculation model

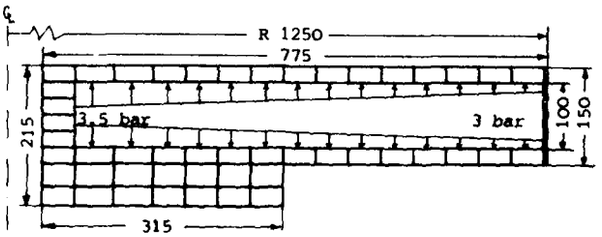


Fig.21 A model cross section

The model possesses less opposite pairs of nodal points than rods exist. Therefore, a certain lot of rods is thought to be comprised in these locations. In the real structure the rods are located on 37 radii to which we assign the names R1 to R37, counting in the proton direction from the larger radii to the smaller ones.

10. Some Calculation Results

Fig.22 exhibits the housing deformation calculated for the case that no traverses are present. The deformation was enhanced by a factor 200, likewise as with all the following pictures. The distribution of the appropriate reference stresses in the lid is shown in fig. 23. Fixing throughbolts at the points of the largest clearance of the deformation (fig.22), at the radii R16 and R18, delivers a deformation pattern as shown in the fig.24. This is already a design to live with. In this case every second rod on the two radii was fastened, which leads to a number of 272 fixed rods. The due reference stresses can be seen in fig.25.

11. The Optimization Procedure

Supposedly a fully stressed design (FSD) with concern to the rods would satisfy the given demand. We started with connecting rods in all possible positions, i.e. between all opposite node point pairs, giving all these rods identical cross areas (according to the AlMg3 cross sections). During the iteration procedure the cross areas were changed according to eq.(1), etc. The

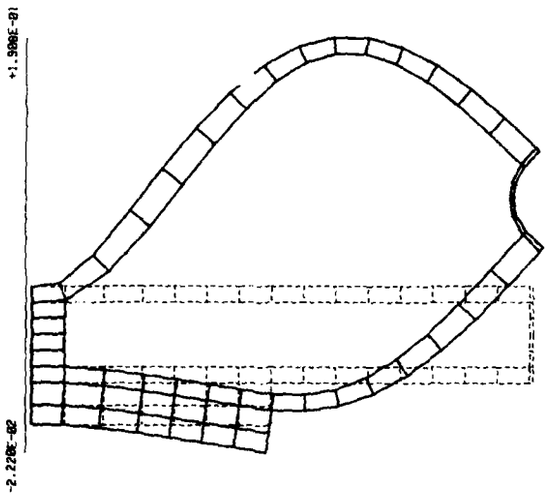


Fig.22 Deformation of the housing if no traverses are present. Deformation enhancement factor 200.

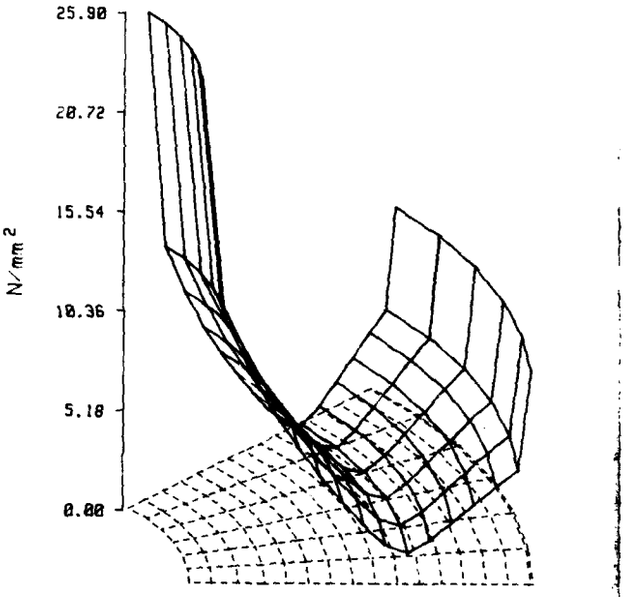


Fig.23 Distribution of the reference stresses in the lid of the housing if no traverses present

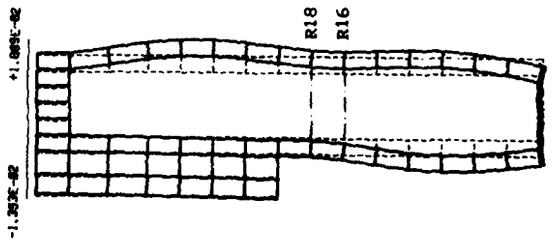


Fig.24 Deformation of the housing with traverses at two radii (R16 and R18). Deformation enhancement by a factor 200

iteration converged after 7 iteration steps, with equal stresses in all rods. The in this way received cross section areas were part of the simplyfied model and must be transferred to the real design. This was done by dividing the calculated cross section areas by the value of one real rod cross section area. Thus the number of necessary transverse rods in the region of a certain model rod could be got. The results are given in table 1. The notified radii are the in the model regarded ones, counting in a row from the small radius to the largest one.

Table 1: Amount of necessary connecting rods along the 360 deg circumference

radius name	location in mm	necessary rods
R33	596	none
R30	657	none
R28	700	3
R26	741	8
R23	797	13
R21	837	15
R18	901	15
R16	945	22
R13	998	23
R11	1035	20
R8	1093	11
R7	1113	none
R3	1197	none

Now, an amount of 130 connecting rods is required (272 in the case of fig.24 and fig.25). Fig.26 shows the deformation of the optimized housing.

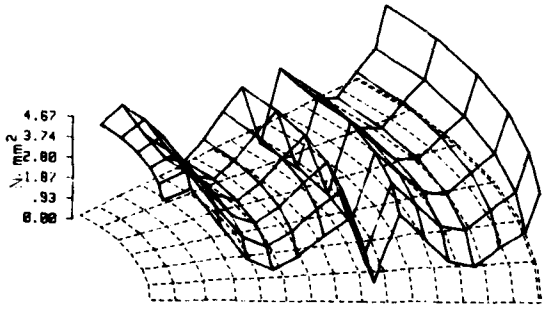


Fig.25 Reference stress distribution in the lid of the housing with traverses in the radii R16 and R18

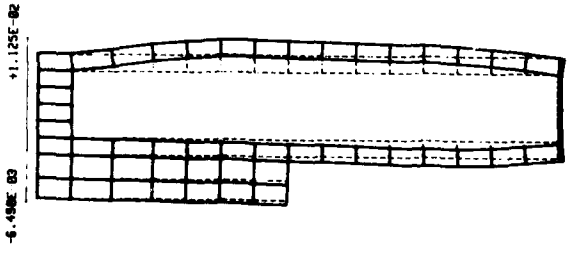


Fig.26 Deformation of the housing with traverses according to the optimum structural design

By the optimization procedure the wanted reductions of the stresses in the lid and the bottom of the casing took place. Also the beam window which is formed by the outer vertical wall is less charged. Table 2 gives a surview over the maximum stresses at different housing locations for the 3 treated cases.

Table 2: Maximum reference stresses at different locations of the housing in the cases of fig.22, fig.24 and fig.26

Location	case of fig.22	fig.24	fig.26 (optim.)
lid	25.9	7.72	4.3
bottom	12.7	3.39	2.5
window	15.5	8	6.34

The stress distribution in the upper and downside parts of the housing is now almost equalized, as fig.27 displays. Consequently, the optimized design offers highest stability and longevity.

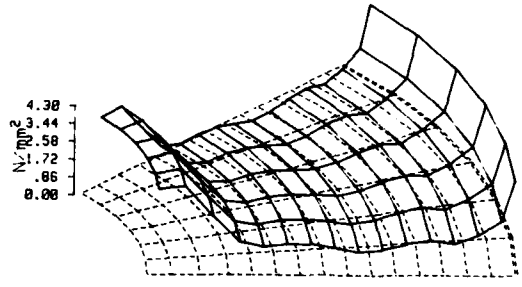


Fig.27 Reference stress distribution in the lid of the housing for the optimized design. The scale is the same as in figs.23 and 25.

References

(1) Stelzer,J.F.,Sievers,A. and Welzel,R.,"Large Magnetic Coils", Report no.Jül-1349, Kernforschungsanlage Jülich, W.Germany, 1976

(2) Hsu,N.N. and Tauchert,T.R.,"Conditions for Zero Thermal Stresses in Anisotropy Multiply Connected Thermo-Elastic Bodies", Acta Mechanica 24, 179-190,1976

(3) Lekhnitskii,S.G.,Theory of Elasticity of an Anisotropic Elastic Body, Holden-Day Inc., San Francisco, 1963

(4) Hearmon,R.F.S., An Introduction to Applied Anisotropic Elasticity, University Press, Oxford, 1961

(5) Nowinski,J. and Olszak,W.,"On Thermoelastic Problems in the Case of a Body of an Arbitrary Type of Curvilinear Orthotropy", Archivum Mechaniki Stosowanej 7, Vol.2, pp.247-265, 1955

(6) Barker,R.M., Fu-Tiin Lin, Dana,J.R.,"Three Dimensional Finite Element Analysis of Laminated Composites" Computers & Structures Vol.2, pp.1013-1029, 1972

(7) Gallagher,R.H.,"Fully Stressed Design" in Optimum Structural Design edited by R.H.Gallagher and O.C. Zienkiewicz, Wiley & Sons, London, 1973

(8) Bauer,G.S., Sebening,H., Vetter, J.E. and Willax,H. (editors), SNQ Study to the Realization of a Spallation Neutron Source, report Jül-Spez-113, Jülich, 1981 (in German)

Acknowledgment. This paper could not have been written without the friendly and helpful assistance of my coworkers E.Graudus, K.Groth, A.Sievers and R.Welzel, all with the Kernforschungsanlage Jülich.

AD-P000 031

OPTIMALITY CRITERIA DESIGN AND STRESS CONSTRAINT PROCESSING

R. Levy

Member of Technical Staff, Jet Propulsion Laboratory, California Institute of Technology
4800 Oak Grove Drive, 511-210A, Pasadena, California, 91109

Abstract

Methods for pre-screening stress constraints into either primary or side-constraint categories are reviewed; a projection method, which is developed from prior cycle stress resultant history, is introduced as an additional screening parameter. Stress resultant projections are also employed to modify the traditional stress-ratio, side-constraint boundary. A special application of structural modification reanalysis is applied to the critical stress constraints to provide feasible designs that are preferable to those obtained by conventional scaling. Sample problem executions show relatively short run times and fewer design cycle iterations to achieve low structural weights; those attained are comparable to the minimum values developed elsewhere.

Introduction

Design optimization of linear structures through optimality criterion method approaches has been established during the past decade as superior to the more formal approaches of nonlinear mathematical programming. The advantage of optimality criteria methods is in problem-size potential and computation effort (1, 2, 3, 4) because of the capability to reduce the solution space from a large design variable space to a much smaller subspace of active constraints. The original design space is retrieved through the application of optimality criteria that supply the desired design variables in terms of Lagrange multipliers associated with the active constraints. The most challenging requirement then becomes the determination of the set of Lagrange multipliers.

The usual objective of the design problem is to minimize the total structure weight, which is adopted as a convenient, although possibly imperfect, measure of cost. The two most frequently-encountered types of constraints in the design of structures for static loadings are compliance constraints, which are applied to limit specific functions of the structure's displacements; and stress constraints, which are applied to ensure structural integrity.

Satisfying the stress constraints is usually a more difficult mathematical requirement than satisfying the compliance constraints because stresses are a direct function of strains while displacements are integral functions. Thus, for a non-optimum design with some of the design variables (member sizes) undersized and some oversized, the undersized members will be overstressed and the design will be considered inadequate to the extent of the overstress, no matter how great the understresses on other members. On the other hand, the oversized members will contribute to reducing constrained displacements so that, even if the design variables are non-optimum, the compliance constraints could be satisfied.

Although the structures most frequently considered for design optimization are linear with respect to analysis, the design process, unless trivial, is always nonlinear. Consequently, the design solutions are obtained by an iterative sequence of analysis-redesign cycles. Hence, the computation efforts and costs can be significantly larger than for conventional structural analysis. Therefore, in practical applications, the extra effort in extending or adjusting the procedures to obtain small improvements is weighed against the value of the improvement.

Fundamental to obtaining an effective solution is the identification of constraints either as belonging to a critical set that will be actively processed by the optimization algorithms or to a benign set treated by elementary mathematical operations. Members of this last set are considered to be passive during optimization algorithm applications, which are presumed to satisfy their requirements automatically. Solution efficiency and stability are enhanced by keeping the active set small and the passive set large. Nevertheless, when the active set is too small, the passive set could produce undesired violations of their constraint requirements. When constraints are violated during the current design iteration, conventional practice is to identify an alternative feasible design that is obtained by scaling the current (raw) structure weight upwards in proportion to the maximum constraint violation. On the other hand, when the active set is overly large, and although the penalties for scaling the structure weight to feasibility could be small, the advantages of reduction of the design space disappear; and mathematical programming approaches (5) become competitive for solution processing. Fortunately, recent discussions (6, 7) of substantive approaches for partitioning the constraint set provide steps to overcome this identification problem.

This paper describes these and other steps to restrict the numbers of primary constraints and adjusted requirements for the passive constraints. Specific items covered are screening of potentially active constraints to reduce their number, a projection method to modify the conventional stress-ratio side constraint boundaries for the passive constraints, and the addition of supplementary structural modification reanalysis procedures to reduce the feasible scaled weight of designs with constraint violations. Results of example executions of standard sample test problems are presented for assessment. Although occasionally penalized by accompanying structural weights that may exceed known minimums by fractions of a percent, these examples often show desirable execution efficiency as measured either by the numbers of design cycles required to achieve low feasible structure weights or by the required computer time.

Mathematical Formulations

The following discussions are simplified to consider applications for 3-dimensional truss-type structures that consist of only one-dimensional rod finite elements. The associated design variables are cross-sectional areas of rods and the stress resultants are the axial forces. They can represent individual rod member areas or common areas for groups of members. The formulation, nevertheless, can readily be modified (7, 8) to include additional membrane plate elements.

Optimality Criteria Method

A brief overview of the optimality criteria method formulation is supplied for convenient reference. Additional details and specific variations are described in a number of other references (1, 2, 4, 9).

A common density for all structural members is assumed here so that the objective to minimize the

structure weight can be replaced by a volume objective V given by:

$$\text{Minimize} \quad V = \sum_{i=1}^{N} L_i a_i \tag{1}$$

in which the design variable a_i is the cross-sectional area, L_i is the lengths of the members, and i is the generic index within a set of N groups.

A virtual work formulation is used to express K primary constraint equations as

$$G_j = \sum_{i=1}^{N} \frac{F_{ij} L_i}{a_i} - C_j^* \leq 0 \quad j = 1,\ldots,K \tag{2}$$

In Eq. (2), F_{ij} is an internal stress resultant virtual work coefficient so that the virtual work of the ith design variable for the jth constraint is $F_{ij}L_i/a_i$. For a group with only a single member, this is computed as the stress resultant for each external loading times the stress resultant for an associated virtual loading divided by Young's modulus. In the case of a group of more than one individual member, the virtual work coefficient is replaced by the length-weighted average for the group of members. C_j^* is a prespecified bound on the virtual work. When the displacement at a single node in a particular direction is to be constrainted, C_j^* is the value of the displacement bound; and the virtual loading is a unit load applied at that node in the corresponding direction. More general forms of compliance constraints (10) can be established from more complex virtual loading vectors. Stress constraints for individual members can be converted to extensional constraints formulated by

$$C_j^* = \frac{\sigma_r^* L_r}{E} \tag{3}$$

in which σ_r^* is the allowable stress, L_r is the length of the rth member, and the virtual loading is a pair of self-equilibrating virtual (11) unit loads at the terminal nodes of the member. The pairs are directed away from each other for tension stress and toward each other for compression stress.

In addition to, or possibly in place of, the primary constraints there are side constraints (4) given by the limits

$$\underline{a_i} \leq a_i \leq \overline{a_i} \qquad i = 1,\ldots,N \tag{4}$$

in which $\underline{a_i}$ and $\overline{a_i}$ are lower and upper side constraint bounds on the design variable a_i.

It is convenient to rewrite Eq. (2) as

$$G_j = C_j - C_j^* \tag{5}$$

where from Eq. (2), C_j is the realized value of the virtual work. That is

$$C_j = \sum_{i=1}^{N} F_{ij} L_i / a_i \tag{6}$$

From this, the constraint ratio is given by

$$D_j = C_j / C_j^* \tag{7}$$

so that ratios greater than unity indicate constraint violations.

By applying either the conventional Lagrange multiplier method or the Kuhn-Tucker conditions, it can be shown (as in most of the previously cited references as well as elsewhere) that the optimality criteria conditions for this problem are

$$a_i^2 = \sum_{j=1}^{K} F_{ij} \lambda_j \qquad j = 1,\ldots,K \tag{8}$$

in which the λ_j are non-negative Lagrange multipliers that are to be determined from the solution of an auxiliary mathematical programming problem given by

$$\lambda_j G_j = 0 \qquad j = 1,\ldots,K \tag{9}$$

This implies obtaining the solution of the simultaneous nonlinear equations

$$G_j = 0 \qquad j \in Q \tag{10}$$

in which the set of indices Q is identified with the currently active constraints, and the remaining indices are associated with a set of passive constraints for which the multipliers are taken as zero. An alternative method of finding the multipliers is by choosing them to maximize a dual objective function (3), but this is a technical rather than a fundamental difference (4). Newton's method, with any of a number of variations or modifications, is the usual method used to solve for the multipliers although primitive earlier research used recursive approximations.

The design procedure iteration cycles terminate when either prespecified convergence criteria are met or maximum numbers of cycles are performed. Each cycle typically consists of two steps:

(1) Analysis of the current design. This includes determination of stress violations and computation of the F_{ij} terms (virtual work coefficients) needed for optimization.

(2) Design optimization. This consists of computation of the multipliers and application of the optimality criteria.

The virtual work coefficients are assumed to be invariant during adjacent design-followed-by-analysis cycles. This assumption is true only for a statically determinate structure, and the associated errors depend on the extent of redundancy of the structure. Redundancy, therefore, provides the requirement for iteration to update these coefficients.

Selection of Candidate Primary Stress Constraints

The set Q (Eq. 10) of constraints active during the optimization step is a subset of candidate constraints established prior to this step. Methods for establishing and updating the Q set have been considered elsewhere (3, 4) and, although worthy of additional research, are not covered here. Nevertheless, this discussion will consider the selection of constraints that are candidates to be included in the Q set. The objective is to compress the solution size for Step 2 by retaining the significant constraints and eliminating the unimportant constraints.

The selection is a screening process that eliminates constraints that fail to meet all of several criteria assumed necessary to qualify for Q set. Stress constraints that do not qualify are treated as side constraints, and minimum design variable size requirements are assigned to be maintained during the optimization step. Usually this minimum size is determined by a stress-ratio requirement. This requires the design variable to be at least as large as its current value times the ratio of current stress to allowable stress.

This is equivalent to, but simpler to compute, than the alternative

$$a_i \geq D_j a_i \qquad (11)$$

Three criteria will be considered here: a stress (constraint) ratio criterion, a stress resultant stability criterion, and a redundancy estimate criterion. None are precise but all are proposed as being rational, at least to this writer and to predecessors who have used either identical formulations or formulations similarly motivated by those to be given. The first two criteria require insignificant computations for application and are applied initially. The third criterion requires the stress resultant vectors for the self-equilibrating virtual loads, which need to be constructed only for the survivors.

In common with many other optional features available to users of prevalent computer optimization programs, numerical values that require subjective or intuitive judgments must be supplied to the computer program by the user. Unfortunately, the efficiency of the design optimization progress, or even the success or failure, can depend upon small variations in the choice of parameters. As with many of the other parameter options that are user-defined, the related parameters for these criteria can have initial values to be applied at the first iteration cycle, multiplier factors to adjust the values for subsequent cycles, and cut-off values that can override unwanted values that can be produced through repeated applications of the factors.

Stress-Ratio Criterion. This criterion is almost self-explanatory and is used in almost every type of optimization procedure. The assumption is that, if the constraint ratio at the current design cycle is small, it might not increase enough during the next cycle to become important. Therefore, it can be moved to the side constraint category at this design cycle. Typical rejection values are in the range from 0.50 to 0.95. The former value ensures little risk of rejecting a constraint that should have been kept. The latter value compresses the number of potential primary constraints with more risk of rejecting a significant one.

Stress Resultant Stability Criterion. This criterion uses the relative change in stress resultants between adjacent design cycles as a measure of current stability. If the change is less than a stability parameter, it is assumed that a side constraint is adequate for the next design step, and the primary stress constraint is rejected. The relative change DP_i for the ith member is computed as

$$DP_i = (P_i^+ - P_i^-)/P_i^+ \qquad (12)$$

in which P_i^+, P_i^- are the current and prior values of the stress resultant.

Typical values used initially for the stability parameter are in the range (0.0, 0.10), with cyclic multiplier factors in the range (0.65, 1.0). Tests are made on the absolute values of DP_i (and on the largest of these in cases of several external loading vectors). To guard against the anomaly of overstressed members that have small relative changes, the relative change can be increased before testing by the amount of over-stress relative to the allowable stress (1.0 minus the stress constraint ratio).

Redundancy Estimate Criterion. The formulation is based upon the approach described in Ref. 7 to identify members that could be regarded as almost statically determinate. These are members with stress resultants that are relatively independent of their associated design variable. The viewpoint here is from a virtual work formulation and provides an equivalent alternative to the preceding reference.

In the case of a statically determinate structure, the matrix of all stress resultant vectors for a full set of self-equilibrating virtual loading vectors is the identity matrix (except for the signs). Therefore, in a redundant structure an "almost statically determinate" member can be identified by a coefficient with magnitude close to unity at the index corresponding to the diagonal element of the self-equilibrating loading stress resultant matrix. Consequently, if that magnitude is larger than an input parameter in the range of, for example, from 0.85 to close to unity, the primary constraint could reasonably be replaced by a stress side constraint. The lower the parameter value, the larger the number of side constraints. It can be observed that this and the preceding redundancy estimate criterion are different formulations with an identical motivation.

Modified Side Constraints

The modifications depend upon the assumption that design variables and stress resultants progress monotonically from initial to final values. Consistent with these assumptions, for example, if a stress resultant has increased in value from the prior cycle, it can be expected to increase in the next cycle; similarly, a decrease would be expected for a prior cycle decrease. Correspondingly, side-constraint, stress-ratio boundaries can be modified to incorporate a projection based upon the difference in stress resultant from the prior cycle. The projected stress resultant P_i^* is

$$P_i^* = P_i^+ + t(P_i^+ - P_i^-) \qquad (13)$$

where t depends upon input parameters and P_i^+ and P_i^- are defined as in conjunction with Eq. (12). An input parameter in the range (0., 1.0) and cyclic multiplier in the same range establish the value of t. The maximum absolute value projected for the stress resultant for any of the members of a design variable group for any of the external loadings from Eq. (13) is used to determine the side constraint.

An examination of about 850 occurrences for one particular design showed that for 85% of these occurrences there was no change in sign of stress-resultant change, which supports the underlying assumption. However, projection parameters at the top of the ranges should be used with caution since there can be adverse effects from too bold projections. Nevertheless, example problems run without projection and also with projection values of about 0.7, both for starting values and multiplier factors applied for decreasing stress resultants, and about half as much applied for increasing, confirm the value of projection in expediting the design process.

The projection just described can be considered as an overrelaxation function and is used here to establish the side constraints. Other forms of overrelaxation (12, 13) or extrapolation (14) functions have been proposed to establish values for the design variables in place of any other type of optimization procedure.

Modifications and Reanalysis

Structural modification reanalysis has been used within optimization procedures (15, 16, 17) to expedite the repeated solutions of the load-deflection analysis equations during redesign iterations. An alternative application described here is to use modification reanalysis after the current stiffness matrix has been decomposed and the analysis for displacements and

stresses has been completed. The purpose is to obtain a feasible design when there are overstresses by resizing only the members that are either overstressed or nearly over-stressed. The design so obtained is anticipated to be more effective than the customary alternative obtained by uniform scaling according to the most critical constraint ratio.

The modifications are performed using the parallel element (17) approach. In terms of rod elements the concept postulates an hypothetical member in parallel with the member to be resized. The area of the parallel member Δa_i is the change in area for the original (parent) member. The concept provides a simple formulation and interpretation, which can also be extended to other types of elements. Although there are alternative approaches (18) to reanalysis, the method here is compatible with the virtual work formulation and requires for application essentially only information already available or information that would be needed independently. Furthermore, there are no mathematical approximations in theory, although, as it will be seen, there can be approximations in the proposed applications.

Mathematical Background. The following explanation of the formulation is abstracted from Ref. 19, which contains additional details. The premise is that displacements of the modified structure U_M are obtained by superposition of displacements of initial structure U_I and the displacements ΔU caused by the internal forces of the parallel members acting as loads on the initial structure. That is,

$$\left[U_M\right] = \left[U_I\right] + \left[\Delta U\right] \tag{14}$$

ΔU can be expressed as the product of the displacements for unit values U_S of the parallel member forces post-multiplied by the forces R of the parallel members, or

$$\left[\Delta U\right] = \left[U_S\right] \left[R\right] \tag{15}$$

In the above equation, U_S, to within the signs, can be extracted from the sets of displacement vectors that result for the self-equilibrating loads that were discussed in conjunction with Eq. (3). Here, however, the signs are based upon loading pairs directed toward each other.

To enforce compatibility of the parent and parallel member, let

e_F = final extensions of parent members = extensions of parallel members

e_I = initial extension of parent member for the external loads

e_S = extension of parent member for unit values of the self-equilibrating loads

e_Q = extension of parallel members for unit forces

For one-dimensional bar members, the extension of a bar along its axis is given by

$$e_i = \frac{S_i L_i}{A_i E_i} \tag{16}$$

where S_i, L_i, A_i, and E_i are the member force, length, area, and modulus of elasticity for the ith member. Therefore, with superposition similar to Eq. (14),

$$\left[e_F\right] = \left[e_I\right] + \left[e_S\right] \left[R\right] \tag{17}$$

But e_F can be determined directly as the extension of the parallel members,

$$\left[e_F\right] = \left[e_Q\right] \left[R\right] \tag{18}$$

Combining and rearranging, R can be obtained by solving

$$\left[\left[e_Q\right] - \left[e_S\right]\right] \left[R\right] = \left[e_I\right] \tag{19}$$

In solution of Eq. (19) for R, the order of the coefficient matrix is equal to the total number of property changes.

The change in stress $\Delta\sigma$, and member force stress resultants ΔS can be obtained from

$$\left[\Delta\sigma\right] = \left[\sigma_S\right] \left[R\right] \tag{20}$$

$$\left[\Delta S\right] = \left[S_S\right] \left[R\right] \tag{21}$$

in which σ_S and S_S are the stress and stress resultant matrices associated with the self-equilibrating loadings. Eq. (21) represents the change in stress resultant for the parent bar. The total change in stress resultant for parent and parallel bar with respect to the original for the parent is obtained by adding the identity matrix to S_S.

Stress Resultant Derivatives. As a by-product, the reanalysis formulation can provide the partial derivatives for stress, displacement, and stress resultants with respect to the area changes.

To obtain the derivatives for stress resultants, let the area of only one bar, bar v, be changed and the change in stress resultant ΔS_{we} be determined for some other bar w where e is the index of the external loading column. That is a_v becomes $a_v + \Delta a_v$ and no other a_i changes. Then from Eqs. (16) and (19) we have

$$(a_v/\Delta a_v - S_{vv})\, R = S_{ve} \tag{22}$$

where S_{vv} is the diagonal element of the stress resultant matrix for unit self-equilibrating loads, S_{ve} is the element at row v, column e of the external loading stress resultant matrix, and R is the magnitude of the self-equilibrating loading associated with the change in bar v.

Eq. (21) then provides

$$\Delta S_{we} = S_{wv} R \tag{23}$$

in which S_{wv} is the row w, column v element of the unit self-equilibrating loading stress resultant matrix.

Then from Eqs. (22) and (23)

$$\Delta S_{we} = S_{wv} S_{ve} \Delta a_v / (a_v - S_{vv} \Delta a_v) \tag{24}$$

and taking limits as the area change approaches zero

$$\partial S_{we} / \partial a_v = S_{wv} S_{ve} / a_v \tag{25}$$

Equations similar to Eq. (25) apply for stress and displacement. When Eq. (25) is used for bar v, it provides the derivative for the portion of the bar associated with the original area. To obtain the total change, unity is added to S_{vv} where it replaces S_{wv} on the right hand side of the equation.

The relationship of the partial derivative in Eq. (25) to the derivative of the constraint equation (Eq. 5) can be shown by recognizing that C_j of

Eq. (6) is equal to the extension of bar w for the loading e in the case of a stress constraint for this bar and loading. That is

$$C_j = S_{we}L_w/(Ea_w) \tag{26}$$

Therefore

$$\partial C_j/\partial a_v = \partial S_{we}/\partial a_v \cdot L_w/(Ea_w) \tag{27}$$

However, in Eq. (25), S_{wv} can be expressed in terms of S_{vw} by using symmetry of the e_S matrix. Therefore, Eq. (27) becomes

$$\partial C_j/\partial a_v = S_{vw}S_{ve}L_v/(Ea_v^2) = \pm F_{vj}L_v/a_v^2 \tag{28}$$

Eq. (28) is the same as if the derivative were computed directly from Eq. (6); thus it actually provides no new information. Nevertheless, the development of Eq. (25) is useful to show the inherent approximation, which is the result of the omitted term in the denominator of Eq. (24). For example, when Eq. (25) is used to estimate the change in stress resultant, the result will usually be biased towards an overestimate of the magnitude of change. This follows because of the term $-S_{vv}\Delta a_v$ in the denominator of Eq. (24); as employed here, Δa_v can be expected to be positive and S_{vv} can be expected to be negative.

Application. This is a two-step procedure. The first step is applied independently for the external loadings to the members with stress ratios that exceed a threshold parameter of unity or slightly less. These members are identified for redesign and a vector of required changes in stress resultants is computed from the current area, stress resultant, and allowable stress. From Eq. (21), for a particular loading column e, and a required change vector of stress resultants ΔS_e, we have

$$\left|\Delta S_e\right| = \left[SS_e\right]\left|R_e\right| \tag{29}$$

in which SS_e is a square matrix of stress resultants for self-equilibrating loads that conforms with the indices of the change vector. Eq. (29) can be solved for R_e, preferably by a solution procedure that can deal with singularities (20), since linear dependencies could be present.

The R_e vector contains the magnitudes of the loadings on the parallel members so that each area change required can be computed as the corresponding component of R_e divided by the allowable stress. Each external loading column is processed the same way, and a record of the area changes is maintained. Whenever the changes for the same bar are made for more than one loading column, the eventual selection is the envelope of maximum area changes.

In the second step, the equation derived from Eq. (19) by converting extensions to stress resultants is solved to obtain a complete R matrix. This is,

$$\left[\left[a/\Delta e\right] - \left[S_S\right]\right]\left[R\right] = \left[S_I\ S_S\right] \tag{30}$$

In Eq. (30) the right-hand side columns include both the external stress resultant matrix and S_S, which is the matrix of stress resultants for unit self-equilibrating loads with columns for all the potential primary constraints that have survived the first two criteria tests. Consequently, all stress resultant vectors needed for the third criteria test and for design optimization can be updated using Eq. (21). Stress resultant vectors so updated will be consistent with the area changes of Eq. (30) and will be exact except for numerical error accumulation.

An alternative to solving for R from Eq. (30) is to use the member extension form of Eq. (19). There would be additional calculations to convert stress resultants, which normally would be at hand, to extensions. There would be advantages, however, of being able to use symmetrical decompositions to solve Eqs. (29) and (30). For either alternative, the coefficient matrix on the left hand side of Eq. (30) will be well conditioned because of the stabilizing effect of the diagonal matrix.

The procedure just described is preliminary and represents the initial application method within a research computer program. Experiences so far have identified future problems to be resolved or opportunities for improvement. Several are discussed briefly in the following:

(1) A negative area change could be derived in Step 1 that could reduce the final area to a lower than acceptable value. The current remedy to remove members with such changes from the set processed in the second step occasionally produces variations from the desired results.

(2) The envelope method employed in Step 1 to obtain the set of area changes for Step 2 could be inefficient because of the need for sequential, rather than combined, processing of the vectors of external stress resultants.

(3) The procedure currently has no provisions to deal with groups of members for which the area changes within the group must be identical. Nevertheless, a tentative approach to provide this capability by using the partial derivative approximations of Eq. (25) is being examined.

(4) Reanalysis will disturb the stress constraint ratios for the unmodified members and the compliance constraint ratios. The current remedy to protect against severe stress ratio disturbances is to use threshold levels of less than unity to select members for modification. However, seriously adverse effects on compliance constraints could be difficult to overcome. As the result, the modification procedure could become questionable for design problems in which compliance constraints are more troublesome than stress constraints.

Numerical Examples

Two well-known demonstration test problems and variations are considered here: 10-bar truss problems, defined in Figure 1; and 63-bar truss problems, shown schematically in Figure 2, is fully defined in Ref. 1.

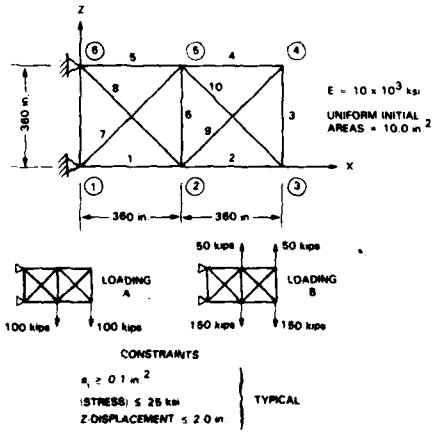


Fig. 1. 10-Bar Truss

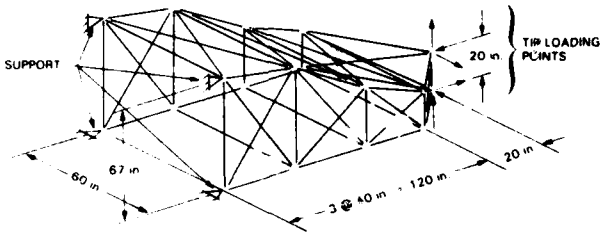


Fig. 2. 63-Bar Space Truss Schematic

Comparisons of results obtained with our present research computer program are made with those obtained with the ACCESS 3 (21) optimization program. Reports in the literature (3, 21) of tests on a number of standard problems, as well our own experiences, indicate this to be among the current best-performing and most efficient structural design computer program.

Comparisons of program efficiency for 10-bar truss design problems can be made only for the numbers of iteration cycles; numerical computation times are so small that they are overwhelmed by the user's printout requests and cannot be identified. The 63-bar truss problems entail a significant amount of numerical computations so that these times can be reasonably estimated. The estimate used here of net computation time is based upon specifying different printout levels for duplicate executions of the same problem. This makes it possible to determine the average number of printed pages that are typically produced by the program. Then the net computation time is estimated from subtractive adjustments dependent upon the page count. All timing comparisons are for execution by a UNIVAC 1100/81 computer.

The numbers of iteration cycles that will be shown in design history tabulations are variable. They depend either upon termination parameters that are equal to a fractional percentage of the change in raw weight between adjacent cycles or upon the lowest feasible weight attained in a few cases where the weight digressed to higher values after the lowest was attained.

10-Bar Truss Problems

Problems with Displacement Constraints. There are two well-studied problems each with the single loading condition of either Case A or of Case B. Minimum weights of 5060.9 lb and 4676.9 lb for the two loadings have been reported in many references and have been achieved with as few as 11 and 7 design cycles. The ACCESS 3 program and the our program incorporating procedures described here (omitting reanalysis) have been shown (4) to arrive at the minimum weights within either the minimum or close to the minimum numbers of cycles. These problems are controlled by the displacement constraints; stresses, except for a few members already at the minimum allowable size, are rarely critical. When we used reanalysis, there was a trivial weight increase for Loading A and a weight increase of about 125 lb for Loading B because the reanalysis caused violations of previously satisfied displacement constraints. A pathological feature of these problems is the increase in displacements caused by increases in the area of bar 6.

Problems with Displacement Constraints Omitted. Three problems for Loading A and one problem for Loading B have been examined previously (1, 22). For Loading A the first problem retains all stress constraints at 25,000 psi, the second allows 30,000 psi for bar 9, and the third allows 50,000 psi for bar 9. Weights of 1593.2 lb, 1545.2 lb, and 1497.7 lb reported in Ref. 22 were obtained in about 16 cycles for each problem and are the known minimums to within trivial differences. In the one problem for Loading B, all stress constraints are 25,000 psi. Weights of 1664.6 lb have been achieved (22, 23) in 11 cycles.

Tables 1 and 2 contain the design histories for these problems obtained by ACCESS 3 and by our program, which included the reanalysis procedure. The tables show that the known minimum weights were achieved and always in fewer cycles than previously. The reanalysis procedure seems to be particularly effective; it usually required fewer cycles to reach the lowest weight it attained, and it provided lower weights during intermediate cycles. Nevertheless, there were initial difficulties with both programs for the third problem with Loading A. The results shown in Table 1 were obtained by setting input parameters for the redundancy estimate criterion to effectively suppress that screening capability.

63-Bar Truss Problems

Problem with Displacement Constraints. The conventional displacement constraints for this problem simulate the torsional rotation for two independent loadings applied at the tip. Ref. 7 reported a weight of 6117 lb attained in 17 cycles; Ref. 21 reported a weight of 6119 lb attained with ACCESS 3 in 13 cycles.

Table 3 shows design histories obtained by the UNIVAC 1100/81 for ACCESS 3 and for our program. Computation times shown at the bottom of the table are the net estimates of the 1100/81 computer central processor unit (CPU) time. The ACCESS 3 run was obtained for a "partially fully-stressed design" mode as described in Ref. 21 with input parameters chosen according to recommendations given there. The usual parameters could provide weights lower than these by fractions of 1% but with added computation time. In fact, but in the spirit of research, all of the problem executions tabulated in the present paper allowed impractically large numbers of iterations. For example, any weight reduction below 6130 lb in Table 3 represents an improvement of at most 0.2%, which is surely only of academic interest.

The table shows that effectively low weights can be achieved comparatively rapidly with program features described here. Reanalysis increases the computation time for runs of the same cyclic duration but usually provides lower weights throughout the run history so that fewer design cycles could be specified. The last column of the table represents an experiment in which only the two displacement constraints were retained in the design optimzation step. That is, after reanalysis to adjust overstresses, all primary stress constraints were replaced by side constraints. The weight attained in 9 cycles is only about 0.7% heavier than the minimum. A problem formulated the same way, but without reanalysis, reached a 20-lb heavier design than this in 11 cycles (4).

Problem with Displacement Constraints Omitted. A weight of 4978 lb reported in Ref. 22 was attained in 14 cycles. Table 4 shows the design histories for problem formulations matching those of Table 3. Since the last column of the table represents a formulation with no primary stress constraints, there are no primary constraints at all. This design, except for using projection-modified side constraints and reanalysis, is equivalent to classical stress-ratio, fully stressed design. This formulation has achieved almost the lowest weight with the smallest computation time. Afterwards, the same runstream was reassembled to permit

Table 1. 10-Bar Truss Design Histories, Loading A

	Allowable Stress, psi					
	25,000 - All Bars		30,000 Bar 9 25,000 Others		50,000 Bar 9 25,000 Others	
	Feasible Weight, lb					
Cycle	Access 3	Present Program	Access 3	Present Program	Access 3	Present Program
1	3435.0	→				
2	1917.5	1799.7	1836.7	1759.0	1733.4	1729.1
3	1949.4	1719.2	1878.8	1675.3	1645.7	1590.5
4	1791.8	1667.6	1685.6	1622.0	1640.9	1534.2
5	1687.9	1628.5	1646.9	1580.6	1534.6	1523.0
6	1609.0	1622.3	1587.5	1574.4	1527.1	1516.4
7	1595.4	1593.2	1556.7	1545.2	1521.5	1510.9
8	1593.5		1548.2		1516.6	1506.3
9	1593.2		1545.6		1512.4	1502.6
10			1545.2		1508.7	1499.7
11					1505.5	1499.0
12					1517.6	1497.6
13					1502.5	
14					1497.6	

Table 2. 10-Bar Truss Design Histories - Loading B

	Feasible Weight, lb	
Cycle	Access 3	Present Program
1	3512.7	3512.8
2	2045.9	1945.3
3	2048.8	1857.5
4	1806.6	1784.8
5	1780.0	1717.0
6	1680.9	1685.4
7	1664.8	1664.5
8	1664.5	

15 analysis cycles. This run provided a further reduction of the weight to 4973.9 lb accompanied by a proportionate increase in computation time.

Additional test runs were made to explore further possibilities of using fully-stressed design methods to completely replace optimization. No reanalysis was used in these runs. Fifteen design cycles produc the following: a weight of 5,082 lb using standard stress-ratio side constraints, a weight of 5,064 lb with stress ratio side constraints modified by projections of the stress resultants. A third run allowed 25 cycles and provided no evidence of further substantial weight reduction.

Summary and Conclusions

Pre-screening of candidate primary stress constraints as described here has the objective of identifying and replacing non-pivotal stress constraints by side constraints that are much easier to process. A stress resultant stability criterion that uses stress resultant projections from prior design cycles was proposed as another criterion to supplement previously used stress ratio and redundancy estimate criteria. Stress resultant projection was also employed to anticipate cyclic progression of stress resultants and to derive modifications to improve the conventional stress ratio side constraints.

A new application of structural modification reanalysis with a virtual work formulation was described. The result is a more effective way to establish feasible designs from designs with stress ratio violations than the traditional method of scaling. The reanalysis procedure is, nevertheless, preliminary and several presently questionable aspects, primarily adverse effects possible for compliance constraints and the current omission of the capability to deal with grouped design variables, were identified for future attention.

Example applications demonstrated the capability of these procedures to provide rapid cyclic descent of the feasible structure weight in relatively low computation times and to achieve structural weights as low (except for occasional trivial differences), or in one case,

Table 3. 63-Bar Truss Design Histories with Displacement Constraints

Cycle	Feasible Weight, lb: Access 3	Present Program: No Reanalysis	Present Program: With Reanalysis	Present Program: With Reanalysis, No Primary Stress Constraints
1	30214.3	→	→	→
2	7625.6	8036.3	6854.2	6854.2
3	7037.3	6694.7	6492.1	6491.0
4	6879.8	6951.7	6297.9	6293.6
5	6510.5	6260.2	6212.0	6203.8
6	6388.3	6245.2	6169.2	6169.2
7	6286.1	6247.1	6163.8	6198.4
8	6216.5	6269.8	6142.3	6161.3
9	6174.8	6239.2	6135.4	6158.4
10	6149.4	6200.1	6130.9	
11	6136.7	6126.1	6126.7	
12	6129.9	6123.7	6122.4	
13	6125.8	6122.4	6121.2	
14	6124.0	6121.8	6119.5	
15			6119.0	
Net CPU Time, s	49	15	20	9

Table 4. 63-Bar Truss Design Histories Without Displacement Constraints

Cycle	Feasible Weight, lb: Access 3	Present Program: No Reanalysis	Present Program: With Reanalysis	Present Program: With Reanalysis, No Primary Stress Constraints
1	30214.3	→	→	→
2	6816.5	6360.2	5633.0	5663.0
3	5877.0	6212.7	5226.4	5312.4
4	5633.2	5531.8	5119.0	5179.1
5	5389.8	5274.7	5061.7	5050.3
6	5180.2	5108.8	5015.4	5019.7
7	5243.2	5095.4	5001.8	5067.1
8	5084.5	5105.7	4994.3	4989.1
9	5031.5	5029.3	4998.4	4983.2
10	4996.2	5019.9	4984.2	4977.9
11	4983.6	5029.2	4982.1	4976.9
12	4979.7	5002.2	4979.3	4976.1
13	4977.8	5005.5	4978.0	
14		4995.6	4976.2	
15		4991.1	4975.9	
Net CPU Time, s	109	29	42	26

lower than the weight achieved by other optimization procedures.

The motivation here was based on the need to deal with practical structural design problems much larger than those dealt with in current research. It appears impractical to be encumbered with hundreds of primary stress constraints. This implies a need for better ways to contend with what could impose overwhelming demands upon computational resources. Industry-oriented approaches to design optimization must emphasize reduction of the numbers of primary stress constraints, the numbers of auxilliary virtual loading (or equivalent) vectors, and the numbers of cycles to obtain feasible designs with significant weight improvements.

Acknowledgment

The research described in this paper was carried out by the Jet Propulsion Laboratory, California Institute of Technology, under NASA contract No. NAS7-100. Martha Strain provided invaluable assistance in converting algorithms to code, developing the computer program, executing innumerable test problems, and analyzing the results.

REFERENCES

1. Berke, L., and Khot, L., "Use of Optimality Criteria Methods for Large Scale Systems," AGARD Lecture Series No. 70, On Structural Optimization, Hampton, Va., pp. 1-29, Oct. 1974.

2. Khot, N., Berke, L., and Venkayya, V., "Comparison of Optimality Criteria Algorithms for Minimum Weight Design of Structures," AAIA Journal, Vol. 17, No. 2, pp. 182-190.

3. Schmit, L.A., and Fleury, C., "Structural Synthesis by Combining Approximation Concepts and Dual Methods," AAIA Journal, Vol. 18, No. 10, pp. 1251-1260.

4. Levy. R., and Parzynski, W., "Optimality Criteria Solution Strategies in Multiple Constraint Design Optimization," AIAA/ASME/ASCE/AHS 22nd SDM Conference, Paper 81-0551, Atlanta, Ga., April 6-8, 1981.

5. Schmit, L.A., and Miura, H., "An Advanced Structural Analysis/Synthesis Capability - Access 2," International Journal for Numerical Methods in Engineering, Vol. 12, 1978, pp. 353-377.

6. Fleury, C., "An Efficient Optimality Criteria Approach to the Minimum Weight Design of Elastic Structures," Computers and Structures, Vol. 11, pp. 163-173, Pergamon Press, Ltd. 1980.

7. Sander, G., and Fleury, C., "A Mixed Method in Structural Optimization," International Journal for Numerical Methods in Engineering, Vol. 13, pp. 385-404.

8. Levy, R., "Computer-Aided Design of Antenna Structures and Components," Computers and Structures, Vol. 6, 1976, pp. 419-428.

9. Schmit, L., and Fleury, C., "An Improved Analysis/Synthesis Capability Based on Dual Methods, St. Louis, Mo., April 4-6, 1979.

10. Levy, R., and Melosh, R.J., "Computer Design of Antenna Reflectors," Journal of the Structural Division, Proc. ASCE 99(ST-11), Proc. Paper 10178, pp. 2269-2285, Nov. 1973.

11. Melosh, R., and Luik, R., "Approximate Multiple Configuration Analysis and Allocation for Least Weight Structural Design," AFFDL-TR-67-59, Wright-Patterson AFB, Apr. 1967.

12. Gallagher, R., "Full Stressed Design," Optimum Structural Design, John Wiley, London, 1973, Ch. 3.

13. Melosh, R., "Structural Design, Frailty Evaluation and Redesign," AFFDL TR-70-15, July 1970, Vol. 1.

14. Khan, M., "Optimality Criterion Techniques Applied to Frames Having Nonlinear Cross-Sectional Properties," AIAA/ASME/ASCE/AHS 22nd SDM Conference. Paper 81-0552, Atlanta, GA., April 6-8, 1981.

15. Von Hoerner, S., "Homologous Deformations of Tiltable Telescopes," Journal of the Structural Division, Proc. ASCE 93(ST-5), Proc. Paper 5529, pp. 461-485, Oct. 1967.

16. Cella, A., and Logcher, R., "Automated Optimum Design from Discrete Components," Journal of the Structural Division, Proc. ASCE 97(ST-1), Proc. Paper 7845, pp. 175-189, Jan. 1971.

17. Storasli, O., and Sobieszczanski, J., "Design Oriented Structural Analysis," AIAA/ASME/SAE 14th SDM Conference Paper 73-338, Williamsburg, Va., March 1973.

18. Kavlie, D., and Powell, G.H., "Efficient Reanalysis of Modified Structures, Journal of the Structural Division, Proc. ASCE 97(ST-1), pp. 377-392, Jan. 1971.

19. Levy, R., "A NASTRAN Postprocessor for Structural Modification Reanalysis," NASA TM X-2378, Vol. II, pp 737-743, Sept. 1971.

20. Forsythe, G., Malcolm, M., and Moler, C., Computer Methods for Mathematical Computation, Prentice-Hall, Englewood Cliffs, N.J., 1977, Ch. 8.

21. Fleury, C., and Schmit, L., "Dual Methods and Approximation Concepts for Structural Synthesis," NASA CR 3226.

22. Schmit, L., and Miura, H., "Approximation Concepts For Structural Synthesis," NASA CR-2552, Mar. 1976.

23. Venkayya, V., "Design of Optimum Structures," Computers and Structures, Vol. 1, 1971, pp. 265-309.

SESSION #2

DYNAMICS AND RELIABILITY BASED DESIGN

AD-P000 032

OPTIMUM STRUCTURAL DESIGNS IN DYNAMIC RESPONSE

Hiroshi Yamakawa

Assistant Professor
Mechanical Engineering Department
Science and Engineering Faculty
Waseda University
Tokyo, Japan

Summary

In this study, general two methods of the optimum structural designs in dynamic response are newly presented and the validity and effectiveness of the methods are revealed by several numerical examples. The proposed two methods respectively consist of the following combined algorithms after discretizing the objective structural system by a certain method of discretization, for example, the finite element method :

(1) Method I (step-by-step integration procedure and optimization technique using gradients)
(2) Method II (modal analysis and optimization technique using gradients).

Emphasis is put on the derivation of convenient computation procedure of gradient of response quantities (displacement, velocity, acceleration, stress, strain) with respect to design variables. Two basic types of problems are considered in beams and framed structures which are subjected to the prescribed impulsive forces and ground motions. One is the problem to find optimum shapes of structures which minimize the r.m.s. values of the prescribed displacements in a certain fixed duration under the condition of constant total structural mass. The other is the problem to find optimum shapes of structures which minimize the total energy of the system at the end of impulse under the condition of constant total mass.

Several kinds of numerical solutions for such problems are obtained by utilizing the proposed two methods where the gradient projection method is adopted for one of optimization techniques.

1. Introduction

Recent advances in the field of computer technology, matrix method of structural analysis and linear and nonlinear optimization techniques have provided all the necessary tools for the optimum structural designs. Many papers concerned with structural optimization have appeared in recent year (1),(2). Much of those has been concerned with static behaviors of structures. However, prctical structural systems are often subjected to various types of dynamic loadings such as a periodic loadings by rotating machines, loadings by an earthquake, a blast, collision. The number of studies are comparatively few which concerns with optimum designs of structures subjected to such dynamic loadings.

Two basically different approaches are avilable to evaluate structural response to such dynamic loadings: deterministic(prescribed) and nondeterministic(random) In the former case, it is more convenient to devide the loadings into two categories from an analytical standpoint:

periodic loading and nonperiodic loading

An approach to avoid resonance phenomena is often effective for the designs of structures subjected to periodic loadings. That is based on natural frequency analysis. Some studies on optimum structural designs from such points of view have been done by Niordson (3), Turner (4) and et al (5)~(9) Their main interests are to obtain optimum shapes of column, beam, simple frame by taking note of the natural frequency. Auther has also presented general effective methods of such opttimum designs which were able to apply to complex structural systems and has shown sorts of numerical examples (10)~(14).

On the other hand, the designs of structures subjected to nonperiodic loading are generally done by checking out the results from dynamic response analysis with the design criteria. Quite a few existing investigations from such a standpoint of view have appeared because of the difficulties in practical computations (15)~(20).

In this paper, the dynamic response of strucutres subjected to certain prescribed loadings and ground motion is of interest and general two methods of optmium designs will be newly presented. The validity and the effectiveness of the proposed methods will be also examined in detail by several numerical examples.

2. Optimum Structural Designs in Dynamic Response

Consider the objective structural systems have been already discretized by a certain method, for instance, a finite element method. The equation of motion for such discretized systems can be, in general, written as follows :

$$M\ddot{q} + C\dot{q} + Kq = 0 \qquad (1)$$

where M , C , K are the mass, damping, stiffness matrices respectively, the order of those matrices corresponding to the number of degrees of freedom, m , used in q describing the displacements of the system. A vector Q is an applied load vector and dots represent differentiation with respect to time.

Now let's consider the case in which M, C, K, q can be expressed as functions of a vector X whose components are n design variables , $x_1, x_2, \ldots, x_n$, which specify the main design of the structure. The design variables usually are postulated to be constrained to maintain the safty requirements and utilities of the structure and form the feasible region to determine the design variables which minimize or maximize the objective quantity. This objective quantity can also be described by the function of design variables (objective function) and is the most important single property of the design, such as the cost, weight, maximum values of velocity or acceleration or r.m.s. value of displacement, especially, for the optimum design of structures in dynamic response.

3. Optimum Design Methods in Dynamic Response

To solve the optimum design problems of structures in dynamic response always involves great difficulties since displacements, velocities, accelerations are often related to objective function and conditions of constraints and they are in general implicit nonlinear functions of design variables. Matrix structural methods and nonlinear optimization techniques which have been developed recently enable us to obtain numerical solutions although they are not in closed forms. Step-by-step integration technique and modal analysis are generally known to be very effective methods for dynamic response analysis. Among many optimization techniques, the technique using gradients of some quantities with respect to the design variables give a powerful device to solve the complicated optimum design problems , for example, problems with a large number of design variables or some nonlinear constraints of the objective function. The gradient projection method is one of the typical methods.

Consequently two new methods of optimum designs of structures in dynamic response will be introduced in the following which utilize aforementioned useful methods. The proposed methods respectively are composed of the following combined algorithms :

(1) Method I
  (a) dynamic resonse analysis ... step-by-step integration procedure
  (b) optimization technique ... any optimization techniques using gradients

(2) Method II
  (a) dynamic response analysis ... modal analysis
  (b) optimization technique ... any optimization techniques using gradients

Primary emphasis will be placed on deriving the convenient computation procedure of gradient of response quantities for example, displacement, velocity , acceleration, stress, strain with respect to design variables.

In the context that follows the presented methods will be detailed. The step-by-step integration techniques and modal analysis ,as themselves, are well known methods. However, some brief explanations will be given to present the methods.

3.1. Method I (Step-by-step Integration Procedure and Optimization Techniques using Gradients)

The step-by-step integration pocedure is the method to obtain the solution of Eq.(1) by numerical integration and is suitable for not only use with linear systems but also use with nonlinear systems. The response is evaluated for a series of short time increments Δt generally taken of equal length for computation convenience. Among sorts of step-by-step integration techniques, Newmark's β method and Wilson's θ method are widely used typical methods. Thus let's introduce the new methods reffering mainly to those two procedures. A similar argument, of course , will be applied to the case using other step-by-step integration techniques.

3.1.1. Newmark's β method

Letting M, C, K, Q, q at the time t be known, the equation of motion at the time t is written by :

$$M(t)\ddot{q}(t) + C(t)\dot{q}(t) + K(t)q(t) = Q(t) \qquad (2)$$

In the method, displacements and velocities at the time t+Δt, a short time increment Δt later than at the time t, are assumed as follows :

$$q(t+\Delta t)=q(t)+\Delta t\dot{q}(t)+\frac{(\Delta t)^2}{2}\ddot{q}(t)+\beta(\Delta t)^2\{\ddot{q}(t+\Delta t)-\ddot{q}(t)\} \qquad (3)$$

$$\dot{q}(t+\Delta t)=\dot{q}(t)+\frac{\Delta t}{2}\{\ddot{q}(t)+\ddot{q}(t+\Delta t)\} \qquad (4)$$

where β is a parameter which takes the value of $0\leq\beta\leq 1/6$. Setting $\beta=1/6$, then the procedure becomes identical to the linear acceleration method. Substituting Eqs.(3),(4) into Eq.(2) and solving for the unknown $\ddot{q}(t+\Delta t)$,

$$\ddot{q}(t+\Delta t)=\{M+\frac{\Delta t}{2}C+\beta(\Delta t)^2K\}^{-1}[Q(t+\Delta t)-C\{\dot{q}(t)+\frac{\Delta t}{2}\ddot{q}(t)\}$$
$$-K\{q(t)+\Delta t\dot{q}(t)+(\frac{1}{2}-\beta)(\Delta t)^2\ddot{q}(t)\}\ ] \qquad (5)$$

By substitution of the obtained $\ddot{q}(t+\Delta t)$ into Eqs.(3),(4) $q(t+\Delta t)$, $\dot{q}(t+\Delta t)$ are also given.

By the way, the gradients of accelerations can be calculated in the following manner. Differentiating Eq.(5) with respect to x_j and rearranging it leads to

$$\frac{\partial\ddot{q}(t+\Delta t)}{\partial x_j}=-\{M+\frac{\Delta t}{2}C+\beta(\Delta t)^2K\}^{-1}\{A_1 q(t)+A_2\dot{q}(t)+A_3\ddot{q}(t)$$
$$+A_4\frac{\partial q}{\partial x_j}+A_5\frac{\partial\dot{q}}{\partial x_j}+A_6\frac{\partial\ddot{q}}{\partial x_j}+A_7 q(t+\Delta T)\} \qquad (6)$$
$$; (j=1,2,\ldots,n)$$

where $A_1 \sim A_7$ are the matrices as shown in Table 1. Similarly the gradients of velocities and diplacements at the time t+Δt are expressed as

$$\frac{\partial\dot{q}(t+\Delta t)}{\partial x_j}=\frac{\partial\dot{q}(t)}{\partial x_j}+\frac{\Delta t}{2}\{\frac{\partial\ddot{q}(t)}{\partial x_j}+\frac{\partial\ddot{q}(t+\Delta t)}{\partial x_j}\} \qquad (7)$$

$$\frac{\partial q(t+\Delta t)}{\partial x_j}=\frac{\partial q(t)}{\partial x_j}+\Delta t\frac{\partial\dot{q}(t)}{\partial x_j}+\frac{(\Delta t)^2}{2}\frac{\partial\ddot{q}(t)}{\partial x_j}+(\Delta t)^2\{\frac{\partial\ddot{q}(t+\Delta t)}{\partial x_j}$$
$$-\frac{\partial\ddot{q}(t)}{\partial x_j}\} \quad ; (j=1,2,\ldots,n) \qquad (8)$$

The gradients of the displacements,velocities,acceleration at the time t+Δt, all of them, thus are able to be evaluated by Eq.(6) to Eq.(8). It should be noted that the initial values of these gradients can be easily determined by letting the gradients at the time before the change of the design equal to zeros.

There exists no investigation on optimum structural designs using such step-by-step integration procedure.

3.1.2. Wilson's θ method

Several different unconditionally stable methods have been used for the dynamic analysis. Wilson's θ method is one of the simplest and the best of these and is a modification of the linear acceleration method. This modification is that the acceleration varies linearly over an extended interval $\theta\Delta t$ where $\theta > 1.37$. The displacements and velocities at the time t+$\theta\Delta$t are assumed as follows :

$$q(t+\theta\Delta t)=q(t)+\theta\Delta t\dot{q}(t)+\frac{(\theta\Delta t)^2}{3}\ddot{q}(t)+\frac{(\theta\Delta t)^2}{6}\ddot{q}(t+\theta\Delta t) \qquad (9)$$

$$\dot{q}(t+\theta\Delta t)=\dot{q}(t)+\theta\Delta t\frac{\ddot{q}(t)+\ddot{q}(t+\theta\Delta t)}{2} \qquad (10)$$

Substitution of these into Eq.(2) gives

$$q(t+\theta\Delta t)=\{K+\frac{3}{\theta\Delta t}C+\frac{6}{(\theta\Delta t)^2}M\}^{-1}[M\{2\ddot{q}(t)+\frac{6}{\theta\Delta t}\dot{q}(t)$$
$$+\frac{6}{(\theta\Delta t)^2}q(t)\}+C\{\frac{\theta\Delta t}{2}\ddot{q}(t)+2\dot{q}(t)+\frac{3}{\theta\Delta t}q(t)\}$$
$$+Q(t+\theta\Delta t)] \qquad (11)$$

Thus accelerations,velocities,displacemnts at the time t+Δt are found to be

$$\ddot{q}(t+\Delta t)=(1-\frac{1}{\theta})\ddot{q}(t)+\frac{1}{\theta}\ddot{q}(t+\theta\Delta t) \qquad (12)$$

$$\dot{q}(t+\Delta t)=\dot{q}(t)+\frac{\Delta t}{2}\{\ddot{q}(t)+\ddot{q}(t+\theta\Delta t)\} \qquad (13)$$

$$q(t+\Delta t)=q(t)+\Delta t\dot{q}(t)+\frac{(\Delta t)^2}{6}\{2\ddot{q}(t)+\ddot{q}(t+\theta\Delta t)\} \qquad (14)$$

The gradients of these quantities with respect to the design variables at the time t+ t are able to be obtained by differentiating both sides of Eq.(11) with respect to x :

$$\frac{\partial q(t+\theta\Delta t)}{\partial x}=\{K+\frac{3}{\theta\Delta t}+\frac{6}{(\theta\Delta t)^2}M\}^{-1}\{B_1 q(t)+B_2\dot{q}(t)+B_3\ddot{q}(t)$$
$$B_4\frac{\partial q}{\partial x}+B_5\frac{\partial\dot{q}(\theta\Delta t)}{\partial x}+B_6\frac{\partial\ddot{q}}{\partial x}+B_7 q(t+\theta\Delta t)\}$$
$$; (j=1,2,\ldots,n) \qquad (15)$$

Table 1

A_1	$\frac{\partial K}{\partial x}$	A_5	$C+(\Delta t)K$
A_2	$\frac{\partial C}{\partial x}+\Delta t\frac{\partial K}{\partial x}$	A_6	$\frac{\Delta t}{2}C+(\frac{1}{2}-\beta)(\Delta t)^2K$
A_3	$\frac{\Delta t}{2}\frac{\partial C}{\partial x}+(\frac{1}{2}-\beta)(\Delta t)^2\frac{\partial K}{\partial x}$	A_7	$\frac{\partial M}{\partial x}+\frac{\Delta t}{2}\frac{\partial C}{\partial x}+\beta(\Delta t)^2\frac{\partial K}{\partial x}$
A_4	K	—	—

where $B_1 \sim B_7$ are the matrices shown in Table 2 and then also by differentiating Eq.(12) to Eq.(14) with respect to x_j.

The initial values of these gradients can be determined in the same manner as mentioned in the section 3.1.1.

3.2. Method II (Modal Analysis and Optimization Technique using Gradients)

The modal analysis is one of the best and the most effective methods in dynamic response analysis though it can be applied only to linear systems. The methods to be proposed is basically similar to the method by Fox and Kapoor (15). However, details are different in the practical calculation, for instance, the calculation of gradients of eigenvectors with respect to design variables.

For undamped free vibration, the equation (1) can be reduced to eigenvalue equation.

$$K u_r - \lambda M u_r = 0 \qquad ; (r=1,2,\ldots,m) \tag{16}$$

where m is aforementioned the degrees of freedom of the system and u_r is an eigenvector corresponding to r-th eigenvalue. Modal coordinate expressions

$$q = U \phi \tag{17}$$

in which U is the mode-shape matrix and ϕ is the general coordinate vector will be intoduced.
Premultiplying Eq.(1) by the transpose of r-th mode-shapevector- u_r leads to

$$u_r^T M U \ddot{\phi} + u_r^T C U \dot{\phi} + u_r^T K U \phi = u_r^T Q \qquad ; (r=1,2,\ldots,m) \tag{18}$$

It was noted above that the orthogonality conditions :

$$u_r^T M u_s = 0 \tag{19}$$

$$u_r^T K u_s = 0 \qquad (r \neq s) \tag{20}$$

cause all components except r-th mode term in the mass and stiffness expressions of Eq.(18) to vanish.
A similar reduction will apply to the damping expression if it is assumed that the cooresponding orthogonality conditions also apply to the damping matrix, that is, assume that

$$u_r^T C u_s = 0 \qquad (r \neq s) \tag{21}$$

Thus Eq.(18) then may be reduced to uncoupled simple equations of motion :

$$\ddot{\phi}_r + 2\zeta_r \omega_r \dot{\phi}_r + \omega_r \phi_r = P_r \qquad ; (r=1.2,\ldots,l) \tag{22}$$

in which l is the number of adopted modes ($l \leq m$) and ω_r , ζ_r , P_r are given in the following relation :

Table 2

B_1	$\frac{6}{(\theta\Delta t)^2}\frac{\partial M}{\partial x} + \frac{3}{\theta\Delta t}\frac{\partial C}{\partial x}$	B_5	$\frac{6}{\theta\Delta t} M + 2 C$
B_2	$\frac{6}{\theta\Delta t}\frac{\partial M}{\partial x} + 2\frac{\partial C}{\partial x}$	B_6	$2M + \frac{\theta\Delta t}{2} C$
B_3	$2\frac{\partial M}{\partial x} + \frac{\theta\Delta t}{2}\frac{\partial C}{\partial x}$	B_7	$-\frac{\partial K}{\partial x} - \frac{3}{\theta\Delta t}\frac{\partial C}{\partial x} - \frac{6}{(\theta\Delta t)^2}\frac{\partial M}{\partial x}$
B_4	$\frac{6}{(\theta\Delta t)^2} M + \frac{3}{\theta\Delta t} C$	—	——

$$\frac{u_r^T K u_r}{u_r^T M u_r} = \omega_r^2 = \lambda_r \tag{23}$$

$$\frac{u_r^T C u_r}{u_r^T M u_r} = 2\zeta_r \omega_r \tag{24}$$

$$\frac{u_r^T Q}{u_r^T M u_r} = P_r \tag{25}$$

The eigenvector u_r may be nolmarlized as follows :

$$u_r^T M u_r = 1 \tag{26}$$

3.2.1 Caluculations of Displacements, Velocities, Accelerations

By Duhamel integral, the solution of Eq.(22) is of the form :

$$\phi_r = \frac{1}{\omega_r'}\int_0^\tau P_r(\tau) \exp(-\zeta_r \omega_r' (t-\tau)) \sin \omega_r (t-\tau) d\tau \qquad (\omega_r' = \omega_r\sqrt{1-\zeta_r^2}) \tag{27}$$

From Eqs.(17), (27) the displacement vector q can be calculated.

Let S be a matrix consists of partial differential operators in the spatial coordinates, the strain vector ε is then expressed as

$$\varepsilon = S q = \Sigma S u_r \phi_r = \Sigma \varepsilon_r \tag{28}$$

The stress vector σ may be related to the strain vector ε by use of elasticity modulus matrix E :

$$\sigma = E \varepsilon \tag{29}$$

3.2.2. Calculations of Gradients of Displacements, Velocities, Accelerations, Stress

(a) Gradients of Displacements

By diffrentiation of Eq.(17) with respect to x_j ,

$$\frac{\partial q}{\partial x_j} = \frac{\partial}{\partial x_j}(\Sigma u_r \phi_r) = \Sigma\left(\frac{\partial u_r}{\partial x_j}\phi + u_r\frac{\partial \phi_r}{\partial x_j}\right) \qquad (r=1,2,\ldots,l) \tag{30}$$

where $\mu_r = \zeta_r \omega_r$. Using Eq.(23) to Eq.(25) and the relation $\omega_r'^2 = \omega_r^2 - \mu_r^2$,

$$\frac{\partial \omega_r'}{\partial x_j} = \frac{1}{2}\left(\frac{\partial \lambda_r}{\partial x_j} - 2\mu\frac{\partial \mu_r}{\partial x_j}\right)(\lambda_r - \mu^2)^{-\frac{1}{2}} \tag{31}$$

$$\frac{\partial \mu}{\partial x_j} = u_r^T C\frac{\partial u_r}{\partial x_j} + \frac{1}{2} u_r^T \frac{\partial C}{\partial x_j} u_r \tag{32}$$

$$; (r=1,2,\ldots,l) \ , (j=1,2,\ldots,n)$$

Consequently, it will be noted that the calculation of gradients of eigenvalues and eigenvectors with respect to the design variables is indispensable for the evaluation of these gradients. The way of calculation will be discussed next.

(i) Gradients of Eigenvalues

Differentiating the both sides of the eigenvalue equation (16) by x_j gives

$$(K - \lambda_r M)\frac{\partial u_r}{\partial x_j} + \left(\frac{\partial K}{\partial x_j} - \lambda_r\frac{\partial M}{\partial x_j}\right)u_r - \frac{\partial \lambda_r}{\partial x_j} M u_r = 0 \qquad ; (j=1,2,\ldots,n) \tag{33}$$

Premultiplying Eq.(33) by u_r and making use of the properties of symmetry leads to the calculation of the gradients of eigenvalues :

$$\frac{\partial \lambda_r}{\partial x_j} = u_r \left(\frac{\partial K}{\partial x_j} - \lambda_r \frac{\partial M}{\partial x_j} \right) u_r \quad ; (j=1,2,\ldots,n) \tag{34}$$

in which Eq.(1) was also used.

(ii) Gradients of Eigenvectors

Putting $T = K - \lambda_r M$ and assuming all eigenvalues are different, that is, the rank of T is $m-1$ leads to the partition of the matrix T :

$$\left[\begin{array}{c|c} T_{11} & T_{12} \\ \hline T_{21} & T_{22} \end{array}\right] \left\{\begin{array}{c} u_r^2 \\ \hline u_r^1 \end{array}\right\} = 0 \tag{35}$$

On the diffrentiation of Eq.(35) with respect to x_j

$$\left[\begin{array}{c|c} \frac{\partial T_{11}}{\partial x_j} & \frac{\partial T_{12}}{\partial x_j} \\ \hline \frac{\partial T_{21}}{\partial x_j} & \frac{\partial T_{22}}{\partial x_j} \end{array}\right] \left\{\begin{array}{c} u_r^1 \\ \hline u_r^2 \end{array}\right\} + \left[\begin{array}{c|c} T_{11} & T_{12} \\ \hline T_{21} & T_{22} \end{array}\right] \left\{\begin{array}{c} \frac{\partial u_r^1}{\partial x_j} \\ \hline \frac{\partial u_r^2}{\partial x_j} \end{array}\right\} = 0 \tag{36}$$

Eq.(36) leads to

$$\frac{\partial u_r}{\partial x_j} = a \frac{\partial u_r}{\partial x_j} + A_j u_r \tag{37}$$

where

$$a = \left[\begin{array}{c|c} -T_{11}^{-1} T_{12} & \\ \hline T_{22}^{-1} T_{21} T_{11}^{-1} T_{12} & \end{array}\right] \tag{38}$$

$$A_j = \left[\begin{array}{c|c} -T_{11}^{-1} \frac{\partial T_{11}}{\partial x_j} & -T_{11}^{-1} \frac{\partial T_{12}}{\partial x_j} \\ \hline -T_{22}^{-1} \frac{\partial T_{21}}{\partial x_j} + T_{22}^{-1} T_{21} T_{11}^{-1} \frac{\partial T_{11}}{\partial x_j} & -T_{22}^{-1} \frac{\partial T_{22}}{\partial x_j} + T_{22}^{-1} T_{21} T_{11}^{-1} \frac{\partial T_{12}}{\partial x_j} \end{array}\right] \tag{39}$$

When Eq.(26) is differentiated with repect to x_j, the relation :

$$2 u_r^T M \frac{\partial u_r}{\partial x_j} + u_r^T \frac{\partial M}{\partial x_j} u_r = 0 \tag{40}$$

is valid . By the substitution of Eq.(37) into Eq.(40) and rearrangement of it, the gradients of eigenvectors are finally able to be calculated as follows :

$$\frac{\partial u_r^2}{\partial x_j} = \frac{2 u_r^T M A_j u_r + u_r^T \frac{\partial M}{\partial x_j} u_r}{2 u_r^T M a} \tag{41}$$

$\partial u_r^1 / \partial x_j$ in Eq.(41) can be given from Eq.(36) as

$$\frac{\partial u_r^1}{\partial x_j} = -T_{11}^{-1} \frac{\partial T_{11}}{\partial x_j} u_r - T_{11}^{-1} \frac{\partial T_{12}}{\partial x_j} u_r - T_{11}^{-1} T_{12} \frac{\partial u_r}{\partial x_j} \tag{42}$$

(b) Gradients of velocities, Accelerations and Stresses

The gradients of velocities and accelerations can be able to be calculated assuming the commutation of the partial differentiation operators of time and design variables.

On the other hand, the gradients of stresses can be given from Eq.(29) by

$$\frac{\partial \sigma}{\partial x_j} = E S \frac{\partial \varepsilon}{\partial x_j} \tag{43}$$

4. Numerical Examples

4.1. Optimum Design Problems

Several types of optimum design problems of structures are of interest from practical engineering standpoints of view and many discussion should be given. However, the detail discussions have been eliminated because of the restriction of this paper.

Two types of optimum design problems treated in this study are summarized in Table 3.

Beams and framed structures are taken as a simple and handy structures in the following numerical examples. Those structures are idealized as connected systems of n uniform finite beam elements by the finite element method. In each element, the flexural diplacement is assumed by the cubic hermitian polynominal in the longitudinal coordinate. The dynamic anlysis here is on the basis of usual finite element method.

The length, density, Young's modulus, common in all element, are designated by ℓ, ρ, E respectively. But the cross sectional areas and the second moments of inertia, different in each element, are expressed by A_j, I_j $(j=1,2,\ldots,n)$.

In every case of the following designs, the mass ratios $x_j = \rho A_j \ell / M$ (element mass/structural mass) ; $(j=1,2,\ldots,n)$ are taken as the design variables for computational convenience.

Table 3

model	beam and framed structures
loading	impulsive loading ground acceleration
design variable	$x_j = \frac{\text{j-th element mass}}{\text{total structural mass}}$ $(j=1,2,\ldots,n)$
codtion of costraints	total structural mass constant $x_j > 0 \quad \Sigma x_j = 1$
objective function	r.m.s.value of displacement $\bar{u}$, $\bar{\ddot{u}}$ ...(A) total energy H ...(B)
optimum design ptoblem	minimization of $\bar{u}$, $\bar{\ddot{u}}$, H

4.2. Numerical Examples by Method I

4.2.1. Optimum Designs of Beams

Consider first the optimum design problems in the type-A Among several step-by-step integration methods, Wilson's θ method, unconditionally stable procedure, is adopted for the dynamic response anlysis because the design variables may be changed at each design step of the optimization. The gradient projection method is used as one of powerful methods in optimization.

Fig.1 and Fig.2 illustrate the relation between a design variable x_j and a displacement at the free end of the cantilever or the r.m.s value of the displacement

during a prescribed time interval. The cantilever with a similar cross section is there modeled by two uniform beam elements and subjected to a half-sine impulsive loading at its free end. The variation of the response displacements cooresponding to the change of design variables is considerablly complicated. However the curves of the variation of the r.m.s. values of these displacements show simple convex and the r.m.s. value is found to be very suitable for the objective fuction of optimum design. In those figures, the optimum point obtained by the proposed method is also shown by refference.

The profiles of the objective functions in the same case are also shown in Fig.3.

The shapes and response displacements of the obtained optimum beams are shown in Fig.4 to Fig.8
It is shown that almost all response displacement levels can be reduced in the prescribed time intervals.
The Rayleigh type damping is considered in the example shown in Fig.7. The proposed method proved to apply to such a damped system.

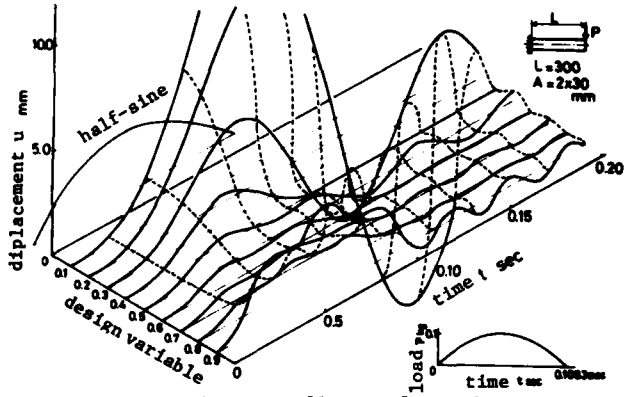


Fig.1 displacement of beam at free end (2-elements-model)

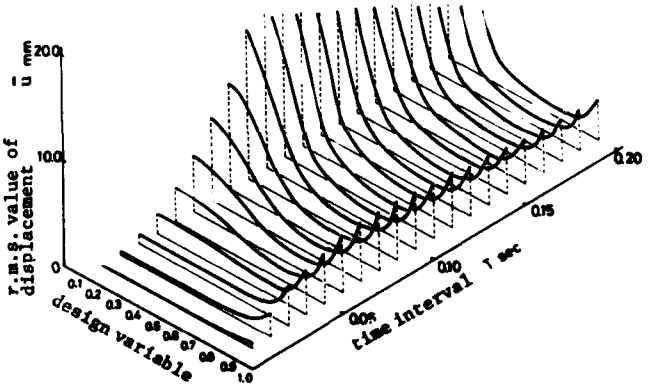


Fig.2 r.m.s. value of displacement at free end (2-elements-model)

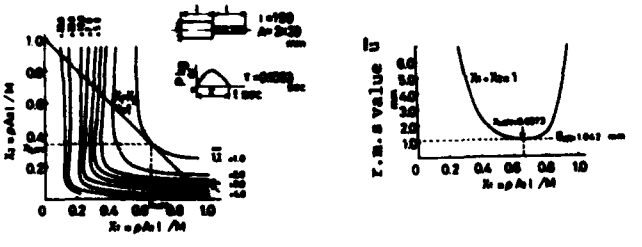


Fig.3 profile of objective function (2-elements-model)

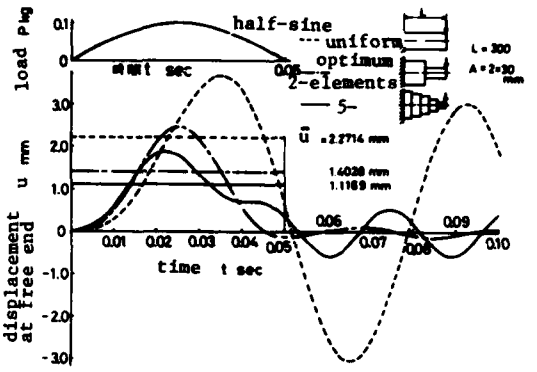
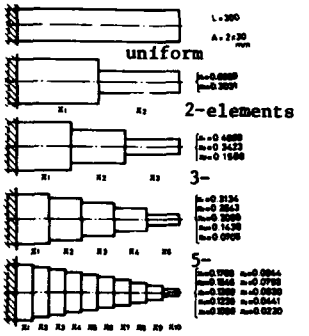


Fig.4 optimum beam



10-

Fig 5 optimum beam

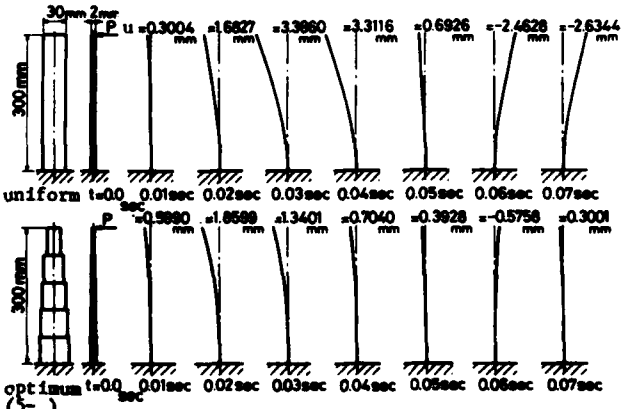


Fig 6 dynamic response of optimum beam

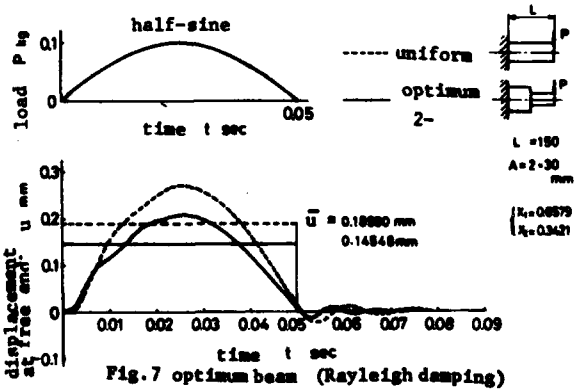


Fig.7 optimum beam (Rayleigh damping)

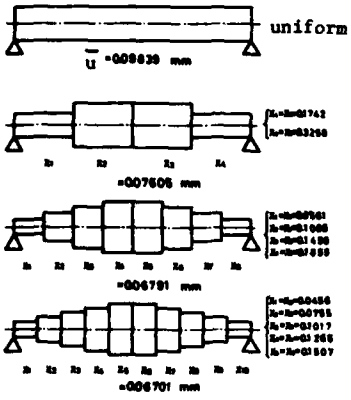


Fig.8 optimum beam (simply supported)

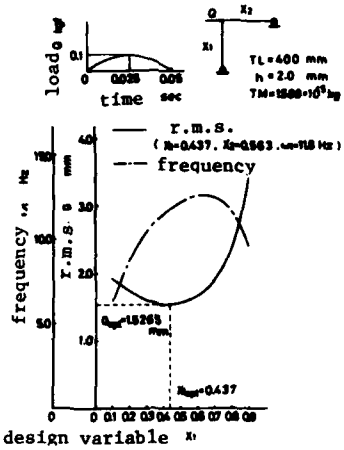


Fig.9 profile of objective function

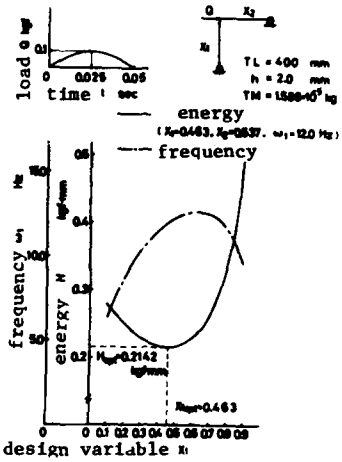


Fig.10 profile of objective function

4.2.2. Optimum Designs of Framed Structures

In this section, two types of optimum design problems, A and B, will be considered and comparisons in both types will be made.

The objective functions and fundamental natural frequencies are shown in Fig.9 and Fig.10 which were obtained for the simple frame modeled by two elements. The frame is subjected to a half-sine impulsive loading to its corner. The calculated optimum design points provides good agreement with the minimum point of the objective function.

Fig.11 compares the optimum response displacements for various numbers of elements. The maximum displacement and the amplitude of free vibration, both of them, are found to be decreased as the numbers of elements increase.

The optimum shapes and response displacements in framed structures in plane are shown in Fig.12 to Fig.15. It appeares from these results that the type-A problems can reduce the value of maximum displacement, On the other hand, the type-B problems can decrease the amplitude of the free vibration.

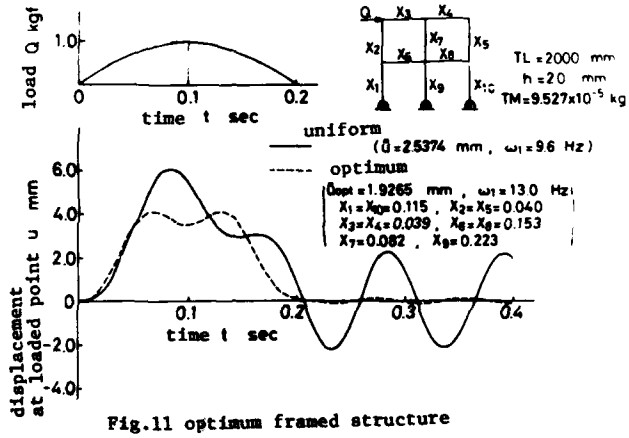


Fig.11 optimum framed structure

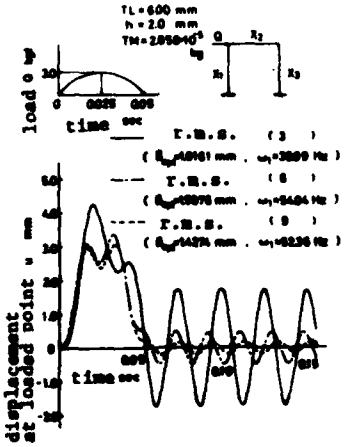


Fig 13 optimum framed structure

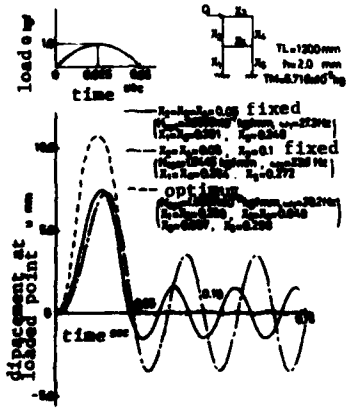


Fig.14 optimum framed structure

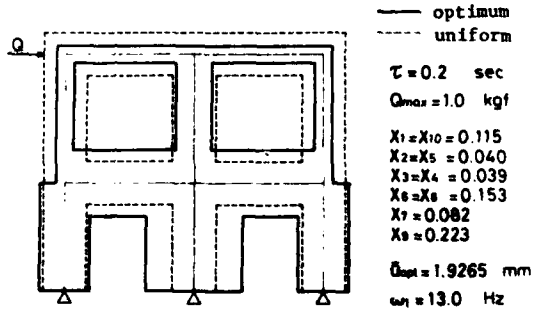


Fig.12 optimum shape of framed structure

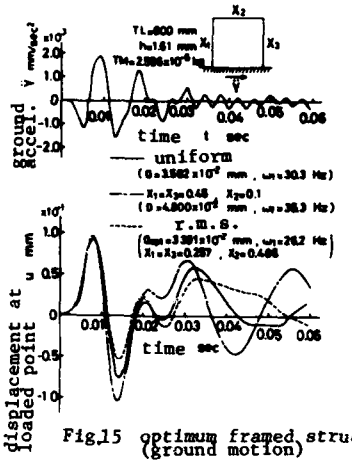


Fig.15 optimum framed structure (ground motion)

4.3. Numerical Examples by Method II

To examine the validity and the effectiveness of the Method II, the same examples in the optimum design problems of cantilevers as in the section 4.2.1 will be taken again and comparisons will be made between the Method I and the Method II. The optimum design results are shown in Fig.16 to Fig.18.

Fig.16 shows the relation between the displacements and the number of elements. The computation was carried under the condition that the number of the adopted mode No= 4 and the number of time increments Nt=100. With the increase of the number of elements, the optimum shape and the response displacement converge gradually. The results obtained presicely agree with the results by the Method I (c.f. Fig.4).

Fig.17 shows the response displacement at the free end corresponding to the number of time increment under the condition that the number of elements N=5 and the number of the adopted modes No=4. As the number of time increment increses, the response displacement converges asymptotically.

The relationship between the displacement at the free end and the number of the adoptedmodes is shown in Fig.18 in which the conditions N=5 , Nt=100 are imposed.

Taking an example in 10-elements-model to compare the computation time in both proposed methods leads to the conclusion that the computation time in the Method II can be reduced by one ninetieth. Thus in linear systems subjected to comparatively simple type impulsive loadings the computation time by the Method II is considerably efficient.

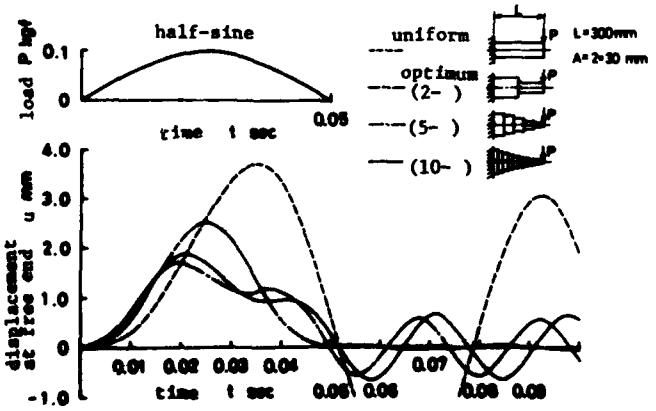


Fig.16 optimum beam

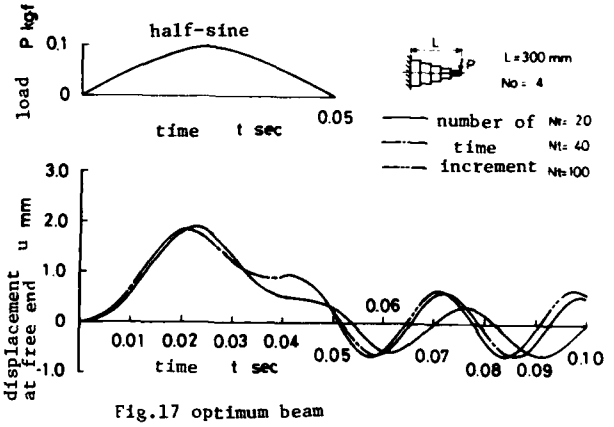


Fig.17 optimum beam

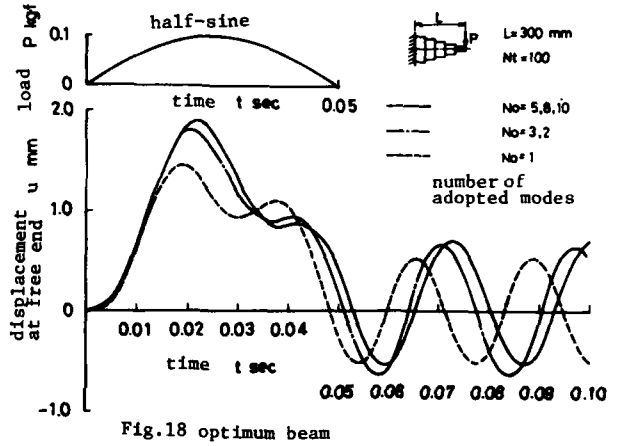


Fig.18 optimum beam

5. Conclusions

The two methods of optimum designs of structures in dynamic response were newly presented. The proposed methods consist of the combined two algorithms, an optimization technique by use of grsdients in nonlinear programming and a step-by-step integration procedure or a modal analysis in dynamic analysis.

The convenient and effective computation procedure of gradients of response quantities with respect to design variables was shown which is able to be applied to any optimization techniues using gradients.

The computed several numerical examples of optimum designs of beams and framed structures led to the following conclusions :

Method I

(1) This method is able to be applied to structural systems subjected to arbitary types of prescribed impulsive loadings expressed in time history.
(2) The maximum displacement is decreased by the selection of the r.m.s. value of displacement for the objective function. On the other hand, the amplitude of displacement in free vibration can be reduced by the adoption of the total energy for the objective function.
(3) When the r.m.s. value is taken for the objective function, the calculation of gradients at every time increment leads to considerable increase in computation time. An appropriate consideration should be given to those countermeasures.

(4) When the total energy is adopted for the objective function. the computation time can be reduced greatly . for example , by one fourth in the cantilever case.

Method II

(1) This method provides to reduce the computation time of gradients exceedingly in comparison with the Method I though the application is restricted only to linear systems.
(2) The computation time of gradients can be further reduced by proper selections of the number of adopted modes and the number of time increments.

Acknowledgements

The auther would like to acknowledge the advice of Dr. A. Okumura in Waseda University. And thanks are due to the following people who helped in the developement of the computer program used the proposed methods and provided several numerical examples for this paper
: H. Wakabayashi, H. Hirose, M. Ichimonji,
A. Ohhashi. K. Hamada.

References

(1) E. Wasiutyski and A. Brandt, " The present state of knowledge in the field of optimum design of structures ", Applied Mechanics Reviews,(1963-5).
(2) W. Prager and C. Sheu, " Recent developement in optimal structural design ", Applied Mechanics Reviews, (1968-10), 985.
(3) F.I. Niordson, " On the optimum design of a vibrating beam ", Quarterly of Applied Mathematics, (1965-4), 47.
(4) M.J. Turner, "Design of minimum-mass structures with specified natural frequencies ", AIAA J, (1967-5),406.
(5) J.E. Taylor, " Minimum-mass bar for axial vibration at specified natural frequencies ", AIAA J, 5,(1967), 1911.
(6) C.Y. Sheu " Elastic minimum weight design for specified fundamental frequency ", Int.J.Solids Struc.,4,(1968),953.
(7) B.R. McCart, E.J. Haug and T.O. Streeter, "Optimal design of structures with constraints on natural frequency ", AIAA J., 8, (1970), 1012.
(8) C.P. Rubin, " Minimum weight design of complex structures subjected to a frequency constraint ", AIAA J., 8, (1970), 923.
(9) M.S. Zaghamee, " Optimum frequency of structures", AIAA J., 6, (1968), 749.
(10) H. Yamakawa and A. Okumura, " Optimum designs of structures with regard to their vibrational characteristic (1st Rep.) ", Bull of JSME, 19-138, (1976-12),1458.
(11) H. Yamakawa and A. Okumura, " Optimum designs of structures with regard to their vibrational characteristic (2nd Rep.) " ,Bull of JSME, 20-141, (1977-3), 292.
(12) H. Yamakawa and A. Okumura, " Optimum designs of structures with regard to their vibrational characteristic (3rd Rep.) " Bull of JSME, 20-141, (1977-3), 300.
(13) H. Yamakawa and et al, " Optimum designs of structures with regard to their vibrational charecteristic (4-th Rep.) ", Bull of JSME, 21-154,(1978-4, 637.
(14) H. Yamakawa and et al, " Optimum designs of structures with regard to their vibrational characteristic (5-th Rep.) ", Bull of JSME, 22-169,(1979-7),
(15) R.L. Fox and M.P. Kapoor, " Structural optimization in the dynamic response regime ". AIAA J.. 8 . (1970),1798
(16) R.M. Brach, " Optimum design of beams for sudden loading ", Proc. of ASCE , EM6, (1968-12),1395.
(17) T.T. Feng, J.S. Arora and E.J. Haug, " Optimal structural design under dynamic loads ", Int. J. Numerical Methods Engnrs, 11, (1977),39.
(18) F.Y. Cheng and M.E. Botkin. " Nonlinear optimum design of dynamic damped frames " Proc. of ASCE, ST3, (1976-3), 609.
(19) V.B. Venkayya and N.S. Khot, " Design of optimum structures to impulse type loading ", AIAA J., 13-8, (1975-8), 989.
(20) R.M. Brach, " Minimum dynamic response for a class of simply supported beam shapes ", Int. J. Solids & Struct, 10, (1968), 430.

INTERACTIVE OPTIMAL DESIGN OF DYNAMICALLY LOADED STRUCTURES USING THE OPTNSR SOFTWARE SYSTEM

R. Balling, V. Ciampi, and K. S. Pister
University of California, Berkeley
and
M. A. Bhatti
University of Iowa

PUBLISHED IN SESSION 12

AD-P000 033

STRUCTUAL OPTIMIZATION ON GEOMETRICAL CONFIGURATION AND ELEMENT SIZING WITH STATICAL AND DYNAMICAL CONSTRAINTS

J. H. Lin,* W. Y. Che,** and Y. S. Yu**

Abstract

In this paper, a bi-factor α-β algorithm based on Kuhn-Tucker criteria about the minimal weight design of structure under statical and dynamical constraints is presented. Among the constraints, "frequency prohibited band" is a new formulation which demands any characteristic frequency of the structure not to fall into a given frequency region. The design variables may cover sizes of the elements and/or coordinates of the nodes. The upper and lower bounds of each variable are specified. And the stress constraints based on full-stress criteria may also be taken into account. Satisfactory results have been obtained over various examples wherein the stiffness and/or mass matrices of the structure may be highly nonlinear about the design variables.

Introduction

The dynamical optimization of structures as a newly developed field is still in its teens. But it has attracted many scholars' attention because of its remarkable importance to engineering. In 1965, Niordson (5) contributed in this field the first paper. Since then, a lot of contributions were made by, e.g., Turner (6), Zarghamee (7), Rubin (8), McCart (9), Venkayya (10), Khot (11), Pierson (12), Kiusalaas (1), and so on. Due to the highly nonlinear property in the dynamical optimality design of structure, the main efforts have been focused on the optimality criteria algorithm with structure subjected to some kind of natural frequency constraints. So far, however, the speed and stability of convergence are still not quite satisfactory, and the solvable structures and selectable variables are still very limited too. The optimization on geometrical configuration has been quite seldom mentioned although it may be of special importance in practical engineering designs.

In 1978, Kiusalaas and Shaw (1) presented a finite element method for minimum weight design of structures with lower-bound constraints on the natural frequencies, and upper and lower bounds on the design variables. The authors of the paper allowed the stiffness matrix of the structure to be optimized to contain up to cubic items of the variables, while the mass matrix was allowed to contain only linear ones.

In this paper, two "damping factors" α,β with clear mechanical meanings are suggested. With these two factors, Kuhn-Tucker criteria is developed into an effective iteration algorithm such that the speed and stability of convergence are remarkably improved. The above-mentioned nonlinear difficulties are all overcome. Many examples including those with coordinates of nodes as variables manifest that the algorithm suggested by this paper is quite flexible and effective.

The dynamical constraints in this paper are appointed to be a "frequency-prohibited band" because of its obvious engineering significance. However, the algorithm itself can be easily extended to other types of frequency constraints -- either equality constraints or nonequality ones, even those with several frequency prohibited bands.

α-β Algorithm

In this paper, only the topological arrangement of the structure to be optimized has to be specified in advance. Design variables are permitted to be the sizes of elements, the coordinates of nodes, or both. On the one hand, each variable can control the change of a number of sizes or coordinates which is known as linking of the design variables. On the other hand, each element can be controlled by several design variables which is one of the features of this algorithm. If for a structure the number of its elements is M, and that of its design variables is BM, then M may be greater than, less than, or equal to BM. The upper bound $A_n^{(u)}$ and lower bound $A_n^{(\ell)}$ of each variable are specified in advance. The upper and lower bounds of the "frequency prohibited band" are denoted by $\bar{\omega}$ and $\underline{\omega}$. Any variable A_n has to be within the region $(A_n^{(\ell)}, A_n^{(u)})$, while any natural frequency of the structure be outside the region $(\underline{\omega}, \bar{\omega})$. To minimize the weight of the structure under all those constraints refers to a problem of conditional extreme value as follows:

$$\min W(A) \tag{1}$$

subject to

$$\omega_i \leq \underline{\omega} \tag{2}$$

$$\omega_j \geq \bar{\omega} \tag{3}$$

$$A_n \geq A_n^{(\ell)} \tag{4}$$

$$A_n \leq A_n^{(u)} \tag{5}$$

$$\underset{\sim}{K}\,\underset{\sim}{u} = \omega^2\,\underset{\sim}{M}\,\underset{\sim}{u} \tag{6}$$

$$n = 1,2,\ldots,BM$$

$$j = i+1$$

where $\underset{\sim}{A} = \{A_1, A_2, \ldots, A_{BM}\}^T \quad \underset{\sim}{A} \in R^{BM}$

$\underset{\sim}{K}$ structural stiffness matrix

$\underset{\sim}{M}$ structural mass matrix

$\underset{\sim}{u}$ natural mode

ω natural angular frequency

ω_i^2, ω_j^2 the ith and j^{th} eigenvalues of equation (6)

$\underline{\omega}$ $\bar{\omega}$ the lower and upper bounds of the frequency-prohibited band

A_n the nth design variable

$A_n^{(\ell)}, A_n^{(u)}$ the lower and upper bounds of A_n

BM the number of independent design variables.

---

*Lecturer, Engineering Mechanics Institute, Dalian Institute of Technology. Visiting Fellow, Civil Engineering Dept., Princeton Univ.

**Graduate students, Engineering Mechanics Institute, Dalian Institute of Technology.

The specification of the frequency-prohibited band (F.P.B.) is according to the demand of avoiding resonance. Once $\underline{\omega}$ and $\bar{\omega}$ has been determined, an experienced engineer is usually able to judge the orders i and j reasonably. If this is somewhat difficult, a suggestion in Ref. [2] for justifying i and j may be of help.

The Lagrangian of the extreme value problem described as equations (1) - (6), is

$$L(\underset{\sim}{A},\underset{\sim}{\xi},\underset{\sim}{\eta},\mu_1,\mu_2) = W(\underset{\sim}{A}) + \mu_1(\omega_i^2 - \underline{\omega}^2) - \mu_2(\omega_j^2 - \bar{\omega}^2) - \sum_{n=1}^{BM} \xi_n(A_n - A_n^{(\ell)}) + \sum_{n=1}^{BM} \eta_n(A_n - A_n^{(u)}) \quad (7)$$

where

$$\underset{\sim}{\xi} = \{\xi_1, \xi_2, \ldots, \xi_{BM}\}^T$$
$$\underset{\sim}{\eta} = \{\eta_1, \eta_2, \ldots, \eta_{BM}\}^T \quad (8)$$

To apply the Kuhn-Tucker criterion, equation (7) should be differentiated with respect to A_n. This gives

$$\frac{\partial L}{\partial A_n} = \frac{\partial W(\underset{\sim}{A})}{\partial A_n} + \mu_1 \frac{\partial \omega_i^2}{\partial A_n} - \mu_2 \frac{\partial \omega_j^2}{\partial A_n} - \xi_n + \eta_n = 0 \quad (9)$$

and the following constraints should also be satisfied:

$$\mu_1(\omega_i^2 - \underline{\omega}^2) = 0 \quad (10.1)$$

$$\mu_2(\omega_j^2 - \bar{\omega}^2) = 0 \quad (10.2)$$

$$(\omega_i^2 - \underline{\omega}^2) \leq 0 \quad (10.3)$$

$$-(\omega_j^2 - \bar{\omega}^2) \leq 0 \quad (10.4)$$

$$\xi_n(A_n - A_n^{(\ell)}) = 0 \quad (10.5)$$

$$\eta_n(A_n - A_n^{(u)}) = 0 \quad (10.6)$$

$$-(A_n - A_n^{(\ell)}) \leq 0 \quad (10.7)$$

$$(A_n - A_n^{(u)}) \leq 0 \quad (10.8)$$

$$\mu_1 \geq 0 \quad (10.9)$$

$$\mu_2 \geq 0 \quad (10.10)$$

$$\xi_n \geq 0 \quad (10.11)$$

$$\eta_n \geq 0 \quad (10.12)$$

$n=1,2,\ldots,BM$

Equations (9) and (10.1) - (10.12) can be rewritten in more compact form

$$\frac{\partial W(\underset{\sim}{A})}{\partial A_n} + \mu_1 \frac{\partial \omega_i^2}{\partial A_n} - \mu_2 \frac{\partial \omega_j^2}{\partial A_n} \begin{cases} = 0 & A_n^{(\ell)} < A_n < A_n^{(u)} \\ \geq 0 & A_n = A_n^{(\ell)} \\ \leq 0 & A_n = A_n^{(u)} \end{cases} \quad (11)$$

$$\mu_1 \begin{cases} = 0 & \text{when } \omega_i^2 < \underline{\omega}^2 \quad (12.1) \\ > 0 & \text{when } \omega_i^2 = \underline{\omega}^2 \quad (12.2) \end{cases}$$

$$\mu_2 \begin{cases} = 0 & \text{when } \omega_j^2 > \bar{\omega}^2 \quad (12.3) \\ > 0 & \text{when } \omega_j^2 = \bar{\omega}^2 \quad (12.4) \end{cases}$$

After multiplying both sides of equation (11) by $(1-\alpha)A_n$ and simplifying, the following expression is obtained:

$$\begin{cases} A_n = f_n A_n & \text{when } A_n^{(\ell)} < A_n < A_n^{(u)} \\ A_n \geq f_n A_n & \text{when } A_n = A_n^{(\ell)} \\ A_n \leq f_n A_n & \text{when } A_n = A_n^{(u)} \end{cases} \quad (13)$$

in which

$$f_n = \alpha + \frac{1-\alpha}{\dfrac{\partial W(\underset{\sim}{A})}{\partial A_n}} \left\{ -\mu_1 \frac{\partial \omega_i^2}{\partial A_n} + \mu_2 \frac{\partial \omega_j^2}{\partial A_n} \right\} \quad (14)$$

The recursive design formulas can be derived from equations (13), as follows:

$$\begin{cases} A_n' = f_n A_n & \text{when } A_n^{(\ell)} < f_n A_n < A_n^{(u)} \\ A_n' = A_n^{(\ell)} & \text{when } f_n A_n \leq A_n^{(\ell)} \\ A_n' = A_n^{(u)} & \text{when } f_n A_n \geq A_n^{(u)} \end{cases} \quad (15)$$

$n=1,2,\ldots,BM$

A_n and A_n' are the design variables before and after the recurrence; f_n is a modification factor which depends not only upon the Lagrangian multipliers μ_1 and μ_2, but also upon α; α is a user-specified parameter ($0<\alpha<1$). The revised extend of A_n depends greatly on α. When α increases up to 1, the revision is completely "damped out", i.e., A_n' exactly equals to A_n. Therefore, α can be regarded as a "geometrical damping factor". Sizing constraints will never be violated because of the enforcement of equation (15). Hence, any intermediate design will be a feasible one if the frequency constraints (2) and (3) are also not violated. Design variables revised according to the first expression of (15) are referred to as active design variables, and those to the other two expressions of (15) referred to as passive ones.

In the equation (14), μ_1 and μ_2 are determined according to the frequency constraints. Let us first assume that ω_i and ω_j are all within the F.P.B. In order to "draw" them to the bounds of the band, the revised frequencies increments are respectively:

$$\Delta\omega_i^2 = (\underline{\omega}^2 - \omega_i^2) \quad (16)$$

$$\Delta\omega_j^2 = (\bar{\omega}^2 - \omega_j^2) \quad (17)$$

These amounts are contributed by the changes of all variables. If the first approximation of a Taylor expansion is taken, the following expressions result:

$$\Delta\omega_i^2 = \sum_{n=1}^{BM} \frac{\partial \omega_i^2}{\partial A_n}(A_n' - A_n) \quad (18)$$

$$\Delta\omega_j^2 = \sum_{n=1}^{BM} \frac{\partial \omega_j^2}{\partial A_n} (A_n' - A_n) \tag{19}$$

For most practical problems, the first approximation is not accurate enough. Over-revision of the concerned frequencies will often occur, which leads to an unstable oscillation of the concerned frequencies about the frequency-constraint surfaces, especially for highly nonlinear problems such as the examples given in this paper.

In order to overcome the above difficulty, a reduction on the revised amounts of concerned frequencies by a factor β is suggested; i.e., the revised amounts are taken as

$$\Delta\omega_i^2 = \beta(\underline{\omega}^2 - \omega_i^2) \tag{16'}$$

$$\Delta\omega_j^2 = \beta(\bar{\omega}^2 - \omega_j^2) \tag{17'}$$

instead of equations (16) and (17), where $0.4 \leq \beta \leq 0.6$ may be a good choice for most structures with highly nonlinear properties. After this reduction, the concerned frequencies will approach the constraint surfaces steadily and almost monotonically with reduced paces. Therefore, β may be termed a "frequency damping factor".

From equations (16'), (17'), (18) and (19), one obtains

$$\sum_{n=1}^{BM} \frac{\partial \omega_i^2}{\partial A_n} (A_n' - A_n) = \beta(\underline{\omega}^2 - \omega_i^2) \tag{20}$$

$$\sum_{n=1}^{BM} \frac{\partial \omega_j^2}{\partial A_n} (A_n' - A_n) = \beta(\bar{\omega}^2 - \omega_j^2) \tag{21}$$

where the A_n' (n=1,2,...,BM) may be active design variables if they obey the first expression of equation (15), or passive ones if they obey one of the other two expressions of equation (15). Thus, equations (20) and (21) can be expressed as

$$\sum_{n_{act.}} \frac{\partial \omega_i^2}{\partial A_n} (f_n - 1)A_n + (\Delta\omega_i^2)_{pass.} = \beta(\underline{\omega}^2 - \omega_i^2) \tag{22}$$

$$\sum_{n_{act.}} \frac{\partial \omega_i^2}{\partial A_n} (f_n - 1)A_n + (\Delta\omega_j^2)_{pass.} = \beta(\bar{\omega}^2 - \omega_j^2) \tag{23}$$

where the incremental frequency shifts due to passive variables are

$$(\Delta\omega_p^2)_{pass.} = \sum_{n_{pass.}} \frac{\partial \omega_p^2}{\partial A_n} (A_n' - A_n) \qquad (p=i,j) \tag{24}$$

Substituting (14), (24) into (22), (23), yields the following equations for μ_1 and μ_2:

$$\begin{aligned} a_{11}\mu_1 + a_{12}\mu_2 &= b_1 \\ a_{21}\mu_1 + a_{22}\mu_2 &= b_2 \end{aligned} \tag{25}$$

$$a_{11} = \sum_{n_{act.}} \frac{A_n}{\frac{W(A)}{\sim}} \left(\frac{\partial \omega_i^2}{\partial A_n}\right)^2 \tag{26}$$

$$a_{22} = \sum_{n_{act.}} \frac{A_n}{\frac{W(A)}{\sim}} \left(\frac{\partial \omega_j^2}{\partial A_n}\right)^2$$

$$a_{12} = a_{21} = -\sum_{n_{act.}} \frac{A_n}{\frac{W(A)}{\sim}} \left(\frac{\partial \omega_i^2}{\partial A_n}\right)\left(\frac{\partial \omega_j^2}{\partial A_n}\right)$$

$$b_1 = -\sum_{n_{act.}} \frac{\partial \omega_i^2}{\partial A_n} A_n - \frac{\beta(\underline{\omega}^2 - \omega_i^2) - (\Delta\omega_i^2)_{pass.}}{1-\alpha}$$

$$b_2 = \sum_{n_{act.}} \frac{\partial \omega_j^2}{\partial A_n} A_n - \frac{\beta(\bar{\omega}^2 - \omega_j^2) - (\Delta\omega_j^2)_{pass.}}{1-\alpha}$$

The partial derivatives $\frac{\partial \omega_p^2}{\partial A_n}$ can be calculated by virtue of the well-known formula

$$\frac{\partial \omega_p^2}{\partial A_n} = \underset{\sim}{u}^T \frac{\partial \underset{\sim}{K}}{\partial A_n} \underset{\sim}{u} - \omega_p^2 \underset{\sim}{u}^T \frac{\partial \underset{\sim}{M}}{\partial A_n} \underset{\sim}{u} \tag{27}$$

in which ω_p^2 and $\underset{\sim}{u}$ are the pth order of eigenvalue and corresponding normalized eigenvector.

The expressions $\frac{\partial \underset{\sim}{W(A)}}{\partial A_n}$, $\frac{\partial \underset{\sim}{K}}{\partial A_n}$, $\frac{\partial \underset{\sim}{M}}{\partial A_n}$ should be specially derived according to the types of structures and variables.

μ_1 or μ_2 in (25) will vanish if ω_i or ω_j is outside F.P.B. In this case, only a part of expressions in (25), (26) are used.

Frequency Modification Operation (F.M.O.)

Repeated applications of the α-β algorithm will usually result in an optimal design. When frequency constraints are severely violated, however, the adoption of the "frequency modification operation" (F.M.O.) may be advantageous wherein the design point is first "drawn" near the bound of the feasible band before the α-β algorithm is applied. By doing so, more intermediate designs will be within or near the feasible band, and in addition, there may be an acceleration in convergence. To illustrate this, let us consider in n-dimensional vector space two supersurfaces defined by expressions (2) and (3) which are assumed to intersect. In the vicinity of the intersection A', the space is divided into four parts, as shown in Fig. 1. They are:

(1) Feasible band, where $\omega_i^2 \leq \underline{\omega}^2$, $\omega_j^2 \geq \bar{\omega}^2$

(2) Unfeasible band (FPB), where $\omega_i^2 > \underline{\omega}^2$, $\omega_j^2 < \bar{\omega}^2$

(3) Unfeasible band, where $\omega_i^2 \leq \underline{\omega}^2$, $\omega_j^2 < \bar{\omega}^2$

(4) Unfeasible band, where $\omega_i^2 > \underline{\omega}^2$, $\omega_j^2 \geq \bar{\omega}^2$

Now, assume current design point A to lie outside the feasible band as shown in Figure 2. The gradient vectors of ω_i^2 and ω_j^2 at point A are, respectively,

$$\vec{N}_i = \left\{\frac{\partial \omega_i^2}{\partial A_n}\right\} \qquad \vec{N}_j = \left\{\frac{\partial \omega_j^2}{\partial A_n}\right\} \tag{28}$$

Generally speaking, if neither constraints (2) or (3) are currently satisfied, it is naturally hoped that both of them will be satisfied after F.M.O. This can be attained by moving point A to A'. Let us further denote the modification vector by $\Delta\vec{A}$, which can be expressed as a linear combination of $\vec{N}_i$ and $\vec{N}_j$ as follows:

$$\Delta = \lambda_1 \vec{N}_i + \lambda_2 \vec{N}_j \tag{29}$$

of which the component form is

$$\Delta A_n = \lambda_1 \frac{\partial \omega_i^2}{\partial A_n} + \lambda_2 \frac{\partial \omega_j^2}{\partial A_n} \tag{30}$$

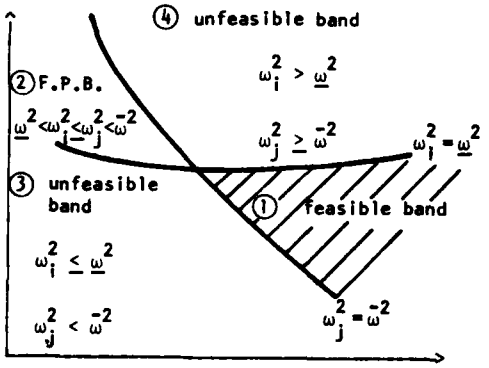


Figure 1

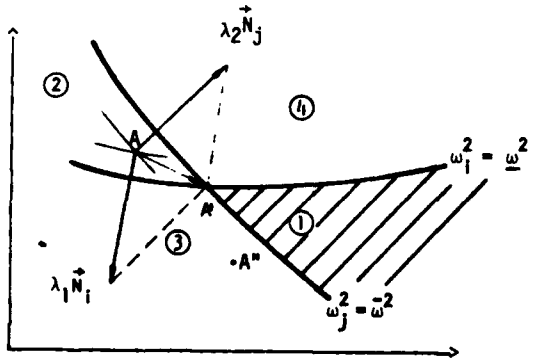


Figure 2

It applies only when A_n is an active design variable. If A_n is a passive one, the modification increment would be

$$\Delta A_n = A_n^{(\ell)} - A_n \tag{31}$$

or

$$\Delta A_n = A_n^{(u)} - A_n \tag{32}$$

Analogous to the derivation of equation (15), the general formulas for modifications of design variables will be

$$A_n' = \begin{cases} A_n + \Delta A_n & \text{when } A_n^{(\ell)} < A_n + \Delta A_n < A_n^{(u)} \\ A_n^{(\ell)} & \text{when } A_n + \Delta A_n \leq A_n^{(\ell)} \\ A_n^{(u)} & \text{when } A_n + \Delta A_n \geq A_n^{(u)} \end{cases} \tag{33}$$

Factors λ_1 and λ_2 in equation (30) are determined by the following equations:

$$\begin{aligned} g_{11}\lambda_1 + g_{12}\lambda_2 &= h_1 \\ g_{21}\lambda_1 + g_{22}\lambda_2 &= h_2 \end{aligned} \tag{34}$$

in which

$$\begin{aligned} g_{11} &= \sum_{n_{act.}} \left(\frac{\partial \omega_i^2}{\partial A_n}\right)^2 \\ g_{22} &= \sum_{n_{act.}} \left(\frac{\partial \omega_j^2}{\partial A_n}\right)^2 \\ g_{12} &= g_{21} = \sum_{n_{act.}} \left(\frac{\partial \omega_i^2}{\partial A_n}\right)\left(\frac{\partial \omega_j^2}{\partial A_n}\right) \end{aligned} \tag{35}$$

$$\begin{aligned} h_1 &= \gamma(\underline{\omega}^2 - \omega_i^2) - \sum_{n_{pass.}} \frac{\partial \omega_i^2}{\partial A_n}(A_n^{(\ell)} - A_n) \\ &\quad - \sum_{n_{pass.}} \frac{\partial \omega_i^2}{\partial A_n}(A_n^{(u)} - A_n) \\ h_2 &= \gamma(\bar{\omega}^2 - \omega_j^2) - \sum_{n_{pass.}} \frac{\partial \omega_j^2}{\partial A_n}(A_n^{(\ell)} - A_n) \\ &\quad - \sum_{n_{pass.}} \frac{\partial \omega}{\partial A_n}(A_n^{(u)} - A_n) \end{aligned}$$

where γ is another frequency damping factor ($0 < \gamma \leq 1$). Its function is quite similar to that of β.

If only one of constraints (2) and (3) is violated severely, such as at design point A" in Figure 2, it may be better to modify only the corresponding unsatisfied frequency by F.M.O. In that case, λ_1 and λ_2 in equation (29) should accordingly be determined in a different manner. A more detailed discussion on F.M.O. is presented in Ref. [5].

Stress Constraints

Stress constraints can be taken into account according to the full-stress criterion. Here, take a truss as example. First, the structure with current design variables is analyzed statically to work out the maximum internal forces of its elements under various loading cases. If the maximum internal force of the nth type of bar is N_n, then the minimal acceptable sectional area for that type will be

$$A_n^* = \left| \frac{N_n}{[\sigma_n]} \right| \tag{36}$$

where $[\sigma_n]$ is the allowable stress of the nth-type of bar. Then, compare A_n^* with $A_n^{(\ell)}$; the larger will be taken as the lower bound of the next iteration.

Example Problems

The algorithm presented in this paper is indeed applicable to all types of structures and design variables. A number of examples have been successfully calculated. Because of length limitations to the paper, only four of them are given here.

Example 1

A stepped steel arbor has a length of 10^m which is divided into 10 segments with equal lengths. The diameter of each segment is taken as an independent design variable of which the original value is 1^m, the lower and upper bounds are respectively 0.5^m and 2^m. A non-structural mass with 10% the magnitude of the original structural mass is attached at the midpoint of the arbor. A consistent mass matrix is adopted, and it contains items with the second power of the variables. The stiffness matrix, however, contains items with the fourth power of these variables. The first angular frequency of the structure must not be greater than $\underline{\omega} = 200$ sec $^{-1}$, while the second one must not be less than $\bar{\omega} = 600$ sec^{-1}. The Young's Modulus is $E = 2 \cdot 10^7$ t/m^2. The specific gravity is $\rho = 7.84$ t/m^3. The process and and result are shown in Figure 3 and Table 1.

TABLE 1

OPTIMIZATION PROCESS OF A STEPPED STEEL ARBOR

Iters. No.	Weight*	ω_1	ω_2	α	β	Remarks
Initial	6.28	250	771	--	--	No F.M.T. is used
1	3.94	209	659	0.75	0.40	
2	2.72	178	596	0.75	0.40	
3	2.42	153	581	0.80	0.40	
4	2.50	160	595	0.80	0.40	
5	2.52	161	598	0.85	0.40	
6	2.52	162	600	0.85	0.40	
7	2.52	162	600	0.90	0.40	

*Multiplying the above-listed weights by g = 9.8 (m/sec^2) yields actual weights.

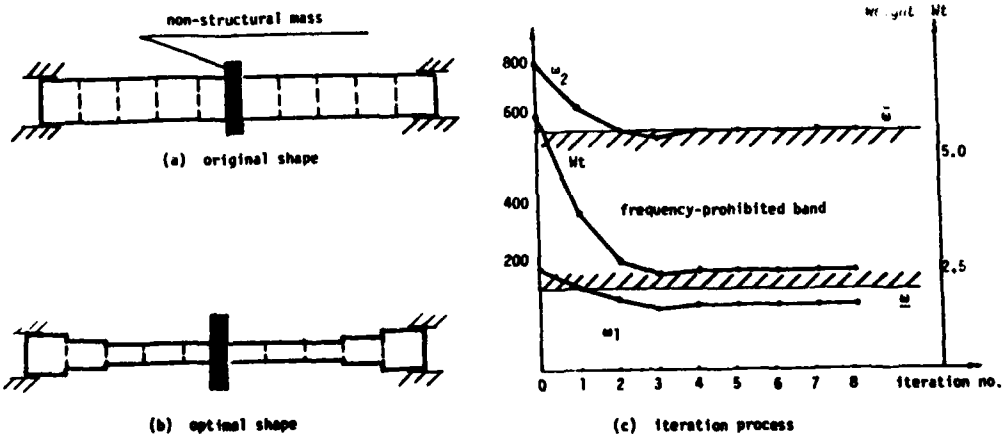


FIGURE 3

Stepped Steel Arbor

Example 2

A plane frame has 5 elements as shown in Figure 4(a). The 12 coordinates of all 6 nodes are linked into 7 types of variables: (X_1, X_3), (X_2, X_4), X_5, X_6, (Y_1, Y_2), (Y_3, Y_4), (Y_5, Y_6). The section areas of the elements are linked into 3 types of variables: (A_1, A_5), (A_2, A_4), A_3. There are 10 independent design variables in all. The original values of the coordinates are shown in Figure 4(a), and the range of variability of each coordinate is $\pm$ 1 m. The original values of all section areas are $S_o = 0.5\ m^2$, the upper and lower bounds are $\bar{S} = 1\ m^2$, $\underline{S} = 0.25\ m^2$. A consistent mass matrix is adopted. The first angular frequency must not be greater than $\underline{\omega} = 50\ sec^{-1}$, the second one not less than $\bar{\omega} = 200\ sec^{-1}$. The aspect ratio of each section remains $\frac{h}{b} = 2.5$. $E = 2.4 \cdot 10^6\ t/m^2$, $\rho = 2.45\ t/m^3$. A nonstructural mass $M_p = 2.7$ t is added to node 6. The process and result are shown in Figure 4(b) and Table 2.

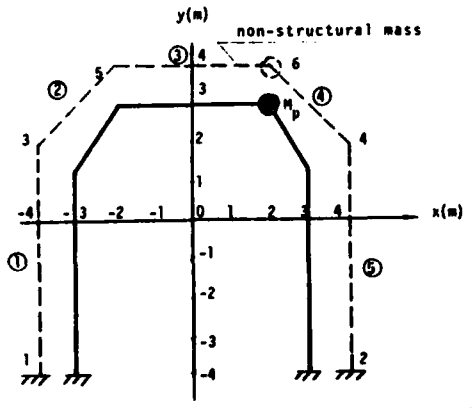
Example 3

A plane truss (bridge panel) has 40 bars as shown in Figure 5(a). The vertical coordinates of all 8 upside nodes are taken as independent design variables. Their upper and lower bounds are all 5 m and 1 m. The section areas of the 40 bars are linked into 19 types of variables, so that there are 27 independent design variables in all. The original values of the section areas are all $0.005\ m^2$, and they can vary only between $0.0025\ m^2$ and $0.05\ m^2$. The four support bars have fixed section areas $0.05\ m^2$ and fixed lengths 0.5 m. At each node on the lower side is exerted a downward force of 10 t as shown in Figure 5(a). A lumped mass matrix is adopted. The first angular frequency must not be greater than $\underline{\omega} = 100\ sec^{-1}$, and the second one not less than $\bar{\omega} = 200\ sec^{-1}$. $E = 2 \cdot 10^7\ t/m^2$, $\rho = 7.8\ t/m^3$. Of the bars, working stress is limited to $[\sigma] = 16000\ t/m^2$.

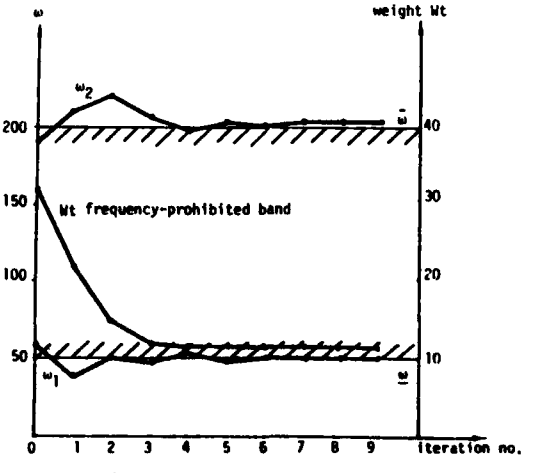
TABLE 2

OPTIMIZATION PROCESS OF 5-ELEMENT FRAME

Itera. No.	Weight	ω_1	ω_2	α	β	Remarks
Initial	27.1	60	189	--	--	F.M.O. with
1	22.2	43	211	0.80	0.40	$\gamma = 0.40$
2	14.5	50	220	0.85	0.40	is used when
3	12.0	48	208	0.85	0.40	the upper bound
4	11.4	52	194	0.90	0.40	frequency
5	11.6	49	202	0.90	0.40	constraint is
6	11.5	50	200	0.90	0.40	violated.
7	11.6	50	201	0.90	0.40	
8	11.6	50	201	0.90	0.40	
9	11.6	50	201	0.90	0.40	



(a) Original shape (broken line) and optimal shape (solid line)



(b) Iteration process

FIGURE 4

5-Element Plane Frame

TABLE 3

OPTIMIZATION PROCESS OF BRIDGE PANEL

Itera. No.	Weight	ω_1	ω_2	α	β	Remarks
Initial	5.62	129.2	255.5	--	--	
1	7.09	88.4	225.1	--	--	F.M.O. with = 1
2	5.58	67.9	201.0	0.85	1.0	
3	4.65	55.3	196.0	0.85	1.0	
4	3.98	49.2	196.7	0.85	1.0	
5	3.49	48.9	199.2	0.85	1.0	
6	3.12	51.2	199.5	0.85	1.0	
7	2.88	54.0	199.5	0.85	1.0	
8	2.70	57.2	199.4	0.85	1.0	
9	2.70	60.8	199.6	0.85	1.0	
10	2.57	63.8	199.7	0.85	1.0	
11	2.56	65.7	199.9	0.85	1.0	
12	2.55	65.6	200.0	0.90	1.0	
13	2.55	65.5	200.0	0.90	1.0	

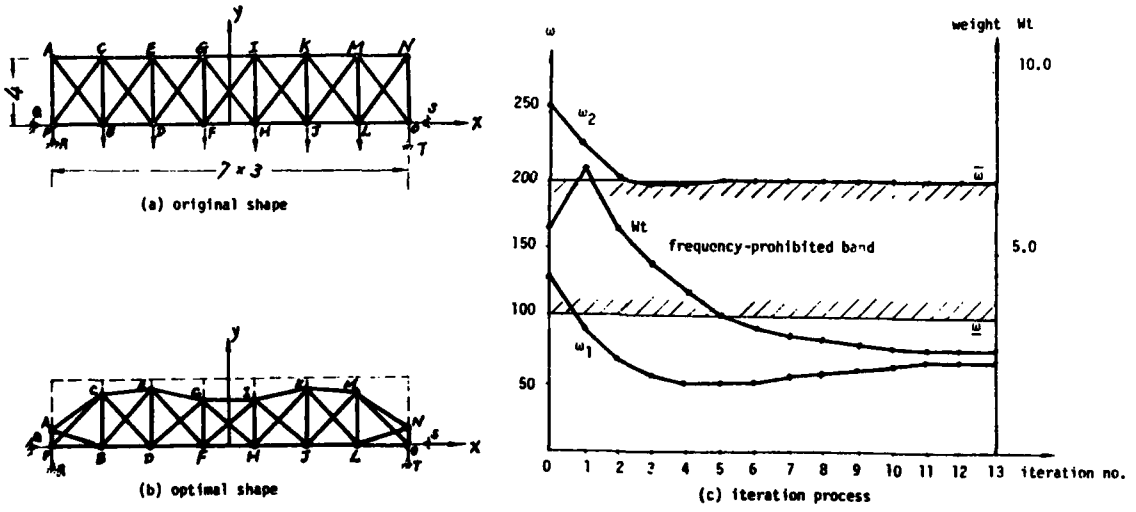


FIGURE 5

Plane Truss (Bridge Panel)

For the final design, the first and seventh types of bars have reached the fully-stressed state. The process and result are shown in Figure 5 and Table 3, above.

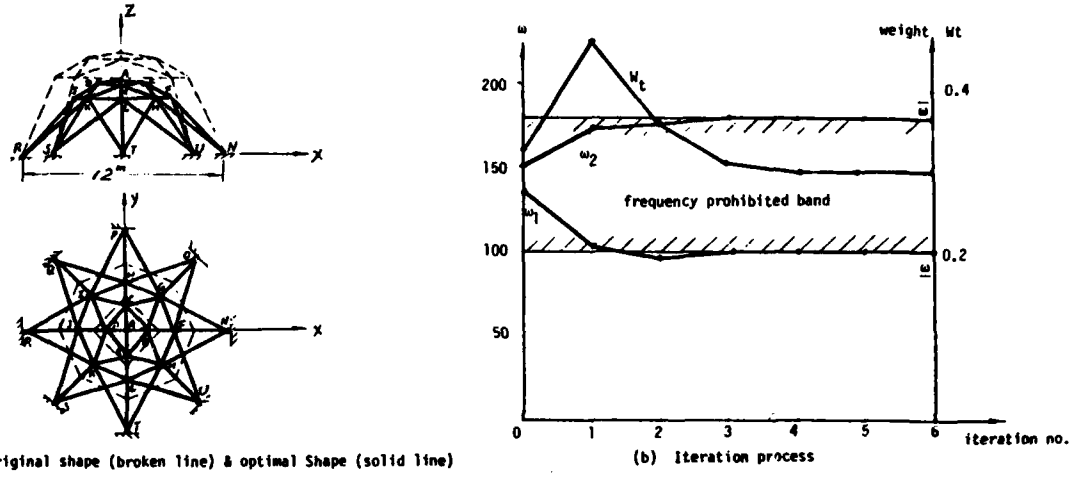
Example 4

A hemispherical space truss (roof) has 52 bars as shown in Figure 6(a). A non-structural mass of 0.05 t is attached to each moveable node. The section area of each bar is originally 0.0002 m^2, and is permitted to vary between 0.0001 m^2 and 0.001 m^2. The 52 bars are linked into 8 types. In addition, the three coordinates of each moveable node are all taken as independent variables. The moveable range of each coordinate is $\pm$ 6 m. Therefore, there are 47 independent design variables in all. The first angular frequency must not be greater than $\underline{\omega} = 100$ sec^{-1}, and the second one must not be less than $\bar{\omega} = 180$ sec^{-1}. A lumped mass matrix is adopted. $E = 2 \cdot 10^7$ t/m^2, $\rho = 7.8$ t/m^3. Working stress of the bars is $[\sigma] = 16000$ t/m^3. Only about 4 passes are needed in this example to obtain the optimum design. The process and result are shown in Figure 6(b) and Table 4.

TABLE 4

OPTIMIZATION PROCESS OF HEMISPHERICAL SPACE TRUSS

Itera. No.	Weight	ω_1	ω_2	α	β	Remarks
Initial	0.339	135.9	150.6	--	--	
1	0.477	104.2	174.6	--	--	F.M.O. with = 1
2	0.371	96.6	176.1	0.90	1.0	
3	0.320	100.2	179.1	0.95	1.0	
4	0.298	99.9	178.9	0.95	1.0	
5	0.298	100.0	179.4	0.95	1.0	
6	0.298	100.0	179.7	0.95	1.0	



(a) Original shape (broken line) & optimal Shape (solid line)

(b) Iteration process

FIGURE 6

Space Truss (roof)

Summary

The α-β algorithm given by this paper is an effective method for highly nonlinear optimization problems with certain frequency constraints which not only can be a frequency-prohibited band, as in this paper, but also can be a set of arbitrary frequency constraints with forms of equality and/or inequality. The rate of convergence depends greatly on the values of α and β. For general problems, α = 0.8∿0.95, β = 0.4∿0.6 may probably lead to a fairly stable convergence. If the extent of nonlinearity is low, then small values of α and (1-β) sometimes lead to a faster convergence.

If one or more frequency constraints are severely violated, the F.M.O. can first be applied before the α-β algorithm is executed. That may hopefully result in a reduction of effort.

Five or ten reanalyses are needed for general problems to reach the optimal solutions. The effort of each reanalysis is mainly for solving a partial generalized eigenproblem, and that is quite acceptable in engineering.

Acknowledgements

The authors are all grateful to their advisor, Professor Qian Lingxi, who has provided constant encouragement and guidance throughout this work. Our thanks and appreciation are extended to Professor F.Y. Cheng and R.H. Scanlan, for their detailed examination of this paper. Special thanks to Mrs. Susan Alston for her help, and Betty Kaminski, for the skillful typing of this paper. We would also like to thank the Department of Civil Engineering of Princeton University, the Engineering Mechanics Institute of D.I.T., and the computer centers of D.I.T. and Princeton University, for their support.

References

1. Kiusalaas, J., Shaw, R.C.J., An Algorithm for Optimal Strucutral Design with Frequency Constraints, Int. J. for Numer. Meth. in Engng., 13, 283-295, 1978.
2. Lin, J.H., Optimum Design of Structure with Specified Frequency-Prohibited Band, J. of Dalian Institute of Technology (in Chinese), 1981.
3. Che, W.Y., "α-β-γ Algorithm and Optimum Design of Plane Frame with Specified Frequency-Prohibited Band," postgraduate dissertation of D.I.T. (in Chinese), 1981.
4. Yu, Y.S.,"Optimal Design of Space Truss on Geometrical Configuration and Element Sizing with Specified Frequency-Prohibited Band," postgraduate dissertation of D.I.T. (in Chinese), 1981.
5. Niordson, F.I., On the Optimal Design of a Vibrating Beam, Quart. Appli. Math., 23, 47-53, 1965.
6. Turner, M.J., Design of Minimum Mass Structures with Specified Natural Frequencies, AIAA J.5, 406-412, 1967.

7. Zarghamee, M.S., Optimum Frequency of Structures, AIAA J.6, 749-750, 1968.

8. Rubin, C.P., Minimum Weight Design of Complex Structures Subject to a Frequency Constraint, AIAA J.8, 923-927, 1970.

9. McCart, B.R., Huag, E.J., and Streeter, T.O., Optimal Design of Structures with Constraints on Natural Frequency, AIAA J.8, 1012-1019, 1970.

10. Venkayya, V.B., Khot, N.S., Tischler, V.A., and Taylor, R.F., Design of Optimum Structures for Dynamic Loads, Third Conf. Matrix Math. Struct. Mech., Wright-Patterson A.F.B., Ohio 619-658, 1971.

11. Khot, N.S., Berke, L., and Venkayya, V.B., Comparison of Optimality Criteria Algorithms for Minimum Weight Design of Structures, AIAA J. 17, 78-469, 1978.

12. Pierson, B.L., Survey of Optimal Structural Design under Dynamic Constraints, Int. J. for Num. Math. Engng., 4, 491-499, 1972.

13. Qian Lingxi, Zhong Wanxie, Sui Yun Kang and Zhang Jindong, Optimum Design of Structures with Mulitiple Types of Element Under Multiple Loading Cases and Multiple Constraints: Program System DDDU, J. of D.I.T., 19, 1-17 (in Chinese), 1980.

14. Wang, S.H., Minimal Weight Design of Structure with Frequency Constraints, Proc. of Chinese National Symposium on Computational Mechanics (in Chinese), 1980.

15. Washizu, K. and Hanaoka, M., Application of the Finite Element Method to Minimum Mass Design of a Bar with Two Specified Natural Frequencies, Computers & Structures, 10, 539-545, 1979.

16. Levy, R. and Chai, K., Implementation of Natural Frequency Analysis and Optimality Criterion Design, Computers & Structures, 10, 277-282, 1979.

17. Yamakawa Hiroshi and Atsubumi Okumura, Optimum Design of Structures with Regard to Their Vibrational Characteristic, Bulletin of the JSME, 20, 300-306, 1977.

18. Cheng, F.Y., and Botkin, Mark E., Nonlinear Optimum Design of Dynamic Damped Frames, ASCE 102, ST3, 609-627, 1976.

AD-P000 034

OPTIMUM DISTRIBUTION OF ADDITIVE DAMPING FOR VIBRATING BEAM STRUCTURES

Roger Lundén and Bengt Åkesson
Division of Solid Mechanics and Strength of Materials
Chalmers University of Technology
S-412 96 Gothenburg, Sweden

Summary

Cost and weight effectiveness of concentrated and distributed additive damping has been studied for linear systems (discrete and continuous) under prescribed harmonic loads and/or displacements. Increases in stiffness and mass due to the additive damping are included. Redistribution of an initially uniformly applied additive damping (viscoelastic layer) has been numerically and experimentally investigated for beam structures. An optimal redistribution has typically been found to reduce amplitudes of resonant responses by about 50 percent (level reduction by 6 dB) with the cost or weight of the damping treatment kept constant. One application has been to vibration isolation of a damped skeletal light-weight machine foundation.

Introduction

Resonant vibrations in a structure can be suppressed by applying additive damping to its members. For ship structures different damping measures were discussed in Reference (1). Additive damping being distributed over the structure is often preferable to concentrated such damping. A required damping treatment can be realized using layers of viscoelastic materials in different physical arrangements, see Reference (2).

In many cases it may be practical to apply a distributed additive damping uniformly over the structure. In other cases it may be profitable to optimize the spatial distribution of an additive damping in order to reduce its cost or weight, see Reference (3).

A numerical method for automatic optimization of damping distributions has been developed by Lundén (4). The method will briefly be presented in this paper. In Reference (4) the method was applied to a beam on spring supports (results summarized here), and in Reference (5) to a plane frame for which also confirming experiments were performed. In Reference (6) the general results of these two studies were used in an optimization by trial and error of the damping distribution over a light-weight skeletal machine foundation (results summarized here).

Theory of Vibration

A damped uniform beam member for computerized FEM (Finite Element Method) calculations of harmonically vibrating general space frame structures has been developed by Lundén and Åkesson (7). This beam member vibrates in simultaneous tension, torsion, bending and shear. Among several other options (ambient medium, second-order theory, external damping etc), the member includes uniformly distributed viscous and hysteretic dampings along its length dissipating energy in bending of the beam in its two principal planes. A frame composed of several such beam elements can be analyzed by the displacement method being implemented in a computer program. The results obtained will then be exact (except for round-off errors) within the differential equation theory applied.

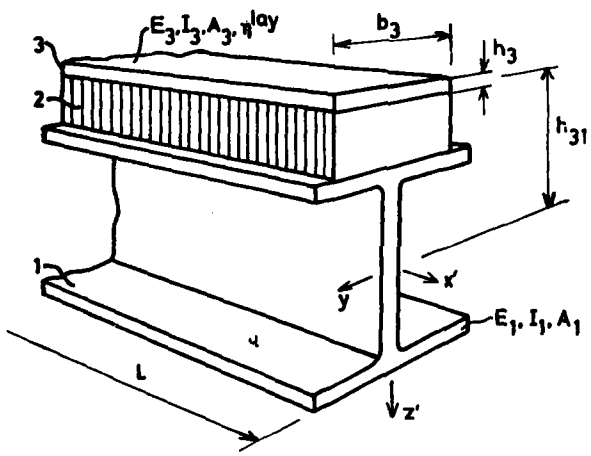


Figure 1. Uniform beam member with spaced free damping layer working in bending vibration about y-axis. Base structure 1. Spacer 2 is rigid in shear and has negligible bending stiffness. Damping layer 3 dissipates energy in tension and compression. Elastic moduli E_1 and E_3, area moments of inertia I_1 and I_3, cross-sectional areas A_1 and A_3, and loss factor $\eta_3=\eta^{lay}$.

For a harmonically vibrating damped space frame a general single-figure response quantity $f(\underset{\sim}{\eta}^b, \omega)$ (the amplitude of a local displacement, velocity, acceleration, stress, support reaction etc, or a weighted sum of such amplitudes) can be calculated. The matrix column vector $\underset{\sim}{\eta}^b$ contains the hysteretic damping loss factors η_i^b, $i=1,2,\ldots,n$, in bending of the n beam elements of the frame. The angular frequency of the exciting prescribed forces and/or displacements is ω. It is noted that the frame vibration will usually be nonsynchronous.

Keeping the amplitudes of the exciting harmonic forces and/or displacements constant, the maximum response F in a given frequency interval $[\omega_\ell, \omega_u]$ can, for a given damping distribution $\underset{\sim}{\eta}^b$, be written as

$$F(\underset{\sim}{\eta}^b) = \max_{\omega \in [\omega_\ell, \omega_u]} f(\underset{\sim}{\eta}^b, \omega) \qquad (1)$$

The response F will here be called a resonant response if the corresponding value of the angular frequency ω is such that $\partial f/\partial\omega=0$ (this definition thus excludes end point maxima). The function F in Equation (1) will serve as objective function in the optimization to follow. Note that the components of the exciting harmonic load on the structures discussed may very well be out of phase with each other.

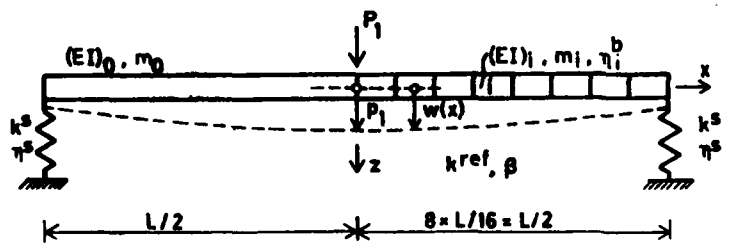


Figure 2. Beam on spring supports subject to a stationary harmonic central load $P_1 \exp i\omega t$. Beam displacement $w(x)\exp i\omega t$. Central displacement amplitud $w(0)$ is denoted by p_1. Spring supports have stiffness k^s and loss factor η^s. Undamped beam (base structure) has uniform bending stiffness (EI_0) and uniform mass per unit length m_0. For analysis, half beam is divided into 8 uniform members (symmetry is used) of equal length as shown on right half of beam. This implies piecewise constant properties of structure. Composite beam member i has bending stiffness $(EI)_i$, mass per unit length m_i, and loss factor η_i^b. Reference elastic stiffness is $k^{ref}=\pi^4(EI)_0/2L^3$. Frequency parameter referring to base structure is $\beta=\omega/\pi^2[(EI)_0/m_0L^4]^{\frac{1}{4}}$.

Objective Function with Constraints

The objective is to choose the set of beam loss factors η_i^b contained in the vector $\underline{\eta}^b$ so as to minimize resonant vibration levels in the loaded frame structure while keeping the amount (cost or weight) of additive damping constant. Mathematically, this can be formulated as

$$\text{Minimize } F(\underline{\eta}^b) \tag{2a}$$

subject to the constraints

$$\eta_i^b \geq 0, \quad i = 1,2,\ldots,n \tag{2b}$$

$$\sum_{i=1}^{n} G_i(\eta_i^b) = C_{damp} \tag{2c}$$

Here C_{damp} denotes the prescribed total cost or weight to be used for additive damping treatment. The function G_i relates the local loss factor η_i^b to the local cost or weight.

Two types of functions G_i have been used to model the cost or weight penalty for a free damping layer as shown in Figure 1. The linear type is

$$G_i(\eta_i^b) = c_i L_i \eta_i^b/\eta^{lay} \tag{3a}$$

The nonlinear type is

$$G_i(\eta_i^b) = c_i L_i \eta_i^b/(\eta^{lay} - \eta_i^b) \tag{3b}$$

Here L_i is the length and c_i a constant (depending on material and geometry parameters) of the beam member i. The loss factor of the damping material itself is denoted by η^{lay}.

It has been found practical to express the total cost of weight C_{damp} of additive damping in terms of a fictitious uniform damping $\eta_i^b=\eta^{bu}$, i=1,2...,n, over the structure, as defined by

$$\sum_{i=1}^{n} G_i(\eta^{bu}) = C_{damp} \tag{4}$$

Additive damping will be accompanied by stiffness and mass increases in the structures. These effects have been included in the vibration analysis and they will affect the objective function F in Equation (2a), see Reference (4) for further information.

Optimization Method

The constrained optimization problem as defined in Equations (2a,b,c) can be turned into a sequence of unconstrained ones by application of a Sequential Unconstrained Minimization Technique, SUMT, see Reference (8). In Reference (4) a sequence of unconstrained objective functions F_u with so called exterior penalty terms was defined as

$$F_u(\underline{\eta}^b,r_k) = F(\underline{\eta}^b) + \frac{1}{r_k}\{\sum_{i=1}^{n}[\min(0, \eta_i^b)]^2 + [\sum_{i=1}^{n} G_i(\eta_i^b) - C_{damp}]^2\}, \quad k=1,2,\ldots,k_{max} \tag{5}$$

The auxiliary parameter r_k was chosen as

$$r_k = r_{k-1}/d, \quad d > 1 \tag{6}$$

Suitable values of r_1 and d were selected by numerical experiments. A typical result was r_1=0.20 and d=10.0. For each value of k, the vector $\underline{\eta}^b$ minimizing F_u was calculated with a standard optimization computer algorithm, see Reference (9). The result found in Step k of the sequence is used as the starting point in Step k+1, and a new optimum is found.

When the change of F_u and of the elements η_i^b in $\underline{\eta}^b$ between two consecutive steps k and k+1 was within preset limits, the optimization procedure was terminated (typically, k_{max}=4). Different starting approximations of $\underline{\eta}^b$ should be tried to avoid results representing only local minima of the objective function $F(\underline{\eta}^b)$ in Equation (1) under the constraints in Equations (2b) and (2c).

Example A: Beam on Spring Supports

The centrally loaded beam in Figure 2 will be studied. The damping distribution along the beam shall be optimized in order to reduce the response amplitude $|p_1|$ maximally while keeping the cost or weight of the damping treatment constant. A parametric study will be performed considering different values of the spring stiffness k^s and loss factor η^s. In Case 1 the cost model in Equation (3a) is applied, and changes in stiffness and mass are neglected. In Case 2 the

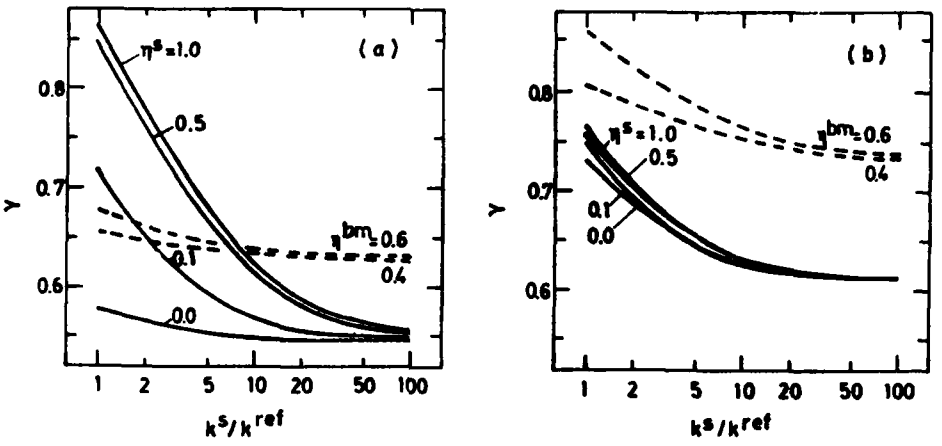


Figure 3. Reduction factor γ for response $|p_1|$ in Figure 2. ———, Case 1; -----, Case 2. (a) η^{bu}=0.1; (b) η^{bu}=0.5.

cost model in Equation (3b) is applied, and the increase of bending stiffness and mass per unit length of the 16 beam elements is observed in the vibration analysis.

Figures 3 and 4 account for results of the optimization considering a frequency interval $[\omega_\ell, \omega_u]$ enclosing only the first symmetric resonant mode of vibration. Different values of the stiffness ratio k^s/k^{ref} and of the loss factor η^{bu} of an initially uniformly distributed damping are investigated, see Equation (4). The optimization leads to a reduction of the central deflection amplitude from $|p_1|$ to $\gamma|p_1|$. The reference value η^{bm} is defined as that loss factor η^b which would make the damping treatment double the weight of the original beam (Case 2 only).

The diagrams in Figure 3 show that the optimization will in Case 1 reduce the amplitudes $|p_1|$ by up to 46%. Case 2 (which is deemed to be the more realistic one) gives a reduction by up to 37%. From the distribution charts in Figure 4 it can be concluded that the damping should (as expected) mainly be located where the bending curvature of the beam is the largest.

The second and third symmetric resonant modes of the beam in Figure 2 were also studied. The reductions came out with similar values as for the first mode. Also other response quantities than $|p_1|$ were investigated. As long as small values (about 0.1) of η^{bu} were considered, the reductions were about the same as above.

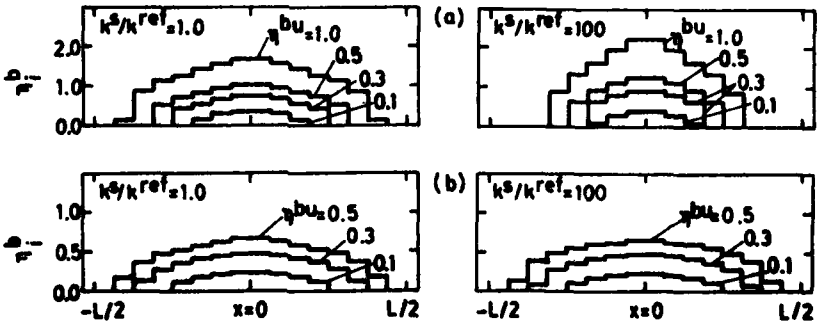


Figure 4. (a) Optimum damping distributions for Case 1 with η^s=0.0. Parameters k^s/k^{ref} and η^{bu} are varied. (b) Optimum damping distributions for Case 2 with η^s=0.0 and η^{bm}=0.4. Parameters k^s/k^{ref} and η^{bu} are varied.

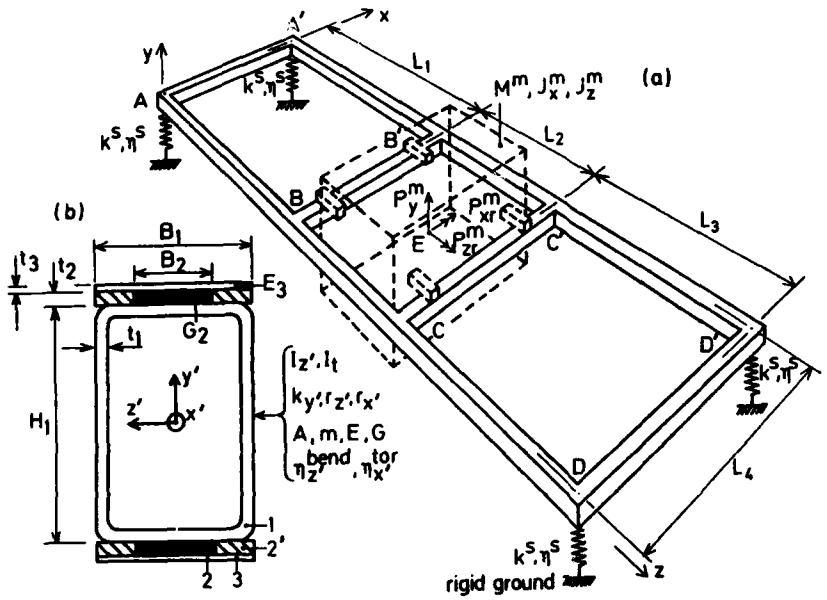


Figure 5. (a) Machinery set-up containing a machine body (dashed) connected to a grillage frame AA'-DD' mounted on four springs. Springs are supported by rigid ground. Global coordinate system is Axyz. Grillage dimensions are L_1=L_3=0.700 m, L_2=0.400 m, and L_4=0.600 m. Machine is modelled as a rigid body with mass centre MC at point E located centrally in frame. Machine has mass M^m=200 kg. Grillage consists of ten beam members AA', AB, BB', etc of equal cross sections. Grillage is supported by four equal massless springs each of stiffness k^s=56.0 kN/m and loss factor η^s (to be varied) giving total machinery set-up a lowest eigenfrequency of about 5 Hz. 'Blocking masses' will be introduced at joints A, A', D and D' (not indicated). Each 'blocking mass' has mass M^b=5.00 kg. Structure is submitted to a combined harmonic external loading P^m_y=1.00 N, P^m_{xr}=0.200 Nm and P^m_{zr}=0.300 Nm (with common time factor $e^{i2\pi ft}$).

(b) Cross-section of grillage beam. Base structure 1 (RHS beam) has dimensions H_1=60.0 mm, B_1=40.0 mm, and t_1=2.90 mm. Structural steel means m=4.29 kg/m, E=210 GPa, and G=80.8 GPa. Natural structural damping is estimated at $\eta^{bend}_{z'}$=$\eta^{tor}_{x'}$=0.005.

Example B: Damped Light-weight Machine Foundation

A grillage beam structure resting on spring supports and carrying a vibrating machine is shown in Figure 5. Reference (6) reports good agreement between numerically and experimentally obtained admittances for the freely suspended grillage (without the machine). In Reference (6) also a numerical parametric study was performed for the full set-up in Figure 5. The vibration transmission from the machine through the grillage to the supports was then of special interest.

Different means of reducing the vibration transmission were tried. Damping at the spring supports was found to be effective for frequencies up to about 75 Hz. 'Blocking masses' of 5 kg above each of the four support joints of the grillage were shown to suppress response levels above about 100 Hz. However, sharp resonance peaks are still present when 'blocking masses' have been introduced.

Additive damping of the beams of the grillage structure was found to give reduced transmission for the whole frequency range studied (0-1000 Hz). Applying the general experience from References (4) and (5), a partial damping treatment was tried for the grillage. From plots of bending moment distributions in the grillage beams for different eigenmodes it was found that high bending moments dominate in the two long beams.

Figure 6a shows the effect of applying damping (η^s=0.200) to the spring supports and uniform damping ($\eta^{bend}_{z'}$=0.010) to the grillage beams. In Figure 6b the damping treatment of the grillage is located only along portions of some beams thus spending only 37% of the damping material used for the situation in Figure 6a. For lower frequencies it was found that response levels are changed very little from Figure 6a to Figure 6b although several of these levels are strongly dependent on the damping of the grillage. For the higher frequencies the effectiveness of the partial treatment differs between the modes. Such a treatment may thus be applicable only when the machine vibrates in some limited frequency interval.

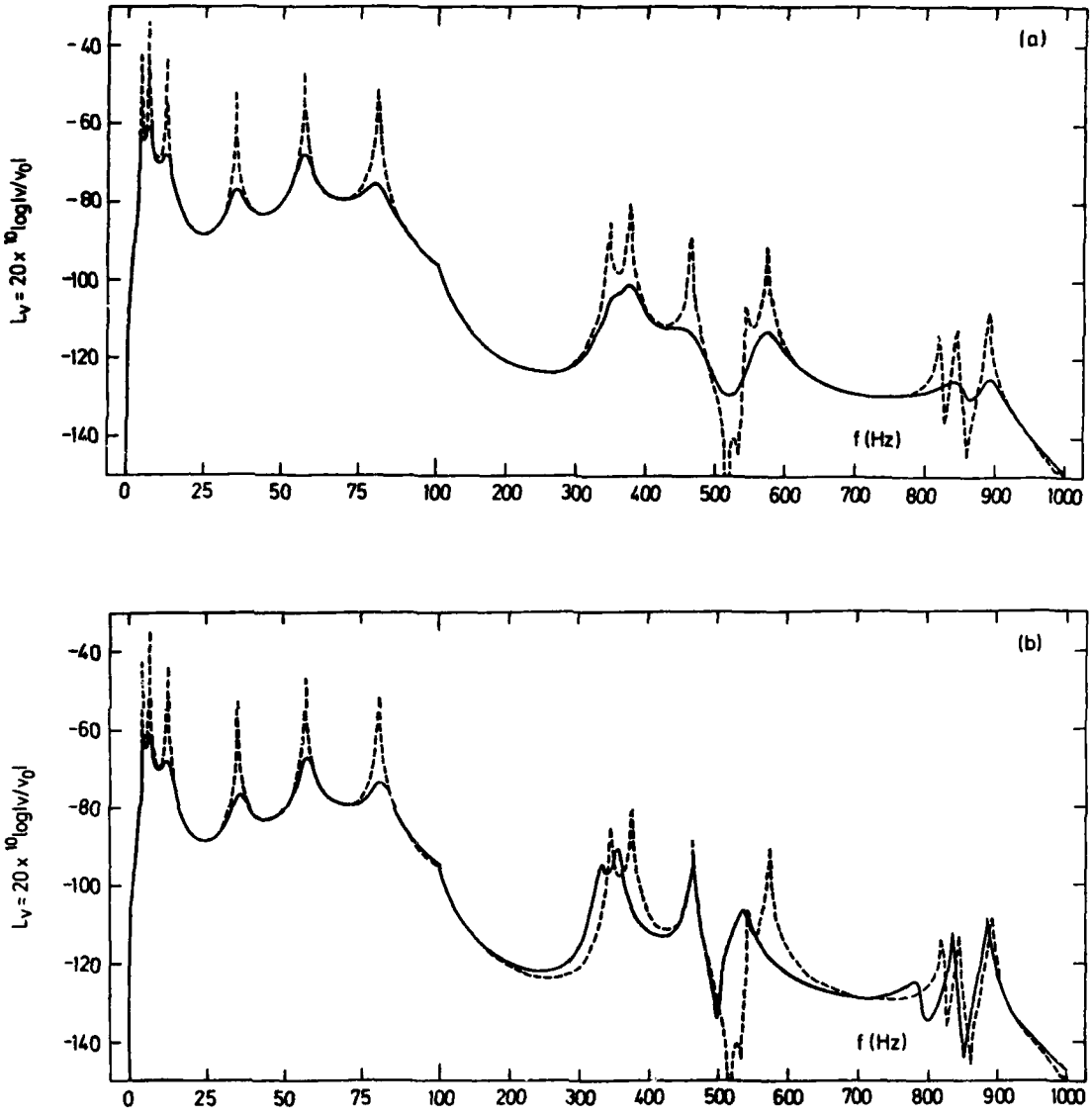


Figure 6. Calculated vertical translational velocity levels L_v (*in dB*, v_0=1 *m/s*) *at joint A of machinery* set-up in Figure 5 under combined loading described versus circular frequency f.
(a) ———, with additive damping at springs and at full length along all beams (η^s=0.200, $\eta_{z'}^{bend}$=0.100) and with 'blocking masses'; -----, without additive damping (natural damping η^s=0.010 and $\eta_{z'}^{bend}$=0.005 only) and with *'blocking masses'*.
(b) ———, with additive damping at springs (η^s=0.200) and along portions of some beams ($\eta_{z'}^{bend}$=0.100 along 1.1 m for each of beams AD and A'D', centrally placed); ------, without additive damping (same curve as in figure a).

Concluding Remarks

Optimum spatial distributions of additive damping for harmonically vibrating structures have been demonstrated in the examples of this paper. It is concluded that an optimal redistribution from an initially uniform additive damping can reduce response levels by about 50%. This general result has also been experimentally confirmed in a separate study of a one-bay two-storey frame reported in Reference (5).

Several numerical studies have shown that the optima obtained are rather flat. This means that a 'good guess' of an optimum damping distribution often gives satisfactory results. This approach was successfully applied in Example B.

In conclusion it is suggested that general results as obtained from extensive (and expensive) idealized optimization studies be used to estimate optimum damping distributions in practical design work instead of performing a full mathematical optimization procedure for each special problem at hand.

References

(1) Lundén, R., "Ship Vibration Attenuation Using Unconventional Methods," Report No. 5612:20, The Swedish Ship Research Foundation, Gothenburg, Sweden, 1977. 51 pp.

(2) Beranek, L.L. (editor), Noise and Vibration Control, McGraw-Hill, New York, 1971. 650 pp.

(3) Lundén, R., Damping of Vibrating Continuous Mechanical Systems (Mathematical modelling, numerical analysis, and experimental verification for optimal design of beam structures), PhD Thesis, Division of Solid Mechanics and Strength of Materials, Chalmers University of Technology, Gothenburg, Sweden, 1981. 162 pp.

(4) Lundén, R., Optimum Distribution of Additive Damping for Vibrating Beams. Journal of Sound and Vibration, Vol. 66, 25-37, 1979.

(5) Lundén, R., Optimum Distribution of Additive Damping for Vibrating Frames. Ibidem, Vol. 72, 391-402, 1980.

(6) Lundén, R. and Kamph, E., "Vibration Isolation of a Damped Skeletal Machine Foundation - Theory and Experiment," Paper No. F69, Division of Solid Mechanics and Strength of Materials, Chalmers University of Technology, Gothenburg, Sweden, 1981 (submitted for international publication). 28 pp.

(7) Lundén, R. and Åkesson, B., "Damped Second-Order Rayleigh-Timoshenko Beam Vibration in Space - An Exact Complex Dynamic Stiffness Matrix," Paper No. F68, ibidem, 1981 (submitted for international publication). 45 pp.

(8) Fiacco, A.V. and McCormick, G.P., Nonlinear Programming: Sequential Unconstrained Minimization Techniques, Wiley, New York, 1968. 210 pp.

(9) Fletcher, R., "FORTRAN Subroutines for Minimization by Quasi-Newton Methods," Report No. 7125, U.K. Atomic Energy Research Group, Harwell, 1972. 28 pp.

AD-P000 035

AN ITERATIVE EIGENVECTOR TECHNIQUE FOR OPTIMIZATION ANALYSIS

Paul S. Jensen
Lockheed Palo Alto Research Laboratory 5233/255
3251 Hanover St.
Palo Alto, CA 94304

ABSTRACT

Certain structural optimization analyses require the repeated generation of sparse, symmetric linear systems of equations for which a few eigenpairs (eigenvalues and corresponding eigenvectors) are to be determined. Typically, these linear systems have similar spectra. Consequently, eigenpairs for one system tend to be reasonably close approximations to those of another "next" linear system. An iterative eigenvector analysis technique that utilizes the available approximate eigenpairs in order to reduce computation costs is described. It is based on Rayleigh quotient iteration with a Lanczos type iterative equation solver. A rational transformation of the initial forms of the linear systems is used in order to overcome the adverse matrix conditions that typically ruin the convergence of the iterative equation solver.

INTRODUCTION

Structural optimization analyses involving certain types of constraint conditions, such as buckling and vibration, require repeated generation of sparse, symmetric linear systems of equations for which a few eigenpairs (eigenvalues and corresponding eigenvectors) are to be determined. An important characteristic of the eigenvector problems in this context is the availability of reasonably good approximate eigenpairs at the outset of each evaluation cycle. This characteristic is a result of the iterative nature of common optimization processes that requires the analysis of a sequence of perturbations of an initial design.

This paper describes an iterative eigenvector algorithm for large, sparse, generalized, symmetric eigenproblems commonly arising in structural analysis (finite element analysis) that exploits the availability of good initial approximate eigenvectors. The algorithm is based on the well known Rayleigh quotient iteration [1], and uses an iterative equation solver based on the Lanczos algorithm [2 and 3] and a preconditioning to enhance convergence.

The cubic convergence of Rayleigh quotient iteration has tantalized analysts ever since its discovery and exposition in the late fifties by Ostrowski [1]. However, the fact that it requires repeated solution of "shifted" linear systems of equations of the form

$$(K - rM)x = y, \qquad (1)$$

where K and M are the coefficient matrices of the eigenvector problem, r is a scalar Rayleigh quotient and x and y are vectors, has thwarted many vigorous efforts to utilize the iteration. Matrix factorization is too expensive and iterative solution algorithms tend to require successivly more time (iterations) to converge as the solution to the eigenvector problem is approached. In fact, if the eigenvector solution is achieved, r becomes the corresponding eigenvalue and the linear equation becomes singular. This singularity (or a near singularity) typically devastates the functionality of iterative solvers.

One valuable characteristic of iterative solvers that are based on the principles of conjugate gradient or conjugate direction methods is that the number of iterations required is relatively small if the coefficient matrix has many eigenvalues of equal modulus. Of course, equation (1) does not generally have this characteristic. In fact, if K and M are generated from a finite element analysis of a structure, the spectrum of (K - rM) tends to be extremely large with only minor duplication. This property, however, implies that the preconditioned matrix

$$S = P'(K - rM)^{-1} P,$$

where P is a factor of (kK - mM) for certain scalars k and m with P' the transpose of P, has the desirable property. The further an eigenvalue of the original problem is from r, the closer the corresponding eigenvalue of S is to k. So all of the distant (usually large) eigenvalues of the original problem coalesce to the value k in the transformed problem.

Although it is not reasonable to repeatedly factor (kK - mM), it is generally acceptable to factor such a matrix once.

Also, the factorization does not need to be accurate and so it is often possible to use a given factorization for several intermediate eigenvector problems in an optimization analysis. Thus, even though K and M may change slightly from one optimization step to the next, the same factor P may be retained. Considerations germane to the rational transformation S are discussed in the next section.

This is followed by a brief discussion of the Rayleigh quotient iteration algorithm for the transformed problem. No discussion of the theory of Rayleigh quotient iteration is included here. For completeness, the algorithms used for the linear systems are briefly discussed in the fourth section. The reader should study the references for details in this area.

The rational transformation greatly enhances the behavior of a good iterative linear equation solver in the early stages of the Rayleigh quotient iteration, but it does not address the problem of approaching singularity as the Rayleigh quotient approaches an eigenvalue. As this happens, however, the angle between the initial vector available to the iterative solver and the solution vector decreases. It turns out that the component of the solution that lies in the direction of the initial vector can be analytically removed so that the iterative solver only needs to determine the component normal to the initial vector. The linear equation system tends to be well posed in terms of this component. This topic is discussed further in the fifth section.

Another approach to the final stages of the Rayleigh quotient iteration is to simply apply the Lanczos algorithm for the desired eigenvector. This is most appropriate when the desired eigenvalues are near the extremes of the spectrum of S. Some of the advantages and disadvantages of this approach are discussed in the sixth section. Some numerical results are given in the last rection.

RATIONAL TRANSFORMATION

In this section we consider a transformation of the coefficient matrices for the generalized, symmetric linear eigenvalue problem

$$Kx = \lambda Mx \qquad (2)$$

that improves the convergence properties of the iterative solution procedure. Consider a factorization of the form

$$kK - mM = PDP' \qquad (3)$$

where P is lower triangular with transpose P', $D = \mathrm{diag}(d_i)$ with $d_i = \pm 1$ and scalars k and m are such that (3) is nonsingular. For any scalar r that is not an eigenvalue of (2), we consider the matrix

$$S = P'(K - rM)^{-1} P. \qquad (4)$$

If we denote the matrix of eigenvectors of (2) by X and the diagonal matrix of eigenvalues by Λ, then it can easily be verified that

$$SW = DW\Theta, \qquad (5)$$

where $PW = DX$

and $\Theta = (k\Lambda - mI)(\Lambda - rI)^{-1} = \mathrm{diag}(\theta_i)$

with $\theta_i = (k\lambda_i - m)/(\lambda_i - r)$

$= k + (kr - m)/(\lambda_i - r)$, $i=1,\ldots,n.$

Thus, for any eigenvalue λ_i of (2) such that the magnitude of $\lambda_i - r$ is large, the corresponding eigenvalue θ_i of (5) is approximately equal to k. Conversely, eigenvalues of (2) that are near r correspond to eigenvalues of (5) that have very large magnitude. In passing, we note that if kr is approximately equal to m, then S is approximately equal to kD, which is a very simple matrix to solve but which reveals very little about the spectrum of (2). This observation suggests that care should be exercised in determining the eigenvectors of (2) from those of (5). For convenience, values k=0, m=1 or k=1, m=0 are frequently chosen when eigenvalues of (2) near the low or high ends of the spectrum are required.

RAYLEIGH QUOTIENT ITERATION

Each step of Rayleigh quotient iteration updates an eigenpair (θ, w) approximation to the transformed problem (5) and the Rayleigh quotient r of the original system (2). It involves the following four computations:

$$y := SDw$$
$$\theta := (y,Dy)/(y,Dw)$$
$$r := (r\theta - m)/(\theta - k)$$
$$w := y/\|y\|$$

where the symbol := is read "is replaced by" and $\|y\|$ is the Euclidean norm of y.

Because S involves the inverse of (K - rM), see (4), it is not explicity determined. Instead, the effect of a matrix-vector product y = Sv is achieved by solving an equation system Ay = v, where A is the inverse of S.

Matrix A is not determined explicitly either because of the resulting computational cost. It is retained in product form, which means that a matrix-vector product v = Ay is determined formally as follows:

solve $P'v = y$

$y := (K - rM)v$

solve $Pv = y$.

The cost of the actual computation of v is reduced somewhat by noting that

$$A = [D + (m - rk)P^{-1}MP'^{-1}]/k$$

which leads to the following algorithm:

```
solve    P'v  = y
          u   := Mv
solve    Pv   = u
          v   := (1/k)Dy + (m/k - r)v
```

The solution of the matrix equation Ay = v is achieved by an iterative process described in the next section. This process requires repeated matrix-vector products of the form Ay.

ITERATIVE SOLUTION OF LINEAR SYSTEMS

Forms of generalized conjugate gradients based on the approachs described in [2 and 3] are currently being used for the inner loop solution. In order to solve an n by n symmetric system

$$Ay = v, \tag{6}$$

a series of n by j, j=1,2, ..., matrices

$$Q_j = [q_1, q_2, \ldots, q_j]$$

with orthonormal columns q_i are developed such that

$$AQ_j = Q_j T_j + E_j, \tag{7}$$

where T_j is j by j tri-diagonal and n by j matrix E_j is nonzero only in the last column. The projection u of the solution to ( ) onto Q is obtained by solving

$$Q'AQ\,u = Q'v$$

which, from (7), is formally equivalent to solving

$$T_j u = Q_j' v \tag{8}$$

since, as it turns out, Q_j is orthogonal to E_j.

The iterative development of the q's and elements of T follows the familiar Lanczos process (see e.g., [2]). For stability, (8) is solved using the LQ factorization. One of the most perplexing difficulties with this algorithm arises from the fact that the columns of Q do not remain orthonormal. The algorithm MINRES, described in [2] and used here, ignores this difficulty and lumbers on using brute force to obtain the solution. The algorithm LANSOL, described in [3] and also used here, handles the difficulty by "selective orthogonalization" as described in [4].

LANSOL generally requires fewer iterations to converge but incurs a nontrivial overhead cost for the selective orthogonalization. At this point, neither algorithm appears to be universally superior for the problem at hand.

For either method, it is prudent to simplify the problem as much as is practical in order to reduce the cost of the solution. In particular, the quality of the initial approximation to the solution must be fully exploited. A general technique, which happens to be particularly effective for the eigenproblem at hand, for using a good initial approximation is described in the next section.

CONDITIONING WITH THE INITIAL APPROXIMATE

The considerations of this section apply to the iterative solution of linear systems of equations in general. Basically, we are to determine the solution of

$$Ay = v \tag{9}$$

given an initial approximation $\bar{y}$ such that $A\bar{y} = \bar{v}$ is a reasonably good approximation to a scalar multiple cv of the given right hand side. For numerical efficacy, we choose to solve

$$Az = cv - \bar{v} \tag{10}$$

instead of (9), followed by setting $y = (z+\bar{y})/c$. In order for the right hand side of (10) to be orthogonal to v, we must choose

$$c = (v,\bar{v})/(v,v)$$

where (.,.) represents an appropriate vector inner product, e.g., Euclidean dot product. If v is approximately an eigenvector of A, then the solution y will be approximately parallel to it. Consequently, the solution z of (10) will be nearly orthogonal to that eigenvector since the right side of (10) is orthogonal to it.

LANCZOS EIGENVECTOR ALGORITHM

For the determination of eigenvalues near the ends of the spectrum of S (with fixed r, see (4)), Lanczos iteration can be used to determine the eigenpairs directly. This approach also applies to the determination of interior eigenpairs as well if good initial approximate eigenvectors are available. This approach was apparently applied successfully in [5].

In order to use this approach, it is necessary for (kK - mM) to be positive definite so that diagonal matrix D of (3) is the identity. Also, it is necessary to factor (K - rM) for some astutely chosen r so that matrix-vector products of the form Sv can be determined directly.

The Lanczos algorithm is then used to determine extreme eigenpairs of S, see (5), and the results are mapped to the corresponding eigenpairs of (2). Suitable implementations of the Lanczos algorithm for large, sparse matrices may be found in [6-9] and a variety of other places.

The obvious disadvantages of this approach have already been noted, i.e., extra factorizations and restrictions on the choice of k and m. The advantage of the approach is its superior convergence rate.

The reason it has a superior convergence rate follows from a reasonably simple argument. Whether Lanczos iteration is used in the inner loop of Rayleigh quotient iteration to solve a system of equations or it is used to determine eigenpairs, it must generate a set of vectors that represent a basis for a corresponding Krylov space. The result produced is then the projection onto this space of either the solution to the equation system or the desired eigenpair, depending upon the application. Since the fundamental objective here is to determine eigenpairs, the latter result is the more direct utilization of the set of "Lanczos" vectors for the basic problem.

One aspect of the Lanczos eigenvalue algorithm that is under active study is the monitoring of the linear independence of the basis vectors. Current methods solve increasingly larger tri-diagonal eigenvalue problems for this purpose. If only a few basis vectors are needed, the monitoring cost is minor; however, in our studies, the numbers of basis vectors needed led to rather large monitoring costs.

TEST RESULTS AND CONCLUSIONS

The three approaches discussed in previous sections have been implemented and tested on problems generated by a pseudo-random number generator and the one dimensional harmonic operator. Links to matrices from actual structural analyses have not been completed as of this writing. The results presented in this section pertain to the harmonic operator.

The initial vector used in these tests was a purturbation of the true eigenvector in the middle of the spectrum given by

$$y_i = (1 + db_i)x_i, \quad i = 1,\ldots,n$$

where x is the true eigenvector, d is the purturbation factor (d = 1/8 in this case), and for each i, b_i is a random number in the range [-1,1]. The actual expression for the components of the true vector in this case is

$$x_i = \sin(ic)$$

where c = [n/2] /(n+1) with [.] interpreted as the largest integer not exceeding the bracketed quantity. Thus, the initial vector is accurate to about one decimal place.

The scale factors k=0, m=1 were used for convenience, see (3). For the straight Lanczos iteration, r=0 was selected in order to illustrate the difficulty in obtaining eigenvalues from the interior of the spectrum of S. A subsequent test seeks the eigenvalue nearest r=0 in order to illustrate the rapid convergence of the Lanczos iteration for extreme eigenvalues of S. Because of the choice of starting vector, it was satisfactory to use the harmonic operator in place of its inverse as prescribed in the definition of S, see (4).

The test results are given in Table 1. The stopping criteria in each case was a residual norm less than 0.0005 using single precision on a DEC VAX11/70 computer having floating point accuracy 0.0000000596. The timer is affected by system load and so several runs were made for each case and the average is given.

Table 1. Results for interior eigenvector refinement

MINRES - Minimum residual method [2]
LANSOL - Lanczos equation solver [3]
LANEIG - Lanczos eigenvalue iteration

N	MINRES		LANSOL		LANEIG	
	Iter	Time	Iter	Time	Iter	Time
50	41	1.15	24	4.57	64	4.48
100	46	2.40	41	9.18	103	17.51
200	46	3.98	29	6.85	151	52.03

The rapid growth in time as n increases for LANEIG illustrates the cost in monitoring linear independence of the basis vectors. This cost was mitigated by stopping the iteration when mildly poor independence was detected and restarting with the resulting approximate eigenvector. This resulted in a larger total number of iterations in some instances, but a smaller total elapsed time.

This same overhead cost is reflected to a lessor degree in the times for LANSOL. However, since the double loop Rayleigh quotient iteration permitted solution in relatively few iterations, the overhead is hardly noticed. As noted earlier, MINRES ignores linear dependence and, therefore, normally requires more iterations than LANSOL. In this problem, each iteration is extremely inexpensive and so MINRES looks relatively appealing.

As promised above, we also present results in Table 2 for LANEIG seeking an extreme eivenvalue of S. Results are not included for the double loop Rayleigh quotient iteration methods because, of course, they automatically adjust all problems (via the Rayleigh quotient) so that they are seeking extreme eigenvalues.

Table 2. Results for refinement of extreme eigenvectors

N	LANEIG	
	Iter	Time
50	15	.54
100	17	.86
200	18	.93

This is clearly the case for which Lanczos iteration shines. For typical application to structural optimization, however, it appears that the cost of forming the product form of S, see (4), together with the resulting losses in sparsity and accuracy due to the factorization of (K - rM) will overpower the benefits of straight Lanczos iteration.

ACKNOWLEDGEMENTS

The author is indebted to Messrs. Bahram-Nour Omid and Horst Simon for the implementation of LANSOL and several delightful discussions relating to Lanczos iteration. He is also indebted to Prof. Beresford Parlett for stimulating discussions on Lanczos based techniques for both equation solving and eigenvalue determination. Finally, thanks go to Prof. David Scott for providing an excellent set of Lanczos eigenvalue analysis programs, ideas from which contributed substantially to this work. This effort was sponsored primarily by the Air Force Office of Scientific Research under grant 76-3019 and secondarily by the independent research program of Lockheed Missiles and Space Co., Inc.

REFERENCES

1. Ostrowski, A. M., "On the Convergence of the Rayleigh Quotient Iteration for the Computation of the Characteristic Roots and Vectors," Arch. Rational Mech. Anal. I (1958) 233-241, II (1958/59) 423-428, III (1959) 153-165, IV (1959) 341-347, V (1959) 472-481

2. Paige, C. C. and M. A. Saunders, "Solution of Sparse Indefinite Systems of Linear Equations," SIAM J. Num. Anal. 12,4 (1975) 617-629

3. Parlett, B. N., "A New Look at the Lanczos Algorithm for Solving Symmetric Systems of Linear Equations," Lin. Algebra and its Applic. 29 (1980) 323-346

4. Parlett, B. N., and D. S. Scott, "The Lanczos Algorithm with Selective Orthogonalization," Math. of Comp. 33, 145 (1979) 217-238

5. Ericsson, Thomas and Axel Ruhe, "The Spectral Transformation Lanczos Method for the Numerical Solution of Large Sparse Generalized Symmetric Eigenvalue Problems," Math. of Comp. 35, 152 (1980) 1251-1268

6. Ruhe, Axel, "Implementation Aspects of Band Lanczos Algorithms for Computation of Eigenvalues of Large Sparse Symmetric Matrices," Math. of Comp. 33, 146 (1979) 680-687

7. Paige, C. C., "Computational Varients of the Lanczos Method for the Eigenproblem," J. Inst. Math. Appl. 10 (1972) 373-381

8. Scott, D. S., "Block Lanczos Software for Symmetric Eigenvalue Problems," Report ORNL/CSD-48, Union Carbide Corp., Oak Ridge National Laboratory, Oak Ridge, Tenn. (1979)

9. Underwood, R., "An Iterative Block Lanczos Method for the Solution of Large Sparse Symmetric Eigenproblems," STAN-CS-75-496, Computer Sciences Dept., Stanford University, Stanford, Calif. (1975)



AD-P000 036

OPTIMUM STRUCTURAL DESIGN UNDER DYNAMIC FORCES WITH UNCERTAINTIES

Kunihito Matsui
Department of Civil Engineering, Tokyo Denki University
Hatoyama, Hiki, Saitama 350-03 Japan
Kazuyuki Yamamoto
Department of Civil Engineering, Tokyo Sibaura Institute of Technology
Shibaura Minato-ku Tokyo 108 Japan
Yukio Kikuta
Department of Civil Engineering, Kokushikan University
Setagaya Setagaya-ku Tokyo 154 Japan
Yasuo Niinobe
Department of Civil Engineering, Tohyo University
Kujirai, Kawagoe, Saitama 350 Japan

Summary

Optimization algorithm is presented on a structure which sustains a time dependent force from an indefinite direction. Stresses and displacements are given by parametric forms of both time and direction of force. The direction is treated as uncetainty and is called enviromental parameter here.

To compute stresses and displacements, equations of motion are formulated based on finite element method with consistent mass matrix and solved by modal analysis. Since the stresses and displacements depend on time and enviromental paramerters, their maximum values have to be found in the domain of the both parameters. Then the weight of structure will be minimized meeting all requirements. Hence the optimization procedure in this paper consists of two alternating processes of maximization and minimization. The maximization is carried out analytically and the minimization process by a gradient projection method.

As example problems three truss structures are considered: one is plane truss and the other two are space trusses. A time dependent force is given by sine function, hence all members of the structures undergo from tensile state to compressive state. The design critera are taken to be 1) in tensile state, stress in a member should be less than an allowable stress, 2) in compressive state, stress must not exceeds the smaller of an allowable stress and Euler buckling stress, 3) displacement is within allowable limit, and 4) design variable is between its upper and lower limits. Time dependent force is allowed to change its direction within the range of 180 degrees. Although this paper treats the case that the force is applied at a single node, loadings on multiple nodes can be handled similarly as long as their directions are same.

Numerical results are presented to demonstrate the validity of the algorithm and the dynamic characteristics of the problems.

Introduction

For many years numerous amount of research work has been conducted on the optimization of structural systems. Most common problems are weight minimization of various structures subject to static loadings. Extensive effort has been made mainly on the development of efficient algorithms (1-7) and partially their applications to other area of engineering problems; inverse problems (8), contact problems (9), stephan problems(10) and so on. There are two main streams on the approach to structural optimization techniques; that is, one is a mathematical programing method (1-7) and the other is optimality criteria method (5-7). Many variations of both methods are also available. The discussion on the two approaches is found in ref. (11) and is beyond the scope of this paper. Among the optimization techniques available, the method adopted herein is a gradient projection method (3),whch is a version of mathematical programings,simply due to the reason that the method is one of the most frequently used and can handle complex constraints.

With marked developments of high strength materials and remarkable progresses on structural analyses and designs, there is a trend toward constructing large flexible structures. To design thse structures, one needs not only static analysis but also dynamic analysis to assure the safety, serviceability and possibly human comforts. Hence from the point of rational designing of the structures, optimum design in dynamic domain is essential. In the past numerous papers have been published in the area of dynamic optimization where design is made to satisfy a specific frequency (12,13). Much less work has been conducted on dynamic response constraints where constraints on stresses and displacements are given in time parametric form (14-16). In this regard some publications (17-20) have been made on optimum earthquake resistant design. Frequently time dependency of the dynamic quantity is removed by using response spectrum technique. Further structural control (21-25) has drawing the attention of structural engineers. The idea behind it is to install a control device composed of spring and damping such that it will prevent a structure from undergoing excessive displacements and accelerations.

On most structural optimization problems, direction and location of loading(both static and dynamic) are given in advance. However in real world problems they are not necessarily known (26,27). Wind load, tidal wave and earthquake can hit structures from any direction. Under such circumstances a design will be made based on an engineer's experience or his intuition. Rational design method is not available yet. The purpose of this paper is to present an optimal design of structures under uncertainty of loading as mentioned above. Hence the problem treated here contains two sets of parameters;one is called environmental parameter which implies a direction of force and the other time parameter. The optimization problem is devided into two processes. First process is maximization which finds the worst states of stresses and displacements due to the direction of force and the second process is minimization process on the weight of structure. Considering characteristics of structural analysis, maximization is carried out analytically but minimization process is solved iteratively by a gradient projection method. Numerical results are presented to demonstrate and the validity of the algorithm and characteristics of example problems.

Formulation of Problem

Optimum design problem consdered herein is minimum weight design of structural system subject to dynamic forces whose magnitude are constant but whose direction can vary within certain range. The problem of this type will be expressed in a mathematical form as:

minimize : $\phi_0(b)$ (1)

subject to the equations of motion

$$M(b)\ddot{\mathbf{x}} + C(b)\dot{\mathbf{x}} + K(b)\mathbf{x} = Q(\alpha, t) \quad (2)$$

$$\mathbf{x}(0) = \mathbf{x}_0 \quad (3)$$

$$\dot{\mathbf{x}}(0) = \dot{\mathbf{x}}_0 \quad (4)$$

and constraints

$$\max \eta_i(b, \mathbf{x}, \alpha) \le 0, \ (i = 1, 2, \cdots, g_1) \quad (5)$$
$$\alpha \in A, \ t \in (0, T)$$

$$\eta_i(b) \le 0, \ (i = g_1+1, \cdots, g_2) \quad (6)$$

where

$$A = \{\alpha \mid g_k(\alpha) \le 0, \ k = 1, 2, \cdots, r\} \quad (7)$$

The notations used above are

$b = [b_1, b_2, \cdots, b_m]^T$: design variable

$\mathbf{x} = [x_1(t), x_2(t), \cdots, x_n(t)]^T$: state variable

$\alpha = [\alpha_1, \alpha_2, \cdots, \alpha_l]^T$: environmental parameter

$K(b)$: stiffness matrix

$M(b)$: mass matrix

$C(b)$: damping matrix

T : upper limit of time parameter

$\dot{z}$ and $\ddot{z}$ imply first and second order derivatives of z with respect to time parameter t. The constraints on stresses, bucklings and displacements are expressed by eq.(5), where a set A defined by eq.(7) is a range that α is allowed to take. Eq.(6) is a sizing constraint, i.e. lower and upper bound of design variable b.

In order to solve the optimization problems stated by eqs.(1) - (7), it will be divided into two levels: one is maximization process wich will find the worst state of stresses and displacements due to the change of environmental parameter α, and the other is maximization process which, meeting all the constraint requirements, will reduce the value of objective function as much as possible. The former process is, hereafter, called an inner problem and the other an outer problem.

Inner problem can be defined as:

maximize $\eta_j(b, \mathbf{x}, \alpha), \ (j = 1, 2, \cdots, g_1)$ (8)
$\alpha \in A, \ t \in (0, T)$
subject to
$M(b)\ddot{\mathbf{x}} + C(b)\dot{\mathbf{x}} + K(b)\mathbf{x} = Q(\alpha, t)$ (2)
$\mathbf{x}(0) = \mathbf{x}_0$ (3)
$\dot{\mathbf{x}}(0) = \dot{\mathbf{x}}_0$ (4)

where

$$A = \{\alpha \mid g_k(\alpha) \le 0, \ k = 1, 2, \cdots, r\} \quad (7)$$

The maximization process will be conducted with a fixed value of $b = b^{(0)}$ to find $\bar{\alpha}_j$ and $\bar{\mathbf{x}}_j(t)$ which maximize η_j for each j,(j = 1,2,$\cdots\cdots$,q_1). Even after $\bar{\alpha}_j$ which maximize η_j , (j = 1,2,$\cdots$,q_1) is found, eq.(5) is still parametric in the sense that they require satisfaction over a range of time parameter. The parametric constraints may be transformed to functional form,

$$\phi_j = \int_0^T h_j(b, \mathbf{x}(t))\,dt \quad (9)$$

where

$$h_j = \begin{cases} \eta_j(b, \mathbf{x}, \bar{\alpha}_j) & \text{if } \eta_j \ge 0 \\ 0 & \text{if } \eta_j < 0 \end{cases} \quad (10)$$

α_j is consdered fixed.

Then outer problem is defined as follows:

minimize $\phi_0(b)$ (11)

subject to

$$M(b)\ddot{\mathbf{x}} + C(b)\dot{\mathbf{x}} + K(b)\mathbf{x} = Q(\bar{\alpha}, t) \quad (12)$$
$$\mathbf{x}(0) = \mathbf{x}_0 \quad (13)$$
$$\dot{\mathbf{x}}(0) = \dot{\mathbf{x}}_0 \quad (14)$$
$$\phi_i = \int_0^T h_j(b, \mathbf{x})\,dt \le 0, \ (j = 1, 2, \cdots, g_1) \quad (15)$$
$$\phi_i = \eta_j(b) \le 0, \ (j = g_1+1, \cdots, g_2) \quad (16)$$

As can be seen, the environmental parameter α is removed in the problem. Alternative approach is to set

$$\phi_i = \max \eta(b, \mathbf{x}, \alpha), \ (i = 1, 2, \cdots, g_1) \quad (17)$$
$$\alpha \in A, \ t \in (0, T)$$

then eq.(9) will be replaced by

$$\phi_i \le 0, \ (i = 1, 2, \cdots, g_1) \quad (18)$$

Although it may be mathematically more regorous to treat the parametric constraint eq.(5) as eqs.(17), (18), eq.(9) is adopted for the sake of simplicity on computational algorithm. The solution procedure for the original problem consists of alternating maximization and minimization processes.

Optimization Procedure

The most common approach to the structural optimization is an adaptation of nonlinear programing method. The inner and outer problems stated in the previous section can be solved by employing the method. However, considering a computational efficency, it is more reasonable to make a full use of the knowledge on structural analysis without getting into optimization scheme. If dynamic force is loaded at one node, it is possible to find a maximum value of eq.(5) without maximization algorithm.

Dynamic Analysis

The optimization problem in a dynamic domain reqires to solve the equations of motion,

$$M\ddot{\mathbf{x}} + C\dot{\mathbf{x}} + K\mathbf{x} = Q(t) \quad (19)$$

$$\mathbf{Z}(0) = \mathbf{Z}_0 \tag{20}$$

$$\dot{\mathbf{Z}}(0) = \dot{\mathbf{Z}}_0 \tag{21}$$

where M, C and K are mass, damping and stiffness matrices, z is state variable and Q(t) is an external force. If one considers N dominant modes of

$$M\ddot{\mathbf{Z}} + K\mathbf{Z} = 0 \tag{22}$$

where M and k are n x n symetric matrices. Then z is approximated by

$$\mathbf{Z} = \sum_{i=1}^{N} y_i p_i(t)$$

$$= [y_1, y_2, \cdots, y_n]^T \begin{bmatrix} p_1(t) & & 0 \\ & p_2(t) & \\ 0 & & \ddots \\ & & p_N(t) \end{bmatrix} \tag{23}$$

where $N \leq n$.

Substituting eq.(23) into eq.(19) and premultiplying by y_i, then one will obtain

$$y_i^T M y \ddot{p} + y_i^T C y \dot{p} + y_i^T K y p = y_i^T Q(t) \tag{24}$$

Since y_i, ($i = 1,2,\cdots,N$) are orthogonal to each other with respect to M and K,

$$y_i^T M y_j = \begin{cases} m_i & i = j \\ 0 & i \neq j \end{cases} \tag{25}$$

and

$$y_i^T K y_j = \begin{cases} k_i & i = j \\ 0 & i \neq j \end{cases} \tag{26}$$

hold. If C is proportional to either M or K matrix, the second term of the left-hand side of eq.(24) is also orthogonalized, i.e.

$$y_i^T C y_j = \begin{cases} C_i & i = j \\ 0 & i \neq j \end{cases} \tag{27}$$

Putting

$$q_i = y_i^T Q(t) \tag{28}$$

and taking into account the orthogonality conditions of eqs.(25) — (27), eqs.(19) — (21) will be rewritten as

$$\ddot{p}_i + 2\xi_i \dot{p}_i + \omega_i^2 p_i = \frac{q_i(t)}{m_i}, \quad (i = 1, 2, \cdots, N) \tag{29}$$

$$p_i(0) = p_{i0} \tag{30}$$

$$\dot{p}_i(0) = \dot{p}_{i0} \tag{31}$$

where

$$k_i = \omega_i^2 m_i, \quad C_i = 2\xi_i \omega_i m_i$$

$$p_{i0} = y_i^T M \mathbf{Z}_0 / m_i, \quad \dot{p}_{i0} = y_i^T M \dot{\mathbf{Z}}_0 / m_i$$

The general solution of eqs.(29) — (31) is

$$p_i(t) = e^{-\xi_i \omega_i t}\left[\frac{\dot{p}_{i0} + p_{i0}\xi_i\omega_i}{\omega_i}\sin\omega_{Di}t + p_{i0}\cos\omega_{Di}t\right.$$

$$\left. + \frac{1}{m_i\omega_{Di}}\int_0^t q_i(t) e^{-\xi_i(t-\tau)} \sin\omega_{Di}(t-\tau)\,d\tau\right] \tag{32}$$

where

$$\omega_{Di} = \omega_i\sqrt{1-\xi_i^2}$$

However if C is not orthogonalized with respect to y_i, numerical integration method such as Newmark's β - method should be adopted to find z(t).

Inner Problem

In the inner problem, design variable is held constant (initially assumed to be $b = b^{(0)}$), and $\bar{\alpha}_j$, and $\bar{\mathbf{Z}}_j(t_0)$ are determined, which, satisfying the requirements of eqs.(9) and (10), maximize eq.(8). This could be done by using any optimization technique, but it is more efficient and exact to use the properties of structure. To explain the latter approach, it is assumed that time dependent force is applied at a single node and is restrained to change its direction on a given plane(for example x-y plane). Let the force is expressed by $P\sin\omega t$ which intersect with x-axis at an angle of α. Then its components in x and y directions are $P\sin\omega t\cos\alpha$ and $p\sin\omega t\sin\alpha$. If $\mathbf{Z}_x^{(0)}$ and $\mathbf{Z}_y^{(0)}$ corresponds to the solutions of eqs.(19) — (21) with the right hand side equall to $\sin\omega t$ in x and y directions respectively, the solution of eqs.(2) — (4) is given by

$$\mathbf{Z} = P\mathbf{Z}_x^{(0)}\cos\alpha + P\mathbf{Z}_y^{(0)}\sin\alpha \tag{33}$$

The quantities $\mathbf{Z}_x^{(0)}$ and $\mathbf{Z}_y^{(0)}$ are obtained from eqs.(23) and (32) by substituting

$$q_i(t) = \begin{cases} y_i^{(\delta)}\sin\bar{\omega}t & (34) \\ y_i^{(\delta+1)}\sin\bar{\omega}t & (35) \end{cases}$$

where δ and $\delta + 1$ indicate δth and $(\delta + 1)$th degree of freedom, and $y_i^{(\delta)}$ and $y_i^{(\delta+1)}$ are δth and $(\delta + 1)$th components of ith eigenvector respectively. If damping matrix is zero and initial conditions z_0, $\dot{z}_0$ are zero, $\mathbf{Z}_x^{(0)}$ and $\mathbf{Z}_y^{(0)}$ become

$$\mathbf{Z}_x^{(0)} = \sum_{i=1}^{N} \frac{y_i^{(\delta)}}{k_i} \frac{1}{\left[1-\left(\frac{\bar{\omega}}{\omega_i}\right)^2\right]}\left\{\sin\bar{\omega}t - \left(\frac{\bar{\omega}}{\omega_i}\right)\sin\omega_i t\right\} \tag{36}$$

$$\mathbf{Z}_y^{(0)} = \sum_{i=1}^{N} \frac{y_i^{(\delta+1)}}{k_i} \frac{1}{\left[1-\left(\frac{\bar{\omega}}{\omega_i}\right)^2\right]}\left\{\sin\bar{\omega}t - \left(\frac{\bar{\omega}}{\omega_i}\right)\sin\omega_i t\right\} \tag{37}$$

The substitution of eqs.(36) and (37) into eq.(8) yields

$$\eta_i(b, \mathbf{Z}, \alpha) = \psi_x(t)\cos\alpha + \psi_y(t)\sin\alpha - 1 \tag{38}$$

If η_i is a stress constraint, $\psi_x(t)$ and $\psi_y(t)$ are stresses due to force $P\sin\omega t$ in x and y directions divided by an allowable stress. Eq.(38) can be written as :

$$\eta_i(\mathbf{z}, b, \alpha) = \sqrt{\psi_x^2 + \psi_y^2}\,\sin(\alpha + \theta(t)) \tag{39}$$

where

$$\theta(t) = \frac{\psi_x(t)}{\psi_y(t)} \tag{40}$$

Then

$$\max_{\alpha\in A,\, t\in(0,T)} \eta_i = \left\{\max_{t\in(0,T)} \sqrt{\psi_x^2+\psi_y^2}\right\}\left\{\max_{\alpha\in A} \sin(\alpha+\theta(t))\right\} \tag{41}$$

If the range of α is whole plane, eq.(41) becomes

$$\max_{\alpha\in A,\, t\in(0,T)} \eta_i = \max_{t\in(0,T)} \sqrt{\psi_x^2(t)+\psi_y^2(t)} \tag{42}$$

Let eq.(41) be maximum when $\alpha = \bar{\alpha}_i$, $z = \bar{z}_i(t)$ at $t = t^*$, then

$$\max_{\alpha\in A} \eta_i(b, \mathbf{z}, \alpha) = \eta_i(b, \bar{\mathbf{z}}_i(t), \bar{\alpha}_i) \tag{43}$$

Eq.(43) is still a function of time parameter t.

Outer Problem

The solution procedure of optimization problem is iterative process. In outer problem, amount of design variable improvement δb will be found in such that the constraints eqs.(16) — (20) are met and the objective function reduces as much as possible. For this purpose a modified gradient projection method is employed.
To derive an iterative scheme, the first order variation of eqs.(15) — (20) are needed. They are

$$\delta\phi_o = \phi_{o,b}\,\delta b \tag{44}$$

$$M\delta\ddot{\mathbf{z}} + (M\ddot{\mathbf{z}})_{,b}\delta b + C\delta\dot{\mathbf{z}} + (C\dot{\mathbf{z}})_{,b}\delta b + K\delta\mathbf{z} + (K\mathbf{z})_{,b}\delta b = 0 \tag{45}$$

$$\delta\mathbf{z}(0) = 0 \tag{46}$$

$$\delta\dot{\mathbf{z}}(0) = 0 \tag{47}$$

$$\delta\phi_i = \int_o^T \left\{h_{i,b}\,\delta b + h_{i,\mathbf{z}}\,\delta\mathbf{z}\right\} dt, \quad (i = 1, 2, \cdots, g_1) \tag{48}$$

$$\delta\phi_i = \phi_{i,b}\,\delta b \tag{49}$$

In the above expressions eqs.(44) — (49), the following matrix differentiation convention is used

$$\phi_{,b} = \left[\frac{\partial\phi_i}{\partial b_j}\right] \tag{50}$$

where ϕ is a column vector of functions of vector variable b. Eq.(50) results in a matrix with row index i and column index j. So the derivative of a scalar function becomes .row vector.

By rewritting eq.(45), one obtains

$$M\delta\ddot{\mathbf{z}} + C\delta\dot{\mathbf{z}} + K\delta\mathbf{z} = -\left\{(M\ddot{\mathbf{z}})_{,b} + (C\dot{\mathbf{z}})_{,b} + (K\mathbf{z})_{,b}\right\}\delta b \tag{51}$$

Upon consideration of the solution of eqs.(19) — (21), the solution of eq.(51) will be given by

$$\delta\mathbf{z} = \sum_{i=1}^{N} y_i\,\delta p_i(t) \tag{52}$$

where with the initial conditions of eqs.(46) and (47)

$$\delta p_i(t) = C_i(t)\,\delta b \tag{53}$$

$$C_i(t) = -\frac{1}{m_i\omega_{Di}}\int_o^t \left\{(M\ddot{\mathbf{z}})_{,b} + (C\dot{\mathbf{z}})_{,b} + (K\mathbf{z})_{,b}\right\} e^{-\xi_i(t-\tau)} \times \sin\omega_{Di}(t-\tau)\,d\tau, \quad (i = 1, 2, \cdots, N) \tag{54}$$

From eqs.(52) — (54), eq.(48) becomes

$$\delta\phi_i = \left[\int_o^T \left\{h_{i,b} + h_{i,\mathbf{z}}\,C_i(t)\right\} dt\right]\delta b \tag{55}$$

To initiate the iterative process, an estimate is made of the design variable $b^{(0)}$. Then the inner problem is solved to find $\max\eta_j(b,z,\alpha)$ and the coresponding $\bar{\mathbf{z}}_j(t)$, $\bar{\alpha}_j$. The inequality constraints eqs.(19),(20) are checked and the indices of tight and violated constraits index sets B_1 and B_2

$$B_1 = \left\{j \,|\, \phi_j(b, \bar{\mathbf{z}}_j, \bar{\alpha}_j) \geq 0,\ j \leq g_1\right\} \tag{56}$$

and

$$B_2 = \left\{j \,|\, \phi_j(b) \geq 0,\ j \leq g_1+1, \cdots, g_2\right\} \tag{57}$$

Let the amount of vioration for eqs.(19) and (20) be $\Delta\phi_j$, $(j\in(B_1 \cup B_2))$, then $\Delta\phi_j$ can be taken

$$\Delta\phi_j = -\,\phi_j, \quad (j\in(B_1 \cup B_2)) \tag{58}$$

Furthermore introducing the following notations:

$$l_o^T = \phi_{o,b} \tag{59}$$

$$l_j^T = \int_o^T \left\{h_{i,b} + h_{i,\mathbf{z}}\,C_i(t)\right\} dt \tag{60}$$

$$\hat{l} = \left\{l_j \,|\, j\in(B_1 \cup B_2)\right\} \tag{61}$$

$$\Delta\hat{\phi} = \left\{\Delta\phi_j \,|\, j\in(B_1 \cup B_2)\right\} \tag{62}$$

the outer problem will reduce to;

minimize $\delta\phi_o = l_o^T\,\delta b$ (63)

subject to

$$\hat{l}^T\delta b - \Delta\hat{\phi} \leq 0 \tag{64}$$

$$\delta b^T W\,\delta b - \xi^2 \leq 0 \tag{65}$$

where ξ^2 is a small positive number and W a positive definite weighting matrix. A new constraint eq.(65) is added due to the reason that the changes of all the equations in the outer problem can be approximated by the first order variations. The Kuhn-Tucker conditions applied to the reduced problem yield:

$$\frac{\partial L}{\partial b} = l_o^T + \gamma^T\hat{l}^T + 2\nu\,\delta b^T W = 0 \tag{66}$$

$$\gamma_j(l_j^T\delta b - \Delta\phi_j) = 0, \quad (j\in(B_1 \cup B_2)) \tag{67}$$

$$\nu(\delta b^T W\,\delta b - \xi^2) = 0 \tag{68}$$

where

$$L = l_o^T\delta b + \gamma^T(\hat{l}^T\delta b - \Delta\hat{\phi}) + \nu(\delta b^T W\,\delta b - \xi^2) \tag{69}$$

and γ is a vector multiplier in which $\gamma_j \geq 0$ for all j

in $B_1 \cup B_2$, a schalar multplier $\nu \geq 0$.

Solving eq.(66) for δb ,

$$\delta b = -\frac{1}{2\nu} W^{-1} (\ell_0 + \tilde{\ell} \gamma) \tag{70}$$

Assuming $\gamma_j \neq 0$ and substituting eq.(70) into eq.(67), one will obtain

$$\tilde{\ell}^T W^{-1} \tilde{\ell} \gamma = -\tilde{\ell} W^{-1} \ell_0 - 2\nu \Delta \bar{\phi} \tag{71}$$

By rewriting γ ,

$$\gamma = \gamma_0 + 2\nu \gamma_1 \tag{72}$$

where γ_0 and γ_1 are the solutions of

$$\tilde{\ell}^T W^{-1} \tilde{\ell} \gamma_0 = -\tilde{\ell}^T W^{-1} \ell_0 \tag{73}$$

$$\tilde{\ell} W^{-1} \tilde{\ell} \gamma_1 = -\Delta \bar{\phi} \tag{74}$$

eq.(70) can be given as

$$\delta b = -\frac{1}{2\nu} \delta b_0 + \delta b_1 \tag{75}$$

where

$$\delta b_0 = W^{-1} (\ell_0 + \tilde{\ell} \gamma_0) \tag{76}$$

$$\delta b_1 = -W^{-1} \tilde{\ell} \gamma_1 \tag{77}$$

The parameter ν still remains undetermined,which can be computed from eq.(69) on the assumption $\nu \neq 0$ or more effective technique is explained in ref.(3).

Computational Algorithm

The optimization procedure stated before can be summarized as follows:

Step 1. Make best possible estimate of $b^{(i)}$where i implies the iteration.

Step 2. Compute eigenvector y_j, (j=1,2,···,N) to obtain $z_x^{(\omega)}$, $z_y^{(\omega)}$and z(t) in eq.(33).

Step 3. $\bar{z}_i$, $\bar{\alpha}_j$ which maximize eq.(8).

Step 4. Compute constraint eqs.(19) and (20), and if violated, form index sets B_1 and B_2 and compute amount of corrections

Step 5. Compute $C_j(t)$, (i=1,2,···,N) from eq.(54) and δz from eq.(52).

Step 6. Calculate ℓ_0 in eq.(55) and ℓ_j in eq.(60).

Step 7. Compute γ_0 and γ_1 from eqs.(73) and (74). Then assuming the value of ν , obtain γ .

Step 8. If any component of ν is negative, delete the corresponding index in B_1 and B_2 and return to Step 4.

Step 9. Calculate $\delta b_0$and δb_1 of eqs.(76) and (77) to obtain δb in eq.(75). Put

$$b^{(i+1)} = b^{(i)} + \delta b$$

Step 10. If constraints are satisfied,$|\delta \phi_\omega|$and$|\delta b_0|$ are sufficiently small, terminate an iteration. Otherwise return to Step 1.

The above algorithm is applied to three truss structures and the results are presented in the following section.

Example Problems

Aforementioned optimization procedure is applied to three truss structures illustrated in Figs.1,7,12. Dynamic model of each structure is formulated by using a finite element method and no damping is assumed. Time dependent force of 20 sin 24 t ton force(tf) is applied at a node of each structure as shown in the figures. The range of time considered is from 0.0 to 0.2 second,which complete two cycles of oscilation. In all example problems,allowable stress is taken to be 1400 kgf/cm , density of material is 0.00785 kgf/cm³, and minimum crossectinal area is chosen to be 0.01 cm . Design variable linking is done consdering a symmetry of structure,hence variables are 6,6, and 7 respectively.

Ten Member Truss

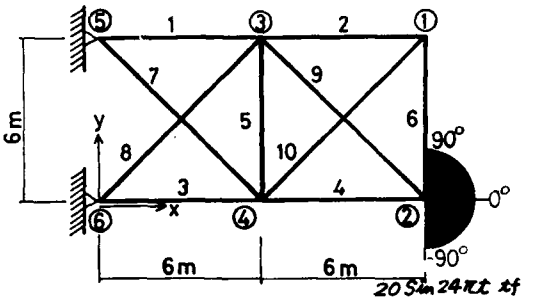


Fig. 1. 10 member Truss

Table 1. Optimum ten member truss

Group	Area (cm²)	Member	Stress(kgf/cm²) Tension	Stress(kgf/cm²) Compression	Angle (deg.)
1	39.1	1	1310	1241	81.8
		3	1375	1402	64.3
2	21.4	2	594	649	-90.0
		4	1215	1236	40.7
3	7.6	5	430	442	-20.5
4	12.6	6	699	726	77.9
5	31.1	7	823	825	84.8
		8	882	898	-90.0
6	28.3	9	787	816	-88.7
		10	623	664	76.6

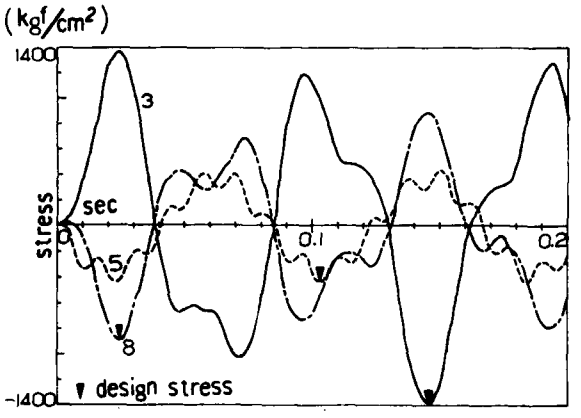


Fig. 2. Stress response of 10 member truss (member no. 3,5 and 8)

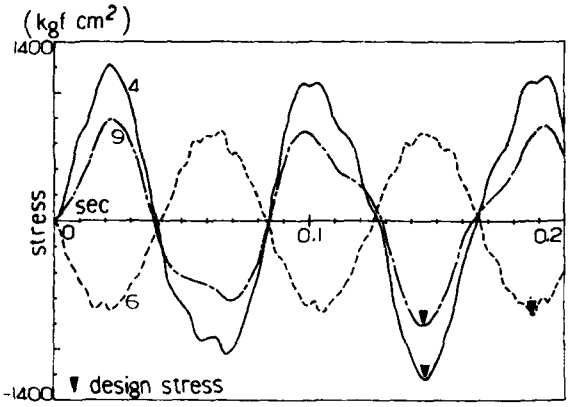


Fig. 3. Stress response of 10 member truss (member no. 4,6 and 9)

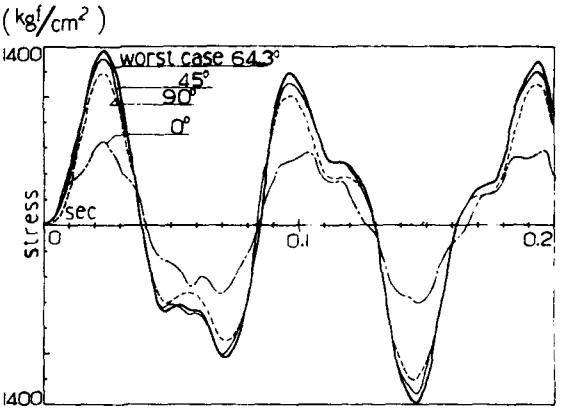


Fig. 6. Stress response of member 3 in 10 member truss with the values of α=0°,45°,64.3°,90°

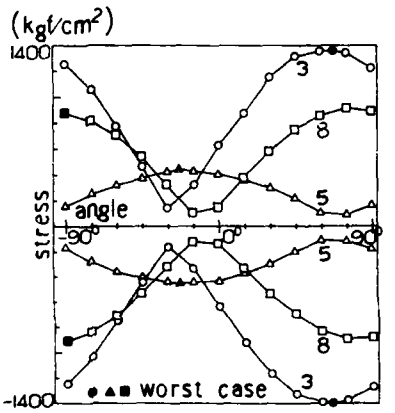


Fig. 4. Variations of maximum and minimum stresses due to the change of α. (member no. 3,5 and 8)

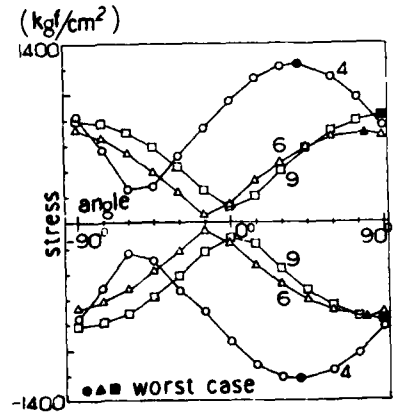


Fig. 5. Variations of maximum and minimum stresses due to the change of α. (member no. 4,6 and 9)

Twenty Four Member Truss

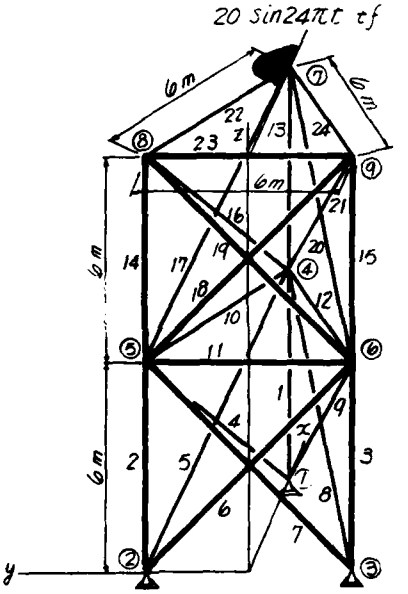


Fig. 7. Twenty four member truss

Table 2. Optimum 24 member truss

Group	Area (cm²)	Member	Stress (kgf/cm²) Tension	Stress (kgf/cm²) Compression	Angle (deg.)
1	60.4	1	1112	912	0.0
		2	1156	944	119.3
		3	944	1156	60.7
2	33.6	4	871	910	140.8
		5	962	969	114.3
		6	529	472	102.1
		7	467	535	69.6
		8	962	969	59.0
		9	895	888	49.5
3	10.0	10	491	579	77.5
		11	352	441	180.0
		12	579	492	105.1
4	23.2	13	739	899	180.0
		14	741	625	120.7
		15	625	740	59.3
5	31.6	16	602	614	132.8
		17	910	868	114.3
		18	273	278	103.8
		19	274	277	67.0
		20	866	912	61.7
		21	613	603	50.5
6	13.4	22	724	682	126.7
		23	109	125	180.0
		24	677	732	62.0

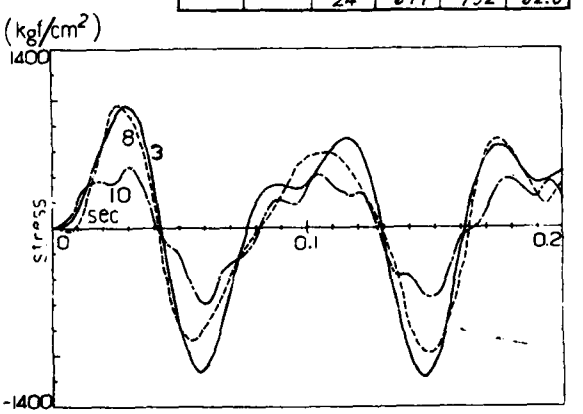


Fig. 8. Stress response of 24 member truss (member no. 3,8 and 10)

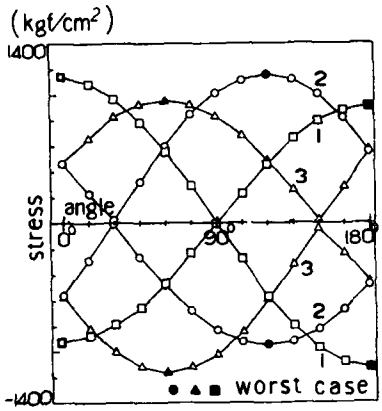


Fig. 9. Variations of maximum and minimum stresses due to the change of α. (member no. 1,2 and 3)

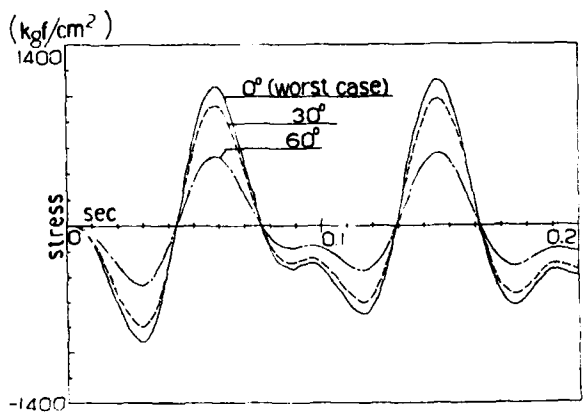


Fig. 10. Stress response of member 1 in 24 member truss with the values of α = 0°,30°and 90°

Twenty Five Member Truss

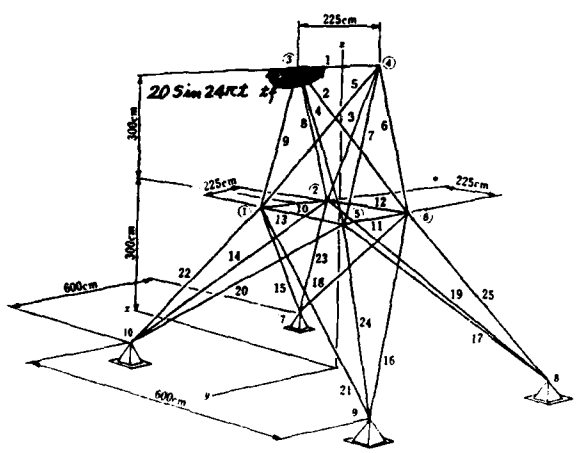


Fig. 11. Twenty five member truss

Table 3. Optimum 25 member truss

Group	Area (cm²)	Member	Stress(kgf/cm²) Tension	Stress(kgf/cm²) Compression	Angle (deg.)
1	11.0	1	808	798	0.0
2	19.8	2	910	905	50.0
		3	488	488	16.1
		4	906	910	130.0
		5	488	488	163.9
3	17.0	6	470	467	173.5
		7	467	470	6.5
		8	1156	1143	118.3
		9	1143	1156	61.7
4	1.4	10	442	448	180.0
		11	500	505	0.0
		12	346	342	61.0
		13	341	347	121.9
5	9.1	14	637	643	140.1
		15	643	637	41.6
		16	573	559	34.9
		17	557	575	139.9
6	12.5	18	288	275	159.9
		19	873	868	105.5
		20	271	291	35.3
		21	867	875	71.2
7	15.2	22	1248	1253	39.8
		23	1253	1248	140.2
		24	1392	1400	141.9
		25	1400	1392	38.1

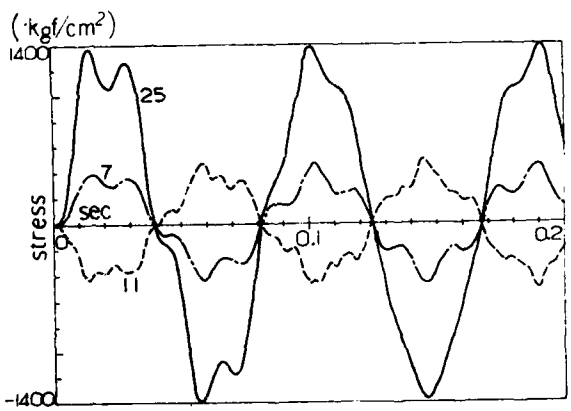


Fig. 12. Stress response of 25 member truss (member no. 7,11, and 25)

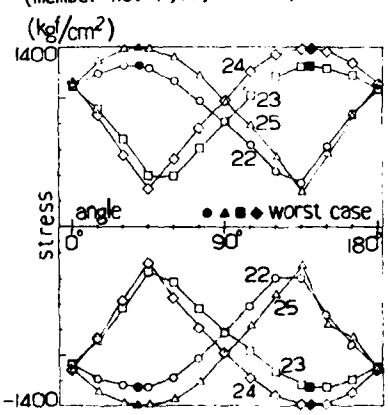
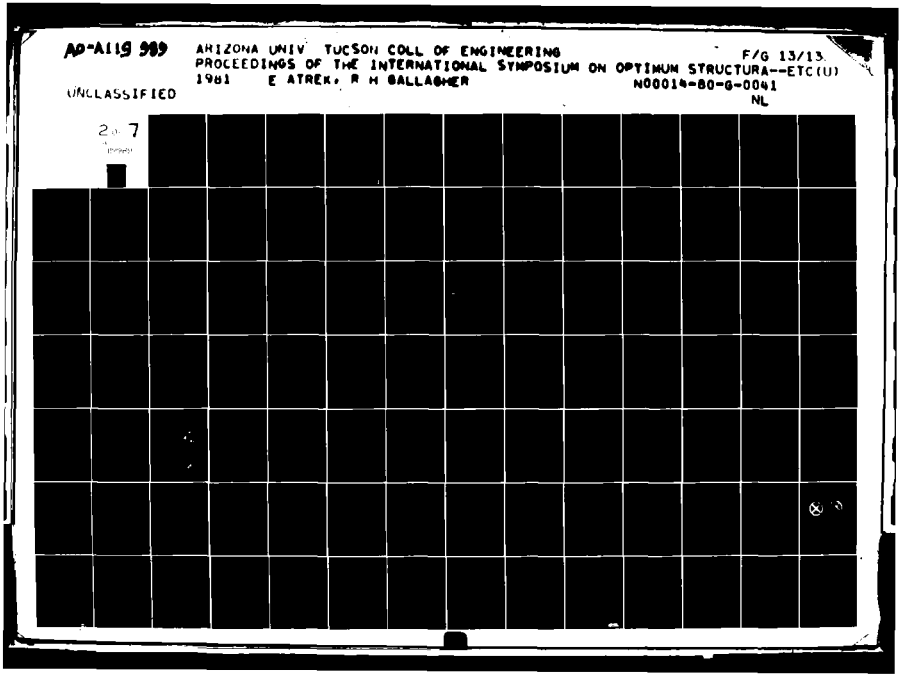


Fig. 13. Variations of maximum and minimum stresses due to the change of α.


AD-A119 989
ARIZONA UNIV TUCSON COLL OF ENGINEERING
PROCEEDINGS OF THE INTERNATIONAL SYMPOSIUM ON OPTIMUM STRUCTURA--ETC(U)
F/G 13/13
1981 E ATREK, R H GALLAGHER
N00014-80-G-0041
UNCLASSIFIED
NL
2 of 7

Tables 1 3 show optimum cross sectional area of structures and the direction of force which control the designs of truss members. As can be seen, the worst loading directions is different depending on members. Figs. 2,3,8 and 12 show stress response of members under their most unfavorable loadings. For 10 member truss, at least one member of every design group is tight, but in the cases of the space truses, this is not necessaryly true. Figs. 4,5,9 and 13 present variations of maximum(tension) and minimum(compresion) stresses of members ,when the direction of time dependent force changes. In Figs. 6 and 10, plotted are stress responses of member 3 in 10 member truss and member 1 in 24 member truss at their worst directions and at a few other directions.

Conclusions

The numerical results show the most unfavorable loading direction is different depending on members. Most structures on the earth are frequently exposed to disturbances from indefinite direction. Hence design has to be made with great care. Optimization algorithm presented appear to be very useful when designing structures under such loading conditions. The results in preceeding section could differ greatly if the frequency of external force changes.

References

(1) Brown, D. M. and Ang, A. H.-S., Structural Optimization by Nonlinear Programming, J. of Structural Division, ASCE,Vol.92, No.ST6, December 1966, pp. 93 - 102.

(2) Frind, E. O. and Wright, P. M., Gradient Methods in Optimum Structural Design, J. of Structural Division, ASCE, Vol.101, No. ST4, April 1974 pp. 939 - 956

(3) Haug, E. J., Arora, J. S. and Matsui, K., A Steepest-Descent Method for Optimization of Mechanical Systems, J. of Optimization Theory and Applications, Vol.19, No.3 July 1976

(4) Gallagher, R. H.,and Zienkiewicz, O. C., Optimum Structural Design : Theory and Appications, John Wiley and Sons, New York, 1973

(5) Dobbs, M. W. and Nelson, R. B., Application of Optimality Criteria to Automated Structural Design, AIAA Journal, Vol.14, No.10, October 1976, pp.1436 - 1443.

(6) Fleury, C. and Geradin, M., Optimality Criteria and Mathematical Programming in Structural Weight Optimization, Computers and Structures, Vol.8 1978, pp.7 -17.

(7) Fleury, C. and Schmidt, L. A., Primal and Dual Method in STructural Optimization, J. of Structural Division, ASCE, Vol.105, No.ST1, January 1979, pp.85 - 99.

(8) Trujillo, D. M., Application of Dynamic Progrmming to the General Inverse Problem, International J. for Numercal Methods in Engineering, Vol.12, 1978, pp.613 - 624.

(9) Chand, R., Haug, E. J. and Rim,K., Analysis of Unbonded Contact Problems by Means of Quadratic Programming, J. of Optimization Theory and Applications, Vol.20, No.2 October 1976, pp.171 - 189.

(10) Yanagisawa, I. and Yoshikawa, H., Numercal Analysis of Freezing Domain around Underground Storage Tank for Cryogenic Liquid using Integrated Penalty and Finite Difference Methods (in Japanese), JSCE, No.272, April 1978, pp.93 - 102.

(11) Arora, J. S. and Haug, E. J., Efficient Hybrid Methods of Optimal Structural, J. of Engineering Mechanics Divison, ASCE, Vol.104,No.EM3, June 1978, pp.663 - 680.

(12) Zarghamee, M. S., Optimum Freauency of Structures. AIAA Journal, Vol.6, No.4, April 1968, pp.749 - 750.

(13) Rubin, C. P., Minimu Weight Design of Complex Structures Subject to a Frequency Constraint, AIAA Journal, Vol.8, No.%, May 1970, pp.923 - 927

(14) Fox, R. L. and Kapoor, M. P.,Structural Optimization in the Dynamic Response regime· A Computational Approach, AIAA Journal, Vol.8, No.10, October 1970, pp.1798 - 1804

(15) Cassis, J. H. and Schmodt, L. A., Optimum Structural Design with Dynamic Constraints, J. of the Structural Division, ASCE, Vol.102, No.ST10, October 1976, pp.2053 - 2071.

(16) Feng, T. T., Arora, J. A. and Haug, E. J., Optimal Structural Design under Dynamic Loads, International J. for Numerical Methods in Engineering, Vol.11,No.1, 1977, pp.35 - 53.

(17) Gurpinar, A and Yao, J. T. P., Design of Columns for Seismic Loads, Journal of Structural Division ASCE, Vol.99, No.ST9, pp.1875 - 1889.

(18) Vitiello, E. and Pister, K. S., Optimal Earthquake Resistant Design, ASCE National Structural Engineering Meeting, April 22 - 26, 1974 (reprint)

(19) Rosenblueth E., Optimum Desigh to Resist Earthquakes, J. of Engineering Mechanics Division, ASCE, Vol.105, No.EM1, February 1979, pp.159 - 176

(20) Ajorinde, E. O. and Warburton, G. B., Minimizing Structural Vibrations with Absobers, Earthquake Engineering and Structural Dynamics, Vol.8, pp.219 -236.

(21) Yang, J.-N., Application of Optimal Control Theory to Civil Engineering Structures, J. of the Engineering Division, ASCE, Vol.101, No.EM6, December 1975, pp819 - 839

(22) Yang, J.-N. and Giannopoulos,F. Active Tendon Control of Structures, J. of the Engineering Mechanics Division, ASCE, Vol.104, No.EM3, June 1978, pp.551 - 568

(23) Abdel-Rohman,M. and Leipholtz, H. H. E., Active Control of Flexible Structures, J. of the Structural Division, ASCE, Vol.104, No.ST8, August 1978, pp.1251 - 1266.

(24) Abdel-Rohman, H. and Leipholtz, H. H. E., General Approach to Active Structural Control, J. of the Engineering Mechanics Division, ASCE, Vol.105, No.EM6, December 1979, pp.1007 - 1023.

(25) Leipholtz, H. H. E. ed. Structural Control, Proceedings of the International IUTAM Symposium on Structural Control, June 4 - 7, 1980.

(26) Kwak, B. M. and Haug, E. J., Optimum design in the Presence of Parametric Uncertainty, Journal of Optimization Theory and Applications, Vol.19 No.4, August 1976,pp.527 - 546.

(27) Kwak, B. M. and Haug, E. J., Parametric Optimal Design, Journal of Optimization Theory and Applications, Vol.20, No.1, September 1976, pp.13 - 35.

AD-P000 037

LIFETIME COST EARTHQUAKE RESISTANT DESIGN: AN ALGORITHM FOR AUTOMATION

Norman D. Walker, Jr.
Kaiser Aluminum & Chemical Corp.
Center for Technology
Pleasanton, Calif. 94566

Summary

An automated design methodology is proposed which exploits the principal features of a lifetime cost approach to earthquake resistant design developed in a previous paper. Several examples are presented which explore the lifetime cost formulation and the proposed design algorithm.

Introduction

The usual approach to multistory building frame optimization utilizes least weight (minimum construction cost) as the design objective, with numerous constraints typically imposed following local building codes. For structures located in seismically active regions, least weight remains the design objective with additional constraints employed to suitably restrict structural response to earthquake loading. Unfortunately, for buildings located in seismic regions, structural related expenses are not confined to construction. Earthquake damage incurred throughout the life of the building is directly related to structural adequacy. With this in mind, a lifetime cost (LC) approach to the design of earthquake resistant multistory steel building frames has been proposed and explored in some detail in previous work [1, 2]. In the LC approach, the design objective is the minimization of lifetime costs including construction related expenses and maintenance and repair costs associated with earthquake damage. A methodology for the computation of lifetime cost estimates has been developed along with associated design constraints for the class of structure being considered. This formulation is briefly reviewed here before turning to the central thrust of this paper, namely, the construction of a computer-based automated/optimal design algorithm.

Background

The problem addressed here is the selection of member sizes for single-bay, multistory, unbraced steel building frames with fully rigid connections. Member selection is restricted to the set of A-36 rolled steel wide flange economy sections. Moment of inertia of the member cross-section is used as the design variable. The collection of design variables for the complete frame is referred to as the design vector.

Performance constraints under operating loads are introduced through typical building code requirements. Considered here, under uniformly distributed beam loads, are stress limitations on the beams and columns, beam deflection allowables and sidesway stability.

Earthquake loading is introduced through the imposition of horizontal ground motion with structural response computed using mode superposition techniques. Design limitations are based on a dual criterion involving both moderate and strong earthquake responses. Under moderate earthquake loading elastic structural response is required; during strong earthquake motions collapse must be avoided. Strong and moderate design earthquakes are selected on the basis of their probability of occurrence.

The design objective is cost minimization over the entire life of the structure, wherein only costs strongly related to the design vector are considered. The LC associated with multistory framed buildings separates into two categories: (1) cost of construction and (2) cost of damage associated with structural overload, here assumed to result from earthquake exposure.

Design vector dependent construction costs include the structural members, beam-column connections including welding, structural metal transportation, field painting, project overhead and profit.

Damage costs resulting from earthquake-induced structural overload can be divided into three categories: structural and nonstructural damage and down-time costs. For steel framed buildings structural damage is usually negligible and is assumed so here. Items susceptible to nonstructural damage and accommodated here are interior drywalls, glazing and masonry. Down-time costs are taken as a percentage of damage costs.

To compute lifetime cost an expected earthquake profile for the particular site and planned service life of the building must be developed. The damage cost for each earthquake in the profile is then computed and the resultant costs summed over all expected earthquakes.

The LC formulation outlined above, and elucidated in more detail in [1, 2], was explored in a recent paper using the example of a one-story frame [2]. Through this mechanism prominent features of the problem were identified. Taking advantage of this problem structure a three-phase design methodology is proposed. In the first phase initial designs are formulated based on the unconstrained optimal, i.e., the optimal design is found disregarding the design constraints. The second phase develops usable designs from unusable designs. That is, all unsatisfied constraints for a particular design are resolved. The third phase provides for design improvement, producing better designs, in terms of the design objective, from usable designs.

These three phases are integrated into a complete design algorithm which calls upon each as necessary in a march toward the optimal. In addition, each phase is accessible individually to aid in the design process on a more limited basis.

In the sequel each phase is discussed alone and as part of the complete algorithm. A computer code based on this approach is then applied to some examples to further explore the LC approach to earthquake resistant design.

Initial Design

The essential characteristics of an initial design are that it be relatively inexpensive to obtain and that it represent a good estimate of the optimal (i.e., final) design. Based on previous work it is known that the unconstrained LC optimal lies in close proximity to the constrained LC optimal. In addition, the LC objective function is close to being uncoupled in form, that

is, the principal directions in the cost surface are nearly parallel to the coordinate axes formed by the components of the design vector. Hence, locating the unconstrained optimal should be relatively straightforward. The unconstrained optimal thus represents a good choice as an initial design.

When dealing with uncoupled objective functions, coordinate descent algorithms have been found to be very effective in determining the optimal [3, 4]. A variant of such procedures is adopted here.

Let f represent the cost function, then the essence of the coordinate descent approach is contained in the expression

$$\min_{x_i} f(x) \quad \text{for all } i \ , \qquad (1)$$

where x is the design vector with components x_i. As the expression indicates, the unconstrained optimal is sought by searching in turn in each coordinate direction x_i. For n components in the design vector, n line searches are required to find the optimal. If each of these line searches is conducted independently, then at the very least, one new analysis for each line search is required, for a total of n+1 analyses to find the optimal. For large structural systems this represents an enormous number of expensive analyses and is clearly unacceptable.

In order to improve upon this situation, a simultaneous coordinate search procedure is adopted. In this approach, searches in all coordinate directions remain independent of one another. However, every new point in each coordinate search is analyzed simultaneously with each new point in all the other coordinate searches. Thus, instead of a new structure being $(x_1, x_2 \ldots, x_i + \Delta x_i, \ldots, x_n)$ as would result from a pure coordinate search it is instead $(x_1 + \Delta x_1, x_2 + \Delta x_2, \ldots, x_n + \Delta x_n)$. To conduct each of the individual coordinate searches the method of bisection is employed. The signs of the directional derivatives of f are used to motivate each coordinate search.

Let x^k represent the present design vector with components x_i^k. The gradient of the cost function at the present design is represented as $\nabla f(x^k)$ with components ∇f_i. A simple algorithm for completing the simultaneous coordinate search is as follows:

Step 0. Set vectors β and ϵ .

Step 1. Compute Δx where $\Delta x_i = -\beta_i \ \nabla f_i(x^0)$; set k = 0 and go to step 3.

Step 2. Compute $\nabla f(x^k)$.

Step 3. For all x_i^k in x^k: if $\nabla f_i(x^k) > 0$ then $u_i = x_i^k$; if $\nabla f_i(x^k) < 0$ then $\ell_i = x_i^k$; otherwise, $u_i = \ell_i = x_i^k$.

Step 4. For all x_i^k in x^k: if u_i and ℓ_i have been established for x_i^k then $x_i^{k+1} = (u_i + \ell_i)/2$; otherwise, $x_i^{k+1} = x_i^k + \Delta x_i$.

Step 5. If $u - \ell \leq \epsilon$ stop, x^{k+1} is the initial design vector, else go to step 6.

Step 6. Set k = k+1 and go to step 2.

where the inequality in step 5 implies component by component comparison.

This algorithm completes two tasks. It begins by establishing an initial set of bounding intervals about the optimal. It then proceeds via the method of bisection to reduce these bounding interval lengths to a sufficiently small size such that the midpoints of all the final intervals represent a satisfactory estimate of the unconstrained optimal.

The vector Δx computed in step 1 is a search vector used in establishing the initial bounding intervals. Its components are taken to be proportional to the corresponding components of the gradient of the objective function at the starting vector x^0. The constants of proportionality are contained in the vector β. Through this mechanism the magnitudes of the components of the search vector are set according to how far away from the optimal value each component is estimated to be.

In step 3 the coordinates of the present design vector are determined to represent either upper or lower bounds for a new set of bounding intervals. The upper bound point is contained in the vector u and the lower bound point in the vector ℓ.

A new design vector for the next iteration is determined in step 4. This determination is made at the component level according to whether or not a bounding interval has been established or not. If one has, the present interval is bisected; if not the search continues.

The procedure terminates when all the bounding intervals are smaller than some required length. The set of stop lengths is contained in the vector ϵ.

This constitutes phase 1 of the design procedure. This phase can be called upon to supply an initial design vector in lieu of a user supplied initial design.

Usable Designs

The next portion of the algorithm, phase 2, deals with the generation of usable designs from unusable ones. A design is unusable when one or more of the system constraints is violated. The task of phase 2 is to adjust the initial design so as to satisfy the violated constraints.

If the initial design is the unconstrained optimal generated by phase 1, then the constrained optimal will lie on the surfaces of the violated constraints. Minimal satisfaction of the violated constraints is thus desirable and serves as the mode of operation for phase 2. Phase 2 thus amounts to a search for the surfaces of violated constraints.

In the case of user supplied initial designs the above apparatus works equally well.

As noted in previous work [1, 2] the constraint functions dealt with here display little design variable coupling, that is, each is essentially dependent on only one component of the design vector. Therefore, coordinate search procedures are again appropriate. Because the constraint functions tend to be very smooth and uniform, curve fitting along fixed lines should be extremely efficient. This, coupled with the expectation that only a few constraints will be violated, dictates that standard coordinate search procedures be used rather than the simultaneous search method used in phase 1.

Let g represent the vector of constraint functions with components g_i then the constraint surfaces are given by $g_i(x) = 0$ for each i. Phase 2 thus involves finding the roots of nonlinear equations. Initially,

in the search for these roots information is available at only one point, the initial design. Assuming only function value and gradient data are supplied at this point, Newton's method must be employed in the line search to obtain the first estimate of an x which satisfies $g_i(x) = 0$. If x^k is the present design and x^{k+1} is the estimated root then Newton's iteration formula can be expressed as

$$x^{k+1} = x^k - \lambda^k h(x^k) \tag{2}$$

where

$$\lambda^k = g_i(x^k) / g_i'(x^k) \tag{3}$$

with

$$g_i'(x^k) = \nabla g_i(x^k)^T h(x^k) \tag{4}$$

where a line search along the vector h emanating from x^k is assumed. To conduct a pure coordinate search h is taken to be the unit base vector e_j which corresponds to the coordinate x_j which is to be searched.

When the constraint function is evaluated at x^{k+1}, information at two points is available. At this juncture, the derivative estimated iteration formula [5] given by

$$\lambda^k = \frac{g_i(x^k)}{g_i'(x^k)} + \frac{\left[g_i(x^k)\right]^2}{2\left[g_i'(x^k)\right]^3} \bar{g}_i'' \tag{5}$$

where

$$\bar{g}_i'' = \frac{-6}{(\lambda^{k-1})^2}\left[g_i(x^k) - g_i(x^{k-1})\right] + \frac{2}{\lambda^{k-1}}\left[2\, g_i'(x^k) + g_i'(x^{k-1})\right] \tag{6}$$

can be employed in equation (2), where g_i' is again found from (4). If necessary, this formula can be reused on the last two points of the sequence $\{x^k\}$ until a satisfactory estimate of the root is obtained.

During the line search, to avoid violating constraints which lie close to the present design vector, an additional mechanism is utilized. Rather than conduct the search along a coordinate base vector, the base vector is instead projected onto the surface of active constraints (all constraints i for which $g_i(x^k) = 0$) and this projection then serves as the search line. The search thus takes place along a tangent to the active constraint surface thereby reducing the possibility that these active constraints will be violated. To present the projection operator, an additional definition is required.

Let A be a matrix whose columns are composed of the gradients of the active constraints at x^k, that is

$$A = \left[\nabla g_i(x^k) \;\ldots\ldots\; \nabla g_j(x^k)\right] \tag{7}$$

where g_i through g_j are active constraints and ∇g_i is a column vector.

The gradient projection operator is given by

$$P = I - A\,(A^T A)^{-1} A^T \tag{8}$$

where I is the identity matrix. The search vector h in equation (2) is found from $h = Pe_j$ where e_j is the appropriate unit base vector.

In the case where the initial design is given by the unconstrained optimal, further refinement is called for. Intuitively, it would seem that the constrained optimal should lie close to the projection of the unconstrained optimal onto the violated constraint surface. Hence, for this case, several additional steps have been added to the end of phase 2 which adjust the phase 2-determined usable design to the usable design given by the above projection.

The algorithm for completing all of the aforementioned operations is as follows:

Step 1. Determine A at x^k from (7) and P from (8).

Step 2. If x^k is usable go to step 7; else select one violated constraint and the e_i which corresponds to the design vector component which this constraint governs and compute $h = Pe_i$.

Step 3. Compute x^{k+1} from (2) and (3).

Step 4. Set k = k+1.

Step 5. If constraint now satisfied, go to step 1.

Step 6. Compute x^{k+1} from (2) and (5) and go to step 4.

Step 7. Compute $h = P(x^i - x^k)$ and $x = x^k + h$.

Step 8. If x is usable, stop; else, determine α such that $x^k + \alpha h$ is usable.

Step 9. Set $x^{k+1} = x^k + \alpha h$; k = k+1 and go to step 1.

If the initial design is supplied by the user, then the algorithm terminates with a usable design in step 2. Thus, the last three steps are entered only if the initial design is the unconstrained optimal generated in phase 1. For this case, the last three steps and step 1 constitute an adjustment operation. The usable design which results from the first six steps is adjusted to approximate the projection of the unconstrained optimal onto the surface of violated constraints as discussed previously. The design vector x^i referred to in step 7 is the initial (i.e., unconstrained optimal) design. If phase 1 is employed in conjunction with phase 2, then at the conclusion of phase 2 what should result is a good estimate of the location of the optimal design.

Note that if the initial design is found to be usable, then almost all of the phase 2 apparatus is skipped and control is passed onto phase 3. Thus, the above algorithm is used only in the case of an unusable initial design.

At the close of phase 2, at the very least, a usable design is available and, at best, a good estimate of the optimal design. The scene is thus set for a formal search for the optimal design which brings the design automation procedure to phase 3.

Optimal Design

Phase 3 is the design improvement portion of the automated design algorithm. This phase begins with a usable design which, if supplied by phase 2, resides on a surface of active constraints. Since the optimal design is in general expected to be partially constrained, a computational method which is efficient in moving along constraint surfaces would appear to be called for.

An appropriate approach to this phase is provided by the gradient projection method [3, 4]. In this procedure, the gradient of the cost function, ∇f, at the present design, x^k, is projected onto the surface of active constraints. This projected gradient then serves as a direction vector for one iteration in the search for the optimal. The algorithm searches along the surface of the present set of active constraints until a candidate optimal is found. The first-order necessary conditions (Kuhn-Tucker), are then checked at this point to see if they are satisfied. If they are, the procedure stops; otherwise, the current projection operator is appropriately modified and the search continues. Thus, the gradient projection algorithm proceeds roughly as follows:

Assume x^k is usable, then

Step 1. Find the set of active constraints at x^k and form A as given by (7).

Step 2. Compute P from (8) and $d = -P\,\nabla f(x^k)$.

Step 3. If $d = 0$, go to step 5, otherwise find $\bar{\alpha}$ such that $f(x^k + \bar{\alpha}d) = \min \{ f(x + \alpha d) \mid \alpha \geq 0$ and $x + \alpha d$ is usable$\}$.

Step 4. Set $x^{k+1} = x^k + \bar{\alpha}d$; $k = k + 1$ and go to step 1.

Step 5. Compute $\beta = -(A^T A)^{-1} A^T \nabla f(x^k)$.

Step 6. If $\beta_j \geq 0$ for all β_j in β then stop, x^k is the optimal, otherwise go to step 7.

Step 7. Delete the column from A corresponding to the constraint with the most negative component of β and go to step 2.

Refinements are obviously necessary in order to make this algorithm implementable. For example, the "ϵ procedure" of [4] is employed for computational reasons [6] and to insure convergence [4]. In addition, a means of establishing $\bar{\alpha}$ in step 3 is required. To this end, a cubic equation is fit [3] through two points on the line $x + \alpha d$ with the minimum of this cubic being used to define $\bar{\alpha}$. One point on the line is obviously the present design. The second point is selected through the use of a heuristically maintained step size variable. Using the value and gradient of the objective function at these two points, the next point is selected using the equations

$$x^{k+1} = x^k + \alpha d \tag{9}$$

where

$$\alpha = -p\left[\frac{f'(x^k) + v - u}{f'(x^k) - f'(x^{k-1}) + 2v}\right]$$

$$u = f'(x^{k-1}) + f'(x^k) + \frac{3}{p}\left[f(x^{k-1}) - f(x^k)\right]$$

$$v = \left[u^2 - f'(x^{k-1})\, f'(x^k)\right]^{\frac{1}{2}}$$

with $\quad f'(x^k) = \nabla f(x^k)^T d$

where p is the step size variable used in selecting the second point x^k, thus, p is given by $pd = x^k - x^{k-1}$.

In order to procure an $x + \alpha d$ which is usable, the constraint location apparatus of phase 2 is employed to modify α whenever $x + \alpha d$ makes an excursion into the unusable design space. This suitably modified α becomes $\bar{\alpha}$ and the algorithm proceeds on.

The stop criterion in the above computational sequence is that $d = 0$. In actual implementation this condition is impossible to satisfy and must be replaced with the more appropriate requirement that $d \leq \eta$ where η is a vector of small values.

The result of phase 3 is an estimate of the optimal design which is as refined as the user cares to specify and pay for.

The three phases presented in this and previous sections have been collected into a computer based automated/optimal design algorithm. Most of the features of this algorithm have been presented. Some further refinements have been added to enhance the program's flexibility, however.

If the user specifies an initial design, phase 1 is skipped entirely. Furthermore, if an initial design is usable most of phase 2 is passed over. The process can be terminated at the conclusion of phase 2 if desired, yielding simply a usable design; if phase 1 was employed then the result of phase 2 is a good estimate of the optimal design. Alternatively, design improvement can be attempted using the apparatus of phase 3. All of the designs generated in phase 3 are usable, thus, this process can be stopped at any time. The design improvement procedure can be terminated in two ways. The user can either specify the number of design improvement iterations desired or an acceptable accuracy for the optimal design estimate. Thus, phase 3 can be tailored to fit the needs and pocket book of the user.

A phase 4 is also present in the algorithm. This phase facilitates the option of specifying that only a subset of the full set of constraint functions be checked for violation during the design process. With this mechanism, constraint functions which are known to be unimportant in the design definition, can be eliminated from consideration at the outset. A full check of all system constraints is made only on the final design. A detailed discussion on the order of importance of constraints and the use of phase 4 can be found in [1].

Note that derivative information for the lifetime cost and system constraints has been assumed throughout this presentation. While specific derivative information has not been developed herein, it is quite straightforward to obtain. A fairly complete discussion of similar derivative computations can be found in [6].

Examples

To explore the LC formulation and the automated design algorithm developed here, three example problems are investigated. The one-story frame introduced in [2] is briefly explored along with a four-story frame and an eight-story frame.

One-Story Frame

The principal specifications for the one-story frame are given in [2] and will not be reiterated here.

As the optimal design for this problem is known to be unconstrained, only the apparatus of phase 1 is required in the design search. Applying the design algorithm to this problem results in the sequence of intervals shown in Fig. 1. The starting point for the search, selected simply for the sake of illustration, is labeled (1) and is a considerable distance away from the optimal. The large rectangles in the figure repre-

sent attempts to establish bounding intervals. Once a bounding interval is found subsequent intervals are nested within it. Thus, the nested rectangles represent bisected intervals obtained as the procedure converges about the optimal. The sequence of analysis points in this operation are given as the circled numbers and extend only through (5) to avoid further confusing the figure. The cost lines given in the figure are computed from the relationship

$$\text{Cost} = \frac{100\ [LC(X) - LC(X^*)]}{\text{Construction Cost at Optimal}} \qquad (10)$$

where LC(X) is the lifetime cost as a function of the present design vector X and X* is the optimal (minimum LC) design vector.

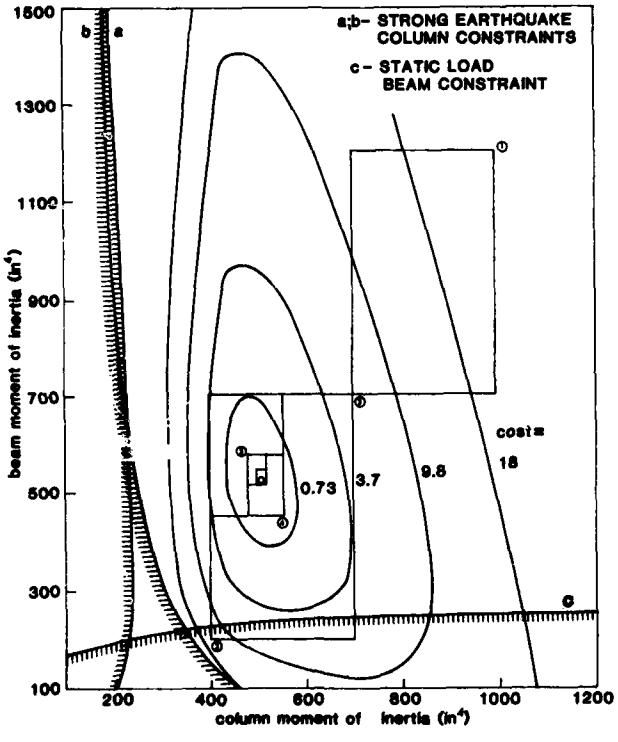


Fig. 1. Solution sequence: one-story frame.

Although it is not shown in the figure, it is not necessary for all of the bounds on each coordinate to be established before the bisection process can begin. Since each of the coordinate searches is conducted, essentially independently of one another, some coordinate intervals may be bisecting while others are still in the bound search mode. If the available search parameters are properly adjusted, this type of activity should not be very prevalent, however.

Four-Story Frame

A somewhat more interesting problem is found with a four-story frame. This frame will be used to further explore the design space which results from the LC approach to design, a task started in [2]. A very good initial design was available for this particular problem and thus it did not represent an adequate test of the automated design algorithm. Observations on the operating characteristics of the automated design algorithm will, thus, be reserved for the more difficult problem of the eight-story frame.

The principal characteristics of the four-story frame, other than its height, are similar to the one-story structure introduced in [2] and discussed in the previous section. A detailed description of the four-story frame is given in [1].

The optimal design is depicted in part in Figs. 2 and 3. Each of these figures was constructed around the optimal frame design by varying two components of the design vector while fixing the remainder, thereby obtaining a two-dimensional view of a portion of the design space. The constraint functions illustrated are those associated with the selected design vector components, thus, many of the system constraint functions are not shown. In particular the single active constraint at the optimal is not illustrated. It is a strong earthquake load limitation on the second-story column.

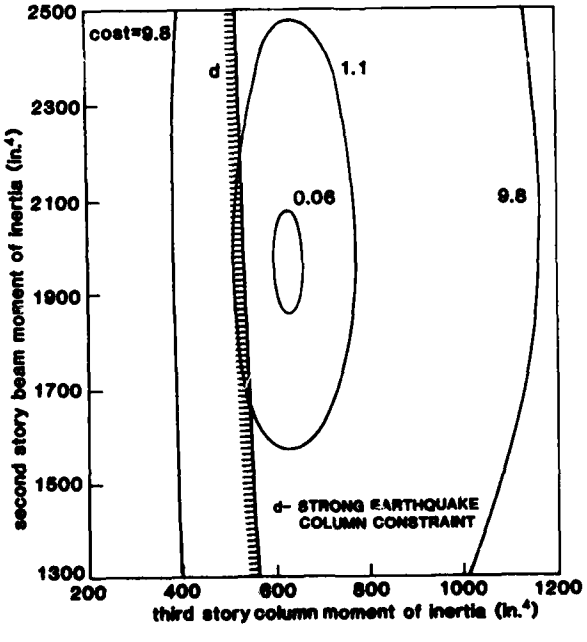


Fig. 2. Beam versus column design space.

The principal observations of [2], made on the basis of a one-story frame, can be clearly seen in Figs. 2 and 3.

First, the optimal design is only partially constrained. Thus, the optimal design is defined only in part by design limitations and in the main by the objective function. This is in striking contrast to least

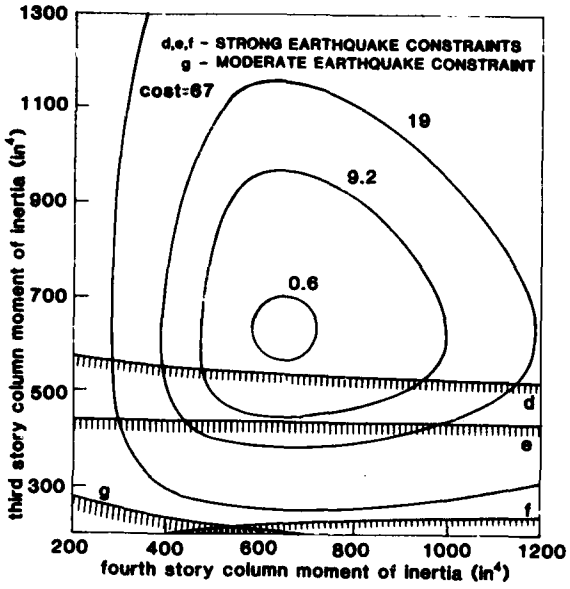


Fig. 3. Column versus column design space.

weight optimals which are typically fully constrained, as they must be, since the least weight criterion contains no extremum.

Second, it is apparent that the constraint functions are nearly uncoupled as each is roughly parallel to one axis or the other. This characteristic of the constraint functions, i.e., the lack of dependency on all but one component in the design vector, forms the basis for the constraint search mechanism of phase 2.

Third, the cost surfaces displayed in these figures carry the appearance of uncoupled functions. That is, the principal directions in the cost surface (eigenvectors of the Hessian of the cost function) are nearly parallel to the axes. This is the same result as was obtained for the one-story frame shown in Fig. 1, the effect is clearly more pronounced, however, for the four-story objective function, as was anticipated [2].

Note that the cost lines in Figs. 2 and 3 were computed using equation (10) with the construction cost in the denominator representing the individual frame members being examined.

One final feature is worthy of comment. The initial design mechanism of phase 1 is based on the assumption that the constrained and unconstrained optimals lie close to one another in the design space. For the four-story frame this was indeed found to be the case with the constrained and unconstrained designs differing essentially only in the size of the second story column. This result is easily anticipated since the two optimals are separated by only a single design limitation.

The minimum construction cost (weight) frame for the same set of conditions was also computed. As expected it was found to be fully constrained. The construction cost for this frame is 28% less than that for the minimum LC frame. Its LC, however, is 10% higher than for the LC based results. Both designs represent acceptable practice, they are strikingly different, however, with the minimum weight frame substantially more flexible than the optimal LC frame, reflecting a very real difference in design philosophy.

Based on the results of this section the automated design algorithm developed herein appears to offer a viable methodology for design on the basis of a minimum lifetime cost objective. Evaluation of the numerical efficiency of this algorithm is reserved for the eight-story frame analysis of the next section.

Eight-Story Frame

The eight-story frame examination serves a two-fold purpose. First, it is of interest to determine what effect, if any, frame height has on the results ascertained to this point. Second, a clear test of the design algorithm is in order. The eight-story frame examined here is identical to the previous four-story structure except that eight stories are involved instead of four. A complete description of the eight-story frame can be found in [1].

The initial design selected for the analysis is given by $X = 1000\,u$ where u is the unit vector (vector of ones). Despite such a poor starting vector, phase 1 of the automated design algorithm required only nine analyses to locate the unconstrained optimal. Included in these nine analyses is the interval establishment and interval bisection operations. The simultaneous coordinate search procedure would thus appear to work quite well.

An additional nine analyses were required to complete phase 2 of the algorithm. It was necessary to resolve four violated constraints in this phase: four strong earthquake loading limits dealing with the second, third and fourth story columns. Thus, the optimal was again found to be only partially constrained. During this phase the LC increased only 0.35%, clearly indicating the close proximity of the constrained and unconstrained optimals.

Phase 3 produced minor changes in the phase 2 result, lending support to the conjecture that projection of the unconstrained optimal onto the violated constraint surface results in a good estimate of the constrained optimal. Despite this, phase 3 consumed 25 analyses. The explanation for this seeming inconsistency is two-fold.

First, it is a reflection on the poor convergence rate of the method of steepest descent, which is the technique used in the active constraint space (projected gradient space) to pursue the optimal (see step 3 in the gradient projection algorithm). As can be seen in Figs. 2 and 3, the design space is somewhat ill-conditioned. This situation carries over into the active constraint space. The method of steepest descent is a poor choice under these conditions. Better use of the projected gradient in the active constraint space would most certainly shorten phase 3.

Another probable cause for the longevity of phase 3 is what appears to be an unrealistically small stop criterion (the η in $d \leq \eta$). The criterion used herein was chosen with investigation in mind, rather than design, and thus is smaller than what would be employed in a design office.

One further item of note is the superb performance of the constraint function search apparatus which was presented as part of the phase 2 development. Despite repeated tests of these procedures at sometimes considerable distances from violated constraint surfaces, more than two iterations were never required

and in actual operation one iteration usually proved to be sufficient. This is in direct contrast to the difficulties encountered in [6] using alternative procedures. It would be difficult to improve upon this performance.

In general the overall number of analyses required during each phase of the algorithm depended greatly on the numerical tolerances which were specified. These tolerances are given as recommended values in [1] and should be accommodated in any future algorithmic comparison.

It must be stated that the algorithm as developed here does not represent a final polished product. It is composed of essentially off-the-shelf items, usually in their most rudimentary forms. It is presented primarily to demonstrate the inherent simplicity and efficiency which results from developing solution procedures specifically suited for the problem being addressed. The algorithm is also presented as a possible methodology for automation of the LC approach to design. The algorithm is operational and thus provides a foundation for further developments in this direction. In addition there is considerable room for improvement in this algorithm. It seems very probably that the operational cost of this automated design program could be brought in line with design office budgets.

Conclusion

An automated design methodology has been presented which is specifically tailored to the lifetime cost design approach for multistory building frames in seismically active regions. The design algorithm takes advantage of the principal characteristics of the LC formulation, resulting in an efficient computer code which holds promise of eventually achieving operational cost levels compatible with design office budgets. Much work remains to be done in this regard. It is hoped that what has been presented here will provide a firm foundation for this endeavor.

In conjunction with [1, 2], this effort has shown in a limited fashion the potential viability of the lifetime cost design philosophy. The lifetime cost approach results in a distinctly different design alternative to standard minimum weight (construction cost) procedures. A definite choice is thus available with the LC approach deserving serious consideration in this context.

Acknowledgement

The author would like to express his appreciation to Professor Karl S. Pister of the University of California, Berkeley, for his contributions and continuous support throughout the conduct of this effort. This research was sponsored by the National Science Foundation through grants to the University of California, Berkeley.

References

1. N. D. Walker, Jr., "Automated Design of Earthquake Resistant Multistory Steel Building Frames," University of California, Berkeley, Report No. EERC 77-12 (1977).

2. N. D. Walker, Jr. and K. S. Pister, A Lifetime Cost Approach to Automated Earthquake Resistant Design. Proc. of the Seventh World Conference on Earthquake Engineering. Istanbul, Turkey (1980).

3. D. G. Luenberger, Introduction to Linear and Nonlinear Programming, Addison-Wesley (1973).

4. E. Polak, Computational Methods in Optimization, Academic Press (1971).

5. A. Ralston, A First Course in Numerical Analysis, McGraw-Hill (1965).

6. N. D. Walker, Jr. and K. S. Pister, "Study of a Method of Feasible Directions for Optimal Elastic Design of Framed Structures Subjected to Earthquake Loading," University of California, Berkeley, Report No. EERC 75-39 (1975).



AD-P000 038

A COMPARISON OF RELIABILITY BASED OPTIMUM DESIGNS AND AISC CODE BASED DESIGNS

by

Kamal B. Rojiani
Assistant Professor
Department of Civil Engineering
Virginia Polytechnic Institute and State University
Blacksburg, Virginia 24073

and

Gregory L. Bailey
Structural Engineer
Union Carbide Corporation
South Charleston, W VA 25303

Summary

A comparison of designs of steel frames using a reliability based optimization procedure and the deterministic AISC code procedure is presented. The reliability based optimization procedure utilizes an iterative method to produce designs for each structure at various prescribed risk levels. The optimum risk level, expressed in terms of the probability of failure of the structural system, is then obtained as that value which results in the minimum total expected cost. The total cost is taken as the sum of the initial cost and the expected cost of failure. The factors considered in the computation of the expected cost of failure include: replacement cost of the structure, business losses, and liability due to death and injury. The reliability analysis is based on a first order second moment approach treating loads and resistances as statistically independent random variables. Several modes of failure for both beams and columns are considered in the reliability analysis. Upper and lower bounds on the probability of failure of the structural system and on the total cost are computed.

The results indicate that there are significant differences in designs obtained by the two methods for the five and ten story steel frames considered. The AISC design results in a structure with lower initial cost than the reliability based method. However, the reliability based method produces designs with lower total expected cost. It is also found that designs based on the AISC specifications do not result in a consistent system failure probability.

Introduction

Many proposals for the introduction of probabilistic methods in design codes have been made in recent years. This is due to an awareness of the advantages that a reliability based procedure has over a deterministic design procedure. In the probabilistic approach, the loads and the structural resistance are treated as random variables rather than fixed deterministic constants, and failure is defined as the event that the load effect exceeds the structural resistance. The safety measure that corresponds to this is the probability of failure (or the reliability index) which is obtained from a systematic analysis of the uncertainties in all the variables. It is thus possible to include the effect of the uncertainties in the load and structural resistance in the design process. Such a method can also provide a uniform and consistent level of safety among similar structures. Furthermore, the level of safety can be adjusted by the designer according to the type, location, and importance of the structure.

Several schemes for structural optimization based on reliability have been suggested. These include: minimization of the cost or weight for an allowable failure probability, minimization of the probability of failure for a fixed cost and, minimization of the total overall cost. Most studies concerning reliability based optimum design consider the first two procedures. Also, the analysis is usually limited to either statically determinate structures, or to a consideration of member failure rather than system failure for statically indeterminate structures.

Hilton and Feigen [1] and Switzky [2] developed a minimum weight design based on a given total structural system probability of failure. Their studies included statically determinate or one member structures for which the system failure probability could easily be determined. It was shown that for these types of structures an overall minimum weight is approached when the individual probabilities of failure of the components of the structure are made proportional to their weight.

Turkstra [3] developed a method whereby a reasonable level of safety could be determined based on the design situation. He developed an approach based on the statistics of success and failure of a structure and the minimum loss criteria for decision. In his formulation the optimum design occurred when the expected loss due to failure was minimized. Thus a means for including loss due to failure for a particular structure in question was developed.

This optimization method was extended by Rosenblueth and Mendoza [4], Moses [5], and Sexsmith and Mau [6]. In their formulation the total cost was defined as the sum of the initial cost and the expected loss due to failure. This total cost was calculated at various levels of failure probability, and the minimum value was taken as the optimum design.

In this paper a procedure for the determination of the optimum probability of failure of indeterminate rigid frame steel structures used the expected loss criterion is presented. The objective function to be minimized is the total expected cost of failure which includes the initial structural cost as well as the loss due to failure. Uncertainties in the loads and structural resistance as well as modeling and prediction errors are included in the reliability analysis which is based on a first order second moment approach.

Loads and Load Combinations

The loads considered are the dead, live and wind loads. The dead load is assumed to be constant in time. The live and wind loads are both time and space dependent and are generally modeled as stochastic processes. However, only simplified formulations are considered herein. Live loads are modeled at three different levels: lifetime maximum total live load, lifetime maximum sustained live load, and instantaneous sustained live load. The wind loads considered are the lifetime maximum, annual maximum and daily maximum wind loads. The transformation of a particular load intensity into the appropriate load effect such as shear, bending moment or axial load is accomplished by means of an influence coefficient obtained through structural analysis. Statistics of the various load effects are summarized in Refs. [7,8].

The following load combinations are considered:

1. Dead Load + Lifetime Maximum Total Live Load
2. Dead Load + Lifetime Maximum Sustained Live Load + Annual Maximum Wind Load
3. Dead Load + Instantaneous Sustained Live Load + Lifetime Maximum Wind Load
4. Dead Load + Lifetime Maximum Total Live Load + Daily Maximum Wind Load
5. Dead Load - Lifetime Maximum Wind Load

For each loading combination the mean total load effect, $\bar{Q}$, due to the combined action of dead, live, and wind loads can be expressed as

$$\bar{Q} = \bar{Q}_D + \bar{Q}_L + \bar{Q}_W \tag{1}$$

in which $\bar{Q}_D$ is the mean dead load effect, and $\bar{Q}_L$, and $\bar{Q}_W$ the appropriate mean live and wind load effect respectively. It is assumed that the loads are statistically independent. The coefficient of variation of the total load effect is [7]

$$V_Q = \left[\frac{1}{\bar{Q}^2}\left\{\bar{Q}_D^2 V_{Q_D}^2 + \bar{Q}_L^2 V_{Q_L}^2 + \bar{Q}_W^2 V_{Q_W}^2 + (2)(0.10)^2(\bar{Q}_D\bar{Q}_L + \bar{Q}_D\bar{Q}_W + \bar{Q}_L\bar{Q}_W)\right\}\right]^{1/2} \tag{2}$$

Analysis of Resistance and Failure Modes

The resistance capacity of steel members is a function of several variables such as the section dimensions and mechanical properties. The statistics of the various member capacities such as the yield moment M_y, the yield load P_y, the axial load capacity P_{cr}, the Euler buckling load P_E, and the critical moment causing lateral torsional buckling M_{cr}, can be determined from the statistics of the section properties and the yield strength F_y. The uncertainties in the various member capacities used in the analysis of the resistance of steel members have been estimated in Ref [7,9]. The factors considered in the analysis of the statistics of member resistance included variabilities in section properties, material strength, fabrication and inaccuracies in the strength prediction equations. A systematic analysis of the contribution of these factors to the total uncertainty in the member resistance was conducted based on available data. The statistics of the member capacities used in this study were obtained from the results of the above mentioned study.

Failure Modes

Column Failure. Columns are typically subjected to both axial thrust and bending moment. Thus, the possible failure modes for a column are:

a) failure by yielding at the ends

b) failure by instability in the plane of bending without twisting

c) failure by lateral torsional buckling.

Each of these failure modes can be expressed as an interaction between the axial force and the end moments. These interaction equations are

$$\theta_1 = \frac{P}{P_y} + \frac{M}{M_y} \tag{3}$$

$$\theta_2 = \frac{P}{P_{cr_x}} + \frac{C_m M}{M_y(1 - P/P_E)} \tag{4}$$

$$\theta_3 = \frac{P}{P_{cr_y}} + \frac{C_m M}{M_{cr}(1 - P/P_E)} \tag{5}$$

in which P and M are the applied axial load and bending moment, C_m is an equivalency factor for different support and loading conditions, and θ_i is a nondimensional parameter representing the ratio of the load to the strength of the member in a given failure mode i.

The probability of failure in a given mode i is

$$P_{f_i} = Pr(\theta_i > 1) \tag{6}$$

For certain prescribed probability distributions, P_{f_i} can be evaluated in terms of the first two moments (i.e., the mean and the coefficient of variation) of θ_i. The statistics of θ_1 can be obtained using a first order approximation. For example, the mean and coefficient of variation of θ_1 are [7,8]

$$\bar{\theta}_1 = \bar{N}_{\theta_1}\left[\bar{P}/\bar{P}_y + \bar{M}/\bar{M}_y\right] \tag{7}$$

$$V_{\theta_1}^2 = V_{N_{\theta_1}}^2 + \frac{1}{\bar{\theta}_1^2}\left\{(\bar{P}/\bar{P}_y)^2(V_P^2 + V_M^2) + (\bar{M}/\bar{M}_y)^2(V_M^2 + V_{M_y}^2) + 2(\bar{P}/\bar{P}_y)(\bar{M}/\bar{M}_y)(\rho_{P_yM_y}V_{P_y}V_{M_y} + \rho_{PM}V_PV_M)\right] \tag{8}$$

in which the bar indicates that the variables are evaluated about the mean values, V is the coefficient of variation, ρ the correlation coefficient and

$\bar{N}_{\theta_1}$ and $V_{N_{\theta_1}}$ the bias and prediction uncertainty respectively in the prediction equation.

The probability of failure of the column can be expressed as

$$P_{f_{col}} = Pr(\theta_1 > 1 \cup \theta_2 > 1 \cup \theta_3 > 1) \quad (9)$$

where $\cup$ represents the union of the events. A procedure which considers the correlation between the various failure modes [10] is used for evaluating bounds on the probability of failure of columns. The application of this procedure to the analysis of failure probabilities of beam columns and the expressions for the evaluation of the correlations between the failure modes are given in Ref [7,8].

Beams. Beams which are not laterally supported and which are subjected to high levels of concentrated loads may fail in one of several different modes. These include yielding due to flexure, yielding due to shear, lateral-torsional buckling, and local buckling. However, in typical office frame systems beams are usually adequately braced and are not subject to heavy concentrated loads. Hence, in this study yielding due to flexure is considered as the only likely failure mode. The statistics of this failure mode may be obtained using an approach similar to that presented for columns.

Optimum Reliability Based Design

The optimum reliability based design procedure consists of two steps:

1) Designs are obtained for specified values of the allowable member probability of failure using an iterative procedure which optimizes the weight of the structure.

2) The optimal risk level expressed in terms of the system probability of failure is determined by minimizing the total expected cost.

Design for a Prescribed Risk Level. The design procedure consists of specifying an allowable member failure probability, P_{fa}, and then selecting trial configurations until each member satisfies this constraint. For members capable of multimodal failure, the upper bound on the probability of failure of the member is compared to the allowable risk level to insure a conservative design solution. Designs are obtained for values of the allowable member failure probability ranging from 10^{-2} to 10^{-7}.

Two factors hinder the use of classical optimum design procedures in the design of steel structures. These are:

1). In order to achieve a practical design, member selections are limited to wide flange rolled shapes from the AISC steel construction manual [11]. Thus, no continuous function of a design variable is available. The optimum design point of such a variable may or may not fall close to a given structural shape.

2). Since the structures considered are indeterminate, the forces and hence the probability of failure of each member is dependent on the size of the other members. This is especially true in the case of columns which are particularly sensitive to the size of the beams connecting to each end. No explicit relationship exists between the column and beam sizes.

These two factors are further complicated by the desire for practicality in the design solution. It is normally considered good practice to keep the columns, within a row, identical in nominal depth, change column size only at alternate story heights, and to design the structure symmetrically. For beams the problem is not as critical and usually only involves keeping the beams symmetric within each story height. In this study the above guidelines are applied to both the AISC code design procedure and the reliability based optimization procedure.

With the preceding additional practical constraints, the optimization problem becomes a minimization of the weight of the structure with the mathematical constraint

$$P_{fd} \leq P_{fa} \quad (10)$$

where P_{fa} is the allowable probability of failure, and P_{fd} is the calculated design probability of failure for the ith member of the structure. Equation (10) must be satisfied for each member of the structure before a given design is acceptable.

To insure conformity with the mathematical and practical constraints, an iteration procedure was developed based on iterations beginning at the smallest possible design and iterating upward. First, each available member size was given an index number, with the smallest member being index number one. Each member in the structure was then given an initial count number of one and the probability of failure of each member was calculated and compared to the allowable failure probability. The count number was then adjusted upward by single steps until each member satisfied the specified risk level. Finally, each member was checked for overdesign by iterating downward one step at a time. It was found that generally some member sizes could be decreased because of the dependence on the size of surrounding members. Once a count number was repeated twice, the member remained at this size.

Optimal Risk Level

Several schemes for the determination of the optimal risk level based on a relaibility analysis have been suggested. These include: (a) minimization of the probability of failure for a fixed cost [12] and (b) minimization of the total overall cost, which is taken as the sum of the initial cost and the expected consequences of failure [3]. In this study the second approach is taken and applied to statically indeterminate rigid steel frames. The objective function to be minimized is given by [4]

$$C_T = C_I + C_{EL} - C_B \quad (11)$$

where C_T = total cost, C_I = initial cost which is a function of the design variables, C_{EL} = expected loss due to failure, C_B = the benefit derived from the system while it survives. Since the benefit derived from the system is essentially constant over a reasonable range of safety levels, it can be eliminated from the objective function. Thus,

$$C_T = C_I + C_{EL} = C_I + P_{fs}C_f \qquad (12)$$

in which P_{fs} is the system probability of failure and C_f the expected cost of failure. The variables in Equation (12) are estimated as follows:

Initial Cost, C_I is a function of the design variables and the specified risk level. It comprises of structural material cost, and miscellaneous systems cost [13]. For a structure of constant dimensions, only structural material cost [14] changes significantly with varying allowable probability of failure.

Probability of Failure, P_{fs} The estimation of system failure probability is quite complicated. Hence, the probability is approximated by means of upper and lower bounds. A lower bound on the system failure probability based on the assumption that all members are perfectly correlated is given by [15,16]

$$P_{fs} \geq \max[P_{f_1}, P_{f_2}, \ldots, P_{f_n}] \qquad (13)$$

where n is the number of members in the structure. The upper bound on the system failure probability, based on the assumption that all members are independent is expressed as [15,16]

$$P_{fs} \leq 1 - \prod_{i=1}^{n} (1 - P_{f_i}) \qquad (14)$$

Expected Cost of Failure, C_f is the total loss incurred if the structure were to collapse. This includes replacement cost, business losses, and liabilities due to death and injury. The above quantities vary considerably with time and geographical location and are in general difficult to determine. Herein, the expected cost of failure is estimated based on the following assumptions:

1). Replacement cost is taken as equal to the initial cost of the structure plus a fifty five percent additional cost to account for removal of the collapsed structure and inflation until replacement.

2). Business losses are taken to be the total loss of the companies operating in the office building. A replacement period of four years is assumed for the businesses to resume normal operations [17]. The losses during this period are approximated as the sum of the salaries of all workers [18] in the building plus two percent of the initial cost for office equipment.

3). Liabilities due to death and injury are taken to only include those incurred by the people present in the building at the time of collapse. The statistics of the number of deaths and injuries are described in detail in Ref. [19]. Cost of each death is based on the assumption of an average death age of thirty and is taken to be the sum of the persons salary until he would have reached sixty-five years of age. Costs for injuries are divided into two parts, the first being those injuries of serious or disabling nature. The costs for disabling injuries are obtained from Ref. [18]. The second type of injury are those which do not have a permanent effect and require short periods of hospitalization. An average cost for this type of injury is taken to be five thousand dollars [18].

Upper and lower bounds on the cost of failure are computed using bounds on the system failure probability. It should be noted that the computed expected cost of failure, and hence the optimal risk level depends on the assumptions made in establishing monetary values for the various items which contribute to the cost of failure. Due to the uncertainty in estimating these values a sensitivity study was performed to determine if the computed optimal risk level is altered significantly by variation in the estimated cost of failure.

Results

The reliability based optimization procedure was applied to the design of a five and a ten story rigid steel frame office building. The first story of each frame is 18 ft high and the upper stories are each 12 ft high. The spacing between adjacent columns as well as between adjacent frames is 25 ft. A typical interior frame of the five story building is shown in Figure 1. Designs were also obtained using the AISC code specifications so that a comparison could be made between the reliability based design procedure and the current deterministic code procedure.

Results of Reliability Based Design

Using the iterative procedure described earlier, member sizes were obtained for specified values of the member failure probability ranging from 10^{-2} to 10^{-7}. Since only bounds on the system failure probability can be realistically determined, two optimum designs are found for each building. One optimum design corresponds to the lower bound on system failure probability while the other corresponds to the upper bound on the system failure probability.

Initial Cost. The initial cost versus the lower bound on the system failure probability for the five story structure is shown in Figure 2. A definite, steadily increasing trend is observed. The data approximates a straight line. The apparent discontinuity in data points is due to the practical restrictions on member dimensions and the difficulty in obtaining an exact continuous function for the member dimensions of available standard sections. This member dimension discontinuity, inherent primarily in metal structures,

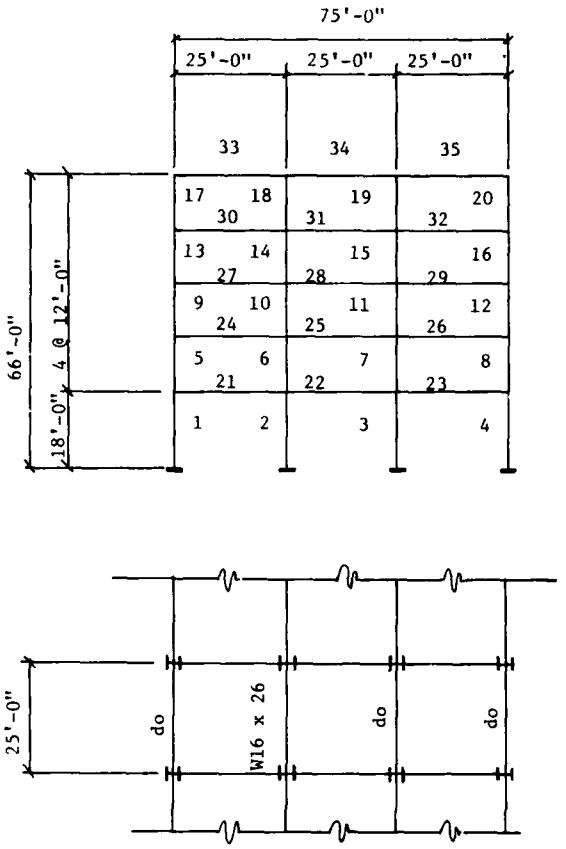


Figure 1. Plan and Elevation of Five Story Building Considered.

is the main cause of the small fluctuations in the data points throughout this study.

The results for the ten story frame were similar to those of the five story frame. A straight line trend was again observed over the range of member failure probabilities. The fluctuations in the data points were greater due to the greater influence of the discontinuities in member dimensions.

Total Cost and Optimal Risk Level. The total cost versus the lower and upper bounds on system failure probability for the five story building is shown in Figure 3. The optimum system failure probability computed using the lower bound on the total cost was found to be 0.94×10^{-4}. This corresponds to an allowable member failure probability of 10^{-4} for both beams and columns. The optimum value of the system probability of failure based on the upper bound on the total cost was 0.54×10^{-4} which corresponds to an allowable member failure probability of 10^{-5}. Member sizes and the probability of failure of members at the optimum design are presented in Table 1.

The computed failure probabilities of the members differ from the allowable values because of two practical considerations. First, the member

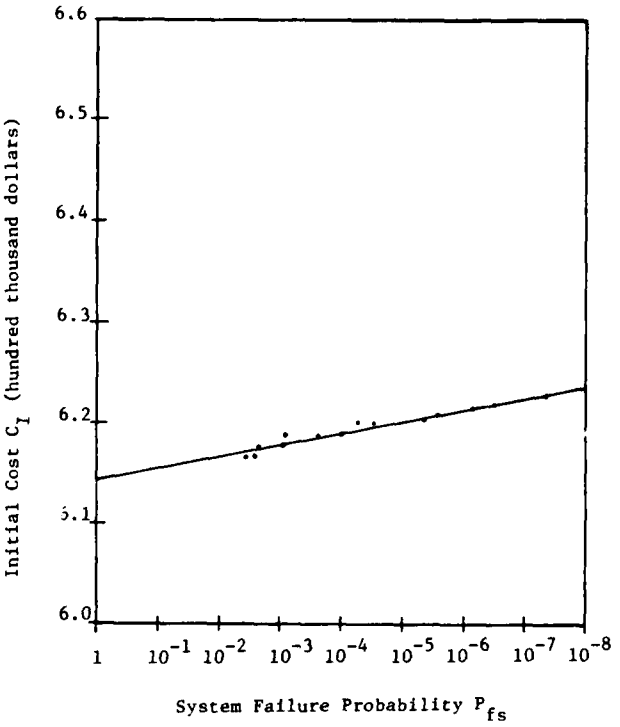


Figure 2. Initial Cost Versus Lower Bound on System Probability of Failure for Five Story Building.

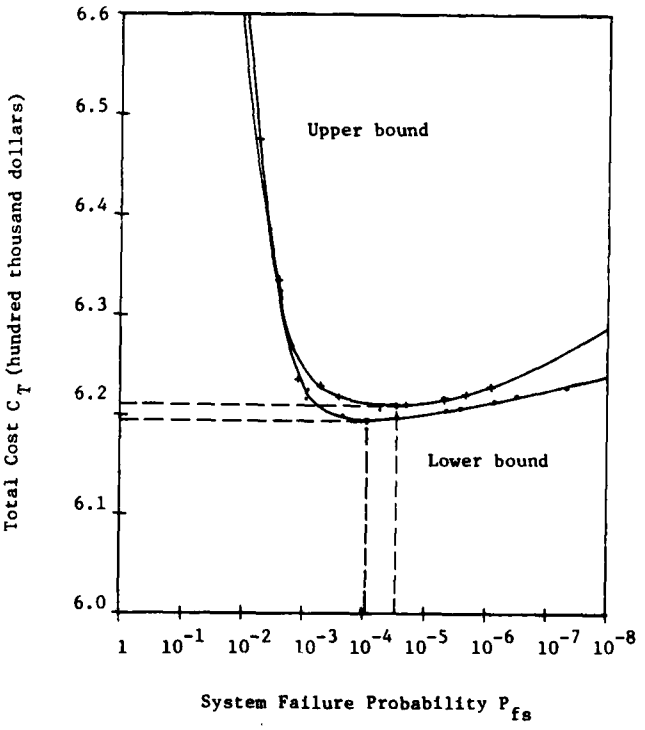


Figure 3. Total Cost Versus System Probability of Failure for Five Story Building.

sizes are limited to a finite number of sections taken from the AISC tables of dimensions and properties [1]. Second, the structure is kept symmetric and the column size is only changed every two stories. These two factors are especially important in column design. For the columns, the critical failure mode is usually buckling about the weak axis which is dependent on the moment of inertia, I_y, a property which may double between consecutive available member sizes. This accounts for the small failure probabilities of some of the members. Although the failure probability of the members is sensitive to this section property the cost of the member does not change significantly.

The structural cost and the total cost for the bounds on the optimum design were found to be close. For the structural cost, a 7.8% increase was found between the lower and upper bound optimum designs. The difference in the total cost was 0.2%, which is negligible.

The total cost versus the lower and upper bounds on the system probability of failure for the ten story building is shown in Figure 4. For this structure, the optimum system failure probability based on the upper bound on the total cost was 0.46×10^{-3} which is slightly higher than that for the five story building. However, the optimum system failure probability computed using the lower bound on the total cost was found to be 0.46×10^{-4}, which compares very favorably with the five story design. As with the five story frame the optimum upper bound design corresponds to an allowable member failure probability of 10^{-5}.

The structural cost and the total expected cost for the bounds on the optimum design were again close. For the structural cost, an 8.2% increase was found between the lower and upper bound optimum designs. The total expected cost for the lower and upper bound designs was found to differ by 0.35% which is negligible.

A sensitivity study was performed on each building to determine the effect of changes in the total expected cost on the computed optimum risk level. The results for the five story building are presented in Figure 5. It can be seen that no significant change in the optimum design occurs within a range of one half the calculated failure cost lower and two times the failure cost higher than the calculated expected cost of failure. Hence, for the five story building, the optimum deisgn is, for practical purposes, insensitive to the expected cost of failure. The sensitivity study for the ten story building indicates a higher degree of sensitivity to the expected cost of failure. However, at expected failure costs greater than ten times the initial cost, this design was also found to be insensitive to failure cost.

Results of AISC Based Design

Each building was designed using the current AISC specifications [20] for the same loading conditions described above to assure a fair comparison. However, the nominal rather than the mean yield stress was applied to the specified safety factors. Also, the AISC design was subjected to the same limiting design assumptions needed to insure a practical solution.

Member sizes and member failure probabilities for the five story structure for both the AISC and the reliability based design are presented in Table 1. It was found that for the five story structure the AISC design was extremely close to the lower bound optimum design. The lower bound on

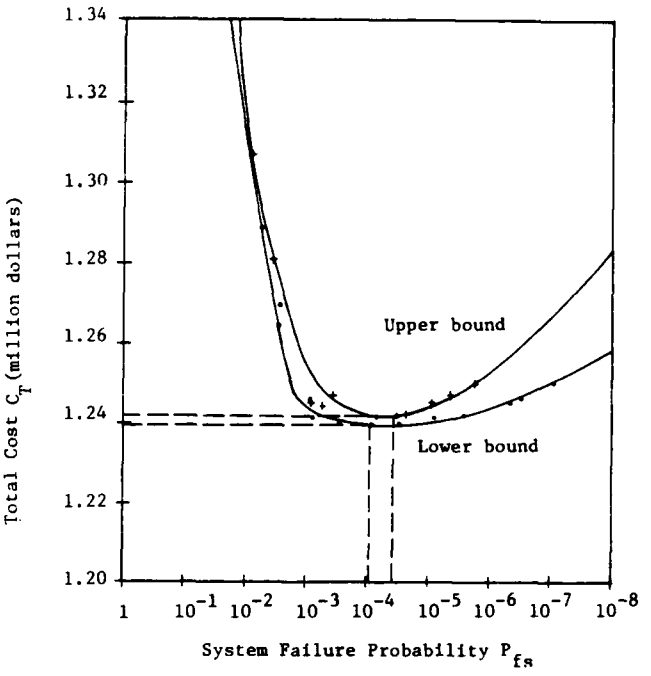


Figure 4. Total Cost Versus System Probability of Failure for Ten Story Building.

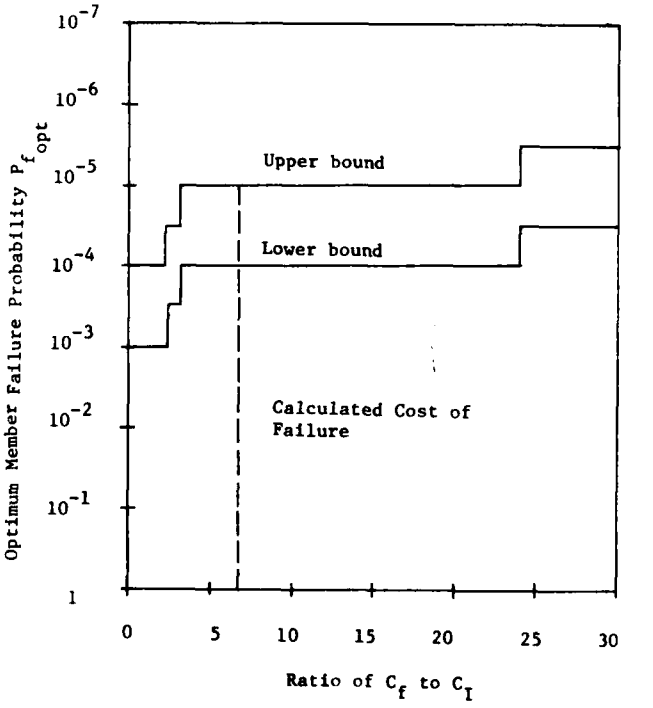


Figure 6. Optimum Member Probability of Failure Versus Ratio of Cost of Failure to Initial Cost for Five Story Building.

the system failure probability for the AISC design was found to be 0.55×10^{-3} and the upper bound 0.27×10^{-2}. Each of these values is higher than those obtained from the reliability based design. The structural cost for the AISC design was found to be 4.3% lower than the lower bound optimum design. The total cost for the AISC design was, however, 1.3% higher than the lower bound reliability based optimum design.

For the ten story building the lower bound on the system failure probability of the AISC design was found to be 0.97×10^{-3} and the upper bound 0.77×10^{-2}. These values are only slightly higher than those obtained for the lower bound optimum design. The structural cost for the AISC design was 10.3% lower than the lower bound reliability based design. The total cost was 4.1% higher than the lower bound optimum design.

Conclusions

A reliability based optimum design procedure was presented. With this procedure it is possible to include uncertainties in modeling the design parameters, the inherent randomness of the loads and the structural resistance and the idealizations involved with the analysis procedure. Also, the level of safety and the consequences of failure can be directly included in the optimization procedure.

From the results of the study the following conclusions can be made:

1). The reliability based optimization procedure results in consistent risks in terms of both the member probability of failure and the system failure probability. Furthermore, it allows optimization based on the type, location and importance of the structure.

2). For the type of structures considered, the optimum member failure probability is of the order of 10^{-4} to 10^{-5} for both beams and columns.

3). The computed optimal risk level is relatively insensitive to the estimated cost of failure.

4). Member sizes obtained using the AISC specifications are comparable to those obtained by the reliability based design procedure at the lower bound on the system failur. probability.

5). For the structures qonsidered the designs obtained using the AISC specifications consistently resulted in a structure with lower initial cost than the reliability based designs. However, the total expected cost for the AISC designs was higher.

6). Designs based on the AISC specifications did not result in a consistent system failure probability.

Table 1

Member Sizes and Member Failure Probabilities for Five Story Frame

Optimum Design at Upper Bound			Optimum Design at Lower Bound		AISC Design	
Member	Member Size	Prob. of Failure	Member Size	Prob. of Failure	Member Size	Prob. of Failure
1,4	W14x61	0.1239×10^{-7}	W14x53	0.4826×10^{-4}	W14x61	0.9060×10^{-7}
2,3	W14x90	0.2283×10^{-5}	W14x82	0.4911×10^{-4}	W14x90	0.2869×10^{-5}
5,8	W14x61	0.1938×10^{-6}	W14x53	0.9679×10^{-5}	W14x53	0.9597×10^{-5}
6,7	W14x68	0.2263×10^{-5}	W14x61	0.2699×10^{-4}	W14x61	0.4049×10^{-4}
9,12	W14x61	0.1055×10^{-9}	W14x53	0.2123×10^{-7}	W14x53	0.2127×10^{-7}
10,11	W14x68	0.4128×10^{-9}	W14x61	0.9556×10^{-8}	W14x61	0.1415×10^{-7}
13,16	W14x43	0.4092×10^{-8}	W14x38	0.3534×10^{-6}	W14x38	0.3624×10^{-6}
14,15	W14x34	0.9703×10^{-5}	W14x34	0.9540×10^{-5}	W14x34	0.5537×10^{-3}
17,20	W14x43	0.1089×10^{-7}	W14x38	0.1109×10^{-5}	W14x38	0.5600×10^{-6}
18,19	W14x34	0.8327×10^{-15}	W14x34	0.1180×10^{-14}	W14x34	0.3603×10^{-10}
21,23	W21x57	0.6318×10^{-5}	W21x57	0.8225×10^{-5}	W21x50	0.2696×10^{-3}
22	W21x57	0.7749×10^{-6}	W21x50	0.4774×10^{-4}	W21x50	0.4506×10^{-4}
24,26	W21x57	0.1371×10^{-5}	W21x50	0.9352×10^{-4}	W21x50	0.9120×10^{-4}
25	W21x57	0.4768×10^{-6}	W21x50	0.3690×10^{-4}	W21x50	0.3338×10^{-4}
27,29	W21x57	0.9537×10^{-6}	W21x50	0.6753×10^{-4}	W21x50	0.6717×10^{-4}
28	W21x57	0.5960×10^{-6}	W21x50	0.3791×10^{-4}	W21x50	0.3767×10^{-4}
30,32	W21x57	0.5364×10^{-6}	W21x50	0.4500×10^{-4}	W21x50	0.4578×10^{-4}
31	W21x57	0.4172×10^{-6}	W21x50	0.3004×10^{-4}	W21x50	0.3034×10^{-4}
33,35	W21x57	0.2742×10^{-5}	W18x55	0.6938×10^{-4}	W21x50	0.1733×10^{-3}
34	W21x57	0.1073×10^{-5}	W21x50	0.6634×10^{-4}	W21x50	0.6485×10^{-4}

References

(1) Hilton, H. H. and Feigen, M., "Minimum Weight Analysis Based on Structural Reliability," Journal of the Aerospace Sciences, Vol. 27, No. 9, pp. 641-652, September, 1960.

(2) Switzky, H., Minimum Weight Design with Structural Reliability," Proceedings, Fifth Annual Structures and Materials Conference, AIAA, Palm Springs, California, April, 1964.

(3) Turkstra, C. J., "Choice of Failure Probabilities," Proceedings of the ASCE, Vol. 93, No. ST6, December, 1967, pp. 189-200.

(4) Rosenblueth, E. and Mendoza, E., "Reliability Optimization in Isostatic Structures," Proceedings of the ASCE, Vol. 97, No. EM6, December, 1971, pp. 1625-1642.

(5) Moses, F., "Structural System Reliability and Optimization," Computers and Structures, Vol. 7, pp. 283-290, Pergamon Press, 1977.

(6) Sexsmith, R. G. and Mau, S-T., "Reliability Design with Expected Cost Optimization," Proceedings, Specialty Conference on Safety and Reliability of Metal Structures, ASCE, Pittsburgh, Pennsylvania, November, 1972.

(7) Rojiani, K. B., "Evaluation of the Reliability of Steel Buildings to Wind Loadings," Ph.D. Thesis, Department of Civil Engineering, University of Illinois at Urbana-Champaign, 1978.

(8) Rojiani, K. B. and Woeste, F. E., "A Probabilistic Analysis of Steel Beam Columns," submitted for publication in Engineering Structures.

(9) Rojiani, K. B. and Wen, Y. K., "Reliability of Steel Buildings Under Winds," Proceedings of the ASCE, Vol. 107, No. ST1, January, 1981, pp. 203-221.

(10) Vanmarcke, E. H., "Matrix Formulation of Reliability Analysis and Reliability Based Design," Computers and Structures, Vol. 3, pp. 757-770, Pergamon Press, 1971.

(11) Dimensions and Properties New W, HP and WT Shapes, Publ. No. S325-(1P 100M578), AISC, New York, New York, 1977.

(12) Moses, F., and Kinser, D. E., "Optimum Structural Design with Failure Probability Constraints," AIAA Journal, Vol. 5, No. 6, June, 1967, pp. 1152-1158.

(13) Manufacturing/Office/Warehouse Building Costs, Dodge Research Report, McGraw Hill Information Systems Company, New York, N.Y., 1976.

(14) Building Cost File, Central Edition, Compiled by McKee-Berger-Manseuto Inc., Van Nostrand Reinhold Company, New York, N.Y., 1979.

(15) Cornell, C. A., "Bounds on the Reliability of Structural Systems," Proceedings of the ASCE, Vol. 93, No. ST1, February, 1967, pp. 171-200.

(16) Ang, A. H-S. and Amin, M., Reliability of Structures and Structural Systems, Proceedings of the ASCE, Vol. 94, No. EM2, April, 1968, pp. 671-691.

(17) Mortimer, T. J. Insurance: A New Look at an Old Subject, The Building Economist, December, 1979.

(18) Pauls, J. L., Management and Movement of Building Occupants in Emergencies, Proc. Conf. on Designing to Survive Severe Hazards, IIT Research Institute, Chicago, Illinois, November, 1977.

(19) Wiggens, J. H., National Losses and Migitation Effects for Air, Earth and Waterborne Natural Hazards, Proc., Conf. on Designing to Survive Severe Hazards, IIT Research Institute, Chicago, Illinois, November, 1977

(20) Specification for the Design, Fabrication and Erection of Structural Steel for Buildings, AISC, New York, New York, 1977.

SESSION #3

OPTIMAL CONTROL METHODS

EXISTENCE OF SOLUTIONS OF THE PLATE OPTIMIZATION PROBLEM

Jean-Louis Armand
Institut de Recherches de la Construction Navale
47 rue de Monceau
75008 Paris, France
and
Ecole Polytechnique
91128 Palaiseau Cedex, France

Konstantin A. Lurie and Andrej V. Cherkaev
A.F. Ioffe Physico-Technical Institute, Leningrad
The U.S.S.R. Academy of Sciences, U.S.S.R.

Introduction

The theory of optimal control represents the modern extension of the classical calculus of variations allowing relaxed requirements on the control functions and dealing with the presence of restrictions other than equalities. The powerful numerical methods developed within its scope have proven their usefulness in providing numerical solutions to some extremely challenging problems of optimum structural design (see, for example, Refs. 1 and 2). The theory of optimal control also provides answers to fundamental questions such as the existence and characterization of solutions and, when necessary, provides insight into the regularization of the original formulation, that is the attempt to construct a proper extension of the set of admissible control functions which guarantees the existence of a solution. The recent recognition of analytical difficulties associated with the occurence of singular designs in the case of simple structural members (Ref. 3) has demonstrated the need for satisfactory answers to such fundamental questions, which can no longer be ignored by the practical designer.

The present paper, presented here in extended abstract form only, focuses on the latter aspect in describing some of the difficulties encountered in the problem of optimum design of plates, shown to be related to the non-existence of a solution to the optimization problem within the scope of the traditional formulation. A regularized formulation is presented, guaranteeing existence to a broad class of optimal design problems for plates, in which tensor-valued controls representing anisotropic properties of the material are introduced within the classical plate theory.

Optimum design of plates

The problem of optimum design of plates has within the past decade received sufficient attention to justify a recent comprehensive review listing as many as 111 papers on the subject, Ref. 4. However, numerical difficulties reported by early investigators, as well as the radically different designs obtained for the same problem by different researchers, are evidence of the singular nature of the problem. Smooth, stationary solutions obtained to geometrically unconstrained formulations for optimal design must be considered as local optimal solutions only (Ref. 5). Upper and lower bounds imposed on the control (design) variable, taken as the thickness t or bending rigidity D, have not helped to improve the situation.

In fact, for the axisymmetric, one-dimensional case of a circular plate, the numerical solutions reported rapidly oscillate between the upper and lower bounds on the thickness prescribed in advance, exhibiting the characteristic features of so-called relaxed control (Ref. 6). A regularized formulation has been offered for that case based on an alternative physical plate model allowing for a distribution of infinitely thin integral stiffeners, the variable density of which being introduced as a control (design) variable, Ref. 7. The allowance for stiffeners is consistent with a tendency exhibited by numerical solutions to concentrate the material along discrete stiffeners. For the same amount of material being used, the superiority of the stiffened plate over the smooth one has in fact been recognized for a long time.

However, generalization of this analogy to cover the two-dimensional situation for a plate with arbitrary shape cannot be directly inferred from the above and requires a different type of approach. The absence of optimal solutions for controls belonging to the initial class U of scalar control functions D is intimately related to the impossibility to satisfy the Weierstrass necessary condition at almost every point of the region delimited by the plate boundary (Ref. 8). One ingenious approach overcoming this difficulty has been to prescribe in the design stiffeners of arbitrarily specified shape and to derive directly the necessary conditions of optimality, yielding their optimal stiffness distributions (Ref. 9).

Regularization through the allowance for anisotropy

Non-existence of a solution to the traditional optimum plate design may in fact be directly linked to previous investigations of optimal control problems governed by linear elliptic equations which have led to a number of non-trivial examples where the minimum of the functional is not attained. In order to guarantee the existence of solutions to such problems, it has been proposed in Ref. 10 that the set of admissible control functions be extended by introducing tensor controls. Within the scope of structural optimization, this suggestion may be interpreted as being equivalent to a relaxation of the severe restriction imposed by the isotropic nature of the material and which is present in the traditional formulation; it allows for the inclusion of anisotropy in the design, such as may be achieved by the use of composite materials. The initial set of admissible materials U is within this assumption extended to include composites of appropriate layered microstructure. Such an extended set, composed of arbitrary combinations of the elements of the initial set U, will be called the G-closure of U and designated as GU (Ref. 11). The G-closure may then be viewed as the set of composites assembled from compounds belonging to the set U.

G-closure of the fourth-order plane operator $\nabla\nabla_{..} D_{..}\nabla\nabla$ arising in the classical theory of plates and involving self-adjoint tensors D of rank four (Ref. 12) regularizes the initial optimization problem by guaranteeing the existence of a solution to the extended optimization problem which preserves the infimum of the functional being minimized. Such extensions GU of sets of admissible control functions have been constructed for a set $U(K_-, K_+)$ of two isotropic media with the same value μ of shear modulus and different values K_-, K_+ of bulk moduli ($K_- < K_+$, K_- and K_+ given), as well as for a set $U(\mu_1,\mu_2,\theta)$

of materials possessing cubic symmetry with the same value K of bulk modulus, the shear moduli μ_1 and μ_2 and angle θ between the principal axes of elasticity and some reference axes being allowed to vary between given bounds.

This result guarantees the existence of solutions to two broad classes of optimal design problems for plates which are built from materials belonging either to the set $U(K_-, K_+)$ or to the set $U(\mu_1, \mu_2, \theta)$. These two classes correspond, respectively, to the problem of optimal distribution of shear modulus for an anisotropic plate, and to the problem of optimal orientation of the principal axes of elasticity of an orthotropic plate.

Complete regularization of the plate optimization problem, that is the construction of the G-closure for the most general initial set U of admissible materials, has not been obtained yet and is presently being investigated by the authors.

References

(1) McIntosh, S.C., Jr., Structural Optimization via Optimal Control Techniques: A Review. Structural Optimization Symposium, AMD, Vol. 7, edited by L.A. Schmit, Jr., ASME, New York, 1974, pp. 49-64.

(2) Pierson, B.L. and Genalo, L.J., Minimum Weight Design of a Rectangular Panel Subject to a Flutter Speed Constraint. Computer Methods in Applied Mechanics and Engineering, Vol. 10, 1977, pp. 45-62.

(3) Olhoff, N., On Singularities, Local Optima and Formation of Stiffeners in Optimal Design of Plates. Optimization in Structural Design, edited by A. Sawczuk and Z. Mroz, Springer-Verlag, Berlin, Heidelberg, New York, 1975, pp. 82-103.

(4) Haftka, R.T. and Prasad, B., Optimum Structural Design with Plate Bending Elements - A Survey. AIAA Journal, Vol. 19, No. 4, April 1981, pp. 517-522.

(5) Seiranyan, A.P., A Study of an Extremum in the Optimal Problem of a Vibrating Circular Plate. Mechanics of Solids (MTT), Vol. 13, No. 6, 1978, pp. 99-104.

(6) Warga, J., Optimal Control of Differential and Functional Equations, Academic Press, New York and London, 1972.

(7) Cheng, K.T. and Olhoff, N., "Regularized Formulation for Optimal Design of Axisymmetric Plates," DCAMM Report No. 203, The Technical University of Denmark, February 1981.

(8) Lurie, K.A. and Cherkaev, A.V., Prager Theorem Application to Optimal Design of Thin Plates, Mechanics of Solids (MTT), Vol. 11, No. 6, 1976, pp. 139-141.

(9) Samsonov, A.M., Necessary Optimality Conditions for Stiffness Distribution of a Rib on an Elastic Plate. Mechanics of Solids (MTT), Vol. 15, No. 1, 1980, pp. 122-129.

(10) Lurie, K.A., On the Optimal Distribution of the Resistivity Tensor of the Working Substance in a Magnetohydrodynamic Channel. Journal of Applied Mathematics and Mechanics (PMM), Vol. 34, No. 2, 1970, pp. 255-274.

(11) Lurie, K.A., Cherkaev, A.V. and Fedorov, A.V., Regularization of Optimal Design Problems for Bars and Plates. Journal of Optimization Theory and Applications (to appear).

(12) Lurie, K.A., Some Problems of Optimal Bending and Extension of Elastic Plates. Mechanics of Solids (MTT), Vol 14, No. 6, 1979, pp. 71-78.

AD P000 039

STABILITY IMPLICATIONS AND THE EQUIVALENCE OF STABILITY AND OPTIMALITY CONDITIONS IN THE OPTIMAL DESIGN OF UNIFORM SHALLOW ARCHES

W. Stadler
Division of Engineering
San Francisco State University
1600 Holloway Avenue
San Francisco, CA 94132

Summary

The simple arch and the uniform shallow arch are used to illustrate the possible coalescence of optimality and stability conditions. The calculations for the simple arch are carried out with the initial rise of the arch used as a design variable. It is shown that the necessary conditions for the constrained minimum weight arch are sufficient for instability, that the minimum stored energy problem has no solution, and that the necessary conditions arising in the calculation of the natural shapes of the arch, involving the simultaneous "minimization" of mass and stored energy, turn out to be sufficient for stability. A summary of the results of similar calculations for the optimal design of uniform shallow arches with initial curvature and the axial load as controls is also presented.

Introduction

The optimal design of structures is one area where there is a great amount of leeway for a designer to express his own views and approaches to a "best" design. There are two fundamentally different philosophical viewpoints: one which reduces every problem to an economic one, where the designer ultimately minimizes the expense or maximizes the profit; the other may best be expressed in viewing nature as an optimal designer through evolution, the task of the designer being the deduction of a shortcut to evolution through the discovery of minimum or maximum principles. This is not meant to be understood in the Leibnizian sense that this is the best of all possible worlds; rather, the intent is to encourage a discretionary look at nature's designs in order to discover those which may have evolved to a state which is optimal for some particular purpose. It is in this latter context that the concept of natural structural shapes was proposed in Ref. (1). Such shapes are the result of the simultaneous "minimization" of the mass and of the strain energy of the proposed structure; the implication is that nature would evolve such a design for a given set of boundary conditions and loads.

These differences in philosophy, however, do not affect the procedural aspects of optimal design. Thus, every optimal structural design may be based on the following four steps:

(i) The selection of a sufficiently general mathematical model of the physical structure. Usually this concerns the particular theory within which the design is to be accomplished, such as beam theory, shell theory, etc. Naturally, any postulated laws and limitations of such a theory carry over as limitations imposed upon the optimal design.

(ii) The selection of the given "parameters" and of the design or control "parameters." In its most general sense, the term "parameter" here is used to identify anything which serves to characterize a particular design of a structure. Usually, the selection of design parameters is constrained in some manner; that is, the possible choices are presumed to belong to some set of admissible decisions, $\mathcal{D}$.

(iii) The selection of a precise meaning of the term "optimal." This always involves the introduction of a preference relation $\preceq$ on the decision set $\mathcal{D}$; that is, some manner of prescribing that a member d_1 of $\mathcal{D}$ is better than or equivalent to some other member d_2 of $\mathcal{D}$. This is then denoted by $d_1 \succeq d_2$, in analogy with the usual ordering on $\mathbb{R}$. The preference may be introduced on $\mathcal{D}$ directly or, as is most often the case, indirectly by using a criterion $f(\cdot): \mathcal{D} \to \mathbb{R}$ with $d_1 \succeq d_2$ iff $f(d_1) \geq f(d_2)$. Another related possibility consists of the use of several criteria with mapping $g(\cdot): \mathcal{D} \to \mathbb{R}^n$ defined by $g(d) = (g_1(d),\ldots,g_n(d))$, $d \in \mathcal{D}$. An appropriate preference on $\mathbb{R}^n$ then induces a corresponding preference on $\mathcal{D}$. The most often used preference on $\mathbb{R}^n$ in this connection is the standard ordering "$\leqq$" on $\mathbb{R}^n$ defined by: For $i = 1,\ldots,n$

$$x \leqq y \Leftrightarrow x_i \leq y_i,$$

$$x < y \Leftrightarrow x_i \leq y_i, \quad x \neq y,$$

$$x << y \Leftrightarrow x_i < y_i.$$

"Minimizing" no longer has meaning in this context, and one needs the more general concept of a minimal element with respect to a preference; such elements are also termed Pareto-optimal in honor of the political economist Vilfredo Pareto, who introduced the concept.

[1] Definition (Pareto-optimality). A decision $d^* \in \mathcal{D}$ is Pareto-optimal iff $d \in \mathcal{D}$ and $g(d) \leqq g(d^*) \Rightarrow g(d) = g(d^*)$, for every d^*-comparable $d \in \mathcal{D}$.

These and other aspects of multicriteria decision making are reviewed in Ref. (1) and in a survey of the subject, Ref. (2).

(iv) The selection of the analytical or numerical methods used to obtain a solution of the "minimization" problem which has been posed. These may consist of methods from the calculus or the calculus of variations, or, more recently, of methods in control and in programming. When several criteria are present, the theory of multicriteria decision making becomes a necessary tool.

[2] Remark. The question of statical determinacy or indeterminacy of a structure is an irrelevant one as far as the application of the methods of control and of programming are concerned. However, a statically determinate problem may often be easier to work because of the absence of coupling between design and equilibrium requirements.

[3] Remark. In all problems of optimal design in the sciences, the postulated laws and principles of a particular discipline may impose restrictions on the design possibilities. In static structural design, one such condition is the required equilibrium of the final structure. Often this is only an implicit condition in the design process; in fact, it should always appear as an explicit constraint on the design variables, although the constraint may be inactive.

As a consequence of this requirement, one has an optimal equilibrium state of the structure corresponding to each optimal design. The question of the stability of such optimal equilibria thus is an essential part of any structural optimization problem.

The inclusion of stability phenomena in optimal design appears to fall within four categories:

(a) It is known a priori or from previous calculations that some structure possesses certain optimality attributes; it is then pointed out that this same structure has undesirable characteristics with respect to imperfections or post-buckling behavior.

Basically, this category involves no interaction between stability and optimality conditions, although one may, somewhat artificially, relate these discussions to optimization problems by using the imperfection parameter as a design variable. These and other aspects, together with a summary, are the content of Ref. (3).

(b) This category differs from the previous one in that the optimization is carried out at a critical point; either the mass is minimized for a specified critical load or the critical load is maximized while the mass is held constant. Two types of critical point are involved: divergence (buckling or static instability) or flutter (oscillation with increasing amplitude or dynamic instability). The former problem type is reviewed in Ref. (4) and in several similar papers by the same author; the latter is reviewed in Ref. (5).

In this category, the question of stability enters only insofar as the optimization is carried out at a critical point.

(c) Instability is avoided by the explicit inclusion of inequality constraints on the loads, deflections, or eigenvalues of the structure. These constraints then must be satisfied in addition to any optimality conditions which arise due to the optimization process. Generally, such constraints are introduced in numerical algorithms for optimal structural design, as exemplified by Ref. (6).

(d) The conditions for stability (or instability) turn out to be the same as the optimality conditions. That is, a necessary condition for optimality may be identical with a condition assuring the onset of instability or, more ideally, it may be the same as a sufficient condition for stability. It is this category which is a major part of this paper.

Throughout, it suffices to use the definition of stability in its usual form.

[4] Definition (Stability). A structure is stable at an equilibrium position iff the potential energy of the structure has a (weak) minimum for this equilibrium.

There are a great many papers dealing with the stability of shallow arches. The extensive report by Fung and Kaplan (Ref. (7)) is used here for comparison purposes and as a basic reference on this topic.

According to the survey by Wasiutynski and Brandt (Ref. (8)), the first steps in optimal arch design were made by Levy (Ref. (9)), who published a detailed study of trusses and arches of uniform strength, including the determination of the axis of an arch of uniform strength. There are about ten more papers cited in Ref. (8) which appear to be concerned with the optimal design of arches, including minimum weight design. Unfortunately, most of these references were either unobtainable or could not be found on the basis of the abbreviated citations. However, all of these date prior to 1961; hence, they certainly differ in method, although some of the results might be the same. More recent optimal design of arches is exemplified by the work of Wu (Ref. (10)), who used perturbation methods to determine that shape of a hinged circular arch which has the largest critical buckling pressure of all circular arches of given radius, central angle, and volume (he assumed that the cross-sections were rectangular and of constant width with the variation in depth used as the design "parameter"). There are a number of additional papers dealing with the optimal design of non-shallow arches. The optimal design of shallow arches is considered in Refs. (11) and (12). Both authors consider a shallow arch of specified volume, length, and initial shape, loaded symmetrically in the plane. They then seek to maximize the buckling load, the first author analytically by variational methods, the second numerically by formulating the problem in displacement terms and discretized as a finite element problem. Control theory and multicriteria decision making are used in Refs. (13) and (14) to determine optimal initial curvatures and axial loads for the shallow arch problems indicated in the titles. The stability implications of these designs are treated in Refs. (15) and (16). The present paper serves to summarize and extend the results in these last two papers.

The Simple Arch

This is the simplest problem which exhibits some of the aspects of the more complicated shallow arch problem. The initial shape (dashed line) and the deflected shape (solid line) of the arch are illustrated in Fig. 1. Assume that the arch is composed of

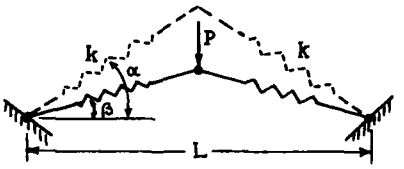


Fig. 1. The Simple Arch

two linear extensional springs with stiffness k which are pinned to each other and to the rigid supports as shown. The springs are assumed to resist both tension and compression. The distance between the supports is taken to be L. The initial angle of the springs is α and the central pin is loaded by a dead vertical force with magnitude P. Only the symmetric deformation of the arch is considered; thus, the final deflected shape of the arch may be characterized by the single angle β. The mass per unit length of the arch is ρ. It will also be assumed that the arch is shallow. This assumption does not diminish the conceptual results, and it simplifies the algebra. However, for convenience, $(-\pi/2, \pi/2)$ will be kept as the ambient interval for the parameters α and β.

It is instructive to pose the problems within the classifications (i) - (iv) given earlier.

(i) The theory is that for the so-called simple shallow arch composed of two linear compression members as indicated in Fig. 1. Strictly speaking, all of the final results must thus be interpreted within this shallowness assumption.

(ii) The given parameters are ρ, k, L, and $P > 0$. The initial rise of the arch, α, is chosen as the control or design parameter, with $-\frac{\pi}{2} < \alpha < \frac{\pi}{2}$. An additional restriction is imposed

by the equilibrium requirement

$$P = kL \sin\beta(\sec\alpha - \sec\beta) \cong \tfrac{1}{2}kL\beta(\alpha^2 - \beta^2). \quad (1)$$

These two conditions together define the decision set $\mathcal{D}$.

(iii) The previously indicated indirect approach is used to introduce a preference on $\mathcal{D}$. The criteria are the mass

$$\mathcal{M}(\alpha) = \rho L \sec\alpha \cong \rho L(1 + \tfrac{1}{2}\alpha^2), \quad (2)$$

and the strain energy

$$\mathcal{E}(\alpha) = \tfrac{1}{4}kL^2(\sec\alpha - \sec\beta)^2 \cong \tfrac{1}{16}kL^2(\alpha^2 - \beta^2)^2. \quad (3)$$

These criteria are then used to define the following three problems:

A. Minimize $\mathcal{M}(\alpha)$ subject to $\alpha \in \mathcal{D}$.

B. Minimize $\mathcal{E}(\alpha)$ subject to $\alpha \in \mathcal{D}$.

C. Obtain Pareto-optimal decisions $\alpha^* \in \mathcal{D}$ for $g(\alpha) = (\mathcal{M}(\alpha), \mathcal{E}(\alpha))$, subject to $\alpha \in \mathcal{D}$.

In addition, the potential energy

$$\mathcal{V}(\alpha) = \tfrac{1}{16}kL^2(\alpha^2 - \beta^2)^2 - \tfrac{1}{2}PL(\alpha - \beta) \quad (4)$$

will be used for comparisons concerning the stability of the arch.

(iv) The present problem is ideal for illustrative purposes, since it requires no more than the use of related rates from calculus and some results from multicriteria decision making.

The Minimum Mass Problem

If no further restrictions are imposed, the optimal design is obviously given by $\alpha^* = 0$ with minimum weight $\mathcal{M}(\alpha^*) = \rho L$. The corresponding optimal equilibrium is obtained from equation (1) as $\beta^* = -\left(\frac{2P}{kL}\right)^{1/3}$. The equilibrium is unique and it clearly is stable.

Suppose now one were to insist on $\alpha > 0$. In that case, the problem has no solution if one allows $\beta < 0$ as a possible deflected state, since one may choose α arbitrarily close to zero, resulting in $\mathcal{M}(\alpha)$ arbitrarily close to ρL with ρL not a possibility. This result also is evident from a graph of α versus β shown in Fig. 2.

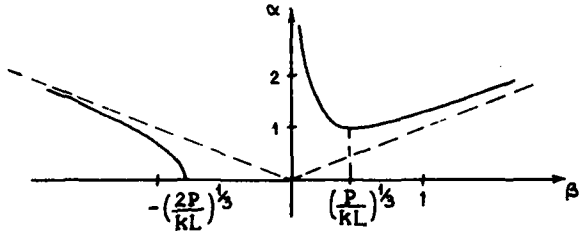


Fig. 2. Deflection versus Initial Shape

Usually, the intended use of an arch is one for which the arch does not sag upon loading; that is, one imposes both $\alpha \geq 0$ and $\beta \geq 0$ as design constraints. This is a so-called state constrained problem and the possible combinations of α and β now are restricted to the positive quadrant in Fig. 2. It follows that the final state β which implies the smallest initial angle α is the optimal one. The condition

$$\frac{d\alpha}{d\beta} = \frac{3\beta^2 - \alpha^2}{2\alpha\beta} = 0 \quad (5)$$

implies $\alpha = \sqrt{3}\beta$. Substitution into equation (4) results in $\alpha^* = \sqrt{3}\left(\frac{P}{kL}\right)^{1/3}$ with corresponding optimal equilibrium $\beta^* = \left(\frac{P}{kL}\right)^{1/3}$. The minimum mass is given by $\mathcal{M}(\alpha^*) = \rho L\left(1 + \frac{3}{2}\left(\frac{P}{kL}\right)^{2/3}\right)$. The use of the word "optimal" is justified because one also has

$$\frac{d^2\alpha}{d\beta^2}(\alpha^*) = \sqrt{3}\left(\frac{kL}{P}\right)^{1/3} > 0.$$

It follows that α^* solves the problem: Minimize $\mathcal{M}(\alpha)$ subject to equation (1), $0 \leq \alpha < \frac{\pi}{2}$, $\beta \geq 0$.

[5] Remark. Generally, for a given load P, and a given design α, there may be one, two, or three corresponding equilibria β. Here, there is a unique equilibrium determined by condition (5) which is the same as the usual critical loading condition given by

$$\frac{dP}{d\beta}(\beta) = \tfrac{1}{2}kL(\alpha^2 - 3\beta^2) = 0;$$

β^* is the critical equilibrium position indicated for the load-deflection curve (Fig. 3). From an energy viewpoint, a look at the total potential energy $\mathcal{V}(\cdot)$ indicates that $\mathcal{V}(\cdot)$ is locally cubic at $\beta = \beta^*$, so that the optimal equilibrium is unstable.

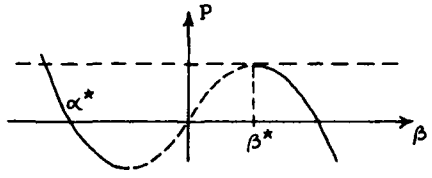


Fig. 3. Load-Deflection Curve

[6] Remark. Note that only the explicit inclusion of a stability condition such as $\mathcal{V}(\beta^*) \leq \mathcal{V}(\beta)$ for some neighborhood of β^*, or $\beta > \beta^*$ or $H > H^*$, H being the axial load in the spring, could have avoided this result. A simple constraint on the maximum deflection or on the maximum axial stress would not suffice, in general, to eliminate the possibility of unstable optimal equilibria.

The Minimum Stored Energy Problem

This problem serves as an excellent example for a standard approach to nonexistence proofs in optimization.

The substitution of equation (1) into the expression for the strain energy yields $\mathcal{E}(\alpha) = \frac{1}{4}\frac{P^2}{k}\frac{1}{\beta^2}$. As a consequence of $-\frac{\pi}{2} < \beta < \frac{\pi}{2}$ one has $\mathcal{E} = P^2/k\pi^2$ as the greatest lower bound which is, however, unattainable. It follows that the minimum $\mathcal{E}^*$, if it exists, must satisfy $\mathcal{E}^* > P^2/k\pi^2$.

Let $\bar{\mathcal{E}}$ be such that $P^2/k\pi^2 < \bar{\mathcal{E}} < \mathcal{E}^*$, take $\bar{\beta} = \frac{P}{2}\frac{1}{\sqrt{k\bar{\mathcal{E}}}}$ and let $\bar{\alpha} = \sqrt{\bar{\beta}^2 + \frac{2P}{kL}\frac{1}{\bar{\beta}}}$.

Thus, there exists an $\bar{\alpha}$ satisfying all constraints, such that $\mathcal{E}(\bar{\alpha}) < \mathcal{E}^*$, a contradiction. Furthermore, this result is not affected by including the additional constraints $\alpha \geq 0$ and $\beta \geq 0$, or by including the shallowness assumption restricting β to $-\beta_0 < \beta < \beta_0$.

The Natural Shapes of the Simple Arch

Some general comments concerning Pareto-optimality with two criteria may be helpful. The mapping $g(\cdot): \mathcal{D} \to \mathbb{R}^2$, given by $g(d) = (g_1(d), g_2(d))$, maps the decision set $\mathcal{D}$ into an attainable criteria set $g(\mathcal{D}) = \mathcal{A} \subset \mathbb{R}^2$, as shown in Fig. 4. The set of Pareto-optimal criteria values, $\mathcal{A}^*$, consists of the

boundary points indicated by the heavy line; the corresponding set of Pareto-optimal decisions $d^* \in \mathcal{D}$ is given by $\mathcal{D}^* = g^{-1}(\mathcal{A}^*)$.

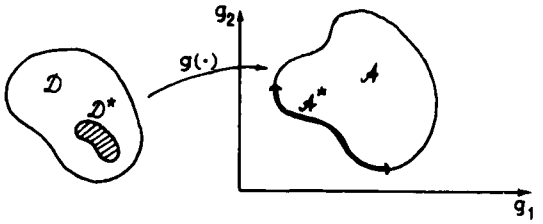


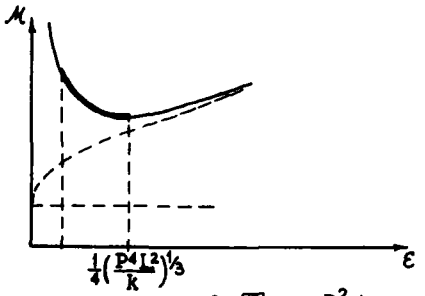
Fig. 4. The Attainable Criteria Set

In Ref. (1) the natural shapes of a structure were defined as those Pareto-optimal decisions $d^* \in \mathcal{D}$ which remained when the minimum mass decision and the minimum stored energy decision were excluded. This restriction can be enforced in terms of certain requirements included in the necessary conditions of the control or the programming problem. Here, this goal may be accomplished by using the necessary condition $\frac{dg_2}{dg_1}(d^*) \leq 0$, derived in Ref. (16), by requiring that the strict inequality be satisfied.

The restrictions $0 \leq \alpha < \frac{\pi}{2}$, $0 \leq \beta < \frac{\pi}{2}$ are again imposed. The mapping $g(\cdot)\colon [0, \frac{\pi}{2}) \rightarrow \mathbb{R}^2$ here is defined by $g(\alpha) = (\mathcal{M}(\alpha), \mathcal{E}(\alpha))$ so that the attainable set $\mathcal{A}$ is a curve in $\mathbb{R}^2$ (see Fig. 5). The use of the expressions (1), (2), and (3) yields the necessary condition

$$\frac{d\mathcal{M}}{d\mathcal{E}} = \frac{4\rho(\alpha^2 - 3\beta^2)}{kL(\alpha^2 - \beta^2)^2} < 0. \tag{6}$$

The condition $\alpha^2 - 3\beta^2 < 0$ together with the equilibrium equation (1) result in the requirements $\alpha^* > \sqrt{3}\left(\frac{P}{kL}\right)^{1/3}$ and $\beta^* > \left(\frac{P}{kL}\right)^{1/3}$ to be satisfied by the Pareto-optimal arch-rises α^* and the corresponding Pareto-optimal equilibria.



$$\mathcal{M}(\mathcal{E}) = \rho L\left[1 + \frac{2}{L}\sqrt{\frac{\mathcal{E}}{k}} + \frac{1}{8}\frac{P^2}{k}\frac{1}{\mathcal{E}}\right]$$

Fig. 5. Mass-Strain Energy Criteria Space

The term Pareto-optimal, rather than Pareto-exremal, is justified in view of the following argument. Among the conditions presented in Ref. (1), the sufficient condition for Pareto-optimality which is easiest to use here may be stated in the form: Suppose $d^* \in \mathcal{D}$ minimizes $G(d) = c_1 g_1(d) + c_2 g_2(d)$ subject to $d \in \mathcal{D}$, for some $c_1, c_2 > 0$. Then $d^* \in \mathcal{D}$ is a Pareto-optimal decision.

The second derivative of $G(\alpha) = \mathcal{M}(\alpha) + r\,\mathcal{E}(\alpha)$, $r > 0$, is

$$\frac{d^2G}{d\alpha^2} = \rho L + \frac{1}{4}rkL^2\frac{(\alpha^2-\beta^2)(3\beta^2+\alpha^2)(3\beta^4+\alpha^4)}{(3\beta^2-\alpha^2)^3} \tag{7}$$

which is greater than zero for all choices of α such that $3\beta^2 > \alpha^2$. It follows that the family of designs specified by $\sqrt{3}\left(\frac{P}{kL}\right)^{1/3} < \alpha^* < \frac{\pi}{2}$ is Pareto-optimal.

[7] Remark. A further look at the use of the preceding sufficient condition may be helpful. The minimizing choice α^* of course depends on the particular r which has been used. For each choice of $r > 0$, $\alpha^*(r)$ is a minimizing decision as long as one uses that corresponding equilibrium $\beta^*(\alpha^*)$ which satisfies the condition $3\beta^{*2} > \alpha^{*2}$.

[8] Remark. Condition (7) above leads to the same requirements for α and β as the condition

$$\frac{\partial^2 \mathcal{V}}{\partial \beta^2}(\beta) = \frac{1}{4}kL^2(3\beta^2 - \alpha^2) > 0 \tag{8}$$

assuring a minimum of the potential energy. Thus, a necessary condition for optimality is sufficient for stability. This is an ideal result; in view of the example in the next section, however, this is not generally the case.

The Uniform Shallow Arch

The details and generalizations of the following example may be found in Refs. (15) and (16); only the problem formulation and major results are presented here.

Consider a uniform shallow arch of span L and loaded by a transverse load $w(x)$. In addition, there may be a given axial load or one may arise as a reaction due to the boundary conditions. With initial shape and final shape specified by $y_0(\cdot)\colon [0,L] \rightarrow \mathbb{R}$ and $y(\cdot)\colon [0,L] \rightarrow \mathbb{R}$, respectively, the equilibrium equations of the arch have the form

$$\frac{d^2y}{dx^2} + \frac{H}{EI}y = \frac{d^2y_0}{dx^2} - \frac{M_0(x)}{EI} \tag{9}$$

for the transverse direction, and

$$\frac{dz}{dx} = -\frac{H}{AE} - \frac{dy_0}{dx}\frac{dy_1}{dx} - \frac{1}{2}\left(\frac{dy_1}{dx}\right)^2, \quad y(x) = y_0(x) + y_1(x) \tag{10}$$

for the axial direction. Here, E is the elastic modulus for the linearly elastic arch, I and A are the cross-sectional moment of inertia and area, z is the displacement of a point on the arch in the axial direction, and $M_0(x)$ is the moment due to the transverse load only.

The relevant criteria are the mass,

$$\mathcal{M} = \rho\left\{L + \frac{1}{2}\int_0^L\left[\frac{dy_0}{dx}\right]^2 d\xi\right\} \tag{11}$$

with mass per unit length ρ, and the strain energy

$$\mathcal{E} = \frac{1}{2}EI\int_0^L\left[\frac{d^2y}{dx^2} - \frac{d^2y_0}{dx^2}\right]^2 d\xi + \frac{1}{2}\frac{H^2L}{AE}. \tag{12}$$

The total potential energy is given by

$$\mathcal{V} = \frac{1}{2}\int_0^L\left\{EI\left[\frac{d^2y_1}{dx^2}\right]^2 + EA\left[\frac{dz}{dx} + \frac{dy_0}{dx}\frac{dy_1}{dx} + \frac{1}{2}\left(\frac{dy_1}{dx}\right)^2\right]^2 - 2w(\xi)y_1(\xi)\right\} d\xi \tag{13}$$

to be used in statements concerning the stability of the arch. Throughout, the initial curvature and the axial load are used as control parameters in optimizing the criteria mass and strain energy.

Control-theoretic and programming results are most easily applied when the problem is formulated in a standard form. This is accomplished by nondimensionalizing and by introducing some auxiliary variables as follows:

$$t = \frac{x}{L},\quad x_1(t) = \frac{y(tL)}{L},\quad x_2(t) = \frac{y_0(tL)}{L},\quad x_5(t) = \frac{z(tL)}{L}$$

$$\frac{d^2y_0}{dx^2} = \frac{1}{L}u(t) = \frac{1}{L}\dot{x}_4,\quad m(t) = \frac{M_0(tL)}{\bar{q}L},\quad q(t) = \frac{L^3}{2EI}w(tL)$$

along with $\dot{x}_1 = x_3$, $\dot{x}_2 = x_4$. In terms of these new variables one may then define the modified criteria

$$g_1(u(\cdot);\beta) = \int_0^1 x_4^2(\xi)\,d\xi \tag{14}$$

as the nondimensional mass, and

$$g_2(u(\cdot);\beta) = \int_0^1 [\pi^2\beta x_1(\xi) + \gamma^2 m(\xi)]^2 d\xi + \frac{1}{2}\frac{\pi^4\beta^2}{k^2} \tag{15}$$

with

$$\beta = \frac{HL^2}{\pi^2 EI}\ (H>0 \text{ for compression}),\quad \gamma^2 = \frac{\bar{q}L^2}{EI},\quad k^2 = \frac{L^2A}{2I}$$

as the nondimensional strain energy. The total potential energy has the form

$$g_3(x_1(\cdot), x_5(\cdot)) = \int_0^1 \Big\{[\ddot{x}_1(\xi) - \ddot{x}_2(\xi)]^2 + 2k^2[\dot{x}_5(\xi) + \tfrac{1}{2}(\dot{x}_1^2(\xi) - \dot{x}_2^2(\xi))] - 4q(\xi)[x_1(\xi) - x_2(\xi)]\Big\} d\xi \tag{16}$$

where the dependence on $x_1(\cdot)$ and $x_5(\cdot)$ has been emphasized because of the intended stability applications.

The nondimensionalized equilibrium equations and boundary conditions are given by

$$\begin{aligned}
&\dot{x}_1 = x_3 && x_1(0) = x_1(1) = 0;\\
&\dot{x}_2 = x_4 && x_2(0) = x_2(1) = 0;\\
&\dot{x}_3 = u - \pi^2\beta x_1 - \gamma^2 m && x_3(0) \text{ and } x_3(1) \text{ arbitrary};\\
&\dot{x}_4 = u && x_4(0) \text{ and } x_4(1) \text{ arbitrary};\\
&\dot{x}_5 = -\tfrac{1}{2}\frac{\pi^2\beta}{k^2} + \tfrac{1}{2}(x_4^2 - x_3^2) && x_5(0) = 0,
\end{aligned} \tag{17}$$

with $x_5(1)$ either arbitrary or specified as $x_5(1) = \delta$, some given displacement.

One of the control parameters is the initial curvature $u(\cdot)$; the axial load may either be specified as a given β, or it may be used as an additional control parameter. Collectively, it is assumed that

$$|u(t)| < \infty \quad \text{and} \quad |\beta| < \infty. \tag{18}$$

[9] Remark. There seems to be no consensus concerning the bound on slope which constitutes a shallow arch. The mathematical model itself is a mixture of seemingly contradictory assumptions. In the expression for the curvature it is assumed that $\left(\frac{dy}{dx}\right)^2$ is negligible in comparison to unity; in the expression for the axial strain the term $\frac{1}{2}\left(\frac{dy_1}{dx}\right)^2$ is assumed to be of the same order as $\frac{dz}{dx}$. Here, no further limitations have been imposed on $u(t)$ and β in order to allow for the full range of stability phenomena. Their physical applicability, of course, ultimately depends on the geometric and constitutive limitations of the mathematical model as obtained from experimental observations.

Concise general problem statements may now be given in terms of the nondimensional expressions above:

A. Minimize $g_1(u(\cdot);\beta)$ subject to the equilibrium conditions (17) and the control constraints (18).

B. Minimize $g_2(u(\cdot);\beta)$ subject to the equilibrium conditions (17) and the control constraints (18).

C. Obtain the remaining Pareto-optimal decisions for $g_1(u(\cdot);\beta)$ and $g_2(u(\cdot);\beta)$ subject to the equilibrium conditions (17) and the control constraints (18).

Collective Necessary Conditions and Problem Restrictions

The necessary conditions for each case consist of the appropriate formulations of the maximum principle and of Kuhn-Tucker conditions in programming. Summary conditions for all may be given in terms of those for Pareto-optimality. The general Hamiltonian has the form

$$\begin{aligned}
\mathcal{H}(x,\lambda,\beta,u) = {}& \lambda_0[c_1x_4^2 + c_2(\beta\pi^2x_1 + \gamma^2 m)^2] + \lambda_1 x_3 + \\
& \lambda_2 x_4 + \lambda_3[u - \beta\pi^2 x_1 - \gamma^2 m] + \lambda_4 u + \\
& \lambda_5\left[-\tfrac{1}{2}\frac{\beta\pi^2}{k^2} + \tfrac{1}{2}(x_4^2 - x_5^2)\right]
\end{aligned} \tag{19}$$

with $c_1 \geq 0$, $c_2 \geq 0$, not both zero, and with $\lambda_0 \leq 0$. The adjoint variables λ_i satisfy the equations

$$\lambda_i = -\frac{\partial \mathcal{H}}{\partial x_i},\quad i = 1,\ldots,5.$$

With $x_5(1) = 0$, the use of the condition $\frac{\partial H}{\partial u} = 0$ in combination with the adjoint equations eventually yields the differential equation

$$\begin{aligned}
&2\lambda_0 c_1 u^{IV} + 2\pi^2\beta[\lambda_5 + 2\lambda_0 c_1 - \lambda_0 c_2\pi^2\beta]\ddot{u} + \\
&\pi^4\beta^2[\lambda_5 + 2\lambda_0 c_1]u = [2\lambda_0 c_2\pi^2\beta - \lambda_5]\gamma^2 m^{IV}
\end{aligned} \tag{20}$$

which must be satisfied by an optimal initial curvature $u(\cdot)$. The necessary condition for an optimal selection of the parameter β is

$$\int_0^1 x_1[2\lambda_0 c_2(\beta\pi^2 x_1 + \gamma^2 m) - \lambda_3]\,d\xi = \frac{1}{2k^2}[\lambda_5 - 2\lambda_0 c_2\pi^2\beta]. \tag{21}$$

[10] Remark. Note that these results are restricted to $x_5(1) = 0$ and that one has $\lambda_5(t) = \lambda_5 = \text{const.}$ as a consequence of the adjoint equations. Note also that the present problems are formulated for particular boundary conditions. Naturally, one may also consider clamped arches or a mixture of clamped and hinged with corresponding changes in the necessary conditions (20) and (21).

The preceding formulation is given for an arbitrary loading $w(x)$. The remainder of the article is devoted to a summary of the results for the particular loading

$$w(x) = -q_0 \sin\frac{\pi x}{L} \tag{22}$$

with $\gamma^2 m(t) = -a \sin\pi t$, $a = (q_0L^3)/(\pi^2 EI)$.

In all cases the solution of equation (20) eventually yields only sinusoidal arches of the form

$$x_2(t) = A(\beta)\sin\pi t \tag{23}$$

as candidates for optimal designs. The problems thus reduce to the selection of an optimal axial load for the family of hinged sinusoidal arches subjected to a sinusoidal load.

[11] Remark. All of the results are stated in terms of the optimal equilibria and ranges of the applied load. To allow an easy comparison of the results with the stability conditions for shallow arches, the notation of Ref. (7) is used. The use of p_1 instead of λ_1 for the amplitude of the initial shape is an exception, since λ_1 is used as an adjoint variable here. The terms B_1, R, and p_1 are related to the nondimensional variables by

$$x_1(t) = \frac{\sqrt{2}}{k}B_1\sin\pi t,\quad x(t) = \frac{\sqrt{2}}{k}p_1\sin\pi t \quad \text{and} \quad R = \frac{ka}{\sqrt{2}\pi^2}.$$

The critical parameters for the shallow arch are

$$B_1^{\pm I} = \sqrt{\tfrac{1}{3}(p_1^2 - 1)},\quad R^I = p_1 + \sqrt{\tfrac{4}{27}(p_1^2 - 1)^3},\quad \beta^I = \tfrac{1}{3}(1 + 2p_1)$$

for $p_1 < \sqrt{\frac{\pi}{2}}$, and for $p_1 \geq \sqrt{\frac{\pi}{2}}$ they are

$$B_1^{II} = \sqrt{p_1^2 - 4},\quad R^{II} = p_1 + 3\sqrt{p_1^2 - 4},\quad \beta^{II} = 4.$$

The main goal here is qualitative results; quantitative results are found in Refs. (15) and (16).

The Minimum Mass Arch

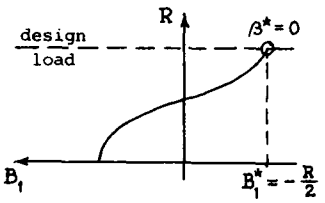
The corresponding necessary conditions are obtained with $c_1 = 1$ and $c_2 = 0$ in equations (19), (20), and (21).

Similar to the results for the simple arch, the admission of tensile axial loads implies $u^*(t) \equiv 0$, the flat arch, as the unique optimal solution of the problem with obviously stable optimal equilibrium. The inclusion of the additional constraint $\beta \geq 0$ yielded some unexpected results, depending on the ranges of the load parameter R of the applied sinusoidal load.

All of the results are illustrated in terms of load-deflection curves. Solid lines denote stable equilibria, dashed lines unstable equilibria, and the small circles denote the optimal equilibria.

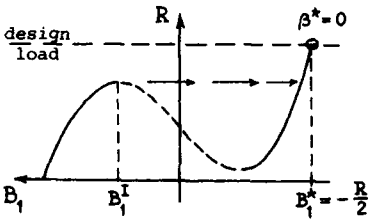
For $0 \leq R \leq 4$ one has $p^* = \frac{R}{2}$ with corresponding optimal equilibrium $B^* = -\frac{R}{2}$ and $\beta^* = 0$.

$0 \leq R \leq 2$



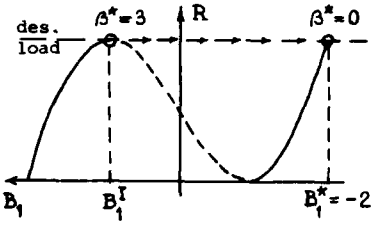
Upon loading, the arch passes through a sequence of stable equilibria; the optimal equilibrium is stable.

$2 < R < 4$



Upon loading, the arch passes through a sequence of stable equilibria until B_1^I is reached; it then snaps through. The optimal equilibrium is stable.

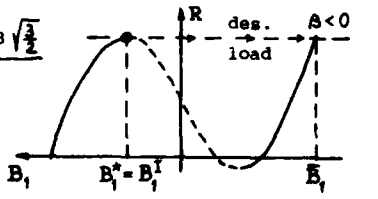
$R = 4$



There now are two optimal equilibria corresponding to $\beta^* = 3$ and $\beta^* = 0$, the former unstable, the latter stable. Obviously, the arch will snap through to the stable equilibrium.

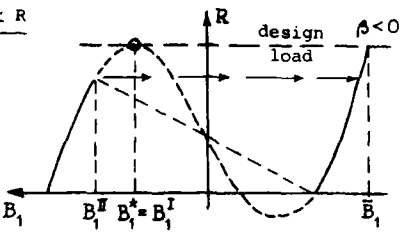
For $R > 4$, p_1^* is obtained by solving $R = p_1 + \sqrt{\frac{4}{27}(p_1^2 - 1)^3}$. The corresponding optimal equilibrium and axial load are given by $B_1^* = \sqrt{\frac{1}{3}(p_1^{*2} - 1)} = B_1^I$ and $\beta^* = \frac{1}{3}(1 + 2p^{*2}) = \beta^I$, respectively.

$4 < R < \sqrt{\frac{11}{2}} + 3\sqrt{\frac{3}{2}}$



In this range the arch still buckles symmetrically. Loading proceeds through stable equilibria to the unstable optimal equilibrium B_1^*. The arch snaps through to the non-optimal equilibrium $\bar{B}_1$; in fact, the equilibrium is excluded as a solution possibility by the assumption $\beta \geq 0$.

$\sqrt{\frac{11}{2}} + 3\sqrt{\frac{3}{2}} < R$



In this range the arch fails asymmetrically. The optimal equilibrium still is at B_1^*; however, upon loading, the arch passes through stable equilibria until it reaches B_1^{II}, snaps through, and is then loaded up to $\bar{B}_1$ which is stable, not optimal, and excluded by $\beta \geq 0$.

[12] Remark. Thus, depending on the magnitude of the load parameter R, the optimal equilibrium may be stable or unstable, it may be non-unique, it may be reached after snap-through, or it may not be attainable at all by the usual loading process. Note that only the explicit inclusion of stability constraints such as $B_1 \geq B_1^I$ or $\beta \geq \beta^I$ could have avoided these difficulties.

[13] Remark. The necessary condition (21) for an optimal selection of β is

$$R = \frac{\sqrt{2}}{2}\left[(\beta-1)^{3/2} \pm (3\beta - 1)^{1/2}\right].$$

This optimality condition is the same as the usual condition for the critical load, $\frac{dR}{dB_1} = 0$, as obtained from the load-deflection curve

$$R = p_1 - B_1^3 + (p_1^2 - 1)\,B_1 .$$

The Minimum Strain Energy Arch

The corresponding necessary conditions are obtained with $c_1 = 0$, $c_2 > 0$ in equations (19), (20), and (21).

The solution of equation (20) consists of a family of sinusoidal arches. However, the use of necessary conditions only is misleading here, since one can show that the minimum does not exist. An expression for the curvature satisfying all conditions eventually leads to the expression

$$g_2(u(\cdot);\beta) = \frac{\pi^4}{k^2}\left\{\left[\frac{R - \sqrt{R^2 - \beta^2(2-\beta)}}{2-\beta}\right]^2 + \frac{1}{2}\beta^2\right\} \quad (24)$$

for the strain energy as a function of β. Evidently, $g_2(u(\cdot);\beta) \geq 0$, and $\beta = 0$ is necessary to attain the absolute minimum. However, $\beta = 0$ in the equilibrium equations yields $g_2(u(\cdot);0) = \frac{\pi^4}{k^2}R^2$ so that the minimum, if it exists, must satisfy $g_2(u^*(\cdot);\beta^*) = g > 0$. Note now that $\lim_{\beta \to 0} g_2(u(\cdot);\beta) = 0$ so that $g_2(u(\cdot);\beta)$ can be made arbitrarily small and hence smaller than g, a contradiction.

The Natural Shapes of the Arch

The corresponding necessary conditions are obtained with $c_1 > 0$ and $c_2 > 0$ in equations (19), (20), and (21).

The use of necessary and of sufficient conditions for Pareto-optimal control ultimately implies that the solution of equation (20) leads to arches of the form

$$x_2(t) = \frac{\sqrt{2}}{k} p_1(\beta) \sin \pi t$$

and corresponding deflection

$$x_1(t) = \frac{\sqrt{2}}{k} B_1(\beta) \sin \pi t .$$

This reduces the problem to the multicriteria programming problem:

Obtain Pareto-optimal β^* for

$$g_1(\beta) = \frac{\pi^2}{k^2} p_1^2(\beta) \quad \text{and} \quad g_2(\beta) = \frac{\pi^4}{k^2}\left\{[B_1(\beta) - p_1(\beta)]^2 + \frac{1}{2}[p_1^2(\beta) - B_1^2(\beta)]^2\right\}$$

subject to $|\beta| < \infty$, where

$$p_1(\beta) = \frac{1}{\beta(2-\beta)}\left[R + |\beta - 1|\sqrt{R^2 + \beta^2(\beta - 2)}\right]$$

and

$$B_1(\beta) = \frac{R - p_1(\beta)}{\beta - 1} .$$

If no further constraints are imposed upon p_1 (that is, on the control $u(\cdot)$) and on β, then the globally Pareto-optimal solution is characterized by $p_1^*(\beta^*) = -p$, $p \geq 0$, where β^* is obtained from the solution of $\beta^* = p^2 - B_1^{*2}$, B_1^* being the real root of

$$B_1^3 - (p^2 - 1) B_1 = -p - R .$$

All of these arches are stable, sagging, and relatively uninteresting. They do, however, give rise to the following conjecture.

[14] Conjecture. All of the equilibrium states of a natural structure are stable when based on a global unconstrained concept of Pareto-optimality.

As for the simple arch, the situation becomes more interesting when an additional constraint is introduced. Here, this is done by insisting that the initial shape of the arch be a proper arch with $p_1 > 0$.

The necessary condition (21) for an optimal selection of the parameter β may be written in the form

$$r = \frac{3(B_1 - B_1^I)(B_1 - B_1^{-I})}{2(B_1 - p_1)^2 (B_1 - B^+)(B_1 - B^-)} = \frac{c_2 \pi^2}{2 c_1} ,$$

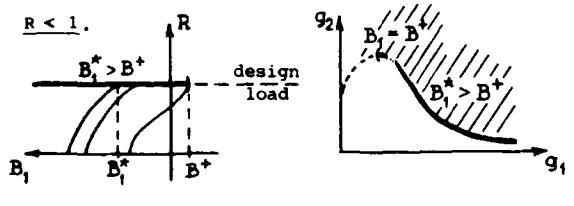
where

$$B^{\pm} = \frac{1}{p_1}\left[-(1 + p_1^2) \pm \sqrt{1 + 2p_1^2}\right] .$$

Sufficient conditions are used to show that one must have $B_1 > B_1^I$ for $p_1 > 0$, $r > 0$, eliminating the possibility $B_1 < B^{-I}$. Thus, the condition $r > 0$ leaves one with the requirement $(B_1 - B^+)(B_1 - B^-) > 0$ as the final constraint to be satisfied by the equilibrium parameter B_1.

The results of the analysis again depend on the ranges of the load parameter R, and they are most easily summarized in terms of the admissible values of the equilibrium parameter B_1; the ranges are illustrated in terms of the load-deflection curve and the corresponding boundary points of the attainable set.

$R < 1$.



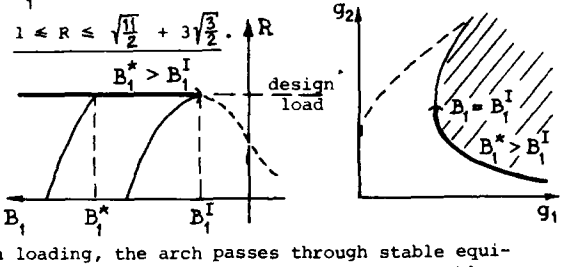
For $p_1 < 1$, one has the optimality condition given by $B_1^* > B^+$. Let $\hat{p}_1$ be the solution of

$$(B^+)^3 - (p_1^2 - 1)(B^+) = p_1 - R ,$$

then the condition implies that $p_1^* > \hat{p}_1$ must be the case. For $p_1^* \geq 1$, the natural equilibria satisfy $B_1^* > B_1^{I*}$ which simply means that the largest root of the load-deflection curve is to be chosen. The loading sequence and the natural equilibria are stable.

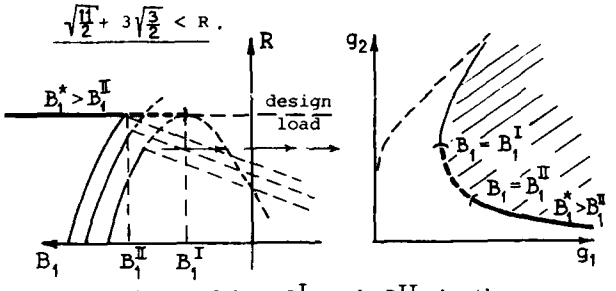
For $R \geq 1$, let $\hat{p}_1$ be the solution of $R = p_1 + \sqrt{\frac{4}{27}(p_1^2 - 1)^3}$; then the natural arches satisfy $p_1^* > \hat{p}_1$, and for any such p_1^* the corresponding natural equilibria satisfy $B_1^* > B^{I*}$. That is, for any p_1^* one has three equilibria $B^3 > B^2 > B^1$, and $B_1^* = B^3$.

$1 \leq R \leq \sqrt{\frac{11}{2}} + 3\sqrt{\frac{3}{2}}$.



Upon loading, the arch passes through stable equilibria; all of the natural equilibria are stable.

$\sqrt{\frac{11}{2}} + 3\sqrt{\frac{3}{2}} < R$.



Let R be given and let B_1^I and B_1^{II} be the corresponding critical equilibria; that is, $B_1^I = \sqrt{\frac{1}{3}(\hat{p}_1^2 - 1)}$, where $\hat{p}_1$ is the solution of $R = p_1 + \sqrt{\frac{4}{27}(p_1^2 - 1)^3}$ and $B_1^{II} = \sqrt{\bar{p}_1^2 - 4}$, where $\bar{p}_1$ is the solution of $R = p_1 + 3\sqrt{p_1^2 - 4}$. Then the natural shapes may be characterized as follows:

For p_1^* such that the corresponding B_1^* satisfies $B_1^I < B_1^* \leq B_1^{II}$, the loading sequence consists of stable equilibria until B_1^{II*} is reached; then the arch snaps through in the asymmetric mode and eventually settles at $\tilde{B}_1$ which is stable but not optimal.

For p_1^* such that $B_1^* > B_1^{II}$, the loading sequence and the natural equilibria are stable.

[15] Remark. The condition $r > 0$ is the same as $\frac{dg_2}{dg_1} < 0$. Both correspond to the stability requirement $\frac{d^2 g_2}{dB_1^2} > 0$ for the loading range in which the deflection is given by $x_1^*(t) = \frac{\sqrt{2}}{k} B_1^* \sin \pi t$ only; that is, for $R < \sqrt{\frac{11}{2}} + 3\sqrt{\frac{3}{2}}$.

References

(1) Stadler, W., Natural Structural Shapes (The Static Case), Quarterly Journal of Mechanics and Applied Mathematics, Vol. 31, No. 2, pp. 169-217, May 1978.

(2) Stadler, W., A Survey of Multicriteria Optimization or the Vector Maximum Problem, 1776-1960, Journal of Optimization Theory and Applications, Vol. 29, No. 1, pp. 1-52, September 1979.

(3) Thompson, J. M. T. and Hunt, G. W., Dangers of Structural Optimization, Engineering Optimization, Vol. 1, pp. 99-110, 1974.

(4) Olhoff, N., Optimal Design with Respect to Structural Eigenvalues, Proceedings of the 15th International Congress of Theoretical and Applied Mechanics, Toronto, Canada, August 1980.

(5) Weisshaar, T. A. and Plaut, R. H., Structural Optimization Under Nonconservative Loading, Proceedings of the NATO Advanced Study Institute on Optimization of Distributed Parameter Structural Systems, The University of Iowa, May 20-June 4, 1980.

(6) Petiau, C. and Lecina, C., Finite Elements and Optimization of Aeronautical Structures, AGARD Symposium on the Use of Computers as a Design Tool (in French), 1979, Translation in Foreign Technology Division, ID(RS)T-1604-79.

(7) Fung, Y. C. and Kaplan, A., Buckling of Low Arches or Curved Beams of Small Curvature, NACA Technical Note 2840, 1952.

(8) Wasiutynski, Z. and Brandt, A., the Present State of Knowledge in the Field of Optimum Design of Structures, Applied Mechanics Reviews, Vol. 16, No. 5, 1963.

(9) Levy, M. M., La Statique Graphique et Ses Applications aux Constructions, Gauthier-Villars, Paris, France, 1874.

(10) Wu, C. H., The Strongest Circular Arch--A Perturbation Solution, Journal of Applied Mechanics, Vol. 35, No. 3, 1968.

(11) Christensen, E. N., Optimal Design of Shallow Arches Against Buckling, Ph.D. Dissertation, Rensselear Polytechnic Institute, June 1975.

(12) Caldwell, H. McM., Optimization of Shallow Arches Against Snap-Through Buckling, Ph.D. Dissertation, Georgia Institute of Technology, 1977.

(13) Stadler, W., Uniform Shallow Arches of Minimum Weight and Minimum Maximum Deflection, Journal of Optimization Theory and Applications, Vol. 23, No. 1, pp. 137-165, September 1977.

(14) Stadler, W., Natural Shapes of Shallow Arches, Journal of Applied Mechanics, Vol. 44, No. 2, pp. 291-298, June 1977.

(15) Stadler, W., Stability Implications of the Optimal Design of Shallow Arches--Part I: (A) The Minimum Mass Arch; (B) The Minimum Stored Energy Arch. Submitted for publication.

(16) Stadler, W., Stability Implications of the Optimal Design of Shallow Arches--Part II: The Natural Shape of a Shallow Arch. Submitted for publication.

AD-P000 040

HYBRID OPTIMIZATION OF TRUSS STRUCTURES WITH STRENGTH AND BUCKLING CONSTRAINTS

Prabhat Hajela* and Holt Ashley**
Department of Aeronautics and Astronautics
Stanford University
Stanford, California

Summary

The problem of minimum weight truss layout is studied via a feasible usable search direction algorithm. For specific material allowable stresses in tension and compression, constraints on strength and stability are imposed. The idea of folding several constraints into a single cumulative measure of design specification violation is used. In addition to fixed geometry, node location movement is permitted through addition of design variables. Contrary to the usual practice of using uniform-cross-section members for all elements of the truss, optimally tapered bars are adopted for those elements sized by an Euler buckling criterion. Such tapered sections are obtained through a closed-form solution resulting from the application of a distributed parameter method and incorporated in the solution process via preprocessors. Significant weight savings are demonstrated.

A degree of complexity is added as a result of introducing redundancy in the structure through insertion of more elements. A statically determinate truss under a single load condition is optimal in a fully stressed configuration. However, both the presence of multiple loading conditions and the addition of redundancy drive the optimal design away from this configuration. Starting from a redundant truss and obtaining the global minimum weight by omitting certain elements is often difficult through conventional non linear programming algorithms. Practical side constraints such as those introduced from stability considerations, render the design space disjointed, concealing the true optima. Moreover, hardening of certain constraints as a result of diminishing a particular design variable value almost invariably moves the design to a non-global optima. As demonstrated here, the cumulative constraint idea, coupled with an artificial 'softening' of critical constraints, has permitted some of these difficulties to be overcome in the context of the nonlinear-programming (NLP) methodology.

The optimization algorithm is coupled to a finite-element analysis program through pre- and post-processors. In addition, further computational resource savings are obtained by piecewise linear approximations to the objective function and constraint information.

* Graduate Research Assistant

** Professor, Department of Aeronautics & Astronautics and Mechanical Engineering.

Introduction

The minimum weight design of truss structures has been an active area of research over the last two decades. Reference 1 is a comprehensive survey citing published work in this area up until the late 60's. Truss structures afford simple test examples for new optimization algorithms, while retaining complexities that sometimes require special treatment. It is recognized that an optimal nonredundant truss sized for stress constraints, is one that conforms to Michell's (Ref. 2) criterion of maximum allowable strain energy. The introduction of redundancies, side constraints and multiple load conditions moves the design away from a fully-stressed configuration. The resulting problem then requires a more involved design strategy.

Pedersen (Ref. 3 & 4) has solved the minimum weight layout problem with strength and stability constraints, via a linear programming algorithm. The present paper approaches the problem by using a feasible usable search-direction algorithm coupled with a finite-element analysis program. Constraints relating to strength in tension and compression are enforced. Side constraints on design variable size are introduced to exclude failure due to an Euler buckling instability. Both free and fixed node designs are generated.

A scheme, involving a modified cumulative constraint formulation, is proposed to adequately handle the problem of obtaining a minimum weight structure, starting from a highly redundant configuration. This problem was examined in detail in Ref. 5 and an iterative bounding technique solution proposed.

The aforementioned scheme has been used in designing a cantilever truss with varying degrees of redundancy. Optimal nonuniform section bars are used for all elements of the truss sized by the buckling criterion, so as to further enhance the weight savings. These optimal shapes are generated by the use of state-space methods as in reference 6.

Problem Statement

The design problem addressed in this study is the optimum sizing of planar truss structures for prescribed static loading conditions. For simplicity, idealized pin-jointed bar elements are assumed to comprise the truss, with material allowable limits on axial loading under tension and compression. The objective is to minimize the total weight of the structure. The problem can be mathematically formulated as

$$\text{Minimize} \quad W = \sum_i \rho_i A_i L_i \qquad i=1,2,..n \qquad (1)$$

Subject to the constraints

$$g_j \leq 0 \qquad j=1,2,..m \qquad (2)$$

$$A_i^u \geq A_i \geq A_i^L \qquad i=1,2,..n$$

where,

$$g_j \equiv \frac{|\sigma_j|}{\sigma_{al}} - 1 \qquad (3a)$$

or equivalently,

$$g_j \equiv \frac{|F_j|}{\sigma_{al}} \frac{1}{A_j} - 1 \qquad (3b)$$

ρ_i is the weight density of the material. Equation 2 establishes lower and upper bounds on the design variables. For purposes of this study, the cumulative constraint formulation of Ref. 7 is adopted, which allows the folding of 'm' constraints into a single measure of constraint violation 'Ω'.

$$\Omega \equiv -\varepsilon + \sum_{i=1}^{m} \langle g_i \rangle^r \qquad (4a)$$

$$\langle g_i \rangle \equiv \begin{cases} g_i & g_i > 0 \\ 0 & g_i \leq 0 \end{cases} \qquad (4b)$$

'ε' is a small positive initialization number. Side constraints can also be included in the cumulative constraint definition. In addition to the cross-sectional areas of the bar sections A_i, node locations can be established as additional design variables. The above formulation casts the minimum weight problem in the most general nonlinear-programming format.

Redundant Truss Structures

Shou & Schmit (Ref. 5) examine the problem of minimum-weight design of elastic redundant trusses for multiple loading conditions. For simple strength constraints and a single loading case, a given set of nodes can be connected by elements stressed to the maximum allowable limits, in a determinate configuration. For multiple loading cases and in the presence of other constraints such as stability, this is no longer valid. One way to approach this problem would involve connecting the prescribed nodes in all possible ways and searching the resulting highly redundant structure for the optimum. Constraints would have to be enforced to keep the final configuration stable.

If a standard NLP scheme is employed to dictate the search strategy, convergence to an incorrect optimum has been demonstrated in previous work with such structures. Two basic problems have been identified with using conventional gradient based search methods

(1) A process of constraint stiffening is identifiable in most problems. As some cross-sectional areas approach zero values, the ratio $|F|/\sigma_{al}$ (Eqn 3b) tends to a finite value, resulting in a corresponding constraint violation. Such constraint stiffening drives the design away from the true optimum.

(2) Side constraints on the design variable, such as those resulting from stability considerations, render the design space disjoint. These constraints conceal the true global optimum for an improper initial choice of the design variables.

Ref. 5 discusses an iterative bounding technique to deal with the above problems. By establishing lower and upper bounds on the optimum weight of the structure, the authors isolate a reduced number of stable truss configurations. An extensive search of these candidate designs yields the true optimum. To make the problem more amenable to standard nonlinear-programming methods, a constraint redefinition is proposed. The modified constraints become

$$g_i' \equiv \left\{ \frac{|\sigma_i|}{\sigma_{al}} - 1 \right\} \frac{A_i}{A_{ref}} \qquad (5)$$

Where A_{ref} is a prescribed softening factor, taking on values between 5 and 10 times the starting design variable values. This parameter is reduced as the optimum is approached, in order to counter any suppression of constraint violation. The cumulative constraint is then defined in terms of g_i'. Note that, as g_i approaches a finite value, the ratio A_i/A_{ref} approaches zero, removing the constraint stiffening influence from Ω. The cumulative constraint also includes the side constraints. In all such problems, caution must be exercised to prevent the design from attaining an unstable configuration.

Use of Non-Uniform Optimal Bars

As an illustration of how optimal control solutions can be adapted in a more practical NLP type optimization algorithm, truss elements critical in buckling were sized by a function space formulation similar to that of reference 6. For simplicity, this study was limited to the use of solid circular convex sections with the property

$$I_i(x) = K A_i^2(x) \qquad (6)$$

Here $I_i(x)$ is the moment of inertia and K is the shape factor ($K=1/4\pi$ for a circular section). Any other regular polygonal section could be prescribed and would afford a higher weight saving than the circular section. For a pin-ended column of length l and under a compressive load P, the differential equation describing the lateral deformation of the bar in buckling is

$$EI(x)\frac{d^2w}{dx^2} + PL^2w = 0 \qquad (7)$$

with the boundary conditions

$$w(0) = w(L) = 0 \qquad (8)$$

The Euler buckling load is given as

$$P_{cr} = \frac{E r^4 \pi^3}{4L^2} \qquad (9)$$

where 'r' is the radius of the circular cross section. Also, for a given load P and an allowable compressive stress σ_{al}, we have

$$P = \pi r^2 \sigma_{al} \tag{10}$$

Combining Eqns. 9 & 10 we have the design relationship

$$P_{cr} = \frac{E\pi P^2}{4\sigma_{al}^2 L^2} \tag{11}$$

$$P < \frac{4\sigma_{al}^2 L^2}{\pi E} \quad , \text{ design for buckling}$$

$$P > \frac{4\sigma_{al}^2 L^2}{\pi E} \quad , \text{ design for strength}$$

For a non dimensional area distribution a(x), the suboptimization problem can be formulated as follows. Minimize the non dimensional mass,

$$M = \int_0^1 a(x)\, dx \tag{12}$$

subject to the constraints given by Eqns. 7 & 8. The Hamiltonian formulation (Ref. 8) was used to derive the necessary conditions required for the optima. In addition, minimum gage constraints are enforced to eliminate the unrealistic designs marked by the appearance of zero cross-sectional areas along the column length. Such constraints provide a minimum area to handle the compressive stresses at all sections. The solution procedure to satisfy the optimality conditions results in a closed-form transcendental equation that yields the area distribution along the column length for a prescribed end load. Details of this solution are presented in an Appendix of reference 9. The optimal tapered column appears as in Fig. 1. A uniform cross section at the ends is followed by a gradually tapered area distribution with the maximum at the center. A plot of M against a measure of the load level is shown in Fig. 2.



$a_m = 0.25$

Fig. 1. Optimally tapered column to withstand compressive load P. Both buckling and compressive strength failures are excluded.

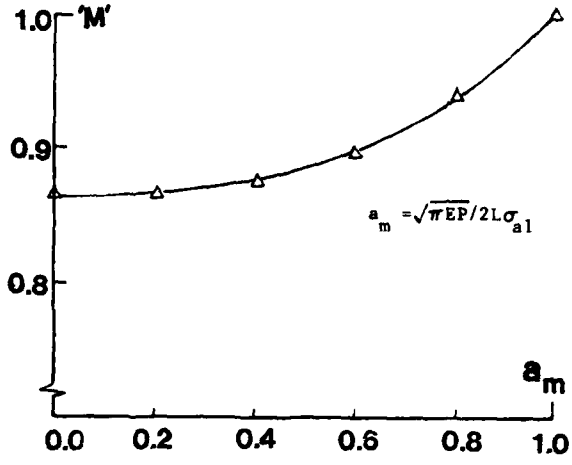


Fig. 2. Ratio of optimal weight to the weight of a uniform reference column 'M' versus a_m.

Numerical Implementation

A finite-element program was coupled to a feasible usable search direction algorithm (Ref. 10), via pre- and post-processors. The sequence of flow through these processors is illustrated in Fig. 3. To further augment savings of computational resources, a strategy involving piecewise linear approximations to the objective function and constraint information was adopted.

$$W^{new} = W_o + \left.\frac{\partial W}{\partial \bar{A}}\right|_{\bar{x}=\bar{x}_o} \Delta\bar{A}$$

$$\Omega^{new} = \Omega_o + \left.\frac{\partial \Omega}{\partial \bar{A}}\right|_{\bar{x}=\bar{x}_o} \Delta\bar{A} \tag{14}$$

Limits on design variable move of ±20% were imposed to preserve the effectiveness of the above approximations. The factor 'r' in Eqn. 4b introduces a non linearity in the constraint which requires special treatment of the constraint gradients, instead of a simple finite difference approximation for $\nabla\Omega$.

$$\frac{\partial \Omega}{\partial A_j} = \sum_{i=1}^{m} r\, [< g_i' >]^{r-1} \frac{\partial g_i'}{\partial A_j} \tag{15}$$

$$\frac{\partial g_i'}{\partial A_j} = \frac{\delta_{ij}}{A_{ref}}\, g_i + \frac{A_i}{A_{ref}} \frac{\partial g_i}{\partial A_j} \tag{16}$$

δ_{ij} is the Kronecker delta function. Using updated information for g_i' and g_i in equations 15 & 16 permits better approximations to $\nabla\Omega$ required in the linear extrapolation of Eqn. 14. For the design of truss structures with simple stress constraints, the choice of reciprocal variables provides further improvement in the constraint approximations.

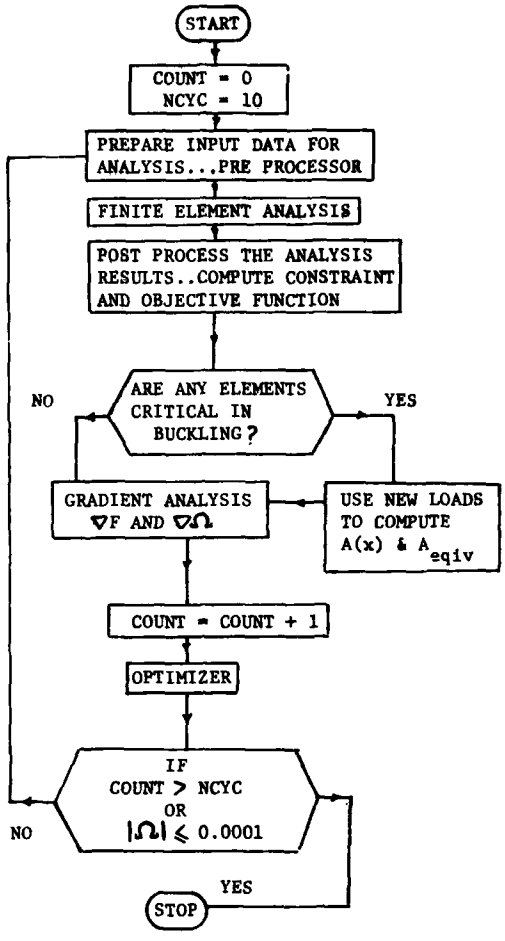


Fig. 3. Flowchart illustrating the flow between the pre- and post-processors.

Non Uniform Sections For a uniform, circular cross section column in critical compression, the minimum radius required for stability is given by

$$r_{cr} = \sqrt[4]{\frac{4L^2 P_{cr}}{\pi^3 E}} \qquad (17)$$

Since the finite element analysis program had the capability of accepting uniform sections only, an equivalent area obtained as

$$A_{eq} = \pi M r_{cr}^2 \qquad (18)$$

was used as an input to compute the stiffness matrices. 'M' is the non dimensional optimum mass ratio obtained as a suboptimization (Eqn. 12). A_{eq} was also used as a lower bound for the size of design variables critical in buckling.

Results

The first step in the study was to validate the procedure of suppressing the constraint stiffening effect. Truss examples from Ref. 5 were used to facilitate comparison. These examples typify the problems associated with using gradient based NLP techniques in redundant structures. The resulting designs are radically different from the true optima.

Three-Bar Truss. The classical three bar truss was sized for three alternative loading conditions depicted in Fig. 4. The design is subject to simple stress constraints only. There were no side constraints other than a design variable non-negativity constraint, allowing a continuous design space. Results of the present study with those reported in Ref. 5 are shown in Table 1. Excellent agreement in both the design variables and the objective function is observed.

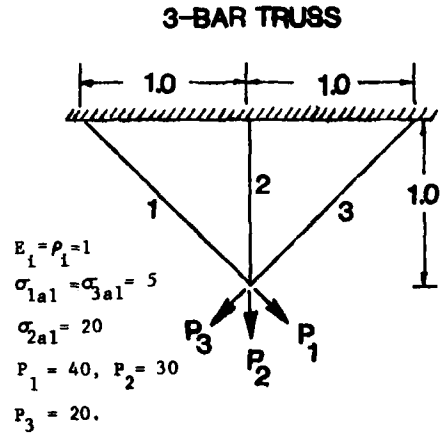


Fig. 4. Three Bar Truss example from Ref. 5. Material properties and allowable are also shown.

	A_1	A_2	A_3	WEIGHT
Sheu & Schmit Reference 5	8.0	1.5	0.0	12.8137
Proposed Method	8.03	1.495	0.0	12.8153

Table 1. A comparison of results from the proposed method with those reported in Ref. 5. (3 Bar Truss)

This example also provides the opportunity to visualize the cumulative constraint as a 3-dimensional surface plot. A region of interest, encompassing both the true and the local optima, was discretized into cubic elements and the constraint value Ω computed at the node points. A linearly interpolating contour plotting package was subsequently used to generate the surface plots for fixed Ω values. Plots for three values of Ω are shown in Fig. 5. As the optimum is approached (Ω tends towards zero), the constraint surface exhibits sharp slope discontinuities. This discontinuity in the design space makes it virtually impossible for a gradient-based search routine to locate the optimum. The constraint definition used in the present formulation suppresses the discontinuity, allowing the optimizer to converge to the correct result.

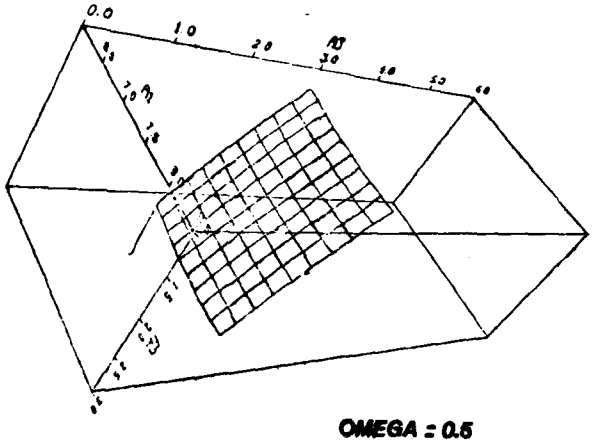


Fig. 5a. Cumulative constraint surface plot for Ω=0.5. A large continuous surface with a disjoint region of satisfaction on surface A_3=0.0.

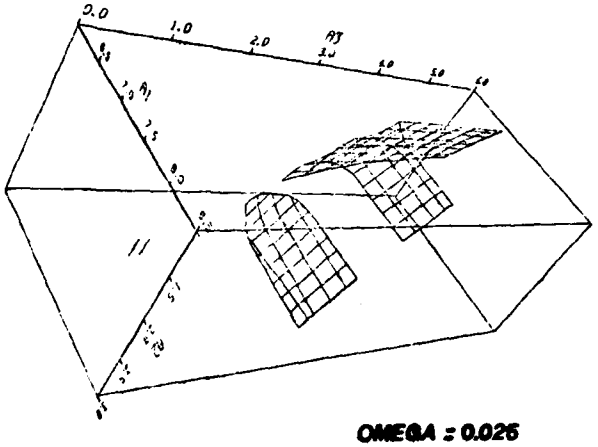


Fig. 5b. Cumulative constraint surface plots for Ω=0.025. Discontinuity appears on the surface.

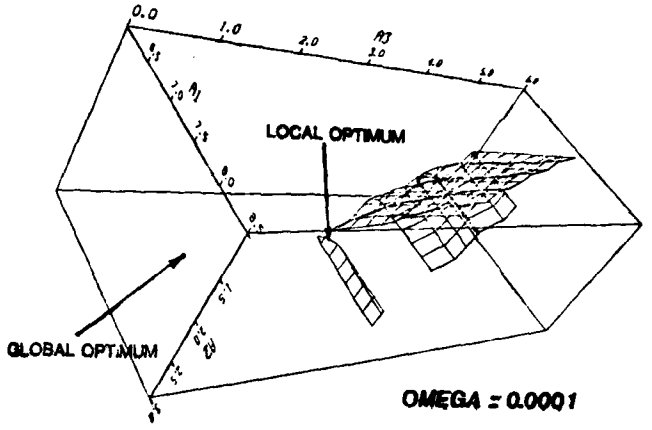
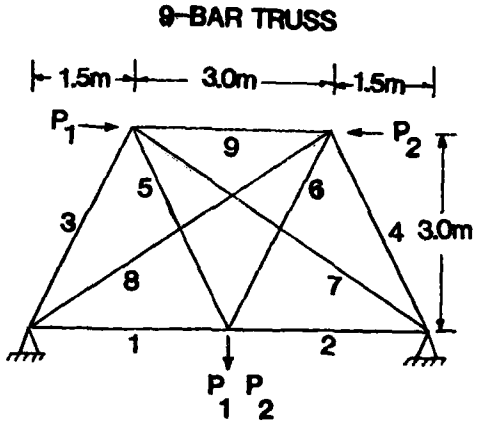


Fig. 5c. Cumulative constraint surface plot for Ω=.0001. Designs on this surface are accepted as feasible. Note that the global optima is on plane A_3=0.0.

Nine-Bar Truss. This five node, nine element truss is shown in Fig. 6. The structure was sized for two loading conditions. The symmetry of the loading conditions permits reduction of the size of the problem to five design variables. Lower limits on cross sectional areas, designed to keep the final configuration stable, render the design space disjoint. A comparison of results obtained with those of Ref. 5 are presented in Table 2.



$E_i = 2.04 \times 10^6$ Kg/cm^2, $\rho_i = .00785$ kg/cm^2

$\sigma^t = 1410$ Kg/cm^2, $\sigma_1^c = \sigma_2^c = \sigma_9^c = 1,270$ Kg/cm^2

$\sigma_7^c = \sigma_8^c = 846$ Kg/cm^2, $\sigma_3^c = \sigma_4^c = \sigma_5^c = \sigma_6^c = 1128$ Kg/cm^2

193.5 cm$^2 \geq A_i \geq 12.9$ cm^2

Fig. 6. Nine Bar Truss example from Ref. 5. Material properties, allowable stresses and side constraints are as shown above.

Figures 7 & 8 show the convergence histories for the three-bar and nine-bar trusses respectively. Both histories show an identical trend, with the structural weights converging from below to the true optima. The constraint 'softening' procedure initially suppresses the constraint violation, allowing the weight to fall below the optimum level. As the parameter A_{ref} is slowly relaxed, the weight converges to the correct optimum value.

	$A_1=A_2$	$A_3=A_4$	$A_5=A_6$	$A_7=A_8$	A_9	WEIGHT
		CM^2				KGS
Sheu & Schmit Refrence 5	17.92	90.16	72.13	0.0	71.67	1125.56
Proposed Method	17.88	89.98	72.32	0.0	71.58	1125.47

Table 2. A comparison of results with those reported in Refrence 5 for the five-node, nine-bar truss.

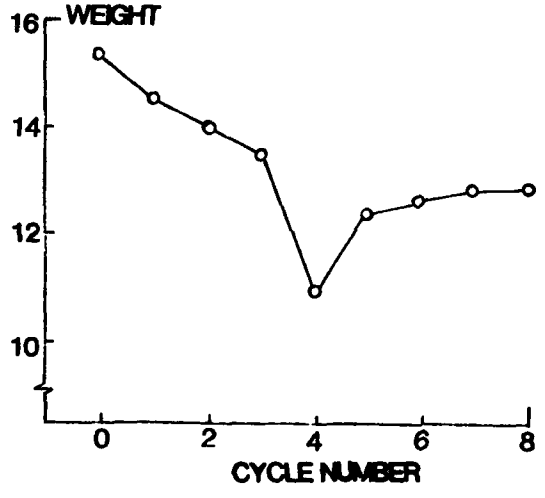


Fig. 7. Weight convergence history for the three-bar truss.

Fourteen-Bar Truss. With the validation of the sizing algorithm complete, a fourteen bar planar cantilever truss of Ref. 3 was selected as the candidate test structure. The initial structure and the loading condition were as shown in figure 9a. This structure was statically determinate and had a fixed geometry. A large initial tip load of 2,000,000 Kg was first applied. For this loading, all members were sized by the material allowable strength criterion. As the tip load F was decreased, the members continued to be sized proportionately by the above strength criterion up to a value of F=995,000 Kgs. At this load, the Euler buckling criterion, which depends on A^2 as opposed to the strength criterion dependence on A, begins to dominate the design. Four members with the lowest compressive load demonstrate the onset of a linear elastic instability (Fig. 9b), dictating the need for an additional constraint in the design process. Several optimal truss designs

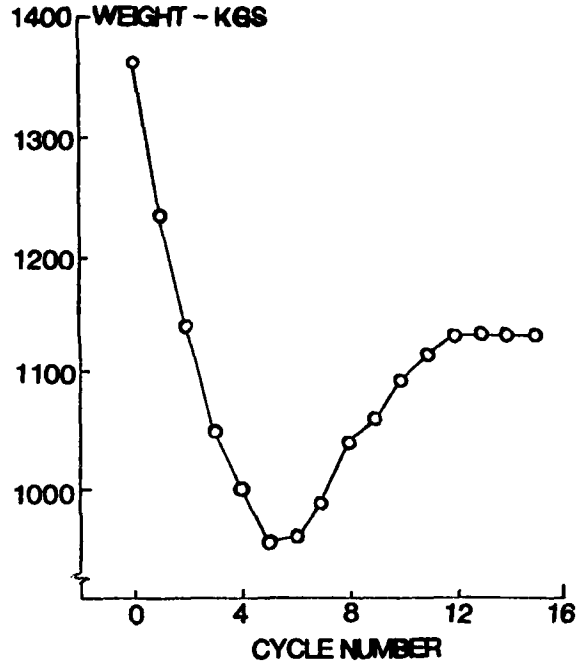


Fig. 8. Weight convergence history for the nine-bar truss.

were generated for different values of the tip load F. Results for a load level of 40,000 Kg are presented here, and these adequately demonstrate the trend observed for other loads. Figure 9c shows the optimal design for this load using uniform circular cross sectional elements. Elements are marked 'b' and 's' indicating if the corresponding sizing criterion was strength or buckling. Figure 9d shows the same configuration but with optimal tapered elements substituted for members sized via a buckling criterion. As shown in the figure, a weight saving of 9.5% is achieved over the conventional uniform-member optimal design.

To examine the variation of the optimum weight with the addition of redundancy in the structure, elements were added between selected nodes. This approach is one of adding 'seed' elements in the structure and examining the resulting stiffness increase versus the penalty incurred in terms of a weight increase. Fig 10a shows the optimal truss with one redundant element. This reflects a weight decrease of 6% over the corresponding optimum determinate structure. Further weight savings are demonstrated by the addition of two more redundancies in the structure. For this design, shown in Fig. 10b, one of the original elements drops out of the optimum configuration. An intermediate design with two redundancies yields an optimum weight of 706 Kgs.

More freedom was allowed in the design process by introducing the vertical locations of nodes 1,3,5 & 7 as additional design variables. This results in an optimal weight of 729 Kgs (Fig. 10c) as opposed to the fixed node design of 754 Kgs. Progressive increase in weight savings were observed with the addition of redundant elements to the free node configuration. Fig. 10d shows an optimal configuartion with four free nodes and three redundant elements. Here, as in the fixed-

node case, one of the original members drops out of the final configuration.

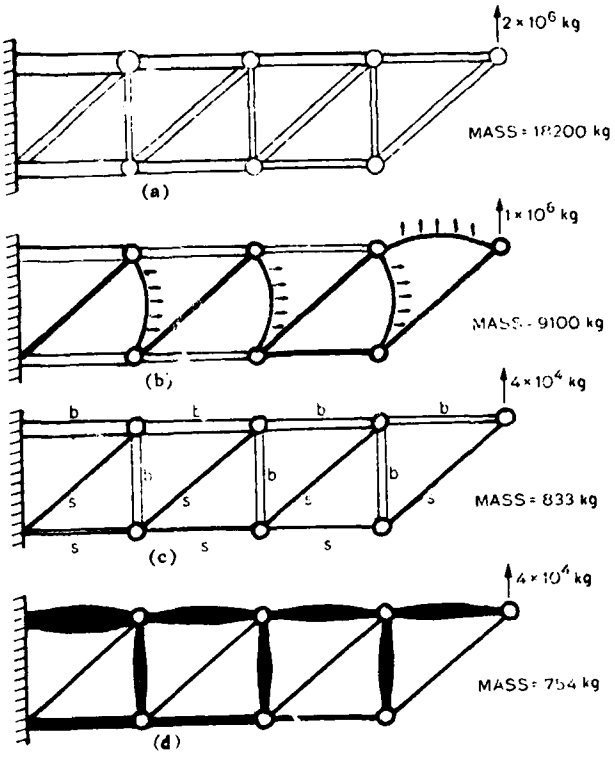
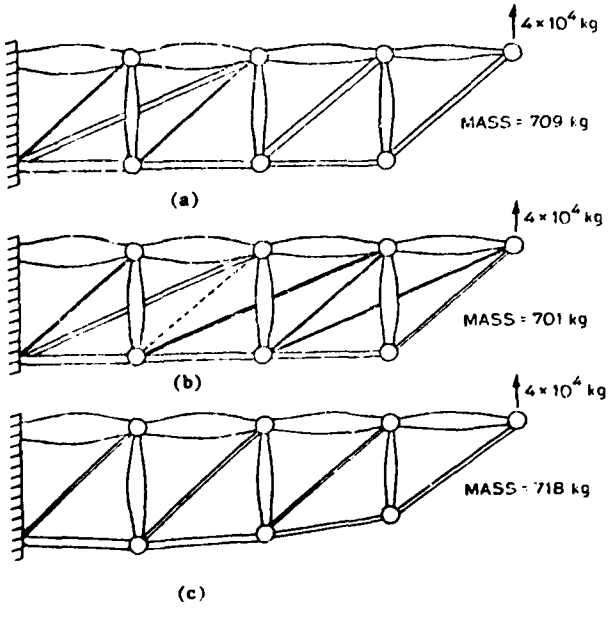


Fig. 9. Optimal configurations for the fourteen-bar truss structure.



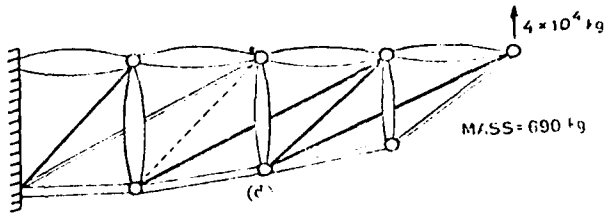


Fig. 10. Optimal truss configurations obtained through addition of redundancies to the fourteen bar truss.

Conclusions

An efficient scheme in the context of NLP methodology is proposed for the optimal design of elastic, redundant structures with strength and buckling constraints. Numerical examples demonstrate how the method, involving a constraint redefinition, successfully overcomes certain problems typical to such structures.

The scheme is applied to the design of a cantilever truss with strength and buckling constraints. Optimal nonuniform cross section columns are used for all elements critical in buckling, to further enhance the weight savings. Permitting node movement and the addition of redundancies are shown to lower the weight of the structure for the prescribed design constraints. It is noteworthy that the node excursions in this configuration are relatively small. This can be explained on the basis of an efficient 45° starting configuration for the truss. Also, although an increased depth at the root would offer greater bending strength, the weight penalty incurred as a result of increasing length of members critical in buckling limits such excursions. For excessively high tip loads, in which the strength design condition dominates, larger node movement would be observed.

Acknowledgements

The first author would like to acknowledge the valuable discussions with Dr. J. Sobieski of the NASA Langley Research Center.

This reasearch was supported under the the grant NGL 05020243 from the NASA Langley Research Center, Hampton, VA.

References

(1) Sheu, C.Y. and Prager, W., Recent Developments in Optimal Structural Design. Applied Mechanics Reviews, Vol. 21, No. 10, October 1968.

(2) Michell, A.G.M., The Limits of Economy of Material in Frame Structures. Philosophical Magazine, Ser. 6, Vol. 8, no. 47, Nov 1904, pp 589-597.

(3) Pedersen, P., On the Minimum Mass Layout of Trusses. Symposium on Structural Optimization, AGARD-CD-36-70.

(4) Pedersen, P., On the Optimal Layout of Multi-Purpose Trusses. DCAMM, Report No. 18, 1971.

(5) Sheu, C.Y. and Schmit, L.A., Jr. Minimum Weight Design of Elastic Redundant Trusses Under Multiple Static Loading Conditions. AIAA Journal, Vol. 10, No. 2, Feb 1972.

(6) Keller, J.B., The Shape of the Strongest Column. Archive of Rational Mechanics and Analysis, Vol. 5, 1960, pp 275-285.

(7) Hajela, P. and Sobieski-Sobieszczanski, J., The Controlled Growth Method-A Tool for Structural Optimization. AIAA Paper No. 81-0549, presented at the 22nd SDM Conference, Atlanta, Georgia, April 6-8, 1981.

(8) Bryson, A.E., Jr. and Ho, Y.C., Applied Optimal Control, Hemisphere Publishing Corp., Washington DC, 1975.

(9) Ashley, H., On Making Things the Best-Aeronautical Uses of Optimization. The 44th Wright Brothers Lecture, Paper No. 81-1738 , presented at the AIAA Aircraft Systems & Technology Conference, Dayton, Ohio, Aug 11-13, 1981.

(10) Vanderplaats, G.N., CONMIN - A FORTRAN Program for Constrained Function Minimization, NASA TM-X-62,282, 1973.

AD-P000 041

STOCHASTIC CONTROL IN STRUCTURAL DESIGN

D.G. Carmichael
Department of Civil Engineering
University of Western Australia
Nedlands 6009
Western Australia

Summary

Deterministic optimal control has contributed to the field of structural optimization through the introduction of new concepts, alternative ways of viewing design problems and a systematic methodology for solving design problems. It remains to show the applicability of stochastic control to the probabilistic structural optimization problem. Here the applicability is not so self evident but its usefulness can be demonstrated. The paper examines open-loop, closed-loop, open-loop feedback and m-measurement feedback control policies and gives the optimal result for the general nonlinear structural optimization problem. The special linear-quadratic problem is examined along with numerical approaches to solving the general nonlinear problem, including the method of stochastic approximation. The design of members in flexure and compression is used to illustrate the methodology.

1. Introduction

The use of deterministic control theory is now well established in the structural optimization literature. Although the original introduction of the theory involved the designer in learning new terminology and new concepts, the designer was rewarded with new solution techniques and a systematic methodology for problem solving [1]. The applicability, however, of stochastic control theory to the structural design problem has yet to be shown. The aim of the present paper is to show the applicability of the stochastic theory to structural optimization.

Stochastic control theory is the theory of control in the presence of uncertainty [2, 3]. Uncertainty may arise due to unknown constant or parameter values of the structural system, the environment or environment-structural system interaction (boundary and terminal conditions and loading). The uncertainty is reflected through characteristic system variables, the state, becoming stochastic or random variables. The relevant theory therefore deals with stochastic difference or differential equations. The presence of uncertainty is also reflected in the design problem solutions which are fundamentally different from the deterministic case. In particular the ideas of closed-loop and feedback control policies (as compared with open-loop policies) are introduced in order to handle the uncertainty.

Probabilistic structural design, in common with all systems design, exhibits characteristic variable groupings and characteristic problem components. The variable groupings are according to a state variable/control variable distinction where the state variables are descriptors of behaviour, such as deflections, rotations, internal actions, ... while the control (design) variables are the quantities directly at the disposal of the designer to vary. The characteristic problem components are a system model, design constraints and an optimality criterion.

The system model is an expression of how the environment and system variables interact. Of concern here are Markov assumptions on the state and system models in terms of stochastic difference equations. Difference equations are preferred over stochastic differential equation models as the former are conceptually simpler and analytically and computationally more tractable. Difference equations correspond with the so called discrete or sampled data systems while differential equations correspond with the so called continuous systems. Design constraints exist in a problem formulation in order to ensure that the resulting design solution satisfies such requirements as Code provisions, construction processes, manufacturing tolerances and the like. An optimality criterion (objective, performance index, merit function, ...) provides a measure of how good a particular design solution is compared with other solutions. Example criteria may be weight, performance, cost, ... The general form of each of these problem components is detailed in the following section (Section 2).

A derivation of the conditions for optimality for the general stochastic problem is given in Section 3. Generally it is seen, that some approximating numerical process is needed to solve these general conditions. There is, however, one specific problem which admits a closed form solution, namely the so called 'linear-quadratic' problem. The form of the components for the linear-quadratic problem are given in Section 4 along with the specific conditions for optimality applicable to this problem. Section 5 presents an alternative view of the solution of the general stochastic problem, namely one in terms of stochastic approximation. Illustrations throughout are in terms of beam and column members subjected to loading which is probabilistic.

2. Problem Statement

Consider systems whose states develop according to

$$x(k+1) = F[x(k),\ u(k),\ v(k),\ k] \qquad k = 0,\ 1,\ \ldots,\ N-1 \qquad (1)$$

where $x(k) = (x_1, \ldots, x_n)^T$ is an n dimensional state vector at stage k (total of N stages),
$u(k) = (u_1, \ldots, u_r)^T$ is an r dimensional control vector,
$v(k) = (v_1, \ldots, v_m)^T$ is a vector of random quantities,
and $F = (F_1, \ldots, F_n)^T$ is a general nonlinear n-vector function of the arguments shown. Boundary or terminal conditions (probabilities) on the state at k = 0 and/or k = N are also required.

Example Consider the beam equation

$$\frac{d^2}{dy^2}\left(\overline{EI}\,\frac{d^2w}{dy^2}\right) = p \qquad y \in [0,L]$$

converted to state equation form and discretized using a finite difference approximation over an interval size Δ. This gives

$$x_1(k+1) = x_1(k) + \Delta x_2(k)$$
$$x_2(k+1) = x_2(k) + \Delta x_3(k)/u(k)$$
$$x_3(k+1) = x_3(k) + \Delta x_4(k)$$
$$x_4(k+1) = x_4(k) + \Delta v(k) \qquad k = 0,\ 1,\ \ldots,\ N-1$$

where the states are deflection, slope, bending moment and shear force respectively, the control is the beam rigidity and the loading $v(k) \triangleq p(k)$ is taken as being a random quantity.

Additional to (1), stochastic control theory includes a measurement or observation equation, but for structural design purposes, the states may be regarded as being directly observable and hence this additional measurement equation may be omitted.

Constraints, typically, for the stochastic control problem are not handled separately. Rather, augmented optimality criteria are adopted using penalty function, weightings or Lagrange multiplier concepts. This is in contrast to the deterministic problem where much effort is spent in characterizing the effects of particular constraint types.

Consider an optimality criterion (including any constraint information) of the form

$$J' = g[x(N)] + \sum_{k=0}^{N-1} G[x(k), u(k), k] \qquad (2a)$$

where g and G are scalar functions of their arguments. Because x(k) is random through (1), J' is random and hence an unsuitable measure. A suitable deterministic measure (among others), however, may be obtained by taking the expectation of J' to give

$$J = E\{ g[x(N)] + \sum_{k=0}^{N-1} G[x(k), u(k), k] \} \qquad (2b)$$

Special cases are those of weight, where J is a function of u only, of serviceability where J is a function of x only, and others. Minimization of J is adopted without loss of generality. Probabilistic criteria other than (2) may be postulated.

A statement of the stochastic design problem is then: To determine the controls u(k), k = 0, 1, ..., N-1 so as to minimize the criterion (2b) while satisfying the system model (1) (including any boundary or terminal conditions). In essence the problem is a multistage decision problem if the analogy of decision with control is made.

A special case of (1) and (2b) will be considered later in Section 4. The problem is referred to as the linear-quadratic problem and is for the case where the system equations are linear and the criterion is a quadratic. This is a particularly tractable problem compared with the general nonlinear stochastic problem and its solution can frequently be used as a guide to design.

3. Optimal Stochastic Control

The conditions for optimality for the general problem defined by (1) and (2b) may be derived using Bellman's principle of optimality. The optimality result is in terms of a recursive expression involving conditional expectations. It is assumed that the loading and system parameters, which are random, have known probability laws or statistical moments. The loading and random system parameters are taken without loss of generality as being independent from one stage to the next. (Dependence may be accounted for by augmenting the state space [2, 4].) This gives the state as a first order Markov sequence and makes dynamic programming directly applicable to the problem.

Assume that the boundary values (probabilistic) of x at k = 0 are known. Consider the computations for the optimization firstly associated with the last interval from k = N-1 to k = N where it is assumed that x(N-1) is known and it only remains to evaluate the control u(N-1). Consider secondly the computations associated with the last two intervals where x(N-2) is assumed known and u(N-2) is to be evaluated. This process is repeated for the last three intervals, and so on.

Define

$$J_{N-1} \triangleq E\{G[x(N-1), u(N-1), N-1] + g[x(N)] \mid x(N-1), u(N-2)\}$$

$$J_{N-2} \triangleq E\{G[x(N-2), u(N-2), N-2] + J_{N-1} \mid x(N-2), u(N-3)\} \qquad (3)$$

etc., and the optimal return functions,

$$S_{N-1} \triangleq \min_{u(N-1)} J_{N-1}$$

$$S_{N-2} \triangleq \min_{u(N-2),\, u(N-1)} J_{N-2} \qquad (4)$$

...

$$S_{N-j} \triangleq \min_{u(N-j),\, \ldots,\, u(N-1)} J_{N-j} \qquad j = 3,4,..,N$$

Here S_{N-j} is the minimum value of the criterion for the j interval case, k = N-j to k = N.

Applying Bellman's principle of optimality leads to the recurrence relationship

$$S_{N-j}\,[x(N-j)] = \min_{u(N-j)} E\{ G[x(N-j), u(N-j), N-j] + S_{N-j+1}\,[x(N-j+1)] \mid x(N-j), u(N-j-1)\}$$

$$\text{where } x(N-j+1) = F[x(N-j), u(N-j), v(N-j), N-j] \qquad (5)$$

The computations proceed by evaluating $S_{N-j}\,[x(N-j)]$ and $\hat{u}(N-j)$ backward for j = 1 to N and proceeding forward after using the known values for x at k = 0. The sequence $\hat{u}(0), \ldots, \hat{u}(N-1)$, where the superposed $\hat{}$ denotes optimality, is the required optimal control sequence or policy. The end condition, from the definition of S is

$$S_N\,[x(N)] = E\{ g[x(N)] \mid x(N), u(N-1) \} \qquad (6)$$

All minimizations are carried out subject to any constraints present in the problem.

The result (5) implies that the optimal control policy is a closed-loop control policy, that is the control at any stage depends on the current state values while also anticipating further information from the stages that have yet to be processed.

Alternative classes of control policies may be defined, and in the stochastic control literature are introduced typically to simplify the computations over those involved assuming a fully closed-loop policy. The solutions using these alternative policies are necessarily suboptimal for the general nonlinear problem. The alternative classes of control policies are the open-loop and feedback policies. Briefly an open-loop policy prespecifies the control to be implemented at each stage while feedback and closed-loop policies incorporate new information during the solution process. The distinction between feedback and closed-loop policies is that while both utilize information that is available at the current stage of the solution process, feedback policies do not anticipate further information from the stages that have yet to be processed. In deterministic problems, 'future' stages are perfectly predictable and hence there is no distinction between open-loop, feedback or closed-loop policies. Two particular control policies belonging to the feedback class are the m-measurement feedback policy and the open-loop optimal feedback policy. The m-measurement feedback policy is based on using current stage information and anticipating future stage information up to m stages ahead. The open-loop optimal feedback policy utilizes only present stage information and assumes that the remaining stages follow an open-loop policy.

Solutions to certain stochastic control policies exhibit a property known as the certainty equivalence property. This prope is said to hold if the deterministic optimal control (using expected values for all the random variables) is the same as the closed-loop optimal control. The certainty equivalence property can be shown to hold for the linear-quadratic problem (Section 4). Commonly this property is assumed to hold in order to obtain a ready, but necessarily suboptimal, solution. (For the stochastic structural design problem with directly observable states, the so-called separation property of estimation and control theory is equivalent to the certainty equivalence property.)

The numerical solution of the general nonlinear stochastic control problem is delayed until Section 5 where the technique of stochastic approximation is discussed. The solution of certain specific control problems in closed form is however possible; the most widely referenced being the linear-quadratic problem which is discussed next.

4. The Linear-Quadratic Problem

The general nonlinear design problem given by (1) and (2b) may take special forms, the most common and most tractable of which is the so-called linear-quadratic problem. Here the system equations are

$$x(k+1) = A(k)\,x(k) + B(k)\,u(k) + v(k) \qquad k = 0, 1, \ldots, N-1 \tag{7}$$

(together with boundary or terminal conditions on x at k = 0 and k = N) where A(k) and B(k) are matrices of appropriate dimensions. A(k), B(k) and v(k) are random variables assumed independent of k and each other, and with known first and second moments. For v(k) white noise sequence properties are assumed,

$$E[v(k)] = 0$$
$$E[v(k)\,v^T(j)] = V(k)\,\delta_{kj} \tag{8}$$

The independence assumption on v(k) can be altered by augmenting the state space [2, 4].
The quadratic criterion is taken as

$$J = E\{\, x^T(N)\,Q(N)\,x(N) + \sum_{k=0}^{N-1} x^T(k)\,Q(k)\,x(k) + u^T(k)\,R(k)\,u(k) \,\} \tag{9}$$

where the matrices $Q(k) \geq 0$ and $R(k) \geq 0$.

Consider firstly the deterministic case. The result

$$\hat{u}(k) = -C(k)\,x(k)$$
$$S[x(k)] = x^T(k)\,M(k)\,x(k) \tag{10}$$

where C and M are $r \times n$ and $n \times n$ matrices, can be shown to hold [1, 5] using any of the several optimization methods available. This result implies a feedback or closed-loop control policy. However the matrices C and M, which depend on A, B, Q, R and on the state boundary conditions, may be calculated a priori, and hence the result is equivalent to an open-loop control policy.

For the stochastic case, a result similar to (10) can be shown to hold [2]. For the special case of A and B deterministic, the relevant relationships are

$$\hat{u}(k) = -C(k)\,x(k)$$
$$S[x(k)] = x^T(k)\,M(k)\,x(k) + m(k) \tag{11}$$

The uncertainty is reflected in an increased value (the scalar m(k)) of the optimality criterion over the equivalent deterministic case. The gain matrix C, the matrix M and the scalar m may be computed recursively from [5]

$$C(k) = [\, R(k) + B^T(k)\,M(k+1)\,B(k) \,]^{-1}\, B^T(k)\,M(k+1)\,A(k)$$
$$M(k) = A^T(k)\,M(k+1)\,A(k) + Q(k) - C^T(k)\,[\, R(k) + B^T(k)\,M(k+1)\,B(k) \,]\,C(k)$$
$$m(k) = m(k+1) + \mathrm{tr}[\, M(k+1)\,V(k) \,] \tag{12}$$
$$\text{with } M(N) = Q(N) \text{ and } m(N) = \mathrm{tr}\,[\, Q(N)\,V(N) \,]$$

Similar, but more general, optimality conditions for the case of A and B random are given in Aoki [2]. The equation in M is a discrete matrix Riccati equation. The linear-quadratic problem exhibits the certainty equivalence property. The uncertainties don't affect the control law but the performance of the system may be strongly affected.

Example. Consider the design of a cantilever beam. The relevant system equations are

$$x_1(k+1) = x_1(k) + \Delta x_2(k)$$
$$x_2(k+1) = x_2(k) + \Delta v(k)/u(k)$$

with $x_1(0) = x_2(0) = 0$. where the states are deflection and slope, v is the bending moment and the control u is the flexural rigidity. These equations may be linearized about some reference solution given by $x^o(k)$, $u^o(k)$ and $v^o(k)$, k = 0, 1, ..., such that

$$x = x^o + \delta x$$
$$u = u^o + \delta u$$
$$v = v^o + \delta v$$

For small deviations δx, δu and δv

$$\begin{bmatrix} \delta x_1 \\ \delta x_2 \end{bmatrix}_{k+1} = \begin{bmatrix} 1 & \Delta \\ 0 & 1 \end{bmatrix} \begin{bmatrix} \delta x_1 \\ \delta x_2 \end{bmatrix}_k + \begin{bmatrix} 0 \\ \Delta v^o \end{bmatrix}_k [\delta u] + \begin{bmatrix} 0 \\ \frac{\Delta}{u^o} \end{bmatrix}_k [\delta v]$$

Consider as an example a criterion of the form

$$J = E\{\, \delta x^T(N)\,Q(N)\,\delta x(N) + \sum_{k=0}^{N-1} \delta x^T(k)\,Q(k)\,\delta x(k) + \delta u^T(k)\,R(k)\,\delta u^T(k) \}$$

which may be used to give a desired response or rigidity by varying the weights Q and R.

For this illustration let the reference moment be that produced by a uniformly distributed load of 1 kN/m, let the length of the cantilever be 1 m, made up of 100 subintervals and let the reference rigidity be a quadratic as for the moment. Let Q and R be unit matrices.

The calculations begin at k = 100. Here

$$M(100) = \begin{bmatrix} 1 & 0 \\ 0 & 1 \end{bmatrix}.$$

At k = 99

$$A(99) = \begin{bmatrix} 1 & 0.01 \\ 0 & 1 \end{bmatrix},\quad B(99) = \begin{bmatrix} 0 \\ 0.5\times10^{-2} \end{bmatrix},\quad R(99) = [1],\quad Q(99) = \begin{bmatrix} 1 & 0 \\ 0 & 1 \end{bmatrix}$$

giving, through the use of (12),

$$C(99) = [0 \quad 0.4\times10^{3}] \text{ and } M(99) = \begin{bmatrix} 2 & 0.01 \\ 0.01 & 1.8 \end{bmatrix}$$

At k = 98, 97, ..., 0 the routine is repeated. At k = 0 the known boundary values of the state

$$E\begin{bmatrix} \delta x_1(0) \\ \delta x_2(0) \end{bmatrix} = \begin{bmatrix} 0 \\ 0 \end{bmatrix}$$

are used to give the control δu(0). The process then works forward using E[δx(k)] and δu(k) together with

the system equations to derive E[$\delta x(k+1)$] which in turn defines $\delta u(k+1)$. The whole process is then repeated up to k = N.

5. Stochastic Approximation

The general stochastic problem typically requires a solution by numerical means and some form of approximations. Various schemes have been proposed for the solution of this problem [2, 3] along the format of the general conditions for optimality outlined in Section 3. An alternative and promising numerical solution scheme is that of stochastic approximation [6] which may be regarded as a stochastic gradient algorithm.

For a control u(k) to minimize (2b) while satisfying (1), an iterative algorithm is sought such that

$$u^{i+1} = u^i - K_u^i \frac{\partial H^i}{\partial u^i} \qquad (13)$$

where the superscript i is the iteration step, K_u is a 'gain' term and H is the Hamiltonian of the problem defined by (1) and (2b) with the random variables taking some value in their sample spaces. Convergence of the solution can be shown to occur if K_u^i is chosen to satisfy certain requirements such as

$$\lim_{i \to \infty} K_u^i = 0 \quad , \quad \sum_{i=1}^{\infty} K_u^i = \infty \quad , \quad \sum_{i=1}^{\infty} (K_u^i)^2 < \infty \qquad (14)$$

A suitable K_u^i value is $^c/_i$, where c is a constant, but the convergence rate of the solution may be improved by alternative or mixed choices of K_u^i.

Example Consider the design of a column, assumed for illustration purposes to be pinned at each end and axially loaded. The relevant system equations are

$$x_1(k+1) = x_1(k) + \Delta x_2(k) \qquad (a)$$

$$x_2(k+1) = x_2(k) - \Delta P x_1(k)/\bar{E}u(k) \quad k = 0, 1, .., N-1$$

with $p[x_1(0)]$ and $p[x_1(N)]$ known. Here the states are deflection and slope, P is the applied axial load (assumed random with a known probability law), $\bar{E}$ is the material modulus of elasticity and the control u is the column moment of inertia. Take the optimality criterion as one of area (= constant x I^{-1})

$$\min J = E \sum_{k=0}^{N-1} u^{-1}(k) \qquad (b)$$

The solution process starts by sampling the distribution for P to give a value P^i and sampling the distributions for $x_1(0)$ and $x_1(N)$ to give values $x_1^i(0)$ and $x_1^i(N)$. The Hamiltonian for this situation is

$$H^i = u^{-1}(k) + \lambda_1(k+1)\,[\,x_1(k) + \Delta x_2(k)\,] + \lambda_2(k+1)\,[\,x_2(k) - \Delta P^i x_1(k)/\bar{E}u(k)\,] \qquad (c)$$

where λ_1 and λ_2 are costate variables.

The costate equations and costate boundary conditions follow,

$$\lambda_1(k) = \lambda_1(k+1) - \Delta\lambda_2(k+1)\,P^i/\bar{E}u(k)$$

$$\lambda_2(k) = \Delta\lambda_1(k+1) + \lambda_2(k+1) \qquad (d)$$

with $\lambda_2(0) = \lambda_2(N) = 0$.

The control is chosen to minimize the Hamiltonian. For a stationary value

$$0 = \frac{\partial H^i}{\partial u(k)} = -\tfrac{1}{2}\, u^{-2}(k) + \Delta\lambda_2(k+1)\,P^i x_1(k)/\bar{E}u^2(k) \qquad (e)$$

Equations (a), (d) and (e), together with the boundary values on x and λ, represent five equations in five unknowns x_1, x_2, λ_1, λ_2 and u. Following their solution the control is updated according to (13) and new boundary values for x, and a new value for P are selected. The whole process is repeated until a solution sufficiently close to the optimum is obtained. Sample calculations and results for framed structures are given in [7].

6. Closure

The problem of the probabilistic optimal design of structures is one of an order of magnitude greater difficulty than the deterministic problem. However, as deterministic control theory has demonstrated its usefulness and applicability to deterministic structural optimization, so too is stochastic control theory applicable to and useable for the probabilistic structural problem.

It is seen that the general nonlinear stochastic problem requires a numerical solution usually involving approximations of some form. Several methods and philosophies of solution were outlined in this regard. However there is one stochastic problem, namely the linear-quadratic problem, which does admit a closed form solution and may be used as a guide or benchmark solution to related problems.

When employing stochastic control theory, all structural variables retain their physical significance whether they be behaviour or geometry/material type variables. Similarly the design problem components retain their distinction and meaning.

References

1. Carmichael, D.G., Structural Modelling and Optimization, Ellis Horwood (Wiley), Chichester, 1981.

2. Aoki, M., Optimization of Stochastic Systems, Academic Press, New York, 1967.

3. Bar-Shalom, Y. and Tse, E., Concepts and Methods in Stochastic Control, in Control and Dynamic Systems (ed. C.T. Leondes), V.12, pp. 99-172, 1976.

4. Gelb, A. (ed.), Applied Optimal Estimation, M.I.T. Press, Massachusetts, 1974.

5. Sage, A.P. and White, C.C., Optimum Systems Control, Prentice-Hall, New Jersey, 2nd ed. 1977.

6. Sage, A.P. and Melsa, J.L., System Identification, Academic Press, New York, 1971.

7. Carmichael, D.G., Probabilistic Optimal Design of Framed Structures, Computer Aided Design, Sept., 1981.

AD P000 042

APPLICATION OF PERTURBATION METHOD TO OPTIMAL DESIGN OF STRUCTURES

N.V.Banichuk

Institute for Problems of Mechanics, USSR Academy of Sciences, Moscow, U.S.S.R.

SUMMARY

The paper presents results concerned with the use of perturbation method in optimal design of structures. An essential attention is given to optimization problems described by non-homogenuous boundary value problems for ordinary and partial differential equations. Different schemes for application of perturbation method in eigenvalue problems and in two dimensional optimization problems with unknown boundaries are described. Some aspects of obtaining successive approximations to optimal solution are given. The efficiency of perturbation technique application is illustrated by solving some particular problems. Some conclusions concerning practical application of the method and accuracy of used two-term expansions are drawn.

INTRODUCTION

Optimal structural design problems are very complicated. Thus, in some cases optimal design is reduced to solving variational problems with unknown boundaries and different types of singularities. The essential difficulties arise from the non-linear nature of the structural optimization problems. Even optimization problems for linear elastic structures are non-linear. The non-linearity of these problems are explained by non-linear nature of optimality conditions. Complexity of the structural optimization is the main reason why today the basic attention is given to development of numerical methods and use of computers. Application of techniques, based on numerical optimization methods (linear and non-linear programming) and simulation on computer give us the possibility to obtain the optimal solution for actual structures. At present our hopes are connected with development of numerical optimization methods and computers Undoubtedly, thatin sequal the high-speed computers will also play a basic part in optimal design of structures.
However, it should not be supposed that the application of the numerical optimisation methods is always effective. For a wide class of problems numerical approaches don't permit to establish general properties and to study the typical singularities of the optimal structures. These approaches are proved to be non effective to show the principal features, determining the shape of the optimal structure, and to investigate the solution on basic parameters. As an example we shall indicate the multiparameter optimal design problems. In this case for investigation of optimal structure and analysis of it's sensitivity to disturbances it is necessary to perform a lot of computations. It is worth whille mentioning, that the essential difficulties arise from the tabulation and storage of the obtained optimal solutions of multiparameter problems. Therefore the tools which are given by analytical methods should not be forgotten. To obtain more powerfull methods for optimal structural design it is natural to combine numerical calculation with analytical techniques.
The perturbation methods are proved to be very efficient for analytical researhes of nonoptimal problems. These methods are the most powerful tools of applied mathematics. Application of perturbation methods permits to obtain the approximate analytical representation of solutions of very complicated linear and non-linear boundary value problems both for ordinary and for partial differential equations. Perturbation methods are widely used for obtaining the asymptotics and analysis of singular points, for determination of analytical solution of the test problems. It should be noted that in some cases the perturbation techniques are the foundation for development of computing methods. Essentially, these techniques are the foundation for all methods of succesive approximations (*Ref.* 1).

The application of perturbation methods in optimization theory and, in particularly, in optimal structural design were started comparatively recently and at present these methods are not widely recognized and routinely employed. Only a few papers have appeared in the literature, concerning application of perturbation techniques to optimal structural design. Apparently a paper (Ref. 2) was the one of the first, where the perturbation method was used for determining the optimal solution. Note a paper (Ref.3) where the perturbation method was applied to optimization of weakly controlled mechanical system, described by ordinary differential equations. Applications of perturbation technique to the optimization problems with partial derivatives and unknown boundaries were given in papers (Refs.4, 5). Perturbation methods were used in (Refs.6-10) for solving optimal problems of hydro and aeroelastisity. Another examples of application of these methods to structural optimization are contained in book (Ref. 8). Note also a recent paper (Ref. 11) in which the optimal problem on reinforcement of the hole contour in plate was solved by the perturbation method.

Note some methodical aspects of perturbation technique application to the structural optimization problems. Let state vector-function $u(x)$ and control vector-function $h(x)$ be defined on the domain Ω in s-dimensional space. Let J denote the optimized performance criteria and $J_1(h, u)$, $J_2(h,u),\ldots,J_r(h,u)$ be the integral

functionals depending on h and u

$$J = F(J_1, J_2, \ldots, J_r)$$
$$J_i = \int_\Omega g_i(h, u, u_x)dx \qquad (1)$$

Equality type constraints are imposed on the values of J_i

$$F_j(J_1, J_2, \ldots, J_r) = 0$$
$$j = 1, 2, \ldots, k \qquad (2)$$

where F, F_j, g_i are given functions of their arguments. Function u satisfies the equations and the boundary conditions of the boundary value problem

$$L(h, \varepsilon)u = f \qquad (3)$$

Here $L(h, \varepsilon)$ is the operator of differentiation with respect to space coordinates, f is vector-function describing, for example, the external forces applied to the structure. Further we shall consider only the small deformations of elastic structures and so L will be a linear operator. Coefficients of the operator depend on control function h and small parameter ε. Let us write also the equation for small variations $L(h,\varepsilon)\delta u + M(h,u,\varepsilon)\delta h = 0$, corresponding to the equation (3). Here $M(h,u,\varepsilon)$ is operator applied to the vector δh.

The optimization problem consists in finding $h(x)$ amond the functions that satisfy the constraints (2), (3), such that the functional J is minimized.

For optimization problem (1) - (3) let us write the necessary optimality conditions (see, for example, (Ref. 8))

$$M^*(h,u,\varepsilon)v + \varphi(h,u,\lambda) = 0 \qquad (4)$$

$$\varphi \equiv \sum_{l=1}^{r} \frac{\partial \Phi}{\partial J_l} \frac{\partial g_l}{\partial h}$$

where $\Phi = F + \lambda_1 F_1 + \ldots + \lambda_k F_k$ and $M^*(h,u,\varepsilon)$ - operator which is conjugate to $M(h,u,\varepsilon)$. Optimality condition (4) connects the values of state function, control variable h, Lagrange multipliers $\lambda_1, \lambda_2, \ldots, \lambda_k$ and conjugate variable v. Lagrange multipliers correspond to conditions (2) and are determined through these conditions. Conjugate vector-function $v(x)$ is determined as a solution of the boundary value problem for equation

$$L^*(h,\varepsilon)v + \psi(h,u,\lambda) = 0 \qquad (5)$$

$$\psi \equiv \sum_{l=1}^{r} \frac{\partial \Phi}{\partial J_l}\left(\frac{\partial g_l}{\partial u} - \sum_{j=1}^{s} \frac{\partial}{\partial x_j}\frac{\partial g_l}{\partial u_{x_j}}\right)$$

with appropriate boundary conditions (see (Ref. 8)). Here the operator $L^*(h,\varepsilon)$ is conjugate to $L(h,\varepsilon)$ and s is the dimension of a vector of space coordinates.

Dimension of v is equal to dimension of u.

System of relations (2) - (5) represent the closed problem for determining h, u, v, λ.

Suppose that the solution of the optimization problem exists for any $\varepsilon < 1$, the differential equations and boundary conditions depend analytically on ε and that the solution of the problem with $\varepsilon = 0$ is known or can be obtained by means of simple analytical or numerical technique. Then the solution can be represented in the form of the power series with respect to ε for small ε. Since the differential equations and boundary conditions depend analytically on parameter ε and the solution is determined through analytical procedures, then it is naturally to suppose that the solution is analytic function of ε and that the application of perturbation technique is correct.

The values h, u, v, λ and J will be sought in the form of series expansions with respect to the small parameter ε

$$h = h^0(x) + \varepsilon h^1(x) + \varepsilon^2 h^2(x) + \ldots$$
$$u = u^0(x) + \varepsilon u^1(x) + \varepsilon^2 u^2(x) + \ldots$$
$$v = v^0(x) + \varepsilon v^1(x) + \varepsilon^2 v^2(x) + \ldots \qquad (6)$$
$$\lambda = \lambda^0 + \varepsilon\lambda^1 + \varepsilon^2\lambda^2 + \ldots$$
$$J = J^0 + \varepsilon J^1 + \varepsilon^2 J^2 + \ldots$$

where values h^i, u^i, v^i, λ^i, J^i don't depend on ε; and h^0, u^0, v^0, λ^0, J^0 - the solution of the optimization problem for $\varepsilon = 0$. To obtain the basic relations for h^1, u^1, v^1, λ^1, J^1 the series (6) must be substituted into the equations (2) - (5). The next step is to expand (2) - (5) for small ε and to arrange into groups the coefficients for each power of ε. Since these equations must be satisfied for arbitrary values of ε and the sequence of powers of ε a linearly independent, then the coefficients at any power of ε are equal to zero. Usually we obtain comparatively simple equations for desired functions. These equations must be successively solved. Original optimization problem is reduced to a set of more simple problems. Solving these problems permits to determine the optimal solution with any desired accuracy. So the zeroth order approximation is the solution of the problem

$$L(h^0, 0)u^0 = f, \qquad (7)$$
$$L^*(h^0,0)v^0 + \psi(h^0,u^0,\lambda^0) = 0$$
$$M^*(h^0,u^0,0)v^0 + \varphi(h^0,u^0,\lambda^0) = 0$$
$$F_i(J_1^0, J_2^0, \ldots, J_r^0) = 0,$$
$$J_j^0 = J_j(h^0, u^0)$$

and for determining the first approximation we have

$$L(h^0,0)u^1 + M(h^0,u^0,0)h^1 + N(h^0,u^0) = 0 \qquad (8)$$

$$L^*(h^0,0)v^1 + \psi^h(h^0,u^0,v^0,\lambda^0)h^1 + \psi^u(h^0,u^0,\lambda^0)u^1 + \psi^\lambda(h^0,u^0)\lambda^1 + \psi^\varepsilon(h^0,v^0) = 0,$$

$$M^*(h^0,u^0,0)v^1 + \varphi^h(h^0,u^0,v^0,\lambda^0)h^1 + \varphi^u(h^0,u^0,v^0,\lambda^0)u^1 + \varphi^\lambda(h^0,u^0)\lambda^1 + \varphi^\varepsilon(h^0,u^0,v^0) = 0$$

$$\sum_{j=1}^{r} \frac{\partial F}{\partial J_j}(J_1^0, J_2^0, \ldots, J_r^0) J_j^1 = 0$$

By means of $\varphi^h(h^0,u^0,v^0,\lambda^0)h^1$, $\psi^h(h^0,u^0,v^0,\lambda^0)h^1$, $\varphi^u(h^0,u^0,v^0,\lambda^0)u^1$, ..., $\varphi^\lambda(h^0,u^0)\lambda^1$, $\psi^\lambda(h^0,u^0)\lambda^1$ we denote the expressions, obtained as a result of expanding of the equations (4), (5) and separation of the members, which are linear with respect to h^1, u^1 and λ^1.

There is also another approach to solving optimization problems by perturbation methods. In the frame of this approach the next operation are carried out. Desired variables h, u, J, J_i of the problem (1) - (3) are expanded in power series with respect to small parameter ε. Optimality condition and the equations for the conjugate variables are not considered at the first stage. The expansions for h, u, J, J_i are substituted into the relationships (1)-(3) and the coefficients of like power in ε are summed and equate to zero. Then the optimization problems for the zeroth, first, second and more higher order approximations are formulated. The problems consist of optimization of the functional J^0, J^1, J^2,... with respect to h^0, h^1, h^2, ... At this stage Lagrange multipliers and the conjugate variables are introduced and the necessary optimality conditions are derived for every problems to be solved. This approach is completely equivalent to the approach discussed above. There are only methodological distinctions between these two approaches.

APPLICATION OF PERTURBATION METHOD TO OPTIMAL DESIGN PROBLEMS WITH ORDINARY DIFFERENTIAL EQUATIONS

Consider the problem of optimal design of the beam lying on elastic foundation (Fig. 1).

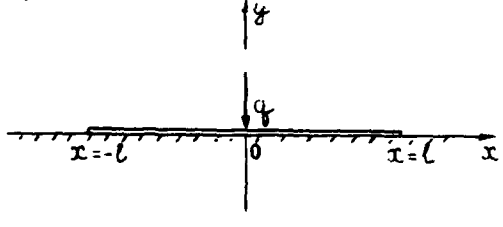


Fig. 1

The beam is simply supported at the points $x = \pm 1$ of the x axis and is loaded at the midpoint by the concentrated load $q = P\delta(x)$, where $\delta(x)$ is Dirac function. The foundation reaction is supposed to be directly proportional to the value of the beam deflection w with the proportionality coefficient C. Let the beam have rectangular cross-section of constant width b and variable height $h = h(x)(-l \le x \le l)$. The lenght 2l and the volume V of the beam are assumed to be given. It gives rise to the isoperimetric condition imposed on the cross-section area distribution $S(x) = bh(x)$.

When the beam shape (i.e., the function h(x)) is varied, the value of the integral stiffness will change. The optimization problem consists in finding the function h(x), satisfying the isoperimetric condition and maximizing the integral stiffness function with respect to h. In the case under consideration the maximization of the integral stiffness functional means the maximization of force value P which induce the given deflection w_0 at the point of load application. Let us write the basic relations of the problem

$$J = P = \frac{1}{w_0}\int_{-l}^{l}(Dw_{xx}^2 + cw^2)dx \longrightarrow \max_h \qquad (9)$$

$$(Dw_{xx})_{xx} + cw = q, \quad D = EI = \frac{1}{12}Ebh^3$$

$$(w)_{x=\pm 1} = (Dw_{xx})_{x=\pm 1} = 0, \quad w(0) = w_0$$

$$\int_{-l}^{l} S dx = V, \quad S = bh$$

where E is the Young's modules of the beam material; I is the moment of inertia of the beam cross-section; w_x, w_{xx} are respectively, the first and the second derivatives of deflection function w with respect to the variable x. The first relation (7) is the equality of the work produced by the force on the displacement w_0 to the potential energy accumulated by the beam and the elastic foundation in the deformation process. Note that the problem of weight (volume) minimization for given value of integral stiffness and the problem (9) are dual. The solutions of these problems can be obtained one from another by simple scaling. Optimality condition for the problem (9) and dual optimization problem can be obtained by usual variation technique and has the form

$$h^2 w_{xx}^2 = \lambda^2 \qquad (10)$$

Here λ^2 denotes the Lagrange multiplier corresponding to the isoperimetric condition.

Using the optimality condition (10) let us obtain the solution of the formulated problem in the case of small c. Apply the perturbation technicue for determination of unknown variables. With this purpose let us represent h, w, λ, P in the form of series expansions with respect to parameter c

$$h = h^0(x) + ch^1(x) + c^2h^2(x) + \dots$$

$$w = w^0(x) + cw^1(x) + c^2w^2(x) + \dots$$

$$\lambda = \lambda^0 + c\lambda^1 + c^2\lambda^2 + \dots$$

$$P = P^0 + cP^1 + c^2P^2 + \dots$$

Substitute these expansion into the basic relations and equate the coefficients of like power in C. For detrmining the unknown functions of zeroth order, corresponding to the case of absence of foundation reaction ($c = 0$), we obtain the system of equations, which solution has the form (the solution is written for $0<x<1$)

$$h^0 = \frac{3V}{4bl}\sqrt{1 - \frac{x}{l}}\,, \qquad P^0 = \frac{27Ew_0V^3}{256\,b\,l^6} \tag{11}$$

$$w^0 = w_0(1 - \frac{x}{l})(3 - 2\sqrt{1 - \frac{x}{l}}), \quad \lambda^0 = -\frac{9w_0V}{8bl^3}$$

Taking into account the properties of the zeroth order approximation lrt us write the boundary value problem for detrmining the firsr order approximation

$$\frac{bE}{12}((h^0)^2\left[h^0w_{xx} + 3h^1w^0_{xx}\right])_{xx} + w^0 = 0$$

$$w^1(0) = w^1_x(0) = w^1(1) = 0$$

$$(w^1_{xx}(h^0)^3 + 3w^0_{xx}h^1(h^0)^2)_{x=1} = 0$$

$$h^1w^0_{xx} + h^0w^1_{xx} = \lambda^1\,, \quad \int_0^l h^1dx = 0$$

$$P^1 = \frac{P}{w_0}(\frac{1}{12}\lambda^0\lambda^1 EV + \int_0^l (w^0)^2dx)$$

Detrmine the functions w^1 and h^1 using the equations described in the first and fourth line. The constants of integration and the value λ^1 are detrmined through boundary conditions and isoperimetric condition. As a result we obtain the corrections to the thickness distribution and the value of the force (in the first approximation)

$$h^1 = \frac{32bl^6}{9EV^2}\sqrt{1 - \frac{x}{l}}\left[(1 - \frac{x}{l})^2(1 - \right.$$

$$\left. - \frac{16}{35}\sqrt{1 - \frac{x}{l}}) - \frac{9}{35}\right], \quad P^1 = \frac{8}{7}lw_0 \tag{12}$$

From the obtained formulas (11), (12) it follows that the thickness of the beam at the middle part increases, but the beam thickness at the ends decreases (beam ends become pointed) when the parameter C increases.

The first approximation determined by the perturbation methods is in a good agreement with the exact solution found numerically (Ref. 8) with application of the successive optimization algorithm. Note, that the results of calculations for finite c are also presented in (Ref. 8).

APPLICATION OF PERTURBATION METHOD TO THE EIGENVALUE PROBLEM

The perturbation technique is very effective for the optimization problems governed by non-linear eigenvalue problems, for which closed solutions cannot be expected. As an example of the perturbation technique application to design of structures, described by the eigenvalue problems, let us consider the optimal problem of a wing of minimum weight under aeroelastic constraint on aileron efficiency (Ref. 10). It should be noted, that the decrease of elastic efficiency of aileron is one of the basic aeroelastic phenomenon, that make worse the maneuverability characteristics. The purpose of the problem consists in an investigation of this constraint influence on optimal distribution of structural material along the wing span. Suppose that the wing has a large aspect ratio (Fig. 2) and for determining wing deformation let us use the beam model of the wing structure.

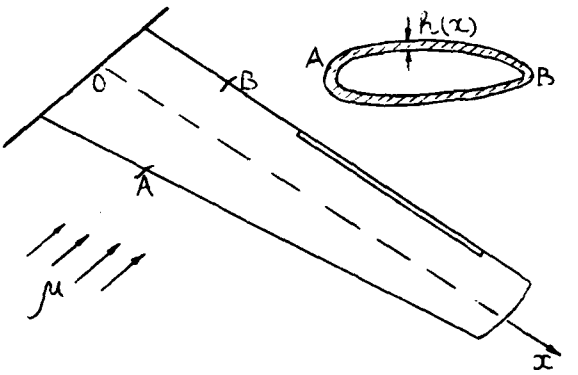


Fig. 2

The aileron is supposed to be rigid. Aerodinamic strip theory is used and the dominating contribution to the torsional stiffness comes from the skin, the thickness of which is assumed to vary along the span. Thickness distribution $h = h(x)$ along the span is considered as the "control" function. In terms of nondimensional variables (see (Ref. 10)) the equilibrium equation for wing with aileron in gas flow and the boundary conditions have the form

$$(h\theta_x)_x + \mu\theta = \varkappa\mu\int_0^1 \theta\,dx$$

$$\theta(0) = (h\theta_x)_{x=1} = 0$$

where θ is the angle of twist of the wing relative to elastic axis; μ is nondimensional pressure head playing the eigenvalue role in the problem under consideration; $\varkappa$ is the basic parameter depending on aileron efficiency and aerodynamic coefficients.

The dependence of $\mathcal{K}$ on these variables is presented in (Ref. 10)where it is also shown that the parameter $\mathcal{K}$ is small for cases which are interesting in practice.

Optimization problem consists in seeking the thickness function that minimizes the weight functional

$$J = \int_0^1 h \, d x \to \min_h$$

and is such that the minimum positive eigenvalue μ is equal or greater than given limit value μ_0 ($\mu_0 > 0$) for fixed value of $\mathcal{K}$

Necessary optimality condition has the form

$$\theta_x \varphi_x = \lambda \qquad (15)$$

where the conjugate function satisfies the following equation and boundary conditions

$$(h\varphi_x)_x + \mu\varphi = \mathcal{K}\mu x \int_0^1 \varphi \, d x \qquad (16)$$

$$\varphi(0) = (h\varphi_x)_{x=1} = 0$$

For the stated optimization problem the next normalization conditions are used

$$\int_0^1 \theta^2 d x = \int_0^1 \varphi^2 d x = \frac{1}{3}$$

Taking into account that the parameter $\mathcal{K}$ is small let us use the perturbation technique and represent the solution of the optimal problem in the form of series expansions with respect to small parameter $\mathcal{K}$

$$h = h^0(x) + \mathcal{K} h^1(x) + \mathcal{K}^2 h^2(x) + \ldots$$

$$\theta = \theta^0(x) + \mathcal{K} \theta^1(x) + \mathcal{K}^2 \theta^2(x) + \ldots$$

$$\varphi = \varphi^0(x) + \mathcal{K} \varphi^1(x) + \mathcal{K}^2 \varphi^2(x) + \ldots$$

$$\lambda = \lambda^0 + \mathcal{K}\lambda^1 + \mathcal{K}^2\lambda^2 + \ldots$$

Substituting the expansion into the relations (13)-(16) and normalization conditions and equating the coefficient of like power in $\mathcal{K}$ we obtain the relations for determining the zeroth, first, second ... order approximations. In particular, for the zeroth order approximation we obtain the same relations as for the optimal problem with divergence constraint (Ref. 12). The solution has the form

$$h^0 = \tfrac{1}{2}\mu_0(1 - x^2), \qquad \theta^0 = \varphi^0 = x \qquad (17)$$

For determining the unknown function of the first order approximation we have

$$(h^0\theta^1_x)_x + \mu_0\theta^1 = \mu_0 \int_0^1 \theta^0 \, dx - (h^1\theta^1_x)_x \qquad (18)$$

$$\theta^1(0) = (h^1\theta^0_x + h^0\theta^1_x)_{x=1} = 0$$

$$(h^0\varphi^1_x)_x + \mu_0\varphi^1 = \mu_0 x \int_0^1 \varphi^0 \, dx - (h^1\varphi^0_x)_x$$

$$\varphi^1(0) = (h^1\varphi^0_x + h^0\varphi^1_x)_{x=1} = 0$$

$$\int_0^1 \theta^0\theta^1 dx = 0, \qquad \int_0^1 \varphi^0\varphi^1 dx = 0,$$

$$\theta^1_x\varphi^0_x + \varphi^1_x\theta^0_x = \lambda^1$$

From the expressions for θ^0, φ^0 and the last equality (17) it follows that $\theta^1_x + \varphi^1_x = \lambda^1$. As far as $\theta^1(0) = \varphi^1(0) = 0$, then $\theta^1 + \varphi^1 = \lambda^1 x$. Let us multiply both sides of this equation by θ^0 and integrate with respect to x from 0 to 1. Using the (17) and the boundary conditions for function φ^1, we obtain $\lambda^1 = 0$.

From the boundary conditions for θ^1 and φ^1 at point $x = 1$ it follows that $h^1(1) = 0$. Let us sum the equation for θ^1, φ^1 and use the relation $\theta^1 = -\varphi^1$ and the properties of zero order approximation. Integrating the resulting equation and taking into account the boundary condition $h^1(1) = 0$, we obtain

$$h^1 = -\frac{\mu_0}{24}(7 - 4x - 3x^2)$$

Determine the function $\theta^1(x)$. To this end we use the (17), (19) and transform the equation (18) (first line) for θ^1 to the form $1/2((1 - x^2)\theta^1_x)_x + \theta^1 = \psi$, where $\psi \equiv (4 - 6x)/24$, $x \in (0, 1)$. Note that the equation $((1 - x^2)\theta_x)_x + \nu\theta = 0$, $x \in (-1,1)$ represents the Legendre equation The Legendre polynomials and the quantities $\nu_i = i(1 + i)$, $i = 0, 1, 2, \ldots$ are respectively the eigenfunctions and eigenvalues of this equation. The Legendre polynomials with odd indexes satisfy the conditions $P_{2i+1}(0) = 0$, $i = 0, 1, 2, \ldots$. Let us define the function $\psi(x)$ for $x \in [-1, 0]$. Using the odd extension of a definition of function ψ for $x \in [-1, 0]$ we represent it and $\theta^1(x)$ in the form of series expansions with respect to Legendre polynomials. Performing the standart calculation we obtain

$$\theta^1 = \sum_{i=1}^{\infty} \frac{(-1)^{i+1}(4i+3)1\,3\ldots(2i-1)}{6i(2i+3)(i+1)\;2^{i+1}} P_{2i+1}(x)$$

It is possible to prove that this series and the series composed from the derivatives are absolutely and uniformly convergent. Consequently, $\theta^1(x)$ is continuously differentiable function.

Similarly, the solution of the boundary value problem of the second order approximation furnishes the quantities h^2, θ^2, φ^2, λ^2, J^2 (Ref.10). For the sake of brevity we present only the final result for nondimensional weight, calculated to within the

the second order terms

$$J = J^0 + \varkappa J^1 + \varkappa^2 J^2 = \tfrac{1}{3}\mu_0(1 - \tfrac{1}{2}\varkappa - 0.0022\varkappa^2)$$

Comparison of the solution obtained by means of perturbation technique with the direct numerical solution of the optimal problem shows a good agreement between analytical and numerical results, contribution of the second order approximation to the functional being negligible. Thus, with a high accurasy we can take the first order approximation

$$h = \tfrac{1}{2}\mu_0(1-x)\left[1 + x - \tfrac{1}{12}\varkappa(7 + 3x)\right]$$

as the solution of the optimal problem of aileron efficiency.

APPLICATION OF THE PERTURBATION TECHNIQUE TO THE OPTIMIZATION PROBLEMS WITH PARTIAL DERIVATIVES AND UNKNOWN BOUNDARIES

An effective approach to solving two-dimensional optimization problems with unknown boundaries is a perturbation method. Application of this method implies expansion in power series both state variables (displacements, strains, stresses, etc.) and control functions describing the shape of the body. A shape optimization is reduced to the set of more simple problems and the solutions of these problems permits to determine the best shape with any desired accuracy.

In the problems with unknown boundaries these expansions are similar to the expansions in the problems with unknown coefficients of equations. Peculiarity of the problems with unknown boundaries consists in expansion of boundary conditions and optimality condition on the unknown boundaries. For these problem not only the state variables, defined at the points of the boundaries but also the functions giving the position of the boundary itself, must to be expanded. Thus, we must use the double expansions. Let us explain this on example. Let the condition $u(x, y) = 0$ is given on the unknown boundary Γ, described by the equation $y = y(x)$. Here $u = u(x,y)$ is the unknown state function. Let us represent the functions u and y in the form of series expansions with respect to the small parameter

$$u = u^0(x,y) + \varepsilon u^1(x,y) + \varepsilon^2 u^2(x,y) + \ldots$$
$$y = y^0(x) + \varepsilon y^1(x) + \varepsilon^2 y^2(x) + \ldots \qquad (21)$$

Taking into account that the functions u^i argument y is also represent in the form of series (21) we shall write the following full expansion for u

$$u = u^0(x,y^0) + \varepsilon\left[u^1(x,y^0) + u^0_y(x,y^0)y^1\right] + \varepsilon^2\left[u^2(x,y^0) + u^1_y(x,y^0)y^1 + u^0_y(x,y^0)y^2 + \tfrac{1}{2}u^0_{yy}(x,y^0)(y^1)^2\right] + \ldots \qquad (22)$$

Therefore the following conditions for the zeroth, first and second order approximations aries from the equality $(u(x,y))_\Gamma = 0$ and the expansion (22)

$$u^0(x,y^0) = 0\,, \quad u^1(x,y^0) = -u^0_y(x,y^0)y^1$$
$$u^2(x,y^0) = -u^0_y(x,y^0)y^2 - \tfrac{1}{2}u^0_{yy}(x,y^0)(y^1)^2 - u^1_y(x,y^0)y^1$$

It should be noted, that in applications of this method to shape optimization different degenerations are possible. Investigation of these cases lead to certain purely mathematical problems which havn't been solved. We shall not consider singular cases and present here general mathematical comments and proofs. We confine this discussion only to illustration of perturbation method possibilities for the example of a well-posed problem of cross-sectional shape optimization of a twisted bar.

Consider a homogeneous isotropic bar with a doubly-connected cross-section subjected to the twisting (Fig.3).

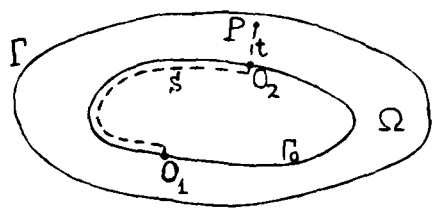


Fig. 3

Let Γ_0 and Γ denote, respectively, the inner and the outer boundaries of the region Ω. By means of φ and K we shall denote a stress function and torsional rigidity. In the sequel it is convenient to employ a curvilinear coordinate system s, t related to the contour Γ_0. The coordinate t of a point $P \in \Omega$ is the distance along the normal O_2P from the point P to the contour Γ_0, while s is the distance along the contour measured from a certain fixed point O_1 to the point O_2. Let $h = h(s)$ is the equation of the contour Γ and $R = R(s)$ the radius of curvature of the contour Γ_0 and l_0 its length. It will be assumed that the bar is thin-walled and that the minimum radius of curvature is of the order of the contour length l_0 (consideration is limited to only weakly curved contours), i.e. $\max_s h(s) = H \ll l_0$, $\min_s R(s) \sim l_0$. Consequently $\varepsilon = H/l_0$ is a small parameter ($\varepsilon \ll 1$).

The inner contour Γ_0 is considered to be given, but the outher boundary is to be determined. The optimization problem solved below consists of seeking a function $h(x)$ satisfying the isoperimetric condition of constant cross-sectional area of the bar and maximizing the torsional rigidity K.

The optimality condition for this problem is obtained in (Refs. 4, 5, 13). It means that the derivative of stress function φ along the normal is constant along the contour Γ.

In terms of the dimensionless variables equation for stress function φ, boundary conditions for φ on Γ_0 and Γ, Bredt condition, optimality condition for unknown boundary Γ isoperimetric condition of constant cross-sectional area of the bar and formula for torsional rigidity take the form (ref. 4)

$$(T\varphi_t)_t + \varepsilon^2 (T^{-1}\varphi_s)_s = -2\varepsilon T \qquad (24)$$

$$\varphi(s,0) = C\,, \quad \varphi(s,h) = 0$$

$$[\nabla\varphi(s,h)]^2 = \lambda^2\,, \quad T = 1 + \frac{\varepsilon t}{R}$$

$$\int_0^1 \varphi_t(s,0)ds = -2S_0\,, \quad \int_0^1 (h + \frac{h^2}{2R})ds = S$$

$$K = 2\left(\varepsilon \int_0^1 \int_0^h T\varphi\, dtds + CS_0\right)$$

where S is the area of domain Ω, S_0 is the area of the domain bounded by the contour Γ_0, C is the unknown constant determined with the help of Bredt condition, is the unknown Lagrange multiplier corresponding to the isoperimetric condition.

The solution of this problem will be sought in the form of series expansions with respect to the small parameter ε

$$\varphi = \varphi^0(s,t) + \varepsilon\varphi^1(s,t) + \varepsilon^2\varphi^2(s,t) + \ldots$$

$$h = h^0(s) + \varepsilon h^1(s) + \varepsilon^2 h^2(s) + \ldots$$

$$C = C^0 + \varepsilon C^1 + \varepsilon^2 C^2 + \ldots$$

$$\lambda = \lambda^0 + \varepsilon\lambda^1 + \varepsilon^2\lambda^2 + \ldots$$

$$K = K^0 + \varepsilon K^1 + \varepsilon^2 K^2 + \ldots$$

For finding the zeroth, first and second order approximate solution it is sufficient to substitute these expansions into the relation (24), take into account (21)-(23), and to equate the coefficients of like power in ε. The resulting boundary value problems serve to determine the unknown functions. Thus, for determining the unknown functions of zeroth order we have

$$\varphi^0_{tt} = 0\,, \quad \varphi^0(s,0) = C^0\,, \quad \varphi^0(s,h^0) = 0 \qquad (25)$$

$$\varphi^0_t(s,h^0) = -\lambda^0$$

$$\int_0^1 \varphi^0_t(s,0)ds = -2S_0\,, \quad \int_0^1 h^0 ds = S$$

Similarly the first approximation is the solution of the boundary-value problem

$$\varphi^1_{tt} = -2 - \frac{1}{R}\varphi^0_t\,, \quad \varphi^1(s,0) = C^1\,, \qquad (26)$$

$$\varphi^1(s,h^0) = \lambda^0 h^1$$

$$\varphi^1_t(s,h^0) = -\lambda^1$$

$$\int_0^1 \varphi^1_t(s,0)ds = 0\,, \quad \int_0^1 h^1 ds = -\frac{1}{2}\int_0^1 \frac{(h^0)^2}{R}\,ds$$

and the second approximation - that of the problem

$$\varphi^2_{tt} = -\frac{1}{R}\left[(t\varphi^1_t)_t + 2t\right] - \varphi^0_{ss}\,, \qquad (27)$$

$$\varphi^2(s,0) = C^2\,, \quad \varphi^2(s,h^0) = \lambda^1 h^1 + \lambda^0 h^2$$

$$\varphi^2_t(s,h^0) = (2 - \frac{\lambda^0}{R})h^1 - \lambda^2$$

$$\int_0^1 \varphi^2_t(s,0)ds = 0\,, \quad \int_0^1 h^2 ds = -\int_0^1 \frac{h^0 h^1}{R}\,ds$$

From the zeroth, first and the second order approximate solutions we can define the torsional rigidity of the bar

$$K = K^0 + \varepsilon K^1 + \varepsilon^2 K^2 + \ldots = 2C^0 S_0 +$$

$$+ 2\varepsilon\left(\int_0^1 \int_0^{h^0} \varphi^0 dtds + C^1 S_0\right) + 2\varepsilon^2\left(\int_0^1 \int_0^{h^0} \varphi^1 dtds + C^2 S_0\right) + O(\varepsilon^3)$$

Let us proceed with the solution of the above boundary-value problems. We start with the zeroth order terms. From equation and boundary condition (25) (the first line) we find the function. Using the obtained expression for φ^0 and the optimality condition (25) (the second line) we determine h^0. Thus we have $h^0 = C^0/\lambda^0$, $\varphi^0 = C^0(1 - t/h^0)$. Substituting the obtained functions into the isoperimetric equalities (25) (the third line) and performing elementary transformation we find the constants λ^0 and C^0. Finally, the zeroth order solution takes the form

$$h^0 = S\,, \quad \varphi^0 = 2SS_0(1 - \frac{t}{S})\,, \quad K^0 = 4SS_0^2$$

$$\lambda^0 = 2S_0\,, \quad C^0 = 2\,S\,S_0 \qquad (28)$$

Thus, in the zeroth order approximation for hollow bars with fairly shallow (large radius of curvature), inner contours the optimal bar will be of constant thickness.

Determine the values of the first order approximation. To do this we integrate the equation (26) for φ^1 and determine the constants of integration from boundary conditions. Then using the optimality condition and the isoperimetric conditions we find the function h^1 and the constants λ^1, C^1. As a result, we obtain the following expressions for the unknown values of the first order approximation

$$\varphi^1 = t^2\left(\frac{S_o}{R} - 1\right) + 2SS_o\left(\int_0^i \frac{ds}{R} - \frac{1}{R}\right) + \quad (29)$$

$$+ S^2 - 2S_o S^2 \int_0^i \frac{ds}{R}$$

$$h^1 = -\frac{S^2}{2R}, \quad K^1 = 4S_o S^2\left(1 - S_o \int_0^i \frac{ds}{R}\right)$$

$$C^1 = S^2\left(1 - 2S_o \int_0^i \frac{ds}{R}\right), \quad \lambda^1 = 2S\left(1 - S_o \int_0^i \frac{ds}{R}\right)$$

The influence of the internal contour curvature on the optimal form of the external boundary Γ_1 is described by the formula (29) for h^1. Thus, to within the terms of the order ε^2, we have

$$h = h^o + \varepsilon h^1 = S\left(1 - \varepsilon \frac{S}{2R}\right) \quad (30)$$

From the formula (30) for h it is evident that the wall thickness of the optimal bar decreases as we move along the inner contour in the direction of increasing curvature.

In order to determine the terms of order ε^2 it is necessary to integrate the equation (27) and to find the arbitrary constants of integration from the the boundary and the isoperimetric conditions. Finally, we get

$$h^2 = -\frac{S^3}{2R^2}\left(3 + \frac{R}{S_o} - 4R^2 \int_0^i \frac{ds}{R^2} - \frac{R^2}{S_o}\int_0^i \frac{ds}{R}\right) \quad (31)$$

Then we determine the value K^2. Using the obtained expressions for K^o, K^1, K and returning to the original dimensioned quantities, we get the following expression for the torsional rigidity of the optimal bar

$$K = \frac{4SS_o^2}{l_o^2} + \frac{4S_o S^2}{l_o}\left(1 - \frac{S_o}{l_o^2}\int_0^{l_o} \frac{ds}{R}\right) + \frac{4S^3}{3l_o^6}\Big[\, 3S_o^2 \times$$

$$\times \left(\int_0^{l_o} \frac{ds}{R}\right)^2 + S_o^2 l_o \int_0^{l_o} \frac{ds}{R^2} - 4S_o l_o^2 \int_0^{l_o} \frac{ds}{R} + l_o^4 \,\Big] \quad (32)$$

SOME NOTES AND CONCLUSIONS

The efficiency of the perturbation methods was illustrated above on example of solving of concrete problems. Considerations, which were carried out, and also the results of other works show that the one terms of expan sions (the zeroth and first order approximations), determined by the perturbation technique, give us a good approximation to the exact solution. Thus, for practical solution of the problems it is possible to restrict our calculations to first order approximations, the high accurasy being achieved as a rule.

Another important property discovered under the perturbation technique application consists in that although the expansions are constructed under the assumption that the parameter is small, the obtained approximations prove to be in a agreement with exact solutions not for only the small values of parameter. By the same token the domain of applicability of obtained solutions is found essentially more wide, that enhance the effi ciency of the method and permit to use it under the constructing quasioptimal solutions for finite values of the parameter also.

This paper is concerned with optimization problems with distributed parameters, for which the state variables are described by the differential or integro-differential equations. However the perturbation technique is applicable to the optimization prob lems with difference or difference-differential equation, arised under the use of the incremental approach.

The possitilities of a perturbation technique are not exhausted by the optimization problem considered here. Likewise, the perturbation technique may be used to solve the problems of optimizing the thickness distributions of a thinwalled structures. Various other constraints can be accounted for within the framework of the technique used.

In this paper attention is focused on applications of the perturbation technique to the optimization of structural elements. Note that the use this method for optimal design of complex structures is also perspective. Really, we can often conventionally devide the real complex structure on parts, weakly interacting with each other. Then by means of perturbation technique the original problem is reduced to a set of more simple optimization problems for separate parts and to synthesis of the structure from these parts. Detection of "weak" relations for complex structure and splitting of it compose the impor tant problem of decomposition. The problem of decomposition is one of the most actial modern problems in structural optimization. At present approaches to the optimal design of complex structures, based on decomposition and application of perturbation technique, are only started to develop. However their efficiency is doubtless.

The perturbation methods applications are not restricted to such cases, when the basic relation of the problems are contained the small parameter in explicit form. There are a lot of methods permitting to introduce the small parameter into the problem artificially. One general method of introducing the small parameter into the problem was discussed in (Ref.1). An affective schemes of the small parameter method, intended for the nimerical solution on computers, are also given in (Ref.1).

One of the basic part of optimal structural design is the sensitivity analysis. The traditional method of design sensitivity analysis is to simply change the design, and reanalyze the structure. Analytical and numerical aspects of design sensitivity analysis are developing at present. Important results have been obtained recently and are treated in the modern engineering literature (see, for example, (Ref. 14, 15)). Design sensitivity analysis gives us the tools for investigation of the influence of the initial perturbation on the optimal solution and

shows how to regularize the optimal problem. Note that even an optimum design exists, numerical methods for its solution are often quite sensitive to initial disturbances and for such cases it is very diffucult to determine the optimal design. Prior to developing a numerical algorithm it is necessary to determine the effect of perturbation in design on the functionals and to regularize the optimal problem. In this relation note that design sensitivity analysis rests implicitly on a foundation of perturbation techniques and that a convenient basis for its development is provided by these techniques.

In the paper the attention is focused on the optimal solutions fully based on perturbation techniques. It is worthwhile mentioning however, that there are several papers, where the perturbation techniques are exploited particularly (in combination with another methods, for separated parts of the problems, at the final stages of solving).

REFERENCES

1. Dorodnitsin A.A., Use of small parameter method for numerical solving of the mathematical physics equations. Lectures of summer school on numerical methods in Kiev (1966), Computer Center of AN SSSR, Moscow, 1966.
2. Wu C.H., The strongest circular arch-a perturbation solution. J. Appl. Mech. Trans. ASME, vol. 35, N 3, 1968.
3. Chernous'ko F.L., Some optimal control problems with small parameter. Prikl. Mat. Mekh. (USSR), vol. 32, N 1, 1968.
4. Banichuk N.V., On a variational problem with unknown boundaries and determination of the optimal shapes of elastic bodies. Prikl. Mat. Mekh. (USSR), vol. 39, N 6, 1975.
5. Banichuk N.V., Optimization of elastic bars in torsion. Int. J. Solids and Struct., vol. 12, N 4, 1976.
6. Banichuk N.V. and Mironov A.A., Optimal design of plate in dynamical problems of hydroelasticity. Proc. of All-union conference on the theory of shells and plates. Metsniereba, Tbilisi, 1975.
7. Banichuk N.V. and Mironov A.A., Optimization problems for plates that vibrate in an ideal fluid. Prikl. Mat. Mekh. (USSR), vol. 40, N 3, 1976.
8. Banichuk N.V., Optimization of shape of elastic bodies, Nauka, Moscow, 1980.
9. Seiranyan A.P., The problem of weight minimization of swept wing with the constraint on divergence speed. Uch.-zap TsAGI, N 6, 1979.
10. Seiranyan A.P. An optimal problem of aileron efficiency. Izvestija of Arm. SSR Academy of Sciences. Mech., vol. 33, N 1, 1980.
11. Kurshin L.M. and Rastorguev G.I., On reinforcing of hole contour in plate. Izvestija of USSR Academy of Sciences. Mech of Solids., N 6, 1979.
12. Ashley H. and Mcintosh S.C., JR, Application of aeroelastic constraints in structural optimization. Proc. 12 th Internat. Congress of Theoret. and Appl. Mech., Stanford, Berlin, Springer-Verlag 1968.
13. Kurshin L.M., On the problem of determining the shape of a bar section of maximum torsional stiffness. Dokl. Acad. Nauk, SSSR, vol. 223, N 3, 1975.
14. Haug E.J. and Arora J.S., Applied optimal design. John Wiley, New York, 1979.
15. Haug E.J. and Rousselet B, Design sensitivility analysis in structural mechanics I, static response variations. J. Structural Mechanics, vol. 8, N 1, 1980.



SESSION #4

SHAPE OPTIMIZATION I

AD-P000 043

SHAPE OPTIMAL DESIGN OF ELASTIC STRUCTURES

E. J. Haug
K. K. Choi
J. W. Hou
Y. M. Yoo

Division of Materials Engineering
College of Engineering
The University of Iowa
Iowa City, Iowa 52242

ABSTRACT

This paper investigates a relatively new class of structural optimization problems that are expected to be important in future applications. Instead of selecting explicit design parameters or functions defining dimensions of a distributed parameter structure over one or two space dimensions, as is normally done in structural optimization, the shape of the elastic solid under consideration plays the role of the design variable. The shape design formulation, for two and three dimensional elastic structures, is essential when load and support conditions lead to fully planar or three dimensional displacement fields that can not adequately be modeled by assumptions arising in beam, plate, or shell theory.

One of the first treatments of a general problem of selection of shape of a structure as the design variable is presented by Zienkiewicz and Campbell [1]. They formulate the shape optimal design problem using a finite element model of the structure and treat the location of nodal points of the finite element model as design variables. They employ sequential linear programming for numerical solution, presenting examples associated with dams and rotating turbine machinery. Ramakrishnan and Francavilla [2] employ a similar finite element formulation, but use a penalty function method for numerical optimization. Francavilla, Ramakrishnan, and Zienkiewicz [3] employ the finite element method of Refs. 2 and 3 for fillet optimization to minimize stress concentration. Schnack [4] and Oda [5] use a finite element formulation for stress calculation in the neighborhood of a stress concentration and iteratively modify the contour to minimize the peak stress.

More basic approaches for surface contouring to minimize stress concentration are presented by Tvergaard [6] and Kristensen and Madsen [7] in selecting the optimum shape of a fillet [6]. He employs a stress field model of the fillet, with a finite dimensional family of orthogonal polynomials defining the boundary shape, and a sequential linear programming method to construct an optimum design.

Bhavikatti and Ramakrishnan [8] present a refinement of the formulation of Refs. 1, 2, and 3 for optimum design of fillets in flat and round tension bars. They also use a polynomial, with coefficients taken as the design variables to characterize the shape of the fillet, and a finite element model to calculate stress with the body. They investigate minimization of stress concentration factor, minimum volume design, and design for uniform stress distribution along the fillet boundary as optimality criterion. Derivatives of response measures with respect to design parameters are calculated using a finite element model. Sequential linear programming is employed for numerical solution.

A function space gradient projection method for optimal design of the shape of two-dimensional elastic bodies is presented by Chun and Haug [9,10], using design sensitivity analysis methods similar to those presented by Rousselet and Haug [11] and a gradient projection optimization method. The design objective in this work is weight minimization, with constraints on Von Mises yield stress and shear stress distribution on the boundary. Dems and Mroz [12] present a related, but more general approach to shape optimal design. They use a boundary perturbation analysis to derive optimality criteria and a finite element numerical method to determine optimum boundaries.

Banichuk [13,14] formulates a general problem of selecting the optimum shape of the cross-section of a nonhomogeneous shaft, to maximize torsional stiffness, with a given amount of material available. He uses the fact that the functional minimized by the warping potential in a variational formulation of the boundary-value problem is proportional to the torsional stiffness of the shaft to obtain an optimality criteria. He treats both simply-connected and multiply-connected cross-sections. Kurshin and Onoprienko [15] treat the same problem of maximum torsional stiffness of a shaft with doubly-connected cross-section, using a complex variable method to determine the optimum boundary. Banichuk [16] subsequently presents an extension of the torsional stiffness maximization problem for rods, using optimal distribution of a given amount of stiffening material around the boundary. Gurvitch [17] presents an alternate analytical technique for optimizing the shape of an interior boundary that is associated with inhomogeneity in material, using a coordinate system associated with the warping function and obtaining necessary and sufficient conditions of optimality. Quite recently, Dems [18] uses the method of Ref. 12 to formulate and numerically solve a variety of problems of shaft cross section shape optimization for torsional stiffness. While there is related literature on specialized shape optimization problems, the above noted literature contains most of the basic methods used to date.

In the formulation presented here, the domain Ω of the elastic body under consideration is taken as the design variable, with the cost function to be minimized written in the form

$$\Psi_0 = \iint_\Omega f_0(z)\, d\Omega \tag{1}$$

subject to functional inequality constraints written in the form

$$\Psi_i = \iint_\Omega f_i(z)\, d\Omega \leq 0, \quad i = 1, \ldots, m \tag{2}$$

and the state variable z is determined as the solution of a boundary-value problem of the form

$$Kz = Q \quad , \quad x \in \Omega \tag{3}$$

$$Bz = q \quad , \quad x \in \Gamma \tag{4}$$

where z is a displacement in the elastic system, Q are body forces acting, K is the elasticity differential operator, q are boundary tractions, and B is a dif-differential operator prescribing boundary conditions on the boundary Γ of the body. The objective is to select the domain Ω (or its boundary Γ) to minimize Ψ_0, subject to constraints of Eqs. 2-4.

This problem is complicated by the fact that the effect of a domain (or shape) change enters into the functionals of Eqs. 1 and 2 in two different ways. First, since the functionals are integrals, a domain variation will directly influence the value of the integral. More subtly, and more complex, the state z of the system is the solution of Eqs. 3 and 4, which change when the domain is varied, hence the state $z = z(x;\Omega)$ must be viewed as depending upon the domain Ω.

The effect of domain variation may be defined by using the idea of a velocity field $V(X)$ with $X \in \Omega$ being the reference variable in the undeformed domain. The position coordinate in the deformed domain may then be written as

$$x = X + tV(X) \ , \ X \in \Omega_0 \ , \ x \in \Omega_t \tag{5}$$

where t may be interpreted as a small time-like parameter and Ω_t denotes the deformed domain. The transformation of Eq. 5 may be substituted into functionals of Eqs. 1 and 2 to reflect the effect of a domain change. Taking the first variation (derivative with respect to t), much as in derivation of the material derivative of continuum mechanics, one obtains the following expression for the variation of a typical functional Ψ_i:

$$\delta\Psi_i = \iint_{\Omega} \frac{\partial f_i}{\partial z} \delta z \, d\Omega + \int_{\Gamma} f_i(z) \, V\cdot n \, ds \tag{6}$$

where δz is the change in state due to the domain change and n is the outward unit normal to the boundary Γ. Denoting the normal movement of the boundary as $\delta D = V\cdot n$ and using an adjoint variable method of design sensitivity analysis, the following simplification of Eq. 6 is obtained:

$$\delta\Psi_i = \int_{\Gamma} [f_i + \lambda^i Q - c(z,\lambda^i)] \, \delta D \, ds \tag{7}$$

where $c(z,\lambda^i)$ is the strain energy bilinear form of the particular system under investigation and λ^i is an adjoint variable satisfying the boundary-value problem

$$\left.\begin{aligned} K\lambda^i &= \frac{\partial f_i}{\partial z} \ , \ x \in \Omega \\ B\lambda^i &= 0 \ , \ x \in \Gamma \end{aligned}\right\} \tag{8}$$

Noting that the boundary-value problem of Eq. 8 is of exactly the same form as the boundary-value problem of Eqs. 3 and 4, one may use the finite element method with the same stiffness matrix for solution of both the state and adjoint equations, leading to essential numerical efficiencies. Having calculated the solution of the state and adjoint equations, the design sensitivity coefficient in the integral of Eq. 7 may be defined on Γ. This provides a design sensitivity result that is needed for optimization.

Optimality criterion and direct numerical methods for structural shape optimization are developed using the design sensitivity result of Eq. 7. Optimality criterion are shown to lead to free boundary problems of elliptic differential equations. This class of problems is shown to be extremely difficult to solve. An iterative optimization method, based on function space and finite dimensional gradient projection methods, is presented and computational algorithms summarized. These algorithms are compared with non-linear programming methods based on discrete finite element models of the structure, with nodal coordinate variables as design. It is suggested that substantial computational advantages are gained using the distributed parameter domain optimization algorithm, rather than the variable nodal coordinate finite element formulation.

An elementary problem of shape optimization of the cross-section of a shaft in torsion is first treated, using the methods discussed previously in the paper, as a means of studying the methods and their application. A general two and three dimensional elasticity formulation of shape optimal design, with constraints on boundary location, stress, and deflection is presented. The computational algorithm obtained is illustrated through solution of two planar structural optimization problems.

REFERENCES

1. Zienkiewicz, O.C. and Campbell, J.S. "Shape Optimization and Sequential Linear Programming" Optimum Structural Design (Ed. R.H. Gallagher and O.C. O.C. Zienkiewicz) Wiley, New York, 1973, pp. 109-126.

2. Ramakrishnan, C.V. and Francavilla, A. "Structural Shape Optimization Using Penalty Functions," Journal of Structural Mechanics, Vol. 3, No. 4, 1975, pp. 403-432.

3. Francavilla, A., Ramakrishnan, C.V. and Kienkiewicz, O.C. "Optimization of Shapte to Minimize Stress Concentration" Journal of Strain Analysis, Vol. 10, 1975, pp. 63-70.

4. Schnack, E. "An Optimization Procedure for Stress Concentrations by the Finite Element Technique" International Journal for Numerical Methods in Engineering, Vol. 14, 1979, pp. 115-124.

5. Oda, J. "On A Technique to Obtain an Optimum Strength Shape by the Finite Element Method" Bulletin of the JSME, Vol. 20, 1977, pp. 160-167.

6. Tvergaard, V. "On the Optimum Shape of a Fillet in a Flat Bar with Restrictions" Optimization in Structural Design (Ed. A. Sawczuk and Z. Mroz), Springer-Verlag, New York, 1975, pp. 181-195.

7. Kristensen, E.S. and Madsen, N.F. "On the Optimum Shape of Fillets in Plates Subjected to Multiple In-Plane Loading Cases" International Journal of Numerical Methods in Engineering, Vol. 10, 1976, pp. 1007-1019.

8. Bhavikatti, S.S. and Ramakrishnan, C.V. "Optimum Design of Fillets in Flat and Round Tension Bars" ASME Paper, 77-DET-45, 1977.

9. Chun, Y.W. and Haug, E.J. "Two Dimensional Shape Optimal Design" International Journal of Numerical Methods in Engineering, Vol. 13, 1978, pp. 311-336.

10. Chun, Y.W. and Haug, E.J. "Shape Optimal Design of an Elastic Body of Revolution" Preprint No. 3526, ASCE Annual Meeting, Boston, April 1979.

11. Rousselet, B. and Haug, E.J. "Design Sensitivity Analysis of Shape Variation" Optimization of Dis-Distributed Parameter Structures (Ed. E.J. Haug and J. Cea) Sijthoff & Noordhoff, Alphen aan den Rijn, Netherlands, 1981, pp. 1415-1460.

12. Dems, K. and Mroz, Z. "Multiparameter Structural Shape Optimization by the Finite Element Method," International Journal of Numerical Methods in Engineering, Vol. 13, 1978, pp. 247-263.

13. Banichuk, N.V. "Optimization of Elastic Bars in Torsion," International Journal of Solids and Structures, Vol. 12, 1976, pp. 275-286.

14. Banichuk, N.V. "On a Variational Problem with Unknown Boundaries and the Determination of Optimal Shapes of Elastic Bodies" PMM, Vol. 39, No. 6, 1975, pp. 1037-1047.

15. Kurshin, L.M. and Onoprienko, P.N. "Determination of the Shapes of Doubly Connected Bar Sections of Maximum Torsional Stiffness" PMM, Vol. 40, No. 6, 1976, pp. 1020-1026.

16. Banichuk, N.V. "On a Two Dimensional Optimization Problem in Elastic Bar Torsion Theory" Soviet Applied Mechanics, Vol. 11, No. 5, 1976, pp. 38-44.

17. Gurvitch, E.L. "On Isoparametric Problems for Domains with Partly Known Boundaries" Journal of Optimization Theory and Applications, Vol. 20, No. 1, 1976, pp. 65-79.

18. Dems, K. "Multiparameter Shape Optimization of Elastic Bars in Torsion," International Journal for Numerical Methods in Engineering, Vol. 15, 1980, pp. 1517-1539.

AD-P000 044

MAXWELL'S THEOREM FOR FRAMES

by Ovadia E. Lev
Merritt CASES, Inc., P.O. Box 1206 Redlands, California 92373

Abstract

Maxwell's Theorem (1890) for trusses $\sum L_i F_i = \sum P_j Q_j = C$ is extended to rigid frames through an extended definition of the length L and the coordinates Q. An expression L = NQ for the length in terms of Q and the geometry/topology matrix N is derived in the process. Simple examples are presented. The extension facilitates uniform numerical manipulation and processing. Implications on optimum material volume and topology of frames remain to be investigated.

Introduction

The following theorem by Maxwell (Reference 1)

$$\sum_{i=1}^{m} L_i F_i = \sum_{j=1}^{2n} Q_j P_j = C \qquad (1)$$

is well known to students of structural optimization. In this theorem, F_i and L_i are the respective force and length of the i-th member of the truss. Q_j and P_j are the respective geometrical coordinate and load component, corresponding to the j-th degree of freedom of the truss joints. The truss is assumed to be two-dimensional and pin-jointed with m members and n nodes. C is a constant independent of the truss configuration (geometry and topology) provided that the member force vector F is in equilibrium with a constant external load vector P. By definition P includes n_a applied load components, P_a, as well as n_r reaction components, P_r, such that $n_a + n_r = 2n$. If Q is partitioned into coordinates of joints which may be loaded by P_a, Q_a (n_a x 1), and support coordinates Q_r (n_r x 1), then Equation (1) may be written as

$$\tilde{Q}P = \begin{bmatrix}\tilde{Q}_a \mid \tilde{Q}_r\end{bmatrix}\begin{bmatrix}P_a \\ P_r\end{bmatrix} = \tilde{Q}_a P_a + \tilde{Q}_r P_r = \tilde{L}F = C \qquad (2)$$

In this paper, the extension of this theorem to frames with rigidly joined members is presented. For simplicity, only two dimesional frames will be considered. Before doing so, a convenient expression for the length of the truss member L will be derived.

Trusses

Consider the plane member shown in Figure 1a. For every member, i, of the truss define a corresponding row in an (m x 2n) matrix, N, which contains (1 x 2) matrices, N_{i+} and N_{i-}, defined below, at the row corresponding to the i-th truss member and at the columns corresponding to node (+) and node (-), respectively:

$$N_{i+} = \begin{bmatrix}\cos\alpha \mid \sin\alpha\end{bmatrix}; \quad N_{i-} = \begin{bmatrix}-\cos\alpha \mid -\sin\alpha\end{bmatrix} \qquad (3)$$

All other elements of row i, corresponding to nodes not incident on member i, are zero. Thus, the matrix N incorporates the geometry as well as the topology of the truss. Using this notation, which was introduced by Spillers (References 2 and 3), Friedland (Reference 4) showed that N may be derived as the gradient of the length vector L ($N = \nabla_Q L$), where the differentiation is carried out with respect to the nodal coordinates Q.

Lev, in Reference 5, expressed the length L as a product of N and Q

$$L = NQ = \begin{bmatrix}N_a \mid N_r\end{bmatrix}\begin{bmatrix}Q_a \\ Q_r\end{bmatrix} \qquad (4)$$

where N_a and N_r are partitions of N corresponding to regular nodes and supports respectively. For example, the equilibrium condition using this notation may be expressed as $\tilde{N}_a F = P_a$.

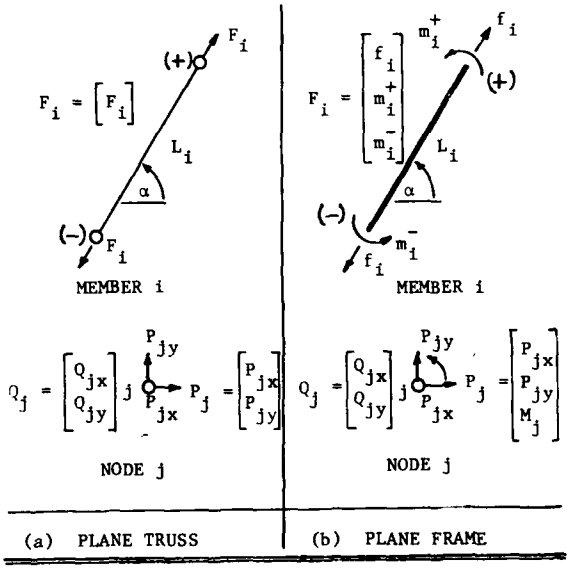


Fig. 1 Notation

Frames

To the plane frame member i shown in Figure 1b, there corresponds a member force vector F_i which has three components: F_i, m_{i+} and m_{i-}. The force vector P_j at node j also has three components: P_{jx}, P_{jy} and M_j:

$$F_i = \begin{bmatrix} f_i \\ m_{i+} \\ m_{i-} \end{bmatrix} \quad ; \quad P_j = \begin{bmatrix} P_{jx} \\ P_{jy} \\ M_j \end{bmatrix} \qquad (5)$$

Using the node method notation (References 4 and 5), the non-zero entries of row (member) i of N are, in analogy to trusses:

$$N_{i+} = \begin{bmatrix} 1 & 0 & 0 \\ 0 & -1/L & 1 \\ 0 & -1/L & 0 \end{bmatrix} \cdot \begin{bmatrix} \cos\alpha & \sin\alpha & 0 \\ -\sin\alpha & \cos\alpha & 0 \\ 0 & 0 & 1 \end{bmatrix}$$

and (6)

$$N_{i-} = \begin{bmatrix} -1 & 0 & 0 \\ 0 & 1/L & 0 \\ 0 & 1/L & 1 \end{bmatrix} \cdot \begin{bmatrix} \cos\alpha & \sin\alpha & 0 \\ -\sin\alpha & \cos\alpha & 0 \\ 0 & 0 & 1 \end{bmatrix}$$

The advantages of this notation is that identical equations may be used to describe equilibrium, compatibility and constitutive relations in trusses as well as frames. For example, the equilibrium equation for frames is, again, $\tilde{N}_a F = P_a$.

Extensions

To extend Maxwell's Theorem (Equation 1) to frames, the definitions of L and Q are extended through the (3m x 1) vector L^* and the (3n x 1) vector Q^* such that for a member i and a node j

$$L^*_i = \begin{bmatrix} L_i \\ 1 \\ 1 \end{bmatrix} \quad ; \quad Q^*_j = \begin{bmatrix} Q_{jx} \\ Q_{jy} \\ 1 \end{bmatrix} \tag{7}$$

Thus, for frames the relation analagous to Equation 4 is

$$L^* = NQ^* \tag{8}$$

where N is defined by Equation 6.

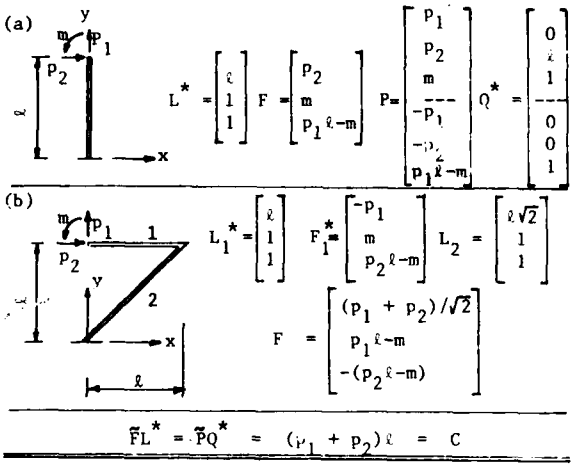
Maxwell's Theorem for frames can now be expressed as

$$\tilde{Q}^* P = \tilde{L}^* F = C \tag{9}$$

The proof of this theorem involves straightforward algebraic manipulations. Conceptually, the result follows directly from the equilibrium requirement that when all the free-body-diagrams of the structure members are assembled, the sum of all moments must vanish. A simple example is given in the following section.

Examples

Figure 2 shows two statically determinate plane frames with identical loads and reactions applied at the same coordinates. The quantities of Equation 9 are calculated and the equation is shown to hold. It is quite easy to make up examples of determinate frames which illustrate the theorem. It is more difficult, however, to make up such examples of indeterminate frames unless they are externally determinate, since both loads and reactions must be respectively equal.



$$\tilde{F}L^* = \tilde{P}Q^* = (p_1 + p_2)\ell = C$$

Fig. 2 A Numerical Example

Figure 3 also illustrates that Equation 1, which holds for trusses, can be extended through Equation 9 to frames. The structures shown in this figure are characterized by the same constant C.

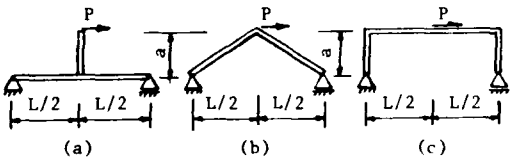


Fig. 3 Frames With Same Constant C

Conclusions

Maxwell's Theorem has its applications, most of them theoretical, in structural optimization and in particular in conjunction with Michell-type structures, and particularly trusses. Some implications of the theorem on optimal volume and topology of certain trusses were discussed by Lev (Reference 5). The extension of the theorem to rigid frames, presented in the paper, facilitates uniform numerical manipulations and processing. The implications of this extension on optimum material volume and topology remains to be investigated.

References

1. Maxwell, J.C., The Scientific Papers of James Clerk Maxwell, 1890, Dover Publications, Inc., New York, N.Y., 1952, pp. 175-177.

2. Spillers, W.R., "Network Analogy for the Truss Problem," Journal of the Engineering Mechanics Division, ASCE, Dec. 1962, pp. 33-40.

3. Spillers, W.R., Automated Structural Analysis: An Introduction, Pergamon Press, New York, N.Y., 1972.

4. Friedland, L.R., "Geometric Structural Behavior," Thesis presented to Columbia University, New York, in 1971, in partial fulfillment of the requirements of Doctor of Philosophy.

5. Lev, O.E., "Topology and Optimality of Certain Trusses," Journal of the Structural Division, ASCE, Vol. 107, No. ST2, Proceedings Paper 16054, February 1981, pp. 383-393.

AD-P000 045

DEVELOPMENTS IN MICHELL THEORY

by

Jean-Marie LAGACHE
Centre Expérimental du Bâtiment & des Travaux Publics
Service Etudes & Recherches Théoriques
12 , rue BRANCION 75015 PARIS (FRANCE)

The design of trusses of minimum volume is considered, subject to the conditions that members are included in some feasible region and safely carry a given system of loads to a rigid foundation. Because there is no difficulty to extend the results to dissymetrical tensile and compressive allowable stresses, one will consider, for the sake of brevity, that the two yield stresses have the same value σ_0 .

Michell Theory (1 to 9) then relates upon virtual feasible displacements, which are shrinking on the foundation and meet with the additional requirement that the overall strain for any segment in the feasible region, lies between two opposite infinitesimal constants. One will assume, by linearity, that these constants are of unit magnitude.

Three theorems about feasible displacements are given in the present paper :

1. *There exists at least one extremal feasible displacement, which makes the work of external loads a maximum upon the class of all feasible displacements.*

2. *Should an optimal truss exist or not, the minimum volume for trusses, V_{min} , and the maximum feasible work , W_{max} , satisfy : $W_{max} = \sigma_0 V_{min}$.*

3. *The computation of only one extremal displacement allows all optimum frames to be synthetized by a converse application of Michell Criterion. Specially, there is no optimum frame at all when the Criterion is inapplicable.*

From a theoritical standpoint, the three theorems carry the implication that maximizing the feasible work is actually the very principle for Optimal Synthesis (3) . In addition, optimal trusses, should such structures exist, are necessarily Michell Trusses.

Prior to the theoritical proof,- which was already given in (11) ,- practical implications of the theorems are discussed on three examples :

Example 1 relates to single loads and convex polygonal foundations. Optimal Synthesis is performed by local methods related to Michell Optimality Criterion (1 to 10). A possible application to Nearly Optimal Design (8,9) is shortly described. A proof that there cannot be any other solution to the problem than the devised cantilevers, is given. Except for the very beginning, the demonstration follows that of Th. 3 .

Example 2 relates to a single load which, this time is inside a concave square foundation. Since local methods reveal inapplicable, Optimal Synthesis is achieved through a direct maximization of the feasible work, which is followed by an application of Th. 3 . A special Graphical Procedure involving geometrical inversions is recalled from (13).

In Example 3 , a load is to be carried to a straight support inside a bounded trapezoidal area. An exact synthesis seems out of reach and Th. 2 is used to check the accuracy of some admissible trusses by resolution of finite dimensional variational problems.

Practical Implications Before the Theoritical Proof

Preliminaries

Feasible displacements. As a consequence of the Principle of Virtual Work, feasible displacements naturallly introduce themselves in Layout Theory because of the inequality :

(1) $$W \leq \sigma_0 V$$

between the external work , W , in any feasible displacement and the volume, V , of any admissible truss.

When an admissible truss and a feasible displacement exist, such that ties undergo the maximum positive feasible strain and struts the negative one, the truss is optimal because inequality (1) is satisfied as an equality (Michell Criterion ; 1 to 9). At the same time, the external work attains its maximum feasible value.

Because earlier treatments have only prooved Michell Criterion to be a sufficient condition of optimality, the problem is reconsidered from the last "variational" standpoint. Results of the theoritical investigation are summarized by the preceding three theorems.

Practical feasibility conditions. In spite of a rather chaotic prior definition, feasible displacements constitute a family of *holderian* applications (11). Piecewise differentiabilitytherefore appears as a quite natural assumption which only involves a slight loss of generality. In fact, density of analytical feasible displacements into the set of all feasible displacements has been obtained in ref.(11) from standard regularization techniques.

Apart from the nuliity on the support, feasibility of a differentiable displacement equivaults to the condition that the principal strains lie within the range -1 , $+1$. The later condition is perfectly suited to the systems of curvilinear coordinates of the standard Michell Approach (2 to 9). For the purpose however, of maximizing the external work without any any information about principal strain lines, the following conditions are preferrable. Given the strain invariants, I_1 , I_2 , I_3 , the principal strains are the roots the characteristic poly omial $P(x) = -x^3 + x^2 I_1 - x I_2 + I_3$ and it results from a mere algebraic discussion that they are comprised between -1 et $+1$ iff :

(2) $$\begin{aligned} |I_1 + I_3| &\leq 1 + I_2 \\ |2 I_1| &\leq 3 + I_2 \\ |I_1| &\leq 3 \end{aligned}$$

In two dimensions, the feasibility conditions reduce to :

(3) $$\begin{aligned} |I_1| &\leq 1 + I_2 \\ |I_1| &\leq 2 \end{aligned}$$

Example 1

Content. One considers the problem of the optimum cantilever supported on a fixed convex polygon. A standard Michell approach is briefly described. Moreover, such structures also ensure optimal transmission to a finite number of points; possibilities of application in the field of Nearly Optimal Design (8,9) are discussed. The following corollary of theorem 3 will be directly prooved with the only basic notions of Michell Theory : *given one Michell Truss T^*, the associated Michell displacement w^* and an optimum truss T ; then, w^* is also a Michell displacement for the truss T* . This brings a rapid answer to the question of unicity : because the Michell Strain Field for a Cantilever problem only yields but one Michell Truss, any other optimum frame coincides necessarily with this Michell Truss. What is prooved is not that the particular method of Synthesis yields a sole solution (5) but that quite different and unformulated methods cannot yield other optimum frames than the devised solution...

Optimum Synthesis. Regardless of the statical conditions of Michell Criterion, a Michell Strain Field with maximum opposite principal strains is synthetized (Fig.1).

1. Rectangular networks expand in the vicinity of the foundation (5) .

2. Because $b\ c$ and $b\ d$, by example, are not orthogonal, the construction could not be continued, unless circles and radii(10) expand in the fans $b\ c\ e$ and $b\ d\ f$, with the first condition that $b\ e$ and $b\ f$ must be orthogonal. In addition, rotations at b of these lines must coincide, in order the displacement to be computable in the fan $e\ b\ f$. A precise kinematical analysis shows the later condition to be fulfilled when angles $c\ b\ e$ and $d\ b\ f$ are equal.

3. There is no difficulty, at this stage to complete the network by successive resolutions of standard boundary problems of Slip-Line Theory (10 : two orthogonal principal lines given).

Examples of Michell Trusses are given on the Figure. Optimum frames for loads which are not consistent with the preceding field may be obtained from auxiliary "unrolled foundations".

Application to Nearly Optimal Design. The main elements in the networks of Fig. 1 are bundles of straight lines which, according to Hencky's first theorem, have a constant magnitude and obey to the following rule of mutual deviation : *when a bundle of the magnitude α meets with a bundle of the magnitude β , lines in the former are deviated by an amount of β and lines in the later by an amount of α* . The preceding rule is sufficient for the drawing of bundles of small magnitude, because the deviation is almost punctual. This explains the following graphical procedure:

1. Pair of equal bundles are first drawn from the wedges, according to the theoritical study.

2. Each bundle is eventually divided into elementary bundles of small magnitude.

3. Elementary bundles being provisorily assimilated with their mean lines, a first approximate network may be drawn by application of the rule of mutual deviation.

4. To complete the network, one may assume that the successive deviations of any other line occur at the intersections with the mean lines.

A mere application of Michell Criterion shows that the considered network also carry the loads to a finite number of points. Thus, for the purpose of synthetizing Nearly Optimum Frames with a finite number of joints upon a smooth convex foundation (8,9), an approximation, by mean of the preceding procedure, of the strain field related to a close polygonal contour may be preferred to the approximation of the true Michell Field. The 10-bar truss of Fig. 2 is based on an hexagon and carry a load to a circular core. The relative increasement in the volume is only about 5% .

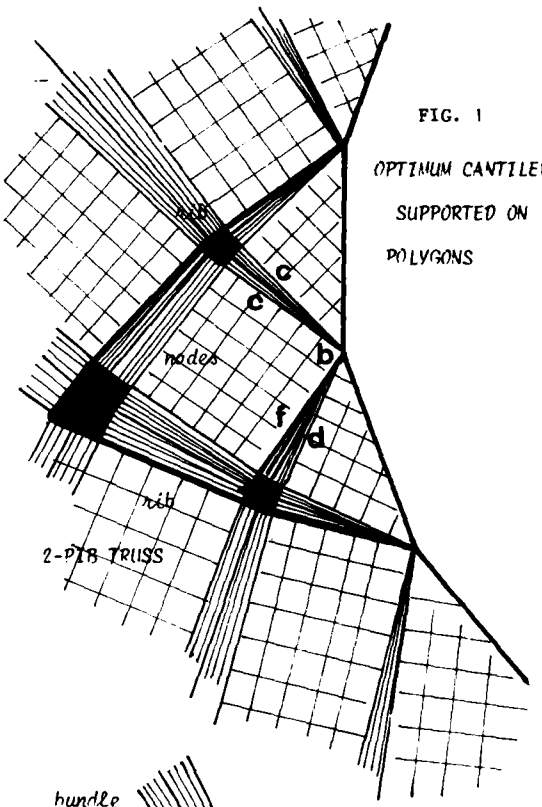
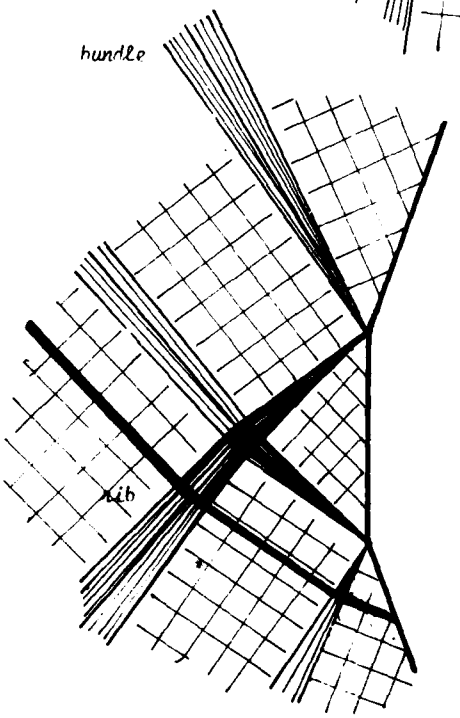


FIG. 1

OPTIMUM CANTILEVERS SUPPORTED ON POLYGONS



Direct Proof of Unicity. Undoubtless, a single application of Michell Procedure for the Cantilever Problem yields a single Michell displacement w^* (Unicity theorem of ref.5). The corresponding strain field being statically determinated, the Michell displacement generates a single Michell Truss T^*. Nevertheless, the question of unicicity is entire because it is not prooved that another method than Michell Procedure cannot yield another optimum structure T .

1. Because the main steps of the calculation will be reproduced in the demonstration of Th. 3 with symetrical allowable stresses, let us suppose in this paragraph that the two stresses have distinct values σ_t and σ_c .

2. One introduces the following notations for the optimum structeure T . Let be :

L , the length of a bar ;
N , the actual effort inside the bar ;
e^* , the overall strain of the bar in the Michell displacement w^*.

B , the cross-sectional area ;

k , the safety ratio, defined by :

$$\begin{cases} \sigma_t \quad B = k\,|N| \quad \text{if} \quad N > 0 \\ \sigma_c \quad B = k\,|N| \quad \text{if} \quad N < 0 \\ \qquad k \geq 1 \end{cases}$$

3. The conventional allowable range for feasible strains being taken as $[-1/\sigma_c\ ,\ 1/\sigma_t]$, one knows that the external work in the Michell displacement is equal to the volume of the Michell truss and, thus, *to the volume of the optimum truss* T .

4. Mere calculations and an application of the Principle of Virtual Work then yields :

$$\sum_{N>0} k\,|N|\,L\,/\sigma_t + \sum_{N<0} k\,|N|\,L\,/\sigma_c = \sum k\,N\,L\,e^*$$

5. The right hand sommation splits in two parts to yield :

$$\sum_{N>0} L\,N\,(-e^* + k/\sigma_t) = \sum_{N<0} L\,N\,(e^* + k/\sigma_c)$$

6. Because w^* is feasible and because k is greater than 1 , terms in the left hand summation are positive while terms in the right hand summation are negative. Obviously, every term in the preceding equation is null. Thus :

$$e^* = k\,/\,\sigma_t \quad \text{if} \quad N > 0$$

$$e^* = -k\,/\,\sigma_c \quad \text{if} \quad N < 0 \ .$$

7. The only admissible value of the safety ratio which is compatible with the preceding conditions and with the definition of a feasible displacement is $k = 1$.

8. The optimal truss, T , is fully-strained ($k = 1$) . Moreover, it verifies :

$$e^* = 1\,/\,\sigma_t \quad \text{if} \quad N > 0$$

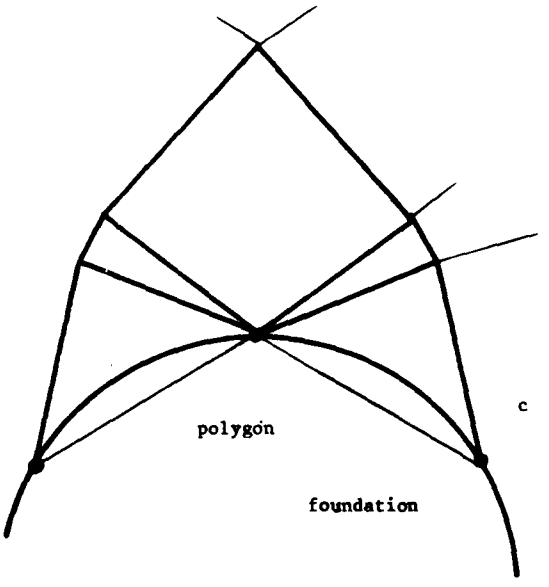
$$e^* = -1\,/\,\sigma_c \quad \text{if} \quad N < 0 \ .$$

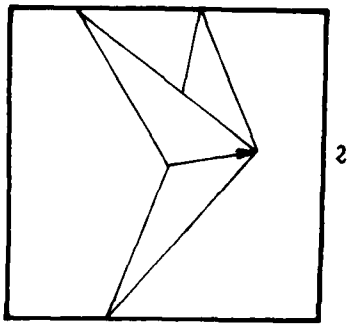
9. The preceding conditions show that the considered optimum truss is a Michell Truss associated with the *Michell displacement* w^* . Because there cannot be two distinct states of tension in the considered network :

$$\boxed{T = T^*}$$

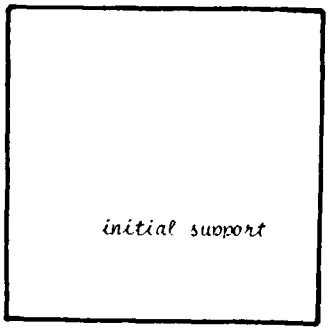
The proof is complete.

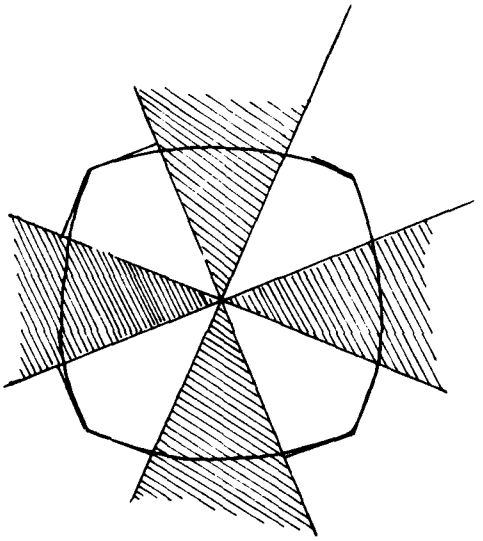
FIG.2 *NEARLY OPTIMUM CANTILEVER*
5 %

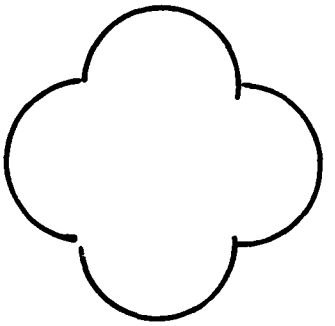


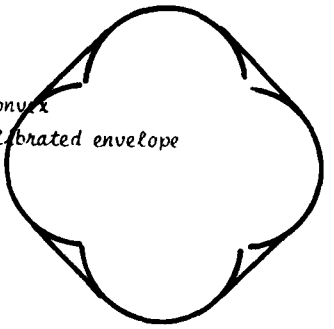


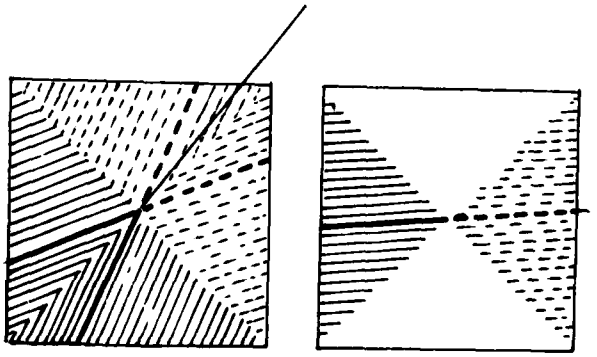
Feasible Subclass



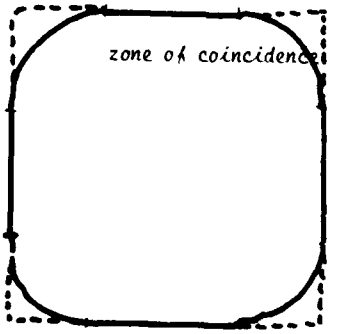








Optimum frames



GEOMETRICAL PROCEDURE

FIG.3 CONCAVE SUPPORT

Example 2

Content. Imagine that an inextensible sheet presents a perfectly smooth aspect when submitted to a given system of loads. If one bends the support, a new kind of equilibrium position appears : stability is now insured by a finite number of isolated folds and the sheet hangs loosely everywhere else. Determination of the equilibrium position demands a simultaneous knowledge of the whole support and loading system, and would scarcely result from the analysis and matching of possible local kinematical regimes of the sheet... There is a quite similar change in the nature of optimal frames and computations methods when one considers concave foundations instead of convex ones.

The transmission of a single load from the inside to the outside of a square cavity is considered on Fig. 3 . Optimal trusses now have a finite number of bars whose position is found by a direct maximization of the feasible work, but not by the method of progressive synthesis of Example 1 . Because of the practical impossibility of taking into account all possible feasible displacements, the first question lies in the reduction of the problem to some suitable feasible subclass. Maximization of the external work is then performed on that special subclass, which yields optimum frames by application of Th. 3 . A practical method of drawing is described.

Feasible Subclass Consider feasible displacements of the square region, with a linear variation along any segment joining the loading point to the rigid support. These are piecewise linear continuous displacements which are fully determinated by the value $w = (w_1, w_2)$ which is taken at the loading point. Formulae (3) and a mere computation of the strain - invariants yield the following feasibility conditions :

$$(4) \qquad w_1^2 \pm 4a w_2 - 4a^2 \leq 0$$
$$w_2^2 \pm 4a w_1 - 4a^2 \leq 0$$

Indeed, maximizing the external work upon the preceding subclass is not the true maximization problem which should be considered for a strict application of theorems 1 to 3 . Because of the piecewise linearity of the considered displacements, however, it may be thought that the set of fully-strained segments in any solution of the partial maximization problem will necessarily include segments issued from the loading point which will allow Michell Criterion to be applied. A rigourous proof is given in ref. (11) for a cubic support is generalized in ref. (12) to any concave support. The considered subclass therefore suffices to Optimal Synthesis.

Optimal Synthesis. Maximization of the external work upon the region Γ which is delineated by inequalities (4) is performed by a graphical technique.

Two basic optimal configurations are obtained :

1. When the action line is inside the shaded area on the second diagram of Fig. 3 , the maximum work is attained at a current point on the boundary. Fully strained segments are parallel to the action line and Michell Criterion is fulfilled by two single-bar and the family of statically indeterminated frames which results from convex interpolation.

2. When the action line is outside the shaded area, the maximum work is attained at a vertex. It may be seen by continuity with the preceding case, that fully-strained segments now arrange parallely to two independant directions. Michell Criterion is fulfilled by four statically admissible trusses and the family which results from convex interpolation.

Because the networks of Fig. 3 do not show any other possibility of statical decompositions of the loads, theorem 3 shows that the list of solutions is complete.

Practical Drawing. A rapid graphical procedure,- which is suited to the transmission of a single load to any concave support,- has been deduced in ref. (13) from the preceding analysis. The procedure involves the following steps (lower diagrams on Fig. 6) :

1. Take inverse of the support about the loading point.

2. Construct the convex equilibrated envelope of the inverse support.

3. Define a modified support by taking again inverse of the preceding envelope.

4. Comparing the initial with the modified support, one can observe a general removal of settlement points towards the loading point. Select the points which did not move inwards and adjoin to the corresponding set its reflection about the loading point. According to notations of (13) , the result is called Equilibrated Zone of Coincidence : E Z C .

5. It is prooved in ref.(13) that the E Z C is the intersection of the support with the shaded zone of Fig. 6 . Single bars are therefore optimal when the action line intersects with the E Z C ; otherways, optimal frames are based upon the nearest points on the E Z C .

When applied to non-concave foundations the method yields nearly optimum frames consisting of bars from the loading point to the boundary. Step 3 of the procedure defines a curve whose radius vector is proportional in any direction to the volume of the associated nearly optimal truss.

When applied to a convex set included in the feasible region, the first three steps yield a curve whose radius vector provides a lower bound to the true minimum volume. Efficiency may thus be checked by purely graphical procedures.

Example 3

Content. One considers the transmission of a vertical load to a straight support, with the additionnal requirement that admissible trusses are included in the trapezoidal area of Fig. 4 . Because of the later condition, it is now almost impossible to imagine convenient kinematical regimes for a Michell displacement to be synthetized. On the other hand, an *exact* maximization of the external work is presently

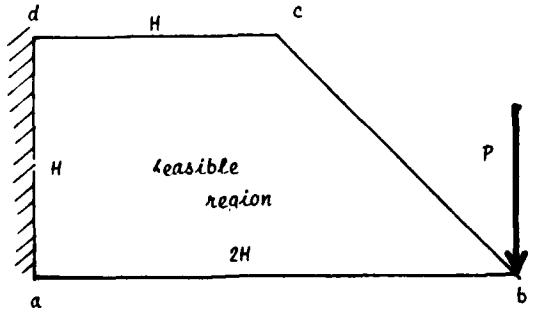


FIG.4 TRAPEZOIDAL AREA

out of reach because there are no particular characteristics in the data which would allow, as before, any reduction of the general maximization problem to a practically suitable one.

A numerical maximization of the feasible work is however described, whose purpose is no longer the definition of some ideal geometry but,- according to theorem 2 ,- the computation of significative lower bounds to the minimum structural volume. The procedure involves finite-dimensional variational problems with a linear objective and algebric inequality constraints of the second degree which may be linearized for the numerical treatment. Results are finally compared with the volume of particular admissible trusses, which brings a practical answer to the considered problem.

Finite Element Computation of the Minimum Volume.

1. The admissible region is shared into triangular elements, as shown on Fig. 5 .

2. For the numerical computation of the maximum work, one only considers feasible displacements with a linear variation inside any triangle.

3. One then formulates a finite-dimensional variational problem. Because feasible displacements are continuous, the only variables are the nodal components of the displacement. The objective,- i. e. the external work,- is linear with respect to the variables. Conditions (3) show that four inequalities hold on each triangle. A graphical interpretation is given on Fig. 5 , in terms of the strain tensor components ϵ_{ij} . Formulation of the constraints in terms of the nodal displacements is a tedious but quite simple task which is left to the reader's attention. It's worth noting that in spite of the convexity of the problem, half the constraints are non convex quadratic inequalities of the hyperbolic type.

4. Constraints of the preceding approximate problem are linearized, as indicated on the figure. Significative lower bounds to the maximum feasible work,- and thus to the minimum volume,- then deduce from the resolution of a Linear Programming Problem.

5. It is shown in ref. (11) that convergence towards the true minimum volume may be obtained from a progressive refinement of the mesh, provided triangles do not degenerate into segments.

Application of the method to the rather coarse network of Fig. 5 yields the following estimation

$$6.123\ P\,H \leq \sigma_0\ V_{min} \quad .$$

It is important to note that an inequality holds because a special care has been brought in the definitions of both approximate and linearized problems so as not to violate the feasibility conditions.

Measurement of Truss Efficiency. Consider one or other of the admissible trusses. The previous analysis yields an overestimation of the fraction of the volume which could be saved if an exact resolution was performed :

$$\Delta V / V \leq (V - 6.123\ P\,H) / V \quad .$$

By example, the preceding fraction is less than 1/4 for the 4-bar truss of the volume $8\ P\,H / \sigma_0$ which is drawn on Fig. 6 .

FIG.5 NUMERICAL COMPUTATION

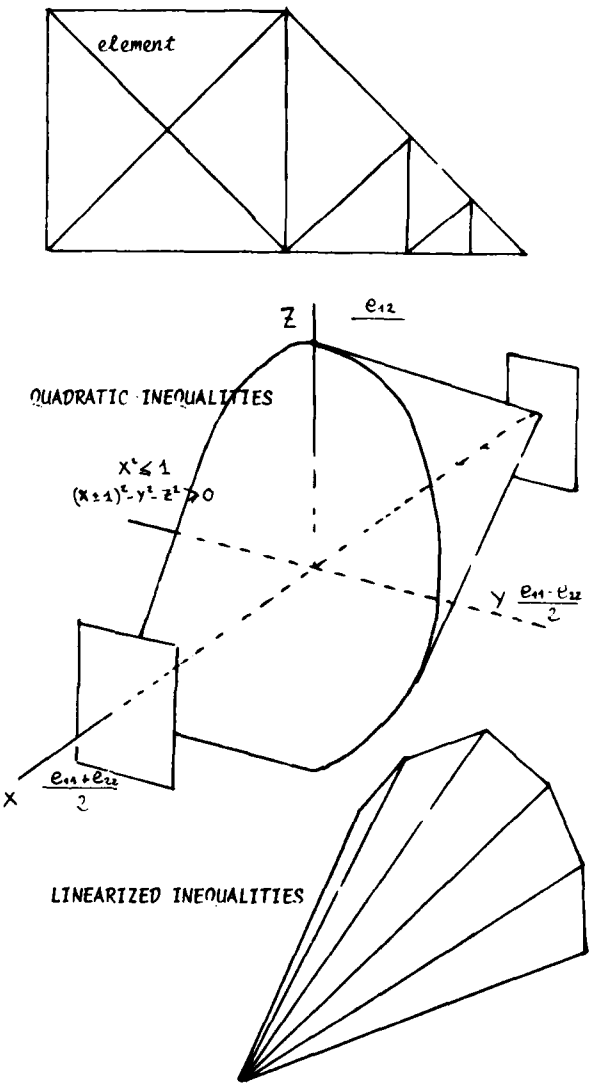
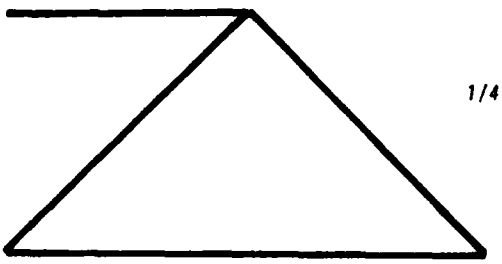


FIG.6 ADMISSIBLE 4 - BAR TRUSS



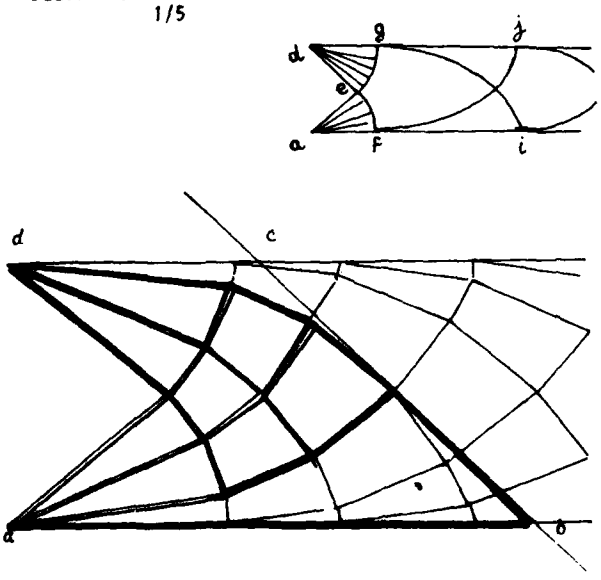
A more efficient 20-bar truss, which is partially based upon a Michell Strain Field is displayed on Fig. 7 . Getting provisorily rid of the geometrical constraints related to segment $b\ c$, one first synthetizes the Michell Strain Field inside the strip delineated by lines $a\ b$ and $c\ d$. A rectangular network, $a\ e\ d$, expands in the vicinity of the foundation, while circular networks inoccupy fans $e\ d\ g$ and $f\ a\ e$. Central networks,- $e\ f\ g\ h$ and the following,- are based upon two orthogonal principal lines. Networks along the boundary,- $i\ f\ h$, $j\ g\ h$ and the following,- are singular networks based upon a principal line and a tangent straight line (6,10). The graphical method of Example 1 is suited to the practical drawing, with the additional rule that *the intersection of any elementary bundle with the free lines $a\ b$ or $c\ d$ generates a "transverse" bundle of the same width along the considered line* (once again, it is a consequence of Hencky's first theorem and of the decomposition in small bundles). The synthetized Michell truss lies partially outside the given trapeze. Nevertheless, a mere comparison between the theoritical network and the 20-bar truss shows that this later is almost a Michell truss. Maxwell diagram shows that the material consumption is about $7.5\ P\ H\ /\sigma_o$. Inequality (5) then shows that the efficiency ratio $\Delta V\ /\ V$ is less than $1/5$.

Because simplicity in the layout is most of the time preferrable to a strict decreasement in the weight, one may consider that the practical solution is attained.

Anyway, more accurate underestimations of the minimum volume would result from a more refined discretization of the feasible area. At the same time, Nearly Optimal Design Procedures could be used either to improve efficiency (14,15) or to define trusses which are likely close to the optimum (16,17).

Remark 1 . The choice of piecewise linear displacements for the computation of the maximum feasible work is not essential. Several examples in ref.(10) show that one may take advantage of particular characteristics of the considered problems (symmetries,...) to obtain rapid analytical evaluations of the maximum work. That kind of approach generally involves ordinary differential inequalities instead of algebraic ones.

FIG.7 20 - BAR CANTILEVER
1/5



Remark 2 . Three-dimensional problems involve so many possibilities of local kinematical regimes that the standard Michell Approach is almost unpracticable. By contrast, the only difficulty in the present method is that conditions (2) involve inequality constraints of the third degree. Several analytical examples have been given in ref.(11) ; numerical examples are on preparation.

Theoritical Part

Proof of theorems 1 and 2

Bounded regions.

1. One considers, as in the practical method which was first described by Hemp (16) and Dorn, Gomory and Greenberg (17), a nested sequence of feasible ground structures submitted to the conditions that :

i) every ground structure includes, for a given number of nodes, as many feasible connections as possible ;

ii) the union, N , of the nodes and the union, , of the supports of all considered ground structures are respectively dense into the feasible region and the support.

2. Unuseful connexions in the k-th ground structure are eliminated by Linear Programming (16,17) ; at the same time, convenient cross-sections are allocated to the remaining connections. This defines a sequence of admissible trusses of the decreasing volume V_k .

3. *Finite-dimensional Duality Theorems* show that theorems 1 and 2 hold for any ground structure. Thus :

$$(6) \qquad W_k = \sigma_o\ V_k \quad ,$$

where W_k denotes the external work which is developed in *some* kinematically admissible displacement, w_k , of the k-th ground structure, which fulfills the overall strain feasibility condition along any connection of the ground structure.

4. Because ground structures are highly redundant (maximum connection hypothesis), the sequence w_k may be seen to be bounded at any point of N . Since the later set is countable, it is possible to extract a convergent "Diagonal Subsequence". The limit, w , which is defined at any point of the dense set N , shrinks on the dense support A and satisfies the overall strain feasibility conditions on a dense lattice of feasible connections (maximum connection hypothesis). From (6), the corresponding external work W meets with :

$$(7) \qquad W = \lim \sigma_o\ V_k \quad .$$

5. Provided the considered bounded region is sufficiently regular, displacements of the preceding type are uniformly continuous (11). Therefore, w admits a continuous extension, w^* , which is defined on the whole feasible region. It is easily seen that w^* is a feasible displacement. According to equation (7), the corresponding work, W^* , meets with :

$$W^* = \lim \sigma_o\ V_k \quad .$$

6. Remember inequality (1), at the beginning of the paper. The preceding equality holds iff $\lim V_k$ coincides with the minimum volume and W^* is the maximum feasible work. Displacement w^* is an extremal displacement, which prooves theorem 1 . At the same time, $\lim \sigma_o\ V_k$ is simultaneously equal to

σ_o V_{min} and $W^* = W_{max}$, which prooves th. 2 .

Remark. There is no proof in ref.(16,17) that under the sole assumptions of Maximal Connection and Density, the sequence of volumes converges to the absolute minimum volume.

Unbounded Regions. An extension of the theorems to unbounded regions is given in ref.(11). The procedure is quite similar, except that finite ground structures are replaced by a nested sequence of regular bounded regions. Extraction of a subsequence at Step 4 is still valid because a generalized compacity theorem for feasible displacements of a regular bounded region (11) substitutes to the finite-dimensional boundedness property.

Proof of theorem 3

1. Given one extremal displacement, W , and some truss of minimum volume, if any, denote :

- e , the overall strain of any member of the truss in the considered displacement ;
- L , the length of the member ;
- N , the actual positive or negative effort inside the member ;
- $k = \sigma_o B / N$, the safety ratio, where B denotes the cross-sectional area.

2. Because the considered truss is of minimum volume, theorem 2 and the Principle of Virtual Work yield :

$$\sigma_o \sum k L |N| / \sigma_o = \sum N L e .$$

3. Depending upon the sign of efforts, summations are split in two parts :

$$(8) \quad \sum_{N>0} N L (k - e) = \sum_{N<0} N L (k + e)$$

4. By definition of feasibility, e lies between -1 and $+1$ and, thus, between $-k$ and $+k$, since the safety ratio in the member is necessarily greater than one . Terms in the left hand summation in equality (8) are thus positive while terms in the right hand summation are negative. This obviously prooves that every term in both summations is null. Finally, the conclusion holds that the overall strain e equals $+k$ when the effort is positive or $-k$ when the effort is negative.

5. The only admissible value of the safety ratio which is compatible with the preceding condition and the definition of a feasible displacement is $k = 1$.

6. Thus, the considered truss,- which, truely speaking is any of the optimal trusses,- is fully-stressed ($k = 1$) ; every bar a unit overall strain in the considered displacement ($e = k$) and efforts and virtual strains are of the same sign. The proof of theorem 3 is complete.

Concluding Remark.

Consider the transmission of a torque from an infinite rigid plane to another parallel one (ref. 11):

1. A mere statical analysis shows that there exists a sequence of admissible trusses whose volumes tend to zero :

$$V_{min} = 0$$

2. A mere kinematical analysis shows the rotation of one plane about the other to be null in every feasible displacement :

$$W_{max} = 0 .$$

3. Obviously, there cannot exist any Michell truss for such a problem.

4. Nevertheless, Th. 1 holds since the null displacement is obviously an extremal feasible displacement.

5. TH. 2 holds since

$$W_{max} = \sigma_o V_{min} \quad (= 0)$$

6. Th. 3 holds in a negative form : because Michell Criterion cannot apply to the empty network associated with the null displacement, Th.3 stipulates that there is no optimum frame at all, which is perfectly well the case.

REFERENCES

(1) A.G.M. MICHELL, The Limits of Economy of Material in Frame-Structures. *Phil Mag* 8 , 589-597 (1904)

(2) H.L. COX, *The Design of Structures of Least Weight*. Pergamon Press, Oxford (1965)

(3) W.S. HEMP, *Optimum Structures*. Clarendon Press, Oxford (1973)

(4) J.B.B. OWEN, *The Analysis and Design of Light Structures*. American Elsevier, New-York (1965)

(5) G.A. HEGEMIER & W. PRAGER, On Michell Trusses. *Int J Mech Sci* 11 , 209-215 (1969)

(6) H.S.Y. CHAN, Half-Plane Slip-Line Fields and Michell Structures. *Quart J Mech & Appl Math* XX , (4), 453-469 (1967)

(7) W.S. HEMP, Michell Framework for Uniform Load Between Fixed Supports. *Engineering Optimization* 1 , 61-69 (1974)

(8) W. PRAGER, Nearly Optimal Design of Trusses. *Computers & Structures* 8 , 451-454 (1978)

(9) W. PRAGER, Optimal Layout of Trusses with Finite Number of Joints. *J Mech Phys Solids* 26 , 241-250 (1978)

(10) R. HILL, *The Mathematical Theory of Plasticity*. Clarendon Press, Oxford (1950)

(11) J.M. LAGACHE, Treillis de Volume Minimal dans une Région Donnée. *Journal de Mécanique* 20 (3) , (1981) in french

(12) J.M. LAGACHE, Transmission optimale d'une Charge au Pourtour d'Une Région Convexe. *Mech Res Comm* 6(6) , 333-338 (1979) infrench

(13) J.M. LAGACHE, A Geometrical Procedure to Design Trusses in a Given Area. *Engineering Optimization* 5 , 1-12 (1980)

(14) P. PEDERSEN, Optimal Joint Positions for Spaces Trusses *J. Struct. Div* (A.S.C.E.) 99 (12), 2459-2477 (1973)

(15) G.N. VANDERPLAATS et F. MOSES, Automated Design of Trusses for Optimum Geometry. *J. Struct. Div.* (A.S.C.E.) 98 (3), 671-690 (1972)

(16) W.S. HEMP, Optimum Structures. *Clarendon Press, Oxford.* 70-101 (1973)

(17) W.S. DORN, R.E. GOMERY et H.J. GREENBERG, Automatic Design of Optimal Structures. *J. Mec.* 3, 25-52 (1964).

AD-P000 046

HENCKY-PRANDTL NETS AND CONSTRAINED MICHELL TRUSSES

Gilbert Strang
Department of Mathematics
Massachusetts Institute of Technology
Cambridge, Massachusetts 02139

Robert V. Kohn
Courant Institute of Mathematical Sciences
New York University
New York, New York 10012

The geometry of slip lines is a beautiful part of the theory of plasticity. Parallel to it, and equally remarkable, is the Michell-Prager theory of optimal design. In plane strain both problems lead to Hencky-Prandtl nets, which define orthogonal curvilinear coordinates with a special property: if the coordinates are α and β, and the curve α = constant makes an angle $\theta = \theta(\alpha,\beta)$ with the x-axis, then $\partial\theta/\partial\alpha\partial\beta = 0$. One goal of this note is to suggest a problem in which we anticipate that *Hencky-Prandtl nets of both kinds will appear in the solution.* Part of the region should be covered by a Michell truss, and part by slip lines -- if our conjecture is correct. Since it is a problem of shape optimization, a third part of the original cross-section may carry no stress in the optimal design and be completely removed.

Our plan in this note is to outline the proposed design problem and to describe both its mathematical framework and a possible approach to the computations. The work is by no means completed, and we add a discussion of a related but simpler problem in order to see the analogies with known optimal designs. It seems possible that the anticipated combination of Hencky-Prandtl nets is new, and we hope that this preliminary report will be admissible and useful. It is organized as follows:

1. Statement of the Michell problem and the proposed redesign problem
2. Formulation of the dual problems (in displacement) and the conditions for a pair σ,u to be optimal
3. Analogies with the optimal redesign of plastic rods in antiplane shear.

We adopt the term redesign to suggest the constraints that are imposed on strength and shape in the final design. It has to lie within a prescribed region Ω, and the stress is bounded by $\|\sigma\| \le \sigma_0$; we use either a direct condition on the principal stresses, or the von Mises yield condition on the stress deviator. The implication is that there is an upper bound to the width of truss members, like the thickness bound in plate design, which could come from having started with a given structure and allowing only its substructures as possible designs. In other words, we are only permitted to remove material. There are also other sources for these constraints; what is significant is the way in which they are reflected in the variational statement of the problem and in the optimal design.

We will take the external loads to be surface tractions f distributed along the boundary Γ of the given simply connected cross-section Ω. For body forces and for displacement boundary conditions the modifications are familiar and can be introduced directly into the variational problems.

1. Variational Forms of the Stress Problems

We give a very brief derivation of the Michell problem, in which the stress constraints come from the equilibrium equations:

$$\text{div } \sigma = 0 \text{ in } \Omega, \quad \sigma{:}n = f \text{ on } \Gamma \quad . \tag{1}$$

The stress tensor is represented by the symmetric matrix

$$\sigma = \begin{bmatrix} \sigma_x & \tau_{xy} \\ \tau_{xy} & \sigma_y \end{bmatrix} , \tag{2}$$

and its eigenvalues (the principal stresses) are

$$\lambda_{1,2} = \tfrac{1}{2}\left(\sigma_x+\sigma_y \pm ((\sigma_x-\sigma_y)^2+4\tau_{xy}^2)^{\frac{1}{2}}\right) \quad . \tag{3}$$

We imagine that the bars of a truss, or truss-like continuum, are placed in the directions of principal stress -- which come from the orthogonal eigenvectors of σ. These bars are made from a perfectly plastic material with tensile and compressive yield limits $\pm\sigma_0$. Therefore, the required cross-sectional areas at any point are proportional to $|\lambda_1|$ and $|\lambda_2|$. The total volume of the truss is thus proportional to

$$\Phi(\sigma) = \iint_\Omega \left(|\lambda_1(\sigma)| + |\lambda_2(\sigma)|\right) dx\, dy \quad . \tag{4}$$

Michell's optimal design minimizes this volume. In other words, the shape and thickness of the Michell truss can be determined from the solution to the optimization problem

(P) Minimize $\Phi(\sigma)$ subject to $\text{div } \sigma = 0$, $\sigma{:}n = f$.

To express this in a way that suggests a computational algorithm, we introduce a stress function $\psi(x,y)$. For any divergence-free stress tensor σ there is a function ψ such that

$$\sigma = \begin{pmatrix} \psi_{yy} & -\psi_{xy} \\ -\psi_{xy} & \psi_{xx} \end{pmatrix} \quad . \tag{5}$$

Here the subscripts indicate partial derivatives, and it is immediate that $\text{div } \sigma = 0$. In the first column, for example,

$$\frac{\partial}{\partial x}\sigma_x + \frac{\partial}{\partial y}\tau_{xy} = \frac{\partial}{\partial x}\psi_{yy} + \frac{\partial}{\partial y}(-\psi_{xy}) = \psi_{yyx} - \psi_{xyy} = 0.$$

Clearly ψ is determined only up to a linear function, for which all second derivatives are zero. The boundary conditions $\sigma{:}n = f$ lead to conditions on ψ, if we start at an arbitrary boundary point P_0 and integrate around Γ. We are given the unit normal $n = (n_x,n_y)$, the unit tangent $t = (-n_y,n_x)$, and the conditions

$$\sigma_x n_x + \tau_{xy} n_y = f_1, \quad \tau_{xy} n_x + \sigma_y n_y = f_2.$$

The first translates into

$$\psi_{yy} n_x - \psi_{xy} n_y = f_1, \text{ or } (\text{grad } \psi_y)\cdot t = f_1.$$

Therefore, the tangential derivative of ψ_y is

$$\frac{\partial \psi_y}{\partial t} = f_1, \text{ or } \psi_y(P) = \int_{P_0}^{P} f_1 \, ds. \tag{6}$$

Similarly ψ_x comes from the indefinite integral $-\int f_2 ds$. Assuming that the integrals of f_1 and f_2 around the closed curve Γ are zero -- a necessary condition for the constraints (1) to be compatible -- the boundary values ψ_x and ψ_y are well defined.

This determines ψ_n and ψ_t, the normal and tangential derivatives. We can continue the same process one more step to determine ψ itself, and write the final result as $\psi = g$, $\psi_n = h$.

Now we can restate the minimization of $\Phi(\sigma)$ as a problem in the scalar stress function ψ. The integrand $|\lambda_1| + |\lambda_2|$ is a convex function, and its value depends on whether the two eigenvalues have the same or opposite signs. If the signs are the same then

$$|\lambda_1| + |\lambda_2| = |\lambda_1+\lambda_2| = |\psi_{xx}+\psi_{yy}| \qquad (7)$$

since the sum of eigenvalues is the sum of the diagonal entries (the trace of the matrix). If λ_1 has opposite sign to λ_2, then we find from (3) that

$$|\lambda_1| + |\lambda_2| = |\lambda_1-\lambda_2| = ((\psi_{xx}-\psi_{yy})^2 + 4\psi_{xy}^2)^{\frac{1}{2}} . \qquad (8)$$

Combining these two cases, $|\lambda_1| + |\lambda_2|$ is the larger of (7) and (8). Therefore, Michell's problem becomes:

$$(Q)\quad \text{Minimize} \iint_\Omega \max(|\psi_{xx}+\psi_{yy}|, ((\psi_{xx}-\psi_{yy})^2+4\psi_{xy}^2)^{\frac{1}{2}})\,dx\,dy$$

$$\text{subject to } \psi = g,\ \psi_n = h \text{ on } \Gamma.$$

With distributed surface tractions and no body forces, this seems to provide one approach to the computation of optimal designs. It is certainly not the only approach, and probably not the most efficient. It differs from the numerical construction of a Hencky-Prandtl net, which is suggested by the equivalent displacement problem (the dual of (P)) that we derive in the next section. We understand that Collins has developed an algorithm of that kind in Manchester; we do not know its capabilities. Here one can represent ψ by finite elements,† and the integral is computed by numerical quadrature. A standard minimization algorithm gives the iterations leading to the optimum. If it is expected that one family of bars is in tension and the other in compression, we can suppress $|\psi_{xx}+\psi_{yy}|$; then we confirm at the end that it is smaller than the square root term, so that there are no "hydrostatic" regions in that optimal design. In general, however, the external loads can produce such a region.

This form of the optimal design problem allowed Ω to be specified, but it imposed no constraint on the cross-sectional areas in the truss. Now we add such a constraint. In its simplest form, it places an upper bound on the principal stresses λ_1 and λ_2. The implication is that the bars of the truss cannot be arbitrarily strong -- and in particular, singular members that can carry a concentrated load will be excluded. If we denote by Λ the upper bound on the stresses, the design problem for a *constrained Michell truss* is

$$(P_\Lambda)\quad \text{Minimize} \iint_\Omega |\lambda_1(\sigma)|+|\lambda_2(\sigma)| \text{ subject to } |\lambda_i| \le \Lambda$$

$$\text{and div } \sigma = 0 \text{ in } \Omega,\ \sigma\cdot n = f \text{ on } \Gamma.$$

This can be restated, and analyzed numerically, in terms of ψ.

There is also a second possibility for the constraint. It acts on the stress deviator σ^D instead of σ, and therefore ignores the hydrostatic component of the force. We could imagine working with a composite material, in which the matrix can withstand pure pressure but nothing else, and the design material is to withstand the remaining stress at each point and have minimum volume. In this case, the constraint is of von Mises type:

$$\left(\frac{\sigma_x-\sigma_y}{2}\right)^2 + \tau_{xy}^2 \le k^2 . \qquad (9)$$

The left side is the square of the eigenvalues of $\sigma^D = \sigma - \frac{1}{2}(\sigma_x+\sigma_y)I$, as we see directly from (3).

The matrix σ^D has trace zero, and its eigenvalues are of equal magnitude and opposite sign. Therefore, *the plane strain redesign problem becomes:*

$$(P_k)\ \text{Minimize} \iint_\Omega |\lambda_1(\sigma^D)| + |\lambda_2(\sigma^D)| \text{ subject to}$$

$$(1) \text{ and } (9) .$$

These are the formulations in terms of stresses. They include inequality constraints, and in general such a constraint will be active in one part of Ω (where equality holds) and inactive in the complement. In this latter part the constraint plays no direct role, and we have a Michell truss as before. The active part corresponds to stresses on the yield surface, exactly like a plastic region in Prandtl-Reuss flow. In case the λ_i are of equal magnitude and opposite sign (a typical situation), the velocity field should correspond to a net of slip lines. This part must fit smoothly into the Michell part, giving continuity of the principal stress directions. As Λ and k increase, the solutions of (P_Λ) and (P_k) will approach the solution of the unconstrained problem (P).

We emphasize the coincidence between the quantity in the constraint (9) and the quantity in the integral to be minimized. It is the reappearance of this same expression that leads us to anticipate two Hencky-Prandtl nets at once; in one region the stress achieves its maximum, and in the other region (as we will see in the dual) it is the strain. We rewrite this expression in terms of the stress function ψ, and denote it by $\|\psi\|$:

$$\|\psi\|^2 = \left(\frac{\sigma_{xx}-\sigma_{yy}}{2}\right)^2 + \psi_{xy}^2 . \qquad (10)$$

With this notation, the constrained problem (P_k) takes the special form

$$(Q_k)\ \text{Minimize} \iint_\Omega 2\|\psi\|\,dx\,dy \text{ with } \|\psi\| \le k \text{ in } \Omega,$$

$$\psi = g \text{ and } \psi_n = h \text{ on } \Gamma.$$

After discretization, this is a finite-dimensional optimization with a quadratic inequality constraint.

We call attention to a new possibility that accompanies both constraints $|\lambda_i| \le \Lambda$ and $\|\psi\| \le k$. If k is too small, there may be no statically admissible ψ. In other words, the constraints on ψ may be incompatible, and the same is true of conditions (1) and (9) on σ; the material may be too weak to withstand the load. This is exactly the problem of limit analysis, and it suggests that in the computational algorithm we may increment the load f (equivalently, g and h) and solve a design problem at each stage prior to collapse.

† A C^0 quadratic element is admissible, if we include the contributions from derivative discontinuities between elements. The square root in (8) makes these contributions finite, and the element is "conforming".

2. The Dual Problems and Optimality Conditions

This section begins with an informal derivation of the dual problem (P*), based on the minimax theorem. The dual is a maximization over displacements $u = (u_1(x,y), u_2(x,y))$, and no boundary conditions are imposed -- since $\sigma:n = f$ was prescribed on all of Γ. For every admissible σ and u, the quantity to be maximized is less than or equal to the quantity $\iint|\lambda_1| + |\lambda_2|$ which was minimized; this is "weak duality", and it will be a direct consequence of Green's formula. To achieve full duality the difference between these quantities must vanish, and this yields the condition which connects an optimal σ in (P) to an optimal u in (P*).

This section is inevitably more concerned with formulation of the dual design problems than with explicit solutions, since the framework seems to be new. Therefore we include some optimal designs in the next section, for a problem that also has constraints on the stresses.

The Michell problem minimized $\iint|\lambda_1| + |\lambda_2|$ over divergence-free stresses satisfying $\sigma:n = f$. We introduce a Lagrange multiplier for the constraint $\operatorname{div}\sigma = 0$; this is a system of two equations,

$$\frac{\partial\sigma_x}{\partial x} + \frac{\partial\tau_{xy}}{\partial y} = 0, \quad \frac{\partial\tau_{xy}}{\partial x} + \frac{\partial\sigma_y}{\partial y} = 0 \quad ,$$

and we denote the multipliers by u_1 and u_2. Then

$$\min_{\substack{\operatorname{div}\sigma=0\\ \sigma:n=f}} \iint |\lambda_1|+|\lambda_2| = \min_{\sigma:n=f} \max_{u} \iint |\lambda_1|+|\lambda_2| + u\cdot\operatorname{div}\sigma$$

$$= \max_{u} \min_{\sigma} \iint_{\Omega} |\lambda_1|+|\lambda_2| - \langle\varepsilon(u), \sigma\rangle + \int_{\Gamma} u\cdot f \, ds. \qquad (11)$$

Here ε is the usual deformation tensor that arises in Green's formula, with components $2\varepsilon_{ij} = (u_{i,j}+u_{j,i})$; the inner product $\langle\varepsilon,\sigma\rangle$ is $\Sigma\Sigma\varepsilon_{ij}\sigma_{ij} = \operatorname{trace}(\varepsilon\sigma)$.

The next step is a minimization, for each fixed matrix ε, over all matrices σ:

$$\min_{\sigma} |\lambda_1(\sigma)| + |\lambda_2(\sigma)| - \langle\varepsilon,\sigma\rangle \quad . \qquad (12)$$

For this we first diagonalize ε by a principal axis transformation $\varepsilon = R\varepsilon' R^{-1}$, with $R^{-1} = R^T$; the eigenvalues ε_1 and ε_2 (the principal strains) appear in the diagonal matrix ε'. The inner product $\langle\varepsilon,\sigma\rangle$ and the eigenvalues $\lambda(\sigma)$ are invariant if this transformation is applied at the same time to σ:

$$\langle\varepsilon,\sigma\rangle = \operatorname{trace}(\varepsilon\sigma) = \operatorname{trace}(R^{-1}\varepsilon' RR^{-1}\sigma' R) =$$

$$\operatorname{trace}(\varepsilon'\sigma') = \langle\varepsilon',\sigma'\rangle.$$

Therefore the minimization (12) simplifies to

$$\min|\lambda_1(\sigma')| + |\lambda_2(\sigma')| - \varepsilon_1\sigma'_{11} - \varepsilon_2\sigma'_{22}. \qquad (13)$$

In case $|\varepsilon_1| > 1$, the minimum is $-\infty$; we just take $\sigma'_{11} = K\varepsilon_1$, so that our expression becomes $K|\varepsilon_1| - K|\varepsilon_1|^2 < 0$, and then let $K \to \infty$. Similarly the minimum is $-\infty$ if $|\varepsilon_2| > 1$. In the remaining case $|\varepsilon_1| \le 1$, $|\varepsilon_2| \le 1$, our expression is always nonnegative and *its minimum value is zero.* This is attained by the diagonal matrix σ', provided that

$$\begin{aligned} &\text{if } |\varepsilon_i| < 1 \text{ then } \quad \sigma'_{ii} = 0 \\ &\text{if } |\varepsilon_i| = 1 \text{ then } \quad \sigma'_{ii} = K\varepsilon_i, \ K \ge 0 \ . \end{aligned} \qquad (14)$$

Now if we return to the variational form (11), and substitute the minimum just computed (zero for $|\varepsilon_i| \le 1$, $-\infty$ otherwise), we are left with only the boundary term:

$$\text{(P*) Maximize} \int_{\Gamma} (u_1f_1+u_2f_2)ds \text{ subject to } |\varepsilon_i(u)| \le 1.$$

This is the dual problem. We expect its maximum value to equal the minimum in (P), corresponding to the minimum volume of the truss. The integrand $u\cdot f$ is simpler than the quantity $|\lambda_1| + |\lambda_2|$ in the stress formulation, but there the constraints were linear and here they are not. Nevertheless, the extreme case $|\varepsilon_i| = 1$ can be interpreted, and that is the key to the whole design.

The interpretation is classical: $\varepsilon_1 = 1$ and $\varepsilon_2 = -1$ arises from a Hencky-Prandtl net. The principal strains are of equal and constant magnitude, and opposite sign. This can happen only for a special class of displacement fields u, and their geometry has been studied in great detail [1-4]. The condition $\partial^2\theta/\partial\alpha\partial\beta = 0$ on the angle θ between the horizontal and the direction of the strain $\varepsilon_1 = 1$ was mentioned in the introduction; here we note also the secondary property

$$\varepsilon_1 + \varepsilon_2 = \frac{\partial u_1}{\partial x} + \frac{\partial u_2}{\partial y} = 0 \quad .$$

We emphasize again that the geometrical problem is identical with that of slip lines in plain strain, where it is the eigenvalues of the stress that equal $\pm\sigma_0$. And in the case of equal strains, $\varepsilon_1 = \varepsilon_2 = 1$ (pure stretching) or $\varepsilon_1 = \varepsilon_2 = -1$, there is a similar correspondence with pure hydrostatic pressure in the stress case.

We need to return to the optimality conditions. They can be expressed very concisely: *an admissible pair σ,u is optimal if and only if the last integrand over Ω in (11) is zero.* This integral is always nonnegative, so that for every admissible σ and u

$$\iint_{\Omega}(|\lambda_1(\sigma)| + |\lambda_2(\sigma)|) \, dx \, dy \ge \int_{\Gamma} u\cdot f \, ds \quad .$$

Thus the minimum in (P) cannot be less than the maximum in (P*), and the two are equal (directly from (11)) if the optimality condition is satisfied. With a more precise description of the admissible spaces, given below, the existence of an optimal pair can be proved.

The admissible spaces will include functions which are not smooth, or even piecewise smooth. Nevertheless the optimal design normally decomposes into distinct regions, in each of which one of the possibilities identified by (14) is fulfilled. We can restate those possibilities as follows:

$$\begin{aligned} &\text{if } \lambda_i(\sigma) = 0 \quad \text{then } |\varepsilon_i(u)| \le 1 \\ &\text{if } \lambda_i(\sigma) \ne 0 \quad \text{then } \varepsilon_i(u) = \operatorname{sgn}\lambda_i \ . \end{aligned} \qquad (15)$$

These conditions already appear in the book by

Rozvany [5], which is a valuable contribution to structural optimization. The region of special interest is the one combining tension and compression; the λ_i have opposite signs and $\varepsilon_1\varepsilon_2 = -1$. Prager [2, p. 53] gives the optimal design for a point load transmitted to a foundation arc, partly by a truss-like continuum of this kind (two dense orthogonal families of bars), partly by a region in which $\lambda_2 = 0$ and the members go in only one direction, and partly by a region in which $\lambda_1 = \lambda_2 = 0$ and there are no interior members. It does involve concentrated loads, and will therefore not remain optimal (or admissible) when constraints are imposed.

We come to the dual of the problem (P_Λ), with bounds $|\lambda_i| \le \Lambda$. The steps that led to (11) are essentially unchanged, but the subsequent minimization over σ is now constrained; it becomes

$$\min_{|\lambda_i|\le\Lambda} |\lambda_1(\sigma)| + |\lambda_2(\sigma)| - \langle\varepsilon,\sigma\rangle \ . \qquad (16)$$

The same transformation to principal axes leads to

$$\min_{|\lambda_i|\le\Lambda} |\lambda_1(\sigma')| + |\lambda_2(\sigma')| - \varepsilon_1\sigma'_{11} - \varepsilon_2\sigma'_{22} \ . \qquad (17)$$

We no longer reach $-\infty$ in the cases $|\varepsilon_i| > 1$, since λ_i cannot be arbitrarily large. Instead, for each of the pairs λ_i,σ_i, there are *three alternatives rather than two:*

$$\begin{aligned} &\text{if } |\varepsilon_i| > 1 \text{ then } \lambda_i = \Lambda \operatorname{sgn}\varepsilon_i \\ &\text{if } |\varepsilon_i| = 1 \text{ then } \lambda_i = |\lambda_i|\operatorname{sgn}\varepsilon_i, 0 \le |\lambda_i| \le \Lambda \qquad (18) \\ &\text{if } |\varepsilon_i| < 1 \text{ then } \lambda_i = 0. \end{aligned}$$

The minimum value in (16) and (17) is still zero in the second and third cases; we are back to a region of Michell type. But in the first case, with $|\varepsilon_i| > 1$, the minimum is no longer $-\infty$. Instead we have, when σ' is diagonal with $\sigma'_{ii} = \lambda_i = \Lambda \operatorname{sgn}\varepsilon_i$,

$$|\lambda_i| - \varepsilon_i\sigma'_{ii} = \Lambda(1-|\varepsilon_i|) \ .$$

Therefore, we can write the minimum in (16) and (17) as

$$M_\Lambda = \Lambda \min(0,1-|\varepsilon_1|)+\Lambda \min(0,1-|\varepsilon_2|) \ . \qquad (19)$$

Returning to (11)$_*$ and substituting this result for the inner minimization over σ, we find the dual to (P_Λ):

$$(P^*_\Lambda) \quad \text{Maximize} \iint_\Omega M_\Lambda \, dx\, dy + \int_\Gamma (u_1 f_1 + u_2 f_2) ds \ .$$

M_Λ penalizes the strain at any point where $|\varepsilon_i| > 1$, and as $\Lambda \to \infty$ we recover the Michell constraint $|\varepsilon_i| \le 1$.

It is the three alternatives in the optimality conditions (18) that lead us to anticipate a combination of Hencky-Prandtl nets, one coming from slip lines and the other from Michell trusses. There may also be regions of other types; in case both $|\varepsilon_i| < 1$, for example, we are completely controlled by the third alternative and the stress is zero. This appears as a hole in the optimal design. But the cases of greatest interest arise when one family of bars is in tension and the other in compression, $\lambda_1\lambda_2 < 0$. The slip line net will occur when both strains are governed by the first alternative:

$$\varepsilon_1 > 1, \varepsilon_2 < -1, \ \lambda_1 = \Lambda, \ \lambda_2 = -\Lambda \ .$$

In this case the quantity denoted earlier by $\|\varepsilon\|$, representing the difference $1/2(\lambda_1-\lambda_2)$, has the constant value Λ -- and this is the yield surface in plane strain. The other net occurs when both strains are governed by the second alternative:

$$\varepsilon_1 = 1, \ \varepsilon_2 = -1, \ \lambda_1 > 0, \ \lambda_2 < 0 \ .$$

This is the Michell situation, already discussed. And we now see the possibility of transition regions, in which *one principal stress and the other principal strain are constant*, say $\varepsilon_1 = 1$, $\lambda_2 = -\Lambda$. We do not know the geometrical implications of such a pairing.

Perhaps it would be reasonable not to work through the dual to the other constrained problem (P_k)[†]. We mention only that because the constraint acts on the deviator, and ignores the trace of σ, the condition $\partial u_1/\partial x+\partial u_2/\partial y = 0$ will appear in the dual. And symmetrically, since the rotation $\partial u_i/\partial y-\partial u_2/\partial x$ is ignored in the strain tensor ε, there must have been an equation constraining the stress tensor. It was $\sigma_{12} = \sigma_{21}$, assumed from the beginning but only now justified.

We do want to describe the space of admissible functions in each of the variational problems given above. For the original Michell problem in stresses, the equivalent form (Q) suggests the right space: the integrand involves second derivatives of the stress function ψ, and we take the largest space in which the integral to be minimized is finite. This allows all ψ whose second derivatives (the stress components) are bounded measures; singularities are permitted. The boundary values for $\sigma:n$ are expected to be integrable, so that $f_i \in L^1(\Gamma)$. (In a proper theory the boundary conditions need to be put in a relaxed form, as in [6].) The dual problem (P*) includes the constraint $|\varepsilon_i| \le 1$, and therefore the components $\varepsilon_{ij} = 1/2(u_{i,j}+u_{j,i})$ should be in $L^\infty(\Omega)$. This does not imply that each of the partial derivatives $u_{i,j} = \partial u_i/\partial x_j$ is bounded; as in [7], where Korn's inequality was shown to fail in the L^1 norm, it is only the symmetric combinations that go into ε_{ij} that must be bounded. The rotation $u_{1,2} - u_{2,1}$ can be unbounded because it is ignored.

We call u *a function of bounded strain* if $|\varepsilon_{ij}| \le$ constant, in order that (by popular demand) we can denote the admissible space by $BS(\Omega)$. We intend to study it elsewhere in more detail. It is analogous to the space $BD(\Omega)$ introduced in [7], where the combinations ε_{ij} are measures and $\int\int|\varepsilon_{ij}| < \infty$. In fact, BD is the admissible space for the dual (P^*_Λ) of our constrained problem. It allows the strains to be unbounded (the restriction $|\varepsilon_i| \le 1$ has been lifted) but it maintains the condition $\int\int|\varepsilon_i| < \infty$ which implies $\int\int M_\Lambda < \infty$. Finally, the admissible space for the new problem (P_Λ) is composed of bounded and divergence-free stresses. These come from functions ψ in the space $W^{2,\infty}(\Omega)$, with second derivatives in L_∞. And for (P_k), it is only the combinations $\psi_{xx} - \psi_{yy}$ and ψ_{xy} that must be bounded -- leading to a space that can survive for the present without a name.

3. Optimal Design in Antiplane Shear

We conclude by describing the solution of a simpler problem. It begins in the same way, with an infinite cylinder of cross-section Ω, but the surface

[†] It comes out more neatly, in terms of a strain function and a stress function, than (P^*_Λ).

forces now act *against* the plane of the cross-section. Earlier f_1 and f_2 were parallel to the plane; now the force is $f = f_3(x,y)$, in the axial direction, and it produces *antiplane shear*. It is still true that all stresses and displacements are independent of z, but a completely different subset of their components will be nonzero. For stress it is the shear components σ_{xz} and σ_{yz} which enter, and the equilibrium equation (without body forces) is

$$\operatorname{div} \sigma = \frac{\partial \sigma_{xz}}{\partial x} + \frac{\partial \sigma_{yz}}{\partial y} = 0 \quad . \tag{20}$$

There is still a stress function ψ that yields the general solution to (20), but now the relation is

$$\sigma_{xz} = \frac{\partial \psi}{\partial y}, \quad \sigma_{yz} = -\frac{\partial \psi}{\partial x} \quad . \tag{21}$$

Thus $\sigma = (\sigma_{xz}, \sigma_{yz})$ is a rotation of the gradient $\nabla\psi$ through $-\pi/2$, and the magnitudes are equal: $|\sigma|^2 = \sigma_{xz}^2 + \sigma_{yz}^2 = |\nabla\psi|^2$. The displacement is in the z direction, $u = u_3(x,y)$.

The design problem is to find the lightest structure that can withstand the boundary load $\sigma\cdot n = f$. This leads to a minimization of the stress volume:

$$\text{(P)} \quad \text{Minimize} \iint_\Omega |\sigma| dx\, dy \text{ subject to } \operatorname{div}\sigma = 0 \text{ in } \Omega, \quad \sigma\cdot n = f \text{ on } \Gamma \quad .$$

Problem (P) is the analogue for antiplane shear of Michell's problem for trusses. Its equivalent, written in terms of the stress function ψ, is

$$\text{(Q)} \quad \text{Minimize} \iint_\Omega |\nabla\psi| dx\, dy \text{ subject to } \psi = g \text{ on } \Gamma.$$

The boundary value g comes from f exactly as in equation (6), by integrating along Γ. We are not far from the minimal surface problem, which has the square root of $1 + |\nabla u|^2$ in the integrand; the disappearance of the constant brings a major simplification. These design problems (P) and (Q) are derived more properly in [8]; we are concerned here only with their solution, and their relationship to the original (P) and (Q) in the first section.

The differences are clear; σ reduces to a vector instead of a matrix, and therefore it has one distinguished direction instead of two. In place of a truss, with bars in both directions of principal stress, there is now a single family of stress trajectories across Ω. And the special properties of a Hencky-Prandtl net are replaced by an even simpler geometry: *the trajectories are straight lines*. The optimal design of the cross-section is composed of fibers that connect one boundary point to another, possibly leaving holes within Ω where the optimal σ vanishes and no material is needed.

We give an example that starts from a circular cylinder; Ω is the unit circle. The boundary force $\sigma\cdot n$ is distributed according to $f = \sin 2\theta$, pushing up in the first and third quadrants and down in the second and fourth. (The net force is $\int f\, ds = 0$, as required by the equilibrium equation $\operatorname{div}\sigma = 0$). The integral of f is $g = -\cos 2\theta/2$, and the optimal function ψ is the one that agrees with g on the boundary and has the smallest possible value of $\iint|\nabla\psi|$. By the "coarea formula", this integral can be computed from the lengths $|\gamma_t|$ of the level curves of ψ [8-9]; if γ_t is the set on which $\psi = t$, then

$$\iint_\Omega |\nabla\psi| dx\, dy = \int_{-\infty}^{\infty} |\gamma_t| dt \quad . \tag{22}$$

Therefore the curves γ_t are as short as possible for the minimizing ψ; they are straight lines. The two boundary points at angles $\pm\theta$ share the same value of g, and ψ takes this value along the line $x =$ constant connecting the two points:

$$\psi(x,y) = \tfrac{1}{2}(1-2x^2), \text{ with } \psi = \tfrac{1}{2}(1-2\cos^2\theta) = g \text{ on } \Gamma.$$

The same holds on the left side of the circle, connecting the points at angles $\pi \pm \theta$. At the top of the circle, beyond the angle $\theta = \pi/4$, there is a change. In this case the most efficient way to connect the four points on the circle that share a common value of g is by horizontal lines -- between the upper pair of points at θ and $\pi - \theta$, and the lower pair at $-\theta$ and $\pi + \theta$. In these regions, ψ is a function only of y.

$$\psi(x,y) = \tfrac{1}{2}(2y^2-1), \text{ with } \psi = \tfrac{1}{2}(2\sin^2\theta - 1) = g \text{ on } \Gamma \ .$$

Thus the circle is cut into five regions by the inscribed square whose vertices are at $\theta = \pm\pi/4, \pm 3\pi/4$. To the right and left of the square, the stress trajectories are vertical:

$$\psi = \tfrac{1}{2}(1-2x^2) \text{ and } \sigma = (\psi_y, -\psi_x) = (0, 2x) \quad .$$

Above and below the square, σ acts horizontally: $\sigma = (2y, 0)$. Inside the square ψ is zero and so is σ; no stress trajectories enter, and it is left unused in the optimal design. The stress magnitude reaches $|\sigma| = 2$ where $x = \pm 1$ and where $y = \pm 1$.

Now we introduce a *constrained design problem*, with the restriction $|\sigma| \le \Lambda$. Its variational form is analogous to the constrained Michell truss:

$$(P_\Lambda) \quad \text{Minimize} \iint |\sigma| \text{ subject to } |\sigma| \le \Lambda, \quad \operatorname{div}\sigma = 0, \ \sigma\cdot n = f.$$

In our example with $f = \sin 2\theta$, the design is not affected if the yield stress Λ exceeds 2. But as Λ decreases beyond that point, the stress trajectories must begin to curve toward the center of the circle. At $\Lambda = 1$ they are completely curved, and their form is computed in [8]. For $\Lambda < 1$ the constraints become incompatible (we could not have $\sigma\cdot n = f = 1$ at $\theta = \pi/4$) and limit analysis intervenes; the structure cannot support the load without violating the yield condition $|\sigma| \le \Lambda$, and it must collapse.

The dual problems will take a familiar form:

$$(P^*) \quad \text{Maximize} \int uf\, ds \text{ subject to } |\nabla u| \le 1$$

$$(P_\Lambda^*) \quad \text{Maximize} \iint_\Omega \min(0, \Lambda(1-|\nabla u|)) + \int_\Gamma uf\, ds.$$

They are linked to (P) and (P_Λ) by optimality conditions, and we write out the three alternatives in the constrained case:

$$\begin{aligned} &\text{if } |\nabla u| > 1 \text{ then } \sigma = \Lambda\, \nabla u/|\nabla u| \\ &\text{if } |\nabla u| = 1 \text{ then } \sigma = |\sigma| \nabla u,\ 0 \le |\sigma| \le \Lambda \\ &\text{if } |\nabla u| < 1 \text{ then } \sigma = 0. \end{aligned} \tag{23}$$

The parallels with (18) are clear, and for (P*) the first alternative disappears ($\Lambda \to \infty$) and the others

correspond completely to (15). In the dual problem (P*) on the circle, the optimal u is equal to y and $-y$ on the right and left of the square, and to x and $-x$ above and below. The second alternative holds, and the minimum in (P) equals $4\sqrt{2}/3$, which is the maximum in (P*).

We have to refer to [8] for a more detailed (and more leisurely) discussion, and to [9] for a second example. There is a similar theory when the cylinder is twisted rather than sheared; the torsional rigidity is maximized and the dual variable u is the warping function [10]. But the one point still to be made in this note is the analogy, in the antiplane context, to the conjectured coexistence of two Hencky-Prandtl nets. We close with a brief explanation of that analogy.

The optimality conditions (23) for antiplane shear make ∇u parallel to σ, so that the curves u = constant are orthogonal to the stress trajectories. The latter can be described by ψ = constant, so that u and ψ are orthogonal curvilinear coordinates. It can be proved that in a region where one family of coordinate curves is straight, the other must have constant gradient -- and conversely. In polar coordinates, for example, θ = constant is straight and $|\nabla r| = 1$. In our constrained problems we expect regions of both kinds: $|\nabla u| = 1$ when the second alternative holds, and $|\sigma| = |\nabla\psi| = \Lambda$ for the first alternative. Each of the orthogonal families is straight in one part and curved in the other, and smooth everywhere. It is a mixture of this kind, which can be illustrated by examples in antiplane shear and in torsion, that we look for also in plane strain.

References

(1) Michell, A. G. M., The Limits of Economy of Macerial in Frame-Structures, Phil. Mag. 8, 1904, 589-597.

(2) Prager, W. Introduction to Structural Optimization, Udine Lecture Notes, Springer-Verlag, 1974.

(3) Prager, W. Transactions, Royal Institute of Technology, Stockholm (1953), no. 65.

(4) Hill, R. The Mathematical Theory of Plasticity, Oxford University Press, 1950.

(5) Rozvany, G. I. N., Optimal Design of Flexural Systems, Pergamon, 1976.

(6) Temam, R. and Strang, G., Duality and Relaxation in the Variational Problems of Plasticity, J. de Mécanique 19, 1980, 493-528.

(7) Matthies, H., Strang, G. and Christiansen, E., The Saddle Point of a Differential Program, Energy Methods in Finite Element Analysis, R. Glowinski, E. Rodin, O. Zienkiewicz, eds. John Wiley, 1979.

(8) Kohn, R. and Strang, G. Optimal Design and Convex Analysis, in preparation.

(9) Strang, G. and Kohn, R. Optimal Design of Cylinders in Shear, Proc. MAFELAP Conference Brunel University, J. Whiteman, Ed., 1981.

(10) Kohn, R. and Strang, G., Optimal Design for Torsional Rigidity, Proc. Conf. on Mixed and Hybrid Finite Element Methods, S. Atluri, ed., Atlanta, 1981.

AD-P000 047

OPTIMUM GEOMETRY OF STEPPED-TAPER BEAMS

Leonard Spunt*
Department of Mechanics, Civil & Industrial Engineering
California State University, Northridge
Northridge, CA 91330 USA

Summary

An application of the parametric load index approach is presented which yields a general least weight formulation for stepped taper beams optimized for any prescribed number of stepped segments. The method provides for treating all cross-sectional dimensions dependent on the step lengths as the only independent variables. Results for both cantilevered and simply supported uniform loading demonstrate that only a two or three segment stepped beam can realize about one half of the maximum weight reduction obtainable through a continuous taper. For example, a two segment cantilever is shown to yield a 30% weight reduction with the continuous taper representing a maximum of 57% weight reduction, both being compared to a uniform cross section.

Stepped-taper configurations of up to 10 variable length segments are optimized for both simply supported and cantilever examples. These numerical results are presented in nondimensional form and are shown to be independent of the numerical value of load environment parameters or type of cross section.

For each prescribed number of steps, comparisons are made between optimized step lengths as opposed to equal length divisions. For the cases considered, it is found that optimizing individual step lengths realizes only small benefit compared to equal length steps.

Nomenclature

A	=	Gross-sectional area
C_B	=	Material and configurational coefficient in beam component optimum design equation
i	=	Subscript which defines the ith interval in a stepped beam
k_i	=	$M_i/(qL^2)$, a parameter which nondimensionalizes the maximum bending moment for the ith interval.
L	=	Total beam length
L_i	=	Length of the ith interval in a stepped-taper beam
$M(x)$	=	Bending moment function for $0 < x < L$
M_i	=	Maximum bending moment in the ith interval
M_{max}	=	Maximum bending moment over total beam span
N	=	Number of stepped intervals
opt	=	Subscript defining an optimum condition
W_c	=	Weight of the continuous taper beam
W_i	=	Weight of the ith interval in a stepped-taper beam
W_s	=	Total beam weight for stepped-taper
W'_s	=	Total beam weight for stepped-taper with equal interval lengths
W_u	=	Weight of the uniform beam
x	=	Longitudinal coordinate axis
α_i	=	Nondimensional step length variables
ρ	=	Material weight density

Introduction

The least weight cross-sectional properties of practical beams such as the I-shape was given by Cox (1). The present writer employed such results to evaluate the weight savings realized through continuous taper (2). It was shown that continuous taper offers great potential for reducing weight as compared to a uniform cross-section (from a minimum of 24% for simply supported/uniformly loaded, to a maximum of 57% for cantilevered/uniformly loaded). Although such weight savings would be desirable, the application of continuous beam taper is often not cost effective, and especially so in light of the continuously varying thickness required.

One practical alternative is to employ a stepped taper whereby the beam is considered a combination of segments, each of which has a set of uniform dimensions. In the present reporting the stepped-beam problem is formulated with the number of steps as a prescribed parameter, N, where step lengths may be set equal (fixed geometry), as well as an N variable problem treating each of N step lengths as subject to optimization. In both types of evaluations, parametric load index results (2) provide for linking all cross-sectional dimensions as dependent on the step variables, thus reducing the problem to an unconstrained search in a greatly reduced design space.

General Formulation for Stepped-Taper

The analysis is applied to the case of pure symmetric bending. It is further assumed that under the suppression of local plate buckling and yield stresses, the cross-section can be proportioned so as to justify elimination of the lateral buckling mode from consideration. This can be readily done since, under these conditions, the weight merit function is relatively insensitive to the width to depth ratio for thin wall cross-sections such as the I or box. For example, in the weight optimization of an I-beam, ignoring lateral buckling, the flange width can be sized at 50% of the section depth with only a 2% weight penalty over least weight (2). At this width to depth ratio it is unlikely that lateral buckling would occur under general loading conditions.

Based on these conditions it has been shown that the weight optimum cross-section may be expressed as (2)

$$(\rho A)_{opt} = C_B M(x)^{2/3} \qquad (1)$$

*Professor of Engineering

where C_B is a coefficient which depends on cross-sectional type and material. Through Eq. (1) the least weight cross-section is defined continuously as a function of the bending moment. To proportion the beam on a step taper basis, as illustrated in Fig. 1, the ith step, A_i, must be evaluated for the maximum bending moment in the corresponding interval, M_i. To insure an index formulation, it will be convenient to define the peak bending moments in terms of dimensionless parameters, k_i, as shown

$$M_i = k_i q L^2 \qquad (2)$$

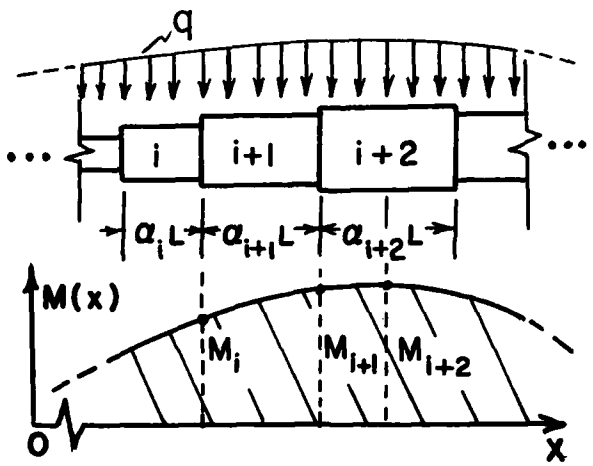


Fig. 1 - Variable Description of the Stepped-Taper Beam

where q is the transverse loading function in units of force per unit length and L is the total beam length. Defining the step length variables nondimensionally as $\alpha_i = L_i/L$, the step length for the ith interval can be written as

$$L_i = \alpha_i L \qquad (3)$$

Since uniform conditions exist over each step interval length, the weight of the ith step can be expressed as

$$W_i = (\rho A)_{opt_i} L_i \qquad (4)$$

Now combining Eqs. (1) through (4) and summing over N prescribed steps we obtain

$$W_s = C_B q^{2/3} L^{7/3} \sum_{i=1}^{N} \left(k_i^{2/3} \alpha_i\right) \qquad (5)$$

where division by L^3 yields the index result

$$\frac{W_s}{L^3} = C_B \left(\frac{q}{L}\right)^{2/3} \sum_{i=1}^{N} \left(k_i^{2/3} \alpha_i\right) \qquad (6)$$

Eq. 6 represents a general index expression in which N-1 of the prescribed number, N, of step variables, α_i, may be optimized subject to some defined load state expressed in terms of the k_i, Eq. (2). Note from Fig. 1 that in addition to the external load state, the k_i's will depend on the α_i's. Thus the α_i's are seen to be the only independent design variables.

Equal Step Lengths

For the stipulation of equal step lengths each α_i reduces to 1/N and Eq. (6) becomes

$$\frac{W_s'}{L^3} = \frac{C_B}{N} \left(\frac{q}{L}\right)^{2/3} \sum_{i=1}^{N} k_i^{2/3} \qquad (7)$$

Eq. (7) is valid for fixed geometry, i.e., each $L_i = L/N$.

Continuous Taper Comparator

The evaluation of the continuous taper ideal may be obtained by specifying a given bending moment function, M(x), and integrating Eq. (1) over the beam length. Whereby

$$W_c = \int_0^L C_B \left[M(x)\right]^{2/3} dx \qquad (8)$$

Uniform Beam Comparator

To obtain an expression for the least weight of a uniform beam, M(x), in Eq. (1), is replaced with the maximum bending moment obtained throughout the beam length, M_{max}, which, upon multiplication by the beam beam length, yields

$$W_u = C_B M_{max}^{2/3} L \qquad (9)$$

Examples

Cantilever Beam/Uniform Loading

Variable Step Lengths - Fig. 2 shows the parametric descriptions for an N step cantilever subjected to uniform loading. Treating the α_i's as variables, the k_i's are evaluated in these terms from the moment diagram of Fig. 2. Noting from Eq. (2) that $k_i = M_i/qL^2$ it follows from the moment diagram of Fig. 2 that

$$k_i = 1/2 \left[\sum_{p=1}^{i} \alpha_p\right]^2 \qquad (10)$$

Eq. (10) can be shown to result from the cantilever moment equation $M(x) = 1/2q\, x^2$. Substitution of $x_i = \sum_{p=1}^{i} L_p$ and employing Eq. (3) yields the required maximum bending moment for the ith interval, M_i. Lastly, one applies the defining equation for the k_i's, Eq. (2).

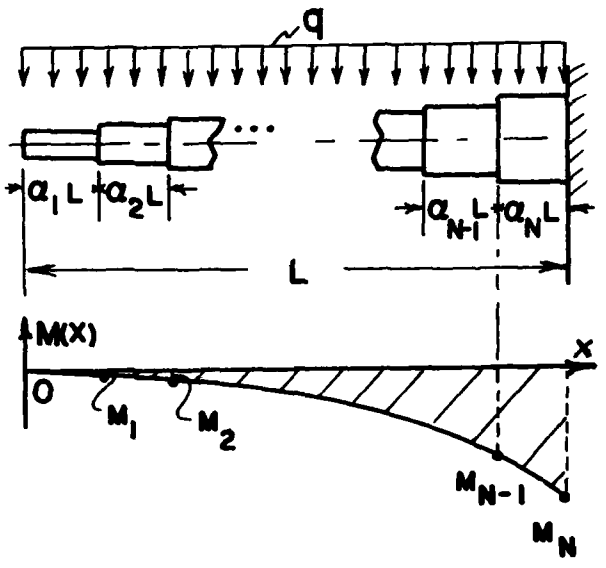


Fig. 2 - Stepped-Taper Cantilever Beam Subjected to Uniform Loading

Substituting into Eq. (6) yields

$$\frac{W_s}{L^3} = \frac{C_B}{(2)^{2/3}} \left(\frac{q}{L}\right)^{2/3} \sum_{i=1}^{N} \left(\alpha_i \left[\sum_{p=1}^{i} \alpha_p \right]^{4/3} \right) \quad (11)$$

Equal Step Lengths - Noting that for equal step lengths $\alpha_i = 1/N$, Eq. (10) becomes

$$k_i = 1/2 \left(\frac{i}{N}\right)^2 \quad (12)$$

whence from Eq. (7)

$$\frac{W_s'}{L^3} = C_B \left(\frac{q}{L}\right)^{2/3} \frac{\sum_{i=1}^{N} (i)^{4/3}}{(2)^{2/3} N^{4/3}} \quad (13)$$

Uniform Beam - From Fig. 2 the maximum bending moment, $M_{max} = 1/2 (q L^2)$. Substituting this into Eq. (9) and dividing by L^3 yields

$$\frac{W_u}{L^3} = C_B \left(\frac{q}{L}\right)^{2/3} \frac{1}{(2)^{2/3}} \quad (14)$$

Continuous Taper - For the loading function of Fig. 2, $M(x) = 1/2 (q x^2)$. Therefore, from Eq. (8) and division by L^3 we obtain

$$\frac{W_c}{L^3} = \frac{C_B q^{2/3}}{(2)^{2/3} L^3} \int_0^L x^{4/3} dx = 0.270 C_B \left(\frac{q}{L}\right)^{2/3} \quad (15)$$

For purposes of comparsion, the weight merit function in Eqs. (11), (13), (14) and (15) can be taken as the nondimensional factor of $C_B (q/L)^{2/3}$. Thus the optimum values of the α_i's are seen to be independent of beam cross-sectional type and material, C_B, and load index, (q/L).

Simply Supported Beam/Uniform Loading

Variable Step Lengths - Fig. 3 shows the parametric description for an N step simply supported beam subjected to uniform loading. For this symmetrical case the k_i's need to be evaluated for i = 1, (N + 1)/2, where i = (N + 1)/2 corresponds to the center section. It is only necessary to apply the summation in Eq. (6) for i = 1, (N - 1)/2. Accordingly, for any symmetric loading the number of independent variables may be reduced from N to (N - 1)/2, where the center section step length variable may be expressed as

$$\alpha_{\frac{N+1}{2}} = 1 - 2 \sum_{i=1}^{\frac{N-1}{2}} \alpha_i \quad (16)$$

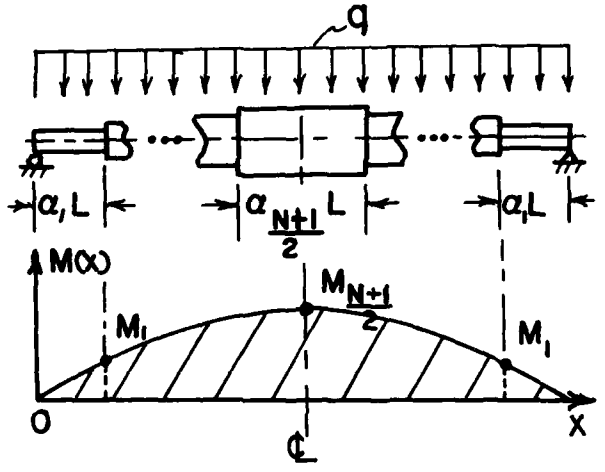


Fig. 3 - Stepped-Taper Simply Supported Beam Subjected to Uniform Loading

Therefore, for the symmetric loading case Eq. (6) may be rewritten as

$$\frac{W_s}{L^3} = C_B \left(\frac{q}{L}\right)^{2/3} \left\{ 2 \sum_{i=1}^{\frac{N-1}{2}} \left(k_i^{2/3} \alpha_i \right) + k_{\frac{N+1}{2}}^{2/3} \alpha_{\frac{N+1}{2}} \right\} \quad (17)$$

Eq. (17) will apply to any symmetric loading case. From the moment diagram of Fig. 3 the k_i's for the present loading case are found to be*

$$k_i = 1/2 \left[\sum_{p=1}^{i} \alpha_p - \left(\sum_{p=1}^{i} \alpha_p \right)^2 \right] \quad (18)$$

Equal Step Length - With the equal step length requirement of $\alpha_i = 1/N$, Eq. (18) becomes

$$k_i = 1/2 \left[\frac{i}{N} - \left(\frac{i}{N}\right)^2 \right] \quad (19)$$

*with the exception of $k_{\frac{N+1}{2}} = 1/8$, since maximum bending moment occurs at the midpoint of this segment.

Modifying the equal step length weight formation, Eq. (7), for the symmetric loading case we obtain

$$\frac{W_s'}{L^3} = \frac{C_B}{N}\left(\frac{q}{L}\right)^{2/3}\left\{2\sum_{i=1}^{\frac{N-1}{2}} k_i^{2/3} + k_{\frac{N+1}{2}}^{2/3}\right\} \qquad (20)$$

Continuous Taper - For the loading function of Fig. 3, $M(x) = 1/2\,(q\,Lx - qx^2)$. Therefore from Eq. (8) and division by L^3 we obtain

$$\frac{W_c}{L^3} = \frac{C_B\, q^{2/3}}{(2)^{2/3} L^3}\int_o^L (Lx - x^2)^{2/3}\, d_x \qquad (21)$$

Integrating by Simpson's Rule yields

$$\frac{W_c}{L^3} = 0.1864\, C_B \left(\frac{q}{L}\right)^{2/3} \qquad (22)$$

Uniform Beam - From Fig. 3, $M_{max} = q\,L^2/8$. Whence from Eq. (9) with division by L^3.

$$\frac{W_u}{L^3} = 1/4\;\; C_B \left(\frac{q}{L}\right)^{2/3} \qquad (23)$$

Once again the form of the merit function can be taken as the nondimensional factor of $C_B\,(q/L)^{2/3}$.

Tables 1 through 4 lists results for various specifications of the number of stepped segments, N, with Figs. (4) and (5) showing plots of merit function in terms of N. The data was obtained by use of a Random Vector search algorith on a CDC 3170 (3).

TABLE 1 - MERIT FUNCTIONS FOR CANTILEVER/UNIFORM LOADING (FIG. 2)

N	MERIT FUNCTIONS		PERCENT DIFFERENCE
	OPTIMIZED LENGTH SECTIONS	EQUAL LENGTH SECTIONS	
1		0.63	--
2	0.4393	0.4400	.16
3	0.3801	0.3808	.18
4	0.3514	0.3521	.20
5	0.3346	0.3352	.18
6	0.3235	0.3240	.15
7	0.3156	0.3161	.16
8	0.3098	0.3103	.16
9	0.3053	0.3057	.13
10	0.3017	0.3021	.13
∞		0.2699	--

TABLE 2 - OPTIMIZED STEP LENGTHS FOR CANTILEVER/UNIFORM LOADING (FIG. 2)

N	α_i	OPTIMUM VALUE OF α_i
2	α_1	0.52968
3	α_1	0.3677
	α_2	0.3265
4	α_1	0.2346
	α_2	0.2526
	α_3	0.2366
5	α_1	0.2333
	α_2	0.2074
	α_3	0.1942
	α_4	0.1858
6	α_1	0.1989
	α_2	0.1764
	α_3	0.1653
	α_4	0.1581
	α_5	0.1527
7	α_1	0.1736
	α_2	0.1541
	α_3	0.1444
	α_4	0.1380
	α_5	0.1334
	α_6	0.1298

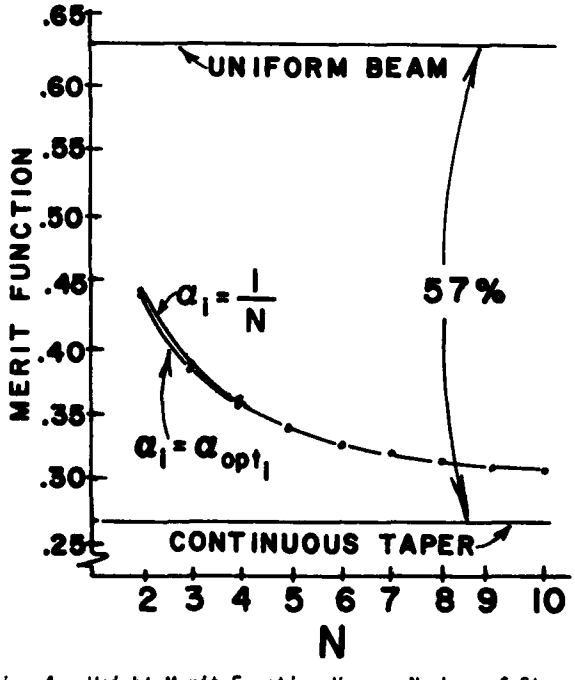


Fig. 4 - Weight Merit Function Versus Number of Steps for Cantilever/Uniform Loading

TABLE 3 - MERIT FUNCTIONS FOR SIMPLY SUPPORTED/UNIFORM LOADING (FIG. 3)

N	MERIT FUNCTIONS		PERCENT DIFFERENCE
	OPTIMIZED LENGTH SECTIONS	EQUAL LENGTH SECTIONS	
1		0.25	
3	0.2229	0.2374	6.51
5	0.2119	0.2216	4.58
7	0.2060	0.2129	3.35
9	0.2022	0.2076	2.67
11	0.1995	0.2040	2.26
13	0.1976	0.2013	1.87
15	0.1961	0.1993	1.63
17	0.1950	0.1978	1.44
19	0.1940	0.1965	1.29
∞	0.1864	0.1864	

TABLE 4 - OPTIMIZED STEP LENGTHS FOR SIMPLY SUPPORTED/UNIFORM LOADING (FIG. 3)

N	α_i	OPTIMUM VALUE OF α_i
3	α_1	0.1538
5	α_1	0.0955
	α_2	0.1292
7	α_1	0.06864
	α_2	0.08713
	α_3	0.11154
9	α_1	0.05319
	α_2	0.06566
	α_3	0.07878
	α_4	0.09872
11	α_1	0.04316
	α_2	0.05245
	α_3	0.06117
	α_4	0.07185
	α_5	0.08901

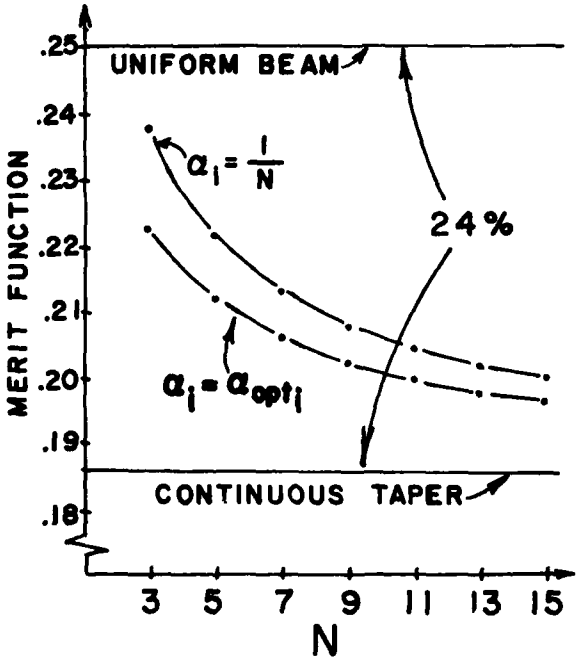


Fig. 5 - Weight Merit Function Versus Number of Steps for Simply Supported/Unform Loading

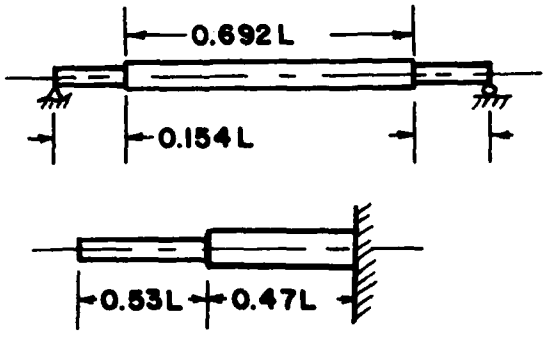


Fig. 6 - Optimum Geometry at the Lowest Step Number

Discussion of Results

The decision to employ a step taper in the practical design of beams entails considerations other than the theoretical weight variation with respect to number and relative size of the stepped segments. Primary amongst these would be the inclusion of fastening weight and the adjustment of the local dimensions to account for the stress concentrations that would accompany a stepped geometry. The ignoring of such considerations in this study in no way minimizes their importance, rather it reflects the fundamental methodology that these matters are best incorporated by way of specific modification of generalized results. In this way, least weight formulations such as presented herein may be obtained for whole classes of problems. Certainly when such results are applied to an actual numerical design, one can at that time include the weight increments associated with, and based on, the specific attachment schemes such as mechanical fasteners, weldment, or slip joints. Realizing that the following observations must in this way be tempered in the arena of real world detail design, it can be concluded from the analysis presented that:

Cantilever Example (Fig. 2)

1) Even at the lowest step number, N=2, a substantial weight reduction of 30% is obtained. This is fully one half of the maximum possible (57%) at the continuous taper, N = ∞ (Fig. 4).

2) Negligible differences in weight merit are found between optimized and equal stepped lengths, being less than 0.2% for all N (Table 1). It can be seen from Fig. 6 that the optimized step lengths for the cantilever are very nearly equal, explaining the small difference.

Simply Supported Example (Fig. 3)

1) For this case, the lowest step number, N=3, yields an 11% reduction in weight at optimized step lengths compared to the uniform beam. This corresponds to just under one half of the maximum possible (24%) at the continuous taper (Fig. 5).

2) Some small differences are found between optimized and equal stepped lengths, being at most 6.5% at N=3. This is reflected in substantially different optimized interval lengths as shown in Fig. 6.

As to the benefit of employing larger values of N, Figs. 4 and 5 indicate a relative flattening of the merit function beyond N=4 for the cantilever and beyond N=7 for the simply supported case. When proper account is taken of attachment weight increments, undoubtedly these values would be near the practical limit for step number.

It may be observed that the continuity of the merit function in Figs. 4 and 5 lends a level of confidence to the globality of the found minimums. Other examples of this can be found in Ref. (4).

References

1. Cox, H. L., The Design of Structures of Least Weight, Pergamon Press, London, 1965.

2. Spunt, L., Optimum Structural Design, Prentice-Hall, New Jersey, 1971.

3. Absher, G. W., Weight Optimization of Stepped Beams, M.S. Thesis, California State University at Northridge, 1977.

4. Spunt, L., A Programming Approach to Optimal Structural Design Using Structural Indices. AIAA Jr. of Air., Vol. 12, No. 6, June 1974.

Acknowledgements

Thanks to George Absher for running the computer evaluations for the examples and to Patti Neighbors for her skillful typing of this manuscript.

AD-P000 048

PATTERN TRANSFORMATION METHOD FOR SHAPE OPTIMIZATION AND ITS APPLICATION TO SPOKED ROTARY DISKS

Juhachi Oda and Kouetsu Yamazaki

Department of Mechanical Engineering
Kanazawa University,
Kodatsuno, Kanazawa, 920, Japan

Summary

A technique to determine effectively an uniformly stressed shape of two-dimensional design bodies under body force, which has been suggested already by the authors and is so-called "Pattern Transformation Method", will be explained plainly. This technique is one of the stress-ratio methods and based on an iterative method consisting of the following steps. In the first step, the deviation of a given shape from the design object is judged by the comparison with the stress at each point on the boundary and the design objective stress. In the next step, the given shape is modified to approach that to an optimum shape by the proportional transformation of the finite elements constituting the boundary.

By applying this technique the optimum strength shapes of the rotating disks with some spokes such as the flywheel, the belt wheel and the gear of large diameter are obtained. Furthermore the validity of the obtained shape is examined experimentally by the spinning fracture test.

Introduction

Up to this day, optimum design field has made a remarkable progress with the developement of space engineering. But optimum design of continuum has not been studied so much as that of structure such as framed or truss structure, because of the difficulties involved in representing mathematically the geometrical shape of continuum and the fact that the problem is generally a large-scale nonlinear one.

But in recent years, some techniques to obtain an optimum shape of elastic continuum have been developed by applying the finite element method. The technique transforming the shape of element near the boundary surface, i.e., "Pattern Transformation Method", is suggested and applied to two dimensional and axisymmetric problems by Oda and Yamazaki (1-3). Furthermore, the growing-reforming technique (4) and the technique applying the inverse variational principle (5) are also developed in Japan. These techniques consist of relatively simple processes and are essentially equal to one another because the shape modification is carried out by comparison with the local stress or strain energy distribution and the standard value. On the other hand, Francavilla et al. (6) and others (7, 8) developed the techniques of applying mathematical programming method. Experimental techniques for reducing the stress concentration are also suggested (9-11).

In this paper, the Pattern Transformation Method for body force problems suggested in Ref. (3) is explained plainly and applied to the practical engineering problems such as the design of spoked rotary disks. Moreover the validity of the obtained shape is examined experimentally by spinning fracture test of the specimens made from resin mortar.

Optimization technique

Design procedure

In the optimum design of a continuous body under arbitrary loading and supporting conditions, if a volume of design body or an allowable stress is specified in advance, the optimum shape satisfying these design constraints will be the nearest one to the uniformly stressed shape. Then, when boundaries S_σ of a design body Ω, on which the external loads are applied or the displacements are specified, are given as illustrated in Fig.1, our design object is to determine the uniformly stressed shape of Ω by changing the free boundaries S_F. For instance, if the volume of Ω is specified, we must minimize the ratio of the maximum stress to the minimum stress on the boundaries. On the contrary, if the allowable stress is specified, the volume of Ω has to be minimized under the stress constraint.

Now, an iterative method to obtain optimum shapes for two dimensional bodies and its application to the body force problem have been previously proposed by the authors (1-3). Figure 2 plainly shows the design procedure for the body force problem. That is, the optimizing steps for body force problem are as follows :

(i) At the first step an original shape which satisfies the given design conditions is assumed.

(ii) The original shape is subdivided into the finite elements. The stresses $\{\sigma\}_j$ and an equivalent stress $\bar{\sigma}_j$ in each element are calculated by the finite element method considering the body force.

(iii) A standard stress σ_a is set according to the design constraints, that is, when the volume V of Ω has to be kept constant, σ_a is determined approximately from the mean value of $\bar{\sigma}_j$ in the element region Ω_F constituting the design boundaries S_F. On the other hand, when the allowable stress is specified, σ_a is set equal to the specified value.

(iv) The superiority or inferiority of the given shape is judged by a deviation from the stress provided with the design object, that is, the deviation is calculated by comparison with the design stress σ_a and the equivalent stress in each element.

(v) The pattern transforming values considering the effect of body force for each element in Ω_F are determined by applying a proportional transformation method of element shape. The values are transformed into the shifting vectors to move the nodes on the boundaries S_F and the shape of them are modified.

(vi) At the final step, the new shape of the design

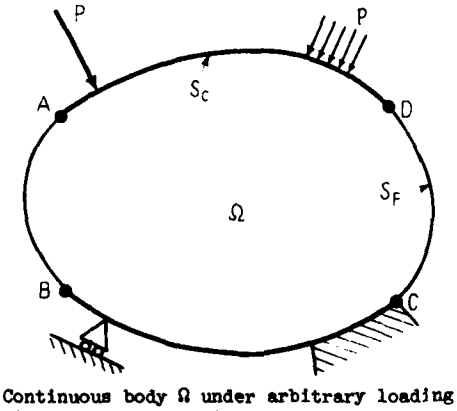


Fig.1 Continuous body Ω under arbitrary loading and displacement conditions.

boundaries S_F should be faired up by the continuous curves. The modified shape is adopted as a new original shape in the next optimization cycle.

By the iteration of the above mentioned steps the optimum shape can be obtained finally. The pattern transformation method and the determination of the shifting vectors are most important in this technique and described in detail in the next section.

Pattern transformation method

If a shape Ω_{n-1} at the cycle $n-1$ changes to a shape Ω_n at the cycle n under an arbitrary dynamical condition, the following relation will be held between these shapes.

$$\Omega_n = \phi_n \Omega_{n-1} \tag{1}$$

in which ϕ_n is called as transforming function and must be determined from the dynamical law between Ω_{n-1} and Ω_n. Moreover ϕ_n should be selected according to the design object.

Now, let's consider to determine a concrete form of ϕ_n by using the following simple example and estimate an effective pattern transformation method in the two-dimensional stress field. Figure 3(a) shows a rectangular plate of $a \times b$ in size and t in thickness. The plate is loaded uniformly with P_x and P_y in two directions of coordinate axes, respectively. If F_x and F_y denote the equivalent components of body force in this plate, the stress components of σ_x and σ_y are given as follows :

$$\sigma_x = (P_x + F_x)/bt \quad , \quad \sigma_y = (P_y + F_y)/at \tag{2}$$

Then, maintaining the loading conditions of P_x, P_y and thickness t constant, we can modify the shape of the plate so as to bring the coordinate stresses closer to the object stress by using the proportional transformation given as

$$\phi = (x \to \xi x \ , \ y \to \eta y) \tag{3}$$

The parameter ξ and η of transformation can be determined from the equation of equilibrium for forces. Figure 3(b) shows a new shape of the plate transformed by Eq.(3).

If body force distributes uniformly, the force will be proportional to the volume of the plate. Therefore the components of body force after transformation are given as

$$F_x^* = \xi\eta F_x \quad , \quad F_y^* = \xi\eta F_y \tag{4}$$

where the values marked with an asterisk denote that after transformation. Then the stress components are changed as follows :

$$\begin{aligned} \sigma_x^* &= (P_x + \xi\eta F_x)/\eta bt \\ \sigma_y^* &= (P_y + \xi\eta F_y)/\xi at \end{aligned} \tag{5}$$

By using the condition that these new coordinate stresses are in accordance with the standard stress σ_a, the parameters ξ and η must be determined. From Eqs. (2) and (5), the equations to determine ξ and η are

$$\begin{aligned} (1+\alpha_x)\eta &= \beta_x (1+\alpha_x \xi\eta) \\ (1+\alpha_y)\xi &= \beta_y (1+\alpha_y \xi\eta) \end{aligned} \tag{6}$$

where α_x and α_y represent the ratios F_x/P_x and F_y/P_y respectively, moreover β_x and β_y denote the ratios of the stress components to the standard stress. Therefore, it should be noted that a pair of ξ and η can be determined from Eq.(6) and the coordinate stresses can be changed to be equal to the standard stress by executing the pattern transformation.

In general, α_x and α_y are not equal to zero. Then the parameter ξ and η are given by solving Eq. (6) as follows :

$$\begin{aligned} \xi &= \frac{(\alpha_x - 1)(\alpha_y - 1) + (\alpha_x - \alpha_y)\beta_x \beta_y - \Delta}{2\alpha_x (\alpha_y - 1)\beta_x} \\ \eta &= \frac{(\alpha_x - 1)(\alpha_y - 1) + (\alpha_y - \alpha_x)\beta_x \beta_y - \Delta}{2(\alpha_x - 1)\alpha_y \beta_y} \end{aligned} \tag{7}$$

in which

$$\Delta = \{(\alpha_x - 1)^2 (\alpha_y - 1)^2 - 2(\alpha_x - 1)(\alpha_y - 1)\alpha_x \alpha_y \beta_x \beta_y + (\alpha_x - \alpha_y)^2 \beta_x^2 \beta_y^2\}^{1/2}$$

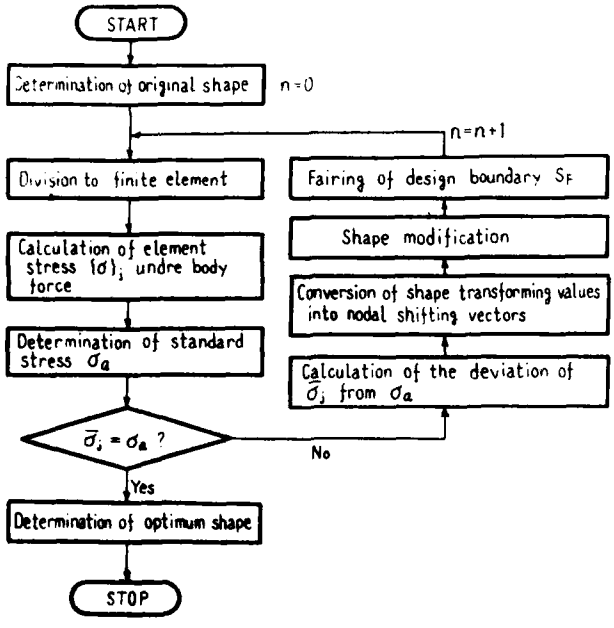


Fig.2 Flow chart to determine an optimum shape for body force problem.

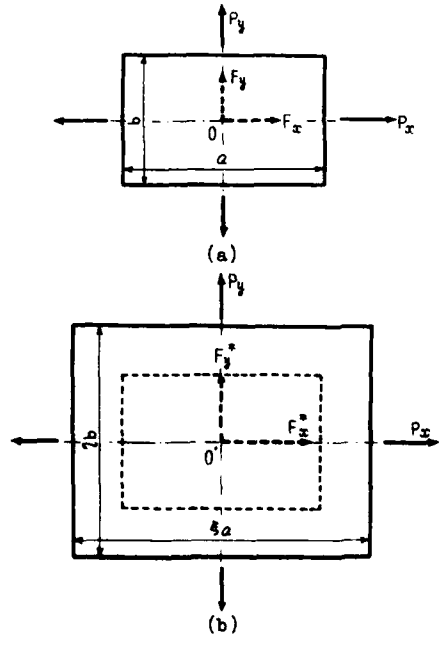


Fig.3 Example of shape transformation in rectangular plate.

In a special case, if body force distributes just in a single coordinate direction, for example $F_x \approx 0 (F_y \neq 0)$, i.e. $\alpha_x = 0$, ξ and η are determined from Eq.(6) as follows :

$$\xi = \frac{\beta_y}{1 + \alpha_y (1 - \beta_x \beta_y)} \quad , \quad \eta = \beta_x \tag{8}$$

Now, in the above mentioned cases the coordinate stresses σ_x and σ_y only are considered and the shear stress is omitted. If the influence of the shear stress is taken into consideration, the parameter ξ and η will be more complicated. When the principal stresses σ_1 and σ_2 ($\sigma_1 \geq \sigma_2$) are considered, however, the pattern transformation described above is applicable to that in the principal directions. Furthermore, if we select linear triangular elements with three nodes for the finite element analysis, the pattern transformation can be applied to each element in the design region Ω_P. The validity of the application can be proved by the mean described in Ref (3).

Shifting vector of node Let us consider to formulate shifting vector of node from the pattern transforming value of element. Figure 4 shows a vector illustration of the pattern transformation of element j, the origin of which situates at the center of gravity of the element. It is recognized that the pattern transformation of the element is to shift the nodes according to the nodal vectors $\boldsymbol{b}_{ji}$ shown in the figure. When the pattern transformation is executed for each element in Ω_P at the same time, the nodal vectors $\boldsymbol{b}_{ji}$ will be produced from each element j that surrounds the node i. Then we assume that the shifting vector $\delta \boldsymbol{X}_i$ of the node i is given by the mean value of $\boldsymbol{b}_{ji}$. If the node i is surrounded by q elements, $\delta \boldsymbol{X}_i$ will be given as follows :

$$\delta \boldsymbol{X}_i = 1/q \sum_{j=1}^{q} \boldsymbol{b}_{ji} \tag{9}$$

Then, the locations of each node on S_F in Ω_{n-1} are changed by $\delta \boldsymbol{X}_i$ formulated in Eq.(9), a new shape Ω_n, the stresses in which must be closed to the required

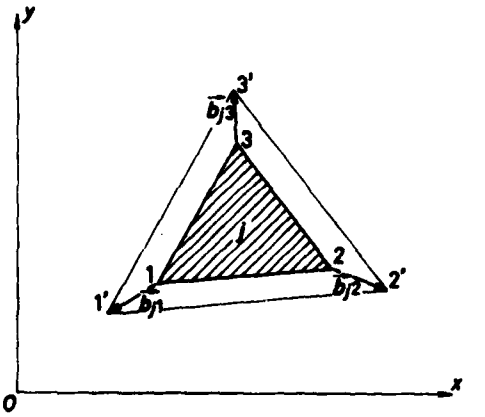


Fig.4 Vector illustration of propotional transformation of element.

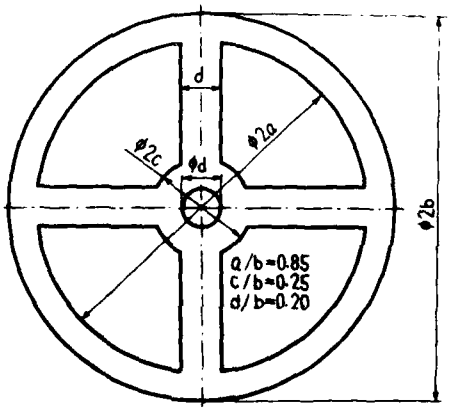
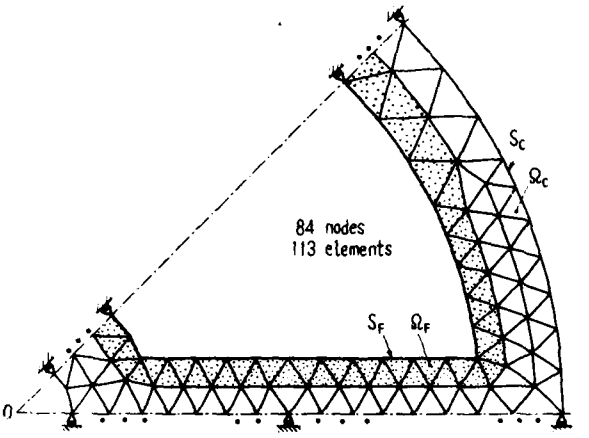
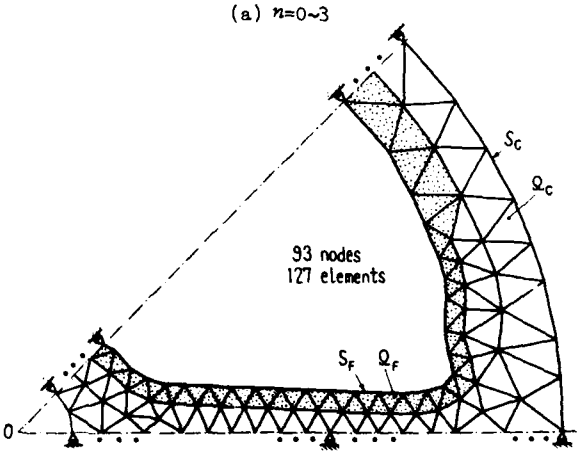


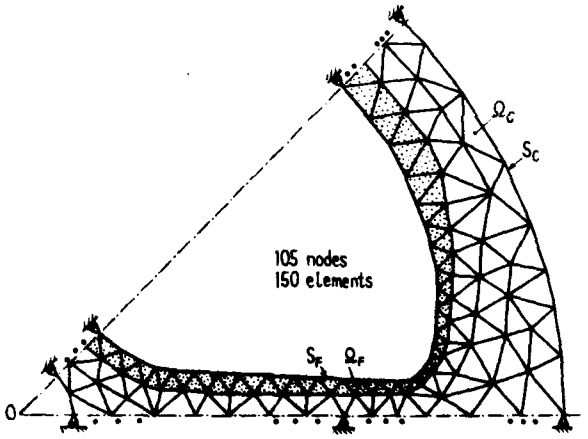
Fig.5 Original shape of four spoked disk.



(a) n=0~3



(b) n=4~11



(c) n=12~13

Fig.6 Element subdivisions of four spoked disk.

stress value, will be produced.

Application to spoked rotary disks

Numerical results

Pattern transformation method described previously is applied to determine optimum shapes of rotary disks with some spokes such as the flywheels, the belt wheels and the gears of large diameter. For the analysis plane stress field is assumed because that the outer diameter is much greater than the thickness of the disk.

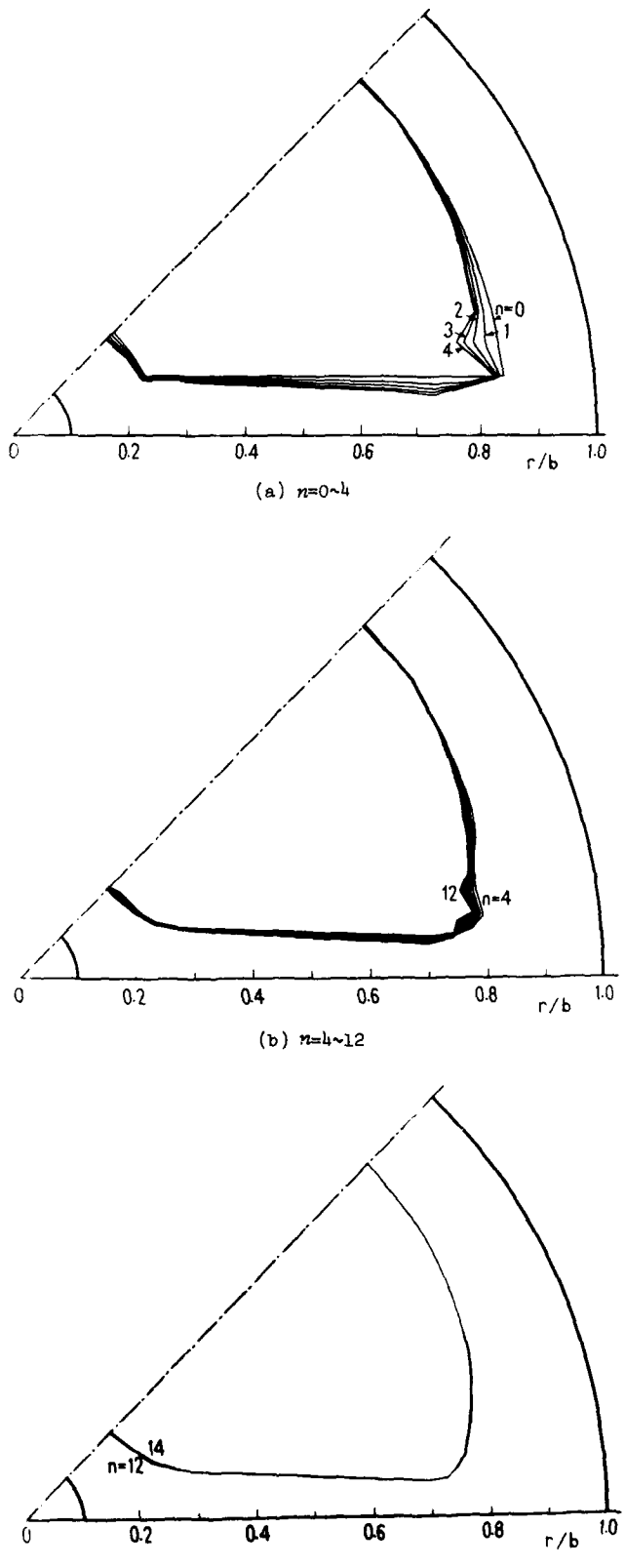
First, we select the rotary disk with four spokes for the original shape of design model as shown in Fig. 5. As for the sizes of this shape, the inner and outer radii of the rim are a and b, respectively, and those of the hub are $d/2$ and c. The width of the spokes are equal to the inner diameter of the hub and wider than one by the general rule of design for the spoked disks. As the design constraints, the sizes of the outer radius of rim and inner radius of hub are specified in advance, and the volume of disk is kept constant. That is, we try to determine an equally stressed shape of disk by modifying the shapes of inner peripheral surface of rim, spokes and outer peripheral surface of hub. The material of disk is assumed resin mortar and the mechanical properties are shown in Table 1. By using the material the spinning fracture test is performed later. Furthermore, the well-known maximum stress theory is adopted as an elastic failure criterion of the brittleness of the material.

The computer implementation is carried out for one-eighth region of the design model because of the symmetry. Figure 6(a) shows the finite element subdivision at the first cycle, which is relatively coarse to promote the fast change of shape. In the figure a dotted area is defined as the design region Ω_F. The pattern transformation is performed in this area, in which the standard stress σ_a is decided from the mean value of the equivalent stresses in the region Ω_F, that is,

$$\sigma_a = \Sigma \bar{\sigma}_j A_j / \Sigma A_j \qquad (10)$$

where A_j is the area of the triangular element j in Ω_F. Figure 7(a) shows the shape changing processes until fourth cycle. At fourth cycle, the element idealization of Ω is changed from (a) to (b) of Fig.6 because each area of element in Ω_F does not satisfy the constraint condition for keeping the precision of analysis (1). At the same time, the shape at the junction part between the spoke and the rim is smoothed to put away an unfavorable shape changing alike saw wave at the stress concentrated parts. This processing is carried out also at 12th cycle. Figure 6(c) shows the element idealization adopted after 12th cycle. Figures 7(b) and (c) show the shape changing processes at n= 4 ~ 12 and n = 12 ~ 14, respectively. From these figures it is recognized that the width of spoke has decreased near the root of the rim, but that of the rim has increased near the root of spoke. Furthermore, the junction parts between the spoke and the rim or the hub have rounded, and at n = 14 the radii of curvature are $r_1 = 0.33d$ and $r_2 = 1.18d$ as shown later in Fig. 15. That is, the width of the spoke has changed to 1/10 tapered shape.

Figure 8 shows the variations of the maximum stress σ_{1max}, minimum stress σ_{1min} and their ratio $\sigma_{1max}/\sigma_{1min}$ (σ_1 means the maximum principal stress at each point in the region Ω and Ω_F, respectively), in which ρ and ω are a material density and angle velocity of rotation. From this figure, the stress ratio in Ω_F has decreased extremely at the earlier cycles and changed from 10.09 to 1.68. The stress distributions on the boundary S_F at the initial and final cycle are shown in Fig.9, in which the distribution of the orig-



(a) n=0~4

(b) n=4~12

(c) n=12~14

Fig.7 Shr changing processes of four spoked disk.

inal shape is obtained by using another fine subdivision of elements. The stress σ_1 concentrates at the junction part between the spoke and the rim in the original shape, but distributes uniformly in the final shape. The volume change is less than one percent during optimization. From these results we may call the shape obtained finally as "optimum shape".

Next, we also try to determine the optimum shape of rotary disk with six spokes. Figure 10 shows the original shape and its subdivision, which has the same volume and the same ratio d/b that the disk with four spokes has and is determined by taking the results mentioned above into consideration. The shape optimization has implemented under the same design constraints that has adopted for the disk with four spokes. Figure 11 shows the shape changing processes. The optimum shape obtained finally is illustrated in Fig.12 in detail, in which $r_1 = 0.43d$ and $r_2 = 0.64d$, and the stress distribution on S_p of the optimum shape is also shown in Fig.13. From these results it is recognized that the radii r_1 and r_2 of curvature differ from that of disk with four spokes, but the taper of the spoke width is nearly equal.

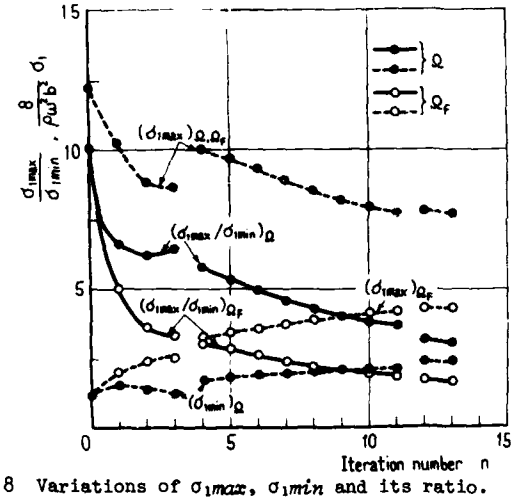
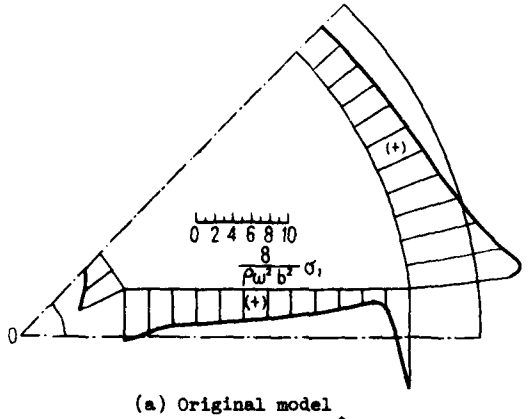
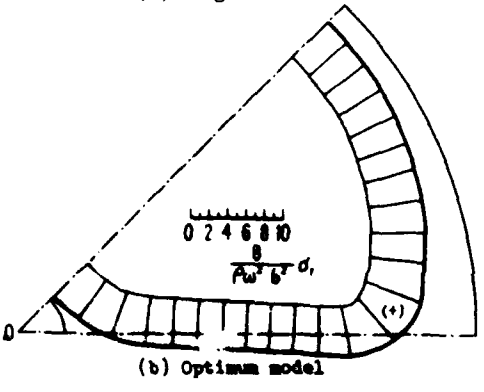


Fig.8 Variations of σ_{1max}, σ_{1min} and its ratio.



(a) Original model



(b) Optimum model

Fig.9 Stress distributions on S_p.

Spinning fracture test

The validity of the numerical results described in the previous section is examined experimentally. That is, the original and optimum shapes of the rotary disks with four spokes are fractured by the spinning test and the results are compared with each other.

Specimens The test specimens of disk are made of resin mortar, which is one of the brittle materials and behaves elastically until fracture. The resin mortar consists of 80 weight-percent fine-grained (0.2 ~ 0.5 mm) sand and 20 weight-percent epoxy resin with

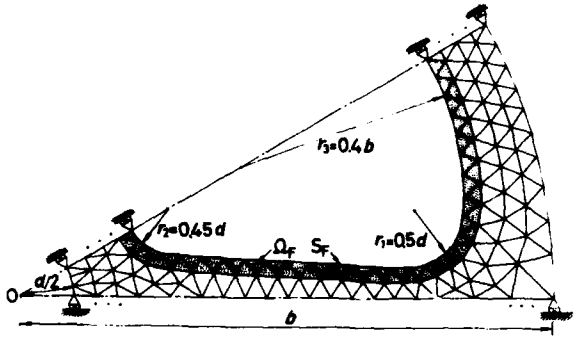


Fig.10 Original shape and finite element subdivision of six spoked disk.

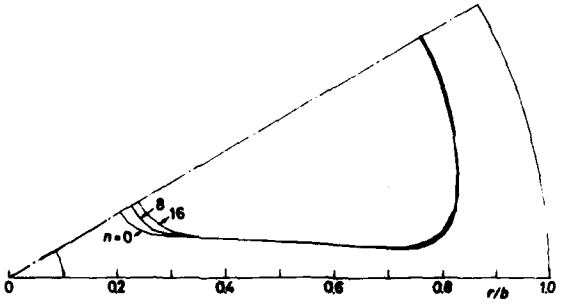


Fig.11 Shape changing processes of six spoked disk.

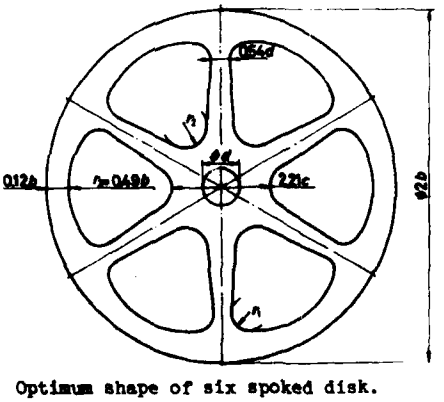


Fig.12 Optimum shape of six spoked disk.

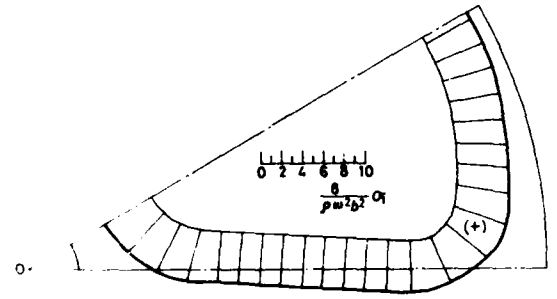


Fig.13 Stress distribution on S_P in optimum shape.

weight composition of Epicoat 828 : Thiokol LP-3 : Diethylentriamine = 100 : 15 : 8. The mechanical properties of resin mortar shown in Table 1 are obtained from tensile tests and the stress - strain relation is shown in Fig.14 .

Now, the configulations of the original and optimum models are shown in Figs.5 and 15, in which practical sizes are determined as $2b = 130$ mm and thickness $t = 10$ mm. The specimens are casted and provided for the test after twenty days to make the strength stable.

Equipment Figure 16 shows an equipment for the spinning fracture test. A specimen is attached directly to the main spindle of a heigh frequency motor , which is lubricated forcibly by the oil mist apparatus. An enameled wire of 0.1 mm in diameter is stretched as a trigger around the position 1 ~ 2 mm apart from the outer peripheral surface of the disk. If the wire is cut, the number of revolutions is memorized by the digital counter. At the same time, a stroboscope is synchronized and a momentary photograph of the cracked specimen is taken by the camera.

Experimental results Ten specimens of each model are fractured by the spinning test and the results are shown in Table 2 . From this table, it is recognized that the bursting speed of the optimum model is 27 percent greater than that of the original model. Furthermore, in this table the values of the bursting speed estimated by using the maximum stress theory and the mean stress theory are also indicated. The estimated values by the mean stress theory are obtained by averaging the normal stress at the cracked section and by using tensile strength σ_B . From these results, neither criterions estimate exactly the actual bursting speed of spoked disk.

From the photographs at fracturing moment as shown in Fig.17, it is obvious that the actual cracks in the original model initiate near the junction part between the rim and the spoke and propagate in the radial direction. On the contrary, the cracks in the optimum model initiate and propagate near each minimum section of rim, spoke and hub. These results are predictable from the stress distribution illustrated in Fig.9.

From these results it is concluded that the uniformly stressed rotary disk with some spokes has higher strength.

Conclusions

In this paper, Pattern Transformation Method to obtain the optimum strength shape of elastic continuum under body force is summarized and applied to the design of spoked rotary disks. From the numerical results it is concluded that the optimum shape of spoked disk under centrifugal force has about 1/10 tapered spokes, the parts near hub of which is wider than that near rim, and the rounded junction parts of a large radius of curvature. Furthermore, the validity of the optimum shape of spoked rotary disks has been con-

Table 1 Mechanical properties of resin mortar.

	Mean value	Standard deviation
Tensile strength σ_B MPa	12.99	0.73
Young's modulus E GPa	12.53	1.30
Poisson's ratio ν	0.279	0.031
Density ρ kg/m³	1.98×10^3	——

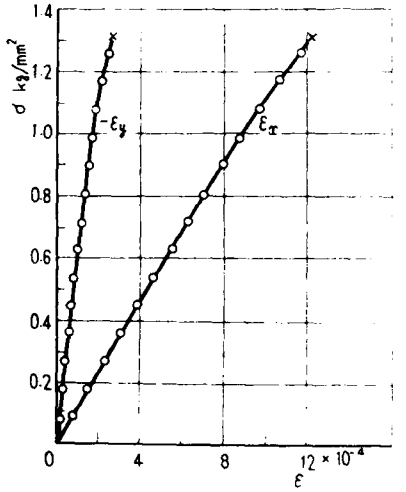


Fig.14 Stress-strain relation of resin mortar.

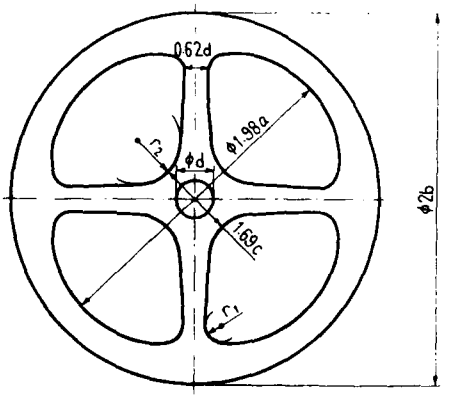


Fig.15 Optimum shape of four spoked disk.

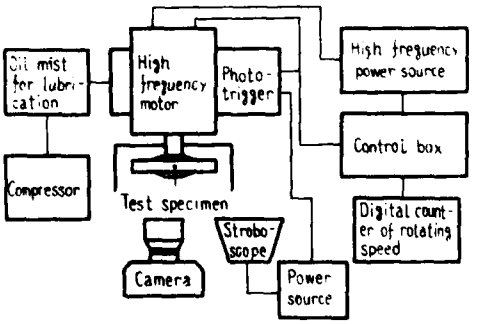
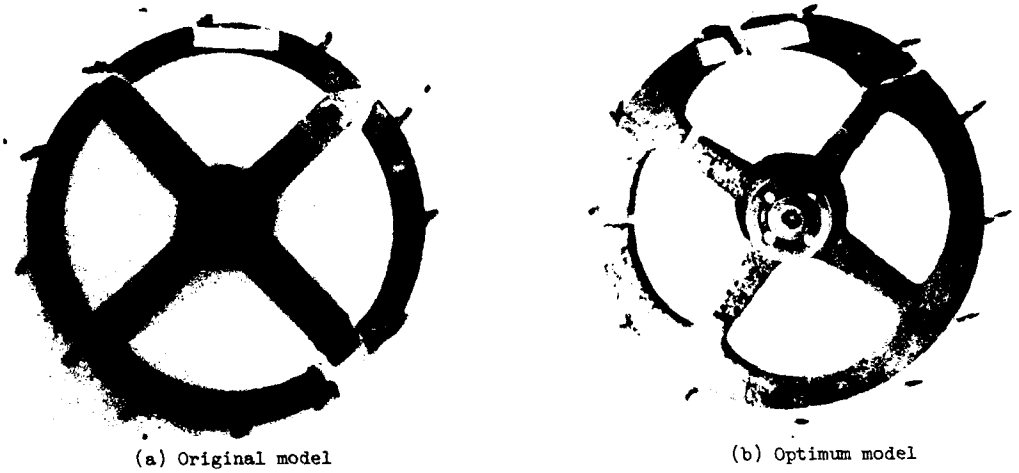


Fig.16 Equipment of spinning fracture test

Table 2 Experimental results and simulated values of fracture spinning test.

Bursting speed	Experimental results		Simulated values	
	Mean value	Standard deviation	Maximum stress theory	Mean stress theory
Original disk $N_{original}$ rpm	11908	239	8401	13690
Optimum disk $N_{optimum}$ rpm	15120	789	12535	14451
$N_{optimum}/N_{original}$	1.270	——	1.492	1.056



(a) Original model (b) Optimum model

Fig.17 Photographs at fracturing moment.

firmed experimentally by the spinning fracture test. Therefore it is also concluded that Pattern Transformation Method is avairable for the practical use of mechanical design procedure.

References

(1) Oda, J. and Yamazaki, K., On a Technique to Obtain an Optimum Strength Shape by the Finite Element Method, Bulletin of Japan Society of Mechanical Engineers, Vol. 20, 160, 1977.

(2) Oda, J. and Yamazaki, K., On a Technique to Obtain an Optimum Strength Shape of an Axisymmetric Body by the Finite Element Method, Bulletin of Japan Society of Mechanical Engineers, Vol. 20, 1524, 1977.

(3) Oda, J. and Yamazaki, K., On a Technique to Obtain an Optimum Strength Shape by the Finite Element Method : Application to the Problem under Body Force, Bulletin of Japan Society of Mechanical Engineers, Vol.22, 131, 1979.

(4) Umetani, Y. and Hirai, S., An Adaptive shape Optimization Method for Structural Material Using the Growing-reforming Procedure, Proceedings of Joint JSME-ASME Applied Mechanics Western Conference, Honolulu, Hawaii, 359, 1975.

(5) Seguchi, Y. and Tada, Y., The Shape Determination Problem of Structure by the Inverce Variational Principle, Transactions of Japan Society of Mechanical Engineers, Vol.44, 1469, 1978.

(6) Francavilla, A., Ramakrishnan, C. V. and Zienkiewicz, O. C., Optimization of Shape to Minimize Stress Concentration, Journal of Strain Analysis, Vol.10, 63, 1975.

(7) Bhavikatti, S. S. and Ramakrishnan, C. V., Optimum Shape Design of Shoulder Fillets in Tension Bars and T-heads, International Journal of Mechanical Sciences, Vol.21, 29, 1979.

(8) Kristenen, E. S. and Maden, N. F., On the Optimum Shape of Fillets in Plates Subjected to Multiple In-plane Loading Cases, International Journal for Numerical Methods in Engineering, Vol.10, 1007, 1976.

(9) Steinchen, W. P., Investigations and Optimization of Stress-relieving Notches, Journal of Strain Analysis, Vol.13, 149, 1978.

(10) Erickson, P. E. and Riley, W. F., Minimizing Stress Concentrations around Circular Holes in Uniaxially Loaded Plates, Experimental Mechanics, Vol.18, 97, 1978.

(11) Durelli, A. J., Brown, K. and Yee, P., Optimization of Geometric Discontinuities in Stress Fields, Experimental Mechanics, Vol. 18, 303, 1978.

AB-P000 049

A GENERAL THEORY OF OPTIMAL STRUCTURAL LAYOUTS

by G.I.N. Rozvany.
Department of Civil Engineering, Monash University,
Clayton, Victoria 3168, Australia.

Summary: A general theory of optimal structural layouts, based on static-kinematic optimality criteria and the concept of structural "universe", is outlined and then illustrated with two simple examples. Finally, the application of this theory to various types of configuration problems is reviewed, giving a state of the art report on analytical solutions for various classes of optimal structural layouts. Particular attention is devoted to a new class of optimal structures termed "Prager structures" which consists of archgrids or cable networks of optimized member layout.

1. Introduction

The problem of optimal structural layouts or configurations has formed the central theme of W. Prager's research work during the last years of his creative life. The degree of complexity of layout problems was summed up in the following remark by Prager [1]: "Most of the literature on structural optimization is concerned with the optimal choice of cross-sectional dimensions. When the layout as well as the cross-sectional dimensions are at the choice of the designer, structural optimization becomes a much more challenging problem."

The theory of optimal structural layouts is based on two fundamental concepts: static-kinematic optimality criteria and the concept of "basic structures" [2] or "structural universe" [3]. The first such optimality criterion was proposed by Prager and Shield [4]; later it was expressed in terms of the generalised gradient operator and extended to a comprehensive set of design criteria by the author [3, 5]. By applying these criteria to a basic structure (or universe) consisting of all potential (feasible) members, the optimal layout can be determined systematically and directly for any structural system.

In this paper, first the theory of optimal layouts is outlined briefly and then it is illustrated with two simple examples. Finally, the present state of knowledge is reviewed, considering various classes of layout problems, namely least weight trusses (Michell structures), beam grids (grillages), archgrids and cable networks (Prager-structures), frameworks subject to combined bending and axial forces, membrane shells and cellular continua consisting of a dense system of intersecting shells. Finally it is explained that the optimal design of solid plates and shells subject to a maximum thickness constraint reduces to a layout problem in which the configuration of densely spaced stiffener-like formations must be optimized.

2. Basic Theory

The problem of layout optimization will be discussed in the context of optimal plastic design in which, by virtue of the lower bound theorem of plastic analysis and design [6], only statical admissibility is required. The resulting design (e.g. Michell structures, optimal grillages), however, often satisfies kinematic admissibility of the elastic strains and constitutes also an optimal elastic design for a given permissible stress, given compliance or given fundamental frequency [5, 7]. Moreover, static-kinematic optimality criteria can be readily extended [7, 8] to any elastic system with permissible stress criteria by optimally understressing some parts of the system with a view to restoring elastic compatibility.

2.1 The Prager-Shield Condition.

Using Prager's terminology [4, 5], the generalised stresses $\underline{Q}$, strains $\underline{q}$, displacements $\underline{u}$ and loads $\underline{p}$ are defined on the structural domain D which is the union of all points of potential centroidal axes or middle surfaces and is referred to the coordinates $\underline{x}$. The specific cost $\psi(\underline{x})$ (i.e. cost per unit length, area or volume) can be represented as a function (termed specific cost function) $\psi[\underline{Q}(\underline{x})]$ of the generalised stress vector, and then the problem of optimal plastic design can be stated as

$$\min \Phi = \int_D \psi(\underline{Q}^s)\, d\underline{x}, \qquad (1)$$

where the superscript "s" denotes statical admissibility and Φ is the total "cost" which is to be minimized. A condition of minimum total cost then becomes [4, 5]

$$\text{(on D)} \qquad \underline{q}^k = \underline{G}[\psi(\underline{Q}^s)], \qquad (2)$$

where the superscript "k" denotes kinematic admissibility and $\underline{G}$ is the generalised gradient operator [5, 9] which reduces to the usual gradient

$$\underline{G} = \underline{\text{grad}} = (\partial/\partial Q_1, \ldots, \partial/\partial Q_n) \qquad (3)$$

for differentiable specific cost functions. Considering now piecewise differentiable cost functions, let $\psi(\underline{Q})$ be differentiable on the interior of subsets of the stress space termed "stress regimes". Then (3) still holds on the interior of the stress regimes but along boundaries contained by more than one stress regime the generalised gradient is given by any convex combination of the limiting gradients for the adjacent stress regimes ([5, 9], see examples in Section 3). Moreover, if $\psi(\underline{Q})$ is discontinuous at a stress value $\underline{Q}^*$ then $G[\psi(\underline{Q}^*)]$ becomes an impulse (Dirac distribution), [5, 9]. Criterion (2) is a necessary and sufficient condition if $\psi(\underline{Q})$ is convex and the equilibrium equations are linear; and it is a necessary condition if the above restrictions are not fulfilled.

Expressing (2) in words, the Prager-Shield condition requires a statically admissible stress field and a kinematically admissible strain field in which at all points of the domain the strains equal the generalised gradients of the specific cost function with respect to such stresses. Static-kinematic optimality criteria convert, in effect, the problem of optimization into a problem of analysis in which the stress-strain relation is furnished by (2).

2.2 The Concept of Basic Structure or Universe.

By applying the Prager-Shield condition (2) to the basic structure or universe, that is, to a system consisting of all potential (feasible) members, the Prager-Shield condition (2) furnishes the optimal strain requirements for members of non-zero cross-sectional area (ie. specific cost). Moreover, it also yields different (and usually less restrictive) strain requirements for members having a zero specific cost (i.e. non-optimal members). If condition (2) is satisfied along all optimal and non-optimal members and $\psi(\underline{Q})$ is convex then a globally optimal layout has been established. This is an important feature of the

PRECEDING PAGE

theory discussed, because the problem is nearly always non-convex when it is formulated in terms of the geometry of the optimal members (i.e. location and orientation of centrelines).

3. Two Simple Examples

3.1 Optimal Beam Layout for a Single Point Load over a Simply Supported Strip.

We consider a horizontal domain (ABCD in Fig. 1a) with a centrally placed vertical point load P and two parallel simple line supports. The optimal beam layout for transmitting the load to the supports is to be determined, if the specific cost function for the beams is $\psi = k|M|$ where k is a given constant and M is the bending moment.

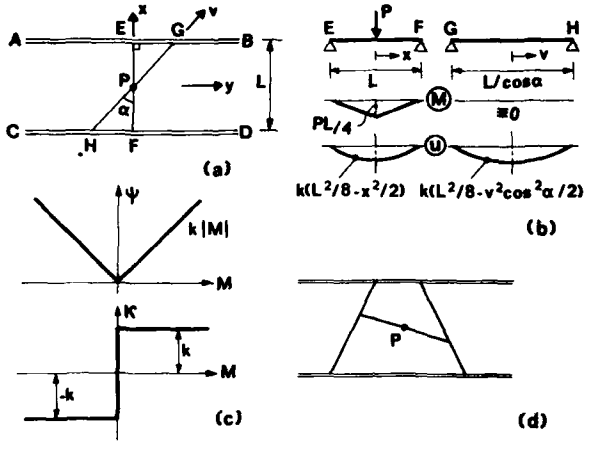


Fig. 1. First example: a beam layout problem.

The purpose of this example is only to illustrate the method described in Section 2. The solution itself is intuitively obvious and consists of a single beam EF normal to the simple supports. The solution will be discussed at three different levels, by increasing the feasible design space progressively.

(a) Structural universe consisting of two beams. Let the only two potential centroidal axes be EF and HG in Fig. 1a. The optimal solution satisfying the Prager-Shield condition (2) is shown in Fig. 1b. For this particular problem, the generalised strain is the curvature $\kappa = -u''$ where u is the beam deflection, primes denote derivation with respect to the distance along the beam axis and the generalised stress is the bending moment M. Thus the Prager-Shield condition (2) furnishes

$$\kappa = k \text{ (for } M > 0), \quad \kappa = -k \text{ (for } M < 0),$$

$$|\kappa| \leq k \text{ (for } M = 0). \tag{4}$$

In the beam EF, $M > 0$ and hence the optimality criterion (4) for this beam yields $\kappa = k$. From Fig. 1b, $-u'' = \kappa = k$ and hence this condition is satisfied. Moreover, in the beam GH $M \equiv 0$ and for the same beam $-u'' = \kappa = k\cos^2\alpha < k$ (for $0 < \alpha < \pi/2$) which satisfies the condition (4). Hence optimality is established. In this subproblem, the only compatibility requirement is equal beam deflections at the point P.

(b) Structural universe consisting of all beams whose centroidal axis contain the point P. For this extended problem, the proof under Section (a) is still valid, but α can take on any arbitrary value within the range $(0 < \alpha < \pi/2)$. The corresponding displacement field u is therefore defined for the entire domain ABCD in which for $0 < \alpha < \pi/2$ $\kappa = -u'' < k$ and hence the only optimal beam direction is EF with $\alpha = 0$.

(c) Structural universe consisting of any beam system over the domain ABCD. One feasible but obviously non-optimal beam system is shown in Fig. 1d. For this problem, the optimal displacement field is

$$\text{(on D)}, \quad u = k(L^2/8 - x^2/2) \tag{5}$$

which is independent of the coordinate y. This means that for any beam running at right angles to the supports, $\kappa = -u'' = k$ and hence from a kinematic point of view all such beams could consitute an optimal system. However, the Prager-Shield condition (2) requires also static admissibility and hence only the beam EF can form part of an optimal beam layout. For beams with $\alpha \neq 0$, the curvature $\kappa < k$ and hence by Eq. (4) M must be zero.

3.2 Prager-Structure for Two Point Loads in between Two Supporting Lines.

In this problem, two vertical point loads $P_1 = P_2$ whose elevation can be chosen arbitrarily, are to be transmitted to two horizontal supporting lines (double lines in Fig. 2a). Moreover, the structural universe shall consist of all possible centroidal axes contained in three vertical planes (AB, CD and EF in Fig. 2a). In Prager-structures, all members are required to be in compression and the specific cost function representing the weight per unit length of a member is $\psi = kF$ where F is the member force (with $F > 0$) and k is a given constant. The specific cost function and the corresponding strain furnished by the Prager-Shield condition is shown in Fig. 2b, the latter being equivalent to the following conditions:

$$\varepsilon = k \text{ (for } F > 0), \quad -\infty < \varepsilon < k \text{ (for } F = 0), \tag{6}$$

where ε is the axial strain in a member. The fact that the elevation of the point loads can be freely chosen is equivalent to having costless (weightless) ties along the vertical lines at P_1 and P_2. For these lines therefore $\psi = 0$ and hence (2) implies $\varepsilon = 0$. It follows that the optimal layout is furnished by a strain field in which along and in the direction of members of non-zero cross-section the strain is $\varepsilon = k$ and at all other points and in all other directions contained in the vertical planes AB, CD and EF,

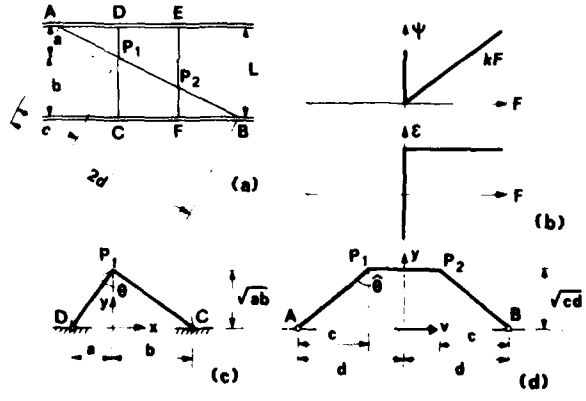


Fig. 2. Second example: a Prager structure.

the strain must be $-\infty \leq \varepsilon \leq k$. In addition, the displacements must be zero at the supporting points A, B, C, D, E and F and the strain along the lines of application of the point loads must be zero. It will be shown subsequently that the optimal solution may take two different forms: for $\sqrt{ab} < \sqrt{cd}$, the optimal elevation of the point loads is $h = \sqrt{ab}$ (Fig. 2a) and the optimal frame consists of two members in both planes CD and EF (Fig. 2c); for $\sqrt{ab} > \sqrt{cd}$, the optimal elevation of the point loads is $h = \sqrt{cd}$ and the optimal frame consists of three members in the plane AB (Fig. 2d.). Moreover, it shall be demonstrated that the total *weight of the system is always*

$$\Phi = 2(P_1 + P_2)kh. \tag{7}$$

The displacement fields (u_x, u_y) and (u_v, u_y) associated with the optimal solution are the following:

Planes CDP_1 and EFP_2 (Fig. 2c).

$$(\text{for } x \leq 0) \quad u_x = k_1(a+x)(b-a)/a, \quad u_y = -2k_1(a+x)\sqrt{b/a}, \tag{8}$$

$$(\text{for } x \geq 0) \quad u_x = k_1(x-b)(a-b)/b, \quad u_y = 2k_1(x-b)\sqrt{a/b}. \tag{9}$$

Plane ABP_1P_2 (Fig. 2d).

$$[\text{for } |v| \leq (d-c)] \quad u_v = -k_2|v|, \; u_y = -2k_2\sqrt{cd} \tag{10}$$

$$[\text{for } |v| \geq (d-c)] \quad u_v = k_2(d-c)(|v|-d)\operatorname{sgn} v/c, \quad u_y = 2k_2(|v|-d)\sqrt{d/c}, \tag{11}$$

$$\text{with } k_2\sqrt{cd} = k_1\sqrt{ab}, \tag{12}$$

$$\text{and } k_1 = k \; (\text{for } \sqrt{cd} \geq \sqrt{ab}), \quad k_2 = k \; (\text{for } \sqrt{cd} \leq \sqrt{ab}). \tag{13}$$

Then considering the plane CDP_1 with $x \leq 0$ for example, the usual expressions for strains, $\varepsilon_x = \partial u_x/\partial x$, $\varepsilon_y = \partial u_y/\partial y$, $\gamma_{xy} = \partial u_x/\partial y + \partial u_y/\partial x$, $\varepsilon_{1,2} = (\varepsilon_x + \varepsilon_y)/2 \pm \{[(\varepsilon_x - \varepsilon_y)/2]^2 + (\gamma_{xy}/2)^2\}^{1/2}$, $\theta = \gamma_{xy}/2(\varepsilon_y - \varepsilon_2)$ furnish $\varepsilon_x = k_1(a-b)/a$, $\varepsilon_y = 0$, $\gamma_{xy} = -2k_1\sqrt{b/a}$,

$$\varepsilon_1 = k_1, \; \varepsilon_2 = -bk_1/a, \; \tan\theta = \sqrt{a/b}. \tag{14}$$

This, together with (13) implies that for the case of $\sqrt{cd} \geq \sqrt{ab}$ the principal strain ε_1 along the member DP_1 in Fig. 2c takes on a value $\varepsilon_1 = k$ and the strain in all other directions satisfies the requirement $-\infty \leq \varepsilon \leq k$ in (6). Similarly, it can be shown readily that along the member CP_1 in Fig. 2c the principal strain ε_1 takes on the value k and the strain in all other directions has a smaller value. In addition, the strain fields in (8) and (9) furnish compatible and constant vertical and horizontal displacements along their common boundary (vertical line through P_1):

$$\Delta_v = 2k\sqrt{ab}, \quad \Delta_h = k(b-a). \tag{15}$$

The above strain fields therefore satisfy all kinematic optimality conditions stated previously. Since for $\sqrt{cd} > \sqrt{ab}$ the members in the plane ABP_1P_2 (Fig. 2d) take on a zero cross-sectional area, it is still necessary to show that $-\infty \leq \varepsilon \leq k$ throughout that plane. The general strain formulae quoted above together with (10) and (11) imply that along P_1P_2, AP_1 and BP_2 in Fig. 2d the principal strain has the value $\varepsilon_1 = k_2$ and in all other directions in all three strain fields in Fig. 2d the relation $-\infty < \varepsilon < k_2$ is satisfied. Moreover, along the vertical lines passing through P_1 and P_2 the displacements are constant and compatible:

$$\Delta_v = 2k_2\sqrt{cd}, \quad \Delta_h = \pm (d-c)k_2. \tag{16}$$

In addition, the inequality $\sqrt{cd} < \sqrt{ab}$, together with (12) and (13) imply $k_2 < k_1 = k$ for this case and hence the strains throughout the plane ABP_1P_2 fulfill the condition $-\infty \leq \varepsilon \leq k$. Compatability of the vertical displacements along intersections of the considered planes is ensured by (12), (15) and (16).

It can be shown similarly that in the case $\sqrt{cd} \leq \sqrt{ab}$ Eqns. (8) - (13) furnish a maximal strain of $\varepsilon = k$ along the polygon AP_1P_2B in Fig. 2d and the condition $-\infty \leq \varepsilon \leq k$ is fulfilled along all non-optimal (vanishing) members of the considered planes.

Note: The horizontal deflections in (15) and (16) introduce displacement components normal to the planes forming the structural universe in this problem. This indicates that larger principal strains than $\varepsilon = k$ may occur in directions outside the considered planes, if the strain fields along these planes were extended to a three-dimensional strain field. However, the kinematic conditions in (6) are only required to be satisfied along potential members of the structural universe and hence the above proof is sufficient in establishing the optimality of the proposed layout. The following argument may also be used for showing that only in-plane strains need to be considered in the current problems.

An additional feature of the Prager-Shield condition implies [5] for the considered class of problems that the sum of the products of the external loads and the corresponding optimal displacements furnishes the total structural weight of the system. The considered problem may, therefore, be split into two subproblems. In one of these, it is assumed that the two point loads P_1 and P_2 are carried fully by members in the planes CP_1D and EP_2F and then the layout along these planes is optimized. In the second subproblem, the entire external load is carried by the optimized layout in the plane AP_1P_2B. In both problems the optimal weight is given by the sum mentioned above. Hence (15) and (16) with $k_2 = k$ furnish the following optimal weights for the two subproblems:

$$\Phi_1 = 2k(P_1 + P_2)\sqrt{ab}, \; \Phi_2 = 2k(P_1 + P_2)\sqrt{cd}. \tag{17}$$

Both weight functions being linear with respect to the external load $(P_1 + P_2)$, in the optimal solution either the entire load is carried by members in the planes CP_1D and EP_2F (if $\sqrt{ab} < \sqrt{cd}$) or the entire load is carried by members in the plane AP_1P_2B (if $\sqrt{ab} > \sqrt{cd}$). If $\sqrt{ab} = \sqrt{cd}$ then an infinite number of optimal solutions exist in which the load can be distributed arbitrarily between the two systems. In this latter case, $k_1 = k_2 = k$ and $\varepsilon = k$ along each of the polygons CP_1D, EP_2F and AP_1P_2B, thus satisfying the requirements of (6). It is obvious from this alternative formulation that in the current problem only in-plane strains along the structural universe need to be considered.

4. Applications: Various Classes of Layout Problems

4.1 Least Weight Trusses or Michell Frames.

This class of optimal layouts was pioneered around the turn of the century by an Australian scientist, A.G.M. Michell [10]. The specific cost function in the considered class of problems is

$$\psi = k|N|, \tag{18}$$

where ψ is the member weight per unit length, N is the member force and k is a given constant. Then (2) furnishes the following optimality criteria:

$$\varepsilon = k \; (\text{for } N > 0), \quad \varepsilon = -k \; (\text{for } N < 0), \quad |\varepsilon| \leq k \; (\text{for } N = 0). \tag{19}$$

Considering now a structural universe consisting of members running in all possible directions at all interior points of the domain, the maximum and minimum strain at any loaded point (with a member in at least one direction) is k and -k, respectively. Since such directional extremum of the strain is known to correspond to principal directions, Michell frames consist of the following type of regions:

$$\begin{aligned}
&R^+: \varepsilon_1 = k,\ |\varepsilon_2| < k, && N_1 > 0,\ N_2 = 0\\
&R^-: \varepsilon_1 = -k,\ |\varepsilon_2| < k, && N_1 < 0,\ N_2 = 0\\
&S^+: \varepsilon_1 = \varepsilon_2 = k, && N_1 > 0,\ N_2 > 0\\
&S^-: \varepsilon_1 = \varepsilon_2 = -k, && N_1 < 0,\ N_2 < 0\\
&T: \varepsilon_1 = -\varepsilon_2 = k, && N_1 > 0,\ N_2 < 0
\end{aligned} \qquad (20)$$

where the subscripts "1" and "2" denote principal strains or forces.

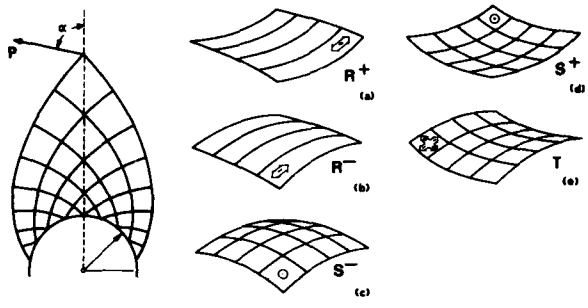


Fig. 3. A Michell Frame.

Fig. 4. Optimal regions for grillages.

In spite of a prolonged international research effort, Michell layouts have only been determined for a few simple loading conditions, most of which are summarised in a perspicuous review by Hemp [11]. In contrast to Prager-structures, the Michell layout is not even known for a simple vertical point load of asymmetric location and two point supports. Hemp [12] has attempted a solution for uniformly distributed load in between two point supports, but his associate Chan [13] has shown that the considered solution is only valid for a certain range of non-uniformly distributed load. More recently, the author and Hill [14] have found that certain superposition principles enable us to derive the optimal Michell layout for four alternate load conditions. The geometrical properties of Michell frames and optimal grillages have been compared by Prager and the author [1]. A Michell frame consisting of a single T-region [cf. Eqn (20)] is shown in Fig. 3, in which $\alpha > \pi/4$.

4.2 Least Weight Beam Systems or Grillages.

The specific cost function for this class of problems is

$$\psi = \kappa|M|, \qquad (21)$$

where ψ is the beam weight per unit length, M is the bending moment and k is a given constant. The theory of optimal beam layout has been explored by the author and his associates [3, 5, 15, 16] and later discussed extensively by Prager and the author [1, 2, 17]. The progress in this field is summarised most appropriately by Prager himself in the following passage [17]: "Although the literature on Michell trusses is quite extensive, the mathematically similar theory of grillages of least weight was only developed during the last decade. Despite its late start, this theory has advanced farther than that of optimal trusses. In fact, grillages of least weight constitute the first class of plane structural systems for which the problem of optimal layout can be solved for almost all loadings and boundary conditions."

Since in both Michell frames and optimal beam layouts the solution often consists of an infinity of densely spaced members, Prager [2] has termed these systems "truss-like continua" and "grillage-like continua". It has been shown [5, 16, 18] that the same grillage layout is optimal in plastic limit design and in elastic design for given permissible stress, or given compliance or given fundamental frequency. For grillages (2) and (21) furnish the following optimality criteria:

$$\kappa = k \text{ (for } M > 0),\ \kappa = -k \text{ (for } M < 0),\ |\kappa| \le k \text{ (for } M = 0). \qquad (22)$$

where $\kappa = -u''$ is the beam curvature, u is the beam deflection and primes denote differentiation with respect to the distance along the beam axis.

Using a structural universe consisting of beams running in all directions at all interior points of the domain, (22) yields the following optimal regions:

$$\begin{aligned}
&R^+: \kappa_1 = k.\ |\kappa_2| < k, && M_1 > 0,\ M_2 = 0\\
&R^-: \kappa_1 = -k,\ |\kappa_2| < k, && M_1 < 0,\ M_2 = 0\\
&S^+: \kappa_1 = \kappa_2 = k, && M_1 > 0,\ M_2 > 0\\
&S^-: \kappa_1 = \kappa_2 = -k, && M_1 < 0,\ M_2 < 0\\
&T: \kappa_1 = -\kappa_2 = k, && M_1 > 0,\ M_2 < 0
\end{aligned} \qquad (23)$$

where the direction and sign of principal curvatures having the absolute value k must match the direction and sign of the corresponding principal moments. The above regions are shown graphically in Fig. 4.

It will be seen that the proposed layout theory has converted a rather complicated layout problem into a simple geometrical problem. In the latter, the structural domain D must be covered with the type of regions given in (23) and Fig. 4 such that along region boundaries the deflection and slope are matched and along simple supports the deflection is zero, whilst along clamped edges the deflection and slope are zero.

Since the present state of the theory of optimal grillage layouts was reviewed at a NATO ASI last year [3], it is sufficient to mention here that the approach described herein enables us to derive analytically by a direct and systematic procedure the optimal

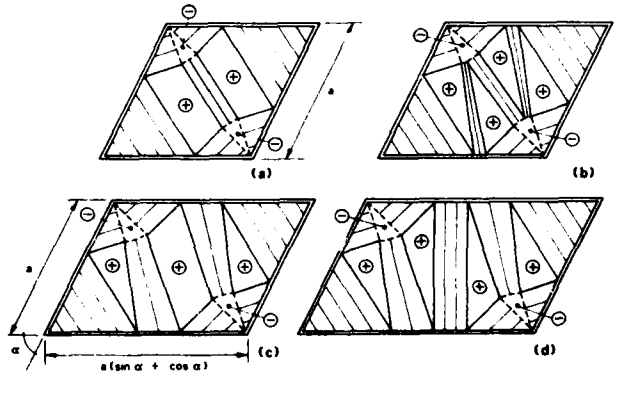


Fig. 5. Some optimal simply supported grillages.

beam layout for all loading conditions and any boundary segments consisting of straight lines or quadratic curves. More recently, a computer algorithm was developed for determining analytically and plotting optimal beam layouts [19]. Examples of optimal beam layouts are given in Fig. 5.

4.3 Optimal Archgrids and Cable Networks or Prager-Structures.

The optimal design of long-span archgrids (and shellgrids) was first investigated by the author and Prager under a government-sponsored research contract in Stuttgart, West Germany in 1978 [20]. In the original project, the directions of the arches were prescribed and only the middle surface of the archgrid was optimized. Because in the case of long-span roof structures the selfweight is a significant load component, the above project was later extended by H. Nakamura and the author to allow for this load component [21]. However, Prager's original intention was to optimize also the layout of the members within the archgrid. Prager repeatedly stressed that there must be some similarity between the optimal layout of archgrids and that of grillages. Unfortunately, his untimely death prevented Prager from completing this joint project with the author. Owing to his contributions to this field, archgrids and cable networks of optimal layout shall be termed Prager-structures. More recently, the author and Wang [22] made significant advances in constructing this particular class of optimal layouts. At present Prager-structures are already available for a much wider range of loadings and boundary conditions than Michell frames.

Prager-structures differ from Michell frames in two respects. Firstly, all members must be in compression (archgrids) or all members must be in tension (cable networks) in Prager structures, whereas the sign of member forces is not constrained in Michell frames. Secondly, only the (usually vertical) line of application of the external forces is prescribed for Prager structures, while the point of application of all loads is also specified for Michell frames. This means, that for Prager structures we consider a system of (usually vertical) forces, whose vertical position (elevation) can be arbitrarily adopted. These forces are to be transmitted by continuously variable members (which are throughout in pure compression or throughout in pure tension) to the supports. The latter usually form the boundary B of a domain D contained by a horizontal plane termed foundation plane N. The specific cost function for Prager-structures is $\psi = kF$ (with $F \gtrless 0$) where F is the member force and k is a given constant. There is also a significant difference between the appearance of a Michell frame and a Prager-structure. For plane domains, a Michell frame usually consists of a system of densely spaced members covering large areas of the domain, whereas a Prager-structure consists of a single curve or polygon. For three-dimensional domains and distributed loads, Michell frames presumably consist of space-frame-like continua (although the actual optimal layout of such frames is not known); Prager-structures, on the other hand, have a single middle surface which contains the centroidal axes of all arches or cables. Two features of Prager-structures make them more practical for many design problems than Michell frames. First, they are surface structures of small structural depth and hence they are suitable for covering large areas. Secondly, the vertical location of the load is determined by the optimal shape of the middle surface which is a realistic assumption for long span roof structures. At this stage, Prager-structures are designed for a stress criterion only. At a later stage, allowance will have to be made for buckling of archgrids and dynamic behaviour (flutter) of cable networks.

4.3a. General Theory of Plane Prager-Structures for a Vertical Loading Consider a finite number of vertical point loads in between two point supports. Since in a Prager-structure all members must be in pure compression (or all members must be in pure tension), the centroidal axes of the system must form a funicular polygon, i.e. it must satisfy the equilibrium conditions at each joint in between two straight segments. However, equilibrium still admits an infinite number of solutions, each of which correspond to a different value of the horizontal reaction H (Fig. 6a). It was explained in Example 3.2 (Fig. 2b) that the strain field in the current problem must fulfill conditions (6), that is, the strain must take on a value of $\varepsilon_1 = k$ along all optimal members and it must be equal or less than k along all members of vanishing cross-section. In addition, the strain must take on a zero value along lines of the vertical loads. Considering the shaded segment in between two point loads in Fig. 6a, let the optimal angle between the member centroidal axis and the vertical be θ_i. Then the optimal strain field shall be shown to consist of the following components

$$\varepsilon_y = 0,\ \varepsilon_x = k(1-\cot^2\theta_i),\ \gamma_{xy} = 2k\cot\theta_i, \tag{24}$$

furnishing

$$\varepsilon_1 = k,\ \varepsilon_2 = -k\cot^2\theta_i, \tag{25}$$

where the inclination of ε_1 with respect to the vertical is θ_i. The above strains give the following relative horizontal and vertical displacements between the two sides of the shaded segment:

$$\Delta_v = 2kL_i\cot\theta_i = 2kh_i,\ \Delta_h = kL_i(1-\cot^2\theta_i). \tag{26}$$

The first equation under (26) obviously results in kinematic admissibility because in Fig. 6a $\Sigma h_i = 0$ if we take the sign of the elevation differences h_i into consideration. The second relation under (26) furnishes

$$\Sigma L_i = \Sigma(L_i\cot^2\theta_i), \tag{27}$$

which implies

$$\int_0^L (dy/dx)^2\,dx/L = 1, \tag{28}$$

where L is the total span between supports and y(x) is the function describing the centroidal axis of the Prager-structure. Relation (28) implies that the mean square slope of the solution must be unity, which condition has already been derived by variational methods earlier [21, 23]. The unit mean square slope condition is still valid if a plane Prager-structure is subject to a distributed load in which case the spacing of loads in Fig. 6a tends to zero ($L_i \to 0$).

4.3b. Prager-structures for Axially Symmetric Vertical Loading and Axially Symmetric Supports. The above conclusions can be readily extended to any axially symmetric system in which the supports and line loads (Q_i) form concentric circles and the intensity of the distributed load q(r) depends on the radial coordinate (r) only (Fig. 6b). For such a system, the optimal displacement field can be constructed by first taking a symmetric version of the strain field in Fig. 6a and Eq. (24) and then generating an axially symmetric equivalent of the same field by rotating it around the axis of symmetry. The actual Prager-structure can be obtained by the following procedure.

(a) Consider a set of simply supported beams having the same span as the radial distance between supports and having the loads formed by the product of the loads on the Prager-structure and their distance from the axis of symmetry, that is $Q_i \cdot r_i$ for line loads and $r \cdot q(r)$ for distributed loads (Fig. 6c).

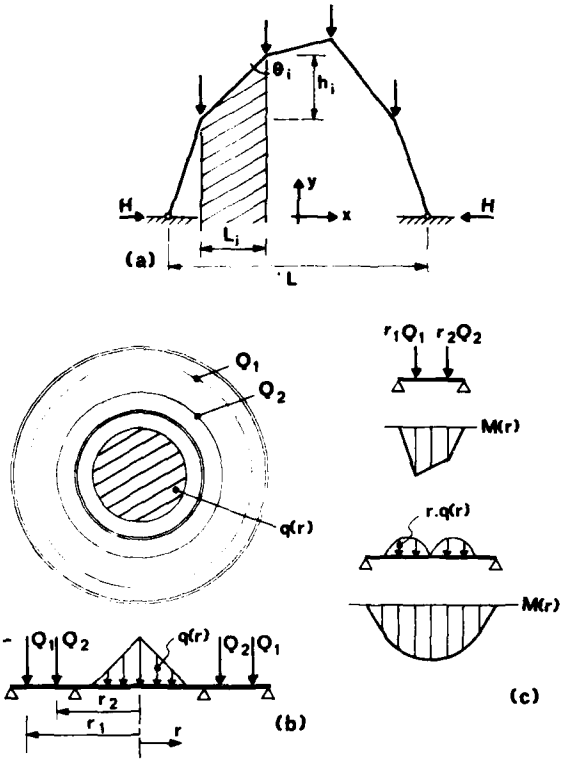


Fig. 6. Plane and axisymmetric Prager structures.

(b) Determine the bending moment diagram M(r) for each equivalent beam.

(c) The optimal elevation of the Prager-structure at any distance (r) from the axis of symmetry is given by $k_j \cdot M(r)$ where k_j is a constant for each span (j) and the curve $k_j \cdot M(r)$ must satisfy the unit mean square slope condition in (28).

4.3c. Prager-Structures for a Quasi-Axisymmetric Loading. The axially symmetric strain fields described in the last section can also be used for establishing the optimality of Prager-structures with axisymmetric supports and point loads located along concentric circles. An example of such a Prager-structure is shown in Fig. 7a in which the magnitude of the point loads is constrained by the relation $P_2 = 2P_1 \cos\alpha$ and $P_4 = 2P_3 \cos\alpha$ with a view to maintaining equilibrium of the three radial member forces at the centre (see also the force diagram in Fig. 7b). Fig. 7c shows a side view (RR) of one "leg" of this structure which must satisfy equilibrium and the unit mean square slope condition (28). Inside the circle containing the loads P_1 and P_2 in Fig. 7a, the strain is $\varepsilon = k$ in all horizontal directions and hence any arbitrary statically admissible system in compression represents an equally optimal layout. In Figs. 7d and 7e, examples of such alternative optimal solutions are given.

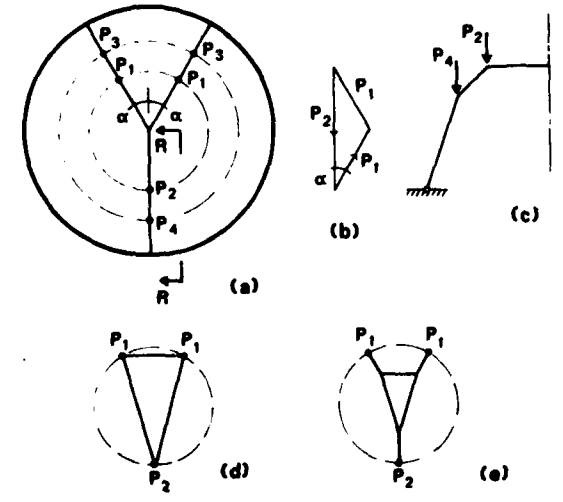


Fig. 7. Prager-structure for quasi-axisymmetric load.

4.3d. Prager-Structures for an Eccentric Point Load and a Circular Support. This problem shall be used later for constructing Prager-structures for a single point load and any arbitrary boundary condition. In Fig. 8a an eccentrically located point load is to be transmitted to a circular support by a Prager-structure whose universe fulfills the following restriction: the centroidal axes of all members are to be contained by vertical planes passing through the point P. Some such planes are indicated in plan view in Fig. 8a (AB, CD and EF). It shall be shown subsequently that the optimal elevation of the point load is

$$h = \sqrt{R^2 - d^2}, \qquad (29)$$

where R is the radius of the circular support and d is the eccentricity of the point load P. This means that the optimal elevation of the point load in this problem is always given by a hemisphere whose base is the circular support. Moreover, it shall be established that an infinite number of structures have the same minimum weight. The set of optimal solutions shall be shown to consist of all layouts in which members connect the point P with the circular support, provided that all such members are in compression (or all members are in tension, if the vertical point load is acting upwards).

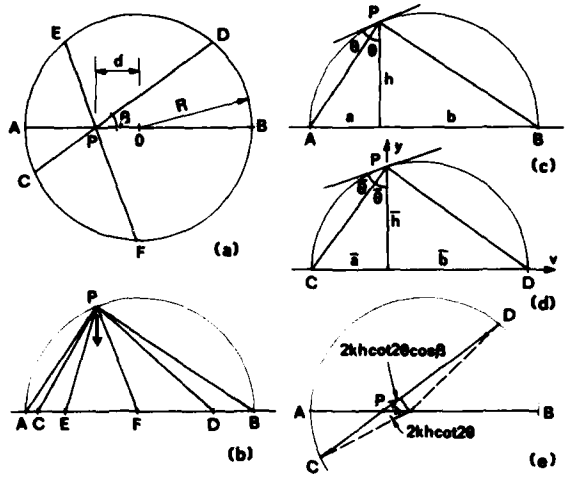


Fig. 8. Prager-structure for an eccentric point load.

Proof. In each vertical plane containing the point P, we shall use the type of strain field given in Fig. 2c and Eqns. (8), (9) and (14). For an arbitrary plane (e.g. CPD in Fig. 8a) through the point P, the angle $\bar{\theta}$ between the direction of the principal strain ε and the vertical (Fig. 8d) can be expressed in terms of such angle θ for the steepest member (AP in Figs. 8a and 8c) and the orientation β of the general plane CD:

$$\cot 2\bar{\theta} = \cot 2\theta / \sqrt{1 + \tan^2\beta} = \cot 2\theta \cos\beta \qquad (30)$$

The strain field in Eq. (14) and Fig. 8d, in which now k_1, a, b and θ are replaced by k, $\bar{a}$, $\bar{b}$ and $\bar{\theta}$, can also be expressed in terms of $h = (\bar{a}\,\bar{b})^{1/2}$ and $\bar{\theta}$ in the following form

$$\varepsilon_y = 0,\ \varepsilon_x = (1-\cot^2\bar{\theta})k,\quad \gamma_{xy} = -2k\cot\bar{\theta},$$

$$\varepsilon_1 = k,\quad \varepsilon_2 = -k\cot^2\bar{\theta}. \tag{31}$$

Then for arbitrary plane CPD the displacements along the vertical line through P (Fig. 8) given originally in Eqs (15) become

$$\bar{\Delta}_v = 2kh,\quad \bar{\Delta}_h = 2kh\cot(2\bar{\theta}). \tag{32}$$

For the particular plane APB with $\beta = 0$, the symbol $\bar{\theta}$ in Eqs. (31) and (32) is replaced by θ. Combining Eqns. (30) and (32), we can expresss $\bar{\Delta}_h$ in terms of θ:

$$\bar{\Delta}_h = 2k\,h\cot(2\theta)\cos\beta. \tag{33}$$

The vertical displacement $\bar{\Delta}_v$ in (32) represents the displacement at the intersection of the considered vertical planes. It is independent of the orientation β and hence satisfies compatibility. Moreover, it can be seen from Fig. 8e that the horizontal displacements of all vertical planes are also compatible, if these planes are permitted to deform in a normal direction (broken line in Fig. 8e). Hence, for the structural universe considered, the requirements of the Prager-Shield condition [Eq. (2)] are completely satisfied and thus optimality of all layouts consisting of straight compression members connecting the point P and the supporting circle is established.

Important Note. The present proof is restricted to a structural universe in which all members are contained in vertical planes passing through the point P, because the normal deformations (broken lines in Fig. 8e) would result in out-of-plane principal strains whose direction does not coincide with that of the assumed optimal members. However, we cannot rule out the possibility that the layout in Figs. 8a and 8b remains optimal when the structural universe consists of all possible member directions at all points. In fact, it seems unlikely that within the constraint of non-negativity of the member forces, a better layout can be found.

4.3e. Prager-Structures for a Point Load and Any Support Condition. It was concluded in the last section that all straight compressive members connecting the loaded point P and a circular support are equally optimal if such a point is contained in a hemisphere whose base is the circular support. It can also be shown easily [22] that the structural weight becomes greater than that of the above solution if some of the load is transmitted to a point outside the considered circular support.

On the basis of the foregoing considerations, we can construct the Prager-structure for a point load and any arbitrary supporting line forming the boundary B or the domain D in the foundation plane N. The optimal elevation h of the loaded point P is always given by Eq. (29) and the members of the Prager-stucture connect this point with the intersections of a circle and the boundary B of a domain D provided that (a) such circle is contained entirely in the domain D and (b) the projection of the point P on the foundation plane is a convex combination of the considered intersections. In Fig. 9a for example, the associated circle furnishes two supporting points (A and B) for the loaded point P_1 and for the point P_2 we have three supporting points (C, E and F). Moreover, for any loaded point within the triangle CEF the Prager-structure consists of three members and for any point of D outside the triangle CEF it contains two members. Regions of a domain D in which a point load is associated with Prager-structures having two and more than two members, respectively, shall be termed R and S regions. It follows from extensions of the Prager-Shield theory [5] and Eq. (7) herein that the weight influence surface (or surface furnishing the optimal elevation of the point load) for the considered Prager-structures consists of a series of circular arcs in vertical planes connecting the two supporting points in R regions, and of hemispherical surfaces (whose base is the inscribed circle) in S regions.

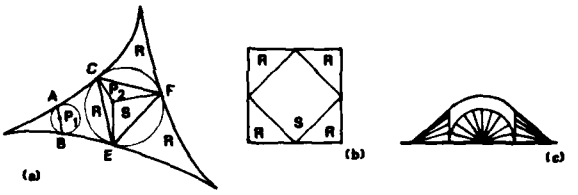


Fig. 9. Prager-structures for noncircular boundaries.

The optimal regions of a Prager-structure for a square domain with a single point load are given in Fig. 9b and the corresponding influence surface in Fig. 9c. The latter consists of cones in the R regions and a spherical surface in the S regions such that slope continuity is satisfied at the region boundaries.

The optimal regions and weight influence surfaces in Fig. 9b and 9c are similar to those for an optimal square simply supported grillage (see Fig. 6.15a on p. 194 in [5]). The only difference is that along lines of optimal force transmission the first order curvature $u'' = \partial^2 u/\partial x^2$ must be constant for grillages and the exact curvature $u''/(1 + u'^2)^{3/2}$ for Prager-structures. It is rather remarkable that the late Professor Prager anticipated this similarity without finding the actual connection between the two theories.

4.4 Optimal Layout of Membrane Shells

In this class of layout problems the specific cost ψ is the shell thickness which depends on the value of the two principal membrane forces F_1, F_2. For shells obeying the Tresca yield condition, for example, the specific cost function becomes

$$\psi = k(|F_1| + |F_2| + |F_1 - F_2|), \tag{34}$$

where k is a known constant. A typical cost contour [representing a constant value of ψ in Eq. (34)] is shown in Fig. 10a and the corresponding cost gradient in Fig. 10b. Assuming that the structural universe consists of shell middle surfaces in all possible directions at all interior points of the domain D, the Prager-Shield condition stipulates that along any middle surface with a non-zero shell thickness, (i) the principal strains (ε_1, ε_2) must have the same directions as the principal forces (F_1, F_2) and (ii) (ε_1, ε_2) must equal the generalised gradient of ψ with respect to the actual values of (F_1, F_2). This means that for a stress point A in Fig. 10a, for example, the admissible strains are furnished by the

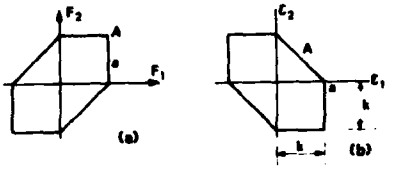


Fig. 10. Cost contour and gradient for membrane shells.

line segment A in Fig. 10b, and for the line segment "a" in Fig. 10a the strains are given by the point "a" in Fig. 10b. Moreover, along any shell of vanishing thickness the principal strains must represent a point on or inside the hexagon in Fig. 10b. The above layout problem would then, in general, furnish a cellular (or "honeycomb") type continuum consisting of an infinity of densely spaced, intersecting shells in several directions.

If for practical reasons we want to restrict the solution to a single surface structure then, as in the case of Prager-structures, we may leave the vertical location of the loads unspecified and/or restrict the principal forces to compression (or tension) throughout the system.

A shell of uniform strength in a broader sense (or "Ziegler-shell"), as defined by Ziegler [24] and Issler [25], fulfills the condition that the principal membrane forces at any point of the middle surface must represent a point on the yield surface. Issler [25] has shown that for a given shape of the middle surface and for a given loading, at most two thickness distributions corresponding to two different segments of the yield surface, satisfy the above requirement. In a shell of uniform strength in the narrower sense (or "Milankovic"-shell), as introduced by Milankovic [26] at the turn of the century, the two prinicpal membrane forces must have the same value ($F_1 \equiv F_2$) at all points of the middle surface. Issler [25] has also demonstrated that this latter condition determines both the thickness variation and the shape of the middle surface for a given load. Examples of such shells are Milankovic's [26] and Dökmeci's [27] solutions for selfweight and snow-load respectively. Prager, the author, Nakamura and Dow [28, 29] have determined the fully stressed thickness variation and the optimal radius of spherical Tresca-shells for a variety of load combinations which all included selfweight. More recently [30], Dow, Nakamura and the author determined the optimal shape of axially symmetric Tresca shells for various load conditions and found that a Ziegler shell of optimized shape turns out to be a Milankovic shell.

4.5 Allowance for Selfweight.

It was shown by the author [31] that a simple modification of the Prager-Shield condition automatically takes care of selfweight when it is modified in the following way:

$$\underline{q}^k = (1+u)\, \underline{G}\, [\psi(\underline{Q})^s]. \qquad (35)$$

Application of Eq. (35) to Prager-structures furnishes, for example, the following modified unit mean square slope condition [c.f. Eq. (28)]:

$$\int_o^L e^{2cy}(dy/dx)^2\, dx \Big/ \int_o^L e^{2cy}\, dx = 1, \qquad (36)$$

where c is γ/σ_o, γ is the specific weight of the material and σ_o is the permissible (or yield) stress.

With the help of Eq. (36) all plane or axially symmetric Prager-structures can be determined readily for an external load plus selfweight.

4.6 Optimal Layout of Frames subject to Combined Bending and Axial Forces.

This problem has been discussed by the author, Wang and Dow [32] considering a single load and two alternate load conditions.

4.7 Optimal Design of Solid Plates.

In investigating the optimal thickness variation of an elastic plate with a maximum thickness constraint by a finite element method, Cheng and Olhoff [33] have discovered that the optimal solution contains rib-like formations of maximum feasible depth when a large number of finite elements is used. Prager has pointed out in a private communication that the layout of such ribs appears to be similar to the optimal grillage layout [15] for the same boundary conditions. Subsequently, the author, Olhoff, Cheng and Taylor [34] have shown that a large number of existing papers on solid plate optimization, based on "smooth" solutions, are in fact erroneous because the global minimum weight solution contains in some regions an infinity of densely spaced stiffeners. The optimal configuration of these stiffeners has been determined for a circular plate [34] and is being investigated for other boundary conditions, using the layout theory described i this paper.

5. Conclusions

It has been demonstrated that the concepts of static-kinematic optimality criteria and basic structure (or structural universe) enable us to determine the optimal layout for various broad classes of design problems. The proposed theory converts in effect an extremum problem into a problem of analysis which becomes essentially a geometrical task. This paper has not covered layout optimization based on repeated redesign and mathematical programming methods because they are dealt with in other papers at this symposium.

A new class of layout problems, viz. Prager-structures (or archgrids and cable networks of optimized member layout) was discussed in detail. In these problems, all members are required to be in compression (or all members are to be in tension) and vertical loads of unspecified elevation are to be transmitted to the boundary of a horizontal domain so that the total structural weight takes on a minimum value. Prager-structures were derived for a wide range of loading and boundary conditions and the surprising conclusion was reached that the optimal weight is always proportional to the sum of the products of the loads and their optimal elevation.

6. References

[1] Prager, W. and Rozvany, G.I.N., "Optimization of Structural Geometry, Proc. Conf. Dynamical Systems, Univ. Florida 1976, Academic Press, New York, 1977, pp. 265-294.

[2] Prager, W., Introduction to Structural Optimization, Springer-Verlag, Vienna, 1974.

[3] Rozvany, G.I.N., "Optimality Criteria for Grids, Shells and Arches", Proc. NATO ASI on Optimzation of Distributed Parameter Structures, Iowa City 1980, pp. 113-152.

[4] Prager, W. and Shield, R.T., "A General Theory of Optimal Plastic Desing", J. Appl. Mech., Vol. 35, 1967, pp. 184-186.

[5] Rozvany, G.I.N., Optimal Design of Flexural Systems, Pergamon, Oxford, 1976; Russian Version: Stroiizdat, Moscow, 1980.

[6] Prager, W., Introduction to Plasticity, Addison-Wesley, Reading 1959.

[7] Rozvany, G.I.N., "Plastic versus Elastic Optimal Strength Design", J. Engng. Mech. Div. ASCE, Vol. 103, 1977, pp. 210-214.

[8] Rozvany, G.I.N., "Optimal Elastic Design for Strength Constraints". Computers and Struct., Vol. 8, 1978, pp. 455-463.

[9] Rozvany, G.I.N., "Variational Methods and Optimality Criteria", NATO ASI on Optimization of Distributed Parameter Structures, Iowa City, 1980, pp. 83-112.

[10] Michell, A.G.M., "The Limits of Economy of Material in Frame Structures", Phil. Mag., Vol. 8, 1904, pp. 589-597.

[11] Hemp, W.S., Optimum Structures, Clarendon, Oxford, 1973.

[12] Hemp, W.S., "Michell Framework for Uniform Load Between Fixed Supports", Eng. Opt., Vol. 1, 1974, pp. 61-69.

[13] Chan, H.S.Y., "Symmetric Plane Frameworks of Least Weight", Proc. IUTAM Symp. Optimization in Structural Design, Warsaw, 1973, Springer, Berlin, 1975, pp. 313-324.

[14] Rozvany, G.I.N. and Hill, R.D., "Optimal Plastic Design: Superposition Principles and Bounds on the Minimum Cost", Comp. Meth. Appl. Mech. Engrg., Vol. 13, 1978, pp. 151-174.

[15] Rozvany, G.I.N. and Adidam, S., "Rectangular Grillages of Least Weight", J. Eng. Mech. Div. ASCE., Vol. 98, 1972, pp. 1337-1352.

[16] Rozvany, G.I.N. and Hill, R.D., "General Theory of Optimal Load Transmission by Flexure", Advances in Appl. Mech., Vol. 16, 1976, pp. 183-308.

[17] Prager, W. and Rozvany, G.I.N., "Optimal Layout of Grillages", J. Struct. Mech., Vol. 5, 1977, pp. 1-18.

[18] Olhoff, N. and Rozvany, G.I.N., "Optimal Grillage Layout for Given Natural Frequency", J. Eng. Mech. Div. ASCE., submitted.

[19] Rozvany, G.I.N. and Hill, R.D., "A Computer Algorithm for Deriving Analytically and Plotting Structural Layout, Proc. NASA Symp.: Future Trends in Computerised Structural Design, Washington, 1978, Pergamon, Oxford, 1978, pp. 295-300; also Computers and Struct., Vol. 10, 1979, pp. 295-300.

[20] Rozvany, G.I.N. and Prager, W., "A New Class of Optimization Problems: Optimal Archgrids", Comp. Meth. Appl. Mech. Engg., Vol. 19, 1979, pp. 127-150.

[21] Rozvany, G.I.N., Nakamura, H. and Kuhnell, B.T., "Optimal Archgrids: Allowance for Selfweight:, Comp. Meth. Appl. Mech. Engg., Vol. 24, 1980, pp. 287-304.

[22] Rozvany, G.I.N., Wang, C.-M. and Dow, M., "Prager-Structures: Archgrids of Optimal Layouts". Comp. Meth. Appl. Mech. Eng., submitted.

[23] Hill, R.D., Rozvany, G.I.N., Wang, C.-M., and Leong, H.K., "Optimization, Spanning Capacity and Cost Sensitivity of Fully Stressed Arches", J. Struct. Mech., Vol. 7, 1979, pp. 375-410.

[24] Ziegler, H., "Kuppeln gleicher Festigkeit", Ing.-Arch., Vol. 26, 1958, pp. 378-382.

[25] Issler, W., "Membranschalen gleicher Festigkeit", Ing.-Arch., Vol. 33, 1964, pp. 330-345.

[26] Milankovic, M. Arbeiten der Jugoslaw Akad der Wissentsch., Agram 175, 1908, p. 140.

[27] Dökmeci, M.C., "A Shell of Constant Strength , ZAMP, Vol. 10, 1966, pp. 545-547.

[28] Prager, W. and Rozvany, G.I.N., "Optimal Spherical Cupola of Uniform Strength", Ing.-Arch., Vol. 49, 1980, pp. 287-294.

[29] Nakamura, H., Dow, M. and Rozvany, G.I.N., "Optimal Spherical Cupola of Uniform Strength - Allowance for Selfweight", Ing.-Arch., in press.

[30] Dow, M., Nakamura, H. and Rozvany, G.I.N., "Optimal Shape of Cupolas of Uniform Strength" to be submitted to Ing.-Arch.

[31] Rozvany, G.I.N., "Optimal Plastic Design: Allowance for Self Weight", J. Eng. Mech. Div. ASCE., Vol. 103, 1977, pp. 1165-1170.

[32] Rozvany, G.I.N., Wang, C.-M. and Dow, M., "Arch Optimization via Prager-Shield Criteria", J. Eng. Mech. Div. ASCE., Vol. 106, 1980, pp. 1279-1282.

[33] Cheng, K.-T. and Olhoff, N., "An Investigation Concerning Optimal Design of Solid Elastic Plates", Int. J. Solids Struct., Vol. 17, 1981, pp. 305-323.

[34] Rozvany, G.I.N., Olhoff, N., Cheng K.-T. and Taylor, J., "On the Solid Plate Paradox in Structural Optimization", DCAMM Rep. No. 212, 1981, J. Struct. Mech., in press.

AD-P000 050

AN OPTIMIZED CONFIGURATION OF AN ENCLOSURE STRUCTURE FOR SAFE CONTAINMENT OF INTERNAL BLASTS

Aaron D. Gupta
Mechanical Engineer

Henry L. Wisniewski
Mathematician
U.S. Army Ballistic Research Laboratory
Aberdeen Proving Ground, Maryland 21005

Abstract

Large deflection elastic-plastic response of a hemispherical containment shell configuration clamped to a horizontal rigid foundation and subjected to an internal blast was analyzed using a finite-difference structural response code PETROS 3 5. Optimization study was conducted based on a minimum amount of material required to elastically contain the first pressure pulse from a specified explosive charge subject to workspace constraints.

The reflected overpressure peak was estimated from a scaled distance of the wall from the point of detonation based on a conservative cube root scaling law and an exponential decay given by the modified Friedlander equation. The residual quasi-static overpressure was obtained from an equation developed by Kinney and Sewell based on the ratio of the available vent area and the internal volume.

Only a quarter segment of the structure was modelled using 18 equal width mesh in one layer and four Gaussian integration points through the thickness in each mesh. The 1020 steel was represented by three sublayers followed by a perfectly-plastic behavior and elastic-plastic unloading resulting in a polygonal approximation.

The results indicated the initiation of flexural waves at the boundary propagating towards the pole and converging thereby altering the spherically symmetric breathing mode of response of the centrally loaded hemisphere. The peak deflection predicted by the code occurred at the pole and permanent deflection was found to be quite small after releasing the load. Transient strain components at the inner and outer surfaces near the clamped edge due to largely elastic oscillations showed the effect of bending deformation superposed on the membrane components. In conclusion the protective structure was found to be efficient and cost effective and capable of blast containment with an adequate margin of safety.

Introduction

The Ballistic Research Laboratory is currently in the process of acquiring a target enclosure to facilitate destructive terminal ballistic testing of chemical explosives (CE), special armor (SA) and kinetic energy (KE) penetrators by safe containment of blast, fragments and resultant harmful combustion products. The present investigation is based on a preliminary concept of the firing range as shown in Figure 1. The target is located inside the hemispherical enclosure at the end of a long concrete pipe-guide. The gun-launched projectile travels through the pipe-guide and enters the enclosure through a .914 m diameter entrance hole. The target interaction with the projectile is monitored photographically with flash X-ray equipment and penetration velocity is obtained using velocity screens and electronic counters. An air exhaust system mounted at the rear of the structure operates during the test and draws back aerosolized material out of the enclosure after a test and traps it in filters in the exhaust ducting. A large sliding door with a configuration to match the curvature of the hemispherical wall allows equipment access inside the enclosure. The door is sealed to the wall with a pressurized hose seal along its perimeter. The entire structure is built to contain blast and fragments, to trap aerosolized materials and to permit photographic observation of the test.

A significant problem associated with the enclosed range tests is the overpressure resulting from shock loading as well as rapid heating of the air within the enclosure as the penetrator and the target are torn apart during their encounter as shown by R. Abrahams et al. [1]. The structure must survive both the reflected and the residual overpressures induced by the interaction until ambient conditions are reached due to venting out to the atmosphere through the exhaust system.

Since the key element of the AHKELS (Advanced High Kinetic Energy Launch System) range is the enclosure structure, the Target Loading and Response Branch was assigned to estimate the overpressure loading on the wall and analyze dynamic response of the preliminary configuration at critical locations and assure structural integrity from a conservative viewpoint. The choice of a hemispherical configuration was confirmed by an earlier investigation by N.J. Huffington et al. [2] who demonstrated the effectiveness of such a protective structure.

In the absence of any available experimental data it was decided to obtain a theoretical estimate of the transient and residual overpressure loading due to a centrally located equivalent charge weight at the base. The subsequent objective was to perform an approximate conservative static analysis for an initial estimate of wall thickness. Finally the dynamic elasto-plastic, large deflection response of the shell configuration clamped to a horizontal rigid foundation was studied to indicate critical locations where peak strains or deflections could occur.

Estimation of Transient Loads

The transient loads were estimated under the assumption that the test firing of penetrator rounds would generate overpressures inside the containment chamber similar to those caused by an internal blast due to an equivalent central charge weight of 29.03 kg at the base of the hemisphere. Assuming the walls to be rigid, the symmetry of the charge and the structure about a vertical axis through the center indicates uniform distribution of internal reflected loading upon the structure. For the estimation of peak reflected overpressure, a conservative cube-root scaling law [3] is employed to compute the scaled distance Z of the wall from the charge location in the form

$$Z = \frac{R}{W_E^{1/3}} \qquad (1)$$

where W_E is the equivalent charge weight and R is the distance of the wall from the charge location.

Once the scaled distance is known the reflected parameters such as peak overpressure, impulse, time of arrival and duration time of the shock loading could be estimated from compiled airblast tables [4,5]. The decay of reflected overpressure is assumed to obey the modified Friedlander exponential decay equation which can be written as

PRECEDING PAGE

$$P_r = P_m[1 - t/t_o]e^{-\alpha t/t_o} \quad (2)$$

where t_o is the positive phase duration of the impulse, P_s is the peak reflected overpressure and t is the elapsed time from impact or detonation. The exponential decay parameter α is given as

$$\alpha = .57\left(\frac{P_m + P_o}{P_o}\right)^{0.65} \quad (3)$$

where P_o is the peak quasi-static overpressure obtained from residual overpressure calculations.

Estimation of Quasi-static Loads

Quasi-static pressures immediately following the reflected pressure were predicted assuming that the heat of combustion of the TNT is used totally to heat the air within the enclosure [6]. A relationship for the resultant increase in pressure is

$$\Delta P = \frac{0.4\ hW_E}{V}, \text{ kPa}, \quad (4)$$

where

$V = 1513.9\ m^3$, the internal volume of the enclosure
$W_E = 29.03$ kg, weight of the explosive charge
$h = 13.5$ KJ/g, the heat of combustion of TNT.

An internally pressurized structure vents the pressure to the surroundings through openings in its walls causing a slow decay to ambient condition as shown by Kinney and Sewell [7] and is computed from

$$\text{Ln } P = \text{Ln } P_o - .315\ (A_v/V)\ t, \quad (5)$$

where

t = elapsed time in ms
P = absolute pressure at t_s
$A_v = 2.33\ m^2$, the available vent area.

The long term duration of the decay is essentially due to the relatively small vent area available causing a slow pressure decay to the atmosphere.

The blow-down time t_s, required to reduce the residual overpressure to ambient conditions developed by Keenan et al. [8] based on the firing of high explosives in chambers with known vent areas and volumes is given as

$$t_s = 6.28\ (A_v/V)^{-.86} \quad (6)$$

The above equation is valid for $A_v/V^{2/3} < 0.21$. In the current design the ratio $A_v/V^{2/3}$ equals .018 and the duration time for the quasi-steady pressure is approximately 1600 ms.

The computation involves determination of peak residual overpressure from Eq. (4) which when combined with Eqs. (5) and (6) yields the quasi-steady part of the loading history. The junction between the reflected overpressure history and the quasi-steady loading is smoothed by a curve interpolation scheme in order to avoid a sharp transition. This loading is applied uniformly at each meshpoint on the inside wall in the radial direction in the finite-difference structural response model in the PETROS 3.5 computer program [9]. The load-time history inside the hemispherical enclosure was zeroed out after 180 ms to facilitate damping of small elastic oscillations and to observe any residual deformation of the hemispheric wall. The peak reflected overpressure was found to be 257.3 kPa while the peak residual overpressure was approximately 100 kPa.

Static Stress Analysis

Prior to a detailed dynamic response study, a static stress analysis estimate in the linear-elastic-small deflection regime was conducted to obtain an initial estimate of the enclosure wall thickness. Since the duration of the reflected pressure is less than 1.5 ms compared to 1600 ms for the duration of the quasi-steady overpressure, an approximate static analysis, based on a minimum factor of safety of 2.0 is considered to be satisfactory. For the preliminary investigation, stress-concentration near holes, cutouts and wall openings was neglected. However the effect of ground-plane reflection of the shock wave was included through a load multiplication factor of $k = 2.0$, which in effect doubled the applied load.

To contain the initial pressure pulse in an elastic manner only the peak reflected overpressure P_r was included in the calculation of stresses and deflections. An equivalent static meridional stress σ can be calculated by equating the resultant upward force due to internal pressurization to the net downward restraining force due to the stress developed at the clamped edge resulting in

$$\sigma = \frac{RkP_r}{2h} \quad (7)$$

where

$R = 8.987$ m, the median radius
k = load multiplication factor.

However for an assumed factor of safety of 2.0 $\sigma = 1/2\ \sigma_y$, where σ_y is the static yield stress. Substituting this value of σ in Eq. (7) and rearranging terms results in an expression for the estimated thickness h in the form

$$h = \frac{RkP_r}{\sigma_y} \quad (8)$$

The yield stress σ_y for the wall material which is 1020 steel is 241.3 MPa. Hence the wall thickness h from Eq. (8) is found to be .019 m.

Up to this point no consideration has been given to the possibility that fragment induced damage to a shell might result in catastrophic rupture when the blast loading is applied. One should estimate the material removal produced by the impact of the worst threat fragment and perform a local three-dimensional analysis of the stress field to determine whether a crack would be propagated under such loading. This problem in fracture mechanics is rather difficult to analyze and can be at least partially circumvented by a conservative selection of wall thickness under the assumption that the residual thickness is capable of withstanding the peak quasi-steady pressure even when a 50% depth of penetration has been achieved by a part-through fragment. The final thickness chosen from a conservative viewpoint was .0254 m (1 in.) which is readily available. The .0254 m thickness corresponds to a stress level of 45.5 MPa which when compared to the yield stress results in a final margin of safety of 4.3 which is satisfactory.

The peak radial deflection ΔR at the pole is estimated from Ref. [10] as

$$\Delta R = \frac{R^2 kP_r(1 - \nu)}{2Eh} \quad (9)$$

where E, ν are elastic material properties.

To detect resonance due to coupling of the duration time of the pressure pulse with the natural vibration period, the time period T was calculated from Ref. [10] as

$$T = \pi R\sqrt{\frac{2\rho(1 - \nu)}{E}} \quad (10)$$

where ρ is the mass density. Further check of any interaction of the reflected pressure pulse due to ground plane reflection with the elastic oscillation of the pole did not reveal a significant problem.

The peak radial elastic deflection at the pole from Eq. (9) was found to be .0011 m which is quite small. The gross weight of the hemispherical enclosure was found to be approximately 96,400 kg based on an .0254 m wall thickness. In this study allowance was made for the weight of flanged material at the base but not for extra weight associated with access provisions, welds or foundations.

Optimization Study

An optimization study based on equivalent strength showed substantial weight saving for a hemispherical configuration at or below 6 m radius but marginal savings at higher radius up to 9 m due to compensating thickness increases. An equation proposed by R. Karpp et al. [11] for the minimum amount of vessel material V_m to contain a specified charge is given as

$$V_m \approx 4\pi M \left(\frac{K}{\varepsilon_y}\right)^{1.0406} \rho^{.0406} \left(\frac{R}{h}\right)^{.0406} \qquad (11)$$

where ε_y is the yield point strain of the vessel material in biaxial tension, M is the charge weight, ρ is the density of the vessel material and K is an empirical curve-fit constant found to be 4.08×10^{-6} m^3/kg. Although the minimum amount of vessel material to contain a specific charge is not the governing design criterion, there may be some interest in determining the optimized value. If the volume of vessel material is plotted as a function of the radius-to-thickness ratio of the container as given in Eq. (11) a slow variation is observed in the amount of vessel material required to contain the dynamic load as a function of the radius-to-thickness ratio R/h. The variation in material volume over the design range of $350 \leq R/h \leq 200$ is only about 3%. Thus, the amount of material required to contain a specified charge in this range of configurations is essentially constant. Very thin wall, large-radius vessels with $R/h \geq 400$ makes inefficient use of material at least for blast wave containment. On the other hand for thick wall, small-radius vessels with $R/h \leq 150$, at least 12% or higher saving in material volume can be realized with judicious choice of reinforcement in critical sections. Unfortunately substantial saving in material could not be achieved due to constraints of minimum workspace and equipment access considerations and the additional requirement of part-through fragment containment with 50% depth of penetration.

The analysis so far applies only to the containment of the initial pressure pulse. However for long term containment the volume of vessel material V_s required to contain the static pressure elastically can be estimated from the semiempirical relationship

$$V_s = C \frac{M}{P} \qquad (12)$$

where C is a constant with a value of about 1.3 m^3 MPa/kg for most solid explosives and P_s is the final static pressure. The material volume appears to be independent of the radius-to-thickness ratio if the internal radius is approximated by the average radius of the vessel and the usual formula for equilibrium of a thin shell is used. Based on Eq. (12) the material volume required to contain the static load was found to be approximately 20% of that required to contain the initial dynamic load.

A comparison of the 9 m hemispherical structure with an equivalent 9 m × 9 m × 7.3 m rectangular parallelepiped all welded depleted uranium (DU) containment structure with a 2.75 in. thick steel armor wall liner and a 2.5 in. thick roof liner indicated an increase of 64 times in containment capacity of equivalent charge weight for the hemispherical structure with a 50% reduction in weight and concurrent doubling of the internal volume capacity without any significant sacrifice in the minimum margin of safety. In addition the simplistic design of the hemispherical enclosure, although somewhat difficult to fabricate, was a significant improvement for static and dynamic load bearing considerations. The down-time for duration of residual overpressure was decreased substantially due to availability of larger entrance hole diameter and vent area.

Dynamic Response Analysis

Response of the structure subjected to transient loads from an instant blast was conducted using the BRL version of the PETROS 3.5 computer program [9], which employs the finite-difference method to solve the nonlinear equations governing finite-amplitude elasto-plastic response of thin Kirchhoff shells. The model is valid for large deflections and can be employed to treat the entire structure rather than a small section.

Material Model

The uniaxial tensile quasi-static stress-strain property of 1020 steel is used for primary vessel material. The material is modelled in the code as a combination of three linear segments followed by perfectly-plastic behavior and linear elastic-plastic unloading, resulting in a polygonal approximation of the experimental data. The strain hardening part of the stress-strain curve is generated by a sublayer hardening model from a weighted combination of elastic perfectly-plastic curves yielding a piecewise multilinear hardening representation. Strain-rate effects were neglected, which is conservative since these effects increase the structural resistance and thus reduce the total deformation.

Finite-Difference Model

Since both the responding structure and the applied loads are symmetric with respect to the vertical axis, it is sufficient to model the response of a single pie-shaped segment of the hemispherical enclosure and generate the entire structure by 360° rotation of the structure about the axis of symmetry resulting in quite economical computer runs.

A total of 18 meshes along the surface and a single layer through the thickness were used to represent the pie-shaped segment. Four Gaussian integration points through the thickness were used at each mesh for computational purpose. The total number of mesh points did not exceed 37. The mesh points at the base were restrained from movement in both axial and transverse directions. However, the pole was allowed to move in the radial direction due to symmetry boundary conditions. Intermediate mesh points were allowed unrestrained movement. Only the internal nodes were subjected to blast pressure in the radially outward direction.

Results and Discussion

The peak deflection of 1.17 mm occurs at the pole of the hemisphere at approximately 36 ms from initial occurrence of internal blast. However, the deflections are, in fact, small enough to be in the linear elastic range, and any residual deflection after elastic oscillations are damped out is probably caused by a numerical artifact of the code.

A maximum deflection of 0.82 mm, essentially radially outward is observed at a point at 45° from the vertical axis of the hemisphere in a meridional plane.

Displacements in general are small everywhere and are less than 4% of the shell thickness so that geometric nonlinearities are insignificant. The larger response at the pole is attributed to focussing of flexural vibratory energy [2].

The PETROS 3.5 code was run for 8000 cycles (192 ms) in an undamped mode, after which artificial damping was introduced to suppress the elastic oscillations, which were positively biased due to residual internal pressure. Fully damped condition was achieved at cycle 8235 (198 ms) when the final configuration was found to be identical to the undeformed configuration with no evidence of residual plastic deformation.

Energy balance studies using the code confirmed absence of plastic work and numerical instability. Both total and kinetic energies were bounded. The fluctuations of kinetic energy appeared to have twice the frequency of the work performed by the internal blast pressure.

Variation of transient strain components on the outer and inner surfaces of the hemisphere at a point near the edge indicates that the meridional strain components on the inner and outer surfaces are almost in phase initially but become out of phase and unequal in magnitude with increasing time signaling the build-up of some flexural deformation. The hemisphere moves outward and inward, except at the fixed boundary in a breathing mode resulting in membrane strains upon which the bending strains are subsequently superposed due to propagation of flexural waves from the fixed boundary towards the pole. Significant difference in strains between the outer and the inner walls at the clamped edge could be primarily attributed to domination of the response by the bending strains. The circumferential strains indicated by continuous lines are zero as expected. Calculations for maximum meridional stress based on peak strain results in a stress level of 48.26 MPa which is equivalent to a safety margin of 4.0. As expected from elastic theory peak strains occurred at the fixed edge while maximum deflection occurred at the pole.

The variation of strain at the inner wall with time at a point near the pole is such that the circumferential strain is in phase and very similar to the meridional strain. The strains at the outer wall near the pole exhibit elastic oscillations of approximately the same magnitude and duration as for the inner wall. This behavior indicates substantial weakening of the flexural wave near the pole and domination of meridional and circumferential strains by the membrane component of strain due to elastic vibration of the wall in the breathing mode. The peak meridional stress at the pole was calculated based on elastic equations and was approximately 25 MPa, which is considerably lower than the maximum stress at the clamped edge. The stress level is equivalent to a safety margin of 3.6 based on the yield stress.

Both strain components are relieved completely upon damping at approximately 198 ms. The coincidence of the final and the initial configurations at a high magnification ratio of 1000 indicates the absence of any plastic deformation and confirms small strains and deformations throughout the structure in accordance with earlier results.

Concluding Remarks

It has been demonstrated, through use of a rigorous nonlinear shell response methodology, that it is possible to design a containment structure with a hemispherical configuration in an efficient and cost effective manner. The methodology could be easily extended to structural optimization studies, resulting in considerable cost savings, provided internal volume and access considerations could be met.

In spite of simplifying assumptions and limitations of the PETROS 3.5 version of the shell response analysis code which neglects transverse shear deformation and rotatory inertia, the analysis gives a clear insight into the initial loading mechanism due to structural resistance and interaction of various components of the response. However, an examination of the characteristics of the hemispherical structure reveals the following:

1. The 9 m radius, .0254 m thick hemispherical enclosure is an efficient protective structure capable of withstanding internal blast from a 29.03 kg TNT charge with assured structural integrity.

2. The structure is capable of successful containment of combustion products and fragments with sufficient mass and velocity to achieve a 50% depth of penetration with a satisfactory margin of safety.

3. Peak deflection occurs at the pole due to elastic oscillations of the structure in the breathing mode resulting in focusing of vibratory energy at the pole.

4. Peak strain occurs at the clamped edge and exhibits considerable difference in straim amplitude between the inner and outer surfaces due to bending waves originating in this region.

5. The ratio of the vent area to the internal volume is small enough to result in a slow rate of venting and an extended venting time of 1600 ms for the quasi-steady residual overpressure to blow-down to the external ambient conditions.

6. Cumulative damage effect due to repeated test firings could conceivably cause low cycle fatigue of the structure and a periodic inspection of the internal surface and joints for cracks in critical regions is recommended.

7. Future work should be directed to modelling of the enclosure structure with wall openings for the equipment and personnel access doors, protective walls for X-ray equipment, detailed analysis of critical joints and stress concentration due to holes and cut-outs in corner regions.

Acknowledgements

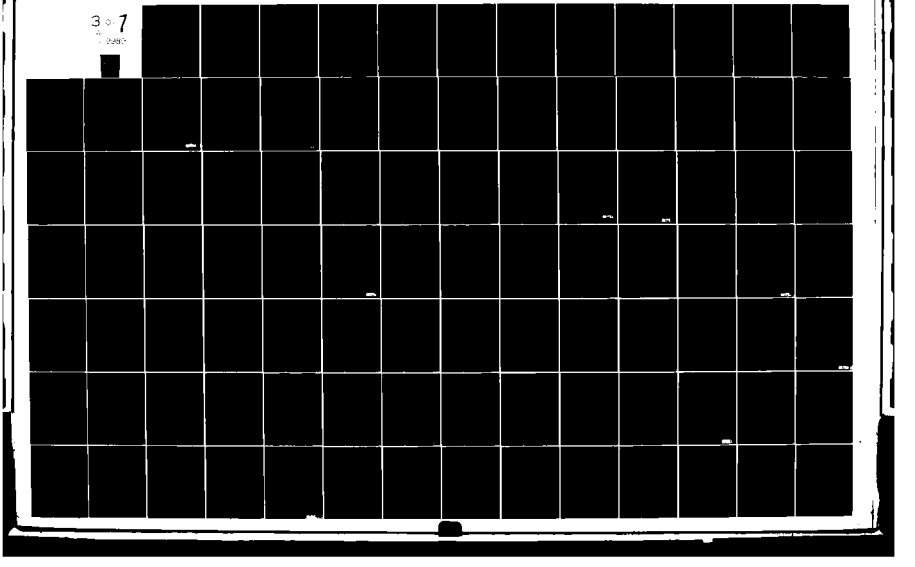
This investigation was performed for Mr. Louis Giglio-Tos, who was the Project Coordinator for Project No. T01400 at R-9. Valuable assistance of Mr. Charles V. Kingery and Dr. Joseph M. Santiago of the Terminal Ballistics Division is gratefully acknowledged.

References

1. Abrahms, R., Peterson, R. and Bertrand, B., "Measurement of Blast Pressure Produced by Impact of Kinetic Energy Penetrator on a Steel Target," BRL Memo Report ARBRL-MR-02983, January 1980, AD #B045141L.
2. Huffington, N.J. and Robertson, S.R., "Containment Structures Versus Suppressive Structures," Memorandum Report BRL-MR-2597, February 1976.
3. Engineering Design Handbook, "Explosions in Air, Part 1," AMC Pamphlet AMCP 706-181, Headquarters, US Army Material Command, pp.3-5, July 1974.
4. Soroka, B., "Air Blast Tables for Spherical 30/50 Pentolite Charges at Side-on and Normal Incidence," Memorandum Report ARBRL-MR-0295 (AD #A080537), December 1979.
5. Goodman, H., "Compiled Free Air Blast Data on Bare Spherical Pentolite," BRL Report 1092, February 1960 (AD #235278).
6. Weyer, E.M., editor-in-chief, Annals of the New York Academy of Sciences, Vol.152, "Prevention of and Protection Against Accidental Explosion of Munitions, Fuels and Other Hazardous Mixtures," published by the Academy, 2 East 63rd Street, New York, NY 10021, p.317.

7. Kinney, G.F. and Sewell, R.G.S., "Venting of Explosives," NWC Tech., Memo 2448, July 1974.
8. Keenan, W.A. and Tamareto, J.A., "Blast Environment from Fully and Partially Vented Explosions in Cubicles," US Naval Civil Engineering Laboratory, Tech. Report No.51-027, February 1974.
9. Pirotin, S.D., Berg, B.A. and Witmer, E.A., "PETROS 3.5: New Developments and Program Manual for the Finite-Difference Calculation of Large Elastic-Plastic Transient Deformations of Multilayer Variable-Thickness Shells," US Army Ballistic Research Laboratories Contract Report No.211, February 1975.
10. Roark, R.J., "Formulas for Stress and Strain," Fifth edition, McGraw-Hill,Book Co., New York, 1975, pp.96,451.
11. Karpp, R.R., Duffy, T.A. and Neal, T.R., "Response of Containment-Vessels to Explosive Blast Loading," Report No. LA-8082, UC-38, Los Alamos Scientific Laboratory, Los Alamos, New Mexico, June 1980.

AD-A119 989 ARIZONA UNIV TUCSON COLL OF ENGINEERING F/G 13/13
PROCEEDINGS OF THE INTERNATIONAL SYMPOSIUM ON OPTIMUM STRUCTURA--ETC(U)
1981 E ATREK, R H GALLAGHER N00014-80-C-0041
UNCLASSIFIED NL



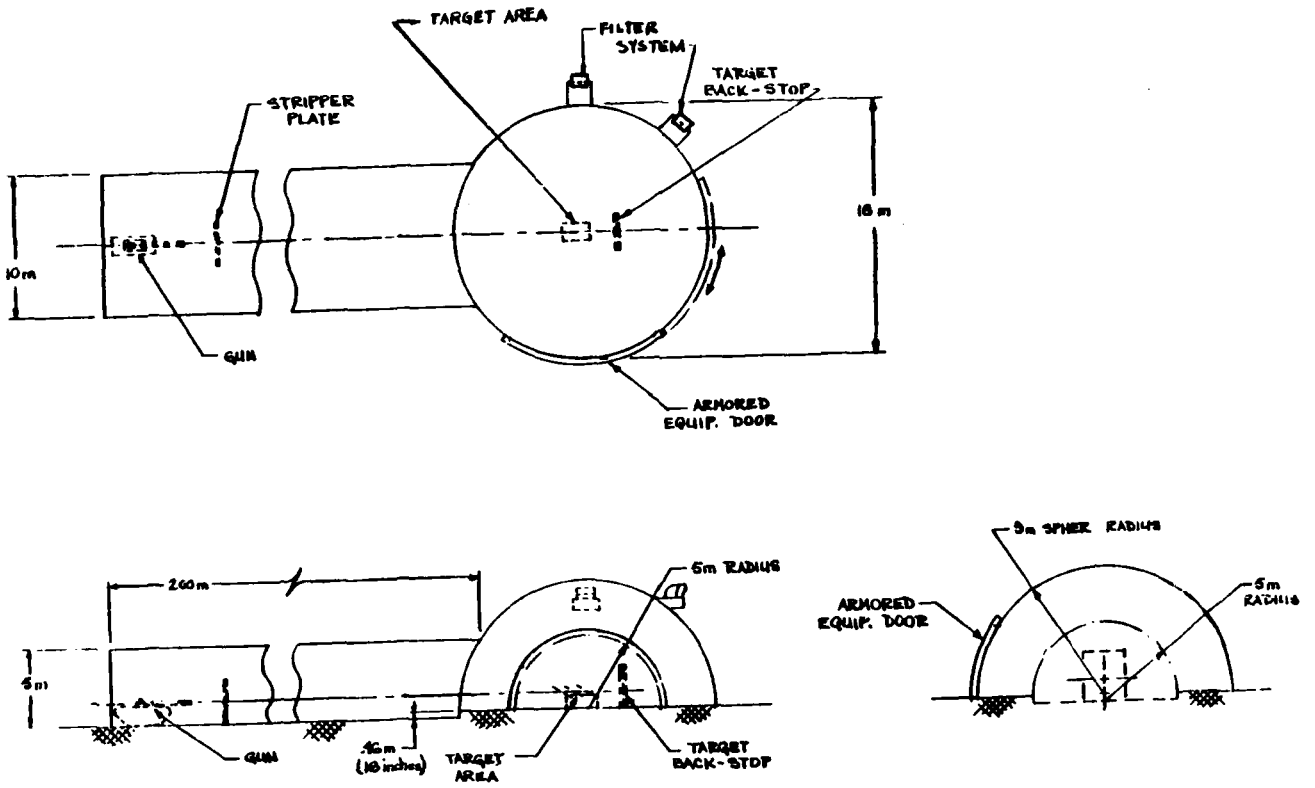


Figure 1. Preliminary concept layout of the AHKELS (Advanced High Kinetic Energy Launch System) range.

AD-P000 051

OPTIMUM COLUMN BUCKLING UNDER AN AXIAL LOAD AND ITS OWN WEIGHT

Sadia M. Makky
Mathematics Department, College Of Science
The University Of Bagdad
Adamya, Bagdad, Iraq

Summary

A vertical column of a given length made of an elastic homogeneous, and isotropic material, is to be designed with circular cross sections of varying radii (or equivalently with any preassigned cross sections that are similar and similarly oriented). The lower end of the column is assumed to be built in, while a vertically copressive force is assumedto be acting on its free upper end. The optimum shape of the columnis determined such that the weight of the column is minimum, and yet the column does not buckle under the action of the prescribed compressive force plus its own weight.
This investigation is similar to that cosi - dered by Keller and Niordson[1] in two aspects: (i) The formulation of the mathe - matical model and the method of its solution are different. (ii) A preassigned compressive force is supposed here to be acting at the upper end of the column. Moreover, this treatment is a generalization of [2], in the sense that it reduces to the problem cosidered in [2] when the external force is taken to be zero.
The linear theory of elasticity is used to express the stress-strain relations, the energy method is applied to define the stability criterion, and calculus of variation is utelized to minimize the weight. The solution of the resulting non-linear two-point boumdary vlue problem is found by a modified method of successive approximations.

Statement of The Problem

Criterion of Stability

Although there are different approuches in determining the critical conditions for structural instability, [3] and [4], we will use the energy approuch. This method is applied for conservative systems, where the work can be expressed in terms of the external forces.
Let the equilibrium configuration be given a small virtual displacement without violating the geometrical boundary cnditions. If the work done by the external load, due to this virtual displacement, does not exceed the increase of the stored strain energy, the body is cosidered stable. Otherwise, the excess energy will appear as kinetic energy. This indicates an instability of the original configuration for the virtual displacement.

The Virtual Displacement

Assume that the axis of the column is along the z- axis, and that its fixed end is at the origin of a rectagular coordinate system. Assume furthermore, that the center line of the column is given a virtual displacement in the x-z plane.

Let (x, y. z) be the coordinates of a point of the column before deformation, let $s_1(x, y, z)$, $s_2(x, y, z)$, and $s_3(x, y, z)$

be the components of the displacement vector of that point. Assuming no elongation along the column axis, and sections normal to the center line remain normal to the deformed center line, it follows that the components of the displacement vector are given by

$$s_1(x, y, z) = u(z) - x[1-\cos \alpha(z)],$$
$$s_2(x, y, z) = 0 , \qquad (1.1)$$
$$s_3(x, y, z) = -x \sin \alpha(z) ,$$

where, u(z) is the lateral displacement of the center line, and α is the angle between the z- axis and the tangent to the curve representing the center line after defor - mation, Assuming α is very small, the components of the displacement vector will be

$$s_1 = u(z) \; ; \; s_2 = 0 \; ; \; s_3 = -x\, u'(z) , \qquad (1.2)$$

where, prime denotes differentiation with respect to z. Let $v_i(r, \theta, z)$, i = 1, 2, 3

be the covariant components of the displacement vector relative to the cylindrical coordinate system. When the tensorial transformation [5], and Eqs(1,2) are used these components take the forms:

$$v_1(r, \theta, z) = u(z) \cos \theta ,$$
$$v_2(r, \theta, z) = -r\, u(z) \sin \theta , \qquad (1.3)$$
$$v_3(r, \theta, z) = -r\, u'(z) \cos \theta .$$

From the defimition of the covariant derivatives [5], and from (1.3) it then follows that

$$v_{1,3} = u' \cos \theta , \; v_{3,1} = -u' \cos \theta ,$$
$$v_{2,3} = -ru' \sin \theta , \; v_{3,2} = ru' \sin \theta , \qquad (1.4)$$
$$v_{3,3} = -ru'' \cos \theta , \; v_{i,j} = 0, \text{ otherwise.}$$

The Stress-Strain Relations

The linear theory of elasticity states that the components of the strain tensor are related to the displacement by [6] :

$$e_{ij} = (v_{i,j} + v_{j,i})/2 . \qquad (1.5)$$

By ussing Eqs(1.4), these relations will take the following form:

$$e_{33} = -r\, u''(z) \cos \theta \qquad (1.6)$$
$$e_{ij} = 0 , \text{ otherwise} .$$

Assuming, to simplify the analysis, that

Poisson's ratio is zero reduces the stress-strain relations to:

$$\sigma_{ij} = 2 G e_{ij} \quad . \tag{1.7}$$

In the above relations σ_{ij} are the components of the stress tensor, and G is a material constant. Upon combining Eq(1.6) and Eq(1.7) the stress components will be given by

$$\sigma_{33} = -2 G r u''(z) \cos\theta \quad ; \qquad \sigma_{ij} = 0 \text{ , otherwise} \quad . \tag{1.8}$$

The Elastic Strain Energy

The elastic strain energy is given by[7]

$$E = \int_V \sigma_{ij} \, e_{ab} \, g^{ia} \, g^{jb} \, dV \quad ; \tag{1.9}$$
$$ij$$

where V is the volume of the column, and g are the contravariant components of the metric tensor, relative to the coordinate system being used. Since all the components of the strain tensor are zero except e_{33} it follows that

$$E = \int_0^L \int_0^{a(z)} \int_0^{2\pi} 2Gr^3 [u''(z)\cos\theta]^2 d\theta \, dr \, dz \quad .$$

In deriving the above equation use is made of Eqs(1.6), (1.8), and (1.9). Finally, upon integrating, as aove indicated with respect to r and θ, the elastic strain energy becomes

$$E = \int_0^L C \, [u''(z) \, A(z)]^2 \, dz, \quad \text{where} \tag{1.10}$$

$$A(z) = a^2(z) \quad ; \quad C = G\pi/2 \quad . \tag{1.11}$$

The Work

The change in the potential energy due to the virtual displacement of the column is

$$T = \int_0^L \pi m \, A(z) \, w(z) \, dz + Q \, w(L) \tag{1.12}$$

where m is the density, w(z) is the vertical drop of points along the center line resulting from the lateral virtual displacement of the column, and Q denotes the external compressive force acting at the upper end of the column. Assuming that the column is built in at its lower end requires that w(0) = 0 ; and consequently Eq(1.12) can be written as

$$T = \int_0^L [D \, A(z) \, w(z) + Q \, w'(z)] \, dz \quad , \tag{1.13}$$

where $D = \pi m$.

Relation Between The Vertical Drop And The Lateral Displacement

Suppose that P is a point on the center line of the undisplaced column, and P' is the position of the point after the virtual displacement. If z is the distance of P to the fixed end of the column; then, since it is assumed that the virtual displacement is inextensional, it follows that the distance along the curve representing the center line after deformation, between P' and the fixed end of the column is z also. Hence

$$\int_0^{z-w(z)} [1 + u'^2(t)]^{1/2} \, dt = z \quad . \tag{1.14a}$$

On the other hand,

$$z = w(z) + \int_0^{z-w(z)} dt \quad . \tag{1.14b}$$

Neglecting powers of u' higher than 2 it follows from (1.14) that

$$w(z) = \int_0^{z-w(z)} [u'(t)]^2/2 \, dt \leq \int_0^z [u'(t)]^2/2 \, dt \quad . \tag{1.15}$$

Finally, differentiation of both members of Eq(1.15) with respect to z yields

$$w'(z) = u'^2(z)/2 \quad . \tag{1.16}$$

Mathematical Statement of The Problem

To determine the optimum shape of the column, a criterion which relates the buckling load to the shape must be given. The criterion which we have adopted is that the column is stable as long as the strain energy is not less than the work done by the external load, due to any infinitesimal virtual displacement [4]. In other words the column is stable when

$$E \geq T \quad ; \tag{1.17}$$

buckling starts when inequality (1.17) is violated, i.e., when E < T. Taking E = T, and using Eq(1.11) and Eq(1.13) one obtains

$$\int_0^L \left[C[A(z)v'(z)]^2 - DA(z)w(z) - Qw'(z) \right] dz = 0, \tag{1.18}$$

where

$$v(z) = u'(z) \quad . \tag{1.19}$$

The total weight of the column is

$$W^* = \int_0^L D \, A(z) \, dz \quad . \tag{1.20}$$

The mathematical problem is to find A, v, and w as functions of z such that W^*, as given by (1.20), is minimized and conditions (1.16) and (1.18) are satisfied. This is a variational problem involving a conditional extremum; the auxiliary funtional is as follows

$$\int_0^L \left[D \, A(z) - B(z) \left[w'(z) - v^2(z)/2 \right] - P[CA^2(z) \, v'^2(z) - DA(z)w(z) - Q\frac{v^2(z)}{2}] \right] dz. \tag{1.21}$$

In the above functional, P and B(z) are the constant and variable Lagrange's multipliers respectively[9]; Eqs(1.16)&(1.19) are used.

The Solution Of The Problem

Euler's Equations

The necessary conditions for the functional defined in the previous section to have an extremum, see[9], are the following Euler's equations:

$$w' - v^2/2 = 0 \quad , \qquad (2.1)$$

$$B' + P\,D\,A = 0 \quad , \qquad (2.2)$$

$$B\,v + 2P\,C\,[A^2\,v']' = 0 \quad , \qquad (2.3)$$

$$D\,(1 + P\,w) - 2P\,C\,A\,v'^2 = 0. \qquad (2.4)$$

The Boundary Conditions

If the column is biult in at the end $z = 0$, it then follows that

$$u(0) = 0 \quad , \quad u'(0) = 0 \; ; \qquad (2.5)$$

$$w(0) = 0 \quad . \qquad (2.6)$$

Using the last condition of (2.5) in connection with Eq(1.19) gives

$$v(0) = 0 \quad . \qquad (2.7)$$

The other boundary conditions are the natural boundary conditions for the variational problem [9]; these conditions are given by:

$$F_{w'} = 0 \quad , \text{ at } \quad z = L \; ;$$

$$F_{v'} = 0 \quad , \text{ at } \quad z = L \quad ,$$

where F is the integrand in (1.21). Utelizing (1.21) with the above two boundary conditions it follows that

$$B(L) = 0 \quad ; \quad A^2(L)\,v'(L) = 0 \quad . \qquad (2.8)$$

Method Of Solution

When one defines

$$H(z) = B(z)/P \quad , \qquad (2.9)$$

$$M(z) = A^2(z)\,v' \quad , \qquad (2.10)$$

the boundary value problem composed of differential equations (2.1)-(2.4), and boundary conditions (2.6)-(2.8) can be replaced by:

$$w' = v^2/2 \quad , \; w(0) = 0; \qquad (2.11)$$

$$H' = -DA \quad , \; H(L) = 0; \qquad (2.12)$$

$$M' = -Hv/2C \quad , \; M(L) = 0; \qquad (2.13)$$

$$A = \sqrt{[M/v']} \quad , \qquad (2.14)$$

$$v' = \sqrt{[D(1 + Pw)/2PCA]}, \; v(0) = 0 \; ; \qquad (2.15)$$

The above system of non-linear differential equations is solved by a modified method of successive approximations. The steps are summarized below:

1. Choose simple expressions for A and v as functions of z, say A_0 and v_0 such that $v_0(0) = 0$.

2. Use Eqs(2.11), (2.12), and the corresponding boundary conditions, with the chosen A_0 and v_0 to determine w_1 and H_1 as functions of z.

3. Use Eq(2.13) and the corresponding boundary condition, taking for v the chosen expression v_0, and for H the expression H_1 found in step 2. above, to find an expression for M as a function of z, call it M_1.

4. With the newly found M_1, and v_0, Eq(2.14) yields a new expression for A, say A_1 a first approximation for the optimum shape.

5. Likewise, using A_1 and w_1 in connection with Eq(2.15) with its corresponding boundary condition, one can determine v_1 as a function of z and P.

6. The value of the parameter P can be determined so that condition (1.18) is satisfied.

7. When the value of P, determined in 6. above is subistituted in v_1, the latter becomes a function of z only.

8. Employing A_1, one can determine through the use of (1.20) a first approximation for the optimum weight.

9. The steps 1. - 9. are repeated using, now A_1 and v_1 to determine A_2, H_2, M_2, and w_2; and so on.

The proof that this method converges is similar to the convergence proof for the usual method of successive approximations.

A Numerical Example

A computer program, based on the above steps, is developed to find the optimum shape of a column with the following specifications:

$m = 0.288 \quad \text{lb/inch}^3$;

$L = 250 \quad \text{inch}$;

$G = 15 \times 10^6 \quad \text{lb/inch}^2$.

Two cases have been considered:

(i) The column is under a compressive force $Q = 10^6$.

(ii) The column is under no compressive force.

The optimum shape for these two cases are plotted below. The optimum weight for the first case is 4542 lbs, while it is 0.5137 lb. for the second case.

For comparison, a uniform column of circular cross section of the same length, which is made of the same material, is cosidered. The critical load for such a column is given by [10]

$$P_c = \pi^2 E^* I/(kL)^2 \quad , \text{ where} \qquad (3.1)$$

E^* = modulus of elasticity = 2G ,

I = moment of inertia of the cross sectio

$= \pi a^4 / 4$ (3.3)

k is a parameter depending on the boundary conditions; for the built in - free case under consideration k = 2.

Taking $P_c = 10^6$, Eq(3.1) gives

$a = 5.726$ inches , (3.3)

from which it follows that the weight of the uniform column , with no consideration to its own weight is 7416.46 lbs. The ratio between the weight of the uniform column to that of the tapered column is 1.63 , thus tapering causes a reduction of 38.75%.

References

[1] Keller, J. B. and Noirdson, F. I., The Tallest Column. J. Math. Mech. , Vol 16, PP.433, 1966.

[2] Abdulla, H. Kh. ," Optimum Shape Of A Column Buckling Under Its Own Weight" , M Sc. thesis, The University Of Bagdad, 1977.

[3] Kachanov, H. M., Foudations Of The Theory Of Plasticity, North-Holland Publishing Co., London, 1971.

[4] Washizu, K. , Variational Methods In Elasticity And Plasticity , 2nd., Pergamon Press, New York, 1975.

[5] Sokolnikoff, I. S., Tensor Analysis And Applications To Geometry And Mechanics, John Wiley, New York, 1964.

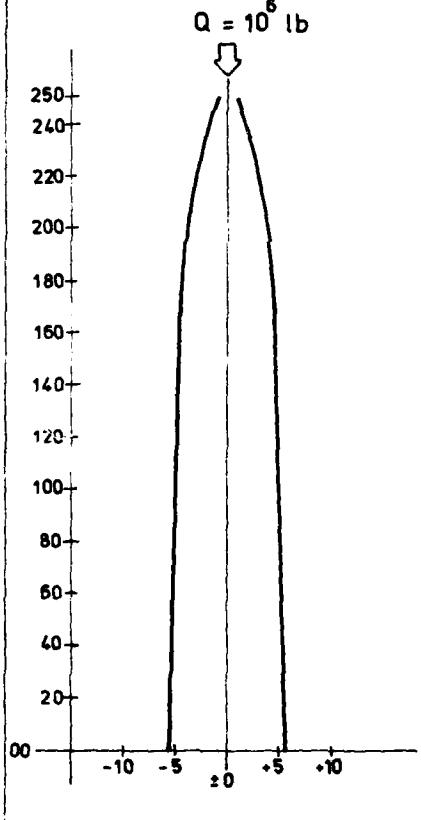
[6] Fung, Y. C., A First Course In Continuum Mechanics, Prentice Hall, Englewood Cliffs, 1969.

[7] Thomas, T. Y.. Plastic Flow And Fracture In Solids, Academic Press, New York, 1961.

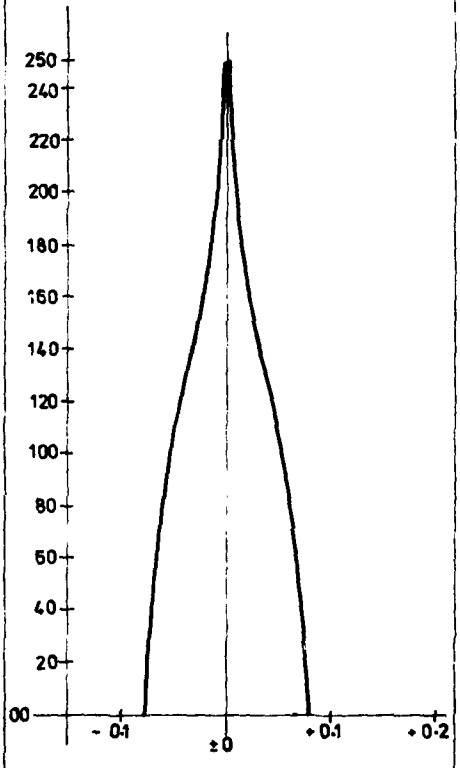
[8] Dym, C. L. And Shames, I. H., Solid Mechanics: A Variational Approach, McGraw-Hill, New York, 1973.

[9] Elsgolc, I. E., Calculus Of Variations, Pergamon Press, New York, 1961.

[10] Johnston, B. G. , Lin, F. J. And Galambos T. V., Basic Steel Design, 2nd. Ed., Prentice-Hall,1980.



[Fig. a]: OPTIMUM COLUMN BUCKLING UNDER ITS OWN WEIGHT PLUS AN AXIAL LOAD



[Fig. b]: OPTIMUM COLUMN BUCKLING UNDER ITS OWN WEIGHT

L = 250 inch
G = 0.15×10^8 lb / inch^2
M = 0.288 lb / inch^3

SESSION #5

SHAPE OPTIMIZATION II

AD-P000 052

SHAPE DETERMINATION OF STRUCTURES BASED ON THE INVERSE VARIATIONAL PRINCIPLE/ THE FINITE ELEMENT APPROACH

by Yukio TADA and Yasuyuki SEGUCHI

Department of Systems Engineering, Kobe University,
Rokkodai, Nada, Kobe, 657, JAPAN

Summary

It is naturally considered that an extremal principle exists in the formation of shape of a body. This idea may be extended to the design of a structural shape.

V. Horák proposed the inverse variational principle. In general, behaviours of a body are described by governing equations derived by variations of the state variables, such as the displacement, strain and stress. In the inverse variational principle, the additional governing equation to determine the structural shape is derived by the variation of the variables which represent the configuration of the body, provided that a constraint is imposed on them so as to specify any global invariant, for example, with respect to the dimension of the body.

In this paper, the numerical shape determination techinique of structures is proposed by combining with the finite element method as an application of the principle. First of all, the optimal shapes of bodies which are subjected to statical loads are determined on the basis of the potential energy principle. The triangular finite element model is employed, and coordinates of the nodal points on the periphery of the body are adopted as shape variables to obtain the optimal shapes independent of preconception. To solve the derived system of nonlinear equations, a new successive reforming procedure referred as "Energy Ratio Method" is proposed. The several numerical examples show that the shape of the body is stably reformed into the optimal one by the method. The structure with the shape obtained is the stiffest one of all the bodies with the same volume. The influences of the loading and the boundary conditions are discussed.

In the second place, the principle is extended to the eigenvalue problems to search the shape of the maximum buckling load and that of the maximum fundamental frequency. Several examples using one-dimensional finite element model are presented and the validity of the Energy Ratio Method is also shown.

1. Introduction

In the structural design, it is necessary to obtain a shape (or, geometry) which will yield a higher efficiency (that is, the minimum volume for a given strength, or the maximum stiffness with a given volume). Among policies to determine those shapes one familiar criterion is an application of extremum principles to the design.

It is often supposed that any behaviour of bodies in the nature is subject to certain laws which are generally called extremum principles. For example, the equilibrium conditions and the kinetic equations of a body are derived from the principle of minimum potential energy and Hamilton's principle, respectively. Accordingly, the existence of similar principles for the formation of the shape of a body is naturally asserted.

Some problems of optimum structural design have been treated as extremum ones by various authors, and were reviewed by Prager & Taylor(1). Taylor called an object of their problems a performance(2). Compliance and stiffness of the body are objectives of extremum problems(3)~(6), and minimum weight design with a constraint to deflections is also considered(7)~(10).

In most of techiniques for optimum structural designs, design variables such as lengths of members and sizes of cross sections of a truss are optimized among a set of prescribed shapes or in given layouts except for particular problems for beams, plates and so on. Otherwise, for a structure, whose shape is specified almost everywhere and is alterable only through some parameters, the optimization of the structure is achieved by searching optimum values of the parameters (11).

Recently, the finite element techinique enters the investigation of the structural optimization, but they are confined within the design region mentioned above (12), or the objects of the optimization are limited to that of a distribution of plate thickness(13),(14).

Meanwhile, other new methods have been proposed(15)~(17), which seek for equi-strength shapes in non-parametric fashion, using finite element method. They are dependent on the stresses of local points, but global evaluation for the behaviour of the body is not considered.

On the other hand, authors formulated a shape determination problem of structures on the basis of the inverse variational principle, proposed by Horák(18), using finite element method. This method can create optimum shapes freely by adopting the coordinates of nodal points as design variables.

In this paper, firstly a method for optimization (19), which uses a new procedure termed as "Energy Ratio Method", is summarized for the two-dimensional elastic problem. Secondly, the principle is extended to eigenvalue problems(20), and thirdly the influences of boundary conditions on the final shapes are discussed for the first case.

2. Inverse Variational Problem

2.1 Principles of Stationary Potential Energy

Variational principles of solid mechanics usually consider the variations of strain, displacement, stress, and force arising in bodies of given shape and given mode of supports, subject to surface and body forces. In the inverse variational problems, an elastic body, whose volume (or, surface area) is given but which is bounded by a closed boundary of a surface not known in advance, is considered(18). Hence, the variation of structural shape is also taken into account. For example, in the inverse variational principle of the minimum potential energy under a subsidiary condition that the volume of the body is constant, the functional to be made stationary is given in the Lagrangian functional as

$$\Omega=\int_V\left(\frac{1}{2}C_{ijkl}e_{ij}e_{kl}-K_iu_i\right)dV-\int_{S_p}P_iu_i\,dS +\lambda\left(\int_V dV-C\right) \quad\longrightarrow \text{stationary}, \quad \text{shape}, u_i, \lambda \tag{1}$$

where u_i, K_i, and P_i are components of the vectors of the displacement, the body force, and the surface force, respectively. The displacement u_i is an admissible function which is related to the strain e_{ij} by

$$e_{ij}=\frac{1}{2}(u_{i,j}+u_{j,i}), \text{ where } u_{i,j}=\frac{\partial u_i}{\partial x_j} . \quad (2)$$

The linear elastic stress-strain relation

$$\sigma_{ij}=C_{ijkl}e_{kl} \quad (3)$$

is assumed in the problem (1). V is an admissible region of the volume integration, S is an admissible one of the surface integration, and S_p is a subregion of S, where tractions are prescribed. C is a given constant for the volume constancy and λ is a corresponding Lagrange multiplier. In Eq.(1), independent variables subject to the variations are the displacement u_i, the Lagrange multiplier λ, and the shape of the body. From the first variation of Eq.(1), the equation of the equilibrium in V, the boundary conditions on S_p, the equation of the volume constancy, and the condition for the optimality of the shape are obtained.

2.2 Discretized Model by Finite Element Method

For the purpose of broad applications to any practical problem, a discrete version of the inverse variational principle is formulated by means of the displacement approach of the finite element method.

In the following, it is assumed that the shape of a body can be described by appropriate variables $\boldsymbol{\Theta}$ [$\boldsymbol{\Theta}=\{\theta_i\}$, $i=1,\cdots,n$]. For example, θ_i is a radius of a circular bar or a height of a cross section of a beam at a joint in the one-dimensional (axial and flexural) elements [Fig.1-(a)]. In the two-dimensional (planar) elements, it is a thickness of an element [Fig.1-(b)], or a coordinate of a nodal point on the outer surface [Fig.1-(c)]. We refer those variables as shape variables.

Then, the functional for the discretized model which is corresponding to Eq.(1) is written as follows.

$$\Omega=\frac{1}{2}w^T K(\Theta) w - w^T p+\lambda\{V(\Theta)-C\} \longrightarrow \text{stationary}, \quad (4)$$
$$w, \Theta, \lambda$$

where K is the stiffness matrix, w the vector of nodal displacements, and p the vector of nodal forces. The stiffness matrix K and the volume V of the body are expressed in terms of the shape variables Θ. The partial differentiation of Eq.(4) with respect to the nodal displacements w, the shape variables Θ, and the Lagrange multiplier λ provide the equilibrium equation, Eq.(5), the equation for the shape determination, Eq.(6), and the equation of the volume constancy, Eq.(7), respectively, which constitute a system of highly nonlinear algebraic equations:

$$\begin{cases} K(\Theta) w = p & (5) \\ \frac{1}{2} w^T \frac{\partial K(\Theta)}{\partial \theta_i} w+\lambda \frac{\partial V(\Theta)}{\partial \theta_i}=0 \quad (i=1,\cdots,n) & (6) \\ V(\Theta)=C . & (7) \end{cases}$$

3. Energy Ratio Method

The system of equations obtained will be solved effectively by the use of an iterative procedure called "Energy Ratio Method"(19). The following is the summary of the procedure.

By the introduction of new quantities λ_i such that

$$\lambda_i=-\frac{1}{2} w^T \frac{\partial K}{\partial \theta_i} w \Big/ \frac{\partial V}{\partial \theta_i} \quad (i=1,\cdots,n), \quad (8)$$

Eq.(6) is reduced to

$$\lambda_i-\lambda=0 \quad (i=1,\cdots,n). \quad (9)$$

In the process of iterative shape reformations, first of all, the numerical analysis to the current structural shape is accomplished by solving Eq.(5). Substituting the resulting displacement w into Eq.(8), the λ_i's are calculated. From the requirement, Eq.(9), an iterative algorithm to make λ_i's equal to each other is

$$\delta\theta_i=\alpha\, sgn\left(\frac{\partial V}{\partial \theta_i}\right) \cdot log|\lambda_i/\bar{\lambda}| , \quad (10)$$

where $\bar{\lambda}$ is a mean value of n λ_i's as an approximate value of the real value of Lagrange multiplier λ, $sgn(x)$ is the sign of x, and α is an appropriate coefficient, for example, α is taken as $D_*/20 \sim D_*/10$, where D_* is a representative size of the initial shape in the direction of the shape reformation. The algorithm, Eq.(10), corresponds to thickening the body when $|\lambda_i|$ is greater than $|\bar{\lambda}|$ and otherwise to thinning it.

The new body thus obtained may violate the volume constraint, then, in the second place, the shape variables Θ are modified in equal ratio with the use of Taylor's expansion so that its volume may be equal to a given constant C. By this iterative method which is composed of two stages of shape modification, the optimal shapes will be obtained stably.

4. Numerical Examples

As a practically useful model, two-dimensional (planar) elements subject to the variations of nodal coordinates are discussed through two examples.

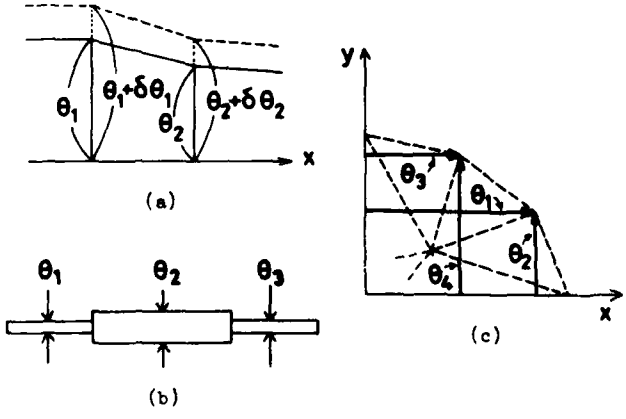


Fig.1 Shape Variables
(a) sizes at joints
(b) thicknesses
(c) nodal coordinates

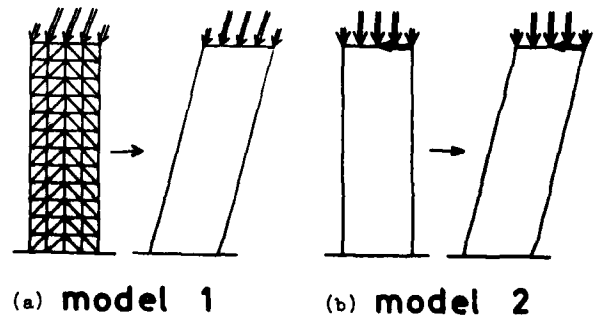


Fig.2 Column
(a) model 1
(b) model 2

Fig.2(a) shows a column subject to a uniformly distributed load on its upper surface. Abscissae of the nodes on the column sides are selected as the shape variables. It is assumed that nodes along the foundation are active, but nodes on the upper surface are inactive. Internal nodes on the horizontal cross sections are always located with equal spacing. The final shape of uniform strength is shown on the right of the initial shape. The central axis of the final shape is parallel with the direction of the load.

The second example is a Γ-shaped structure subject to a load on its protrudent head [Fig.3(a)]. Abscissae of nodal points on the right side of the body are shape variables in this case. Internal points are dealt with in the similar manner as in the previous example. In the final shape, the stress distribution is uniform along the right side [Fig.3(b)].

Fig.4 shows the behaviour of the potential energy, Π_s, with the number of iterations. It is seen that the potential energy increases toward its maximum as the shape reformation process.

From these two and another examples, the following is concluded: the shape obtained by the proposed method is the stiffest one in the sense that the strain energy is minimum among those of all structures with the given volume, and each quantity $|\lambda_i|$, which corresponds to the strain energy density at a part of the structure, is equal to a certain quantity $|\lambda|$.

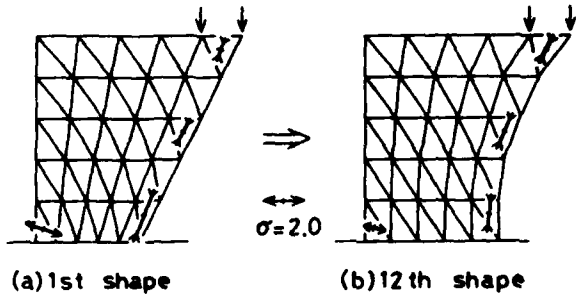


Fig.3 Γ-shaped structure
(a) initial
(b) final

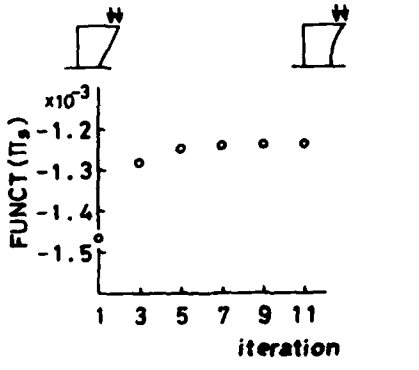


Fig.4 Process to convergence

5. Problem of Maximizing Eigenvalue

From the character of the inverse variational principle that it considers the extremum of a quantity which is defined on the whole structure, the principle is applicable to the optimal shape determination problems for a body with the highest buckling load or fundamental frequency.

5.1 Eigenvalue Problem

In a body V, let x be a variable representing location, $s(x)$ a function expressing a shape of the body, and $v(x)$ a displacement function. We define two energy functionals $D(s,v)$ and $T(s,v)$ dependent on the above two functions. D is a strain energy, and T stands for the work done by a unit load in the buckling problem or a kinetic energy in the free vibration problem. In order to formulate the problem of maximizing eigenvalue by the inverse variational principle, the following inverse variational problem is set up, referring to the method under the static load condition in the former chapter.

"Determine the shape $s(x)$, the eigenvalue μ, and the eigenfunction $v(x)$ which make the functional $D(s,v)$ stationary under the subsidiary conditions that another functional $T(s,v)$ and the volume $V(s)$ are constant",

which is written in the Lagrangian functional as [(21)]

$$\Omega=D(s,v)-\mu\{T(s,v)-k_T\}+\lambda\{V(s)-C\} \xrightarrow[v,s,\mu,\lambda]{} \text{stationary.} \quad (11)$$

The stationary conditions of Eq.(11) are

$$\begin{cases} \dfrac{\partial D}{\partial v}-\mu\dfrac{\partial T}{\partial v}=0 & (12)\\ \dfrac{\partial D}{\partial s}-\mu\dfrac{\partial T}{\partial s}+\lambda\dfrac{dV}{ds}=0 & (13)\\ T(s,v)=k_T & (14)\\ V(s)=C\ . & (15) \end{cases}$$

Equations (12)~(15) are identical with those of conventional formulations which maximize Rayleigh's quotient [(1),(22)~(24)].

5.2 Functional

5.2.1 Buckling Problem Consider a column with length l, and denote its axial coordinate and transverse deflection by x and $w(x)$, respectively. In the buckling problem, the change in the potential energy during the buckling is investigated. In other words, the increase in the strain energy by bending and the decrease in the potential energy of the axial load P are taken as the functionals D and T, respectively. Then, the inverse variational problem that aims to maximize the buckling load P is written as

$$\Omega=\frac{1}{2}\int_0^l EI\left(\frac{d^2w}{dx^2}\right)^2dx-P\left\{\frac{1}{2}\int_0^l\left(\frac{dw}{dx}\right)^2dx-k_T\right\}+\lambda\left(\int_0^l A\,dx-C\right) \xrightarrow[s,w,P,\lambda]{} \text{stationary,} \quad (16)$$

where E, I, and A are Young's modulus, the second moment of area, and the cross-sectional area of the column, respectively.

5.2.2 Free Vibration Problem In the free transverse vibration of an elastic beam, its deflection is denoted by $y(x,t)$. The strain and kinetic energies of the beam for the infinitesimal deformation are given as

$$U=\frac{1}{2}\int_0^l EI\left(\frac{\partial^2 y}{\partial x^2}\right)^2dx \quad (17)$$

and

$$K=\frac{1}{2}\int_0^{\ell}\rho A\left(\frac{\partial y}{\partial t}\right)^2 dx \quad , \tag{18}$$

respectively, where ρ is a density. Denoting the amplitude of the deflection by $w(x)$, it is assumed that

$$y(x,t)=w(x)g(t) \ . \tag{19}$$

Then, from the Hamilton's principle, the energy functional for $w(x)$ is expressed as

$$\Omega=\frac{1}{2}\int_0^{\ell}EI\left(\frac{d^2w}{dx^2}\right)^2 dx-\mu\left(\frac{1}{2}\int_0^{\ell}\rho Aw^2 dx-k_T\right)$$
$$+\lambda\left(\int_0^{\ell}A dx-C\right) \quad \longrightarrow \ \underset{s,w,\mu,\lambda}{\text{stationary}} . \tag{20}$$

When a certain shape s is given, the stationary condition of Eq.(20) with respect to w makes μ be the minimum eigenvalue for the shape, μ_s, where the square root ν_s of μ_s, that is,

$$\nu_s=\sqrt{\mu_s} \tag{21}$$

is the fundamental frequency for the shape s.

5.3 Discretization

The above mentioned problems are solved by discretizing a bar into flexural elements. In the first place, it is assumed that the bar consists of n elements, in which their contours vary linearly [Fig.1(a)]. Thus, if the bar has a circular cross section, the radius distribution of the cross section in an element, $a(x)$, is expressed in terms of the values at nodal points of the element [Fig.5].

In the second place, the transverse displacement in an element is assumed to be cubic, so that the deflection $w(x)$ in the i-th element is expressed in terms of the deflections at the nodes and of deflection angles there [Fig.6]. Substituting these interpolation functions into the functionals (16) or (20), and arranging the resulting equation in terms of the nodal deflection W^i, the nodal deflection angle θ^i, and the shape variable a^i, then the objective function, which is to be stationary, is written as

$$\Omega=\frac{1}{2}\mathbf{w}^T K(a^1,a^2,\cdots,a^{n+1})\mathbf{w}-\mu\left\{\frac{1}{2}\mathbf{w}^T M(a^1,\cdots,a^{n+1})\mathbf{w}-k_T\right\}$$
$$+\lambda\left\{V(a^1,\cdots,a^{n+1})-C\right\} \longrightarrow \underset{\{a^i\},\mathbf{w},\mu,\lambda}{\text{stationary}} , \tag{22}$$

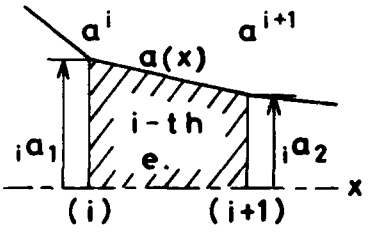


Fig.5 Model of bar

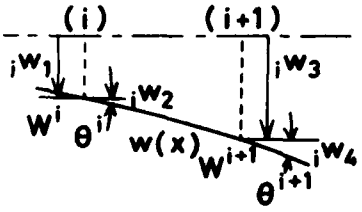


Fig.6 Deflection

where $\mathbf{w}$ is given by

$$\mathbf{w}=\{W^1,\theta^1,\cdots\cdots,W^{n+1},\theta^{n+1}\}^T \ . \tag{23}$$

In the buckling problem, μ is regarded as the axial load P. From the variation of Ω in Eq.(22) with respect to the nodal displacements $\mathbf{w}$, the shape variable a^i, and the Lagrange multipliers μ and λ, the stationary conditions of Eq.(22) are obtained as

$$\begin{cases} K\mathbf{w}=\mu M\mathbf{w} & (24)\\ \frac{1}{2}\mathbf{w}^T\frac{\partial K}{\partial a^i}\mathbf{w}-\mu\frac{1}{2}\mathbf{w}^T\frac{\partial M}{\partial a^i}\mathbf{w}+\lambda\frac{\partial V}{\partial a^i}=0 \quad (i=1,\cdots,n+1) & (25)\\ \frac{1}{2}\mathbf{w}^T M\mathbf{w}=k_T & (26)\\ V(\{a^i\})=C \ . & (27) \end{cases}$$

Equation (24) is an eigenvalue equation, Eq.(25) is an equation for the shape determination, and Eq.(27) is of the volume constancy. The norm of the eigenfunction is given by Eq.(26), and λ in Eq.(25) is dependent on it. We solve the above system of nonlinear equations by the Energy Ratio Method proposed in Ch.3.

5.4 Numerical Examples

Fig.7 illustrates the results of the buckling problem for columns with circular cross section; Fig. 7(a) being the case of clamped-free condition, (b) both-end-hinged, (c) clamped-hinged, and (d) both-end-clamped. In the last case, only the left side is considered for symmetry. The abscissa ξ is a non-dimensional axial coordinate x/l, and the ordinate r represents a/a_{uni}, where a_{uni} is the radius of uniform radius column, that is, $a_{uni}=\sqrt{C/(\pi l)}$. P_{uni} is the buckling load for a uniform radius column, and P is that for an obtained column.

Fig.8 shows the results of the problem of maximizing the fundamental frequency in the free vibration. ν/ν_{uni} is the ratio of the fundamental frequency of the optimal beam to that of the uniform radius beam.

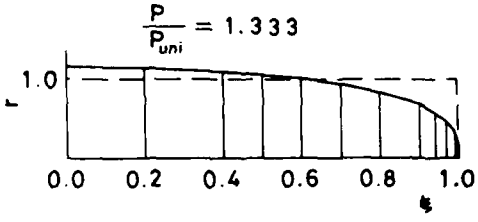
The above results are in good agreement with the analytical and numerical solutions by the conventional methods (22),(23).

6. Effects of Boundary Conditions on the Optimum Shapes

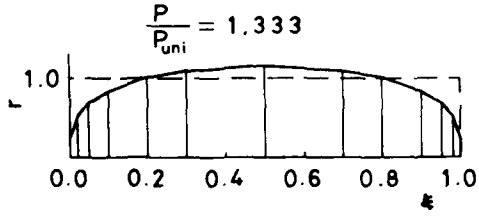
In practical situations, structures may become to be subject to load and support conditions which are different from those which were set in the (original) design. If the behaviours of the bodies are sensitive to their boundary conditions, the safety of the structures may be damaged in some cases. Accordingly, in this study, it is examined how optimum shapes will be affected by changes in boundary conditions.

6.1 Compression of Column

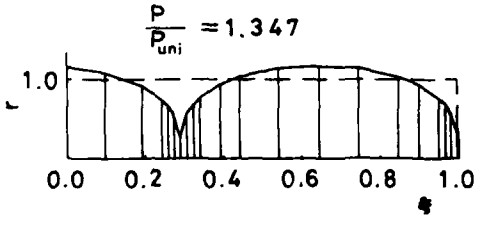
The first example is a similar model to Fig.2(a), except that instead of uniformly distributed horizontal load, an equivalent, concentrated load acts at the center of the upper surface [Fig.2(b)]. The final shape is almost the same as that of Fig.2(a). This similarity between the two models is able to be interpreted by the Saint-Venant principle. In this example, the difference of modeling of loads doesn't have effect on optimum shapes.



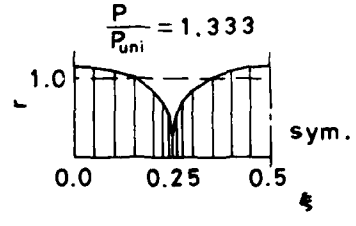
(a)



(b)

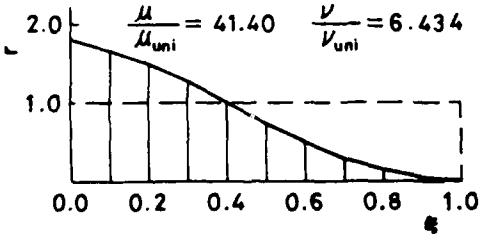


(c)

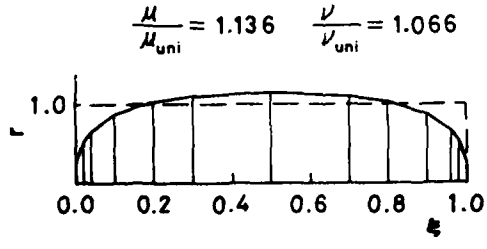


(d)

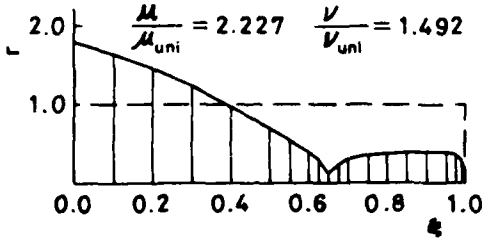
Fig.7 Optimum columns
(a)clamped-free (b)hinged-hinged
(c)clamped-hinged (d)clamped-clamped



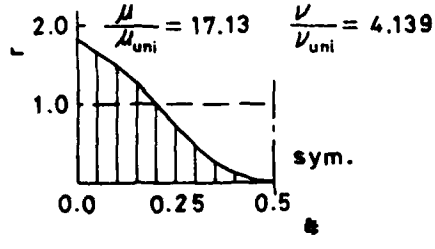
(a)



(b)



(c)



(d)

Fig.8 Optimum beams
(a)clamped-free (b)hinged-hinged
(c)clamped-hinged (d)clamped-clamped

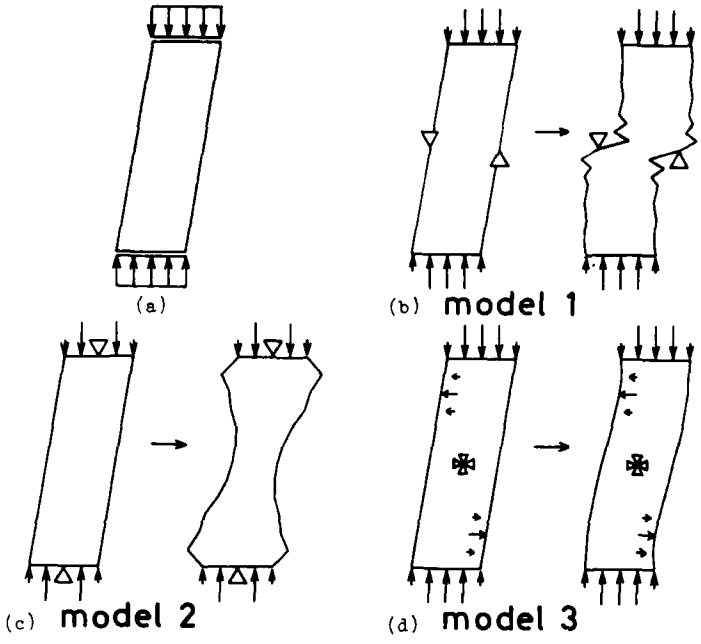


Fig.9 Oblique columns
(a) basic condition
(b)model 1 (c)model 2 (d)model 3

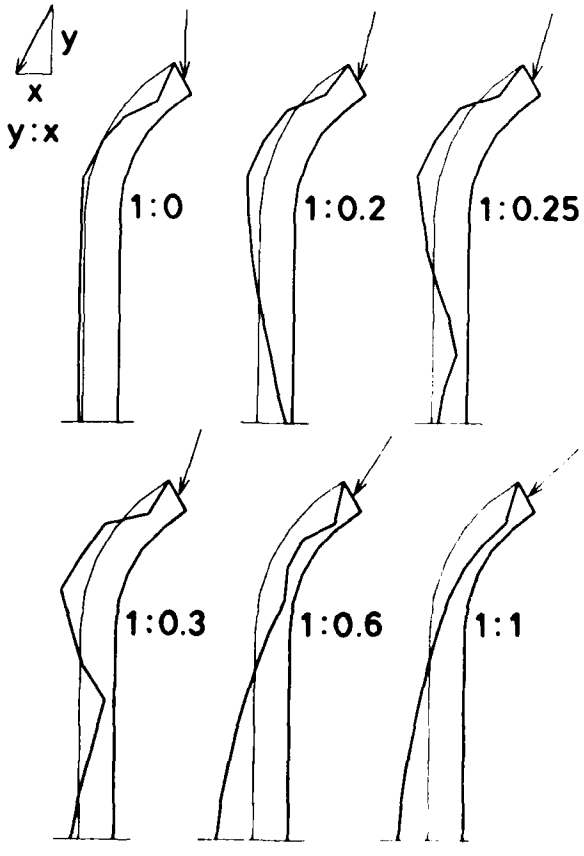


Fig.10 Curved beams

6.2 Oblique Column

An oblique column is subject to uniformly distributed compressive load on its upper and lower surfaces. We want to determine the optimum shape of this structure under the condition that the nodes on its upper and lower surfaces are inactive [Fig.9(a)]. To meet static equilibrium requirement, the following three models are examined:

Model 1. As shown in Fig.9(b), two supporting points are provided on the centers of both sides.

Model 2. It is assumed that this structure is jointed with other members by pins. Thus, two supporting points are set on the centers of both upper and lower surfaces [Fig.9(c)].

Model 3. The centroid of the body is fixed, and then the coupling forces are applied [Fig.9(d)].

These results show that among the statically equivalent loading conditions, the possible different modelings produce different shapes and it is necessary to pay careful attention to modeling of boundary conditions not given in advance.

The above example is introduced to the analysis of a shape for a collarbone of human being. The model 3 suggests the optimality of the shape of the collarbone.

6.3 Curved Beam

In Fig.10, optimum shapes for curved beams are shown against various concentrated loads, where only nodal points on the left surface are active shape variables. These curved beams are simple models for femurs of human being. Fig.10 shows that depending on the direction of the applied concentrated load, the optimum shape varies.

7. Conclusions

A numerical shape determination procedure based on the inverse variational principle and the finite element method is summarized, and the advantages of the variational approach and the effectiveness of the Energy Ratio Method to solve a system of nonlinear equations obtained are shown for static and eigenvalue structural problems. The effects of boundary conditions on optimum shapes are also discussed. It is shown that the analyses of several models selected from the statically equivalent loading conditions may yield different optimum shapes. This suggests that even if a structure is optimum with respect to certain boundary conditions set initially, the optimality might be violated with changes in boundary conditions or loading conditions after the lapse of years.

The optimal shape based on the inverse variational principle is a limiting case of the natural structural shape(25). In this sense, the shapes obtained can be useful for designers to evaluate various engineering optimal shapes of structures or to search better structural shapes in design process.

References

(1) Prager, W. & Taylor, J. E., Problems of Structural Design, Trans. ASME, Ser.E, 35-1(1968-3), 102.

(2) Taylor, J. E., Optimal Design of Structural Systems: An Energy Formulation, AIAA J., 7-7(1969-7), 1404.

(3) Huang, N. C. , Optimal Design of Elastic Structures for Maximum Stiffness , Int. J. Solids Struct., 4-7(1968-7), 689.

(4) Chern, J. M. & Prager, W. , Optimal Design of Beams for Prescribed Compliance under Alternative Loads, JOTA, 5-6(1970-6), 424.

(5) Masur, E. F. , Optimum Stiffness and Strength of Elastic Structures , Proc. ASCE , J. Engng. Mech. Div., 96-EM5(1970-10), 621.

(6) Martin, J. B. , The Optimal Design of Beams and Frames with Compliance Constraints , Int. J. Solids Struct., 7-1(1971-), 63.

(7) Huang, N. C. & Tang, H. T., Minimum-Weight Design of Elastic Sandwich Beams with Deflection Constraints, JOTA, 4-4(1969-10), 277.

(8) Shield, R. T. & Prager, W. , Optimal Structural Design for Given Deflection , ZAMP, 21-4(1970-7), 513.

(9) Huang, N. C. , On Principle of Stationary Mutual Complementary Energy and its Application to Optimal Structural Design, ZAMP, 22- (1971-), 608.

(10) Huang, N. C. , Minimum Weight Design of Elastic Cables, JOTA, 15-1(1975-1), 37.

(11) Umetani, Y., J. Japan Soc. Mech. Engrs. (in Japanese), 79-693(1976-8), 749.

(12) Gallagher, R. H. & Zienkiewicz, O. C. (Ed.), Optimum Structural Design--Theory and Applications, (1973), John Wiley & Sons.

(13) Hegemier, G. A. & Tang, H. T., (Ed. Sawczuk, A. & Mróz, Z.) , "A Variational Principle, the Finite Element Method, and Optimal Structural Design for Given Deflection", Optimization in Structural Design , IUTAM Sympo. , Poland, (1973-8), Springer-Verlag, 464.

(14) Rossow, M. P. & Taylor, J. E. , A Finite Element Method for the Optimal Design of Variable Thickness sheets, AIAA J., 11-11(1973-11), 1566.

(15) Umetani, Y. & Hirai, S. , An Adaptive Shape Optimization Method for Structural Material Using the Growing-Reforming Procedure , JSME Papers (1975 Joint JSME-ASME Applied Mechanics Western Conf.), Honolulu, (1975-3), 359.

(16) Oda, J., J. Japan Soc. Mech. Engrs. (in Japanese), 79-691(1976-6), 494.

(17) Tsuta, T. & Yamaji, S. , "Finite Element Analysis of Thick-Walled Structure by Using Legendre Function and its Shape Optimization", Proc. Sympo. on Appl. of Comp. Meth. in Engng., (Ed. by Wellford, L. C. Jr.), vol. II, (1977-8), 859, USC.

(18) Horák, V., Inverse Variational Principles of Continuum Mechanics, (1969), 26, Rozpravy Československé Akad. Věd.

(19) Seguchi, Y. & Tada, Y. , "Shape Determination Problems of Structures by Inverse Variational Principle/ The Finite Element Formulation", ACTA TECHNICA ČSAV, 24-2(1979-), 139, Proc. Sympo. on Appl. of Comp. Meth. in Engng., (Ed. Wellford, L. C. Jr.), vol. II, (1977-8), 899, USC.

(20) Hamada, M., Seguchi, Y. & Tada, Y. , Shape Determination Problems of Structures by the inverse Variational Principle (2nd Report, Buckling and Vibration Problems) , Bull. of JSME, 23-184(1980-10), 1581.

(21) Hayashi, T. & Mura, T. , Calculus of Variations (in Japanese), (1958), 130, Corona.

(22) Tadjbakhsh, I. & Keller, J. B., Strongest Columns and Isoperimetric Inequalities, Trans. ASME, Ser. E, 29-1(1962-3), 159.

(23) Niordson, F. I. , On the Optimal Design of a Vibrating Beam , Quart. Appl. Math. , 23-1(1965-4), 47.

(24) Yamakawa, H. and Okumura, A. , Trans. Japan Soc. Mech. Engrs. (in Japanese), 42-356(1976-4), 1109.

(25) Stadler, W., Natural Structural Shapes (The Static case), Q. Jl. Mech. Appl. Math., 31-2(1978-5), 169.

AD-P000 053

OPTIMAL SHAPE DESIGN

OF TURBINE AND COMPRESSOR BLADES

J.P. QUEAU - Assistant

P. TROMPETTE - Professor - ASME Member

Laboratoire de Mécanique des Structures. ERA - CNRS 911 -

Bâtiment 113 - INSA -

69621 Villeurbanne

ABSTRACT

In this paper a general engineering method to minimize the weight of rotating turbine or compressor blades is presented. The cross section shapes are optimized using the design variables selected by the areodynamicists. The contraints originate from either aerodynamic or solid mechanic specifications. As the problem is reformated after a first finite element analysis the optimization process is quite inexpensive. A large variety of blades can be designed by this method and here, two examples are given which lead to continuous optimal profiles and demonstrate the efficiency of the method.

NOMENCLATURE

a_i, b_j, c_k	design variables
c	chord of a cross section
e	maximum thickness of a cross section
f	deflection of a cross section
f_m, f_M	limit values of e/c(x)
F_c	centrifugal force
g_ℓ	constraints
g_o	transition parameter
g_m, g_M	limit values of $c^2(x)$
H	Hessian matrix
I_m, I_M	minimum and maximum flexural inertia
J	torsional inertia
k_ℓ	added concentrated stiffness
K	stiffness matrix
K_G	geometric stiffness matrix
L	length of the blade
m_k	added concentrated mass
M	mass matrix
M_G	supplementary mass matrix
N_i	resonance frequency
R	root abscissa of the blade
r_p	response factor
S	area of a cross section
u,v,w	local displacements
W	weight of the blade
x	abscissa
α	stagger angle
θ	twist
ϕ_i	mode shape
ρ	mass per unit of volume
Ω	speed of rotation
σ_c	centrifugal stress
$\sigma_{\ell_1}, \sigma_{\ell_2}$	limit values of centrifugal stresses

INTRODUCTION

This paper describes an engineering approach to minimize the weight of compressor or turbine blades, by selecting optimal cross section shapes. The followed procedure offers some practical and significant advantages particulary specially in regards to several previous papers |1|, |2|, |3| : first the design variables are those selected by the aerodynamicists, second no assumptions on the cross section blade profiles are formulated and finally the computer calculations are very economical. Nevertheless it cannot be postulated that the final solution is mathematically the best and unique but this lack in the process has only minor disatvantages from an engineering point of view.
In such a design there are two parts : the analysis of the structure and the optimization process itself. Here the analysis of the structure is performed in two steps: at start the finite element analysis, then a reduction technique are used . In order to decrease the number of design variables, to obtain continuous blade profiles, polynomial fittings of all the mechanical characteristics are retained and the optimization process is conducted on the coefficients of these polynomials. In this part a well known interior extended penalty function |4| is used. The constraints are either aerodynamic or mechanic. Two applications concerned with actual compressor or turbine blades and various boundary conditions are presented. The details of the optimization algorithm, the computer program and the method itself have been described in |5|.

DESIGN VARIABLES - OBJECTIVE FUNCTION - CONSTRAINTS

In aeronautics, compressor or turbine blades are decided upon by aerodynamic design engineers for jet engine efficiency reasons. The variables used by these designers are the chord c, the thickness/chord ratio e/c, and the deflection chord ration f/c (Figure 1).
The relations between these variables and the mechanical characteristics of the blades, namely the maximum and minimum flexural inertia I_M, I_m, the cross section area S and constant torsion J are generally empiric.

PRECEDING PAGE

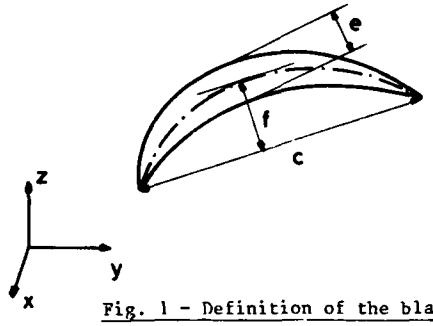


Fig. 1 - Definition of the blade

Noting :

$$y = e/c\ (x) \tag{1}$$

$$z = c^2\ (x) \tag{2}$$

$$z_1 = (f/c)^2(x) \tag{3}$$

where x is the abscissa of a cross section, it can be established that convenient formula for the presented applications are :

$$S = A_1 yz + B_1 yzz_1 \tag{4}$$

$$I_M = A_2 yz^2 + B_2 yz^2 z_1 \tag{5}$$

$$I_m = A_3 y^3 z^2 + B_3 y^3 z^2 z_1 + C_3 yz^2 z_1 + D_3 yz^2 z_1{}^2 \tag{6}$$

$$J = A_4 y^3 z^2 \tag{7}$$

Constants A_i, B_i, C_i, D_i are either known (N.A.C.A. profiles) or searched by a best approximation fitting technique.

It could seem logical and efficient to select these aerodynamical variables, e/c, f/c, as design variables but in practical applications they are only rarely analytical functions of x. This difficulty can be overcome by selecting numerical point data tables, such nodal values. This approach results in many design variables, increases the size of the problem and during the optimization process leads to numerous, computer time consuming F.E. calculations. That are the reasons why polynomial fittings have been retained, thus is it written :

$$e/c = y = \sum_{i=o}^{n} a_i x^i \tag{8}$$

$$c^2 = z = \sum_{i=o}^{m} b_j x^i \tag{9}$$

$$(f/c)^2 = z_1 = \sum_{k=o}^{p} c_k x^k \tag{10}$$

Consequently the coefficients a_i, b_j, c_k, are now the design variables. Their initial values are obtained from the fitting of the initial blade shape data which is satisfactory as a first approximation. Inserting (8), (9), (10) in (4), (5), (6) gives S, I_M, I_m and J as functions of a_i, b_j, c_k.

OBJECTION FUNCTION

The objective function is the weight of the blade which is given by the integral :

$$W = \int_R^{R+L} \rho\ S(x)\ dx \tag{11}$$

where R is the root abscissa, L the length, ρ the mass per unit of volume. Using (4) W can be written :

$$W(a_i,b_j,c_k) = \sum_{\ell=o}^{n+m+p} \rho\ d_\ell\ (a_i,b_j,c_k) \left| \frac{(R+L)^{\ell+1} - R^{\ell+1}}{\ell+1} \right|$$

Here coefficients d_ℓ are polynomial functions of the design variables a_i, b_j, c_k.

CONSTRAINTS

Constraints originate from either aerodynamic or solid mechanic specifications. At first the relative pitch, which is a function of the chord c and of the number N_b of blades, is allowed to vary in a relatively narrow interval at the root and the top of the blade. These limitations lead to upper and lower bounds on c and e/c at x = R and R + L. It is assumed that in the interval (R, R + L) the variations noted f_M, g_M, f_m, g_m are either linear or quadratic. Thus :

$$f_m(e/c(x)) \leq e/c(x) \leq f_M(e/c(x)) \tag{13}$$

$$g_m(c^2(x)) \leq c^2(x) \leq g_M(c^2(x)) \tag{14}$$

$$h_m(f/c^2(x)) \leq f/c^2(x) \leq f_M(f/c^2(x)) \tag{15}$$

$R \leq x \leq R + L$ (figure 2)

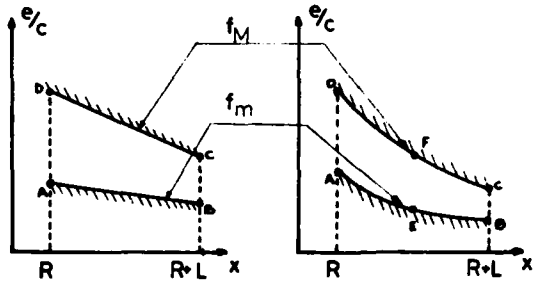


Fig. 2 - Limitations of e/c(x)

The mechanical constraints are relative to the centrifugal stress and to the first resonance frequencies N_i, (i = 1,2, ...). It is supposed that the maximum of the centrifugal stress for x > R is less than a limiting value $\sigma_{\ell 1}$ and that for x = R, σ_c is less than $\sigma_{\ell 2}$.

$$\max |\sigma_c| \leq \sigma_{\ell 1} \quad R < x \leq R + L \tag{16}$$

$$\sigma_c \leq \sigma_{\ell 2} \tag{17}$$

The relation between σ_c and the design variables is obtained by :

$$\sigma_c = F_c/S \tag{18}$$

in which F_c is the centrifugal force calculated by :

$$F_c(x) = \int_x^{L+R} \rho\ S(y)\Omega^2\ y\ dy + \sum_{k=1}^{M} m_k\ \Omega^2\ x_k \tag{19}$$

m_k possible added concentrated mass in the interval (x, L + R).

The last mechanical constraints are introduced by assuming a relative stability of the first resonance frequencies of the blade during the optimization. These limitations can be written :

$$N_{\ell m} < N_\ell < N_{\ell M} \quad \ell = 1,2,\ldots \qquad (20)$$

with

$$N_{\ell m} \neq N_{\ell M}$$

The resonance values N_ℓ are the eigenvalues of the matrix equation :

$$(M + K + K_G - M_G\Omega^2)\{\delta\} = 0 \qquad (21)$$

which has been already used in several previous papers |6|.

δ is the nodal displacement vector,
M is the finite element mass matrix,
K the stiffness matrix, M_G the supplementary mass matrix, K_g the geometric stiffness matrix.
$\lambda = 4\pi^2 N^2$.

In (21) the Coriolis effects have been neglected.

It can be mentionned that all the derivatives of λ, σ_c , F_c which are needed in the optimization procedure, are easily obtained. For example (18) leads to :

$$\frac{\partial \sigma_c}{\partial a_i} = \frac{\partial F_c}{\partial a_i} \cdot \frac{1}{S} - \frac{F_c}{S^2} \cdot \frac{\partial S}{\partial a_i} \qquad (22)$$

and (20) after premultiplying by the vector $\{\delta\}^t$:

$$\frac{\partial \lambda_\ell}{\partial a_i} = \frac{\{\delta_\ell\}^t \,|\partial K/\partial a_i + \partial K_G/\partial a_i - \Omega^2 \partial M_G/\partial a_i - \lambda_\ell \partial M/\partial a_i|\{\delta_\ell\}}{\{\delta_\ell\}^t \,|M|\{\delta_\ell\}} \qquad (23)$$

δ_ℓ, eigenvector associated to λ_ℓ .

BLADE ANALYSIS

In order to determine the mode shapes which will be used in the following analysis, the initial rotating blade is discretized in finite beam elements (six DOF per node). The general integral expressions of the kinetic and potential energies calculated by this method are :

$$T = \frac{1}{2}\int_R^{L+R} \rho S(\dot{u}^2 + \dot{v}^2 + \dot{w}^2)dx + \frac{1}{2}\int_R^{L+R} \rho I_O \dot{\theta}^2 \, dx$$
$$+ \frac{1}{2}\int_R^{L+R} \rho\, \Omega^2 S(w^2\sin^2\alpha + v^2\cos^2\alpha + 2\, wv\cos\alpha)dx$$
$$+ \int_R^{L+R} \rho S\Omega^2\, u(R+x)dx + \frac{1}{2}\sum_k m_k\,(\dot{u}_k^2(x_k) + \dot{v}_k^2(x_k) + \dot{w}_k^2(x_k) \qquad (24)$$

and :

$$U = \frac{1}{2}\int_R^{L+R} ES(u^2{}_{,x})dx + \frac{1}{2}\int_R^{L+R} E(I_M v^2{}_{,xx} + I_m w^2{}_{,xx})dx$$
$$+ \frac{1}{2}\int_R^{L+R} G\,J\,\theta^2{}_{,x}\,dx + \frac{1}{2}\int_R^{L+R} ES(w_{,x}+v)^2{}_{,x}dx \qquad (25)$$
$$+ \frac{1}{2}\sum k_\ell(u^2(x_\ell) + w^2(x_\ell) + v^2(x_\ell) + \theta^2(x_\ell)$$

In which,

α is the stagger angle (it may be a function of x)
$I_o = I_M + I_m$

u,v,w, the displacements in a local coordinate system, Ox' y' z', (figure 3)

θ the twist,

$u_{,x} = \frac{\partial u}{\partial x}$, $u_{,xx} = \frac{\partial^2 u}{\partial x^2}$, $\dot{u} = u_{,t}$

E Young's modulus, G shear modulus, k_ℓ possible added local stiffnesses, m_k possible added concentrated masses.

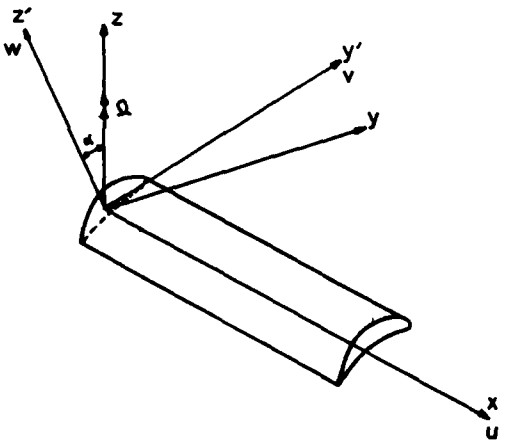


Fig.3 : local coordinate system

The detail of the proofs of (24) and (25) can be found in |7|. Note that non linear terms of strain-displacement relations are taken into account in U (third integral of (25) and that the cross section gravity centers are supposed to be situated along Ox. The discretized form of the Lagrange's equations deduced from the integrals (24) and (25) is the equation (21).

After the first finite element calculation the p mode shapes of the initial blade :

$$\phi_1 , \phi_2, \ldots, \phi_p$$

with the component ϕ_{1u}, ϕ_{1v}, ϕ_{1w}, $\phi_{1\theta}$, ... are known at the nodal points of the mesh. They are fitted by polynomials :

$$\phi_{1_u} = \sum_{k=0}^{\ell_1} \beta_{uk}\, x^k \qquad (26)$$

$$\phi_{1_v} = \sum_{k=0}^{\ell_2} \beta_{vk} \, x^k \qquad (27)$$

and used to make the classical variable change

$$\{\delta\} = |\phi| \, \{q\} \qquad (28)$$

This means that (24) and (25) are calculated in all the following steps of the optimization sheme by new formula. For example it is obtained for T :

$$T = \frac{1}{2}\int_R^{L+R} \rho \, \{\dot{\delta}\}^t |\phi|^t \begin{vmatrix} S & S & 0 \\ 0 & & I_o \end{vmatrix} |\phi| \, \{\dot{q}\} \, dx$$

$$= \frac{1}{2} \int_R^{L+R} \rho\Omega^2 S \, \{q\}^t \, |\phi|^t \begin{vmatrix} 0 & 0 & 0 & 0 \\ & c & cs & 0 \\ & & s & 0 \\ \text{sym.} & & & 0 \end{vmatrix} |\phi| \, \{q\} \, dx$$

$$+ \int_R^{L+R} \Omega^2 \rho S \, (R+x) \, \{\phi_{1u}, \ldots, \phi_{pu}\}^t \, \{q\} \, dx$$

$$+ \frac{1}{2} \Sigma \, m_k \, \{\dot{q}\}^t \, |\phi(x_k)| \, \{\dot{q}\} \qquad (29)$$

$c^2 = \cos^2\alpha$, $cs = \cos\alpha \sin\alpha$, $s^2 = \sin^2\alpha$

After the calculation of the derivatives of (26), (27) with respect to x, a similar transformation is easily applied to the integral form (25) of U.

It must be pointed out that these new integrals which yield T and U are computationally inexpensive, as they are composed of polynomials. Further the different powers of x are integrated only once by the numerical Gauss point method.

OPTIMIZATION PROCESS

It has been mentionned in the introduction that the optimization process uses an extended interior penality function - i. e. the function of Kavlie |4|. The search of the minimum of the objective function $W(a_i, b_j, c_k)$ which is constrained by the different limitations $g_j(a_i, b_j, c_k)$ is replaced by the search of the minima of the sequence of the unconstrained functions :

$$\phi(a_i,b_j,c_k,r_p) = W(a_i,b_j,c_k) + r_p \left[\sum_{\ell=1}^{J_A} \frac{1}{g_\ell} + \sum_{\ell=J_A+1}^{J} \frac{2 - g_\ell/g_o}{g_o} \right] \qquad (30)$$

Where J is the total number of limitations, J_A the number of these which are satisfied ; g_o is the transition parameter and r_p the response factor. Each value of r_p in the process defines a response surface. Here the method retained to find the minimum of ϕ is due to Davidon Broyden |8|.It can for a given r_p, be briefly summarized in the six following steps :

1 - the choice of a starting point x_o,
2 - the determination $\phi(x_o, r_k)$, $\nabla\phi(x_o, r_k)$. The initial hessian matrix H_o (second derivatives) is the unity matrix,
3 - the calculation of the minimizing direction at the step q by :

$$S_q = - H_q \, \nabla\phi_q \quad (S_o = - \nabla\phi_o) \qquad (31)$$

4 - the calculation of the step α_q in this direction by :

$$x_{q+1} = x_q + \alpha_q \, S_q \qquad (32)$$

in which three formulas for α_q are available,

5 - the determination of the modified hessian, and of the new value of $\phi(x_{q+1}, r_k)$,
6 - return in (4) or stop and take if necessary a new value of r_p.

For all details or this part and also for the strategy in choosing the evolution of r_p, the value of g_o,... the reader can consult the papers |8|, |9|, |10|.

APPLICATIONS

The proposed method has been applied to the determination of the optimal design of two actual turbine and compressor blades manufactured by SNECMA. In these two examples the ratio f/c is not allowed to vary during the optimization process, So the design variable are the coefficients ai and b_j. The numerical values of the characteristics of the initial blades are given in a non dimensional form.

a) Turbine blade

The relative variations of c and e/c from top to the root of the initial blade are :

$$1 < c(x) < 0.92$$
$$1 < e/c\,(x) < 0.76 \qquad \text{Fig. 4}$$
$$\alpha_{top} - \alpha_{root} = 27°$$

The material characteristic are :

$E = 0.2\ E + 12\ N/m^2$, $\nu = 0.3$, $\rho = 7900\ kg/m^3$

The exact and fitted values of S.Im, IM, J are in satisfactory agreement as it has been show in |11|.

The specifications given by the manufacturer are :

$e/_c$ (root)		- 1,2 % ,+ 15 %
$e/_c$ (top)		- 7,3 % ,+ 50 %
c (root)		- 6 % ,+ 15 %
c (top)		- 20% ,+ 10 %
N_1 first N_2 second	bending frequencies	- 1,3%,+ 5,4% - 3,2%,+ 0,5%

First the blade is clamped-free. The results of the optimization process are summarized in table (1) at rest and at the nominal speed of rotation Ω_N. Either the first , the second or the both frequencies can be controlled. When the blade rotates the centrifugal stress is limited to 30 h bars. It has ben concluded in this configuration that the influence of the ration e/c is small in comparison with those of c

which is closed from its limiting value |5|, |11|

	Constraints	deviation of N_1 and/or N_2 %	weight% gain	Number of analysis
optimal blade Ω=0	N_1	2.5	21.5	14
	N_2	0.5	21.5	22
	N_1 and N_2	1.6 and 0.8	21.2	23
$\Omega = \Omega_N$	N_1 and N_2	0.4 and 1.5	20.4	21

Table (1)

In the following the blade is clamped supported, i.e the displacement in the direction oy' and the torsion of the top are restrained. The results of the design are given in table (2) and in the figures 4a) and 4b).

	Constraints	deviation %	weight gain %	Number of analysis
optimal blade $\Omega = \Omega_N$	N_1	1.56	14.5	16
	N_2	1.48	19.6	19
	N_1 and N_2	1.56 and 3	12.1	18

Table (2)

It is noted (see figures 4a and b) that the effects of the two frequency constraints are opposed with respect to variations of c which is shown to be the more sensitive design variable; The weight gain is also less than in the preceding example.

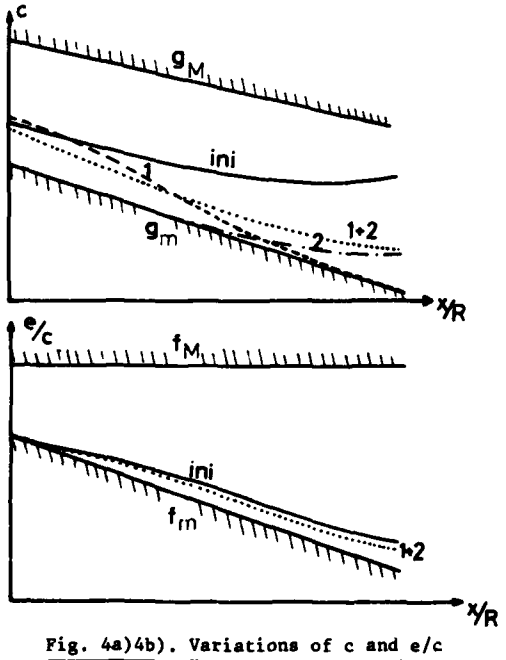


Fig. 4a)4b). Variations of c and e/c

b) Compressor blade

The same procedure has been applied to an actual new compressor blade which is longer than the turbine blabe and very twisted. This example can be considered as a more severe test of the method.

The limitations are :

c root	- 17 %	+ 6 %		
c top	- 0,5%	+ 5,4%		
e/c root	- 8 %	+ 8%		
e/c top	- 3 %	+ 5%		
N_1	- 5 %	+ 2,6%	(Ω=o)	- 6,2% + 2% ($\Omega=\Omega_N$)
N_2	- 5,6%	+ 1,4%		- 3,8% + 0,6%

The fitted values of S, Im. IM have been also found satisfactory (Figures 5 a.b.c). The maximum of the relative error is about 1.2 %. The reduced basis used the six first bending frequencies at rest. The boundary conditions are the following : clamped at the root, θ, V_y = 0 at the top. Table (3) and figures 6a,6b) give the evolutions of the blade shape and the weight gain at the nominal speed.

	Constraints	deviation %	Weight gain %	number of analysis
optimal blade $\Omega = \Omega N$	N_1 and N_2	-6,2 and 2,1 %	19.3	15

table (3)

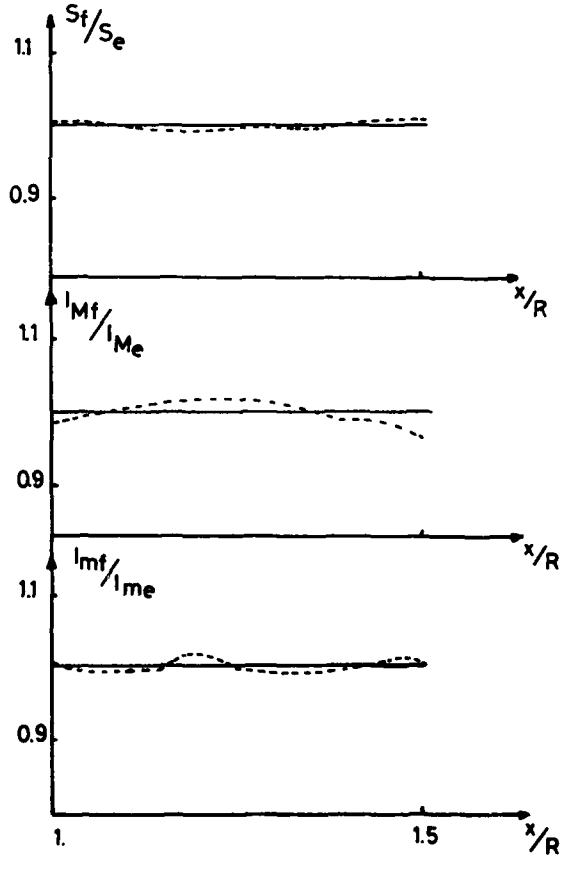


Fig. 5 a.b.c. The fitted values of $S.I_M.I_m$

CONCLUSION

A general method to minimize the weight of actual compressor or turbine blades has been presented. It a shown to give satisfactory results. As the problem has been reformated the number of finite element analyses has been reduced to two. Thus the optimization process is quite inexpensive and can be applied, to a large variety of blades with only minor changes in the relations (4), (5), (6).

ACKNOLEDGEMENTS

The authors are grateful to the S.N.E.C.M.A. in authorizing the publication of this paper.

REFERENCES

|1| B.M.E. DE SILVA, B. NEGUS, B. WORSTER
Penalty function type optimal control methods for the design of turbine blade profiles.
N.A.S.A. Report N76 11464, 1975.

|2| B.M.E. DE SILVA, G.N.C. GRANT, B.L. PIERSON
Conjugate gradient optimal control methods for the design of turbine blades.
N.A.S.A. Report N76 11463, 1975

|3| B.M.E. DE SILVA, G.N.C. GRANT
Comparison of some optimal control method for the design of turbine blades.
A.S.M.E. Paper No 77 Det 43, 1978.

|4| D. KAVLIE
Optimum design of statically indetermined structures.
Ph. Thesis, Berkeley, 1971

|5| J.P. QUEAU
Quelques problèmes d'optimisation en mécanique des structures.
Thèse, 1981.

|6| R. HENRY, M. LALANNE
Vibration analysis of rotating compressor blades.
Journal of Eng. for Industry, A.S.M.E., 1028-1035, 1974.

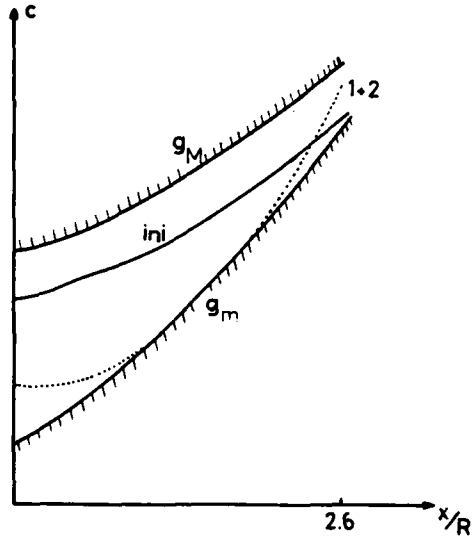
|7| M. LALANNE, P. TROMPETTE, G. FERRARIS
Vibration des ensembles disques-aubes.
Rapport D.R.M.E. n° 7734433, 1978.

|8| C.G. BROYDEN
A class of methods for solving non linear simultaneous equations.
Math. Comput., (19), 92, 577-593, 1965.

|9| J.H. CASSIS, L.A. SCHMIT
On implementation of the extended interior penalty function.
Int. J. for Num. Methods in Eng., (10), 3-23, 1976.

|10| T.A. STRAETER
Davidon Broyden Rank one minimization methods in Hilbert Space with application to optimal control problems .
Langley Research Center, N.A.S.A.

|11| J.P QUEAU, Ph TROMPETTE
Optimal shape design of turbine blades.
A.S.M.E. Vibration Conferences. Septembre 81 Hartford.



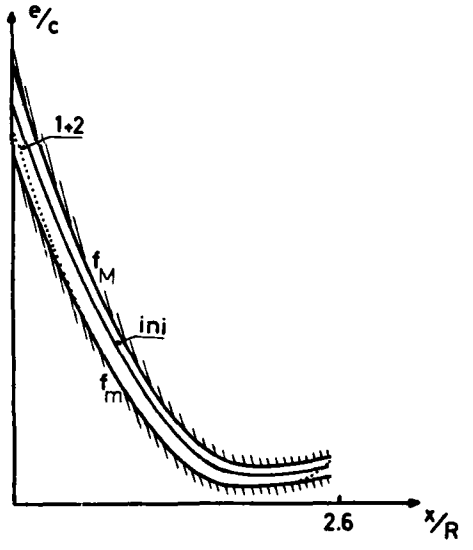


Fig. 6 a.b. Variations of c and e/c

AD-P000 054

APPLICATION OF OPTIMIZATION TO AIRCRAFT ENGINE DISK SYNTHESIS

Ji Oh Song* and Richard E. Lee**

Pratt & Whitney Aircraft Group
Government Products Division
West Palm Beach, FL 33402

ABSTRACT

An automated optimum disk synthesis technique for aircraft gas turbine engines is developed using a mathematical programming method. The optimum synthesis program constructs a minimum-weight disk while meeting burst speed, stress and geometric constraints. A general purpose optimization program is used in synthesizing piece-wise hyperbolically shaped disks in which thermal gradient effects in the radial direction are taken into account. For conceptual design purposes, the disk analysis is simplified based on elastic plane stress assumption. The feasibility of this approach is demonstrated through example problems of a typical disk from the preliminary design phase.

INTRODUCTION

The design of an advanced gas turbine engine begins in a preliminary design phase when the engine designer is challenged with selecting the best engine configuration for the defined customer requirements. This "best" configuration is the result of an extensive study of numerous candidate engines of varying sizes, operating at different speeds, at different temperatures, different pressures, etc. The designer must review a large number of these candidate engines against the customer's requirements in order to arrive at the optimum configuration.

To study a large number of candidate engines in a preliminary design phase with a limited amount of time requires design tools which can do a preliminary design of engine components literally overnight. Reference [1] described a preliminary design tool used at Pratt & Whitney Aircraft's Government Products Division to do preliminary designs of gas turbine disks. This tool has been further developed by the addition of an optimization program which extends the disk synthesis procedure to a point closer to the final disk design weight.

During the last two decades, significant efforts have been made in the application of optimization to the engineering field, particularly structural problems. Some researchers have successfully used both linear[2,3] and nonlinear[4] programming techniques to solve formulated structural optimization problems. The application of mathematical programming techniques is comprehensively reviewed in reference[5]. Others have pursued the optimality criteria approach based on the fully stressed design concept[6,7]. More recently, the state-space method has been introduced from the optimal control theory[8]. This method is primarily aimed at efficient sensitivity analysis, and has been successfully applied in mechanical and structural systems[9]. However, the nonlinear programming technique is believed the most suitable application to the optimum disk synthesis. This is because the optimum disk synthesis problem can be easily formulated as the standard form of the nonlinear programming, and a well-developed solution algorithm can be exploited.

The objective of this paper is, therefore, to apply the existing optimization technique in synthesizing gas turbine engine disks with minimum weight while meeting burst margin, stress and geometric constraints. For this purpose, a general purpose optimization program, CONMIN[10], is used in this study. CONMIN was designed primarily to solve nonlinear programming problems with inequality constraints, and is widely applied in practical engineering problems[11-14]. The disk analysis procedure used in the synthesis program is reviewed to acquaint the reader who is not familiar with gas turbine design procedures, and the disk analysis program is interfaced with the optimizer, CONMIN, to provide a more efficient disk synthesis tool for the early stage of disk design. In this paper, we refer to the resulting synthesized disk as the "optimum disk design." As the term "optimum" is used here, it is intended to be an optimum disk for the preliminary design phase of the engine. This synthesized disk is used as the starting point for further analysis leading to the final design configuration. More sophisticated analysis techniques are used during final analysis to account for disk plastic deformation, out-of-plane loading, system vibrations, and complex mission usage.

DISK ANALYSIS

For preliminary disk design the analysis used is less rigorous than the analysis required for a final production configuration. The intent is to arrive at an answer that is correct enough to indicate real trends in weight, size, life, etc., without incurring unnecessary expense due to analysis sophistication. Since the application of optimization theory to gas turbine engine preliminary design has only recently been undertaken, the appropriate level of analysis sophistication is still undetermined. For the purpose of this study it was concluded that a simple elastic formulation to calculate stress would be a reasonable approximation. Among the classical disk analysis tools available in the literature, a hyperbolically shaped disk was chosen as the analyzer. The well-established solution procedure for this disk is summarized in the appendix, and the results are used for further derivations in this section. This disk shape represents a slightly more sophisticated configuration than our earlier synthesis-analysis which was discussed in [1]. The stress distribution for an axisymmetrically loaded disk is analyzed by assuming that the disk is piece-wise hyperbolically shaped; whereas, in reference [1] we had initially used straight-sided rings. Burst margin and cross-section profile slopes of the disk are also derived so that they could be used as constraints to be satisfied in the optimizing process. Finally, the disk weight, which is the objective function to be minimized, is calculated.

A disk with varying thickness was divided into a number of ring elements, as shown in figure 1. Each element has the cross-section profile of a hyperbola represented as

$$t = cR^a \qquad (1)$$

where a and c are constants to be determined from the geometry. Plane stress assumption is made in this analysis. Temperature is assumed to be constant within each ring element, but can vary from element to element.

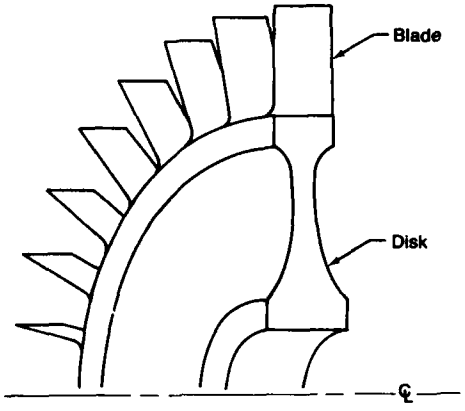
Denoting the outer and inner boundaries of each element by subscripts o and i, respectively, and using the equation (A-8) derived in the appendix, one can get stresses at the outer and inner boundaries of each element as follows:

*Senior Research Engineer
**Senior Design Engineer

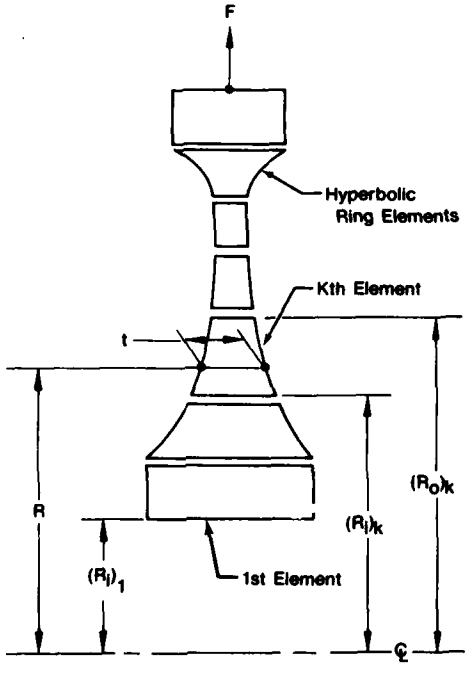
$$\sigma_{R_\delta} = \frac{A}{c} R_\delta^{m_1-a-1} + \frac{B}{c} R_\delta^{m_2-a-1} - \frac{3+\nu}{8+(3+\nu)a} \rho\omega^2 R_\delta^2$$

$$\sigma_{T_\delta} = \frac{A}{c} m_1 R_\delta^{m_1-a-1} + \frac{B}{c} m_2 R_\delta^{m_2-a-1} - \frac{1+3\nu}{8+(3+\nu)a} \rho\omega^2 R_\delta^2 \quad (2)$$

where δ = o,i, and constants a, c are given in Equation (A-1) and m_1, m_2 defined in Equation (A-8). A and B for each element are determined from the boundary conditions.



(a) Bladed Disk Segment



(b) Disk Model

Fig. 1. Typical bladed disk shape

By applying the continuity of radial displacement, u, and radial stress at the boundary of the elements k and k+1, the following conditions may be obtained.

$$\begin{aligned} (u_o)_k &= (u_i)_{k+1} \\ (\sigma_{R_i})_1 &= 0 \\ (\sigma_{R_o})_k &= (\sigma_{R_i})_{k+1} \\ (\sigma_{R_o})_n &= F/(\text{Rim circumferential area}) \end{aligned} \quad (3)$$

where k = 1, 2, ..., n-1, F is the rim pull due to the centrifugal force of blades, and n is the total number of ring elements. The expression for the radial displacement, u, may be written in terms of A and B from Equations (A-4), (A-5), and (A-8) in the appendix. u_i and u_o are radial displacements at inner and outer boundaries, respectively.

Then 2n unknowns of A's and B's for n ring elements can be determined from the 2n equations of boundary conditions in Equation (3). As a result, stresses at the boundaries can be obtained from Equation (2) and stresses at any radial station from Equation (A-8) by substituting A and B.

Using the radial and tangential stresses, additional quantities related to the disk design criteria are derived. These are constrained in the optimum disk synthesis.

Effective stress is an important variable to be considered in disk design. Effective stress, based on the Von Mises yield criterion, is defined as

$$\sigma_{e_\delta} = \left(\sigma_{R_\delta}^2 - \sigma_{R_\delta}\sigma_{T_\delta} + \sigma_{T_\delta}^2\right)^{1/2} \quad (4)$$

where δ = i,o, and σ_{e_i} and σ_{e_o} are effective stresses at inner and outer boundaries, respectively.

Another important consideration for the gas turbine engine disk design is the speed at which the disk will burst. A reliable estimate of the burst speed may be obtained from the average tangential stress, $\sigma_{T_{avg}}$. The ratio of the speed at which the stress reaches ultimate stress to the design speed may be used as a design criterion and called "Burst Margin." Burst margin (BM) may be defined by

$$BM = \left(MUF \cdot \sigma_u / \sigma_{T_{avg}}\right)^{1/2} \quad (5)$$

where MUF is a material utilization factor which is determined experimentally, and σ_u is ultimate tensile strength. $\sigma_{T_{avg}}$ can be obtained from the simple free body of the half disk.

$$\sigma_{T_{avg}} = \frac{F_f + F}{2\pi A_r} \quad (6)$$

where F_f is the body force due to the centrifugal force of the disk, and A_r the disk cross-sectional area. F_f can be written as

$$F_f = 2\pi\omega^2 \sum_{k=1}^{n} \left[\int_{(R_i)_k}^{(R_o)_k} \rho R^2 t dR \right] \quad (7)$$

In addition, geometric constraint should be considered in the disk design. Slope angles of the cross-section profile, as shown in figure 2, need to be constrained to maintain the validity of plane stress assumption. Experience shows that a large angle $(\theta_i)_2$ in figure 2 tends to decrease the utility of the material at bore edge because of nonuniform stress distribution in bore section.

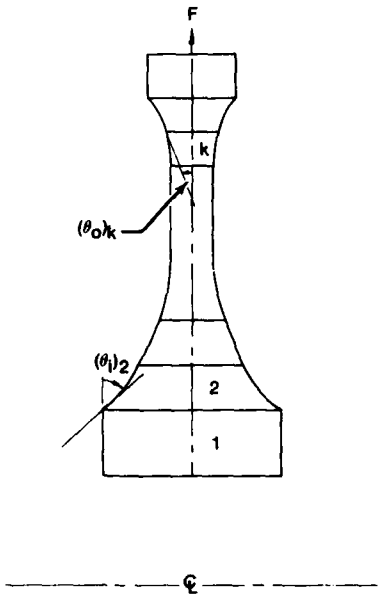


Fig. 2. Slope constraint

The angle $(\theta_\delta)_k$ can be obtained from differentiation of Equation (1)

$$(\theta_\delta)_k = \tan^{-1}\left[\frac{1}{2}\, c\, a\, (R_\delta)_k^{a-1}\right] \tag{8}$$

where δ = o, i implies outer and inner boundary of the element respectively. Finally, the disk weight, WT, may be given as

$$WT = 2\pi \sum_{k=1}^{n} \left[\int_{(R_i)_k}^{(R_o)_k} \rho\, R t dR\right] \tag{9}$$

OPTIMUM DISK SYNTHESIS

With the disk analysis derived in the previous section, all the necessary information required for disk design can be obtained if the disk geometry is given. Optimum disk synthesis is to choose the disk dimensions of the minimum weight disk while meeting given design criteria. The optimization program simply guides design improvement by interfacing with the analysis program until the optimum disk is obtained. This is the fundamental difference between the use of optimization theory to size the disk and the alternative, iterative practice summarized in reference [1]. The general purpose optimization program, CONMIN, is used here. CONMIN is organized to solve the classical nonlinear programming problem with inequality constraints, i.e., in mathematical terminology,

Find D such that

minimize J(D)

subject to (10)

$\Phi(D) \le 0$

and D is bounded or unbounded.

Where $D = \{D_j, j=1, 2, ..., \ell\}$ is the vector of design variables, $\Phi = \{\Phi_j, j=1, 2, ..., m\}$ the vector of constraints, and J the objective function (or cost function). ℓ and m represent the number of design variables and constraints, respectively. Design improvement then can be made as:

$$D^{q+1} = D^q + \gamma S^q \tag{11}$$

where D^q is current design, D^{q+1} updated design, γ stepsize and S^q direction vector for design improvement.

The major function of CONMIN is to find the direction vector S^q using the feasible direction method[15,16] and stepsize γ at each iteration by interfacing with the analysis program to guide the design to the optimum point.

The optimum disk synthesis problem can be formulated using the equations derived in previous section as

Find $D = \{t_1, ..., t_{n+1}, (R_i)_1, ..., (R_i)_n\}$ such that

minimize WT

subject to

$$BM^L \le BM \le BM^U$$

$$(\sigma_{T_i}{}^L)_k \le (\sigma_{T_i})_k \le (\sigma_{T_i}{}^U)_k$$

$$(\sigma_{T_o}{}^L)_k \le (\sigma_{T_o})_k \le (\sigma_{T_o}{}^U)_k$$

$$(\sigma_{R_i}{}^L)_k \le (\sigma_{R_i})_k \le (\sigma_{R_i}{}^U)_k$$

$$(\sigma_{R_o}{}^L)_n \le (\sigma_{R_o})_n \le (\sigma_{R_o}{}^U)_n \tag{12}$$

$$(\sigma_{e_i}{}^L)_k \le (\sigma_{e_i})_k \le (\sigma_{e_i}{}^U)_k$$

$$(\sigma_{e_o}{}^L)_k \le (\sigma_{e_o})_k \le (\sigma_{e_o}{}^U)_k$$

$$(\theta_i{}^L)_k \le (\theta_i)_k \le (\theta_i{}^U)_k$$

$$(\theta_o{}^L)_k \le (\theta_o)_k \le (\theta_o{}^U)_k$$

and

$$t_j{}^L \le t_j \le t_j{}^U$$

$$(R_i{}^L)_k \le (R_i)_k \le (R_i{}^U)_k$$

where k = 1, 2, ..., n, j = 1, 2, ..., n+1, t_1, ..., t_{n+1} are the disk thicknesses at various radial stations, and $(R_i)_1$ is the bore radius. n is the total number of ring elements. Superscripts L and U represent lower and upper limits of the variables considered, respectively. The Equation (12) can be converted to the standard form of Equation (10).

The disk synthesis procedure may be summarized as follows:

Step 1. Initialize design variables based on engineering guess.

Step 2. Do disk analysis using Equations (1) to (9).

Step 3. Check the constraints of Equation (12).

Step 4. If no constraints are violated and no design improvement is made, the result is optimum. Then stop here. Otherwise go to Step 5.

Step 5. Obtain the improved design from Equation (11) and go to Step 2.

Steps 3, 4, and 5 are carried out by the optimizer.

EXAMPLES AND RESULTS

Four different variations on a typical turbine disk are presented to illustrate the capability of this approach. The disk is divided into ten elements with thermal gradients. As shown in figure 3, disk elements and stations are enumerated from the bore to rim in ascending order.

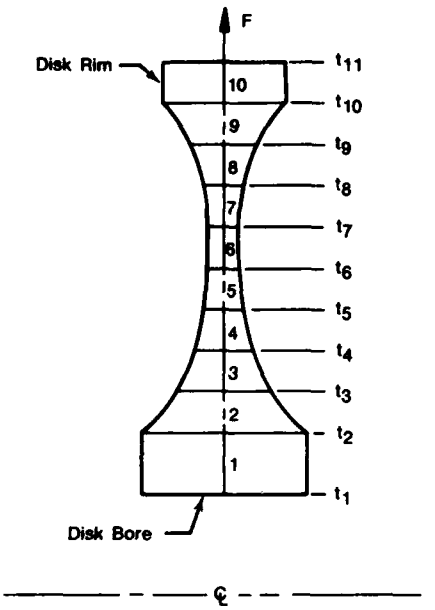


Fig. 3. Configuration of example

Constant variables used in the analysis are:

$E = 27.1 \times 10^6$ psi
Specific weight = 0.284 lb/in.^{3}
$\alpha = 7.39 \times 10^{-6}$ in./in. °F
$\nu = 0.3$
MUF = 0.8
σ_u = 210,000 psi
Rotational speed = 11,500 rpm
$F = 1.393 \times 10^6$ lb.

The radius at each station and temperature of each element are tabulated in table 1. Radius and temperature are held constant in first three cases. In the fourth case, radius is designated as a design variable.

Disk rim thicknesses t_{10} and t_{11} are fixed to accommodate the blade. In this example, therefore, t_1, ..., t_9 are taken as design variables and $t_{10} = t_{11} = 1.415$ in. Constraint limits used in common for four cases are:

$BM^L = 1.3$

$(\sigma_{T_o}{}^U)_{10} = 93{,}000$ psi

$(\sigma_{T_o}{}^U)_k = 114{,}000$ psi, k = 1, 2, ..., 9

$(\sigma_{T_i}{}^U)_k = 114{,}000$ psi, k = 1, 2, ..., 10

$(\sigma_{R_o}{}^U)_{10} = 126{,}000$ psi

$(\sigma_{R_i}{}^U)_k = 126{,}000$ psi, k = 1, 2, ..., 10

$(\sigma_{e_o}{}^U)_k = 114{,}500$ psi, k = 1, 2, ..., 10

$(\sigma_{e_i}{}^U)_k = 114{,}500$ psi, k = 1, 2, ..., 10

$(\theta_o{}^U)_9 = 56°$

$(\theta_o{}^L)_9 = -56°$

$(\theta_o{}^U)_k = 46.3°$, k = 2, 3, ..., 8

$(\theta_o{}^L)_k = -46.3°$, k = 2, 3, ..., 8

$(\theta_i{}^U)_k = 46.3°$, k = 2, 3, ..., 9

$(\theta_i{}^L)_k = -46.3°$, k = 2, 3, ..., 9

$t_k{}^L = 0.25$ in., k = 1, 2, ..., 9

BM^U, $(\sigma_{T_o}{}^L)_k$, $(\sigma_{T_i}{}^L)_k$, $(\sigma_{R_o}{}^L)_k$, $(\sigma_{R_i}{}^L)_k$, $(\sigma_{e_o}{}^L)_k$, $(\sigma_{e_i}{}^L)_k$ and $t_j{}^U$ are unbounded, where k = 1, 2, ..., 10 and j = 1, 2, ..., 9.

In order to show the effectiveness of the program developed here, extreme initial configurations are taken. Cases 1, 3 and 4 start at a very conservative configuration, while case 2 starts at lower bounds of design variables. All of these initial configurations are outside of the range of choices which a designer would realistically consider. The reason they are selected here is to illustrate the versatility of the optimizer in arriving at an optimum configuration.

Case 1

Thicknesses at station 1 and 2 are linked so that $t_1 = t_2$ in the synthesizing process. Hence, the number of independent design variables is 8 instead of 9. This implies that the cross section near the bore is rectangular. Disks with rectangular shaped bore sections may be observed in many engines. Initial design variable values are $t_1 = t_2 = 2.2$ in., $t_3 = 1.5$ in., $t_4 = ... = t_9 = 1.2$ in. and $t_{10} = t_{11} = 1.415$ in.

Case 2

Case 2 is same as case 1 except that initial design is chosen at the other extreme for bore and web geometry. The classic disk shape is intentionally avoided to test the optimizer. Initial design variable values are $t_1 = ... = t_9 = 0.25$ in. and $t_{10} = t_{11} = 1.415$ in.

Case 3

In case 3, t_1 and t_2 are not linked anymore, and are independent design variables. Initial design variable values are same as those in case 1. Additional constraints $(\theta_o)_1$ and $(\theta_i)_1$ are imposed such that $(\theta_o{}^U)_1 = (\theta_i{}^U)_1 = 46.3°$ and $(\theta_o{}^L)_1 = (\theta_i{}^L)_1 = -46.3°$.

Case 4

Radial locations of ring elements are included as design variables in addition to the thicknesses of case 1. $(R_i)_1$ is taken as the independent design variable, while $(R_i)_2$, ..., $(R_i)_9$ are linked such that the height of each element in the radial direction is proportional to that of the initial configuration. $(R_i)_{10}$ and $(R_o)_{10}$ are fixed because of the blade attachment requirement. Except for some additional design variables and constraints, the initial configuration, design variables and constraints are the same as those of case 1. In this case, bore radius is constrained such that $(R_i{}^L)_1 = 2.5$ in. and $(R_i{}^U)_1 = 5.0$ in.

In cases 1, 3 and 4, the initial design is so conservative that no constraints are violated, while initial design of case 2 is not feasible. Initial and converged final values of design variables are given in table 2 for the first three cases, and in table 3 for case 4. Initial and final configurations are depicted in figures 4, 5, 6, and 7. Disk weight history in terms of the number of iterations is given in figure 8. Note that case 1 and case 2 have converged to virtually the same optimum disk, which

Table 1. Radii and Temperature Distribution of Example

	1	2	3	4	5	6	7	8	9	10	11
Radius (inch)	3.750	4.615	5.048	5.480	5.913	6.345	6.778	7.210	7.640	8.076	8.459
Temperature (°F)	703	711	724	742	767	798	835	877	925	975	

may, therefore, be considered to be the global minimum disk for given constraints. In case 2, even though 38 out of 83 constraints are initially violated, the program successfully corrected the violations. Case 3 converges to a disk that is 7% lighter than cases 1 and 2. As might be expected, it can be observed that the disk weight can be reduced if the requirement for a rectangular bore element is eliminated. It should be noted, however, that bore thickness in case 3 is greater than cases 1 and 2. It might be necessary to constrain bore thickness to a smaller value in some applications. In practical design, the bore section of the optimum disk shown in figure 7 would be made as the smooth shape illustrated by dotted lines in the figure. In case 4 where bore radius is a design variable, disk weight, bore section thickness and bore radius are reduced compared to cases 1 and 2.

Table 2. Design Variables for Case 1, 2 and 3

	Case 1		Case 2		Case 3	
	Initial	*Final*	*Initial*	*Final*	*Initial*	*Final*
t_1*	2.2	2.022	0.25	2.030	2.2	2.846
t_2*	2.2	2.022	0.25	2.030	2.2	1.614
t_3*	1.5	1.318	0.25	1.325	1.5	0.944
t_4*	1.2	0.683	0.25	0.691	1.2	0.376
t_5*	1.2	0.315	0.25	0.316	1.2	0.316
t_6*	1.2	0.302	0.25	0.301	1.2	0.301
t_7*	1.2	0.286	0.25	0.286	1.2	0.286
t_8*	1.2	0.273	0.25	0.274	1.2	0.270
t_9*	1.2	0.556	0.25	0.553	1.2	0.555
t_{10}*	1.415	1.415	1.415	1.415	1.415	1.415
t_{11}*	1.415	1.415	1.415	1.415	1.415	1.415

*Unit is in inch.

Table 3. Design Variables for Case 4

	R (inch)		t (inch)	
Position	*Initial*	*Final*	*Initial*	*Final*
1	3.750	2.5	2.2	1.523
2	4.615	3.615	2.2	1.523
3	5.048	4.173	1.5	0.772
4	5.480	4.730	1.2	0.346
5	5.913	5.288	1.2	0.331
6	6.345	5.845	1.2	0.315
7	6.778	6.403	1.2	0.296
8	7.210	6.960	1.2	0.280
9	7.640	7.514	1.2	0.423
10	8.076	8.076	1.415	1.415
11	8.459	8.459	1.415	1.415

The solution of the simultaneous equations for the disk analysis is provided through the program LEQT1B of the IMSL[17] library. Computations are carried out in double precision using the IBM 3033 computer. Computing time is approximately 5 CPU seconds for each case.

CONCLUDING REMARKS

An optimization technique has been applied to the synthesis for compressor and turbine disks of conceptual aircraft gas turbine engines. A simple elastic disk analysis program is combined with the general purpose optimization program, CONMIN, to minimize disk weight while meeting burst margin, stress and geometric constraints. This expedites preliminary design work where disk configurations are being studied and initially sized.

The feasibility and effectiveness of this approach are demonstrated by numerical example problems. The synthesis program constructs optimum disks which may not otherwise be possible because of the engineer's limited intuition. It is also shown that the implication of certain constraints can be readily evaluated.

The program presented here can be used to provide quick design guidance in the preliminary design phase and can provide the starting point for a more elaborate (for example, plastic) final solution.

The most important feature of the program is that it can not only improve design quality but also can drastically reduce disk design time.

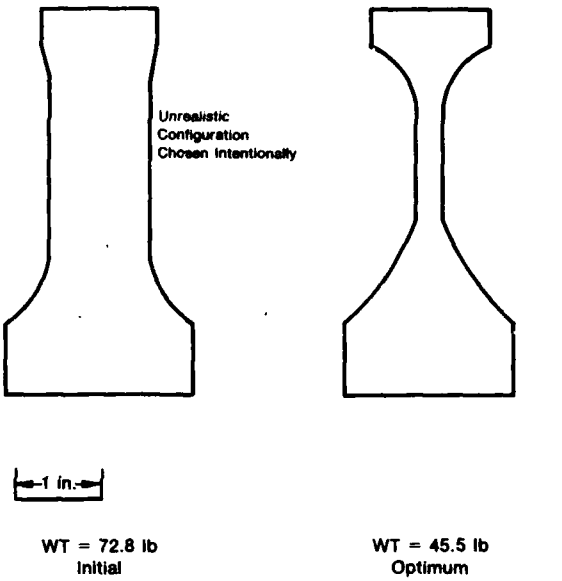


Fig. 4. Initial and optimum disks, Case 1

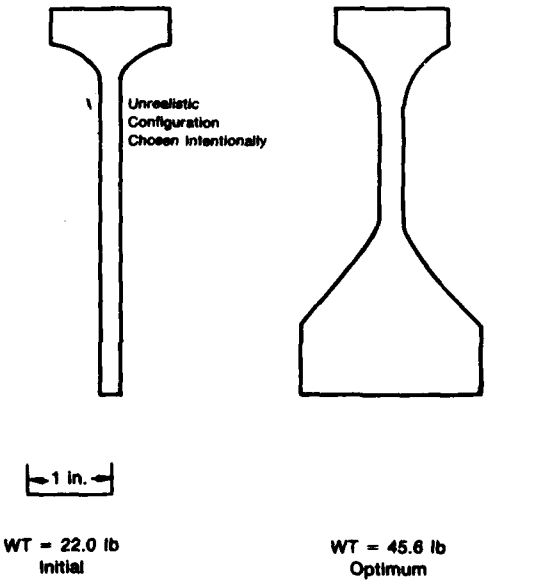


Fig. 5. Initial and optimum disks, Case 2

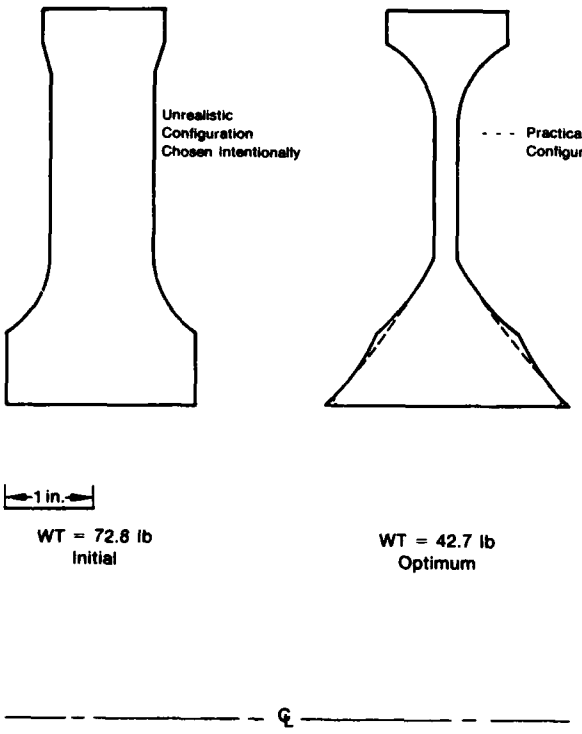


Fig. 6. Initial and optimum disks, Case 3

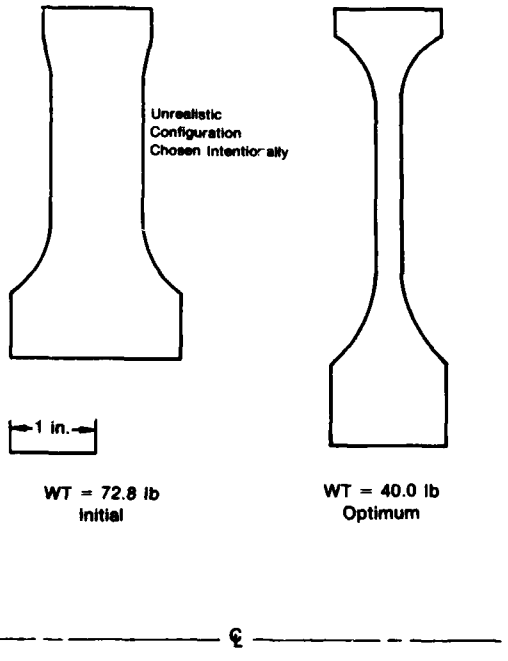


Fig. 7. Initial and optimum disks, Case 4

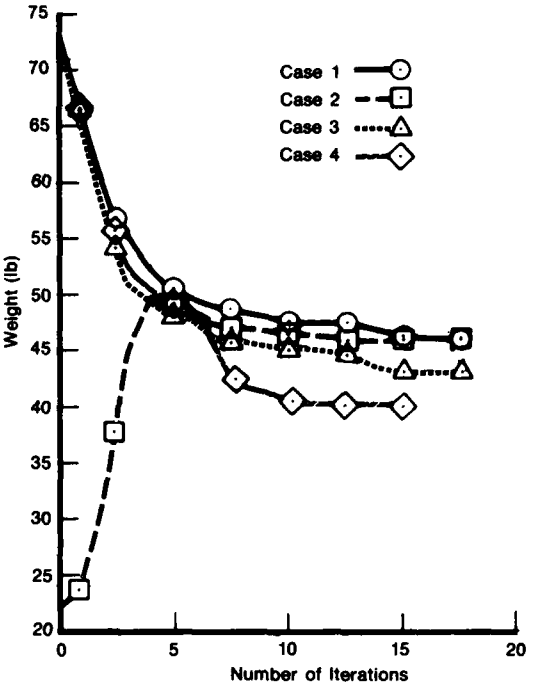


Fig. 8. Disk weight history

REFERENCES

1. Osmer, J., Novotny, R. J., and Blevins, E. G., "Engine Life Methodologies for Conceptual Design," AIAA-81-1398, July 1981.

2. Moses, F., "Optimum Structural Design Using Linear Programming," *J. of Structural Div.*, Proc. ASCE, Vol. 90, No. ST6, pp 89-104, Dec 1964.

3. Schmit, L. A. and Farshi, B., "Some Approximate Concepts for Structural Synthesis," *AIAA J.* 12, pp 692-699, 1974.

4. Brown, D. M. and Ang, A. H. S., "Structural Optimization by Nonlinear Programming," *J. of Structural Div.*, Proc. ASCE, Vol. 92, No. ST6, pp 319-340, Dec 1966.

5. Pope, G. G., and Schmit, L. A., (Editors), *Structural Design Applications of Mathematical Programming Techniques*, AGARDograph 149, Feb 1971.

6. Venkayya, V. B., Khot, N. S., and Berke, L., "Application of Optimality Criteria Approaches to Automated Design of Large Practical Structures," presented at AGARD 2nd Symposium on Structural Optimization, Milan, Italy, Apr 1973.

7. Fleury, C., "An Efficient Optimality Criteria Approach to the Minimum Weight Design of Elastic Structures," *Computers and Structures*, Vol. 11, Pergamon, pp 163-173, 1980.

8. Haug, E. J. and Arora, J. S., "Design Sensitivity Analysis of Elastic Mechanical Systems," *Computer Method in Applied Mechanics and Engineering* 15, pp 35-62, 1978.

9. Haug, E. J. and Arora, J. S., *Applied Optimal Design*, John Wiley and Sons, New York, 1979.

10. Vanderplaats, G. N., "CONMIN — A FORTRAN Program for Constrained Function Minimization," NASA TMX-62,282, 1973.

11. Garberoglio, J. E., Song, J. O., and Boudreaux, W. L., "Optimization of Compressor Vane and Bleed Settings," AFWAL-TR-81-2046, June 1981

12. Vanderplaats, G. N., "Efficient Algorithm for Numerical Airfoil Optimization," *J. Aircraft*, Vol. 16, No. 12, pp 842-847, Dec 1979.

13. Bennett, J. A., Lin, K. H., and Nelson, M. F., "The Application of Optimization Techniques to Problems of Automotive Crashworthiness," General Motors Research Publication GMR-2316R, Apr 1977.

14. Sobieszczanski-Sobieski, J. and Bhat, R. B., "Adaptable Structural Synthesis Using Advanced Analysis and Optimization Coupled by a Computer Operating System," *J. Aircraft*, Vol. 18, No. 2, pp 142-149, Feb 1981.

15. Zoutendijk, G. G., *Methods of Feasible Directions*, Elsevier, Amsterdam, 1960.

16. Vanderplaats, G. N., and Moses, F., "Structural Optimization by Methods of Feasible Directions," *Computers and Structures*, Vol. 3, Pergamon, pp 739-755, 1973.

17. IMSL Library Reference Manual, 8th Edition, 1980; IMSL, Inc., Houston, Texas.

APPENDIX

Let the radial section thickness of the disk of figure A-1 be represented by the hyperbolic formula

$$t = cR^a \tag{A-1}$$

where $a = \dfrac{\ln (t_i/t_o)}{\ln (R_i/R_o)}$

and $\ln c = \ln t_i - a \ln R_i$

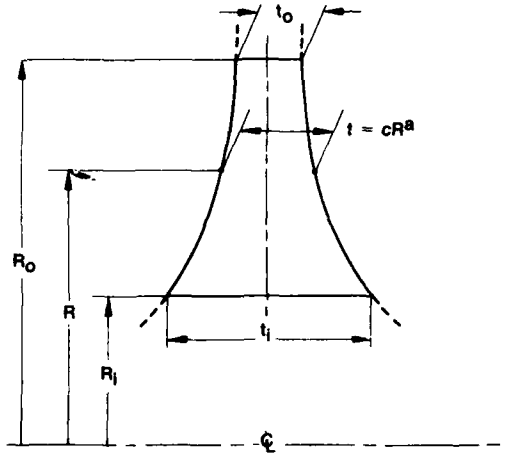


Fig. A-1. Disk ring element of hyperbolic section

By assuming plane stress, the equilibrium equation and compatibility equation can be written as

$$\frac{d}{dR}(t\,R\,\sigma_R) - t\,\sigma_T + t\,\rho\,\omega^2R^2 = 0 \tag{A-2}$$

$$R\,\frac{d\epsilon_T}{dR} + \epsilon_T - \epsilon_R = 0 \tag{A-3}$$

where ρ is the material density and ω the angular speed of the disk. σ_R and σ_T denote the radial and tangential stresses, respectively. ϵ_R and ϵ_T are radial and tangential strains, respectively.

Constitutive equation may be written

$$\epsilon_R = \frac{1}{E}\,(\sigma_R - \nu\,\sigma_T) + \alpha\,(T - T_o)$$

$$\epsilon_T = \frac{1}{E}\,(\sigma_T - \nu\,\sigma_R) + \alpha\,(T - T_o) \tag{A-4}$$

where T_o and T are reference and current temperatures, respectively. α is the coefficient of linear thermal expansion, E is the modulus of elasticity, and ν is the Poisson's ratio.

And the relationship between the strains and displacements may be expressed as

$$\epsilon_R = \frac{du}{dR}$$

$$\epsilon_T = \frac{u}{R} \tag{A-5}$$

where u is the radial displacement.

Introduce the following stress function that satisfies Equation (A-2)

$$\psi = tR\sigma_R$$

$$\frac{d\psi}{dR} + t\,\rho\,\omega^2R^2 = t\,\sigma_T \tag{A-6}$$

Then by using Equations (A-4) and (A-6) and assuming that T is constant, the compatibility equation (A-3) becomes

$$\frac{d^2\psi}{d\beta^2} - a\,\frac{d\psi}{d\beta} - (1 - \nu a) = -(3 + \nu)\,c\,\rho\,\omega^2\,e^{(3+a)\beta} \tag{A-7}$$

where $\beta = \ln R$

From Equations (A-6) and (A-7) one has

$$\sigma_R = \frac{A}{c}R^{m_1-a-1} + \frac{B}{c}R^{m_2-a-1} - \frac{3+\nu}{8+(3+\nu)a}\rho\omega^2R^2$$

$$\sigma_T = \frac{A}{c}m_1R^{m_1-a-1} + \frac{B}{c}m_2R^{m_2-a-1} - \frac{1+3\nu}{8+(3+\nu)a}\rho\omega^2R^2 \tag{A-8}$$

where

$$m_1 = \frac{a}{2} + \left[\frac{a^2}{4} - \nu a + 1\right]^{1/2}$$

$$m_2 = \frac{a}{2} - \left[\frac{a^2}{4} - \nu a + 1\right]^{1/2}$$

$R_i \le R \le R_o$

A and B are constants to be determined from the boundary conditions.

NOMENCLATURE

A_r	Disk cross-sectional area
BM	Burst margin
D	Vector of design variables
E	Modulus of elasticity
F	Disk rim pull
F_f	Body force due to centrifugal force
J(D)	Objective function (or cost function)
L	Superscript denoting lower bound of constraint
MUF	Material utilization factor
$(R_i)_k$, $(R_o)_k$	Inner and outer radii of k-th element, respectively
S	Direction vector for design improvement
t	Disk thickness
T_o, T	Reference and current temperatures, respectively
u	Radial displacement
U	Superscript denoting upper bound of constraint
WT	Disk weight
α	Coefficient of linear thermal expansion
γ	Stepsize in design improvement
Φ(D)	Vector of constraints
θ	Angular constraint
ν	Poisson's ratio
ρ	Material density
σ	Stress
ω	Angular speed



AD-P000 055

OPTIMAL SHAPE DESIGN TO MINIMIZE STRESS CONCENTRATION FACTORS IN PRESSURE VESSEL COMPONENTS

J. Middleton
Lecturer
Department of Civil Engineering
University College of Swansea
Singleton Park
Swansea SA2 8PP, U.K.

Summary

The problem of shape optimization to minimize stress concentration factors is presented. Design variables are chosen such that optimal configurations can be produced for a cylindrical pressure vessel with an end closure and nozzle intersection.

A system model is formed in which the stress gradients are calculated numerically using the finite element method and optimization is performed by the penalty function technique. Various examples of the design algorithm are presented showing optimal geometries together with plots of boundary stress concentrations for the sequence of designs generated.

1. Introduction

The design of cylindrical pressure vessels and associated components has been the subject of considerable attention due to the many severe requirements of industry. As a consequence of complicated geometries and the complex problem of stress analysis design in the past have been largely formulated from empirical rules and it is only recently that optimal configurations for such components has been attempted.

In this presentation a more rational design technique is adopted which is of a general nature. The basis of this formulation is a two-dimensional isoparametric finite element for the analysis phase and a penalty function procedure for the optimization of the objective or merit function.

The most important problem associated with pressure vessel design is the production of components which have minimum stress concentration effects. The basis of this requirement is to ensure enhanced fatigue behaviour since it has been shown (1) that as stress concentrations are minimized the safe working life of the component will be substantially increased.

In this treatment a cylindrical vessel with torispherical end cap and nozzle intersection is considered. The geometrical shape of the component is described by a set of design variables x_n such that the maximum stress concentration factor (SCF) occurring within the body is reduced to a minimum value for a given set of loading conditions.

Although the problem of determining stress concentrations has received much attention (2,3) it is only recently that researchers have devoted themselves to the solution of optimal shapes to minimize stress concentration effects. Much of this recent work was centred on the optimization of notches and fillets (4,5) and the success of these investigations has lead onto the more general design applications such as considered here (6,7,8). Of these recent papers all use high degree polynomial approximations to give an accurate description of the stresses and the only major difference lies in the geometrical description of the boundary shape. In this formulation the boundary description is such that evolved shapes will satisfy the ASME and European pressure vessel requirements and also geometries will allow the ease of production from the manufacturing point of view.

2. Component Geometry

The configuration to be studied is shown in Fig. 1. This is basically an assembly of three axisymmetric components, namely a torispherical end closure, which can be formed from a two or three radii end cap, a cylindrical portion which forms the main body of the vessel and a hemispherical end closure which is pierced by a protruding nozzle. The torispherical head formed from two radii is defined by the head radius x_1, knuckle radius x_2, closure height x_3 and head and cylindrical wall thicknesses of x_4 and x_5 respectively. In this case the design variables are to be defined by the vector

$$x_n = \begin{Bmatrix} x_2 \\ x_3 \\ x_4 \\ x_5 \end{Bmatrix} \qquad (1)$$

In the case of the three radii torispherical head the geometry is defined by the head radius x_1^1, two knuckle radii, x_2^1 and x_3^1 and head and cylinder wall thicknesses x_5^1 and x_6^1. The angle θ is also required to ensure that the knuckle radii x_2^1 and x_3^1 remain tangential. Here the design vector is defined by the following six variables

$$x_n^1 = \begin{Bmatrix} x_2^1 \\ x_3^1 \\ x_4^1 \\ x_5^1 \\ x_6^1 \\ \theta \end{Bmatrix} \qquad (2)$$

In the cylindrical portion of the vessel the diameter D cylindrical length L_c, and the transition lengths L_F are treated as constant dimensions.

A somewhat different problem is posed by the nozzle head intersection in that unlike the torispherical heads where the whole of boundary may be subject to change we are only concerned here with the reinforcement of the nozzle where it intersects the hemispherical closure. The general configuration adopted is one that can produce balanced reinforcement since it is well known that such geometries offer good structural behaviour.

Here the variable P defines the protrusion into the end closure, the radius R_1 angle θ and distance S describe the internal reinforcement and the radius R_2 defines the external reinforcement. It should be noted that in the geometry of Fig. (1) the dimensions R_3 and w depend explicitly on the choice of the design vector $\underset{\sim}{x}_n$. For the optimization of the nozzle intersection the design variables are chosen as

$$x_n = \begin{Bmatrix} R_1 \\ \theta \\ P \\ S \\ R_2 \end{Bmatrix} \qquad (3)$$

Equations (1), (2) and (3) define the design vectors for which optimal sets will be sought. It should be emphasized that the choice of these design vectors is very important indeed in that overcomplication of the geometry may prove restrictive in computer time and also design shapes may evolve which may be difficult to manufacture. On the contrary oversimplification may restrict boundary evolution and therefore only trivial solutions may be forthcoming due to the type of configuration defined.

3. Method of Stress Analysis

Due to the complex geometry of the vessel shown in Fig. (1) its structural response cannot in general be defined explicitly in terms of the design vector x_n therefore a system model must be introduced which physically describes the behaviour of the component in terms of the design parameters. To achieve an accurate system model the method of analysis used must be capable of accurately predicting the behaviour of the structure under the conditions of arbitrary geometry together with applied mechanical and thermal loading conditions.

These requirements can be adequately met by the application of the finite element technique. Here the eight noded isoparametric parabolic formulation will be used which is fully described elsewhere (9). In order to give an accurate description of the stress field the stresses are sampled at the 2x2 Gauss points throughout the mesh and linearly extrapolated to give stress values at the boundary. This type of formulation has received increasing attention for the solution of the optimization of continuum structures and many excellent results obtained (6,7,8,10).

3.1 Automated mesh generation

In general the application of the finite element technique involves considerable computing time especially, where accurate results are required and a fine mesh becomes essential. Here it is proposed to substructure the components such that mesh refinement can be controlled and the benefits of simplified discretization used during the early iterations of the design scheme.

This technique has further advantages in that areas which are known intuitively to have low stresses may be specified with a low mesh density and vice versa for areas where peak stresses are likely to occur.

Typical component substructures are shown in Fig. (2). In the case of the nozzle intersection once the boundary elements have been specified the internal region is meshed automatically such that element compatibility is maintained.

A prerequisite of this type of scheme is that an automated mesh generator is required. This has been developed such that once the geometry and mesh densities have been defined all other input and loading conditions are generated automatically although this may be over stepped if some special input type is required.

4. The Optimization Problem

As mentioned previously the most important design criterion for pressure vessels and related components is the reduction of stress concentration factors such that failure by fatigue is minimized. Morrison et al (11) have shown that the fatigue failure of such pressurised components can be predicted with good accuracy using the maximum shear stress theory or Tresca theory. Furthermore this theory has been adopted by the ASME pressure vessel codes (12) and in particular is a requirement for designs based on a numerical procedure.

Thus using the notation of (12) if σ_1, σ_2 and σ_3 are the three principal stresses at a point with $\sigma_1 > \sigma_2 > \sigma_3$ algebraically then the stress intensity for the Tresca theory is defined as the largest of the three stress differences and is defined as the largest of the three stress differences and is defined as

$$S = \sigma_1 - \sigma_3 \qquad (4)$$

Therefore using equation (4) the criterion for optimization can be stated as "given an initial design vector x_n which defines the component geometry find the optimal set x_n^* such that the maximum value of stress intensity S, occuring in the body is a minimum".

The usual classical approach of minimizing $Z(x_n)$, n=1, N where N is the number of design variables is not applicable in this treatment since optimization is based on a discrete element technique where only a finite number i of stress sampling points will be considered. The reformulated discretized objective function may be written as a minimum-maximum problem, thus

$$\text{Min } Z(x_n) = \min_{x_n} \left\{ \max_i S \right\} \qquad (5)$$

In equation (5) the stress intensity S is sampled at a finite number of locations i throughout the body and extrapolted to the boundary and x_n describes the boundary region which is subject to variation.

The objective of equation (5) requires that the maximum SCF occurring within the given component is brought to a minimum value therefore no behavioural constraints are required on the stresses. In this treatment the only constraints required are geometrical constraints $g(x_n)$ and technological constraints $t(x_n)$. Constraints of the type $g(x_n)$ are required to ensure that designs evolved remain compatible and undistorted while constraints of the type $t(x_n)$ allow the designer to prescribe fixed limits which may be a mandatory requirement of the design. The application of constraints $g(x_n)$ and $t(x_n)$ render the problem one of constrained optimization although it should be noted that the basis for these constraints is to prevent unusable designs from being produced thus essentially the technique still retains its unconstrained nature.

4.1 Mathematical Modelling

As mentioned in section 3, it is invariable when optimizing a continuum type structure that the analytical effort required predominates over the optimization phase. If optimization was directly applied to a five variable probler such as the 3 radii head of Fig. (1), then approximately 1200 re-analyses would be required for solution and obviously this is very restrictive indeed considering the amount of numerical work required.

To reduce this number of analyses to a reasonable number the technique of sequential modelling (13) incorporating move limits will be used. This involves generating an approximation to the objective function near some current design point x_n^j. Since this approximation is only valid near the current design points x_n^j then limits must be placed on x_n to control the accuracy of the system model generated. Optimization is then performed sequentially after establishment of each new approximate model. These limits are prescribed by adding a set of constraints on the design space as follows

$$\ell(x_n) = x_n^j - |\Delta^L x_n| \leq x_n^{j-1} \leq x_n^j + |\Delta x_n^U|, \quad n=1,N \quad (6)$$

where Δx_n^L and Δx_n^U denote the upper and lower moves limits respectively.

The constraints $\ell(x_n)$ ensure that the system model generated is accurately defined since optimization is restricted to the design space defined by Δx_n^L and $\Delta^U x_n$. Applications of this technique have shown convergence to optimal solutions in approximately 8 to 10 design steps (7) with only 70 reanalyses required compared with 1200 reanalyses for the direct application of optimization.

5. Formulation of the Objective Function

The formulation of the system model is simply an artifice to create an approximate mathematical model on which optimization may be performed. Many such models have been based on linear formulations due to the simplicity and ease by which solutions may be obtained. However this linear treatment can cause severe restrictions in the loss of design space available and problems can also arise due to lack of convergence especially when nearing the optimal design point.

To move away from total linear representations the objective function proposed will be based initially upon a linear approximation and on subsequent iterations extended to form a second order polynomial approximation. The linear form of the objective function is written as

$$Z(x_n) = \sum_{h=1}^{N} (a_n x_n + a_{N+1}) \quad (7)$$

in which the coefficients a_n are derived numerically with respect to the maximum stress intensity S as

$$a_n = \frac{\partial S(x_n)}{\partial x_n}, \quad n=1,N \quad (8)$$

Once the terms a_n, n=1, N have been found the constant term in equation (7) is derived as

$$a_{N+1} = \max_{S} (x_n) - \sum_{n=1}^{N} (a_n x_n) \quad (9)$$

The updated objective function is defined as

$$Z(x_n) = \sum_{n=1}^{N} (a_n x_n^2) + \sum_{n=1}^{N} \{(a_{n+N} x_n) + a_{2N+1}\} \quad (10)$$

In equation (10) the coefficients a_n are determined by the quadratic fitting of the stress gradients $\frac{\partial S}{\partial x_n}$ which are calculated at successive design points. This procedure is carried out as follows. Store the partial derivatives $\frac{\partial S(x_n)^{j-1}}{\partial x_n}$ from some previous design point x_n^{j-1}. Differentiating equation (10) at the j-1th design point yields

$$\frac{\partial S(x_n)^{j-1}}{\partial x_n} = 2 a_n x_n^{j-1} + a_{N+n} \quad n=1,N \quad (11)$$

then reconsidering equation (10) at the updated design point gives a new set of equations

$$\frac{\partial S(x_n)^{j}}{\partial x_n} = 2a_n x_n^{j} + a_{N+n} \quad n=1,N \quad (12)$$

The required unknowns a_n are then found from

$$a_n = \frac{\frac{\partial S(x_n)^{j}}{\partial x_n} - \frac{\partial S(x_n)^{j-1}}{\partial x_n}}{2(x_n^j - x_n^{j-1})} \quad n=1,N \quad (13)$$

and a_{n+N} is solved for by substituting the known terms a_n into equation (11). Finally the constant term in equation (10) is expressed as

$$a_{2N+1} = \max_{S} (x_n) - \sum_{n=1}^{N} (a_n x_n^2)^j - \sum_{n=1}^{N} (a_{n+N} x_n)^j \quad (14)$$

Since the objective function and constraints are of a general nonlinear form the optimization algorithm used must be capable of efficient and effective solution of such nonlinear systems. A method which has found wide usage for the solution of such problems is the penalty function method which transforms the usual classical approach into one of unconstrained minimization by adding the constraints to the objective function through a penalty parameter r_K. This formulation is fully treated in reference (14) and only a brief description will be given here.

The unconstrained minimization form may be written

$$\min\Omega (x_n, r_K) = Z(x_n) - r_K \sum_{m=1}^{M} G(g_m(x_n)) \quad (15)$$

where M is the number of constraints and $G(g_m(x_n))$ is the penalty function. Optimization is performed by minimizing $\Omega(x_n, r_K)$ as an unconstrained function of x_n and r_K for a sequence of decreasing values of r_K such that $r_K \to 0$ as $K \to \infty$.

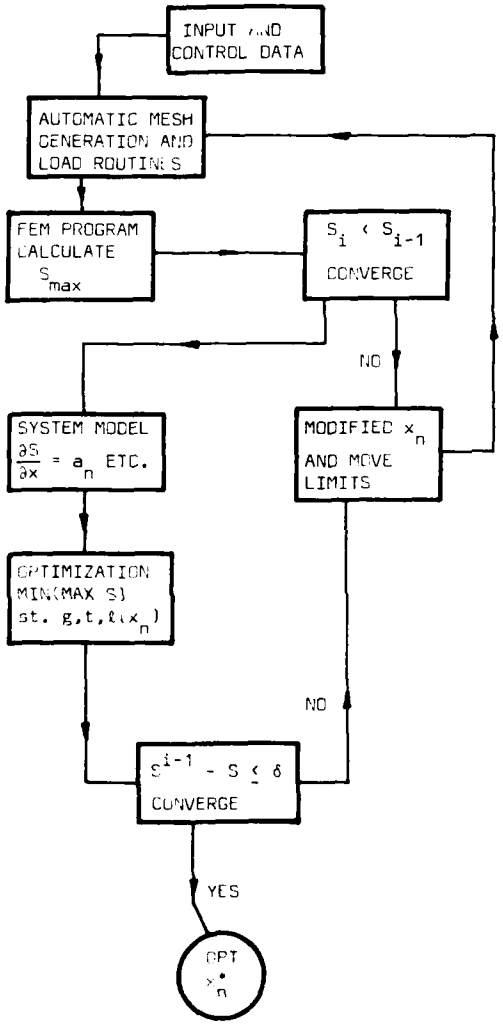
The optimization scheme completes the requirements needed to form the optimum design algorithm. Thus we have a design system which consists of four major segments as follows:

1. Geometrical input and automated mesh generation.
2. Analysis of the component by the finite element method.
3. Formulation of a system model which mathematically

describes the optimization problem.

4. Optimization of the system model by the penalty function approach.

The application of the design algorithm is shown below in the form of a flow chart. Before considering examples of the application of this system it should be noted that the analyses and optimization solutions chosen are by no means the only possible routines but at the present time seem to be the most favourable means of treating continuum type structures.



FLOW CHART SHOWING APPLICATION OF ANALYSIS, SYSTEM MODEL AND OPTIMIZATION SEGMENTS.

6. Design Examples

In this section various design examples are considered to show the application of the optimization scheme. Two and three radii heads are treated and comparisons are made between SCF produced for both heads under internal pressure loading. Optimal nozzle reinforcement is also treated under the combined conditions of internal pressure loading and nozzle thrust.

In all examples considered a two point Gauss rule was used for numerical integration and Poisson's ratio ν and the elastic modulus E were taken as 0.3 and 30×10^6 lb/in² respectively. For thermal loading conditions the coefficient of linear expansion was taken as 12×10^{-6} /°C, and where results are expressed in terms of SCF this is defined as $\frac{St}{PD}$.

6.1 Two radii head

Before considering the optimal design of the two radii head constraints of the type g(x) must be defined. These constraints form a linear set as follows using the notation of Fig. (1).

$$\begin{aligned} g_1(x) &= x_3 - x_2 \geq 0 \\ g_2(x) &= D/2 - x_2 \geq 0 \\ g_3(x) &= D/2 - x_3 \geq 0 \\ g_4(x) &= x_5 - x_4 \geq 0 \end{aligned} \qquad (16)$$

Also the vector x_n must be non-negative.

In this case the head radius x_1 is dependent explicitly on the variables x_2 and x_3 and may be calculated from the following expression

$$x_1 = \frac{x_3^2 + \left(\frac{D}{2}\right)^2 - (D.x_2)}{2(x_3 - x_2)} \qquad (17)$$

The loading conditions for this example were internal pressure and a thermal load of 300°C applied to the internal surface. This simulates the important stage of start-up conditions where temperature stresses may be more important than mechanical loading.

Initial and final design shapes for this case are shown in Fig. (3.1). The optimum shape shows a reduction in the head thickness due to thermal loading and also a significant change in the head radius x_1. Fig. (3.2) shows the reduction of stress for each design step with the optimal solution being reached in six redesigns. The shear stress was lowered from 285 lb/in² to 204 lb/in² which is a reduction of 29%.

6.2 Three radii head

The applied geometrical constraints for this configuration are somewhat more complicated due to the fact that a further radius has been included in the knuckle region. These constraints may be written as follows:

$$\begin{aligned} g_1^1(x) &= x_1^1 - x_2^1 \geq 0 \\ g_2^1(x) &= D/2 - x_2^1 \geq 0 \\ g_3^1(x) &= D/2 - x_1^1 \geq 0 \\ g_4^1(x) &= x_1^1 - x_3^1 \geq 0 \\ g_5^1(x) &= \frac{\pi}{2} - \theta \geq 0 \end{aligned} \qquad (18)$$

/cont....

$$g_6^1(x) = \theta \geq 0 \qquad (18)\ \text{cont..}$$

$$g_7^1(x) = \frac{\pi}{2} - \left\{\frac{\text{SIN}\left(\frac{D}{2} - x_3^1 - (x_2^1 - x_3^1)\right)\cos\theta}{(x_1^1 - x_2^1)}\right\} - \theta \geq 0$$

$$g_8^1(x) = (x_2^1 - x_3^1)\,\text{SIN}\theta + x_4^1 - x_2^1 \geq 0$$

In this configuration the head radius x_1^1 can be defined in terms of x_2^1, x_3^1, x_4^1, D and θ as follows:

$$x_1^1 = \frac{P_z^2 + P_r^2 + 2x_4^1 x_2^1 - (x_4^1)^2 - (x_2^1)^2}{2(x_4^1 - x_2^1 + P_z) + x_4^1} \qquad (19)$$

where

$$P_r = \frac{D}{2} - x_3^1 - (x_2^1 - x_3^1)\cos\theta \qquad (20)$$

and

$$P_z = (x_2^1 - x_3^1)\,\text{SIN}\theta \qquad (21)$$

Results for the three radii head are shown in Fig. (4). In this case internal pressure loading only was applied and the closure height and thicknesses were held constant. As seen from Fig. (4) appreciable reductions in SCF were obtained. Fig. (4) also shows results for the two radii head under the same loading conditions such that comparisons can be made between the two head types. Considerable stress levelling is achieved in both cases with the SCF for the three radii head being approximately 16% lower than the two radii head.

6.3 Protruding nozzle

The geometry of the protruding nozzle is shown in Fig. (1). Again constraints must be applied to control the geometry such that slope continuity between the various radii forming the reinforcement is achieved. Constraints for this case are written as

$$g_1^2(x) = R_3 - R_1 - \left\{\frac{(D - (D-R_1)\cos\beta - P}{\text{SIN}(\frac{\pi}{2} - \theta - \beta)}\right\} \geq 0 \qquad (22)$$

$$g_2^2(x) = W - \{D - \left[D-P-(D-R_2)\text{COS}\beta\right] - P\}\tan\beta$$
$$- \{D - \left[D-R_1\right]\text{COS}\beta - P\}\tan\gamma - \frac{d}{2} - R_3 \geq 0 \qquad (23)$$

together with x_n being non-negative.

An example is shown in Fig. (5) of a typical nozzle under internal pressure loading and nozzle thrust. The initial design consisted of the material defined by the inside surface of the hatching shown in Fig. (5). Reinforcement was subsequently added to this as optimization progressed and this is shown by the internal and external hatched areas. Plots of SCF are shown for the inside and outside surfaces of the nozzle reinforcement. The major reduction in SCF occurred on the outside surface where the initial SCF was reduced from 5.06 to 3.19 which is a reduction of 36.8%. It was noted that little change of SCF took place on the internal boundary throughout the design changes.

7. Conclusions

The optimization of shape to reduce stress concentration factors in a typical pressure vessel configuration has been successfully treated. A mathematical model was formed by calculating structural sensitivities which were based on the finite element method of analysis.

The penalty function approach was used to optimize the discrete nonlinear programming problem and this method can be used regardless of the technique employed in analysis.

Examples of different configurations under various loading conditions were examined and very promising results were obtained. Results were generally obtained in six to eight design steps but this obviously depends on how close the initial design vector is to the optimal solution.

The versatility of the optimization scheme and the generality of the finite element method in solving arbitrary geometries allows the application of the technique to many different problems. Here the method could produce optimal configurations without the use of parametric studies which usually form the basis of many designs and loading cases.

Finally it should be mentioned that the procedure developed is not intended to completely replace the design engineer but allows him to have at his disposal a most powerful technique which fully analyses and outputs the structural response of the component at each stage of the optimization process.

8. References

(1) Harvey, J. F., Theory and design of modern pressure vessels. New York, Van Nostrand Reinhold, 1974.

(2) Peterson, R. E., Stress concentration factors, Wiley, New York, 1974.

(3) Neuber, H. and Hahn, H. G., Stress concentration in scientific research and engineering. Applied Mech. Rev. 19131. p.107, 1966.

(4) Schnack, E., An optimization procedure for stress concentration by the finite element technique. Int. J. Num. Meth. Engng. Vol.14, p.115, 1979.

(5) Bhavikatti, S. S. and Ramakrishnan, C. V., Optimum design of fillets in flat and round tension bard. ASME publication 77-DET-45, 1977.

(6) Francavilla, A., Ramakrishnan, C. V. and Zienkiewicz, O. C., Optimization of shape to minimize stress concentration. Journal of Strain Analysis, Vol. 10, No.2, pp.63-70, 1975.

(7) Middleton, J. and Owen, D. R. J., Automated design optimization to minimize shearing stress in axisymmetric pressure vessels. Nuclear Eng. and Design, 44, p.357, 1977.

(8) Queau, J. P. and Trompette, P. Two-dimensional shape optimal design by the finite element method. Int. J. Num. Meth. Engng. Vol.15, p.1603, 1980.

(9) Zienkiewicz, O. C., The Finite Element Method, 3rd Edition, McGraw-Hill, U.K. 1977.

(10) Kristensen, E. S. and Madsen, N. F., On the optimum shape of fillets in plates subjected to multiple in plane loading cases. Int. J. Num. Meth. Engng. Vol.10, p.1007, 1976.

(11) Morrison, J. L. M., Crossland, B. and Parry, J. S. C., The strength of thick cylinders subjected to repeated pressures. ASME Trans. Paper 59-A-167, 1959.

(12) ASME Boiler and Pressure Vessel Code 1980.

(13) Romstad, K. M. and Wang, C. K., Optimum design of framed structures, ASCE, Str. Div., 94, p.1219, 1968.

(14) Fiacco, A. V. and McCormick, G. P., Nonlinear Programming: Sequential Unconstrained Minimization Techriques. J. Wiley & Sons, New York, 1968

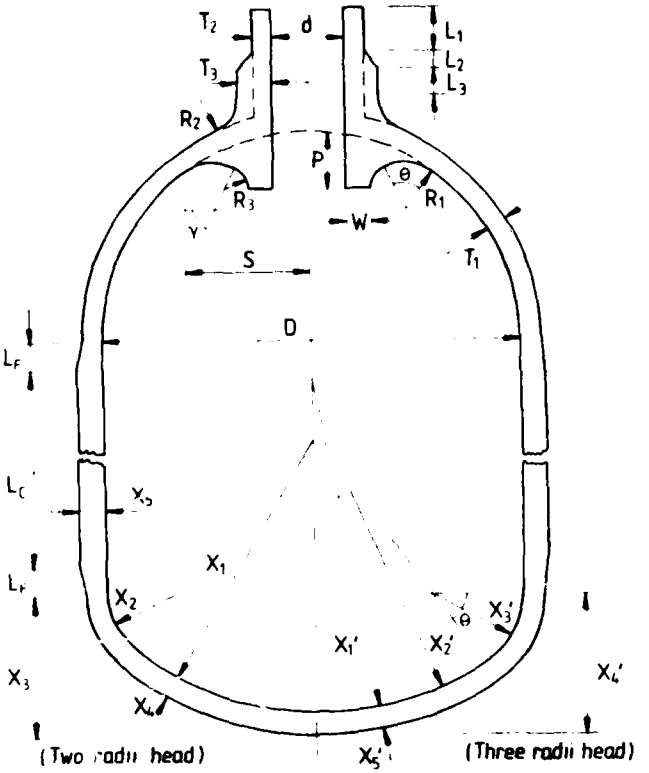


FIGURE 1 VESSEL GEOMETRY AND DESIGN VARIABLES

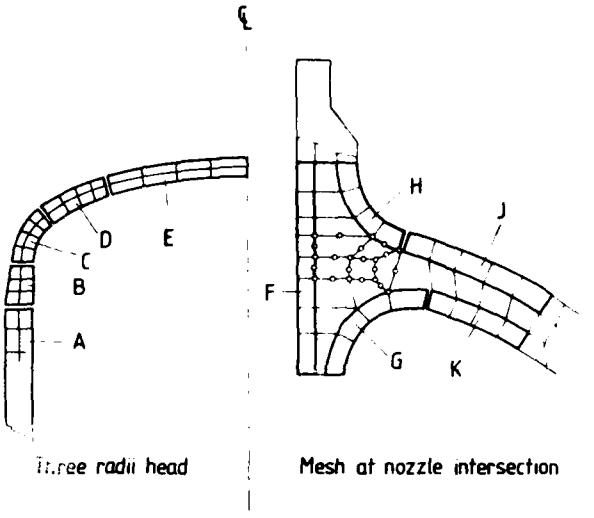


FIGURE 2 TYPICAL COMPONENT MESHING. REGION A-E IN HEAD AND F-K IN NOZZLE ALLOW CONTROL OF MESH DENSITIES

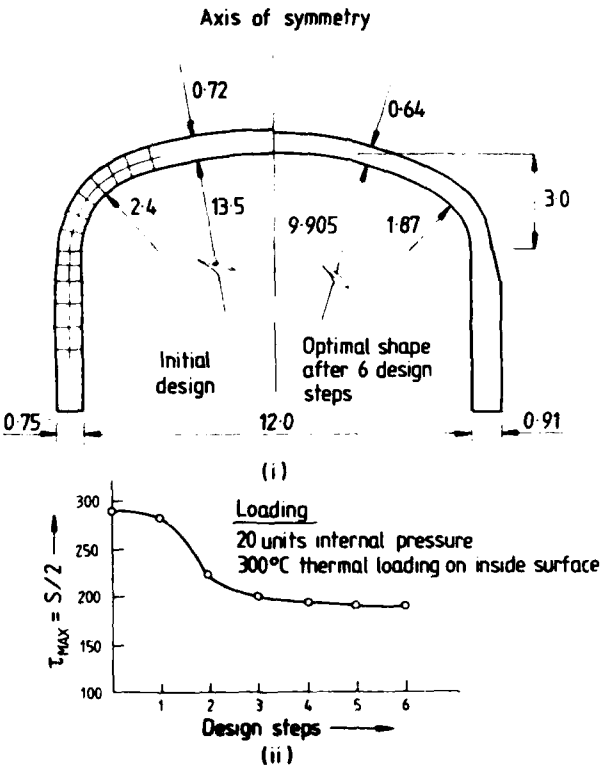


FIGURE 3 TWO RADII TORISPHERICAL HEAD SUBJECT TO PRESSURE AND THERMAL LOADING

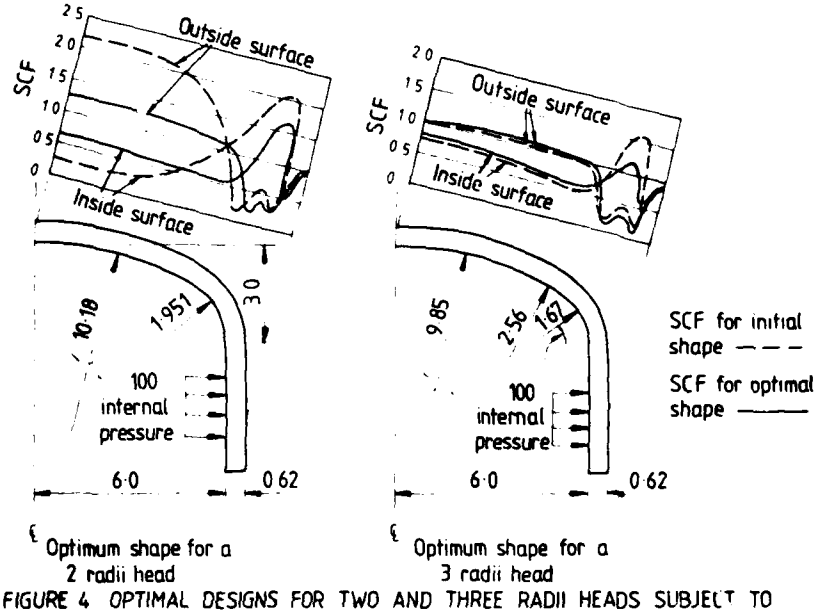


FIGURE 4 OPTIMAL DESIGNS FOR TWO AND THREE RADII HEADS SUBJECT TO INTERNAL PRESSURE LOADING

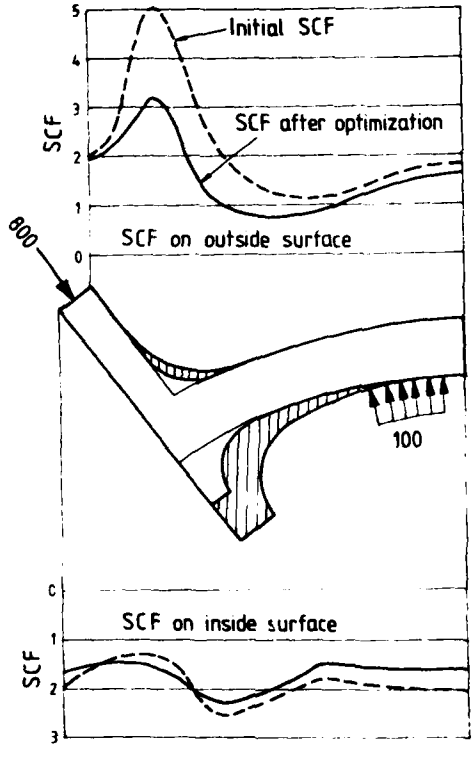


FIGURE 5 NOZZLE INTERSECTION UNDER INTERNAL PRESSURE AND NOZZLE THRUST

NUMERICAL METHODS FOR SHAPE OPTIMIZATION
AN ASSESSMENT OF THE STATE OF THE ART

G. N. Vanderplaats
Naval Postgraduate School
Monterey, California

Abstract

Numerical techniques for structural optimization have seen extensive development over the past twenty years. This was motivated, in large part, by the classic work of Schmit whereby he showed that the minimum weight design of a statically indeterminate structure, designed to support multiple loading conditions, need not be fully-stressed. The design variables were member cross-sectional areas. Using a simple three-bar truss, the design obtained by the common stress-ratio method was statically determinate and weighed approximately seven percent more than the optimum indeterminate truss which he designed using nonlinear programming techniques.

Following this work, major advances in structural optimization have been made. However, the vast majority of this effort has been devoted to the member sizing (fixed shape) problem where the design variables are the cross-sectional areas of truss members or membrane or web thicknesses as in aircraft wing skins and stiffeners. The key to the high degree of design efficiency today is in the ability, for a large class of problems, to provide high quality approximations to the response variables as functions of the member sizing design variables.

Relatively little effort has been devoted to the shape optimization problem where the nodal positions of the finite element structure are treated as design variables. However, it is intriguing to note that by allowing for reasonable geometric changes, the optimum three-bar truss reduces to a statically determinate two-bar truss of even lighter weight and which is fully-stressed under the specified loading conditions. This satisfies our intuition that the optimum structure should make the best use of material and provides motivation to study the shape optimization problem.

In discussing numerical methods for shape optimization, it is necessary to provide a logical progression to our discussion so that the similarities and differences with fixed-shape optimization may be identified. To this end, the basic design task is first outlined as a mathematical programming problem. It is assumed that the finite element method will be used as the analysis tool. Using the displacement method, the mathematical nature of the analysis problem is discussed. From this it is seen that the major efficiency improvements in fixed-shape structural optimization have come from the recognition that, for many problems, the element stiffness matrix is the product of a single design variable and an invarient matrix. This leads to the ability to create high quality approximations to the analysis which can then be used to improve the optimization efficiency. However, this feature does not exist when considering elements where the stiffness matrix is not of this form. Shape optimization (as well as some fixed-shape problems such as frames) falls into this category, and this requires an approach which is different than that used for fixed-shape design. A close look at sensitivity computations using the finite element method will identify the difficulties which arise when the shape is allowed to change.

Shape optimization problems are classified into discrete and continuous structures, where discrete structures are defined here to include truss and frame structures and continuous structures include machine castings and arch dams as examples. The significant consideration here is that the finite element model used in the analysis must be modified during the optimization of continuous structures if the analysis is to remain valid.

A review of the available literature in shape optimization is presented. Several fundamentally different, approaches to the problem are reviewed and compared. These include direct approaches where the geometric variables are included in the same set as the member sizing variables as well as multi-level approaches where the fixed-shape problem is solved as a sub-problem within the configuration design process.

In reviewing the state of the art, it is seen that, for a large class of problems, the fixed-shape design problem is efficiently solved using modern optimization techniques. When the structural shape or geometry is treated as a design variable, the state of the art is not so well developed. Given sufficient resources, many shape optimization problems can be solved. However the methods presently available for their solution lack the efficiency desirable for everyday use.

With major design improvements achievable through the use of shape variables, this is clearly a subject requiring concentrated research and development efforts. It is hoped that the insight gained from this review will served to generate ideas and advances in this very timely topic.

PRECEDING PAGE

AD-P000 056

MULTILEVEL OPTIMIZATION OF ARRAYS OF PROTECTIVE STRUCTURES

S. GINSBURG and U. KIRSCH
Department of Civil Engineering,
Technion - Israel Institute of Technology
Haifa 32000, Israel.

Summary

The present study deals with optimal design of arrays of protective structures. The structures, intended for storage of explosive materials, consist of rectangular reinforced concrete (RC) plates, beams, and doors.

The design variables include: a) The elements' cross sectional dimensions; b) The structural configuration; c) The glometric location of the structure. The constrains are related to safety distances, functional requirements, and structural behavior. The objective function represents the cost, including cost of materials, real estate, subgrade, maintenance, etc.

The main difficulties involved in this problem stem from the complex analysis and the nature of the design variables, constraints, and objective function. The various types of variables are of fundamentally different nature, and some of the variables are discrete. The objective function is neither differentiable nor continuous.

Approximate behavior models are employed in order to simplify the analysis. Since it is not practical to optimize all the design variables simultaneously, it is proposed to use a multilevel optimization procedure. The variables are optimized in different levels, according to their type and nature. Considerations for choosing the levels are discussed and numerical examples illustrate the approach and its practicality.

1. Introduction

Protective structures, intended to resist the effects of explosions, are usually expensive due to the nature of the loadings and design criteria. Therefore, improved designs may lead to considerable savings in the total cost of the structure. While much work has been done in the last two decades on optimum structural design [1,2], most applications are limited to cross sections optimization. Examples of previous work on optimal design of protective structures include: cross sections design [3] or optimization of geometry and cross sections [4] of RC slabs subjected to impulse loadings; and optimal (average) strength of magazine doors [5].

The main difficulties involved in design of protective structures stem from the complex analysis and the nature of the design variables, constraints, and objective function. In general, the nonlinear dynamic analysis must be repeated many times and the various types of variables involved are often of fundamentally different nature, from both the mathematical and the physical points of view.

The present study deals with optimal design of arrays of protective structures, intended for storage of explosive materials. The structure consists of RC rectangular plates, and the design variables include:

(a) The elements cross sectional dimensions (plate thicknesses and amounts of steel);
(b) The structural configuration (length and width);
(c) The geometric location of the structure (distances between adjacent structures).

Due to functional requirements the configurational variables are discrete and the objective function, representing the cost, is neither differentiable nor continuous.

To simplify the analysis, approximate behavior models are employed. These include empirical loading expressions, idealized constitutive laws, and simplified dynamic models. A multilevel optimization procedure, in which the different types of variables are treated separately, is proposed. Several authors, e.g. [6], proposed separate design spaces for geometry and cross sections in truss optimal design. In general, such a solution may be viewed as a multilevel approach [2,7,8]. In the formulation presented in this study, the cross sectional dimensions are optimized in the first level for a given configuration and location of the structure. As a result, the structural elements can be optimized independently in a simple manner. Data banks of optimal elements are introduced, to be used in the higher levels of the optimization. In the second level the structural configuration is optimized for a given location of the structure. For each candidate geometry the optimal cross sectional dimensions are chosen from the data banks. The geometric location of the structure is selected in the third level. For each selected location, both the structural configuration and the cross-sections are optimized.

The proposed approach combines efficient suboptimization for cross sectional variables, reduction in the number of design variables optimized simultaneously, and improved convergence.

2. Problem Statement

Consider the array of RC rectangular magazines shown in Fig. 1. The object is to minimize the cost of storing a unit weight of explosive material. It is assumed that the number of structures is large and all the structures are identical; i.e., the optimal design represents a standard magazine. The preassigned parameters include: materials properties, unit costs, height of the structure, and spacings between beams. Uniform cross sectional dimensions of the RC elements and standard steel doors have been assumed. The optimal design problem can be stated as follows: find the vector of design variables $\{X\} = \{D\},\{L\},\{TC\},\{AS\}$ where

$$\begin{aligned} \{D\} &= \{D_1, D_2\} && \text{(distance between adjacent structures)} \\ \{L\} &= \{L_1, L_2\} && \text{(length and width of the structure, } L_1 \in \Lambda_1,\ L_2 \in \Lambda_2) \\ \{TC\} &= \{TC_1, \ldots TC_I\} && \text{(thickness of concrete plates)} \\ \{AS\} &= \{AS_1, \ldots AS_I\} && \text{(amount of steel in plates)} \end{aligned} \tag{1}$$

such that

$$C = \sum_{j=1}^{J} C_j/W \rightarrow \min. \quad \text{(objective function)} \tag{2}$$

$$\{D^L\} \leq \{D\} \leq \{D^U\} \quad \text{(bounds on distances)} \tag{3}$$

PRECEDING PAGE

$$\{L^L\} \le \{L\} \le \{L^U\} \quad \text{(bounds on structural geometry)} \quad (4)$$

$$\{TC^L\} \le \{TC\} \le \{TC^U\} \quad \text{(bounds on concrete thickness)} \quad (5)$$

$$\{\rho^L\} \le \{\rho\} \le \{\rho^U\} \quad \text{(bounds on steel percentage)} \quad (6)$$

$$\{V\} \le \{V^U\} \quad \text{(deflection constraints)} \quad (7)$$

$$\{\theta\} \le \{\theta^U\} \quad \text{(rotation constraints)} \quad (8)$$

$$\{\sigma^L\} \le \{\sigma\} \le \{\sigma^U\} \quad \text{(bending stress constraints)} \quad (9)$$

$$\{\tau^L\} \le \{\tau\} \le \{\tau^U\} \quad \text{(shear stress constraints)} \quad (10)$$

In the above formulation

Λ_1, Λ_2 = sets of allowable discrete values of L_1 and L_2, respectively
I = number of elements in the structure
L,U = superscripts denoting lower and upper bounds, respectively
C = total cost of a magazine per unit stored explosive material
W = quantity of explosive material in a magazine
C_j = the j-th component of the objective function
J = number of components of the objective function
ρ = steel percentage
V = deflection
θ = rotation at the supports
σ = bending stress
τ = shear stress

It should be noted that $\{D^L\}$ is a function of W. The behavior constraints (Eqs. (7) to (10)) are implicit functions of the design variables, given by the analysis equations.

Two types of structures, earth covered and uncovered (Fig. 2) have been considered. The cost function (Eq. (2)) includes: cost of materials (concrete, steel, doors), real estate, subgrade, maintenance, etc. Due to functional requirements the variables $\{L\}$ are discrete. The behavior constraints restrict the amount of damage due to possible explsions in adjacent structures.

3. The Analysis Model

In the discussion that follows only blast loadings have been considered. It is assumed that other effects (such as fragments) are secondary and may be checked after the optimization process. Modifications in the design can then be made, if necessary. An approximate analysis model has been employed with the following features.

a) Loadings

The explosive materials are represented by an equivalent TNT charge at the center of gravity of the charge [9,10]. The blast loadings due to a possible explosion are computed by the methods described in TM 5-1300 [11]. The model is based on experimental results and idealized (such as piecewise-linear) pressure-time relations.

b) Constitutive equations and resistance-deflection functions

Idealized elaso-plastic behavior models have been employed. Also, it is assumed that cracking (but not spalling) may occur in the concrete. The piecewise linear resistance-deflection functions for the various elements are detemined by the yield line theory, considering dynamic values of material constants [11].

c) Dynamic response of elements

To compute displacements and stresses in the elements the medium is discretized, resulting in systems of lumped masses and nonlinear springs. A single degree of freedom system is assumed for each RC element, with the following equation of motion [11]

$$F - P = K_{Lm}\, ma = m_e a \quad (11)$$

in which F = time dependent external force; P = internal force (resistance); m = mass of the element; a = acceleration; K_{Lm} = a factor relating the value of the actual mass m and the equivalent mass m_e. The value of K_{Lm} is determined from the principal mode of vibration. For example, consider the sector of a plate shown in Fig. 3. The equation of motion (rotation about the support) is

$$Fc - (\Sigma M_N + \Sigma M_p) = \frac{I_m}{\ell} a \quad (12)$$

where c = distance of the resultant force from the support; M_N, M_p = negative and positive internal moments, respectively; I_m = moment of inertia; ℓ = width of the element. From Eqs. (11),(12) we obtain

$$K_{Lm} = \frac{I_m}{c\ell m} \quad (13)$$

For an element consisting of a number of sectors

$$K_{Lm} = \frac{\Sigma(I_m/c\ell)}{\Sigma m} \quad (14)$$

For earth covered elements the corresponding mass of the cover is also considered in the equation of motion [12]. Multi-degree-of-freedom systems may be considered for each element if better approximations are required. Numerical algorithms (such as Runge-Kutta) or available results [11] are used to solve the equations of motion and to evaluate displacements and stresses.

d) Computational considerations

Analysis of a single element, including calculation of the loadings and solution of the equations of motion, involves much computational effort (up to 10 sec CPU on IBM 370/168 were reported for complex loading histories). There are several elements in a structure and the analysis usually must be repeated many times during optimization. Therefore, it is proposed to reduce the number of analyses in the solution process by introducing data banks of preoptimized elements for sequences of given loadings and element configurations.

4. Multilevel Optimization

Design of a large complex system usually involves decomposition into a number of smaller subsystems, each with its own goals and constraints [2]. In general, an integrated problem cannot be decomposed into subproblems which can be independently optimized. There may be many different ways of transforming an optimization problem into a multilevel problem. In the model coordination approach [2,7,8] used in this study, we choose certain variables called coordinating or interaction variables to control the lower level systems. For fixed values of the coordinating variables the lower level problems often become independent and simple to optimize. The task in the higher levels is to choose the coordinating variables in such a way that the independent lower level solutions are optimal. The term "model coordination" derives from the circumstance that a constraint is added to the

problem in the form of certain fixed interaction variables.

Define the vector of cross sectional design variables {Q} as

$$\{Q\} = \{TC\},\{AS\} \tag{15}$$

and the vector of configurational and geometric variables {R} by

$$\{R\} = \{D\},\{L\} \tag{16}$$

It has been noted earlier in section 2 that the vector of design variables {X} can be partitioned (Eq. (1))

$$\{X\} = \{R\},\{Q\} \tag{17}$$

In this formulation {R} is the subvector of coordinating variables between the subsystems and {Q} is the vector of subsystem variables, in turn partitioned as follows

$$\{Q\} = \{Q_1\},\ldots,\{Q_i\},\ldots,\{Q_I\} \tag{18}$$

The subvector $\{Q_i\}$ represents the cross sectional variables associated with the i-th element (subsystem) and I is the number of elements. With these definitions, the objective function of Eq. (2) and the constraints of Eqs. (3) to (10) can be expressed in the general form

$$C = F(\{X\}) = \sum_{i=1}^{I} F_i(\{R\},\{Q_i\}) \tag{19}$$

$$g_k(\{X\}) = g_k(\{R\}) \leq 0 \tag{20}$$

$$h_i(\{X\}) = h_i(\{R\},\{Q_i\}) \leq 0 \tag{21}$$

in which g_k are constraints on the {R} variables (i.e., Eqs. (3),(4)) and h_i are constraints associated with the i-th element (Eqs. (5) to (10)). That is, the variables {R} may appear in all expressions, while the variables $\{Q_i\}$ appear only in the constraints associated with the i-th element, and in the corresponding term of the objective function. Specifically, it is assumed that the cross sectional variables of a given element affect only the constraints and objective function component of that element.

The general optimization problem can now be formulated as the following two level problem.

First-level problem. Determine a fixed value for {R} through the constraints

$$\{R\} = \{R^o\} \tag{22}$$

Then the integrated problem can be decomposed into the following I independent first-level subproblems: find $\{Q_i\}$ (i=1,...,I) such that

$$C_i = F_i(\{R^o\},\{Q_i\}) \rightarrow \min. \tag{23}$$

$$h_i(\{R^o\},\{Q_i\}) \leq 0 \tag{24}$$

Second-level problem. The task in the second level problem is to find $\{R^o\}$ such that

$$H(\{R^o\}) = \sum_{i=1}^{I} H_i(\{R^o\}) \rightarrow \min. \tag{25}$$

$$g_k(\{R^o\}) \leq 0 \tag{26}$$

where $H_i(\{R^o\})$ is defined by

$$H_i(\{R^o\}) = \min C_i \tag{27}$$

An additional constraint on $\{R^o\}$ is that the first-level problem has a solution, i.e., that $H(\{R^o\})$ exists.

The two-level problem is solved iteratively as follows:

1. Choose an initial value for the coordinating variables $\{R^o\}$.
2. For a given $\{R^o\}$ solve the I independent first-level problems.
3. Modify the value of $\{R^o\}$ so that $H(\{R^o\})$ is reduced.
4. Repeat steps 2 and 3 until min $H(\{R^o\})$ is achieved.

If all intermediate values for {R},{Q} are feasible, the iteration can be terminated always with a feasible-even though nonoptimal-solution, whatever the number of cycles. This is advantageous from an engineering point of view and may considerably reduce the computational effort, particularly if the object is to achieve a practical optimum rather than the theoretical one.

Since the second level variables ({D} and {L}, see Eq. (16)) are of fundamentally different nature, it is proposed to decompose the second-level problem into two-levels, such that only the configurational variables {L} are optimized in the second level, while the geometric location variables {D} are treated in a new third-level problem. The three problems are solved iteratively until the optimum is achieved. Note that the I first-level subproblems remain unchanged (Eqs. (22) to (24)). The modified second and third-level problems are formulated as follows (Fig. 4).

Second-level problem. For a given geometric location

$$\{D\} = \{D^o\} \tag{28}$$

find $\{L^o\}$ such that

$$C(\{D^o\},\{L^o\},\{Q\}) \rightarrow \min \tag{29}$$

$$g_k(\{D^o\},\{L^o\}) \leq 0 \tag{30}$$

Third-level problem. Find $\{D^o\}$ such that

$$C(\{D^o\},\{L\},\{Q\}) \rightarrow \min \tag{31}$$

$$g_k(\{D^o\},\{L\}) \leq 0 \tag{32}$$

The proposed solution procedure is possible since the system by its very nature can be decomposed. The loadings depend only on the {R} variables, therefore the first level problems can be solved for fixed loadings. The main advantage is that I independent simple subproblems are obtained in this level. It has been noted that $\{D^L\}$ is a function of W, which in turn is a function of {L}. Thus, Eqs. (3) are the only explicit constraints which are functions of both {D} and {L}. The main reason for choosing {L} as the second-level variables is their discrete nature. For any given $\{D^o\}$ only a limited number of {L} values must be considered. The solution process is shown in Fig. 5.

5. Optimization Methods for the Various Levels

First-level. For the relevant ranges of loadings and element dimensions, data banks of preoptimized elements have been prepared. As a first step a sequence of loadings, with fixed peak pressure and variable duration, is computed for a given element configuration. The cross sectional dimensions are optimized by a direct search technique. For each selected concrete thickness the amount of reinforcing steel is minimized, and the optimal thickness is evaluated by quadratic interpolation. The data banks, to be used in the higher level optimization, are obtained by repeating

this process for several element configurations. Intermediate solutions may be evaluated by interpolation.

Second-level. The optimization method in this level is based on a direct search in the space of the discrete variables {L}. For each assumed L_1 value the optimal L_2 is selected. L_1 is then modified, with the current optimal L_2 (or the nearest feasible value) chosen as the initial design. The L_1 values are modified until the optimum is reached.

Third-level. Powell's direct search method [13] is applied in this level with the convergence criterion

$$|C(\{X_q\}) - C(\{X_{q+1}\})|/C(\{X_q\}) < \varepsilon_c \qquad (33)$$

where ε_c is a predetermined parameter and q is the iteration number in the third level. An additional criterion

$$|\{X_q\} - \{X_{q+1}\}| < \varepsilon_x \qquad (34)$$

ensures that the iteration is terminated only if the condition of Eq. (34) holds for two successive iterations.

6. Numerical Examples

Two types of magazine have been considered [14]: earth covered structure with a standard cover thickness and an uncovered structure. Fig. 6 shows some reasible combinations of the {L} variables (a = standard spacing, b = required spacing to satisfy functional requirements, c = required spacing for doors). Fig. 7 shows a typical design space for the cross sectional variables, in which A_s and A'_s are the amounts of reinforcing steel required for tensile and compressive forces, respectively. A direct search in the space of d (the effective depth of the cross section), as shown in Fig. 8, provides the optimal element for the given loading and configuration. This procedure is repeated for all relevant loadings and element configurations. Typical optimal costs for a sequence of triangular pulses are shown in Fig. 9, in which p is the peak pressure and the time axis denotes the duration.

Since the second level variables are discrete, the objective function in the third level is not continuous (Fig. 10). It can be noted that local optimum points may exist and the search is terminated only after checking the objective function in a number of points, to ensure that the true optimum is achieved. For each point in the {D} variables space an optimal structure is selected. For larger values of {D} the feasible region in the {L} variables space is increased, and the result might be a change in the discrete optimal {L} values. The computational effort in the second level optimization may be reduced considerably by interactive design. Convergence display programs may be used for this purpose. Fig. 11 demonstrates the relative cost against the number of calculated {R} vectors (Eq. (16)). The latter number is equal to the number of accesses to the data banks. Search in {D} space is shown in Fig. 12. Different initial designs or directions in this space provided an identical optimum. Earth covered structures were optimized in a similar manner, with convergence demonstrated in Fig. 13. This type of structure was found to be cheaper than the uncovered structure.

The possibility of choosing the structural configuration {L} as the third-level variables was also checked. While an identical optimum was obtained, the convergence rate was much slower; the number of iterations was about 50% larger. This can be explained by the difficulties encountered in searching the optimum in the discrete variables space. Choosing {L} as the second-level variables, the number of checked points for a given {D} value is limited by the constraints of Eq. (3).

7. Concluding Remarks

A multilevel approach for optimal design of protective structures has been presented. The solution method, which is based on a simplified analysis model and decomposition of the integrated problem into a number of smaller subproblems, is motivated by the following difficulties:

a. Nonlinear dynamic analysis is needed to describe the structural response even when approximate models are used.
b. The various types of design variables are of fundamentally different nature from both the physical and the mathematical points of view.
c. The objective function is neither differentiable nor continuous.
d. The problem size (numbers of variables and constraints) may be large in practical problems.

A simple optimization model is proposed for the cross-sectional variables. Preoptimized elements are introduced for a set of given element configurations and loadings. This information is then used for efficient optimization of the higher level variables. The approach is general and is not restricted to a specific problem, analysis model, or optimization algorithms. Rather, other types of structure (such as steel or composite structures having non-rectangular shape), different analysis models (dependong on the type of approximations and simplifications used) and optimization methods (such as optimality criteria) can be employed.

The numerical examples indicate that efficient solutions which do not involve much computational effort, can be achieved for complex optimal design problems by the proposed approach.

Acknowledgement

This work was supported by the Vice-President Fund for Research at the Technion - Israel Institute of Technology.

References

[1] Haug, E.J., and Arora, J.S., Applied Optimal Design, Mechanical and Structural Systems, John Wiley & Sons, 1979.

[2] Kirsch, U., Optimum Structural Design, Concepts, Methods, and Applications, McGraw-Hill Book Company, 1981.

[3] Ferritto, J.M., Optimization of Reinforced Concrete Slabs, The Shock and Vibration Information Bulletin, 49(3), 1979.

[4] Kirsch, U., "Optimization of Protective Structures," Report No. 010-598, Technion Research and Development Foundation, (in Hebrew), 1974.

[5] Tancreto, J.E., An Economic Decision Model to Optimize Magazine Door Design, Minutes of the 18th Explosives Safety Seminar, 1978.

[6] Vanderplaats, G.N., and Moses, F., Automated Design of Trusses for Optimum Geometry, J. Struct. Div., ASCE, Vol. 98, ST3, March 1972.

[7] Kirsch, U., Multilevel Approach to Optimum Structural Design, J. Struct. Div., ASCE, Vol. 101, ST4, April 1975.

[8] Kirsch, U. and Moses, F., Decomposition in Optimum Structural Design, J. Struct. Div., ASCE, Vol.105, ST1, January 1979.

[9] Hokanson, J.C., and Wenzel, A.B., Reflected Blast Measurements Around Multiple Detonating Charges, Minutes of the 18th Explosives Safety Seminar, 1978.

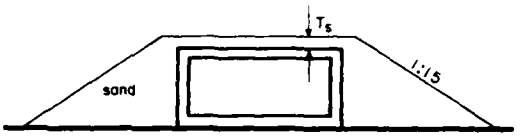
[10] Reeves, H.J., Hazard Classification Test of Complete Round 155mm Pallets, Minutes of the 18th Explosives Safety Seminar, 1978.

[11] TM 5-1300/NAVFAC P-397/AFM 88-22, Structures to Resist the Effects of Accidental Explosions, 1969.

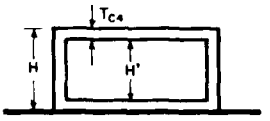
[12] Hill, W.V., Practical Aspects of Soil as a Protective Construction Material, Minutes of the 18th Explosives Safety Seminar, 1978.

[13] Powell, M.J.D., An Efficient Method for Finding the Minimum of a Function of Several Variables without Calculating Derivatives, Computer J. 7(4), 1964.

[14] Ginsburg, S., and Kirsch, U., Optimization of Protective Structures, Report No. 010-810, Technion Research and Development Foundation, (in Hebrew), 1981.



(a) EARTH-COVERED MAGAZINE



(b) UNCOVERED MAGAZINE

FIG. 2

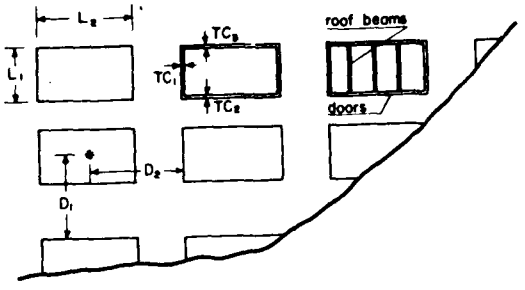
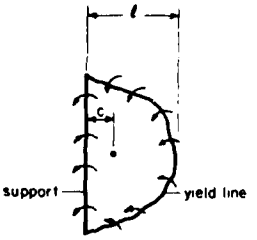
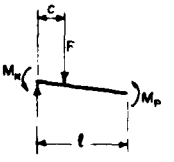


FIG. 1



(a) PLAN



(b) SECTION

FIG. 3

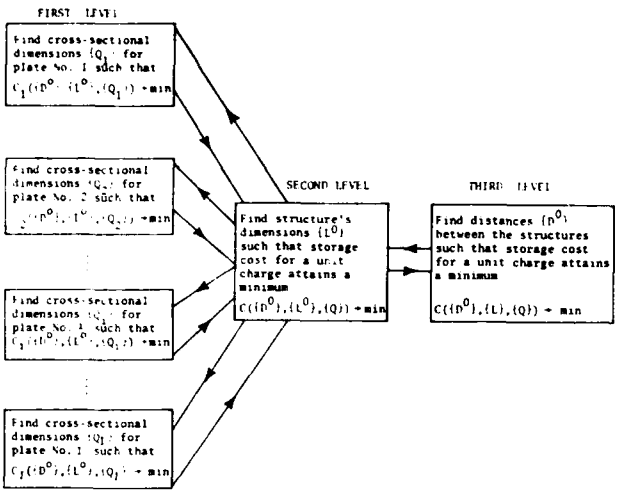


FIG. 4

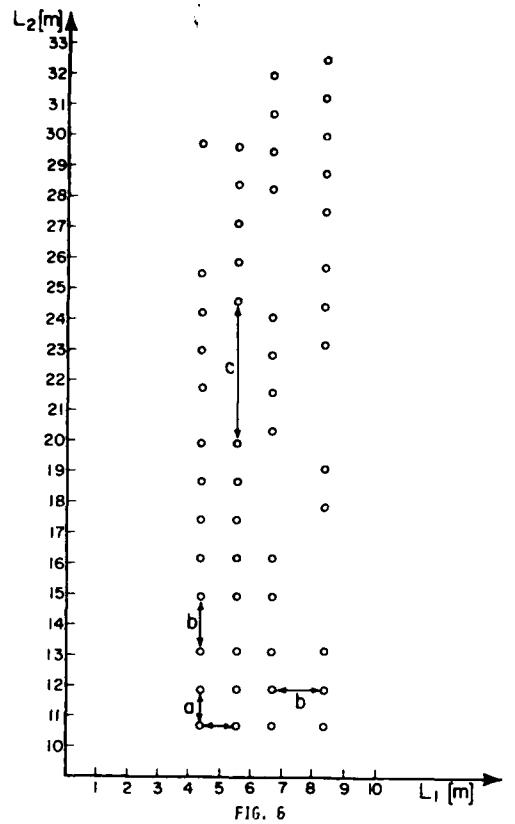


FIG. 6

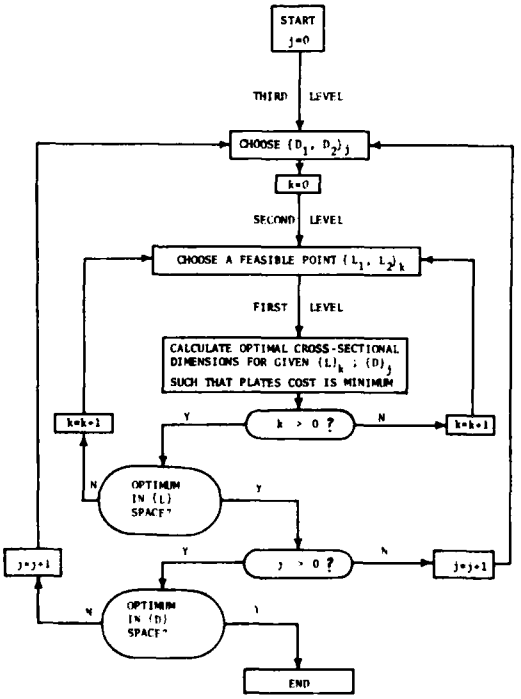


FIG. 5

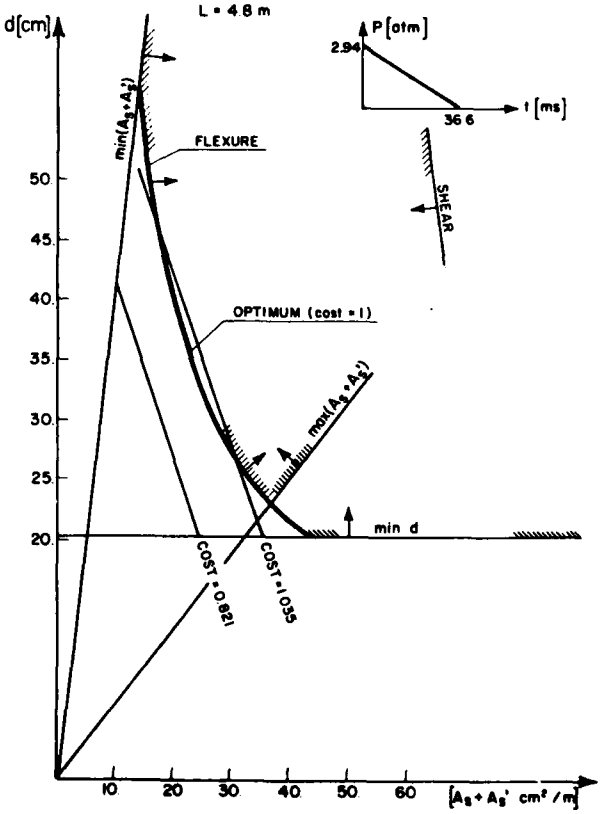


FIG. 7

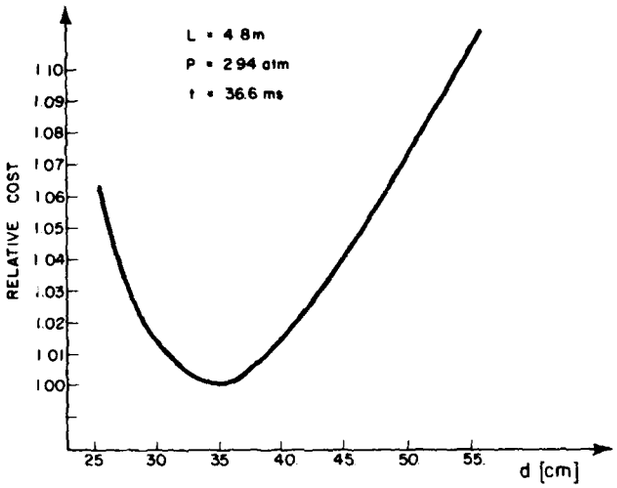


FIG. 8

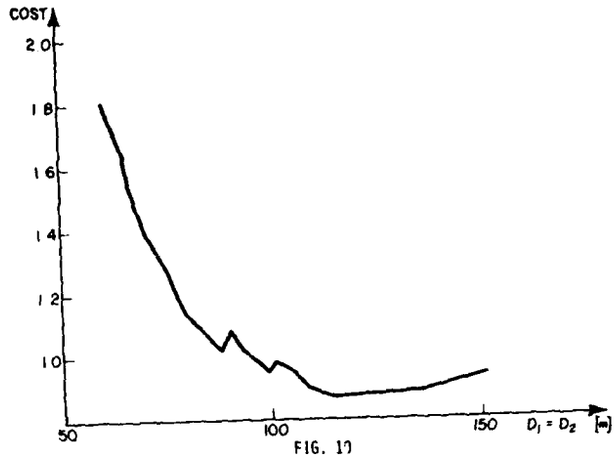


FIG. 10

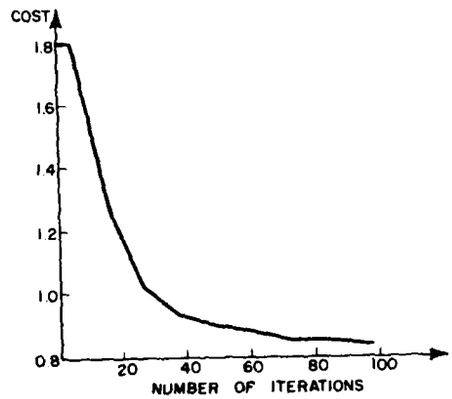


FIG. 11

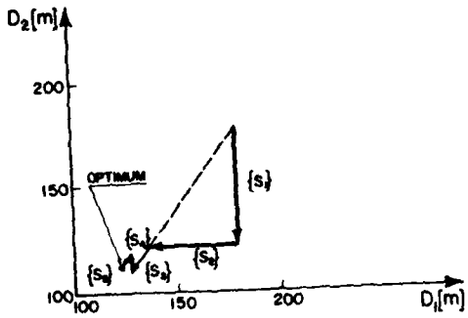


FIG. 12

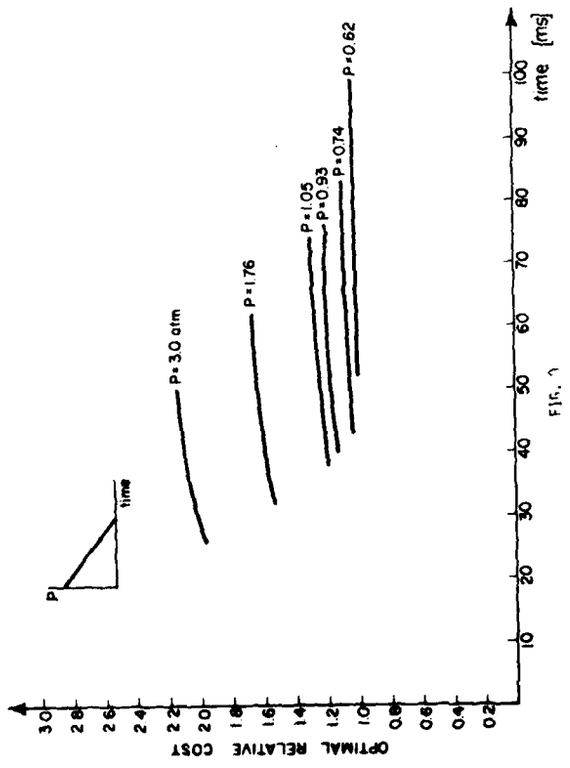


FIG. 9

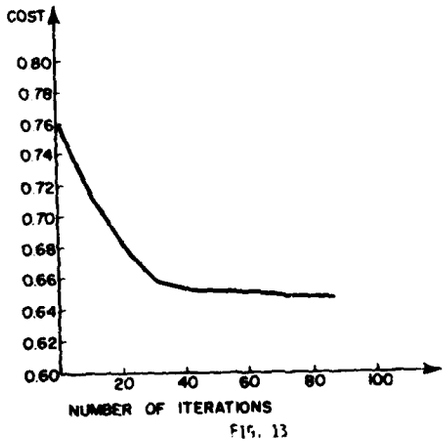


FIG. 13

SESSION #6

LOCAL AND GLOBAL OPTIMA

RIGOROUS SIMPLIFICATION AND BOUNDING OF OPTIMIZATION MODELS WITH OBSCURED MONOTONICITY

by

Douglass J. Wilde and Meldon Human

Design Division, Department of Mechanical Engineering
STANFORD UNIVERSITY, Stanford CA 94305

EXTENDED ABSTRACT

Nonlinear equations constraining an optimization problem often confound analytic and numerical procedures that work well when all constraints are inequalities. A rigorous theory is developed for constructing simpler approximating problems that not only reveal hidden monotonicity, but also give both upper and lower bounds on the optimum. This permits postponing solving exact constraint equations until an almost feasible, nearly optimal design has been located.

In optimization problems constrained by inequalities, monotonicity analysis has been used to identify constraints which must be satisfied as strict equations at the optimum . When such "binding" constraints are easily solved in closed form, they can be used to eliminate variables, producing, if not the optimum sought, then at least a simpler problem.

Although there are other advantages to knowing which constraints are binding, this particular one is lost on binding constraints that are not solvable. In engineering design problems, a constraint is often made unsolvable by small terms or factors appended to improve the accuracy of a basically simple physical relation. Then it becomes attractive to neglect or cancel such refinements (here named "obscurants") to obtain a solvable, though perhaps inaccurate, approximation.

This article shows how to construct approximations that achieve solvability while retaining most of the original accuracy. Each obscurant is replaced by a bounding function which is either a constant or a function having the same form as some underlying part of the constraint. The replacement bounds the obscurant either from above or below, depending on the direction of the inequality. In this manner an approximating problem is constructed whose optimal solution bounds the original minimum from below.

Although every binding constraint still must be satisfied as a strict equality at the true optimum, approximate designs can easily be adjusted to produce nearly optimal ones on the feasible side of the inequalities. Being upper bounds on the true minimum, their comparison with results of the lower bounding approximation gives rules for accepting a design as satisfactory.

This procedure is more difficult to apply to equality constraints. One cannot tell whether an obscurant is to be bounded from above or from below until its equation has been replaced by an inequality identifying the equation's non-optimal side. This in turn requires monotonicity analysis, but the monotonicity needed is often hidden by the obscurants. A way out of this dilemma will be demonstrated on part of a magnetodynamic power plant design problem having for constraints 12 equations and NO inequalities.

A further difficulty is that, unlike inequalities, equations do not have a feasible side obtainable simply by adjusting approximate designs. Hence upper bounds for termination rules are not readily available. One can, however, construct an approximating problem giving an upper rather than lower bound on the true minimum. This is done by replacing each obscurant with a function bounding it on the side opposite from that used in the lower bounding approximating problem.

Before developing these ideas, the article defines and discusses the underlying concepts of minimum and infimum, critical, redundant, and binding constraints, boundedness and monotonicity. This permits stating the two principles of monotonicity analysis more precisely than in previous publications.

These monotonicity principles are then applied to designing a magnetohydrodynamic power plant described briefly in engineering terms. This requires directing the 12 constraint equations and then constructing lower and upper bounding approximating problems, for which supporting theory is presented.

AD-P000 057

ON LOCAL AND GLOBAL MINIMA IN STRUCTURAL OPTIMIZATION

Krister Svanberg
Contract Research Group for Applied Mathematics
Royal Institute of Technology
S-100 44 Stockholm, Sweden

0. Summary

This paper deals with convexity properties in structural optimization, and with the closely related question of local versus global optima.

The problem we investigate is that of minimizing the structural weight subject to constraints on displacements, stresses and natural frequencies. It is assumed that the structure is described by a finite element model, and that the transverse sizes of the elements, e.g. thicknesses of membrane plates, are the design variables. This implies that both the objective function, i.e. the weight, and the structural stiffness matrix depend linearly on the design variables. The constraint functions, however, become nonlinear and they may in the general case give rise to a nonconvex feasible region in the design space. Then there is a risk that a local, but not global, mimimum is attained when any of the various existing methods for numerically solving the problem is applied. This fact is illustrated by examples of nonconvex problems.

However, as shown in this paper, there are some special cases where the feasible region always becomes convex, so that, due to the linearity of the objective function, each local optimum is in fact also a global one. Three examples of constraints which are proved to possess such convexity properties are: i) a natural kind of "symmetric" displacement constraint, where the magnitude of the displacement is measured in the direction of the applied load, ii) a "global" displacement constraint, which may be interpreted as a lower bound of the smallest eigenvalue of the structural stiffness matrix, and iii) a lower bound on the lowest natural frequency.

1. Introduction

When an "optimal" solution of a structural optimization problem is obtained, by some numerical method, it is often very difficult to decide if it is the "global" optimal solution or just a "local" one. If, however, the considered problem is known to be convex, then some strong statements about the global nature of obtained solutions can be made. This is the main reason for the investigation of convexity properties in structural optimization accomplished in this paper. A second reason, which we do not go into details about, is that if the considered problem is known to be convex, then methods specially developed for convex problems could be used. Such methods might be more efficient than methods developed for more general nonlinear problems.

The problem we consider is to minimize the structural weight subject to constraints on displacements and stresses, under multiple statical load conditions, and on natural frequencies. It is assumed that the considered structure is described by a linearly elastic finite element model, and that the transverse sizes of the elements (cross section areas of bars, thicknesses of membrane plates etc.) are the design variables. The elements may be linked together in groups, so that the j:th design variable x_j determines the sizes of all the elements in the j:th group. Also, some elements may have fixed sizes.

Under these assumptions the structural weight w is a linear function of the design variables: $w(x) = w_o + \sum w_j x_j$. The structural stiffness matrix K and the structural mass matrix M are also linear functions of x, i.e. $K(x) = K_o + \sum x_j K_j$ and $M(x) = M_o + \sum x_j M_j$, where K_j and M_j (j=0,1,..,n) are constant symmetric matrices. It is further assumed that each design variabel x_j is restricted between given bounds: $x_j^{min} \le x_j \le x_j^{max}$, where x_j^{min} and x_j^{max} are constant positive real numbers. This may be written: $x \in X$, where $x = (x_1,..x_n)^T$ is the vector of variables and $X = \{x \in R^n \mid x_j^{min} \le x_j \le x_j^{max},\ j=1,..n\}$. For each $x \in X$, the structure is assumed to be non-degenerate, so that K(x) and M(x) are symmetric and positive definite.

It should be noted that since the weight w is a linear function in x, it is also a convex function in x. Thus, when investigating if the minimum weight problem is convex, it suffices to investigate if the imposed constraints (on displacements, etc.) give rise to a convex feasible domain in the design space. (This statement is made clear in section 2.)

We will occasionally use the notation $\|v\|$, to denote the euclidean norm of the vector v. If $v = (v_1,..v_n)^T \in R^n$, then $\|v\|^2 = \sum v_j^2$. We also use the notation S for the "unit sphere" (of suitable dimension apparent from the context), i.e. $S = \{v \mid \|v\| = 1\}$.

2. Convex optimization problems

In this section we bring together some basic definitions and results, concerning nonlinear optimization in general and convex problems in particular, which will be frequently referred to in the forthcoming sections. The results collected in this section have been known for several decades, and we therefore omit the proofs. A more exhaustive description of the matter may be found in refs [1] and [2].

We consider here the following general optimization problem P:

$$P: \quad \min f(x) \ , \ x \in R^n$$

$$\text{subject to } g_i(x) \le \alpha_i, \ i=1,..m$$

$$x_j^{min} \le x_j \le x_j^{max}, \ j=1,..n$$

f and g_i are real-valued functions. α_i, x_j^{min} and x_j^{max} are constant real numbers. To shorten the notation we will also write:

$$P: \quad \min f(x)$$

$$\text{subject to } x \in \Omega$$

where Ω, the feasible set, is defined by $\Omega = \{x \in X \mid g_i(x) \le \alpha_i, \ i \in I\}$, where $X = \{x \in R^n \mid x_j^{min} \le x_j \le x_j^{max}, \ j=1,..n\}$ and $I = \{1,..m\}$.

PRECEDING PAGE

Definition 2.1: A point $x^* \in \Omega$ is said to be a global minimum point of P if $f(x^*) \leq f(x)$ for all $x \in \Omega$.

A global minimum point is what we normally are searching for. However, algorithms for numerically solving nonlinear problems of realistic sizes can not, in the general case, be expected to find anything better than a local minimum point:

Definition 2.2: A point $x^* \in \Omega$ is said to be a local minimum point of P if there is an $\varepsilon > 0$ such that $f(x^*) \leq f(x)$ for all $x \in \Omega$ such that $\|x-x^*\| < \varepsilon$.

If x^* is a global minimum point then x^* is obviously also a local minimum point, but the converse is in general not true.

Definition 2.3: A set C in R^n is said to be convex if $\mu x + (1-\mu)y \in C$, for every $x, y \in C$ and every real number μ such that $0 < \mu < 1$.

The following property is fundamental for convex sets:

Lemma 2.4: Let C_ν, $\nu \in V$, be a collection of convex sets in R^n. Then the intersection set $C = \bigcap_{\nu \in V} C_\nu = \{x \in R^n \mid x \in C_\nu \text{ for all } \nu \in V\}$ is convex. (If C is empty then C is by definition convex.)

V may be a finite or infinite index set. The lemma is illustrated in fig 2.1.

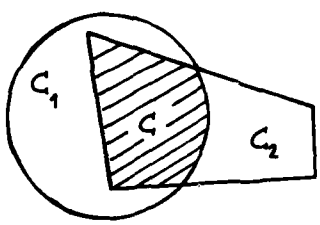


Fig 2.1 $C = C_1 \cap C_2$ is convex if C_1 and C_2 are convex.

Definition 2.5: A real-valued function φ, defined on a convex set C, is said to be convex over C if $\varphi(\mu x+(1-\mu)y) \leq \mu\varphi(x) + (1-\mu)\varphi(y)$, for every $x, y \in C$ and every μ such that $0 < \mu < 1$.

For twice continuously differentiable functions there is an alternative characterization of convexity:

Lemma 2.6: Assume that the function φ has continuous second partial derivatives on a convex set C in R^n. Then φ is convex over C if and only if the Hessian matrix Φ (= the matrix of second derivatives) of φ is positive semidefinite throughout C, i.e. if and only if:

$h^T\Phi(x)h = \sum_j \sum_k \frac{\partial^2 \varphi}{\partial x_j \partial x_k} h_j h_k \geq 0$ for all $x \in C$ and every vector $h \in R^n$.

The following property is fundamental for convex functions:

Lemma 2.7: Let g_ν, $\nu \in V$, be a collection of functions which are convex over the convex set C. Assume that, for each $x \in C$, $\max_{\nu \in V} \{g_\nu(x)\}$ exists. Then the "pointwise maximum function" g, defined by $g(x) = \max_{\nu \in V} \{g_\nu(x)\}$, is convex over C.

V may be a finite or infinite index set. The lemma is illustrated in fig 2.2.

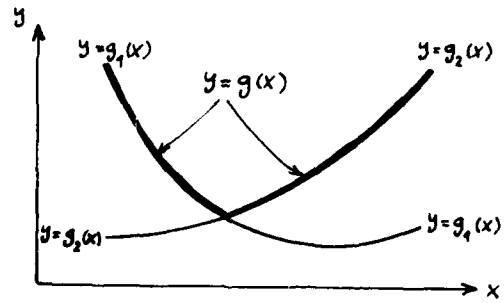


Fig 2.2 $g(x) = \max\{g_1(x), g_2(x)\}$. g is convex if g_1 and g_2 are convex.

We now come to what, in this paper, will be meant by a convex problem:

Definition 2.8: If, in problem P, the feasible set Ω is convex and the objective function f is convex over Ω, then P is said to be a convex (optimization) problem.

Lemma 2.9: A sufficient condition for P to be a convex problem is that the objective function f and the constraint functions g_i, $i \in I$, are convex over X.

The following theorem is of obvious practical importance:

Theorem 2.10: Assume that P is a convex problem and that x^* is a local minimum point of P. Then x^* is also a global minimum point of P.

Most of the methods commonly used in structural optimization, see e.g. ref [3], do not explicitly use definitions 2.1 and 2.2 when searching for a minimum point. Instead they search for, and usually end up with, a point which satisfies the so called KT-conditions (= Kuhn-Tucker conditions).

Definition 2.11: Assume that f and g_i are differentiable functions. A point $x^* \in \Omega$ is said to be satisfying the KT-conditions of problem P if there are non-negative real numbers λ_i, $i \in I$, such that the following two conditions are satisfied:

i) $$\frac{\partial f}{\partial x_j} + \sum_{i \in I} \lambda_i \frac{\partial g_i}{\partial x_j} \begin{cases} \geq 0 \text{ if } x_j^* = x_j^{min} \\ = 0 \text{ if } x_j^{min} < x_j^* < x_j^{max} \\ \leq 0 \text{ if } x_j^* = x_j^{max} \end{cases}$$

for all $j \in \{1,..,n\}$, where the derivatives are evaluated at $x = x^*$.

ii) $\lambda_i(g_i(x^*)-\alpha_i) = 0$ for all $i \in I$.

In the general case, such a "KT-point" x^* may fail to be even a local minimum point of P. In the convex case, however, the situation is completely satisfactory:

Theorem 2.12: Assume that P is a convex problem and that x^* satisfies the KT-conditions of P. Then x^* is a global minimum point of P.

Convex problems possess a variety of other interesting and useful properties, see e.g. ref [4], but we believe that the above theorems, 2.10 and 2.12, suffice to point out that convex problems are well-behaved compared to nonconvex ones.

3. Displacement- and stress constraints

Displacement constraints are usually of the form $q^T u \leq \alpha$, where u is the nodal displacement vector, q is a given constant vector and α is a given real number. u is obtained from the system $Ku = p$, where p is the load vector and $K = K_o + \sum x_j K_j$ is the structural stiffness matrix. Thus $u = K^{-1}p$, and a given displacement constraint may be written:

$$d(x) = q^T K^{-1} p \leq \alpha$$

q is in the literature often considered to be a "virtual load" vector, a convention we will follow in this paper. Note that q and p are both assumed to be given constant vectors, while K^{-1} depends on x. We will therefore occasionally (when we want to emphasize this dependence) write $q^T K^{-1}(x)p$ instead of the shorter $q^T K^{-1} p$. The meaning is however always the same.

Unfortunately, displacement constraints are not always convex:

Proposition 3.1: Displacement- and stress constraints may give rise to a nonconvex feasible set.

We prove this statement by presenting an example of a nonconvex problem, where the chosen displacement constraint is equivalent to a stress constraint. Consider the two-dimensional truss structure shown in fig 3.1.

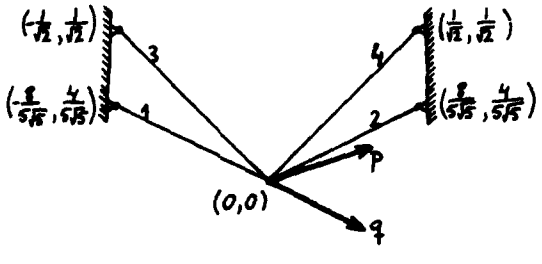


Fig 3.1 Two-dimensional 4-bar truss.

The structure has only got 2 degrees of freedom, namely the horizontal and vertical displacements of the single non-fixed node. The elements are linked together two by two, so that we have the following variables:

x_1 = cross section area of elements 1 and 2.

x_2 = cross section area of elements 3 and 4.

The lower and upper bounds on the variables are $x_1^{min} = x_2^{min} = 0.1$ and $x_1^{max} = x_2^{max} = 1.5$

There is only one displacement constraint. The corresponding load vector p and "virtual load" vector q, which are shown in fig 3.1, are:

$$p = \frac{1}{\sqrt{10}}\begin{pmatrix}3\\1\end{pmatrix} \quad \text{and} \quad q = \frac{1}{\sqrt{5}}\begin{pmatrix}2\\-1\end{pmatrix}$$

Note that, since q is parallel to element 1, the considered displacement constraint is equivalent to a constraint on the tensile stress in element 1.

After some calculations we obtain the following structural stiffness matrix:

$$K = E \cdot \begin{pmatrix} 2x_1 + x_2 & 0 \\ 0 & \frac{x_1}{2} + x_2 \end{pmatrix}$$

where E = Young's modulus of elasticity. We then get the following displacement constraint:

$$d(x) = q^T K^{-1} p = \frac{1}{\sqrt{50}E}\left(\frac{6}{2x_1+x_2} - \frac{2}{x_1+2x_2}\right) \leq \alpha$$

Assume, for simplicity, that $\alpha = \frac{4}{3\sqrt{50}E}$. The constraint then becomes:

$$\frac{3}{2x_1+x_2} - \frac{1}{x_1+2x_2} \leq \frac{2}{3}$$

The feasible set implied by this constraint, together with the lower and upper bounds on the variables, is shown in fig 3.2. It is clearly nonconvex.

To see what consequences this might lead to, assume that x_1 has been fixed to the value 1.0. The feasible set is then reduced to the two line segments:

$$0.1 \leq x_2 \leq 0.25 \text{ and } 1.0 \leq x_2 \leq 1.5$$

(see the dotted lines in fig 3.2). The global minimum weight solution of this, restricted, problem is obviously $x_2 = 0.1$ (and $x_1 = 1.0$), but it is also clear that $x_2 = 1.0$ is a local minimum solution. If a starting point with $x_2 \geq 1.0$ is chosen, then this latter solution is the one which most likely will be found by a standard method for solving the problem.

It should be noted that this undesirable existence of a non-global local minimum can not be avoided by any transformation of the design variables. If the problem is formulated in e.g. the reciprocal variables $\xi_1 = 1/x_1$ and $\xi_2 = 1/x_2$ we get the situation illustrated in fig 3.3.

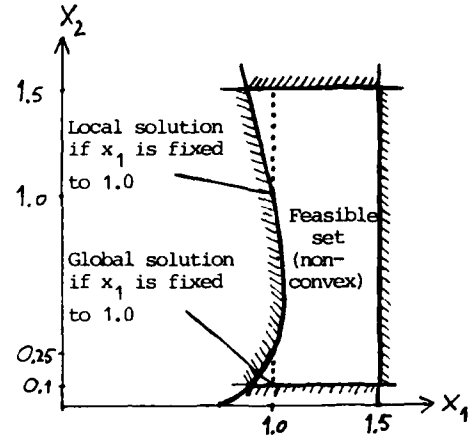


Fig 3.2 Feasible set of the 4-bar problem.

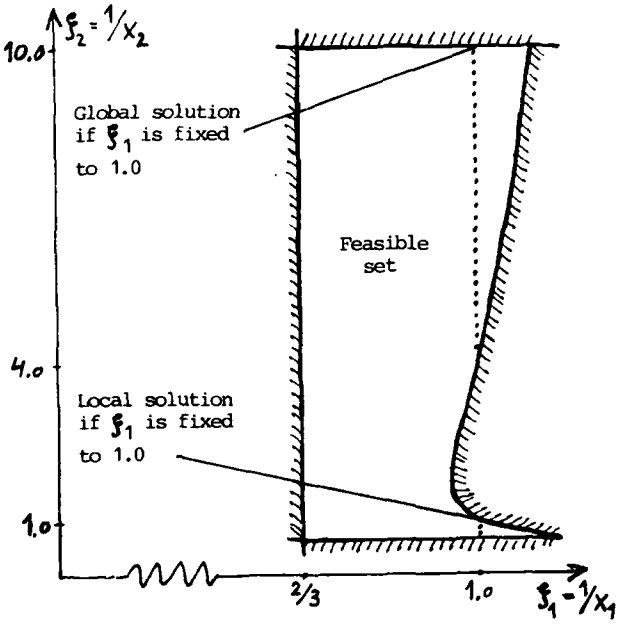


Fig 3.3 Feasible set in the reciprocal variables.

4. Symmetric displacement constraints

When defining a displacement constraint, it is sometimes natural to let the "virtual load" vector q be parallel to the load vector p. We will call such a displacement constraint "symmetric":

Definition 4.1: The constraint $d(x) = q^T K^{-1} p \leq \alpha$ is said to be a symmetric displacement constraint if $q = \gamma p$ for some positive real number γ.

As a typical example, consider the famous 10-bar cantilever truss in fig 4.1. Assume that one of the loadcases consists of a single vertical force in node 6. A reasonable constraint is then to place a limit on the vertical displacement of node 6, under this loadcase. This clearly becomes a symmetric displacement contraint.

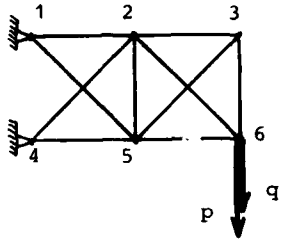


Fig 4.1 Example of a symmetric displacement constraint.

Symmetric displacement constraints can be given an alternative interpretation. Since $q = \gamma p$ and $p = Ku$, we have:

$d(x) = q^T K^{-1} p = \gamma p^T K^{-1} p = \gamma u^T K u = 2\gamma U$, where $U = \frac{1}{2} u^T K u$ is the strain energy in the structure when the given load p has been applied. A symmetric displacement constraint may thus be formulated: "For a given load p, the resulting strain energy must not exceed a given quantity".

We now prove that symmetric displacement constraints possess an attractive convexity property:

Theorem 4.2: Let $d(x) = q^T K^{-1} p$ and assume that $q = \gamma p$ for some real number $\gamma > 0$. Then d is a convex function over X.

Proof: We prove this theorem by showing that the Hessian matrix of d is positive semidefinite for all $x \in X$, cf. lemma 2.6. We also use the formula:

$\frac{\partial K^{-1}}{\partial x_j} = - K^{-1} \frac{\partial K}{\partial x_j} K^{-1}$, which is immediately obtained by differentiating the identity $K^{-1}K \equiv$ the unity matrix.

If we differentiate $d = q^T K^{-1} p$ twice, we get:

$$\frac{\partial d}{\partial x_j} = - q^T K^{-1} \frac{\partial K}{\partial x_j} K^{-1} p = \text{(using } K = K_o + \sum x_j K_j) =$$

$$= - q^T K^{-1} K_j K^{-1} p$$

$$\frac{\partial^2 d}{\partial x_j \partial x_k} = q^T K^{-1} \frac{\partial K}{\partial x_k} K^{-1} K_j K^{-1} p + q^T K^{-1} K_j K^{-1} \frac{\partial K}{\partial x_k} K^{-1} p =$$

$$= q^T K^{-1} (K_k K^{-1} K_j + K_j K^{-1} K_k) K^{-1} p.$$

We must prove that $\sum \sum \frac{\partial^2 d}{\partial x_j \partial x_k} h_j h_k \geq 0$

for all $h = (h_1, .. h_n)^T$. But

$$\sum \sum \frac{\partial^2 d}{\partial x_j \partial x_k} h_j h_k = \sum \sum q^T K^{-1} (h_k K_k K^{-1} h_j K_j +$$

$$+ h_j K_j K^{-1} h_k K_k) K^{-1} p = 2 q^T K^{-1} H K^{-1} H K^{-1} p, \text{ where the}$$

introduced matrix $H = \sum h_j K_j$ is symmetric. With $q = \gamma p$ we then get:

$$\sum \sum \frac{\partial^2 d}{\partial x_j \partial x_k} h_j h_k = 2\gamma p^T K^{-1} H K^{-1} H K^{-1} p =$$

$$= 2\gamma (H K^{-1} p)^T K^{-1} (H K^{-1} p) \geq 0, \text{ since } K^{-1} \text{ is positive definite.}$$

As a consequence of this theorem we get:

Corollary 4.3: The minimum weight problem subject to a collection of symmetric displacement constraints (e.g. one for each loadcase) is a convex problem.

5. Global displacement constraints

Consider a displacement constraint $q^T K^{-1} p \leq \alpha$. We may "normalize" this constraint by normalizing the vectors p and q:

$$\left(\frac{q}{\|q\|}\right)^T K^{-1} \left(\frac{p}{\|p\|}\right) \leq \frac{\alpha}{\|p\| \|q\|}$$

An arbitrary displacement constraint may thus, without any loss of generality, be written:
$q^T K^{-1} p \leq \alpha$, where $\|p\| = \|q\| = 1$. Such a (normalized) displacement constraint is symmetric if and only if $q = p$.

Now, assume that, for a given value of α, we require that $q^T K^{-1} p \leq \alpha$ for all vectors p and q such that $\|p\| = \|q\| = 1$. This infinite set of constraints may equivalently be written:

$$\max_{p,q \in S} \{q^T K^{-1}(x) p\} \leq \alpha$$

where S is the unit sphere, so that, for each $x \in X$, the maximum on the left hand side is taken over all vectors p and q such that $\|p\| = \|q\| = 1$. (This maximum clearly exists since, for each $x \in X$, $q^T K^{-1}(x) p$ is continuous in p and q, and the set over which the maximum is taken in compact.) We will call this constraint a "global displacement constraint":

Definition 5.1: The constraint $d_G(x) \leq \alpha$, where α is a given real number and the function d_G is defined by $d_G(x) = \max_{p,q \in S} \{q^T K^{-1}(x) p\}$, is called a global displacement constraint.

A global displacement constraint implies e.g. that: for any unit load applied on the structure, the displacement of any node in any direction does not exceed α.

Using some well-known rules for vector and matrix calculus, see e.g. ref [5], we get:

$$d_G(x) = \max_{p \in S} \{\max_{q \in S} \{q^T K^{-1} p\}\} = \max_{p \in S} \left\{\frac{(K^{-1}p)^T K^{-1} p}{\|K^{-1}p\|}\right\} =$$

$$= \max_{p \in S} \{\|K^{-1}p\|\} = \|K^{-1}\| = 1/\lambda_K(x)$$

where $\lambda_K(x)$ is the smallest eigenvalue of the stiffness matrix K. It also follows that

$$d_G(x) = \max_{p \in S} \{p^T K^{-1} p\}.$$

A global displacement constraint $d_G(x) \leq \alpha$ is thus equivalent to a lower limit on the smallest eigenvalue of K: $\lambda_K(x) \geq \lambda_K^{min}$ where $\lambda_K^{min} = 1/\alpha$, but also to the infinite set of symmetric displacement constraints: $p^T K^{-1} p \leq \alpha$ for all p such that $\|p\| = 1$.

Theorem 5.2: The global displacement constraint function d_G is convex over X.

Proof: From theorem 4.2 we know that $p^T K^{-1}(x) p$ is convex (in x) over X, for every vector p, and according to lemma 2.7 the pointwise maximum function of a collection of convex functions is convex. Since $d_G(x) = \max_{p \in S} \{p^T K^{-1}(x) p\}$, it thus follows that d_G is convex over X.

As a consequence of this theorem we get:

Corollary 5.3: The set $\{x \in X | d_G(x) \leq \alpha\}$, which alternatively can be expressed as $\{x \in X | \lambda_K(x) \geq \lambda_K^{min}\}$, is convex.

The convexity of the set $\{x \in X | \lambda_K(x) \geq \lambda_K^{min}\}$ alternatively follows from the following theorem:

Theorem 5.4: Let $\lambda_K(x)$ be the smallest eigenvalue of the stiffness matrix K. Then λ_K is a concave function over X.
(Note: a function φ is concave if and only if $-\varphi$ is convex.)

Proof: $\lambda_K(x) = \min_{s \in S} \{s^T K(x) s\} = \min_{s \in S} \{s^T K_o s + \sum x_j s^T K_j s\}$

$$\Rightarrow -\lambda_K(x) = \max_{s \in S} \{-s^T K_o s - \sum x_j s^T K_j s\}$$

For a fixed vector s, the function within the brackets is linear, and thus convex, in x. From lemma 2.7 it then follows that $-\lambda_K$ is convex, i.e. that λ_K is concave, over X.

6. Semiglobal displacement constraints

Assume that, for a given value of α and a given load vector p, we require that $q^T K^{-1} p \leq \alpha$ for all virtual load vectors q such that $\|q\| = 1$. This is a sort of "compromise" between an ordinary and a global displacement constraint, and we therefore use the name "semiglobal":

Definition 6.1: The constraint $\max_{q \in S} \{q^T K^{-1} p\} \leq \alpha$, where α is a given real number and p is a given vector, is called a semiglobal displacement constraint.

The maximizing $q \in S$ in definition 6.1 is easily seen to be $q = \frac{K^{-1}p}{\|K^{-1}p\|}$. The semiglobal displacement constraint may thus be written: $\|K^{-1}p\| \leq \alpha$ or, equivalently, $\|u\| \leq \alpha$. (As before, u is the nodal displacement vector.)

Since $\|u\|^2 = u^T u = p^T K^{-2} p$, and since $p^T K^{-1} p$ is convex over X (as was shown in section 4), one might guess that also $\|u\|^2$ is convex over X. Then the set $\{x \in X \mid \|u\|^2 \leq \alpha^2\} = \{x \in X \mid \|u\| \leq \alpha\}$ would be convex. However, as will be shown by the example to follow, this is not always true. Instead, we can state the following:

Proposition 6.2: Semiglobal displacement constraints may give rise to a nonconvex feasible set. Also, $\|u\|$ and $\|u\|^2$, i.e. $\|K^{-1}(x)p\|$ and $p^T K^{-2}(x) p$, may be nonconvex functions in x.

Consider the two-dimensional 3-bar truss shown in fig 6.1.
There are two variables:

x_1 = cross section area of elements 1 and 2 (not elements 1 and 3!).

x_2 = cross section area of element 3.

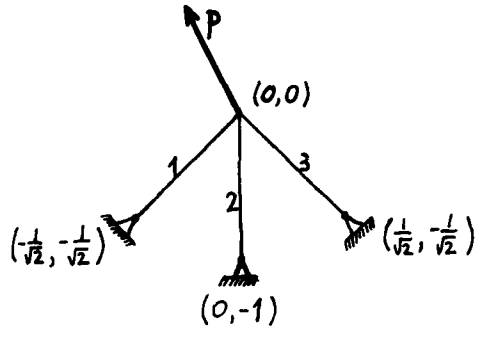


Fig 6.1 Two-dimensional 3-bar truss.

The load vector, applied in the non-fixed node, is $p = (-1\ ,\ 2)^T$. After some calculations we obtain the following displacement vector:

$$u = \frac{1}{E(x_1^2+3x_1x_2)} \cdot \begin{pmatrix} x_2-5x_1 \\ x_2+3x_1 \end{pmatrix}$$

(The two components of u are respectively the horizontal and vertical displacements of the nonfixed node.)

Assuming (for simplicity) that $\alpha = \frac{1}{E}$, the semiglobal displacement constraint $\|u\|^2 \leq \alpha^2$ becomes:

$$(x_2-5x_1)^2 + (x_2+3x_1)^2 \leq (x_1^2+3x_1x_2)^2$$

The feasible set implied by this constraint is shown in fig 6.2. By direct calculations it is seen that the two points:

$$(\frac{\sqrt{74}}{3}, \frac{\sqrt{74}}{9}) \text{ and } (\frac{\sqrt{410}}{5}, \frac{\sqrt{410}}{35})$$

are feasible, i.e. satisfy the above constraint. However, their midpoint is, also by direct calculations, seen to be unfeasible. The feasible set is thus nonconvex.

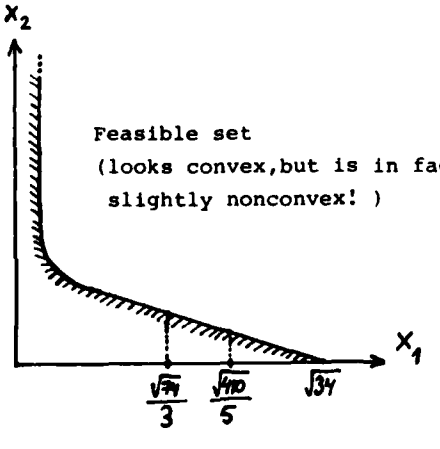


Fig 6.2 Feasible set of the 3-bar problem.

7. Natural frequency constraints

The natural frequencies ω_i of a structure are obtained from the generalized eigenvalue problem:

$$Ky = \omega^2 My$$

, where $K = K_o + \sum x_j K_j$ is the structural stiffness matrix and $M = M_o + \sum x_j M_j$ is the structural mass matrix.

An important example of a frequency constraint, the only one that will be considered here, is that no natural frequency should be less than a given number ω^{min}. This may be written $\omega(x) \geq \omega^{min}$, where $\omega(x)$ is the lowest natural frequency of the structure (i.e. the smallest number ω for which there exists a vector $y \neq 0$ such that $Ky = \omega^2 My$).

In general, constraints on natural frequencies may give rise to a nonconvex feasible set. The constraint mentioned above, however, possesses the following attractive property:

Theorem 7.1: Let $\omega(x)$ be the lowest natural frequency and let ω^{min} be a given positive real number. Then the set $\{x \in X | \omega(x) \geq \omega^{min}\}$ is convex.

To prove this theorem we need the following well-known result, which may be found in e.g. chapter 3 of ref [5].

Lemma 7.2: If λ is the smallest solution of the eigenvalue problem $Ky = \lambda My$, where K and M are symmetric and positive definite, then:

$$\lambda = \min_{y \neq 0} \left\{ \frac{y^T K y}{y^T M y} \right\}$$

Proof of theorem 7.1: According to the above lemma we have:

$$\omega^2(x) = \min_{y \neq 0} \left\{ \frac{y^T K y}{y^T M y} \right\} = \min_{y \neq 0} \left\{ \frac{k(x,y)}{m(x,y)} \right\}$$

, where the introduced functions $k(x,y) = y^T K_o y + \sum_j x_j y^T K_j y$ and $m(x,y) =$ $= y^T M_o y + \sum x_j y^T M_j y$ are linear in x and quadratic in y. We also have $k(x,y) > 0$ and $m(x,y) > 0$ for all $x \in X$ and $y \neq 0$.

Now, consider $\Omega = \{x \in X | \omega(x) \geq \omega^{min}\} =$

$= \{x \in X | \omega^2(x) \geq \lambda^{min}\}$, where $\lambda^{min} = (\omega^{min})^2$, $=$

$= \{x \in X | \frac{k(x,y)}{m(x,y)} \geq \lambda^{min} \text{ for all } y \neq 0\} =$

$= \{x \in X | k(x,y) \geq \lambda^{min} m(x,y) \text{ for all } y \neq 0\} =$

$= \bigcap_{y \neq 0} \{x \in X | k(x,y) \geq \lambda^{min} m(x,y)\}.$

For any fixed $y \neq 0$, the set $\{x \in X | k(x,y) \geq \lambda^{min} m(x,y)\}$ is convex, since k and m are linear functions in x. But according to lemma 2.4 the intersection of any collection of convex sets is convex, and it thus follows that Ω is a convex set.

8. Conclusions

In this paper an investigation concerning convexity properties in structural optimization has been accomplished. The investigation is not claimed to be exhaustive. It has been shown that, although the problems in general may be nonconvex, there are some nontrivial special cases where the convexity of the problem can be proved, e.g. when the structural weight should be minimized subject to a collection of symmetric displacement constraints and/or a global displacement constraint and/or a lower bound on the lowest natural frequency.

It is reasonable to believe that there are other special cases, than the ones discussed in this paper, which also possess important convexity properties. Further research concerning these questions is thus recommended.

Acknowledgement

This work has been carried out under research contract with the Swedish Institute of Applied Mathematics.

References

[1] Zangwill, W.I., Nonlinear Programming: A Unified Approach, Prentice-Hall, Englewood Cliffs, New Jersey, 1969.

[2] Luenberger, D.G., Introduction to Linear and Nonlinear Programming, Addison-Wesley, Reading, Massachusetts, 1973.

[3] Fleury, C., A Unified Approach to Structural Weight Minimization", Computer Methods in Applied Mechanics and Engineering, Vol 20, pp 17-38, 1979.

[4] Rockafellar, R.T., Convex Analysis, Princeton, New Jersey, 1970.

[5] Lancaster, P., Theory of Matrices, Academic Press, New York, 1969.

AD-P000 058

A SELF-CONTAINED THEORY FOR OPTIMUM DESIGN OF SKELETAL STRUCTURES AND THE GLOBAL OPTIMUM

Erdal Atrek*

İnşaat Bölümü, Mühendislik-Mimarlık Fakültesi,
İstanbul Teknik Üniversitesi, Maçka, İstanbul, Turkey

SUMMARY

The minimum weight design of truss and frame systems is considered. Constraints are on stresses, displacements, and cross-sectional areas. Each constraint is coupled to inverses of all design variables. The objective function is applied in two forms. A modified form yields the Lagrange multipliers associated with active constraints. Then the new design variables are computed using the other expression for objective function. An algorithm for adding and deleting constraints within an active set is developed. The solution proceeds without recursive relationships between re-analyses, and some steps may not need optimization procedure. The disjoint optimum of the ten bar truss problem is found during solution. An approach to generate starting vectors towards the global optimum of flexural systems is discussed. The theory is illustrated with a numerical example.

Introduction

Two main methods for optimum design of structures are seen to be gaining increased popularity with regard to the literature on the subject. One is the mathematical programming approach wherein a mathematical programming code (optimizer) is coupled with a structural analysis routine (simulator). The popularity of this approach perhaps lies to a degree in its convenience. The optimizers are mainly written with a general purpose in mind and are available in package form for many search algorithms. Further, the input towards development of such algorithms and programs is by no means restricted to the structural engineering community. This, on the other hand, exacts a penalty in that structural theory may not always be utilized to its fullest extent for efficiency of the design process. Still, the simplicity of coupling an optimizer with a simulator that has a re-solution facility is very attractive, particularly in light of the fact that the theory for optimum design of structures has not yet realized its potential to the degree structural analysis theory has.

The second method, the optimality criteria approach, enjoys the reputation of being based more on structural theory, although the dividing line between the two approaches may grow rather thin sometimes. For example, many structural design applications with mathematical programming methods include derivation of constraint gradients through the use of structural theory (e.g., (1)), and resort to mathematical programming tools such as step sizes are encountered in optimality criteria applications (2). Mixed methods develop as a result (3).

The work described herein would fall in the category of optimality criteria methods in that it is mainly based on structural theory with the possibility of no need for step sizes, but with still the requirement for an understanding of constraint surfaces.

The main features include direct computation of the Lagrange multipliers, efficient derivation of stress constraints, derivation of interaction relations for fabricational constraints, and a new derivation for displacement constraints. Additionally, some ideas regarding the global optimum are set forth based on numerical experience with small-scale problems.

The classical ten bar truss example presented to supplement the theoretical material.

Theory

An optimization problem with a single objective would be presented as the minimization of the objective function.

$$W = \underset{\sim}{\ell}^T \underset{\sim}{a} \qquad (1)$$

subject to a set of constraints which may be nonlinear in the design variables $\underset{\sim}{a}$. Again, Equation 1 may reflect only the linearized form of the actual objective function. Here, $\underset{\sim}{\ell}$ is a column vector of weighting coefficients.

In optimum design of a skeletal structure, such as a truss or a frame, for minimum volume, $\underset{\sim}{a}$ would be the column vector of cross-sectional areas and $\underset{\sim}{\ell}$ would be the member lengths. Optimization for minimum weight would proceed by including the unit weights in $\underset{\sim}{\ell}$.

Frequently met constraints in structural design are on stresses ($\underset{\sim}{\sigma}$), displacements ($\underset{\sim}{\delta}$) and member sizes (a). These can be represented in the following basic form:

$$\sigma_k \leq \sigma_k^* \qquad , k = 1, \ldots \qquad (2a)$$

$$\delta_m \leq \delta_m^* \qquad , m = 1, \ldots \qquad (2b)$$

$$a_j \leq a_j^* \qquad , j = 1, \ldots \qquad (2c)$$

where absolute values have been implied for the stresses and the displacements. For the fabricational constraints 2c, lower limits may also be required:

$$a_j \geq \bar{a}_j^* \qquad (2d)$$

In Equations 2, the right hand sides (RHS) are the limiting values for the unknowns on the LHS. These may be prescribed or variable, such as for design with stability considerations.

It is now noted that, all LHS variables are, in general, actually nonlinear functions of the design variables $\underset{\sim}{a}$. Thus

$$\begin{aligned} \sigma_k &= \sigma_k(\underset{\sim}{a}) \\ \delta_m &= \delta_m(\underset{\sim}{a}) \\ a_j &= a_j(\underset{\sim}{a}) \end{aligned} \qquad (3)$$

While the first two functions above are obvious, the third one follows rather implicitly from structural interaction. In optimality criteria approaches, the constraint expressions 3 are linearized with respect to the inverses of the design variables.

* Currently visiting at Department of Civil Engineering, University of Arizona, Tucson, Arizona, U.S.A.

PRECEDING PAGE

Thus, for an unknown x_i, the linearized expression at a given design would be

$$x_i(\underset{\sim}{a}) = \sum_{j=1}^{n} \frac{c_{ij}}{a_j} \leq x_i^* \qquad (4)$$

where c_{ij} are constants to be computed (while for trusses a_j would be the cross-sectional areas, a_j in Equation 4 will be taken as the moments of inertia for flexural members in this work).

Such expressions for displacement and stress constraints may readily be obtained by application of the virtual work principle (3, 4, 5). The expressions for fabricational considerations will then follow from that for the stresses (5).

After division by x_i^* and rearrangement, Expression 4 will take the form

$$f_i(\underset{\sim}{a}) = \frac{1}{x_i^*} \sum_{j=1}^{n} \frac{c_{ij}}{a_j} - 1 \leq 0 \qquad (5)$$

Acting from principles of variational calculus, the usual procedure is to associate each constraint expression f_i with a Lagrange multiplier λ_i, to set the expression equal to zero

$$\lambda_i f_i(\underset{\sim}{a}) = 0 \qquad (6)$$

and to add the resulting expressions to the objective function

$$W = \underset{\sim}{\ell}^T \underset{\sim}{a} + \underset{\sim}{\lambda}^T \underset{\sim}{f}(\underset{\sim}{a}) \qquad (7)$$

The objective function is then differentiated with respect to the design variables and the result set equal to the zero vector $\underset{\sim}{0}$, to obtain a linearized form of the optimality criteria.

For purposes of the present work, Equation 7 will now be written in the following form:

$$W = \underset{\sim}{1}^T \underset{\sim}{L}\, \underset{\sim}{a} + \underset{\sim}{1}^T \underset{\sim}{\Lambda}\, \underset{\sim}{f}(\underset{\sim}{a}) \qquad (7a)$$

where the coefficients $\underset{\sim}{\ell}$ and the Lagrange multipliers $\underset{\sim}{\lambda}$ have been placed diagonally in $\underset{\sim}{L}$ and $\underset{\sim}{\Lambda}$, respectively, and where $\underset{\sim}{1}$ is a column vector of unit values.

Substitution for $\underset{\sim}{f}(\underset{\sim}{a})$ from Equation 5 yields

$$W = \underset{\sim}{1}^T \underset{\sim}{L}\, \underset{\sim}{a} + \underset{\sim}{1}^T \underset{\sim}{\Lambda} (\underset{\sim}{Y}^* \underset{\sim}{C}\, \underset{\sim}{a}_I - \underset{\sim}{1}) \qquad (8)$$

Here $\underset{\sim}{Y}^*$ is a diagonal matrix of the reciprocals of the limiting values x_i^* and $\underset{\sim}{C}$ is, in general, a fully populated matrix of the coefficients c_{ij}. The column vector $\underset{\sim}{a}_I$ consists of the reciprocals of the design variables $\underset{\sim}{a}$, i.e., $(\underset{\sim}{a}_I)_j = 1/a_j$.

Performing the differentiation and equating to zero will give, for truss structures

$$\left\{\frac{\partial W}{\partial \underset{\sim}{a}}\right\} = -\underset{\sim}{L}\underset{\sim}{a}_s + \underset{\sim}{C}^T \underset{\sim}{Y}^* \underset{\sim}{\lambda} = \underset{\sim}{0} \qquad (9)$$

where $\underset{\sim}{a}_s$ is a column vector of the squares of the design variables, i.e., $(\underset{\sim}{a}_s)_j = a_j^2$.

With Equation 9, the design variables $\underset{\sim}{a}$ are related to the Lagrange multipliers $\underset{\sim}{\lambda}$. On the other hand, the Lagrange multipliers are also unknown.

In the literature, several techniques for iterative solution of Equation 9 are given (2, 6, 7). Here, however, a direct solution will be attempted. One method may proceed as follows:

Assuming that, for a given design, the active constraints are identified, then the Lagrange multipliers for the inactive (passive) constraints are known to be zero. Setting

$$\underset{\sim}{G} = \underset{\sim}{L}^{-1} \underset{\sim}{C}^T \underset{\sim}{Y}^* \qquad (10)$$

and partitioning Equation 9 with respect to active and passive constraints, one obtains

$$\begin{Bmatrix} \underset{\sim}{a}_{s_1} \\ \underset{\sim}{a}_{s_2} \end{Bmatrix} = \begin{bmatrix} \underset{\sim}{G}_{11} & \underset{\sim}{G}_{12} \\ \underset{\sim}{G}_{21} & \underset{\sim}{G}_{22} \end{bmatrix} \begin{Bmatrix} \underset{\sim}{\lambda}_1 \\ \underset{\sim}{\lambda}_2 \end{Bmatrix} \qquad (11)$$

where subscript 1 is associated with the active constraints. Then $\underset{\sim}{\lambda}_2 = \underset{\sim}{0}$, and the first equation in (11) can be solved for $\underset{\sim}{\lambda}_1$

$$\underset{\sim}{\lambda}_1 = \underset{\sim}{G}_{11}^{-1} \underset{\sim}{a}_{s_1} \qquad (12)$$

after which $\underset{\sim}{a}_{s_2}$ can be found by

$$\underset{\sim}{a}_{s_2} = \underset{\sim}{G}_{21} \underset{\sim}{\lambda}_1 \qquad (13)$$

This procedure has the effect of keeping $\underset{\sim}{a}_1$ constant and varying $\underset{\sim}{a}_2$, as long as no negative values are obtained for the squares of the variables $\underset{\sim}{a}_2$.

A generalization of this technique is discussed after consideration of the constraint expressions.

Stress Constraints

It has already been noted that stress expressions will be linearized in the form

$$\sigma_k = \sum_{j=1}^{n} \frac{c_{kj}}{a_j} \qquad (14)$$

To attribute a meaning to the coefficients c_{kj} it is sufficient to invoke the principle of virtual work. Since σ_k is directly proportional to a displacement quantity which can be obtained through use of two load vectors, one actual and one virtual, it is obvious that c_{kj} contain the actual forces s_j.

Setting

$$c_{kj} = z_{kj} s_j \qquad (15)$$

and substituting in Equation 14 one obtains

$$\sigma_k = \sum_{j=1}^{n} z_{kj} \frac{s_j}{a_j} \qquad (16)$$

But the indicated ratio (s_j/a_j) is the stress σ_j. Therefore,

$$\sigma_k = \sum_{j=1}^{n} z_{kj}\, \sigma_j \qquad (17)$$

In fact, if the stress expressions were written similarly for the entire structure, one would have (5)

$$\underset{\sim}{\sigma} = \underset{\sim}{Z}\ \underset{\sim}{\sigma} \tag{18}$$

This matrix $\underset{\sim}{Z}$ will be very important in the rest of the theoretical presentation.

The most important property $\underset{\sim}{Z}$ has is that it satisfies Equation 18 no matter what changes the stresses $\underset{\sim}{\sigma}$ go through*, so long as small displacements and no geometrical changes are considered. Thus, it seems sufficient, at this time, to derive $\underset{\sim}{Z}$ only for the starting design and to keep it constant throughout the solution.

It can now be seen that to derive column j of $\underset{\sim}{Z}$, one needs to apply a load corresponding to a unit value of the stress σ_j. Thus, for truss members, this load will be equal to the cross-sectional area, and for purely flexural members (see footnote) it will be equal to the moment of inertia, in numerical value. For example, for the classical three-bar truss, the first column of $\underset{\sim}{Z}$ is obtained as a result of the loading case shown on Figure 1. However, it is not necessary to apply a load to obtain each column. It is easily observed that for a statically determinate structure, $\underset{\sim}{Z}$ would be the unit matrix $\underset{\sim}{I}$, since there is no interaction. Then, to define $\underset{\sim}{Z}$ completely for a statically indeterminate structure, load cases corresponding to redundants should be sufficient.

The derivation of $\underset{\sim}{Z}$ would proceed as follows (5): Partition Equation 18 with respect to the redundants R:

$$\begin{Bmatrix} \underset{\sim}{\sigma}_R \\ \underset{\sim}{\sigma}_D \end{Bmatrix} = \begin{bmatrix} \underset{\sim}{Z}_{RR} & \underset{\sim}{Z}_{RD} \\ \underset{\sim}{Z}_{DR} & \underset{\sim}{Z}_{DD} \end{bmatrix} \begin{Bmatrix} \underset{\sim}{\sigma}_R \\ \underset{\sim}{\sigma}_D \end{Bmatrix} \tag{19}$$

Then obtain columns R by application of loads corresponding to unit values of the stresses $\underset{\sim}{\sigma}_R$. This would involve R load cases, preferably applied after solution for actual load so that only the right-hand sides need to be modified, and since more computer core is available for multiple load cases after initial reduction of the stiffness matrix.

$\underset{\sim}{Z}_{RD}$ can now be obtained from $\underset{\sim}{Z}_{DR}$ by direct application of the Maxwell-Betti Theorem. For truss members, the relationship is in the form

$$z_{ij} = \frac{a_i \ell_i E_i}{a_j \ell_j E_j}\ z_{ji} \tag{20}$$

where E is the elastic modulus.

For flexural members, since stress at a point rather than along the member is considered, and since the stress considered is the one at unit distance to the neutral axis, the relationship is somewhat more different, but is not difficult to derive:

$$2z_{im} + z_{jm} = \frac{(i\,\ell/E)mn}{(i\,\ell/E)ij}\ (2z_{mi} + z_{ni}) \tag{21}$$

where i and j are two ends of member ij and m and n are two ends of member mn, and where i is the moment of inertia.

* For flexural members, the stresses are those at unit distance from the neutral axis.

The next step is to compute $\underset{\sim}{Z}_{DD}$. Solving the first of Equations 19 for $\underset{\sim}{\sigma}_R$:

$$\underset{\sim}{\sigma}_R = (\underset{\sim}{I} - \underset{\sim}{Z}_{RR})^{-1}\ \underset{\sim}{Z}_{RD}\ \underset{\sim}{\sigma}_D \tag{22}$$

and substuting in the second equation gives

$$\underset{\sim}{\sigma}_D = [\underset{\sim}{Z}_{DR}\ (\underset{\sim}{I} - \underset{\sim}{Z}_{RR})^{-1}\ \underset{\sim}{Z}_{RD} + \underset{\sim}{Z}_{DD}]\ \underset{\sim}{\sigma}_D \tag{23}$$

This procedure has the effect of condensing away the redundants, therefore reducing the structure to a determinate one. Thus, the bracketed expression in Equation 23 should be equal to the unit matrix $\underset{\sim}{I}$. Noting this equality and solving for $\underset{\sim}{Z}_{DD}$,

$$\underset{\sim}{Z}_{DD} = \underset{\sim}{I} - \underset{\sim}{Z}_{DR}\ (\underset{\sim}{I} - \underset{\sim}{Z}_{RR})^{-1}\ \underset{\sim}{Z}_{RD} \tag{24}$$

is obtained.

The derivation of matrix $\underset{\sim}{Z}$ is thus completed. Returning to Equation 18 and separating the forces from $\underset{\sim}{\sigma}$ on the right-hand side, the stress expressions can be rewritten as

$$\underset{\sim}{\sigma} = \underset{\sim}{Z}\ \underset{\sim}{S}\ \underset{\sim}{a}_I \tag{25}$$

where $\underset{\sim}{S}$ is obtained by placing the forces s_j diagonally. Thus, the procedure for obtaining the coefficients c_{kj} (Equation 14), will be to keep $\underset{\sim}{Z}$ constant and to modify $\underset{\sim}{S}$ at each step.

Fabricational Constraints

From Equation 25, separating the forces $\underset{\sim}{S}$ on the left-hand side as well, one obtains (8)

$$\underset{\sim}{S}\ \underset{\sim}{a}_I = \underset{\sim}{Z}\ \underset{\sim}{S}\ \underset{\sim}{a}_I \tag{26}$$

from which

$$\underset{\sim}{a}_I = \underset{\sim}{S}^{-1}\ \underset{\sim}{Z}\ \underset{\sim}{S}\ \underset{\sim}{a}_I \tag{27}$$

Again, Z would remain constant while the diagonal matrix $\underset{\sim}{S}$ is modified at each redesign.

In addition to providing sensitivity coefficients for fabricational constraints, Equation 27 has significance for three main reasons:

1. It will be used to modify the objective function for direct computation of the Lagrange multipliers.

2. For design of flexural systems, the relation between the cross-sectional areas and moments of inertia needs to be linearized at each step. Equation 27 will then be inserted into the linearized relation to provide some global information regarding sensitivities.

3. If an expression such as Equation 13 would give some imaginary design variables, these variables can be resurrected by means of Equation 27.

Displacement Constraints

It is very interesting that the first constraint considered in the development of optimality criteria methods is the case of a limit on a single displacement (9). Multiple displacement constraints can now be treated with ease. However, the trend noted in the literature has been the application of one unit load case for each displacement expression. For a large struc-

ture with many degrees of freedom that may displace more than a tolerable amount, efficiency of this type of derivation would not be very high.

Here, an alternative method which requires no unit load applications is derived in the case stress constraints are already present. If stress constraints are not present, then load cases equal in number to the redundants need to be applied.

It is noted that for an elastic skeletal structure, the displacements of the degrees of freedom can be found from the stresses associated with some arbitrarily selected basic statically determinate system D, i.e.,

$$\underset{\sim}{\delta} = \underset{\sim}{Q}_D^T \; \underset{\sim}{F}_D^e \; \underset{\sim}{A}_D \; \underset{\sim}{\sigma}_D \tag{28}$$

Here $\underset{\sim}{A}_D$ is a diagonal matrix of cross-sectional areas (or moments of inertia), $\underset{\sim}{F}_D^e$ is composed by diagonally placing element flexibility "matrices", and $\underset{\sim}{Q}_D$ is the inverse of the equilibrium matrix for system D.

From Equation 19 it is known that

$$\underset{\sim}{\sigma}_D = \underset{\sim}{Z}_{DR} \underset{\sim}{\sigma}_R + \underset{\sim}{Z}_{DD} \underset{\sim}{\sigma}_D \tag{29}$$

By substitution into Equation 28, the following expression results:

$$\underset{\sim}{\delta} = \underset{\sim}{Q}_D^T \; \underset{\sim}{F}_D^e \; \underset{\sim}{A}_D \; \left[\underset{\sim}{Z}_{DR} \; \underset{\sim}{Z}_{DD}\right] \begin{Bmatrix} \underset{\sim}{\sigma}_R \\ \underset{\sim}{\sigma}_D \end{Bmatrix} \tag{30}$$

or separating the forces $\underset{\sim}{S}$ from the stresses

$$\underset{\sim}{\delta} = \underset{\sim}{Q}_D^T \; \underset{\sim}{F}_D^e \; \underset{\sim}{A}_D \; \left[\underset{\sim}{Z}_{DR} \quad \underset{\sim}{Z}_{DD}\right] \underset{\sim}{S} \; \underset{\sim}{a}_I \tag{31}$$

This equation can now be simplified into

$$\underset{\sim}{\delta} = \underset{\sim}{V} \; \underset{\sim}{S} \; \underset{\sim}{a}_I \tag{32}$$

where $\underset{\sim}{V}$ is similar to $\underset{\sim}{Z}$ in that keeping it constant throughout the design changes will not affect the satisfaction of Equation 32. Of course, if the multiplication $\underset{\sim}{V} \; \underset{\sim}{S}$ is carried out, the coefficients c_{mj} in the well-known expression

$$\delta_m = \sum_{j=1}^{n} \frac{c_{mj}}{a_j} \tag{33}$$

will result.

The only bothersome proposal here is the requirement for computation of $\underset{\sim}{Q}$, and ease may depend on selection of system D. Since numerical experimentation with large problems is lacking, no comments on efficiency may yet be provided.

Computation of the Lagrange Multipliers

Due to slight differences between treatment, the derivation will first be shown for truss systems, then the derivation for flexural systems will be built on the one for trusses.

The objective function of Equation 1 can be alternatively written:

$$W = \underset{\sim}{l}^T \; \underset{\sim}{L} \; \underset{\sim}{A}_s \; \underset{\sim}{a}_I \tag{34}$$

where $\underset{\sim}{A}_s$ is a diagonal matrix of squares of member cross-sectional areas. It is now proposed to use to the current values for $\underset{\sim}{A}_s$ while keeping $\underset{\sim}{a}_I$ variable. Obviously, this amounts to some type linearization with respect to inverses of design variables, and has already been tried in Ref. (1). However, since generality is lost by this linearization, the interaction expression Equation 27 is now substituted for a_I providing additional information. Then

$$W = \underset{\sim}{l}^T \; \underset{\sim}{L} \; \underset{\sim}{A}_s \; \underset{\sim}{S}^{-1} \; \underset{\sim}{Z} \; \underset{\sim}{S} \; \underset{\sim}{a}_I \tag{35}$$

As a rule of thumb, whenever a linearization is made, appropriate coupled expression will be made use of.

Performing the multiplication of the matrices in Equation 35 and setting equal to a matrix $\underset{\sim}{M}$:

$$W = \underset{\sim}{l}^T \; \underset{\sim}{M} \; \underset{\sim}{a}_I \tag{36}$$

and adding the constraint expressions to this objective function

$$W = \underset{\sim}{l}^T \; \underset{\sim}{M} \; \underset{\sim}{a}_I + \underset{\sim}{l}^T \; \underset{\sim}{\Lambda} \; (\underset{\sim}{Y}^* \; \underset{\sim}{C} \; \underset{\sim}{a}_I - \underset{\sim}{1}) \tag{37}$$

one obtains the objective function in terms of the inverses of design variables. Taking the derivative with respect to $\underset{\sim}{a}_I$ will yield an expression only in the Lagrange multipliers:

$$\left\{\frac{\partial W}{\partial \underset{\sim}{a}_I}\right\} = \underset{\sim}{M}^T \; \underset{\sim}{1} + \underset{\sim}{B}^T \; \underset{\sim}{\lambda} = 0 \tag{38}$$

or, simplifying

$$\underset{\sim}{B}^T \underset{\sim}{\lambda} = \underset{\sim}{m} \tag{39}$$

Partitioning 39 with respect to active and passive constraints:

$$\begin{bmatrix} \underset{\sim}{B}_{11} & \underset{\sim}{B}_{12} \\ \underset{\sim}{B}_{21} & \underset{\sim}{B}_{22} \end{bmatrix} \begin{Bmatrix} \underset{\sim}{\lambda}_1 \\ \underset{\sim}{\lambda}_2 \end{Bmatrix} = \begin{Bmatrix} \underset{\sim}{m}_1 \\ \underset{\sim}{m}_2 \end{Bmatrix} \tag{40}$$

and setting $\underset{\sim}{\lambda}_2 = 0$ will give

$$\underset{\sim}{\lambda}_1 = \underset{\sim}{B}_{11}^{-1} \; \underset{\sim}{m}_1 \tag{41}$$

which can then be substituted in Equation 9 to find $\underset{\sim}{a}_s$ and therefore $\underset{\sim}{a}$.

There is one immediate difficulty in this process, and this is the possibility of obtaining some negative values in $\underset{\sim}{a}_s$. At this time, such variables are resurrected by using Equation 27. For the positive variables the new variables, and for variables with negative a^2 the old values are used on the right-hand side. If, again this time the variable itself should come out negative, the prescribed value of zero is assigned to the variable at this time.

Modification for Flexural Systems

For flexural systems, the initial objective function of Equation 1 would be in terms of cross-sectional areas while the constraint expressions would be written in terms of the moments of inertia (or both if axial effects are also considered). Clearly, some linearization of the relationship between cross-sectional areas a and moments of inertia $\underset{\sim}{i}$ need to be made at each step, such as

$$a_j = \eta_j \, i_j \tag{42}$$

where η_j is a constant to be evaluated at each step. If this is substituted in the first term of Equation 8, a further modification is made by substitution of Equation 27 in the following form:

$$\underset{\sim}{i}_I = \underset{\sim}{S}^{-1} \; \underset{\sim}{Z} \; \underset{\sim}{S} \; \underset{\sim}{i}_I \tag{43}$$

Here the vector $\underset{\sim}{i}_1$ is composed of inverses of moments of inertia.

Also, Equation 34 will then take the form

$$W = \underset{\sim}{l}^T \underset{\sim}{L} \underset{\sim}{I}_s \underset{\sim}{i}_1 \qquad (44)$$

where $\underset{\sim}{I}_s$ is a diagonal matrix of squares of current values for the moments of inertia. Thus, the problem is converted to one totally in terms of moments of inertia. After new values are found for $\underset{\sim}{i}$, the cross-sectional areas can be computed based on the linearization in Equation 42.

It should be noted here that the numerical experimentation with flexural systems is not yet sufficient to bring out the full significance of the above relationships.

Stress Constraints for Flexural Systems

When span loads exist in the structure, one would need to work with the equivalent nodal loads in a finite element approach. Furthermore, since the moments of inertia are the variables, the stress constraints need to be written in the form

$$(\underset{\sim}{Z}\,\underset{\sim}{S} - \underset{\sim}{S}_o)\,\underset{\sim}{i}_1 \leq \underset{\sim}{X}^*\,\underset{\sim}{T}\,\underset{\sim}{i}_1 \qquad (45)$$

Where $\underset{\sim}{S}$ are the equivalent nodal moments, $\underset{\sim}{S}_o$ are the work equivalent nodal loads (moments), and $\underset{\sim}{T}$ is a diagonal matrix of section moduli. The $\leq$ sign holds for each expression separately. Thus, it is observed that the limiting stress becomes variable in this case. It is not exactly clear how one should proceed at this point. It is, however, possible to use the instantaneous values for the section moduli $\underset{\sim}{T}$, and to simplify the constraint expression into a homogeneous one:

$$(\underset{\sim}{Z}\,\underset{\sim}{S} - \underset{\sim}{S}_o - \underset{\sim}{X}^*\,\underset{\sim}{T})\,\underset{\sim}{i}_1 \leq \underset{\sim}{0} \qquad (46)$$

after which the solution may proceed in the usual manner.

Solution Procedure

It is very important to observe that the proposed theory will not produce magic results. The gradients obtained by differentiation of the objective function are only as good as the linearization at a particular design would indicate.

Furthermore, since the solution proceeds based on active constraints only, no consideration is taken of those constraints which may be violated by advance in the computed direction. Perhaps this situation will be remedied in the future. However, for the time being, the following procedure has been adopted:

Suppose constraint j is active; i.e. when the design is scaled to the constraint surface, j is exactly satisfied. Upon advance with the gradients, constraint i is violated. Now the weight may either increase or decrease, depending on the particular problem. If a decrease is observed, j is deleted and solution continues with i. On the other hand, if an increase in weight is noted, for a convex problem*, the best solution between i and j would lie on the intersection of the constraint hypersurfaces. Thus, a decrease in weight should be obtained if this intersection hyperline can be found. Then further advance will be along this intersection until a new constraint is violated.

In philosophy, this sounds simple enough. The main problem is to find the constraint intersections accurately. Otherwise, at each step, the adding up of the errors will slow down the progress. In the solution of the ten-bar truss example, a weighting procedure has been used to generate an intermediate design vector to bring the solution close to the required intersection. Again, the convergence rate may depend on selection of weighting factors.

If the two successive designs are ascertained to be rather close to such a constraint intersection, a more powerful alternative can then be based on the observation that the intersection of two constraint surfaces is really the two constraints molded into one along that intersection. Thus, solution of the two constraint expressions together should give the expression for the intersection. In order to do this, the two successive approximations to the constraint surfaces have to be handled together. This procedure has not yet been programmed.

Disjoint Optima of Indeterminate Trusses

It is known that indeterminate truss systems under a single loading condition and under stress constraints only, will have, as an optimum solution, a statically determinate configuration; i.e., some cross-sectional areas will disappear. Recursive relations used in optimality criteria approaches are quite sensitive to such behavior since division by the cross-sectional area is required. However, the direct approach presented herein will not be affected by the disappearance of a cross-sectional area.

It is suggested that if a variable cannot be resurrected by Equation 27, it is probably tending strongly toward zero. For example, in design of the ten-bar truss (Figure 2), this behavior has been observed for the middle upright, member 5.

Setting the cross-sectional area of this member equal to zero, after when thus appropriate, results in the design further moving on to the minimum weight statically determinate structure. It is not known, however, under what general conditions this behavior will be observed and what refinements in the theory are needed for more generality.

Multiple Optima of Frameworks

The two-bar grid of Figure 4 is known to have three optima (Figure 5) arising from the nonconvex properties of the problem. The usual approach in such a case is to select different starting points so as to try several regions of possible optima, and thus perhaps arrive at the global optimum. While this is perfectly acceptable, the choice of starting points is based mainly on intuition and experimentation.

It is therefore desirable to be able to select starting points not in the region of the previously obtained optimum.

For example, writing the equation for the reaction R between the two beams of Figure 4.

$$R = a\left(\frac{b}{i_1} + \frac{c}{i_2}\right)^{-1}\left(\frac{d}{i_1} - \frac{e}{i_2}\right) \qquad (47)$$

where a to e are constants, it is observed that R will change sign depending on the relative values of the moments of inertia i_1 and i_2. In the given case, using reciprocals of i_1 and i_2. will provide this result at an optimum. Alternatively, if R is known, its sign may be changed and the corresponding force distribution may be approximated from the current design point.

The second alternative was adopted in an attempt to investigate this problem, resulting in a move from the local optimum (point A on Figure 5) to point B. Obviously, the optimization process may proceed by any method from this point on, to result in the global optimum (point C).

The problem that may be encountered will be proper definition and computation of such redundants in a stiffness method of solution. Again, although the philosophy is simple, programming requires more insight and numerical experimentation.

* The situation for a nonconvex problem is not clear to the author.

Numerical Example

Ten Bar Truss (Figure 2)

This ten bar truss is now a classical test problem for new methods. The material density is 0.1 and the stress limits are 25 for all bars except for bar 9, for which the limit is 50. Minimum cross-sectional area requirement is 0.1.

Since treatment of fabricational constraints with the use of expressions in the form of Equation 27 has not yet been coded into the program (although this equation is used for the other purposes indicated previously), it was decided to assign the value (0.1/RATMAX) to variables which cannot be saved by use of Equation 27. Here, RATMAX is the scaling factor to the constraint surface. Near convergence, RATMAX would not change appreciably and hence 0.1 would be attained.

That this approach is rather artificial, without the use of supporting explicit fabricational constraint expressions, is indicated by the solution progress on Figure 3. After the seventh step, a negative value is obtained for a_5^2 and application of Equation 27 again gives a negative value for a_5.

If a_5 is then set equal to zero, the solution proceeds very efficiently toward the statically determinate optimum solution with members 2, 5, 6 and 10 removed.

However, if a_5 is set equal to (0.1/RATMAX), the rest of the steps result in a struggle between this artifice and the theory. Although there is progress at the completion of each descent, this progress is extremely slow. The broken lines on the figure indicate the use of an alternative weighting factor.

Conclusions

A theory based on optimality criteria has been proposed. There is, at this time, limited numerical experimentation, since the relevant computer program has not been completed to perform all the necessary tasks.

A decrease in structural weight is definitely obtained under stress constraints and there is also the possibility of arriving at the disjoint statically determinate optimum. On the other hand, it is felt that further refinements may be necessary for generality of the task of finding the statically determinate optimum. More insight will probably be gained after explicit use of fabricational constraints during solution.

The additional considerations for design of gridworks are almost completed and numerical experimentation is expected in the near future.

At the present, design for multiple load cases is believed to proceed based on relative values of Lagrange multipliers for each load case, and this aspect is still in the programming phase.

Displacement constraints have not yet been programmed, but are being planned for future implementation.

While it is obvious that the work presented represents only a start into uncovering the possibilities posed by the derived equations, the initial results are quite encouraging. Completion of the computer program would result in a large quantity of numerical data, which upon compilation should yield valuable information regarding extension and refinements for the proposed approach.

Acknowledgement

A major portion of the computer program was developed using the CDC-Cyber and DEC-10 computer facilities at the University of Arizona.

References

1. Reinschmidt, K. F., Cornell, C. A., and Brotchie, J. F., "Iterative Design and Structural Optimization", Jour. Struct. Div., ASCE, V. 92, No. ST6, Dec. 1966, p. 281.

2. Khot, N. S., Berke, L., and Venkayya, V. B., "Comparison of Optimality Criteria Algorithms for Minimum Weight Design of Structures", AIAA Jour., V. 17, No. 2, Feb. 1979, p. 182.

3. Sander, G. and Fleury, C., "A Mixed Method in Structural Optimization", Inter. Jour. Numer. Methods Engrg., V. 13, 1978, p. 385.

4. Berke, L., Khot, N. S., "Use of Optimality Criteria Methods for Large Scale Systems", AGARD Lect. Ser. 70, Structural Optimization, NATO, Sept. 1974, p. 1.1.

5. Atrek, E., "On Stress Constraints in Structural Optimization", Mechs, Res. Comms., V. 8, No. 2, 1981, p. 61.

6. Gellatly, R. A., Helenbrook, R. G., and Kocher, L. H., "Multiple Constraints in Structural Optimization", Inter. Jour. Numer. Methods Engrg.,V. 13, 1978, p. 297.

7. Taig, I. C. and Kerr, R. L, "Optimisation of Aircraft Structures with Multiple Stiffness Requirements", AGARD, Second Symp. Struct. Optim., Milan, Italy, April 1973, p. 16.1.

8. Atrek, E., "Yapısal Optimizasyonda Optimumluk Koşulları Üzerine", TÜBİTAK, VII. Science Congr., Engrg. Div. Kuşadası, Turkey, Oct. 1980.

9. Venkayya, V. B., "Design of Optimum Structures", Jour. Comps. Structs., V. 1, 1971, p. 265.

10. Moses, F., and Onoda, S., "Minimum Weight Design of Structures with Application to Elastic Grillages", Inter. Jour. Numer. Methods Engrg., V. 1, 1969, p. 311.

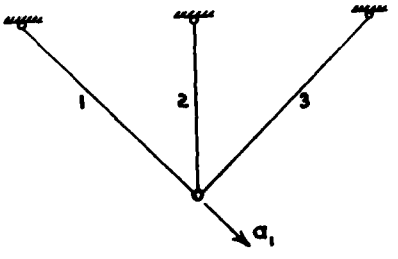


Figure 1. "Redundant" Loading for Three Bar Truss.

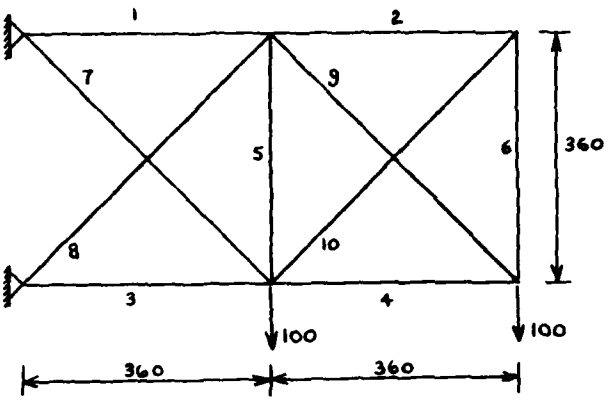


Figure 2. Ten Bar Truss.

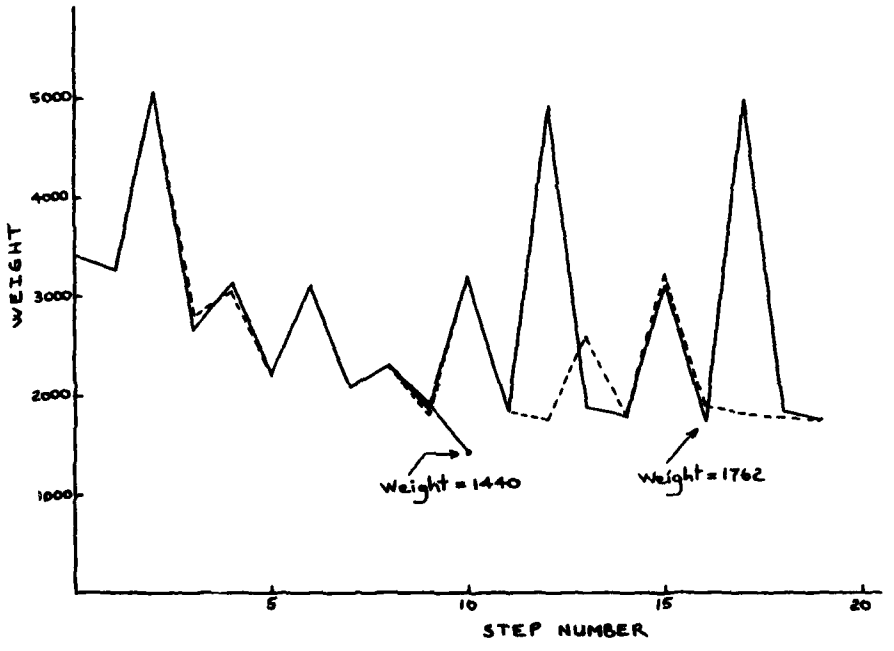


Figure 3. Solution Progress for Ten Bar Truss.

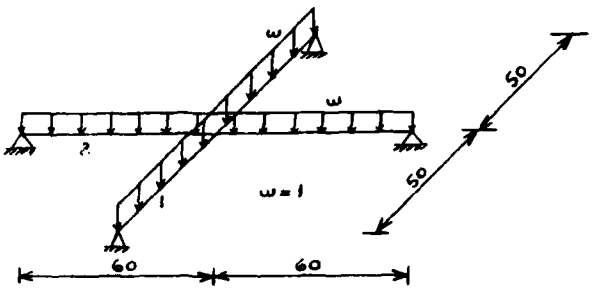


Figure 4. Two Bar Grid (Reference 10).

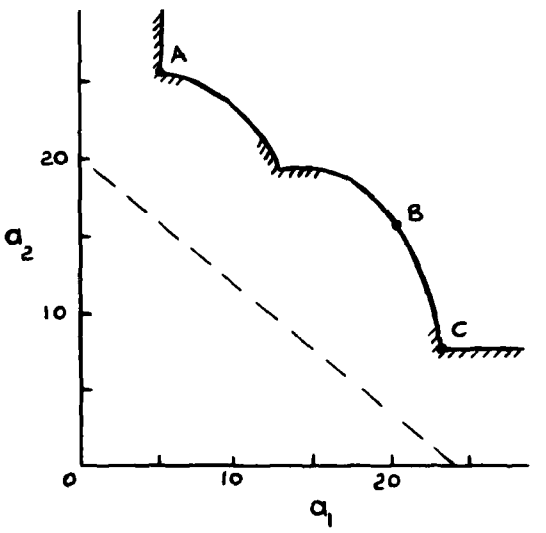


Figure 5. Constraint Surface and Objective Function for Two Bar Grid (Reference 10)

A STUDY OF GLOBAL BUCKLING EFFECTS ON OPTIMUM RISER DESIGN

M.M. Bernitsas
Assistant Professor
Dept. of Naval Architecture
and Marine Engineering

P. Papalambros
Assistant Professor
Dept. of Mechanical Engineering
and Applied Mechanics

The University of Michigan, Ann Arbor, Michigan 48109

Summary

Marine risers used in offshore drilling and mining are long, tubular structures subjected to tension, internal and external static pressure and hydrodynamic loads. Design optimization of risers for general static loads has been studied by the authors in an earlier paper. The present paper examines the influence of global buckling on the optimum design.

The optimization studies conducted earlier use a non-linear programming formulation and show that in the case of generalized static loads with high tension applied at the top of the riser two local optima are possible. One corresponds to optimum design for drilling and production risers and the other for mining risers. Even though in practice high tension is used at the top of the riser, it has been proven that risers may buckle globally while in tension all along their length, due to excessive internal static pressure.

A new optimization model with a minimum weight objective is formulated. The method of monotonicity analysis is applied to identify possible combinations of active constraints. Monotonicity arguments allow the analytical determination of the global optimum by proving that there exist only two local optima both constraint-bound. One of the local optima corresponds to the case where buckling is not critical but instead, the stress due to the internal and external static pressure at the riser's lower end becomes critical. The other local optimum is obtained by making buckling critical along with tensile stresses at the riser's upper end and static pressure stresses at the riser's lower end. In both cases lower limits on mud density and inside diameter of the riser are binding.

This method of analysis provides explicit expressions for the design variables at the optimum and can be used readily for sensitivity analysis.

Introduction

An important element of the offshore drilling, mining and production systems is the riser structure, a long tube connecting the platform with the sea bed. Drilling or production risers are currently 16"-42" in diameter, up to 4,000 feet in length and contain drill string and circulating mud or petroleum. Mining risers have smaller diameters, lengths about 10,000 feet and are used for suction of ore-rich mud.

The riser is supported by a tensioning system housed in the offshore platform and by buoyancy modules properly distributed (see Figure 1). This structure should sustain the external hydrostatic and hydrodynamic load, the internal static pressure and its own weight. Several studies have been conducted on modeling the structural and hydrodynamic problem [1,2,3,4,5,6]. The design problem and subsequent optimization studies were initiated by the authors [7,8]. In this previous work, the riser response under generalized static load was analyzed and an exact solution was obtained in terms of Airy functions. Analytic approximations involving a cable response with end corrections were derived in order to make the solution more amenable to optimization. The derived constraint functions reveal fairly explicitly the dependence of riser behavior on the design variables and parameters, thus allowing successful application of monotonicity analysis [9,10]. Attention in [7,8] was focused on risers subjected to significant external loads, thus requiring high tensions at the top of the riser and eliminating the possibility of buckling. However, global buckling failures may occur for relatively low external loads and high mud densities and riser weight. This problem is the subject of the present paper. The buckling constraint is formulated based on an earlier derivation of the buckling loads [11]. The design model is derived and treated with monotonicity analysis to identify active constraints and locate the global optimum.

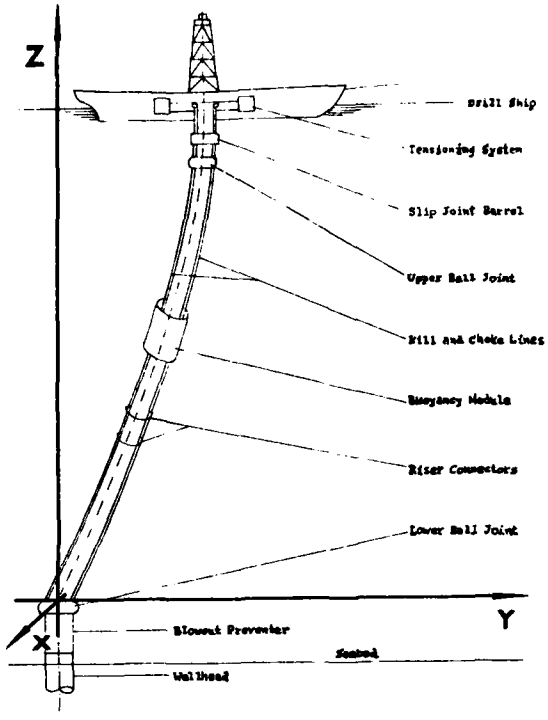


FIGURE 1: OFFSHORE DRILLING SYSTEM

Riser Global Buckling Model

The global buckling loads of a riser can be evaluated using the small slope, small deflection linear equations of static equilibrium. Risers can be modelled as slender tubular open-ended columns subjected to internal and external fluid static pressure.

Studying the equilibrium of the differential element dz (see Figure 2) we derive the following equations [5]:

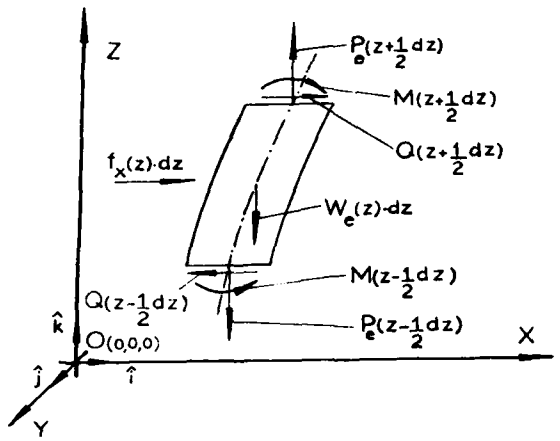


FIGURE 2: FREE BODY DIAGRAM FOR A DIFFERENTIAL ELEMENT DZ LINEARIZED MODEL

Equilibrium of forces in the x direction:

$$\frac{dQ}{dz} = f_x \tag{1}$$

where

$Q(z)$ is the shear force in the x direction,

$f_x(z)$ is the external force per unit length exerted on the riser.

Equilibrium of forces in the z direction:

$$\frac{dP_e}{dz} = W_e \tag{3}$$

where

$$W_e \equiv W_R + W_m + W_B - B$$

$$P_e(z) \equiv T(z) + \gamma_w \frac{\pi D_0^2}{4} (h_w - z) - \gamma_m \frac{\pi D_i^2}{4} (h_m - z) \tag{4}$$

$T(z)$ is the actual tension in the riser,

$$W_R = \gamma_R \frac{\pi}{4} (D_0^2 - D_i^2) \tag{5}$$

is the weight of the riser per unit length,

$$W_m = \gamma_m \frac{\pi}{4} D_i^2. \tag{6}$$

is the weight of the drilling mud per unit length,

$$W_B = \gamma_B \frac{\pi}{4} (D_B^2 - D_0^2) \tag{7}$$

is the buoyancy of the buoyancy modules per unit length and

$$B = \gamma_w \frac{\pi}{4} D_B^2 \tag{8}$$

is the buoyancy of the riser and modules per unit length.

Equilibrium of moments:

$$\frac{dM}{dz} - P_e \frac{dU}{dz} + Q = 0 \tag{9}$$

where

$M(z)$ is the bending moment in the y direction,

U is the deflection of the riser in the x direction.

Finally the linear constitutive relation of bending is:

$$M(z) = EI \frac{d^2U}{dz^2} \tag{10}$$

where

$$I = \frac{\pi}{64} (D_0^4 - D_i^4) \tag{11}$$

Elimination of $M(z)$, $Q(z)$ and $P_e(z)$ from equations (1), (2), (9) and (10) yields the linear fourth order differential equation with variable coefficients which describes the riser static response to external loads:

$$\frac{d^2}{dz^2}\left[EI \frac{d^2U}{dz^2} \right] - \frac{d}{dz}\left[(W_e z + P_e(0)) \frac{dU(z)}{dz} \right] = f_x(z) \tag{12}$$

In order to derive the buckling loads we set

$$f_x(z) = 0 \tag{13}$$

and solve equation (12) subject to the proper boundary conditions. In this application the riser was considered as a vertical column simply supported at both ends. That is,

$$U(0) = 0 \tag{14} \qquad U(L) = 0 \tag{15}$$

$$\frac{d^2U(0)}{dz^2} = 0 \tag{16} \qquad \frac{d^2U(L)}{dz^2} = 0 \tag{17}$$

The above boundary value problem (BVP) can be recast in dimensionless form as follows:

$$\frac{d^4U}{dp^4} - \frac{d}{dp}\left[(\beta p + \tau) \frac{dU}{dp} \right] = 0 \tag{18}$$

$$U(0) = 0 \tag{19} \qquad U(1) = 0 \tag{20}$$

$$\frac{d^2U(0)}{dp^2} = 0 \tag{21} \qquad \frac{d^2U(1)}{dp^2} = 0 \tag{22}$$

where

$$\tau = \frac{P_e(0)L}{EI} \tag{23} \qquad \beta = \frac{W_e L^3}{EI} \tag{24}$$

and $$p = \frac{z}{L} \tag{25}$$

This BVP has been solved in two ways in [11]. Analytically, in terms of Airy functions of the first and second kind and numerically using infinite series. The results, that is the critical buckling loads τ_{crit}, are plotted versus the design parameter β, for the first six buckling modes in Figure 3 [11]. The first mode buckling loads provide a lower bound for τ. Thus if we denote these loads by $f(\beta)$ the buckling constraint becomes

$$\tau \geq -f(\beta)/N_2 \tag{26}$$

where N_2 is a buckling safety factor.

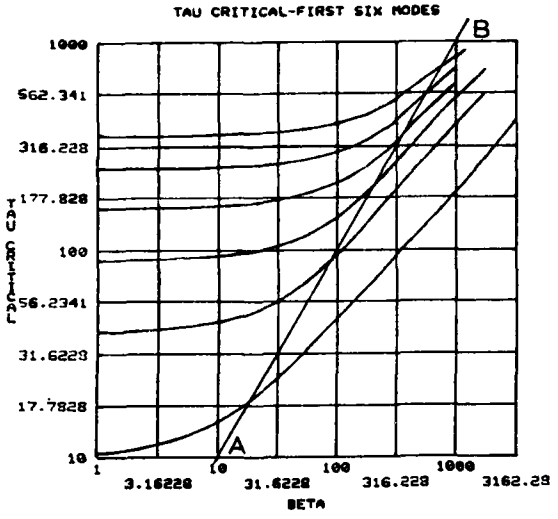


FIGURE 3: CRITICAL BUCKLING LOADS VERSUS BETA

Combined Stresses in the Riser

In the present analysis we are concerned about the possibility of global riser buckling that is likely to occur for low values of the tension applied at the top of the riser and high values of the drilling mud density and the riser weight per unit length. This design problem arises for very low values of the external loads [8]. Consequently, the bending stress component, which in the general static problem is significant [7], is negligible in the buckling problem.

Let (z,r,t) be the local coordinate system in the riser where r and t are local radial and tangential directions and z is the axial direction. Considering the riser tube as a thin cylindrical shell we can derive the following expressions for the local shear stresses

$$\tau_{tz} = \frac{Q}{I}\frac{D\delta}{4}\cos\phi \equiv 0 \qquad (27)$$

where

δ is the thickness of the riser tube

D is the average riser tube diameter

and ϕ is the polar ordinate

$$0 \leq \phi \leq 2\pi \qquad (28)$$

$$\tau_{tr} = 0 \qquad (29) \qquad \tau_{zr} = 0 \qquad (30)$$

The normal stresses are:

$$\sigma_z = \sigma_e + \sigma_p \qquad (31)$$

$$\sigma_r = \sigma_p - \tilde{\tau} \qquad (32) \quad \text{and} \quad \sigma_t = \sigma_p + \tilde{\tau} \qquad (33)$$

where

$$\sigma_p = \frac{\tilde{p}_i D_i^2 - \tilde{p}_0 D_0^2}{(D_0^2 - D_i^2)} \qquad (34) \qquad \tilde{\tau} = \frac{(\tilde{p}_i - \tilde{p}_0) D_i^2 D_0^2}{(D_0^2 - D_i^2) 4r} \qquad (35)$$

$$\sigma_e = \frac{P_e}{A} \qquad (36)$$

$$\tilde{p}_i = \gamma_m (h_m - z) \qquad (37) \qquad \tilde{p}_0 = \gamma_w (h_w - z) \qquad (38)$$

and $$A = A_0 - A_i = \frac{\pi D_0^2}{4} - \frac{\pi D_i^2}{4} \qquad (39)$$

Finally the Tresca criterion gives the limit stress σ_T

$$\sigma_T = \max \left\{ \frac{1}{2}\left|\sigma_z - \sigma_r\right| , \frac{1}{2}\left|\sigma_z - \sigma_t\right| , \frac{1}{2}\left|\sigma_t - \sigma_r\right| \right\} \qquad (40)$$

or

$$\sigma_T = \max \left\{ \frac{1}{2}\left|\sigma_e + \tilde{\tau}\right| , \frac{1}{2}\left|\sigma_e - \tilde{\tau}\right| , \left|\tilde{\tau}\right| \right\} \qquad (41)$$

The maximum local value of the stress is a function of p and can be derived from (42)

$$\sigma_T = \max \left\{ \frac{1}{2} \left| \frac{EI}{L^2 \frac{\pi}{4}(D_0^2 - D_i^2)} (\beta p + \tau) + (\gamma_m - \gamma_w)(1-p) \frac{LD_i^2}{D_0^2 - D_i^2} \right| , \left| (\gamma_m - \gamma_w)(1-p) \frac{LD_0^2}{D_0^2 - D_i^2} \right| \right\} \qquad (42)$$

Optimum Design

The optimization model can now be assembled in the form of a nonlinear programming problem. The design criterion used as objective is the riser weight W_R :

$$\min W_R = \gamma_R \frac{\pi}{4}(D_0^2 - D_i^2) \qquad (43)$$

The constraint functions are developed following previous practice [8]. There are three stress constraints corresponding to the possible local stress maxima along the riser. The first constraint refers to maximum stress due to tension at the upper end of the riser (see eq (42)) and is expressed as:

$$\frac{4EI(\beta+\tau)}{\pi L^2 (D_0^2 - D_i^2)} \leq \frac{S_y}{N_1} \qquad (44)$$

where S_y is the yield strength in tension and N_1 is a safety factor. The other two constraints refer to maximum stresses due to tension and static pressure at the lower end of the riser. They can be derived from (42) and expressed as

$$\frac{4EI\tau}{\pi L^2 (D_0^2 - D_i^2)} + (\gamma_m - \gamma_w)\frac{LD_i^2}{D_0^2 - D_i^2} \leq \frac{S_y}{N_1} \qquad (45)$$

$$(\gamma_m - \gamma_w)\frac{LD_0^2}{(D_0^2 - D_i^2)} \leq \frac{S_y}{2N_1} \qquad (46)$$

The buckling constraint is expressed in terms of the nondimensional variables τ and β as derived in the previous section eq. (26), i.e.

$$\tau \geq -\frac{f(\beta^+)}{N_2} \qquad (47)$$

There are several practical constraints that must be observed. A minimum inside diameter for the riser tube is required for proper mud circulation, i.e., $D_i > D_{imin}$. Upper and lower limits for the mud density are required for drill string protection and blow out prevention, i.e. $\gamma_{m_1} < \gamma_m < \gamma_{m_2}$. Acceptable design practice requires that there is some positive tension at the top of the riser, i.e. TTR>0 is a strict inequality; also, partial buoyancy implies the strict inequality

$$W_R = \frac{\pi}{4}\gamma_{wB}(D_B^2-D_0^2) > 0 \qquad (48)$$

An obvious geometric constraint is that the buoyancy module diameter D_B must be strictly greater than the riser outside diameter D_0. Finally, the design variables must satisfy the relations and definitions described earlier, which leads to equality constraints (49) to (52):

Equation (24) which defines β becomes

$$\frac{EI\beta}{L^3} = W_R + \gamma_m \frac{\pi}{4} D_i^2 - \gamma_w \frac{\pi}{4} D_B^2 + \gamma_B \frac{\pi}{4}(D_B^2-D_0^2) \qquad (49)$$

where W_R is the weight of the riser per unit length

$$W_R = \frac{\pi}{4}\gamma_R(D_0^2-D_i^2) \qquad (50)$$

I is the area moment of inertia

$$I = \frac{\pi}{64}(D_0^4-D_i^4) \qquad (51)$$

and TTR is given by

$$(\tau+\beta)\frac{EI}{L} = TTR + \frac{\pi}{4}\gamma_w L(D_B^2-D_0^2) \qquad (52)$$

This concludes the model description. Note that all the design variables are positive with the exception of τ which can be negative. The solution procedure is facilitated by examining two different cases:

Problem P1: $0 \geq \tau \geq -f(\beta)/N_2$ (53)

Problem P2: $\tau \geq 0$ (54)

Problem P1 is examined first. Introducing the transformation

$$t \triangleq -\tau \qquad (55)$$

and eliminating I, TTR and W_R using equality constraints (49) to (51) we define the following optimization problem in normalized form:

Problem P1

$$\min \; W_R = \frac{\pi}{4}\gamma_R(D_0^2-D_i^2)$$

subject to:

$$R_1: \; \frac{E(D_0^2+D_i^2)(\beta-t)N_1}{16L^2S_y} \leq 1$$

$$R_2: \; -\frac{E(D_0^2+D_i^2)tN_1}{16L^2S_y} + \frac{(\gamma_m-\gamma_w)LD_i^2N_1}{(D_0^2-D_i^2)S_y} \leq 1$$

$$R_3: \; \frac{2(\gamma_m-\gamma_w)LD_0^2N_1}{(D_0^2-D_i^2)S_y} \leq 1$$

$$R_4: \; tN_2/f(\beta) \leq 1$$

$$R_5: \; D_{imin}D_i^{-1} \leq 1$$

$$R_6: \; \gamma_{m_1}\gamma_m^{-1} \leq 1$$

$$R_7: \; \gamma_m\gamma_{m_2}^{-1} \leq 1$$

plus the inactive constraints

$$R_8: \; W_R^{-1}\left[\frac{\pi}{4}\gamma_{wB}(D_B^2-D_0^2)\right] \leq 1 \qquad \text{(from eq. (48))}$$

$$R_9: \; \gamma_{wB}D_0^2\left[\gamma_R(D_0^2-D_i^2) + \gamma_m D_i^2 - \gamma_B D_0^2 - E\beta(D_0^4-D_i^4)/16L^3\right]^{-1} \leq 1 \qquad \text{(since } D_B>D_0\text{)}$$

$$R_{10}: \; \gamma_w(D_B^2-D_0^2)\left[\frac{E(D_0^4-D_i^4)(\beta-t)}{16L^3}\right]^{-1} \leq 1 \qquad \text{(because TTR>0)}$$

and the nonnegativity constraints

$$D_0,\; D_i,\; \beta,\; \gamma_m > 0 \quad , \quad t \geq 0$$

Examining the monotonicity with respect to (wrt)β in Problem P1 it can be seen that, if a solution exists, then either both constraints R_1 and R_4 are active, or they are both inactive. Thus Problem P1 is reduced to two subcases, where each of the above alternatives is considered separately. Note that the symbol "$\overset{=}{<}$" indicates an active constraint, while "$<$" is reserved for constraints with possible, yet unknown, activity.

Subproblem P1.1 corresponds to having both R_1 and R_4 active. Given the activity of the stress constraint R_1 we then consider the possibility of dominance between R_1 and the other stress constraint R_2. Direct comparison shows that R_1 dominates R_2 whenever

$$W_R - \gamma_{wB}\frac{\pi}{4}(D_B^2-D_0^2) > \frac{\pi}{4}\gamma_w(D_0^2-D_i^2) \qquad (56)$$

Condition (56) dominates constraint R_8, which can thus be dropped from sub-problem P1.1. Note that if condition (56) is not satisfied, R_2 would dominate R_1 which would then be inactive, a situation assumed for subproblem P1.2. Good design practice requires use of some buoyancy modules. Thus D_B is assumed strictly greater than D_0 and R_9 becomes inactive. Finally note that monotonicity wrt γ_m shows constraint R_6 to be active and R_7 inactive, i.e. the mud density must be set always equal to its lower limit γ_{m_1}. In order to reveal monotonic behavior of the remaining variables a transformation is introduced, viz.

$$D_R^2 \triangleq D_0^2 - D_i^2 \qquad (57)$$

$$D_A^2 \triangleq D_0^2 + D_i^2 \qquad (58)$$

This transformation allows a simplification of some expressions by assuming $D_A^2 >> D_R^2$ with a maximum induced error of 5%. This is true because the thickness of the riser tube is generally very small compared to either the inside or the outside diameter. Thus we have:

Problem P1.1

$$\min \quad W_R = \frac{\pi}{4}\gamma_R D_R^2$$

subject to:

$$R_1: \quad \frac{EN_1 D_R^2(\beta - t)}{16L^3 S_y} \leq 1$$

$$R_3: \quad (\gamma_{m1}-\gamma_w)\frac{N_1 L D_A^2}{D_R^2 S_y} \leq 1$$

$$R_4: \quad t\left[f(\beta)\right]^{-1} N_2 \leq 1$$

$$R_5: \quad 2D_{imin}^2 D_A^{-2} \leq 1$$

plus the inactive constraints R_{10}, R_{11} and condition (56) appropriately expressed in terms of D_A and D_R. Expressing problem P1.1 in terms of functional monotonicities we have:

$$\min W_R(D_R^+)$$

subject to:

$$R_1(D_R^+, \beta^+, t^-) \leq 1 \qquad R_4(\beta^-, t^+) \leq 1$$
$$R_3(D_A^+, D_R^-) \leq 1 \qquad R_5(D_A^-, D_R^+) \leq 1 \qquad (59)$$

From (59) it is concluded that R_3 must be active due to monotonicity wrt D_R and therefore R_5 must be also active due to monotonicity wrt D_A. Thus the optimum for Problem P1.1 is constraint bound, determined by simultaneous activity of constraints R_1, R_3, R_4, R_5. This solution is a local optimum for Problem P1, provided it satisfies the above mentioned inactive constraints.

Next we examine subproblem P1.2 corresponding to R_1 and R_4 being inactive. Using transformations (57) and (58) we get

Problem P1.2

$$\min \quad W_R = \frac{\pi}{4}\gamma_R D_R^2$$

subject to:

$$R_2: \quad \frac{-ED_R^2 N_1}{16L^3 S_y} t + (\gamma_m-\gamma_w)\frac{LN_1 D_A^2}{2D_R^2 S_y} \leq 1$$

$$R_3: \quad (\gamma_m-\gamma_w)\frac{N_1 L D_A^2}{D_R^2 S_y}$$

$$R_5: \quad 2D_{imin}^2 D_A^{-2} \leq 1$$

$$R_6: \quad \gamma_{m_1}\gamma_m^{-1} \leq 1$$

$$R_7: \quad \gamma_m\gamma_{m_2}^{-1} \leq 1$$

Monotonicity wrt γ_m shows that R_6 is again active and R_7 inactive, i.e. $\gamma_{m*} = \gamma_{m_1}$. Constraint R_2 is the only one containing t providing a lower bound on t. Therefore

$$t_* > \max\{0, \phi_2(D_{A*}, D_{R*})\} \qquad (60)$$

where

$$\phi_2(D_{A*}, D_{R*}) \triangleq \frac{(\gamma_{m1}-\gamma_w)LN_1 D_{A*}^2/2D_{R*}^2 S_y}{ED_{R*}^2 N_1/16L^2 S_y} \qquad (61)$$

is the solution of R_2 wrt t. Thus constraint R_2 is considered inactive. Then monotonicity wrt D_A and D_R shows that constraints R_3 and R_5 must be active. Therefore the solution of Problem P1.2 is constraint bound given by simultaneous activity of R_3, R_5 and R_6. Of course all the variables must be checked against the inactive constraints to assure feasibility. This case then gives a second local optimum for problem P1.

Now Problem P2 is examined, i.e. the case with $\tau > 0$.

Problem P2

$$\min \quad W_R = \frac{\pi}{4}\gamma_R D_R^2$$

subject to:

$$R_1: \quad \frac{EN_1(D_0^2+D_i^2)(\beta+\tau)}{16L^2 S_y} \leq 1$$

$$R_2: \quad \frac{EN_1}{16L^2 S_y}(D_0^2+D_i^2)\tau + (\gamma_m-\gamma_w)\frac{LD_i^2 N_1}{(D_0^2-D_i^2)S_y} \leq 1$$

$$R_3: \quad (\gamma_m-\gamma_w)\frac{2LD_0^2 N_1}{(D_0^2-D_i^2)S_y} \leq 1$$

$$R_5: \quad D_{imin} D_i^{-1} \leq 1$$

$$R_6: \quad \gamma_{m_1}\gamma_m^{-1} \leq 1$$

$$R_7: \quad \gamma_m\gamma_{m_2}^{-1} \leq 1$$

and $\tau \geq 0$

and the inactive constraints R_9, R_{10}, R_{11}.

Since R_1 and R_2 provide only upper bounds on τ, one possibility is that R_1 and R_2 are both inactive and $\tau > 0$. However, this leads to an unbounded problem wrt D_0. Thus $\tau_* = 0$ and at least one of R_1 and R_2 must be active. But R_1 is the only constraint containing β therefore it need not be active which leaves R_2 as the active one. As in the previous cases R_6 is also active due to monotonicity wrt γ_m. The problem P2 is thus reduced to:

Problem P2'

$$\min \quad W_R = \frac{\pi}{4}\gamma_R(D_0^2-D_i^2)$$

subject to:

$$R_2: \quad (\gamma_{m_1}-\gamma_w)\frac{LD_i^2 N_1}{(D_0^2-D_i^2)S_y} \leq 1$$

$$R_3: \quad (\gamma_{m_1}-\gamma_w)\frac{2LD_0^2 N_1}{(D_0^2-D_i^2)S_y} \leq 1$$

$$R_5: \quad D_{imin} D_i^{-1} \leq 1$$

It can be seen immediately that R_3 always dominates R_2 and therefore it is active due to monotonicity wrt D_0. Solving R_3 for D_0 and substituting in the objective we get an increasing function wrt D_i which then makes R_5 active. Thus the optimum for problem P2

as constraint bound given by simultaneous activity of R_3 , R_5 , R_6 and $\tau = 0$.

Discussion

In order to study the effect of global buckling on optimum riser design, we have formulated the appropriate nonlinear optimization problem with ten constraints and six degrees of freedom. Three possible local optima have been identified corresponding to the solutions of problems P1.1, P1.2 and P2'. All three problems are constraint bound with constraints R_6 , R_5 and R_3 active. From the design point of view this means that (1) The density of the drilling mud must be set in all cases equal to its lower limit; that is:

$$\gamma_m^* = \gamma_{m_1} \tag{62}$$

(2) The internal riser diameter must be set to its lower limit which is dictated from practical constraints; vis.

$$D_i^* = D_{imin} \tag{63}$$

(3) The stress due to internal and external static pressure at the lower end of the riser must be critical. This results in an explicit expression for D_0 in terms of the parameters of the problem:

$$D_0^* = D_{imin}/\sqrt{1-\omega} \tag{64}$$

where

$$\omega \triangleq \frac{2(\gamma_{m1}-\gamma_w)\ LN_1}{S_y} \tag{65}$$

and

$$\omega < 1 \tag{66}$$

Using equations (62), (63) and (64) we can prove that the lower bound for t derived from constraint R_2 is always negative. Consequently, as inequality (60) shows, τ becomes zero in problem P1.2 and the solutions to P1.2 and P2 become identical. Thus the local optima reduce to the following two:

1) The first local optimum is the solution to problem P1. From the activity of R_1 and R_4 we get respectively

$$\beta^* - \frac{f(\beta^*)}{N_2} = \frac{16L^2S_y\ (1-\omega)}{ED^2_{imin}N_1(2-\omega)} \tag{67}$$

and

$$t^* = \frac{f(\beta^*)}{N_2} \tag{68}$$

It can be seen from Figure 3 that equation (67) always has a unique positive solution for β . The sixth design variable of the problem, that is D_B , does not influence the objective W_R . Problem P1 will have a solution as long as there is a feasible D_B value satisfying the inactive constraints for the values of the other five design variables defined by equations (62), (63), (64), (67) and (68). Constraint R_2 (or condition (56)) dominates R_8 and yields an upper bound for D_B

$$\frac{D_B^{2*}}{D^2_{imin}} < \frac{1}{1-\omega}\left[\omega\frac{\gamma_R-\gamma_w}{\gamma_{wB}} + 1\right] \tag{69}$$

R_9 sets a lower bound for D_B

$$\frac{1}{1-\omega} < \frac{D_B^{2*}}{D^2_{imin}} \tag{70}$$

and R_{10} sets a second upper bound for D_B

$$\frac{D_B^{2*}}{D^2_{imin}} < \frac{1}{1-\omega}\left[1 + \omega\frac{S_y}{N_1\gamma_w L}\right] \tag{71}$$

Obviously, there is always a feasible range for D_B since both upper limits for D_B are greater than the lower limit. For long risers, that is for

$$L > \frac{S_y}{N_1\gamma_w}\ \frac{\gamma_R-\gamma_w}{\gamma_{wB}} \tag{72}$$

constraint R_{10} (TTR > 0) becomes dominant and the upper limit for D_B is given by (71). If (72) is not satisfied, R_2 becomes dominant, and the upper limit for D_B is given by (69).

2) The second local optimum is the solution to problems P1.2 and P2. The values of γ_m^* , D_i^* and D_0^* are given by equations (62), (63) and (64) respectively and

$$\tau^* = 0 \tag{73}$$

The other two design variables, β and D_B , do not affect the objective at the optimum. A solution will exist if there are feasible values for β and D_B , for the derived values of γ_m , D_i , D_0 and τ .

Constraints R_8 and R_9 yield the feasible range for D_B :

$$\frac{1}{1-\omega} < \frac{D_B^{2*}}{D^2_{imin}} < \frac{1}{1-\omega} + \frac{\gamma_{wB}}{\gamma_R}\ \frac{\omega}{1-\omega} \tag{74}$$

which is not null.

Finally, constraints R_1 and R_{10} give the feasible range for β :

$$\frac{16L^3\gamma_w}{ED^2_{imin}}\ \frac{(1-\omega)^2}{\omega(2-\omega)}\left(\frac{D_B^2}{D^2_{imin}} - \frac{1}{1-\omega}\right) < \beta^* < \frac{16L^2S_y}{EN_1D^2_{imin}}\ \frac{1-\omega}{2-\omega} \tag{75}$$

This solution to problems P1.2 and P2 is similar to the solution to problem P2 in reference [8]. In both cases the bending stresses are not critical.

Conclusions

The nonlinear design problem for investigation of the effects of buckling on the optimum static design of risers was formulated. Monotonicity analysis was used to find active constraints of the optimum. Two local optima were identified as solutions to constraint bound problems. In both problems explicit values of the design variables or feasibility ranges were derived in terms of the design parameters. These explicit expressions can readily be used for sensitivity analysis.

Both local optima occur for the minimum allowable values of the drilling mud density and internal riser diameter, and when the stress at the lower end of the riser due to the internal and external static pressures becomes critical. One of the two local optima occurs when the buckling constraint becomes active. In this

case the optimal values of design variables β and τ are influenced by the buckling constraint.

Acknowledgements

The work of the authors has been supported by Faculty Research Grant Nos. 387565 and 387569 respectively, from the Horace H. Rackham School of Graduate Studies of The University of Michigan. The work of the second author has been supported by NSF Grant No. CME80-06687.

Nomenclature

BVP	Boundary Value Problem
D	Average diameter of riser
D_B	Outer diameter of buoyancy modules
$D_{B\ max}$	Maximum allowable D_B
D_i, D_0	Inner and outer riser diameters
$D_{i\ min}$	Minimum allowable D_i
E	Young's Modulus
$f(x_1^+, x_2^-)$	Function f increasing with respect to x_1 and decreasing with respect to x_2
I	Riser cross-sectional area moment of inertia
L	Riser's length
M	Bending moment
P_e	Effective tension
Q	Shear force
R_i	Constraint no. i
S_y	Riser's material yield strength
$T(0)$	Actual tension at the riser's lower end
TTR	Tension at the top of the riser
U	Riser's lateral displacement
W_e	Effective weight of riser per unit length
W_m	Weight of drilling mud per unit length
W_R	Weight of riser per unit length
h_m	Total height of mud column
H_w	Total water depth
f_x	External hydrodynamic load per unit length
p	Dimensionless vertical coordinate along the riser
P_t, P_0, P_1	Position of maximum total stress
$\bar{P}_0$, $\bar{P}_i$	External and internal local static pressure
wrt	With respect to

Greek Symbols

β	Dimensionless effective riser weight
γ_B, γ_R, γ_W	Specific weight of buoyancy modules material, riser wall material, water
γ_m	Specific weight of circulating mud
γ_{m_1}, γ_{m_2}	Lower and upper limits for γ_m

References

1. Azar, J.J. and Soltveit, R.E., "A Comprehensive Study of Marine Drilling Risers," ASME Paper, Petroleum Division, PET-61, 1978.

2. Sparks, C.P., "Mechanical Behavior of Marine Risers Mode of Influence of Principal Parameters," Deepwater Mooring and Drilling, ASME O.E.D., Vol. 7, 1979.

3. Bernitsas, M.M., "Three Dimensional, Non Linear Large Deflection Model of Dynamic Response of Risers, Pipelines and Cables," Journal of Ship Research, 1981.

4. Rapel, K.H., "Structural Analysis for a Long Drilling Riser," Interocean '76. (In German)

5. Bernitsas, M.M., "Static Analysis of Marine Risers," Department of Naval Architecture and Marine Engineering, The University of Michigan, Report No. 234, May 1981.

6. BSRA, "A Critical Evaluation of the Data on Wave Force Coefficients," Report W278, Aug. 1976.

7. Bernitsas, M.M. and Papalambros, P., "Design Optimization of Risers Under Generalized Static Load," Intermaritec '80, Hamburg, W. Germany, Sept. 1980.

8. Papalambros, P. and Bernitsas, M.M., "Monotonicity Analysis in Optimum Design of Marine Risers," Trans. ASME Journal of Mechanical Design. (to appear)

9. Wilde, D.J., Globally Optimal Design, Wiley Interscience, New York, 1978.

10. Papalambros, P. and Wilde, D.J., "Global Non-Iterative Design Optimization Using Monotonicity Analysis," Trans. ASME, J. of Mech. Design, Vol. 101, No. 4, 1979.

11. Bernitsas, M.M., "Riser Top Tension and Riser Buckling Loads," ASME AMD, Vol. 37, 1980.

12. Papalambros, P., "Monotonicity in Goal and Geometric Programming," Trans. ASME, J. of Mech. Design (to appear).



AD-P000 060

CONNECTEDNESS CRITERION AND THE UNIQUE OPTIMUM OF THE IZO-STATIC TRUSSES

M.Bayer

Dept. of Aeronautics, Mechanical Engineering Faculty,
Istanbul Technical University, Istanbul

Summary. This paper deals with the uniqueness of the optimum of the least-weight izo-static elastic trusses which have given layouts and have members that are made of different materials. The trusses under consideration are subject to sets of static loads where the member cross-sectional areas, the member stresses and the nodal displacements are to remain within the prescribed bounds. Connectedness criterion is utilized to show the uniqueness of the optimum.

Symbols

A_j	cross-sectional area of member j
A_j^1, A_j^2	A_j values at points 1 and 2 respectively
A_j^ℓ, A_j^u	lower and upper bounds on A_j respectively
$\tilde{A}^1$, $\tilde{A}^2$	vectors whose elements are A_j^1 and A_j^2 respectively
E_j	elastic modulus of the material of member j
F_{jk}	member force in member j under load set k
$\tilde{F}_k$	vectors whose elements are F_{jk}
(D)	direction-cosine matrix
$(D)^T$	(D) transposed
f(x)	a function of variables x
$f(\tilde{x})$	function value at position vector $\tilde{x}$
$f(\tilde{x}^1)$, $f(\tilde{x}^2)$	function values at position vectors $\tilde{x}^1$ and $\tilde{x}^2$ respectively
(I_E)	diagonal matrix whose elements are E_j/L_j
i	subscript indicating the nodal displacement number, and also the equilibrium equation number
j	subscript indicating the member number
k	subscript indicating the load set number
L_j	length of member j
m	total number of the members
n	total number of the nodal displacements, and also the equilibrium equations
P_{ik}	external load that is parallel to u_{ik} at the relevant node
$\tilde{P}_k$	vectors whose elements are P_{ik}
p(t)	a path expressed in terms of parameter t
p(0), p(1)	the path values at points 1 and 2 respectively
q	total number of the load sets
S	a solution domain
t	a parameter such that $0 \leq t \leq 1$
u_{ik}	nodal displacement i for load set k
u_{ik}^ℓ, u_{ik}^u	lower and upper bounds on u_{ik} respectively
$\tilde{u}_k$	vectors whose elements are u_{ik}
W	total weight of the truss
W^1, W^2	total weights of the truss af points 1 and 2 respectively
w_j	weight of member j
w_j^1, w_j^2	weights of member j at points 1 and 2 respectively
$\tilde{x}$	a position vector whose elements are variables x
$\tilde{x}^1$, $\tilde{x}^2$	position vectors at points 1 and 2 respectively
ρ_j	specific-weight of the material of member j
σ_{jk}	member stress in member j for load set k
σ_{jk}^ℓ, σ_{jk}^u	lower and upper bounds on σ_{jk} respectively
$\tilde{\sigma}_k$	vectors whose elements are σ_{jk}
σ_{jk}^1, σ_{jk}^2	σ_{jk} values at points 1 and 2 respectively
$\tilde{\sigma}_k^1$, $\tilde{\sigma}_k^2$	vectors whose elements are σ_{jk}^1 and σ_{jk}^2 respectively
λ	a parameter such that $0 \leq \lambda \leq 1$

Introduction

The least-weight elastic truss design, as a Mathematical Programming Problem, has been a topic to many research programmes since 1960[1] and many researchers have been engaged in devising suitable computer methods that will find the optimum. There is no doubt that this kind of research is very important for the practical applications, but it is also essential to investigate the mathematical

PRECEDING PAGE

characteristics of the design problem.

In this paper a very important mathematical character of the truss, namely the connectedness character, will be shown for the izo-static trusses. There is a marked difference between the izo-static trusses and the hyper-static trusses. It suffices to mention here that the former can be formulated as Non-linear Programming Problems where as the latter can only be formulated as Non-linear Combinatorial Problems[2]. Therefore these problems may posses multiple optima and to determine the global optimum constitutes the most important aspect of the least-weight truss design.

As for the least-weight izo-static trusses, this issue can be settled by showing the uniqueness of the optimum. It is well known that a convex optimization problem posseses a unique optimum[3]. The convexity criterion was first applied to the izo-static trusses by A.R.Toakley[4] and independently from him, with a different approach, by the author[2]. In both approaches the optimization problem is expressed in terms of variables that are the reciprocals of the member cross-sectional areas. That is to say, the minimization problem is transformed to a new space so that a convex formulation of the least-weight truss design is obtained, and only by then, the uniqueness of the optimum is claimed. This transformation is only possible for the izo-static trusses and not for the hyper-static trusses.

The convexity criterion is only a sufficient condition for the unique optimum[5], where as the connectedness criterion is the necessary and the sufficient condition for the unique optimum[6] and therefore it is the most general way of showing uniqueness. In this paper, for the first time, the connectedness criterion will be used to show the uniqueness of the optimum of the least-weight izo-static elastic trusses.

Formulation of the Problem

This paper concerns in showing the uniqueness of the optimum belonging to the least-weight izo-static elastic trusses whose members are made of different materials. The trusses have given layouts and they are subject to sets of external static loads such that the member cross-sectional areas, the member stresses and the nodal displacements are to remain within the prescribed bounds. The problem formulation follows[2]:

Objective function:

$$\text{Min } W = \sum_{j=1}^{m} \rho_j L_j A_j \qquad (1a)$$

Subject to:

$$\begin{aligned}
&(D)\ \tilde{F}_k = \tilde{P}_k && k=1,\ldots,q && (1b)\\
&(I_E)\ (D)^T \tilde{u}_k = \tilde{\sigma}_k && k=1,\ldots,q && (1c)\\
&F_{jk} = A_j \sigma_{jk} && j=1,\ldots,m;\ k=1,\ldots,q && (1d)\\
&A_j^{\ell} \le A_j \le A_j^{u} && j=1,\ldots,m && (1e)\\
&\sigma_{jk}^{\ell} \le \sigma_{jk} \le \sigma_{jk}^{u} && j=1,\ldots,m;\ k=1,\ldots,q && (1f)\\
&u_{ik}^{\ell} \le u_{ik} \le u_{ik}^{u} && i=1,\ldots,n;\ k=1,\ldots,q && (1g)
\end{aligned} \qquad (1)$$

The total weight of the truss is a linear function of the member cross-sectional areas (1a). The equilibrium equations (1b) and the compatibility equations (1c) are linear constraints, where as the member force definitions (1d) are non-linear constraints. Due to this non-linearity the least-weight elastic trusses are classified as Non-linear Programming Problems. The remainder of the constraints are the inequalities that enforce upper and lower limits onto the variables of the problem.

The problem outlined in formulation (1) may be expressed in a fewer dimensional space where the nodal displacements may be dispensed with. In this paper however, it will be left as it is casted in formulation(1).

If the nodal displacements are not constrained then the problem outlined in formulation (1) becomes a trivial Linear Programming Problem[2]. It can be easily solved by the conventional methods and at the optimum either the member cross-sectional area or the member stress for a particular load set is critical for a member.

Connectedness

A connected minimization problem is defined below[6]:

$$\begin{aligned}
&\tilde{x} \in S && (2a)\\
&\tilde{x} = p(t);\ \tilde{x}^1 = p(0),\ \tilde{x}^2 = p(1);\ 0 \le t \le 1 && (2b)\\
&f(\tilde{x}) \le \text{Max}\{f(\tilde{x}^1),\ f(\tilde{x}^2)\} && (2c)
\end{aligned} \qquad (2)$$

In relations (2), $\tilde{x}$ is a position vector showing any feasible point in solution space S (2a), and p(t) is an arbitrary path between any two feasible points such as $\tilde{x}^1$ and $\tilde{x}^2$ (2b). f(x) is said to be a connected function in S provided that there exists a path p(t) between $\tilde{x}^1$ and $\tilde{x}^2$ on which the function value $f(\tilde{x})$ is less than or equal to the higher of the function values at either end of the path (2c).

In order to put the connected functions into perspective the following comparisons will be made[6]: In relation (2b), if p(t) is asked to be a linear path then relations (2) define a quasi-convex function f(x) in S. In addition to this, in relation (2c), if $f(\tilde{x})$ is asked to be less than or equal to the linear combination of $f(\tilde{x}^1)$ and $f(\tilde{x}^2)$ then relations (2) define a convex function f(x) in S.

In relations (2), if function f(x) is to be minimized in solution domain S then it is referred to as a connected minimization problem and it posseses a unique optimum[6].

Uniqueness of the Optimum

The least-weight izo-static elastic truss formulated in relations (1) can be shown to be a connected minimization problem as defined in relations (2). In order to show this a linear path p(t) is proposed in the member stress and the nodal displacement sub-space. Due to this linearity and also to the linearity of constraints (1c, 1f, 1g) the proposed path remains feasible between any two solution points in the related sub-domain.

A_j can be defined by re-arranging constraints (1d):

$$A_j = F_{jk}/\sigma_{jk} \qquad j=1,\ldots,m;\ k=1,\ldots,q \tag{3}$$

In these relations F_{jk} are the member forces, which are constants, and can be determined from equations (1b).

Let $(\tilde{A}^1, \tilde{\sigma}^1_k)$ and $(\tilde{A}^2, \tilde{\sigma}^2_k)$ indicate the values of the variables at two arbitrary feasible solutions of the problem. The variables at these points must satisfy relations (3), so by re-arranging them the followings are obtained:

$$\left.\begin{aligned}\sigma^1_{jk} &= F_{jk}/A^1_j \\ \sigma^2_{jk} &= F_{jk}/A^2_j\end{aligned}\right| \quad j=1,\ldots,m;\ k=1,\ldots,q \tag{4}$$

On the proposed path the following relations hold for σ_{jk} variables since it is a linear path in the member stress sub-space.

$$\left.\begin{aligned}&\sigma_{jk} = \lambda\sigma^2_{jk} + (1-\lambda)\,\sigma^1_{jk} \qquad j=1,\ldots,m;\ k=1,\ldots,q \\ &0 \le \lambda \le 1\end{aligned}\right| \tag{5}$$

The following relations are obtained after substituting σ^1_{jk} and σ^2_{jk} of the above equations by those of equations (4):

$$\sigma_{jk} = (\lambda F_{jk}/A^2_j) + (1-\lambda)\,F_{jk}/A^1_j \quad j=1,\ldots,m;\ k=1,\ldots,q \tag{6}$$

If σ_{jk} in equations (3) are substituted by those of equations (6) then the followings are obtained:

$$A_j = 1/\{(\lambda/A^2_j) + (1-\lambda)/A^1_j\} \qquad j=1,\ldots,m \tag{7}$$

The above non-linear relations define the proposed path in the member cross-sectional area sub-space. To prove that it remains feasible in the relevant sub-domain, it is sufficient to show that A_j defined in relations (7) satisfy constraints (1e). In order to show this, the following relations will be first proved to hold for A_j:

$$A_j \le \lambda A^2_j + (1-\lambda)A^1_j \qquad j=1,\ldots,m \tag{8}$$

Substituting the above A_j values by those of (7) and re-arranging relations (8) give the following inequalities:

$$0 \le \lambda(1-\lambda)(A^1_j - A^2_j)^2/A^1_jA^2_j \qquad j=1,\ldots,m \tag{9}$$

The above relations hold since all the terms at the right-hand side of the inequalities are positive. Therefore the inequalities in relations (8) hold. It can be deduced from relations (8) that A_j are bounded by A^1_j and A^2_j. This naturally means that they are also bounded by A^ℓ_j and A^u_j. Thus, A_j defined in relations (7) satisfy constraints (1e) and therefore the proposed non-linear path remains feasible in the relevant sub-domain.

Hence, the proposed path is shown to be feasible

in the solution domain defined by the constraints of the minimization problem (1). To complete the proof that it is a connected minimization problem, the objective function (1a) must be shown to satisfy relation (2c).

Inequalities (8) will be used in showing the objective function (1a) satisfying (2c). Multiplying relations (8) by $\rho_j L_j$ and adding them on j, the following expression is obtained in terms of the member weights:

$$\sum_{j=1}^{m} w_j \leq \lambda \sum_{j=1}^{m} w_j^2 + (1-\lambda) \sum_{j=1}^{m} w_j^1 \qquad (10)$$

The above expression can be also written in terms of the total truss weights:

$$W \leq \lambda W^1 + (1-\lambda) W^2 \qquad (11)$$

From inequality (11) it is apparent that on the proposed path the total weight of the truss is less than or equal to the linear combination of the total weights at both ends of the path. This also means that the total weight on the path is less than or equal to the higher of the total weights at either end of the path:

$$W \leq \text{Max}\{W^1, W^2\} \qquad (12)$$

Thus, the objective function of the minimization problem outlined in formulation (1) is shown to satisfy relation (2c). This completes the connectedness proof of the problem.

The least-weight izo-static elastic truss of formulation (1) is shown to satisfy relations (2). Hence, it is a connected minimization problem and therefore it posseses a unique optimum.

Discussion

The available Mathematical Programming methods used in solving the non-linear optimization problems basically apply the Kuhn-Tucker optimization test. It is a first-order test which is a sufficient condition for the optimum[7], and therefore the global optimum is not guaranteed. Due to this fact, it is very important to show the uniqueness of the optimum of a problem. The uniqueness can be shown by proving the problem being connected or being special form of connected, such as convex, quasi-convex, pseudo-convex[6].

In this paper the uniqueness of the optimum of the least-weight izo-static elastic truss is proved by the connectedness criterion. Connectedness is the necessary and the sufficient condition for the unique optimum, therefore it is the most general criterion. This general criterion may also be applied to the hyper-static elastic trusses so that the global optimum of these Combinatorial Non-linear Programming Problems may be identified[2]. Identifying the global optimum constitutes one of the most important theoretical aspects of the truss optimization.

Although the least-weight izo-static elastic truss posseses a unique optimum, some Mathematical Programming methods may find difficulties in reaching the optimum. This may be due to their suitability to the convex problems rather than the non-convex problems.

If the nodal displacement constraints are not present then the least-weight izo-static elastic truss becomes a trivial Linear Programming Problem, hence the uniqueness of the optimum is apparent for this case. However, the conventional methods rather than the Linear Programming methods should be used in solving these problems.

Acknowledgement. The author would like to express sincere thanks to Dr.E.Yarımer of University College London for his instructive suggestions during the early stages of this research.

References:

[1] Schmit,L.A., "Structural design by systematic synthesis", Proc.2nd. National Conference on Electronic Computation, Struct.Div.ASCE, Pittsburgh, Pa., pp.105-132, 1960.
[2] Bayer,M., Bilinear Formulations in Structural Optimization, Ph.D.Thesis. Univ.of London, March 1978.
[3] Lasdon,L.S., Optimization Theory for Large Systems, The Macmillan Company, 1970.
[4] Toakley,A.R., "The Optimum design of triangulated frameworks", Int.J.Mech.Sci., Vol.10, pp.115-122, 1968.
[5] Kunzi,H.P., Tzschach,H.G. and Zehnder,C.A., Numerical Methods of Mathematical Optimization, Academic Press, 1971.
[6] Ortega,J.M. and Rheinboldt,W.C., Iterative Solutions of Nonlinear Equations in Several Variables, Academic Press, 1970.
[7] Bazaraa,M.S. and Shetty,C.M., Lecture Notes in Economics and Mathematical Systems, Vol.122, Foundations of Optimization, Springer-Verlag, 1976.

SESSION #7

LINEARIZATION AND CONDENSATION METHODS

AD-P000 061

PARAMETERIZATION IN FINITE ELEMENT ANALYSIS

B. P. Wang and W. D. Pilkey

Department of Mechanical and Aerospace Engineering
University of Virginia
Charlottesville, Virginia 22901

Summary

Techniques are developed for expressing structural response of a finite element model as a function of design parameters. Analytical formulations are derived for the displacement response as well as for the rate of change of the response with respect to the design parameter values of an updated design. A 10 member truss system is used to illustrate the computations required by these formulations.

Introduction

In optimal structural design, the goal is usually to find the value of a set of design parameters such that the structure is optimized in some sense while satisfying prescribed constraints. The analysis for the structural response needed in forming objective functions or constraints is often handled by the finite element method (1). In this paper, methods of expressing the response as a function of design parameters are developed for linear finite element models. In particular, the following three topics will be discussed:

(1) Expression of the displacement response as an explicit function of the design parameters and of a set of reduced active degrees of freedom (dof).

(2) Computation of derivatives of responses as a function of design parameters.

(3) Expression of displacement responses as explicit functions of a single design parameter.

The computation of response derivatives is a straightforward procedure if the derivatives are taken at the original trial design(2). If the derivatives at the updated design state are desired, it would appear that the updated system has to be solved. In this paper, the derivative calculation is based on a reanalysis formulation and permits the computation of the derivative at any updated design state without the need to resolve the updated system. This is achieved using an exact reanalysis formulation (3,4) to express the responses as explicit bilinear functions of the design parameter and the unknown response of a set of active dof. These active dof are defined as those that are physically contained in the modified portion of the structure. This approach will simplify an optimal structural design computation which employs an integrated formulation (1,5) in which the design and analysis problem are solved simultaneously. This simplification results from the analysis equations being replaced by a system of bilinear equations with a reduced number of unknowns. It is shown that once the required information for exact reanalysis is established, the computation of derivatives at an updated design can be accomplished with little effort. The availability of these derivatives permits an optimal design using, for example, a first order Taylor expansion (1) to linearize the system to be carried out efficiently.

When the design modification involves only a single parameter, the displacement responses can be expressed as explicit functions of the design parameter. This will facilitate a parametric study in a design analysis. The explicit functional relationship can be found by various techniques, including explicit matrix inversion for a case with less than 3 active dof, the use of Leverrier's algorithm, or the use of a spectral expansion technique.

The general formulation for expressing responses as functions of design parameters is developed in the following section. A truss example is given. The derivative formations are presented in the next section. The same truss is employed to illustrate the use of the derivatives. In the final section, various techniques of expressing a response as an explicit function of a single design parameter are presented. A frame example is provided.

Static Response as a Function of the Design Parameters

When doing structural designing, such as for a spacecraft structure, a preliminary design is usually chosen based on previous experience with similar structures. We will suppose that such a preliminary design exists. Furthermore, let us assume the structure is modeled by finite element methods so that the static behavior of the structure is governed by the following system of linear equations

$$[K_o](U_o) = (P) \qquad (1)$$

where

$[K_o]$ = system stiffness matrix, nxn

(U_o) = system displacement vector, nx1

(P) = system loading vector, nx1

n = number of dof of the discretized structure

The upper case quantities are referred to as the global coordinates. In practical design situations, there may be more than one loading vector to be considered. Here, to illustrate the formulation, we will assume that there is only one loading vector.

This preliminary design, more often than not, will not meet all the design specifications. Thus, the designer normally chooses to modify the design in order to achieve a feasible design. In theory, optimal design procedures can be applied to resize all of the members of the system to achieve an optimal design. In practice, however, this approach is usually avoided due to the computational difficulty of solving a large-order, nonlinear, programming problem. Rather, the designer usually modifies the structure locally to improve its performance. This approach has a minimum impact on the project schedule due to design changes and would make maximum use of

structural components that have been proved in other projects.

Let us assume that the designer chooses to modify the system locally and uses m design parameters to characterize the design modifications. The new finite element equation of motion would appear as

$$[K_o + \Delta K]\{U\} = \{P\} \qquad (2)$$

where

$\{U\}$ = displacement vector of the modified system. nx1

$[\Delta K]$ = contribution to the global stiffness matrix due to design modifications.

It should be noted that in applying Eq. (2), we are making the assumption that the loading vector is independent of design modifications. The case wherein $\{P\}$ is a function of the design parameters can be handled in a similar fashion. This will be discussed in the next subsection.

We proceed by condensing the system of equations. Let

$[\Delta K_i(\alpha_i)]$ = contribution to the global stiffness matrix due to design parameters α_i. nxn

$\{\hat{U}_{oi}\}, \{\hat{U}_i\}$ = displacement vectors of dof that are connected to the portion of structure defined by parameter c_i x1

= active dof associated with parameters α_i

c_i = number of active dof associated with parameters α_i.

Normally, $[\Delta K_i(\alpha_i)]$ is a linear function of the design parameter α_i. For this case,

$$[\Delta K_i(\alpha_i)] = \alpha_i[\Delta K_i^*] \qquad (3)$$

where

$[\Delta K_i^*] = [\Delta K_i]$ with $\alpha_i = 1.0$. Thus by definition

$$[\Delta K] = \sum_{i=1}^{m} [\Delta K_i] = \sum_{i=1}^{m} \alpha_i [\Delta K_i^*] \qquad (4)$$

Futhermore, define

$[\overline{\Delta K_i}]$ = condensed global stiffness matrix associated with parameter α_i. c_i x c_i

= $[\Delta K_i]$ with all rows and columns containing only zeros deleted

Similarly,

$$[\overline{\Delta K_i}] = \alpha_i [\overline{\Delta K_i^*}] \qquad (5)$$

in which

$[\overline{\Delta K_i^*}] = [\overline{\Delta K_i}]$ with $\alpha_i = 1.0$

Note that

$$\{\hat{U}_i\} = [B_i]\{U\} \qquad (6)$$

and

$$[\Delta K_i] = [B_i]^T [\overline{\Delta K_i}][B_i] \qquad (7)$$

$$[\Delta K_i^*] = [B_i]^T [\overline{\Delta K_i^*}][B_i] \qquad (8)$$

where

$[B_i]$ = Boolean matrix. c_i xn

Substituting Eq. (4) into Eq. (2) and rearranging

$$[K_o]\{U\} = \{P\} - \sum_{i=1}^{m} \alpha_i [\Delta K_i^*]\{V\} \qquad (9)$$

or

$$\{U\} = [K_o]^{-1}\{P\} - \sum_{i=1}^{m} \alpha_i [K_o]^{-1}[\Delta K_i^*]\{V\} \qquad (10)$$

Examine the term $[K_o]^{-1}[\Delta K_i^*]\{U\}$. From Eqs. (6) and (8)

$$[K_o]^{-1}[\Delta K_i^*]\{U\}$$

$$= [K_o]^{-1}[B_i]^T [\overline{\Delta K^*}][B_i]\{U\}$$

$$= [K_o]^{-1}[B_i]^T [\overline{\Delta K^*}]\{\hat{U}_i\} \qquad (11)$$

Define

$$[D_i] = [B_i]^T [\overline{\Delta K_i^*}]$$

$$= n \times c_i \text{ pseudoload matrix} \qquad (12)$$

$$[Y_i] = [K_o]^{-1}[D_i]. \; n \times c_i \qquad (13)$$

Also, note that

$$[K_o]^{-1}\{P\} = \{U_o\} \qquad (14)$$

Equations (11) - (14) permit Eq. (10) to be written as

$$\{U\} = \{U_o\} - \sum_{i=1}^{m} \alpha_i [Y_i]\{\hat{U}_i\} \qquad (15)$$

Equation (15) is a relationship between the modified system responses, the original system responses $\{U_o\}$, the design parameters and the response of the active dof associated with all of the design parameters.

Let t be the total number of active dof. Then

$$t \leq \sum_{i=1}^{m} c_i \qquad (16)$$

The inequality is needed because some dof may be active dof for several design parameters. Based on Eq. (15), optimal design using the integrated approach will involve (t+m) variables as compared with (n+m) variables when Eq. (2) is used. When $t << n$, this may lead to considerable computational efficiency. Furthermore, Eq. (15) is bilinear in the unknowns $\alpha_1, \alpha_2, \ldots \alpha_m$ and $\{\hat{U}\}$, where

$$\{\hat{U}\} = \{\hat{U}\}_{(1)} \quad u\{U\}_{(2)} \cdots u\{U\}_{(m)} \qquad (17)$$

Equation (15) can be further reduced for the purpose of reanalysis. Define

$$\{\hat{U}_i\} = [b_i]\{\hat{U}\} \qquad (18)$$

where $[b_i] = c_i \times t$ Boolean matrix. Then, Eq. (15) can be written as

$$\{U\} = \{U_o\} - [W]\{\hat{U}\} \qquad (19a)$$

where

$$[W] = \sum_{i=1}^{m} \alpha_i \; [Y_i][b_i] \qquad (19b)$$

Define another Boolean matrix [E], txn, such that

$$\{\hat{U}\} = [E]\{U\} \qquad (20)$$

Premultiply Eq. (19a) by [E]

$$\{\hat{U}\} = \{\hat{U}_o\} - [\hat{W}]\{\hat{U}\} \qquad (21)$$

or

$$\{\hat{U}\} = ([I] + [\hat{W}])^{-1}\{\hat{U}_o\} \qquad (22)$$

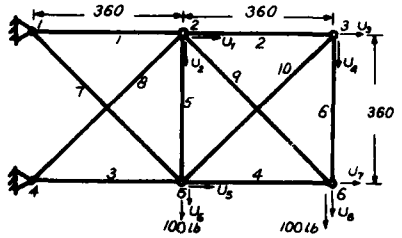
where

$$[\hat{W}] = [E][W] = \sum_{i=1}^{m} \alpha_i \; [E][Y_i][b_i] \qquad (23)$$

Note that, in practice, the various Boolean matrices need not be defined and the product involving Boolean matrices involves the selection of the proper rows and columns as when assembling the global stiffness matrix in a finite element analysis. For a given set of parameter values, Eq. (21) can be used to compute $\{\hat{U}\}$ and then Eq. (19a) provides $\{U\}$. Thus, the desired reanalysis is carried out. Equation (21) will be used to derive the derivative of responses as functions of the design variables.

Example 1

The 10-member truss system shown in Fig. 1 will be used to illustrate the above formulation.



$E = 10^7$ psi

Original Design: $A = 1.0$ in^2 for all members

Fig. 1 Ten Member Truss

Suppose the cross-sectional areas of member 5 and 8 are to be modifed. As shown, the system has 8 dofs.

For this system, the active dof for member 5 is $\{\hat{U}_{(1)}\} = [U_3 \; U_4]^T$, while $\{\hat{U}_{(2)}\} = [U_1 \; U_2]^T$ are the active dof associated with member 8. Thus, $c_1 = 2$ and $c_2 = 2$. Then $\{\hat{U}\} = \{\hat{U}_{(1)}\}U\{U_{(2)}\} = [U_1 \; U_2 \; U_3 \; U_4]^T$ and $t = 3$. Also, it can be readily identified that

$$[B_1] = \begin{bmatrix} 0 & 1 & 0 & 0 & 0 & 0 & 0 & 0 \\ 0 & 0 & 0 & 0 & 0 & 1 & 0 & 0 \end{bmatrix}$$

$$[B_2] = \begin{bmatrix} 1 & 0 & 0 & 0 & 0 & 0 & 0 & 0 \\ 0 & 1 & 0 & 0 & 0 & 0 & 0 & 0 \end{bmatrix}$$

$$[b_1] = \begin{bmatrix} 0 & 0 & 0 \\ 0 & 1 & 0 \\ 0 & 0 & 1 \end{bmatrix}$$

$$[b_2] = \begin{bmatrix} 1 & 0 & 0 \\ 0 & 1 & 0 \end{bmatrix}$$

$$[E] = \begin{bmatrix} 1 & 0 & 0 & 0 & 0 & 0 & 0 & 0 \\ 0 & 1 & 0 & 0 & 0 & 0 & 0 & 0 \\ 0 & 0 & 0 & 0 & 0 & 1 & 0 & 0 \end{bmatrix}$$

For the loading conditions shown, the solution of the original system is:

$$\{U_o\} = \begin{Bmatrix} 0.007033 \\ 0.016744 \\ 0.008477 \\ 0.037951 \\ -0.007367 \\ 0.018021 \\ -0.009522 \\ 0.039396 \end{Bmatrix}$$

Furthermore,

$$[\overline{\Delta K}^*_{(1)}] = \begin{bmatrix} a & -a \\ -a & a \end{bmatrix}$$

in which $a = 27777.78$ and

$$[\overline{\Delta K}^*_{(2)}] = \begin{bmatrix} b & -b \\ -b & b \end{bmatrix}$$

with $b = 9820.828$. Then $[Y_{(1)}]$ and $[Y_{(2)}]$ can be computed from (13). The results are

$$[Y_1] = [\{y\} - \{y\}]$$

$$[Y_2] = [\{z\} - \{z\}]$$

where

$$\{y\} = \begin{Bmatrix} 0.104807 \\ 0.401246 \\ 0.197507 \\ -0.463501 \\ 0.104807 \\ -0.401246 \\ 0.197597 \\ 0.0463501 \end{Bmatrix} \qquad \{z\} = \begin{Bmatrix} 0.116914 \\ -0.552404 \\ 0.104807 \\ -0.493947 \\ 0.116914 \\ -0.447569 \\ -0.104807 \\ -0.506053 \end{Bmatrix}$$

Equation (15) can be expressed as

$$\{U\} = \{U_o\} - \alpha_1[\{y\} \; \sim \; \{y\}]\begin{Bmatrix} U_1 \\ U_6 \end{Bmatrix}$$

$$- \alpha_2[\{z\} \; \sim \; \{z\}]\begin{Bmatrix} U_1 \\ U_2 \end{Bmatrix}$$

or

$$\{U\} = \{U_o\} + \left[-\alpha_2\{z\} \,\vdots\, (\alpha_2\{z\} - \alpha_1\{y\}) \,\vdots\, \alpha_1\{y\}\right]\begin{Bmatrix} U_1 \\ U_2 \\ U_6 \end{Bmatrix} \quad (a)$$

Equation (a) expresses the response $\{U\}$ in terms of the original responses $\{U_o\}$, the 2 design parameters α_1, α_2 and the unknown displacements at the active dof U_1, U_2 and U_6.

For given values α_1 and α_2, the first, second, and sixth equations are used to evaluate $\{\hat{U}\}^T$.

$$\{\hat{U}\}^T = [U_1 \; U_2 \; U_6]^T$$

These values are inserted in Eq. (a) to find the displacements at other dof. In Fig. 2, the displacement U_8 (y displacement at node 6) is plotted for various values of $\alpha_1 = \alpha_2 = \alpha$.

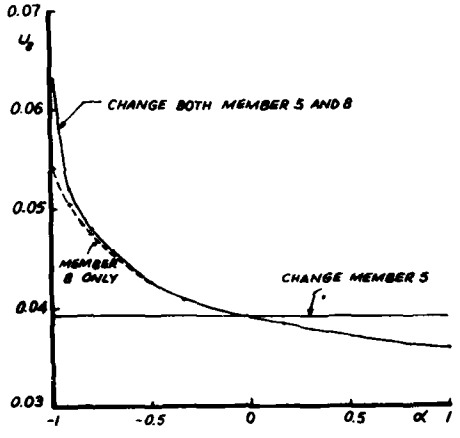


Fig. 2 Displacement U_8 as Function of Design Parameter

Example 2

For the special case of modifying only member 5 (or member 8), we can find an explicit equation for the modified system response in terms of the design parameters.

For modifying member 5 only, $\alpha_2 = 0$. Then, in Eq. (a) of the previous example, set $\alpha_1 = \alpha$ and solve for U_2 and U_6 from the second and sixth equations. Substitute the results back into Eq. (a). The results are

$$\{U\} = \{U_o\} + \frac{0.0012777\alpha_1}{1 + 0.802492\alpha}\{y\} \quad (b)$$

or

$$U_8 = 0.0393957 + \frac{5.9189\times10^{-5}\alpha_1}{1 + 0.802492\alpha_1} \quad (c)$$

Note that stiffening member 5 will increase the displacement U_8.

In order to modify member 8 only, set $\alpha_1 = 0$ and $\alpha_2 = \alpha$ in Eq. (a). Use the first two relations in Eq. (a) to solve for U_1 and U_2. Substitute the results into (a).

$$\{U\} = \{U_o\} + \frac{0.00971036\,\alpha_2}{1 + 0.669318\alpha_2}\{z\} \quad (d)$$

For the displacement at dof 8

$$U_8 = 0.0393957 - \frac{4.91396\times10^{-3}\alpha_2}{1 + 0.669318\alpha_2} \quad (e)$$

Equations (c) and (b) are also plotted in Fig. 2. It should be noticed that the stiffness of member 5 has little effect on U_8 by itself or when stiffening simultaneously with member 8. In contrast, the effects are quite noticeable when softening (reducing the cross-sectional area) simultaneously with member 8.

Rate of Change of Responses

Take the derivative of $\{U\}$ of Eq. (19a) with respect to .

$$\{U\}_{,\alpha_i} = -[W]_{,\alpha_i}\{\hat{U}\} - [W]\{\hat{U}\}_{,\alpha_i} \quad (24)$$

where $X_{,\alpha_i} = \dfrac{\partial X}{\partial \alpha_i}$.

From Eq. (19b)

$$[W]_{,\alpha_i} = [Y_i][b_i] \quad (25)$$

Thus, if $\{\hat{U}\}_{,\alpha_i}$ is known, $\{U\}_{,\alpha_i}$ can be computed using Eq. (24). From Eq. (19)

$$\{\hat{U}\}_{,\alpha_i} = -[\hat{W}]_{,\alpha_i}\{\hat{U}\} - [\hat{W}]\{\hat{U}\}_{,\alpha_i} \quad (26)$$

Thus,

$$\{\hat{U}\}_{,\alpha_i} = -([I] + [\hat{W}])^{-1}[\hat{W}]_{,\alpha_i}\{\hat{U}\} \quad (27)$$

where

$$[\hat{W}]_{,\alpha_i} = [E][Y_i][b_i] \quad (28)$$

Using Eq. (22)

$$\{\hat{U}\}_{,\alpha} = -([I] + [\hat{W}])^{-1}[\hat{W}]_{,\alpha}([I] + [\hat{W}])^{-1}\{\hat{U}_o\} \quad (29)$$

with $[\hat{W}]$ and $[\hat{W}]_{,\alpha}$ defined in Eq. (23) and (28) respectively.

Equations (29) and (24) define the derivative, or rate of change, of responses with respect to a design parameter at any design state (α_i values) in terms of the parameter values, system characterics, and original system responses.

It should be noted that the classical method of computing the response derivative (2) is a special case of the present formulation. Let $\alpha_i = 0$ for i = 1 to m in Eq. (24). Then

$$\{U\}_{,\alpha} = -[W]_{,\alpha_i}\{\hat{U}\} \quad (30)$$

From (22), we have

$$\{\hat{U}\} = \{\hat{U}_o\} \quad (31)$$

Since $[\hat{W}] = [0]$. Also $[\hat{W}]_{,\alpha_i} = -[\hat{Y}_i][b_i]$. Thus,

$$\begin{aligned}(U)_{,\alpha} &= -[Y_i][b_i](\hat{U}_o) \\ &= -[Y_i](\hat{U}_{o_i}) \qquad (32) \\ &= -[Y_i][B_i](U_o)\end{aligned}$$

Using definitions (12) and (13),

$$\begin{aligned}(U)_{,\alpha} &= -[K_o]^{-1}[B_i]^T[\overline{\Delta K}^*][B_i](U_o) \\ &= -[K_o]^{-1}[\Delta K_i^*](U_o) \qquad (33)\end{aligned}$$

Note that

$$[\Delta K_i] = \alpha[\Delta K_i^*]$$

Thus,

$$[K]_{,\alpha} = [K_o + \sum \alpha_i \Delta K_i^*]_{,\alpha_i} = [\Delta K_i^*]$$

Hence Eq. (33) is equivalent to the classical formula

$$(U)_{,\alpha} = -[K_o]^{-1}[K_o]_{,\alpha}(U_o)$$

Example 3

Return to the structure of Fig. 1. To illustrate the use of Eq. (28), the rate of change of responses with respect to the changes in the cross-sectional areas of members 5 and 8 will be calculated. For this case,

$$[W] = \alpha_1[Y_{(1)}][b_{(1)}] + \alpha_2[Y_{(2)}][b_{(2)}]$$

and

$$[\hat{W}]_{,\alpha_i} = [E][Y_{(i)}][b_{(i)}]$$

Using the data given in Example 1.

$$[\hat{W}]_{,\alpha_1} = \begin{bmatrix} 0 & 0.104807 & -0.104807 \\ 0 & 0.401246 & -0.401246 \\ 0 & 0.197507 & -0.197507 \end{bmatrix}$$

$$[\hat{W}]_{,\alpha_2} = \begin{bmatrix} 0.116914 & -0.116914 & 0 \\ -0.552404 & 0.552404 & 0 \\ -0.447296 & 0.447596 & 0 \end{bmatrix}$$

These quantities are independent of α_i. For $\alpha_1 = 1.0$, $\alpha_2 = 3.0$

$$[\hat{W}] = [E][W] = \begin{bmatrix} 0.350742 & -0.245935 & -0.104807 \\ -0.1657212 & +1.2058458 & -0.401246 \\ -1.342788 & 0.9415542 & 0.401246 \end{bmatrix}$$

With this information, Eq. (29) leads to

$$(\hat{U})_{,\alpha_1} = \begin{Bmatrix} 0.000440 \\ -0.002703 \\ -0.001683 \end{Bmatrix}$$

$$(\hat{U})_{,\alpha_2} = \begin{Bmatrix} -0.001873 \\ 0.010053 \\ 0.007172 \end{Bmatrix}$$

Explicit Functions for the Response as a Function of a Single Design Parameter

Suppose all the design parameters are equal, i.e.,

$$\alpha_1 = \alpha_2 = \ldots = \alpha_m = \alpha \qquad (34)$$

Then, Eq. (18) becomes

$$(U) = (U_o) - \alpha[\hat{W}^*](\hat{U}) \qquad (35)$$

where

$$[W^*] = \sum_{i=1}^{m}[Y_i][b_i] \qquad (36)$$

Also, Eq. (22) becomes

$$(\hat{U}) = ([I] + \alpha[\hat{W}^*])^{-1}(\hat{U}_o) \qquad (37)$$

where

$$[\hat{W}^*] = [E][W^*] \qquad (38)$$

Substitute Eq. (37) into Eq. (35)

$$(U) = (U_o) - \alpha[W^*]([I] + \alpha[\hat{W}^*])^{-1}(\hat{U}_o) \qquad (39)$$

For $t \leq 3$, the matrix inversion of Eq. (39) can be carried out explicitly. This permits (U) to be expressed as an explicit function of . For $t \geq 4$, the inversion of the the "λ-matrix" $([I] + \alpha[\hat{W}^*])$ can be accomplished by one of the following procedures.

Leverrier's Algorithm

Leverrier's algorithm (6) was developed as an analytical inverse of the matrix $(s\,I - A)$. Let $s = -1/\alpha$, or $\alpha = -1/s$. Then

$$([I] + \alpha[\hat{W}^*])^{-1} = s(sI - [\hat{W}^*])^{-1} \qquad (40)$$

Applying Leverrier's algorithm to the matrix inversion on the right hand side of Eq. (40) gives

$$([I] + \alpha[W^*])^{-1} = \frac{s^n[P_1] + s^{n-1}[P_2] + \ldots + s[P_n]}{1 + Q_1\alpha + \ldots + Q_n\alpha^n}$$

Multiplying both the numerator and denominator

$$([I] + \alpha[\hat{W}^*])^{-1} = \frac{(-1)^n[P_1] + \alpha(-1)^{n-1}[P_2] + \ldots - \alpha^{n-1}[P_n]}{(-1)^n + (-1)^{n-1}Q_1\alpha + \ldots + \alpha_n Q_n} \qquad (41)$$

where the scalars Q_i and matrices $[P_i]$ are computed using the recursive relationships

$$[P_1] = [I]$$

$$Q_1 = -\mathrm{tr}[A][P_1] \qquad (42)$$

where $[A] = [\hat{W}^*]$ and for $j = 2$ to n

$$[P_j] = [A][P_{j-1}] + Q_{j-1}[I]$$

$$Q_j = -\mathrm{tr}([A][P_j])/j \qquad (43)$$

tr = trace of a matrix

When the order of the matrix $[W^*]$ is high, Leverrier's algorithm may lose its accuracy due to excessive multiplication. In this case, spectral representation can be used.

Spectral Decomposition

In this representation,

$$(I + \alpha[\hat{W}^*])^{-1} = \sum_{i=1}^{m} \frac{\frac{1}{\alpha}\{\varphi_i\}\{\psi_i\}^T}{\frac{1}{\alpha} + \lambda_i} \qquad (44)$$

where $\{\varphi_i\}$ and $\{\psi_i\}$ are the right and left eigenvectors of $-[\hat{W}^2]$ and λ_i are the corresponding eigenvalues. The vectors $\{\varphi_i\}$ and $\{\psi_i\}$ are normalized such that

$$\{\psi_i\}^T\{\varphi_i\} = 1.0$$

Use of Eq. (41) or (44) in Eq. (39) permits the responses to be expressed as explicit functions of the design parameter α.

Example 4

To illustrate the use of Leverrier's algorithm, consider the case of a change in the cross-sectional area of member 5 only. For this problem,

$$[W^*] = [Y_{(1)}] = [\{y\} \quad -\{y\}]$$

Thus,

$$[\hat{W}^*] = [B_{(1)}][W^*] = \begin{bmatrix} a & -a \\ a & -a \end{bmatrix}$$

in which

$$a_1 = y_2 = 0.401246$$

$$a_2 = y_6 = -0.401246 = -a_1$$

Thus,

$$[\hat{W}^*] = a\begin{bmatrix} 1 & -1 \\ -1 & 1 \end{bmatrix} = [A]$$

$$[P_1] = [I] = \begin{bmatrix} 1 & 0 \\ 0 & 1 \end{bmatrix}$$

$$Q_1 = -\mathrm{tr}[A][P_1] = -2a$$

$$[P_2] = [A][P_1] + Q_1[I] = \begin{bmatrix} -a & -a \\ -a & -a \end{bmatrix}$$

$$Q_2 = -\mathrm{tr}([A][P_2])/2 = -\mathrm{tr}\begin{bmatrix} 0 & 0 \\ 0 & 0 \end{bmatrix}/2 = 0$$

Then, for n = 2, Eq. (41) becomes

$$([I] + \alpha[\hat{W}^*])^{-1} = \frac{[P_1] - \alpha[P_2]}{1 + Q_1\alpha + Q_2\alpha^2}$$

or

$$([I] + \alpha[\hat{W}^*])^{-1} = \frac{\begin{bmatrix} 1 & 0 \\ 0 & 1 \end{bmatrix} - \alpha\begin{bmatrix} -a & -a \\ -a & -a \end{bmatrix}}{1 + 2a\alpha}$$

or

$$([I] + \alpha[\hat{W}^*])^{-1} = \frac{\begin{bmatrix} 1+a\alpha & a\alpha \\ a\alpha & 1+a\alpha \end{bmatrix}}{1 + 2a\alpha}$$

$$= \frac{\begin{bmatrix} 1 + 0.401246\alpha & 0.401246\alpha \\ 0.401246\alpha & 1 + \alpha(0.401246) \end{bmatrix}}{1 + 0.802492\alpha}$$

Example 5

Continue the previous example, except use the spectral representation. The eigenvalues are $\lambda_1 = 0$ and $\lambda_2 = 2a$. The corresponding right and left eigenvectors are

$$\{\varphi_1\} = \begin{Bmatrix} 1 \\ 1 \end{Bmatrix} \qquad \{\psi_1\} = \begin{Bmatrix} 1/2 \\ 1/2 \end{Bmatrix}$$

$$\{\varphi_2\} = \begin{Bmatrix} 1 \\ -1 \end{Bmatrix} \qquad \{\psi_2\} = \begin{Bmatrix} +1/2 \\ -1/2 \end{Bmatrix}$$

Thus, Eq. (44) leads to

$$([I] + \alpha[\hat{W}^*])^{-1} = \frac{\{\varphi_1\}\{\psi_1\}^T}{1 + \alpha\lambda_1} + \frac{\{\varphi_2\}\{\psi_2\}^T}{1 + \alpha\lambda_2}$$

$$= \frac{\begin{bmatrix} 1/2 & 1/2 \\ 1/2 & 1/2 \end{bmatrix}}{1} + \frac{\begin{bmatrix} 1/2 & -1/2 \\ -1/2 & 1/2 \end{bmatrix}}{1 + 2a\alpha}$$

$$= \frac{\begin{bmatrix} 1 & 0 \\ 0 & 1 \end{bmatrix} + \begin{bmatrix} a & a \\ a & a \end{bmatrix}\alpha}{1 + 2a\alpha}$$

This is the same result as found in Example 4.

Conclusions

In this paper techniques are considered for expressing the modified response of a linear structural system as functions of the design parameters and the displacements of a reduced set of

active dof. This should be useful in the optimal design procedures utilizing local modifications. For a given number of active dof, the method becomes more effective as the order of the system increases. Furthermore, the rate of change of responses with respect to the design parameters has been derived. Such a relationship can be used effectively in the first order Taylor series expansion frequently employed in iterative optimal design. Finally, when the design involves only a single parameter, the responses can be expressed explicitly as a function of that parameter. This simplifies greatly a design trade-off study.

To fully explore the potential of these formulations, computer software should be developed. This could take the form of a postprocessor that relies on an existing analysis code to provide the information needed in the formulation. With such a program available, optimal design by local modification using the present formulation, could be further studied.

Acknowledgment

This work is supported by the Office of Naval Research.

References

1. Kirsch, U., Optimum Structural Design, McGraw-Hill, New York, 1981.

2. Noor, A.K., and Lowder, H.E., "Approximate Techniques of Structure Reanalysis," International Journal of Computers and Structures, Vol. 4, No. 4, 1974, pp. 801-812.

3. Wang, B.P., Palazzolo, A.B., and Pilkey, W.D., "Reanalysis, Modal Synthesis and Dynamic Design," Chapter 8 of State of the Art Review of Finite Element Methods, edited by A. Noor and W. Pilkey, ASME, New York, 1982.

4. Wang, B.P., and Pilkey, W.D., "Efficient Reanalysis of Modified Structures," Proceedings of the First Chautuqua on Finite Element Modeling, Schaeffer Analysis, 1980.

5. Fox, R.L., and Schmit, L.A., "Advances in the Integrated Approach to Structure Synthesis," Journal of Spacecraft and Rockets, Vol. 3, No. 6, 1966.

6. Wiberg, D.M., State Space and Linear Systems, Schaum's Outline Series, McGraw-Hill, New York, 1971.

AD-P000 062

APPLICATION OF LINEAR CONSTRAINT APPROXIMATIONS TO FRAME STRUCTURES

by

J. A. Bennett
Engineering Mechanics Department
General Motors Research Laboratories
Warren, Michigan 48090

Abstract

The use of structural approximation techniques coupled with mathematical programming methods has proved to be an efficient way to handle structural optimization problems. Approximating the constraints with first order Taylor series implies that the effectiveness of the approximation is dependent on the linearity of the active constraint over some segment of the design space. This is accomplished by choosing either a simple element, such as a truss or shear panel, or by using an intermediate design variable chosen for the particular application. Some structures such as frames do not easily lend themselves to either of these approaches. One approach to this problem is to retain the concept of linear approximations for the constraints but to accept that the move regions will be somewhat smaller than those used for a more linearized problem.

This approach has been applied to frame models of the automotive skeleton. The beams were thin-walled box and channel sections in which thickness, widths, and heights were used as design variables. It was found that approximately 20-25 finite element solutions were required to find minimum mass solutions for reasonably complex structures with approximately 500 degrees of freedom and 100 design variables with both stress and stiffness constraints. Since the majority of the analyses are required in the convergence portion of the problem, the effect of changing the move limits was minimal. However, if the move limits were too large, the process did not converge.

Introduction

The development of structural optimization as a design tool has continually emphasized the need to provide efficient ways of accomplishing minimum mass design. It was realized fairly early in this development that straightforward application of classical mathematical programming techniques required excessive computer time to be considered for large scale structural optimization problems. Therefore much of the thrust of more recent work has been to develop more efficient classes of structural optimization methods. The most common approaches are the approximation concepts (1) and the optimality criteria (2) methods. Very recently the essential similarity of these methods has been demonstrated (3,4). In essence, all of these approaches exploit the quasi-linear response behavior of many structural idealizations. This permits the effective use of linear extrapolation of the constraint behavior in the neighborhood of a known solution.

Much of the literature in the area of efficient structural optimization codes has therefore been limited to structural elements which can be fairly easily linearized in some design variable such as truss or shear elements. Significantly less experience has been developed for structures for which the linearization is not so obvious such as frame structures. Much of the existing work with frame structures has involved expressing the section properties as functions of a single design variable (5,6), typically for wide flanged I beams. It is the intention of this paper to explore the application of simple approximation techniques to more general thin-walled beam sections.

Nature of the Approximations

The general structural optimization problem is given by

$$\text{minimize } M(\vec{x})$$
$$\text{subject to } g_i(\vec{x}) \leq 0 \qquad (1)$$

where M is the mass, the g_i's are constraints on displacements, stresses frequencies, and member sizes, and $\vec{x}$ is the vector of design variables, typically member sizes.

If one uses a first-order Taylor series to express the constraints,

$$g_i(\vec{x}) = g_{io}(\vec{x}) + \sum_j \frac{\partial g_i}{\partial x_j} \Delta x_j \quad . \qquad (2)$$

It is possible to pose the problem stated in eq. (1) as a series of approximate structural optimization problems in which the constraints are evaluated using eq. (2) rather than a full structural analysis (1).

After each approximate structural optimization problem is solved, a full finite element analysis is conducted to generate the g_{io}'s and $\frac{\partial g_i}{\partial x_j}$'s for the next approximate problem. The x_i are restricted to be less than some move limits so that the design remains in the neighborhood of the initial design. Thus there is a relationship between the nonlinearity of the constraints and the appropriate values of the move limits which will allow an efficient solution.

Clearly one desirable goal is to choose as quantities to expand the constraints, variables which will linearize the constraints. For a simple truss member, for example, the displacement is given by

$$\delta = \frac{PL}{AE} \quad . \qquad (3)$$

The displacement δ is nonlinearly dependent on the obvious choice of design variable, A. However, if one makes the change of variable $\beta = \frac{1}{A}$, the constraint now becomes linearly dependent on the variable β

$$\delta = \frac{PL}{E}\beta \quad . \qquad (4)$$

Thus for a statically determinate truss problem, the displacement and stress constraints will be linear functions of the β_i's, although the mass will be a nonlinear function of the β_i's. The assumption is that for an indeterminate truss the constraint nonlinearities will be slight and fairly large move limits will be possible. Similarly, for simple plate or beam bending problems, an expansion in the inverse of the inertia term is effective for displacement constraints and in the section modulus for the stress constraints.

If one now considers frame structures, the problem becomes more complicated since the structure is now dependent on the bending as well as the axial deflections of the structure. There is probably no single quantity which will render the expansions for displacements and stresses of frame structures as close to linear as will the reciprocal area variable for trusses.

PRECEDING PAGE

In addition, the selection of a single independent variable to describe both the area and the section moment of inertia usually will imply some relationship among the section external dimensions such as has been determined for wide flanged I beams (5,6). A second approach would be to consider second order expansions; however, as the number of design variables increases, the computational burden may become excessive. A remaining option is to continue to use the linear expansions in the approximate problem with a simple but admittedly nonlinear choice of expansion variables. This will require a reduction of the move limits such that the sequence of approximate problems will converge to a minimum mass design. If the increased computational cost is not too excessive, this may be an acceptable approach.

Class of Problems Considered

The type of structures that are to be optimized are those structures which are found in an automotive structure. This structure is a complex assembly of components which are stamped sheet metal (Fig. 1).

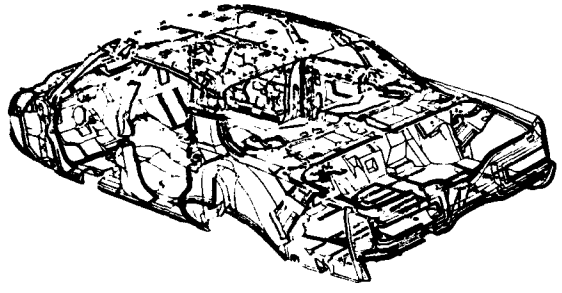


Fig. 1 Typical automotive structure

For modeling purposes these components can be represented as beam elements or plate elements. The beam elements form a skeleton frame structure which carries the major structural loads (Fig. 2). The plate elements which are integral parts of the body typically are designed by local conditions. The removable panels such as hoods, deck lids, and doors are treated as rib stiffened panels. Therefore, it is convenient to handle most panel structures on a component level optimization and to handle the beam skeleton optimization on a global level with a simple representation for the inplane stiffness of the panels (7). Therefore, the two types of models as shown in Figs. 2 and 3 arise. The structure shown in Fig. 2 is clearly a frame structure in which both bending and axial loads will occur.

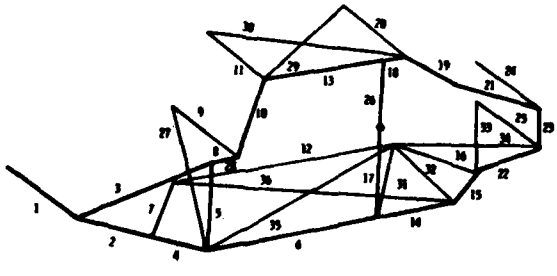


Fig. 2 Typical simplified beam model

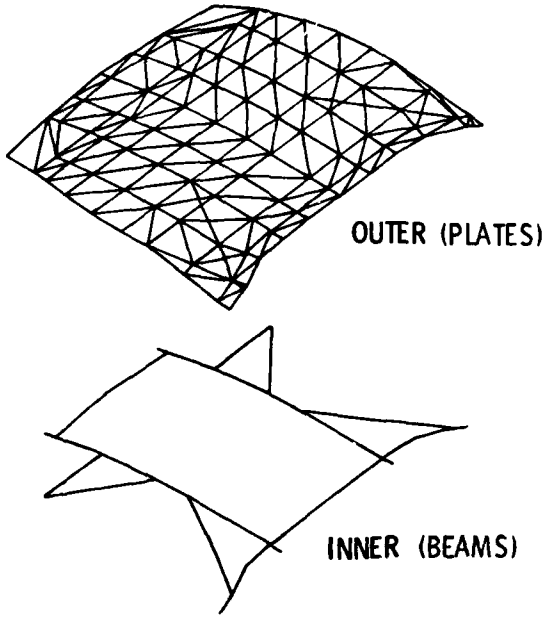


Fig. 3 Hood structure

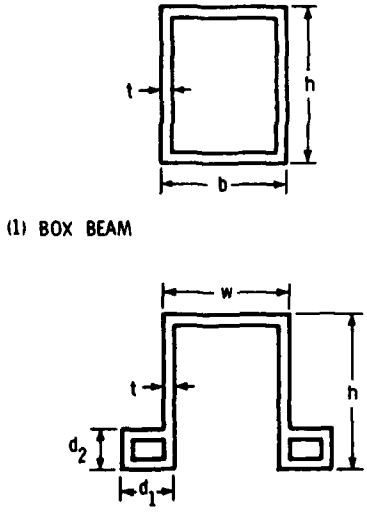


Fig. 4 Typical beam sections

The beam members in this structure are typically thin-walled beams with exterior to thickness ratios of the order of 100 to 200. During the early part of the design process, the width, height, and thickness of the beams are variable. Therefore, it is appropriate to use thin-walled rectangular sections for that part of the design process where the exterior dimensions may vary. These types of elements are shown in Fig. 4. As the design progresses, the cross sections will take a more contorted shape for manufacturing or packaging considerations. At this point thickness is the only appropriate design variable.

The structure is typically subjected to load inputs though the suspension as well as impact loads through the bumper, both of which lead to stress and displacement constraints. In addition, there are usually lower bounds on the first bending and torsional frequencies. These frequency constraints are usually stated in terms of the complete vehicle which has a significant amount of nonstructural mass. Typical load conditions and constraints are shown in Fig. 5.

SYMMETRIC BOUNDARY CONDITIONS

1. H-point beaming
   3340 N vertical at B-pillar, deflection at B-pillar less than 0.102 cm
2. Rear beaming
   1110 N vertical at rear bumper, deflection at rear bumper less than 0.645 cm
3. Front bumper
   33400 N rearward at front bumper
4. 3g bump both front wheels
   10030 N front wheel, 3800 N rear wheel
5. Rear bumper
   31200 N forward at rear bumper
6. Roof loading
   4450 N downward at top of A-pillar
7. Cowl loading
   4450 N rearward at outside edge of cowl
8. 3g bump both rear wheels
   3440 N front wheel, 11550 N rear wheel
9. 2g panic brake
   9700 N rearward, 6140 N up at front wheel
   4930 N rearward, 1180 N up at rear wheel

ASYMMETRIC BOUNDARY CONDITIONS

1. Torsional stiffness
   1110 N vertical at rear wheel, deflection at rear wheel less than 0.165 cm

COMBINED LOADING

1. 3g bump one front wheel
2. 3g bump one rear wheel

FREQUENCY CONSTRAINTS

1. Symmetric
   First mode > 16.0 hz
2. Asymmetric
   First mode > 16.0 hz

Fig. 5 Load conditions and constraints

Expansion Approach

The extensive set of constraints discussed in the previous section suggest that either one must develop an extensive set of approximations appropriate for each constraint type or try to identify a single expansion type that is reasonably robust. This latter approach was taken in the present work.

Clearly the simplest approach is to expand the constraints in terms of each of the physical design variables, x_i, or possibly their reciprocals, $\beta_i = \frac{1}{x_i}$. The reciprocal relationship is attractive based on the reciprocal nature of the relation between the stresses and the physical design variables for simple frame members. On the other hand, for a frequency constraint the physical variables would be more attractive since

$$\omega^2 \propto \frac{K}{m+m_o} \tag{5}$$

where m_o is the nonstructural mass. Since in general for the global structure $m_o >> m$, this becomes

$$\omega^2 \propto K. \tag{6}$$

Because of this difference in constraint behavior, example problems will be run with two different sets of design variables

1) $\frac{1}{t}$, b, h

2) $\frac{1}{t}$, $\frac{1}{b}$, $\frac{1}{h}$.

An alternate approach to varying all dimensions simultaneously is to note that since thin-walled beams are being used, expanding in the reciprocal of the thickness while keeping the remaining design variables fixed should lead to very high quality approximations for displacements or stresses, whereas the approximations may not be as accurate when all variables are considered. This suggests a two-step procedure in which the optimization is first run with the reciprocal thickness variable. Once an optimum to this problem is reached, the problem is restarted considering all design variables possibly with tighter move limits. This approach may be extremely attractive in the situation where the upper bounds on the exterior dimensions will be active on several of the major structural members. In this case, if the thickness only design is run with all members at their largest dimension, a design that is quite close to the final optimum will be obtained at the end of this step. In the step where all design variables are considered, the major size changes will be primarily in those members which are lightly loaded (i.e., the external sizes can decrease), and the inaccuracies in the constraint approximations will not be critical to the convergence. This will be called the combined method.

The selection of an appropriate move limit is clearly critical to the success of the approximation scheme. If the move limit is too small, an excessive number of analyses will be required, whereas too large a move limit may introduce instabilities which can preclude convergence. In addition, move limits for physical and reciprocal variables are not directly comparable. For example, if the move limit is ± a and the reciprocal variable is

$$\beta = \frac{1}{b} , \tag{7}$$

then the maximum change in b is

$$b = \frac{1}{\beta_o(1\pm a)} = b_o\left(\frac{1}{1\pm a}\right) . \tag{8}$$

Thus if a=.5 for reciprocal variables this implies a maximum 33% decrease or 100% increase in the physical variable since

$$b = b_o \frac{1}{1+.5} = b_o\ (.667)\ ,$$

$$b = b_o \left(\frac{1}{1-.5}\right) = b_o\ (2) \qquad (9)$$

whereas if physical variables are used throughout, a 50% change in both directions will result. Since dimensions more frequently decrease in an optimization process, there is some difficulty in choosing comparative move limits. The move limits of .3 and 1.0 chosen in the examples for the $\frac{1}{b}$ and $\frac{1}{h}$ expansion give decreasing limits of .23 and .5, respectively, in the physical variables, which is quite similar to the move limits of .2 and .5 which will be used in the physical variables examples.

Optimization Method

The evaluations of these various approaches were carried out using the GM structural optimization code, ODYSSEY (Optimum DYnamic and Static Structurally Efficient SYstems). This program allows both constraint approximation methods and full mathematical programming methods with exact constraint evaluation to be used as required. The design variable may be any integer power of the physical variable. A feasible directions algorithm (CONMIN (8)) is used as an optimizer in both cases. A design library of thin-walled beam elements and triangular plate bending and membrane elements is available. Multiple load conditions and multiple boundary conditions may be applied. For purposes of derivative calculations, stresses are assumed to depend only on the design variables of the local element. The displacement and frequency constraints are dependent on all design variables.

Comparative Examples

Example 1. This is a seven bar frame problem whose dimensions, loading, and constraints are shown in Fig. 6. The iteration history of an all-variable, mathematical programming optimization run is shown in Fig. 7. The iteration history is plotted in terms of function evaluations. Each function evaluation requires a finite element evaluation of all constraints. The optimum mass is 8.18 kg. At the optimum, one displacement constraint and several stress constraints are active.

Figure 8 shows the results of a t only (the actual design variable is $\frac{1}{t}$) approximate optimization with a move limit (Δ) of ±25% (.25) followed by an all-variable approximate optimization. Points identified with a dot have a maximum constraint violation of 3%, those with an open circle of between 3% and 10%, and those with a closed box are greater than 10%. The program does not force an absolutely feasible solution, so a 3% maximum violation has been taken as an acceptable design. Using the approximations usually produces a final design that is not strictly feasible but close enough for practical design considerations. The transition between the t only and the all-variable segments occurs after the flattening in the curve where the $\frac{1}{t}$ segment is converging.

Figure 8 indicates that with move limits of .1 and .2 (10% and 20%) that the optimum was obtained in 25 and 15 function evaluations, respectively, as compared with 70 for the full optimization (Fig. 4). However, for a move limit of .5, the program was unable to find a solution. This is primarily caused by the nonlinearity of the constraints in that the approximate

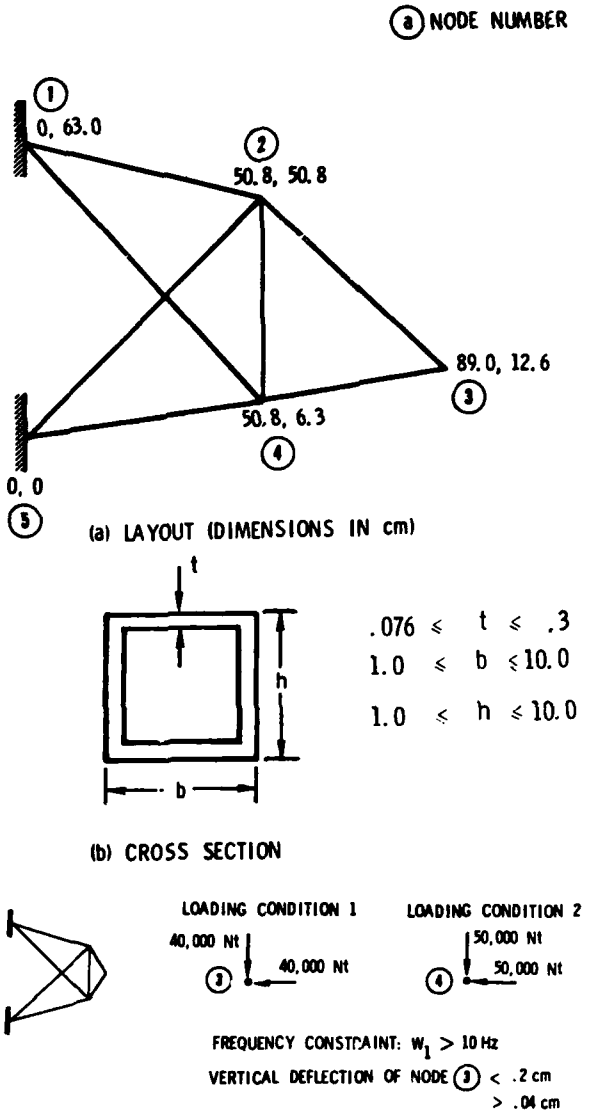


Fig. 6 7 bar frame

problem will indicate a feasible minimum has been obtained, but when the constraints are reevaluated by the full finite element analysis, they are not satisfied.

Figure 9 shows the solutions for an all-variable approximate solution throughout the optimization. The results in this case are quite similar to those of the combined optimization. Move limits of .2 proved to converge most quickly and move limits of .5 did not converge. Fifteen to twenty total function evaluations were needed to find the solution. It does appear that this approach could be slightly more efficient since the convergence process only occurs once. Figure 10 shows similar results for the $\frac{1}{t}, \frac{1}{b}, \frac{1}{h}$ combination. This choice clearly gives better approximations for the higher move limits than does the $\frac{1}{t}$, b, h expansion. However, there is a very little difference in the number of function evaluations required for convergence. Even though the move limits affect the size of the first few steps, the moves during the final convergence are quite small and

are not greatly affected by the move limits. Since the final convergence process usually required the majority of the function evaluations, there is not a significant reduction in the number of function evaluations by using the larger move limits.

The previous examples have all converged to approximately the same minimum mass in that the maximum scatter was less than 2% of the full optimization mass. Figure 11 presents a comparison of the final designs between the mathematical programming optimization and the combined optimization using b and h as design variables with Δ=.2. It is clear that the final dimensions are quite different in some cases, although the mass distributions are basically similar. These types of differences were observed in the results from all of the varying schemes and are indicative of the well known flatness in the neighborhood of the optimum of statically indeterminate problems.

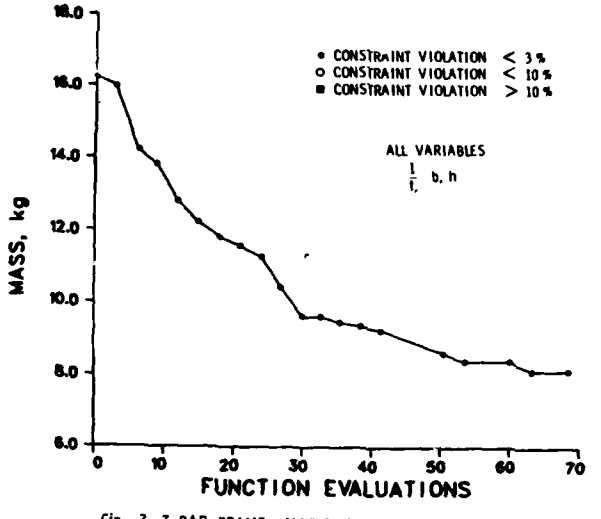


Fig. 7 7 BAR FRAME. MATHEMATICAL PROGRAMMING SOLUTION

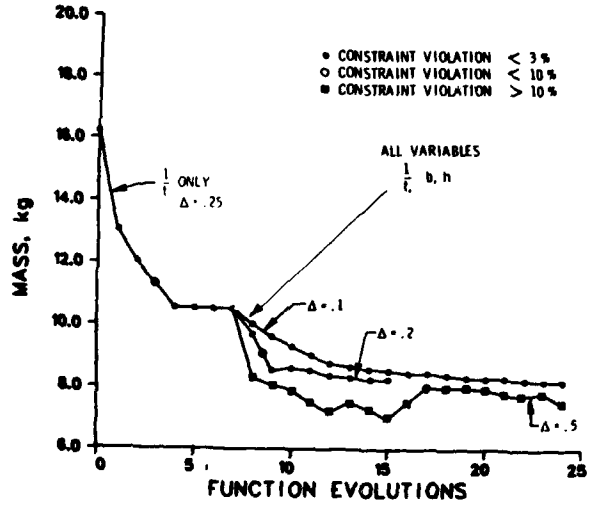


Fig. 8 7 bar frame

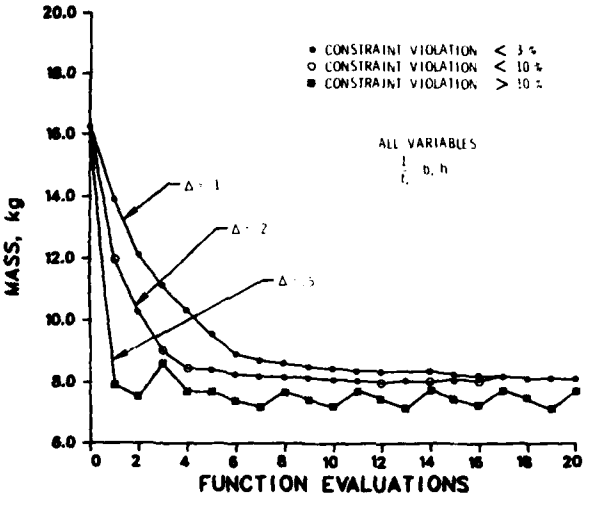


Fig. 9 7 bar frame

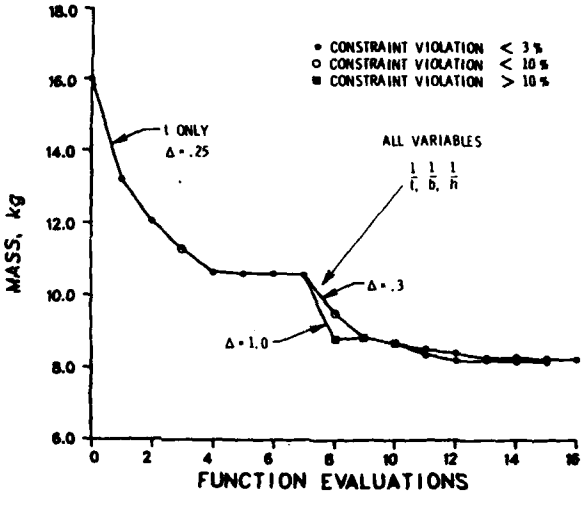


Fig. 10a 7 bar frame

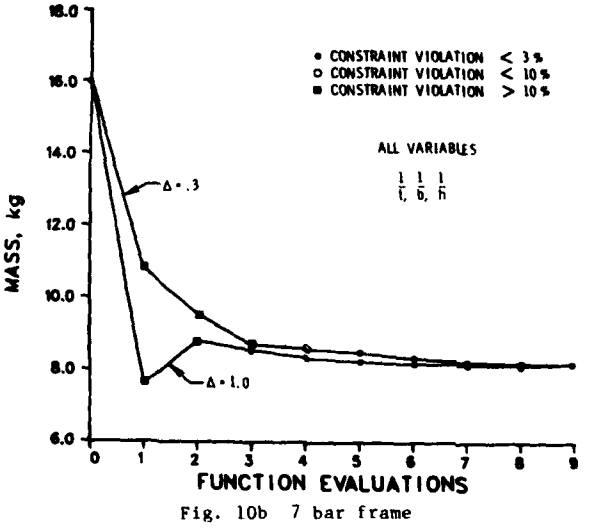


Fig. 10b 7 bar frame

Combined Optimization, 1/t, b, h (Fig. 7)

Element		Mass (kg)	t(cm)	w(cm)	h(cm)
1		1.80	.165	10.00	3.73
2		1.61	.096	10.00	10.00
3		1.17	.110	7.81	10.00
4		2.42	.201	10.00	5.49
5		.14	.076	1.50	1.32
6		.22	.076	1.28	1.28
7		.88	.076	5.31	5.13
	Total	8.25			

Mathematical Programming, 1/t, b, h(Fig. 8)

1		1.74	.205	8.39	2.42
2		1.67	.143	7.31	6.76
3		1.19	.138	7.41	7.15
4		2.09	.268	9.01	1.28
5		.12	.076	1.00	1.50
6		.17	.078	1.00	1.00
7		1.21	.095	5.83	5.74
	Total	8.18			

Fig. 11 Final optimized sizes for 7 bar frame

Example 2. This example is based on modeling the load-carrying skeleton of the automobile by beam members as shown in Fig. 2 and under the load conditions of Fig. 5. This example had 77 total design variables and 154 degrees of freedom. The all-variable, full optimization approach required 200 function evaluations and produced an optimum mass of 78 kg. Results for combined and approximate optimizations using both physical and reciprocal variables are shown in Fig. 12-12d. In general the results are similar to those for the seven bar frame except that smaller move limits were required. In addition, the combined approach appeared to converge better than the all-variable approach. Further reduction of the move limits would improve the convergence at the expense of more function evaluations. Approximately twenty function evaluations were required to obtain a minimum mass feasible solution. Although there are some convergence difficulties, these seem quite acceptable in light of the order of magnitude decrease in the number of function evaluations with the approximation methods. Currently the combined approach with move limits of .25 and .1 are routinely being used on problems of this type.

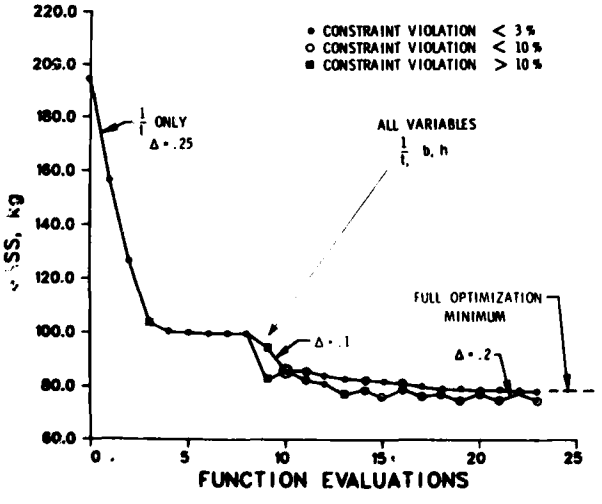


Fig. 12a 33 bar frame

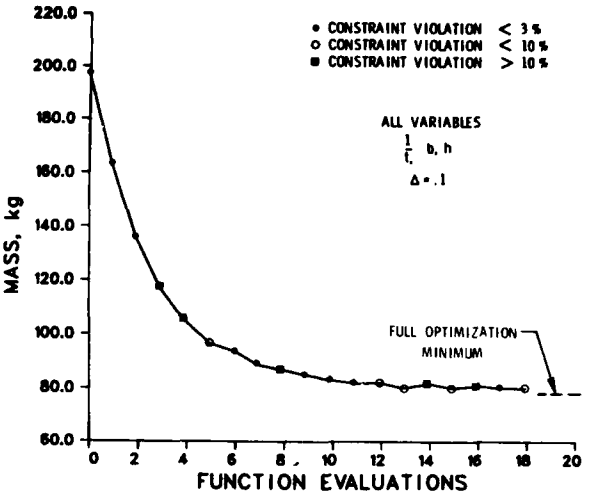


Fig. 12b 33 bar frame

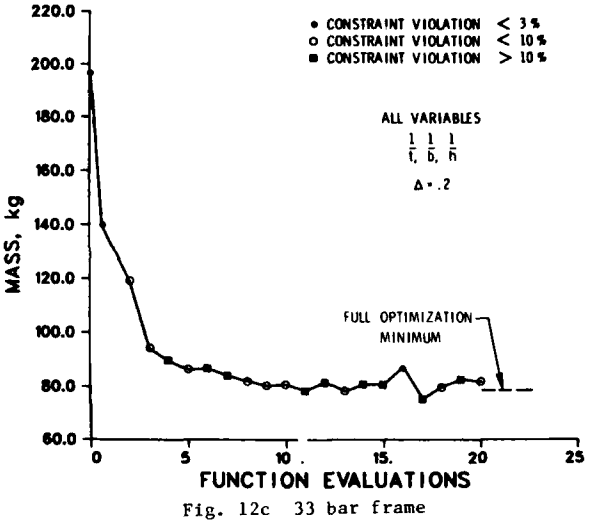


Fig. 12c 33 bar frame

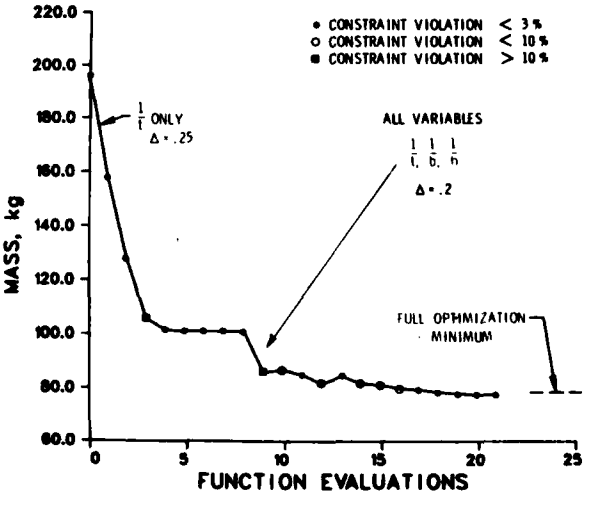


Fig. 12d 33 bar frame

Summary

It is clear that use of the approximate methods can lead to acceptable results even when the constraints being approximated cannot be strictly linearized in the design variables or some intermediate variable. Minimum mass designs are obtained for frame structures in fifteen to twenty finite element solutions, which is approximately twice the number required for more linearized problems. The number of finite element solutions required appears to be independent of the number of design variables. For a full mathematical programming approach, the number of function evaluations is known to be dependent of function evaluations. Therefore, the efficiency improvements realized from the approximation methods increased as the size of the problem increased.

The second example, a fairly realistic model of an automobile structure, clearly indicates that it is possible to obtain optimum designs using all variables necessary to describe the physical dimensions of a beam cross section. Although only one realistic automotive structural example was given, we are using these approaches routinely on problems of up to 500 degrees of freedom and 150 design variables.

Finally, while reciprocal design variables should be used for thickness types of physical variables, it does not appear to be necessary to use reciprocal design variables for the other physical variables for thin-walled sections for this general class of problems.

References

(1) L. A. Schmit and H. Miura, "An Advanced Structural Analysis/Synthesis Capability -- ACCESS-2," Int. J. for Numerical Methods in Engineering, Vol. 12, pp. 353-377, 1978.

(2) V. B. Venkayya, "Structural Optimization: A Review and Some Recommendations," Int. J. for Numerical Methods in Engineering, Vol. 13, pp. 203-228, 1978.

(3) C. Fleury, "A Unified Approach to Structural Weight Minimization," Computer Methods in Applied Mechanics and Engineering, Vol. 20, pp. 17-38, 1979.

(4) J. S. Arora, "Analysis of Optimality Criteria and Gradient Projection Methods for Optimal Structural Design," Computer Methods in Applied Mechanics and Engineering, Vol. 23, pp. 185-213, 1980.

(5) D. M. Brown and A. H.-S. Ang, "Structural Optimization by Nonlinear Programming," Journal of the Structural Division, ASCE, Vol. 92, No. ST6, pp. 319-340, 1966.

(6) M. R. Khan, "Optimality Criteria Techniques Applied to Frames Having Nonlinear Cross Section Properties," AIAA Paper No. 81-0552.

(7) H. Miuro, R. V. Lust, and J. A. Bennett, "Integrated Panel and Skeleton Automotive Structural Optimization," Proceedings of SAE 4th International Conference on Vehicle Structural Mechanics, Detroit, MI, November 1981.

(8) G. N. Vanderplaats, "CONMIN - A FORTRAN Program for Constrainted Function Minimization," NASA TM-X-62.282, August 1973.

AD-P000 063

APPROXIMATE BEHAVIOR MODELS FOR OPTIMUM STRUCTURAL DESIGN

U. Kirsch and B. Hofman
Department of Civil Engineering
Technion - Israel Institute of Technology
Haifa 32000, Israel.

Summary

Efficient reanalysis models, which provide high quality explicit approximations for the structural behavior, are introduced. The presented algorithms are based on a series expansion which is shown to be equivalent to a simple iteration procedure. To preserve efficiency, only methods which do not involve matrix inversion have been considered. Only the decomposed stiffness matrix, known from exact analysis of the initial design, is required to obtain the approximate expressions. Two approaches of accelerated convergence are proposed to improve the quality of the approximations:

a) An approach where a scalar multiplier, used for scaling of the initial design, is chosen prior to the solution as the accelerating parameter.

b) An approach where information gathered during calculations of the series coefficients is used to improve the convergence rate.

Numerical examples illustrate the efficiency and the quality of the proposed approximations. A special attention is focused on reanalyses along a line, a problem typical to many optimal design procedures. The computational effort in this case is considerably reduced, since only a single independent variable is involved.

1. Introduction

In most optimal design procedures the behavior of the structure must be evaluated many times for successive modifications in the design variables. This operation, which involves much computational effort, is one of the main obstacles in applying optimization methods to large structural systems. Reanalysis methods, intended to analyze efficiently new designs using information obtained from previous ones, can broadly be classified as [1]:

(a) Direct methods, giving exact solutions and applicable to situations where a relatively small proportion of the structure is modified (for example, only a small number of elements are changed).

(b) Iterative methods [2,3], suitable for cases of relatively small changes in the structure. The known solution of a given design is usually used as an initial value for the iterative process. Problems of slow convergence rate or even divergence may arise for large changes in the design.

(c) Approximate methods [4-8], usually based on series expansion and require less computational effort. One problem often encountered is that the accuracy of the solution may not be sufficient. Under certain assumptions, some approximate methods are shown to be equivalent to iterative procedures.

In this study reanalysis methods for optimum structural design, based on explicit approximations of the structural behavior in terms of the independent design variables, are presented. Once the explicit model has been introduced, it can be used for multiple reanalyses of designs obtained by successive changes in the variables. The presented algorithms are based on a series of expansion which is shown to be equivalent to a simple iteration procedure.

Two conflicting factors should be considered in choosing an approximate behavior model for a specific optimal design problem:
(a) The computational effort involved, or the efficiency of the method.
(b) The accuracy of the calculations, or the quality of the approximation.
To preserve the efficiency, the presentation is limited to methods which do not involve matrix inversion. Only the available decomposed stiffness matrix, known from exact analysis of the initial design, is required to obtain the explicit expressions. However, since the proposed models are based on a single exact analysis, the accuracy of the approximations might be sufficient only for a limited region.

Two approaches of accelerated convergence are proposed, to improve the quality of the approximations:

(a) An approach where a scalar multiplier, used for scaling of the initial design, is chosen prior to the solution as the accelerating parameter. Several algorithms for selecting the value of this multiplier are proposed and their merit is demonstrated.

(b) An approach where the accelerated parameters are calculated from results obtained during the solution process. Information gathered during calculation of the series coefficients is used to improve the convergence rate.

Some numerical examples illustrate applications of the proposed procedures. A special attention is focused on reanalyses along a given line in the design space, a problem common to many optimal design procedures. The efficiency and the quality of the proposed approximations are demonstrated.

2. Problem Statement

The displacement analysis equations for a given design variables vector $\{\overset{*}{X}\}$ are

$$[\overset{*}{K}]\{\overset{*}{r}\} = \{R\} \tag{1}$$

where $[\overset{*}{K}]$ = stiffness matrix corresponding to the design $\{\overset{*}{X}\}$; $\{R\}$ = load vector whose elements are assumed to be independent of the design variables; and $\{\overset{*}{r}\}$ = nodal displacements computed at $\{\overset{*}{X}\}$. The elements of the stiffness matrix $[K]$ are some functions of the design variables $\{X\}$. Assuming a change $\{\Delta\overset{*}{X}\}$ in the design variables so that the modified design is

$$\{\overset{**}{X}\} = \{\overset{*}{X}\} + \{\Delta\overset{*}{X}\} \tag{2}$$

the corresponding stiffness matrix is given by

$$[\overset{**}{K}] = [\overset{*}{K}] + [\Delta\overset{*}{K}] \tag{3}$$

where $[\Delta\overset{*}{K}]$ = the matrix of changes in the stiffness matrix due to the change $\{\Delta\overset{*}{X}\}$.

The object in this study is to present explicit models for efficient calculation of the displacements $\{\overset{**}{r}\}$

PRECEDING PAGE

corresponding to designs $\{\overset{**}{X}\}$, obtained by changing the value of the design variables. It is assumed that the displacements $\{\overset{*}{r}\}$ are known from analysis of the initial design. Also, $[\overset{*}{K}]$ is given in the decomposed form

$$[\overset{*}{K}] = [\overset{*}{U}]^T[\overset{*}{U}] \tag{4}$$

where $[\overset{*}{U}]$ is an upper triangular matrix.

Approximations along a given line in the design space are often required in optimal design procedures. This problem is common to many mathematical programming methods such as flasible directions or penalty function. A set of lines (or direction vectors) in the design space are determined successively by the optimization method used. In each of the given directions it is usually necessary to evaluate the constraint functions, or to repeat the analysis, many times. A line in the design space can be defined in terms of a single independent variable Y by

$$\{X\} = \{\overset{*}{X}\} + Y\{\Delta\overset{*}{X}\} \tag{5}$$

where $\{\overset{*}{X}\}$ is the given initial design, $\{\Delta\overset{*}{X}\}$ is a given direction vector in the design space, and the variable Y determines the step size. Approximations along a line require much less computations since only a single variable is involved.

In general, the elements of the stiffness matrix are some functions of Y. One common case is that the modified stiffness matrix can be expressed as

$$[K] = [\overset{*}{K}] + f(Y)[\Delta\overset{*}{K}] \tag{6}$$

In truss structures where $\{X\}$ are the cross-sectional areas or in beam elements where the moments of inertia are chosen as design variables, the elements of the stiffness matrix are linear functions of Y and Eq. (6) becomes

$$[K] = [\overset{*}{K}] + Y[\Delta\overset{*}{K}] \tag{7}$$

If the elements of [K] are functions of aZ_i^b (Z_i being the naturally chosen design variables and a,b are given constants) we may use the transformation

$$X_i = aZ_i^b \tag{8}$$

and obtain the linear relationship (7). The expression of Eq. (8) is suitable, for example, for standard joists [9]. In cases where such transformations are not possible (for example, in frame elements where the stiffness matrix is a function of both moments of inertia and cross-sectional areas), still linear approximations may be used for the nonlinear terms of the stiffness matrix [10].

3. Explicit Behavior Models

The analysis equations at $\{\overset{**}{X}\}$ are

$$[\overset{**}{K}]\{\overset{**}{r}\} = \{R\} \tag{9}$$

Based on Eq. (3),

$$([\overset{*}{K}] + [\Delta\overset{*}{K}])\{\overset{**}{r}\} = \{R\} \tag{10}$$

Premultiplying by $[\overset{*}{K}]^{-1}$ and substituting

$$\{\overset{*}{r}\} = [\overset{*}{K}]^{-1}\{R\} \tag{11}$$

$$[\overset{*}{B}] \equiv [\overset{*}{K}]^{-1}[\Delta\overset{*}{K}] \tag{12}$$

yields

$$([I] + [\overset{*}{B}])\{\overset{**}{r}\} = \{\overset{*}{r}\} \tag{13}$$

Premultiplying by $([I] + [\overset{*}{B}])^{-1}$ and expanding

$$([I] + [\overset{*}{B}])^{-1} = [I] - [\overset{*}{B}] + [\overset{*}{B}]^2 - [\overset{*}{B}]^3 + \ldots \tag{14}$$

Eq. (13) becomes

$$\{\overset{**}{r}\} = ([I] - [\overset{*}{B}] + [\overset{*}{B}]^2 - [\overset{*}{B}]^3 + \ldots)\{\overset{*}{r}\} \tag{15}$$

The coefficients of this series can readily be calculated. Defining

$$\{\overset{*}{r}_1\} \equiv -[\overset{*}{B}]\{\overset{*}{r}\} \tag{16}$$

$$\{\overset{*}{r}_2\} \equiv -[\overset{*}{B}]\{\overset{*}{r}_1\} \tag{17}$$

etc., the series of Eq. (15) becomes

$$\{\overset{**}{r}\} = \{\overset{*}{r}\} + \{\overset{*}{r}_1\} + \{\overset{*}{r}_2\} + \ldots \tag{18}$$

For the given triangularization of Eq. (4), the calculation of the coefficient vectors $\{\overset{*}{r}_1\},\{\overset{*}{r}_2\},\ldots$ requires only forward and back substitutions. The calculation of $\{\overset{*}{r}_1\}$, for example, is carried out as follows. Substituting Eq. (12) into Eq. (16) and rearranging gives

$$[\overset{*}{K}]\{\overset{*}{r}_1\} = -[\Delta\overset{*}{K}]\{\overset{*}{r}\} \equiv \{\overset{*}{R}_1\} \tag{19}$$

We first solve for $\{\overset{*}{P}\}$ by a forward substitution

$$[\overset{*}{U}]^T\{\overset{*}{P}\} = \{\overset{*}{R}_1\} \tag{20}$$

$\{\overset{*}{r}_1\}$ is then calculated by the backward substitution

$$[\overset{*}{U}]\{\overset{*}{r}_1\} = \{\overset{*}{P}\} \tag{21}$$

The coefficient vectors $\{\overset{*}{r}_2\},\{\overset{*}{r}_3\}$ etc., can be calculated in a similar manner.

It is instructive to note that the series of Eq. (15) is equivalent to the simple iteration procedure [7,8]

$$\{\overset{**}{r}^{(k)}\} = [I] - [\overset{*}{B}]\{\overset{**}{r}^{(k-1)}\} \tag{22}$$

where k denotes the iteration cycle and

$$\{\overset{**}{r}^{(o)}\} = \{\overset{*}{r}\} \tag{23}$$

In the case of approximations along the line defined by Eq. (5), the expression of Eq. (15) will become explicit function of $\{r\}$ in terms of Y. Assuming the relationship (6), we obtain

$$\{r\} = ([I] - f(Y)[\overset{*}{B}] + f^2(Y)[\overset{*}{B}]^2 - \ldots)\{\overset{*}{r}\} \tag{24}$$

If the linear dependence of Eq. (7) holds, this explicit expression becomes

$$\{r\} = ([I] - [\overset{*}{B}]Y + [\overset{*}{B}]^2Y^2 - [\overset{*}{B}]^3Y^3 + \ldots)\{\overset{*}{r}\} \tag{25}$$

or (see Eq. (18))

$$\{r\} = \{\overset{*}{r}\} + \{\overset{*}{r}_1\}Y + \{\overset{*}{r}_2\}Y^2 + \ldots \tag{26}$$

This equation can readily be used for multiple reanalyses along a line. Also, it can be shown that Eq. (26) and Taylor series expansion of the displacements are equivalent [7,8]. Other approximate methods can be used [7,8], however, these usually involve matrix inversion.

While the methods discussed so far are based on a single exact analysis at $\{\overset{*}{X}\}$, it should be recognized that better approximations could be obtained if results of two exact analyses (at $\{\overset{*}{X}\}$ and $\{\overset{**}{X}\}$) were considered. Assuming for example, quadratic and cubic interpolations, respectively, we find

$$\{r\} \approx \{\overset{*}{r}\} + \{\frac{\partial\overset{*}{r}}{\partial Y}\}Y + (\{\overset{**}{r}\} - \{\overset{*}{r}\} - \{\frac{\partial\overset{*}{r}}{\partial Y}\})Y^2 \tag{27}$$

$$\{r\} = \{\overset{*}{r}\} + \{\frac{\partial \overset{*}{r}}{\partial Y}\}Y + (3\{\overset{**}{r}\} - 3\{\overset{*}{r}\} - 2\{\frac{\partial \overset{*}{r}}{\partial Y}\} - \{\frac{\partial \overset{**}{r}}{\partial Y}\})Y^2 + (2\{\overset{*}{r}\} - 2\{\overset{**}{r}\} + \{\frac{\partial \overset{*}{r}}{\partial Y}\} + \{\frac{\partial \overset{**}{r}}{\partial Y}\})Y^3 \quad (28)$$

The derivatives $\{\frac{\partial r}{\partial Y}\}$ can readily be computed by several methods [1]. One possibility is to differentiate Eq. (1) with respect to Y. The result is

$$[K]\{\frac{\partial r}{\partial Y}\} = -[\frac{\partial K}{\partial Y}]\{r\} \quad (29)$$

in which both $\{r\}$, and $[K]$ in the decomposed form of Eq. (4), are known from the analysis. Thus, solution for $\{\frac{\partial r}{\partial Y}\}$ involves only calculation of the right hand side vector of Eq. (29) and forward and backward substitutions.

4. Behavior of Scaled Designs

Scaling of the initial design $\{\overset{*}{X}\}$ to obtain a modified design $\{X_\alpha\}$ is given by

$$\{X_\alpha\} = \alpha\{\overset{*}{X}\} \quad (30)$$

where α is a positive scalar multiplier. If the elements of the stiffness matrix are assumed to be linear functions of the design variables then

$$[K_\alpha] = \alpha[\overset{*}{K}] \quad (31)$$

and the displacements of the modified design are (Eq. (1))

$$\{r_\alpha\} = \frac{1}{\alpha}\{\overset{*}{r}\} \quad (32)$$

The significance of this relation is that a given design $\{\overset{*}{X}\}$ can easily be scaled by modifying α so that any desired displacement be equal to a predetermined value, an operation called scaling of the design. (The line $\alpha\{\overset{*}{X}\}$ is called a design line).

In optimal design problems it is often necessary to find the design $\{X_c\}$ along the design line $\alpha\{X\}$, with a displacement r equal to its limiting value r^u. That is (see Fig. 1)

$$\frac{1}{\alpha}\overset{**}{r} = r^u \quad (33)$$

or

$$\alpha = \frac{\overset{**}{r}}{r^u} \quad (34)$$

In cases where $\overset{**}{r}$ is calculated by an approximate behavior model (such as Eq. (15)), we may evaluate the accuracy of the displacements of the approximated design $\{\tilde{X}_c\}$ as follows. $\{\tilde{X}_c\}$ is given by

$$\{\tilde{X}_c\} = \tilde{\alpha}\{\overset{**}{X}\} \quad (35)$$

where $\tilde{\alpha}$ is determined from

$$\frac{1}{\tilde{\alpha}}\overset{\tilde{**}}{r} = r^u \quad (36)$$

or

$$\tilde{\alpha} = \frac{\overset{\tilde{**}}{r}}{r^u} \quad (37)$$

in which $\overset{\tilde{**}}{r}$ is the approximated value of $\overset{**}{r}$ at the point $\{X\}$. The approximated displacement of $\{\tilde{X}_c\}$ is $\tilde{r}(\{\tilde{X}_c\}) = r^u$ and the exact displacement at this point is (Eq. (37))

$$r(\{\tilde{X}_c\}) = \frac{1}{\tilde{\alpha}}\overset{**}{r} = \frac{\overset{**}{r}}{\overset{\tilde{**}}{r}}r^u \quad (38)$$

That is, the ratio between the approximated and the exact displacements at $\{\tilde{X}_c\}$ is

$$\frac{\tilde{r}(\{\tilde{X}_c\})}{r(\{\tilde{X}_c\})} = \frac{\overset{\tilde{**}}{r}}{\overset{**}{r}} \quad (39)$$

This result indicates that the error in the approximations at $\{\tilde{X}_c\}$ depends only on the ratio $\overset{\tilde{**}}{r}/\overset{**}{r}$ (and not on $\tilde{\alpha}$, the distance between $\{\overset{**}{X}\}$ and $\{\tilde{X}_c\}$). The combination of approximate behavior models and scaling can be used to introduce efficient optimal design procedures [10]. It will be shown in the next section how selection of the scaling multiplier α may improve the approximate behavior models.

5. Improved Approximations by Scaling

The modified design $\{\overset{**}{X}\}$ can be expressed as (see Fig. 2)

$$\{\overset{**}{X}\} = \{\overset{*}{X}\} + \{\Delta\overset{*}{X}\} = \{X_\alpha\} + \{\Delta X_\alpha\} \quad (40)$$

and the corresponding stiffness matrices are (Eq. (31))

$$[\overset{**}{K}] = [\overset{*}{K}] + [\Delta\overset{*}{K}] = [K_\alpha] + [\Delta K_\alpha] = \alpha[\overset{*}{K}] + [\Delta K_\alpha] \quad (41)$$

Substituting Eq. (41) into Eq. (9), premultiplying by $[\overset{*}{K}]^{-1}$ and rearranging yields

$$([I] + \frac{1}{\alpha}[\overset{*}{K}]^{-1}[\Delta K_\alpha])\alpha\{\overset{**}{r}\} = \{\overset{*}{r}\} \quad (42)$$

Substituting $[\Delta K_\alpha]$ from Eq. (41) into Eq. (42) gives

$$([I] + \frac{1-\alpha}{\alpha}[I] + \frac{1}{\alpha}[\overset{*}{K}]^{-1}[\Delta\overset{*}{K}])\alpha\{\overset{**}{r}\} = \{\overset{*}{r}\} \quad (43)$$

Defining

$$[B_\alpha] \equiv \frac{1-\alpha}{\alpha}[I] + \frac{1}{\alpha}[\overset{*}{K}]^{-1}[\Delta\overset{*}{K}] = \frac{1-\alpha}{\alpha}[I] + \frac{1}{\alpha}[\overset{*}{B}] \quad (44)$$

substituting into Eq. (43) and expanding $([I]+[B_\alpha])^{-1}$, we obtain the following series for $\{\overset{**}{r}\}$ in terms of α (see Eq. (15))

$$\{\overset{**}{r}\} = \frac{1}{\alpha}([I]-[B_\alpha]+[B_\alpha]^2-[B_\alpha]^3+\ldots)\{\overset{*}{r}\} \quad (45)$$

For $\alpha = 1$ we find $[B_\alpha] = [\overset{*}{B}]$ and the series of Eqs. (45) and (15) become equivalent. Different direction vectors $\{\Delta X_\alpha\}$ may be selected in the plane of $\{\overset{*}{X}\}$ and $\{\overset{**}{X}\}$ for various α values. While it is usually difficult to predict which α will provide improved convergence, some possibilities are summarized in Table 1. In cases a,b,c, the value of α is chosen so that the resulting direction $\{\Delta X_\alpha\}$ is perpendicular to $\{\overset{*}{X}\}$, $\{\overset{**}{X}\}$, and to the bisector of angle θ, respectively. The criterion in cases d,e is chosen such that the elements on the principal diagonal of $[\Delta K_\alpha]$ or the second term in the series of Eq. (45) be equal zero. In both cases the multipliers α_i are chosen separately for each displacement. Results obtained for different α values will be compared in the numerical examples of section 7.

The scaling multiplier α affects both the direction vector $\{\Delta X_\alpha\}$ and the step size $|\Delta X_\alpha|$, where (see Eqs. (30) and (40))

$$\{\Delta X_\alpha\} = \{\overset{**}{X}\} - \alpha\{\overset{*}{X}\} \quad (46)$$

The smallest step size is determined by (case a Table 1)

$$\alpha\{\overset{*}{X}\}^T\{\Delta X_\alpha\} = 0 \quad (47)$$

or, after rearranging

$$\alpha = \frac{\{\overset{*}{X}\}^T\{\overset{**}{X}\}}{\{\overset{*}{X}\}^T\{\overset{*}{X}\}} \tag{48}$$

and the corresponding step size is

$$|\Delta X_\alpha| = (|\overset{**}{X}|^2 - \alpha^2|\overset{*}{X}|^2)^{\frac{1}{2}} \tag{49}$$

Another parameter which represents the step size for a given direction is the angle θ, where

$$\cos\theta = \frac{\{\overset{*}{X}\}^T\{\overset{**}{X}\}}{|\overset{*}{X}|\ |\overset{**}{X}|} \tag{50}$$

Evidently, for any given direction $\{\Delta X_\alpha\}$ a better convergence will be obtained for smaller θ values.

It is instructive to note that a scalar multiplier β can be chosen instead of α such that (Fig.2)

$$\{X_\beta\} = \beta\{\overset{**}{X}\} \tag{51}$$

Defining

$$[B_\beta] \equiv (\beta-1)[I] + \beta[\overset{*}{B}] \tag{52}$$

we may obtain the series

$$\{\overset{**}{r}\} = \beta([I] - [B_\beta] + [B_\beta]^2 - [B_\beta]^3 + \ldots)\{\overset{*}{r}\} \tag{53}$$

Comparing Eqs. (52),(53) with Eqs. (44),(45), it can be observed that identical results would be obtained by both series if $\alpha = 1/\beta$. In this case the directions $\{\Delta X_\alpha\}$ and $\{\Delta X_\beta\}$ are parallel, and the convergence rate will be identical for any given θ.

6. Convergence Considerations

Problems of slow convergence or divergence may be encountered in applying the series of Eq. (15). The series converges if, and only if [11],

$$\lim_{k\to\infty} [\overset{*}{B}^k] = [0] \tag{54}$$

A sufficient criterion for the convergence of the series is that

$$\|\overset{*}{B}\| \leq 1 \tag{55}$$

where $\|\overset{*}{B}\|$ is the norm of $[\overset{*}{B}]$. It can be shown that

$$\rho([\overset{*}{B}]) \leq \|\overset{*}{B}\| \tag{56}$$

in which $\rho([\overset{*}{B}])$ is the spectral radius of matrix $[\overset{*}{B}]$, defined as the largest eigenvalue $|\lambda_1|$

$$\rho([\overset{*}{B}]) = |\lambda_1| = \max_i |\lambda_i| \tag{57}$$

From Eqs. (55) and (56) we have

$$\rho([\overset{*}{B}]) \leq 1 \tag{58}$$

It should be noted that the existence of a norm such that $\|\overset{*}{B}\| > 1$ does not preclude the convergence of the series.

Some procedures have been proposed to predict the eigenvalue λ_1. One possibility, based on the use of Rayleigh quotient, is [12]

$$\lambda_1 \simeq \frac{\{\overset{*}{r}_k\}^T[\overset{*}{B}]\{\overset{*}{r}_k\}}{\{\overset{*}{r}_k\}^T\{\overset{*}{r}_k\}} = -\frac{\{\overset{*}{r}_k\}^T\{\overset{*}{r}_{k+1}\}}{\{\overset{*}{r}_k\}^T\{\overset{*}{r}_k\}} \tag{59}$$

where $\{\overset{*}{r}_k\}$ are the vectors of the series (see Eq. (18)). A better estimation would be obtained for large k values.

Dynamic acceleration

In cases of slow convergence rate dynamic acceleration methods, which make use of previous terms in the series, can be employed. If the iterative process has a slow convergence rate, successive errors will generally exhibit an exponential decay in the later stages of the iteration (see Fig. 3). Aitken's δ^2 process [13] is one approach to predict the asymptotic limit to which the predictions for each displacement r_j is tending. Assume the extrapolation expression

$$\overset{**}{r}_j \simeq a + be^{-kc} \tag{60}$$

where a, b, c are constants and k is the iteration number (or number of terms in the series). The final solution ($k\to\infty$) is determined from the three successive estimates

$$\begin{aligned} r_j^{(k)} &= a + be^{-kc} \\ r_j^{(k+1)} &= a + be^{-(k+1)c} \\ r_j^{(k+2)} &= a + be^{-(k+2)c} \end{aligned} \tag{61}$$

The result is

$$\overset{**}{r}_j \simeq a = \frac{r_j^{(k)}\, r_j^{(k+2)} - (r_j^{(k+1)})^2}{r_j^{(k)} - 2r_j^{(k+1)} + r_j^{(k+2)}} \tag{62}$$

or. alternatively

$$\overset{**}{r}_j \simeq a = r_j^{(k+2)} + s_j(r_j^{(k+2)} - r_j^{(k+1)}) \tag{63}$$

where

$$s_j = \frac{r_j^{(k+1)} - r_j^{(k+2)}}{r_j^{(k)} - 2r_j^{(k+1)} + r_j^{(k+2)}} \tag{64}$$

If Aitken's acceleration is applied at the wrong time the denominator of Eq. (62) could be zero or very small. In such circumstances the method will either fail to yield a prediction or else give a predicted value which is grossly in error. The "wrong time" may be interpreted as either too soon, before an exponential decay is established, or too late when rounding errors affect the predictions.

Jennings[12] proposed a modified version of Aitken's acceleration, used by several authors [14,15]. While the prediction of Eq. (62) is calculated for each displacement r_j separately, a common acceleration parameter is introduced for all variables in the modified method. The result is

$$\{\overset{**}{r}\} \simeq \{r^{(k+2)}\} - \frac{\lambda_1}{1+\lambda_1}(\{r^{(k+2)}\} - \{r^{(k+1)}\}) \tag{65}$$

in which

$$\frac{\lambda_1}{1+\lambda_1} = \frac{(\{r^{(k)}\} - \{r^{(k+1)}\})^T(\{r^{(k+1)}\} - \{r^{(k+2)}\})}{(\{r^{(k)}\} - \{r^{(k+1)}\})^T(\{r^{(k)}\} - 2\{r^{(k+1)}\} + \{r^{(k+2)}\})} \tag{66}$$

or

$$\lambda_1 = -\frac{(\{r^{(k+2)}\} - \{r^{(k+1)}\})^T(\{r^{(k+1)}\} - \{r^{(k)}\})}{(\{r^{(k+1)}\} - \{r^{(k)}\})^2} \tag{67}$$

The convergence rate is governed by the magnitude of λ_1. This method is particularly effective when only one eigenvalue of matrix $[\overset{*}{B}]$ has modulus close to unity. It is possible to apply the acceleration after two or more iterations and to repeat the procedure frequently.

7. Numerical Examples

Ten-bar truss. The truss shown in Fig. 4 is subjected to a single loading condition (all dimensions are in kips and inches) and the initial design is $\{X\} = \{6.0\}$. The following three cases of changes in the design were solved:

Case 1: $\{\overset{*}{\Delta X}\}^T = \{4.0,4.0,4.0,4.0,6.0,6.0,$
$1.2,1.2,1.2,1.2\}$

Case 2: $\{\overset{*}{\Delta X}\}^T = \{-3.0,-3.0,-3.0,-3.0,9.0,9.0,9.0,$
$9.0,9.0,9.0\}$

Case 3: $\{\overset{*}{\Delta X}\}^T = \{18.0,18.0,18.0,18.0,18.0,18.0,$
$36.0,36.0,36.0,36.0\}$

The angles θ for the three cases (Eq. (50)) are 11.3^o, 30°, and 11.5^o, respectively.
Results obtained for cases 1,2, by Aitken's δ^2 method (Eq. (62)) and the modified acceleration method (Eq. (65)), assuming $k = 2,3,4$, are given in Table 2. While the approximations for case 1 are excellent, some errors can be observed in case 2. The iteration history for the latter case, with Aitken's δ^2 method applied after iterations 4 and 6, is shown in Figs. 5 and 6. It can be seen that no convergence of the vertical displacements could be achieved without Aitken's method. Applying scaling by the five methods of Table 1 combined with Aitken's process ($k = 2,3,4$) for case 2 may improve the convergence, as shown in Table 3. The best results have been obtained by methods b and d. The effect of α on the spectral radius (Eq. (59)) is illustrated in Fig. 7. The divergence for $\alpha=1$ is explained by the relatively large $|\lambda_1|$ value ($|\lambda_1|=1.5$). Assuming $\alpha=1.96$, the value of $|\lambda_1|$ is reduced to 0.75.

The effect of scaling on the convergence is demonstrated in case 3 (Table 4). Applying the modified acceleration method ($k=2,3,4$), no convergence could be obtained for $\alpha=1$. Assuming $\alpha=4.94$ (method c, Table 1), the convergence is fast; a solution very close to the exact one is obtained for three terms in the series. Similar results could be reached with the criterions of methods a,b in Table 1.

Forty-seven-bar truss. The truss shown in Fig. 8 was solved for the following data (all dimensions are in kips and inches):
Initial design $\{X\} = \{0.5\}$.

$\Delta\overset{*}{X}_i = 0.5$ $\quad$ $(i=1,\ldots,8)$
$\Delta\overset{*}{X}_i = 0$ $\quad$ $(i=9,10,27\text{-}30,37\text{-}40,45\text{-}47)$
$\Delta\overset{*}{X}_i = 0.2$ $\quad$ $(i=11\text{-}20,41\text{-}44)$
$\Delta\overset{*}{X}_i = 0.4$ $\quad$ $(i=21\text{-}26)$
$\Delta\overset{*}{X}_i = -0.15$ $\quad$ $(i=31\text{-}36)$

Notation of the displacements is as follows: $r_1, r_3, \ldots$ are the horizontal displacements and $r_2, r_4, \ldots$ are the vertical ones. Results obtained by Aitken's method and the modified acceleration method (in both cases $k=2,3,4$) are given in Table 5. It can be noted that despite the different order of magnitude of the various displacements, relatively small errors have been obtained. To illustrate the effect of the step size Y, the displacements r_{39}, r_{41}, r_{43} have been calculated along the line $\{X\} = \{\bar{X}\}+Y\{\overset{*}{\Delta X}\}$ for $Y = 0.25, 0.50, 0.75, 1.0$. Results obtained after four iterations ($k=4$) are shown in Fig. 9. The effect of Aitken's δ^2 method on the iteration history for $Y=1.0$ is illustrated in Fig. 10 and the evaluation of $|\lambda_1|$ is demonstrated in Fig. 11. The final value $|\lambda_1| = 0.99$ explains the slow convergence rate of the series.

8. Concluding Remarks

Approximate behavior models for efficient reanalysis have been presented. The algorithms are based on a series expansion which is equivalent to a simple iteration procedure. A single exact analysis is sufficient to introduce the series coefficients and matrix inversion is not required throughout. The proposed approximations might be sufficient only for a limited region, in the neighborhood of the initial design.
Two approaches have been proposed to improve the quality of the approximations:

a) An approach where a scalar multiplier, used for scaling of the initial design, is chosen prior to the solution as the accelerating parameter. Several algorithms for selecting the value of this multiplier are proposed and their potential for improving the series convergence is demonstrated. It is shown how the scaling multiplier affects both the direction vector in the design space and the step size.

b) An approach where the accelerated parameters are determined from results obtained during the solution process. Information gathered during calculations of the series coefficients is used to introduce extrapolation expressions. The two methods of Aitken's δ^2 process and a modified method of Aitken's acceleration are presented. It is shown how these methods provide high quality results in cases of poor convergence rate or divergence of the series.

In the typical problem of reanalyses along a given line in the design space, the methods discussed in this study involve much less computational effort. Multiple reanalyses along a line can efficiently be introduced in terms of a single independent variable.

Acknowledgement

The authors are indebted to the "Fund for the promotion of research at the Technion" for supporting this work.

References

(1) Kirsch, U., Optimum Structural Design - Concepts, Methods, Applications, McGraw-Hill, New York, 1981.

(2) Kirsch, U. and Rubinstein, M.F., Structural Reanalysis by Iteration, Computers and Structures, 2, 497-510, 1972.

(3) Phansalkar, S.R. Matrix Iterative Methods for Structural Reanalysis, Computers and Structures, 4, 779-800, 1974.

(4) Noor, A.K. and Lowder, H.E., Approximate Techniques of Structural Reanalysis, Computers and Structures, 4, 801-812, 1974.

(5) Noor, A.K. and Lowder, H.E., Structural Reanalysis Via a Mixed Method, Computers and Structures, 5, 9-12, 1975.

(6) Noor, A.K. and Lowder, H.E., Approximate Reanalysis Techniques with Substructing, Journal of the Structural Division, ASCE, 101, ST8, Paper 11523, 1687-1698, 1975.

(7) Kirsch, U., Approximate Structural Reanalysis Based on Series Expansion, to be published, Computer Methods in Applied Mechanics and Engineering, 1981.

(8) Kirsch, U., Approximate Structural Reanalysis for Optimization along a Line, to be published, International J. for Numerical Methods in Engrg. 1981.

(9) Clarkson, J., The Elastic Analysis of Flat Grillages, Cambridge University Press, 1965.

(10) Kirsch, U., Optimal Design based on Approximate Scaling, to be published, J. of the Structural Division, ASCE, 1981.

(11) Wilkinson, W., The Algebraic Eigenvalue Problem, Oxford University Press, 1965.

(12) Jennings, A., Matrix Computation for Engineers and Scientists, John Wiley & Sons, 1977.

(13) Aitken, A.C., On the Iterative Solution of a System of Linear Equations, Proc. Roy. Soc., Edinburgh, 63, 52-60, 1950.

(14) Lawther, R., Modification of Iterative Processes for Improved Convergence Characteristics, International J. for Numerical Methods in Engrg., 15, 1149-1159, 1980.

(15) Atrek, E., Note on the Modified Aitken Accelerator for use in the Residual Force Method," International J. for Numerical Methods in Engrg., 15, 1857-1872, 1980.

Table 1: Various Possibilities for the Selection of α

	Criterion for Determining α	Condition	α
a	$\{\Delta X_\alpha\}$ perpendicular to $\alpha\{\overset{*}{X}\}$	$\alpha\{\overset{*}{X}\}^T\{\Delta X_\alpha\} = 0$	$\frac{\{\overset{*}{X}\}^T\{\overset{**}{X}\}}{\{\overset{*}{X}\}^T\{\overset{*}{X}\}}$
b	$\{\Delta X_\alpha\}$ perpendicular to $\{\overset{**}{X}\}$	$\{\overset{*}{X}\}^T\{\Delta X_\alpha\} = 0$	$\frac{\{\overset{**}{X}\}^T\{\overset{**}{X}\}}{\{\overset{*}{X}\}^T\{\overset{**}{X}\}}$
c	$\{\Delta X_\alpha\}$ perpendicular to the bisector of θ	$\lvert\alpha\overset{*}{X}\rvert = \lvert\overset{**}{X}\rvert$	$(\frac{\{\overset{**}{X}\}^T\{\overset{**}{X}\}}{\{\overset{*}{X}\}^T\{\overset{*}{X}\}})^{\frac{1}{2}}$
d	$\Delta K_{ii_\alpha} = 0$	$\Delta K_{ii_\alpha} = \overset{**}{K}_{ii} - \alpha_i \overset{*}{K}_{ii} = 0$	$\alpha_i = \frac{\overset{**}{K}_{ii}}{\overset{*}{K}_{ii}}$
e	second term in the series = 0	$(1-\alpha_i)\overset{*}{r}_i + \{\overset{*}{B}_i\}^T\{\overset{*}{r}\} = 0$	$\alpha_i = 1 + \frac{\{\overset{*}{B}_i\}^T\{\overset{*}{r}\}}{\overset{*}{r}_i}$

Table 2: Results (×100), Ten-Bar Truss.

Case	Method	$\overset{**}{r}_1$	$-\overset{**}{r}_2$	$-\overset{**}{r}_3$	$-\overset{**}{r}_4$	$\overset{**}{r}_5$	$-\overset{**}{r}_6$	$-\overset{**}{r}_7$	$-\overset{**}{r}_8$
1	Eq. (62)†	0.086	0.440	0.094	0.453	0.071	0.207	0.073	0.219
	Eq. (65)†	0.086	0.439	0.094	0.453	0.071	0.207	0.073	0.220
	Exact	0.086	0.440	0.094	0.453	0.071	0.207	0.073	0.219
2	Eq. (62)†	0.290	0.813	0.310	0.824	0.237	0.284	0.243	0.294
	Eq. (65)†	0.275	0.818	0.295	0.827	0.225	0.278	0.231	0.287
	Exact	0.290	0.876	0.310	0.887	0.237	0.303	0.243	0.313

† k = 2,3,4.

Table 3: Results (×100), Ten-Bar Truss Case 2 Eq. (62)†, for Various α Values.

Case††	α	$\overset{**}{r}_1$	$-\overset{**}{r}_2$	$-\overset{**}{r}_3$	$-\overset{**}{r}_4$	$\overset{**}{r}_5$	$-\overset{**}{r}_6$	$-\overset{**}{r}_7$	$-\overset{**}{r}_8$
a	1.70	0.291	3.041	0.309	19.000	0.237	0.194	0.243	0.214
b	2.26	0.292	0.878	0.309	0.889	0.237	0.304	0.243	0.314
c	1.96	0.291	0.915	0.309	0.929	0.237	0.335	0.243	0.350
d	separate	0.290	0.877	0.310	0.887	0.237	0.303	0.243	0.313
e	separate	0.290	0.756	0.310	0.757	0.237	0.222	0.243	0.217
Exact	-	0.290	0.876	0.310	0.887	0.237	0.303	0.243	0.313

† k = 2,3,4

†† See Table 1.

Table 4: Effect of Scaling, Ten-Bar Truss, Case 3 (×100)

j	α = 1		α = 4.90		Exact Solution
	$r_j^{**(4)}$	Eq. (65)†	$r_j^{**(4)}$	Eq. (65)†	
1	9.928	-0.762	0.035	0.035	0.035
2	-155.200	-0.150	-0.137	-0.137	-0.137
3	-8.372	0.859	0.040	0.040	0.040
4	-157.600	-0.019	-0.143	-0.143	-0.143
5	7.561	-0.632	0.029	0.029	0.029
6	-94.430	-0.870	-0.056	-0.056	-0.056
7	-7.079	0.665	-0.031	-0.031	-0.031
8	-97.040	-0.756	-0.061	-0.061	-0.061

† $k = 2,3,4$

Table 5: Results 47-Bar Truss (×100)

j	r_j^*	r_j^{**}			j	r_j^*	r_j^{**}		
		Eq. (62)†	Eq. (65)†	Exact			Eq. (62)†	Eq. (65)†	Exact
5	1.34	1.31	1.31	1.31	25	3.63	4.07	4.04	4.04
6	0.32	0.24	0.24	0.24	26	-4.51	-3.82	-3.84	-3.84
7	1.56	1.49	1.49	1.49	27	3.17	3.61	3.57	3.57
8	-1.21	-1.19	-1.19	-1.19	28	-0.02	-0.78	-0.78	-0.78
9	3.87	3.50	3.50	3.50	29	0.99	2.20	2.16	2.16
10	0.14	0.08	0.08	0.08	30	-12.94	-9.84	-9.83	-9.85
11	4.04	3.73	3.72	3.73	31	0.19	1.62	1.59	1.58
12	-1.96	-1.92	-1.92	-1.92	32	5.94	3.19	3.19	3.20
13	6.33	5.79	5.79	5.79	33	-4.78	-1.64	-1.63	-1.67
14	-0.56	-0.85	-0.85	-0.86	34	-27.64	-19.78	-19.64	-19.78
15	6.74	6.39	6.38	6.39	35	-3.89	-1.15	-1.16	-1.18
16	-2.25	-2.28	-2.28	-2.28	36	12.94	-9.84	-9.83	-9.85
17	7.76	7.48	7.47	7.48	37	-3.01	-0.65	-0.68	-0.69
18	-2.26	-2.71	-2.71	-2.71	38	-4.95	-4.14	-4.15	-4.15
19	7.73	7.43	7.42	7.43	39	-2.56	-0.20	-0.24	-0.24
20	-1.48	-1.50	-1.50	-1.50	40	0.42	-0.46	-0.46	-0.46
21	6.42	6.00	5.98	5.98	41	-2.56	-0.20	-0.24	-0.24
22	-3.29	-3.21	-3.22	-3.22	42	5.94	3.19	3.19	3.20
23	6.58	6.08	6.06	6.06	43	-2.56	-0.20	-0.24	-0.24
24	-0.90	-1.21	-1.21	-1.21	44	11.45	6.84	6.84	6.85

† $k = 2,3,4.$

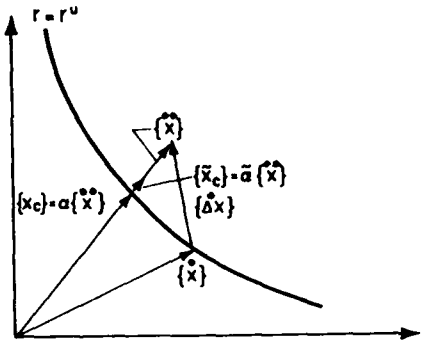


FIG. 1

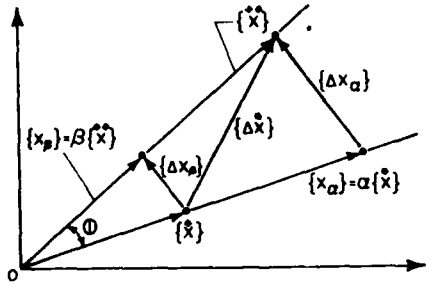


FIG. 2

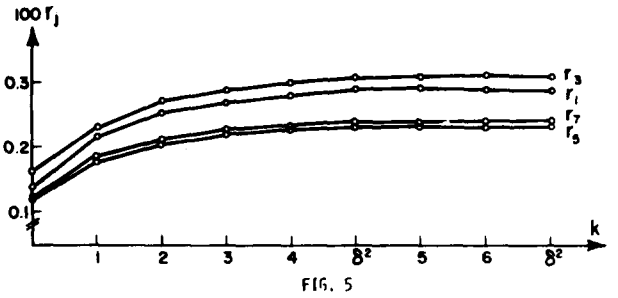


FIG. 5

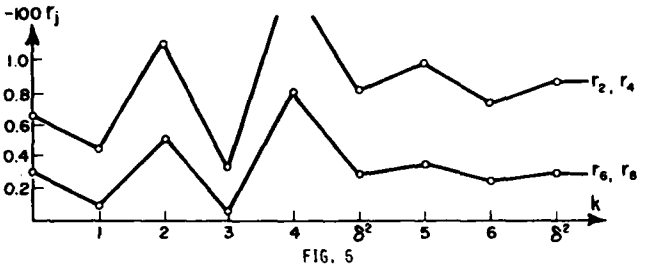


FIG. 6

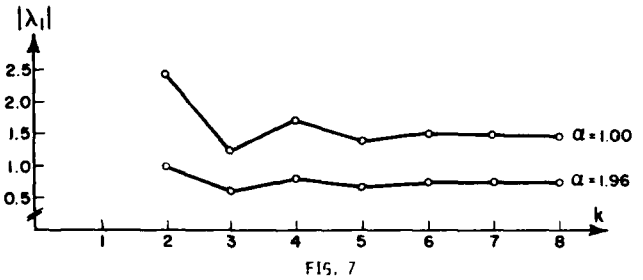


FIG. 7

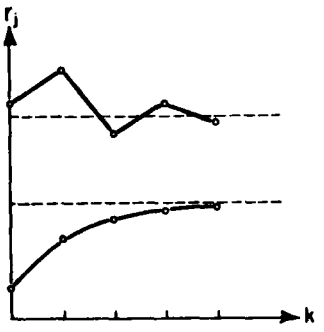


FIG. 3

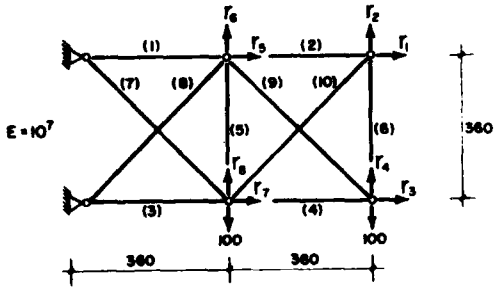


FIG. 4

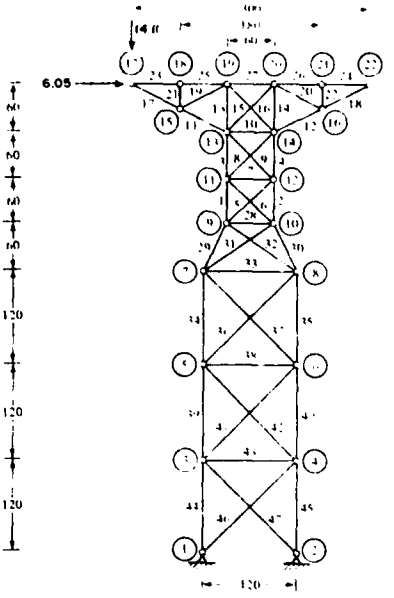


FIG. 8

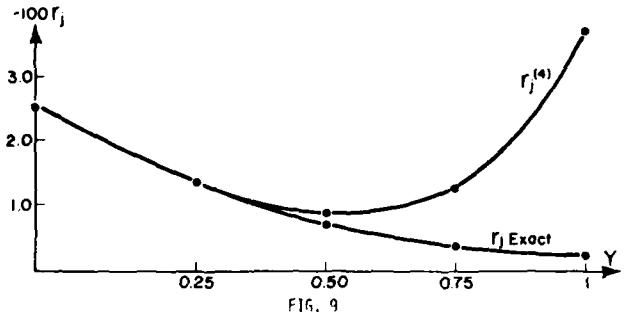


FIG. 9

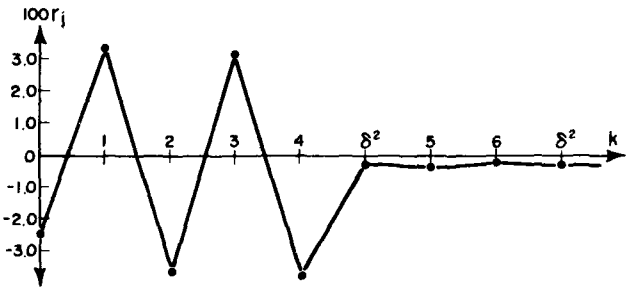


FIG. 10

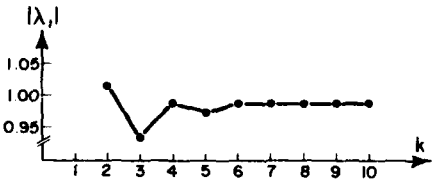
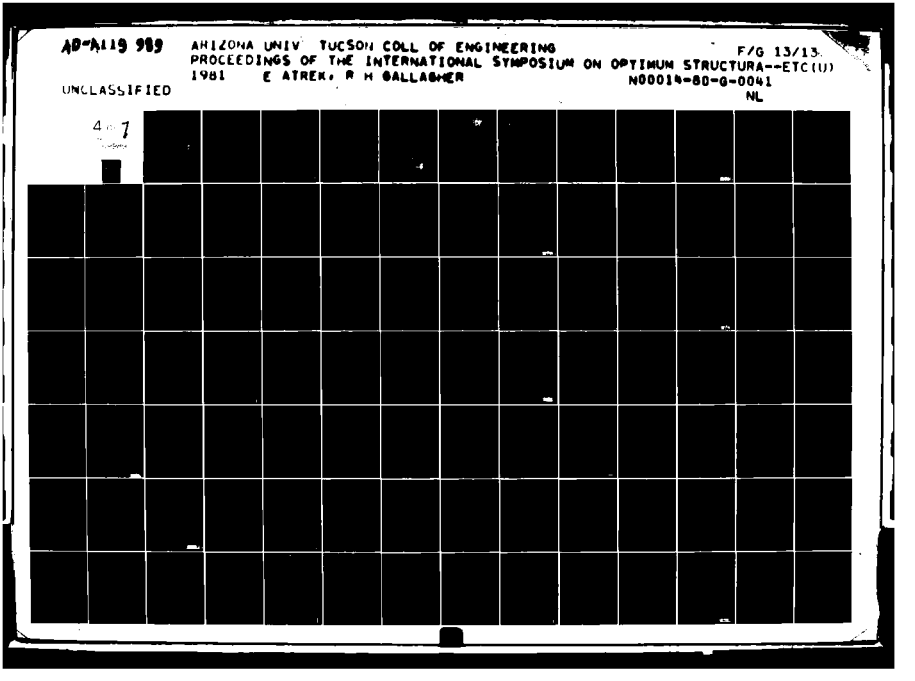


FIG. 11

AD-A119 989 ARIZONA UNIV TUCSON COLL OF ENGINEERING F/G 13/13
PROCEEDINGS OF THE INTERNATIONAL SYMPOSIUM ON OPTIMUM STRUCTURA--ETC(U)
1981 E ATREK, R H GALLAGHER N00014-80-G-0041
UNCLASSIFIED NL



AD-P000 065

WEIGHT OPTIMIZATION OF MEMBRANE STRUCTURES

Björn Esping
Linköping Institute of Technology
Dept or Mechanical Engineering
Div of Solid Mechanics
S-581 83 Linköping, Sweden

1. Summary

Algorithms to find the minimum weight design for a 3-dimensional composite membrane structure are presented. Constraints are on strength and displacements. Variables are plythicknesses, angles of orthotropi and node point co-ordinates in a FE approximation. Analytical derivatives with respect to the variables are derived for a constant strain triangle.

To solve the optimization problem a sequence of strictly convex subproblems are created. "Boxes" around each preceding design point stabilize the algorithm. Each subproblem is solved by using the duality theory for convex programming. In this article the interest is focused on the presentation of the analytical derivatives for the constant strain triangle. It begins with a brief formulation of the optimization problem and its solution. A more detailed presentation is found in (1).

2. Formulation of the Optimization Problem

The problem is to minimize the weight (w) of a 3-dimensional composite membrane structure subject to

- displacement (d_i) constraints and
- strain-stress (ε_i, σ_i, Ts_i) constraints

under multiple load conditions. (Ts is the equivalent stress Tsai).

There are three kind of variables in the optimization

- thicknesses of each ply ℓ of the composite stack for each element e ($t_{\ell e}$)
- reference directions for the material properties for each element (ϕ_e, v_e)
- co-ordinates of the nodes (c_j)

Besides from the implicit constraints above there may be explicit constraints like

- min-max sizes of the ply thicknesses
- min-max values of the reference directions
- min-max values of the co-ordinates

There may as well be some practical linking restrictions, for instance

- the thickness in a certain area, a *group of elements*, is prescribed to be constant or to have a linear variation
- the reference directions in a *group of elements* is prescribed to be either constant or vary linearly (to avoid kinks at the element boundaries)
- the structure is supposed to be symmetric or the co-ordinates in a *group of nodes* are supposed to vary linearly

and

- some thicknesses, reference directions or co-ordinates are fixed

For a single stacked triangular membrane element the variables can be visualized as

t - thicknesses of the plies (t_1, ... t_{NL})

ϕ - angle to the reference direction p (for the layup angles β_i)

c - co-ordinates of the nodes (R_{X1}, R_{Y1}, R_{Z1}, ..., R_{X3}, R_{Y3}, R_{Z3})

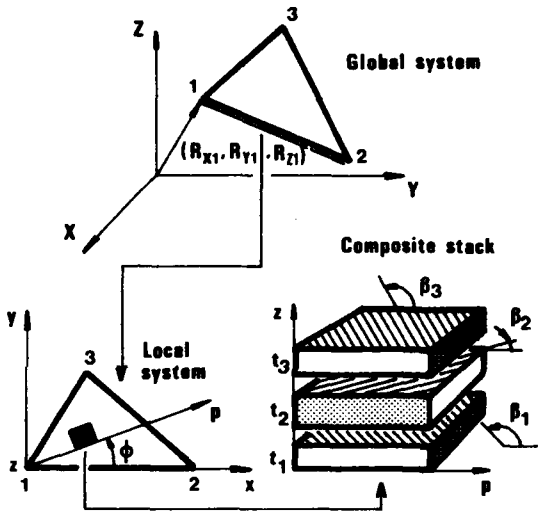


Fig 1 Design variables

Instead of using the angle, ϕ, directly as a design variable, a vector, v, may be used. The vector, v, is then projected on the element to give ϕ.

v - reference vector (v_x, v_y, v_z). (Notice: it is no limitation to set one of the components to one)

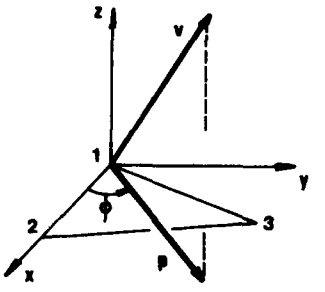


Fig 2 Projection of the reference vector

Let t, ϕ, v and c denote the vectors of $t_{\ell j}$, ϕ_j, v_j and c_j. The linking restrictions can be expressed

$$t = t_o + N_1\alpha$$

$$\begin{bmatrix} \phi \\ v \\ c \end{bmatrix} = \begin{bmatrix} \phi_o \\ v_o \\ c_o \end{bmatrix} + N_2\gamma \qquad (2.1)$$

where t_o, ϕ_o, v_o and c_o are vectors of constant terms. $\alpha = (\alpha_1, \ldots, \alpha_{n1})^T$ and $\gamma = (\gamma_1, \ldots, \gamma_{n2})^T$ are the new *independent variables*. N_1 and N_2 are constant matrices where at most one term in each row is non zero.

The optimization problem we consider can mathematically be formulated as follows:

P: min $w(\alpha,\gamma)$

subject to:

$d_i(\alpha,\gamma) \le d_i^{max}$ $\quad i = 1, .., m_d$

$\varepsilon_i(\alpha,\gamma) \le \varepsilon_i^{max}$ $\quad i = 1, .., m_\varepsilon$

$\sigma_i(\alpha,\gamma) \le \sigma_i^{max}$ $\quad i = 1, .., m_\sigma$

$Ts_i(\alpha, \gamma) \le Ts_i^{max}$ $\quad i = 1, .., m_{Ts}$

$\alpha_j^{min} \le \alpha_j \le \alpha_j^{max}$ $\quad j = 1, .., n_1$

$\gamma_j^{min} \le \gamma_j \le \gamma_j^{max}$ $\quad j = 1, .., n_2$

3. Gradients

The optimization algorithm used here will need information about the gradients of the weight function ∇w and the constraints ∇d_i, $\nabla \varepsilon_i$, $\nabla \sigma_i$, ∇Ts_i with respect to the design variables.

The derivatives with respect to (α, γ) are derived by the chain rule

$$\frac{\partial w}{\partial \alpha_j} = \sum_i \frac{\partial w}{\partial t_i} \frac{\partial t_i}{\partial \alpha_j} \quad \text{etc} \qquad (2.2)$$

Let ξ be an arbitrary variable, i e $\xi = t_{\ell e}$, ϕ_e, v_e or c_j.

3.1 Weight Function

The total weight of the structure w is the sum of the weights of the separate finite elements w_e

$$w(t, \phi, v, c) = \sum_{e=1}^{NELEM} w_e(t, \phi, v, c) \qquad (3.1)$$

Differentiate w with respect to ξ

$$\frac{\partial w}{\partial \xi} = \sum \frac{\partial w_e}{\partial \xi} \qquad (3.2)$$

$\frac{\partial w_e}{\partial \xi}$ is derived in Chapter 5.3.

Notice that $\frac{\partial w_e}{\partial \xi} \neq 0$ *only* if $\xi = t_{\ell e}$ where $t_{\ell e}$ is the thickness of one of the plies in element e, or if $\xi = c_j$ where c_j is a co-ordinate for one of the nodes of element e.

3.2 Displacement Constraints

For this section see for example ref (3).

Consider a given displacement constraint $d_i \le d_i^{max}$. d_i is the displacement of a given node in a given direction in a given load case or a linear combination of such displacements.

The FE problem can be formulated

$$Ku = p \qquad (3.3)$$

Let q be a chosen vector such that

$$d_i = q^T u = u^T q \qquad (3.4)$$

Differentiate (3.4) with respect to ξ and use (3.3)

$$\frac{\partial d_i}{\partial \xi} = (\frac{\partial p^T}{\partial \xi} - u^T \frac{\partial K}{\partial \xi})K^{-1}q + u^T \frac{\partial q}{\partial \xi} \qquad (3.5)$$

For displacement constraint q is independent of the design variables $\Rightarrow \frac{\partial q}{\partial \xi} = 0$.

Let

$$v = K^{-1}q \qquad (3.6)$$

or

$$Kv = q \qquad (3.7)$$

v is derived by solving (3.7). q may appear as additional load case in the FE-calculations.

So

$$\frac{\partial d_i}{\partial \xi} = \frac{\partial p^T}{\partial \xi} v - u^T \frac{\partial K}{\partial \xi} v \qquad (3.8)$$

but K is assembled of the different element stiffness matrices k_e. Thus

$$K = \sum_{e=1}^{NELEM} k_e \qquad (3.9)$$

The load vector p can usually be split in one "fix" part p_o and contributions from the different elements p_e, thus

$$p = p_o + \sum_{e=1}^{NELEM} p_e \qquad (3.10)$$

Let u_e and v_e be the node displacements for the e:th element.

Combine (3.9), (3.10) with (3.8)

$$\frac{\partial d_i}{\partial \xi} = \sum_e \frac{\partial p_e^T}{\partial \xi} v_e - \sum_e u_e^T \frac{\partial k_e}{\partial \xi} v_e \qquad (3.11)$$

For $\frac{\partial p_e}{\partial \xi}$ and $\frac{\partial k_e}{\partial \xi}$ see Chapter 5.5 and 5.2.

Notice that $\frac{\partial p_e}{\partial \xi} \neq 0$ and $\frac{\partial k_e}{\partial \xi} \neq 0$ *only* if $\xi = t_{\ell e}$, $\xi = \phi_e$ or $\xi = v_i$ where v_i is one of the components of the reference direction vector for element e or if $\xi = c_j$ where c_j is a co-ordinate for one of the nodes of element e.

In many cases p_e is independent of $\xi \Rightarrow \frac{\partial p_e}{\partial \xi} = 0$. This is always true if $\xi = \phi_j$ or v_j.

3.3 Strain and Stress Constraints

Consider a given strain constraint $\varepsilon_i \le \varepsilon_i^{max}$. ε_i is one of the strain components $(\varepsilon_x, \varepsilon_y, \gamma_{xy})$ at a given element e in a given load case.

Now, let q be the vector such that

$$\varepsilon_i = q^T u = u^T q \tag{3.12}$$

Vector q consists of the corresponding row in matrix Q in Chapter 5.6.

Differentiate (3.12) with respect to ξ and use (3.3)

$$\frac{\partial \varepsilon_i}{\partial \xi} = (\frac{\partial p^T}{\partial \xi} - u^T \frac{\partial K}{\partial \xi})K^{-1}q + u^T \frac{\partial q}{\partial \xi} \tag{3.13}$$

with

$$v = K^{-1}q \tag{3.14}$$

or

$$Kv = q \tag{3.15}$$

v is derived by solving (3.15). q may appear as additional load case in the FE-calculations.

$$\frac{\partial \varepsilon_i}{\partial \xi} = \frac{\partial p^T}{\partial \xi} v - u^T \frac{\partial K}{\partial \xi} v + u^T \frac{\partial q}{\partial \xi} \tag{3.16}$$

with (3.9) and (3.10)

$$\frac{\partial \varepsilon_i}{\partial \xi} = \sum_e \frac{\partial p_e^T}{\partial \xi} v_e - \sum_e u_e^T \frac{\partial k_e}{\partial \xi} v_e + u_e^T \frac{\partial q_e}{\partial \xi} \tag{3.17}$$

where q_e is the vector for the e:th element. $\partial q_e/\partial \xi \neq 0$ only if $\xi = c_j$, where c_j is a co-ordinate for one of the nodes of element e. The derivatives $\partial p_e/\partial \xi$, $\partial k_e/\partial \xi$ and $\partial q_e/\partial \xi$ are derived in Chapters 5.5, 5.2 and 5.6.

In a membrane the strains are constant through the thickness. In case the membrane is a composite stack of orthotropic materials the strains and stresses in the directions of orthotropy in each ply are the governing ones for failure.

Let

ε_x, ε_y, γ_{xy}: strain components in a given element for a given load case derived according to (3.12) and their derivatives according to (3.17) (x, y are the element local co-ordinate axes)

and

$$\varepsilon = \begin{bmatrix} \varepsilon_y \\ \varepsilon_y \\ \gamma_{xy} \end{bmatrix}$$

Strains $\varepsilon_\ell = (\varepsilon_1, \varepsilon_2, \gamma_{12})^T$ in ply ℓ in the directions of orthotropy

$$\varepsilon_\ell = T_\ell \varepsilon \tag{3.18}$$

Differentiate (3.18) with respect to

$$\frac{\partial \varepsilon_\ell}{\partial \xi} = \frac{\partial T_\ell}{\partial \xi} \varepsilon + T_\ell \frac{\partial \varepsilon}{\partial \xi} \tag{3.19}$$

T_ℓ and $\partial T_\ell/\partial \xi$ are derived in Chapters 5.1 and 5.2.

$\partial T_\ell/\partial \xi \neq 0$ only if $\xi = \phi_e$ or $\xi = v_j$ where v_j is one of the components of the reference direction vector for element e or if $\xi = c_j$ where c_j is a co-ordinate for one of the nodes of element e.

Stresses $\sigma_\ell = (\sigma_1, \sigma_2, \tau_{12})^T$ in ply ℓ in the directions of orthotropy

$$\sigma_\ell = C_\ell \varepsilon_\ell \tag{3.20}$$

C_ℓ is the constitutive matrix of the material.

Differentiate eq (3.20) with respect to ξ and notice that C_ℓ is independent of ξ, i e $\partial C_\ell/\partial \xi = 0$

$$\frac{\partial \sigma_\ell}{\partial \xi} = C_\ell \frac{\partial \varepsilon_\ell}{\partial \xi} \tag{3.21}$$

An equivalent normalized dimensionless stress frequently used for orthotropic materials is Tsais number Ts.

$$Ts_\ell = [(\frac{\sigma_1}{F_1})^2 + (\frac{\sigma_2}{F_2})^2 - \frac{\sigma_1\sigma_2}{\rho F_1 F_2} + (\frac{\tau_{12}}{F_{12}})^2]^{1/2} \tag{3.22}$$

where, depending on the sign of σ_1 and σ_2, the constants F_1 and F_2 are the stresses of failure in uniaxial tension or compression.

F_{12} is the stress of failure in pure shear and ρ is a constant usually around 10.

Differentiate

$$\frac{\partial Ts_\ell}{\partial \xi} = \frac{1}{2Ts_\ell}(\frac{2\sigma_1}{F_1^2}\frac{\partial \sigma_1}{\partial \xi} + \frac{2\sigma_2}{F_2^2}\frac{\partial \sigma_2}{\partial \xi} - \frac{\partial \sigma_1}{\partial \xi}\frac{\sigma_2}{\rho F_1 F_2} - \frac{\sigma_1}{\rho F_1 F_2}\frac{\partial \sigma_2}{\partial \xi} + \frac{2\tau_{12}}{F_{12}^2}\frac{\partial \tau_{12}}{\partial \xi}) \tag{3.23}$$

where $\partial\sigma_1/\partial\xi$, $\partial\sigma_2/\partial\xi$ and $\partial\tau_{12}/\partial\xi$ are evaluated in (3.21).

4. Method for Solving the Optimization Problem

A sequence of strictly convex subproblems $\bar{P}^{(k)}$ are created. Each subproblem is a first order approximation, based on gradient information of the original problem. "Boxes" around the iteration point, i e the optimum $(\alpha^{(k)}, \gamma^{(k)})$ of the preceding subproblem are created to stabilize the algorithm.

I e

$$\frac{1}{2}\alpha_j^{(k)} \leq \alpha_j \leq 2\alpha_j^{(k)}$$

$$\gamma_j^{(k)} - h_j^{(k)} \leq \gamma_j \leq \gamma_j^{(k)} + h_j^{(k)} \tag{4.1}$$

$h_j^{(k)}$ is chosen such that $h_j^{(k)} \to 0$, when $k \to \infty$, but $h_j^{(k)}$ must not approach zero "too fast". The weight function (w) is made linear in the variables (α, γ) by a Taylor expansion around the iteration point $(\alpha^{(k)}, \gamma^{(k)})$. w is indeed linear in the variable α which means that derivatives with respect to α only depend on γ.

The constraints, on the other hand, are made linear in the variables (y, z) where

$$y_j = \frac{\alpha_j^{(k)}}{\alpha_j} \text{ and } z_j = \frac{\gamma_j - \gamma_j^{(k)}}{h_j^{(k)}} \tag{4.2}$$

Variable y_j is, except for the constant $\alpha_j^{(k)}$, the reciprocal of the thickness variable α_j. Deformations and strains-stresses are often close to linear in y. When convergence is reached $y_j = 1$ and $z_j = 0$. To make the problem strictly convex, small terms $\varepsilon_j^{(k)} z_j^2$ are added to the weight function. $\varepsilon_j^{(k)}$ are small positive parameters. Constant terms are dropped in the expression for w.

Expressed in variables (y, z) the subproblem $\bar{P}^{(k)}$ finally becomes

$$\bar{P}^{(k)}: \min_{y,z} \sum_j \frac{\partial w}{\partial \alpha_j} \frac{\alpha_j^{(k)}}{y_j} + \sum_j \left(\frac{\partial w}{\partial \gamma_j} h_j^{(k)} z_j + \varepsilon_j^{(k)} z_j^2\right)$$

subject to

$$g_i^{(k)} - \sum_j \frac{\partial g_i}{\partial \alpha_j} \alpha_j^{(k)} (y_j - 1) + \sum_j \frac{\partial g_i}{\partial \gamma_j} h_j^{(k)} z_j \le g_i^{max}$$

$$i = 1, .. m = m_d + m_\varepsilon + m_\sigma + m_{Ts}$$

$$y_j^{min} \le y_j \le y_j^{max} \quad j = 1, .., n_1$$

$$z_j^{min} \le z_j \le z_j^{max} \quad j = 1, ... n_2$$

where all derivatives are evaluated in $(\alpha^{(k)}, \gamma^{(k)})$ and g_i represents the different constraints.

$$y_j^{min} = \max \{\frac{1}{2}, \frac{\alpha_j^{(k)}}{\alpha_j^{max}}\}$$

$$y_j^{max} = \min \{2, \frac{\alpha_j^{(k)}}{\alpha_j^{min}}\}$$

$$z_j^{min} = \max \{-1, \frac{\gamma_j^{min} - \gamma_j^{(k)}}{h_j^{(k)}}\}$$

$$z_j^{max} = \min \{1, \frac{\gamma_j^{max} - \gamma_j^{(k)}}{h_j^{(k)}}\} \qquad (4.3)$$

Problem $\bar{P}^{(k)}$ can as well be expressed

$$\bar{P}^{(k)}: \min_{y,z} \sum_{j=1}^{n_1} \frac{e_j}{y_j} + \sum_{j=1}^{n_2} (f_j z_j + \varepsilon_j z_j^2)$$

subject to

$$\sum_{j=1}^{n_1} a_{ij} y_j + \sum_{j=1}^{n_2} b_{ij} z_j \le d_i \qquad i = 1, \ldots, m$$

$$y \in Y \qquad z \in Z$$

It can be shown that if the sequence of solutions to the subproblems $\bar{P}^{(k)}$ converges to $y_j = 1$ and $z_j = 0$ for all i then the sequence $(\alpha^{(k)}, \gamma^{(k)}$ converges to a point which satisfies the Kuhn-Tucker condition of the original problem P. The subproblem $\bar{P}^{(k)}$ is solved by using the duality theory for convex programming. The Lagrangian is

$$L(y,z,\lambda) = \sum_{j=1}^{n_1} \frac{e_j}{y_j} + \sum_{j=1}^{n_2} (f_j z_j + \varepsilon_j z_j^2) +$$

$$+ \sum_{i=1}^{m} \lambda_i \left(\sum_{j=1}^{n_1} a_{ij} y_j + \sum_{j=1}^{n_2} b_{ij} z_j - d_i \right) \qquad (4.4)$$

The dual objective function is

$$\phi(\lambda) = \min_{y \in Y,\ z \in Z} L(y, z, \lambda) \qquad (4.5)$$

ϕ is concave in λ.

$\bar{D}^{(k)}$: max $\phi(\lambda)$

subject to:

$\lambda_i \ge 0$

Because L is separable, $y_j(\lambda)$ and $z_j(\lambda)$ are easily calculated

$$y_j(\lambda) = \begin{cases} y_j^{min} & \text{if } \delta_j \ge \frac{e_j}{(y_j^{min})^2} \\ \sqrt{\frac{e_j}{\delta_j}} & \text{if } \frac{e_j}{(y_j^{max})^2} \le \delta_j \le \frac{e_j}{(y_j^{min})^2} \\ y_j^{max} & \text{if } \delta_j \le \frac{e_j}{(y_j^{max})^2} \end{cases} \qquad (4.6)$$

for $j = 1, \ldots, n_1$ $\left(\delta_j = \sum_{i=1}^{m} \lambda_i a_{ij}\right)$

$$z_j(\lambda) = \begin{cases} z_j^{min} & \text{if } \rho_j \ge -f_j - 2\varepsilon_j z_j^{min} \\ -\frac{f_j + \rho_j}{2\varepsilon_j} & \text{if } z_j^{min} \le -\frac{f_j+\rho_j}{2\varepsilon_j} \le z_j^{max} \\ z_j^{max} & \text{if } \rho_j \le -f_j - 2\varepsilon_j z_j^{max} \end{cases} \qquad (4.7)$$

for $j = 1, \ldots, n_2$ $\left(\rho_j = \sum_{i=1}^{m} \lambda_i b_{ij}\right)$

It is also very easy to calculate the derivatives of ϕ

$$\frac{\partial \phi}{\partial \lambda_i} = \sum_{j=1}^{n_1} a_{ij} y_j(\lambda) + \sum_{j=1}^{n_2} b_{ij} z_j(\lambda) - d_i \qquad (4.8)$$

with $y_j(\lambda)$ and $z_j(\lambda)$ as in (4.6) and (4.7). If $\bar{\lambda}$ is the optimal solution of $\bar{D}^{(k)}$, then we get the optimal solution $(\bar{y}, \bar{z})$ of $\bar{P}^{(k)}$ by simply letting $\bar{y}_j = y_j(\bar{\lambda})$, $\bar{z}_j = z_j(\bar{\lambda})$. $\bar{D}^{(k)}$ may be solved by an arbitrary gradient method. References (1) and (2).

5. Derivation of the Stiffness Matrix, Weight, Load Vector, Strains and Stresses and Their Derivatives for a Triangular Composite Finite Element of the Constant Strain Type

Locally in Chapter 5 we drop the subindex e of the design variables.

5.1 Stiffness matrix k_e

The co-ordinates of a node i can be expressed in global co-ordinates $R_i = (R_{Xi}, R_{Yi}, R_{Zi})^T$ or in local co-ordinates $r_i = (r_{xi}, r_{yi}, r_{zi})$.

The transformation is

$$R_i = R_1 + L r_i \qquad (5.1)$$

where

$$L = (\hat{x}, \hat{y}, \hat{z}) \qquad (5.2)$$

and $\hat{x}$, $\hat{y}$, $\hat{z}$ are the unit vectors of the local x, y, z axes expressed in global co-ordinates, i e

$$\hat{x} = \frac{R_2 - R_1}{\|R_2 - R_1\|} \qquad (5.3)$$

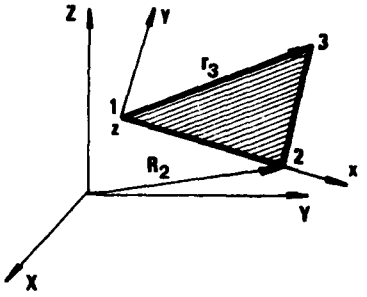


Fig 3 Global and local co-ordinate systems

$$\hat{z} = \frac{\hat{x}\times h}{\|\hat{x}\times h\|} \quad \text{and } h = R_3 - R_1 \tag{5.4}$$

$$\hat{y} = \hat{z}\times\hat{x} \tag{5.5}$$

Notice that $L^{-1} = L^T$.

The stiffness matrix k_e may be written

$$k_e = \lfloor L,\ L,\ L \rfloor\ M k M^T\ \lfloor L^T,\ L^T,\ L^T \rfloor \tag{5.6}$$

where

$$\lfloor L,\ L,\ L \rfloor = \begin{pmatrix} L & 0 & 0 \\ 0 & L & 0 \\ 0 & 0 & L \end{pmatrix} \tag{5.7}$$

and

$$M = \begin{pmatrix} 1&0&0&0&0&0 \\ 0&0&0&1&0&0 \\ 0&0&0&0&0&0 \\ 0&1&0&0&0&0 \\ 0&0&0&0&1&0 \\ 0&0&0&0&0&0 \\ 0&0&1&0&0&0 \\ 0&0&0&0&0&1 \\ 0&0&0&0&0&0 \end{pmatrix} \tag{5.8}$$

The "degrees of freedom" are supposed to be in the following order

$$u = (u_{X1},\ u_{Y1},\ u_{Z1},\ u_{X2},\ u_{Y2},\ u_{Z2},\ u_{X3},\ u_{Y3},\ u_{Z3})^T \tag{5.9}$$

k is the stiffness matrix expressed in the local co-ordinates

$$k = H^T A H \Delta \tag{5.10}$$

where

$$H = G F^{-1} \tag{5.11}$$

and

$$G = \begin{pmatrix} 0&1&0&0&0&0 \\ 0&0&0&0&0&1 \\ 0&0&1&0&1&0 \end{pmatrix} \tag{5.12}$$

and

$$F = \begin{pmatrix} F_1 & 0 \\ 0 & F_1 \end{pmatrix} \quad \text{and } F_1 = \begin{pmatrix} 1 & 0 & 0 \\ 1 & r_{x2} & 0 \\ 1 & r_{x3} & r_{y3} \end{pmatrix} \tag{5.13}$$

the inverse F^{-1} is

$$F^{-1} = \begin{vmatrix} F_1^{-1} & 0 \\ 0 & F_1^{-1} \end{vmatrix} \tag{5.14}$$

and

$$F_1^{-1} = \frac{1}{2\Delta} D \tag{5.15}$$

$$D = \begin{pmatrix} (r_{x2}\cdot r_{y3}) & 0 & 0 \\ -r_{y3} & r_{y3} & 0 \\ (r_{x3} - r_{x2}) & -r_{x3} & r_{x2} \end{pmatrix} \tag{5.16}$$

and Δ is the area of the element

$$\Delta = \frac{1}{2} \det F_1 = \frac{1}{2} r_{x2}\, r_{y3} \tag{5.17}$$

A is the constitutive matrix connecting the stress resultants $N = (N_x, N_y, N_{xy})^T$ to the strains $\varepsilon = (\varepsilon_x, \varepsilon_y, \gamma_{xy})$, i e

$$N = A\varepsilon \tag{5.18}$$

$$A = \sum_{\ell=1}^{NL} t_\ell\, T_\ell^T\, C_\ell\, T_\ell \tag{5.19}$$

where t_ℓ is the thickness and C_ℓ is the constitutive matrix for ply ℓ.

$$T_\ell = \begin{pmatrix} \cos^2\psi_\ell & \sin^2\psi_\ell & \sin\psi_\ell\cos\psi_\ell \\ \sin^2\psi_\ell & \cos^2\psi_\ell & -\sin\psi\ \cos\psi_\ell \\ -2\sin\psi_\ell\cos\psi_\ell & 2\sin\psi_\ell\cos\psi_\ell & \cos^2\psi_\ell - \sin^2\psi_\ell \end{pmatrix} \tag{5.20}$$

ψ_ℓ is the angle from the x-axis to the first main axis of orthotropy of the material in ply ℓ. ψ_ℓ can be expressed as

$$\psi_\ell = \phi + \beta_\ell \tag{5.21}$$

where β_ℓ is a fix angle from a reference axis p to the first main axis. The reference axis p makes an angle ϕ with the x-axis.

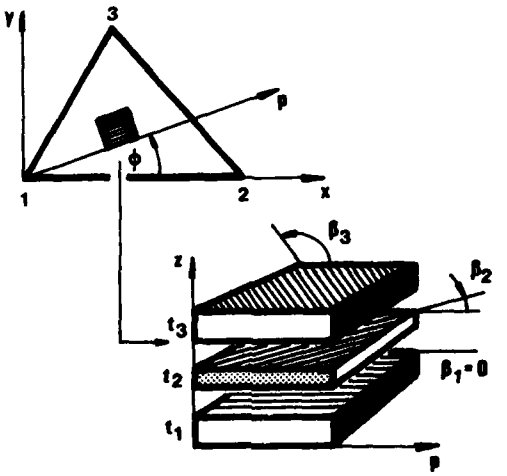


Fig 4 A composite element

ϕ is either given explicitly or derived from the projection p of a vector v on the plane of the element (see Fig 2). ϕ is then the angle from the x-axis to the vector p.

Instead of using p we introduce a vector q which is perpendicular to p and in the x-y-plane.

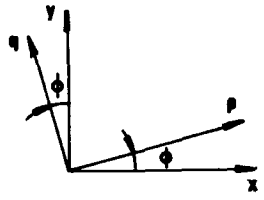


Fig 5 q-vector

$$\hat{q} = \frac{\hat{z}\times v}{\|\hat{z}\times v\|} \tag{5.22}$$

$$\sin\phi = -\hat{q}_x \tag{5.23}$$

$$\phi = \arcsin(-\hat{q}_x) \tag{5.24}$$

$$-1 \le \hat{q}_x \le 1 \Rightarrow -\frac{\pi}{2} \le \phi \le \frac{\pi}{2}$$

References (4) and (5).

5.2 Derivatives of the Stiffness Matrix k_e

$\xi = t_\ell$, the thickness of ply ℓ of element e.

The thickness appears only in the expression for A, so

$$\frac{\partial k_e}{\partial t_\ell} = \left[L,\ L,\ L\right] M \frac{\partial k}{\partial t_\ell} M^T \left[L^T,\ L^T,\ L^T\right] \tag{5.25}$$

$$\frac{\partial k}{\partial t_\ell} = H^T \frac{\partial A}{\partial t_\ell} H\,\Delta \tag{5.26}$$

$$\frac{\partial A}{\partial t_\ell} = T_\ell^T C_\ell T_\ell \tag{5.27}$$

$\xi = \phi$, the angle of reference direction for element e

ϕ_e appears only in A.

$$\frac{\partial k_e}{\partial \phi} = \left[L,\ L,\ L\right] M \frac{\partial k}{\partial \phi} M^T \left[L^T,\ L^T,\ L^T\right] \tag{5.28}$$

$$\frac{\partial k}{\partial \phi} = H^T \frac{\partial A}{\partial \phi} H\,\Delta \tag{5.29}$$

$$\frac{\partial A}{\partial \phi} = \sum_{\ell=1}^{NL} t_\ell\left[\left(T_\ell^T C_\ell \frac{\partial T_\ell}{\partial \phi}\right)^T + T_\ell^T C_\ell \frac{\partial T_\ell}{\partial \phi}\right] \tag{5.30}$$

$$-\frac{\partial T_\ell}{\partial \phi} = \frac{\partial T_\ell}{\partial \psi_\ell}\frac{\partial \psi_\ell}{\partial \phi} \tag{5.31}$$

$$\frac{\partial T_\ell}{\partial \psi} = \begin{bmatrix} -2\sin\psi_\ell\cos\psi_\ell & 2\sin\psi_\ell\cos\psi_\ell & \cos^2\psi_\ell-\sin^2\psi_\ell \\ 2\sin\psi_\ell\cos\psi_\ell & -2\sin\psi_\ell\cos\psi_\ell & -(\cos^2\psi_\ell-\sin^2\psi_\ell) \\ -2(\cos^2\psi_\ell-\sin^2\psi_\ell) & 2(\cos^2\psi_\ell-\sin^2\psi_\ell) & -4\sin\psi_\ell\cos\psi_\ell \end{bmatrix} \tag{5.32}$$

$$\frac{\partial \psi_\ell}{\partial \phi} = 1 \tag{5.33}$$

ϕ is used as a design variable (instead of v) when there are no constraints on continuity of the derivative of the material main axis of orthotropy between different finite elements. The main axis can make kinks in the element boundaries. As long as the *geometry is not changed* (i e the co-ordinates are not variables) linking of the variables ϕ_e inside a group of element can avoid this.

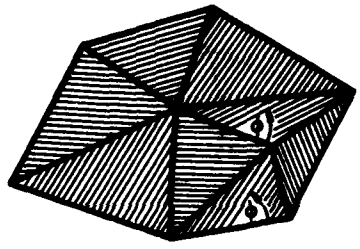


Fig 6 Kinks of the reference direction

$\xi = v_x$, v_y or v_z, the reference direction vector of element e

(Notice: At least one of the components v_x, v_y or v_z is fixed.) Consider one of the components, e g v_x

$$\frac{\partial k_e}{\partial v_x} = \left[L,\ L,\ L\right] M \frac{\partial k}{\partial v_x} M^T \left[L^T,\ L^T,\ L^T\right] \tag{5.34}$$

$$\frac{\partial k}{\partial v_x} = H^T \frac{\partial A}{\partial v_x} H\,\Delta \tag{5.35}$$

$$\frac{\partial A}{\partial v_x} = \sum_{\ell=1}^{NL} t_\ell\left(\left(T_\ell C_\ell \frac{\partial T_\ell}{\partial v_x}\right)^T + T_\ell C_\ell \frac{\partial T_\ell}{\partial v_x}\right) \tag{5.36}$$

$$\frac{\partial T_\ell}{\partial v_x} = \frac{\partial T_\ell}{\partial \phi}\frac{\partial \phi}{\partial v_x} \tag{5.37}$$

for $\frac{\partial T_\ell}{\partial \phi}$. See (5.31.)

With $\phi = \arcsin(-\hat{q}_x)$ see (5.24).

$$\frac{\partial \phi}{\partial v_x} = -\frac{1}{1-\hat{q}_x^2}\frac{\partial \hat{q}_x}{\partial v_x} \tag{5.38}$$

with

$$\hat{q}_x = \frac{(\hat{z}\times\hat{v})_x}{\|\hat{z}\times v\|} \tag{5.39}$$

$$\frac{\partial \hat{q}_x}{\partial v_x} = \frac{1}{\|\hat{z}\times v\|}\left(\frac{\partial}{\partial v_x}(\hat{z}\times v)\right)_x - \frac{(\hat{z}\times v)_x}{\|\hat{z}\times v\|^2}\frac{\partial}{\partial v_x}\|\hat{z}\times v\| \tag{5.40}$$

as

$$\frac{\partial \hat{z}}{\partial v_x} = 0 \tag{5.41}$$

$$\frac{\partial}{\partial v_x}(\hat{z}\times v) = \hat{z}\times\frac{\partial v}{\partial v_x} \tag{5.42}$$

$$\frac{\partial v}{\partial v_x} = \begin{bmatrix}1\\0\\0\end{bmatrix} \tag{5.43}$$

$$\frac{\partial}{\partial v_x}\|\hat{z}\times v\| = \frac{\left(\hat{z}\times\frac{\partial v}{\partial v_x}\right)(\hat{z}\times v)}{\|\hat{z}\times v\|} \tag{5.45}$$

$\frac{\partial k_e}{\partial v_y}$ and $\frac{\partial k_e}{\partial v_z}$ are calculated similarly.

v is used as design variable (instead of ϕ) when continuity of the derivative of the material main axis is wanted between the elements. The reference direction

vector v, within a group of elements, may be linked and the main axis keeps straight even if the geometry is changed.

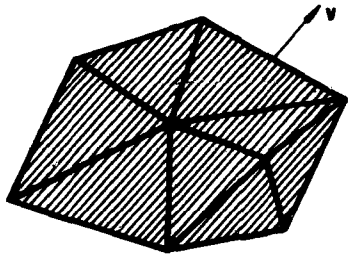


Fig 7 Reference direction vector

$\xi = c_j$, *co-ordinates of the nodes of element e*

c_j represents one of the nine global co-ordinates of the element (R_{X1}, R_{Y1}, R_{Z1}, R_{X2}, R_{Y2}, R_{Z2}, R_{X3}, R_{Y3}, R_{Z3})

$$\frac{\partial k_e}{\partial c_j} = \left[\frac{\partial L}{\partial c_j}, \frac{\partial L}{\partial c_j}, \frac{\partial L}{\partial c_j}\right] MkM^T \left[L^T, L^T, L^T\right] +$$
$$+\left[\left[\frac{\partial L}{\partial c_j}, \frac{\partial L}{\partial c_j}, \frac{\partial L}{\partial c_j}\right] MkM^T \left[L^T, L^T, L^T\right]\right]^T +$$
$$+ \left[L, L, L\right] M \frac{\partial k}{\partial c_j} M^T \left[L^T, L^T, L^T\right] \qquad (5.46)$$

$$\frac{\partial L}{\partial c_j} = \left(\frac{\partial \hat{x}}{\partial c_j}, \frac{\partial \hat{y}}{\partial c_j}, \frac{\partial \hat{z}}{\partial c_j}\right) \quad \text{See (5.2).} \qquad (5.47)$$

$$\frac{\partial \hat{x}}{\partial c_j} = \frac{1}{\|R_2-R_1\|} \frac{\partial}{\partial c_j}(R_2-R_1) - \frac{(R_2-R_1)}{\|R_2-R_1\|^2} \frac{\partial}{\partial c_j} \|R_2-R_1\| \qquad (5.48)$$

$$\frac{\partial}{\partial c_j}(R_2-R_1) = \frac{\partial}{\partial c_j}\begin{bmatrix} R_{2X}-R_{1X} \\ R_{2Y}-R_{1Y} \\ R_{2Z}-R_{1Z} \end{bmatrix}$$

for $c_j = R_{1X}$ (x-co-ordinate of node No. 1)

$$\frac{\partial}{\partial R_{1X}}(R_2-R_1) = \begin{bmatrix} -1 \\ 0 \\ 0 \end{bmatrix} \qquad (5.49)$$

The derivatives of (R_2-R_1) with respect to c_j where c_j are the co-ordinates in the order above become

$$\begin{bmatrix} -1 & 0 & 0 & 1 & 0 & 0 & 0 & 0 & 0 \\ 0 & -1 & 0 & 0 & 1 & 0 & 0 & 0 & 0 \\ 0 & 0 & -1 & 0 & 0 & 1 & 0 & 0 & 0 \end{bmatrix} \qquad (5.50)$$

$$\frac{\partial}{\partial c_j}\|R_2-R_1\| = \frac{\partial}{\partial c_j}((R_{2X}-R_{1X})^2 + (R_{2Y}-R_{1Y})^2 +$$
$$+ (R_{2Z}-R_{1Z})^2)^{1/2} =$$
$$= \frac{(R_{2X}-R_{1X})\frac{\partial}{\partial c_j}(R_{2X}-R_{1X}) + (R_{2Y}-R_{1Y})\frac{\partial}{\partial c_j}(R_{2Y}-R_{1Y})}{\|R_2-R_1\|^2} +$$
$$+ \frac{(R_{2Z}-R_{1Z}\frac{\partial}{\partial c_j}(R_{2Z}-R_{1Z})}{\|R_2-R_1\|^2} \qquad (5.51)$$

$$\frac{\partial \hat{z}}{\partial c_j} = \frac{\partial \hat{z}}{\partial c_j} \times \hat{x} + \hat{z} \times \frac{\partial \hat{x}}{\partial c_j} \qquad (5.52)$$

$$\frac{\partial \hat{z}}{\partial c_j} = \frac{1}{\|\hat{x}\times h\|} \frac{\partial}{\partial c_j}(\hat{x}\times h) - \frac{(\hat{x}\times h)}{\|\hat{x}\times h\|^2} \frac{\partial}{\partial c_j}\|\hat{x}\times h\| \qquad (5.53)$$

$$\frac{\partial}{\partial c_j}(\hat{x}\times h) = \frac{\partial \hat{x}}{\partial c_j} \times h + \hat{x} \times \frac{\partial h}{\partial c_j} \qquad (5.54)$$

$$\frac{\partial h}{\partial c_j} = \frac{\partial}{\partial c_j}(R_3-R_1) \qquad (5.55)$$

Those derivatives are in the same order

$$\begin{bmatrix} -1 & 0 & 0 & 0 & 0 & 0 & 1 & 0 & 0 \\ 0 & -1 & 0 & 0 & 0 & 0 & 0 & 1 & 0 \\ 0 & 0 & -1 & 0 & 0 & 0 & 0 & 0 & 1 \end{bmatrix}$$

$$\frac{\partial}{\partial c_j}\|\hat{x}\times h\| = \frac{1}{\|\hat{x}\times h\|^2}\left(\frac{\partial \hat{x}}{\partial c_j} \times h + \hat{x} \times \frac{\partial h}{\partial c_j}\right)(\hat{x}\times h) \qquad (5.56)$$

$$\frac{\partial k}{\partial c_j} = (\eta^T A \frac{\partial H}{\partial c_j} \Delta)^T + H^T A \frac{\partial H}{\partial c_j} \Delta +$$
$$+ H^T \frac{\partial A}{\partial c_j} H \Delta + H^T A H \frac{\partial \Delta}{\partial c_j} \qquad (5.57)$$

$$\frac{\partial H}{\partial c_j} = G \frac{\partial F^{-1}}{\partial c_j} \qquad (5.58)$$

$$\frac{\partial F^{-1}}{\partial c_j} = \begin{bmatrix} \frac{\partial F_1^{-1}}{\partial c_j} & 0 \\ 0 & \frac{\partial F_1^{-1}}{\partial c_j} \end{bmatrix} \qquad (5.59)$$

with

$$F_1 F_1^{-1} = E \qquad (5.60)$$

$$\frac{\partial F_1}{\partial c_j} F_1^{-1} + F_1 \frac{\partial F_1^{-1}}{\partial c_j} = 0 \qquad (5.61)$$

$$\frac{\partial F_1^{-1}}{\partial c_j} = - F_1^{-1} \frac{\partial F_1}{\partial c_j} F_1^{-1} \qquad (5.62)$$

where F_1^{-1} is derived in (5.15)

$$\frac{\partial F_1}{\partial c_j} = \begin{bmatrix} 0 & 0 & 0 \\ 0 & \frac{\partial r_{x2}}{\partial c_j} & 0 \\ 0 & \frac{\partial r_{x3}}{\partial c_j} & \frac{\partial r_{y3}}{\partial c_j} \end{bmatrix} \qquad (5.63)$$

With (5.1) the local co-ordinates become $r_i = L^T(R_i-R_1)$

$$\frac{\partial r_i}{\partial c_j} = \frac{\partial L^T}{\partial c_j}(R_i-R_1) + L^T \frac{\partial}{\partial c_j}(R_i-R_1) \qquad (5.64)$$

where $\frac{\partial L}{\partial c_j}$ and $\frac{\partial}{\partial c_j}(R_i - R_1)$ are derived above

and

$$\frac{\partial A}{\partial c_j} = \sum_{\ell=1}^{NL} t_\ell \left((T_\ell^T C_\ell \frac{\partial T_\ell}{\partial c_j})^T + T_\ell^T C_\ell \frac{\partial T_\ell}{\partial c_j} \right) \tag{5.65}$$

$$\frac{\partial T_\ell}{\partial c_j} = \frac{\partial T_\ell}{\partial \phi} \frac{\partial \phi}{\partial c_j} \tag{5.66}$$

$\frac{\partial T_\ell}{\partial \phi}$ is derived in (5.31).

$$\frac{\partial \phi}{\partial c_j} = \frac{\partial}{\partial c_j}(\arcsin(-\hat{q}_x)) = -\frac{1}{1-\hat{q}_x^2} \frac{\partial \hat{q}_x}{\partial c_j} \tag{5.67}$$

$$\frac{\partial \hat{q}_x}{\partial c_j} = \frac{1}{\|\hat{z}\times v\|} \left(\frac{\partial}{\partial c_j}(\hat{z}\times v)\right)_x - \frac{(\hat{z}\times v)_x}{\|\hat{z}\times v\|^2} \frac{\partial}{\partial c_j} \|\hat{z}\times v\| \tag{5.68}$$

as

$$\frac{\partial v}{\partial c_j} = 0 \tag{5.69}$$

$$\frac{\partial}{\partial c_j}(\hat{z}\times v) = \frac{\partial \hat{z}}{\partial c_j} \times v \tag{5.70}$$

for $\frac{\partial \hat{z}}{\partial c_j}$. See (5.53).

$$\frac{\partial}{\partial c_j} \|\hat{z}\times v\| = \frac{1}{\|\hat{z}\times v\|} \left(\frac{\partial \hat{z}}{\partial c_j} \times v\right)(\hat{z}\times v) \tag{5.71}$$

If ϕ is either fix or the design variable, instead of v, then $\partial T_\ell / \partial c_j = 0$, which means that the reference direction in the global system will change when the co-ordinates change.

$$\frac{\partial \Delta}{\partial c_j} = \frac{1}{2} \frac{\partial}{\partial c_j} \det F_1 = \frac{1}{2}\left(\frac{\partial r_{x2}}{\partial c_j} r_{y3} + r_{x2} \frac{\partial r_{y3}}{\partial c_j}\right) \tag{5.72}$$

where $\partial r_{x2}/\partial c_j$ and $\partial r_{y3}/\partial c_j$ are derived in (5.64).

5.3 Weight w_e

The weight of element e becomes

$$w_e = \left(\sum_{\ell=1}^{NL} \rho_\ell t_\ell\right) \Delta \tag{5.73}$$

where

ρ_ℓ = density of ply No. ℓ in the element

Δ = area of the element

5.4 Derivatives of the weight w_e

$\xi = t_\ell$, the ply thickness

$$\frac{\partial w_e}{\partial t_\ell} = \rho_\ell \Delta \tag{5.74}$$

$\xi = \phi$ *or* $\xi = v_x$, v_y *or* v_z, *the reference direction*

w_e is not dependent on these variables, i e

$$\frac{\partial w_e}{\partial \phi} = \frac{\partial w_e}{\partial v_x} = \frac{\partial w_e}{\partial v_y} = \frac{\partial w_e}{\partial v_z} = 0 \tag{5.75}$$

$\xi = c_j$, *co-ordinates of the nodes of element e*

$$\frac{\partial w_e}{\partial c_j} = \left(\sum_{\ell=1}^{NL} \rho_\ell t_\ell\right) \frac{\partial \Delta}{\partial c_j} \tag{5.76}$$

for $\frac{\partial \Delta}{\partial c_j}$. See (5.72).

5.5 Load vector p_e and its derivatives

Load caused by eigenweight - the load is distributed equally between the nodes, i e

$$p_e = \begin{bmatrix} p_e^{(1)} \\ p_e^{(1)} \\ p_e^{(1)} \end{bmatrix} \tag{5.77}$$

$$p_e^{(1)} = \frac{1}{3} w_e g \tag{5.78}$$

where g is the gravity vector

$$g = \begin{bmatrix} g_x \\ g_y \\ g_z \end{bmatrix} \tag{5.79}$$

The derivatives with respect to ξ become

$$\frac{\partial p_e^{(1)}}{\partial \xi} = \frac{1}{3} \frac{\partial w_e}{\partial \xi} g + \frac{1}{3} w_e \frac{\partial g}{\partial \xi} \tag{5.80}$$

where $\frac{\partial w_e}{\partial \xi}$ are derived in Chapter 5.4.

In most cases g is independent of ξ, i e $\partial g/\partial \xi = 0$ but e g g is dependent of the co-ordinates c_j in a quasi-static problem like a structure rotating with a constant angular velocity ω around a fix axis.

Area loads (e g wind) - the load is distributed equally between the nodes

$$p_e = \begin{bmatrix} p_e^{(1)} \\ p_e^{(1)} \\ p_e^{(1)} \end{bmatrix} \tag{5.81}$$

The area loads are supposed to be proportional to the area and directed perpendicular to the surface. Only the projection of the area load intensity (a) on this direction contributes.

$$p_e^{(1)} = \frac{1}{3} \Delta (a \hat{z}) \hat{z} \tag{5.82}$$

The derivatives with respect to ξ become

$$\frac{\partial p_e^{(1)}}{\partial \xi} = \frac{1}{3}\frac{\partial \Delta}{\partial \xi}(a\ \hat{z})\ \hat{z} + \frac{1}{3}\Delta\frac{\partial}{\partial \xi}(a\ \hat{z})\ \hat{z} + \frac{1}{3}\Delta\ (a\ \hat{z})\frac{\partial \hat{z}}{\partial \xi} \qquad (5.83)$$

where $\frac{\partial \Delta}{\partial \xi}$ and $\frac{\partial \hat{z}}{\partial \xi}$ are derived in Chapter 5.2.

$$\frac{\partial}{\partial \xi}(a\ \hat{z}) = \frac{\partial a}{\partial \xi}\hat{z} + a\frac{\partial \hat{z}}{\partial \xi} \qquad (5.84)$$

In most cases a is independent of ξ, i e $\partial a/\partial \xi = 0$, but a can very well be a function of the co-ordinates, i e a = a(c).

5.6 Strains and stresses

The strains $\varepsilon = (\varepsilon_x, \varepsilon_y, \gamma_{xy})^T$ in the directions of the local co-ordinate axes are derived from

$$\varepsilon = Q^T u_e \qquad (5.85)$$

where

$$Q^T = HM^T\left[L^T, L^T, L^T\right] \qquad (5.86)$$

and H, M and L are derived in Chapter 5.1. The derivative of Q with respect to ξ is

$$\frac{\partial Q}{\partial \xi} = \left[\frac{\partial L}{\partial \xi}, \frac{\partial L}{\partial \xi}, \frac{\partial L}{\partial \xi}\right] MH^T + \left[L, L, L\right] M\frac{\partial H^T}{\partial \xi} \qquad (5.87)$$

where $\partial L/\partial \xi \neq 0$ only if $\xi = c_j$ which is derived in (5.47) and $\partial H/\partial \xi \neq 0$ only if $\xi = c_j$ which is derived in (5.58).

References

(1) Esping B. and Svanberg K., "Weight Optimization of Membrane Structures - Part 1", LiTH-IKP-R-186. Linköping Institute of Technology, Linköping, Sweden, 1981.

(2) Svanberg K., "Optimal Geometry in Truss Design", TRITA-MAT-1980-17, Royal Institute of Technology, Stockholm, Sweden, 1980

(3) Gallagher R. and Zienkiewicz O. C., Optimum Structural Design, Theory and Applications, John Wiley & Sons, 1973

(4) Cook R, Concepts and Applications of Finite Element Analysis, John Wiley & Sons, 1974

(5) Calcote L, The Analysis of Laminated Composite Structures, van Nostrand Reinhold Company, 1969

P000 065

ABOUT DETERMINATION OPTIMAL – WEIGHT STATICALLY INDETERMINATE BAR STRUCTURES OF COMPLEX STRESS BY USING EXPLICIT FORMS OF THE CONDITIONS

Emil Halmos
Traffic and Telecommunications
Technical College
Győr, Hungary

Designing minimum-weight bar structures are usually made only by implicit functions of the conditions. In this essay we formulate the conditions as an explicit functions of the cross-sectional characteristics in order to have better applicability of mathematical programming algorithms. For this purpose we decompose the large-sized structure of optional geometry into substructures. With the help of this decomposition we can substitute the dimensioning of the whole structure for dimensionings of several small and easy handling structures. Then we move back the dimensioned large structure within the appropriate degree of tolerance used in practice.

The form of the stress vector of a bar we trace back to algebraic summing of some displacement vector components. So we get a formula which is suitable to produce the functions of the conditions both at the structures having rigid connections at the nodes and at some special cases as the trusses.

Introduction

In this essay we deal with the optimum dimensioning of statistically indeterminate trusses. The dimensioning of trusses – as mentioned in the title – is a design process, in the course of which the most economical resolution is chosen from several structures adequate to the functional requirements.

The economical condition of our investigations is the structure weight.

On the basis of the dimensioning model we can calculate those values of the structure's cross section characteristics which ensure the bearing of stress induced by an external load and result a structure the weight of which is the least of all the possible versions.

A more precise definition of the design – process of the trusses is as follows: It is an iteration – succassive approximation – method, which is carried out from a t_o starting point of the n-dimencional design space to the t_{opt} point containing the dimensional variables *of the minimum – weight structure. Consequently it can be ascertai*ned that in this stage of the design – work the iteration must be carried out with the help of an algorithm suitably composed for a computer, instead of using the traditional „design iteration" method.

The following schematic outline is added to the above mentioned:

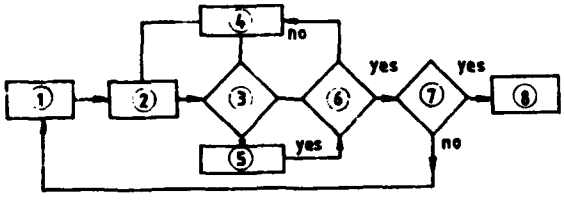


fig. 1.

1 The t_o values of the original structure
2 The defining of Y(t) stresses
3 Are the constraints $g_i(t) \leq 0$ fulfilled or not?
4 The modification of design variables
5 The defining of the structure's W(t) weight
6 Is the W(t) = Min condition fulfilled?
7 The evaluation of design and technological considerations
8 The structure of minimum (optimal) weight.

On the basis of the outline it can be proved that if the starting data of dimensioning satisfy the constraints $g_i(t) \leq 0$ the structure is convenient from the point of view of combined strength. It has to be modified only if these conditions aren't fulfilled. If required this step can be repeated several times. We determine the structure weight by replacing the convenient from the point of view of strength vector t_o, which results the starting value of weight reducing process.

The algorithm set up on the basis of the above mentioned taking into consideration both the $g_i(t) \leq 0$ and the objective function W(t) = *Min results an iteration method, which, after all, by the continuous* changing of the structure's t_o variable creates a construction of optimal weight, the weight of which cannot be reduced any more.

The aim of this essay is to determine the relations, schematically ennumerated above, with the help of which the dimensioning task is attributed to a non-linear optimization problem.

The main advantage of the model is that the tension constraints can be formulated as an explicit function of the cross-sectional characteristics of trusses and thus the task can be solved by the aid of the already known optimization methods.

Finally we add that our essay is a generalized development of the *basic principle worked out in the essey (4) (5).*

Thus the dimensioning method can be developed more broadly and applicated also for the mechanical model of complex stress, which will be discussed in Chapter 1. (1)

1. General Characteristics of the Mechanical Model (1)

In the course of discussing this topic we try to find connections between the nodal displacements, the stresses and the external load of trusses, placed in plane and loaded in their own plane. The sets of equations, describing the equilibrium of displacements and stresses are *formulated considering the following reducing conditions:*

- A trussing is a complex of rod – members jointed by prismatic rods
- The rod – members are of constant rigidity and the distribution of stresses arising under the influence of different loads is steady.
- *The interconnecting points of rod-members are the nodes and the* external load is transferred to the construction at these nodal points. The members joining at the nodes are connected rigorously.
- The internal stresses of the rod-members are unanimously decided by the loads operating on the rod- ends(nodes).
- The nodal displacements are superposed by the displacements of the rod members in the nature of rigid – body and by the deformation of the flexible construction.
- Only differentially little displacements are supposed, so the structure – deformation doesn't react on the clearance of force of the structure.

So as to make the following statements unambiquous we lay down here some fundamental conceptions and markings which will be used regularly during the treatment of our subject.

Accordingly the structure is examined in such a right – hand sided (x; y; z) co- ordinate system, the rod – members of which meet each other in the (x; y) plane. The position of rods in the plane are given by the (u, v .w) self co-ordinates attached to the rod-members in the following way: The u axis points towards the direction of the centroidal axis of the rod and the v and w axes point towards the main inertial directions of the prismatic rod's crossectional area.

The position of the rod-members can be unambiquously determi*ned by the cosines of the angles closed by the correspondent axes of* the co-ordinate system.

The motional characteristics and stresses of the structure in question we consider a special version of the general case, because out of the six motional characteristics values and stress values – from the vector pairs summarized in the following chart – there are only 3 ones each in our model.

PRECEDING PAG

	Stresses	Vector Pairs Belonging Together		Rigidity of Rod
1.	Forces in rod direction	N_u; u		$0 < AE < \infty$
2.	Bending in the (u, v) plane	M_w; φ_w,	T_v; v	$0 < I_w E < \infty$
3.	Twisting	M_u; u		$I_u G = \infty$
4.	Bending in the (u, w) plane	M_v; v	T_w; w	$I_v E = \infty$

So our investigations relate to the stresses and deformations containing the first two lines of the chart, where

u – the tensile or compression strain resulted by the N force of rod – direction

v – the displacement resulted by the T shear force

φ_w – the angular displacement caused by the M_w bending moment with the w axis.

Summing up what has been said it can be ascertained that the chosen mechanical model can be regarded as inflexible against the twisting moment and in the (u, w) plane against the bending moment. Its motions are produced in the (u, v) plane by a translation of u and v direction and by the rotation around the w axis.

The indexes shown in the chart refer to the co-ordinate axes, but because of the already mentioned reductions they can be disregarded without offending against the unanimity of the treatment.

It is why the deformations in question and the stresses, which they are induced by, can be replaced by vectors

$$X = u\,e_1 + v\,e_2 + \varphi\,e_3 \qquad \text{and}$$

$$Y = N\,e_1 + T\,e_2 + M\,e_3$$

where e_1; e_2; e_3 are unit vectors, pointing towards the direction of (u v w) co-ordinates, while u, v φ and N, T, M, are the scalar components of the X, resp. those of the Y vectors.

2. Stress Function of Trussing (2) (3)

In order to determine the tensions and the nodal displacements let us consider the following equation:

$$\begin{bmatrix} \mathbf{R} & \mathbf{A} \\ \mathbf{A}^T & \mathbf{0} \end{bmatrix} \begin{bmatrix} Y \\ -X \end{bmatrix} = \begin{bmatrix} 0 \\ q \end{bmatrix}, \tag{2.1}$$

where

$\mathbf{A}$ – matrix related to the nodal displacements,

$\mathbf{A}^T$ – the transposed of $\mathbf{A}$,

$\mathbf{R}$ – elasticity matrix of the construction elements,

X – vector of the nodal displacements,

Y – vector of the tensions,

q – vector of the load conditions.

The system of linearly independent equations (2.1) consists of the equilibrium and the compatibility equations of the structure. Because an elastic truss is considered, the determinant of $\mathbf{R}$, denoted by $|\mathbf{R}|$ is not zero, i.e. $|\mathbf{R}| \neq 0$.

Let us define now the following matrix:

$$\mathbf{C} = \mathbf{A}^T \mathbf{R}^{-1} \mathbf{A}. \tag{2.2}$$

This is a symmetric, square matrix and it can be verified that the determinant of $\mathbf{C}$ is not zero, i.e. $|\mathbf{C}| \neq 0$. It is clear that (2.1) is the Kuhn–Tucker system for the following quadratic problem:

$$\min \tfrac{1}{2} Y^T \mathbf{R} Y \tag{2.3}$$

$$\text{subject to } \mathbf{A}^T Y = q,$$

where the function $\frac{1}{2} Y^T \mathbf{R} Y$ is strictly convex. Thus $\frac{1}{2} Y^T \mathbf{R}^{-1} Y$ is also strictly convex and as the rows of $\mathbf{A}$ are linearly independent, $\mathbf{C}$ is a positive definite matrix and $|\mathbf{C}| > 0$.

Since $|\mathbf{R}| \neq 0$, $|\mathbf{C}| \neq 0$, system 2.1 has a unique solution.

System (2.1) can be rewritten as

$$\mathbf{A}^T Y = q \tag{2.4}$$

$$\mathbf{R} Y - \mathbf{A} X = 0$$

and using the previous relations we get

$$Y = \mathbf{S}\mathbf{A}\mathbf{C}^{-1} q, \tag{2.5}$$

here $\mathbf{S} = \mathbf{R}^{-1}$. In this expression $\mathbf{C}^{-1}$ can be written as a function of $|\mathbf{C}|$.

As the elements of t vector occur in $\mathbf{S}$ and in $\mathbf{C}$ as well, the X vector is a function of the t variable. The t variable cannot be expressed from the $Y(t)$ in an explicit formula. It is the consequence of the above mentioned characteristics of the function that there are other structures, too, with the same geometrical arrangement but different from the point of view of strength, which are suitable for bearing the given external load. Out of these structures must be chosen the structure of minimum weight.

3. An Explicit Formulation of Stress Function

3.1 Disintegration of the Structure to Equal Partial Systems

On the basis of the non-linear programming task described in the Introduction and the detailed characteristics of the mechanical mod it can be admitted that both the computation technique and the str ture analysis require such formulas which can bo set up by functio expressed in an explicit form. This is why we deal in brief with the introduction of the functions used for solving the task.

We want to determine a function – relation between the stress – and cross-sectional characteristics of the rod elements. So similarly to the already mentioned (4) (5) model the analysis of the whole structure can be deduced to the analysis of the structure elements devided into units. The moving off nodal points and the rod-elements connecting to them are regarded as such units. (We remark that the units have the same mechanical characteristics as the whole structure has.)

Illustrating this let us examine the simple structure given below (fig. 2.)

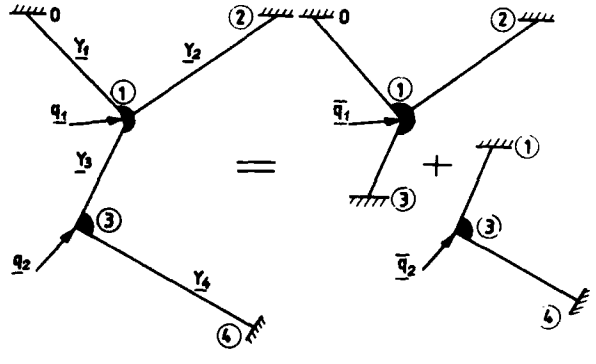


fig. 2.

which contains two moving off nodal points and according to this we decomposed it to the sum of two part-systems. As a straight consequence of this attlitude, the rodelement connecting the two nodal points occur in both part-systems. Further on we examine how the basic equation regarding to the two part-systems is connected with the basic equation system of the original structure.

According to the points of view detailed in the previous chapter, using the markings of fig. 2. we set up the basic equation system of the whole structure.

$$\begin{bmatrix} R_{01} & 0 & 0 & 0 & -Q_{01} & 0 \\ 0 & R_{12} & 0 & 0 & A_{12}Q_{12} & 0 \\ 0 & 0 & R_{13} & 0 & A_{13}Q_{13} & -Q_{31} \\ 0 & 0 & 0 & R_{34} & 0 & A_{34}Q_{34} \\ -Q_{01}^T & Q_{12}^T A_{12}^T & Q_{13}^T A_{13}^T & 0 & 0 & 0 \\ 0 & 0 & -Q_{31}^T & Q_{34}^T A_{34}^T & 0 & 0 \end{bmatrix} \begin{bmatrix} Y_1 \\ Y_2 \\ Y_3 \\ Y_4 \\ X_1 \\ X_2 \end{bmatrix} + \begin{bmatrix} 0 \\ 0 \\ 0 \\ 0 \\ q_1 \\ q_2 \end{bmatrix} = \begin{bmatrix} 0 \\ 0 \\ 0 \\ 0 \\ 0 \\ 0 \end{bmatrix}$$

When dividing the whole structure into parts we observe the basic principle, according to which the ends of the rods connecting to a moving off nodal point are fixed rigidly, so the matrix equation describing the whole structure breaks up to equation systems of the same type, independent from each other.

$$\begin{bmatrix} R_{01} & 0 & 0 & -Q_{01} & & & \\ 0 & R_{12} & 0 & A_{12}Q_{12} & & & \\ 0 & 0 & R_{13} & A_{13}Q_{13} & & & \\ -Q_{01}^T & Q_{12}^T A_{12} & Q_{13} A_{13} & 0 & & & \\ & & & & R_{31} & 0 & -Q_{31} \\ & & & & 0 & R_{34} & A_{34}Q_{34} \\ & & & & -Q_{31}^T & Q_{34}^T A_{34} & 0 \end{bmatrix} \begin{bmatrix} Y_1 \\ Y_2 \\ Y_3 \\ X_1 \\ Y_3 \\ Y_4 \\ X_2 \end{bmatrix} + \begin{bmatrix} 0 \\ 0 \\ 0 \\ \bar{q}_1 \\ 0 \\ 0 \\ \bar{q}_2 \end{bmatrix} = \begin{bmatrix} 0 \\ 0 \\ 0 \\ 0 \\ 0 \\ 0 \\ 0 \end{bmatrix}$$

So the Q_{jk} matrix of the co-ordinate transformation.

$$Q_{jk} = \begin{bmatrix} \cos\alpha & -\sin\alpha & 0 \\ \sin\alpha & \cos\alpha & 0 \\ 0 & 0 & 0 \end{bmatrix}$$

shaped ortogonal matrix, and a factoring with it results the α angle rotation of the rod-element's self coordinate system around the e_3 vector.

The relation between the two systems is provided with the reservation that the displacements of the nodal points before the breaking up are equal to the displacements that can be determined by the

$$X = C^{-1} q$$

equation. The difference is indicated by the $\bar{q}_1$; $\bar{q}_2$ artificial loads operating at the nodal points of the partunits, which can be calculated on the basis of

$$\bar{q}_\alpha = C_\alpha X_\alpha \qquad (\alpha = 1, 2)$$

connection, on condition that they induce the same displacement as the real loads did before decomposition. C_α-can be determined on the basis of the factor- and the springmatrices of the part systems.

The double direction of the rod-member, which connects the two moving off nodal points, depending on which nodal point system is examined. The beginning and end of the rod are also transformed according to this on the basis of the basic principles given is the previous chapter.

Making use of the partial results received hitherto the scalar components of $Y(t)$ function can be determined. The forming of $C_\alpha^{-1} \bar{q}_\alpha$ and S A products are necessary for this. Therefore we are analysing the C_α matrix in a more detailed way.

By way of illustration we examine the example of the nodal points marked by 1 and 3 then we generalise the received results.

So the matrix of rigidity of the part-system belonging to 1 nodal point is as follows:

$$C_1 = \left[-Q_{01}^T \,\middle|\, Q_{12}^T A_{12}^T \,\middle|\, Q_{13}^T A_{13}^T \right] \begin{bmatrix} R_{01}^{-1} & & \\ & R_{12}^{-1} & \\ & & R_{13}^{-1} \end{bmatrix} \begin{bmatrix} -Q_{01} \\ \hline A_{12}Q_{12} \\ \hline A_{13}Q_{13} \end{bmatrix} =$$

$$= Q_{01}^T R_{01}^{-1} Q_{01} + Q_{12}^T A_{12}^T R_{12}^{-1} A_{12} Q_{12} + Q_{13}^T A_{13}^T R_{13}^{-1} A_{13} Q_{13}$$

Having performed the operations pointed out in a quadratic form just like this we receive for the nodal point 3 the

$$C_3 = Q_{31}^T R_{31} Q_{31} + Q_{34}^T A_{34}^T R_{34} A_{34} Q_{34}$$

result. On the basis of the received expressions we can make two general remarks regarding the structure of the C_α matrix.

- The C_α matrix consists of two kinds of quadratic products independently from the number of rods connecting to the nodal points.
- The connecting rods are distinguished by their direction examined in the surroundings of the nodal points. To be more exact the rod directioned towards the nodal point is with negative sign in its own nodal-point-system. Consequently the structure of the matrix product determining its own rigidity differs from that of the rods with positive sign.

3.2 Definition of Rigidity Matrix

After derivating the components of C matrix and clearing up its physical contents we are to examine the characteristics of the C_α matrix, which characterises the rigidity of the rods being connected at one nodal point, resp. the rigidity of the node itself.

In the preceeding we could see that two possible versions containing the elements of C matrix can be determined for one rod member.

$$C'_\alpha = Q^T S Q = C_0 - C_1 = \begin{bmatrix} C_{0x} & -C_{0xy} & 0 \\ -C_{0yx} & C_{0y} & 0 \\ 0 & 0 & C_{0z} \end{bmatrix} - \begin{bmatrix} 0 & 0 & M_{xz} \\ 0 & 0 & M_{yz} \\ M_{zx} & M_{zy} & 0 \end{bmatrix}$$

$$C''_\alpha = Q^T A^T S A Q = C_0 + C_1 = \begin{bmatrix} C_{0x} & -C_{0xy} & 0 \\ -C_{0yx} & C_{0y} & 0 \\ 0 & 0 & C_{0z} \end{bmatrix} + \begin{bmatrix} 0 & 0 & M_{xz} \\ 0 & 0 & M_{yz} \\ M_{zx} & M_{zy} & 0 \end{bmatrix}$$

where C'_α denotes the rigidity of that rod (one of the rods being connected at the i nodal point) which is directed from i to j according to the $i < j$ relation, C''_α is valid in case of opposit direction of the same rod. The relation also contains the definition of the interrelationship between the respective nodal point systems. The contents of the matrix elements are detailed below.

$$C_{0x} = \frac{AE}{l}\left[12\frac{i^2}{l^2} + \left(1 - 12\frac{i^2}{l^2}\right)\cos^2\alpha\right]$$

$$C_{0y} = \frac{AE}{l}\left[12\frac{i^2}{l^2} + \left(1 - 12\frac{i^2}{l^2}\right)\sin^2\alpha\right]$$

$$C_{0z} = \frac{AE}{l}\,4\,i^2$$

$$-C_{0xy} = -C_{0xy} = -\frac{AE}{l}\,\frac{1}{2}\left(1 - 12\frac{i^2}{l^2}\right)\sin 2\alpha$$

$$M_{xz} = M_{zx} = \frac{AE}{l}\,6\,\frac{i^2}{l^2}\,l\sin\alpha$$

$$M_{yz} = M_{zy} = \frac{AE}{l}\,6\,\frac{i^2}{l^2}\,l\cos\alpha$$

In the expressions of string rigidities the C_{0x}, C_{0y} and C_{0z} mean the components of string rigidity vector co-ordinate system of the trussing. $C_{0xy} = C_{0yx}$ is the centrifugal string rigidity calculable in the (x; y) plane for both axles.

Finally we construe the $M_{xz} = M_{zx}$ and $M_{yz} = M_{zy}$ elements as the statical moment of the force-giving $6\frac{i^2}{l^2}$ value calculated for the x and y axles.

The identity of the certain elements refers to the symmetry related to the principal diagonal.

Some special characteristics of the problem follow from the general result defined for the C_α. Here we call the attention only to two of them.

a) In the course of examining the elements of $C_{0\alpha}$ matrix it can be ascertained that if the $\left(1 - 12\frac{i^2}{l^2}\right)$ value of the coefficient $\sin^2\alpha$, $\cos^2\alpha$, $\sin 2\alpha$ is equal to 1, the $C_{0\alpha}$ contains the rigidity characteristics of the rod member with an articulated joint at the two ends. It results from the $\left(1 - 12\frac{i^2}{l^2}\right) = 1$ condition that

$$12\frac{i^2}{l^2} = 0$$

The physical contents of this is easy to see if multiplying with the tensile rigidity (which can be uniformly factored o_{ut} from the matrix)

$$12\frac{IE}{l^3} = 0$$

which is true only if in the lattice mesh structure connected with ideal joints the flexural rigidity exerted against bending is JE = 0. It follows from the foregoing that $C_{1\alpha} = 0$ (after the performance of the mentioned multiplication).

b) Continuing the analysing of the characteristics of coefficient examined within the a) point we change the expression in the following way:

$$\left(E - 12\frac{E}{\lambda^2}\right) = \left(E - 12\frac{E\pi^2}{\lambda^2\pi^2}\right) = \left(E - \frac{12}{\pi^2}\sigma_k\right)$$

where

$\lambda = \frac{l}{i}$ is the slenderness of the rod member

$\sigma_k = \frac{\pi^2 E}{\lambda^2}$ is the critical tension arising when the rod buckles.

The critical tension only depends on the quality of the material and the geometric data of the rod. The geometric data can be characterised by the slenderness ratio. It can be easily ascertained that if we put the rod material far from the centre of gravity of the cross-section the load capacity of the rod will grow. This is restricted by the validity-limit of the Hooke law, so we calculate with the

$\lambda = \lambda_p = \pi\sqrt{\frac{E}{\sigma_p}}$ value, where

$\sigma_k \leqq \sigma_p$ is the limit of elasticity of the material.

In this way the material is utilized up to the limit of buckling as concerns stability and by fixing the (i) radius of inertia

$$i_{min} = \frac{l}{\pi}\sqrt{\frac{\sigma_p}{E}}$$

the most favourable material arrangement can by provided, then by determining the A (cm^2) independent variable the necessary moment of inertia can be computed on the basis of

$$I_{min} = A\,i^2\ (cm^4)$$

After these preliminary remarks the rigidity of any nodal points of the trussing can be determined by a simple mechaninical summation if we take into consideration the already laid down condition regarding the signs of the rods. Accordingly it is a symmetrical quadratix matrix with the shape

$$C = \left[\begin{array}{c|c|c} C_1 & C_4 & C_5 \\ \hline C_4 & C_2 & C_6 \\ \hline C_5 & C_6 & C_3 \end{array}\right]$$

the certain elements of which we determine by the following summation

$$C_1 = \sum_{i=1}^{m} C_{0xi} = \sum_{i=1}^{m} A_i\,(k_{i1} + k_{i2}\cos^2\alpha_i)$$

$$C_2 = \sum_{i=1}^{m} C_{0yi} = \sum_{i=1}^{m} A_i\,(k_{i1} + k_{i2}\sin^2\alpha_i)$$

$$C_3 = \sum_{i=1}^{m} C_{0zi} = \sum_{i=1}^{m} A_i\,k_{i3}$$

$$C_4 = \sum_{i=1}^{m} C_{0xyi} = -\frac{1}{2}\sum_{i=1}^{m} A_i k_{i2} \sin 2\alpha_i$$

$$C_5 = \sum_{i=1}^{m} M_{xzi} = \frac{1}{2}\sum_{i=1}^{m} A_i k_{i1} l_i \sin \alpha_i$$

$$C_6 = \sum_{i=1}^{m} M_{yzi} = \frac{1}{2}\sum_{i=1}^{m} A_i k_{i1} l_i \cos \alpha_i$$

The constans used in the relations are the following:

$$k_{1i} = 12\frac{\sigma_p}{\pi^2 l_i}$$

$$k_{2i} = \frac{E}{l_i} - 12\frac{\sigma_p}{\pi^2 l_i}$$

$$k_{3i} = 4\frac{l_i}{\pi^2}\frac{\sigma_p}{E}$$

i is the serial number of the rods being connected to the nodal point and the summation has to be carried out for all the rods (m-number) being connected to the node.

3.3 Definition of the explicit function of condition

For the explicit formulation of the (2.5) th equation determined in the 2. chapter it is necessary to have the explicit forms of $X = C^{-1}\tilde{q}$ and S A products.

As a first step with the help of symbols used in the previous chapter we determine the C^{-1} inverse matrix in the following shape

$$C^{-1} = \frac{1}{|C(t)|}\begin{bmatrix} C_1(t) & C_4(t) & C_5(t) \\ C_4(t) & C_2(t) & C_6(t) \\ C_5(t) & C_6(t) & C_3(t) \end{bmatrix}$$

where

$$C_1(t) = C_2C_3 - C_6^2 \qquad C_4(t) = -(C_4C_3 - C_5C_6)$$

$$C_2(t) = C_1C_3 - C_5^2 \qquad C_5(t) = C_4C_6 - C_2C_5$$

$$C_3(t) = C_1C_2 - C_4^2 \qquad C_6(t) = -(C_1C_6 - C_4C_5)$$

Examining from the point of view of the vector variabletit can be proved that both the elements of the adjungated matrix and the $|C(t)|$ determinant of the matrix are the functions of higher degree of the independent variable different from the linear.

By using the C^{-1} matrix the replacement-components of certain nodes of the trussing can be determined if we solve the following matrix equation:

$$\begin{bmatrix} x_1 \\ x_2 \\ x_3 \end{bmatrix} = \frac{1}{|C(t)|}\begin{bmatrix} C_1(t) & C_4(t) & C_5(t) \\ C_4(t) & C_2(t) & C_6(t) \\ C_5(t) & C_6(t) & C_3(t) \end{bmatrix}\begin{bmatrix} \tilde{q}_x \\ \tilde{q}_y \\ \tilde{q}_\varphi \end{bmatrix}$$

The elements of $\tilde{q}$ vector denote the x; y directioned component of the already defined artificial force and its turning moment around Z axle.

We can get the final result by performing the S A matrix multiplication. Similarly with the setting up of the C matrix we get two alternative solutions depending on the direction of the rod members. taking into consideration the structure of S and A matrices given for the nodal structures in : 3.1 chapter resp. the partial for the products as the result of factoring them

$$SQ = \frac{AE}{l}\begin{bmatrix} \cos\alpha & -\sin\alpha & 0 \\ 12\frac{i^2}{l^2}\sin\alpha & 12\frac{i^2}{l^2}\cos\alpha & -12\frac{i^2}{l^2}l \\ -12\frac{i^2}{l^2}\sin\alpha & -12\frac{i^2}{l^2}\cos\alpha & 4i^2 \end{bmatrix}$$

$$SAQ = \frac{AE}{l}\begin{bmatrix} \cos\alpha & -\sin\alpha & 0 \\ 12\frac{i^2}{l^2}\sin\alpha & 12\frac{i^2}{l^2}\cos\alpha & -12\frac{i^2}{l^2}l \\ -12\frac{i^2}{l^2}l\sin\alpha & -12\frac{i^2}{l^2}\cos\alpha & -2i^2 \end{bmatrix}$$

The results reached in this way are substituted into the $Y = SAX$ relation. For the sake of lucidity only the components of X are used for establishing the function. In this way, depending on the direction of the rod member we get the following result:

$$Y' = SQX' = \begin{bmatrix} N' \\ T' \\ M' \end{bmatrix} \text{ and } Y'' = SAQX'' = \begin{bmatrix} N'' \\ T'' \\ M'' \end{bmatrix}$$

The N; T; M components of the Y' and Y''vectors are the following:

$$N' = \frac{AE}{l}(X_1'\cos\alpha - X_2'\sin\alpha)$$

$$T' = 12\frac{JE}{l^3}(X_1'\sin\alpha + X_2'\cos\alpha - \frac{1}{2}X_3')$$

$$M' = 6\frac{JE}{l^2}(-X_1'\sin\alpha - X_2'\cos\alpha + \frac{2}{3}X'_3)$$

$$N'' = \frac{AE}{l}(X_1''\cos\alpha - X_2''\sin\alpha)$$

$$T'' = 12\frac{JE}{l^3}(X_1''\sin\alpha + X_2''\cos\alpha + X_3''\frac{1}{2})$$

$$M'' = 6\frac{JE}{l^2}(-X_1''\sin\alpha - X_2''\cos\alpha - X_3''\frac{1}{3})$$

The X' and X'' values are the displacement vectors of the two connecting nodes of the rod element.

As a consequence of the above mentioned the rod members of the trussing generally connect two moving off nodal points. In accordance

with this the Y (t) vector can be defined as the resultant of two partial systems of different character. Utilizing the two alternative fundamental relations we set up the stress function of the rod connecting the moving off nodes by producing the following summations:

$$Y(t) = Y'(t) + Y''(t) = \begin{bmatrix} N \\ T \\ M \end{bmatrix} = \begin{bmatrix} N' + N'' \\ T' + T'' \\ M' + M'' \end{bmatrix}$$

Substituting in the expressions determined for the respective components we get the results as seen below:

$$N = \frac{AE}{l}\left[(X'_1 + X''_1)\cos\alpha - (X'_2 + X''_2)\sin\alpha\right]$$

$$T = 12\frac{IE}{l^3}\left[(X'_1 + X''_1)\sin\alpha + (X'_2 + X''_2)\cos\alpha - (X'_3 + X''_3)\frac{l}{2}\right]$$

$$M = 6\frac{IE}{l^2}\left[-(X'_1 + X''_1)\sin\alpha - (X'_2 + X''_2)\cos\alpha + (\frac{2}{3}X'_3 - \frac{1}{3}X''_3)\,l\right]$$

With this we have reduced the producing of stress function to the algebraic summation of the displacement components of the nodal points.

The case when one end of the trussing is rigorously fixed i. e. cannot move off can be considered as a special application of the general formule. In such a case-depending on the direction of the rod in question by substituting the values of X' or X'' for zero we get the stress function resp. its appropriate components.

The tension which comes into being as a result of the loading can be determined on the basis of the unindirectional complex stress of the rod member. On the basis of the normal power influencing on the rod the

$$\sigma_1 = \frac{N}{A} = \frac{E}{l}\left[(x'_1 + x''_1)\cos\alpha - (x'_2 + x''_2)\sin\alpha\right]$$

tension comes into being. The σ_2 tension emerging under the influence of the bending moment must be added to it.

The effective stress is the greatest moment loading the rod, in the cross-section of the capture, which can be calculated from the sum of the components of thet moment which is on the left side of it. The resultant force which is on the left of the cross-section is T' resp T'', depending on the location of the origin of the co-ordinate system – i. e. on which end-point of the rod we suppose it is. The moment of the T force supposing that both ends of the rod are rigid

$$\frac{T'\,l}{2} \text{ resp. } \frac{T''\,l}{2}$$

By adding them to the adequate M' and M'' concentrated moment values we get the

$$M'_2 = \frac{T'\,l}{2} + M' = 6\frac{IE}{l^2}(\frac{2}{3}x'_3 - \frac{1}{2}x'_3)\,l = \frac{IE}{l}x'_3 \text{ resp.}$$

$$M''_2 = \frac{T''l}{2} + M'' = 6\frac{IE}{l^2}(\frac{1}{2}x''_3 - \frac{1}{3}x''_3)\,l = \frac{IE}{l}x''_3$$

expressions, from which it is easy to see that their size is decided by the rate of the X_3 angular displacement. So from the point of view of the tension-maximum the

$$\sigma_2 = \frac{M_{2max}}{l}e = \frac{E}{l}e\,|x_3|_{max}$$

relation is valid, where

e – is the exterior fibre distance of the cross-section.

The value of e is also given with the knowledge of the radius of inertia elready discussed in the 3.2 chapter, consequently it can be determined on the basis of

$$\sigma_{max} = \pm\sigma_1 \pm \sigma_2 = \frac{E}{l}\left[(x'_1 + x''_1)\cos\alpha - (x'_2 + x''_2)\sin\alpha + e\,x_{3max}\right]$$

The summation is performed only covering the tensions of the same signs and we require the equation

$$|\sigma_{max}| \leqq \sigma_{meg}$$

for the greater tension (as regards its absolute value) σ_{meg} is characteristic of the material of the trussing and means the tension which can be allowed in the material without damage.

After these preparations and using them we put down the equiponderate of condition of the rod member connecting the two nodal points

$$\sigma'_i(t) = |C'|p_i\left[Z''_{1i}(t)\cos\alpha - Z''_{2i}(t)\sin\alpha\right] + |C''|p_i\left[Z'_{1i}(t)\cos\alpha - Z'_{2i}(t)\sin\alpha + Z'_{3i}(t)\right] - |C'|\,|C''|\sigma_{meg} \leqq 0$$

which has been determined on the basis of the displacement components substituted in the σ_{max} expression and the arrangement of

$$|\sigma_{max}| - \sigma_{meg} \leqq 0$$

The contents of the used narkings will be detailed as follows:

$|C'|$ and $|C''|$ – the determinant of the matrix of rigidity concerning the two end-points of the rod member

$$Z'_{1i}(t) = C'_1(t)\tilde{q}'_x + C'_4(t)\tilde{q}'_y + C'_5(t)\tilde{q}'_z$$

$$Z'_{2i}(t) = C'_4(t)\tilde{q}_x + C'_2(t)\tilde{q}'_y + C'_6(t)\tilde{q}'_z$$

$$Z_{3i}(t) = C'_5(t)\tilde{q}'_x + C'_6(t)\tilde{q}'_y + C_3(t)\tilde{q}'_z$$

means the product-sums. The expressions with '' index are accordingly equal to the above expressions.

$p_i = \frac{E}{l_i}$ is the constant referring to the i-th rod.

In connection with the addition of $Z'_{3i}(t)$ we call the attention to the fact that when setting up the function we supposed the $(x'_3) > (x''_3)$ inequality. Inversely it is obvious that $Z''_{3i}(t)$ must be taken into consideration in the expressions of gi (t)' and in this case $Z'_{3i}(t)$ does not occur in the function. Here we mention an already discussed special version of the task. – i. e. one of the two end-points of the rod memeber is fixed, consequently unable to move off. In this case the equiponderate of condition can be formulated in the following simpler form without making any difference between the 'and'' signs.

$$g_i(t) = p_i\left[Z_{1i}(t)\cos\alpha - Z_{2i}(t)\sin\alpha + Z_{3i}(t)\right] - |C|\sigma_{meg} \leqq 0$$

Summarizing the characteristics of the scalar function determined for the $g_i(t) \leqq 0$ inequality we can state that only one $g_i(t)$ i = 1, 2 ... m) function belongs to each occuring t vector. The function defined in this way unambiguously contains all the stressing and dimensioning variables of a given structural solution. The $Z_1(t)$; $Z_2(t)$ and $Z_3(t)$ expressions occuring in the function are the quadratic functions of the independent variable so the non-linear characteristics of the $g_i(t)$ function are determined by the $|C| = |C(t)|$ determinant function.

4. Algorithms Suitable for Definition of Optimum Weight

The problems occuring in practice generally lead to a nonlinear conditional extreme-value task solution when a minimum weight of statically indeterminate structure has to be determined in case of continuons independent variables.

There are three basical groups of computer technique methods applied this time:

a) They transform the non-linear programming problem into a linear one. (6) (7) (8) These procedures are based on the fact that the steps of approximation are approaching to the solution being on the limit of permissible range.

b) Using the gradient methods (9) (10) (11) they decide such directions passing along which the value of the objective function is gradually reducing,

c) The third group of non-linear programming solutions is based on the so called „penalty" function technique (12) (13) (14) (15). A common feature of these procedures is that they transform the objectional extreme-value-tasks into non-conditional ones.

Summing up the solution-methods of the enumerated non-linear programming tasks it can be proved that the application of linearing formules and grandient methods is justified first of all when the functions of condition of the structure to be optimized can be well approached by means of a linear function. The application of correctional functions are effective when neither the objective function nor the functions of condition are linear.

The bus carcass elements are of mixed construction i.e. they contain structural elements of both compression-tension and complex load. So there can be found characteristics of two kinds: either characteristics approaching to the linear or other ones different from it at a great extent.

For solving these problems the linearized centre-method is used, worked out by P Huard (16). Namely according to this method in the course of optimization in each step we perform only one simplex procedure and one minimalization along section. This makes possible that the method is well applicable also in case of a great number of independent variables and, on the other hand, because of the already mentioned mechanical characteristics of the task it is well adjusted to the special characteristics of the task.

We got computational experiences in cases of different structures and different load conditions. One of these solved problems was a minimum-weight design of a bar structure being part of a Hungarian IKARUS bus.

References

(1) Gallagher R.H., Finite-Element-Analysis, Springer-Verlag Berlin Heidelberg New York 1976.

(2) Pestel, E.C., Leckie, A., Matrix metjods in elastomechanics, McGraw-Hill, New York (1963).

(3) Szabó, J., Roller, B., Rúdszerkezetek elmélete és számítása, Műszaki Könyvkiadó, Budapest (1963).

(4) Halmos, E., Rapcsák, T., Minimum weight design of the statically indeterminate trusses, Mathematical Programming Study 9,109–119 (1978).

(5) Bernau H., Halmos E., Dimensioning of Statistically Indeterminate Lightweight Structures of Complex Stress on the Basis of Minimum – Weight Conditions, MTA SZTAKI Working paper MO/17. (1980)

(6) Reinschmidt, K.F., Russel, A.D., Application of Linear Programming in Structural Layout and Optimization, Computer and Structures, Vol. 4(855–869). Pergamon Press (1974).

(7) Farshi, B., Schmidt, L.A., Minimum weight design of trusses, Journal of the Structural Division I (1974).

(8) Moses, F., Optimum structural design using linear programming, Journal of the Structural Division 12 (1964).

(9) Avriel, M., Nonlinear Programming, Analysis and Methods, Prentice Hall, Englewood, New Jersey (1976).

(10) Bazaraa, M.S., Shetty, C.M., Nonlinear Programming, Theory and Algorithms, John Wiley and Sons; New York (1979).

(11) Gill, P.E., Murray, W., Methods for constrained Optimization, Academic Press, London–New York–San Francisco (1974).

(12) Fiacco, A.V., McCormick, G.P., Nonlinear sequential unconstrained minimization techniques, John Wiley and Sons, New York (1968).

(13) Pierre, D.A., Lowe, M.J., Mathematical programming via augmented Lagrangians. An introduction with computer programs, Addison–Wesley Publ. Comp., Reading, Mass. (1975).

(14) Biggs, M.C., On the convergence of some constrained minimization algorithms based on recursive quadratic programming, J.Inst. Maths.Appls. Vol.21, No.1., 67–82 (1978).

(15) Miele, A., Cragg, E.E., Iver, R.R., Levy, A.V., Use of the augmented penalty function in mathematical programming problems, Part I and Part II, J.Optimization Theory and Appl. 8(115–153) (1971).

(16) Huard, P., Programmation mathematique convex, Revue Francaise d' Informatique et de Recherche Operationelle 7, 43–59 (1968).

SESSION #8

MATHEMATICAL PROGRAMMING I

THE UTILITY OF NONLINEAR PROGRAMMING METHODS FOR ENGINEERING DESIGN

K. M. Ragsdell, P.E.
School of Mechanical Engineering
Purdue University
West Lafayette, Indiana
U.S.A.

AD-P000 046

Abstract

Herein is considered the relative merits of modern optimization methods for engineering design applications. The design and implementation of two major comparative experiments is reviewed in detail. These studies took place at Purdue University. The first, an investigation of the merits of general purpose nonlinear programming codes with major funding from the National Science Foundation, was conducted over the period 1973 to 1977. The second, an investigation of the relative merits of verious geometric programming strategies and their code implementations with funding from the Office of Naval Research, was conducted over the period 1974 to 1978. The various major decisions associated with such studies are discussed; such as the selection and collection of problems and codes, the nature of data to be collected, evaluation criteria, ranking schemes, presentation and distribution of results, and the technical design of the experiment itself. The statistical implications of the results in light of the experiment design are examined; as are the effects of various experiment parameters such as number of variables, number of constraints, degree of nonlinearity in the objective and constraints, and starting point placement.

The NSF Study

In this study we considered methods which address the *nonlinear programming problem* (NLP):

$$\text{MINIMIZE:} \quad f(x) \quad ; \quad x \in R^N \tag{1}$$

$$\text{subject to:} \quad g_j(x) \geq 0 \qquad j=1,2,3,\ldots,J \tag{2}$$

$$h_k(x) \equiv 0 \qquad k=1,2,3,\ldots,K \tag{3}$$

$$\text{and} \quad x_i^{(\ell)} \leq x_i \leq x_i^{(u)} \qquad i=1,2,3,\ldots,N \tag{4}$$

given $x^{(0)}$, an initial estimate of the solution, x^*, a Kuhn-Tucker point.

Before coming to Purdue, I, as most others interested in nonlinear programming, was aware of the pioneering work of Al Colville of IBM [1]. Colville sent eight problems having from three to sixteen design variables and a standard timing routine to the developers of thirty codes. Each participant was invited to submit his "best effort" on each problem, and the time required to execute the standard timing routine on his machine. One can only marvel at the economic wisdom of Colville's decision to send the problems around rather than collect the codes and run the tests himself. Unfortunately, this approach contains at least three flaws. Eason [2] has shown that Colville's *timing routine does not adequately remove the effect of compiler and computing machine selection on code performance.* Accordingly, the data collected at one site in the Colville study is not comparable to data collected at another. Furthermore, each participant was allowed to attack each problem as many times as he felt necessary in order to optimize the performance of his code. Thus another investigator could not reasonably expect to produce similar results with the same code in the absence of the special insight which only its originator would possess. Finally, and possibly most importantly, no two participants reported solutions to the same accuracy, which in our experience is a major difficulty in fair comparison. These shortcomings cast a very real shadow on the validity of the Colville results and conclusions. Quite unfortunately from the scientific point of view the Colville experiment was not repeatable, so that it was essentially impossible for latter investigators to confirm his findings directly. In 1974 Eason and Fenton [3] reported on a comparative study of twenty codes on thirteen problems. Dr. Eason did his testing on one machine, and included in his test set the Colville problems plus several problems from mechanical design. The major contribution of the Eason study is the introduction of error curves, which allow convenient comparison of codes at exactly the same error criteria. The major shortcomings are the lack of difficulty in the problem set and the failure to include the more powerful algorithms. There have been other important studies reported [4,5,6,7,8,9,10,11], but the work of Colville and Eason have had the most profound impact on the work reported here.

Major Objectives of Study:

The major goal of this study was to discern the utility of the world's leading NLP methods for use in engineering design. A secondary objective was to design the experiment and present the results so as to enhance the utility of the results and conclusions in an industrial environment. Theoretical convergence rates were and are of little importance to me. I wanted to rate the methods in a manner that would allow a typical designer to choose the appropriate method or possibly class of methods for his particular problem. It seemed desirable to include an many current industrial problems and codes in the experiment as possible. Industry supported the work by contributing codes, problems and by direct financial support of visits in the summers. I spent two summers in industry during the study helping to formulate problems and collecting codes. The companies who contributed most to the study are Whirlpool Corporation, Honeywell Corporation, York Division of Borg Warner, and Gulf Oil Corporation. The same person, Eric Sandgren, performed all of the numerical experiments, and all calculations were performed on the same machine using the same compiler, a CDC-6500 at Purdue University. Furthermore, the student was not involved in algorithm development. The major steps in the study were:

1. assemble codes and problems.
2. qualify codes via preliminary test set of 14 problems.
3. apply 24 qualified codes to full 35 problem test set.
4. eliminate problems on which fewer than 5 codes were successful.
5. compile and tabulate results for 24 codes on 23 problems.
6. prepare individual and composite utility curves.

Results are presented graphically, as seen in Figure 1 and hopefully in a useful form for engineering designers.

Major Conclusion:

We were able to confirm the major conclusion of the Colville study; that is, that the Generalized Reduced Gradient codes are superior as a class to the others tested. Sandgren [12] shows that the trends are statistically significant.

The ONR Study

In this study we considered methods which address the prototype posynomial geometric programming problem (GP):

MINIMIZE: $g_o(x)$; $x \epsilon R^N$ (5)

subject to $g_k(x) \leq 1$ $k=1,2,3,\ldots,K$ (6)

and $x_i > 0$ $i=1,2,3,\ldots,N$, (7)

where the posynomial functions $g_k(x)$ are defined as:

$$g_k(x) = \sum_{t=s_k}^{T_k} c_t \prod_{n=1}^{N} x_n^{a_{nt}} \quad (8)$$

with specified positive coefficients c_t and specified real exponents a_{nt}. The term indices t are defined as:

$$s_0 = 1 \quad (9)$$

$$s_{k+1} = T_k + 1 \quad (10)$$

$$T_K = T \quad (11)$$

This problem is in general a non-convex programming problem which because of the nonlinearities of the constraints can be expected to severely tax conventional nonlinear programming codes. However, despite the apparent difficulty of the primal problem, there are structural features of the generalized posynomial functions which can be exploited to facilitate direct primal solutions. In addition various transformations can be employed to give equivalent formulations. The additional formualtions which we considered in this study are:

1. The Convexified Primal

   This formulation results from the transformation $x_i = e^{z_i}; i=1,2,3,\ldots,N$.
   The new functions of z become convex functions.

2. The Transformed Primal

   The additional transformation, $w = A^T Z + \ell nc$ gives this formulation.

3. The Dual

   The relationship of the dual and primal is well known.

4. The Transformed Dual

   An alternate way of formulating the dual program is to eliminate the linear equality constraints by solving them for the dual variables in parametric form. Using this device the dual variable δ_t can be expressed as the sum of a particular solution and a linear combination of T-N-1 homogeneous solutions of the N+1 dual constraints.

Major Objectives of Study:

The goals of this study were to determine:

1. Whether the constructions resulting from GP theory offer any computational advantages over conventional NLP methodology.
2. Which of the various equivalent GP problem formulations are preferable and under what conditions.
3. Which GP algorithm/formulation combination is most likely to be successful for a given problem.
4. Whether a criteria can be defined by means of which GP problem difficulty can be gauged.

In designing this experiment, we attempted to rectify some of the inadequacies of previous studies. In particular we did the following:

1. Used a large number (42) of problems, with randomly generated starting points (up to 20 per problem).
2. Results were obtained at several precise error levels.
3. Execution time is measured such that starting point generation and extraneous I/O is excluded.
4. Designed the tests such that formulation effects can be separated from algorithm effects.
5. Finally appropriate statistical tests were used for the comparisons.

The Major Conclusions of This Study are:

1. the convex primal is inherently the most advantageous formulation for solution.
2. a general purpose GRG code applied to the convex primal will dominate even the reputedly best specialized GP codes currently available.
3. the differences between the primal and convex primal formulations lie mainly in scaling and function evaluation time.
4. transformed primal solution approaches are not likely to lead to more efficient GP solution than the convex primal.
5. the dual approaches are only likely to be competitive for small degree of difficulty, tightly constrained problems.
6. posynomial GP problem difficulty as measured in solution time is best correlated to an exponential of the number of variables in the formulation being solved and is proportional to the total number of multi-term primal constraints.

Other Experiments

Schittkowski [13] has recently completed an experiment which is similar in many ways to the Sandgren study. He gives results for the latest successive quadratic programming algorithms [14] and has proposed a model [15] for the conduct of future studies. In addition the recent comparison of "reduction methods" of G. Van der Hoek [16] is examined. Finally the work of Root [17] and Gabriele [18] is considered in light

of structural applications. In particular Gabriele's modification of the Generalized Reduced Gradient method to exploit sparcity in structural applications is reviewed.

References

1. Colville, A.R., "A Comparative Study on Nonlinear Programming Codes", Proceedings of the Princeton Symposium on Mathematical Programming, Kuhn, H.W., ed., Princeton, N.J., pp. 481-501, 1970.

2. Eason, E. D., "Validity of Colville's Time Standardization for Comparing Optimization Codes", ASME Design Engineering Technical Conference, Chicago, September 1977, 77-DET-116.

3. Eason, E. E. and Fenton, R. G., "A Comparison of Numerical Optimization Methods for Engineering Design", ASME Journal of Engineering for Industry, Series B, Vol. 96, No. 1, Feb. 1974, pp. 196-200.

4. Stocker, D. C., "A Comparative Study of Nonlinear Programming Codes", M.S. Thesis, The University of Texas, Austin, Texas, 1969.

5. Himmelblau, D. M., Applied Nonlinear Programming, McGraw-Hill, New York, 1972, pp. 368-369.

6. Pearson, J. D., "Variable Metric Methods of Minimization", Computer Journal, Vol. 12,1969, pp. 171-178 178.

7. Huang, H. Y., and Levy, A. V., "Numerical Experiments on Quadratically Convergent Algorithms for Functional Minimization", JOTA, Vol. 6, 1970, pp. 269-282.

8. Murtagh, B. A., and Sargent, R. W. H., "Computational Experience with Quadratically Convergent Minimization Methods", Computer Journal, Vol. 13, 1970, pp. 185-194.

9. Pappas, M. and Moradi, J. Y., "An Improved Direct *Search Mathematical Programming Algorithm*", Journal of Engineering for Industry, Trans, ASME, Series B, Vol. 97, No. 4, Nov. 1975, pp. 1305-1310.

10. Schuldt, S. B., Gabriele, G. A., Root R. R., Sandgren, E. and Ragsdell, K. M., "Application of a New Penalty Function Method to Design Optimization", Journal of Engineering for Industry, Trans. ASME, Series B, Vol. 99, No. 1, Feb. 1977, pp. 31-36.

11. Gabriele, G. A. and Ragsdell, K. M., "The Generalized Reduced Gradient Method: A Reliable Tool for Optimal Design", Journal of Engineering for Industry, Trans. ASME, Series B, Vol. 99, No. 2, May 1977, pp. 394-400.

12. Sandren, E. "A Statistical Review of the Sandgren-Ragsdell Comparative Study", Mathematical Programming Society COAL Meeting, Boulder, CO, Jan. 5-6, 1981.

13. Schittkowski, K., "Nonlinear Programming Codes: Information, Tests, Performance", Lecture Notes in Economics and Mathematical Systems, Vol. 183, Springer-Verlag, Berlin, 1980.

14. Powell, M. J. D., "A Fast Algorithm for Nonlinearly Constrained Optimization Calculations," Proceedings of the 1977 Dundee Conference on Numerical Analysis, Springer-Verlag, Berlin, 1978.

15. Schittkowski, K., "A Model for the Performance Evaluation in Comparative Studies", Mathematical Programming Society COAL meeting, Boulder, CO., Jan. 1981.

16. Van der Hoek, G., Reduction Methods in Nonlinear Programming, Mathematical Centre Tract 126, Mathematisch Centrum, Amsterdam, 1980.

17. Root, R. R., "An Investigation of the Method of Multipliers", Ph.D. Dissertation, Purdue University, 1977.

18. Gabriele, G. A. and Ragsdell, K. M., "Large Scale Nonlinear Programming Using the Generalized Reduced Gradient Method", ASME Journal of Mechanical Design, Vol. 102, No. 3, July 1980, pp. 566-573.

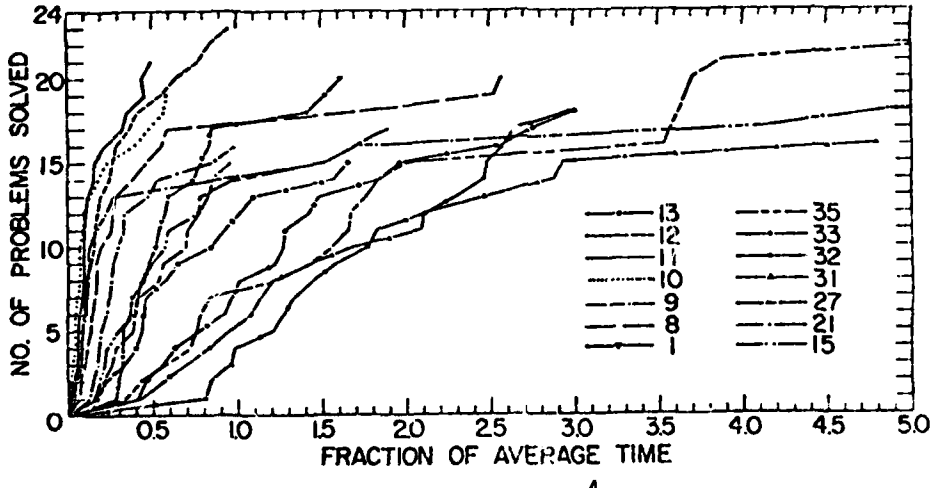


Fig. 1 Algorithm utility ($\epsilon_t = 10^{-4}$)

AD-P000 067

APPLICATION OF A REDUCED QUADRATIC PROGRAMMING TECHNIQUE TO OPTIMAL STRUCTURAL DESIGN

Nien-Hua Chao , Graduate student , Mechanical Engr
S. J. Fenves , University Professor, Civil Engr. Dept.
A. W. Westerberg , Professor , Chemical Engr. Dept.
Carnegie-Mellon University , Pittsburgh, Pa. 15213

Abstract

A recently developed optimization technique of great practical potential will be presented. The technique is based on two developments. First, it utilizes a successive Quadratic Programming algorithm originally presented by Han and implemented by Powell for solving nonlinear constrained optimization problems. A Quasi-Newton method is used to approximate the Hessian matrix, resulting in near- quadratic convergence to at least a local optimum. Second, the procedure uses the work of Berna et al., who developed a decomposition procedure for the Han-Powell algorithm. The procedure partitions the original design variables into independent and dependent variables, eliminates the dependent variables, and thus yields a much reduced Quadratic Programming problem to be solved at each iteration.

Results obtained with the technique for a number of standard test problems, which include the 10 bar truss, the 25 bar truss and the 72 bar truss problems, are in agreement with previous results and show a general reduction of the number of cycles to convergence, especially for the optimal structural design problems with stress constraints only.

Introduction

The general optimal structural design problem is to minimize a measure of the cost of the structure subject to applicable performance requirements. In most of the literature, the cost function is taken as the weight (or volume) of the structure, the design variables are separated into element size parameters (e.g., cross-sectional area) and structure configuration parameters (e.g., joint coordinates), and the performance requirements include behavior constraints on the stress in each element and on the displacements of certain joints, as well as the usually implicit equality constraints arising from the joint equilibrium equations.

One popular approach for solving optimal structural design problems is to formulate them as a sequence of mathematical programming subproblems . Numerous papers ([1] - [11]) use a variety of such mathematical programming techniques.

The purpose of this paper is to introduce and illustrate a recently developed optimization technique of great practical potential. The technique is based on two developments. First, it utilizes a fast successive quadratic programming algorithm originally stated by Han [12] and implemented by Powell ([13]-[20]) for solving nonlinear constrained optimization problems. The algorithm uses a Quasi-Newton method to approximate the Hessian matrix, resulting in near-quadratic convergence to at least a local optimum. Second, the technique uses the work of Berna et al.[21], who developed a decomposition procedure for Powell's algorithm which partitions the original design variables into independent and dependent variables and eliminates the dependent variables, thus yielding a much reduced quadratic programming subproblem at each step.

The technique is first derived and then illustrated using problems previously presented in the structural optimization literature. The examples all deal with the simplest structural application of the technique, namely element size parameter optimization for trusses. Extensions of the technique, including additional structural types (plane frames and systems of finite elements) combined with configuration optimization, will be presented in later papers.

Optimization Problem

The optimal structural design problem is stated as follows:

(P1) Find the vector of variables Y which minimizes an objective function F(Y) subject to the constraints

$$g_i(Y) = 0 \qquad i = 1,\ldots,m \tag{1a}$$

$$h_i(Y) \le 0 \qquad i = m+1,\ldots,m \tag{1b}$$

Where $F, g_1,\ldots,g_m, h_{m+1},\ldots,h_m$ denote real-valued functions of the vector Y in N-dimensional Euclidean space R^N.

In the specific case of element size parameter optimization using an elastic finite element model, the vector Y contains both the element size parameters and the joint displacements. In this case, the equality constraints (1a) are given by the system equilibrium equations:

$$g = [\,K\,]\{\,u\,\} - \{\,P\,\} \tag{2}$$

where K = structure stiffness matrix
u = vector of joint displacements
P = vector of applied joint loads.

The inequality constraints (1b) are of the form

$$h_i = s_i - s_{iL} \quad \text{or} \quad s_{iU} - s_i \tag{3}$$

where s_{iL} and s_{iU} are upper and lower limits on the behavior variable s_i. For structural optimization, the constraints pertain to element stresses and joint displacements. In the former case, the controlling stresses in element i can be computed as

$$s_i = [\,\Pi_i\,]\,T_i\,a_i\,\{\,u\,\} \tag{3a}$$

where Π_i = modulus matrix
T_i = coordinate transformation matrix of element i
a_i = branch-node incidence matrix of element i

The equality constraint equations (2) are bi-linear in the variables Y, as the element stiffnesses k_i entering into [K] are linear functions of the element size parameters. The modulus matrices Π_i for certain element types, e.g. trusses, are independent of the element size parameters, which can be demonstrated as follows:

a) In a basic local coordinate system, the element force, R_i, is

$$R_i = [\,k_i\,]\,T_i\,a_i\,\{\,u\,\} = [\,EA_i/L_i\,]\,T_i\,a_i\,\{\,u\,\} \tag{4}$$

where E = Young's modulus

A_i = cross-sectional area of element i

L_i = length of element i

b) The controlling bar stress, s_i, is

$$s_i = R_i/A_i = (1/A_i)\,[\,EA_i/L_i\,]\,T_i\,a_i\,\{\,u\,\} = E/L_i\,T_i\,a_i\,\{\,u\,\} = \Pi_i\,T_i\,a_i\,\{\,u\,\} \tag{5}$$

where $\Pi_i = E/L_i$

The inequality constraints are thus linear functions of the joint displacements u, and therefore of Y.

The non-linearity of equations g in the variables Y and the very large number of constraint equations makes the direct solution

PRECEDING PAGE

of (P1) infeasible or economically impractical. One step that may be taken to reformulate (P1) so as to reduce the problem dimensions is to take advantage of symmetry and repetition of identical components to link together some design variables Y_i as a function of distinct design variables X_j, i.e., to set

$$\{ Y \} = [L] \{ X \} \tag{6}$$

$$i = 1,2,\ldots\ldots\ldots,n,$$
$$j = 1,2,\ldots\ldots\ldots,n$$
$$n << n$$

It is to be noted that only the element size parameters A_i may be linked together by Equation (6) ; all the joint displacements must be retained as distinct design variables in X. Further steps in reducing the problem dimensions will be introduced later.

The design problem now becomes :

$$\begin{aligned} &(P2) \text{ Minimize } F(X) \\ &\quad \text{Subject to } g(X) = 0 \\ &\qquad\quad h(X) \le 0 \end{aligned} \tag{7}$$

The general form of the vector { X } is { A^T ; u^T }

where { A } = vector of element size parameters
(cross-sectional areas for trusses)
{ u } = vector of joint displacements

The Lagrangian function of problem (P2), which will be used later, is

$$L(X, \mu, \eta) = F(X) + \mu^T * g(X) + \eta^T * h(X) \tag{8}$$

where μ , η are vectors of Lagrangian and Kuhn-Tucker multipliers, respectively.

Quadratic Problem Formulation

Han [12] has suggested that the nonlinear optimization problem (P2) can be solved by generating a sequence of points { X^k } which are the solutions to the following quadratic approximation programming subproblem:

(P3) Minimize

$$\nabla F(X^k)^T * (\Delta X) + 1/2 * (\Delta X)^T * H_k * (\Delta X)$$

subject to :

$$\begin{aligned} &g(X^k) + \nabla g(X^k)^T * (\Delta X) = 0.0 \\ &h(X^k) + \nabla h(X^k)^T * (\Delta X) \le 0.0 \end{aligned} \tag{9}$$

where $\Delta X = X^{k+1} - X^k$

$$\nabla F = \frac{\partial F}{\partial X}$$
$$\nabla g = \frac{\partial g}{\partial X^T}$$
$$\nabla h = \frac{\partial h}{\partial X^T}$$

The n x n matrix H_k is intended to be an approximation of the Hessian matrix of the Lagrangian function of problem (P2). In Han's original work, the Hessian matrix is updated by the Davidon-Fletcher-Powell [22] method. Powell has used Han's method to solve optimization problems with nonlinear constraints [13]-[20] with the Hessian matrix approximated by a Quasi-Newton method. Powell suggests an emprical rule so that the updated Hessian matrix remains positive definite or positive semi-definite. A Quasi-Newton method which was simultaneously presented by Broyden, Fletcher, Goldfarb and Shanno (BFGS) [22] has been used in his study. Numerical results have proven that the efficiency of Han's method can be improved by Powell's modifications [13].

Reduced Quadratic Problem Formulation

Berna et al. have suggested a decomposition procedure whereby the optimization problem (P3) can be solved more efficiently [21]. In Berna's work, the design variables { ΔX } are partitioned into two subvectors, the vector { ΔA } of independent variables and the vector {Δu} of dependent variables.

The necessary conditions for solving the quadratic approximation problem (P3) are as follows :

(1) Stationary condition of the Lagrangian function of the quadratic approximation problem (P3):

$$\left[H_k \right] \begin{Bmatrix} \Delta A \\ \Delta u \end{Bmatrix} + \begin{bmatrix} \frac{\partial g}{\partial A}^T \\ \frac{\partial g}{\partial u}^T \end{bmatrix} \{ \mu \} + \begin{bmatrix} \frac{\partial h}{\partial A}^T \\ \frac{\partial h}{\partial u}^T \end{bmatrix} \{ \eta \} = - \begin{Bmatrix} \frac{\partial F}{\partial A} \\ \frac{\partial F}{\partial u} \end{Bmatrix} \tag{10}$$

(2) Satisfaction of the linearized original constraint equations:

$$\begin{aligned} &\frac{\partial g}{\partial A^T} \Delta A + \frac{\partial g}{\partial u^T} \Delta u + g = 0 \\ &\frac{\partial h}{\partial A^T} \Delta A + \frac{\partial h}{\partial u^T} \Delta u + h \le 0 \end{aligned} \tag{11}$$

(3) Complementary slackness and nonnegativity of the Kuhn-Tucker multipliers:

$$\eta^T \left[\frac{\partial h}{\partial A^T} \Delta A + \frac{\partial h}{\partial u^T} \Delta u + h \right] = 0 \tag{12}$$

$$\eta \ge 0$$

It is easier to present the remainder of the derivation if the following notation is adopted :

$$H_{AA} = \frac{\partial^2 L}{\partial A \partial A^T} \qquad H_{Au} = \frac{\partial^2 L}{\partial A \partial u^T}$$
$$H_{uA} = \frac{\partial^2 L}{\partial u \partial A^T} \qquad H_{uu} = \frac{\partial^2 L}{\partial u \partial u^T}$$
$$G_A = \frac{\partial g}{\partial A^T} \qquad G_u = \frac{\partial g}{\partial u^T}$$
$$h_A = \frac{\partial h}{\partial A^T} \qquad h_u = \frac{\partial h}{\partial u^T}$$
$$F_A = \frac{\partial F}{\partial A} \qquad F_u = \frac{\partial F}{\partial u}$$

Using the above notation, the necessary conditions given by Equations (10) through (12) are as follows (rows and columns of the coefficient matrix are numbered for later reference):

$$\begin{array}{c} \\ (1) \\ (2) \\ (3) \\ (4) \end{array} \begin{array}{c} \begin{array}{cccc} (1) & (2) & (3) & (4) \end{array} \\ \begin{bmatrix} H_{AA} & H_{Au} & G_A^T & h_A^T \\ H_{uA} & H_{uu} & G_u^T & h_u^T \\ G_A & G_u & 0 & 0 \\ h_A & h_u & 0 & 0 \end{bmatrix} \end{array} \begin{Bmatrix} \Delta A \\ \Delta u \\ \mu \\ \eta \end{Bmatrix} \begin{array}{c} = \\ = \\ = \\ \le \end{array} \begin{Bmatrix} -F_A \\ -F_u \\ -g \\ -h \end{Bmatrix} \tag{13}$$

$$\eta^T \begin{bmatrix} h_A & h_u & I \end{bmatrix} \begin{Bmatrix} \Delta A \\ \Delta u \\ h \end{Bmatrix} = 0 \quad \text{and} \quad \eta \ge 0$$

The size of the coefficient matrix in Equation (13) is extremely large. The major contribution by Berna et. al. is the *procedure for eliminating the dependent variables {u} efficiently*, resulting in a much reduced quadratic programming problem. The reduction is accomplished in two steps.

The rows and columns in Equation (13) are first rearranged as shown:

$$
\begin{array}{c}
(2)\ (3)\ (1)\ (4) \\
\begin{matrix}(3)\\(2)\\(1)\\(4)\end{matrix}
\begin{bmatrix} G_u & 0 & G_A & 0 \\ H_{uu} & G_u^T & H_{uA} & h_u^T \\ H_{Au} & G_A^T & H_{AA} & h_A^T \\ h_u & 0 & h_A & 0 \end{bmatrix}
\begin{Bmatrix} \Delta u \\ \mu \\ \Delta A \\ \eta \end{Bmatrix}
\begin{matrix} = \\ = \\ = \\ \le \end{matrix}
\begin{Bmatrix} g \\ -F_u \\ -F_A \\ -h \end{Bmatrix}
\end{array}
\qquad (14)
$$

$$
\eta^T \begin{bmatrix} h_A & h_u & I \end{bmatrix} \begin{Bmatrix} \Delta A \\ \Delta u \\ h \end{Bmatrix} = 0 \quad \text{and} \quad \eta \ge 0
$$

Next a reduction or condensation is performed on the first two matrix columns of Equation (14), producing :

$$
\begin{bmatrix} I & 0 & M_1 & 0 \\ 0 & I & M_2 & N_1 \\ 0 & 0 & \hat{H} & Q \\ 0 & 0 & Q^T & 0 \end{bmatrix}
\begin{Bmatrix} \Delta u \\ \mu \\ \Delta A \\ \eta \end{Bmatrix}
\begin{matrix} = \\ = \\ = \\ \le \end{matrix}
\begin{Bmatrix} m_1 \\ m_2 \\ \hat{q} \\ \hat{h} \end{Bmatrix}
\qquad (15)
$$

The terms appearing in Equation (15) are defined in Appendix A.

The conditions that the quadratic programming problem must satisfy are then given by the last two rows of Equation (15) :

$$
\begin{bmatrix} \hat{H} & Q \\ Q^T & 0 \end{bmatrix}
\begin{Bmatrix} \Delta A \\ \eta \end{Bmatrix}
\begin{matrix} = \\ \le \end{matrix}
\begin{Bmatrix} \hat{q} \\ \hat{h} \end{Bmatrix}
\qquad (16)
$$

The original complementary slackness conditions, Equation (12), become

$$\eta^T * (Q^T * \Delta A - \hat{h}) = 0$$

Again, nonnegativity of the Kuhn-Tucker multipliers in Equation (12) gives $\eta \ge 0$

The reduced QPP is, therefore :

(P4) Minimize

$$F(\Delta A) = \hat{q}^T * \Delta A + 1/2 * \Delta A^T * \hat{H} * \Delta A \qquad (17)$$

subject to

$$Q^T * \Delta A \le \hat{h}$$

The corresponding Lagrangian function is

$$L (\Delta A, \eta) = \hat{q}^T * \Delta A + 1/2 * \Delta A^T * \hat{H} * \Delta A + \eta^T * (Q^T * \Delta A - \hat{h}) \qquad (18)$$

The optimization design problem(P4) can now be solved in terms of the independent design variables { ΔA }. The results,{ ΔA } and { η }, of problem (P4) can then be used to calculate the vectors { Δu } and { μ } in the first two rows of the Equation (15), thus completing the solution of the quadratic approximation subproblem.

Active Constraints

In applying the reduced quadratic programming technique presented above to optimal structural design, the number of constraint equations $Q^T * \Delta A \le \hat{h}$ may be 10 to 100 times larger than the number of independent design variables { ΔA }. To further reduce the problem dimensions, in each iteration only the critical and potentially critical constraint equations are included, so that only about 5% to 30% of the original number of constraint equations is used in each iteration.

Controlling the Step Size

In optimal structural design problems which include both stress and displacement constraints, the optimal solution is usually found at an interior point of the design space such that the total number of active constraint equations is less than the total number of independent design variables. In such situations, Powell's algorithm [13] may not converge.

To control the step size of the independent design variables and to stablize the algorithm, a constraint of the form

$$1/2 \{ \Delta A^T \} * \{ \Delta A \} \le \epsilon \qquad (19)$$

may be added to the problem (P4).

Adding constraint (19) to the problem results in adding a diagonal matrix $\pi * [I]$ to the Hessian of the reduced quadratic problem, where π (≥ 0) is the Kuhn-Tucker multiplier for the above constraint. Rather than chosing ϵ we can treat π as an adjustable parameter, to be increased if we wish to reduce the step size and decreased if we wish to allow for larger steps. A minimum value of zero for π releases the step size constraint completely.

No automatic adjustment algorithm for π has been developed to date, but one similar to that used by Reid [23] and Westerberg [24] could be devised. Such an algorithm would increase π if the actual change in the Lagrangian function for the step taken is significantly different from the value predicted by the linearized Lagrangian function, hold π fixed if the linearization is moderately acceptable, and decrease π (to zero perhaps) if the linearization is excellent. The addition of a diagonal matrix to the approximated Hessian matrix H_k also stabilizes the algorithm. The updating procedure assures that the Hessian matrix H_k remains symmetric and positive definite (see Appendix C), but in the limit it may make H_k nearly singular (positive semi-definite). We have on occasion found it effective to have a small diagonal term in the approximated Hessian matrix to control the conditioning.

Inconsistent Constraints

In solving the reduced quadratic programming problem (P4), inconsistent constraints may exist among the set of linearized constraint equations ($Q^T * \Delta A \le \hat{h}$). This inconsistency arises from using the linearized constraints to substitute for the original constraints, when the initial guess or an itermediate solution is too far from the optimum solution. Powell [13] introduced a dummy variable ξ ($0.0 \le \xi \le 1.$) to the quadratic programming problem to solve this problem.

By adding the variable ξ to the reduced QPP , Equation (16) can be rewritten as follows:

$$
\begin{bmatrix} \hat{H} & 0 & Q_1 & Q_J \\ 0 & 1 & \hat{h}_1^T & 0 \\ Q_1^T & \hat{h}_1 & 0 & 0 \\ Q_J^T & 0 & 0 & 0 \end{bmatrix}
\begin{Bmatrix} \Delta A \\ \xi \\ \eta_1 \\ \eta_J \end{Bmatrix}
\begin{matrix} = \\ = \\ \le \\ \le \end{matrix}
\begin{Bmatrix} \hat{q} \\ C \\ \hat{h}_1 \\ \hat{h}_J \end{Bmatrix}
\qquad (20)
$$

where C = large negative constant

$$\hat{h}_1 < 0.0$$

$$\hat{h}_j \ge 0.0$$

and a feasible solution can always be found for Equation (20).

Implementation

The complete algorithm for applying the reduced quadratic programming technique to optimal structural design is described in Appendix B. A modular software system is being developed to implement the technique. The main feature of the system is that only the subroutines for generating the matrices k_1, T_1 and Π_1 and their derivatives need to be compiled with the system for each different structural type.

Examples

Three truss examples previously reported in the literature have been chosen to test the accuracy and efficiency of the program.

Example 1 is a ten bar planar cantilever truss shown in Figure 1, previously used by Schmit[3],Khan[25] and others. Design and loading data are given in Table 1.

Example 2 is a twenty-five bar transmission tower truss, shown in Figure 2, previously studied by Schmit[3],Arora[4] and others. The design data and the two loading conditions applied are given in Table 2. The elements are linked into eight groups as in Reference [3].

Example 3 is a seventy-two bar space truss, shown in Figure 3, previously studied by Schmit[3],Arora[4] and others. Design and loading data are given in Table 3. The elements are linked into sixteen groups as in Reference [3].

For each of the three examples, two cases were investigated: **Case 1**, using element stress constraints only and **Case 2**, with displacement constraints included.

Results

The results obtained for the three examples are shown in Tables 4 through 6, showing the final areas, the total weight, and the number of cycles to convergence. The optimal results for Case 2 of the three examples are compared to published results in Tables 7 through 9.

It can be seen from the tables that the technique presented converges in all cases to the same optimum point as the previous studies. It can also be seen that with one exception (Venkayya [1] on Example 2), the present technique requires fewer cycles to converge to an approximate optimal point[1] than the fastest of the previous methods.

Conclusion

A fast optimization technique for optimal structural design has been presented. The speed of the technique derives from two key factors: first, the dependent design variables are eliminated or condensed out of the quadratic approximation subproblems, and second, near-quadratic convergence for the independent design variables is obtained. The technique appears to be particularly attractive for large-scale optimal structural design problems, since all joint displacements (a subvector of length equal to the number of degrees of freedom times the number of loading conditions) are eliminated, resulting in a reduced quadratic programming subproblem involving only the distinct element sizing parameters as design variables.

Results obtained with the technique for a number of standard test problems are in agreement with previous results and show a general reduction in the number of cycles to convergence.

We are currently extending the algorithm and software system to handle additional structural types, as well as configuration optimization combined with parameter optimization. At the same time, we are exploring additional techniques to further increase speed and capacity, such as the use of sparse matrix techniques for the elimination of the dependent variables.

An interesting consequence of the optimization technique described is that the solution of each quadratic approximation subproblem may not be a feasible one unless the optimum is reached. Specifically, a trial solution given in terms of the current variables { A } and { u } is not in equilibrium with the applied joint loads P.

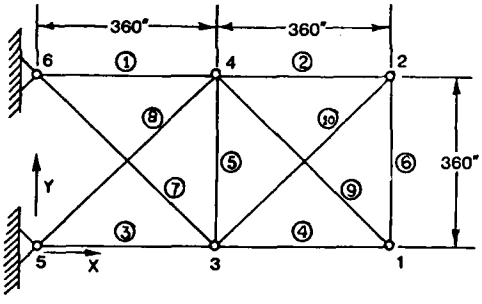


Figure 1. 10 Bar Truss

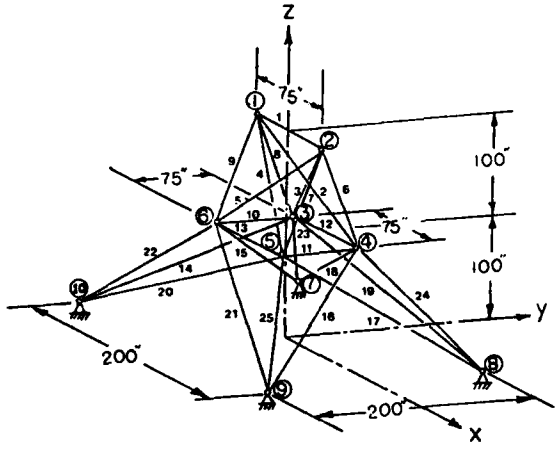


Figure 2. 25 Bar Transmission Tower

[1]Defined as $\max|g_i|/\max|P_i| \leq 10^{-5}$

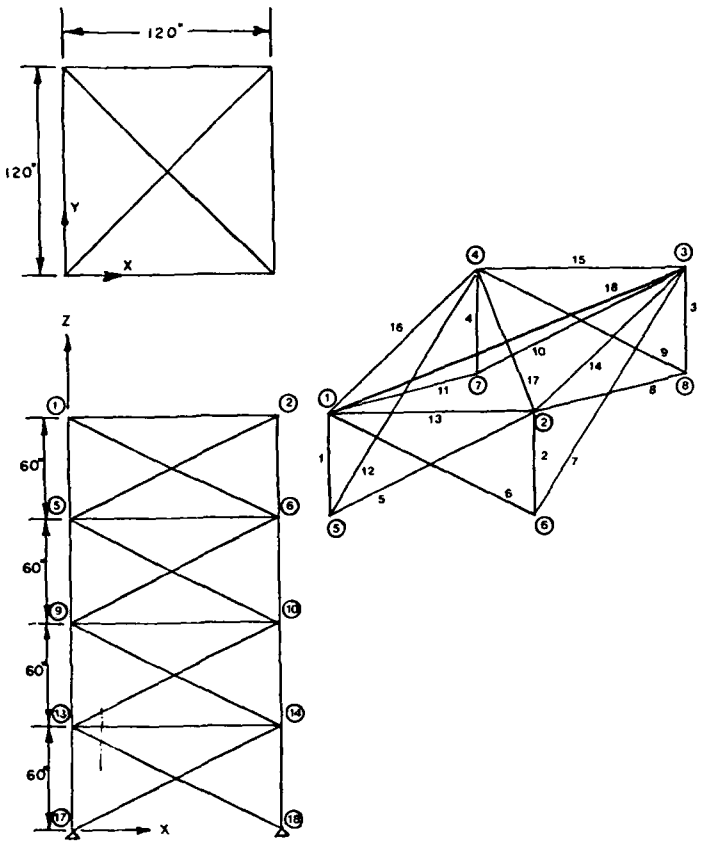


Figure 3. 72 Bar Truss

Table 1. Design Data for 10 bar truss

Modulus of Elasticity	=	10^4 ksi
Material Density	=	0.10 lb/in^3
Stress limits	=	±25 ksi
Lower limit on cross-sectional areas	=	0.10 in^2
Upper limit on displacements	=	2.0 in
Number of loading conditions	=	1

	Magitude of load (Kips)	
Node	X	Y
1	0.0	-10.0
3	0.0	-10.0

Table 2. Design Data for 25 bar transmission tower

Modulus of Elasticity	=	10^4 ksi
Material Density	=	0.10 lb/in^3
Stress limits	=	±40 ksi
Lower limit on cross-sectional areas	=	0.10 in^2 *
		0.01 in^2 **
Upper limit on displacements	=	0.35 in
Number of loading conditions	=	2

		Magnitude of load (Kips)		
Load cond.	Node	X	Y	Z
1	1	-1.0	-10.0	-5.0
	2	0.0	-10.0	-5.0
	3	-0.5	0.0	0.0
	4	-0.5	0.0	0.0
2	1	0.0	-20.0	-5.0
	2	0.0	20.0	-5.0

* Stress constraints only
** Stress and displacement constraints

Table 3. Design Data for 72 bar truss

Modulus of Elasticity	=	10^4 ksi
Material Density	=	0.10 lb/in^3
Stress limits	=	±25 ksi
Lower limit on cross-sectional areas	=	0.10 in^2
Upper limit on displacements	=	0.25 in
Number of loading conditions	=	2

		Magnitude of load (Kips)		
Load cond.	Node	X	Y	Z
1	1	5.0	5.0	-5.0
2	1	0.0	0.0	-5.0
	2	0.0	0.0	-5.0
	3	0.0	0.0	-5.0
	4	0.0	0.0	-5.0

Table 4. Optimum 10 bar truss

	Final area (in^2)		
Member number	case 1	case 2	Group No.
1	7.9379	30.7928	1
2	0.1000	0.1000	2
3	8.0621	23.9655	3
4	3.9379	14.7038	4
5	0.1000	0.1000	5
6	0.1000	0.1000	6
7	5.7447	8.5321	7
8	5.5690	20.9519	8
9	5.5690	20.8014	9
10	0.1000	0.1000	10
Final weight (lb)	1593.18	5076.64	Final weight(lb)
Number of iterations	3	10	Number of iterations

Table 7 Optimum designs for ten-bar truss

	Final area (in^2)						
Member number	Schmit & NEWSUMT	Miura(3) CONMIN	Schmit & Farshi(2)	Venkayya(1)	Arora & Haug(4)	Khan & Willmert(25)	This paper
1	30.6700	30.5700	33.4320	30.4160	***	30.9800	30.7928
2	0.1000	0.3690	0.1000	0.1280	***	0.1000	0.1000
3	23.7600	23.9700	24.2600	23.4080	***	24.1690	23.9655
4	14.5900	14.7300	14.2600	14.9040	***	14.8050	14.7038
5	0.1000	0.1000	0.1000	0.1010	***	0.1000	0.1000
6	0.1000	0.3640	0.1000	0.1010	***	0.4060	0.1000
7	8.5780	8.5470	8.3880	8.6960	***	7.5470	8.5321
8	21.0700	21.1100	20.7400	21.0840	***	21.0460	20.9519
9	20.9600	20.7700	19.6900	21.0770	***	20.9370	20.8014
10	0.1000	0.3200	0.1000	0.1860	***	0.1000	0.1000
Final weight(lb)	5076.85	5107.30	5089.00	5084.90	***	5066.98	5076.64
Number of iterations	13	14	23	25	***	18	10

*** data not available

Table 5 Optimum 25 bar transmission tower

Group No.	Member numbers	Final area (in**2) case 1	case 2
1	1	0.1000	0.0100
2	2 3 4 5	0.3761	2.0415
3	6 7 8 9	0.4709	3.0011
4	10 11	0.1000	0.0100
5	12 13	0.1000	0.0100
6	14 15 16 17	0.1000	0.6836
7	18 19 20 21	0.2773	1.6248
8	22 23 24 25	0.3801	2.6716
Final weight (lb)		91.13	545.03
Number of iterations		3	8

Table 8 Optimum designs for 25-bar transmission truss

Group No.	Final area (in**2) Schmit & NEWSUMT	Miura(3) CONMIN	Schmit & Farshi(2)	Venkayya(1)	Arora & Haug(4)	Khan & Willmert(25)	This paper
1	0.0100	0.1660	0.0100	0.0280	0.0100	0.0100	0.0100
2	1.9850	2.0170	1.9640	1.9420	2.0476	1.7550	2.0415
3	2.9960	3.0260	3.0330	3.0810	2.9965	2.8690	3.0011
4	0.0100	0.0870	0.0100	0.0100	0.0100	0.0100	0.0100
5	0.0100	0.0970	0.0100	0.0100	0.0100	0.0100	0.0100
6	0.6840	0.6750	0.6700	0.6930	0.6853	0.8450	0.6836
7	1.6770	1.6360	1.6800	1.6780	1.6217	2.0110	1.6248
8	2.6620	2.6690	2.6700	2.6270	2.6712	2.4780	2.6716
Final weight(lb)	545.17	548.47	545.22	545.50	545.04	553.94	545.03
Number of iterations	10	9	16	7	12	9	8

Table 6. Optimum 72 bar truss

Group No.	Member numbers	Final area (in**2) case 1	case 2
1	1 2 3 4	0.1688	0.1565
2	5 6 7 8 9 10 11 12	0.1000	0.5493
3	13 14 15 16	0.1000	0.4061
4	17 18	0.1600	0.5550
5	19 20 21 22	0.1904	0.5127
6	23 24 25 26 27 28 29 30	0.1000	0.5289
7	31 32 33 34	0.1000	0.1000
8	35 36	0.1000	0.1000
9	37 38 39 40	0.1987	1.2521
10	41 42 43 44 45 46 47 48	0.1000	0.5214
11	49 50 51 52	0.1000	0.1000
12	53 54	0.1000	0.1000
13	55 56 57 58	0.2941	1.8321
14	59 60 61 62 63 64 65 66	0.1000	0.5119
15	67 68 69 70	0.1000	0.1000
16	71 72	0.1000	0.1000
Final weight (lb)		96.637	379.62
Number of iterations		3	8

Table 9 Optimum designs for 72-bar truss

Group No.	Final area (in**2) Schmit & NEWSUMT	Miura(3) CONMIN	Schmit & Farshi(2)	Venkayya(1)	Arora & Haug(4)	Khan & Willmert(25)	This paper
1	0.1565	0.1558	0.1580	0.1610	0.1564	0.1519	0.1565
2	0.5458	0.5484	0.5940	0.5570	0.5464	0.5614	0.5493
3	0.4105	0.4105	0.3410	0.3770	0.4110	0.4378	0.4061
4	0.5699	0.5614	0.6080	0.5060	0.5712	0.5317	0.5550
5	0.5233	0.5228	0.2640	0.6110	0.5263	0.5814	0.5127
6	0.5173	0.5161	0.5480	0.5320	0.5178	0.5273	0.5289
7	0.1000	0.1000	0.1000	0.1000	0.1000	0.1000	0.1000
8	0.1000	0.1133	0.1510	0.1000	0.1000	0.1583	0.1000
9	1.2670	1.2680	1.1070	1.2460	1.2702	1.2526	1.2521
10	0.5118	0.5111	0.5790	0.5240	0.5124	0.5244	0.5241
11	0.1000	0.1000	0.1000	0.1000	0.1000	0.1000	0.1000
12	0.1000	0.1000	0.1000	0.1000	0.1000	0.1000	0.1000
13	1.8850	1.8850	2.0780	1.8180	1.8656	1.8589	1.8321
14	0.5125	0.5118	0.5030	0.5240	0.5131	0.5259	0.5119
15	0.1000	0.1000	0.1000	0.1000	0.1000	0.1000	0.1000
16	0.1000	0.1000	0.1000	0.1000	0.1000	0.1000	0.1000
Final weight(lb)	379.64	379.79	388.63	381.20	379.62	387.67	379.62
Number of iterations	9	8	22	12	12	10	8

References

1. V. B. Venkayya, "Design of Optimum Structures," *Computer & Structures*, Vol. 1, 1971, pp. 265-309.
2. L. A. Schmit and B. Farshi, "Some Approximation Concepts for Structural Synthesis," *AIAA Journal*, Vol. 12, No. 5, 1974, pp. 692-699.
3. L. A. Schmit and H. Miura, "Approximation Concepts for Efficient Structural Synthesis," Tech. report CR-2552, NASA, 1976.
4. Arora, J. S. and Haug, E. J. Jr., "Efficient optimal design of structures by generalized steepest descent programming," *Int. J. Num. Meth. Engng*, Vol. 10, 1976, pp. 747-766.
5. Arora, J. S. and Govil, A. K., "An efficient method for optimal structural design by substructuring," *Computers & Structures*, Vol. 7, 1977, pp. 507-515.
6. Govil, A. K. Arora, J. S. and Haug, E. J., "Optimal design of wing structures with substructures," *Computers & Structures*, Vol. 10, 1979, pp. 899-910.
7. Arora, J. S. and Haug, E. J., "Methods of design sensitivity analysis in structural optimization," *AIAA Journal*, Vol. 17, 1979, pp. 970.
8. R. T. Haftka & J. H. Starnes Jr., "Application of a Quadratic Extended Interior Penalty Function for Structural Optimization," *AIAA Journal*, Vol. 14, No. 6, 1976, pp. 718-724.
9. R. T. Haftka & B. Prasad, "Programs for Analysis and Resizing of Complex Structures," *Computers & Structures*, Vol. 10, 1979, pp. 323-330.
10. B. Prasad & R. T. Haftka, "A Cubic Extended Interior Penalty Function for Structural Optimization," *Int. J. for Numerical Methods in Engineering*, Vol. 14, 1979, pp. 1107-1126.
11. G. N. Vanderplaats & F. Moses, "Structural Optimization by Methods of Feasible Directions," *Computers & Structures*, Vol. 3, 1973, pp. 739-755.
12. S. P. Han, "A Globally Convergent Method for Nonlinear Programming," *Journal of Optimization Theory and Applications*, Vol. 22, No. 3, July 1977, pp. 297-309.
13. M. J. D. Powell, "A fast algroithm for nonlinear constrainted optimization calculations", Presented at the 1977 Dundee Conference on numerical Analysis
14. M. J. D. Powell, "The convergence of variable metric methods for nonlinear constrained optimization calculations", Presented at the Nonlinear Programming 3 symposium held at Madison, Wisconsin 1977
15. M. J. D. Powell, "Variable metric methods for constrained optimization", Presented at the Third International Symposium on Computing Methods in Applied Sciences and Engineering (Paris) 1977
16. M. J. D. Powell, "Contraint optimization by a variable metric method," Tech. report, DAMTP University of Cambridge , 1978.
17. M. J. D. Powell, "Gradient conditions and Lagrange multipliers in nonlinear programming," Tech. report, DAMTP University of Cambridge, 1979.
18. M. J. D. Powell, "Quasi-Newton formulae for sparse second derivative matrices," Tech. report, DAMTP University of Cambridge, 1979.
19. M. J. D. Powell, "Optimization algorithm in 1979", Presented at the Ninth IFIP Conference on Optimization Techniques (Warsaw) 1979
20. R.M. Chamberlain, C. Lemarechal, H.C. Pedersen and M.J.D. Powell, "The Watchdog Technique for Forcing Convergence in Algorithms for Constrained Optimization", Tenth International Symposium on Mathematical Programming August, 1979
21. T. J. Berna, M. H. Locke and A. W. Westerberg, "A New Approach to Optimization of Chemical Processes," *AIChE. Journal*, Vol. 26, January 1980, pp. 37-43.
22. J.E.Dennis and Jorge J. More, "Quasi-Newton Methods,Motivation and Theory," *SIAM Review*, Vol. 19, No. 1, January 1977, pp. 46-89.
23. J. K. Reid, "Least squares solution of sparse systems of

nonlinear equations by a modified Marquardt algorithm," *Decomposition of Large-Scale Problems*, 1973, pp. 437-445.

24. A. W. Westerberg and S. W. Director, "A Modified Least Squares Algorithm for Solving Sparse N X N Sets of Nonlinear Equations," *Computers and Chemical Engineering*, Vol. 2, 1978, pp. 77-81.
25. Khan, M. R. , Willmert, K. D. and Thornton, W. A., "An optimality criterion method for large-scale structures," *AIAA Journal*, Vol. 17, 1979, pp. 753.
26. C. Fleury and M. Gerardin, "Optimality Criteria and Mathematical Programming in Structural Weight Optimization," *Computer & Structures*, Vol. 8, 1978, pp. 7-17.
27. G. Sander and C. Fleury, "A Mixed Method in Structural Optimization," *Int. J. Numer. Meth. Eng.*, Vol. 13, 1978, pp. 385-404.
28. C. Fleury, "A Unified Approach to Structural Weight Minimization," *Comp. Meth. Appl. Mech. and Eng.*, Vol. 20, 1979, pp. 17-38.
29. C. Fleury, "Structural Weight Optimization by Dual Methods of Convex Programming," *Inter. J. Numer. Meth. Eng.*, Vol. 14, 1979, pp. 1761-1783.
30. C. Fleury and L. A. Schmit, "Primal and Dual Methods in Structural Optimization," *ASCE J. Structural Div.*, May 1980, pp. 1117-1135.
31. R. Fletcher, "The calculation of feasiable point for linearly constrained optimization problems," Tech. report AERE R.6354, U.K.A.E.A. Research Group, April, 1970.
32. R. Fletcher, "A Fortran Subroutine for General Quadratic Programming," Tech. report AERE R.6370, U. K. A. E. A. Research Group, June, 1970.
33. R. Fletcher, "A General Quadratic Programming Algorithm," *J. Inst. Maths Applics*, Vol. 7, 1971, pp. 76-91.

Appendix A. Terms Appearing in Equation (15)

The terms appearing in the condensed Equation (15) are obtained as follows:

Define:

$$G_1 = (G_u)^{-1}$$

$$G_2 = (G_u^T)^{-1} = G_1^T$$

$$C_{uuu} = G_2 * H_{uu} * G_1$$

Then:

$$M_1 = G_1 * G_A$$

$$M_2 = -G_2 * H_{uA} - C_{uuu} * G_A$$

$$N_1 = G_2 * h_u$$

$$\hat{H} = H_{AA} - H_{Au} * G_1 * G_A - G_A^T * G_2 * H_{uA} + G_A^T * C_{uuu} * G_A$$

$$Q^T = h_A - h_u * G_1 * G_A$$

$$\hat{q} = -F_A + H_{Au} * G_1 * g - G_A^T * G_2 * C_{uuu} * g + G_A^T * G_2 * F_u$$

$$\hat{h} = -h + h_u * G_1 * g$$

$$m_1 = -G_1 * g$$

$$m_2 = -G_2 * F_u + C_{uuu} * g$$

Appendix B. Algorithm Implementation

The procedure for performing optimal design is described by the following algorithm.

Step 0 Initialization

i) Set k (iteration index) = 0 and the Hessian matrix H_k = [I] (results in the first step in the steepest descent direction)

ii) Initialize vector { A } and solve Equation (2) for vector { u }

Step 1 Compute right hand side and derivatives for approximation problem (Equations (10) - (12))

i) k = k + 1

ii) Compute matrices G_A and G_u and vector g

iii) Compute vectors F_A and F_u

iv) Compute matrices h_A and h_u and vector h

v) *If k = 1 go to Step 2*

vi) Compute

$$\left(\frac{\partial L}{\partial X}\right)_2 = \begin{pmatrix} F_A \\ F_u \end{pmatrix} + \begin{bmatrix} G_A^T \\ G_u^T \end{bmatrix} \mu + \begin{bmatrix} h_A^T \\ h_u^T \end{bmatrix} \eta$$

vii) Compute

$$\begin{bmatrix} H_{AA} & H_{Au} \\ H_{uA} & H_{uu} \end{bmatrix} = [I] + \sum_{j=1}^{n} (-1)^j \begin{Bmatrix} W_{A_j} \\ W_{u_j} \end{Bmatrix} [\, W_{A_j}^T \; W_{u_j}^T \,]$$

Where $n = (k - 1) * 2$

$$\gamma = \left(\frac{L}{X}\right)_2 - \left(\frac{L}{X}\right)_1$$

$$\sigma_j = [\, W_A^T \; W_u^T \,]_j \, \delta \qquad j = 1, \ldots, n$$

$$\sigma = \sum_{j=1}^{n} (-1)^j * \sigma_j^2 + \delta^T \delta$$

$$\theta = \begin{cases} 1. & \text{if } \delta^T \gamma \geq 0.2\, \sigma \\ .8\sigma/(\sigma - \delta^T\gamma) & \text{otherwise} \end{cases}$$

$$\zeta = \theta\gamma + (1. - \theta)\, \delta + (1. - \theta) \sum_{j=1}^{n} (-1)^j \begin{Bmatrix} W_{A_j} \\ W_{u_j} \end{Bmatrix} \sigma_j$$

$$\begin{Bmatrix} W_A \\ W_u \end{Bmatrix}_{n+1} = \delta + \sum_{j=1}^{n} (-1)^j \begin{Bmatrix} W_A \\ W_u \end{Bmatrix}_j \sigma_j \Big/ \sqrt{\sigma}$$

$$\begin{Bmatrix} W_A \\ W_u \end{Bmatrix}_{n+2} = \frac{\zeta}{(\delta^T \zeta)^{1/2}}$$

viii) Update Hessian matrix H_k (see Appendix C)

Step 2 Reduction(Condensation) and setup of Quadratic Programming problem

i) Compute matrices $\hat{H}$ and Q^T (see Appendix A)

ii) Compute vectors $\hat{q}$ and $\hat{h}$ (see Appendix A)

iii) Select critical and potentially critical constraints for problem (P4)

Step 3 Optimization

i) Solve problem (P4) for vectors { ΔA } , { η }

ii) Backsubstitute in the first two rows of Equation (15) for vectors { Δu } and { μ }

iii) Compute

$$\left(\frac{\partial L}{\partial X}\right)_i = \begin{pmatrix} F_A \\ F_u \end{pmatrix} + \begin{bmatrix} G_A^T \\ G_u^T \end{bmatrix} \mu + \begin{bmatrix} h_A^T \\ h_u^T \end{bmatrix} \eta$$

Step 4 Determine step size parameter.

i) For k = 1

$\nu_i = 0.0 \qquad i = 1,.....m$

ii) For $i = 1,.....m^*$

$\nu_i = \max \{ |\mu_i| , 0.5 * (\nu_i + |\mu_i|) \}$

iii) For $i = m^*+1,...,m$

$\nu_i = \max \{ \eta_i , 0.5 * (\nu_i + \eta_i) \}$

iv) Select the largest value of α, $0.0 \le \alpha \le 1.0$,

a) If $\Psi(\tilde{A},\tilde{u},\nu) > \Psi_k$ go to b)

a1) If $\Psi(\tilde{A},\tilde{u},\nu) < \Psi(A,u,\nu)$ or $L(\tilde{A},\tilde{u},\mu,\eta) < L(A,u,\mu,\eta)$ go to vi)

b) If $\Psi(\tilde{A},\tilde{u},\nu) < \Psi(A,u,\nu)$ go to vi)

c) Go to v) of Step 5

where $\Psi(A,u,\nu) = F(A,u) + \sum_{i=1}^{m'} \nu_i |g_i(A,u)| + \sum_{i=m'+1}^{m} \nu_i \max \{0., h_i\}$

$$\Psi_k = \min \{ \Psi(A^j,u^j,\nu^j) \; ; \; j = 0,1...,k-1 \}$$

$\tilde{A} = A + \alpha \Delta A \qquad \tilde{u} = u + \alpha \Delta u$

vi) Set $A = \tilde{A}$, $u = \tilde{u}$ $\qquad \delta = \alpha \begin{Bmatrix} \Delta A \\ \Delta u \end{Bmatrix}$

Step 5 Check for convergence

i) Let $\varphi = \delta^T \begin{Bmatrix} F_A \\ F_u \end{Bmatrix} + \sum_{i=1}^{m'} \nu_i |g_i(A,u)|$

ii) If $\varphi \le \epsilon$ print result and go to Step 6

iii) Adjust the step controlling parameter π

iv) If $k <$ maximum number of allowed iterations, go to Step 1

v) Print error message and go to Step 6

Step 6 Stop

Appendix C. Updating of the Hessian matrix

In Powell's work [13]-[20], the Hessian matrix was updated by the BFGS rank 2 method. In that updating method, the Hessian matrix H is initially set equal to an identity matrix, and in each iteration on the quadratic approximation subproblem the Hessian matrix is updated by the following formula:

$$H_{k+1} = H_k + \frac{y\, y^T}{\langle y , s \rangle} - \frac{H_k\, s\, s^T\, H_k}{\langle s , H_k\, s \rangle}$$

where $\qquad y = L (X_{k+1}) - L (X_k)$

$s = \Delta X$

$\langle y , s \rangle = y^T s$

Instead of keeping the full matrix H_k, Berna suggested the following expression to update the Hessian matrix:

$$\begin{bmatrix} H_{AA} & H_{Au} \\ H_{uA} & H_{uu} \end{bmatrix} = [I] + \sum_{j=1}^{n} (-1)^j \begin{Bmatrix} W_{A_j} \\ W_{u_j} \end{Bmatrix} [W_{A_j}^T \; W_{u_j}^T]$$

where W_{A_j} and W_{u_j} are defined in Appendix B and $n = (k - 1) * 2$

The following formula, used by Berna, is implemented in the present method to update the reduced Hessian matrix in each iteration . By using this formula, the number of arithmetic operations performed in updating the reduced Hessian matrix is reduced dramatically.

$$H = H_{AA} - H_{Au} * G_3 - G_3^T * H_{uA} + G_3^T * H_{uu} * G_3$$

$$= (I_r + \Sigma W_{A_j} * W_{A_j}^T) - G_3^T * (\Sigma W_{u_j} * W_{A_j}^T)$$

$$+ G_3^T * (I_z + \Sigma W_{u_j} * W_{u_j}^T) * G_3$$

$$= I_r - G_3^T * G_3 + \Sigma (W_{A_j} - G_3^T * W_{u_j}) *$$

$$(W_{A_j} - G_3 * W_{u_j})^T$$

where $G_1 = (G_u)^{-1}$ and $G_3 = G_1 * G_A$

r = number of independent variables

z = number of dependent variables.

AD-P000 068

MODIFIED SUMT FOR STRUCTURAL SYNTHESIS+

Manohar P. Kamat* and Preecha Ruangsilasingha**
Department of Engineering Science and Mechanics
Virginia Polytechnic Institute and State University
Blacksburg, VA 24061

SUMMARY

Fiacco-McCormick's SUMT algorithm offers an easy way of solving nonlinearly constrained problems. However, this algorithm frequently suffers from the need to minimize an ill-conditioned penalty function. An ill-conditioned minimization problem , however, can be solved very effectively by posing the problem as one of integrating a system of stiff differential equations utilizing concepts from singular perturbation theory.

This paper evaluates the robustness and the reliability of such a singular perturbation based SUMT algorithm on two different problems of structural optimization of widely separated scales. The report concludes that whereas conventional SUMT can be bogged down by frequent ill-conditioning, especially in large scale problems, the singular perturbation SUMT has no such difficulty in converging to very accurate solutions.

I. INTRODUCTION

Most problems of structural optimization involve the extremization of an objective function of design variables subject to a set of constraints which are of the geometric and behavioral type. The constraints which stem from limitations on stresses, displacements and the allowable member sizes are implicit functions of the design variables and are often very highly nonlinear.

Perhaps one of the easiest ways of solving such a nonlinearly constrainted problem is the penalty method. In this method, an auxiliary objective function which is a function of the original objective functions and the constraints is constructed. An appropriate unconstrainted extremization of this auxiliary objective function then yields an approximate solution of the original nonlinearly constrained problem. Among the basically two distinct kinds of the penalty methods, namely the exterior and the interior or barrier function methods, the latter is the most often used for structural optimization problems. This is because the method often begins with an initial feasible solution and the successive solutions are never allowed to leave the feasible domain with the result that any immature termination of the process still guarantees a quasi optimum solution but one which is always feasible. The same is not true of the exterior method.

In the context of the interior penalty method the algorithm that is most commonly used is the Sequential Unconstrained Minimization Technique (SUMT) proposed by Fiacco-McCormick [1]. The algorithm involves the use of a sequence of penalty parameters which converts the constrained problem into a sequence of unconstrained problems using the last solution as the initial guess for the next unconstrained problem. The choice of the initial value of the penalty parameter as well as the sequence of its values is very crucial to the success of the algorithm. In fact, a severely ill-conditioned problem will occur if the choice is inappropriate. Furthermore, as a constraint boundary is approached, the Hessian of the penalty function becomes more and more ill-conditioned. Ill-conditioning of the Hessian is also likely to occur as a result of a poor scaling of the variables; this being especially true for large scale problems. It is this ill-conditioning feature of the method that inhibits the determination of reasonably accurate solution of the original nonlinearly constrained problem. Some of the ways through which this method can be made viable are those that resort to measures to overcome the ill-conditioning and permit a smooth passage to the optimum solution.

The last decade has seen the emergence of some of the most sophisticated and robust algorithms for unconstrainted minimization including those that are known as the self-scaling algorithms [2]-[5] and those that utilize the techniques of singular perturbation [6]-[7] to solve ill-conditioned minimization problems. The accuracy of algorithms based on the singular perturbation theory usually improves as the problems become more and more ill-conditioned. In light of this it is only natural to test the effectiveness of such an algorithm in the context of structural optimization problems that use the interior penalty method for solution.

II. DESCRIPTION OF THE METHOD

The objective is simply the unconstrained minimization of a function f of an n-dimensional vector $\underline{x}$ which will be assumed to be twice continuously differentiable in a open convex set containing the point $\underline{x}^*$ such that $\nabla f(\underline{x}^*) = 0$. Furthermore, to allow for possible ill-conditioning of the penalty function in the vicinity of constraint boundaries or because of poor scaling of the variables it will be assumed that the Hessian of f, $\underset{\sim}{H} = \underset{\sim}{f}''(\underline{x})$. has a large condition number.

Following Boggs [6] the approach is to convert the minimization problem into one of integrating a system of 'stiff' differential equations. The relation between the two problems is evident upon an application of the steepest descent to the minimization problem. Accordingly

$$\underline{x}_{k+1} = \underline{x}_k - \alpha_k \nabla f(\underline{x}_k), \quad k = 0,1... \qquad (1)$$

with $\underline{x}_0$ being the initial guess.

Equation (1) may be viewed as Euler's method for integrating the system

$$\frac{d}{d\alpha}(\underline{x}(\alpha)) = -\nabla f(\underline{x}(\alpha)) \text{ with } \underline{x}(0) = \underline{x}_0 \qquad (2)$$

By definition a differential equation of type (2) is said to be stiff if its linearized form has eigen-

+This work was partially supported by NASA Langley Research Center under Grant No. NAG-1-139.

*Associate Professor

**Graduate Student

values that are widely separated. Expansion of the right hand of Eq. (2) in a Taylor series about the optimum solution $\underline{x}^*$ and retention of only the linear terms yields

$$\frac{d}{d\alpha}(\underline{x}(\alpha)) = -\underset{\sim}{f}''(\underline{x})(\underline{x} - \underline{x}^*) = -\underset{\sim}{H}(\underline{x} - \underline{x}^*) \qquad (3)$$

Clearly if the condition number of $\underset{\sim}{H}$ is large the system of differential equations (2) is stiff. This implies that $\underset{\sim}{H}$ has a few eigenvalues or at the very least a single eigenvalue that does not contribute significantly over the domain of interest. This in turn implies a separation of the system into singular and nonsingular components; singular components being those that vary rapidly in a narrow region called the boundary layer.

A method for accurately integrating stiff differential equations of the type (3) is sought but one which permits a large step-length for little computational work. Singular perturbation theory has been used by several investigators [8]-[11] to integrate such systems and the resulting computational methods have the property that their accuracy actually increases as the equations become stiffer. This is in sharp contrast to the Levenberg-Marquardt type methods [12] for direct minimization of f which utilize the Newton's method or quasi-Newton methods that are based on a Taylor's series model of the function f. Boggs [6] claims that models based on singular perturbation theory are better able to 'smooth the geometry' than for instance Powell's method [12] which uses a combination of the steepest descent and quasi-Newton directions where each direction is computed using the entire system.

a. Numerical Integration Technique for Stiff Differential Equations

Consider a two variable set of first-order differential equations in the singular perturbation form

$$\frac{d\underline{x}}{d\alpha} = \underline{g}(\underline{x},\underline{y};\varepsilon) \; ; \; \underline{x}(0) = \underline{\xi} \qquad (4)$$

$$\varepsilon\frac{d\underline{y}}{d\alpha} = \underline{h}(\underline{x},\underline{y};\varepsilon) \; ; \; \underline{y}(0) = \underline{\eta} \qquad (5)$$

Above equations are in the singular perturbation form because as $\varepsilon \to 0$ the system reduces to a combination differential and algebraic system and an inconsistency arises in attempting to satisfy the initial conditions $\underline{y}(0) = \underline{\eta}$. The order of the differential equations drops to that of the $\underline{x}$ components. The $\underline{y}$ components are referred to as the singular components (inner variables) while the $\underline{x}$ components are referred to as the nonsingular components (outer variables).

The solution is first assumed to be a simple expansion in the outer variables as a power series in ε

$$\underline{x} = \sum_{i=0}^{\infty} \underline{x}_i(\alpha)\frac{\varepsilon^i}{i!} \qquad (5\text{-a})$$

$$\underline{y} = \sum_{i=0}^{\infty} \underline{y}_i(\alpha)\frac{\varepsilon^i}{i!} \qquad (5\text{-b})$$

Details on the conditions for the existence of such a solution may be found in references [9] and [10].

Next, Eqs. (5) are substituted into Eqs. (4) with the functions $\underline{g}$ and $\underline{h}$ expanded about the point $\underline{x}_0(\alpha)$ and $\underline{y}_0(\alpha)$ as a power series in ε. Thus

$$\frac{d\underline{x}}{d\alpha} = \frac{d\underline{x}_0}{d\alpha} + \varepsilon\frac{d\underline{x}_1}{d\alpha} + \ldots = \underline{g}(\underline{x}_0,\underline{y}_0;\varepsilon) + \varepsilon[\underset{\sim}{g}_x\underline{x}_1 + \underset{\sim}{g}_y\underline{y}_1] + \ldots$$

$$\varepsilon\frac{d\underline{y}}{d\alpha} = \varepsilon\frac{d\underline{y}_0}{d\alpha} + \varepsilon^2\frac{d\underline{y}_1}{d\alpha} + \ldots = \underline{h}(\underline{x}_0,\underline{y}_0;\varepsilon) + \varepsilon[\underset{\sim}{h}_x\underline{x}_1 + \underset{\sim}{h}_y\underline{y}_1] + \ldots$$

where the matrices $\underset{\sim}{g}_x = [\partial\underline{g}/\partial\underline{x}]$, $\underset{\sim}{g}_y = [\partial\underline{g}/\partial\underline{y}]$, etc., evaluated at $\underline{x} = \underline{x}_0$ and $\underline{y} = \underline{y}_0$, have as their i-jth component the derivative of the ith component of $\underline{g}$ or $\underline{h}$ with respect to the jth component of $\underline{x}$ or $\underline{y}$.

Collection of the coefficients of like powers of ε results in

$$\varepsilon^0: \quad \frac{d\underline{x}_0}{d\alpha} = \underline{g}(\underline{x}_0,\underline{y}_0;\varepsilon) \; ; \; \underline{x}_0(0) = \underline{\xi} \qquad (6\text{-a})$$

$$0 = \underline{h}(\underline{x}_0,\underline{y}_0;\varepsilon) \; ; \; \underline{y}_0(0) = \underline{\eta} \qquad (6\text{-b})$$

and

$$\varepsilon^1: \quad \frac{d\underline{x}_1}{d\alpha} = \underset{\sim}{g}_x\underline{x}_1 + \underset{\sim}{g}_y\underline{y}_1 \; ; \; \underline{x}_1(0) = 0 \qquad (7\text{-a})$$

$$\frac{d\underline{y}_0}{d\alpha} = \underset{\sim}{h}_x\underline{x}_1 + \underset{\sim}{h}_y\underline{y}_1 \; ; \; \underline{y}_1(0) = 0 \qquad (7\text{-b})$$

It is immediately obvious that an inconsistency will arise since Eqs. (6-b) may not be satisfied. This is resolved by the introduction of inner variables which are important in the boundary layer. The inner variables are expressed in terms of the expanded scale $\tau = \frac{\alpha}{\varepsilon}$ since it allows for easier computation. This gives new composite solution approximation valid in the boundary layer.

$$\underline{x}^*(\alpha) = \sum_{i=0}^{\infty} \underline{x}_i(\alpha)\frac{\varepsilon^i}{i!} + \sum_{i=0}^{\infty} \underline{X}_i(\tau)\frac{\varepsilon^i}{i!} \qquad (8\text{-a})$$

$$\underline{y}^*(\alpha) = \sum_{i=0}^{\infty} \underline{y}_i(\alpha)\frac{\varepsilon^i}{i!} + \sum_{i=0}^{\infty} \underline{Y}_i(\tau)\frac{\varepsilon^i}{i!} \qquad (8\text{-b})$$

with

$$\lim_{\tau\to\infty} \underline{X}_0 = \underline{X}_1 = \underline{Y}_0 = \underline{Y}_1 = \ldots = 0$$

Thus Eqs. (1) may be written in terms of τ as

$$\frac{d\underline{x}}{d\tau} = \varepsilon\underline{g}(\underline{x},\underline{y};\varepsilon) \; ; \; \underline{x}(0) = \xi \qquad (8\text{-c})$$

$$\frac{d\underline{y}}{d\tau} = \underline{h}(\underline{x},\underline{y};\varepsilon) \; ; \; \underline{y}(0) = \underline{\eta} \qquad (8\text{-d})$$

From Eqs. (8)

$$\frac{d\underline{x}}{d\tau} = \varepsilon\frac{d\underline{x}_0}{d\alpha} + \varepsilon^2\frac{d\underline{x}_1}{d\alpha} + \frac{d\underline{X}_0}{d\tau} + \varepsilon\frac{d\underline{X}_1}{d\tau} + \ldots$$

$$\frac{d\underline{y}}{d\tau} = \varepsilon\frac{d\underline{y}_0}{d\alpha} + \varepsilon^2\frac{d\underline{y}_1}{d\alpha} + \frac{d\underline{Y}_0}{d\tau} + \varepsilon\frac{d\underline{Y}_1}{d\tau} + \ldots$$

Similarly

$$\underline{g}(\underline{x},\underline{y};\varepsilon) = \underline{g}(\underline{x}_0(\alpha) + \underline{X}_0(\tau),\ \underline{y}_0(\alpha) + \underline{Y}_0(\tau);\varepsilon) + \varepsilon[\underset{\sim}{g}_x^*(\underline{x}_1(\alpha) + \underline{X}_1(\tau)) + \underset{\sim}{g}_y^*(\underline{y}_1(\alpha) + \underline{Y}_1(\tau))] + \ldots$$

$$\underset{\sim}{h}(\underset{\sim}{x},\underset{\sim}{y};\varepsilon) = \underset{\sim}{h}(\underset{\sim}{x}_0(\alpha) + \underset{\sim}{X}_0(\tau),\ \underset{\sim}{y}_0(\alpha + \underset{\sim}{Y}_0(\tau);\varepsilon)$$
$$+ \varepsilon[\underset{\sim}{h}^*_{\underset{\sim}{x}}(\underset{\sim}{x}_1(\alpha) + \underset{\sim}{X}_1(\tau))$$
$$+ \underset{\sim}{h}^*_{\underset{\sim}{y}}(\underset{\sim}{y}_1(\alpha) + \underset{\sim}{Y}_1(\tau))]\ldots$$

where $\underset{\sim}{g}^*_{\underset{\sim}{x}}$, $\underset{\sim}{g}^*_{\underset{\sim}{y}}$, $\underset{\sim}{h}^*_{\underset{\sim}{x}}$ and $\underset{\sim}{h}^*_{\underset{\sim}{y}}$ are evaluated at $\underset{\sim}{x} = \underset{\sim}{x}_0(\alpha)\underset{\sim}{x}_0(\tau)$ and $\underset{\sim}{y} = \underset{\sim}{y}_0(\alpha) + \underset{\sim}{Y}_0(\tau)$.

Substitution of the above expansions into Eqs. (8) followed by a collection of the coefficients of like powers of ε yields in the limit as $\varepsilon \to 0$ the following equations

$$\varepsilon^0: \quad \frac{d\underset{\sim}{X}_0}{d\tau} = 0 \tag{9-a}$$

$$\frac{d\underset{\sim}{Y}_0}{d\tau} = \underset{\sim}{h}\ (\underset{\sim}{x}_0(0) + \underset{\sim}{X}_0(\tau);\ \underset{\sim}{y}_0(0) + \underset{\sim}{Y}_0(\tau)) \tag{9-b}$$

and

$$\frac{d\underset{\sim}{X}_1}{d\tau} = \underset{\sim}{g}(\underset{\sim}{x}_0(0) + \underset{\sim}{X}_0(\tau),\ \underset{\sim}{y}_0(0) + \underset{\sim}{Y}_0(\tau)) - \frac{d\underset{\sim}{x}_0}{d\alpha}$$
$$= \underset{\sim}{g}(\underset{\sim}{x}_0(0) + \underset{\sim}{X}_0(\tau),\ \underset{\sim}{y}_0(0) + \underset{\sim}{Y}_0(\tau)) - g(\underset{\sim}{x}_0(0),\ \underset{\sim}{y}_0(0),0) \tag{10-a}$$

ε^1:

$$\frac{d\underset{\sim}{Y}_1}{d\tau} = \underset{\sim}{h}^*_{\underset{\sim}{x}}\underset{\sim}{X}_1(\tau) + \underset{\sim}{h}^*_{\underset{\sim}{y}}\underset{\sim}{Y}_1(\tau) + \underset{\sim}{h}^*_{\underset{\sim}{x}}\underset{\sim}{x}_1(0)$$
$$+ \underset{\sim}{h}^*_{\underset{\sim}{y}}\underset{\sim}{y}_1(0) - \underset{\sim}{h}_{\underset{\sim}{x}}\underset{\sim}{x}_1(0) - \underset{\sim}{h}_{\underset{\sim}{y}}\underset{\sim}{y}_1(0) \tag{10-b}$$

Where use is made of the known outer solution from Eqs. (6) and (7). Equations (9) and (10) have to be *solved subject to the boundary conditions*

$$\underset{\sim}{x}_0(0) + \underset{\sim}{X}_0(0) = \underset{\sim}{\xi}$$
$$\underset{\sim}{y}_0(0) + \underset{\sim}{Y}_0(0) = \underset{\sim}{\eta}$$
$$\underset{\sim}{x}_1(0) + \underset{\sim}{X}_1(0) = \underset{\sim}{0}$$
$$\underset{\sim}{y}_1(0) + \underset{\sim}{Y}_1(0) = \underset{\sim}{0}$$

$\underset{\sim}{h}^*_{\underset{\sim}{x}}$ and $\underset{\sim}{h}^*_{\underset{\sim}{y}}$ in the above equations are evaluated at $\underset{\sim}{x} = \underset{\sim}{x}_0$ and $\underset{\sim}{y} = y_0$.

b. Miranker's Method for ε-Independent Minimization Problems

In the case of applications of the singular perturbation theory to ill-conditioned minimization problem, the parameter ε is not available. Miranker [11] has developed an ε-independent method. In this case the differential equations are considered to be of the type

$$\underset{\sim}{z}' = \underset{\sim}{f}(\underset{\sim}{x},\varepsilon)\ ;\quad \underset{\sim}{z}(0) = \underset{\sim}{\zeta} \tag{11}$$

where ε is taken to be unidentifiable. The system is solved numerically by taking a steplength α of any self-starting method like the Euler's Method. The resulting $\underset{\sim}{z}$ and $\underset{\sim}{\zeta}$ are compared by testing the inequalities

$$\frac{|z_i - \zeta_i|}{1+|\zeta_i|} > \theta\ ;\quad i = 1,2\ldots n \tag{12}$$

where θ is a given tolerance. If the tolerance is not exceeded by any of the components of $\underset{\sim}{z}$, the value of $\underset{\sim}{z}$ is accepted. On the other hand, if the tolerance is exceeded by a set $J_1, J_2, \ldots J_m$), $m > 0$, the integration is rejected and the following classification into singular and nonsingular components is undertaken

$$x_i = z_i$$
$$\xi_i = \zeta_i \qquad i = 1,\ldots n, i \notin J \tag{13-a}$$
$$g_i = f_i$$

and

$$y_j = z_j$$
$$\eta_j = \zeta_j \qquad j = 1,\ldots m, \quad j \in J \tag{13-b}$$
$$h_j = f_j$$

The system now has the form

$$\frac{d\underset{\sim}{x}(\alpha)}{d\alpha} = \underset{\sim}{g}(\underset{\sim}{x},\underset{\sim}{y})$$
$$\frac{d\underset{\sim}{y}(\alpha)}{d\alpha} = \underset{\sim}{h}(\underset{\sim}{x},\underset{\sim}{y})$$

and the system is regarded as being stiff. Thus, solely for the derivation of expressions for the boundary layer terms the small parameter ε is introduced as

$$\frac{d\underset{\sim}{x}}{d\alpha} = \underset{\sim}{g}(\underset{\sim}{x},\underset{\sim}{y};\varepsilon) \tag{14-a}$$

$$\frac{d\underset{\sim}{y}}{d\alpha} = \underset{\sim}{w}(\underset{\sim}{x},\underset{\sim}{y};\varepsilon)/\varepsilon \tag{14-b}$$

Proceeding in a manner very similar to the one outlined before Miranker [11] derives the following expressions

$$\frac{d\underset{\sim}{x}_0}{d\alpha} = \underset{\sim}{g}(\underset{\sim}{x}_0,\underset{\sim}{y}_0;\varepsilon)\ ,\quad \underset{\sim}{x}_0(0) = \underset{\sim}{\xi} \tag{15-a}$$

$$0 = \underset{\sim}{h}(\underset{\sim}{x}_0,\underset{\sim}{x}_0;\varepsilon) \tag{15-b}$$

$$\varepsilon\frac{d\underset{\sim}{x}_1}{d\alpha} = [\underset{\sim}{g}_{\underset{\sim}{x}} - \underset{\sim}{g}_{\underset{\sim}{y}}\underset{\sim}{h}^{-1}_{\underset{\sim}{y}}\underset{\sim}{h}_{\underset{\sim}{x}}]\varepsilon\underset{\sim}{x}_1 - \underset{\sim}{g}_{\underset{\sim}{y}}\underset{\sim}{h}^{-1}_{\underset{\sim}{y}}\underset{\sim}{h}^{-1}_{\underset{\sim}{y}}\underset{\sim}{h}_{\underset{\sim}{x}}[\underset{\sim}{g} + \underset{\sim}{h}_\alpha] \tag{15-c}$$

$$\varepsilon\underset{\sim}{y}_1 = -\underset{\sim}{h}^{-1}_{\underset{\sim}{y}}\underset{\sim}{h}_{\underset{\sim}{x}}\varepsilon\underset{\sim}{x}_1 - \underset{\sim}{h}^{-1}_{\underset{\sim}{y}}\underset{\sim}{h}^{-1}_{\underset{\sim}{y}}[\underset{\sim}{h}_{\underset{\sim}{x}}\underset{\sim}{g} + \underset{\sim}{h}_\alpha] \tag{15-d}$$

To determine the initial conditions $\varepsilon\underset{\sim}{x}_1(0)$, Miranker [11] proceeds with an ε-independent determination of the boundary layer terms using Eqs. (15). It can be easily verified that $\underset{\sim}{X}_0(0) \equiv \underset{\sim}{0}$ and under reasonable assumptions $\varepsilon\underset{\sim}{x}_1$ and $\varepsilon\underset{\sim}{y}_1$ can be shown to be negligible [11,6]. Miranker [11] then derives an expression for $\underset{\sim}{Y}_0$ and incorporates this into an expression for $\varepsilon\underset{\sim}{x}_1(0)$ yielding

$$\varepsilon\underset{\sim}{x}_1(0) = \frac{\underset{\sim}{g}(\underset{\sim}{\xi},\underset{\sim}{y}_0(0);\varepsilon) - \underset{\sim}{g}(\underset{\sim}{\xi},\underset{\sim}{\eta};\varepsilon)}{\underset{\sim}{g}_{\underset{\sim}{y}}(\underset{\sim}{\xi},\underset{\sim}{\eta};\varepsilon)\underset{\sim}{h}(\underset{\sim}{\xi},\underset{\sim}{\eta};\varepsilon)} \tag{16}$$

where the division is element-wise.

The rest of the details of the final basic algorithm for a step from zero to α when the asymptotic method with the two term aproximations is used may be found in reference [13].

c. Modification for Function Minimization: Basic Algorithm

The basic algorithm for function minimization of general functions like the penalty function $P(\underline{A})$, will be considered next. For the constrained optimization problem

$$\text{Minimize} \quad f(\underline{A}) \tag{17}$$

$$\text{Subject to } G_j(\underline{A}) \geq 0 \quad j = 1,2\ldots m \tag{18}$$

$$H_j(\underline{A}) = 0 \quad j = m+1,\ldots M$$

Fiacco-McCormick's logarithmic quadratic-loss penalty function is given by

$$P(\underline{A}) = f(\underline{A}) + r \sum_{j=1}^{m} \ln G_j + \sum_{j=m+1}^{M} H_j^2 \tag{19}$$

The integration model is assumed to be

$$\frac{d\underline{A}(\alpha)}{d\alpha} = -\underline{\nabla P}(\underline{A})$$

and at the beginning of the kth interaction the following information is assumed to be available.

$\underline{A}^k \equiv$ the current approximation to $\underline{A}^*$, $\underline{A}^0$ being user supplied;

$\underline{\nabla P}^k \equiv \underline{\nabla P}(\underline{A}^k)$

$\underset{\sim}{H}^k \equiv$ an approximation to $[\underset{\sim}{P}''(\underline{A}^k)]^{-1}$

$\underset{\sim}{B}^k \equiv$ an approximation to $[\underset{\sim}{P}''(\underline{A}^k)]$

$\Delta^k \equiv$ an upper bound such that $\|\underline{A}^{k+1} - \underline{A}^k\| \leq \Delta^k$, Δ^0 being user supplied (assumed to be unity in this study).

The above information is updated for the (k + 1)th step. Two additional pieces of information which remain constant throughout the entire process are the error convergence criterion, err and the factor $c > 1$ which is used to control the function change; $\underline{A}^{k+1}$ is accepted if

$$P(\underline{A}^{k+1}) \leq cP(\underline{A}^k) \tag{20}$$

the basic steps of the algorithm [6] may now be briefly outlined as follows:

1. Apply one step of the quasi-Newton method to compute

$$\underline{A}^{k+1} = \underline{A}^k - \underset{\sim}{H}^k \underline{\nabla P}^k \tag{21}$$

If $\|\underline{A}^{k+1} - \underline{A}^k\| < \Delta^k$ and (20) is satisfied then go to step 8; else go to step 2.

2. Apply one step of the steepest descent method and seperate the system into singular and nonsingular components.

$$\underline{A}^{k+1} = \underline{A}^k - \alpha^k \underline{\nabla P}^k \tag{22}$$

where

$$\alpha^k = \begin{cases} 1 & \text{if } \|\underline{\nabla P}^k\| \leq \Delta^k \\ \Delta^k / \|\underline{\nabla P}^k\| & \text{if } \|\underline{\nabla P}^k\| > \Delta^k \end{cases} \tag{23}$$

and then test

$$|A_i^{k+1} - A_i^k| > \theta\Delta^k, \quad i = 1,2,\ldots n, \quad \theta\epsilon[0,1] \tag{24}$$

$\theta = 0.5$ is found to be satisfactory.

Assume

$$\begin{Bmatrix} \underline{x}' \\ \underline{y}' \end{Bmatrix} = -\begin{Bmatrix} \text{components of } \underline{\nabla P}^k \text{ corresponding to nonsingular part} \\ \text{components of } \underline{\nabla P}^k \text{ corresponding to singular part} \end{Bmatrix} = \begin{Bmatrix} \underline{g} \\ \underline{h} \end{Bmatrix} \tag{25}$$

3. For a one term approximation the following differential algebraic system of equations must be solved

$$\underline{x}_0' = \underline{g}(\underline{x}_0, \underline{y}_0; \epsilon); \quad \underline{x}_0(0) = \underline{A}_x^k \tag{26-a}$$

$$0 = \underline{h}(\underline{x}_0, \underline{y}_0; \epsilon); \quad \underline{y}_0(0) = \underline{A}_y^k \tag{26-b}$$

a. Using $\underline{y}_0(0) = \underline{A}_y^k$ as the initial guess apply one step of the quasi-Newton Method to obtain

$$\underline{y}_0(0) = \underline{A}_y^k - \underset{\sim}{H}_{yy} \underline{\nabla P}_y^k \tag{27}$$

b. Apply one step of Euler's Method to the differential equation (26-a) to obtain $\underline{x}_0(\alpha)$

$$\underline{x}_0(\alpha) = \underline{A}_x^k - \alpha \underline{\nabla P}_x^k(\underline{A}_x^k, \underline{y}_0(0)) \tag{28}$$

c. Application of one step of the quasi-Newton Method to Eq. (26-b) yields

$$\underline{y}_0(\alpha) = \underline{y}_0(0) - \underset{\sim}{H}_{yy} \underline{\nabla P}_y^k(\underline{x}_0(\alpha), \underline{y}_0(0)) \tag{29}$$

In the above equations the subscripts x and y denote appropriate partitions of the matrices corresponding to singular and nonsingular components. The matrix $\underset{\sim}{H}$ is updated by the usual BFGS update [14]. Thus a direction $\underline{\delta}^k = (\underline{\delta}_x^k, \underline{\delta}_y^k)^t$ is computed such that $\|\underline{\delta}_x^k\| \leq \Delta^k$ and $\|\underline{\delta}_y^k\| \leq \Delta^k$.

4. Test $\langle \underline{\delta}^k, \underline{\nabla P}^k \rangle \leq 0$ i.e. test for a feasible direction. If the test is not satisfied, then set

$$\underline{\delta}^k = (\underline{\delta}^k / \|\underline{\delta}^k\| + \underline{\nabla P}^k / \|\underline{\nabla P}^k\|) \frac{\Delta^k}{2} \tag{30}$$

5. Compute $\underline{A}^{k+1} = \underline{A}^k + \underline{\delta}^k$ and apply test (20). If successful, go to step 8; else go to step 6.

6. Test the point $\underline{A}^{k+1} = \underline{A}^k + \underline{\delta}^k/i$, $i = 2,4,6,8,16,32$ or until (20) is satisfied. If satisfied, go to step 8; else go to step 7.

7. Set $\underline{\delta}^k = -(\underline{\nabla P}^k / \|\underline{\nabla P}^k\|)\Delta^k$ and repeat step 6. If the test is still not satisfied, set $\Delta^k = \Delta^k/2$ and go to the next iteration.

8. Update $\underset{\sim}{H}^k$, $\underset{\sim}{B}^k$ and Δ^k. Δ^k is updated using the procedure outlined by Powell [12] which requires an estimate of $\underset{\sim}{B}^k$. $\underset{\sim}{B}^k$ in turn, is updated like $\underset{\sim}{H}^k$ using the BFGS update [14].

III. APPLICATION TO OPTIMIZATION OF SPACE TRUSSES

In this section the application of the singular perturbation based procedure outlined in the earlier sections and the SUMT algorithm proposed by Fiacco-McCormick [1] is examined. Both the programs share a lot of features in common. They both use the same penalty function - namely the logarithm quadratic loss interior point penalty function. They share an identical finite element program to analyze stress and displacement constraints and both use the same technique

to evaluate the gradient of the penalty function analytically. In view of the limitations on space the details on the analytical evaluation of the gradients of the penalty function will be omitted since they are available to the interested reader by consulting reference [13]. The only difference between the two algorithms is in essence the unconstrained minimization of the penalty function. In one case the method for minimization is Fiacco-McCormick's modification of Fletcher-Powell's Method as reported in [1], whereas in the other case the method for minimization is one based on the singular perturbation theory.

a. Evaluation Basis

The primary interest in evaluating the two algorithms on the various structural optimization problems is not necessarily to select the one algorithm which is the better of the two but rather to observe these techniques for their robustness and reliability, especially in handling problems which may be ill-conditioned as posed.

The initial choice of the penalty parameter, r^0, and the sequence of its successive values is very crucial since an inappropriate choice may result in a seriously ill-conditioned problem. It is therefore natural that the sensitivity of these two algorithms be examined for several different values of these penalty parameters.

The initial value of penalty parameter is calculated according to

$$r^0 = \frac{f(\underline{A})}{\sum_{i=1}^{m} \ln g_i(\underline{A})} \frac{a}{100} \qquad (31)$$

where 'a' is a specified percentage. The parameter 'a' will be set to 10, 20 and 50.

The next value of r is obtained by

$$r^{k+1} = r^k/\text{ratio} \qquad (32)$$

where ratio is again a preassigned parameter. Fiacco-McCormick [1] recommends a value of 16 for this parameter, however, for the purposes of this evaluation a range of values between 10 and 50 is assumed. Finally, the sensitivity of these algorithms to the initial guess is also examined with the proviso that every initial guess be feasible.

b. Example Problems

In order to evaluate the sensitivity of the algorithms to the scale of the problem, two problems with rather widely separated scales are chosen. One of these is a four-bar truss shown in Figure 1. This space truss defined in Table 1 is reproduced directly from Ref. [15] subjected to a single load system as shown in Table 2. Displacement lines are specified in Table 3.

The modified objective function for this problem is

$$P(\underline{A},r) = \sum_{i=1}^{4} \rho A_i L_i + r \sum_{J=1}^{10} \ln g_J(\underline{A}) \qquad (33)$$

where ρ is the specific weight, A_i and L_i are cross sectional area and the length respectively of the ith member, $g_J(\underline{A})$, J = 1,2,...10, are the constraints defined below:

$$g_i = 25{,}000 - \sigma_i > 0$$

or

$$g_i = 25{,}000 + \sigma_i > 0 \text{ if } \sigma_i < 0$$

for i = 1,2,...,4

$$g_5 = 0.3 - v_5 > 0 \text{ if } v_5 > 0$$

or

$$g_5 = 0.3 + v_5 > 0 \text{ if } v_5 < 0$$

$$g_6 = 0.4 - w_5 > 0 \text{ if } w_5 > 0$$

or

$$g_6 = 0.4 + w_5 > 0 \text{ if } w_5 < 0$$

and

$$g_J = A_\ell - .1 > 0 \; ; \quad \text{for } J = 7,8,\ldots,10 \quad \ell = 1,2,\ldots,4$$

Results for the 4-bar truss problem are presented in Table 4. The second problem is a 25-bar transmission tower. The sketch of the 25-bar tower is shown in Figure 2 and defined in Table 5. This entire figure as well as the loading conditions for this problem are reproduced from Ref. [15]. The two independent loading systems are shown in Table 6. The modified objective function and the constraints for the 25-bar tower may be constructed in a manner similar to that of the 4-bar truss. In this case (assuming symmetry) there are a total of 51 constraints, 25 of which are stress constraints, 18 of which are displacement constraints, and the remaining 8 are the minimum gage constraints. Table 7 summarizes the results for this problem.

The results for the two problems are summarized in the next section. The convergence criterion in each case was assumed to be

$$\text{RSIGMA} = \left| r \sum_{J=1}^{m} \ln g_J(\underline{A}) \right| < \theta_0$$

where θ_0 was assumed to be 1×10^{-3}, the constraints $g_J(\underline{A})$ having been suitably nondimensionalized.

In the tables to follow, NFUN represents the total number of function evaluations, NGRD represent the total number of gradient evaluations and NTIME represents the normalized CPU time for a given problem. Method I is the modified SUMT algorithm; Method II is the original SUMT algorithm.

c. Conclusions

The two separate computer programs used for the implementation of the two algorithms were by no means production programs. No attempt was made to include features like extrapolation which may be hastened the convergence to the final solution. For the two problems considered it was relatively easy to come up with an initial feasible guess. Hence, the need for the implementation of sophisticated features like the extended penalty function [16] did not exist. Likewise no attempt was made to economize on the gradient calculations by restricting such calculations only to those constraints that are active. All such features and a few others can always be implemented to enhance the effectiveness of the respective programs. However, as indicated earlier, the major thrust of this study was to attempt to make the SUMT algorithm more robust and more reliable through the use of the singular perturbation theory.

The results for the 4-bar truss as well as for the 25-bar transmission tower clearly demonstrate that the modified SUMT based on Boggs algorithm is much more robust and has little difficulty in converging to very accurate solutions. Several more cases for many other values of a, ratio and intial guess $\{A\}^0$ may be found in reference [13]. The modified algorithm appears indeed to be much more effective for large scale problems wherein a greater likelihood for ill-conditioning exists simply as a result of the greater probability for the variables to be poorly scaled in such problems. Whether such ill-conditioning is due to the poor scaling of the variables or an inappropriate choice of the penalty parameter, the modified algorithm has a much superior performance as compared with the conventional SUMT both in terms of CPU time and equivalent function evaluations.

Based on Boggs' experiments with mathematical functions [6] it can be safey said that there is very little to be gained in carrying the asymptotic expansion through the second terms. The extra computational effort is likely to outweigh the improved steplength predictions. This is likely to be much more adverse for very large scale problems.

V. REFERENCES

[1] Fiacco, A. V. and McCormick, G. P., Nonlinear Programming; Sequential Unconstrained Minimization Techniques, Wiley, New York, 1968.

[2] Oren, S. S. and Luenberger, D., "Self-Scaling Variable Metric (SSVM) Algorithms, Part I", Management Science, 20, 5, 545-862 (1974).

[3] Oren, S. S. and Spedicato, E., "Optimal Conditioning of Self-Scaling Variable Metric Algorithms", Math. Prog., 10, 70-90 (1976).

[4] Davidon, W. C., "Optimally Conditioned Optimization Algorithms Without Linear Searches", Math. Prog. 9, 1-30 (1975).

[5] Shanno, D. F. and Phua, K. H., "Matrix Conditioning and Nonlinear Optimization", Math. Prog. 14, 149-160 (1978).

[6] Boggs, P. T., "An Algorithm, Based on Singular Perturbation Theory, for Ill-Conditioned Minimization Problems", SIAM, J. Num. Anal., 14, 5, 830-843 (1977).

[7] Boggs, P. T. and Dennis, J. E., "A Stability Analysis for Perturbed Nonlinear Iterative Methods, Math. Comp., 30, 199-215 (1976).

[8] Aiken, R. C. and Lapidus, L., "An Effective Numerical Intergration Method for Typical Stiff Systems", AIChE Journal, 20, 2, 368-375 (1974).

[9] Hoppenstadt, F., "Properties of Solutions of Ordinary Differential Equations with Small Parameters", Comm. Pure Apl. Math. 24, 807-840 (1971).

[10] Flaherty, J. E. and O'Malley, Jr., R. E., "The Numerical Solution of Boundary Value Problems for Stiff Differential Equations", 31, 137, 66-93 (1977).

[11] Miranker, W. L., "Numerical Methods of Boundary Layer Type for Stiff Systems of Differential Equations", Computing, 11, 221-234 (1973).

[12] Powell, M. J. D., "A New Algorithm for Unconstrained Optimization", Nonlinear Programming, J. Rosen, et al [eds.], Academic Press, New York, 31-66 (1970).

[13] Kamat, M. P. and Ruangsilasingha, P., "A Robust Sequential Unconstrainted Minimization Technique for Structural Optimization", VPI-E-80-20, August 1981.

[14] Dennis, J. E. and More, J. J., "Quasi-Newton Methods, Motivation and Theory", SIAM Review, 19, 1 (1977).

[15] Venkayya, V. B., Khot, N. S. and Reddy, V. S., "Energy Distribution in an Optimum Structural Design", AFFDL-TR-68-156, 1968.

[16] Haftka, R. and Starnes, J., "Applications of a Quadratic Extended Interior Penalty Function for Structural Optimization", AIAA Journal, 14, 6, 718-724 (1976).

VI. RESULTS

Table 1
Design Information for the 4-Bar Truss

Material = Aluminum
Stress Limits = 25000 psi
Modulus of Elasticity, $E = 10^7$ psi
Specific Weight = .1 lb/in^3
Lower Limit on Member Sizes $(A_i)_{min}$ = .1 in^2
Displacement Limit - As specified in Table 3

Table 2
Loading System for 4-Bar Truss

Node	Direction and Magnitude of Load (lb)		
	x	y	z
5	10,000	20,000	-30,000

Table 3
Displacement Limits

Node	Displacement		
	x	y	z
5	None	± .3 (inch)	± .4 (inch)

Table 4
Results for the 4-Bar Truss

I.

METH	Final Value # of Element Areas (in^2) $A_0 = \{1\}$ in^2; a = 10; Ratio = 10								
	A_1	A_2	A_3	A_4	RSIGMA	NFUN	NGRD	NTIME	WEIGHT (lb)
I	0.1000	1.0151	0.9545	.2872	$.1486 \times 10^{-3}$	173	107	1.3828	39.2122
II	0.1032	1.0275	0.9593	.2814	$.7777 \times 10^{-1}$	534	26	1.0	39.3959

II.

METH	Final Value # of Element Areas (in^2) $A_0 = \{3\}$ in^2; a = 10; Ratio = 10								
	A_1	A_2	A_3	A_4	RSIGMA	NFUN	NGRD	NTIME	WEIGHT (lb)
I	0.1000	1.0152	0.9547	0.2872	$.1302 \times 10^{-2}$	176	100	.6881	39.212
II	0.1008	1.0184	0.9558	0.2856	$.9049 \times 10^{-2}$	1097	47	1.0	39.2575

III.

METH	Final Value # of Element Areas (in^2) $A_0 = \{1\}$ in^2; a = 1; Ratio = 10								
	A_1	A_2	A_3	A_4	RSIGMA	NFUN	NGRD	NTIME	WEIGHT (lb)
I	.1000	1.0151	0.9547	0.2872	$.1487 \times 10^{-3}$	171	103	.9192	39.2122
II	.1003	1.0172	0.9552	0.2860	$.1019 \times 10^{-1}$	818	39	1.0	39.2297

IV.

METH	Final Value # of Element Areas (in^2) $A_0 = \{3\}$ in^2; a = 1; Ratio = 10								
	A_1	A_2	A_3	A_4	RSIGMA	NFUN	NGRD	NTIME	WEIGHT (lb)
I	0.1000	1.0152	0.9547	0.2872	$.1302 \times 10^{-3}$	151	96	.8276	39.2136
II	0.1008	1.0186	0.9558	0.2855	$.9056 \times 10^{-2}$	887	38	1.0	39.2572

V.

METH	Final Value # of Element Areas (in^2) $A_0 = \{1\}$ in^2; a = 1; Ratio = 50								
	A_1	A_2	A_3	A_4	RSIGMA	NFUN	NGRD	NTIME	WEIGHT (lb)
I	0.1004	0.9889	0.9529	0.30687	$.6598 \times 10^{-4}$	160	84	.699	39.2490
II	0.1001	1.0153	0.9547	0.28711	$.2369 \times 10^{-2}$	878	42	1.0	39.2155

VI.

METH	Final Value # of Element Areas (in^2) $A_0 = \{3\}$ in^2; a = 1; Ratio = 50								
	A_1	A_2	A_3	A_4	RSIGMA	NFUN	NGRD	NTIME	WEIGHT (lb)
I	0.1000	1.0153	0.9547	0.28712	$.4732 \times 10^{-3}$	99	63	.8425	39.2138
II	0.1016	1.0217	0.9570	0.2840	$.1687 \times 10^{-1}$	556	24	1.0	39.3039

Table 5
Ten Node Twenty-Five Bar Transmission Tower

Material: Aluminum
Stress Limits = 40,000 psi
Modulus of Elasticity, $E = 10^7$ psi
Specific Weight $\rho = .1$ lb/in^3
Lower Limit on Member Sizes $(A_i)_{min} = .01$ in^2
Displacement Limits: .35 inch on all nodes in all directions

Table 6
Loading System for 25-Bar Truss

Load Condition	Nodal Point	Direction & Magnitude x	y	z
1	1	1,000	10,000	-5,000
	2	-	10,000	-5,000
	3	500	-	-
	6	500	-	-
2	1	-	20,000	-5,000
	2	-	-20,000	-5,000

Table 7
Results for the 25-Bar Transmission Tower

Ratio	r^o	A^o	Method I			
20	.37892	{3} in^2	NFUN	NGRD	NTIME	WEIGHT (lb)
RSIGMA = 19178x10^{-3}			279	149	1.0	545.04084

El. No.	Area (in^2)	El. No.	Area (in^2)	El. No.	Area (in^2)
1	0.0106	10	0.0100	19	1.6171
2	2.0525	11	0.0100	20	1.6171
3	2.0525	12	0.0101	21	1.6171
4	2.0525	13	0.0101	22	2.6766
5	2.0525	14	0.6815	23	2.6766
6	2.9980	15	0.6815	24	2.6766
7	2.9980	16	0.6815	25	2.6766
8	2.9980	17	0.6815		
9	2.9980	18	1.6171		

Ratio	r^o	A^o	Method II			
20	.3789	{3} in^2	NFUN	NGRD	NTIME	WEIGHT (lb)
RSIGMA = .30346x10^{-2}			2342	110	1.52	545.0514

El. No.	Area (in^2)	El. No.	Area (in^2)	El. No.	Area (in^2)
1	0.0102	10	0.0102	19	1.6331
2	2.0229	11	0.0102	20	1.6331
3	2.0229	12	0.0102	21	1.6331
4	2.0229	13	0.0102	22	2.6687
5	2.0229	14	0.6813	23	2.6687
6	3.0173	15	0.6813	24	2.6687
7	3.0173	16	0.6813	25	2.6687
8	3.0173	17	0.6813		
9	3.0173	18	1.6331		

Ratio	r^o	A^o	Method I			
20	.003789	{3} in^2	NFUN	NGRD	NTIME	WEIGHT (lb)
RSIGMA = .67207x10^{-3}			162	80	1.0	545.0383

El. No.	Area (in^2)	El. No.	Area (in^2)	El. No.	Area (in^2)
1	0.0101	10	0.0100	19	1.6233
2	2.0424	11	0.0100	20	1.6233
3	2.0424	12	0.0100	21	1.6233
4	2.0424	13	0.0100	22	2.6717
5	2.0424	14	0.6835	23	2.6717
6	3.0028	15	0.6835	24	2.6717
7	3.0028	16	0.6835	25	2.6717
8	3.0028	17	0.6835		
9	2.5735	18	1.7659		

Ratio	r^o	A^o	Method II			
20	.003789	{3} in^2	NFUN	NGRD	NTIME	WEIGHT (lb)
RSIGMA = 0.62302x10^{-2}			3416	140	3.77	632.6053

El. No.	Area (in^2)	El. No.	Area (in^2)	El. No.	Area (in^2)
1	1.9577	10	0.9143	19	1.7659
2	2.1453	11	0.9143	20	1.7659
3	2.1453	12	1.8668	21	1.7659
4	2.1453	13	1.8668	22	2.3678
5	2.1453	14	1.3790	23	2.3678
6	2.5735	15	1.3790	24	2.3678
7	2.5735	16	1.3790	25	2.3678
8	2.5735	17	1.3790		
9	2.5735	18	1.7659		

Ratio	r^o	A^o	Method I			
20	.00556	{4} in^2	NFUN	NGRD	NTIME	WEIGHT (lb)
RSIGMA = 9714x10^{-3}			159	89	1.0	545.0401

El. No.	Area (in^2)	El. No.	Area (in^2)	El. No.	Area (in^2)
1	0.0101	10	0.0101	19	1.6283
2	2.0424	11	0.0101	20	1.6233
3	2.0424	12	0.0101	21	1.6233
4	2.0424	13	0.0101	22	2.6716
5	2.0424	14	0.6835	23	2.6716
6	3.0028	15	0.6835	24	2.6716
7	3.0028	16	0.6835	25	2.6716
8	3.0028	17	0.6835		
9	3.0028	18	1.6233		

Ratio	r^o	A^o	Method II			
20	.00556	{4} in^2	NFUN	NGRD	NTIME	WEIGHT (lb)
RSIGMA = 0.93609x10^{-3}			3376	156	3.12	545.5333

El. No.	Area (in^2)	El. No.	Area (in^2)	El. No.	Area (in^2)
1	0.0106	10	0.0101	19	1.6580
2	2.0373	11	0.0101	20	1.6580
3	2.0373	12	0.0100	21	1.6580
4	2.0373	13	0.0100	22	2.6169
5	2.0373	14	0.7399	23	2.6169
6	2.9343	15	0.7399	24	2.6169
7	2.9343	16	0.7399	25	2.6169
8	2.9343	17	0.7399		
9	2.9343	18	1.6580		

Ratio	r^o	A^o	Method I			
50	.72425	{5} in^2	NFUN	NGRD	NTIME	WEIGHT (lb)
RSIGMA = .4489x10^{-3}			217	104	1.0	545.0871

El. No.	Area (in^2)	El. No.	Area (in^2)	El. No.	Area (in^2)
1	0.0100	10	0.0106	19	1.6056
2	2.0395	11	0.0106	20	1.6056
3	2.0395	12	0.0100	21	1.6056
4	2.0395	13	0.0100	22	2.6618
5	2.0395	14	0.6856	23	2.6618
6	3.0457	15	0.6856	24	2.6618
7	3.0457	16	0.6856	25	2.6618
8	3.0457	17	0.6856		
9	3.0457	18	1.6056		

Ratio	r^o	A^o	Method II			
50	.72425	{5} in^2	NFUN	NGRD	NTIME	WEIGHT (lb)
RSIGMA = .91935x10^{-2}			687	24	0.66	682.3302

El. No.	Area (in^2)	El. No.	Area (in^2)	El. No.	Area (in^2)
1	6.3288	10	3.0179	19	1.7365
2	1.8462	11	3.0170	20	1.7365
3	1.8462	12	3.0229	21	1.7365
4	1.8462	13	3.0229	22	2.6270
5	1.8462	14	0.6466	23	2.6270
6	3.1591	15	0.6466	24	2.6270
7	3.1591	16	0.6466	25	2.6276
8	3.1591	17	0.6466		
9	3.1591	18	1.7365		

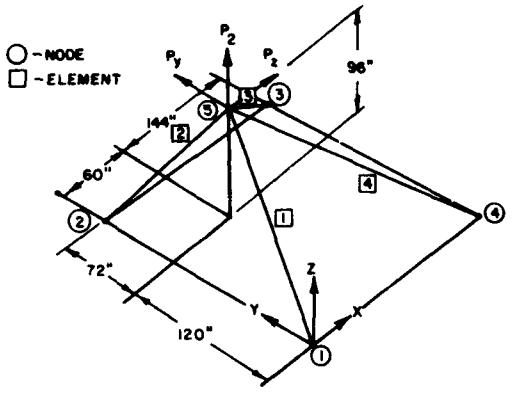


Figure 1 Loading System for the 4-Bar Truss

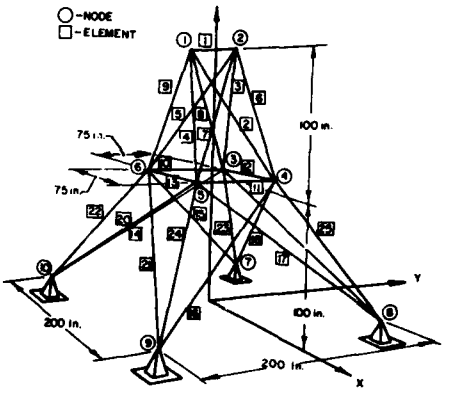


Figure 2 Loading System for the 25-Bar Transmission Tower

AD-P000 069

AN ALGORITHM FOR OPTIMUM STRUCTURAL DESIGN WITHOUT LINE SEARCH

Jasbir S. Arora, Professor
and
Sharad V. Belsare, Research Assistant
Division of Materials Engineering
The University of Iowa
Iowa City, Iowa 52242

Abstract

In this paper, a new optimization algorithm for optimal design of engineering systems is presented. The main feature of the new algorithm is that it does not rely on one dimensional search to compute a step size at any design iteration. Implication of the feature is that algorithm requires evaluation of constraint functions only once at any design iteration. This is highly desirable for optimal design of engineering systems because evaluation of constraints for such systems is very expensive. The reason for the high cost is that many constraints for such design problems are implicit functions of design variables. Thus their evaluation requires solution for a high dimensional finite element model for the system. The new algorithm is based on finding upper and lower bounds on the optimum cost and is derived in the paper. Several new step sizes are introduced and their relation to proper reduced optimal design problems are presented. Numerical aspects for the algorithm are also presented. Based on the new algorithm, a general purpose computer code GRP2 is developed. The code is used to solve several small scale problems to gain experience and insight into the algorithm. Numerical experience with examples is discussed. It is shown that the algorithm has substantial potential for applications in optimal design of engineering systems.

I. Introduction

During the past twenty years, considerable numerical work has been done to show that optimization techniques have potential for practical applications in engineering system design [1-4]. Whereas this is true, several problems remain to be addressed before efficient and effective algorithms can be developed for optimal design of complex systems. A fundamental problem that remains unsolved for application of optimization techniques to large complex engineering systems is that of a proper step length calculation. The step size calculation problem is that after a direction of travel has been determined in the design space, how far should one travel along this direction to determine a new design point. For nonlinear programming problems, this is not difficult, as one dimensional search can be readily used to calculate an optimum step length. However, one dimensional search is quite expensive, if not impossible in engineering design applications. The major reason for this difficulty is that many constraints in such applications are implicit functions of design variables. Evaluation of such constraints requires solution of equilibrium equations for quasi-static problems and integration of equations of motion for dynamic response problems. Thus one dimensional search may require several analyses of the system before a proper step length may be determined. This can lead to a highly inefficient and ineffective algorithm for practical applications in engineering design.

A fundamental hypothesis of this paper is that one dimensional search for optimal design of complex engineering systems is inefficient and should not be used. Therefore other concepts and methods for step size calculation need to be deveoped for such problems. The paper presents a method for step size calculation based on computing bounds on the optimum value of the cost function of the design problem.

The fundamental idea of the method is to first locate lower and upper bounds on the optimum value of the cost function. Once this is done the design space between these bounds is systematically searched to locate feasible designs that are better than the previous design. During this search procedure better upper and lower bounds on the optimum cost function are also established. since different step size selection techniques can yield vastly different optimization algorithms, the algorithm developed in the paper is regarded as a new algorithm for optimal design of engineering systems.

To accomplish the objectives mentioned above several relatively simple concepts are introduced in the paper. These include, a constraint correction vector, a descent direction, and a constant cost direction. An algorithm based on these concepts is then derived. Some properties of the algorithm that are extremely useful in its numerical implementation are derived. Step size ideas are completely developed. Finally, some numerical examples are solved to show effectiveness of the algorithm.

II. Design Optimization Model

The behavior of most engineering systems is governed by some law of physics. This behavior is described analytically by a set of variables called state variables. For structural and elastic mechanical systems, state variables may include displacements and stresses at certain points, eigenvectors, eigenvalues, etc. Let $z \in R^n$ be a state variable representing displacements at key points of the structure, and let the vector $y \in R^n$ represent an eigenvector. There is a second set of variables called design variables that describe the system. These variables are chosen by the designer. The equations that determine the state of structural and mechanical systems generally depend on the design variables; so the two sets of variables are related. Member thickness, cross-sectional area, moment of inertia, flange and web thickness are design variables. Let $b \in R^k$ represent a vector of design variables.

The most practical way of analyzing the behavior of a large and complex structural system is the finite element approach. The governing equilibrium equation for a finite element model of such a structure subjected to quasi-static load is

$$K(b)z = S(b) \tag{1}$$

where

$K(b)$ = an n x n symmetric nonsingular structural stiffness matrix,
$S(b)$ = an n-vector representing equivalent nodal loads for the finite element model.

PRECEDING PAGE

A large number of complex structural systems subjected to a wide variety of loads can be represented by Eq. (1). Examples of these structures include aircraft structures, spacecraft structures, antennae, building frames, bridge structures, various supporting structures, special purpose machine elements etc. The loads that may be included in the vector S(b) are the dead loads supported by the structure, the live loads, thermal loads, loads due to initial imperfections, and g loads. Using the displacements found from Eq. (1), stresses at various points of the structure are computed.

Another equilibrium equation that governs the free vibration response of a structure of its buckling behavior is the eigenvalue problem

$$K(b)y = \zeta M(b)y \tag{2}$$

where

M(b) = an n x n structural mass matrix for the vibration problem and the geometric stiffness matrix for the buckling problem,
ζ = an eigenvalue related to the natural frequency or the buckling load for the problem,
y = an eigenvector.

Note that in Eqs. (1) and (2), K(b) and M(b) are symmetric matrices. For the finite element model of the structure the quantities K(b), M(b), and S(b) are continuously differentiable functions of b. Also, since K(b) is nonsingular, the Implicit Function Theorem can be invoked for Eq. (1) to state that z is a continuously differentiable function of b. Further, since K(b) and M(b) are symmetric and K(b) is positive definite, all eigenvalues of Eq. (2) are real and positive, and the eigenvectors are orthogonal with respect to K and M. Further, if no repeated roots occur, then the eigenvalue ζ and the eigenvector y are continuously differentiable functions of b. These properties are assumed in derivations of subsequent sections.

Now a general mathematical model for optimal design of linearly elastic structural systems is defined as follows:

Problem P1: Find a design variable vector $b \in R^k$ that minimizes a cost function

$$\psi_0(b,z,\zeta), \tag{3}$$

and satisfies the equilibrium equations (1) and (2) and the constraints

$$\psi_i(b,z,\zeta) \leq 0, \quad i = 1, 2, \ldots, m \tag{4}$$

The mathematical model P1 is quite general. For example, the cost function of Eq. (3) may represent weight of the structure, deflection or stress at critical points of the structure, support reaction, natural frequency related function, or any other function of b, z, and ζ. The inequalities of Eq. (4) also represent a wide variety of constraints, such as stress, displacement, von Mises yield criterion, buckling, natural frequency, member size and any other functional relationship between b, z, and ζ. It is noted that equality constraints, if present in any design problem, are routinely treated in the algorithm [4].

It is critically important to realize that function ψ_0 and ψ_i are implicit functions of design variable b because z and ζ are implicit functions of b. To evaluate these functions for any given design b, one must solve Eqs. (1) and (2) for the finite element model of the system. This is a major calculation in any design optimization algorithm. If a one dimensional search is to be performed in an optimization algorithm, designer must solve Eqs. (1) and (2) for each update of design and evaluate all the constraints given in Eq. (4). This can be quite inefficient. Therefore, an objective of the current paper is to develop algorithms that do not rely on one dimensional search.

It is also important to note that algorithm developed in the paper is applicable to dynamic response problems, although these applications are not discussed in the present paper. For more details on how an algorithm, such as the one derived in the paper, is directly applicable to dynamic response problems, refer to Chapter 5 of Ref. 4.

III. Derivation of the Algorithm

In this section some basic derivations for the algorithm are presented. Two results are used in these derivations. The first result involves the use of an efficient method for calculation of gradients of various implicit functions for the problem. This problem has been adequately addressed in the literature [4-8]. Therefore it is assumed in the paper that an efficient method for calculation of gradients of various implicit functions for the problem has been used in numerical calculations. The second result that is used in the paper is the standard set of Kuhn-Tucker necessary conditions of nonlinear programming [4].

The method derived herein falls into the class of direct methods of nonlinear programming in which one starts with an initial estimate b^0 for the design. Constraints of the problem are then checked and design gradients of active and violated constraints are calculated. Using these gradients and the gradient of the cost function, a change in design δb is computed and the design is upgraded as $b^1 = b^0 + \delta b$. The process is continued until convergence criteria are satisfied. The following analysis applies to any design iteration. Therefore the iteration counter is omitted in all derivations. Also arguments for various functions and gradient vectors are omitted. It is understood that these quantities are computed for the most current value of design variables.

To calculate a change δb in the current design b, functions of the problem are linearized and a reduced optimization problem for δb is defined as follows:

Reduced Problem R1: Find δb to minimize a first order change in the cost function as

$$\delta\psi_0 = g^{0^T} \delta b \tag{5}$$

subject to linearized constraints

$$\psi_i + g^{i^T} \delta b \leq 0, \quad i = 1, 2, \ldots, m \tag{6}$$

and a quadratic step size constraint

$$\delta b^T W \delta b \leq \xi^2 \tag{7}$$

For the problem R1, g^0 is the gradient of the cost function and g^i is gradient of the ith constraint function. These gradients may be calculated using methods of Refs. 5-7. In Eq. (7), W is a positive definite weighting matrix and ξ is a small number. Equation (7) is a step size constraint used to obtain a bounded solution for the Problem R1. It represents a hypersphere in the design space with ξ as its radius and origin at the current design point. The step size constraint is tight at the optimal solution for the

reduced Problem R1. Therefore, value of ξ effects convergence of the design algorithm. It is also noted that by selecting W to be Hessian of the Lagrange function for the Problem P1, Newton-like algorithms can be generated [8]. Or by selecting W to be an estimate for the above Hessian matrix quasi-Newton methods can be generated. In the derivations presented here W is included to encompass these possibilities. However, in all the numerical results presented later in the paper, W is taken as an identity matrix.

Reduced Problem R1 has been addressed adequately in the literature [4,8,9]. Therefore, omitting details, an application of Kuhn-Tucker necessary conditions yields the following solution for Problem R1:

$$\delta b = -\eta \delta b^1 + \delta b^2 \tag{8}$$

where vectors δb^1 and δb^2 are given as

$$\delta b^1 = W^{-1}(g^0 + g\mu^1) \tag{9}$$

$$\delta b^2 = -W^{-1} g \mu^2 \tag{10}$$

Here g is a matrix whose each column is the design gradient of a constraint, and μ^1 and μ^2 are solutions of the following linear set of equations:

$$\bar{B}\mu^1 = -g^T W^{-1} g^0, \quad \bar{B}\mu^2 = \psi \tag{11}$$

where

$$\bar{B} = g^T W^{-1} g, \quad \psi = \{\psi_i\} \tag{12}$$

In Eq. (8), η is a step size for the current design iteration. Also, the Lagrange multiplier vector for the Problem R1 is given as

$$\mu = \mu^1 + \mu^2/\eta \tag{13}$$

It is shown in Ref. 4 that the Lagrange multiplier vector μ of Eq. (13) for Problem R1 converges to the Langrange multiplier vector for the Problem P1 as the optimum is reached. Also, it is shown there that as the optimum to P1 is reached, $\delta b^1 \to 0$.

The algorithm derived above has been used successfully to solve several classes of optimal design problems [4]. However, calculation of the step size η in Eq. (8) has been done in an ad hoc manner. Calculation for a step size has been the most difficult part in the algorithm. It has generally required some experience with the class of design problems being considered before a proper step size could be calculated. In order to present better and automatic methods for calculating step size, without doing one dimensional search, it will be highly advantageous to normalize the reduced Problem R1 for change in design δb. The normalized reduced problem leads to results that are extremely useful in numerical implementation of the optimal design algorithm. These aspects are discussed later in the paper.

Since W is a positive definite matrix, it may be decomposed as

$$W = U^T U \tag{14}$$

where U is an upper triangular matrix. Quite often, W is a diagonal matrix with positive elements. Therefore in such a case, $U_{ii} = \sqrt{W_{ii}}$ and $U_{ij} = 0$ for $i \neq j$. Now define a new variable s as

$$s = U \delta b \tag{15}$$

or δb is given as

$$\delta b = U^{-1} s \tag{16}$$

Equation (16) is a simple transformation equation for δb that may be substituted into Eqs. (5) to (7) to transform the reduced Problem R1 in terms of s. Columns of U^{-1} or U are linearly independent, so they form a basis for the k dimensional vector space. Therefore, once s is known, δb is uniquely known from Eq. (16). Or inversely, if δb is known, then s is uniquely known from Eq. (15).

Substitue for δb from Eq. (16) into Eqs. (5) to (7) to obtain

$$\delta\psi_0 = g^{0T} U^{-1} s \tag{17}$$

$$\psi_i + g^{iT} U^{-1} s \leq 0, \quad i = 1, 2, \ldots, m \tag{18}$$

$$s^T s \leq \xi^2 \tag{19}$$

Now dividing Eqs. (17) and (18) by a positive number

$$||U^{-T} g^i|| = [(U^{-T} g^i)^T U^{-T} g^i]^{1/2} = [g^{iT} W^{-1} g^i]^{1/2} \tag{20}$$

for i = 0, 1, 2, ..., m, the normalized reduced problem may be defined as follows:

Reduced Problem R2: find s that minimizes a normalized cost function

$$\bar{\delta\psi}_0 = A^{0T} s \tag{21}$$

subject to the constraints

$$A^{iT} s \leq \Delta_i, \quad i = 1, 2, \ldots, m \tag{22}$$

and constraint of Eq. (19). Here,

$$A^0 = (U^{-T} g^0)/||U^{-T} g^0|| \tag{23}$$

$$A^i = (U^{-T} g^i)/||U^{-T} g^i||, \quad i = 1, 2, \ldots, m \tag{24}$$

$$\Delta_i = -\psi_i/||U^{-T} g^i||, \quad i = 1, 2, \ldots, m \tag{25}$$

Note from Eq. (24) that A^i are unit vectors. Also A^0 is a unit vecto. A first order change in cost is given as

$$\delta\psi_0 = ||U^{-T} g^0|| A^{0T} s \tag{26}$$

The Kuhn-Tucker necessary conditions for the reduced Problem R2 guarantee that there exist multipliers $\nu_i \geq 0$, and $\gamma \geq 0$ such that

$$\frac{\partial}{\partial s}\left[A^{0T} s + \nu^T (A^T s - \Delta) + \gamma(s^T s - \xi^2)\right] = 0$$

or

$$A^0 + A\nu + 2\gamma s = 0; \tag{27}$$

and

$$\nu_i (A^{iT} s - \Delta_i) = 0, \quad i = 1, 2, \ldots, m \tag{28}$$

$$\gamma(s^T s - \xi^2) = 0 \tag{29}$$

where columns of the matrix A are the tansformed design sensitivity vectors of the ε-active constraints. Equations (27) - (29) must be solved for s, ν, and γ.

Assuming $\gamma > 0$ (i.e., constraint 19 is active), s from Eq. (17) is given as

$$s = -\frac{1}{2\gamma}(A^0 + A\nu) \tag{30}$$

Assuming $\nu_i > 0$ for all i, one obtains $A^T s - \Delta = 0$ from Eq. (28). Substituting for s from Eq. (30) into this equation, one obtains

$$B\nu = -2\gamma\Delta - A^T A^0; \quad B = A^T A \tag{31}$$

After calculating ν, the assumption $\nu_i > 0$ for all i is checked and if necessary the matrix A is re-assembled and calculations for ν carried out again. Substituting for ν from Eq. (31) into Eq. (30), one obtains

$$s = -\eta s^1 + s^2; \quad \eta = \frac{1}{2\gamma} \tag{32}$$

where

$$s^1 = PA^0; \quad P = [I - AB^{-1}A^T] \tag{33}$$

$$s^2 = AB^{-1}\Delta \tag{34}$$

Now, one could substitute s from Eq. (32) into $s^T s = \xi^2$ and solve for γ. However, ξ^2 must be chosen by the designer. Therefore, it is appropriate to choose $\gamma > 0$ directly and interpret $1/(2\gamma)$ as a step size. The matrix P of Eq. (33) is a projection matrix since $PP = P$. Also note that P is a symmetric matrix, since B^{-1} is a symmetric matrix. It should be noted that if gradients of all constraints are linearly independent at the current design, then matrix B is positive definite and hence non-singular.

One can avoid explicit computation for B^{-1} in the calculation of s^1 and s^2 if one decomposes the vector ν as

$$\nu = \nu^1 + 2\gamma\,\nu^2 \tag{35}$$

Substituting for ν from Eq. (35) into Eq. (31), one observes that vectors ν^1 and ν^2 are solutions of the following systems of equations:

$$B\nu^1 = -A^T A^0, \quad B\nu^2 = -\Delta \tag{36}$$

Substituting Eqs. (36) into Eqs. (33) and (34), s^1 and s^2 are given in terms of ν^1 and ν^2, as

$$s^1 = [A^0 + A\nu^1]; \quad s^2 = -A\nu^2 \tag{37}$$

IV. Properties of the Algorithm

The algorithm derived in the previous section is a variation of the gradient projection method of nonlinear programming. It has several properties that are extremely useful for its numerical implementation. Also, these properties are utilized in developing step size calculation for the algorithm.

The vectors s^1 and s^2 of Eqs. (33) and (34), or Eq. (37) satisfy the following properties at any design iteration:

$$\text{(i)} \quad s^{1T} s^2 = 0 \tag{38}$$

$$\text{(ii)} \quad A^T s^2 = \Delta \tag{39}$$

$$\text{(iii)} \quad A^T s^1 = 0 \tag{40}$$

$$\text{(iv)} \quad A^{0T} s^1 = ||s^1||^2 \tag{41}$$

$$\text{(v)} \quad A^{0T}(-s^1) \leq 0 \quad \text{and} \quad A^{0T}(-s^1) = 0 \tag{42}$$

if and only if $s^1 = 0$

These properties are proved by direct substitution [10] from Eqs. (33) and (34). Property (i) shows that the directions s^1 and s^2 are othogonal to each other. Property (ii) shows that the vector s^2 gives desired corrections to constraint violations (to first order). This is an extremely useful property as s^2 can be used at any design iteration to just correct constraint violations. Property (iii) indicates that a move in s^1 direction does not effect constraint functions (to first order). Property (iv) shows that the inner product of vectors A^0 and s^1 is non-negative and is equal to $||s^1||^2$. This also implies that the angle between A^0 and s^1 is always between 0 and 90°. Property (v) shows that the direction $(-s^1)$ is one of descent for the cost function. Any move along $(-s^1)$ direction reduces the cost function.

The Lagrange multipliers for the Problem P1 at the optimum point give a very useful information to the designer. The constraint variations sensitivity theorem [4] shows that the values of these multipliers indicate for the designer what the gain in cost for the design problem will be if a particular constraint is slightly relaxed. Conversely, it also tells the designer what the increase in cost will be if a constraint is made more severe. Consequently relative values of the Lagrange multipliers for the tight constraints at the optimum tell the designer which constraint results in a maximum change in cost and which constraint results in a minimum change in cost if he decides to vary limiting values for the constraints. Therefore, it is useful to obtain Lagrange multipliers for the Problem R1 using Lagrange multipliers of the Problem R2. These desired relations can be readily obtained if transformation of Eqs. (23) to (25) are substituted into Eqs. (36) and resulting expressions are compared to Eqs. (11) and (12). Thus, the relations between the Lagrange multipliers for the Problems R1 and R2 are given as

$$\mu_i^1 = ||U^{-T}\ell^0||\,\nu_i^1/||U^{-T}\ell^i|| \tag{43}$$

$$\mu_i^2 = \nu_i^2/||U^{-T}\ell^i|| \tag{44}$$

Another important step in the algorithm is to check for the sign of Lagrange multipliers given by the Eq. (35). Since only first order information is used in the algorithm, large constraint violations can occur at any design iteration. In such a case it is desirable to correct only constraint violations. Therefore, the sign check for the Lagrange multipliers of Eq. (35) cannot be made, as these multipliers are for the reduced Problem R2 which is based on reduction in cost function. However, it is interesting to note that the Lagrange multipliers for the problem of constraint correction are given in the vector ν^2. Therefore, sign check should be made for components of ν^2 during the constraint correction step. This can be shown quite readily.

The problem of constraint correction at any design iteration can be defined as follows:

Reduced Problem R3: Find s to minimize

$$\delta\psi' = {}_0 s^T s \tag{45}$$

subject to the constraints

$$A^{i^T} s \leq \Delta_i, \quad i = 1, 2, \ldots, m \tag{46}$$

By writing the Kuhn-Tucker necessary conditions for the Problem R3, it can be readily shown that the vector s^2 given in Eqs. (37) solves the Problem R3 with the corresponding Lagrange multiplier ν^2 given in Eqs. (36). This analysis then yields an extremely useful criterion for checking signs of Lagrange multipliers at any design iteration. That is, if constraints are to be corrected at any design iteration, then the sign check for components of ν^2 should be made and the constraints corresponding to negative ν^2 components should be deleted from the constraint set. By deleting these constraints what we are saying is that these constraints will be satisfied (to first order) at a reduced value of the cost function given in Eq. (45). Reduction in the cost function of Eq. (45) is not only useful but also desirable, as it implies that we can come into the feasible region at a reduced length of the vector s. Since only first order terms are used in expansions of various functions it is highly desirable to keep s as small as possible.

Another extremely important step in the algorithm is to decide when to take a constraint correction step and when to take a cost reduction step. Such a criterion will also decide whether to check signs of the multipliers ν^2 or ν^1. The criterion for constraint correction step should be based on the severity of constraint violation at any design cycle. There are two ways in which the severity of constraint violations may be checked. The first criterion may be based on the amount of maximum constraint violation. If the maximum constraint violation is greater than a certain percentage of the nominal constraint value, the constraints may be treated as severely violated and a constraint correction step should be taken. This criterion works fairly well for most problems. However, in some cases this criterion may be unnecessarily conservative and may take more constraint correction steps than necessary. Another criterion for checking severity of constraint violation may be based on the increase in the cost function that may result in case constraints are corrected. If the increase in cost to correct constraints is larger than a given percent of the current cost (2-5%) then the constraint correction step should be taken.

Since s^2 is the vector that corrects constraint violations, change in cost $\Delta\psi_{02}$ to correct constraints is given from Eq. (17) as

$$\Delta\psi_{02} = \ell^{0^T} U^{-1} s^2 \tag{47}$$

substituting for s^2 from Eq. (37) and using Eq. (36), Eq. (47) becomes

$$\Delta\psi_{02} = (\ell^{0^T} U^{-1})(A B^{-1} \Delta) \tag{48}$$

Using Eqs. (24) and (36), Eq. (48) can be reduced to

$$\Delta\psi_{02} = -||U^{-T}\ell^0||\,\nu^{1^T}\Delta \tag{49}$$

Equation (49) can be used to calculate change in the cost to correct constraint violations without calculating s^2, and decision can be made whether to take a constraint correction step or not.

Another way of obtaining Eq. (49) is to use the constraint sensitivity theorem [4] for the Problem R2. To use this theorem, one may argue that the constraints of Eq. (22) are first imposed by setting $\Delta_i = 0$. Corresponding optimal solution for this problem is contained in vectors s^1 and ν^1. Now Δ_i's can be interpreted as variations in the right hand side of the constraints $A^{i^T} s \leq 0$, and according to the constraint sensitivity theorem [4] one has:

$$\frac{\partial(\delta\bar{\psi}_0)}{\partial\Delta_i} = -\nu_i^1 \tag{50}$$

Therefore change in cost in adjusting constraint boundaries by Δ_i's is given as

$$\Delta\psi_{02} = ||U^{-T}\ell^0||\,\delta\bar{\psi}_0 = -||U^{-T}\ell^0||\,\Delta^T\nu^1 \tag{51}$$

which is same as Eq. (49).

It is noted that since $\Delta \leq 0$ and if $\nu^1 \geq 0$ are imposed to treat constraints, Eq. (49) shows that there is an increase in cost to correct constraint violations. However, if equality is imposed in Eq. (22) when there are large constraint violations, then ν^1 is free in sign and Eq. (49) may actually give a reduction in cost.

V. Step Size Calculation

Calculation of a proper step size in an optimization algorithm is of critical importance for stable and rapid convergence to an optimum design. A larger step can cause divergence of the algorithm and a smaller step can slow the rate of convergence. The most commonly used step size calculation method - the one dimensional search - is not efficient for structural design problems. This is due to the fact that several structural analyses of the system would be required to compute a step that minimizes the cost function in the desired descent direction. Approximate structural reanalysis methods can be used to some advantage in this regard. However, this requires calculation of gradients of several response quantities which is again inefficient.

In this section a new concept for determination of a proper step size is presented. The new method is based on first calculating upper and lower bounds on the optimum value of the cost function. Then the design space between these bounds is systematically searched by proper moves in the design space. During this process sharper upper and lower bounds on the optimum cost get defined. The process is continued until convergence criteria are satisfied. This concept of design changes is based entirely on the cost function value at a design cycle. Therefore, the cost function for the problem should be well defined.

In the design algorithm, the first step is to establish lower and upper bounds on the optimum cost function. Establishment of an upper bound on the optimum cost is fairly straight forward. Cost function value corresponding to any feasible design point that is not an optimum point, gives an upper bound on the optimum cost. Thus if the starting design is infeasible, the first step is to obtain a feasible design. For this purpose, the s^2 direction from Eq. (34) is used. Or, the Problem R3 is solved. Establishment of a lower bound on the optimum cost function value is more challenging. One way of establishing a lower bound on the optimum cost is to show that at a particular value of the cost a feasible design cannot be obtained. This can be viewed as a problem of trying to enter the constraint set from an infeasible point without any change in cost. This implies that one needs a method for taking constant cost steps in the design algorithm. The present algorithm allows one to take such a step whenever it is

necessary. This will be explained later in the section.

Once lower and upper bounds are established, one simply tries to locate feasible designs at lower cost while keeping all the designs within the established bounds. For further discussion, let ψ_{0u} and $\psi_{0\ell}$ represent upper and lower bounds on optimum value of the cost function, respectiely. Before presenting various step size calculations, several parameters that will be used later need to be defined.

First of all, one needs to determine whether the current design point is feasible or infeasible. One method is to check all constraints and defin. the maximum constraint violation as

$$||\psi||_\infty = \max_i \{\psi_i\}, \text{ for all i with } \psi_i > 0 \qquad (52)$$

If $||\psi||_\infty < \theta_2$ where θ_2 is a small positive number, then the current design is feasible. If $\theta_2 < ||\psi||_\infty < \theta_1$, where θ_1 is (another positive) small number, greater than θ_2, then the current design point is nearly feasible, otherwise it is infeasible.

Many times, when the current design point is infeasible, one would like to know change in the cost to bring the design point into the feasible region (i.e., to correct all the constraint violations). Let $\Delta\bar{\psi}_{02}$ represent a ratio of change in the cost to correct constraints to the current value of cost function. Therefore, from Eq. (26),

$$\Delta\bar{\psi}_{02} = (\Lambda^{0T} s^2)\ ||U^{-T}\ell^0||/\psi_0 \qquad (53)$$

where ψ_0 is the current value of the cost function. Thus, if $\Delta\bar{\psi}_{02}$ positive and small, then the current design point can be easily made feasible without too much penalty on the cost. Negative value for $\Delta\bar{\psi}_{02}$ implies that constraint correction will lead to reduction in cost whereas $\Delta\bar{\psi}_{02} = 0$ suggests no change in cost due to constraint correction.

Several expressions for step size that will be used in optimal structural design are derived in the following:

(i) Advancing Step Size. When the current design is feasible ($||\psi||_\infty < \theta_2$), but is not optimum, an advancing step size may be used to reduce the cost by some desired amount. Since the design is nearly feasible and s^2 corrects constraint violations, $||s^2||$ must be small. Setting $s^2 = 0$ in Eq. (32), one obtains

$$s = -\eta_1 s^1 \qquad (54)$$

where η_1 is a step size. Substituting Eq. (54) into Eq. (26), one obtains a change in the cost as

$$\Delta\psi_0 = -\eta_1 ||U^{-T}\ell^0||\Lambda^{0T} s^1 \qquad (55)$$

A cost function reduction ratio r is selected by the designer. Or, if lower and upper bounds on the cost function have been established then r is selected in such a way that the new cost lies exactly at the mid-point of lower and upper bound. In this r is given as

$$r = \frac{\psi_{0u} - \psi_{0\ell}}{2\psi_{0u}} = (1 - \psi_{0\ell}/\psi_{0u})/2 \qquad (56)$$

Once r has been assigned, the reduction in current cost is also given as

$$\Delta\psi_0 = -r\psi_0 \qquad (57)$$

From Eq. (55) and Eq. (57), one obtains

$$\eta_1 = \frac{r\psi_0}{\Lambda^{0T} s^1 ||U^{-T}\ell^0||} \qquad (58)$$

Since $\Lambda^{0T} s^1 = ||s^1||^2$, the step size η_1 of Eq. (58) is given as

$$\eta_1 = \frac{r\psi_0}{||s^1||^2 ||U^{-T}\ell^0||} \qquad (59)$$

(ii) Step Size When Current Design is Interior to the Constraint Set. If the current design point is in the interior of the constraint set, then $s^2 = 0$ and $s^1 = \Lambda^0$ from Eq. (37). Substituting $s^1 = \Lambda^0$ into Eq. (58), one obtains another step size as

$$\eta_2 = \frac{r\psi_0}{||\Lambda^0||^2 ||U^{-T}\ell^0||} = \frac{r\psi_0}{||U^{-T}\ell^0||} \qquad (60)$$

Comparing Eqs. (59) and (60), one observes that η_2 and η_1 are related as follows:

$$\eta_2 = ||s^1||^2 \eta_1 \qquad (61)$$

Since $||s^1||^2 < 1$ [10] one has from Eq. (61) $\eta_2 < \eta_1$.

(iii) Constant Cost Step Size. At many design iterations, it may be desirable to use a step that leaves the cost unchanged. This type of step size is desirable when the current design point is nearly infeasible. Substituting Eq. (32) into Eq. (26) and setting the change in cost $\Delta\psi_0 = 0$, one obtains

$$\Delta\psi_0 \equiv \Lambda^{0T} (-\eta_3 s^1 + s^2) ||U^{-T}\ell^0|| = 0$$

or

$$\eta_3 = \frac{\Lambda^{0T} s^2}{\Lambda^{0T} s^1} = \frac{\Lambda^{0T} s^2}{||s^1||^2} \qquad (62)$$

Here, η_3 is a step size that changes the design at constant cost function value. Thus, if a constant cost step brings the next design into the feasible region, then the current cost gives an upper bound on the optimum cost. Otherwise, it gives a lower bound to the optimum cost.

The change in design that gives constant cost step can also be obtained by solving the following reduced problem:

Reduced Problem R4: Find s to minimize

$$\delta\psi_0' = s^T s \qquad (63)$$

subject to the constraints

$$\Lambda^{0T} s = 0 \qquad (64)$$

and

$$\Lambda^T s < \Delta \qquad (65)$$

It can be shown by writing the Kuhn-Tucker necessary conditions for the Problem R4, that the step size η_3 of Eq. (62) is related to the Lagrange multiplier for the constraint of Eq. (64).

(iv) Zero Step Size. When the current design point is far from the feasible region, it is desirable to correct only the violated constraints. In the present algorithm, this can be accomplished quite easily by setting $\eta = 0$ in Eq. (32). It should be noted that $\eta = 0$ usually results in an increase in the cost.

(v) Overall Step Size. Step sizes determined in the preceding four paragraphs can result in a large change in design which is undesirable due to linearizations used in the algorithm. Even a zero step size ($\eta = 0$) to correct constraints can result in a large change in design when the design is highly infeasible. Therefore, an overall step size is introduced to limit the change in design. Thus a desirable change in design may be expressed as

$$\delta b = \eta_0 \delta \tilde{b} \tag{66}$$

where $\delta b = U^{-1}s$ is the calculated change in design, η_0 is an overall step size and $\delta \tilde{b}$ is a desired change in design. Several criteria may be used in calculating the step size η_0. One criterion may be that the change in design δb should not be more than a fraction of the current design at any iteration. That is

$$||\delta b|| \leq r_1 ||b|| \tag{67}$$

where r_1 is a desired fractional change in design. (r_1 may be taken between 0.005 and 0.25). Substituting Eq. (66) into Eq. (67), one obtains

$$\eta_0 = \frac{r_1 ||b||}{||\delta \tilde{b}||} \tag{68}$$

In actual computation then, η_0 is given as

$$\eta_0 = \min \left[1.0, \frac{r_1 ||b||}{||\delta \tilde{b}||} \right] \tag{69}$$

Another criterion for determining overall step size may be based on the change in cost predicted by the calculated vector $\delta \tilde{b}$. The idea here is that change in cost predicted by the δb vector should not be more than a fraction of the current cost. That is

$$|g^{0T} \delta b| \leq r_2 \psi_0 \tag{70}$$

where r_2 is a fraction chosen by the designer and ψ_0 is the current value of the cost function. Substituting Eq. (66) into Eq. (70) one obtains

$$\eta_0 \leq \frac{r_2 \psi_0}{|g^{0T} \delta \tilde{b}|} \tag{71}$$

In actual computation, η_0 is then selected as

$$\eta_0 = \min \left[1.0, \frac{r_2 \psi_0}{|g^{0T} \delta \tilde{b}|} \right] \tag{72}$$

Another point that should be noted is that before η_0 is calculated based on the preceding discussion, it may be necessary to scale the vector δb. A reason for this scaling is that $b + \delta b$ may violate some lower or upper bound constraints on the design variables (some variables may even become negative). Therefore, it is necessary to scale the vector $\delta \tilde{b}$ such that no such constraint is violated. A step size can easily be determined to scale the vector δb in this case.

VI. Step-By-Step Algorithm

Figure 1 gives a conceptual flow diagram for step size selection at each design iteration. It is assumed that before entering into this part of calculations, all constraints have been checked and gradients of active constraints have been computed. There are three major paths of calculation in the flow diagram of Fig. 1. These paths are 1-2, 3-4-12, and 5 to 11. Location of the current design relative to the feasible region is checked at first. If the current design is far from the feasible region, then only constraint violations are corrected (Path 1-2). If the current design is not too far from the feasible region, one follows the Path 3-4-12, taking a constant cost step size, η_3. That is, one tries to correct constraint violations without changing the current cost. Once the design is feasible, convergence criterion for the algorithm is checked. If the current design satisfies the convergence criterion, the process is terminated (Path 5-6). If the current design is near the optimum, but does not satisfy the convergence criterion, a smaller step size such as η_2 is used to avoid oscillation in constraint violations in the subsequent iterations (Path 5-7-8-11). Otherwise, a larger step size such as η_1, is used for reducing the cost function more rapidly (Path 5-7-9-10).

Based on the preceding derivations and discussion a computational algorithm is stated as follows:

Step 1. Estimate the optimal design as b^0.

Step 2. Select a positive definite weighting matrix W.

Step 3. Evaluate constraint functions. Active set strategies may be used here to delete some of the constraints.

Step 4. Evaluate gradients of cost and constraint functions as

$$g^i = \frac{\partial \psi_i^T}{\partial b}, \quad i = 0, 1, 2, \ldots$$

Step 5. Evaluate vectors Λ^0 and Λ^i as in Eqs. (23) and (24). Evaluate normalized constraint correction parameters Δ_i as in Eq. (25). $|\Delta_i|$ represent distance from the current design point to constraint hyperplanes. Rearrange vectors Λ^i and the corresponding parameters Δ_i in the descending order of Δ_i.

Step 6. Check if any design sensitivity vectors are parallel. If two are dependent, retain the worst violated constraint. Calculate the matrix B as in Eq. (31), and a vector $A^T\Lambda^0$.

Step 7. Calculate vectors v^1 and v^2 from Eqs. (36). If the system of Eqs. (36) is linearly dependent, then delete the dependent columns from matrix Λ and the corresponding Δ_i from Δ, and repeat this step.

Step 8. Determine the design condition. If only constraints have to be corrected,

calculate s^2 from Eq. (37) and a change in design using Eq. (16) as

$$\delta b = U^{-1} s^2$$

Update the design estimate after imposing the overall step size requirement, as follows

$$b^1 = b^0 + \delta b$$

and return to Step 2. Otherwise, continue.

Step 9. Check sign of v^1 components. Delete columns of A corresponding to negative v^1 components, and the corresponding Δ_i from Δ. Recalculate v^1 and v^2 from Eqs. (36).

Step 10. Calculate vectors s^1 and s^2 from Eqs. (37).

Step 11. If all constraints are satisfied and the convergence parameter $\xi_p = ||s^1||$ is smaller than an acceptable small number, terminate the process. Otherwise, continue.

Step 12. Select a step size based on the flow diagram of Fig. 1 and the discussion of the Section V. Calculate a vector s as

$$s = -\eta s^1 + s^2$$

Determine if the current cost represents an upper or a lower bound on the optimum cost.

Step 13. Calculate a change in design from Eq. (16), as

$$\delta b = U^{-1} s$$

Update the design estimate after imposing the overall step size requirement, as follows:

$$b^1 = b^0 + \delta b$$

and return to Step 2.

VII. Numerical Aspects

Based on the algorithm of previous section, a general purpose computer code GRP2 has been developed [11]. The program can treat equality as well as inequality constraints. Considerable care is required in numerical implementation of the algorithm. This section presents a discussion of the numerical aspects of the computer program and the algorithm.

It can be seen that the step sizes defined by Eqs. (59), (60), and (72) are functions of the current cost ψ_0. If the cost takes a zero or nearly zero value at any iteration, then each of the steps defined by the said equations reduces to zero or almost zero, leaving the current design point unchanged for the next iteration. This stops the progressive improvement of the iterative design process towards the optimum. It is therefore necessary to see that the cost function never takes a zero or nearly zero value during the iterative procedure. This can be easily achieved by adding a positive constant to the cost function.

At optimum, the design must be feasible. That is, Δ in Eq. (34) is a zero vector reducing s^2 to zero and Eq. (32) gives $s = -\eta s^1$. Thus

$$A^{0T} s = \eta A^{0T}(-s^1)$$

represents a change in the normalized cost along $(-s^1)$ vector. Since $(-s^1)$ is a direction of descent for the cost funtion (refer to Eq. (42)). it can be seen that if $s^1 = 0$, then no further reduction in cost is possible. Thus, for a feasible design, $||s^1|| = 0$ implies optimum solution. It is, however, not always possible to attain zero value for $||s^1||$ and hence a tolerance limit on the value of $||s^1||$ is placed in the algorithm. Geometrically, $||s^1||$ is the projection of the normalized cost gradient vector A^0 on a plane tangent to the constraint surface. Since A^0 is a unit vector, $||s^1||$ represents cosine of the angle between the tangent plane and the vector A^0. Theoretically, at optimum, this angle should be 90°. However, if a tolerance limit of 0.0001 is placed on $||s^1||$, then it would mean that an angle of $\cos^{-1}(0.0001) = 89.99427°$ is considered admissible at optimum. For some problems, it is not possible to attain a value as small as 0.0001 for $||s^1||$ and a value as large as 0.05 may be considered acceptable.

The algorithm uses Gaussian elimination procedure to determine rank of the matrix B in Eqs. (36). If at a point in the Gaussian elimination procedure, a scan for pivotal element shows the largest value for the pivotal element as less than a small positive number (say 10^{-7}), then the rank of B gets determined there. The linearly dependent vectors A^1 are ignored and solutions of Eqs. (36) are obtained for the non-singular part of B.

VIII. Design Applications

Several design problems have been solved using the GRP2 Code [11]. Three design examples are presented here.

Design of Tension/Compression Spring

Minimum weight design of a linear spring shown in Fig. 2 is considered. The design requirements are:

(i) Deflection under a 10 lb load must be at least 0.5 in;
(ii) Shear stress in the wire should be no greater than 8×10^4 psi under the 10 lb load;
(iii) The natural frequency of surge waves is at least a factor of 10 higher than the operating frequency of 10 Hz;
(iv) The outside diameter of the spring is no greater than 1.5 in.

Design variables for the coil spring are: d = wire diameter, in; D = mean coil diameter, in; and n = number of active coils. In terms of these variables, optimal design problem is stated as follows:

$$\min \psi_0 = (n + 2) D d^2$$

Subject to

$$\psi_1 \equiv 1.0 - \frac{D^3 n}{7.14 \times 10^4 d^4} \leq 0$$

$$\psi_2 \equiv \frac{4D^2 - dD}{1.257 \times 10^4 (Dd^3 - d^4)} + \frac{1}{5.11 \times 10^3 d^2} - 1.0 \leq 0$$

$$\psi_3 \equiv 1.0 - \frac{140d}{D^2 n} \leq 0$$

$$\psi_4 \equiv \frac{D + d}{1.5} - 1.0 \leq 0$$

The lower and upper bound on design variables are as follows:

$$d^L = 0.05 \text{ in.} \quad , \quad d^U = 0.20 \text{ in.}$$

$$D^L = 0.25 \text{ in.} \quad , \quad D^U = 1.3 \text{ in.}$$

$$n^L = 2.00 \quad , \quad n^U = 15.0$$

Detailed derivation of these equations can be found in several references [4, 11, 12]. It should be noted that all functions of the design problem depend explicitly on design variables. Therefore, implicit differentiation of these functions is not necessary. For a given design any function or its gradient can be readily computed. Several starting designs are tried and optimal solution obtained in each case. At all optimum solutions constraints ψ_1 and ψ_2 are active. Table 1 gives results for a run of the program GRP2 for this design problem. It gives histories for maximum constraint violation ($||\psi||_\infty$), s_1 norm and cost function. The cost function history for the problem is also given in Fig. 3. At the starting design, the cost function is quite far from the optimum point. However, the algorithm reduces the cost by a factor of more than 40 in fifteen iterations. Several upper bounds on optimum cost (feasible designs) are established; e.g., at iterations 3,6,7,10,11,12 and 15. Also, a lower bound on the optimum cost is established at iteration 21.

Several other widely separated design points produced same optimum cost [11]. However, the final design points were different. This indicates that there are several local minimum points having same value of the cost function.

Design of Trusses

Two examples of design of truss structures that have been extensively used in the literature for evaluating algorithms are solved using the GRP2 code. The design problems are:

(1) A ten member cantilever planar truss subjected to on loading condition. It has ten design variables.

(2) A twenty five member three dimensional transmission tower subjected to multiple loading conditions. It has seven design variables.

Formulation for these design problems and their data can be found in several references; for e.g., Refs. 4 and 9, and other references cited there. The cost function for these problems is weight of the structure and constraints are imposed on member stress, nodal displacement, buckling, natural frequency and member sizes. These problems have implicit functions of design variables and require implicit differentiation procedures. Optimum designs for various combination of constraint cases are well known and may be found in references cited above. Same optimum solutions are obtained with the GRP2 code. Cost function histories for various cases are as follows:

1. Ten Member Truss (Case II of Ref. 4)

(i) Stress Constraints only
419.6, 1802, 1802, 1802, 1802, 1792, 1789, 1722, 1722, 1670, 1670, 1670, 1670 lbs.

(ii) Stress and Displacement Constraint Case
419.6, 1802, 2703, 4013, 4013, 4013, 4014, 4657, 4657, 4657, 4657, 4680, 4661, 4661, 4661, 4661, 4704, 4683, 4683, 4683, 4683, 4672, 4678 lbs.

(iii) All Constraints Case
419.6, 1802, 2703, 3610, 4638, 5113, 5113, 5113, 5113, 5096, 5020, 5021, 5014, 4864, 4864, 4864, 4864, 4871, 4872, 4872, 4872, 4800, 4814, 4767, 4784, 4784 lbs.

2. Twenty Member Transmission Tower

(i) Stress Constraints Only
330.7, 90.1, 90.2, 91.4, 91.4 lbs.

(ii) Stress and Displacement Constraints Case
330.7, 87.8, 131.6, 197.5, 296.2, 430.2, 529.1, 529.1, 529.1, 529.1, 546.4, 546.4, 546.4, 540.7, 540.7, 540.7, 540.7, 543.5, 543.5, 543.5, 543.5, 545.2 lbs.

(iii) All Constraints Case
330.7, 87.8, 112.1, 168.1, 252.1, 378.1, 495.7, 558.4, 558.4, 558.4, 564.0, 564.0, 564.0, 577.6, 577.6, 577.6, 577.6, 603.7, 603.7, 603.7, 603.7, 590.7, 590.7 lbs.

For all the problems, several upper and lower bounds on the optimum cost were established. All optimum solutions were obtained by starting the algorithm from a uniform design of 1.0 in^2. No parameters were externally adjusted during the iterative process.

IX. Discussion and Conclusions

In this paper, a new optimization algorithm based on upper and lower bounds on the optimum cost and the gradient projection concept is presented. A general purpose computer program GRP2 has been developed based on the algorithm. The program has been used to solve several small scale optimization problems to study behavior of the new algorithm relative to its ability to obtain optimum point [11]. The new algorithm has several important features that make it particularly attractive for its application to large complex structural and mechanical systems. These features are:

(i) Automatic calculation of a step size at each iteration. The user does not have to select any step size related parameters.
(ii) Cost and constraint functions are evaluated only once at any iteration.
(iii) The starting point can be arbitrary. If the starting point is infeasible, the algorithm finds a feasible design. Also the algorithm successively obtains improved feasible designs until an optimum is reached.

Feature (i) is useful because the algorithm does not require any prior experience by the user in selecting step size and other parameters to use the program. Feature (ii) is extremely useful because any further function evaluation at any iteration for the structural and mechanical design problems requires reanalysis of the system. For statics problems reananlysis means calculations for new stiffness matrix, its decomposition and new displacements and stresses. For the dynamic resonse problems, reanalysis means writing new equations of motion for the system and solving them for the new response. Thus, it is obvious that evaluation of functions only once in an iteration results in substantial savings in the computational

effort for this class of problems. Feature (iii) is very useful from practical standpoint as it yields improved feasible points even if the algorithm does not satisfy the convergence criteria in the specified number of iterations.

The new computer code GRP2 has several useful features that may be noted:

(i) All gradients in the program are normalized with respect to their lengths. This allows an easy numerical check for dependency of constraint. This also gives a very useful and numerically implementable convergence criterion for the algorithm.

(ii) The step size is calculated based on upper and lower bounds on the cost function. Therefore the program first tries to locate these bounds. For many example solutions [11], the convergence criteria were satisfied while the algorithm was trying to locate lower and upper bounds. Several limitations on changes in design at any iteration have been built into the program. These constraints include maximum change in the cost and a maximum change in the design variable vector.

(iii) Explicit lower and upper bound constraints on design variables are imposed automatically in the program. Thus, the user does not have to code these constraints in the user-supplied subroutines. Also, the computed change in design at each iteration is such that the new design does not violate lower and upper bound constraints.

(iv) The program can be coupled to other codes for optimization of various classes of structural and mechanical systems.

There are several other points about the algorithm and the computer code that should be noted. These are:

(i) The step size in the algorithm is calculated based on the cost function value. Therefore the cost function should be well defined at each iteration. It should be always a positive number which can be obtained by adding a large constant to the cost function.

(ii) If the convergence criteria specified by the user are satisfied, the program prints the optimum values of the cost function and design variables. If these criteria are not satisfied, execution of the program stops after specified limit on iterations is exceeded. In such a case the user should scan histories of the maximum constraint violation, s_1-norm and the cost function to locate the best feasible design. Also, if desired, the iterative process may be continued using the restart option of the program.

(iii) Special attention should be given to proper formulation of the problem to avoid singularities in various functions and their derivatives. All functions must be well behaved and differentiable at all points. Also upper and lower bounds on design variables should be carefully specified to avoid physical absurdities.

In conclusion, the new algorithm offers potential for applications to large and complex structural and mechanical design problems.

References

1. Venkayya, V.B., "Structural Optimization: A Review and Some Recommendations", Int. J. for Num. Methods in Engrg., Vol. 13, 1978, pp. 203-228.

2. Krishnamoorthy, C.S. and Mosi, D.R., "A Survey on Optimal Design of Civil Engineering Structural Systems", Engineering Optimization, Vol. 4, 1979, pp. 73-88.

3. Schmit, L.A. and Fleury, C., "Structural Synthesis by Combining Approximation Concepts and Dual Methods", AIAA J., Vol. 18, No. 10, Oct. 1980, pp. 1252-1260.

4. Haug, E.J. and Arora, J.S., Applied Optimal Design: Mechanical and Structural Systems, Wiley Interscience, John Wiley and Sons, N.Y. 1979.

5. Arora, J.S. and Haug, E.J., "Methods of Design Sensitivity Analysis in Structural Optimization", AIAA J., Vol. 17, No. 9, Sept. 1979, pp. 970-74, Vol. 18, No. 11, Nov. 1980, pp. 1406-1408.

6. Haug, E.J. and Arora, J.S., "Design Sensitivity Analysis of Elastic Mechanical Systems", Computer Methods in Applied Mechanics and Engineering, Vol. 15, 1978, pp. 35-62.

7. Arora, J.S. and Govil, A.K., "Design Sensitivity Analysis with Substructuring", J. of Engineering Mechanics Division, ASCE, Vol. 103, No. EM 4, Aug. 1977, pp. 537-548.

8. Gill, P.E. and Murray, W. (Eds.), Numerical Methods for Constrained Optimization, Academic Press, N.Y. 1974.

9. Arora, J.S. and Haug, E.J., "Efficient Optimal Design of Structures by Generalized Steepest Descent Programming", Int. J. for Num. Meth. in Engrg., Vol. 10, No. 4, 1976, pp. 747-766; Vol. 6, No. 6, 1976, pp. 1420-1427.

10. Arora, J.S., "Analysis of Optimality Criteria and Gradient Projection Methods for Optimal Structural Design", Computer Methods in Applied Mechanics and Engrg., Vol. 23, No. 2, Aug. 1980, pp. 185-213.

11. Belsare, S.V. and Arora, J.S., "A General Purpose Computer Code GRP2 BAsed on an Extended Gradient Projection Method", Technical Report No. 66, Division of Materials Engineering, University of Iowa, Iowa City, Iowa, Nov. 1980.

12. Spotts, M.F., Design of Machine Elements, 2nd Ed. Prentice Hall, Englewood Cliffs, N.J., 1953.

TABLE I RESULTS FOR SPRING DESIGN PROBLEM

I	$\|\|\psi\|\|_\infty$	S1 NORM	COST
1	0.7134D 00	0.1907D 00	0.8840D 00
2	0.1689D 00	0.5865D-03	0.4972D 00
3	0.0000D 00	0.1000D 01	0.2878D 00
4	0.1885D 01	0.1172D 00	0.4513D-01
5	0.4970D 00	0.1453D 00	0.7050D-01
6	0.0000D 00	0.1000D 01	0.6243D-01
7	0.0000D 00	0.1000D 01	0.6005D-01
8	0.2390D 00	0.6959D-01	0.3799D-01
9	0.2181D-01	0.7862D-01	0.3778D-01
10	0.2371D-03	0.7968D-01	0.3778D-01
11	0.0000D 00	0.8999D-01	0.2857D-01
12	0.0000D 00	0.1000D 01	0.2399D-01
13	0.3148D 00	0.8825D-01	0.1961D-01
14	0.3571D-01	0.1029D 00	0.1944D-01
15	0.6410D-03	0.1051D 00	0.1944D-01
16	0.0000D 00	0.1126D 00	0.1658D-01
17	0.0000D 00	0.1189D 00	0.1461D-01
18	0.0000D 00	0.7902D-01	0.1338D-01
19	0.4169D 00	0.9126D-03	0.1101D-01
20	0.1273D 00	0.1366D-03	0.9396D-02
21	0.5332D 00	0.9953D-03	0.9637D-02
22	0.6903D-01	0.1136D 00	0.1331D-01
23	0.2324D-01	0.1183D 00	0.1330D-01
24	0.2872D-01	0.1185D 00	0.1330D-01
25	0.4691D-01	0.6266D-04	0.1223D-01
26	0.0000D-00	0.5761D-04	0.1274D-01

Initial design: $d = d^U = 0.2$ in.
$D = D^U = 1.3$ in.
$n = n^U = 15.0$
Initial cost = 0.8840

Optimum design: $d = 0.05037$ in.
$D = 0.3255$ in.
$n = 13.42$
Optimum cost = 0.01274

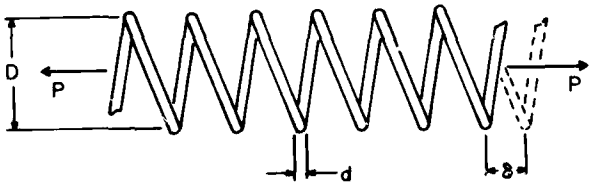


Figure 2. A Coil Spring

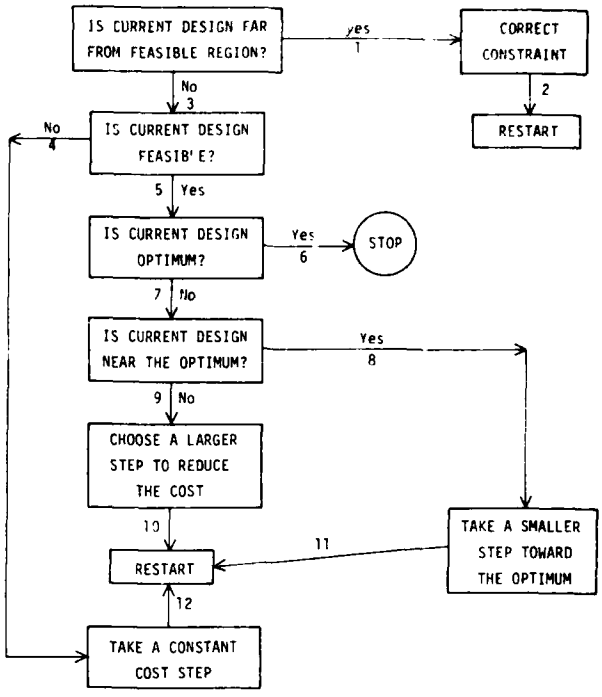


Figure 1. Conceptual Flow Diagram for Step-Size Selection in Optimal Structural Design.

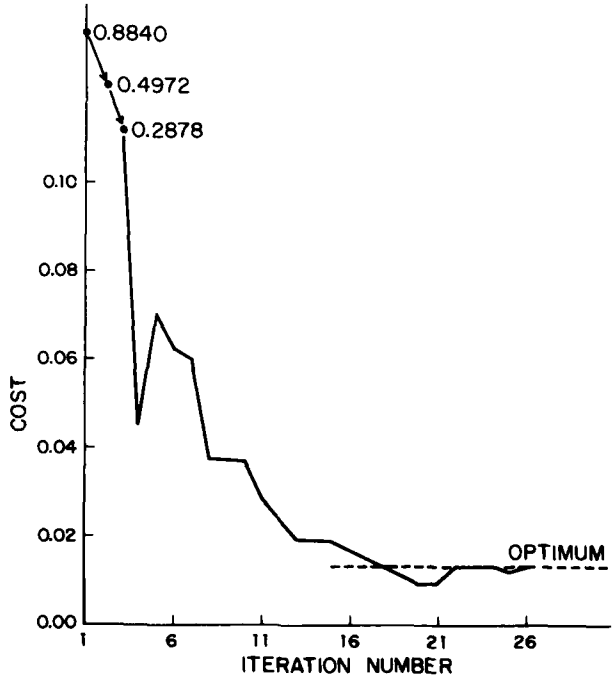


Figure 3. Cost Function History for Spring Design Problem

A BARRIER FORM OF THE METHOD OF MULTIPLIERS

R. R. Root
IBM Corporation
Rochester, Minn.

K. M. Ragsdell
School of Mechanical Engineering
Purdue University
West Lafayette, Indiana

AD P000 070

Abstract

Transformation or penalty function techniques have enjoyed wide popularity for solving nonlinear programming problems in recent years. There have been many methods of this class proposed, among them being the Method of Multipliers. In this paper we develop a barrier penalty function which incorporates penalty multipliers similar to those used in the Method of Multipliers. Two formulae for updating these multipliers are derived and numerical results are presented comparing both multiplier updating schemes with a conventional barrier penalty function algorithm.

Introduction

Interest in nonlinear programming techniques has increased significantly in recent years. Today, as never before, with ever increasing demands and decreasing resources engineers and scientists must face the challenge of finding the "best" solutions to modern problems. We pose the nonlinear programming problem (NLP) in the following form:

$$\text{Minimize} \quad f(x) \tag{1}$$

$$\text{Subject to} \quad g_j(x) \geq 0 \quad j = 1,2,3,\ldots,J \tag{2}$$

$$h_k(x) \equiv 0 \quad k = 1,2,3,\ldots,K \tag{3}$$

$$\text{and} \quad x_i^{(\ell)} \leq x_i \leq x_i^{(u)} \quad i = 1,2,3,\ldots,N \tag{4}$$

We also assume the existence of an initial design, $x^{(0)}$, which is feasible (that is, satisfies all constraints and bounds). Nonlinear programming techniques generate a sequence of points, $x^{(t)}$, which at termination approximates a local minimum, $\tilde{x}$, of the NLP.

Transformation techniques have enjoyed wide spread application [1,2,3]* recently primarily due to their ease of utilization and their dependence upon well developed unconstrained optimization techniques.

Let us define a general penalty function in the following form:

$$P(x) = f(x) + \Omega\,(p,g,h) \tag{5}$$

Here Ω is called the penalty term. Clearly, $P(x)$ is indirectly a function of x, since $f(x)$ and the constraint functions depend upon x. Typically, the penalty parameters, p, are chosen and $P(x)$ is minimized in an unconstrained state. The termination point of this search, $x^{(1)}$, is utilized to recalculate the penalty parameters, p. The updated penalty function is again minimized utilizing $x^{(1)}$ as a starting point. The iterative technique is continued until small changes are observed in the solution sequence.

The Method of Multipliers [1] is an extremely efficient transformation technique which has received considerable attention recently. The penalty function is,

$$P(x) = f(x) + p\sum_{j=1}^{J}\{\langle g_j(x) + \sigma_j\rangle^2 - \sigma_j^2\} + p\sum_{k=1}^{K}\{[h_k(x) + \tau_k]^2 - \tau_k^2\} \tag{6}$$

where the bracket operator, $\langle\cdot\rangle$, is defined

$$\langle\alpha\rangle = \begin{cases} \alpha, & \text{if } \alpha \leq 0 \\ 0, & \text{if } \alpha > 0 \end{cases} \tag{7}$$

At the termination of each unconstrained minimization the multipliers may be updated using the following simple formulae:

$$\sigma_j^{(t+1)} = \langle g_j(x^{(t)}) + \sigma_j^{(t)}\rangle, \quad j = 1,2,\ldots,J \tag{8}$$

$$\tau_k^{(t+1)} = h_k(x^{(t)}) + \tau_k^{(t)}, \quad k = 1,2,\ldots,K \tag{9}$$

where $x^{(t)}$ is the solution to the $t^{\underline{th}}$ unconstrained minimization.

This form of the Method of Multipliers is considered external since the sequence of unconstrained solutions obtained is necessarily infeasible with respect to the inequality constraints. Difficulties may arise, however, when this form of the penalty function is utilized in certain modeling situations. Generally these situations are characterized by certain combinations of the variables which preclude the evaluation of some parts of the model. In the case of a model formulated in the framework of a nonlinear programming problem, this translates to the inability to evaluate $f(x)$ or certain constraint functions in some region of R^N. In such situations, the modeller must formulate additional inequality constraints in order that the feasible region also forms a region in which all elements of the model are capable of evaluation.

Much to a modeller's chagrin, in situations like the one described above, the form of the Method of Multipliers described in (6) does not guarantee the generation of x vectors which remain within the feasible region. In fact, the exterior qualities discussed previously require the algorithm to traverse into the infeasible region. It would seem highly desirable to obtain a Method of Multiplier type penalty function which generates a sequence of solutions to the unconstrained minimizations which are feasible (or very nearly so) with respect to the set of inequality constraints.

* Numbers in brackets cite references listed at the end of the paper.

PRECEDING PAGE

Barrier Penalty Functions

When we use the terms, interior and exterior regions in R^N, we are only speaking of the set of inequality constraints. There does exist a region in which the set of equality constraints ($h_k(x)$) is satisfied, however this region is of smaller dimensionality than R^N. When we speak of barrier functions we will always be concerned with barriers in the full N-space, and hence only the set of inequality constraints may be considered.

There are several existing penalty function algorithms which indeed do generate a sequence of unconstrained solutions which are all contained within the feasible region formed by the inequality constraints. Examples of such functions include

$$P(x) = f(x) + p \sum_{j=1}^{J} \frac{1}{g_j(x)} \quad j = 1,2,3,\ldots, J \qquad (10)$$

and

$$P(x) = f(x) - p \sum_{j=1}^{J} \ell n\, g_j(x) \quad j = 1,2,3,\ldots,J \qquad (11)$$

We see that in both penalty functions, any constraint approaching a value of zero will create a very large value to be added to P(x). In both algorithms the value of p begins at a moderate level and approaches zero as the sequence of minimizations proceeds. Starting from a feasible $x^{(0)}$, the mathematical barrier produced by the penalty term guarantees that the first unconstrained solution, $x^{(1)}$, will also be feasible. As p is reduced at each stage, t, the unconstrained solutions, $x^{(t)}$, will all be feasible while the constraints destined to be satisfied at x^* will become closer and closer to zero in value.

Unfortunately, numerical difficulties can arise due to the value of p approaching zero. As p becomes smaller, each minimization becomes more and more difficult to perform. Moreover, the solution of the NLP may be obtained in the limit of p approaching zero. Computationally, p can only become small within the limits of the accuracy available within the computer. Methods exist which extrapolate the results of successive minimizations to that stage when p would be zero, however they concede the existence of the numerical difficulty and do not rid the algorithm of it.

The intent of this paper is to introduce a multiplier type barrier penalty function. We will find several advantages to be had from such a formulation. Among these are

1. The value of p may remain finite and nonzero as the algorithm generates a sequence of unconstrained solutions, $x^{(t)}$.
2. The true solution of the NLP is contained within the region of the constraint boundaries rather than on them.
3. The gradient of such a penalty function is well defined at the true NLP solution.

Let us consider the following penalty function and determine that it exhibits the advantages mentioned above.

$$P(x) = f(x) + \sum_{j=1}^{J} \frac{p_j}{[g_j(x) + \sigma_j]} \qquad (12)$$

Notice that we have only included inequality constraints, since as we mentioned earlier, there is no barrier function analogy for the equality constraints.

Optimality Results

Let us present the optimality results in the form of a theorem.

Theorem 1: There exists a p'>0 such that if the largest p_j in the set of p_j's is less than p', a constrained minimum of f(x), $\tilde{x}$, is a local minimum of P(x) with respect to x.

Proof: The proof of the theorem is in two parts. First assuming the gradients of the inequality constraints to be independent of one another, we consider the necessary conditions for $\tilde{x}$ to be local constrained minimum of f(x).

$$g_j(\tilde{x}) \geq 0 \qquad j = 1,2,3,\ldots,J \qquad (13)$$

$$\nabla f(\tilde{x}) = Q(\tilde{x})\lambda \qquad (14)$$

$$\lambda_j \geq 0 \qquad j = 1,2,3,\ldots,J \qquad (15)$$

$$\lambda_j\, g_j(\tilde{x}) \equiv 0 \quad j = 1,2,3,\ldots,J \qquad (16)$$

where

λ = the vector of optimal Lagrange Multipliers

Q = a rectangular matrix whose columns represent the gradients of the inequality constraints with respect to x.

$\nabla f(\tilde{x})$ = the gradient of f(x).

Let us now consider the gradient of expression (12) with respect to x.

$$\nabla P(\tilde{x}) = \nabla f(\tilde{x}) - Qq \qquad (17)$$

where

q = the column vector whose $j^{\underline{th}}$ element is

$$q_j = p_j^2/[g_j(\tilde{x}) + \sigma_j]^2 \quad j = 1,2,\ldots,J \qquad (18)$$

If we let q_j equal λ_j and use this fact in expression (17), then from (14) we see that $\nabla P(\tilde{x})$ would be zero.

This, of course, shows us that $\tilde{x}$ is a stationary point of P(x).

The second part of the proof requires that we show the matrix of second partial derivatives of P(x), $\nabla^2 P$, be positive definite. We begin with an expression for $\nabla^2 P$.

$$\nabla^2 P(\tilde{x}) = \nabla^2 f(\tilde{x}) + QTQ^T - \sum_{j=1}^{J} q_j [\nabla^2 g_j(\tilde{x})] \qquad (19)$$

where

T = a diagonal matrix whose nonzero elements are

$$t_{jj} = 2p_j^2/[g_j(\tilde{x}) + \sigma_j]^3 \qquad (20)$$

At $\tilde{x}$, the expression above may be equivalently written as

$$\nabla^2 P(\tilde{x}) = L + QTQ^T \qquad (21)$$

where L is the matrix of second partial derivatives with respect to x of the well known Lagrangian.

Consider now any vector, $\hat{u}$, such that the Euclidean norm is equal to one. The vector, $\hat{u}$, may be decomposed in the following manner:

$$\hat{u} = v + Q^{+T} w \qquad (22)$$

In (21), v is chosen to be orthogonal to the columns of Q and Q^+ is called the pseudo-inverse of Q. This pseudo inverse is equal to $(Q^TQ)^{-1}Q^T$ and projects the vector, w, onto the space spanned by the columns of Q. We use the facts that L and (QTQ^T) are symetric and that v is orthogonal to the columns of Q to show that

$$\hat{u}^T[\nabla^2 P(\tilde{x})]\hat{u} = v^T Lv + 2v^T LQ^{+T} w + w^T Q^+ LQ^{+T} w + w^T Tw \qquad (23)$$

Showing the left side of (22) to be positive insures the positive definite quality of $\nabla^2 P(\tilde{x})$. To accomplish this, we make use of the properties of matrix and vector norms. We utilize the following definition of a matrix norm:

$$||Z||_2 = [\text{maximum eigenvalue of } Z^H Z]^{1/2} \qquad (24)$$

where Z^H implies Z-Hermitian. Also, we will make use of the following matrix norm properties:

$$||Z||_2 \geq 0 \qquad (25)$$

$$||YZ||_2 \leq ||Y||_2 \, ||Z||_2 \qquad (26)$$

We can use these properties to bound the terms in (22).

$$||v^T Lv||_2 \leq ||v||_2^2 \, ||L||_2 \qquad (27)$$

$$||w^T Q^+ LQ^{+T} w||_2 \leq ||w||_2 \leq ||w||_2^2 \, ||Q^+ LQ^{+T}||_2 \qquad (28)$$

$$2||v^T LQ^{+T} w||_2 \leq 2||v||_2 \, ||LQ^{+T}||_2 \, ||w||_2 \qquad (29)$$

and

$$||w^T Tw||_2 \leq ||w||_2^2 \, ||T||_2 \qquad (30)$$

We know that the Lagrangian is positive definite, and hence can state that

$$v^T Lv \geq a \, ||v||_2^2 \qquad (31)$$

for some positive a and any v such that $Q^T v$ is equal to zero (which we have chosen to be the case). We also note that

$$||T||_2 = \text{the largest } |t_{ii}|. \qquad (32)$$

Combining all of this information into expression (23) results in

$$\hat{u}^T[\nabla^2 P(\tilde{x})]\hat{u} \geq a \, ||v||_2^2 - 2||v||_2 \, ||w||_2 ||LQ^{+T}||_2 + [d - ||Q^+ LQ^{+T}||_2] \, ||w||_2^2 \qquad (33)$$

Here, the term, d, denotes the matrix norm of T. The theorem hinges upon finding a value of d large enough to make the right side of (33) positive. To show how this may be true, we consider an alternate expression for t_{ii}.

$$t_{jj} = 2q_j/[g_j(\tilde{x}) + \sigma_j] \qquad (34)$$

We know that at $\tilde{x}$ the Lagrange multipliers are fixed and hence $\bar{q}$ is fixed. Of course, to increase the norm of T, we must increase the value of the largest diagonal element of T. With q_j fixed, the only way to increase t_{jj} is to decrease σ_j, and this may be accomplished by decreasing p_j. We see that the value of any t_{jj} may be increased indefinitely by reduction of the corresponding p_j, and hence there exists a p_j' such that the value of d will insure the positive quality of (33).

The results of this theorem demonstrate that the values of p_j and σ_j at $\tilde{x}$ are indeed nonzero, and more importantly, the gradient of this penalty function exists and is continuous at the true constrained solution of f(x). We can better appreciate this fact with the aid of Figure 1. The dotted line represents a penalty function given by (10) while the solid line represents the analogous multiplier form. Note that in the conventional penalty function, $\tilde{x}$ does not lie <u>within</u> the barrier but <u>on</u> it. The multiplier form includes $\tilde{x}$ within its barrier. As successive minimizations are performed with the multiplier form, the penalty function contour is displaced (<u>without</u> significant distortion)

until its minimum corresponds to the constrained minimum of f(x). We realize that this effect implies successive minimizations of equal difficulty rather than the conventional sequence which we realize becomes increasingly difficult.

Updating the Penalty Multipliers

The updating algorithm for the values of σ_j is based upon the following simple theorem:

Theorem 2: Let $x^{(t)}$ be an unconstrained local minimizer of P(x). $x^{(t)}$ is then a local constrained solution to the problem,

$$\text{Minimize} \quad f(x) \tag{35}$$

Subject to

$$(g_j(x) - g_j(x^{(t)}) \geq 0 \tag{36}$$

The proof follows immediately from the optimality conditions for P(x). First,

$$\nabla f(x^{(t)}) - Q(x^{(t)})\, q(x^{(t)}) = 0 \tag{37}$$

and we let

$$\lambda_j^{(t)} = q_j^{(t)} = \frac{p_j^2}{[g_j(x^{(t)}) + \sigma_j^{(t)}]^2}, \tag{38}$$

then it follows that

$$[g_j(x) - g_j(x^{(t)})] \geq 0 \qquad j = 1,2,\ldots, J \tag{39}$$

$$\lambda_j^{(t)} = q_j^{(t)} \geq 0 \qquad j = 1,2,\ldots, J \tag{40}$$

We also see from (37) that

$$\lambda_j^t\, [g_j(x) - g_j(x^{(t)})] \equiv 0 \qquad j = 1,2,\ldots, J \tag{41}$$

Of course, the expressions (37-41) imply that $x^{(t)}$ is a local constrained minimum of the problem stated by (35) and (36).

We can understand how this theorem provides a means of multiplier update by considering a few simple points. If, for the inequality constraints destined to be equal to zero at the true constrained solution, we could predict $\sigma_j^{(t+1)}$ so that $g_j(x^{(t+1)})$ would equal zero, the theorem would say that part of the conditions for $x^{(t+1)}$ being the constrained solution of f(x) are met. If, for the remaining constraints, we could set q_j equal to zero, we would indeed have the constrained solution in $x^{(t+1)}$.

To achieve this result, we must be able to determine which of the constraints are active (i.e. $g_j(\tilde{x}) \equiv 0$) at the constrained solution of f(x). To this end we will define an active constraint set as those constraints possessing the following two properties:

1. The value of $g_j(x^{(t)})$ is less than some positive number, ε, and the vector dot product of $\nabla f(x^{(t)})$ and $\nabla g_j^{(t)})$ is positive.

2. The value of $g_j(x^{(t)})$ is negative.

The first condition takes into consideration any constraint which can simultaneously display a value close to zero and possibly satisfy expression (37). The second condition must be included because of the lack of exact unconstrained minimization. It is possible to obtain an $x^{(t)}$ for which some of the $g_j(x^{(t)})$ are slightly violated. These constraints are then included in the active set. Let us, define the set of indices belonging to those active constraints as the set, B.

Using a truncated Taylor series expansion, we may express the correction to the active constraint set as

$$0 = g'(x^{(t+1)}) \approx g'(x^{(t)}) + [\frac{\partial g}{\partial \sigma}]' \Delta\sigma' \tag{42}$$

In expression (42), the prime notation signifies that only the active inequality constraints are utilized. We may express (42) equivalently as

$$[\frac{\partial g}{\partial \sigma}]' \Delta\sigma' = -g'(x^{(t)}) \tag{43}$$

We find (43) to be of little use in its present form. We need to be able to evaluate $[\frac{\partial g}{\partial \sigma}]'$. Since this is a square matrix whose rows are the partial derivatives of the constraints with respect to σ, we may write the matrix as

$$[\frac{\partial g}{\partial \sigma}]' = Q'^T D \tag{44}$$

In (44), D is a rectangular matrix whose rows represent the partial derivatives of x with respect to σ'. We may obtain an expression for D by recalling that

$$\nabla P(x) = \nabla f(x) - Q' q' = 0 \tag{45}$$

Operating on (45) by $(\frac{\partial}{\partial \theta})$

$$GD + Q' T' = 0 \tag{46}$$

where

G = the matrix of second derivatives of P(x)

From (46) we see immediately that

$$D = -G^{-1} Q' T', \tag{47}$$

and hence

$$[Q'^T G^{-1} Q' T'] \Delta\sigma' = g'(x^{(t)}) \tag{48}$$

The updating formula is then seen to be

$$\Delta\sigma' = [Q'^T G^{-1} Q' T']^{-1} g'(x^{(t)}) \tag{49}$$

The formula is easily implemented and an approximation to G^{-1} is often available if a variable metric unconstrained search is incorporated.

Sometimes there is no estimate of G^{-1}, and we would like to be able to develop an updating formula which did not require second derivative information. To this end consider increasing the matrix, T', by

adding a diagonal matrix, S, whose elements are all equal to a large positive value. Having done this, we find a new expression for G.

$$G_{T+S} = G_T + Q'SQ'^T \tag{50}$$

Householder [4] gives a formula for expressing the inverse of matrices such as G_{T+S}. Given the matrices W,X,Y,and Z

$$[W + XYZ]^{-1} = W^{-1} - W^{-1}X[ZW^{-1}X + Y^{-1}]ZW^{-1} \tag{51}$$

Utilizing this, we see that

$$[G_T + Q'SQ'^T]^{-1} = G_T^{-1} - G_T^{-1}Q'[Q'^TG_T^{-1}Q' + S^{-1}]Q'^TG_T^{-1} \tag{52}$$

and secondly,

$$Q'^TG_{T+S}^{-1}Q' = Q'^TG_T^{-1}Q' - Q'^TG_T^{-1}Q'[Q'^TG_T^{-1}Q' + S^{-1}]Q'^TG_T^{-1}Q' \tag{53}$$

Close inspection or (53) reveals to us

$$Q'^TG_{T+S}^{-1}Q' = [(Q'^TG_{T+S}^{-1}Q')^{-1} + S]^{-1} \tag{54}$$

Now, if the elements of S are sufficiently large, then

$$[(Q'^TG_{T+S}^{-1}Q')^{-1} + S] \simeq S \tag{55}$$

We then find that

$$[Q'^TG_{T+S}^{-1}Q'] \simeq S^{-1} \tag{56}$$

Noting also that if the elements of S are large, then

$$(T' + S) \simeq S, \tag{57}$$

and (49) may be written as

$$\Delta\sigma' = [S^{-1}S]^{-1}g'(x^{(t)}) \tag{58}$$

or

$$\nabla\sigma' = g'(x^{(t)}) \tag{59}$$

Until now, we have described the multiplier updating only for those constraints in the active set. As stated earlier, optimality depends upon the remaining g_j being zero. We may achieve this in a manner very similar to other barrier penalty function algorithms. At the end of each unconstrained minimization we simply reduce those q_j not corresponding to the active set. This may be very easily accomplished by simultaneously multiplying those $[\sigma_j, j \notin B]$ and dividing the values of $[p_j, j \notin B]$ by an appropriate positive constant.

Computer Implementation

Any implementation of a penalty function requires the same basic components. These components include an unconstrained search algorithm, a penalty function, and a penalty parameter updating routine. The implementation must be able to iteratively invoke the unconstrained search algorithm, update the parameters between successive unconstrained iteractions (stages), and finally recognize when a solution has been obtained. All these components have previously been put together in a computer program called BIAS [1]. BIAS has been developed to incorporate a different multiplier type penalty function, however with some modifications to several of its components we may easily implement our barrier penalty function. First of all, we replace BIAS's penalty function routine with one which evaluates (12). Next we alter the section of code which performs the multiplier updating. We now have an implementation of our barrier penalty function which takes advantage of the Davidon-Fletcher-Powell unconstrained search algorithm and the quadratic interpolation unidimensional search already existing in BIAS.

Numerical Results

The results of three implementations of the barrier penalty function are displayed in Tables 1, 2, and 3. Table 1 contains the results of parameter updating via expression (49). Table 2 contains the results of utilizing (59), and Table 3 contains the results of holding the elements of σ at zero and reducing the p_j at each stage. This third implementation is the algorithm associated with the penalty function given in (10). Except for changing the penalty function and parameter updating algorithms, BIAS was used in its original form. All BIAS parameters were held fixed for each test problem, thus insuring a relatively controlled algorithm environment. The value of ϵ used in determining constraint activity was .01. The values of σ_j were set at zero for the first stage. The test problems comprise a subset of the Sandgren-Ragsdell [5] problems. This subset consists of those problems originally in the Colville [6] and Eason and Fenton [7] test studies. Only the problems exhibiting inequality constrained optimum solutions were considered. The problem numbers used in the tables refer directly to the numbering used in the Sandgren-Ragsdell study.

The results are interesting in several respects. For one, solution times do not differ significantly among the three implementations. Looking at the results of updating formulae (49) and (59), we see solutions of equivalent accuracy. Based upon the slightly higher level of complexity of (49), expression (59) would seem the more advantageous updating algorithm. The superiority of the multiplier technique shows through when we examine the results in Table 3. The only problems in which the penalty function algorithm of (10) was able to reduce constraint violation to less than .0001 were those exhibiting only one active constraint at the solution. On the other problems, this algorithm was totally unable to achieve suitably accurate solutions.

Closure

The intent of this paper has been to develop a barrier penalty function algorithm which exhibits advantages over other existing barrier function algorithms. To this end the paper has been successful. A barrier function has been presented along with two efficient and simple parameter updating formulae. The advantages of the method include convergence of the penalty parameters to finite, nonzero values and a well behaved penalty function gradient at the constrained solution. Practical advantages include the ability to acheive active constraint satisfaction to a high degree of accuracy.

References

1. Root, R. R., "An Investigation of the Method of Multipliers." Ph.D. Dissertation, Purdue University, 1977.

2. Himmelblau, D.M., Applied Nonlinear Programming, McGraw-Hill Co., New York, NY, 1972.

3. Fox, R.L., Optimization Methods for Engineering Design, Addision-Wesley, 1971.

4. Householder, A.S., The Theory of Matrices in Numerical Analysis, Blaisdell Publishing Co., New York, NY, 1964.

5. Sandgren, E., "The Utility of Nonlinear Programming Algorithms," Ph.D. Dissertation, Purdue University, 1977.

6. Colville, A.R., "A Comparative Study of Nonlinear Programming Codes," Proceedings of the Princeton Symposium of Mathematical Programming, ed. by H.W. Kuhn, (Princeton, New Jersey, 1970), pp. 487-501.

7. Eason, E.D., and Fenton, R. G., "Testing and Evaluation of Numerical Methods for Design Optimization," UTME-TP 7204, University of Toronto, September 1972.

Nomenclature

D = a rectangular matrix whose rows are the partial derivatives of x with respect to σ.

f(x) = a scalar objective function.

G = the matrix of 2nd partial derivatives of P(x).

g(x) = $[g_1(x), g_2(x), \ldots, g_J(x)]^T$ = J - dimensional vector of inequality constraint functions.

h(x) = $[h_1(x), h_2(x), \ldots, h_K(x)]^T$ = K - dimensional vector of equality constraint functions.

L = the matrix of 2nd partial derivatives of the Lagrangian function.

N = the number of variables.

P(x) = a scalar penalty function.

Q = a rectangular matrix whose columns represent the gradients of the inequality constraint.

Q^+ = the pseudo-inverse of Q.

p = a vector of penalty parameters.

q = a vector whose j^{th} element is $p_j/(g_j(x) + \sigma_j)^2$

S = a diagonal matrix with large positive elements

T = a diagonal matrix whose elements are $t_{jj} = 2p_j^2 / (g_j(x) + \sigma_j)^3$

$\hat{u}$ = any vector whose norm is 1.

v = a vector orthogonal to the columns of Q.

w = a vector whose dimension equals the rank of q.

$\tilde{x}$ = the solution vector.

$x^{(t)}$ = the tth approximation of $\tilde{x}$.

Δσ = the correction vector for σ.

λ = the vector of Lagrange multipliers.

∇f(x) = the gradient of f(x).

$\nabla^2 f(x)$ = the matrix of 2nd partial derivatives of f(x).

$\nabla^2 P(x)$ = the matrix of 2nd partial derivatives of P(x).

Ω = the penalty term.

σ = $[\sigma_1, \sigma_2, \ldots, \sigma_J]^T$ = a J - dimensional vector of inequality multipliers.

τ = $[\tau_1, \tau_2, \ldots, \tau_k]^T$ = a K - dimensional vector of equality multipliers.

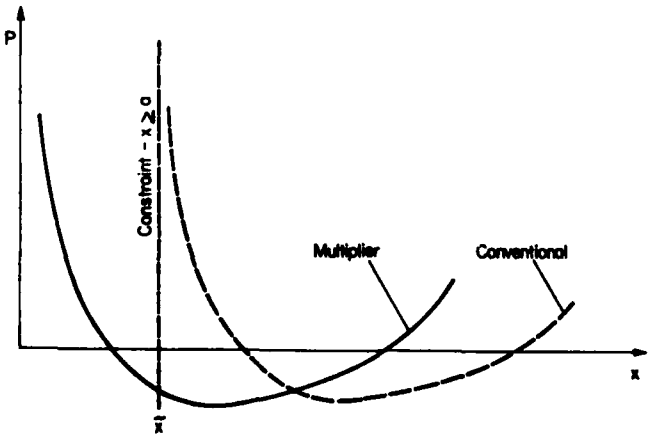


Figure 1. Conventional and Multiplier Barrier Penalty Function.

Table 1

Results of Barrier Method of Multipliers
Using Updating Formula (49)

Problem	CPU time*	No. of Stages	No. of Cycles	No. Obj. Funct. Eval.	No. Const. Eval.	Max. Violation of an Active Constraint
1	3.87	6	57	1197	1190	1.4×10^{-5}
2	.57	11	24	628	616	2.5×10^{-7}
3	2.10	11	55	1461	1449	1.7×10^{-6}
7	.45	8	32	513	504	1.8×10^{-7}
8	.62	7	33	631	623	2.8×10^{-6}
11	54.57	6	33	528	521	9.0×10^{-4}
14	20.68	7	153	4572	4564	1.98×10^{-4}
16	5.95	8	42	898	894	4.0×10^{-6}

Table 2

Results of Barrier Method of Multipliers
Using Updating Formula (59)

Problem	CPU time*	No. of Stages	No. of Cycles	No. Obj. Funct. Eval.	No. Const. Eval.	Max. Violation of an Active Constraint
1	4.48	8	77	1376	1367	3.2×10^{-5}
2	.45	7	21	542	534	1.0×10^{-8}
3	2.17	11	61	1508	1496	1.6×10^{-6}
7	.37	5	29	467	461	2.1×10^{-6}
8	.65	4	45	757	752	2.9×10^{-5}
11	56.5	6	33	553	546	8.0×10^{-4}
14	19.5	7	143	4277	4269	4.3×10^{-4}
16	5.29	6	34	700	692	3.2×10^{-6}

Table 3

Results of Conventional Interior Penalty Function

Problem	CPU time*	No. of Stages	No. of Cycles	No. Obj. Funct. Eval.	No. Const. Eval.	Max. Violation of an Active Constraint
1	3.93	7	67	1228	1220	1.7×10^{-4}
2	.45	8	18	499	490	4.6×10^{-6}
3	1.83	8	56	1359	1350	6.5×10^{-3}
7	.45	7	36	564	556	3.5×10^{-6}
8	.59	3	42	715	711	2.8×10^{-3}
11	56.95	7	35	552	544	8.2×10^{-5}
14	19.6	7	147	4439	4431	2.0×10^{-4}
16	5.99	8	34	865	856	2.3×10^{-8}

* Measured in seconds on the Purdue University CDC 6500.

AD-P000 071

GEOMETRIC PROGRAMMING FOR CONTINUOUS DESIGN PROBLEMS

Alejandro Diaz, Panos Papalambros and John Taylor
College of Engineering
The University of Michigan
Ann Arbor, MI 48109

The present paper examines a certain extension of Geometric Programming for functionals defined in infinite-dimensional space. The intended application is for continuous problems in design optimization. A brief summary of previous work is given and the particular version of the primal problem to be studied is stated. The construction of the dual problem is presented using two approaches, one involving the formulation and reinterpretation of the Lagrangian functional and another utilizing the concepts of conjugate functions. Both approaches give the same results. The (generalized) zero degree of difficulty dual problem is solved exposing the similarities between the continuous case and the more familiar discrete one. Two simple structural design problems are included to illustrate the application of the method.

Introduction

The first concepts of Geometric Programming (GP) were introduced by Zener in 1961 (15) and developed by Duffin, Peterson and Zener in 1967 in their now classic text on the subject (4). Since then, significant progress has been achieved. Recently, a state-of-the-art review was conducted by Ecker (5) and a review and comparative testing of available algorithms was compiled by Sin and Reklaitis (14). Although GP is a relatively specialized technique, its effective application to certain classes of design optimization problems makes it attractive for further study.

The original standard formulation of a GP problem involved the minimization of a posynomial objective function subject to posynomial upper bound inequality constraints. A posynomial was defined as a polynomial with arbitrary real exponents and positive variables and coefficients. This positivity restriction was essential for the use of the arithmetic-geometric mean inequality for real numbers in order to link the primal and dual formulations of the posynomial (prototype) GP problem. The first change in the prototype formulation was the lifting of the sign restriction on the posynomial coefficients (Passy and Wilde (8), Blau and Wilde (2)). The generalized polynomial defined as the difference of two posynomials was called a signomial. Thus, a signomial primal problem (SPP) is a GP problem in which a signomial objective function is minimized subject to signomial inequality constraints. Its standard mathematical formulation is as follows:

$$\text{Minimize } P_o(t)$$

$$\text{subject to } P_k(t) \le s_k, \qquad k=1,2,\ldots,p$$

$$\text{and } t_j > 0, \qquad j=1,2,\ldots,m$$

where P_k is a signomial defined by

$$P_k \triangleq \sum_{i_k} s_i c_i \prod_{j=1}^{m} t_j^{a_{ij}}, \qquad k=0,1,\ldots,p.$$

Here the index set i_k is:

$$i_k = (m_k, m_k+1, \ldots, m_k+n_k-1), \qquad k=0,1,\ldots,p$$

with $m_o \triangleq 1 \le m_1 = m_o + n_o \le \ldots \le m_p = m_{p-1} + n_{p-1}$

where n_k is the number of terms in each signomial p_k, the coefficients c_i are positive and the exponents a_{ij} are real numbers. The signum functions $s_i = \pm 1$ are designed to carry the sign of each term, while the s_k's generalize the right-hand side of the constraints to ± 1. Problem SPP reduces to a posynomial (prototype) program if all the signum functions are +1. Duffin and Peterson (3) have shown that any SPP reduces to a posynomial problem with some reversed inequalities, i.e., lower bound inequalities.

More recently, the theory of convex functions was used to expand the concepts and methodology of geometric programming. Peterson (9) defined the generalized geometric programming (GGP) in n-dimensional Euclidean space and showed that several mathematical programming problems (e.g., linear, quadratic, signomial) may be transformed into a GPP formulation.

A somewhat simplified version of the primal GPP problem is:

$$\text{Minimize } g_o(x^o)$$

$$\text{subject to } g_k(x^k) \le 0 \qquad k=1,2,\ldots,p$$

$$x^k \in C_k \subseteq En_k$$

$$x_l \in X\text{: a cone in En,}$$

where $x = (x^o, x^1, \ldots, x^p)$ is a vector in En with $x^k \triangleq (x_1^k, x_2^k, \ldots, x_{n_k}^k)$.

Both the signomial and the GGP programs presented above are optimization problems in n-dimensional Euclidean space. A GGP formulation in infinite-dimensional space has been constructed by Scott and Jefferson (13). In their development, the authors combine the approach described by Peterson to solve his n-dimensional problem with some theorems and concepts of convex functionals developed by Rockafellar (11). They also show, as an example, a particular version of an infinite-dimensional posynomial (prototype) GP program.

In the infinite dimensional GGP primal problem En is replaced by L, a real, decomposable vector space of measurable functions. The GGP primal problem to be considered in this paper has the form:

$$\text{Minimize } G_o(x^o) = \int_T g_o(t, x^o)dt$$

$$\text{subject to } G_k(x^k) = \int_T g_k(t, x^k)dt - 1 \le 0, \qquad k=1,2,\ldots,p$$

$$x^k \in C_k, \qquad k=0,1,\ldots,p$$

$$x \in X\text{: a cone in L.}$$

Here x^k is a function from T to En_k and g_k is a normal convex integrand (in the sense of Rockafellar (11)).

The intention of this paper is to study the posynomial (prototype) GP problem that corresponds to the above primal formulation. The equivalent dual problem will be derived in two different ways. The first

PRECEDING PAGE

derivation will follow a traditional approach, introducing transformations and interpretations that have been used by Duffin, Peterson and Zener; Wilde; Beightler and Phillips (1) to solve the posynomial and signomial problems. This involves the definition of a Lagrangian functional and the use of a "geometric inequality" for integrals. The second approach will be based on the theory of convex functionals and corresponds to the methodology of GGP developed by Peterson (9), and Scott and Jefferson (13). Once the dual formulation is established, some suggestions will be made on how to solve it. Finally, the process of solution will be illustrated using some simple examples drawn from the field of structural design.

The mathematical formulation of the particular version of the infinite-dimensional posynomial GP problem treated in the rest of this paper is stated as follows:

Program I:

Minimize $P_o(u)$

subject to $P_k(u) \leq 1, \qquad k=1, 2, \ldots, p$

with

$$P_k = \int_T \sum_{i_k} c_i(t) \left(\sum_{j=1}^{m} u_j(t)^{a_{ij}} \right) dt$$

and $u \in U_+ = \{u \mid u(t) > 0 \text{ a.e. in } T\}$. Here u is a continuous function from T to Em and the index set i_k equals $\{m_k, m_k+1, \ldots, m_k+n_k-1\}$. Note that as before $m_o \triangleq 1 \leq m_1 = m_o + n_1 \leq \ldots \leq m_p = m_{p-1} + n_{p-1}$, and n_k equals the number of terms in the integrand of P_k. Coefficients c_i are continuous, positive, and bounded functions from T to R, and the a_{ij}'s are real numbers.

The similarities between the posynomial (prototype) problem and Program 1 are evident. Both share the positivity restriction on coefficients and variables; both have only upper bound inequality constraints. These restrictions insure the convexity of the transformed problem and permit the use of some sort of geometric inequality. Even though the development of a dual GP theory is no longer bound by the geometric inequality or even the sign of the coefficients, for the purposes of this paper positivity of coefficients and variables will be required.

Dual Construction Via the Lagrangian Functional

The dual of Program 1 is obtained here using a "traditional" approach that follows closely the procedure described by Wilde and Beightler (15) and Beightler and Phillips (1). This involves first, a transformation that exploits the linearities present in Program 1 by introducing a new set of primal variables. The intention of this transformation is to reach a primal formulation in which the new variables appear in separable functions. Once this has been achieved, a Lagrangian functional is stated as a function of both primal variables and multipliers. A variation of the Lagrangian with respect to the primal variables gives conditions for optimality. Using these, the Lagrangian is rewritten and interpreted as one associated with another program. This turns out to be the desired dual problem.

The transformed equivalent problem is:

Minimize V_o

subject to:

$$1 - \int_T \sum_{i_o} w_i dt = 0$$

$$1 - \int_T \sum_{i_k} w_i dt \geq 0 \qquad k=1, 2, \ldots, p$$

$$\sum_{j=1}^{m} a_{ij} v_j - V_o = \ln\left(\frac{w_i}{c_i}\right) \qquad i \text{ in } i_o$$

$$\sum_{j=1}^{m} a_{ij} v_j = \ln\left(\frac{w_i}{c_i}\right) \qquad i \text{ in } I$$

$$w_i(t) > 0 \quad \text{a.e. in T} \quad \text{for all i and } I \triangleq \bigcup_{k=1}^{p} i_k$$

The critical feature of the transformed problem is the introduction of the primal weight functions defined by

$$w_i = \frac{c_i \prod_{j=1}^{m} u_j^{a_{ij}}}{P_o} \qquad i \text{ in } i_o$$

$$w_i = c_i \prod_{j=1}^{m} u_j^{a_{ij}} \qquad i \text{ in } I$$

Also $V_o = \ln P_o$ and $v_j = \ln u_j$, u in U_+. For convenience the objective $\exp(V_o)$ is replaced by V_o.

In the following definition of the Lagrangian L, $\ell = (\ell_0, \ell_1, \ldots, \ell_p)$ is the real vector of multipliers associated with the integral constraints and, for each i, d_i is the function multiplier associated with the constraint relating w_i and v. Thus the Lagrangian is stated as:

$$L(V_o, w, v, d, \ell) = V_o - \ell_o \left[1 - \int_T \sum_{i_o} w_i dt\right] -$$

$$- \sum_{k=1}^{p} \ell_k \left[1 - \int_T \sum_{i_k} w_i dt\right] -$$

$$- \sum_{i_o} \int_T d_i \left[\ln\left(\frac{w_i}{c_i}\right) + V_o - \sum_{j=1}^{m} a_{ij} v_j\right] dt -$$

$$- \sum_{k=1}^{p} \sum_{i_k} \int_T d_i \left[\ln\left(\frac{w_i}{c_i}\right) - \sum_{j=1}^{m} a_{ij} v_j\right] dt.$$

Necessary conditions for a stationary point of L are:

$$\sum_{i_o} \int_T d_i dt = 1 \qquad (1)$$

$$A^T d = 0 \qquad (2)$$

and

$$d_i = \ell_k w_i \quad \text{for all i in } i_k \text{ and all k} \qquad (3)$$

where A is the n x m matrix of coefficients a_{ij}.

Combined with the primal constraints, equations (1) and (3) give the additional conditions:

$$\ell_o = 1 \qquad (4)$$

$$d_i = w_i \qquad i \text{ in } i_o \qquad (5)$$

And by the definitions of the weights w_i

$$\int_T \sum_{i_k} d_i dt = \ell_k \qquad k=1, 2, \ldots, p \qquad (6)$$

Using Eqs. (3) through (6) the Lagrangian may be rewritten in the form:

$$L = \sum_{k=0}^{p} \int_T \sum_{i_k} d_i \ln\left(\frac{c_i \ell_k}{d_i}\right) dt + (V_0 - 1)\left[1 - \int_T \sum_{i_o} d_i dt\right]$$

$$+ \sum_{j=1}^{m} \int_T u_j \left[\sum_{k=0}^{p} \sum_{i_k} a_{ij} d_i\right] dt.$$

Following the steps of Wilde and Beightler (15), this Lagrangian may be viewed as a functional associated with the following problem:

$$\text{Optimize } Z(d, \ell) = \sum_{k=0}^{p} \int_T \sum_{i_k} d_i \ln\left(\frac{c_i \ell_k}{d_i}\right) dt$$

$$\text{subject to } \int_T \sum_{i_k} d_i dt = \ell_k \qquad k=0, 1, \ldots, p$$

$$A^T d = 0$$

$$\ell_k > 0, \quad d_i(t) > 0 \text{ a.e. in } T, \quad \ell_o = 1.$$

To determine the nature of this optimization problem, it is useful to introduce the notions of arithmetic and geometric means.

For f and q finite and positive functions of Z in T, and with $\int_T q\, dt = 1$, the arithmetic mean of f with weight q is

$$M(f, q) = \int_T qf dt.$$

The geometric mean is

$$G(f, q) = \exp\left[\int_T q \ln f\, dt\right]$$

and for M finite, $M(f, q) \geq G(f, q)$ where the equality holds iff $f \equiv$ constant.

The counterparts for real numbers are

$$M(f, q) = \sum_{i=1}^{n} q_i f_i$$

$$G(f, q) = \sum_{i=1}^{n} f_i^{q_i}$$

where $f = (f_1, \ldots, f_n) > 0$, $q = (q_1, \ldots, q_n) > 0$ with $\sum_{i=1}^{n} q_i = 1$. Again, $M(f, q) \geq G(f, q)$ and the inequality holds iff $f_i \equiv$ constant for all i.

For convenience define $p_i = \prod_{j=1}^{n} u_j^{a_{ij}}$ for all i and let d_i be a weight function whose integral over T is D_i and such that $\sum_{i_k} D_i = \ell_k$. With $\ell_o = 1$, and using the geometric inequalities

$$P_k^{\ell_k} = \left[\sum_{i_k} \frac{D_i}{\ell_k} M\left(\frac{d_i}{D_i}, \frac{c_i p_i \ell_k}{d_i}\right)\right]^{\ell_k} \geq \left[\sum_{i_k} \frac{D_i}{\ell_k} G\left(\frac{d_i}{D_i}, \frac{c_i p_i \ell_k}{d_i}\right)\right]^{\ell_k}$$

$$\geq \prod_{i_k} G\left(\frac{d_i}{D_i}, \frac{c_i p_i \ell_k}{d_i}\right)^{D_i}$$

$$= \exp\left[\sum_{i_k} \int_T d_i \ln\left(\frac{c_i p_i \ell_k}{d_i}\right)\right]$$

Since $\lambda_k > 0$ and $P_k \leq 1$ for k=1, 2, ..., p, it follows that

$$P_o \geq \prod_{k=0}^{p} P_k^{\ell_k} \geq \exp Z(d) \cdot \exp\left[\sum_{k=0}^{p} \ell_k \int_T d_i \ln p_i\, dt\right].$$

From the definition of p_i and $A^T d = 0$, the term $\exp\left[\sum_{k=0}^{p} \sum_{i_k} \int_T d_i \ln p\, dt\right] = 1$. Therefore

$$P_o(u) \geq D(d) \triangleq \exp Z(d).$$

From the geometric inequalities $P_o(u) = D(d)$ iff

$$\frac{c_i p_i \ell_k}{d_i} = B_k = \text{constant}, \quad k=0, 1, \ldots, p; \ i \text{ in } i_k, \ \ell_o = 1$$

which corresponds to the optimality conditions (3), (4) and (5) obtained from the Lagrangian by setting $B_o = P_o$ and $B_k = 1$, k=1, 2, ..., p. Hence, with $(\ )^*$ denoting the solution point

$$P_o(u) \leq P_o(u^*) = D(d^*) \leq D(d)$$

and the dual problem is:

Program 2:

$$\text{Maximize } D(d) = \exp\left\{\int_T \sum_{k=0}^{p} \sum_{i_k} d_i \ln\left(\frac{c_i \ell_k}{d_i}\right) dt\right\}$$

$$\text{subject to } \int_T \sum_{i_k} d_i\, dt = \ell_k, \qquad k=0, 1, \ldots, p$$

$$A^t d = 0$$

and $d(t) > 0$ a.e. in T, $\ell_o = 1$.

Program 2 is the dual formulation of Program 1 when all the primal constraints are active at the optimum. If a given constraint is loose at the optimum, the formulation is correct if the corresponding dual variables ℓ_k and d_i are zero (identically on T) and $d_i \ln \frac{c_i}{d_i}$ is defined as the identically zero function on T.

Dual Construction Via Conjugate Functions

The dual formulation of Program 1 will be presented here as a particular case of the dual infinite-dimensional GGP problem. Dual GGP statements have been derived by Peterson (9) and Scott and Jefferson (13) using the concepts of conjugate functions and subgradient sets. The fundamental theorems that apply to the infinite dimensional problem appear in Rockafellar (11). The reader is referred to these references for a description of the development of the GGP duality theory. Certain definitions and concepts needed to understand the dual GGP statement are provided here for completeness.

Definition 1. The bilinear form $\langle x, y \rangle$ is defined here as $\int_T x(t) \cdot y(t) dt$ if x and y are real valued functions on T. If x and y are vectors in Em, $\langle x, y \rangle$ is the ordinary dot product $x \cdot y$.

Definition 2. The conjugate function of G(x) defined on C is H defined on D by

$$H(y) = \sup_{x \in C} \{\langle x, y \rangle - G(x)\}$$

$$D = \{y \mid \sup[\langle x, y \rangle - G(x)] < \infty\}.$$

Definition 3. The positive homogeneous extension of H(y) is $H^+(y, \lambda)$ defined on D_+ by

$$H^+(y, \lambda) = \sup \langle x, y \rangle \text{ if } \lambda = 0 \text{ and } \sup_{x \in C} \langle x, y \rangle < \infty$$

$$\lambda H(y/\lambda) \text{ if } \lambda > 0$$

and $D_+ = \{(y, \lambda) \mid \sup \langle x, y \rangle < \infty \ \ \lambda = 0\}$

$$\cup \ \{(y, \lambda) \mid y/\lambda \in D, \ \lambda > 0\}.$$

When G is of the form $G(x) = \int_T g(t, x) dt - 1$ with g a normal convex integrand, H is given by $H(y) = \int_T h(t, y) dt + 1$ where h is the conjugate of g. By

construction

$G(x) + H(y) \geq \langle x, y \rangle \quad x \text{ in } C,\ y \text{ in } D$

$\lambda G(x) + H^{+}(y, \lambda) \geq \langle x, y \rangle \quad x \text{ in } C,\ (y, \lambda) \text{ in } D_{+}.$

The GGP dual to the infinite dimensional primal problem given earlier is:

$$\text{Minimize } H(y, \lambda) = H_o(y^o) + \sum_{k=1}^{p} H_k^{+}(y^k, \lambda_k)$$

$$\text{subject to } y^o \in D^o;\ (y^k, \lambda_k) \in D_{+}^{k},\quad k=1, 2, \ldots, p$$

$$y \in Y\text{: the polar cone of } X.$$

Here y^k is a function from T to En_k. In terms of the primal objective functional G_o, at the solution point

$$G_o(x^o)^* + H(y)^* = 0$$

The dual function just stated, is valid for any infinite dimensional optimization problem that can be put into the standard GGP form. It can be used in particular to solve Program 1 once this problem has been suitably transformed. As before, this can be accomplished by defining a new set of primal variables that brings out the separability exhibited by all posynomial problems. These new variables are given by the transformation

$$x_i = \ln \left[\prod_{j=1}^{m} u_j^{a_{ij}} \right] \text{ for all } i,\ u \text{ in } U_{+}.$$

With these new variables the primal problem becomes

Program 3:

$$\text{Minimize } G^o(x^o) = \int_T \sum_{i_o} c_i \exp x_i \, dt$$

$$\text{subject to } G^k(x^k) = \int_T \sum_{i_k} c_i \exp x_i \, dt - 1 \leq 0,$$

$$k=1, 2, \ldots, p$$

$$x^k(t) \in En_k$$

and

$$x \in X = \{x \mid x_i = \sum_{j=1}^{m} a_{ij} \ln u_j \text{ for all } i,\ u \text{ in } U_{+}\},\ a$$

subspace.

The conjugate function of each G^k and its positive homogeneous extension are obtained using the definitions given above. Once they are found, the dual of Program 3 is written as follows:

Program 4:

$$\text{Minimize } H(y, \lambda) = \int_T \sum_{i_o} [y_i \ln(\frac{y_i}{c_i}) - y_i] dt +$$

$$+ \sum_{k=1}^{p} \int_T [\sum_{i_k} y_i \ln(\frac{y_i}{\lambda_k c_i}) - y_i] dt + \lambda_k$$

$$\text{subject to } A^T y = 0$$

$$y(t) > 0 \quad \text{a.e. in } T$$

$$\lambda > 0.$$

It can be shown that the condition $A^T y = 0$ is equivalent to $\langle x, y \rangle = 0$ for all x in X and it therefore describes the orthogonal complement of X (which is the polar cone of X since X is a subspace).

Program 4 does not yet have the same form as Program 2, the dual formulations with objective D obtained using the Lagrangian approach. However, the two programs are equivalent and at the optimum $D^* = -H^*$. To show this equivalence first introduce the following transformed version of the dual Program 4.

$$\text{Minimize } \bar{H}(Z, z, \mu) = Z \ln Z - Z - ZD(z, \mu) +$$

$$+ Z[\sum_{k=1}^{p} \mu_k - \int_T \sum_{i_k} z_i \, dt]$$

$$\text{subject to } \int_T \sum_{i_o} z_i \, dt = 1$$

$$A^T z = 0$$

$$z(t) > 0 \quad \text{a.e. in } T,\ \mu > 0.$$

Here the transformed variables z and μ are defined by $z_i = y_i / Z$ and $\mu_k = \lambda_k / Z$ where Z is a positive real number chosen so that

$$\int_T \sum_{i_o} z_i dt = 1.$$

Conditions for optimality of $\bar{H}$ with respect to Z and μ are

$$\ln Z = \ln D(z, \mu) - \sum_{k=1}^{p} [\mu_k - \int_T \sum_{i_k} z_i dt]$$

$$\int_T \sum_{i_k} z_i dt = \mu_k, \qquad k=1, 2, \ldots, p.$$

With these conditions the transformed dual problem involving the minimization of $\bar{H}(Z, z, \mu)$ is equivalent to the maximization of $D(d, \ell)$ with

$$\bar{H}(Z, z, \mu) = -D(d, \ell)$$

$$z = d, \qquad \mu = \ell.$$

And the equivalence between Programs 2 and 4 is established thereby.

Solution of the Zero Degree of Difficulty Problem

As is the case with the prototype problem, solving the dual of the infinite dimensional problem has many advantages. In particular, the solution to certain problems may be obtained by just solving the constraint equations. This occurs when n, the number of terms in the primal functionals, equals m, the number of primal unknowns plus one. The number $r = n-m-1$ is called the degree of difficulty.

When r=0 only one function is needed to describe the whole subspace Y. [For instance, all the feasible d_i's may be expressed in terms of d_1 by just solving $A^T d = 0$.] Also, if D_i is the integral of d_i over T, the D_i's satisfy

$$\sum_{i_k} D_i = \ell_k, \qquad k=0, 1, \ldots, p \tag{7}$$

$$\sum_{k=0} \sum_{i_k} a_{ij} D_i = 0, \qquad j=1, 2, \ldots, m$$

$$\ell_o = 1$$

which can be solved for the D's and ℓ's provided that all the constraints are independent, active and r=0. In addition, in terms of d_1,

$$d_i = \frac{D_i}{D_1} d_1, \qquad \text{for all } i \tag{8}$$

and

$$D(d) = \exp\{\int_T \frac{d_1}{D_1} \ln[(\frac{D_1}{d_1})^K \prod_{k=0}^{p} \prod_{i_k} (\frac{c_i \ell_k}{D_i})^{D_i}]dt\} \qquad (9)$$

with

$$K \triangleq \sum_{k=0}^{p} \ell_k, \quad \ell_o = 1.$$

This has the form of the geometric mean of a function f with weight function d_1/D_1, which is maximum for f ≡ constant = B_o.

$$f = (\frac{D_1}{d_1})^K \prod_{k=0}^{p} \prod_{i_k} (\frac{c_i \ell_k}{D_i}) \equiv B_o.$$

Since D_1 is the integral of d_1 over T_1, the solution is

$$B_o = \{\int_T [\prod_{k=0}^{p} \prod_{i_k} (\frac{c_i \ell_k}{D_i})^{D_i}]^{1/K} dt\}^K \qquad (10)$$

$$d_1^* = D_1\{\frac{1}{B_o} \prod_{k=0}^{p} \prod_{i_k} (\frac{c_i \ell_k}{D_i})^{D_i}\}^{\frac{1}{K}} \qquad (11)$$

and

$$D(d^*) = P_o(u^*) = B_o.$$

All optimum dual variables are retrieved from Eq. (8). The primal solution is obtained by solving m of the following equations

$$\sum_{j=1}^{m} a_{ij} \ln u_j^* = \ln(\frac{d_i^* P_o^*}{c_i}), \qquad i \text{ in } i_o$$

$$\sum_{j=1}^{m} a_{ij} \ln u_j^* = \ln(\frac{d_i^*}{\ell_k^* c_i}) \qquad i \text{ in } I \qquad (12)$$

Structural Design Examples

The following simple examples are included here to illustrate the method.

Problem 1. Axial member:

Consider an axial member fixed at one end (t=0) and subject to a distributed load of constant magnitude q_o. Find the area distribution a(t) that minimizes the volume while keeping the tip displacement less than a maximum value u_{max}.

The volume, and the tip displacement are given by

$$V = \int_o^L a\,dt; \quad u(L) = \int_o^L \frac{q_o(L-t)}{E} a^{-1} dt.$$

The mathematical problem statement is

Minimize $\int_o^L a\,dt$

subject to $\int_o^L \frac{q_o(L-t)}{E u_{max}} a^{-1} dt \le 1; \quad a(t) > 0$

This is a zero degree of difficulty problem, and therefore the solution is found simply by solving the constraint equations of the dual problem.

$$D_1 = \ell_o \quad D_2 = \ell_1 \quad (1, -1)(\frac{d_1}{d_2}) = 0 \quad \ell_o = 1$$

whereby

$$D_1^* = D_2^* = \ell_1^* = 1 \text{ and } K = 2.$$

From Eqs. (10), (11) and (8)

$$B_o = V^* = \frac{4}{9} \frac{q_o L^3}{E u_{max}}$$

and

$$d_1^* = d_2^* = \frac{3}{2}(L-t)^{1/2} L^{-3/2}.$$

Finally, the optimum area distribution is found from Eq. (12):

$$a^* = \frac{2}{3} \frac{q_o L^{3/2}}{E u_{max}} (L-t)^{1/2}$$

Problem 2: Cantilevered beam:

Consider a beam cantilevered at one end (t=0) and subject to a tip load of magnitude Q_o at t=L. Let the cross section of the beam be rectangular, of fixed width b and varying height h(t). Find h that minimizes the volume so that the average bending stress does not exceed s_o.

The volume of the stress is given by $V = \int_o^L bh\,dt$. The average stress is

$$s_{avg} = \frac{1}{L}\int_o^L s(t, h/2)dt = \int_o^L \frac{6Q_o(L-t)}{bL} h^{-2} dt.$$

The mathematical problem statement is:

Minimize $\int_o^L bh\,dt$

subject to $\int_o^L \frac{6Q_o(L-t)}{bL\,s_o} h^{-2} dt \le 1, \qquad h \ge 0.$

Again, r=0 and the solution to the dual constraints solves the problem:

$$D_1 = \ell_o, \quad D_2 = \ell_1, \quad (1, -2)(\frac{d_1}{d_2}) = 0, \quad \ell_o = 1$$

whereby

$$D_1^* = 1, \quad D_2^* = 1/2, \quad \ell_1^* = 1/2, \quad K = 3/2.$$

Using Eqs. (10), (11), and (8):

$$B_o = V^* = \frac{9}{4\sqrt{2}} (\frac{bQ_o}{s_o})^{1/2} L^{3/2}$$

$$d_1^* = \frac{4}{3} L^{-4/3}(L-t)^{1/3} \qquad d_2^* = \frac{2}{3} L^{-4/3}(L-t)^{1/3}$$

and the optimum height distribution is:

$$h^* = \frac{3\sqrt{2}}{2} (\frac{Q_o}{b\,s_o})^{1/2} L^{1/6}(L-t)^{1/3}.$$

Conclusion

The infinite-dimensional prototype formulations, both primal and dual, are very similar to the more familiar discrete problems. Solution in the dual space is often easier than in the primal. In the infinite-dimensional problem, the solution functions belong to a subspace that is often small and easy to describe. In the case of the zero degree of difficulty problem,

this subspace is described by multiples of only one function and the solution is immediately available.

The dual problem incorporates all the primal constraints into the objective function, resulting in a set of dual constraints and a subspace condition that are much easier to handle. Local inequality constraints may be added to the primal without difficulty and with very little change in the results (7). The incorporation of state equations, on the other hand, is much more difficult and more research is needed towards this goal.

The interpretation of the dual solution is similar in both the finite and the infinite dimensional problems. At the optimum, the dual functions act as weight functions that measure the contribution of each primal term towards the objective function or towards the satisfaction of the constraints. In fact, the integral over T of each dual function associated with a term in the primal objective is equal to the fraction of the objective carried by that particular term.

References

(1) Beightler, C. S. and D. T. Phillips, Applied Geometric Programming, Wiley, New York, 1976.

(2) Blau, G. and D. J. Wilde, Second Order Characterization of Generalized Polynomial Programs. Paper presented at the Princeton International Symposium on Mathematical Programming, 1967.

(3) Duffin, R. J. and E. L. Peterson, Geometric Programming with Signomials, J. Optimization Theory Appl., 11, pp. 3-35, 1973.

(4) Duffin, R. J., E. L. Peterson and C. Zener, Geometric Programming - Theory and Application, Wiley, New York, 1967.

(5) Ecker, J. G., Geometric Programming: Methods, Computations and Applications, SIAM Review, 22, No. 3, 1980.

(6) Hardy, G. H., J. E. Littlewood and G. Pólya, Inequalities, Cambridge University Press, London, 1964.

(7) Jefferson, T. R., and C. H. Scott, Generalized Geometric Programming Applied to Problems of Optimal Control: Part I, Theory, J. Optimization Theory Appl., 26, pp. 117-129, 1978.

(8) Passy, U. and D. J. Wilde, Generalized Polynomial Optimization, SIAM J. Appl. Math., 15, 1344-1356, 1967.

(9) Peterson, E. L., Geometric Programming, SIAM Review, 18, 1-51, 1976.

(10) Rockafellar, R. T., Conjugate Duality and Optimization, Regional Conference Series in Applied Mathematics, SIAM, 1974.

(11) Rockafellar, R. T., Integrals Which are Convex Functions, Pacific J. Math., 24, 525-539, 1968.

(12) Rockafellar, R. T., Convex Analysis, Princeton University Press, Princeton, N.J., 1970.

(13) Scott, C. H. and T. R. Jefferson, Duality in Infinite Dimensional Mathematical Programming: Convex Integral Functionals, J. Math. Anal. Appl., 61, pp. 251-261, 1977.

(14) Sin, Y. T. and G. V. Reklaitis, On the Computational Utility of Generalized Geometric Programming Solution Method. Part 1: Review and Test Procedure Design; Part 2: Results and Interpretation, 7th ASME Design Automation Conference, Hartford, 1981, to appear in Progress in Engineering Optimization, 1981, ASME Design Division.

(15) Wilde, D. J. and C. S. Beightler, Foundations of Optimization, Prentice-Hall, Inc., Englewood Cliffs, N.J., 1967.

(16) Zener, C., A Mathematical Aid in Optimizing Engineering Designs, Proc. Natl. Acad. Sci., 47, pp. 537-539, 1961.

AD-P000 072

ASSOCIATED SOLUTIONS IN OPTIMIZATION APPLICATIONS TO STRUCTURAL MECHANICS

Pierre BROUSSE
Institut de Mécanique Théorique et Appliquée
Université Pierre et Marie Curie
4 Place Jussieu
75005 Paris

SUMMARY

In a previous article (1) we have defined and studied, sets of two optimization problems that we call associated problems : an optimization problem with one inequality constraint being given, its associated problem is obtained by exchanging the constraint function and the objective function. The main purpose of this paper is to present some connections between the solutions of a problem and those of its associated one, and more particularly to make methods for solving any optimization problem having a suitable form when the solutions of its associated problem are known.

First of all, we present two general theorems about solutions of associated problems. These theorems are very general ; they do not use any properties regarding continuity, differentiability or convexity. The second one concerns problems, often met in practice, the solutions of which are on the boundary of the admissible region. In this event, we actually derive a method for solving one of two associated problems when the solutions of the other are known. In particular, we develop the method in the important case as far as the numerical treatment is concerned. Then, we extend the definition of the associated problem of a given optimization one to problems involving several inequality constraints. We show why optimization problems introduced in practice present often the properties required in the general considerations above ; here, increasing and continuous functions are necessary. At last, two examples concerning structural optimization are completely treated : for an elastic column, minimize the mass when the load is bounded from below, or maximize the load when the mass is bounded from above ; for perfectly plastic frameworks, minimize the mass when the safety factor is bounded from below, or maximize the safety factor when the mass is bounded from above.

I. INTRODUCTION

In this paper, we shall study pairs of optimization problems. Each problem of a pair is deduced from the other one by exchanging the objective function and a constraint function.

Some of such pairs of associated problems (also called dual problems) have been considered by several authors. But, to my knowledge, all these examples concern very particular structures ; for example, for a given bar, or plate, or shell, to minimize the mass when one of the natural frequencies is bounded from below, or to maximize this frequency when the mass is bounded from above. In such examples, as well as in any examples we have seen in literature, the results have been obtained by elaborating particular proves adapted to each particular case, and by using various properties for the problem which is studied : control theory, extremum theorems with differentiability, convexity, etc.. (2 - 7) . Let us note a particular method based only on extremum properties and which permits to prove that a certain condition already known as a necessary one in a problem of mass minimization with a free boundary, is also a sufficient condition for both this problem and its associated problem (8).

In this paper, we make and we prove general optimization theorems valid for all associated problems provided they have a very general form. We do not need any properties regarding continuity, differentiability or convexity. From these theorems we derive methods for solving any optimization problem when the solutions of its associated problem are known. We examine general situations where the assumptions mentioned above on the initial form are automatically verified ; in this event, we need functions which are monotonically increasing and continuous. At last, applications to mechanical optimization problems are given.

2. GENERAL THEOREMS

2.1. NOTATIONS

- Given,

  E : a finite or infinite dimensional space,

  S : a non empty set of E,

  a : the generic point in E,

  f,g: two given real-valued functions defined on S,

m_o, p_o : two constant numbers.

- The following terminology will be used,

$G(p_o)$: the subset of points a in S where $g(a) \geqslant p_o$ (this subset $G(p_o)$ is assumed to be non empty),

$f^{(\downarrow)}_{\uparrow_o}$: the infimum of the function f on $G(p_o)$,

$F(m_o)$: the subset of points a in S where $f(a) \leqslant m_o$.

- The two following problems will be considered,

Problem $P(p_o)$: minimize f on $G(p_o)$

Problem $Q(m_o)$: maximize g on $F(m_o)$

- The following notations will be used,

$X(p_o)$: the set of the solutions of problem $P(p_o)$,

$Y(m_o)$: the set of the solutions of problem $Q(m_o)$

(the sets $X(p_o)$ and $Y(m_o)$ may be empty) .

2.2. THEOREM 1

Theorem 1. i. If problem $P(p_o)$ has at least a solution, then problem $Q(f^{(\downarrow)}_{\uparrow_o})$ is equivalent to the following one : maximize the function g on $X(p_o)$, and any solution of these problems verifies $g(a) \geqslant p_o$

ii. If problem $P(p_o)$ has no solution, then problem $Q(f^{(\downarrow)}_{\uparrow_o})$ has no solution in $G(p_o)$.

Proofs . i. Let us consider in $F(f^{(\downarrow)}_{\uparrow_o})$, the part which is in $G(p_o)$ and the part which is in the complement of $G(p_o)$ with respect to S.

In $G(p_o)$ the only points contained in $F(f^{(\downarrow)}_{\uparrow_o})$ are the points in $X(p_o)$, according to the definition and the existence of the solutions of problem $P(p_o)$. Let us recall that any point a in $X(p_o)$ verifies $g(a) \geqslant p_o$.

In the complement of $G(p_o)$ with respect to S, there may be some points a such that $f(a) \leqslant f^{(\downarrow)}_{\uparrow_o}$; but, all these points verify $g(a) < p_o$

Then, theorem 1.i is proved.

ii. The set $X(p_o)$ is here assumed to be empty : all points a in $G(p_o)$ verify $f(a) > f^{(\downarrow)}_{\uparrow_o}$.

If problem $Q(f^{(\downarrow)}_{\uparrow_o})$ has no solution, the conclusion of the theorem is evident.

If problem $Q(f^{(\downarrow)}_{\uparrow_o})$ has solutions, all these solutions a verify the inequality $f(a) \leqslant f^{(\downarrow)}_{\uparrow_o}$, after the definition of problem $Q(f^{(\downarrow)}_{\uparrow_o})$. Thus no solution of $Q(f^{(\downarrow)}_{\uparrow_o})$ is in $G(p_o)$.

Consequences of theorem 1

- Any solution a^* of problem $Q(f^{(\downarrow)}_{\uparrow_o})$ verifying $g(a^*) \geqslant p_o$ is a solution of problem $P(p_o)$

Proof. According to theorem (1.ii), problem $P(p_o)$ has at least a solution : the set $X(p_o)$ is non empty. Then, according to theorem (1.i), the point a^* is in $X(p_o)$, i.e. is a solution of problem $P(p_o)$.

- If problem $P(p_o)$ has only one solution a^* , then a^* is the unique solution of problem $Q(f^{(\downarrow)}_{\uparrow_o})$.

Proof. The set $X(p_o)$ reduces to a single point a^* ; of course, this point is the unique solution of the problem : maximize g on $X(p_o)$, i.e. the unique solution of problem $Q(f^{(\downarrow)}_{\uparrow_o})$, by theorem (1.i).

2.3. THEOREM 2

In most optimization problems which are formula ted as problem $P(p_o)$, all solutions lie on the boundary $g(a) = p_o$. Therefore, by supposing this is the case, we do not make a very restrictive assumption. This explains the interest of the following theorem.

Theorem 2. If problem $P(p_o)$ has at least a solution and if all its solutions verify $g(a) = p_o$, then problem $Q(f^{(\downarrow)}_{\uparrow_o})$ is equivalent to $P(p_o)$. In other words, we have $X(p_o) = Y(f^{(\downarrow)}_{\uparrow_o})$

Proof. Here, all points a in $X(p_o)$ verify $g(a) = p_o$. Then $X(p_o)$ is the set of the solutions of the following problem : maximize g on $X(p_o)$. By theorem (1.i), the set $X(p_o)$ is also the set of the solutions of problem $Q(f^{(\downarrow)}_{\uparrow_o})$. Therefore, theorem 2 is proved.

Comments - Replacing in the various statements the inequalities by their opposite ones, and, at the same time, exchanging the terms minimize and maximize, lead to a theorem analogous to theorem 2, whose formulation is left to the reader.

- Exchanging problem $P(p_o)$ and problem $Q(m_o)$ in theorem 2 gives a new theorem : if $Q(m_o)$ is not empty, we have $Y(m_o) = X(g^{(\downarrow)}_{\uparrow_o})$, where $g^{(\downarrow)}_{\uparrow_o}$ is the supremum of the function g on $F(m_o)$.

3. APPLICATIONS TO OPTIMIZATION PROBLEMS

3.1. APPLICATION OF THEOREMS 1 AND 2 TO THE RESOLUTION OF PROBLEM $Q(m_o)$ WHEN THE SOLUTIONS OF PROBLEM $P(p_o)$ ARE KNOWN

According to the comments above, problems $P(p_\circ)$ and $Q(m_\circ)$ play the same part. For instance, suppose that we know how to solve problem $P(p_\circ)$. We are going to show how to obtain the solutions of problem $Q(m_\circ)$.

A first result is the following : if the assumptions of theorem 2 are verified, then the solutions of problem $Q(m_\circ)$ with $m_\circ = f^{(\dot{\iota})}_{\underline{\uparrow}_\circ}$ are those of problem $P(p_\circ)$.

The following result is much more important : under suitable conditions, it is possible to obtain the solutions of problem $Q(m_\circ)$ for all $m_\circ$ in certain sets.

Indeed, let us suppose that the assumptions of theorem 2 (existence of at least a solution of problem $P(p_\circ)$, localization of all the solutions on $g(a) = p_\circ$) hold for all numbers $p_\circ$ in a given interval J : $(\underline{p}_\circ , \overline{p}_\circ)$. Let $p_\circ$ and $p'_\circ$ be two numbers in this interval such that $p_\circ < p'_\circ$. The set $X(p_\circ)$ does not intersect $G(p'_\circ)$ because it is in $g(a) = p_\circ$ by assumption. Thus, according to the definition of problem $P(p_\circ)$, the inequality $f(a) > f^{(\dot{\iota})}_{\underline{\uparrow}_\circ}$ holds on $X(p'_\circ)$. But on $X(p'_\circ)$ we have $f(a) = f^{(\dot{\iota})}_{\underline{\uparrow}'_\circ}$. Therefore we obtain $f^{(\dot{\iota})}_{\underline{\uparrow}_\circ} < f^{(\dot{\iota})}_{\underline{\uparrow}'_\circ}$. Thus, the inequality $p_\circ < p'_\circ$ implies $f^{(\dot{\iota})}_{\underline{\uparrow}_\circ} < f^{(\dot{\iota})}_{\underline{\uparrow}'_\circ}$. In other words, we have defined on J a strictly increasing function $f^{(\dot{\iota})}$ of $p_\circ$. Consequently, this function has an inverse function defined on the set I consisting of all numbers $f^{(\dot{\iota})}_{\underline{\uparrow}_\circ}$ when $p_\circ$ describes J : to each number $m_\circ$ in I, there corresponds one number $p_\circ$ in J such that $m_\circ = f^{(\dot{\iota})}_{\underline{\uparrow}_\circ}$.

Now, let $a^*(\underline{\uparrow}_\circ)$ be an arbitrary solution of problem $P(p_\circ)$. For any value $m_\circ$ in I, the maximum of the function g on $F(m_\circ)$ is denoted by $p_\circ(m_\circ)$: the solutions of problem $Q(m_\circ)$ are the $a^* p_\circ(m_\circ))$ obtained in replacing $p_\circ$ by $p_\circ(m_\circ)$ in $a^*(p_\circ)$. In most concrete applications, the function $f^{(\dot{\iota})}$ of $p_\circ$ is continuous. Then, the set I is an interval of $\mathbb{R}$: the interval $(f^{(\dot{\iota})}_{\underline{\uparrow}_\circ} , f^{(\dot{\iota})}_{\overline{\uparrow}_\circ})$. Both following cases are very important.

- Suppose that we can calculate the quantity $p_\circ(m_\circ)$ and the solutions $a^*(p_\circ)$ in terms of $m_\circ$ and $p_\circ$ respectively. Then, for each $m_\circ$ in I, the maximum $p_\circ(m_\circ)$ of g and the solutions of $Q(m_\circ)$ are obtained in terms of $m_\circ$ by substitution (see example 4.1).
- Suppose that we can numerically solve problem $P(p_\circ)$ and compute the corresponding minimum $m_\circ(p_\circ)$ of the function f for each $p_\circ$ in J. Then, for every value of $m_\circ$ in I, we can compute the corresponding value $p_\circ(m_\circ)$ by a numerical interpolation, and thus compute the solutions of problem $Q(m_\circ)$.

3.2. REMARKS ON SOME SITUATIONS WHERE THE PREVIOUS THEOREMS CAN BE APPLIED

Now, we are going to extend the definition of associated problems and to introduce a situation for which either the unique solution of problem $Q(f^{(\dot{\iota})}_{\underline{\uparrow}_\circ})$ is known or the assumptions of theorem 2 are automatically verified.

3.2.1. An extension of theorems 1 and 2.

In the definition of associated problems, it was supposed that problem $P(m_\circ)$ involves only one inequality constraint: $g(a) \geqslant p_\circ$. Now, let us suppose that there are several constraints which do not intervene in the definition of the initial set S : the inequality constraints $g_j(a) \geqslant p_\circ$, $j = 1, \ldots, \overline{j}$ (there is no loss of generality in supposing that the right-hand sides of the $\overline{j}$ previous inequalities have the same value $p_\circ$). Let us consider the greatest lower bound g of the g_j (i.e. such $g(a) = \inf_j g_j(a)$ for any a in S). The $\overline{j}$ constraints $g_j(a) \geqslant p_\circ$ are equivalent to the unique constraint $g(a) \geqslant p_\circ$. We are then led to define for problem :

- minimize f on the intersection of S and of $g_j(a) \geqslant p_\circ$, $j = 1, \ldots, \overline{j}$,
- its associated problem :
- maximize on $F(m_\circ)$ the smallest of the functions g_j.

Then, theorems 1 and 2 can be used with the greatest lower bound function g defined as above.

3.2.2. A general case met in practice

In most practical cases, the subset S of the space E is defined by a bound from below and a bound from above :

$$\underline{a} \leqslant a \leqslant \overline{a} , \qquad (1)$$

where $\underline{a}$ and $\overline{a}$ are given. If E is a finite dimensional space ($E = \mathbb{R}^n$) $\underline{a}$ and $\overline{a}$ are column-matrices, and the double inequality (1) represents 2n inequalities between the components of the matrices $\underline{a}$, a, $\overline{a}$: $\underline{a}_i \leqslant a_i \leqslant \overline{a}_i$, for $i = 1, \ldots n$. If E is an infinite dimensional space of real-valued functions defined on a connected subset Δ of $\mathbb{R}$, $\mathbb{R}^2$ or $\mathbb{R}^3$, then $\underline{a}$ and $\overline{a}$ are given real-valued functions defined on Δ ; the double inequality (1) means $\underline{a}(x) \leqslant a(x) \leqslant \overline{a}(x)$ for all x in Δ.

Here, the function f is assumed to be a strictly

increasing continuous function(as it is the case when f is the volume).

If $\underline{a}$ is in $G(p_0)$, it is the unique solution of problem $P(p_0)$, and, consequently, the unique solution of problem $Q(f^{(\mu)}_{p_0})$ by the second consequence of theorem 1 mentioned in paragraph (2.2).

If $\underline{a}$ is not in $G(p_0)$, and if problem $P(p_0)$ has a solution (such a solution always exists if E is a finite dimensional space), we are going to show that all solutions of $P(p_0)$ lie in the set $g(a) = p_0$. Indeed, if a solution a^* would verify $g(a^*) > p_0$, some point a' such that $a' < a^*$ (i.e. $a' \leqslant a^*$ and $a' \neq a^*$) would exist in $G(p_0)$, the inequality $f(a') < f(a^*)$ would hold, and therefore a^* would not be a solution of problem $P(p_0)$. Then the assumptions of theorem 2 are actually fulfilled.

4. ASSOCIATED SOLUTIONS IN STRUCTURAL MECHANICS

4.1. EXAMPLE 1: MINIMIZATION OF THE MASS OF AN ELASTIC COLUMN AND MAXIMIZATION OF THE LOAD SUPPORTED BY THE COLUMN

4.1.1. Formulation of the problems. The column is pin-jointed at its ends ; it supports a compressive axial load applied at one end. The column is a cylindrical tube ; its height h is fixed. The interior radius and the exterior radius are termed r_1 and r_2 respectively. The column is made of an homogeneous material (mass density ρ, Young modulus E). Its weight is neglected.

The exterior radius r_2 is to be smaller than or equal to a given length c. It is assumed that only two failures can occur ; the compressive stress must not exceed a given stress σ_0, Euler buckling must not appear.

The two following problems are stated.

How to choose r_1 and r_2 in such a way that the maximum load supported by the column be greater than or equal to a given load p_0, and that the mass M of the column be minimum (2)

How to choose r_1 and r_2 in such a way that the mass M of the column be smaller than or equal to a given mass M_0 and that the maximum load supported by the column be maximum (3)

Let us write :

$$C = \pi c^2 \sigma_0 \quad , \quad B = \frac{\pi^3 c^4 E}{4h^2} \quad , \quad m_0 = \frac{M_0}{\pi c^2 h \rho}$$

$$m = \frac{M}{M_0} m_0 \quad , \quad a_1 = \frac{(r_1)^2}{c^2} \quad , \quad a_2 = \frac{(r_2)^2}{c^2}$$

Then, problems (2) and (3) take the following forms :

Minimize $m = a_2 - a_1$ on

$$G(p_0) = \left\{ a_1, a_2 \;\middle|\; 0 \leqslant a_1 \leqslant a_2 \leqslant 1 \,,\; C(a_2 - a_1) \geqslant p_0 \,,\; B\left((a_2)^2 - (a_1)^2\right) \geqslant p_0 \right\} \quad (4)$$

Maximize the smallest of the 2 quantities :

$$C(a_2 - a_1) \,,\; B\left((a_2)^2 - (a_1)^2\right) \text{, on}$$

$$F(m_0) = \left\{ a_1, a_2 \;\middle|\; 0 \leqslant a_1 \leqslant a_2 \leqslant 1 \,,\; a_2 - a_1 \leqslant m_0 \right\} \quad (5)$$

Problems (4) and (5) have the generalized forms presented in paragraph (3.2.1).

4.1.2. Solutions of problem (5)

The second problem, (5), can easy be solved by taking $m = a_2 - a_1$ as a variable. The number and the explicit expressions of the solutions a_1^*, a_2^*, as well as the maximum value P^* of the supported load, depend on the respective values of C and B, and on the values of m_0 :

- If $C \leqslant B$,

  - $0 \leqslant m_0 \leqslant C/B$: $\frac{1}{2}\left((C/B) + m_0\right) \leqslant a_2^* \leqslant 1$; $a_1^* = a_2^* - m_0$; (infinity of solutions) ; $P^* = C m_0$
  - $C/B \leqslant m_0 \leqslant 1$: $m_0 \leqslant a_2^* \leqslant 1$; $a_1^* = a_2^* - m_0$; (infinity of solutions) ; $P^* = C m_0$
  - $m_0 > 1$: no solution

4.1.3. Résolution of problem (4)

In the previous solutions, the maximum values of the supported load (now written p_o instead of P^*) define functions p_o of m_o. Each of these functions has an inverse function in the corresponding interval. By substitution as it was explained in paragraph (3.1), we can directly obtain the solutions a_1^*, a_2^*, of problem (4), in terms of p_o, as well as the minimum values m^* of the reduced mass m :

- If $C \leqslant B$

. $0 \leqslant p_o \leqslant C^2/B$:
$\frac{1}{2}(C/B + p_o/C) \leqslant a_2^* \leqslant 1$
$a_1^* = a_2^* - p_o/C$
(infinity of solutions)
$m^* = p_o/C$

. $C^2/B \leqslant p_o \leqslant C$:
$p_o/C \leqslant a_2^* \leqslant 1$
$a_1^* = a_2^* - p_o/C$
(infinity of solutions)
$m^* = p_o/C$

. $p_o > C$: no solution

- If $C \geqslant B$

. $0 \leqslant p_o \leqslant 2C - C^2/B$:
$\frac{1}{2}(C/B + p_o/C) \leqslant a_2^* \leqslant 1$
$a_1^* = a_2^* - p_o/C$
(infinity of solutions)
$m^* = p_o/C$

. $2C - C^2/B \leqslant p_o \leqslant B$:
$a_2^* = 1$
$a_1^* = \sqrt{1 - p_o/B}$
(one solution)
$m^* = 1 - \sqrt{1 - p_o/B}$

. $p_o > B$: no solution

4.2. EXAMPLE 2 : MINIMIZATION OF THE MASS AND MAXIMIZATION OF THE SAFETY FACTOR OF PERFECTLY PLASTIC FRAMEWORKS

We consider structures which are represented as perfectly planar frames with perfect constraints. The frames are expected to support given concentrated loads lying in their plane. We postulate that all failures derive from the formation of plastic hinges.

The column matrix of cross-sectional areas of bars are taken as a variable ; let a be this matrix. It is assumed that all bars are made of the same homogeneous material. So, the total mass m of bars is : $\rho\, L^T a$, where ρ is the mass density, L the column matrix of lengths of bars, and where T is the symbol of the transpose. For several reasons, in particular technological ones, the matrix a is to be bounded from below and from above : $\underline{a} \leqslant a \leqslant \bar{a}$, where $\underline{a}$ and $\bar{a}$ are given matrices (with positive elements).

It is shown (9) that a safety condition is

$$a^T |D^T \gamma^\alpha| \geqslant p\, \phi^T C^T \gamma^\alpha \quad , \alpha = 1, \dots, \bar{\alpha} \ ,$$

with the following notations,

p : safety factor,

ϕ : load column matrix,

C and D : rectangular matrices depending only on the geometry of the structure,

γ^α : column matrices of certain independent parameters which generate kinematically admissible mechanisms (for all γ^α, the product $\phi^T C^T \gamma^\alpha$ is positive)

It is of interest to consider the two following problems :

Minimize the mass m when the safety factor p is greater than or equal to a given number p_o ,

Maximize the safety factor p when the mass m is smaller than or equal to a given mass m_o .

These two problems can be stated as follows :

- Minimize $m = \rho\, L^T a$ with the constraints
$\underline{a} \leqslant a \leqslant \bar{a}$, $a^T |D^T \gamma^\alpha| \geqslant p_o \phi^T C^T \gamma^\alpha$, $\alpha = 1, \dots, \bar{\alpha}$

- Maximize the smallest (when α varies from 1 to $\bar{\alpha}$) of the quotients $a^T |D^T \gamma^\alpha| \,/\, \phi^T C^T \gamma^\alpha$, with the constraints $\underline{a} \leqslant a \leqslant \bar{a}$, $\rho\, L^T a \leqslant m_o$

Let us suppose that the admissible region of the first problem (minimization of the mass) be non empty. Then, this problem has at least a solution. According to paragraph (3.2) and theorem 2, we have the following result : the solutions of the second problem (maximization of the safety factor) are the same than those of the first one (mass minimization) when m_o is the minimum of the mass in the first problem.

5. CONCLUDING REMARKS

As it has been shown, the notion of associated solutions permits the resolution of numerous optimization problems. We shall give new results for problems of which the solutions are obtained by computors and for problems where E is an infinite dimensional space.

REFERENCES

(1) Brousse, P., Sur les solutions de problèmes associés en optimisation des structures mécaniques, Structural Control, H.H.E. Leipholz, North-Holland, IUTAM, I980.

(2) Taylor, J.E., Minimum mass bar for axial vibration at specified natural frequency, AIAA Journal, 5 (10), I967

(3) Brach, R.M., On optimal design of vibrating structures, J. Optimization Theory and Applications, 11 (6), I973.

(4) Sippel, D.L. and Warner, W.H., Minimum mass design of multi-element structures under a frequency constraint, AIAA Journal, 11 (4), I973.

(5) Cardou, A. and Warner, W.H., Minimum mass design of sandwich structures with frequency and section constraints, J. Optimization Theory and Applications, 14 (6), I974.

(6) Jouron, C., Analyse théorique et numérique de quelques problèmes d'optimisation intervenant en théorie des structures, Thèse, Université de Paris XI, I976.

(7) Vavrick, D.J. and Warner, W.H., Duality among optimal design problems for torsional vibration, J. Struct. Mech., 6 (2), I978.

(8) Brousse, P., Les méthodes d'optimisation dans la construction, Collège international des sciences de la construction, Séminaire tenu à Saint-Rémy-lès-Chevreuse (France) 6-9 nov., I973.

(9) Brousse, P., Réduction of kinematic inequality and optimization of perfectly plastic frameworks, J. Struct. Mech., 8 (2), I980.

AD-P000 073

MULTIOBJECTIVE OPTIMIZATION IN STRUCTURAL DESIGN: THE MODEL CHOICE PROBLEM

Lucien Duckstein
Department of Systems & Industrial Engineering
Department of Hydrology & Water Resources
University of Arizona
Tucson, Arizona 85721

Existing and potential applications of multi-optimization techniques to structural design are reviewed.

Two approaches are available to formulate a multiobjective structural design problem. The first approach starts with a classical design, say minimize weight subject to cost, reliability, risk and other constraints; and then some of the quantities included in the constraints, in particular cost and reliability, are used to define additional objectives. Thus, if $\underline{X}$ denotes the design or decision variable vector, $W(\underline{X})$, $K(\underline{X})$ and $R(\underline{X})$ the weight, cost and reliability objective functions, respectively, and $G(\underline{X})$ is a set of non-negativity constraints, the multiobjective problem is written as

Problem P1:

$$\min_{\underline{X}} \underline{Z}(\underline{X}) = (W(\underline{X}), K(\underline{X}), 1-R(\underline{X})) \qquad (1)$$

subject to

$$G(\underline{X}) \geq 0$$

Note that $G(\underline{X})$ usually includes constraints on the objectives themselves such as allowable maximum cost or minimum reliability.

The second approach consists in modeling the design problem directly in multiobjective form. This formulation may lead not only to problem P1, but also to the inclusion of qualitative objectives into the analysis, expressed by criteria such as aesthetics $A(\underline{X})$ and employment $M(\underline{X})$. Since qualitative (ordinal) objectives are usually defined on a discrete scale, it is convenient to consider a discrete set of alternatives as well. Accordingly, let $\underline{X} = \{\underline{X}(i): i=1,2,\ldots, J\}$ be a discrete set of alternative designs. Then the jth alternative design is evaluated by the criterion vector

$$\underline{C}(j) = (W(j), K(j), 1-R(j), A(j), M(j))$$

and the multiobjective problem now becomes:

Problem P2:

Find an alternative $\underline{X}(j)$ that constitutes a satisfactory trade off between the elements of criterion vector $\underline{C}(j)$.

For example, consider the standard steel-floor design (1) as described in (2), in which cost is to be minimized. The optimization technique used in that model is geometric programming (3), (4). Alternatives may be obtained by minimizing weight, or by probabilistic design (5), (6). Table 1 shows five alternatives obtained from the basic model of (2). Design I represents the original problem, Design IV corresponds to a minimum weight formulation, Designs II, III, V are probabilistic. These alternatives have been obtained by changing constraints into objectives, which means that Table 1 stems from Problem P1.

TABLE I Alternative Steel Floor Designs Versus Four Objectives

	DESIGN				
	I	II	III	IV	V
Cost	3850	3085	2774	4780	4162
V-Ratio	1:1	1:2	1:2	1:1	1:2
Reliability	1.00	0.80	0.95	1.00	.95
Applied Weight	1000	720	570	1000	570

Design I Standard (Deterministic)
Design II Probabilistic, R = .28
Design III Probabilistic, R = .43
Design IV Minimum U_T
Design V Minimum U_T and Probabilistic R = .43

For both problems P1 and P2, a trade-off solution, also called "satisfactum", is to be sought among the set of non-dominated solutions or Pareto-optimum set. Alternative k dominates alternative j if $\underline{C}^*(k) \geq \underline{C}(j)$; the dominance is strict if at least one element of vector $\underline{C}(k)$ is greater than the corresponding element of $\underline{C}(j)$.

Once the multiobjective problem has been formulated as either problem P1 or P2, a solution technique which matches with the type of problem and desiratas of the decision-maker is to be chosen. This model choice problem is examined in a systematic manner and illustrated by setting up a problem with a choice between eleven multiobjective techniques, respectively:

1. Compromise Programming (7), (8)
2. Goal Programming (9), (10)
3. Cooperative Game Theory (11), (12)
4. Multiattribute Utility Theory (13), (14)
5. Surrogate Worth Trade-off (15)
6. ELECTRE (16), (17), (18)
7. Q-analysis (19), (20)
8. Dynamic Compromise Programming (21), (22), (23)
9. PROTRADE (24), (25)
10. STEP Method (26)
11. Local Multiattribute Utility Functions (27).

These techniques can be categorized by means of five binary classification criteria:

a. Marginal versus non-marginal difference between alternatives; are only marginal differences between alternatives being considered? If yes, formulation P1 is applicable; if not, that is, if major differences between alternatives are possible, say an arch versus a gravity dam, then formulation P2 may be preferable. A parallel classification criterion would be design versus maintenance problem.

b. Qualitative versus quantitative criteria: are there qualitative criteria which cannot or should not

be quantified? If so, formulation P2 may be more appropriate than formulation P1.

c. Prior versus progressive articulation of preferences: at which point of the analysis is the decision-maker required to express his preference function, if at all?

d. Interactive versus non-interactive: has the technique been explicitely designed for an interactive mode of application?

e. Comparison of alternatives to a given solution point or to each other; in the former case, the solution point may be an aspiration level, corresponding to a feasible solution, or a goal point, corresponding to a non-feasible (often ideal) solution.

To these five classification criteria are added other criteria describing the characteristics of the problem (size, uncertainty, number of objectives...), the decision maker (level of understanding, time available for interaction) and the techniques themselves (robustness, partial versus complete ranking provided, ease of use...). This procedure leads to defining four categories of choice criteria (23):

1. mandatory binary criteria: for example, under formulation P1, a technique able to solve only discrete problems would be eliminated from further consideration

2. non-mandatory binary criteria: for example, comparison to an aspiration level versus comparison of a goal point

3. technique-dependent criteria: time required from decision-maker, robustness

4. application-dependent criteria: number of objectives, formulation P1 or P2.

To conclude, the advantages of a multiobjective formulation over a single objective one with a sensitivity analysis is that more alternatives can be explored and that explicit trade-offs between criteria can be made. Furthermore, given any problem involving trade-offs between quantitative or even qualitative criteria, an appropriate multiobjective technique can usually be found by following the proposed model choice procedure. The potential use of multiobjective techniques in structural design thus looks quite promising.

References

(1) Rozvany, G. I. N., Optimal Design of Flexural System, Pergamon Press, Oxford, New York, Toronto, Sydney, Paris, Frankfurt, 1976.

(2) Templeman, A. B., Structure Design for Minimum Cost Using the Method of Geometric Programming, Proc. of the Institute of Civil Engineering 46, pp. 459-472, August 1970.

(3) Duffin, R. J., E. L. Peterson and C. M. Zener, Geometric Programming, Wiley, New York, 1967.

(4) Beightler, C. S., D. T. Phillips and D. J. Widel, Foundation of Optimization, Prentice-Hall, Inc., New Jersey, 1979.

(5) Haugen, E., Probabilistic Approaches to Design, Wiley, London, New York, Sydney, 1968.

(6) Ghiocal, D. and D. Lungu, Wind, Snow and Temperature Effects on Structures Based on Probability, Abacus Press, Kent, England, 1975.

(7) Zeleny, M., Compromise Programming, in Multiple Criteria Decision Making, M. K. Starr and M. Zeleny, eds., University of South Carolina Press, Columbia, 1973.

(8) Zeleny, M., Multiple Criteria Decision Making, McGraw-Hill Book Company, New York, 1982.

(9) Lee, S., Goal Programming for Decision Analysis, Auerbach, Philadelphia, 1972.

(10) Ignizio, J., Goal Programming and Extensions, Heath, Lexington, Mass., 1976.

(11) Szidarovszky, F., I. Bogardi and L. Duckstein, Use of Cooperative Games in a Multiobjective Analysis of Mining and Environment, Proc. of the 2nd International Conference on Applied Numerical Modeling, Madrid, Sept. 11-15, 1978.

(12) Szidarovszky, F., M. Gershon and A. Bardossy, A Goal Programming Approach for Dynamic Multiobjective Decision Making, Presented at the CORS-TIMS-ORSA Joint National Meeting, Toronto, Canada, May 3-6, 1981.

(13) Keeney, R. and H. Raiffa, Decisions with Multiple Objectives: Preferences and Value Tradeoffs, Wiley, New York, 1976.

(14) Krzysztofowicz, R. and L. Duckstein, Preference Criterion for Flood Control Under Uncertainty, Water Resources Research, Vol. 15, No. 3, pp. 513-520, June 1979.

(15) Haimes, Y. Y., W. Hall and H. Freedman, Multiobjective Optimization in Water Resources Systems: The Surrogate Worth Tradeoff Method, Elsevier, Amsterdam, 1975.

(16) Benayoun, R., B. Roy and B. Sussman, ELECTRE: Une Methode pour Guider le Choix en Presence de Points de Vue Multiple, Direction Scientifique, Note de travail No. 49, SEMA, Paris, 1966.

(17) Roy, B., Problems and Methods with Multiple Objective Functions, Mathematical Programming, Vol. 1, No. 2, pp. 239-268.

(18) Gershon, M., L. Duckstein and R. McAniff, Multiobjective River Basin Planning with Qualitative Criteria, to appear, Water Resources Research, 1981.

(19) Duckstein, L. and J. Kempf, Multicriteria Q-analysis for Plan Evaluation, Preprint, presented at the 9th Meeting of the EURO Working Group on MCDM, Amsterdam, April 1979.

(20) Pfaff, R. and L. Duckstein, Ranking Alternative Plans that Manage the Santa Cruz River Basin by Using Q-analysis as a Multicriteria Decision Making Aid, Proceedings of the Joint AZ Sect., AWRA, and Hydrology Sect., AZ-Nevada Acad. of Science, May 1-2, 1981, Tucson.

(21) Opricovic, S., An Extension of Compromise Programming to the Solution of Dynamic Multicriteria Problems, 9th IFIP Conference on Optimization Techniques, Warsaw, Poland, September, 1979.

(22) Szidarovszky, F., Some Notes on Multiobjective Dynamic Programming, Working paper No. 79-1, Dept. of Systems & Industrial Engineering, University of Arizona, Tucson, 1979.

(23) Gershon, M., Model Choice in Multiobjective Decision Making in Natural Resource Systems, Unpublished Ph.D Dissertation, Dept. of Systems & Industrial Engineering, University of Arizona, Tucson, 1981.

(24) Goicoechea, A., L. Duckstein and M. Fogel, Multiobjective Programming in Watershed Management: A Study of the Charleston Watershed, Water Resources Research, 12(6), pp. 1085-1092, 1976.

(25) Goicoechea, A., D. Hansen and L. Duckstein, Introduction to Multiobjective Analysis with Engineering and Business Applications, to appear, Wiley, New York, 1981.

(26) Benayoun, R., J. de Montgolfier, J. Tergny and O. Larichev, Linear Programming with Multiple Objective Functions: STEP Method (STEM), Mathematical Programming 1(3), pp. 366-375, 1971.

(27) Oppenheimer, K. R., A Proxy Approach to Multiattribute Decision Making, Management Science 24(6), pp. 675-689, 1978.

Acknowledgement

The help of Kent Youngberg in working out the steel floor design example is greatly appreciated.

AD P000 074

A METHOD FOR NONLINEAR OPTIMUM DESIGN OF LARGE STRUCTURES, AND APPLICATIONS TO NAVAL SHIP DESIGN

by

Prof. Owen Hughes

Dept. of Naval Architecture
University of New South Wales
Sydney

SUMMARY

Over the past several years a methodology for rationally-based optimum design of large structures has been developed. Previous papers have presented some of its features and have shown how it gives substantial savings in structure cost, reduces design time and gives the designer far more power and flexibility, allowing, for example, a much wider investigation of design alternatives. This paper presents the method's dual level formulation of the optimization problem, which is a principal source of its versatility and efficiency. It also demonstrates its use for the structural design of naval ships and presents the results of a realistic design study of a destroyer, showing how the method achieves substantial savings in structural weight and vertical center of gravity compared to current practice designs, while also satisfying constraints on hull girder deflection and fatigue damage.

1. Goals of Structural Optimization

In the field of structural optimization the two principal goals, at least in relation to large complex structures, may be summarized as follows:

(1) the development of an optimization algorithm which can achieve a rapid and efficient solution to the type of problem which a large structure poses: a large-scale, nonlinear, highly constrained problem in which the objective may be any designer-specified nonlinear function of the design variables.

(2) the combination and synthesis of this algorithm with the other basic aspects of structural design which are required for a fully *rationally-based design method*.

A rationally-based design method is one which is based on accurate and efficient methods of structural response analysis, limit state analysis, and optimization, which accounts for uncertainties and reliability, and which achieves an optimum structure on the basis of a designer-selected measure of merit. Thus in addition to the optimization algorithm, a rationally-based design method must include the following:

- an accurate and comprehensive *structural response analysis* to determine all of the load effects (stresses, deflections, etc.) in all of the members. For large complex structures the only analysis method capable of this is the finite element method.
- an accurate and comprehensive *limit state analysis*; i.e. an explicit investigation of all possible modes and levels of failure, in order to determine the limit values of the load effects, $Q_L(\mathbf{X})$. These are usually nonlinear functions of the design variables, $\mathbf{X}$.
- *reliability-based design criteria* for establishing the required margin between each value of Q and Q_L, so as to account for the various uncertainties (in loads, load effects, and limit values of load effects, the latter being due to variations in material quality, workmanship, fabrication, etc.) and also account for the degree of seriousness of all relevant limit states.
- *ability to accommodate any special constraints* which the designer may wish to specify, such as limits on deflection, natural frequency, sizes or proportions of members, need for uniform member sizes, etc.

PRECEDING PAGE

2. Principal Requirements

The creation of such a comprehensive design method requires substantial developments in many areas, but there are two items which are particularly vital:

- a *structure-oriented* optimization method, i.e. a method which meets the particular requirements of structural optimization stated in paragraph (1), and which also, wherever possible, takes advantage of any special features of structural optimization which may not be present for other types of optimization.
- a *design-oriented* finite element method, which has sufficient speed and efficiency as to permit repeated structural analysis, as is required for optimization.

Structure-Oriented Optimization Method

During the past two or three decades many optimization methods have been developed. The majority may be grouped into two categories:

- sophisticated general purpose methods, such as mathematical programming methods and various algorithms for unconstrained minimization;
- rapid special purpose methods, such as fully stressed design and the optimality criteria method.

Most of these methods perform satisfactorily for small or medium size problems (up to say 30 design variables). However, for large and complex structures such as ships both types of methods have been found to have significant limitations:

- general purpose methods involve far too much computation;
- special purpose methods are too restricted; they cannot handle constraints which are highly nonlinear and/or involve many design variables, and they cannot handle an arbitrary (user-specified) nonlinear objective.

Design-Oriented Finite Element Method

The finite element analysis must deal with a large enough portion of the structure to accurately portray all interactions and eliminate doubts about boundary conditions. For a structure with complicated geometry and three-dimensional loading it is necessary to model and analyze a very large portion. For example, for a ship it is generally necessary for the structural analysis to extend over several cargo holds (or compartments of a naval vessel). However, since structural optimization requires that the analysis be repeated many times, the analysis method must be extremely rapid and efficient. The general purpose finite element programs presently available are far too slow for this purpose.

3. A Comprehensive Optimum Design Method For Large Structures

As the result of an eight-year research project, both of the required methods have now been developed. Firstly, a new optimization method has been developed which is capable of solving problems involving a large number of constraints of various types (linear and nonlinear, equality and inequality) and in which the objective may be any user-specified nonlinear function of the design variables. Most importantly the algorithm is very rapid and cost-effective; it involves much less computation than other nonlinear methods. The algorithm is a new form of sequential linear programming and is known as SLIP2. It is not limited to structures; it can be used for any optimization application, and a stand-alone computer program has been developed for this purpose. The theory, mathematical details and complete documentation of SLIP2 are given in reference [1].

Secondly, a special "design-oriented" finite element analysis program has been developed which has been shown [2] to be approximately 15 to 20 times faster than a standard general purpose program, for comparable levels of accuracy. This is achieved mainly by the use of large specially developed elements, each of which corresponds to a principal structural member (stiffened panel, deep girder, etc.) instead of smaller general purpose elements. In this way the level of detail of the analysis matches the level which is required for the optimization. There is no more computation than is absolutely required. Also the one-to-one correspondence between the analysis variables and the design variables simplifies the interfaces between the response analysis, the limit state analysis and the optimization.

On the basis of the SLIP2 optimization method and the design-oriented finite element method, a complete rationally-based methodology has been developed for the preliminary structural design of stiffened plate structures such as ships, box girder bridges, freight cars , container structures, etc. The computer program which implements this method is known as SHIPOPT. Besides the two main features just described the program also contains:

(1) A comprehensive set of subroutines for the accurate estimation of the various modes of ultimate strength and other limit values, nearly all of which are nonlinear functions of the design variables. For the current design (as the optimization proceeds) the method calculates the lowest margin of safety for each limit state, and the location and loadcase where each lowest value occurs; this allows the method to be used for the comprehensive evaluation of a given design, as well as for producing an optimum design.

(2) A complete set of partial safety factors which account for the various uncertainties (in loads, load effects, and limit values of load effects, the latter being due to variations in material quality, workmanship, fabrication, etc.) and which also account for the degree of seriousness of all relevant limit states. These factors are chosen according to the target level of reliability. The method can accommodate multiple loadcases, each with its own set of partial safety factors, in order to allow for any special or unusual conditions or modes of operation.

(3) The automated formulation of the complete set of mathematical constraints arising from the various limit states; these constraints, which incorporate the various partial safety factors, ensure that the target level of reliability is reached. The program can also accommodate any number of user-supplied constraints which represent other design requirements, as described earlier.

The basic theory and methodology of SHIPOPT is presented in reference [3], and the performance of the program is demonstrated in reference [2] in which it is used for the design of a 100,000 ton segregated ballast tanker and a 140,000 ton bulk carrier. These are very large structural optimization problems; for example, the segregated ballast tanker involved 168 design variables, 1080 constraints of which approximately half were nonlinear, and a nonlinear objective function (least cost). SHIPOPT achieved the least cost design in five minutes of computer time on an IBM 370/158 (approximately $60 at commercial rates). In this test problem all of the design particulars (ship dimensions, general arrangements, loading conditions, etc.) were the same as for an actual current practice design. The design produced by SHIPOPT had a 6% lower structural cost than the current practice design, which for a vessel of this size represents a cost savings of over $1 million. Also SHIPOPT gives a dramatic savings in design time, reducing it to manhours instead of manweeks, and it gives the designer far more power and flexibility, allowing, for example, a much wider investigation of design alternatives.

4. Dual Level Optimization of Large Structures

In structural optimization the objective function usually depends on all of the design variables, and some of the constraints may also depend on a large number of design variables because of interactions among the various members, either in the structural response (e.g. a load effect might be a function of many design variables) or in the limit states (a limit value might be a function of many design variables). However, for a structure having over 100 design variables and over 500 nonlinear constraints, together with a nonlinear objective function, it is simply not possible to express these constraints as functions of all of the design variables because the problem size and the computation required would be prohibitive, even for a very rapid and efficient optimization algorithm. Therefore, in addition to an efficient optimization algorithm it is also necessary to have a method for formulating the optimization problem which takes account of the interactions, both in the response and in the limit states, and yet avoids excessive computation. This may be achieved by taking advantage of the fact that for most large structures there are three distinct levels of response and also of limit states: overall, substructure and member. An overall response or limit state involves the structure as a whole, and a substructure response or limit state involves a group of members. For example, at the overall level a ship structure is essentially a box beam or girder (the *hull girder*) and the predominant structural response is bending of the hull girder in the vertical plane. This hull girder bending has two components: a static (or "stillwater") component caused by the unequal longitudinal distribution of weight and buoyancy along the ship's length, and a dynamic component caused by the waves which the ship encounters. The resulting load effects at the overall level are the hull girder bending stresses (both stillwater, σ_s, and wave-induced, σ_w) and hull girder deflection.

An overall response usually consists of the interactive response of a group of substructures, and an overall limit state is usually some maximum permissible value of this collective response. Since the design variables act in a collective manner, both the response and the limit state may be expressed in terms of *substructure variables* which are combinations of the individual design variables and which account for their collective influence. For example, in a ship the hull girder deflection depends on the moment of inertia of the ship's cross section, I, and the maximum hull girder stresses (which occur in the deck and in the bottom) depend on the section modulus, $Z = I/y$. Both I and Z can be expressed in terms of the cross sectional area of the substructures which comprise the ship's cross section. Hence the constraints relating to hull girder deflection or stresses can be expressed in terms of these areas, which are few in number, rather than as a function of the many individual design variables.

The existence of these two distinct levels - overall and substructure - in the structural response and in the limit states makes it possible to divide the optimization problem into several smaller problems, one at the overall level and one for each of the substructures. The first problem contains all of the overall constraints, and the design variables are whichever substructure variables are appropriate for those constraints. Each substructure problem contains all of the constraints relating to that substructure, either as a whole or to its component members, plus a set of constraints which require that the values of the substructure variables for that substructure, which are known functions of the individual design variables, must not decrease below the values which were determined in the first problem. The design variables are optimized and the corresponding values of the substructure variables are calculated. When all of the substructures have been optimized the first problem is repeated, with the additional constraints that the substructure variables cannot decrease below the values corresponding to the optimum solution of the substructure problems. Then each of the substructures is again optimized, with the new values of the substructure variables replacing the old values. This process is repeated until convergence.

This dual level formulation is utilized in SHIPOPT and recent tests on realistic full scale ship designs have shown it to be very successful. The manner of implementation and the test results have not been previously published, and that is the main purpose of this paper. The structure chosen for the test problem is a naval destroyer because naval vessels involve some nonlinear constraints at the overall level which do not occur with commercial vessels. Also, in naval design the objective is maximum mission capability, which is a more complex objective than least cost. The remainder of the paper consists of three sections and an appendix:

- an explanation of the special aspects of naval structural design.
- a summary of the benefits of a rationally-based method, and the results of a SHIPOPT design of a destroyer, for which the design specifications were the same as for an actual, current practice design.
- in the appendix, a description of how the optimization strategy is implemented in SHIPOPT.

5. Special Features of Naval Structural Design

Minimization of Weight and Vertical Centroid

In the optimum design of commercial ships the objective is profitability, which is influenced by structure mainly through initial cost. Hence for these ships the appropriate objective is least cost. For naval ships the objective is to obtain the maximum possible mission capability over the life of the ship, subject to budget limitations. Thus cost is here a constraint instead of an objective. The two aspects of a structural design which have the greatest influence on mission capability are the weight of the structure and its vertical center of gravity (VCG):

- weight savings permits either a higher speed or more mission-related equipment (weapons, sensors, etc.) or increased range and endurance, or some combination of these.
- a low VCG of the hull structure is of great benefit since most of the important weapons and sensor systems involve large topside weight. In fact, the provision of adequate stability is often the limiting factor on the number or size of such systems, particularly as a vessel gets older and it becomes necessary to fit more modern systems.

These objectives tend to produce a structure which is more intricate and involves less material. Hence for naval vessels the structural cost (that is, the cost which is attributable to structure and is a function of the structural design variables) is mainly fabrication cost; the material cost is much smaller and, for a given material, it has little influence in determining final optimum design*. Thus naval design involves a tradeoff between weight, VCG and fabrication cost. The designer seeks to determine the number, arrangement and size of structural members which will give the lowest possible weight and VCG, subject to cost limitations and to a variety of other constraints requiring satisfactory strength, reliability, endurance and functioning of the vessel. The constraint on cost is somewhat different from the other constraints. Rather than being an absolute limit it is a somewhat elastic barrier in which the rigidity of the resistance to further increase in cost depends on the cost/benefit ratio - i.e. how much benefit the increase in cost will yield. Nevertheless, besides the cost/benefit type of constraint, there is often an absolute upper limit on total cost.

The situation is illustrated in Figure 1, in which the coordinates are the three main aspects: weight, VCG and fabrication cost. The curved surface represents the combined and net effect of all of the constraints. It is actually an irregular surface - it is the outer envelope of all of the many individual constraints, each of which is itself a surface consisting of the lowest possible combinations of weight, VCG and cost which just satisfy the requirements of that particular constraint. In different regions of the design space different constraints are the outermost or "active" constraints. Any point in the design space which does not penetrate below this surface is a feasible design, and any point actually on the surface is an optimum design. The surface indicates what sort of tradeoffs are available to the designer.

For example, by raising the height of the strength deck or increasing its thickness the designer may achieve a lower overall weight at no extra fabrication cost, but incur a higher VCG. Alternatively if he is willing to pay more for a more sophisticated and intricate structural arrangement (more stiffeners and thinner plating) he can achieve a lower weight, or a lower VCG, or both . The choice of which tradeoff to make and the selection of the final optimum combination must be left to the designer because this depends entirely on the particular mission requirements, cost limitations and other design requirements and priorities.

The objective function U is a combination of weight W and VCG in the form

$$U = \frac{W}{W_o} + \lambda \frac{VCG}{VCG_o} \qquad (1)$$

where W_o and VCG_o are the weight and VCG of a previous design of approximately the same size, in which the VCG is at a satisfactory height. The value of the parameter λ is then determined by making a few trial optimizations, starting with $\lambda = 1$ and adjusting λ until the resulting optimal design has a satisfactory VCG. If the previous design was smaller or if it is desired to achieve a lower VCG λ should be increased.

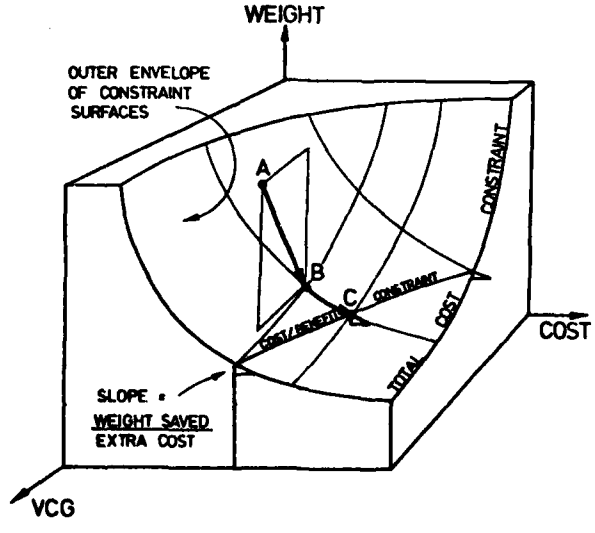


FIGURE 1 DESIGN SPACE

* The possibility of using a very expensive material such as titanium would be investigated by making a separate optimum design using that material and then judging whether the weight/VCG savings was worth the extra cost.

Special Overall Structural Constraints

Besides the usual constraints guarding against structural failure, naval vessels must also satisfy two structural requirements at the overall level which do not arise for commercial vessels. Firstly there is a limit on the amount of hull girder deflection because the weapons tracking and guidance systems impose a limit on the relative angular deflection θ between various points along the ship length; for example, from the inertial navigation set to the aft missile launcher, as shown in Figure 2. Because of their slender shape and their lightweight construction (which is accentuated by least weight optimization) naval vessels tend to be relatively flexible and so the constraint on θ can be of fundamental importance in the design.

Secondly, the slender proportions and lightweight construction of these ships cause the hull girder bending stress to be correspondingly larger. The wave-induced portion, σ_w, is cyclic, and in a ship's lifetime it undergoes approximately 10^8 cycles. Therefore a larger value of σ_w increases the possibility of a fatigue failure in the deck or bottom, where σ_w is maximum. The use of high yield steel does not alleviate the problem because the fatigue characteristics of steel are relatively unaffected by the value of yield stress. Therefore in naval vessels it is necessary to impose a strict upper limit on σ_w. Although in principle this same limit applies to commercial vessels, they are usually much less slender and also, since they are designed for least cost rather than least weight, the optimum design is much heavier, involving thicker plating and fewer stiffeners. This gives a much larger hull girder section modulus Z, and a corresponding decrease in σ_w, *usually bringing it well below the fatigue limit.*

In these two constraints the quantities involved, θ and σ_w, are a property of the ship as a whole, in its hull girder level of response; they are not related to any particular substructure or member. Therefore, unlike the constraints dealing with structural failure of substructures or of members, these constraints cannot be dealt with at the substructure level. They must be dealt with at the overall level and must be expressed in such a way that their dependency on the design variables throughout the structure is accurately accounted for. This can be achieved without generating an excessively large problem by using substructure variables and the dual level formulation outlined earlier. The particular manner in which this is done in SHIPOPT is described in the Appendix.

6. Sample Benefits of Rationally-Based Design of Naval Hulls

As shown above, naval structural design involves several complex and difficult aspects and hence a rationally-based design method can be of great benefit. Current designs are the result of a long evolutionary process of gradual improvement and have now reached the approximate limit of what can be achieved by current practice methods. These methods involve the following features:

- empirical design codes based on accumulated experience
- two-dimensional structural analysis; no finite element analysis as part of preliminary design
- approximate formulas for limit values; no nonlinear computer-based limit state analysis
- very limited optimization - least weight only, few design variables.

Further improvements in naval ship structures can only be achieved by adopting a more powerful and rationally-based design method. This section presents a brief outline and some sample values of the improvements in weight and VCG which are possible. The numerical results given here are from a small design study which was performed with SHIPOPT in order to illustrate and quantify some of the benefits which rationally-based design can provide for naval vessels. In order to make the study as realistic as possible it was based on the same design specifications (ship dimensions, general arrangement, loading conditions, etc.) as for an actual, current practice destroyer design, and the quoted savings in weight and VCG are in comparison to this design. In order to guarantee a fair comparison the precise structural dimensions of the actual design were used as the starting values in the SHIPOPT program and hence all quantities, including weight and VCG, were calculated in the same manner for both designs. Also, whenever an approximation or assumption was required it was made in such a way as to favor the current practice design.

The percentage savings of the rationally-based design method and its other performance statistics are quoted herein because it is these values which are required in order to assess the performance of the method. The detailed specifications of the actual design are not required for this purpose, and although

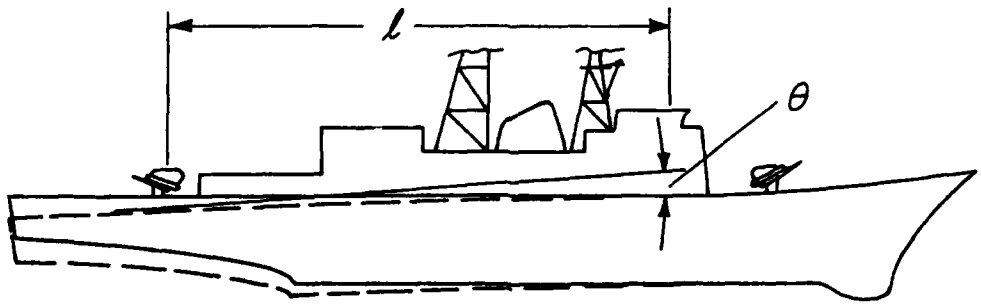


FIG. 2 RELATIVE ANGULAR DEFLECTION OF HULL

they are not classified information they are not given here because of normal design confidentiality. It is expected that a more complete report will be published in future, after further studies have been completed and decisions have been made regarding the information to be published.

For purposes of explanation the benefits of using a rationally-based method are presented as three separate stages, but they can be obtained in any order or combination. Firstly there is a savings in weight and VCG simply because of the greater accuracy of the rationally-based method. In current practice design both the load effects and the limit values of the load effects are only known approximately, and therefore so also are the margins between them. To help prevent the actual margin from becoming less than the required margin (which allows for genuine and unavoidable uncertainties such as wave loads) the design margin is made larger than is actually required. But in rationally-based design the actual margin is known and so it can be set to the required value rather than an inflated value. The result is illustrated in Figure 3, which is an enlargement of Figure 1. Point A represents a current practice design. The calculation and use of actual margins gives an immediate savings in structural weight, and the improved (in fact, optimal) distribution of material gives a reduction in VCG (point B in the figure). Both savings can be achieved with no additional fabrication cost. In the destroyer design study the savings were 8% in weight and 4% in VCG. As indicated earlier the proportion between the two can be altered to any desired figure by modifying the value of the parameter λ in the objective function.

But these savings are just the start; the designer can also investigate the question of cost. He can ease some or all of the cost constraints, which would then allow more intricate and efficient (but costlier) structural arrangements and proportions (point C in Figure 3). The most common example is an increase in the number of stiffeners and a decrease in plate thickness. In the SHIPOPT program the new optimum arrangements and proportions are calculated immediately, as soon as the designer supplies the modified cost constraints (or any other modifications). Still further savings in weight and VCG can be obtained because with such a versatile, rapid and inexpensive design program the designer can examine many other design alternatives and perform parametric studies. For example he can investigate the use of an improved steel or aluminium alloy, with a higher yield stress or an improved fatigue resistance. These changes would have the effect of moving the corresponding constraint surfaces (in Figure 1) closer to the origin, and if one of them had been an active (outermost) constraint for the current optimum design, then the optimal design surface in that region of the design space also moves closer to the origin, and an immediate savings in weight and/or VCG is gained. In present day naval vessels the fatigue constraint *is* one of the active constraints and so knowing the true margin permits an immediate savings, and using a steel with a higher fatigue limit would permit further savings. In the destroyer design study these savings have not yet been investigated, and the 8% and 4% savings do not include these further potential savings.

In the design study the current practice destroyer design was found to be close to the limit on hull girder deflection and in the optimized design this was one of the active constraints. Nevertheless it is still possible to obtain further weight savings by taking account of the contribution of the superstructure. In current practice design this contribution is ignored because it cannot be calculated with sufficient accuracy by the prismatic beam theory on which the current design method is based. Even a modified beam theory which attempts to account for the different radius of (bending) curvature of the superstructure is not sufficiently accurate. The problem is essentially three-dimensional, and only a method which includes a three-dimensional analysis can deal with it adequately. The effect of the superstructure and the savings which can be achieved by allowing for it will be investigated in a further design study.

ACKNOWLEDGEMENTS

The author is grateful to Mr. Andrew Cawsey and Mr. John Donovan for preparing the SHIPOPT data and other assistance in the design study, and to Mrs. Loyce Dalloway for typing the paper. Thanks are also due to Dr. John Gergin, Director of the UNSW Computing Services Unit, and to his staff.

REFERENCES

1. Mistree, F., Hughes, O.F. and Phuoc, H.B., "An Optimization Method for the Design of Large, Highly Constrained Complex Systems", *Engineering Optimization*, Vol. 5, No. 3, August 1981.

2. Liu, D., Hughes, O.F. and Mahowald, J.E., "Applications of a Computer-Aided, Optimal Preliminary Ship Structural Design Method", *Trans. SNAME*, 1981 (Paper to be presented at the SNAME Annual Meeting, November 1981).

3. Hughes, O.F., Mistree, F. and Žanić, V., "A Practical Method for the Rational Design of Ship Structures", *J. Ship Research*. Vol. 24, No. 2, June 1980, pp 101-113.

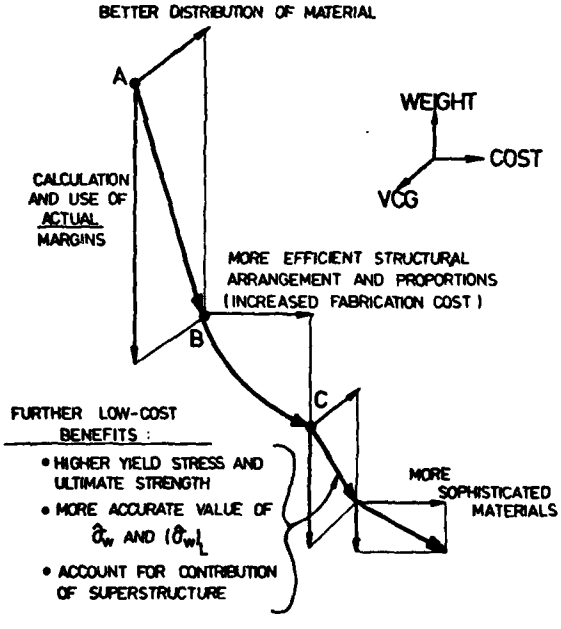


FIG. 3 BENEFITS OF RATIONALLY - BASED DESIGN

APPENDIX

Implementation of Dual Level Optimization in SHIPOPT

In SHIPOPT the principal type of substructure is a "strake", that is, a row of panels and transverse frame segments and an adjacent longitudinal girder, if there is one, extending in the longitudinal direction, as shown in Figure 4. This type of substructure is large enough to encompass nearly all types of structural failure and other types of limit state; in other words, most limit states do not involve a larger extent of structure than a strake, and therefore the majority of the constraints can be dealt with at the strake level. Also, this type of substructure contains many regular and identical members. A group of identical members should always be optimized as a group, and for each limit state the constraint is formulated for the member which has the lowest margin. The total number of constraints per substructure is then the sum of the number of constraints for each different member in that substructure. This approach is not limited to strakes; it can be applied to any substructure such as a transverse bulkhead.

The limit states which cannot be dealt with at the strake level are those relating to structural failure of the hull girder and any other limits on a hull girder load effect, such as the limit on relative angular deflection, θ. Structural failure of the hull girder is defined as collapse of either of its "flanges"; i.e. either the strength deck or the bottom. In most cases each flange consists of only two or three strakes, all of which have approximately the same ultimate strength. Thus if any one of them collapsed the resulting overload on the others would usually cause them to collapse also. Hence the collapse of a flange strake should be classified as hull girder collapse. There are also multi-strake modes of hull girder collapse caused by the formation of a collapse mechanism in the transverse framing of the flange strakes. It will be shown below that by making a slightly conservative approximation it is possible to deal with this type of hull girder collapse at the strake level.

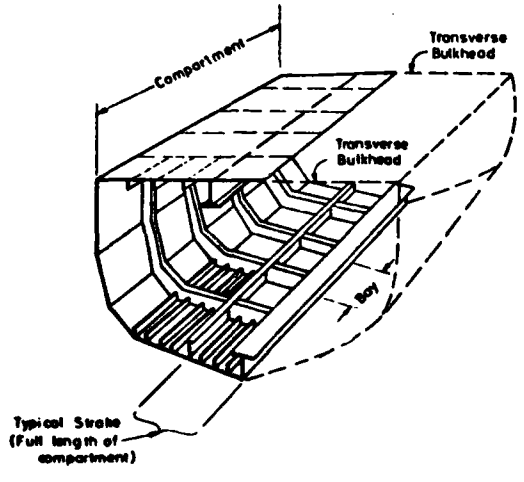


FIG. 4 DEFINITION OF STRAKE

The hull girder collapse constraints can be classified according to the type of load effect which is involved: the total hull girder bending stress, σ_{hg}; the wave-induced stress, σ_w; and the transverse loads due to external fluid pressure and internal loads: cargo, fuel, stores, ship steelweight, etc. The following four subsections give a brief summary of these three types of collapse constraints, and the other hull girder constraint arising from the limit on hull girder deflection.

(1) Collapse due to total hull girder stress

The total hull girder stress σ_{hg} can cause collapse of a strake either in tension, by tensile yield or direct fracture, or in compression, either by compressive yield or instability (and usually by a combination of these two). In the first three cases the limit value $(\sigma_{hg})_L$ is a material property; if instability is involved the limit value is also a function of the individual design variables of that strake. For each type of instability the dependency can be simplified and expressed in terms of a few *substructure variables* (or *strake variables*, in this case). As explained in Section 4, for constraints relating to hull girder stress σ_{hg} the appropriate strake variables are the cross sectional areas of the flange strakes; for convenience these will be denoted as a vector, $\mathbf{A}_s$, and the symbol $\sigma_{hg}(\mathbf{A}_s)$ indicates the dependency of σ_{hg} on these areas. Using these symbols the constraints against collapse caused by σ_{hg} are of the form

$$\sigma_{hg}(\mathbf{A}_s) \leq (\sigma_{hg})_L \qquad (2)$$

where in each case $(\sigma_{hg})_L$ is the limit value for the particular type of collapse.

If the superstructure's contribution is being disregarded then the dependency of σ_{hg} on $\mathbf{A}_s$ can be expressed in terms of the hull girder section modulus, $Z(\mathbf{A}_s)$. The expression is

$$\sigma_{hg} = \hat{M}/Z(\mathbf{A}_s) \qquad (3)$$

in which $\hat{M}$ is the characteristic or design value of hull girder bending moment, which allows for the statistical distribution of bending moment over a ship's lifetime. The general form of the constraints becomes

$$Z(\mathbf{A}_s) \geq \hat{M}/(\sigma_{hg})_L \qquad (4)$$

If the superstructure is being counted the value of σ_{hg} is obtained from the finite element analysis of the hull girder, with $\hat{M}$ as the applied bending moment. The dependency of σ_{hg} on $\mathbf{A}_s$ is obtained numerically, by a systematic perturbation of each value of $\mathbf{A}_s$. The form of each constraint is as given in eq. (2).

(2) Cumulative fatigue failure due to wave-induced stress

Over its lifetime a ship encounters a wide range of values of wave-induced bending moment, M_w, each of which occurs for a different number of cycles. This distribution can be characterized by a characteristic value, $\hat{M}_w$, such as the value of M_w corresponding to $N = 10^8$ cycles. In the fatigue constraint the value of wave-induced bending stress is $\hat{\sigma}_w$, the value resulting from $\hat{M}_w$. If the superstructure is ignored then $\hat{\sigma}_w$ is given by

$$\hat{\sigma}_w = \hat{M}_w / Z(A_s) \tag{5}$$

and the fatigue constraint is of the form

$$Z(A_s) \geq \hat{M}_w / (\hat{\sigma}_w)_L \tag{6}$$

in which $(\hat{\sigma}_w)_L$ is the limit value of $\hat{\sigma}_w$ for a particular steel. This value is established by fatigue tests. Since fatigue failure is the result of accumulated fatigue damage the tests must take into account the complete range of σ_w.

If the superstructure is being taken into account the value of $\hat{\sigma}_w$ is obtained from the finite element analysis of the hull girder, with $\hat{M}_w$ as the applied bending moment. The dependency of $\hat{\sigma}_w$ on A_s is again obtained numerically, as for σ_{hg}. The form of the constraint is then

$$\hat{\sigma}_w(A_s) \leq (\hat{\sigma}_w)_L \tag{7}$$

(3) Collapse due to transverse loads

Collapse of the hull girder can also occur due to the formation of a mechanism in the transverse framing which supports the flange strakes. The mechanism may be caused by plastic hinges or by flexural-torsional buckling of the framing. In this type of collapse the principal load effect is the bending moment in the transverse frames, and the strake variables are the plastic section modulus Z_{pf} and moment of inertia I_f of each of these frames. A mechanism due to plastic hinges may involve more than one strake but flexural-torsional buckling does not, and this type of mechanism can be triggered by the formation of just one or two plastic hinges. Therefore, in order to simplify matters and to be slightly conservative, collapse of the framing is defined as either flexural-torsional buckling within any strake or the formation of *one* plastic hinge in any strake. The occurrence of either of these two failures within a flange strake is regarded as hull girder collapse. This approach gives rise to two constraints for each flange strake, of the form

$$Z_{pf} \geq M_f / \sigma_y \tag{8a}$$

$$M_{cr}(I_f) \geq M_f \tag{8b}$$

in which M_f is the maximum frame bending moment in that strake, $M_{cr}(I_f)$ is the critical bending moment for flexural-torsional buckling as a function of I_f, and σ_y is the yield stress. This approach has the enormous advantage that each pair of constraints relates only to its own strake and therefore all of the constraints corresponding to eq. (8) can be dealt with at the strake level; they do not need to be included in the overall, or hull girder, optimization problem.

(4) Limit on hull girder relative angular deflection

If the contribution of the superstructure is not counted the relative angular deflection between two points along the hull girder separated by a distance ℓ is given to a good approximation by

$$\theta = \frac{1}{EI(A_s)} \int_0^{\ell} M(x)dx = \frac{C}{EI(A_s)} \tag{9}$$

in which $I(A_s)$ is the average value of hull girder moment of inertia, which is a function of the strake cross sectional areas, A_s. Since C/E is a constant (say C_1) the constraint that θ not exceed the limit value θ_L may be written as

$$I(A_s) \geq \frac{C_1}{\theta_L} \tag{10}$$

If the superstructure is counted it is necessary to use a transformed hull girder cross section with moment of inertia I_{tr} and a further correction, obtained by means of a finite element analysis of the combined hull and superstructure, which allows for the non-prismatic nature of this new hull girder. As with the other constraints this is merely an added complication; it does not create any obstacle to the formulation and solution of the overall optimization problem. Hence from this point on we shall ignore the superstructure. It was also ignored in the design study described in Section 6 because current practice design does not account for it, and the purpose of the study was to compare a rationally-based optimum design with a current practice design, using the same design specifications.

Formulation of the Overall Optimization Problem

The three sets of hull girder constraints are given by eqs. (4), (6) and (10). Eqs. (4) and (6) both apply to section modulus $Z(A_s)$ and therefore it is only necessary to use whichever of them has the larger right hand side, which is the required value of section modulus, Z_R. Likewise in eq. (10) the right hand side is the required value of I, denoted as I_R. The objective function is that of eq. (1) expressed in terms of strake areas A_s. The overall optimization problem is then:

> Determine the values of A_s which give the minimum value of $U(A_s)$ subject to the two nonlinear constraints
>
> $$Z(A_s) \geq Z_R$$
>
> $$I(A_s) \geq I_R$$
>
> and the constraints on each strake area A_{si} arising from the individual strake optimization problem for strake i
>
> $$A_{si} \geq (A_{si})_R \qquad i = 1, \ldots n$$
>
> where n is the number of hull girder flange strakes and $(A_{si})_R$ is the strake area resulting from the optimum design of strake i, as obtained in the previous set of strake optimization problems.

In a typical ship structure there are seldom more than eight or ten flange strakes, and so the above problem is solved by SLIP2 in negligible computer time (approximately 1 second on a CDC Cyber 171).

AD-P000 075

OPTIMUM CONFIGURATION OF TRANSMISSION LINE TOWERS IN DYNAMIC RESPONSE REGIME

Dr. M.P. Kapoor
Professor
Department of Civil Engineering
Indian Institute of Technology
Kanpur-208016, INDIA.

Dr. K. Kumarasamy
Assistant Engineer
Ocean Engineering Division
Engineers India Limited
New Delhi-110001, INDIA.

Summary

This paper addresses itself to the automated optimum design of transmission line towers, modelled as a space truss in dynamic response regime. The basic thrust of the investigation is to achieve the optimum configuration of the tower. The objective is to minimize the total weight of the tower including the weight of the secondary members. The design variables chosen in the present work are the base width and the panel heights in the body of the tower. The weight minimization is carried out subject to the limitations on dynamic stresses in the individual members and the requirements of overall compatibility of the tower configuration. The optimum design problem is formulated as an unconstrained minimization problem. All the constraints are handled implicitly. This is necessitated since the objective function is not an explicit function of design variables. Powell's method has been used which turns out to be the obvious choice for seeking the solution of such unconstrained minimization problems. Dynamic analysis of the transmission line tower is carried out through modal superposition technique. Subspace iteration method is used for the extraction of eigenpairs. Optimization study is carried out for 15m, 20m and 25m body heights of transmission line towers under time dependent wind loading. The sensitivity of optimum design to the damping coefficient is also studied in the present work. Some of the salient conclusions of the present study are : (1) rigorous dynamic analysis under wind load should be carried out to obtain more realistic response prediction of transmission line tower as against the conventional practice of considering equivalent static wind load; (2) the optimum configuration of the tower is more sensitive to dynamic loads as compared to the one obtained by merely considering only the static behaviour; (3) the optimum configuration of the tower corresponds to bottom-most panel to be 3.5m high, top-most panel to be 2.0 m high, intermediate panels interpolated in between and the base width varying with the height of the tower body; and (4) the optimum configuration of the tower is insensitive to the admissible changes in the damping coefficient.

Introduction

The enormous increase in the amount of electrical energy to be transmitted coupled with higher and higher voltage of transmission has focussed attention to the optimum design of transmission line towers. Sixties witnessed enough success in optimum structural design. Till early seventies these studies were, by and large, restricted to a fixed geometry of structure. Of late attention is rightly directed towards configuration optimization (1-5). However, the studies on configuration optimization, so far, have been restricted to static behaviour of structures. A detailed study on optimum configuration of transmission line towers, under static behaviour, i.e., using static loading patterns prescribed by design standards, has been carried out and reported by the authors (6). The present study is directed to achieve the optimum configuration of the tower in the dynamic response regime. The tower is modelled as a space truss. The dynamic response is assumed to be linear with or without damping. A time dependent forcing function similar to the one used in Ref. (7) has been considered to model the wind load in the present work. The design variables chosen are the base width and the panel heights in the body of the tower.

Formulation of Optimum Design Problem

The general structural optimization problem can be stated as follows :

$$\text{Minimize } f(\vec{d}) \tag{1}$$

$$\text{Subject to } g_j(\vec{d}) \lesseqgtr b_j,\ j=1,2,\ \ldots,m \tag{2}$$

$$\text{and } d_i^{(l)} \leq d_i \leq d_i^{(u)},\ i=1,2,\ \ldots,n \tag{3}$$

where

- f represents the objective function
- $\vec{d}$ is the vector of design variables
- g_j is the constraint function
- b_j is the known value corresponding to the j-th constraint

and

$d_i^{(l)}$ and $d_i^{(u)}$ are respectively the lower and upper bounds on the design variables.

Design Variables

The geometry of the basket portion of the transmission tower is specified from electrical considerations. Hence this portion of the tower geometry is of no consequence to the present work. Therefore, structurally it is only the geometry below the bottom cross arm, i.e., body of the tower, which can be optimized. The configuration of the tower body is defined from the ensions of the

base, number of panels and the height of each panel. The base of the tower, in general, is square in plan. This, therefore, introduces only one design variable, viz. the width of the base. The number of panels being integers, its incorporation as a design variable leads to a mixed integer programming problem; the solution to which is not easy to obtain. Therefore, it has been dropped from the set of design variables in the present work. However, a parametric study has been carried out to study the influence of number of panels on the optimum configuration of the tower (6). Thus the design variables chosen in the present work are the base width of the tower and the panel heights of the tower body, Fig. 1, to generate an optimum configuration.

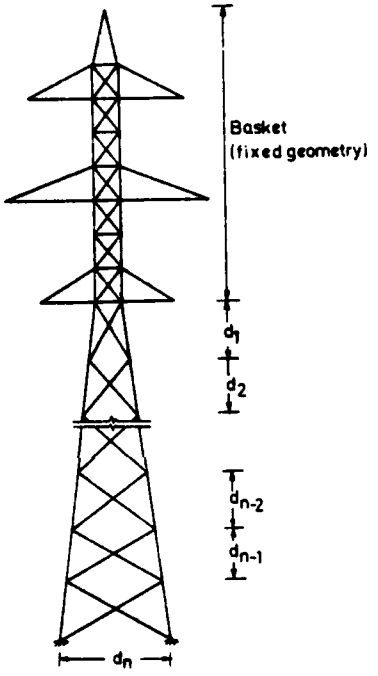


Fig.1 Design variables

Available angle sections are used for the members of the tower. While designing the members, section having an area close to the required one is picked up which satisfies all the stipulations of the design standard (8). Therefore, the cross sectional variables do not appear explicity in the formulation of the optimum design of tower.

Objective Function

The goal of the present work is to study the effect of panel heights and the base width on the minimum weight of the tower. This is justified because towers are made-up of only one material and their fabrication and erection cost goes on tonnage basis. Hence, the objective function, f, representing the total weight of tower, is minimized in the present work. It can be stated as :

$$f = \rho \sum_i A_i \, l_i \, n_i \quad , \quad i = 1 \text{ to } n_g \qquad (4)$$

where

ρ = unit weight of material

l_i = length of members in group i, (all leg members/diagonals in a panel symmetrically located about the tower axis form a group)

A_i = area of members in group i

n_i = number of members in group i

and

n_g = number of groups which is the sum of the groups of primary as well as secondary members.

It is to be noted that l_i and A_i are implicit functions of the design variables, chosen in the present work.

Constraints

The minimum weight design of the tower is to be constrained in a manner such that at no point on the structure the displacement exceeds a specified upper bound, as well as the stress remains below the permissible value in the time domain. Moreover, the natural frequencies of the structure should be away from the resonant frequency (9). Furthermore, the panel heights should add up to the specified body height of the tower. Needless to mention that the base width and panel heights should be positive values. However, no upper bound limit on the design variables is imposed.

While considering the linear dynamic analysis of the tower, consideration of displacement constraint together with stress constraint is redundant unless stability considerations warrant it. Study on the stability of optimum configuration of the tower(6) has obviated the need. The dynamic stress constraint can be easily accounted for, while designing the members of the tower. Therefore, considerations of dynamic displacement and dynamic stress do not impose any explicit constraints on the optimum design formulation.

The time dependent forcing function corresponding to wind load, being aperiodic in nature eliminates the necessity of considering constraints on natural frequencies of the tower. Thus, the formulated optimum design problem has only one explicit constraint to satisfy which can be stated as

$$d_1 + d_2 + \ldots + d_{n-1} + h_{NP} = \text{constant} \qquad (5)$$

where d_i is the height of i-th panel from the top of the body and h_{NP} is height of bottom most panel in the body. To handle this constraint implicity, only the first (NP - 1) panel heights are taken as variables, making the bottom-most panel dependent on the height of the other panels. Thus the formulated configuration optimization of the transmission line tower turns out to be an unconstrained minimization problem.

Method of Optimization

Several methods are available for solving the resulting unconstrained minimization problem. However, the nature of the problem makes the choice limited. In the present formulation, the function to be minimized is not an explicit function of design variables and, therefore, the evaluation of gradient in close form is not possible. An estimate to the gradient can, however, be made using finite difference technique. This, apart from the time required for additional number of function evaluations, may not be an accurate estimate, since the available angle sections (10) that are used for the members of the tower are discrete in nature resulting into the discontinuity of the function. Hence non-gradient method is the best choice for the problem formulated in the present work.

Among the non-gradient methods, Powells method (11) is the most widely used search method since it is quadratically convergent. Therefore, Powells method is chosen in the present work for the unconstrained minimization. The details of the method are well documented in literature (12). For one-dimensional minimization, quadratic interpolation technique (12) has been used.

Dynamic Analysis

The tower is modelled as a space truss, having pin connected joints. The discrete element method of structural analysis is used in the present work. The matrix formulation of the general structural dynamic response problem results in the equation

$$M\ddot{\vec{u}} + C\dot{\vec{u}} + K\vec{u} = \vec{p}(t) \qquad (6)$$

where M,C and K are, respectively, the master mass, damping and the stiffness matrices of the structure and their order n_f corresponds to the elastic degrees of freedom of the system. The vectors $\vec{u}$, $\dot{\vec{u}}$ and $\ddot{\vec{u}}$ represent the displacement, velocity, acceleration of the lumped masses at the panel joints and $\vec{p}(t)$ is the external load. The stiffness matrix is assembled from the corresponding element matrices of the members. The diagonal mass matrix M is obtained by lumping the masses of the members at panel joints. The elements of the C matrix are considered to be linear combinations of corresponding elements of K and M matrices.

The two distinct phases of the dynamic analysis are : (1) an eigenvalue analysis of the structural model and (2) computation of the dynamic response. The eigenvalue problem given by

$$K\vec{\phi} = \omega^2 M\vec{\phi} \qquad (7)$$

is obtained by substituting $\vec{u} = \vec{\phi}\sin\omega(t-t_0)$ and assuming the system to be undamped. The n_f eigenvalues, ω, give the natural frequencies of the system and the corresponding eigenvectors $\vec{\phi}$ represent the modes of vibration.

The eigenvalue problem, Eq.(7), is solved using subspace iteration method (13). First six eigenpairs are extracted in the present work resulting in the following mode shapes (14) :

1. First bending mode in the transverse direction
2. First bending mode in the longitudinal direction
3. First torsional mode
4. Second torsional mode
5. Second bending mode in the transverse direction
6. Second bending mode in the longitudinal direction

Table 1 : Eigenvalues of A Transmission Line Tower

Mode No.	Eigenvalue, ω^2 (rad^2/sec^2)
1.	691.39
2.	710.83
3.	1230.15
4.	6001.15
5.	7042.81
6.	8033.55

Table 1 presents the corresponding eigenvalues of a typical transmission line tower, having 15m body height, with 6 panels in the body and 4.33m base width.

Making the transformation :

$$\vec{u} = \varphi\vec{q} \qquad (8)$$

where $\varphi = [\varphi_1, \varphi_2, \varphi_3, \ldots, \varphi_p]$ and p in many practical situations is taken to be considerably less than n_f as an approximation to save computational effort. The equilibrium equations, Eq.(6), become, in view of the orthonormality of eigenvectors, as

$$\ddot{\vec{q}} + \Delta\dot{\vec{q}} + \Lambda^2\vec{q} = \varphi^T\vec{p}(t) \qquad (9)$$

in which $\Delta = \varphi^T C\,\varphi$ turns out to be diagonal. Eq. (9) consists of p uncoupled equations each one corresponding to a single degree-of-freedom which can readily be solved (15).

The wind load function, $p_i(t)$ at the i-th degree of freedom is expressed as

$$p_i(t) = F_i\, f_i(t) \qquad (10)$$

where F_i is a constant for i-th degree of freedom, being the maximum value of $p_i(t)$. The

time function, $f_i(t)$, as shown in Fig. 2, is same as that considered in Ref. (7). The other loads on the tower, viz. the broken wire loads and dead loads are considered at static maximum values. The broken wire load has been calculated based on the IS recommendations (8) which is the load on the cable at failure.

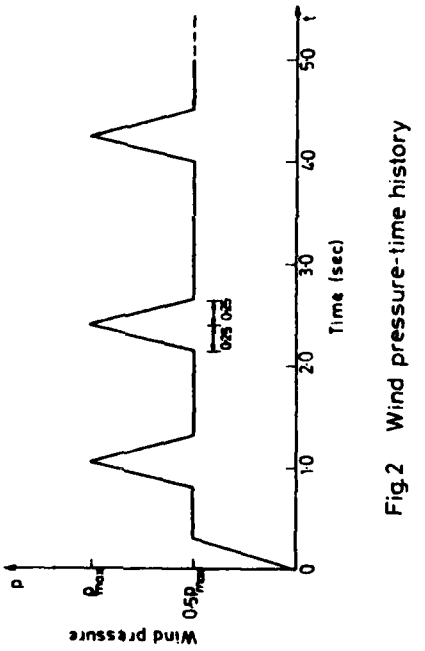


Fig.2 Wind pressure-time history

The uncoupled equation for the j-th mode, Eq. (9), turns out as

$$\ddot{q}_j(t) + 2\beta_j \dot{q}_j(t) + \omega_j^2 q_j(t) = \sum_{i=1}^{n_f} \varphi_{ij} F_i f_i(t) \qquad (11)$$

where suffix i denotes i-th degree of freedom,

$\beta_j = \xi_j \omega_j$, ξ_j is the fraction of critical damping

and

φ_{ij} = i-th component of the j-th mode shape vector.

Assuming initial conditions to be zero, the solution of Eq. (11) is given (15) as

$$q_j(t) = \sum_{i=1}^{n_f} \frac{\varphi_{ij} F_i}{\omega_j^2} \left[\frac{\omega_j^2}{\omega_{jd}} \int_0^t f_i(\tau) e^{-\beta_j(t-\tau)} \sin \omega_{jd}(t-\tau) d\tau\right] \qquad (12)$$

The expression inside square brackets in the above equation is the Dynamic Load Factor (DLF). Taking the maximum value of DLF, the modal participation factor is given as

$$q_{j,max} = \sum_{i=1}^{n_f} \varphi_{ij} F_i (DLF)_{ij,max} / \omega_j^2 \qquad (13)$$

where $(DLF)_{ij,max}$ is defined as the maximum DLF for the unit load $f_i(t)$ due to oscillations under natural frequency ω_j. The upper bound on stress is computed by superimposing the modal contributions as,

$$\sigma_{j,max} = \sum_{j=1}^{p} |\sigma_{ij} q_{j,max}| \qquad (14)$$

where σ_{ij} is the stress in member i due to mode shape j taken as deflection vector. The DLF has been computed by segmentwise integration of the function (16) shown in Fig. 2. For the static loads $(DLF)_{max}$ has been taken as 1.0 in all modes.

The member forces experienced by the leg members of the 15m, 20m and 25m body towers are presented in Table 2. These are the maximum value of stresses obtained by the superposition of the stresses due to the first six eigenmodes. In other words p has been taken to be six in this case. The first 7 rows in Table 2 correspond to the forces in leg members in the basket portion of the tower and the rest are in the body portion, starting from the top. The corresponding member forces under static load conditions are also shown in the same table. It is observed from these results that there is an increase of 33 % in the maximum dynamic stress as compared to maximum static stress in the bottom-most members. For smaller towers, however, the increase is lesser, Table 2.

Results and Discussion

Optimum design is carried out for 15m, 20m and 25m heights of tower body. The optimum configuration design obtained under static loads, presented in an earlier paper (6), is taken as the starting point for the present study in each case.

In order to find a usable search direction, a step size of 0.01 has been used, to check whether the function decreases along a given direction. After the usable direction is obtained, objective function values are evaluated at intervals of 0.3, 0.6, 0.9, ..., or at 0.3/2, 0.3/4, 0.3/8, ... depending upon the situation to bracket the minimum. Then the minimum along this direction within the bracketed range is located through successive quadratic fits.

The first (n-1) variables of the design vector correspond to panel heights starting from top and the n-th design variable correspond to the base width (Fig. 1). Hence, to start with, in the first cycle in Powell's method, the routine finds a better base width locally, goes on to panel heights, once again along base width and then moves along the pattern direction.

The optimization process is terminated

Table 2 Member Force (ton) in the Legs Under Static and Dynamic Loading

Leg member number starting from top	15m body, 6 panels in the body		20m body, 8 panels in the body		25m body, 10 panels in the body	
	Static analysis	Dynamic analysis	Static analysis	Dynamic analysis	Static analysis	Dynamic analysis
1.	7.220	3.214	7.125	2.782	7.048	2.536
2.	10.166	7.194	10.166	6.535	10.166	6.552
3.	15.904	14.995	17.473	15.560	18.691	17.174
4.	20.855	19.106	22.098	19.420	23.039	21.044
5.	26.241	27.209	26.250	25.415	26.261	27.088
6.	34.325	35.671	34.317	34.235	34.308	35.859
7.	36.607	38.850	36.744	38.504	36.902	39.458
8.	43.555	44.764	45.267	47.450	45.847	50.290
9.	49.086	46.257	48.370	49.450	51.194	56.142
10.	50.289	48.375	52.013	50.096	52.428	57.623
11.	53.215	53.037	56.544	55.111	58.200	62.336
12.	53.939	55.841	58.817	60.291	61.115	66.045
13.	55.710	59.132	61.594	65.848	64.862	72.118
14.			63.159	70.311	66.842	78.651
15.			65.186	74.782	69.501	85.669
16.					71.011	91.392
17.					73.051	97.084

when the change in all design variables is less than 0.001 in the search along the pattern direction.

The results of optimum design are presented in Table 3 and Table 4 for undamped system and for a system with 2 percent damping respectively. The time taken on DEC 1090 system for one function evaluation is also given in Table 3. The weight of tower at the end of each iteration is plotted in Fig. 3 and Fig. 4 for undamped case and for a case with 2 percent damping respectively.

Contrary to the results of optimum design under static loads (6), there is considerable variation in the base width corresponding to the optimum tower under dynamic loads, Table 3. Optimum base width increases for increasing height of the tower body. Under static loads the optimum base width (6) was observed to be around 4.0m for all the towers considered herein. Thus, for a realistic optimum configuration design of transmission line towers, considerations in the dynamic response regime seem to be inevitable.

From Table 3, it is observed that the optimum base width varies from 4.34m to 5.49m when the towers are assumed to be undamped. However, the range of optimum base width, Table 4, is 4.02m to 5.20m when 2 percent damping is considered in each case.

The reduction in weight is maximum corresponding to the change in the base width. This can be observed from Fig. 3 and Fig.4 wherein the reduction in weight in the first iteration (which corresponds to changes in base width) is significant. The reduction in weight due to the changes in panel heights is relatively small.

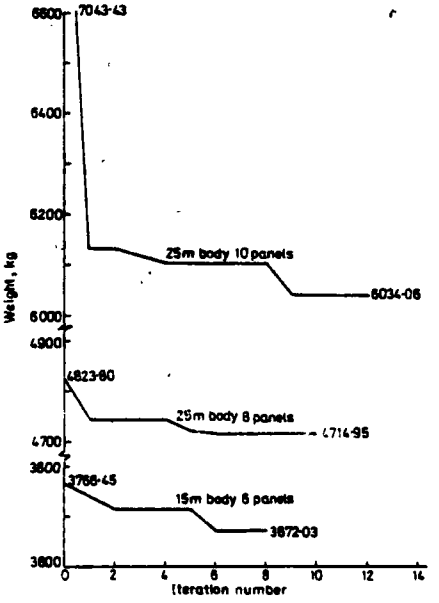


Fig. 3 Weight versus iteration (undamped)

Table 3 Results of Optimization Study (Undamped Case)

	15m body, 6 panels		20m body, 8 panels		25m body, 10 panels	
	Starting Design (S.D.)	Optimum Design (O.D.)	S.D.	O.D.	S.D.	O.D.
	2.00	1.85	1.90	1.90	2.10	2.10
	2.20	2.20	2.10	2.10	2.20	1.58
	2.40	2.40	2.30	2.30	2.30	1.90
	2.60	2.60	2.50	2.30	2.40	2.40
Panel heights(m)	2.80	2.37	2.50	2.35	2.50	2.56
	3.00	3.58	2.70	2.70	2.50	2.45
			2.90	2.90	2.60	2.59
			3.10	3.45	2.70	3.00
					2.80	2.75
					2.90	3.67
Base width(m)	4.00	4.34	4.00	4.60	4.00	5.49
Lowest natural frequency, ω_1	27.756	28.926	22.348	23.349	18.033	20.679
Total weight (kg)	3766.447	3672.028	4823.799	4714.947	7043.425	6034.063
Reeuction in weight(percent)	2.50		2.26		14.35	
CPU time for one function evaluation (sec)	6.83		7.85		11.04	

Table 4 Results of Optimization Study (2 Percent Damping)

	15m body, 6 panels		20m body, 8 panels		25m body, 10 panels	
	S.D.	O.D.	S.D.	O.D.	S.D.	O.D.
	2.00	1.10	1.90	1.90	2.10	1.31
	2.20	1.30	2.10	2.10	2.20	1.84
	2.40	2.10	2.30	2.30	2.30	2.31
	2.60	2.72	2.50	2.50	2.40	2.40
Panel heights(m)	2.80	2.80	2.50	2.50	2.50	2.50
	3.00	3.98	2.70	2.70	2.50	2.50
			2.90	2.90	2.60	2.45
			3.10	3.10	2.70	3.00
					2.80	2.65
					2.90	4.04
Base width(m)	4.00	4.02	4.00	4.30	4.00	5.20
Lowest natural frequency, ω_1	27.289	27.291	21.916	22.879	17.959	20.315
Total weight (kg.)	3688.956	3630.854	4823.799	4716.258	6598.937	5924.535
Reduction in weight(percent)	1.57		2.23		10.2	

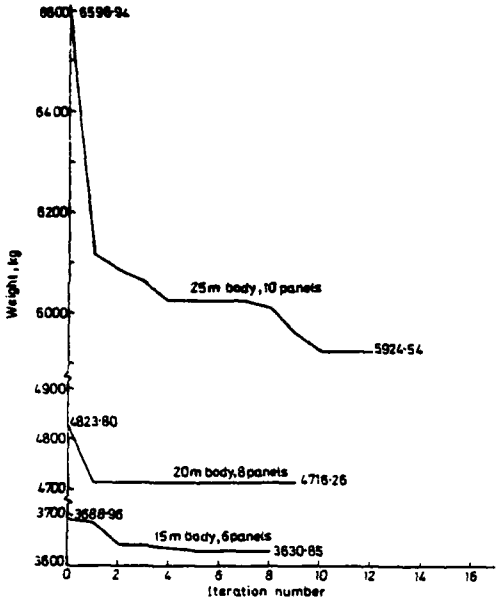


Fig. 4 Weight versus iteration (2% damping)

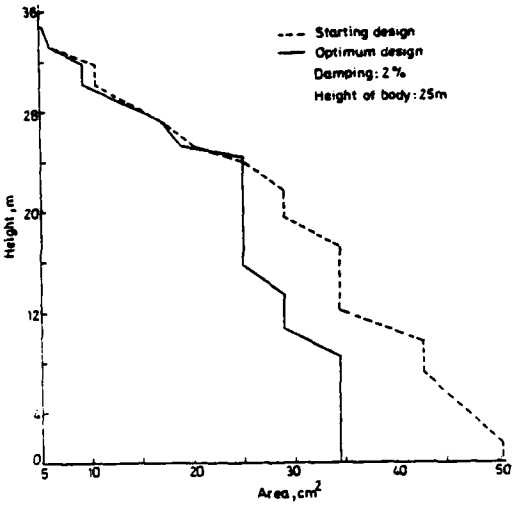


Fig. 5 Area of leg members along the height of tower

The study further reveals (Tables 3 and 4) that for the minimum weight towers, number of panels should be chosen such that the height of the central panel(s) of the body is around 2.5m. For an optimum configuration the panel heights are to be chosen such that the top most has the smallest and the bottom most has the largest panel height. Optimal panel height turns out to be 2.0m and around 3.5m respectively for top and bottom most panels. The intermediate panel heights may be varied linearly. Similar conclusions for the panel heights were arrived at during the configuration optimization study of transmission line towers under static loads (6).

It is observed, by plotting the area of leg members along the height of optimum towers under static and dynamic loads (16), that there is reduction in the area of leg members coupled with increase in the base width in each case. Reduction of the order of 31.7 percent is noted in the leg members of the 25m body tower, Fig.5. There is an increase in the base width of this tower by 30 percent, Table 4. These observations lead us to conclude that at the optimum tower, in dynamic regime, resists the dynamic loading by increased stiffness contribution and with reduced inertia.

A parametric study has been carried out to study the effect of damping on the optimum design. The results are presented in Table 5. From this table, it is observed that there is a general tendency of reduction in optimum weight with increased damping. However, the reduction is negligible. Further, the reduction in weight is not monotonic with increased damping. This is due to the discrete nature of available sections being used as members of the tower.

Conclusions

The following are the salient conclusions based on the present study :

1. In order to have a realistic response prediction for wind loading, considerations of equivalent static loads are insufficient and a rigorous dynamic analysis is inevitable. This is more so when optimum design is the goal.

2. The variation in base width has marked effect on the optimum weight of the tower. The optimum weight is more sensitive to the base width in the dynamic response regime as compared to the static case. From the results, it is observed that the base widths corresponding to optimum tower for 15m, 20m, and 25m body heights are around 4.00m, 4.30m and 5.20m respectively.

3. The number of panels in the body of the tower should be chosen such that the height of central panel(s) of the body is around 2.5m. Further, the top-most panel height may be kept around 2.00m and that of bottom-most panel around 3.5m for achieving minimum weight tower. The intermediate panel heights may be fixed by linear interpolation of heights of top and bottom panels.

4. The reduction in the optimum weight of the tower for the admissible changes in damping coefficient is negligible.

Table 5 Results of Optimum Design with Different Damping Ratios*

Sl.No.	Damping ratio (percent)	15m body		20m body		25m body	
		Optimum base width (m)	Optimum weight (kg.)	Optimum base width (m)	Optimum weight (kg.)	Optimum base width (m)	Optimum weight (kg.)
1.	0	4.34	3674.028	4.60	4714.947	5.49	6034.063
2.	1	4.02	3616.830	4.30	4716.258	5.50	6048.663
3.	2	4.02	3630.854	4.30	4716.258	5.20	5924.535
4.	3	3.95	3668.007	4.56	4712.519	5.41	6036.838
5.	4	3.94	3617.080	3.94	4789.293	5.43	6024.327
6.	5	3.94	3593.230	4.28	4717.968	5.39	6009.267

*Starting base width has been taken as 4.00m for all designs presented in this table.

References

(1) Lipson, S.L., and Gwin, L.B., The Complex Method Applied to Optimal Truss Configuration. Computers and Structures, Vol. 7, No.3, June 1977, pp.461-468.

(2) Lipson, S.L., and Agarwal, K.M.,Weight Optimization of Plane Trusses. Journal of the Structural Division, ASCE,Vol. 100, No.ST5, May 1974,pp.865-879.

(3) Vanderplats, G.N., and Moses, F.,Automated Design of Trusses for Optimum Geometry. Journal of the Structural Division, ASCE, Vol. 98, No.ST3, March 1972, pp.671-690.

(4) Kunar, R.R., and Chan, A.S.L., Method for the Configuration Optimization of Structures. Computer Methods in Applied Mechanics and Engineering, Vol. 7,No.3, March 1976, pp. 331-350.

(5) Bennett, J.A., Automated Design of Truss and Frame Geometry. Computers and Structures, Vol.8, No.6, June 1978, pp. 717-721.

(6) Kapoor, M.P., and Kumarasamy, K.,Optimum Configuration Study of Transmission Line Towers. Irrigation and Power Journal, Vol. 37, No.3, July 1980,pp.359-369.

(7) Yeh,C., and Shieh, W., Stability and Dynamic Analysis of Cooling Towers. Journal of Power Division, ASCE,Vol.99, No.PO2, Nov.1973,pp.339-347.

(8) IS:802 (Part I) - 1973, 'Indian Standard: Code of Practice for Use of Structural Steel in Overhead Transmission Line Towers, Part I-Loads and Permissible Stresses', ISI, New Delhi,Jan.1974.

(9) Rao, S.S., Structural Optimization Under Shock and Vibration Environment. The Shock and Vibration Digest,Vol.11, No.2, Feb.1979, pp.3-12.

(10) IS: Handbook for Structural Engineers-1 Structural Steel Sections, ISI, New Delhi, 1964.

(11) Powell, M.J.D., An Efficient Method for Finding the Minimum of a Function of Several Variables without Calculating Derivatives. The Computer Journal,Vol. 7, No.4, 1964, pp.155-162.

(12) Fox, R.L., Optimization Methods for Engineering Design, Addison-Wesley Publishing Co., Massachusetts, 1971.

(13) Bathe, K.J., and Wilson, E.L.,Numerical Methods in Finite Element Analysis, Prentice-Hall Inc., Englewood Cliffs, N.J., 1976.

(14) Kumarasamy, K., and Kapoor, M.P.,Eigensolution of Transmission Line Towers. Accepted for publication in the International Journal of Structures, Roorkee, India.

(15) Biggs, J.M., Introduction to Structural Dynamics, McGraw-Hill, New York, 1964.

(16) Kumarasamy, K., 'Configuration Optimization of Transmission Line Towers', Ph.D. Thesis, Deptt. of Civil Engineering, I.I.T. Kanpur, Nov. 1979.

AD-P000 076

OPTIMIZATION OF MULTIPLE SAFETY FACTORS IN STRUCTURAL DESIGNS

E. D. Eason, J. M. Thomas, P. M. Besuner
Failure Analysis Associates
750 Welch Road, Suite 116
Palo Alto, California 94304

This paper presents a method for optimization of safety factors and testing procedures to simultaneously minimize weight and maintain acceptable reliability and testing costs. A load combination rule for two categories of load with different safety factors is analyzed by structural reliability methods to estimate the probability of failure as a function of the two safety factors. As a part of this analysis, a procedure is developed for modifying published strength distributions to reflect a successful test to a specified fraction of design ultimate load. A cost model is constructed including the expected cost of failure, the value of saving weight, and the cost of development and/or proof tests. This cost is minimized numerically subject to constraints on maximum failure probability, safety factors, and proof level. The results for an application to the Space Shuttle External Tank show that reduced weight and reduced total cost are possible without any significant decrease in reliability, by increasing development and testing expenditures.

Introduction

The literature on structural optimization has been periodically organized and surveyed over the past two decades (1)-(5). In most cases, the work has emphasized development of computer codes that will specify structural element dimensions, shapes, or behavior to minimize cost or weight, or maximize performance and reliability. The traditional design safety factors (or code requirements) often appear as constraints on the objectives of minimum weight or cost, thereby implicitly controlling reliability. Some recent papers, e.g. (6), explicitly consider reliability, but the emphasis is still to let the optimization code specify the element or structure design.

In contrast, the present study assumes that the elements of complex structures will be designed in the traditional way by large groups of engineers, and the reliability will be controlled by design safety factors, proof test levels, and development testing as is common practice today. A larger-scale optimization problem is considered to find the design safety factors, proof levels, and type of testing that will minimize total cost. This total cost includes the expected consequences of failure as well as development costs, testing costs, and cost and performance penalties associated with structural weight. Such an approach has been applied to several aerospace structures by Thomas, et al. (7),(8), considering the effect of various types of development testing on the strength distribution in a probabilistic design approach. A single safety factor was optimized, and the results showed a wide variation in the optimum value depending on the consequences of failure and the level of proof and development testing.

The present study extends the earlier work (7)-(8) to the practically important case where loads are split into categories, each with its own safety factor. Such an approach has been used in weight reduction efforts on the external tank for the Space Shuttle, and the related load factor approach is in widespread use in civil engineering. The analysis contains three basic parts: probabilistic analysis of structural reliability, cost and weight modeling, and design factor optimization. The probabilistic analysis follows standard approaches (7)-(11), except that an improved method is developed for modifying the strength distribution of previously untested structures to reflect a successful full scale static load test. A simple cost model is developed to assess the relative importance of weight savings, changes in reliability, and cost of various testing schemes. The cost, as calculated by this model, is then minimized subject to a constraint on failure probability and limits on the variables, using a nonlinear minimization computer code.

Reliability Methodology

Load Combination Rule

Two broad load categories are considered in the Space Shuttle application, well defined (thrust, pressure, inertia) and other (dynamic, thermal, and aerodynamic). Each category has its own safety factor, conceptually defined as

$$\nu = \frac{\tilde{R}}{\tilde{S}} \qquad (1)$$

where ν is the safety factor ($\nu > 1$), $\tilde{R}$ is the predicted ultimate strength or resistance, and $\tilde{S}$ is the limit load -- an upper bound or high estimate of the load to be withstood in actual use. Since there are two load categories, a load combination rule (which actually defines ν_1 and ν_2) is necessary. The rule analyzed in this application is

$$\tilde{R} = \nu_1 \tilde{S}_1 + \nu_2 \tilde{S}_2 \qquad (2)$$

where subscript 1 corresponds to well defined, subscript 2 to other loads.

This traditional definition of safety factor is based on an underlying deterministic design assumption that a given design has a predictable, single-valued strength, and the maximum load it will experience is known and similarly single-valued. Probabilistic design begins from a more realistic assumption, that both strength and load may vary between different samples of the same design, under different applications, and at various times during the life of the structure. Most of the time the sample structure will have nearly average strength and the loads will be well below the limit load, so the probability of

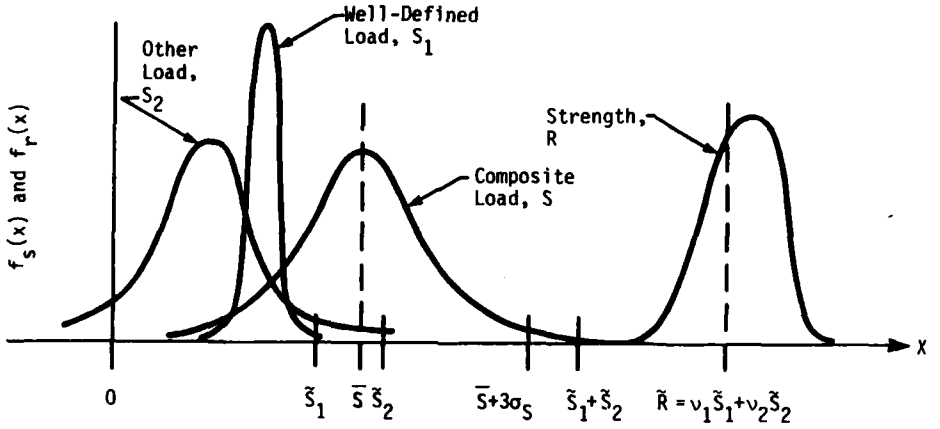


Figure 1 - Diagram of Load Combination Procedure and Strength Distribution.

failure for $\nu > 1$ will be small. However, a sample of a given design or class of designs may fail because it is under-strength, or an unusually large overload may cause average or above-average strength structures to fail. Thus, the probabilistic approach treats a range or distribution of strengths and loads, as occur in practice, and attempts to control the design factors so that the probability of failure is acceptable considering the entire range of possible combinations of strength and load.

Figure 1 shows the two probability density functions (PDF) for load, $f_s(x)$, combined to form a composite load PDF. The upper tail of this load distribution intersects with the lower tail of the strength distribution, $f_r(x)$, and it is in this intersection region where load may exceed strength, resulting in failure. The two-factor analog of Eq (1) is the effective safety factor ν_e

$$\nu_e = \frac{\tilde{R}}{\tilde{S}_1 + \tilde{S}_2} = \frac{\nu_1\tilde{S}_1 + \nu_2\tilde{S}_2}{\tilde{S}_1 + \tilde{S}_2} \qquad (3)$$

where $\tilde{S}_1$ and $\tilde{S}_2$ are the limit loads of the well-defined and other distributions. The composite distribution is obtained by probabilistic combination of the two load distributions, summing the means and variances. The design ultimate strength $\tilde{R}$ is not the mean of the strength distribution; structural engineers typically produce designs that average somewhat stronger than the predicted design ultimate (8),(12)-(14). Figure 1 also shows the fact that when the limit loads $\tilde{S}_1$, $\tilde{S}_2$ are three standard deviations from their respective means $\bar{S}_1$, $\bar{S}_2$, their sum is not three standard deviations from the mean of the composite load, i.e.,

$$\tilde{S}_1 + \tilde{S}_2 \geq \bar{S} + 3\sigma_s \qquad (4)$$

Equality holds only when there is one load component or all components are mutually dependent and in proportion.

The value of the effective safety factor depends on the proportions of well defined and other loads. For convenience, a parameter a is defined as the fraction of well defined load

$$a = \frac{\tilde{S}_1}{\tilde{S}_1 + \tilde{S}_2}, \quad 0 \leq a \leq 1 \qquad (5)$$

With this definition, the effective safety factor is

$$\nu_e = \nu_2 + (\nu_1 - \nu_2)a \qquad (6)$$

In practice, there will be a range of values for a at different locations in the structure and at different times in the launch sequence of the Space Shuttle. Consequently, the cost function must be evaluated at typical values of a, while the constraints must be evaluated over the entire range of a.

Load Distributions

For this study, the load distributions are assumed to be Gaussian. There is some theoretical justification for this assumption, because the load at many points in the structure is the sum of several load components, each of which may take on positive or negative values at various times during launch. Whenever a composite distribution is the sum of many independent distributions, the composite distribution is Gaussian regardless of the shape of the individual distributions (15), provided that none of the individual distributions dominate the composite.

The load distributions are defined as a percentage of design ultimate (i.e. $\tilde{R} = 100$), using the load combination rule, Eq. (2), Eq. (5) and (6), the assumption of Gaussian distribution, and the definition of limit load as q standard deviations above the mean,

$$\tilde{S}_i = \bar{S}_i(1 + q_i\gamma_i) \qquad (7)$$

where γ_i is the coefficient of variation ($\gamma = \sigma/\bar{S}$). It is not necessary to know the mean of the loads $\tilde{S}_1$ and $\tilde{S}_2$ in advance, because they can be calculated as

$$\bar{S}_1 = \frac{100a}{\nu_e (1 + q_1\gamma_1)}, \quad \bar{S}_2 = \frac{100 (1-a)}{\nu_e(1 + q_2\gamma_2)} \tag{8}$$

Combining the means and standard deviations - ($\sigma = \gamma\bar{S}$), the composite load distribution is given by Eq. (8) and

$$\bar{S} = \bar{S}_1 + \bar{S}_2 \tag{9}$$

$$\sigma_s = \left[(\bar{S}_1\gamma_1)^2 + (\bar{S}_2\gamma_2)^2\right]^{1/2} \tag{10}$$

Note that both $\bar{S}$ and σ_s depend only on values of a, ν_i, q_i, and γ_i. Since the range of a is known, ν_i are the design factors to be found, and q_i is typically three standard deviations in aerospace practice, the only problem-specific input data to the load distribution are the values γ_1 and γ_2. The values of γ_i and q_i are treated as sensitivity study variables in the current Space Shuttle application.

Strength Distribution

The basic strength distribution data was collected during the Saturn V program (12). Fifty structures were tested, in most cases to failure, and the failure load was expressed as a fraction of the design ultimate load. Many different types of structures were included, and the loading included the normal range of compression, bending, and concentrated loads (with associated failure modes) found in rocket structures. All of these tests are assumed to belong to a single population that can best be described as previously untested aerospace structures.

The Saturn V strength data compares closely over the critical lower tail region of its distribution with the data collected by the Air Force Materials Laboratory as reported in (10),(16). Much of that data is not readily comparable because it is not reported as a fraction of the design ultimate load. However, selected results of 66 tests are reported this way in (16), including 38 tests in 7 groups that are reported in (10). When these data are plotted together on Weibull paper, the aircraft data fits a cumulative distribution:

$$F(x) = 1 - e^{-(x/103)^{8.5}} \tag{11}$$

compared to the Saturn V distribution:

$$F(x) = 1 - e^{-(x/115.5)^{6.43}} \tag{12}$$

Both distributions are plotted in Figure 2, where it is apparent that there is close agreement up to about 80% of ultimate strength (the region of intersection with the load distribution where most field failures would occur). The Saturn V structures are generally more likely to withstand loads near and above the design ultimate than the aircraft structures.

Effect of Successful Development Testing

It is necessary to adjust the strength distribution of previously untested structures for the fact that one sample of the external tank structure (the Structural Test Article or STA) successfully passed a full scale test. The adjustment is performed by blending the distribution of strengths for identical samples of a particular structure, given in (16) for 341 test items

$$F(x) = 1 - e^{-(x/101.7)^{25}} \tag{13}$$

with the distribution of strengths for a variety of structures given by Eq. (12). The basic issue is, what is the probability that a second (flight hardware) sample of the tested structure will fail at or below strength x, given that the Structural Test Article (STA) survived a test to strength x_1? In probability notation, let

A = the event that a second sample of the design (flight hardware) fails at $R \leq x$

B = the event that the first sample of the design (STA) does not fail at all $R \leq x_1$

Find

$$P(A\backslash B) = \frac{P(A\cap B)}{P(B)} \tag{14}$$

where P(B) is found by normalizing $P(A\backslash B)$ to unity over all x.

$$P(A\cap B) = \int_0^\infty P(A\cap B\backslash v_2)\ PDF(v_2)dv_2 \tag{15}$$

where v_2 is the unknown scale parameter (characteristic strength) for the distribution of samples of a particular structure, to be drawn from a probability density function, $PDF(v_2)$, representing the entire class of similar structures. Note that $v_2 = 101.7$ in Eq. (13).

$$P(A\cap B\backslash v_2) = P(B\backslash v_2) \int_0^x PDF(A\backslash v_2)dx\ , \tag{16}$$

because A and B are independent events from the same distribution, Eq. (13). This can be broken down to

$$P(B\backslash v_2) = e^{-(x_1/v_2)^{k_2}} \tag{17}$$

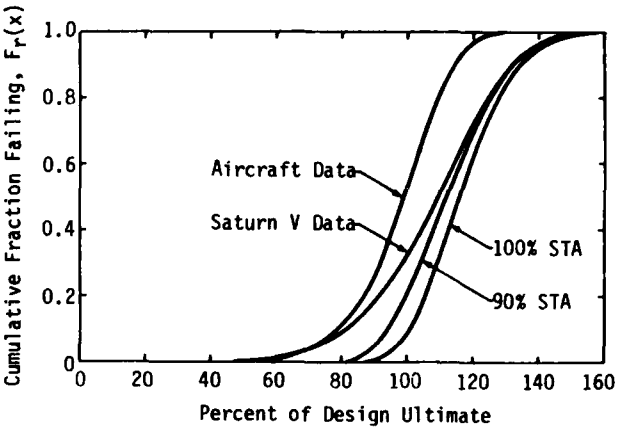


Figure 2 - Comparison of Strength Distributions. Aircraft Data from (10), (16), Saturn V Data from (8).

$$PDF(A\backslash v_2) = \frac{k_2}{v_2}\left(\frac{x}{v_2}\right)^{k_2-1} e^{-(x/v_2)^{k_2}} \quad (18)$$

$$PDF(v_2) = \frac{k_1}{v_1}\left(\frac{v_2}{v_1}\right)^{k_1-1} e^{-(v_2/v_1)^{k_1}} \quad (19)$$

Note Eq. (15)-(19) have been expressed in terms of the same-structure scale parameter v_2; this is effectively an assumption that the Saturn V data is a distribution of scale parameters v_2 for various structures. Because $k_2 = 25$ corresponds to low variability, and the mean of the Weibull distribution is

$$\bar{x} = v_2\,\Gamma\left(1 + \frac{1}{k_2}\right), \quad (20)$$

v_2 can be used in place of the mean with an error that is practically insignificant. Thus, the Saturn data given by Eq. (12), which is actually a distribution of recorded failure loads, can be interpreted as either a distribution of mean failure loads for various types of structures or a distribution of scale parameters for the sample-to-sample distribution of particular structures.

Combining Eq. (14)-(19), the result is an expression for the probability that strength is less than x, given that one sample of the structure survived a test to load level x_1:

$$P(A\backslash B) = F_r(x) =$$

$$\frac{1}{c}\int_0^\infty (1-e^{-(x/v)^{k_2}})\, e^{-(x_1/v)^{k_2}} v^{k_1-1} e^{-(v/v_1)^{k_1}} dv \quad (21)$$

where subscript 2 has been dropped from the variable of integration. The normalization constant

$$c = \int_0^\infty e^{-(x_1/v)^{k_2}} v^{k_1-1}\, e^{-(v/v_1)^{k_1}} dv \quad (22)$$

and $k_1 = 6.43$, $v_1 = 115.5$, $k_2 = 25$ from Eq. (12) and (13). This expression requires numerical integration and is somewhat clumsy to manipulate, but it can be conveniently and accurately approximated by a product of Weibull functions. At $x_1 = 100\%$, the result is

$$F_r(x) = (1-e^{-(x/120.9)^{9.23}})(1-e^{-(x/101.9)^{16.1}}) \quad (23)$$

while at $x_1 = 90\%$, the result is

$$F_r(x) = (1-e^{-(x/117.1)^{8.82}})(1-e^{-(x/92.4)^{16.3}}) \quad (24)$$

This least-squares fit to points generated by Eq. (21) is most accurate in the critical lower tails, yielding deviations from Eq. (21) of 1% or less in those regions.

The distributions for successful tests to 90% and 100% of design ultimate are shown in Figure 2. By comparison with the Saturn V distribution, the modified distributions drop sharply near their respective successful test levels. This is because the narrower distribution for expected variation among samples of the same design dominates in this region.

Effect of Proof Tests

The second test option considered in this study is the proof test. The proof test is an idealization in which all load conditions are fully tested before flight to a particular percentage r_o of design ultimate, and no failures occur in flight below this level if the test is passed. Analytically, this corresponds to truncating the strength distribution below r_o, which affects the probability of flight failure as discussed in the next section and introduces an expected cost of proof test failure. Assuming that the proof test load is deterministic, the probability of proof test failure is simply the probability that strength is below r_o, given by

$$P(\text{fail} < r_o) = F_r(r_o) \quad (25)$$

Failure Probability Calculations

The probability of failure at load x is equal to the probability that the strength is below x and the load is in a small range dx about x, i.e.

$$P(\text{fail @ } x) = F_r(x)\, f_s(x)\, dx \quad (26)$$

where $F_r(x)$ is the cumulative strength distribution given by Eq. (21) and $f_s(x)$ is assumed to be a Gaussian probability density function with parameters given by Eq. (9), (10). The probability of flight failure is the integral of Eq. (26) over all x above the proof level r_o

$$P_f = \frac{1}{\sigma\sqrt{2\pi}[1-F_r(r_o)]}\int_{r_o}^\infty F_r(x) e^{-(x-\bar{S})^2/2\sigma^2} dx \quad (27)$$

where $1/[1-F_r(r_o)]$ is a normalizing term for maximum probability = 1. Eq. (27) is integrated numerically, using the approximations Eq. (23) and (24) for $F_r(x)$ to avoid nested numerical integrations.

Cost Optimization Model

The form of the cost model is

$$C = C_f P_f(v_1, v_2, r_o) + C_W \frac{\partial Wt}{\partial v_e} v_e + C_p F_r(r_o) + C_t \quad (28)$$

where the constants are defined as

- C_f = cost of flight failure
- C_W = cost of launching added weight
- C_p = cost of proof test failure
- C_t = incremental direct cost, including cost of structural tests or proof tests plus cost of re-engineering and manufacturing, less baseline cost for unoptimized design.
- $\frac{\partial Wt}{\partial v_e}$ = sensitivity of weight to changes in effective safety factor

The model is nonlinear in the variables ν_1, ν_2 and r_0 and it depends on the ratio of well defined to total load, a. The absolute values of the constants are less important than the relative values, which establish the relative importance of reliability, weight reduction, and development cost.

Constraints are imposed in addition, placing upper and lower limits on ν_1, ν_2, and r_0 and an upper limit on flight failure probability. These limits are based on factors not included in the model (e.g., fracture mechanics considerations, yield failure mode) and engineering judgement, considering the systems-level assumptions of the present analysis and the fact that flight failure would be life-threatening. The constraints are required to be satisfied at all values of a.

The constrained cost minimization problem can be solved by a variety of constrained nonlinear optimization codes. The functions are not analytic, because of numerical integration for P_f, so it is necessary to choose a code that does not require analytic derivatives. In addition, the limits imposed on the variables by engineering judgement are fairly tight, so a code that is based on local exploration is preferable to one that is based on large-step extrapolation.

The chosen code PATPEN is a revised version of the best algorithm in Eason's study of seventeen codes (17). The original algorithm is due to Hooke and Jeeves (18); the modifications include scaled step lengths, provision for scaled external penalty functions for the constraints, search order permutation, retained information on the direction of successful exploratory steps, and many other details. The code has proved effective and reliable on many similar practical problems characterized by a small number of variables and inequality constraints.

Sample Application

The methods presented above have been applied to the external tank of the Space Shuttle. The original design, referred to as HWT hereafter, performed successfully in the first Space Shuttle flight. It was based on a safety factor of 1.4 throughout and extensive development tests, including a full-scale Structural Test Article (STA) program. In the STA program, the most critical load combinations were tested to *full design ultimate (1.4 S) with no failures.* All loading conditions were successfully tested to at least 90% of design ultimate, so this set of tests is referred to as the 90% STA test option below.

A lighter-weight design called the LWT has been developed based on the results of the successful testing program for the HWT. Several methods of weight reduction are being simultaneously implemented, as discussed in (19), but the one of interest here is the use of multiple safety factors. Well-defined loads in the LWT are subject to a 1.25 safety factor, while other loads are subject to the original 1.4 safety factor. The testing program is considerably less exhaustive than the HWT tests, because the hardware is in most cases similar in configuration, differing only in dimensions. Tests are planned for those areas where design changes are extensive or not covered by the earlier tests. For the purposes of this analysis, this procedure of testing where necessary and otherwise relying on the previous test is assumed to be functionally equivalent to a 90% STA test option.

In both the HWT and LWT designs, the oxygen and hydrogen tanks are pressure proof tested. This cannot be considered a proof test under the assumptions in the Reliability Methodology section, because not all of the load conditions are proofed. That is, all combinations of pressure, aerodynamic, thermal, dynamic, thrust and inertia loading would have to be tested to the proof level to qualify as a proof test option.

Selected results for a typical set of cost constants are shown in Figure 3. Different cost constants and input parameters q_i, γ_i can change the results. Full details and input values are presented elsewhere (20). Figure 3 shows substantial weight reduction from the HWT to the LWT, but not much cost reduction. The optimum solution for the 90% STA test option, with safety factors 1.285 on well-defined load, 1.25 on other load, trades slightly less weight savings for slightly greater reliability, resulting in lower total cost. The optimum solution for 90% STA testing plus full proof testing saves both weight and cost and also increases reliability slightly. The safety factors are 1.25 on both load categories, the

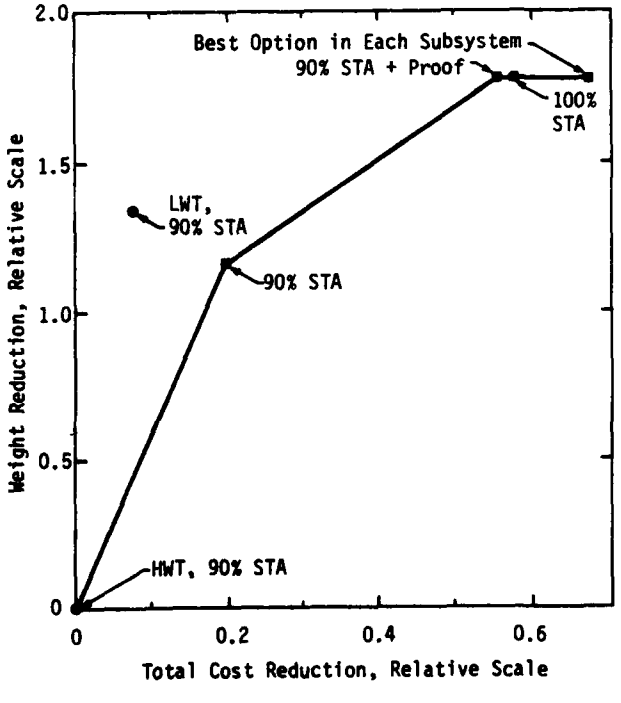


Figure 3 - Locus of Optimized Solutions Compared to Original Design (HWT) and Light-Weight Design (LWT).

minimum allowed by the constraints, and the optimum proof level varies between 74% and 78% of design ultimate, depending on the subsystem.* An even better solution is to perform structural tests that successfully test all load combinations to at least 100% of design ultimate. The 100% STA option assumes this is done with no failures -- quite an achievement since in practice some loads must be applied above the design ultimate to ensure that all load combinations reach the 100% level. Such tests would justify a 1.25 safety factor throughout, and would give slightly better flight reliability with less risk of proof test failures.

The costs of the 90% STA + proof and 100% STA options are as close as shown in Fig. 3 primarily because it was assumed in the 100% STA option that pressure proofing would still be required for the hydrogen and oxygen tanks, so that the risk of proof test failure is not avoided entirely in those subsystems. In fact, an improved strategy compared to either 100% STA or 90% STA + proof is to combine the two. For the hydrogen and oxygen tanks, the proof test strategy is optimal, so it appears worthwhile to expand the pressure proof test to a full static load proof test at about 75% of design ultimate. In the intertank and interface subsystems it is better to perform the more stringent 100% test and avoid proof testing. The result of using the best test option in each subsystem is a significant decrease in expected cost, as shown in Fig. 3. It should be recognized that options involving decreases in expected cost generally involve initial monetary outlays, in particular, additional expenditures for development and testing.

All of the results shown in Fig. 3 are at nominal values of the inputs q_i, γ_i and the cost coefficients. The sensitivity of the results to off-nominal conditions is also investigated in (20), with results such as Fig. 4. The results are rather sensitive to q_i; for instance, if the limit load is less than 3 standard deviations from the mean, the optimal safety factors switch from $\nu_1 > \nu_2$ or $\nu_1 = \nu_2$ (depending on the test option) to $\nu_1 < \nu_2$, and the weight increases dramatically to maintain the same reliability.

Discussion

There are several key assumptions in this analysis. First, the strength distribution is assumed to correspond closely with data from a different set of structures. This is a necessary assumption underlying structural reliability analyses whenever there is insufficient data on the structure in question (especially when there are neither failures in development nor high-load successes in tests of the final structural configuration). The assumption is reasonable because the strength distribution effectively describes the ability of engineers to design and build

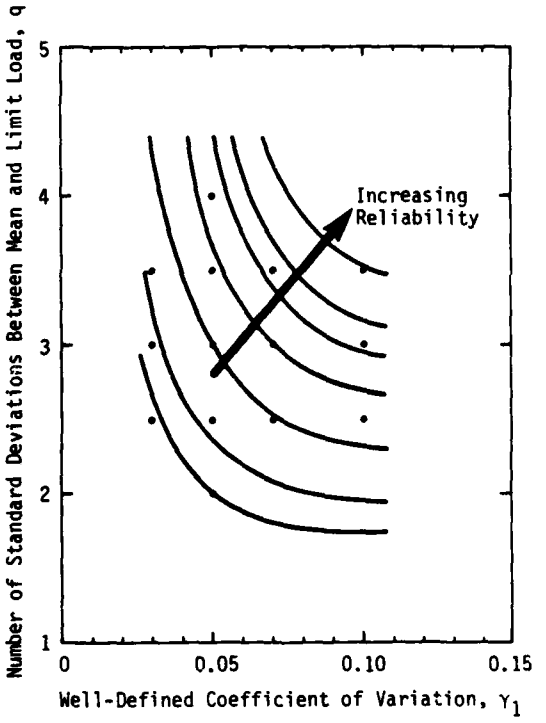


Figure 4 - Sensitivity of Estimated Reliability to Input Parameters (at a=1, ν_1=1.25).

structures that perform as predicted, and this ability is relatively independent of application. However, it is quite possible for one group of engineers to include more or less conservative strength margins above design ultimate, or for fabrication to be better controlled by one company than another, and the present analysis would not reflect these differences.

The second assumption is the idealization of test options. In practical tests, some load conditions are tested to higher levels than others because of the complexity of the load paths and the extremely large number of load conditions. The lower bound on test level is used here for a conservative analysis, but it is known that the loading conditions judged most critical were applied at higher levels. Similarly, no credit for proof tests is given unless all load conditions are specifically proofed, yet the fact that the tanks are pressure proofed does increase their reliability relative to other loads as well.

A third assumption is that the sensitivity of weight to safety factor changes can be modeled by a linear $\Delta Wt/\Delta\nu_e$ calculation from HWT and LWT data. This is a necessary assumption to avoid the massive redesign effort that would be needed to obtain several points on a weight vs. safety factor curve. There is no fundamental reason why $\partial Wt/\partial\nu_e$ should be linear over the domain of ν_e, but linearity is probably a good assumption for the limited range considered.

Finally, many assumptions went into the model parameters and cost constants, some of which have been checked by sensitivity analysis. It is necessary to

* The optimization was carried out separately for each subsystem of the external tank, then combined for the results in Fig. 3.

temper the conclusions of a system study such as this with an awareness of these sensitivities, the importance of imperfect knowledge, and the fiscal constraints that must be considered in efforts to achieve optimum design.

Conclusions

An approach has been presented for determining optimum values of safety factors and test options by structural reliability analysis. An effective technique was derived for modifying existing test data for the fact of a successful structural test. Two load categories and safety factors were considered, and depending on the test option and input data, the optimal values of the two safety factors could be equal or either one larger. The most sensitive input variable was found to be the number of standard deviations between the mean and limit load. Testing was worthwhile for improving reliability, and depending on the subsystem, the best test option could be either enhanced development tests or proof tests. The simple Hooke and Jeeves pattern search optimization code with scaled exterior penalty functions performed well on this problem.

Acknowledgements

The cooperation of many NASA and Martin Marietta personnel was crucial to the successful completion of the Space Shuttle application included in this paper. Funding was received under Martin Marietta contract ASO-704773.

References

1. Wasiutynski, A, and Brandt, A, "The Present State of Knowledge in the Field of Optimum Design of Structures," Applied Mechanics Reviews, Volume 16, No 5, May 1963, pp 341-350.

2. Sheu, C Y, and Prager, W, "Recent Developments in Optimal Structural Design," Applied Mechanics Reviews, Volume 21, No 10, October 1968, pp 985-992.

3. Schmit, L A, "Literature Review and Assessment of the Present Position," Chapter 4, G G Pope and L A Schmit (eds) Structural Design Applications of Mathematical Programming Techniques, AGARDograph No 149, AG-149-71, 1971.

4. Gallagher, R H, and Zienkiewicz, O C, Optimum Structural Design, Wiley, New York, 1973.

5. Krishnamoorthy, C S, and Mosi, D R, "A Survey on Optimal Design of Civil Engineering Structural Systems," Engineering Optimization, Vol 4, No 2, 1979, pp 73-88.

6. Moses, F, "Structural System Reliability and Optimization," Computers and Structures, Vol 7, 1977, pp 283-290.

7. Thomas, J M, Hanagud, S, and Hawk, J D, "Decision Theory in Structural Reliability," Proceedings, 1975 Reliability and Maintainability Symposium, pp 255-262.

8. Thomas, J M, and Hanagud, S, "Reliability-Based Econometrics of Aerospace Structural Systems: Design Criteria and Test Options," NASA TN D-7646, Marshall Space Flight Center, June 1974.

9. Freudenthal, A M, Garrelts, J M, and Shinozuka, M, "The Analysis of Structural Safety," ASCE Structural Division Journal, Vol 92, No ST1, Feb 1966, pp 267-325.

10. Freudenthal, A M, and Wang, P Y, "Ultimate Strength Analysis of Aircraft Structures," J. Aircraft, Vol 7, No 3, May-June 1970, pp 205-210.

11. "Structural Safety - A Literature Review", ASCE Structural Divison Journal, Vol 98, No ST4, April 1972, pp 845-884.

12. Thomas, J M, "Statistical Determination of Safety Factor Requirements for Untested Structures from Saturn V Test Data," Research Achievements Review, Vol IV, Report No 1, NASA TM X-64528, 1970.

13. Galambos, T V, "Probabilistic Approaches to the Design of Steel Bridges," Probabilistic Design, Redundancy, and other Bridge Papers, Transportation Research Record 711, National Academy of Sciences, Washington, D.C., 1979, pp 7-13.

14. Ellingwood, B, "Reliability of Current Reinforced Concrete Designs," Proc. ASCE, Vol 105, ST4, April 1979, pp 699-712.

15. Benjamin, J R, and Cornell, C A, Probability, Statistics, and Decision for Civil Engineers, McGraw-Hill, New York, 1970, pp 249-253.

16. Freudenthal, A M, and Wang, P Y, "Ultimate Strength Analysis," Air Force Materials Laboratory Report AFML-TR-69-60, March 1969.

17. Eason, E D, and Fenton R G, "A Comparison of Numerical Optimization Methods for Engineering Design," J. Engineering for Industry, Transactions ASME, Series B, Vol 96, No 1, February 1974, pp 196-200.

18. Hooke R, and Jeeves, T A, "Direct Search Solution of Numerical and Statistical Problems," Journal of the Association for Computing Machinery, Volume 8, 1961, pp 212-229.

19. Norton, A M, "Space Shuttle External Tank Performance Improvements," Canaveral Council of Technical Societies, 18th Space Congress, April 1981.

20. Eason, E D, Thomas, J M, and Besuner, P M, "Optimization of Space Shuttle External Tank Design Factors and Testing," Failure Analysis Associates Report, FAA-81-8-11, September 1981.

AD-P000 077

MULTICRITERION OPTIMIZATION IN STRUCTURAL DESIGN

Juhani Koski
Tampere University of Technology
Department of Mechanical Engineering
P.O. Box 527
SF-33101 Tampere 10
FINLAND

Summary

A general philosophy of the multicriterion approach is presented, and Pareto optima are defined as solutions to the problem. A structural design problem where the weight and some chosen nodal displacements of the structure are taken as design criteria is formulated for hyperstatic trusses and plane frames. The displacement method is applied, and limits for the stresses as well as for the member areas are imposed. Only elastic structures with constitutive and geometrical linearity are considered.

Special attention is paid to numerical techniques for generating Pareto optima. The weighting method and the constraint method as well as the minimax approach are presented, and two examples of structural design are given to illustrate the theory. Also an interactive method where some parameters are joined with the minimax problem and trade-offs obtained from the Kuhn-Tucker multipliers are used is introduced. In addition, graphic representation of the results, which has become an important question because of the great number of Pareto optima, is discussed.

Introduction

During the last two decades much attention has been paid to exploiting the results of mathematical optimization theory in different fields of engineering. Also in structural design various techniques, mainly based on nonlinear programming, have been widely used to handle problems with a constantly increasing number of design variables and constraints. Usually a scalar-valued objective function is optimized in a feasible set, and the result is then used as a guiding device in striving for the best practicable structure. In mechanical and structural problems, however, there often exist several, usually conflicting, criteria to be considered by the designer. One very promising approach to this specific topic seems to be multicriterion optimization, where a vector-valued objective function is examined. The problem is then stated as

$$\min_{x \in \Omega} f(x) = [f_1(x), f_2(x), \ldots, f_m(x)]^T \quad , \tag{1}$$

where the components $f_i(x)$, $i = 1,2,\ldots,m$, called criteria, may be noncommensurable as well. The design variable vector x belongs to the feasible set $\Omega \subset R^n$, defined by equality and inequality constraints in the following way:

$$\Omega = \{x \in R^n \mid h(x) = 0,\ g(x) \leq 0\} \quad . \tag{2}$$

Usually there exists no unique point which would give an optimum for all m criteria simultaneously. Thus a new optimality concept, different from that used in scalar optimization, is introduced as a solution to the vector optimization problem.

Definition. A vector $x^* \in \Omega$ is called Pareto optimal for problem (1) if and only if $x \in \Omega$ and $f_i(x) \leq f_i(x^*)$ for $i = 1,2,\ldots,m$ imply that $f_i(x) = f_i(x^*)$ for $i = 1,2,\ldots,m$.

Verbally this definition states that x^* is Pareto optimal if there exists no feasible vector x which would decrease some criterion without causing a simultaneous increase in at least one criterion. The notation $z^* = f(x^*)$ is used for the corresponding vector in the criterion space R^m, and it is called a minimal solution. Usually several Pareto optima exist for a vector optimization problem, and additional information is needed to order the Pareto optimal set. This clearly makes it possible to bring in special considerations not included in the optimization model but yet stressed by the designer, thus making the multicriterion approach a flexible technique for most design problems.

Even though vector optimization goes back as far as 1896 (Pareto, [1]), a wider interest in the subject in such areas as optimization theory, operations research and control theory was not aroused until the late 1960s, and since then research work has been very intensive. Also in structural and mechanical design problems vector optimization has been treated by some authors [2] - [8], and the multicriterion approach has now come to occupy an established position in solving economic problems, but its full potential has not yet been exploited in engineering design.

The object of this paper is to briefly present the basic ideas of multicriterion optimization and to apply the theory to a specific structural design problem formulated for trusses and plane frames. Special attention is paid to the numerical calculation of Pareto optima, but also an interactive method for reaching the final design is introduced.

Numerical methods for Pareto optima

Several numerical techniques for solving a general nonlinear vector optimization problem have been presented in the literature [9]. Usually they turn the original problem into a sequence of scalar optimization problems, which may be solved by using standard nonlinear programming routines. Here only three of them are presented, namely the weighting method, the constraint method and the minimax approach. These seem to be suitable basic techniques to be considered in structural optimization as well as in other fields of engineering design.

Weighting method

Perhaps one of the most commonly used approaches to problems with several criteria is to form one scalar objective function as a weighted sum of the criteria. In cases where certain convexity requirements are met, this technique may be used also in generating Pareto optima for multicriterion problems. If the notation $\lambda \in R^m$ is used for the vector of weighting coefficients, the problem takes the form

$$\min_{x \in \Omega} \lambda^T f(x) \quad . \tag{3}$$

Without losing generality λ can be normalized so that

PRECEDING PAGE

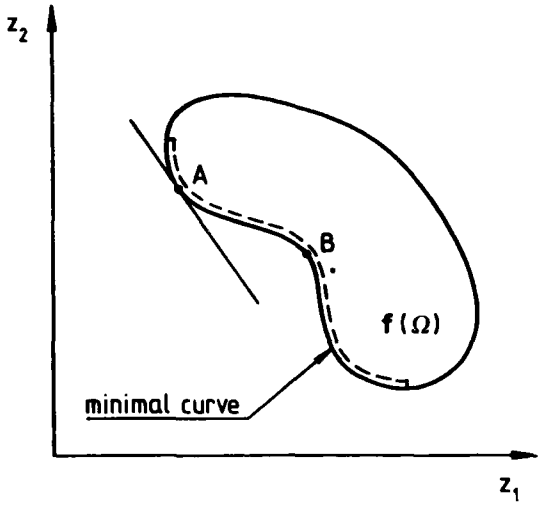


Figure 1. Geometrical interpretation of weighting method in bicriterion case. The minimal point B and the corresponding Pareto optimum are missed no matter what weights are used.

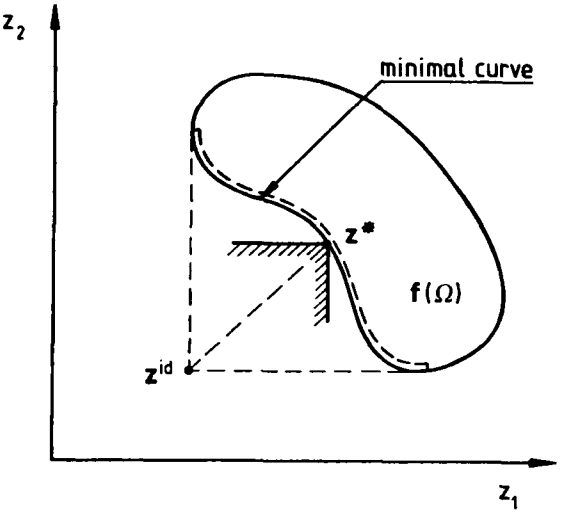


Figure 2. Geometrical interpretation of minimax approach in bicriterion case. All Pareto optima are obtained by this method regardless of the convexity of the minimal curve.

the sum of its components, which are nonnegative and not all zero, is equal to one. Now Pareto optimal solutions can be generated by parametrically varying the weights λ_i in the objective function. The main disadvantage of this technique is its incapability of producing the whole Pareto optimal set for some nonconvex problems. This may be seen by geometrical interpretation of the weighting method in the criterion space, where the problem may be stated as

$$\min_{\mathbf{z} \in \mathbf{f}(\Omega)} \lambda^T \mathbf{z} \qquad (4)$$

With a fixed λ a linear function is minimized in $\mathbf{f}(\Omega)$, which is the image of the feasible set. As is illustrated in fig. 1, even the great majority of Pareto optima may be unattainable by this method if the lower boundary of $\mathbf{f}(\Omega)$ is not convex.

Constraint method

As the second technique for generating Pareto optimal solutions to a multicriterion problem the costraint method is considered. In this approach the original formula (1) is replaced by

$$\min_{\mathbf{x} \in \Omega \cap \Omega_k(\varepsilon)} f_k(\mathbf{x}) \quad , \qquad (5)$$

where

$$\Omega_k(\varepsilon) = \{ \mathbf{x} \mid f_i(\mathbf{x}) \leq \varepsilon_i , \quad i \neq k \}$$

and

$$\varepsilon \in E_k = \{ [\varepsilon_1, \varepsilon_2, \ldots, \varepsilon_{k-1}, \varepsilon_{k+1}, \ldots, \varepsilon_n]^T \mid \Omega_k(\varepsilon) \neq \phi \} .$$

Verbally this states that one criterion is taken as a scalar objective function and the others are constrained by the suitable chosen constants ε_i. By systematic variation of these parameters the entire Pareto optimal set is obtained also in nonconvex cases. The constraint method may be viewed as having an established position as a basic numerical technique in vector optimization, and it is widely discussed in the literature.

Minimax approach

In this section a method based on the l_∞-norm or more properly on the distance function induced by it is presented. This approach leads to a minimax problem, where the largest deflection from the so-called ideal solution is minimized. By introducing certain parameters a method for generating the Pareto optimal set may then be constructed. First the ideal solution needed in this approach is defined by

$$\mathbf{z}^{id} = [\min_{\mathbf{x} \in \Omega} f_1(\mathbf{x}), \min_{\mathbf{x} \in \Omega} f_2(\mathbf{x}), \ldots, \min_{\mathbf{x} \in \Omega} f_m(\mathbf{x})]^T . \qquad (6)$$

In order to determine this point in the criterion space it is necessary to search for the minimum of every f_i in Ω, which calls for solving m scalar optimization problems. Generally the ideal is not feasible, ie $\mathbf{z}^{id} \notin \mathbf{f}(\Omega)$. The distance between $\mathbf{z} \in \mathbf{f}(\Omega)$ and the ideal $\mathbf{z}^{id} \in R^m$ is measured by the metric function

$$d_\infty(\mathbf{z}, \mathbf{z}^{id}) = \max_{i = 1,2,\ldots,m} | z_i - z_i^{id} | . \qquad (7)$$

Because a scale invariant solution to the problem is wanted, a normalized vector objective function

$$\tilde{\mathbf{f}}(\mathbf{x}) = [\tilde{f}_1(\mathbf{x}), \tilde{f}_2(\mathbf{x}), \ldots, \tilde{f}_m(\mathbf{x})]^T , \qquad (8)$$

where the components are defined by

$$\tilde{f}_i(\mathbf{x}) = \frac{f_i(\mathbf{x}) - \min f_i(\mathbf{x})}{\max f_i(\mathbf{x}) - \min f_i(\mathbf{x})} , \qquad (9)$$

is introduced. Thus the values of every normalized criterion are limited to an equal range, ie $\tilde{f}_i(\mathbf{x}) \in [0,1]$. If the notation $\tilde{\mathbf{z}} = \tilde{\mathbf{f}}(\mathbf{x})$ is used, the problem is now looking for the vector $\tilde{\mathbf{z}} \in \tilde{\mathbf{f}}(\Omega)$ which in the sense of d_∞-metric is nearest to the ideal $\tilde{\mathbf{z}}^{id} = 0$, and it may be formulated as

$$\min_{\tilde{\mathbf{z}} \in \tilde{\mathbf{f}}(\Omega)} d_\infty(\tilde{\mathbf{z}}, 0) . \qquad (10)$$

One Pareto optimal point is usually obtained as a solution to this scalar optimization problem, which is next modified to solve the multicriterion problem (1). If certain parameters w_i, $i = 1,2,\ldots,m$, are used as weights for the criteria in the same way as was done in the weighting method, the problem can be written in the form

$$\min_{\mathbf{x}\in\Omega} \max_{i} (w_i \tilde{f}_i(\mathbf{x})) \quad . \tag{11}$$

Now the whole Pareto optimal set may be generated by parametrically varying the weights in the objective function. This method is illustrated in fig. 2, which shows that the minimax approach may be interpreted as searching for that point $\tilde{\mathbf{z}}^* \in \tilde{\mathbf{f}}(\Omega)$ where the rectangular level set just touches $\tilde{\mathbf{f}}(\Omega)$. The corresponding vector $\mathbf{x}^* \in \Omega$ is the Pareto optimum actually needed by the designer. The geometrical meaning of the weight variation is changing the side ratio of the rectangle, which in turn may be viewed as an origo centered ball generated by the d_∞-metric in the criterion space. From this discussion it should be clear that using the minimax approach given in (11) all pareto optima can be obtained regardless of the convexity of the minimal curve.

Several techniques for the numerical treatment of the minimax problems have been presented in the literature, and the one chosen here is that where the scalar problem

$$\begin{aligned} &\min_{\gamma,\ \mathbf{x}\in\Omega} \gamma \\ &\text{subject to} \\ &w_i \tilde{f}_i(\mathbf{x}) \le \gamma, \quad i = 1,2,\ldots,m \end{aligned} \tag{12}$$

is considered. In the sequel this special formula is utilized in developing an interactive algorithm for solving the multicriterion design problem.

General aspects

Each of those three numerical techniques discussed in this chapter includes parameters to be varied in generating Pareto optimal solutions to the multicriterion problem (1). The geometrical interpretation of these parameters facilitates the understanding of the methods and gives a natural basis for future development concerning different interactive approaches. By some parameter values it may happen, however, that the constraint problem (5) has no unique solution. This is due to the so-called weakly Pareto optimal points, which are defined next.

Definition. A vector $\mathbf{x}^* \in \Omega$ is called weakly Pareto optimal for problem (1) if and only if there exists no vector $\mathbf{x} \in \Omega$ such that $f_i(\mathbf{x}) < f_i(\mathbf{x}^*)$ for $i = 1,2,\ldots,m$.

From the definition it may be concluded that every Pareto optimum is also weakly Pareto optimal but the converse is not true. This concept is illustrated in fig. 3, where the flat parts of the boundary of $\mathbf{f}(\Omega)$ which are parallel to the coordinate axes, form the corresponding weakly minimal solutions in the criterion space. In effect, all the numerical techniques considered here meet difficulties in such problems where weakly Pareto optimal solutions exist. It should be noticed, however, that in some cases the designer may be interested in weak Pareto optima as well.

The weighting method, which is a suitable solution technique for convex problems, and the minimax approach, applicable also to nonconvex problems, may be both considered as members of a larger algorithm family called p-norm methods [10]. This is a collection of all those methods which may be obtained by using the distance function d_p induced by the l_p-norm

$$\| \mathbf{w}\mathbf{f} \|_p = \left(\sum_{i=1}^{m} (w_i f_i)^p \right)^{1/p}, \quad 1 \le p \le \infty \quad , \tag{13}$$

where the diagonal matrix

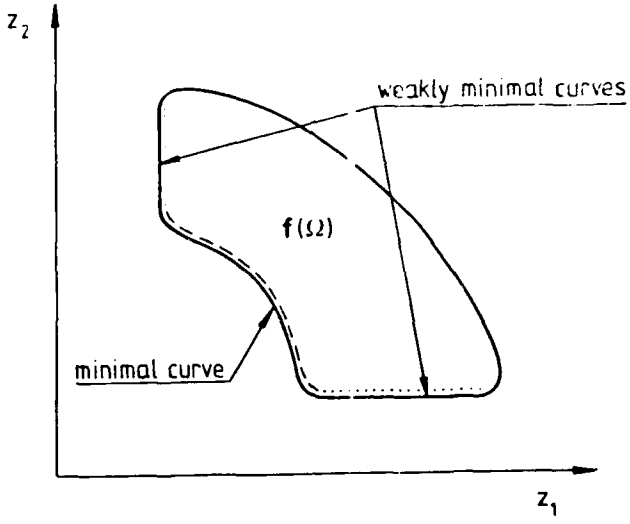


Figure 3. Minimal and weakly minimal solutions in bicriterion case.

$$W = [w_1, w_2, \ldots, w_m], \quad w_i \ge 0 \ ,$$

is used to bring in the parameters w_i. Now the d_p-family thus defined includes the weighting method and the minimax approach as special cases corresponging to the values $p = 1$ and $p = \infty$, respectively.

Multicriterion optimization of structures

Problem formulation

Even though various design criteria may arise in optimizing structures for different operational purposes, a specific multicriterion problem where the weight of the structure and some chosen nodal displacements are taken as components of the vector objective function is discussed in this paper. The same problem has been considered earlier in truss optimization [6], [8], and here it is extended to embrace plane frames as well. The structural design problem is now stated as

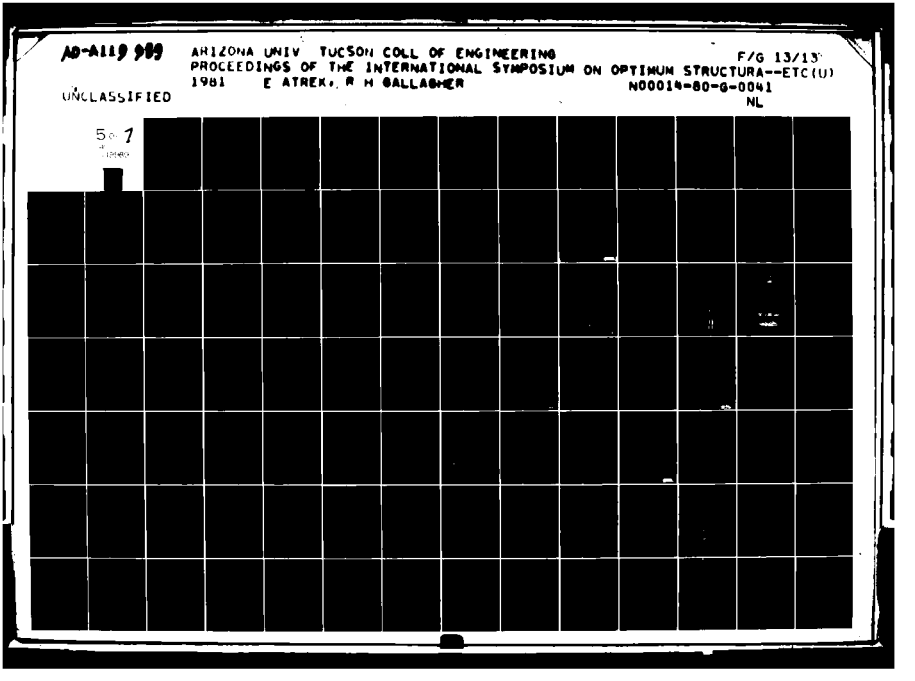
$$\min_{\mathbf{x}\in\Omega} \mathbf{f}(\mathbf{x}) = [W, \Delta_1, \Delta_2, \ldots, \Delta_{m-1}]^T \ , \tag{14}$$

where W is the weight of the structure and Δ_j, $j = 1,2,\ldots,m-1$, are displacement criteria. This multicriterion formula is apparently suitable for elastic structures in general, but only trusses and plane frames with specified geometry and topology are considered here to illustrate the applicability of the vector optimization theory in structural design. If it is further assumed that the members of the structure consist of the same material, which also implies that the minimum weight design and the minimum volume design are equal, it is possible to choose member areas A_i, $i = 1,2,\ldots,k$, as the only design variables. This is true even for plane frames if the well-known expressions

$$\begin{aligned} I &= a A^p \ , \quad a,p \in R \ , \\ Z &= c A^q \ , \quad c,q \in R \ , \end{aligned} \tag{15}$$

where I is the moment of inertia and Z is the section modulus, are used for the members. In addition, constitutive as well as geometrical linearity is assumed throughout this chapter.

The detailed formulation of the problem is only briefly discussed here, and it may be found in reference


AD-A119 909
ARIZONA UNIV TUCSON COLL OF ENGINEERING
PROCEEDINGS OF THE INTERNATIONAL SYMPOSIUM ON OPTIMUM STRUCTURA--ETC(U)
1981 E ATREK, R H GALLAGHER
F/G 13/13
N00014-80-G-0041
NL
UNCLASSIFIED
5 of 7

[11] where the minimum weight design of trusses and plane frames is considered. The only difference is that now the vector valued objective function (14), which includes also displacement criteria in addition to the weight, is used. Comparisons between the two basic techniques of structural analysis [6] suggest that the displacement method appears preferable to the force method because it offers simple linear expressions also for the displacement criteria, as can be seen from

$$W = \sum_{i=1}^{k} A_i L_i \ , \qquad \Delta_j = X_j \ , \quad j = 1,2,\ldots,m-1 \ , \tag{16}$$

where L_i is the length of member i and X_j is a nodal displacement chosen into the objective function. The special numbering of the nodal coordinates used in (16) should cause no confusion in this general presentation, and certainly any numbering system wanted by the designer can be used. The nodal displacements X_i, $i = 1,2,\ldots,\ell$, where ℓ is the number of the nodal degrees of freedom, may now be regarded as additional design variables, also called state variables [12]. Thus the design variable vector

$$\mathbf{x} = [A_1, A_2, \ldots, A_k, X_1, X_2, \ldots, X_\ell]^T \ , \tag{17}$$

typical in structural optimization, is obtained. If limits for the member areas and the stresses are imposed, then the feasible set of the multicriterion problem (14) is defined by

$$\Omega = \{ \mathbf{x} \in R^{k+\ell} \mid \mathbf{P} = \mathbf{KX}, \ \underline{\sigma}_i \le \sigma_i \le \bar{\sigma}_i, \ \underline{A}_i \le A_i \le \bar{A}_i \} \ , \tag{18}$$

where **P** is the loading matrix, **K** is the stiffness matrix and **X** is the displacement matrix, which are the usual notations found in displacement method analysis. In this stiffness equation each column of the matrices **P** and **X** corresponds to one loading condition. Further, the notations $\underline{\sigma}_i$, $\bar{\sigma}_i$, $\underline{A}_i$ and $\bar{A}_i$ are used for the lower and the upper limits of the stresses σ_i and the member areas A_i, respectively. For plane frames member stresses can be calculated from the common expression

$$\sigma_i = \frac{M_i}{Z_i} + \frac{N_i}{A_i} \ , \tag{19}$$

where M_i is the bending moment of member i in the critical section and N_i is the normal force in member i. Thus the stress constraints for plane frames are nonlinear functions of the design variables whereas for trusses, for which $M_i = 0$ in (19), they are linear functions of the nodal displacements X_i. The stiffness equation, however, destroys the linearity and the convexity of the problem in both cases. If also displacement constaints occur, the approach presented is still applicable by simply introducing these quantities into the objective function. This is also motivated by the fact that the limits for the displacements cannot usually be defined exactly.

In the sequel two examples are given to illustrate the multicriterion design theory discussed in this paper. Pareto optimal solutions are generated for both problems by using the numerical techniques presented in the previous chapter. The bicriterion frame example has been chosen so that the results can be represented graphically both in the design space and in the criterion space. On the contrary, the truss example with three criteria has been introduced to illustrate the difficulties which arise in representing the Pareto optimal set and the minimal set when the number of design variables or criteria is increased.

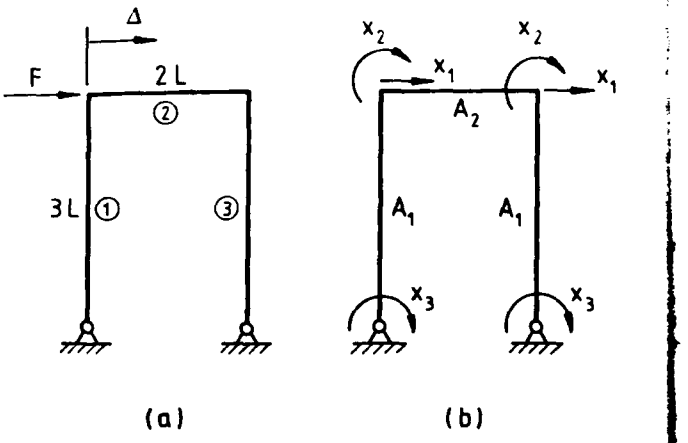
Three-member frame

As an introduction to the multicriterion approach in structural design a three-member plane frame shown in fig. 4 is first considered. The structure is subject to only one loading condition, which consists of a horizontal force F at the left-hand free node of the frame. In addition to the weight of the structure the horizontal displacement of the loaded node is chosen into the objective function. The effect that is caused by extensions of the members is not included in the kinematic model applied to this problem, and it is further assumed that both the vertical members are equal, ie they have the same design variable $A_1 = A_3$. The structure now behaves antimetrically, and the coordinate system shown in fig. 4(b) can be used. In addition, the displacement criterion as well as the constraints imposed on the design variables and the member stresses are presented in the figure. This example has been modified from a scalar optimization problem treated in [11], and the expressions

$$I = 3.200\ A^2 \qquad Z = 1.452\ A^{3/2} \tag{20}$$

are used here for all members. Two criteria, five design variables, three equality constraints, two stress constraints for each member and two inequality constraints for both design variables occur in the design formulation of this bicriterion frame problem.

Even though the structure is hyperstatic, it behaves like an isostatic one, ie the element forces do not depend on the values of the member areas but are constants. Thus the feasible region in the A_1A_2-plane may be easily formed by the upper and the lower limits of the member areas, as is shown in fig. 5. The Pareto optimal polygonal line, which connects the extreme vertices of the feasible set, is also presented in the figure. Most of the Pareto optima lie in the interior of the feasible region, and only a short line segment AE is located on the boundary of the rectangle. The corresponding minimal curve and the whole image $f(\Omega)$ can be seen in fig. 6 where the situation in the criterion space is illustrated.



L = 100 cm $\bar{\sigma}$ = 10 kN/cm² $\bar{A}$ = 30 cm²

E = 2.07 · 10⁴ kN/cm² $\underline{\sigma}$ = -10 kN/cm² $\underline{A}$ = 0 cm²

F = 2.07 kN

Figure 4. Three-member plane frame under one loading condition.

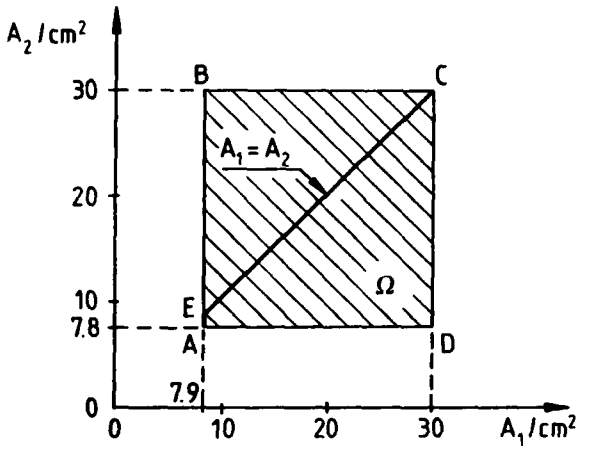


Figure 5. Feasible region ABCD and Pareto optimal polygonal line AEC of three-bar frame.

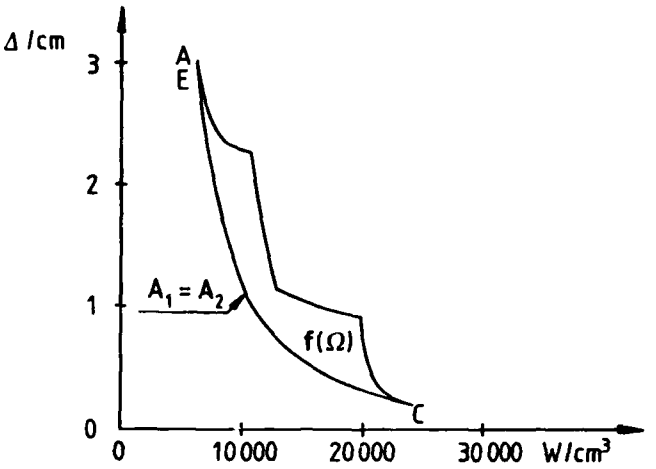


Figure 6. Feasible region in criterion space and minimal curve AEC of three-bar frame.

Four-bar truss

Next a four-bar plane truss shown in fig. 7 is considered. In this example two displacement criteria in addition to the weight of the structure are included. The first is the vertical displacement of the outer loaded node under loading condition 1 and the second is the vertical displacement of the loaded node under loading condition 2. Both these criteria and the corresponding loadings as well as the constraints imposed on the design variables and the member stresses are also presented in the figure.

Because of the great number of Pareto optima there easily arise difficulties in representing the results of a multicriterion problem. The numerical results of this example are given in table 1, and the corresponding graphic illustration is shown in figures 8 and 9. It may be noticed that both the displacement criteria achieve their minimum value in the same point where the member areas are in their upper limits. This need not, however, be the situation in general, but also displacement criteria may be conflictive.

Table 1. Pareto optimal and minimal solutions to four-bar truss problem.

A_1 cm^2	A_2 cm^2	A_3 cm^2	A_4 cm^2	W cm^3	Δ_1 $10^{-2}cm$	Δ_2 $10^{-2}cm$
1.00	1.41	4.24	3.00	2600	7.33	3.00
1.29	1.82	4.24	3.26	2880	6.28	2.92
1.16	1.64	4.44	3.88	2960	6.28	2.69
1.00	1.42	6.14	4.44	3420	6.27	2.06
1.00	1.41	8.00	8.00	4660	5.46	1.44
1.65	2.34	4.24	4.10	3340	5.22	2.73
1.45	2.05	4.97	4.52	3470	5.22	2.37
1.20	1.70	7.08	5.51	4060	5.22	1.74
1.06	1.50	8.00	8.00	4710	5.22	1.44
2.21	3.12	4.50	5.45	4130	4.17	2.44
1.93	2.73	5.61	5.50	4230	4.17	2.06
1.72	2.44	6.87	5.89	4500	4.17	1.74
1.48	2.09	8.00	8.00	5040	4.17	1.44
2.96	4.20	5.99	7.29	5550	3.12	1.83
2.42	3.41	8.00	8.00	5790	3.12	1.44
8.00	8.00	8.00	8.00	9330	2.06	1.44

$w_{min} = 2600\ cm^3$ $\quad \Delta_{1\,min} = 2.06 \cdot 10^{-2} cm$

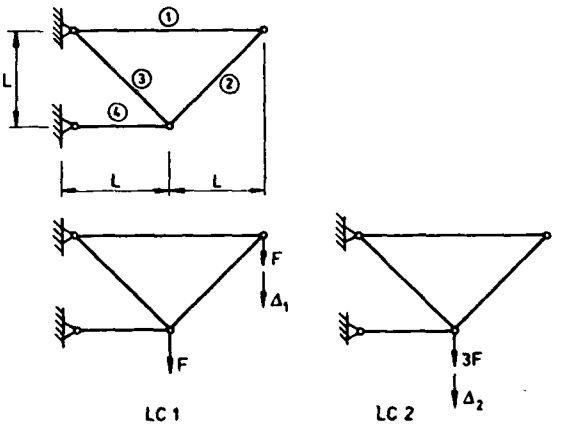
$\Delta_{2\,min} = 1.44 \cdot 10^{-2} cm$

Interactive solution method

In order to lessen the computational and human effort in the design process it seems preferable instead of generating all Pareto optima to restrict the survey only to a certain subset of them. One possibility, which may prove to be a suitable approach also in structural optimization, is to develop interactive algorithms where the designer participates the process in every Pareto optimum achieved to determine the direction of the next step. In this chapter a technique of this category, based on the method of pairwise comparisons given by Saaty [13] and trade-off studies of the minimax formula (12), is introduced.

Method of pairwise comparisons

The aim of this method is to produce the weights w_i for the minimax problem (11) by using pairwise comparisons for the criteria. First a reciprocal matrix **A**, which includes the relative weights of the criteria, is considered. This matrix is defined by



$L = 200\ cm$ $\quad \bar{\sigma} = 10\ kN/cm^2$ $\quad \bar{A} = 8\ cm^2$

$E = 2 \cdot 10^4\ kN/cm^2$ $\quad \underline{\sigma} = -10\ kN/cm^2$ $\quad \underline{A} = 0\ cm^2$

$F = 10\ kN$

Figure 7. Four-bar plane truss under two loading conditions.

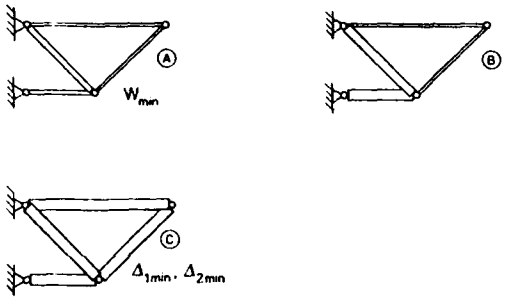


Figure 8. Pareto optimal trusses corresponding to corner points of minimal surface. A different scale is used for the lengths and the widths of the bars.

$$\mathbf{A} = \begin{bmatrix} \frac{w_1}{w_1} & \frac{w_1}{w_2} & \cdots & \frac{w_1}{w_m} \\ \frac{w_2}{w_1} & \frac{w_2}{w_2} & \cdots & \frac{w_2}{w_m} \\ \vdots & \vdots & & \vdots \\ \frac{w_m}{w_1} & \frac{w_m}{w_2} & \cdots & \frac{w_m}{w_m} \end{bmatrix} \qquad (21)$$

and its positive elements satisfy the reciprocal rule $a_{ij} = 1/a_{ji}$. The matrix has the property that if it is multiplied by the vector $\mathbf{w} = [w_1, w_2, \ldots, w_m]^T$ then the vector $m\mathbf{w}$ is obtained, ie

$$\mathbf{Aw} = m\mathbf{w} \ . \qquad (22)$$

This equation has a nonzero solution if and only if m is an eigenvalue of **A**. All the eigenvalues μ_i, i = 1,2,...,m, are zero except one, notated here by μ_{max}, which according to eq. (22) is equal to m. This can be seen immediately from (21) where every row is a constant multiple of the first row, ie **A** has unit rank. The solution **w** of this problem is any column of **A**, and these solutions differ by a multiplicative constant. The vector **w** may be normalized so that its components sum to unity. Then the result is a unique solution of eq. (22) no matter which column is used. Further, the matrix **A** satisfies the cardinal consistency property $a_{ij}a_{jk} = a_{ik}$ and is called consistent.

In the sequel only estimates of the ratios w_i/w_j in the matrix are known and the object is to determine the corresponding weights. The notations **A'** and **w'** are used here for the estimated matrix and its eigenvector, respectively. The elements of **A'** are now obtained by pairwise comparisons of the criteria and the weights $w'_1, w'_2, \ldots, w'_m$ may then be calculated by solving the eigenvalue problem of this matrix. In this case, however, the combined consistency relation given above need not hold, nor need an ordinal relation of the form: $f_i \prec f_j$, $f_j \prec f_k$ imply $f_i \prec f_k$ (notation $\prec$ is used as "more important than") hold. It turns out that **A'** is consistent if and only if $\mu'_{max} = m$. With inconsistency $\mu'_{max} > m$ always, but the ordinal consistency is preserved, ie, if $f_i \preceq f_j$ then $w'_i \geq w'_j$. Finally the departure of μ'_{max} from m can be shown to measure the inconsistency which may call for revising the judgements in the matrix. It should be mentioned that also another consistency criterion, where the computation of the maximum eigenvalue is not needed at all, has been reported [14].

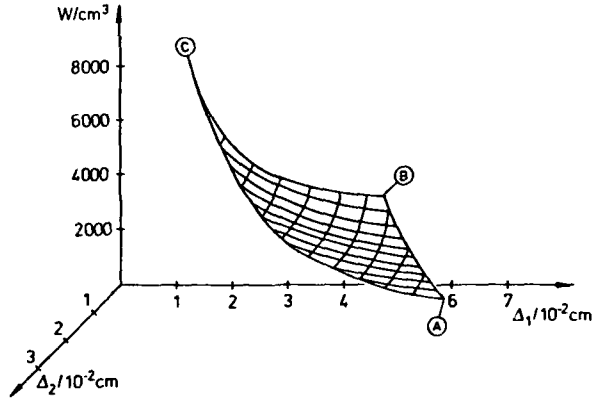


Figure 9. Minimal surface of four-bar truss.

Various applications of this technique, which was only briefly described here, to different decision making problems can be found in the literature [15], [16], and it is now proposed for structural design problems with several criteria as well. The obvious advantage of the method is that the weights are obtained by pairwise comparisons of the criteria which is easier for the designer. Encouraging results have been achieved by using a scale ranging from one to nine, also given by Saaty [13], but an additional examination of different scales is recommended for structural problems.

Trade-off study and interactive design method

A comprehensive trade-off study coupled with the constraint method is presented in reference [17], but it is not applicable to the minimax approach discussed here. The interactive sheme, however, uses trade-off numbers and thus it is necessary to give a preliminary survey on the subject. For convenience a simplified scalar problem

$$\begin{aligned} &\min \gamma \\ &\text{subject to} \\ &f_i(\mathbf{x}) - \gamma \leq 0, \quad i = 1,2,\ldots,m \ , \\ &g_i(\mathbf{x}) \leq 0 \quad , \quad i = 1,2,\ldots,r \ , \\ &h_i(\mathbf{x}) = 0 \quad , \quad i = 1,2,\ldots,s \ , \end{aligned} \qquad (23)$$

instead of the weighted and normalized formula (12) is considered. The Kuhn-Tucker conditions of this problem can be written in the form:

$$\begin{aligned} &\sum_{i=1}^{m} u_i \nabla f_i(\mathbf{x}) + \sum_{i=1}^{r} u_{m+i} \nabla g_i(\mathbf{x}) + \\ &\sum_{i=1}^{s} v_i \nabla h_i(\mathbf{x}) = 0 \ , \\ &1 - \sum_{i=1}^{m} u_i = 0 \ , \\ &u_i \geq 0 \quad , \quad i = 1,2,\ldots,m \ , \end{aligned} \qquad (24)$$

$$u_i\,(f_i(\mathbf{x}) - \gamma) = 0, \quad i = 1,2,\ldots,m \quad ,$$

$$u_{m+i}\,g_i(\mathbf{x}) = 0 \quad , \quad i = 1,2,\ldots,r \quad .$$

In order to find out the trade-off number α_{jk} relating the change of f_k with the change of f_j the first of these equations is divided by u_j which is assumed to be strictly positive. By applying the sensitivity theorem (Luenberger, [18], p. 236) it may be then concluded that

$$\alpha_{jk} = -\frac{u_k}{u_j} \quad . \tag{25}$$

This result is very useful in solving a multicriterion problem because it provides the designer with an additional information about the properties of the minimal surface. Its geometrical interpretation in the criterion space states that the vector

$$\mathbf{u}^* = [u_1^*, u_2^*, \ldots, u_m^*]^T \tag{26}$$

whose components are the Kuhn-Tucker multipliers corresponding to a Pareto optimum $\mathbf{x}^*$, is normal to the tangent plane of the minimal surface at $\mathbf{z}^*$. In convex problems this means that the multipliers u_i^*, $i = 1,2,\ldots,m$, can be regarded as the weighting coefficients used in the scalar formula (3). In nonconvex cases, however, a given vector $\mathbf{u}^*$ as well as the numbers α_{jk} associated with it may correspond to more than one Pareto optimal solution. The trade-off study given here can be easily modified for the original problem (12) which is used as a basis of the interactive design technique discussed next.

In this algorithm the method of pairwise comparisons coupled with the use of trade-off numbers is applied. The object is to determine new weights w_i', $i = 1,2,\ldots,m$, for the minimax problem (11) in every iteration step. These can be obtained as an eigenvector $\mathbf{w}'$ of the matrix $\mathbf{A}'$ which is formed by the designer. Quotients w_j'/w_k', which are the elements of this matrix, may be geometrically interpreted as side ratios of the rectangular level set generated by the d_∞-metric in the criterion space. By using pairwise comparisons of the criteria it is now possible to compute each element a_{jk}' when only the trade-off numbers α_{jk} are known. From the relation

$$\Delta f_j(\mathbf{x}^*) = \alpha_{jk}\,\Delta f_k(\mathbf{x}^*) \tag{27}$$

an estimate for the change of f_j corresponding to the change of f_k at $\mathbf{x}^*$ is obtained. If $\Delta f_k(\mathbf{x}^*)$ is chosen by the designer, as is suggested in this approach, the elements of $\mathbf{A}'$ can be calculated by (27) and

$$a_{jk}' = \frac{\frac{c}{w_k} + \Delta f_k(\mathbf{x}^*)}{\frac{c}{w_j} + \Delta f_j(\mathbf{x}^*)} \quad , \tag{28}$$

where c is the value of the distance function d_∞ at $\mathbf{x}^*$. Geometrically this expression simply gives the new side ratio of the rectangle. By making all the necessary pairwise comparisons the matrix $\mathbf{A}'$ is formed and the corresponding eigenvalue problem may be solved. First the consistency rate of $\mathbf{A}'$, however, should be checked because inconsistency easily appears. Thus it may be necessary to correct the values of the elements a_{jk}' by the designer to improve the consistency rate.

The interactive design method introduced in this chapter is now summarized in the following:

1° Choose the starting weights w_i, $i = 1,2,\ldots,m$, for the normalized criteria $\tilde{f}_i$ by using the method of pairwise comparisons.

2° Solve the corresponding scalar problem (12) with fixed weights for the Pareto optimum $\mathbf{x}^*$.

3° Compute $\mathbf{z}^*$ and consider the result. If it is satisfactory then stop, if it is not then continue.

4° Determine the trade-off numbers α_{jk} at $\mathbf{x}^*$.

5° Impose the allowable changes $\Delta f_k(\mathbf{x}^*)$ and compute the elements a_{jk}' for the matrix $\mathbf{A}'$ by using the relations (27) and (28).

6° Check the consistency rate of $\mathbf{A}'$ and make the necessary corrections for its elements.

7° Determine the new weights w_i', $i = 1,2,\ldots,m$, by solving the eigenvector of $\mathbf{A}'$.

8° Go to 2°.

If some additional requirements not included in the optimization model occur, it is possible to generate more Pareto optima in the neighbourhood of the final design by properly varying the weights w_i in (12).

Conclusions

In this paper the basic principles of multicriterion optimization and three numerical methods for the solution of Pareto optima are presented. In addition an interactive design technique where some parameters are joined with the minimax problem and trade-offs obtained from the Kuhn-Tucker multipliers are used is introduced. A special structural problem where the weight and some chosen nodal displacements are chosen as design criteria is formulated. Especially trusses and plane frames are considered to illustrate the applicability of the vector optimization theory in structural design.

Only elastic structures have been examined here, but also multicriterion plastic design will undoubtedly deserve attention in the future. In order to still more effectively consider the practical design requirements the suitability of new criteria, different from those used in this paper, should be studied as well. Further, effective numerical techniques for generating Pareto optimal solutions to these specific structural problems will be needed. It seems, however, necessary to solve some open questions concerning the graphic presentation of the results before it is reasonable to tackle large problems with several criteria and numerous variables. This is due to the fact that the number of Pareto optima is usually great, and thus a reduced solution set should be considered. Problems arise also in the criterion space where the minimal surface becomes difficult to present as soon as the number of criteria exceeds two.

One way of reducing the number of the Pareto optima considered by the designer is to develop interactive algorithms where only a few Pareto optimal solutions are generated. Sometimes it is preferable, however, to aim at obtaining the whole Pareto optimal set which is then offered to the designer for his final choice. Both these approaches seem suitable for structural problems, and they should be further developed in future research work in this field.

Acknowledgements

This research has been supported by The Academy of Finland and The Emil Aaltonen Foundation. Discussions with Mr. Risto Silvennoinen are gratefully acknowledged.

References

[1] Pareto, V., Cours d'economie politique, F. Rouge, Lausanne, 1896.

[2] Baier, H., Über algorithmen zur ermittlung und charakterisierung Pareto-optimaler lösungen bei entwurfsaufgaben elastischer tragwerke, ZAMM 57, 1977, 318 - 320.

[3] Leitmann, G., Some problems of scalar and vector-valued optimization in linear viscoelasticity, J. Optim. Theory Appl. 23, 1977, 93 - 99.

[4] Osyczka, A., An approach to multicriterion optimization problems for engineering design, Comp. Meths. Appl. Mech. Eng. 15, 1978, 309 - 333.

[5] Rao, S. S. and Hati, S. K., Game theory approach in Multicriteria optimization of function generating mechanisms, J. Mech. Des. Trans. ASME 101 1979, 398 - 405.

[6] Koski, J., "Truss optimization with vector criterion", Tampere University of Technology, Publications 6, Tampere, 1979.

[7] Carmichael, D. G., Computation of Pareto optima in structural design, Int. J. Num. Meths. Eng. 15, 1980, 925 - 929.

[8] Koski, J. and Silvennoinen, R., Pareto optima of isostatic trusses, Submitted for publication.

[9] Hwang, C. L. and Masud, A. S. M., Multiple objective decision-making methods and applications, Lecture Notes in Economics and Mathematical Systems 164, Springer-Verlag, New York, 1979.

[10] Lightner, M. R. and Director, S. W., Multiple criterion optimization for the design of electronic circuits, IEEE Transactions on Circuits and Systems 28 No. 3, 1981, 169 - 179.

[11] Majid, K. I., Optimum design of structures, Newnes-Butterworths, London, 1974.

[12] Haug, E. J. and Arora, J. S., Applied optimal design, mechanical and structural systems, John Wiley & Sons, New York, 1979.

[13] Saaty, T. L., A scaling method for priorities in hierarchical structures, Journal of mathematical psychology 15 No. 3, 1977, 234 - 281.

[14] Vargas, L. G., A note on the eigenvalue consistency index, Applied mathematics and computation 7, 1980, 195 - 203.

[15] Saaty, T. L., Applications of analytical hierarchies, Mathematics and computers in simulation XXI, 1979, 1 - 20.

[16] Wind, Y. and Saaty, T. L., Marketing applications of the analytic hierarchy process, Management science 26 No. 7, 1980, 641 - 658.

[17] Haimes, Y. Y. and Chankong, V., Kuhn-Tucker multipliers as trade-offs in multiobjective decision-making analysis, Automatica 15, 1979, 59 - 72.

[18] Luenberger, D. G., Introduction to linear and nonlinear programming, Addison-Wesley, Reading, Massachusetts, 1973.

AD-P000 078

AN APPROACH TO MULTICRITERION OPTIMIZATION FOR STRUCTURAL DESIGN

Doc.dr hab.inż. Andrzej OSYCZKA
Technical University of Cracow
ul.Warszawska 24
31-155 Kraków
POLAND

SUMMARY

In many structural design tasks the designer's goal is to minimise and/or maximize several functions simultaneously. This situation is formulated as a multicriterion optimization problem. Since optimization tasks in structural design are often modelled by means of nonlinear programming, a multicriterion approach to this programming is discussed in the paper. The problem is formulated as follows: find a vector of design variables which satisfies constraints and optimizes a vector function which represents several noncomparable criteria. The min-max approach to this problem is presented. The aim of this approach is to define the best compromise solution, i.e., the solution that gives such values of the objective functions which are as close as possible to their separately attainable extremes. Then, some methods for seeking the optimum are shortly described. These methods are based on optimization techniques for one-criterion problems.

The optimum defined in the paper gives one solution. However, using the min-max approach we can also influence the priority of the criteria. Seeking the optimum in the min-max sense for different values of priority coefficients a set of evenly distributed solutions which are optimal in the Pareto sense (noninferior solutions) can be easily obtained.

To illustrate the advantages of this approach, the multicriterion optimization problem for an I-beam design is presented. The problem is to find the dimensions of the beam which satisfy strength and geometric constrains and optimize two objective functions: cross-section area which is related to the volume of the beam and the deflection of the beam. Both functions are to be minimised. In this problem the criteria are contrary to each other, i.e., the best solution for the first objective function gives the worst solution for the second function and conversely.

INTRODUCTION

Facing a complex optimisation problem an engineer often has to deal with a situation in which several non-commensurable criteria are to be considered. This leads to a multicriterion optimisation problem which recently evokes a great deal of interest. A lot of different approaches to this problem have been developed such as weighting objective method (1), the trade-off study method (2), the hierarchical optimisation (3) and the goal programming (4),(5). Some other methods are described and reviewed in (6).

In this paper the min-max approach to the multicriterion optimization problem for nonlinear programming is discussed since this programming is very often used to model structural design problems. The aim of this approach is to define the best compromise solution considering all criteria simultaneously and on terms of equal importance.

PROBLEM FORMULATION

The problem is formulated as follows: Find the vector $x^* = [x_1^*, \ldots, x_n^*]^T$ that will satisfy the inequality constraints

$$g_j(x) \geq 0 \qquad j=1,\ldots,m \qquad (1)$$

the equality constraints

$$h_j(x) = 0 \qquad j=m+1,\ldots,p \qquad (2)$$

and optimize the vector function

$$f(x) = [f_1(x), \ldots, f_k(x)]^T$$

where $x = [x_1, \ldots, x_n]^T$ is a vector of variables defined in n-dimensional Euclidean space E^n.

Here $g_j(x)$, $h_j(x)$ are linear or nonlinear functions of variables $x_1, \ldots, x_n$. The constraints given by (1) and (2) define the feasible region X and any point x in X defines a feasible solution. The vector function $f(x)$ is a function which maps the set X into E^k. The k components of the vector $f(x)$ represent the non-commensurable objective functions (performance criteria) which must be considered. We use $I = \{1, \ldots, k\}$ to denote the set of indices for all the objective functions.

We assume that all the objective functions are to be minimised. The maximisation problem for any objective function can be easily converted to a minimisation problem by employing the identity

$$\max f_i(x) = - \min(- f_i(x)) \qquad (3)$$

DEFINITION OF THE OPTIMUM

The points of references for the multicriterion optimisation problem are in all certainty the extremum solutions which can be obtained by solving optimization problems for each criterion separately. Assuming that these extrema can be found let $x^{o(i)} = [x_1^{o(i)}, \ldots, x_n^{o(i)}]^T$ be a vector of variables which minimises the i-th objective function $f_i(x)$. In other words,

the vector $x^{o(i)} \in X$ is such that

$$f_i(x^{o(i)}) = \min_{x \in X} f_i(x) \qquad (4)$$

Assuming that for every $x \in X$, $f_i(x) \neq 0$, the fractional deviation from the extremum for the i-th objective function can be calculated from the formula

$$z_i'(x) = \frac{\mathrm{abs}(f_i(x) - f_i(x^{o(i)}))}{\mathrm{abs}(f_i(x^{o(i)}))} \qquad (5)$$

or from the formula

$$z_i''(x) = \frac{\mathrm{abs}(f_i(x) - f_i(x^{o(i)}))}{\mathrm{abs}(f_i(x))} \qquad (6)$$

It should be mentioned that by applying formula (3) all the functions are minimized. However, for the originally stated problem, the fractional deviations from the extrema have a different physical interpretation for the functions which are to be minimized and for those which are to be maximized. Formula (5) for the functions which are to be minimized defines their fractional increment, whereas, for those to be maximized it defines their fractional decrement. Formula (6) works conversely.

For any $x \neq x^{o(i)}$ the values of $z_i'(x)$ and $z_i''(x)$ for the i-th function will be different. The best compromise solution should give the smallest values of the fractional deviations (both the fractional increments and decrements) for all the objective functions.

Let $z(x) = [z_1(x), \ldots, z_k(x)]^T$ be a vector of the fractional deviations which is defined in E^k. The i-th component of the vector $z(x)$ will be evaluated as follows:

$$z_i(x) = \max\{z_i'(x), z_i''(x)\} \qquad (7)$$

Formula (7) choses the maximum from two values $z_i'(x)$ and $z_i''(x)$.

Using the min-max principle of optimality the best compromise solution can be defined as follows:

The point $x^* \in X$ is optimal in the min-max sense, if for every $x \in X$ the following recurrence formula is satisfied:

step 1 $v_1(x^*) = \min_{x \in X} \max_{i \in I} \{z_i(x)\}$

and then $I_1 = \{i_1\}$, where i_1 is the index for which the value of $z_i(x)$ is maximal.

If there is a set of solutions $X_1 \subset X$ which satisfies step 1, then

step 2 $v_2(x^*) = \min_{x \in X_1} \max_{\substack{i \in I \\ i \notin I_1}} \{z_i(x)\}$

and then $I_2 = \{i_1, i_2\}$, where i_2 is the index for which the value of $z_i(x)$ in this step is maximal.

. . . . . (8)

If there is a set of solutions $X_{r-1} \subset X$ which satisfies step r-1, then

step r $v_r(x^*) = \min_{x \in X_{r-1}} \max_{\substack{i \in I \\ i \notin I_{r-1}}} \{z_i(x)\}$

and then $I_r = \{I_{r-1}, i_r\}$, where i_r is the index for which the value of $z_i(x)$ in the r-th step is maximal.

. . . . . .

If there is a set of solutions $X_{k-1} \subset X$ which satisfies step k-1, then

step k $v_k(x^*) = \min_{x \in X_{k-1}} z_i(x)$ for $i \in I$ and $i \notin I_{k-1}$

where $v_1(x^*), \ldots, v_k(x^*)$ is the set of optimal values of fractional deviations ordered nonincreasingly.

Verbally this optimum can be described as follows. Knowing the extrema of the objective functions which can be obtained by solving the optimization problems for each criterion separately, the desirable solution is the one which gives the smallest values of the fractional increments and decrements of all the objective functions from their extremum values.

The optimum defined above gives us one solution. However, using the min-max approach we can also influence the priority of the criteria. In this case the i-th element of the vector z(x) should be determined from the formula

$$z_i(x) = \max\{\alpha_i z_i'(x), \alpha_i z_i(x)\} \qquad (9)$$

where α_i is a coefficient of the priority of the i-th criterion. Seeking the optimum in the min-max sense for different values of α_i, we can easily obtain a set of evenly distributed solutions which are optimal in the Pareto sense.

METHODS FOR SEEKING THE OPTIMUM

Let us discuss shortly methods for seeking the optimum in the min-max sense. There are numerous methods for seeking the extremum of an objective function subject to constraints. The question arises if these methods can be used for seeking the optimum in the min-max sense. In most of these methods, like the gradient method, the successive linear approximation method and the direct search method, the objective function determines the sequence of the steps which gradually improve the solution. Since the min-max principle of optimality has a recurrence form it is not possible to use these methods in order to find the optimum considering the full form of formula (8). However, the first step of formula (8) can be taken as a new objective function. Thus, the new objective can be written in the form

$$v(x) = \max_{i \in I} \{z_i(x)\} \qquad (10)$$

and the optimization problem is to find $x^* \in X$ such that

$$v(x^*) = \min_{x \in X} \max_{i \in I} \{z_i(x)\} \qquad (11)$$

It is easy to show that in many models the solution determined by the first step of this principle will be the optimum in the min-max sense.

Many one-criterion optimization techniques and programs in FORTRAN allow to use the objective function of the form presented above. The author has adapted and successfully used the following methods:

1. Hooke and Jeeves direct search method (7),
2. Davidon and Fletcher's variable metric method (8),
3. the flexible tolerance method (9).

For the first two methods penalty function was used in order to solve problems with constraints.

Some other methods for seeking the optimum in the min-max sense based upon the Monte Carlo approach and the trade-off study method were described by the author in (10). In these methods the optimum is chosen by comparing solutions which are generated at random (the Monte Carlo approach) or by changing the objective functions into constraints (the trade-off study approach).

Since there is no general method for solving all one-criterion optimization problems, every engineering task has to be treated individually. The same situation occurs when the problem of seeking the optimum in the min-max sense is considered. Therefore, a multicriterion optimization system (MCOS) has been developed at the Technical University of Cracow which allows to try any of several techniques in order to find the optimum in the min-max sense.

NUMERICAL EXAMPLE

Consider the I-beam design problem formulated as follows: Find the dimensions of the beam presented in Fig. 1 which satisfy the geometric and strength constraints and which are optimal considering the following criteria:

1. Cross-section area of the beam,
2. Static deflection of the beam for the displacement under the force P.

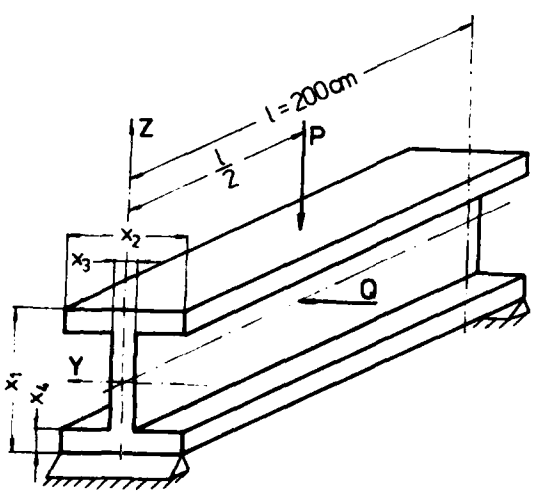


Fig.1

Both criteria are to be minimized. It can be easily noticed that these criteria are contrary to one another, i.e., the best solution for the first objective function gives the worst solution for the second one and conversely.

It is assumed that:

1. Permissible bending stress of the beam material $k_g = 16$ kN/cm^2.
2. Young's Modulus of Elasticity $E = 2 \times 10^4$ kN/cm^2.
3. Maximal bending forces P = 600 kN and Q = 50 kN.

The vector of the decision variable is $x = [x_1, x_2, x_3, x_4]^T$ where the variables will be given in centimeters.

The geometric constraints are as follows:

$$10 \leq x_1 \leq 80, \quad 10 \leq x_2 \leq 50$$
$$0.9 \leq x_3 \leq 5, \quad 0.9 \leq x_4 \leq 5$$

The strength constraint is as follows:

$$\frac{M_y}{W_y} + \frac{M_z}{W_z} \leq k_g$$

where: M_y and M_z are maximal bending moments in Y and Z directions respectively; W_y and W_z are section moduluses in Y and Z direction respectively.
For the forces acting as it is shown in Fig.1, values of M_y and M_z are 30 000 kNcm and 2 500 kNcm respectively. Section moduluses can be expressed as follows:

$$W_y = \frac{x_2x_1^3 - (x_2 - x_3)(x_1 - 2x_4)^3}{6x_1}$$

$$W_z = \frac{2x_4x_2^3 + (x_1 - 2x_4)x_3^3}{6x_2}$$

Thus, the strength constraint is

$$16 - \frac{180\,000x_1}{x_2x_1^3 - (x_2 - x_3)(x_1 - 2x_4)^3} - \frac{15\,000x_2}{2x_4x_2^3 + (x_1 - 2x_4)x_3^3} \geq 0$$

The objective functions can be expressed as follows:

1. Cross-section area

$$f_1(x) = 2x_2x_4 + x_3(x_1 - 2x_4) \quad \text{cm}^2$$

2. Static deflection

$$f_2(x) = \frac{P\,l^3}{48\,E\,I} \quad \text{cm}$$

where I is the moment of inertia which can be calculated from the equation

$$I = \frac{x_2x_1^3 - (x_2 - x_3)(x_1 - 2x_4)^3}{12}$$

After substitution the second objective function is

$$f_2(x) = \frac{60\,000}{x_2 x_1^3 - (x_2 - x_3)(x_1 - 2x_4)^3}$$

Since a factory can produce only I-beams whose dimensions x_3 and x_4 are the multiples of 1 cm we have an additional restriction that for the optimal solution the variables x_3 and x_4 should be integers.

Hooke and Jeeves direct search method (7) was used in order to find the extreme solution for each criterion separately and Hooke and Jeeves method together with branch and bound method were used for seeking the optimum in the min-max sense. A computer program was based on the optimization subroutines described by J.N.Siddal (11). Using this program following results were obtained:

1. The solutions which give the minima of the objective functions for each criterion separately
   a) considering the cross-section area
      $x^{o(1)} = [60.8, 40.5, 0.9, 0.93]^T$
      $f_1(x^{o(1)}) = 128\ cm^2$, $f_2(x^{o(1)}) = 0.062\ cm$
   b) considering the static deflection
      $x^{o(2)} = [80, 50, 5, 5]^T$
      $f_1(x^{o(2)}) = 850\ cm^2$, $f_2(x^{o(2)}) = 0.0059\ cm$
2. The best compromise solution
   $x^* = [80, 50, 1, 2]^T$
   $f_1(x^*) = 276\ cm^2$, $f_2(x^*) = 0.015\ cm$.

The solution x^* was accepted by the designer and it was unnecessary to seek further solutions optimal in the Pareto sense.

For this example CPU time of execution on CYBER 72 computer was 72 sec.

FINAL REMARKS

The approach to the multicriterion optimization problem presented in this paper can be applied to models in which all the criteria have to be considered simultaneously and on terms of equal importance. The main idea consists in finding the compromise solution which gives values of the objective functions as close as possible to their separately attainable extrema.

An application to the typical optimization problem for structural design presented in this paper illustrates usefulness and versatility of the approach discussed.

The min-max principle of optimality which is mathematically formalized has been used in order to define the optimum. By using this principle and the methods for seeking the optimum, the solution can be obtained automatically (decision can be made by a computer). This is important in automation of design problems.

REFERENCES

(1) Leitman, G. and Marzollo, A., Multicriteria Decision Making, Springer-Verlag, New York -Berlin, 1975.

(2) Peschel, M. and Riedel, C., Polyoptimierung, VEB Verlag Technik, Berlin, 1976.

(3) Walz, F. M., An Engineering Approach: Hierarchical Optimization Criteria, IEEE Trans. Auto. Contr., AC 12, 1967.

(4) Ingizio, J. P., Goal Programming and Extensions, Lexington Books, D.C.Heath and Company, Lexington, MA, 1976.

(5) Zeleny, M., Linear Multiobjective Programming, Springer - Verlag, New York - Berlin, 1974.

(6) Hwang, C. L., Paidy, S. R. and Yoon, K., Mathematical Programming with Multiple Objectives: A Tutorial, Comput. and Ops. Res. Vol.7, 1980.

(7) Hooke, R. and Jeeves, T. A., Direct Search Solution of Numerical and Statistical Problems, J. Assoc. Comp. Mach., vol. 8, 1961.

(8) Fletcher, R. and Powell M. J. D., A Rapidly Convergent Descent Method for Minimization, Computer J., Vol. 6, 1963.

(9) Himmelblau, D. M., Applied Nonlinear Programming, McGraw-Hill Book Company, New York, 1972.

(10) Osyczka, A., An Approach to Multicriterion Optimization Problems for Engineering Design, Computer Methods in Applied Mech. and Eng., No. 15, 1978.

(11) Siddal, J. N., "OPTISEP, Designers' Optimization Subroutines", Report No. ME/71/DSN/REP1, Faculty of Engineering, McMaster University, Canada, 1971.

SESSION #9

STEEL AND CONCRETE DESIGN

AD-P000 079

RIGID-PLASTIC MINIMUM WEIGHT PLANE FRAME DESIGN USING HOT ROLLED SHAPES

R. C. Johnson
Associate Professor
Department of Civil Engineering
Auburn University, AL 36849

Summary

Conventional minimum weight structural design methods generally assume that a continuous spectra of shapes are available; however, actual sections consist of a finite set of discrete sizes. By utilizing discrete programming techniques, it is possible to develop design methods which work directly with the properties of the available sections. A design approach based on the static theorem of plastic analysis is formulated herein. The resulting optimization problem is a mixed integer type. Alternatively, a pure integer linear optimization problem results when the kinematic theorem is used to formulate the problem.

A multi-level decision making programming problem is formulated to minimize the frame weight. The algorithm is capable of handling both the pure integer and mixed integer problems; however, focus is restricted to the mixed integer problem associated with the static approach to the design formulation. The algorithm may be classified as a branch and bound type and utilizes ordinary linear programming techniques to test the feasibility of various designs. A FORTRAN computer program has been developed to automate the procedure. An example problem illustrating the method is included.

Introduction

A significant step in the structural design process is the selection of member sizes for a frame of known geometry subjected to a set of known loads. There, of course, exist numerous possible safe designs. A relevant consideration is which of these possible designs represents the optimum design. Comparisons of the total weight of material used in the designs of such a frame are considered to be one method of measuring the relative efficiencies of a number of possible designs. Furthermore, structural weight is a parameter that is readily incorporable into design formulations due to the linear relationship between weight per unit length of a member and the cross sectional area of that member. Connection and labor costs are likely to be quite similar for two designs in which the only differences are the sizes of the individual members. In this respect weight is analogous to cost and also gives to the designer an absolute basis upon which to compare alternative designs.

Conventional minimum weight structural design methods assume that a continuous spectra of shapes are available to the designer; however, available sections consist of a finite set of discrete sizes. By utilizing discrete programming techniques, it is possible to derive design methods which work directly with the properties of the available sections.

Assumptions

Traditionally the minimum weight design problem has been formulated by the direct implementation either of energy considerations based on the kinematic theorem or of a force method based on the static theorem. Problems formulated by either of these approaches become linear programming problems when certain assumptions are made:

1. All members are prismatic and exhibit bilinear moment-curvature relations with strain hardening neglected.

2. The frame is loaded with concentrated loads in its own plane.

3. Collapse involves only inplane deflections which are small compared to the overall structural dimensions.

4. Beam-column action and secondary column moments are neglected.

5. Instability, either in the frame as a whole or in the individual members, does not occur.

6. Member weight is linearly proportional to the member plastic moment capacity.

Assumption 1 is the usual idealization for a ductile material. Assumption 2 is valid since distributed loads can be represented by a series of concentrated loads. Assumptions 3, 4, and 5 pose the most severe limitations on the usage of rigid-plastic theory. In this study attention is restricted to frames of three or fewer stories where the columns are subjected to relatively low axial load and are designed primarily for bending. With this restriction on the type of problem to be considered, a design based upon rigid-plastic theory neglecting the effects of axial force is satisfactory (1). In the technique to be used, the effects of axial force can be included with minor additions to the algorithm. This is accomplished by the introduction of the concept of reduced plastic moment capacities. The fully plastic moment capacity of each section is multiplied by a reduction factor which is a function of the member axial force, the cross sectional area of the section used, and the material yield stress. The discrete section optimization procedure is then cycled; and at the end of each cycle the reduction factors are calculated. When for two successive cycles the reduction factors are the same, the optimum design including the effects of axial force has been achieved.

The total structural weight to be minimized is the sum of the individual member weights as is shown in Equation 1 below

$$W = \sum_{j=i}^{n} \rho_j A_j l_j \qquad (1)$$

where ρ_j = weight per unit length per unit area of member j
A_j = cross sectional area of member j
l_j = length of member j

If all structural members are made from the same grade steel, ρ_j is then a constant and may be moved outside the summation. For the sections listed in Table 1, The following area-plastic moment capacity relationships were derived from a least squares regression analysis:

beam sections $\quad A = 0.31\, M_p^{0.67} \qquad (2)$

column sections $\quad A = 0.37\, M_p^{0.71} \qquad (3)$

Table 1
Plastic Moment Capacities (ft. kips)
(A36 Steel)

Beams

Section	Mp	Section	Mp	Section	Mp
W36x300	3780	W30x108	1040	W16x40	218
W36x280	3510	W30x99	939	W18x35	200
W36x260	3240	W27x94	834	W14x34	164
W36x245	3030	W24x94	759	W16x31	162
W36x230	2830	W24x84	672	W12x31	132
W33x220	2330	W24x76	603	W12x26	132
W36x194	2300	W24x68	528	W14x26	120
W36x182	2150	W21x68	480	W14x22	99
W36x170	2000	W24x62	456	W12x22	88
W36x160	1880	W24x55	402	W12x16.5	61.8
W36x150	1740	W21x55	378	W10x15	48
W33x141	1540	W18x55	336	M10x9	28
W36x135	1530	W21x49	324	M8x6.5	16
W33x118	1250	W21x44	286	M7x5.5	12
W30x116	1130	W18x40	235		

Columns

Section	Mp	Section	Mp	Section	Mp
W14x228	1280	W12x65	291	W8x31	91
W14x193	1065	W10x60	225	W6x25	57
W14x142	765	W10x49	181	W6x20	45
W14x111	588	W8x48	147	W5x16	29
W14x87	453	W8x40	119	W4x13	19
W12x79	359	W8x35	104		

In order to employ linear programming techniques, these area-plastic moment capacity relationships must be linear or piecewise linear. Fortunately, the range in plastic moment capacity for sections which might be used for a particular member is limited. Equations 2 and 3 may be approximated by the linear relations given by Equations 4 and 5 for the k-th beam and the k-th column respectively

$$(A_b)_k = a_k + b_k(M_p)_k \tag{4}$$

$$(A_c)_k = c_k + d_k(M_p)_k \tag{5}$$

When the linear relationships given by Equations 4 and 5 are substituted into the weight function, Equation 1, the structural weight becomes linear in plastic moment capacity. For cases where the identical grade of steel is used for both beams and columns, this substitution yields the following function to be minimized:

$$W = \rho\Big[\sum_{j=1}^{nbm} a_j l_j + \sum_{j=nbm+1}^{nm} c_j l_j + \sum_{j=1}^{nbm} b_j l_j (M_p)_j + \sum_{j=nbm+1}^{nm} d_j l_j (M_p)_j\Big] \tag{6}$$

where nm = total number of members
nbm = number of beam members
nm-nbm = number of column members.

Continuous Spectra Formulation

Objective Function

The common procedure is to simplify the function to be optimized, Equation 6, in order to achieve a simplified function proportional to the weight. The first two terms of Equation 6 are constants for a given problem and may be omitted since they add the same constant to each evaluation of the objective function. Due to the geometric similarity of W sections, the constants b_j and d_j found in the third and fourth terms of Equation 6 differ by only a few percent. These two constants as well as the constant ρ need not be included in the simplified function since optimizing a certain function is identical to optimizing a multiple of that function; thus, a commonly used simplified indicator function for the weight is

$$z = \sum_{j=1}^{nm} l_j (M_p)_j. \tag{7}$$

Constraints

The static theorem of rigid-plastic analysis states that for a given frame and loading, any safe and statically admissible bending moment distribution corresponds to a loading, P, which is less than or equal to the collapse load, P_c. This theorem is employed in design through the implementation of a force method. The first step is to introduce a sufficient number of releases to make the structure statically determinate. The moment at any point, particularly at possible plastic hinge locations, in the structure can be calculated as a function of the applied loads and the redundants at the introduced releases. Subsequently, at each of the NH plastic hinge locations, the absolute value of the moment must not exceed the plastic moment capacity of that particular member where the plastic hinge is located. Mathematically, this is expressed as

$$\Big|\sum_{i=1}^{NR} a_{hi} R_i + (m_e)_h\Big| \leq (M_p)_j \; ; \; (h=1,\ldots,NH; \; j=1,\ldots,nm) \tag{8}$$

where R_i = redendant i
$(m_e)_h$ = moment at h due to external loads
$(M_p)_j$ = plastic moment capacity of member j.

Also, since no member can have a negative weight, the plastic moment capacity of each member must be nonnegative.

$$(M_p)_j \geq 0 \ , \quad (j=1,\ldots,nm) \tag{9}$$

Discrete Section Formulation

The discrete section design problem is to utilize available section sizes in such a manner that the resulting total frame weight is less than all other discrete section combinations. To achieve this end, the following procedure is used in conjunction with the notation used by Livesley (2) and Toakley (3). The set of members is consolidated into NG groups. Each group consists of all members which are to be designed with identical structural sections. For each of the NG groups, NS possible standard rolled structural steel sections are chosen. For convenience in the automated procedure, the number of possible sections is the same for all groups. Only one of the NS sections is used per group. If $(M_p)_j$ is the plastic moment capacity for group j and if mp_{jk} (k=1,...,NS) are the plastic moment capacities of the possible sections for group j, then

$$(M_p)_j = \sum_{k=1}^{NS} mp_{jk}\, \delta_{jk} \ , \quad (j=1,\ldots,NG) \tag{10}$$

$$\sum_{k=1}^{NS} \delta_{jk} = 1 \ , \quad (j=1,\ldots,NG) \tag{11}$$

$$\delta_{jk} = 0 \text{ or } 1 \tag{12}$$

prescribe that only one section is to be used per group. The various plastic moment capacities of the sections being considered are known, and the optimization problem decision variables are the zero-one delta variables, δ_{jk}.

Substitution of the relationships given by Equations 10, 11, and 12 into the continuous spectra problem given by Equations 7 through 9 leads to a mixed integer programming problem nearly identical to that formulated by Toakley (3), namely to

$$\text{minimize} \quad \sum_{j=1}^{NG} \sum_{k=1}^{NS} l_j\, mp_{jk}\, \delta_{jk} \tag{13}$$

$$\text{subject to} \quad \left| \sum_{i=1}^{NR} a_{hi} R_i + (m_e)_h \right| \leq \sum_{k=1}^{NS} mp_{jk}\delta_{jk}$$

$$(j=1,\ldots,NG;\ h=1,\ldots,NH)$$

$$\sum_{k=1}^{NS} \delta_{jk} = 1 \ , \quad (j=1,\ldots,NG)$$

$$\delta_{jk} = 0 \text{ or } 1$$

$$R_i \geq 0.$$

Multiple Loading Cases

When through the solution of a single linear programming problem the static approach is used to find the minimum weight design of a frame subjected to multiple loading conditions, a unique minimum weight is always found. Values obtained for the redundants, however, are not necessarily unique. The result is that absolute knowledge of the member forces for the various loading conditions is not known.

For a problem with k section sizes to be determined and n loading cases, there exist two types of linear programming formulations which may be applied to the static approach. In the first case, one linear program for each loading condition is solved yielding n single loading case designs. Selection of the n largest member sizes for each of the k sections results in a design which is safe for all n loading cases. The redundants are uniquely determined for each separate design.

In the second approach, one linear program is formulated and solved including all n loading cases and n sets of redundants which lead to a coupled constraint set. It is likely that the optimum solution for this second formulation will be some linear combination of the n loading conditions. In such a case, the individual loading conditions still yield statically indeterminate structures; therefore, the constraints at the optimum solution represent n of many statically admissible bending moment diagrams. The mathematical consequence of this is that the redundants associated with each loading condition are not physically meaningful if they are interpreted as reactions for the various loading conditions. Mathematically it is impossible to arrive at unique values for these redundants when in the optimum tableau they appear in a row with a nonzero slack variable. Each row of the tableau represents an equality between the moment at a potential plastic hinge position plus the slack variable and the plastic moment capacity of the member in which the potential plastic hinge is located. There is no way to distribute this slack moment to various redundants without an a priori knowledge of the proper values for the redundants.

Description of Algorithm

The mixed integer linear optimization problem given by Equations 13 is a multiple choice problem in that for each group of members one section which satisfies all the constraints and minimizes the overall structural weight is selected from all those available. Two basic approaches to the problems of this type are cutting plane methods and enumerations methods. Cutting plane methods may be inefficient for certain types of problems. Toakley (3) found that convergence of Gomory's mixed-integer algorithm (4) was unpredictable for discrete section minimum weight rigid-plastic plane frame design. Toakley was forced to terminate Gomory's algorithm and use an approximate random search technique. Enumeration techniques are in certain situations the best methods of solution. This appears to be particularly true for physical problems where the constraint set and function to be optimized are well behaved. Tree search techniques, one class of enumeration approaches, are applicable to problems for which the various states can be represented as connected nodes. The arcs connecting the nodes represent forward or backward steps from one state, or design, to another. There are two important features associated with tree search algorithms. First, they lack mathematical structure and, hence, can be used to solve a wide variety of problems. Second, there is a known upper bound on the number of steps necessary for convergence which is not the case for cutting plane methods. For problems with n zero-one variables, this upper bound is 2^n.

Figure 1 is a graphical representation of a two dimensional all integer minimization problem with a noninteger continuous optima. The region to the right of and above ABCD indicates the area of feasibility. The continuous spectra optimum solution objective function is given by line z_c-z_c. One integer solution may be obtained by rounding up both x_1 and x_2 to the first integer point above the continuous solution. As illustrated by the objective function

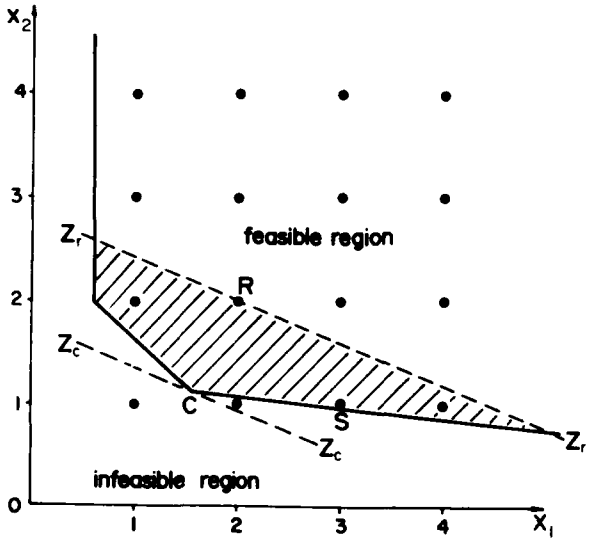


Figure 1. Graphical Representation of Two Dimensional All Integer Problem.

drawn through the rounded up solution, line z_r-z_r, this procedure does not necessarily yield a true integer restrained optimum solution; however, it is known by the convexity of the constraint set that this solution is feasible. Also, the optimum integer solution must lie somewhere in the convex set created by the intersection of line z_r-z_r and the boundary of the constraint set ABCD. See the shaded area of Figure 1. The algorithm to be developed investigates integer solutions within this region.

The continuous spectra minimum weight design problem, given by Equations 7, 8 and 9, is solved in order to obtain an indication of the proper range of discrete sections to be used for each group. This solution represents the absolute minimum weight and is obtainable if, and only if, sections are available having exactly the plastic moment capacities given by this solution. Hence, the continuous spectra solution represents a lower bound on the discrete section design. Next, reasonable sets of discrete sections--some heavier than those required by the continuous spectra solution and some lighter--- are chosen for each group.

By rounding up each nondiscrete member size to the smallest discrete section available above the continuous spectra solution size, a solution is obtained which is known to be feasible by the convexity property of the constraint set. The problem is now to investigate designs whose weight lies between that of the continuous solution (lower bound) and that of the rounded up solution (upper bound). If no such solution is found to be feasible, then the rounded up solution represents the discrete section minimum weight design. When a feasible solution on a specific branch is found between the two bounds, that solution becomes the new provision must be made for zigzagging outside these limits. Point S in Figure 1 represents the integer restrained optimum solution and may be reached by one of two branches. Either x_1 may be increased, followed by a decrease in x_2; or x_2 may be decreased, followed by an increase in x_1. The first branch (increasing x_1 at constant x_2) initially leads to a solution with an objective function value greater than that of the rounded up solution and will not be considered. The first step of the second branch (decreasing x_2 at constant x_1) results in an infeasible solution; however, this is the only avenue by which S can be reached since the first branch was rejected because its first node had an objective function value greater than the upper bound. When a member size decrease is made which leads from a feasible solution to an infeasible solution or to a solution for which the objective function value is less than the lower bound, before investigation along this branch may be terminated the following procedure must be satisfied. Assume that the members of group k were decreased to reach this infeasible state. From the infeasible state, all groups other than group k are increased one at a time; and the resulting states investigated. If all of these states prove to be infeasible or feasible but with objective function values greater than the upper bound, then the currently investigated branch is considered to be completely implicitly enumerated; and control is reverted to the rounded up solution for investigation of other initial branches. If a feasible solution with an objective function value below the upper bound is found, it becomes the new upper bound; and an attempt is made to find a better solution from this point before returning to the rounded up solution.

Allusions have been made to a feasibility test for the determination of whether or not a specific design represents a safe design. In order to assure feasibility for a specific design, the constraints of Equations 13 must be satisfied to insure that at no point does the bending moment exceed the plastic moment capacity of the member in which that point is located. Examination of these inequalities shows that there are NH inequalities and that there are NR unknown redundants, R_i. To test the feasibility of a given design, values of the redundants must be found in order to calculate the bending moments at various potential plastic hinge locations. Physically, if a set of redundant reactions can be found which satisfies the constraint set, then a safe design exists. If such a set of redundant reactions cannot be found for a given design, plastic collapse of this design will occur at a load level less than the desired one; and therefore, this design is unsafe. Since the number of inequalities, NH, and the number of unknown redundant reactions, NR, are not, in general, equal; an infinite number of solutions to the inequality constraints exist. The problem, however, can be expressed as a linear optimization problem as shown below:

Physically, this linear program represents an attempt to find a set of redundant reactions such that a statically admissible moment diagram is obtained based on the static theorem.

If a particular design is unsafe, the attempted solution of Equations 14 by the dual simplex method will fail since primal feasibility cannot be attained for an unsafe design. This becomes evident when a negative pivot element for removal of primal infeasibility cannot be found. When a particular design is a safe design, primal feasibility is obtained along with a set of redundant reactions which yield an admissible bending moment diagram. It must be noted that the values obtained for the redundant reactions associated with a safe design are not necessarily meaningful. In general, the safe discrete design will not be at a collapse state as there are not sufficient plastic hinges. This indicates that the structure is still statically indeterminate and the constraints can be satisfied with nonzero slack variables.

Numerical Results

In the numerical cases investigated in this study, a pseudo weight is assigned to the continuous spectra solution. The area-plastic moment capacity relationships for beam and column sections given by Equations (2) and (3) are used to calculate an area, and hence weight, from the required plastic moment capacities obtained for the continuous spectra problem. A discrete section design having exactly the same weight as the pseudo weight is possible only if discrete sections are available with exactly those plastic moment capacities required by the continuous spectra solution.

In general the weight of the rounded up discrete section solution is found to be ten percent higher than the pseudo weight of the continuous spectra solution. The weight of the best obtained discrete section solution is found to be approximately two percent higher than the pseudo weight of the continuous spectra solution. In all examples problems considered for which an exact discrete section solution is available, the method developed herein converged to the same optimum design. It is suspected that for the majority of typical plane frame problems, convergence to the exact optimum solution will occur when the limited tree search algorithm developed herein is used. In order to assure that the exact optimum discrete section design is obtained, the additional computational effort would increase computer time by an estimated factor of ten for all problems.

Example

The geometric configuration and loading for a single story, two bay frame are shown in Figure 2a. The same section is to be used for both beams. Similarly, all three columns are restricted to be identical. These restrictions lead to two groups for the five members (group b for beams and group c for columns). Potential plastic hinge locations and the choice of redundants are illustrated in Figures 2b and c respectively. Table 2 lists the moment expressions at the potential plastic hinge locations. Positive moment is defined as that which causes tension on the broken line side of the members as shown in Figure 2c.

Solution of the continuous spectra problem results in the required plastic moment capacities and redundants shown below.

beam M_p = 100.00 ft.-kips

column M_p = 33.33 ft.-kips

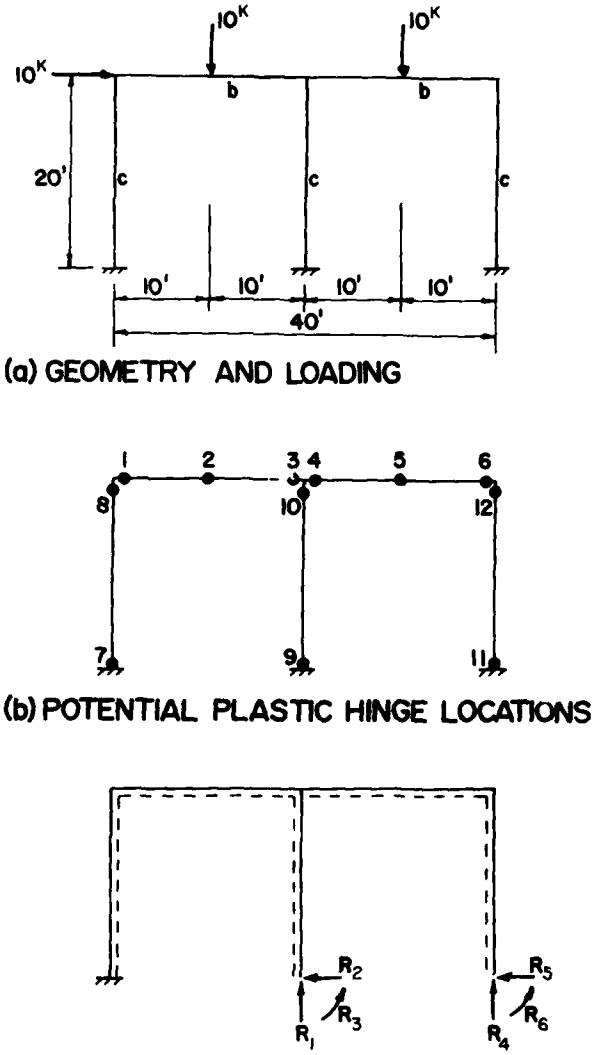


Figure 2. Single Story, Two Bay Frame

R_1 = 25.00 k, R_2 = 3.33 k, R_3 = 33.33 ft.-k

R_4 = 11.67 k, R_5 = 3.33 k, R_6 = 33.33 ft.-k

In order to compare weights of the continuous spectra solution and various discrete section solutions, it is necessary to assign a weight to the continuous spectra solution. This is accomplished using Equations 2 and 3 and the unit weight of steel to calculate a pseudo weight of 1838 lb. For the set of sections chosen, see Table 3, the discrete section optimal design consists of those sections marked with asterisks. The total frame weight for this solution is 2000 lbs. The weight of the rounded-up design (beam - W 14x26, column - W 6x20) is 2240 lbs.

Table 2. Moments at Critical Points

Potential plastic hinge locations	Moment expressions
1	$20R_1-20R_2+R_3-20R_5+R_6-400$
2	$10R_1-20R_2+R_3+10R_4-20R_5+R_6-200$
3	$-20R_2+R_3+20R_4-20R_5+R_6-100$
4	$20R_4-20R_5+R_6-100$
5	$10R_4-20R_5+R_6$
6	$-20R_5+R_6$
7	$20R_1+R_3+R_6$
8	$20R_1-20R_2+R_3-20R_5+R_6-400$
9	R_3
10	$-20R_2+R_3$
11	R_6
12	$-20R_5+R_6$

Conclusion

An implicit enumeration algorithm has been presented in the form of a limited tree search technique for minimum weight rigid-plastic plane frame design using available sections. The algorithm consists of two basic parts. First, a search is conducted for a node which represents a design having a weight between an upper and a lower bound. Second, when such a design is located, an investigation is conducted to determine whether or not the design is safe. Comparisons of the results obtained by this method with those of other reported methods indicates a substantial reduction in computational effort to achieve an optimum integer restrained solution. Also, the significant reduction in frame weight from the weight of the rounded up design is sufficient to make utilization of the automated procedure practical for design purposes.

Table 3. Sections for Example Problem

beam		column	
Section	Mp (ft-k)	Section	Mp (ft-k)
W14x34	164	W8x31	91
W16x31	162	W6x25	57
*W14x26	120	W6x20	45
W14x22	99	*W5x16	29
W12x22	88	W4x13	19

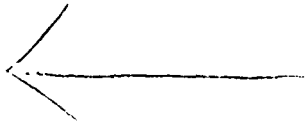
References

(1) Neal, B. G. and Symonds, P.S., "The Rapid Calculation of the Plastic Collapse Load for a Framed Structure," Proceedings of the Institution of Civil Engineers, Vol. 1, No. 1, p. 58, 1952.

(2) Livesly, R. K., "The Automatic Design of Structural Frames," Quarterly of the Journal of Mechanics and Applied Math, Vol. 9, Part 3, p. 257, 1956.

(3) Toakley, A. R., "Studies in Minimum Weight Rigid Plastic Design with Particular Reference to Discrete Sections," Second Report, Study of Analytical and Design Procedures for Elastic and Elastic-Plastic Structures, Department of Civil Engineering, University of Manchester, England, 1966.

(4) Gomory, R. E., "An Algorithm for the Mixed-Integer Problem," Publication P-1885, The RAND Corporation, 1960.



AD-P000 080

LIGHT GAGE STEEL DESIGN VIA THE METHOD OF MULTIPLIERS

Nesrin Sarigul and Richard Gallagher
College of Engineering
University of Arizona
Tucson, AZ 85721

1. Introduction

Cold formed light gage steel shapes would appear to be an attractive target for structural optimization procedures. In contrast with rolled sections, where shapes and dimensions are fixed by the economics of production, there is scope for choice of dimensions in cold formed steel in order to achieve the objective of minimum weight or minimum cost. At the same time, light gage steel shapes are manufactured in relatively large quantities and economies of weight or cost should result in total savings that justify the expense of the numerical optimization effort.

Relatively few optimization procedures for this class of problem have been published. Seaburg and Salmon (1) used a gradient projection scheme for this purpose. Ramamurthy and Gallagher (2) reported the use of the geometric programming approach. Neither of these optimization approaches has been the most popular of mathematical programming tools for structural optimization. That attribute can be assigned to penalty function methods.

Penalty methods have been popular in structural optimization for approximately fifteen years; a good account of past work is given by Moe (3). All methods described in Ref. 3 are in the class of SUMT (Sequence of Unconstrained Minimization Techniques). In these a function is formed by appropriate combination of the constraint conditions, the function is multiplied by a "penalty factor", and the product is added to the basic objective function. An unconstrained minimization is then performed for a chosen value of the penalty factor, resulting in a solution for the set of design variables. These calculated variables, together with a new value of the penalty factor, are then employed as the basis for another unconstrained minimization, and so on until convergence.

Extensive numerical studies of the performance of penalty function methods[4,5] have demonstrated that the traditional approach, outlined above, is not as robust as was earlier assumed. Consequently, new avenues in penalty methods have been explored. One of these, the method of multipliers, has proved to be particularly attractive and is adopted here as a technique for the minimum weight design of light gage steel sections.

The method of multipliers was suggested by Hestenes (6) and Powell (7) and was amplified by Miele (8) for the equality constrained problem. Schuldt, Gabriele, Root, Sandgren and Ragsdell (9) extended it to inequality constraints and thoroughly explored its performance on the Eason and Fenton (4) series of problems. Subsequently, Root and Ragsdell (10) devised enhancements of the method which permitted the treatment of bounds on the variables and which facilitate scaling of the objective function and constraints.

We first outline the method of multipliers, followed by a brief description of the computer program used for calculations based upon it. Then, the nature of the optimization problem of cross-sections of cold formed steel members is described and the relevant merit function and constraint conditions are given in detail. Numerical solutions are obtained for a design problem that was previously solved in Ref. 2 and for a new problem. The method of multipliers is found to be generally effective in these applications, although questions remain as to the choice of the penalty parameter in order to achieve a convergent solution.

2. The Method of Multipliers

The Method of Multipliers is a method in the class of penalty function methods. Consider an optimization problem in which the minimum of a function $W(\underset{\sim}{x})$ is sought, where $\underset{\sim}{x}$ is the set of design variables. Suppose the constraint conditions are of the form:

$$g_j(\underset{\sim}{x}) \geq 0 \qquad (j = 1, \ldots J) \text{ (inequality constraints)} \tag{2.1}$$

$$h_k(\underset{\sim}{x}) = 0 \qquad (k = 1, \ldots K) \text{ (equality constraints)} \tag{2.2}$$

Then a penalty statement of the minimization problem can be written as

$$P = W(\underset{\sim}{x}) + Q(R, g, h) \tag{2.3}$$

where Q is the penalty term, a function of the penalty parameter R and the constraints g and h.

In the SUMT approach the penalty factor R is increased in each successive minimization and the constraints are incorporated in Q as given in the limit $R = \infty$. This increases the curvature of the surface whose minimum is sought and a stage is often reached where the minimization process is difficult to accomplish.

In the Method of Multipliers the following penalty function is constructed

$$P = W(\underset{\sim}{x}) + R\sum_{}^{J}[\langle g_j + \sigma_j\rangle^2 - \sigma_j^2] + R\sum_{k=1}^{K}[(h_k + \tau_k)^2 - \tau_k^2] \tag{2.4}$$

In this, the penalty parameter R is fixed. The adjustable parameters are σ_j and τ_k. The meaning of the bracket operator is that

$$\langle(g_j + \sigma_j)^2\rangle = 0 \quad \text{when } (g_j + \sigma_j) \leq 0 \tag{2.5}$$

$$\langle(g_j + \sigma_j)^2\rangle = (g_j + \sigma_j)^2 \quad \text{for } (g_j + \sigma_j) > 0 \tag{2.6}$$

The parameters σ_j and τ_k are fixed during the execution of a minimization stage. Then, prior to the next stage, these parameters are updated. A suggested rule for updating is, for the mth stage

$$\sigma_j^{(m+1)} = \langle g_j^m + \sigma_j^m\rangle \tag{2.7}$$

$$\tau_k^{(m+1)} = h_k^m + \tau_k^m \tag{2.8}$$

In the limit, σ_j and τ_k go to zero. It has been proved (9) that the solution obtained in the limit is a Kuhn-Tucker point.

As noted above, in the Method of Multipliers R is held fixed and each constraint is supplemented in the manner described in Eq. (2.4). The parameters added to

the constraints are changed from one minimization stage to the next. The effect of this format of the penalty term is that there is only a moderate effect on the surface whose minimum is sought (there is no effect at all for linear constraints). The difficulty of the minimization effort is not increased as the parameters σ_j and τ_k are reduced. Since any difficulty in this process will require the use of the maximum number of significant figures in the computations the method is advantageous for computers with 8 or 16 bit registers.

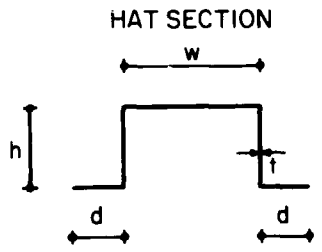
Strategies for performing the minimization and determining when to terminate the computation are embodied in the BIAS computer program used in this work. The program is discussed in Section 4.

3. Problem Data - The Hat Section

3.1 Section Geometry

The geometry of the hat section is shown in Figure 1. The corner radii are taken to be zero. The width of the unstiffened bottom flange is $d = x_1$, and that of the stiffened top flange is $w = x_2$. $h = x_3$ is the depth of the vertical web. The thickness of the section is $t = x_4$. Subsequently, we introduce the effective width $b = x_5$. All design variables must be zero or greater.

FIGURE 1.



3.2 Constraint Conditions

The constraints are principally those which are defined in the AISC Code (13), as follows:

a. Constraints Due to Positive Bending Moment M_p

It should first be noted that the code stipulates that the stress on the extreme fiber of flexural members shall not exceed 0.6 of the material yield stress, F_y.

The condition that the direct stresses in the flanges due to the application of the positive moment M_p (compression in top fiber) are less than the allowable can be written as

$$M_p \bar{y}_p / I_e \leq 0.6F_y \quad \text{(top flange)} \tag{3.1}$$

$$M_p \bar{y}_b / I_e \leq 0.6F_y \tag{3.2}$$

$\bar{y}_p$ and $\bar{y}_b$ are the distances from the horizontal centroidal (1-1) axis and the top center lines of the top and bottom flanges, respectively. I_e is the moment of inertia of the effective cross-section. The effective width of the top flange, x_e, which is used in the calculation of I_e, is obtained from the effective width equation (Eq. 2.3.1.1. Ref. 13).

$$\frac{x_e}{x_4} = \frac{253}{\sqrt{f}}\left(1 - \frac{55.3}{(x_2/x_4)\sqrt{f}}\right) \tag{3.3}$$

Eq. (3.3), which is an equality constraint, is valid when

$$x_2/x_4 \geq 171/\sqrt{f} \tag{3.4}$$

otherwise, $x_e = x_2$.

b. Stress Constraints Due to Negative Bending Moment M_n

The condition that the direct stresses in the flanges due to the applied negative bending moment are less than the allowables ($0.6F_y$) can be written as

$$\frac{M_n \bar{y}_n}{I} \leq 0.6F_y \quad \text{(top flange)} \tag{3.5}$$

$$\frac{M_n \bar{y}_{nb}}{I} \leq F_c \tag{3.6}$$

where F_c is the allowable bending stress, $\bar{y}_n$ is the distance between the centroid and the top center line, $\bar{y}_{nb}$ is the distance between the centroid and the bottom center line, and I is the moment of inertia of the entire section.

The allowable bending stress in compression, F_c, is dependent on the ratio, x_1/x_4 (Eqn. 3.2.b Ref. 13). For the present problem x_1/x_4 must not exceed $\frac{144}{\sqrt{F_y}}$. Thus

$$\frac{x_1}{x_4} \leq \frac{144}{\sqrt{F_y}} \tag{3.7}$$

c. Stress Limitations Due to Shear, V

Similar to F_c, the allowable stress for shear, F_r, is a function of the web depth-to thickness ratio, x_3/x_4. The expressions for F_r are dependent upon the range of values of x_3/x_4 given by Eq. 3.4.1 a and b of Ref. 13. The chosen range for the hat section is

$$\frac{x_3}{x_4} \geq 547\sqrt{F_y} \tag{3.8}$$

For the ranges considered the shearing stress F_r is restricted as follows (Ref. 13)

$$F_r \leq \frac{83{,}700}{(x_3/x_4)^2}$$

and, since the shearing stress is related to the shear V by $F_r = V/2x_3x_4$

$$V \leq \frac{166{,}400\, x_4^3}{x_3} \tag{3.9}$$

Altogether, therefore, there are 8 inequality constraints (3.1, 3.2, 3.4-3.9) and one equality constraint (3.3).

3.3 Objective Function

The weight per unit length is chosen as the objective function. Multiplying the area of the section by the unit weight of steel, we have

$$W = 6.8x_1x_4 + 3.4x_2x_4 + 6.8x_3x_4 \qquad (3.10)$$

4. The Bias Computer Code

In the solution of the problems the BIAS computer code, developed by Root and Ragsdell[11], is used. This code adopts the Method of Multipliers with some computational enhancements (10) which improve the effectiveness of the method. These enhancements are variable bounds and problem scaling.

Variable bounding ($a_i \leq x_i \leq b_i$, i = 1, 2, ...N) keeps the variable at the approximate bound in the case the upper or lower bound is encountered and adjusts the unconstrained search to reflect the bounded variable.

To avoid the difficulty of an ill-scaled variable or constraint BIAS scales the variables and the constraints in a way that the contributions of the individual variable to the gradient of the penalty function are all approximately the same.

Another enhancement is available which helps to update the R value if it has been chosen too small.

In the program, unconstrained minimization has been carried out in the program by the Davidon-Fletcher-Powell method. The calculation of the gradients is done by forward differences, Coggins' algorithm[12] is used for the line search.

The user must give the objective function, the constraints and the following parameters: the number of design variables, number of inequality constraints, number of equality constraints, the overall stopping criterion, the line search convergence criterion. Any legal FORTRAN programming coding is allowed in defining the constraint values. The determination of the value for the overall stopping criterion, the line search convergency criterion and penalty parameter are problem dependent.

The program proceeds as below:

First, the program sets the values of σ_j and τ_k to zero. Then, if there are no equality constraints, and no inequality constraints are violated, it performs the Davidon-Fletcher-Powell unconstrained minimization. Otherwise, it scales the problem. In the unconstrained minimization, termination occurs when either the norm of the gradient becomes small or the changes in the elements of the design vector become small.

Termination occurs if the relative change in the objective function between two consecutive stages is small, or if there are more numbers of unconstrained steps than the allowed maximum steps.

Then, it updates σ_j and τ_k and again repeats the same operation starting with the unconstrained minimization.

Numerical results were obtained using the University of Arizona Interactive Graphics Engineering Laboratory ECLIPSE S/230, 16-bit word (in the single precision) minicomputer system. In the given examples, double precision arithmetic (64-bit word) has been used. This gives approximately 15 decimal places of precision.

5. Numerical Results

We apply this procedure to two different design problems. One of these, solved previously in Ref. 2, is a problem which was suggested by a design analysis problem given by Yu in Ref. 14. In this problem a three-span beam is uniformly loaded on the outer spans resulting in a positive moment M_p of 134.2 in.K. and a negative moment M_n of 66.436 in.K. accompanied by a shear force V of 20.3K. F_y = 40,000 lb./in.^{2}.

The same initial design as in Ref. 2 was employed: x_1 = 2.35, x_2 = 14.5, x_3 = 9.5, and x_4 = 0.105, with W = 13.637 lb./ft. The overall stopping and line search convergence criteria were chosen as 10^{-4}, and the partial derivative parameter was taken as 10^{-7}. A convergent solution, in accordance with these criteria, was achieved in seven stages.

A "stage" is an unconstrained minimization for a given set of values σ_j and τ_k; an iteration is one step within the DFP minimization process. Table 1 shows, for the cumulative number of iterations, spanning all seven stages, the progress of the design variables. This same data is plotted in Fig. 2. The resulting design was x_1 = 1.531, x_2 = 3.677, x_3 = 8.881 and x_4 = 0.103, with W = 8.556 lb./ft. These values agree with the solution reported in Ref. 2.

It should be noted that the values of x_3 and x_4 (the vertical web depth and the thickness of the sheet) did not change after the first stage. In view of the convergence of x_3 and x_4 after the first stage the overall weight did not change significantly thereafter.

In the second design problem we seek the proportions of a hat section for a positive bending moment of 281.25 in.K. and a shear of 3.75 K. These section forces represent a uniformly loaded, simply supported beam. Five different initial solutions are attempted, as defined in Table 2, each with the same value of R and tolerances employed in the previous example. All initial designs except case 3 were feasible.

Every case except 4 converged to a solution in the neighborhood of 12.39 lb./ft. The case 4 initial weight was approximately 44 times larger than any other initial design.

6. Concluding Remarks

The performance of the method of multipliers in the selected examples gives promise for the utility of the method. Considerably greater computational experience in practical problems of cold formed light gage steel design is first needed, however, before this view is confirmed. One difficulty in this is to identify a representative range of such practical problems.

A limitation of the computer program employed in this work is that stationary points of the penalty function are, in general, infeasible. Also, the selection of the convergence criterion, partial derivative criterion, and overall stopping criterion is very important to convergence. In certain examples, not reported here, two different combinations of these parameters were tried, and no convergence was achieved. Since the solution depends on these parameters, more research work on their selection can be done. Also, the programs should be modified in such a way that if the convergence has not achieved in several steps new parameters will be considered.

References

1. Seaburg, P.A. and Salmon, C.G., "Minimum Weight Design of Light Gage Steel Members", Proc. ASCE, Journal of the Structural Division, Vol. 97, No. ST1, 203-222 (1971).

2. Ramamurthy, S. and Gallagher, R.H., "Generalized Geometric Programming in Light Gage Steel Design", Proc. 4th Int. Specialty Conf. on Cold-Formed Steel Structures, Mo, June 1-2, (1978).

3. Moe, J., "Penalty Function Methods", Ch. 9, Optimum Structural Design, R. Gallagher and O.C. Zienkiewicz, Editors. J. Wiley Book Co., 1973.

4. Eason, E. and Fenton, R.G. "A Comparison of Numerical Optimization Methods for Engineering Design", ASME, J.Engrg.Ind., 96, 1974, pp.196-200.

5. Colville, A.R. "A Comparative Study on Nonlinear Programming Codes", Proc. Princeton Symp. on Math. Programming. H. W. Kuhn, Ed., Princeton, N.J. 1970.

6. Hestenes, M.R. "Multiplier and Gradient Methods", J. Optim. Theory and Applic., V. 4, No. 5, 1969.

7. Powell, M.J.D. "A Method for Nonlinear Constraints in Minimization Problems", Ch. 19 in Optimization, R. Fletcher, Editor. Academic Press, 1969.

8. Miele, A. "On the Method of Multipliers for Mathematical Programming Problems", J. Optim. Theory and Applic., V. 10, No. 1, 1972.

9. Schuldt, S.B., Gabriele, G.A., Root, R.R., Sandgren, E. and Ragsdell, K.M. "Application of a New Penalty Function Method to Design Optimization", ASME, Journal of Engineering for Industry, V. 99, No. 1, Feb. 1977, pp. 31-36.

10. Root, R.R. and Ragsdell, K.M. "Computational Enhancements to the Method of Multipliers", Trans. ASME, V. 102, Journal of Mechanical Design, 517-523, July 1980.

11. Root, R. and Ragsdell, K.M. BIAS: A Nonlinear Programming Code in Fortran IV, Purdue Research Foundation, Indiana (1979).

12. Coggins, G.F. "Univariate Search Methods", Imperial Chem. Ind., Central Instr. Lab. Res. Note, 64/11, 1964.

13. American Iron and Steel Institute. "Specification for the Design of Cold-Formed Steel Structural Members", 1968 ed. Parts I, II, III, (1974).

14. Yu, W. -W., Cold-Formed Steel Structures, McGraw Hill Book Co., N.Y. (1973).

Acknowledgement

The authors wish to express their appreciation to Prof. K. Ragsdell of Purdue University and to the Purdue University Research Foundation for the use of the BIAS computer program.

Number of Iterations	Weight	$w = x_2$	$d = x_1$
	Lb/ft	inch	inch
STARTING POINT	13.64	14.50	2.35
1	12.67	14.04	2.24
2	10.24	9.50	1.65
4	9.71	8.19	1.78
8	9.18	7.04	2.15
15	8.44	4.23	1.86
20	8.34	3.67	1.76
25	8.34	3.49	1.74
30	8.37	3.49	1.75
40	8.52	3.52	1.76
50	8.55	3.65	1.58
55	8.56	3.67	1.55
65	8.56	3.68	1.53
69	8.56	3.68	1.53
FINAL VALUE	8.56	3.68	1.53

TABLE 1

TEST		DESIGN VARIABLES					Objective Function (Weight)	Number of Stages	Number of Iterations
		X_1(d)	X_2(w)	X_3(h)	X_4(t)	X_5(b)			
1	I *	1.000	4.267	18.144	12.094	4.247	17.498	3	40
	0**	0.577	3.582	15.394	0.103	3.586	12.396		
2	I	1.000	4.270	18.140	0.150	4.250	21.701	3	54
	0	0.577	3.582	15.394	0.103	3.586	12.396		
3	I	0.500	2.133	9.070	0.061	2.173	4.374	9	85
	0	0.577	3.579	15.387	0.103	3.503	12.384		
4	I	7.300	8.500	1.500	10.000	15.700	887.400		
	0								
5	I	7.300	8.500	20.500	0.100	8.500	21.794	5	76
	0	0.577	3.582	15.393	0.103	3.585	12.394		

* Initial values
** Optimum values

TABLE 2

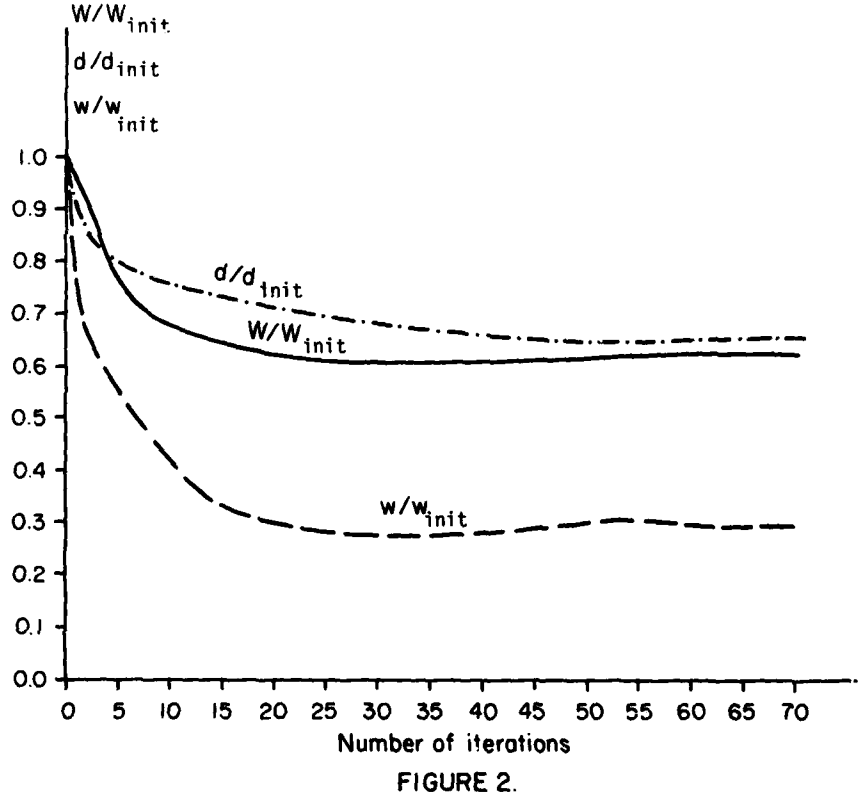


FIGURE 2.

AD-P000 081

OPTIMUM DESIGN OF GRILLAGES INCLUDING WARPING

Dr.Mehmet Polat Saka
Civil Engineering Department
Karadeniz Technical University
Trabzon,Turkey

Summary

A method is presented for optimum design of elastic grillages made of straight thin walled beams. The design problem is formulated by matrix displacement method. Emprical relationships are used to relate the beam cross-sectional properties to each other so that each beam element has only one design variable which is its moment of inertia. Joint displacements are also treated as independent design variables. This requires to include the stiffness constraints as polynomials of the variables in the design problem. Constraints on stresses, displacements and cross-sectional moments of inertia are also considered. The effect of warping is included by employing Vlasov's theory.

The minimum weight design problem obtained by such a formulation turns out to be a nonlinear programming problem. Approximating programming is adopted for its solution, because the constraints involved are in the form of polynomials that can be differentiated automatically. Simplex method is employed after linearization. Move limits are required to obtain the convergence.These are arranged automatically by the program. The examples solved have shown that this way leads to obtain the final design after relatively small number of iterations. Practical examples are given for the application of the method.

Introduction

The rapid development of structural optimization techniques in the last two decades has given sufficient confidence to structural engineers to consider more practical design problems. Among the design procedures presented so far, three types of approaches to structural optimization may be distinguished which are not totaly independent of each other.

In mathematical programming procedures, the objective function is minimized directly by various numerical search techniques while prescribed design constraints are observed to be satisfied. The design problem is handled in general without paying any attention to its physical characteristics. Several reviews are available, some of which contain an extensive reference list. Those by Schmit [1], Niordson and Pedersen [2] cover more than 100 papers. On the other hand, in optimality criteria approaches, a criterion related to the behaviour of structure is generated. A search procedure is then developed to find the design satisfying this specified criteria. When this is achieved, the objective function automatically attains its optimum value. A brief review of structural optimization including optimality criteria approach was presented by Venkayya [3] .In optimum-control approaches the application of calculus of variations are involved. A presentation and review of these techniques was given by McIntosh [4] .

Among these methods, the mathematical programming procedures does not only appear to be extremly general in their range of applicability, but flexible and easy to adopt for computer programming. There are large number of mathematical programming algorithms that can be employed in structural design. Selection of the suitable one for the solution of a design problem is sometimes another optimization problem. However, review of the design algorithms presented so far shows that structural engineers have found the approximating programming quite powerful . This method linearise the nonlinear problem by Taylor expansion and then employs simplex method to obtain its solution. This technique is used in various structural design algorithms by Reinschmit [5], Romstad and Wang [6], Pope [7], Fleury and Schmid [8] and Saka [9,10] . In these works the topology of the structure is considered to be specified and cross-sectional properties of the elements are treated as design variables. Later, the same method is employed in structural shape optimization. Notable in this field are Dorn , et al [11], Majid and Saka [12, 13], Pedersen [14,15] and Saka [16,17] .

In this paper, an application of the approximating programming in the optimum design of elastic grillages is presented. The same design problem was also considered by Moses and Onoda [18] where the results obtained by methods of stress-ratio, cutting-plane and usable-feasible gradient were compared. Kavlie and Moe [19] used SUMT for the solution of the same problem. In both design procedures, the effect of warping was neglected. It is also reported that a large number of analyses are involved in the design process. Present method formulates the design problem by matrix displacement method. Joint displacements are treated as design variables as well as sectional properties. This leads to inclusion of the stiffness constraints as polynomials of the variables in the design problem. Constraints on stresses and displacements are also considered. The number of iterations involved in optimum design

PRECEDING PAGE

is small, generally less than 10. The effect of warping is considered by employing Vlasov's theory.

Warping in grillage elements

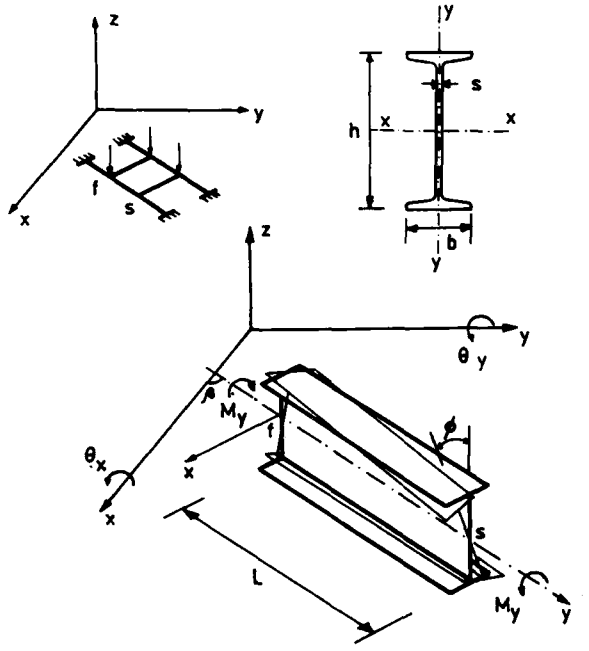


Figure 1. A grillage element

Grillage elements as shown in figure 1 are usually made of thin walled beams such as I, C, T shapes. In such beams, according to Vlasov's theorems [20] , even when no external twisting moments are present, torsional stresses can be present. A torque acting on a such beam is a combination of pure and flexural torques which is given by the following differential equation:

$$G J \frac{d\phi}{dy} - E \Gamma \frac{d^3\phi}{dy^3} = -M_t \qquad (1)$$

where G is the modulus of rigidty and E is modulus of elasticity of the material of beam, J is torsional moment of inertia and Γ is warping constant. ϕ is angle of twist and M_t is the total torque. If equation (1) is derived with respect to y, considering that torque is constant along the beam

$$\frac{d^4\phi}{dy^4} - \alpha \frac{d^2\phi}{dy^2} = 0 \qquad (2)$$

is obtained where $\alpha = \sqrt{\frac{GJ}{E\Gamma}}$.

The general solution of this equation is

$$\phi = A \operatorname{Cosh} \alpha y + C \sinh \alpha y + Dy + H \qquad (3)$$

where A,C,D and H are constants of integration. The following boundary conditions may be used to evaluate the integration constants for the grillage elements rigidly connected to each other.

$$\left.\begin{array}{l} \text{When } y=o\ ,\ \phi = \theta_{by_f} \text{ and } \dfrac{d\phi}{dy} = o \\ \text{When } y=L\ ,\ \phi = \theta_{by_s} \text{ and } \dfrac{d\phi}{dy} = 0 \end{array}\right\} \qquad (4)$$

Where θ_{by_f} and θ_{by_s} are the rotations of beam ends and $\frac{d\phi}{dy}$ is the rate of twist.

Using equations (2), (3) and (4) the torque in the beam is obtained as

$$M_y = -G J \cdot \frac{\alpha \operatorname{Sinh} \alpha L}{2\operatorname{Cosh} \alpha L - \alpha L \operatorname{Sinh} \alpha L - 2} (\theta_{by_s} - \theta_{by_f}) \qquad (5)$$

where L is the legth of the beam. The bimoment in the beam is given by

$$B = -E \Gamma \frac{d^2\phi}{dy^2} \qquad (6)$$

Similarly, by employing the equations (3), (4) and (6) the bimoment at the first end of the beam is obtained as

$$B = GJ \cdot \frac{\operatorname{Cosh} \alpha L - 1}{2\operatorname{Cosh} \alpha L - \alpha L \operatorname{Sinh} \alpha L - 2} (\theta_{by_s} - \theta_{by_f}) \qquad (7)$$

The bimoment at the second end of the beam is

$$B = GJ \cdot \frac{\operatorname{Cosh} \alpha L - 1}{2\operatorname{Cosh} \alpha L - \alpha L \operatorname{Sinh} \alpha L - 2} (\theta_{by_f} - \theta_{by_s}) \qquad (8)$$

It may be noticed that when the beam end rotations are equal to each other, no torque emerges in the beam. On the other hand, if one end of the beam is fixed then the equations (5), (7) and (8) can still be used by only equating the rotation of that end to zero.

In grillage elements with a bending hinge at one end, the torque is obtained as

$$M_y = -G J \cdot \frac{\operatorname{Cosh} \alpha L}{\operatorname{Sinh} \alpha L - \alpha L \operatorname{Cosh} \alpha L} (\theta_{by_s} - \theta_{by_f}) \qquad (9)$$

and the bimoment at the other end of the beam is

$$B = -G J \cdot \frac{\operatorname{Sinh} \alpha L}{\operatorname{Sinh} \alpha L - \alpha L \operatorname{Cosh} \alpha L} (\theta_{by_s} - \theta_{by_f}) \qquad (10)$$

For grillage elements with a different end conditions, similar expressions for torgue and bimoments may be obtained.

Mathematical model

In the formulation of the design problem, the joint displacements are treated as independent design variables in addition to the moments of inertia of grillage elements. The other cross sectional properties of the element are related to its moment of inertia in such a way that each beam element introduces only one design variable.

$$\left.\begin{aligned} J&=a_1 I^{b_1}, \quad I_y = a_2 I^{b_2}, \quad h = a_3 I^{b_3} \\ b&=a_4 I^{b_4}, \quad Z = a_5 I^{b_5}, \quad A = a_6 I^{b_6} \\ s&=a_7 I^{b_7} \end{aligned}\right\} \quad (11)$$

where J, I_y, Z and A are respectively the torsional moment of inertia, sectional moment of inertia about to y-y axes, sectional modulus and area of element. h,b,s are shown in figure 1. The constants (a_i, b_i, i=1,..,7) may be obtained by applying least square approximation to logaritmic values of the above sectional properties which are given in steel manuals such as AISC, DIN [21].

Using the matrix displacement method with the design variables mentioned, it becomes necessary to include the stiffness constraints as polynomials of the variables in the design problem. Therefore, the problem is to minimize

$$W = W(\underset{\sim}{I})$$

Subject to

$$\begin{aligned} &K_i(\underset{\sim}{I}).\underset{\sim}{X}_d - P_i = 0 \quad , i=1, \ldots, k \\ &\sigma_i(\underset{\sim}{I}, \underset{\sim}{X}_d) - \sigma_{pi} \leq 0, \; i=k+1,\ldots,m \\ &\underset{\sim}{X}_d - \underset{\sim}{X}_{pd} \leq 0 \\ &\underset{\sim}{I}_\ell \leq \underset{\sim}{I} \leq \underset{\sim}{I}_u \end{aligned} \quad (12)$$

the first of which is the stiffness constraints, the second is the stress constraints, the third is deflection constraints and the fourth is the upper and lower bounds on moments of inertia. P_i is the external load acting at a joint. $\underset{\sim}{I}$ is the vector of unknown moments of inertia, $\underset{\sim}{X}_d$ is the vector of joint displacements σ_p and $\underset{\sim}{X}_{pd}$ are the permissible values imposed on stresses and displacements respectively.

Using the relationship (11) the objective function will have the form

$$W = \sum_{i=1}^{NG} \rho_i A_i L_i = \sum_{i=1}^{NG} \rho_i L_i a_6 I_i^{b_6} \quad (13)$$

in which ρ_i and L_i are the material density and length of elements in group i, NG is the total number of different groups in grillage.

The stiffness constraints

The stiffness constraints are equalities and they have the form

$$\underset{\sim}{K}(\underset{\sim}{I}).\underset{\sim}{X}_d - \underset{\sim}{P} = 0 \quad (14)$$

where $\underset{\sim}{K}(\underset{\sim}{I})$ is the overall stiffness matrix and $\underset{\sim}{P}$ is the external load matrix. The contribution of a single grillage element, linking joints f and s as shown in figure 1, to the overall stiffness matrix is

$$\underset{\sim}{K}_{fs} = \left[\begin{array}{ccc:ccc} A & B & -Y & -A & B & -Y \\ B & C & D & -B & R & H \\ -Y & D & F & E & H & P \\ \hdashline -A & -B & Y & A & -B & Y \\ B & R & H & -B & C & D \\ -Y & H & P & Y & D & F \end{array}\right] \quad (15)$$

Here,

$$\begin{aligned} &A=\frac{12E}{L^3}I, B=\frac{6E\sin\beta}{L^2}I, C=\frac{4E\sin^2\beta}{L}I+T\cos^2\beta \\ &D=(T-\frac{4E}{L}I)\sin\beta\cos\beta, Y=\frac{6E\cos\beta}{L^2}I, \\ &F=\frac{4E\cos^2\beta}{L}I+T\sin^2\beta, R=\frac{2E\sin^2\beta}{L}I-T\cos^2\beta, \\ &H=-(\frac{2E}{L}I+T)\sin\beta\cos\beta, P=\frac{2E\cos^2\beta}{L}I-T\sin^2\beta \end{aligned} \quad (16)$$

β is shown in figure 1.

If warping is not considered $T = \frac{GJ}{L}$ (17)

If warping is considered

$$T = GJ \cdot \frac{\alpha \sinh\alpha L}{2\cosh\alpha L - \alpha L \sinh\alpha L - 2} \quad (18)$$

In these expressions I and J are respectively the unknown moment of inertia and torsional moment of inertia of grillage element, E and G are modulus of elastisity and modulus of rigidity and L is the length of the element. $\alpha = \sqrt{\frac{GJ}{E\Gamma}}$ and for I sections $\Gamma = \frac{I_y \cdot h^2}{4}$ as given in [20].

Employing the relationships (11), the equations (17) and (18) may be related to unknown moment of inertia as

$$T = \frac{G}{L} a_1 I^{b_1} \quad (19)$$

$$T = c_1 I^{c_2} \frac{\sinh(c_3 I^{c_4})}{2\cosh(c_3 I^{c_4}) - c_3 I^{c_4} \sinh(c_3 I^{c_4}) - 2} \quad (20)$$

where

$$\begin{aligned} c_1 &= \sqrt{\frac{G^2 a_1^2}{0.25 E a_2 a_3^2}}, \quad c_2 = 1.5b_1 - 0.5b_2 - b_3 \\ c_3 &= \sqrt{\frac{G a_1 L^2}{0.25 E a_2 a_3^2}}, \quad c_4 = 0.5b_1 - 0.5b_2 - b_3 \end{aligned} \quad (21)$$

in which values of a_i, b_i are given equation (11). It can be seen from equations (16), (19) and (20) that the contribution of an grillage element to overall stiffness matr. is expressed as only function of its unknown moment of inertia.

The stress constraints

In grillages made of thin walled beams, the governing elastic stress at the outher fibres is a combination of stresses caused by bending moments and stresses caused by bimoments [20].

$$-\sigma_{ci} \leqslant \pm \sigma_{bi} \pm \sigma_{wi} \leqslant \sigma_{ti} \qquad (22)$$

where σ_{ci} and σ_{ti} are the permissible compressive and tensile stresses, σ_{bi} and σ_{wi} are the stresses caused by bending moment and bimoment respectively in member i.

In the grillage element linking joints f and s as shown in figure 1, employing equation (11), the stresses due to bending moments at the first and second ends are expressed in terms of its moment of inertia as

$$\begin{bmatrix}\sigma_{bf}\\ \sigma_{bs}\end{bmatrix} = I^{1-b_5}\left[\begin{array}{ccc:ccc} a_{11} & a_{12} & -a_{13} & -a_{11} & a_{22} & -a_{23}\\ a_{11} & a_{22} & -a_{23} & -a_{11} & a_{12} & -a_{13}\end{array}\right]\begin{bmatrix}\underset{\sim}{X}_{df}\\ \underset{\sim}{X}_{ds}\end{bmatrix} \qquad (23)$$

where

$$a_{11}=\frac{6E}{a_5L^2} \quad a_{12}=\frac{4E\sin\beta}{a_5L} \quad a_{13}=\frac{4E\cos\beta}{a_5L}$$
$$a_{22}=\frac{2E\sin\beta}{a_5L} \quad a_{23}=\frac{2E\cos\beta}{a_5L} \qquad (24)$$

On the other hand, stresses due to bimoments are

$$\sigma_w = \frac{Bw}{\Gamma} \qquad (25)$$

where B is bimoment, w is sectorial area and Γ is warping constant. Bimoment in the element is given by equations (7), (8) and (10). The sectorial area for I section is $w = 0.25\,bh$ where b and h is shown in figure 1. Once again, substituting equation(11) in (7) an (24), the stress due to bimoment is obtained as

$$\sigma_{wi} = \begin{bmatrix} o & -U_i\cos\beta & -U_i\sin\beta & o & U_i\cos\beta & U_i\sin\beta\end{bmatrix}\begin{bmatrix}\underset{\sim}{X}_{df}\\ \underset{\sim}{X}_{ds}\end{bmatrix} \qquad (26)$$

where
$$U_i = c_5 I^{c_6}\frac{\cosh(C_3 I^{c_4}) - 1}{2\cosh(C_3 I^{c_4}) - c_3 I^{c_4}\sinh(C_3 I^{c_4}) - 2} \qquad (27)$$

$$c_5=\frac{Ga_1a_4}{a_2a_3}, \quad c_6 = b_1-b_2-b_3+b_4$$

in which a_i, b_i are given by equation (11), C_3 and C_4 are given by equation (21). In this way, both stresses caused by bending moments and bimoments are related to the moments of inertia of grillage elements by equation (23) and (26). Expression for U similar to (27) may be obtained for different end conditions. Shear stress constraints is also considered.

$$\tau_i = \frac{Q_i}{A_{wi}} \leqslant \tau_{pi} \qquad (28)$$

where Q_i is shear force in element i, A_{wi} is web area and τ_{pi} is the permissible shear stress. Using equation (11), the shear stress in the element may be expressed in terms of its moment of inertia as

$$\tau_i = I^{1-c_8}\begin{bmatrix} b_{11} & b_{12} & -b_{13} & -b_{11} & b_{12} & b_{13}\end{bmatrix}\begin{bmatrix}X_{df}\\ X_{ds}\end{bmatrix} \qquad (29)$$

where

$$b_{11}=\frac{12E}{c_7L^3}, \quad b_{12}=\frac{6E\sin\beta}{c_7L^2}, \quad b_{13}=\frac{6E\cos\beta}{c_7L^2}$$
$$c_7 = a_3\,a_7, \quad c_8 = b_3 + b_7 \qquad (30)$$

Equation (22) implies that for a section of an element, it is necessary to consider four independent stress constraint to cover the possible stress reguirements. However, at each iteration, the joint displacements are available either from the result of analysis or after carrying out the simplex method for the linearised problem. Using these values, it is possible to determine the sign of the maximum longitudinal stress and shear stress at either end of a grillage element. Hence, it becomes possible to introduce only one constraint for the longitudinal stress and one constraint for the shear stress; total of two stress constraints for each member.

The deflection constraints

Inclusion of joint displacements as design variables in the design problem reduces the deflection constraints to upper bounds.

$$\underset{\sim}{X}_d \leqslant \underset{\sim}{X}_{pd} \qquad (31)$$

where $\underset{\sim}{X}_{pd}$ is a vector of permissible displacements. Deflections are unrestricted in sign. Mathematical programming techniques however, operate only with non-negative variables. It is therefore necessary to make the substitution

$$x_j = \gamma_j - e_j \qquad (32)$$

and impose a deflection constraint of the from

$$x_j \leqslant x_{pdj}$$
$$\gamma_j \leqslant x_{pdj} + e_j \qquad (33)$$

where γ_j is a new non-negative variable that replaces x_j and e_j is a constant that is the most negative value x_j can possibly take. The bounds for the vertical displacements can be obtained from specifications. In the case of joint rotations, the bounds are made large enough to cover a wide range. The value of e=0.02 radians is convenient, because linear structural theories are only applicable for small deflections with $|\theta| \leq 0.02$

The approximating programming

It is shown in previous sections that the objective function and the constraints are nonlinear functions of the design variables. This turns the design problem to a nonlinear programming problem. The approximating programming is adopted for its solution. This method makes use of the first two terms of a Taylor expansion. When applied to nonlinear design problem of (12), the following linear programming problem is obtained.

$$\text{Minimize } W = w(\underset{\sim}{Y}^o) + \nabla w(\underset{\sim}{Y}^o)\left[\underset{\sim}{Y}^1 - \underset{\sim}{Y}^o\right]$$

Subject to

$$\begin{aligned} S_i(\underset{\sim}{Y}^o) + \nabla S_i(\underset{\sim}{Y}^o)\left[\underset{\sim}{Y}^1 - \underset{\sim}{Y}^o\right] &= 0 \\ \sigma_i(\underset{\sim}{Y}^o) + \nabla \sigma_i(\underset{\sim}{Y}^o)\left[\underset{\sim}{Y}^1 - \underset{\sim}{Y}^o\right] &\leq 0 \\ \underset{\sim}{X}_d - \underset{\sim}{X}_{pd} &\leq 0 \\ (1-m)\underset{\sim}{I}^o \leq \underset{\sim}{I}^1 &\leq (1+m)\underset{\sim}{I}^o \end{aligned} \qquad (34)$$

where $\underset{\sim}{Y} = [\underset{\sim}{I}\ \underset{\sim}{X}_d]^T$ is the vector of design variables in which the submatrix $\underset{\sim}{I}$ contains the moments of inertia of different groups and $\underset{\sim}{X}_d$ contains displacements of N joints. The i th stiffness constraint has the form

$$S_i(\underset{\sim}{Y}) = K_i(\underset{\sim}{I}).\underset{\sim}{X}_d - P_i = 0 \qquad (35)$$

The stress constraint for member i has the form

$$\sigma_i(\underset{\sim}{Y}) = \underset{\sim}{B}(\underset{\sim}{I}).\underset{\sim}{X}_d - \sigma_{pi} \leq 0 \qquad (36)$$

The values of every function is known at $\underset{\sim}{Y}^o$ and $\underset{\sim}{Y}^1$ is the unknown variable vector. m is the preselected percentage which is known as move limits. These are required to prevent fluctuation of iterations and encourage the convergence of the original nonlinear problem. When the linear programming problem of (34) is rearranged

$$\text{Minimize } W = \nabla \underset{\sim}{w}(\underset{\sim}{Y}^o).\underset{\sim}{Y}^1 + w(\underset{\sim}{Y}^o) - \nabla \underset{\sim}{w}(\underset{\sim}{Y}^o).\underset{\sim}{Y}^o$$

Subject to

$$\begin{aligned} \nabla \underset{\sim}{S}_i(\underset{\sim}{Y}^o).\underset{\sim}{Y}^1 &= \nabla \underset{\sim}{S}_i(\underset{\sim}{Y}^o).\underset{\sim}{Y}^o - S_i(\underset{\sim}{Y}^o) \\ \nabla \underset{\sim}{\sigma}_i(\underset{\sim}{Y}^o).\underset{\sim}{Y}^1 &\geq \nabla \underset{\sim}{\sigma}_i(\underset{\sim}{Y}^o).\underset{\sim}{Y}^o - \sigma_i(\underset{\sim}{Y}^o) \\ \underset{\sim}{X}_d^1 &\leq \underset{\sim}{X}_{pd} \\ \underset{\sim}{I}^1 &\leq (1+m)\underset{\sim}{I}^o \\ \underset{\sim}{I}^1 &\leq (1-m)\underset{\sim}{I}^o \end{aligned} \qquad (37)$$

in which ∇W, ∇S and $\nabla \sigma$ are respectively the gradient vectors of objective function, stiffness and stress constraints.

$$\left.\begin{aligned} \nabla \underset{\sim}{W}(\underset{\sim}{Y}^o) &= \left[\left(\frac{\partial W}{\partial I^o}\right) \quad 0\right] \\ \nabla \underset{\sim}{S}_i(\underset{\sim}{Y}^o) &= \left[\left(\frac{\partial S_i}{\partial I^o}\right) \quad \left(\frac{\partial S_i}{\partial X_d^o}\right)\right] \\ \nabla \underset{\sim}{\sigma}_i(\underset{\sim}{Y}^o) &= \left[\left(\frac{\partial \sigma_i}{\partial I^o}\right) \quad \left(\frac{\partial \sigma_i}{\partial X_d^o}\right)\right] \end{aligned}\right\} \qquad (38)$$

The derivatives of the nonlinear constraints with respect to design variables can be calculated directly. Hence, the derivatives of the stiffness and stress constraints given in (35) and (36) with respect to the moments of inertia and deflections are

$$\left.\begin{aligned} \frac{\partial S_i}{\partial I_j} &= \frac{\partial K_i(\underset{\sim}{I})}{\partial I_j}.\underset{\sim}{X}_d, \quad \frac{\partial S_i}{\partial \gamma_j} = K_{ij}(\underset{\sim}{I}) \\ \frac{\partial \sigma_i}{\partial I_j} &= \frac{\partial B(\underset{\sim}{I})}{\partial I_j}.\underset{\sim}{X}_d, \quad \frac{\partial \sigma_i}{\partial \gamma_j} = B_j(\underset{\sim}{I}) \end{aligned}\right\} \qquad (39)$$

After solving the linear programming problem of (37) by simplex method, new values of design variables $\underset{\sim}{Y}^1$ are obtained. This procedure is repeated until convergence on the objective function is obtained.

The selection of move limits are carried out differently in various research works. In this paper, it is found suitable choose the value of 0.90 for move limits to begin with and then gradually reduce by 0.10 at each iteration. In the case where convergence is not obtained although the value of m is reduced to 0.10 then the iterations are continued with this particular value. Examples solved have shown that the number of iterations required to reach the final design is around 10.

Design procedure

The flow diagram of the design procedure is given in figure 2. The procedure can operate both from a feasible or an infeasible initial design point. The only restriction for this point is that it has to satisfy the stiffness constraints. The initial values of the moments of inertia may be selected by using the engineering judgement.

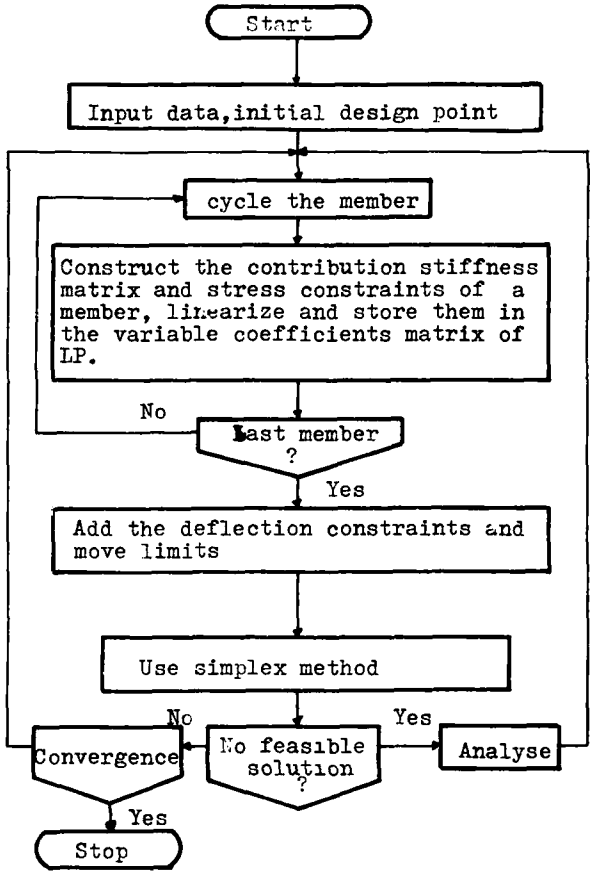


Figure 2. The design procedure

It may be noticed from the flow diagram that the inclusion of the joint displacements as independent design variables leads to a simple computer programming. No matrix inversion is involved. An analysis is only carried out when the current imposed move limits fails to obtain an optimum solution. As a result, one analysis at most may be required at each optimization iteration.

The convergence criterion utilized to end the algorithm is that the change in the objective function on two succesive cycles will be less than preselected small percentage of its current value.

Design examples

In the examples solved in this paper, the value of E,G, σ_c,σ_t, and τ_p were takes as 210 KN/mm^2, 81 KN/mm^2, 0.14 KN/mm^2, 0.14 KN/mm^2 and 0.09 KN/mm^2 respectively throughout. The values of ai and bi of equation (11) are given in table 1. These are obtained for the I shape rolled sections given in [21]. It should be noticed that in the calculation of these elements the values of the sectional properties are taken in the unit of centimetres (1 cm = 10 mm).

i	1	2	3	4
a_i	0.00874	0.1285	2.5758	1.7025
b_i	0.9409	0.887	0.2666	0.2153
i	5	6	7	
a_i	0.778	0.8827	0.1247	
b_i	0.733	0.476	0.23725	

Table 1. The values of a_i, b_i

Example 1

As a demonstration of the method,design of a simple grillage shown in figure 3 is considered. This grillage is subject to vertical load of 100 KN acting at B. The vertical displacement of joint B were limited to 20 mm. The bounds on rotations were taken as 0.02 radians. The beams are made out of the same section.

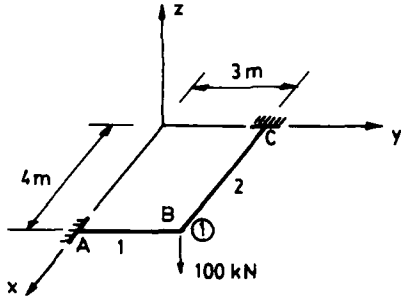


Figure 3. A simple grillage

Iteration No	Without warping		With warping	
	Ix10^{7}mm^4	volume x10^{6}mm^3	Ix10^{7}mm^4	volume x10^{6}mm^3
0	9.800	49.061	9.800	49.061
1	17.349	64.389	17.761	65.112
2	26.358	77.138	26.796	79.190
3	29.720	83.192	32.337	86.602
4	30.461	84.172	33.490	88.058
5	30.477	84.194	33.527	88.104
6	30.477	84.194	33.527	88.104

Table 2. Iteration history

There are four design variables in the design problem. These are $V=[\,I\ z_1\ \theta_{x1}\ \theta_{y1}]^T$. Using the equation (15) the stiffness constraints will have the from

$$(A_1+A_2)Iz_1+(B_1+B_2)I\theta x_1-(Y_1+Y_2)I\theta y_1+10=0$$
$$(B_1+B_2)Iz_1+(C_1(I)+C_2(I))\theta x_1+(D_1(I)+D_2(I))\theta y_1=0 \quad (40)$$
$$-(Y_1+Y_2)Iz_1+(D_1(I)+D_2(I))\theta x_1+(F_1(I)+F_2(I))\theta y_1=0$$

where A_i, B_i and Y_i are linearly related to unknown I as shown in (16), but C_i, D_i and F_i are nonlinear function of I which is also given in (16) and i is the member number. Similarly, the stress constraints are constructed by using the expressions (23), (25) and (29). The following non-negativity substitutions are required as explained in (32)

$$z_1=\gamma_1-20\ ,\quad \theta_{x_1}=\gamma_2-0.02,\ \theta_{y_1}=\gamma_3-0.02 \quad (41)$$

The initial design point is choosen to be infeasible point at which the non-linear stiffness and stress constraints are linearized. After adding the deflection constraints which are only upper bounds and move limits, the linearized problem is solved by simplex method. The iteration history of the design is given in Table 2.

When the effect of warping was neglected, the optimum value of the moment of inertia of the beam was obtained as 30.477×10^7 mm^4. The same value has increased to 33.527×10^7 mm^4 when warping was included. As a result, 10% of increase was required in the value of the moment of inertia in this particular example.

Example 2

A grillage shown in figure 4 was designed both with and without considering the effect of warping. The dimensions and member grouping of the grillage and the loading are also show in the figure. The vertical displacements of joints were limited to 30mm and the bounds on rotations were 0.02 radians.

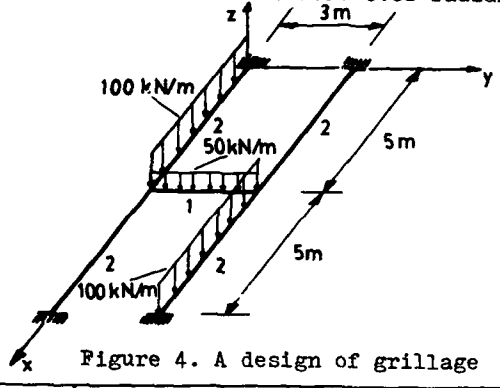


Figure 4. A design of grillage

	Without warping		With warping	
	Initial design	Final design	Initial design	Final design
I_1 $\times 10^7$ mm^4	5.000	4.270	3.000	12.307
I_2 $\times 10^7$ mm^4	50.000	92.326	40.000	96.927
Volume $\times 10^7$ mm^4	31.974	42.185	28.576	44.006

Table 3. Initial and final designs

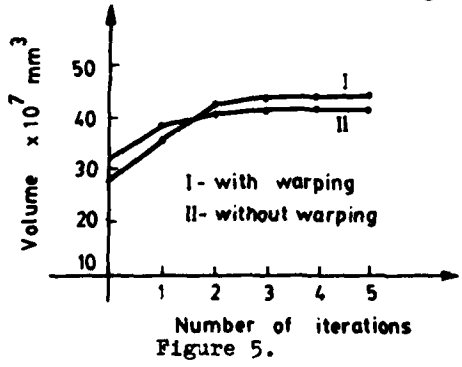


Figure 5.

The design problem has 8 variables which are the moments of inertia of two groups and six displacements of two joints. The same grillage was designed both considering and not considering the effect of warping. As shown in figure 5 convergence was obtained after only 5 iterations in both cases. Initial and final designs are given in table 3. It may be noticed that the moment of inertia of member 1 has increased from 4.27×10^7mm^4 to 12.307×10^7mm^4 when the effect of warping was included. This example clearly shows that depending on the loading, optimum design without including warping will not be adequate.

Example 3

As a final example, design of the grillage shown in figure 6 is presented. The member grouping and loading of the grillage are also shown in the figure. The limitations on the vertical displacements are 40 mm and on the rotations are 0.02 radians.

The design problem was initiated from an infeasible point. There are 21 variables and 68 constraints altogether in the design problem. The minimum volume of 87.7758×10^7mm^3 was obtained after 7 iterations. The optimum values of the moments of inertia are given in table 4. It is noticed that the stress constraints were dominant in the design problem. As a result while, the stresses at points A and B were at their bounds, the displacements of joints were under the limitations. The value of bending stress was 0.127 KN/mm^2 and the warping stress was 0.013 KN/mm^2 at these points.

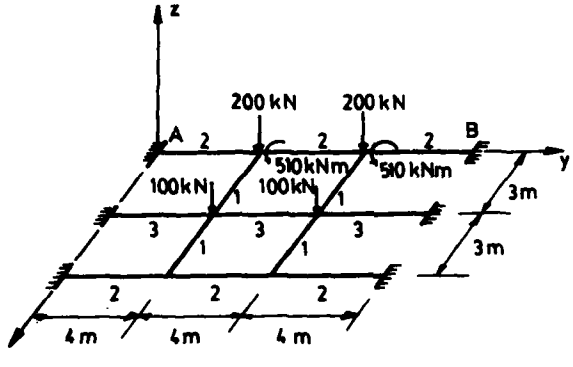


Figure 6.

	Initial design	Final design
I_1 $x10^7 mm^4$	3.000	10.342
I_2 $x10^7 mm^4$	50.000	125.209
I_3 $x10^7 mm^4$	50.000	44.424
Volume $x10^7 mm^4$	59.593	87.774

Table 4. Initial and final design

Conclusions

A general procedure for optimum elastic design of grillages is presented. In the case that the grillage elements are made of thin walled beams, the effect of warping becomes important. It is shown that by making use of the matrix displacement method this effect can easily be included in the formulation of the design problem. The limitations on displacements as well as stresses are also considered. The treatment of the joint displacements as independent variables simplifies the formulation of the design problem and leadsto easy computer programming. Several other examples solved which are not given in this paper showed that the number of iterations required to obtain the final design was small, indicating the efficiency of the method.

Grillages made out of I sections are considered in this paper. However, consideration of [sections or any other shapes does not introduce any difficulty. The only amendment required is to include the necessary relationship among the warping constant, the sectorial area and the moment of inertia of the section considered.

References

1. Schmit, L.A., Structural Synthesis: Univ. of Alabama Press, Huntsville, 1971.
2. Niordson, F.I. and Pedersen, P., A review of optimal structural design , Proc.13 th Int. Cong. Theor. Appl.Mech., Springer-Verlag, Moskova 1973.
3. Venkayya, V.B., Structural optimization: A review and some recommendations, Int. Jour. for Num.Methts. in Engr. Vol. 13, 1978.
4. McIntosh, S.C., Structural optimization via optimal control techniques, AGARD lecture series, 1977.
5. Reinschmidt, K.F., Cornell, C.A. and Brotchie, J.F., Iterative design and structural optimization, ASCE, Struc.Div., Vol.92,ST6, 1966.
6. Romstad, K.M. and Warg, C.K., Optimum design of framed structures, ASCE,Struc. Div., Vol.94, 1968.
7. Pope, G., Application of linear programming techniques in the design of optimum structures, Proc. of AGARD, Symp.Structural optimization, İstanbul,Oct., 1969.
8. Fleury, C. and Schmit, L.A., Primal and dual methods in structural optimization, ASCE,Struc.Div., Vol.106, ST5, 1980.
9. Saka, M.P., Optimum design of structures, Univ. of Aston,Birmingham,U.K., 1975.
10. Saka,M.P., Optimum design of rigidly jointed frames, Computers and Structures, Vol.11,1980.
11. Dorn,M.W. and Felton,L.P., Optimization of truss geometry, ASCE,Struc.Div., Vol. 95, ST10, 1969.
12. Majid,K.I. and Saka,M.P.,Optimum shape design of rigidly jointed frames,Proc.of Symp.on Appl.of Comp.methds.in Engr., Univ.of Southern California,Berkeley, Calif, 1977.
13. Majid,K.I.Saka,M.P. and Çelik,T., The theorems of structural variations generalized for rigidly jointed frames,Proc. ICE,Vol.65,London,1978.
14. Pedersen,P.,On the optimal layout of multi-purpose trusses, Computers and structures, Vol.2, 1972.
15. Pedersen,P., Optimal joint positions for space trusses, ASCE,Struc.Div., Vol.99, ST12, 1973.
16. Saka,M.P., Structural shape optimization -A review, XV th Yugoslav congress of theoretical and applied Mechanics, June, Kupari, 1981.
17. Saka,M.P., Shape optimization of trusses, ASCE, Struc.Div.,Vol.106,ST5, 1980.
18. Moses,F. and Onoda,S., Minimum weight design of structures with application to elastic grillages, Int.J.for num.methds. in engr., Vol. 1, 1969.
19. Kavlie, D. and Moe,J., Application of nonlinear programming to optimum grillage design with noneonvex sets of variables, Int.J.for, num.methds.in engr.,Vol. 1, 1969.
20. Zbirohowski-Koscıa,K., Thin walled beams, Crosby lockwood, London, 1967.
21. Stahl in hochbau, Verlag stahleisen, Püsseldorf, 1967.

AD P000 082

OPTIMUM COST DESIGN OF PRECAST CONCRETE BUILDINGS

J. Knapton,
Nigel Nixon & Partners
Norham House, New Bridge Street,
Newcastle upon Tyne, U.K.

K.A. Andam,
Department of Engineering,
Technical University,
Kumasi, Ghana.

Introduction

For several years, the authors have worked in co-operation with the largest U.K. manufacturer of precast concrete portal framed buildings with the aim of producing a computer design and detailing program for agricultural and industrial buildings. From 1977 to 1979, research was undertaken into costs of fabricating, delivering and erecting portal framed buildings and this work allowed the authors to write a FORTRAN IV program which determines the precast concrete manufacturer's cost of providing a building to a client's specification. During 1979, a design program was written, also in FORTRAN IV, which selected sizes for structural elements and cladding components. By maintaining compatibility of data between these two programs, it became possible by the end of 1979 for a design engineer to enter data describing a building and for the computer to select the sizes of all components and hence determine the cost of a feasible design solution.

These two programs were linked to a third program which uses Rosenbrock's optimization algorithm to iterate towards the least cost building. Finally, during 1981, a fourth program was written which takes the data describing component sizes for the optimum cost building and produces a general arrangement drawing together with a written specification, both on a drum plotter.

During the course of the project, an IBM contouring package was used to investigate the sensitivity of the primary optimization variables. Although this was of little value to the manufacturer, the cost surfaces produced gave the authors invaluable information on the unimodality of the cost response surface and helped in selecting the most appropriate optimization algorithm.

This paper describes the four programs and shows some of the data obtained during the cost response surface sensitivity analysis. It shows the drawings produced by the final program and draws conclusions regarding the merits of cost optimisation.

Manufacture of Precast Concrete Portal Framed Industrial Buildings.

The precast concrete industry in the U.K. has a workforce of about 28,000 which represents nearly 2.3% of the total construction workforce. Between 1971-78 the total outputs of the construction industry and precast concrete industry are respectively estimated at £m42169 and £m1604. That is, the precast concrete industry's output is 3.72% of the total construction industry's output.

Of the 250 precast concrete firms in the U.K. 10 are fabricators of framed structural components on a large scale. Studies carried out on these types of structures show that an average of 0.5 million tonne are fabricated and erected annually. In terms of cost, framed structures form about 15.26% of all precast concrete products. Table 1 shows the quantity of precast concrete for framed buildings during the period 1971 to 1979. The influence of the 1973 oil crisis and the subsequent recession are clearly seen in the table. Indeed, it is the reduction in the total marked size and the resulting manufacturing overcapacity which generated the need for the manufacturer involved in this project to try to increase his market share by applying optimization at the design stage.

TABLE 1. Output of precast concrete for framed buildings in the U.K. (tonnes).

Year	Output (Tonnes)
1971	400000
1972	516700
1973	735000
1974	405000
1975	450000
1976	480000
1977	465000
1978	495000
1979	540000

In order to ensure that the data used in the cost model was accurate, a detailed study was undertaken of the working methods of one typical precast concrete manufacturing plant.

Figure 1 shows the structural elements which comprise the building and this figure shows that each element is manufactured in its own terretory within the plant. Such an arrangement is helpful in allowing time study methods to be applied to each type of element individually. Figure 2 shows the sequence of operations involved in the manufacture of each type of element. These operations form the basis of the cost model program described in the next section. Although figures 1 and 2 apply only to the structural elements, costs are also determined for the remaining components of the building. However, because these components are bought by the precast concrete manufacturer, their price to the precaster is used as their cost. Therefore it is unnecessary to investigate their manufacture. This applies to all cladding components.

For each of the structural elements shown in Figure 2, the following operations were studied:

1. Cut and bend reinforcement to schedule.
2. Assemble reinforcement, ready mould and place cage in mould.
3. Place and vibrate concrete with finishes and stack where necessary.
4. Demould element and stack.

Operation times were approximated to the nearest second. Operations (3) and (4) could not be studied concurrently for lack of personnel. At some instances operation (1) or (2) was executed for more than one element. Each of the four operations was timed for ten cycles and the mean times were taken. Figure 3 shows the results of the study. Sizes of each of the five elements vary according to the particular design. Studies were made on element sizes of weights ranging between 0.14 - 1.28 tonnes. The results presented in Figure 3 assume a linearly proportional weight of one tonne for each element.

Table 2 summarises the work gang and equipment used in each operation. Readying the mould takes the form of cleaning and coating the interior with a thin film of oil. Lifting reinforcement cages is done mainly with gantry cranes, portable wheelers and manually. Vibrating tables are used. Gantry cranes are used to demould column and rafters. Purlins are demculded manually and gutter moulds are dismantled to ensure no damage is done to the delicate sections.

TABLE 2. Work Study Sheet.

Operation	Number of workmen					Equipment
	Col	Raf	Pur	Ral	Gut	
1. Cut and bend reinf. to schedule	1	1	1	1	1	Cutting machine
2. Assemble reinf. Ready Mould	2	2	1	2	1	Gantry cranes used to carry heavy cages
3. Place and Vibrate concrete, dinishes and stack	3	2	1	2	2	Wheelbarrow for concrete distribution, gantry cranes for stacking.
4. Demould and stack	3	2	1	2	2	Gantry cranes for demoulding cols.& rafters

Analsyis of Factory Output.

In order to complement findings of the work study, output of the same factory over a continuous sixty day period has been analysed. The period covers about the same duration as the work study. For each element, output levels and the frequency at which they are manufactured (days) are presented on histograms (Figures 4-9)

Fabrication constant is defined as the number of manhours taken to manufacture one tonne of finished precast concrete, i.e.

TABLE 3. Fabrication Constants for Structural Elements

Structural Element	Daily Output (Tonnes)	Fabrication Constant (Manhour/Tonne)
Column	14.5	5.0
Rafter	12.8	6.33
Purlin	10.9	3.78
Eaves Gutter	5.1	11.36
Sheeting Rail	6.5	5.71

$$\text{Fabrication Constant} = M/(\sum_{i=1}^{J} We)$$

where We represents the weight of every ith type of element summed over the range of all j elements observed and M is the total manhours needed to manufacture all the j elements. Table 3 gives Fabrication Constants for each structural element.

The reliability of the results in Table 3 can be measured from the following statistical analysis. Assume a Gaussian distribution for the overall production levels shown in Figure 3.

$$F(t) = (1/2)I)e^{-2/2}$$

and the standard deviation is given by =

$$s = \sqrt{(\sum(Wi-W)^2/n)}$$

The standard deviation was computed to be 6.76 kg and the mean daily output was 46.144 tonnes.

Haulage Costs

The oldest and simplest hiring system which the haulage contractor uses is the one that makes hiring charges on an hourly basis. There is another system which makes charges on radial mileage basis and which is more popular. With this system trucks having up to 10 tonnes capacity, and trucks having over 10 tonnes capacity are caregorised separately. The haulage cost is then as shown.

$$\text{Haulage Cost} = \text{Rate} * \text{Tonnage}$$

For a given tonnage of structural elements, the number of trips is computed and the appropriate rate used to price the haulier's charges.

Foundation Costs

Foundation problems associated with the structure are generally uncomplicated. There is usually a low contact pressure between column bases and the soil, typically up to 150 kN/m^2. Foundation design for the structure therefore entails provision of column bases which can be easily constructed from standard moulds. A typical column base comprises unreinforced footings of about one meter deep.

Cladding Costs

Various cladding materials may be specified including asbestos, steel profile sheeting and brickwork. A common arrangement is for brickwork to be built to a height of 2m and for lightweight material to be fixed over the remainder of the sides and the roof. The program allows for this and for the inclusion of windows, personnel doors, sliding doors and folding doors. The cost model program costs all cladding panels, fixing components and flashing as required. Fixing costs are included. These were obtained during time study observations and the erection rates are shown in Table 4.

TABLE 4. Rate of erecting cladding

Activity	Rate M^2/Manhour
Fixing roof sheeting	1.3
Fixing Side Sheeting	1.25
Erecting a brickwall	0.278

Erection costs for Structural Elements

Observations were made of several sites throughout the U.K. and the cost of erecting the various structural elements is shown, in terms of manhours, in Table 5.

TABLE 5. Rate of erecting Structural Components

Structural Element	Workmen	Rate (Hours)
Column	4	2.8/pair
Rafter	4	1.8/pair
Purlin	4	0.2/each
Sheeting Rail	4	0.4/each
Gutter Beam	4	0.75/each

The Cost Model Function

The following are the optimisation primary variables:-

Span of the structure	x
Frame spacing	y
Number of bays	n
Number of spans	k
Roof pitch	w
Height to eaves	h

The overall cost of the structure is the sum of the following costs:

1. Fabrication costs
2. Haulage costs
3. Foundation costs
4. Cladding costs
5. Erection costs

that is the global cost of the structure is:

Building cost = (Foundation cost + Haulage cost + Foundation cost + Cladding cost + Erection cost)

Let -

A=0.5xtan (0.01750)

B=0.7Ayn - 3.14yn-0.5A-0.2

C=(yn-0.15)/(A-0.15)

D=2.73(h+0.762) (nk+n+k+1)

In terms of the primary variables alone the terms in the above equation can be written as follows:-

Fabrication Cost = (31.22(0.7h+0.0533) (nk+n+k+1)
+ 78.02(0.0438A+0.0485) (nk+n)
+720.08ynk+375.91yn+418.94(ny+ynk)
+(D+5.45A(k+nk)+73.48ynk+20yn+35.1yn)

Haulage Cost = 7.15((0.07h+0.0533) (nk+n+k+1)
+2(0.0485+0.0438A) (nk+k)+(0.12052ynk)
+(0.124yn)+0.1159(yn+ynk))

Foundation Cost = 29.62(nk+n+k+1)

Cladding Cost = k(8.19A+27.59B+18.81C+1.37yn
+158.09)+516(yn+x-2.25)

Erection Costs = 92.06n+9.49

Therefore the cost model function may be formally stated as:

BUILDING COST = f(x y n k w h)

Structural Design Program

The design procedure is fully automated and excludes the use of design charts. Discrete steel areas are selected during the design procedure. The design algorithm proceeds as follows:

Firstly, analysis routines estimate dead, imposed and wind loads, to be used to estimate bending moments and shear forces. Trial design of the various elements is then carried out. For a column, trial dimensions coupled with other design data are input to the program which computes and selects appropriate design bending moments. The program tests for slenderness and then designs accordingly either for a short or long column case. In the process the neutral axis depth is varied and and at each stage compressive and tensile steel areas are iteratively computed. There exists for each complete iteration an optimum steel area and a corresponding neutral axis depth. By using stored cost data, the least cost column is designed.

Secondly, to design a rafter using a parabolic stress block, the program selects the maximum bending moment along the rafter and tests for the position of the neutral axis in relation to the beam's flange. Accordingly, a design is carried out for a neutral axis depth position either within or outside the flange.

Finally, purlins, sheeting rails and gutters are treated as simply supported beams spanning between bays. As each element must be topologically compatible with the rest of the structure, tests are carried out at each stage to ensure that a functional and stable structure is being designed. Frequently, incompatibility causes the program to reject otherwise feasible designs for individual elements. In the event of a failed design, an option for data adjustment and improvement is offered. The design cycle is repeated as often as necessary until an acceptable design is reached where all constraints are satisfied.

All elements in the structure have to be transported from the factory to the erection site. Unlike in-situ construction the structural frame is erected by connecting various members securely to one another to form a stable unit. For instance, full continuity is required at the rafter/stanchion section which means that the connection at the eaves must be designed to transmit bending moments, shear forces and torsion. Two important factors that govern the design of connections are:

i. A partial safety factor 10% higher than that for adjacent members should be provided against failure to ensure that concrete members fail before the connection.
ii. Connections have to be located at convenient sections in the structure since at certain sections in the structure stress concentrations can occur if connections are used, with consequent spalling and splitting of the concrete at the contact surfaces.

Figure 10 shows a simplified flow chart for the design program. It can be seen that the elements designed correspond with those manufactured as shown in figure 2. This division of the building has been adhered to in each stage of the project.

OPTIMISATION TECHNIQUE

The purpose of this optimization exercise is to

seek a feasible optimum cost design of the building. A number of design variables are identifiable but for practical purposes only six primary variables were isolated namely:

x span of the structure (lateral column to column dimension)
y frame spacing (longitudinal column to column dimension)
n number of bays
k number of spans
w roof pitch
h height to eaves (vertically from ground level)

In terms of these six primary variables the global cost of the structure can be determined. Therefore, objective function is formally stated as

minimize f(x, y, n, k, w, h)

subject to design constraints. Two classes of design constraints are identified:

i. Analytical constraints

ii. Cost and design constraints are built into the design program whilst the cost constraints are essentially the client's requirements. During the field survey it was found that the client's requirements can be restricted to the following primary variables:

1. Building area
2. Height to eaves.

Therefore, the objective function is subject to inequality constraints of the form:

$$g_j(x) \geq 0$$

Most structural design problems are non-linear with constrained optima. A number of algorithms have been used to evaluate different problems and in each case an appropriate justification is offered for the choice of algorithm. Rosenbrock's algorithm has been used in the present work. The algorithm in this case is selected for two reasons:

1. Being one of the pioneer methods it has been tested and found to be powerful in several engineering problems.
2. Being a search technique, Rosenbrocks algorithm can be attached conveniently to a design program without requiring major amendments to either. This factor was of particular relevance in this instance. The original Rosenbrock algorithm is modified to take into account constraints.

The search continues until cost savings become minimal or until 100 iterations are completed. Fig.11 shows the flowchart used. In fig.11 the output node labelled 77 indicates that a further optimization attempt should be undertaken, using a different set of initial primary variables. Therefore, if 77 is reached, before a return to GO, a subroute is entered which generates a new set of starting variables before optimization restarts.

Cost Response Surfaces

Using an IBM contour interpolation package, an investigation was undertaken of the relative sensitivity of the primary variables and the unimodality was investigated. In order to allow data to be presented in a meaningful manner, two primary variables were allowed to vary while the remainder were held constant at sensible values. The following assumptions were made when producing the cost response surfaces:

1. Design wind speed = 45 m/s
2. All prices and costs are at 1979 levels
3. A grid of 100 designs has been used to prepare each surface.
4. Haulage distance = 40 miles

Effect of Varying Frame Spacing and Number of Spans

Lower and upper bounds of 3-12 m for frame spacing were imposed on 1000 m^2 and 2000 m^2 buildings, and 4-22 m on 3000 m^2 and 4000 m^2 buildings. Roof pitch was maintained at 14°. All buildings were clad with single skin sheeting. Variables other than frame spacing and number of spans were held constant.

The cost surfaces in Figues 12 to 16 are strongly unimodal. On the 1000 m^2 surface the optimum resides in a well-defined trough located at (4, 6.0m, £8432.32) lying in the mid-west. There are no local depressions. Buildings with spans below 5 m and above 10 m are uneconomical. The 2000 m^2 surface has a well-shaped optimum located at (5,8.0m, £150 15.04). It is separated by a saddle from two local depressions located in the south-east. In the north-west another saddle separates the optimum from a deep local depression. On the 3000 m^2 surface the optimum is located at (2, 10.0m, £12100.11) in a deep trough separated by a saddle from two local depressions situated in the south-east. North-eastern slopes have become steeper. Buildings with frame spacing below 8.0 m and above 14.0 m are not economical. The optimum for the 4000 m^2 surface is at (2, 12.0 m, 12.0 m, £26092.12). A saddle in the south-east separates the optimum from a shallow local depression and a conical hill has formed in the north-west of the optimum. Another local depression is located north-east of the optimum. Steep sides of the trough to the north-east and south-west of the optimum indicate that designs with frame spacing about 14 m and below 6 m are sensitive to cost.

Response Surfaces for Different Pairs of Primary Variables on 1000 m^2 Buildings.

It is possible to produce cost contours for any two primary variables, whilst keeping the other four variables constant. Four sets are further selected to illustrate the process. In each case the building area is fixed at 1000 m^2.

Building Span and Number of Spans

The lower bound for span is 8 m and the upper bound is 26 m. The number of spans ranges from 1 to 10 The cost surface shown in Figure 16 has an optimum at (2, 20.0 m, £9415.84) in the north-west residing in a U-shaped valley. The wall to the west valley is steep but slopes gently in the east. There are seven local depressions to the south-east of the optimum and another in the north. The most attractive local depression would cost 1.05% more than the optimum.

Roof Pitch and Frame Spacing

The lower bound for roof pitch is 1° and the upper bound is 37°; frame spacing varies from 3 m to 12 m. Sandwich construction roof cladding is used and on the sides of the building a combination of single skin construction and brickwork is used. The 1000 m^2 cost surface shown in Figure 17 has a U-shaped valley with a gentle sloping bed. The optimum resides in the south at (6.0, 4°, £17129.16) and buildings with frame spacings between 4.5 m and 9.0 m are the most economical.

Building Span and number of bays

Roof and vertical cladding types are as used as previously described. The roof pitch is fixed at 14^{0} and only single span buildings were considered. The cost surface shown in Figure 18 has an optimum at (3, 32.0 m, £18874.30) in the north-west lying in an elongated U-shaped valley. Two local depressions appear in the south and hills have formed in the north-east. Single and double bay buildings are very expensive within this range.

Frame Spacing and number of bays

A lower bound of 3 m and an upper bound of 12 m for frame spacing were imposed on 1-10 bay 1000 m^2 buildings. The cost surface shown in Figure 19 is strongly unimodal and has an optimum at (2, 7.0 m, £8789.27) in a V-shaped valley. Two local depressions are formed in the south-east of the optimum. The most economical buildings are those with frame spacing between 5 m and 8m, with 2-4 bays.

General Arrangement Drawings and Specification

The initial general arrangement drawing program was written independently of the optimization programs but the data structure was made compatible. The whole suite has now been linked together to run on a 16 bit 64K bytes NAKED MINI System, driving a 9 cm/sec 90 cm wide BENSON drum plotter (3 pens), using a 10 Mb moveable/fixed plotter disk system for on-line program and data storage. The computer is run by the precast concrete manufacturers who participated in the project and drawings of optimized buildings are produced in response to sales enquiries. The system allows the manufacturer to respond quickly to an enquiry and to produce general arrangement drawings and a price almost immediately. Drawings are produced at a scale of 100:1 as shown in figures 20 and 21. Larger buildings such as that shown on figure 20 are drawn on A0 size paper while smaller buildings are drawn on A1 sheets. The software decides which sheet size to use. The specification for the building is written in the right hand column.

Personnel doors, windows, roller doors and sliding doors are selected interactively from a catalogue of available styles and sizes. Their position is specified by distance from grid lines.

The data to define a building such as that shown in figure 20 requires approximately 25 minutes to generate. The optimization requires approximately 30 minutes computer time and the drawing takes up to 3 hours, but does not require personnel in attendance. The system can process up to 6 such buildings in 24 hours. Previously, drawings such as that in Figure 20 required at least one man week. An editing facility allows the designer to modify locations of archectural detail so that fresh drawings can be provided if a change in building specification is required.

Figure 22 shows an enlarged cross-section and the elevations corresponding with this cross-section are shown in Figure 23. It is perhaps a tribute to the skill of the programmers of this part of the project (3 final year civil engineering undergraduates) that the drawings are often taken to be manual drawings.

Conclusions

This paper shows that it is possible to apply optimization in a commercial situation and that the cost/benefit is considerable. It is interesting that most of the cost of developing the system was in researching data for the cost model and in producing output and input of a robust and commercially acceptable standard. The time spent on programming the optimization algorithm was negligible, although it is of considerable commercial value.

In managing and supervising the development of the programs, the authors paid full attention to the structuring of the data.

In general, data files were constructed prior to writing programs which operated on them. Programs should be seen as means of transforming data rather then ends in themselves. Often, the prior generation of data files greatly facilitated program writing since the latter could then be defined in terms of the transformation required. The authors are of the firm opinion that in all program development, data structure modelling is of the essence.

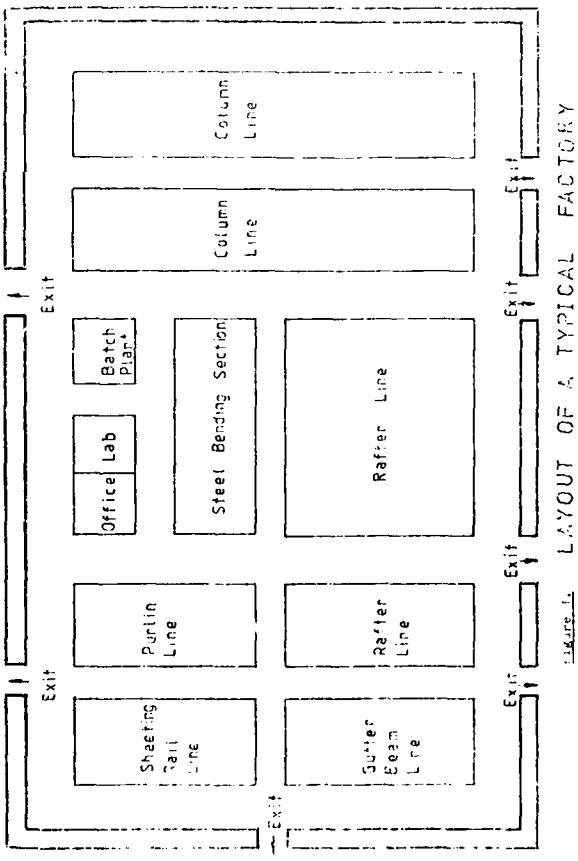
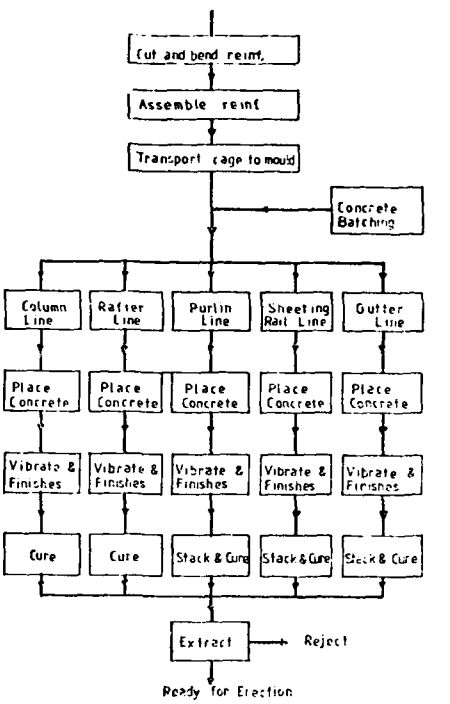


Figure 1. LAYOUT OF A TYPICAL FACTORY

Figure 2. FABRICATION PROCESSES FOR STRUCTURAL COMPONENTS



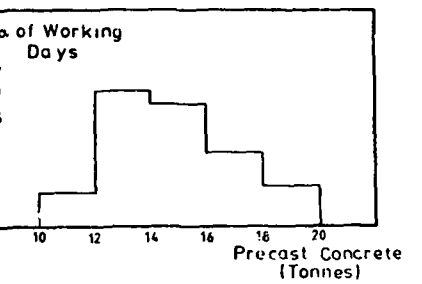


Figure 4. FABRICATION OF COLUMNS

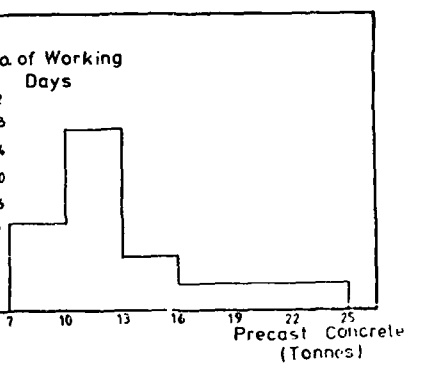


Figure 5. FABRICATION OF RAFTERS

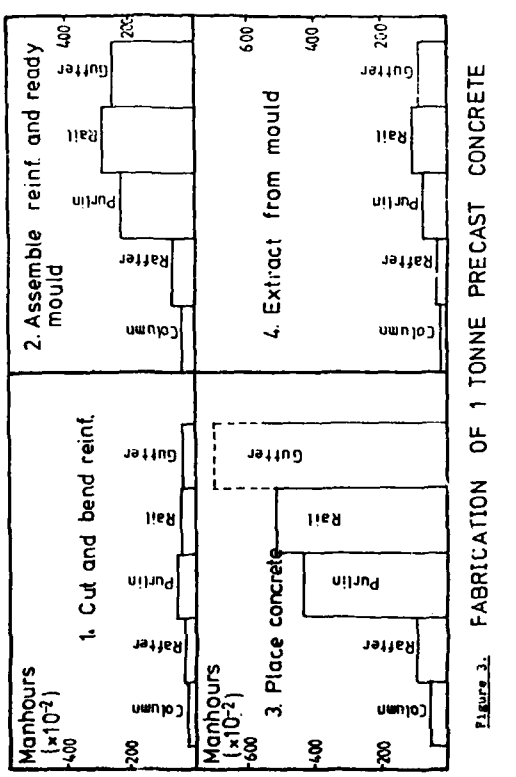


Figure 3. FABRICATION OF 1 TONNE PRECAST CONCRETE

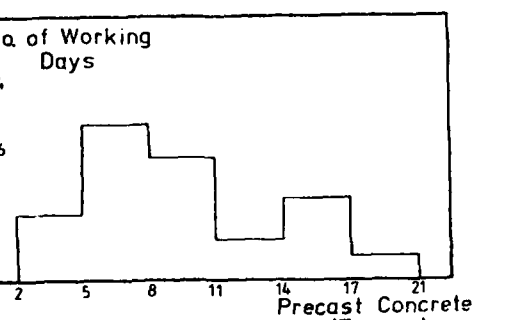
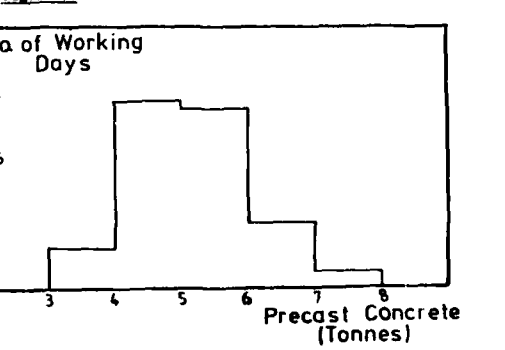


Figure 6. FABRICATION OF PURLINS

Figure 7. FABRICATION OF GUTTERS



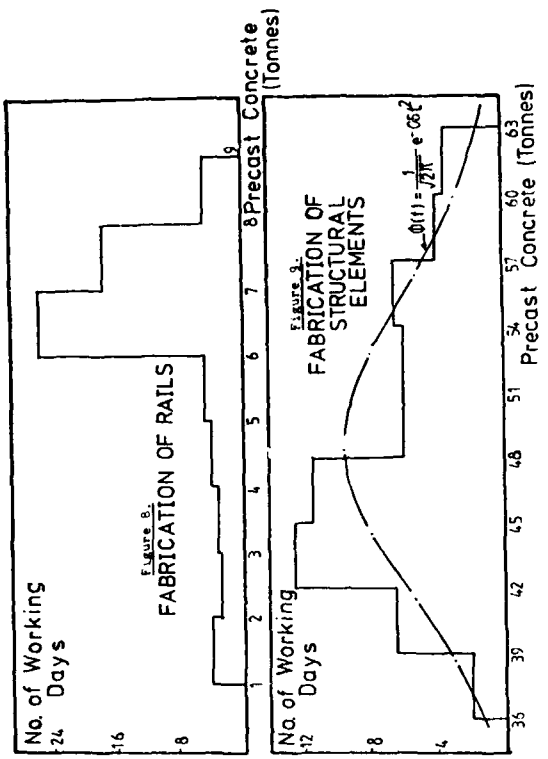


Figure 8.

Figure 9.

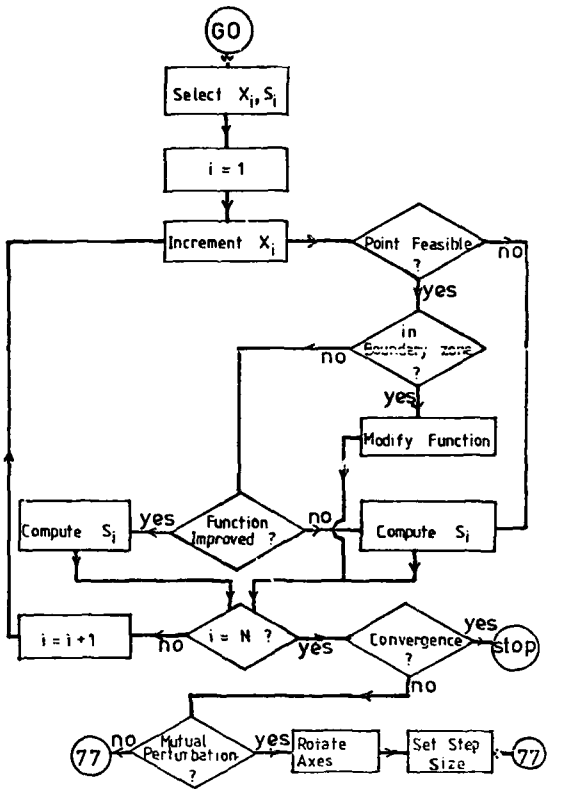


Figure 11. CONSTRAINED ROSENBROCK ALGORITHM

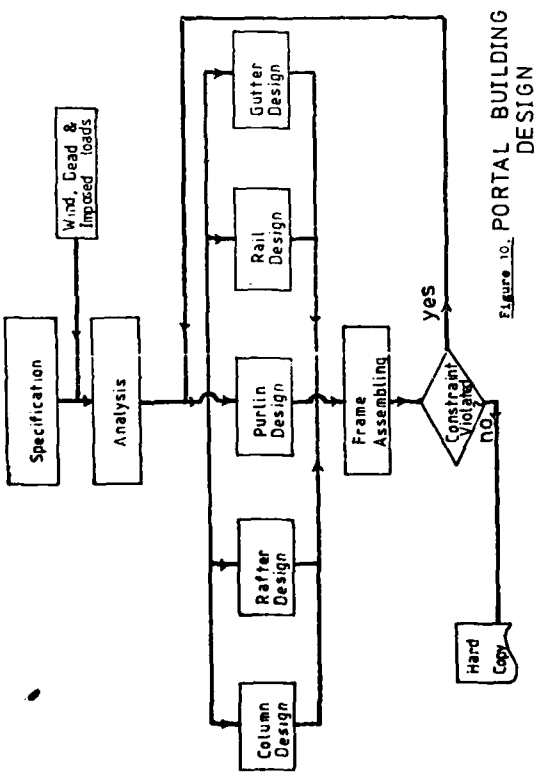


Figure 10. PORTAL BUILDING DESIGN

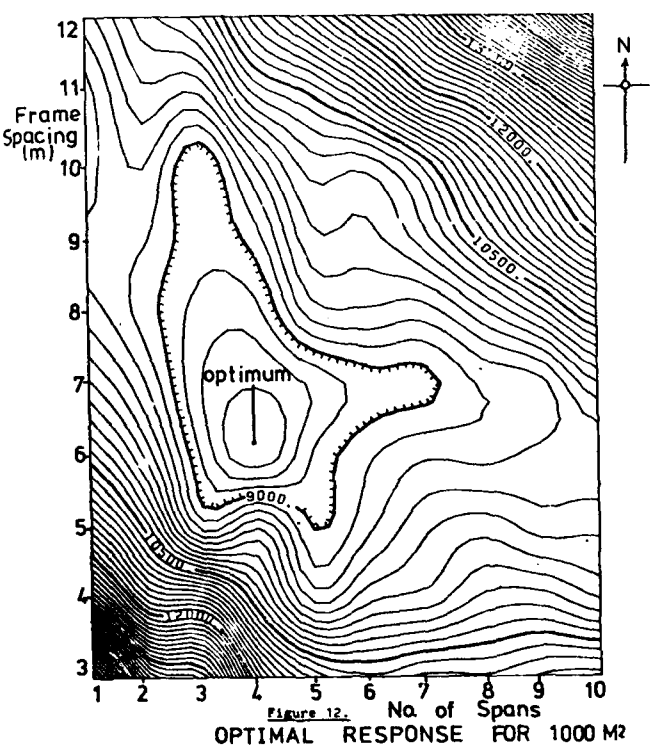


Figure 12. OPTIMAL RESPONSE FOR 1000 M² BUILDINGS

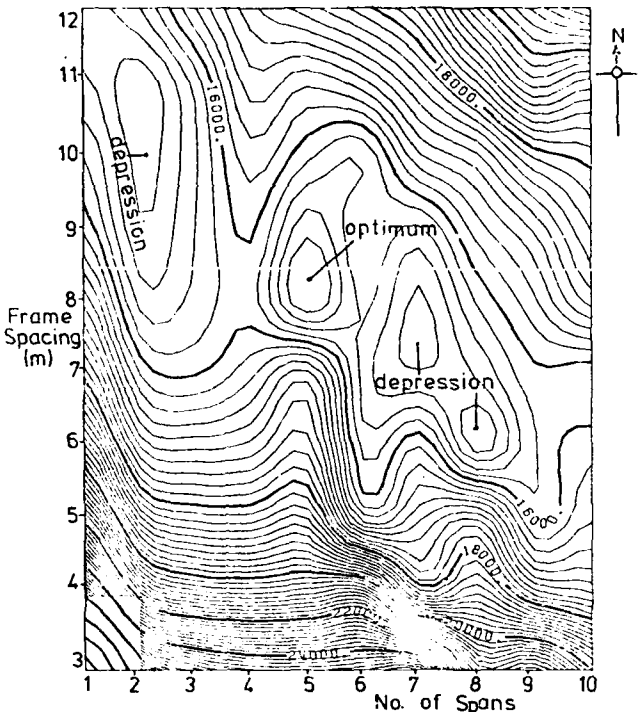


Figure 13. OPTIMAL RESPONSE FOR 2000 M² BUILDINGS

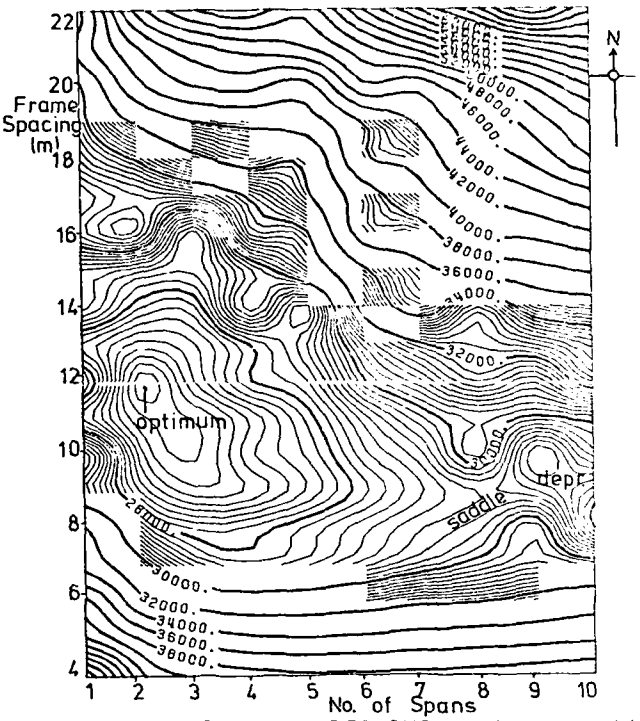


Figure 15. OPTIMAL RESPONSE FOR 4000 M² BUILDINGS

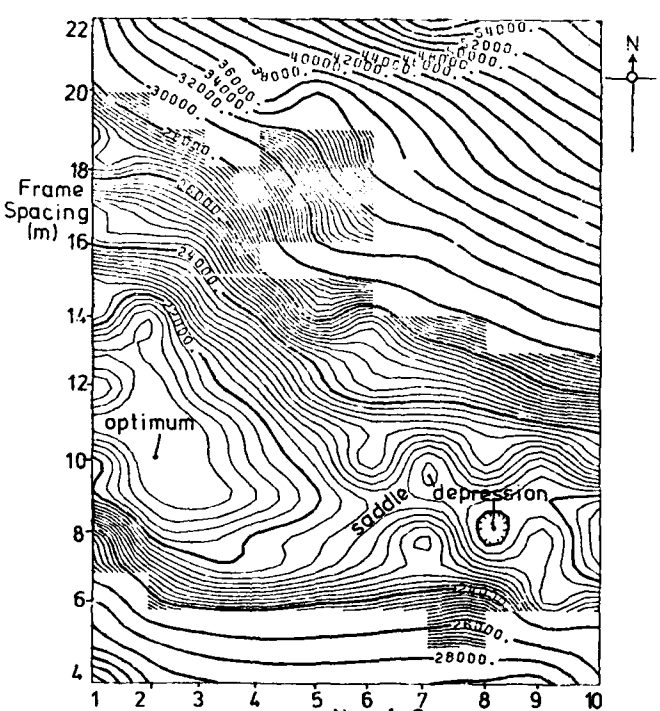


Figure 14 OPTIMAL RESPONSE FOR 3000 M² BUILDINGS

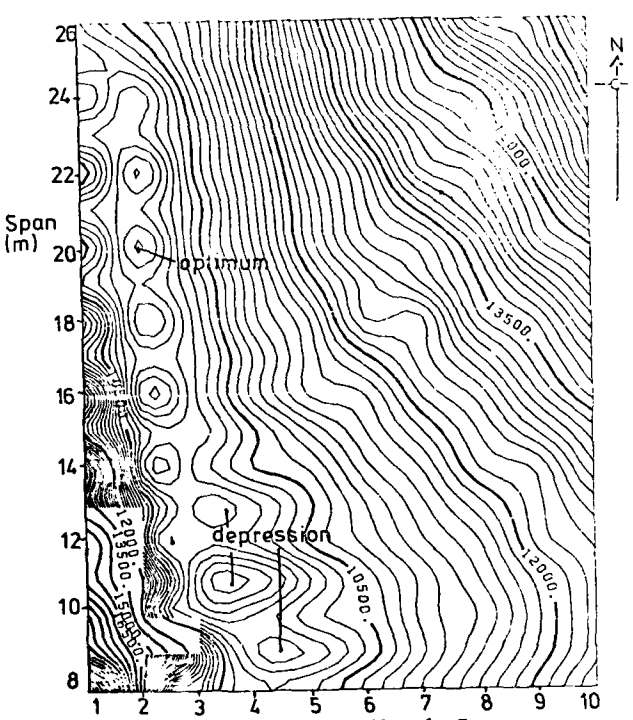


Figure 16. OPTIMAL RESPONSE FOR 1000 M² BUILDINGS

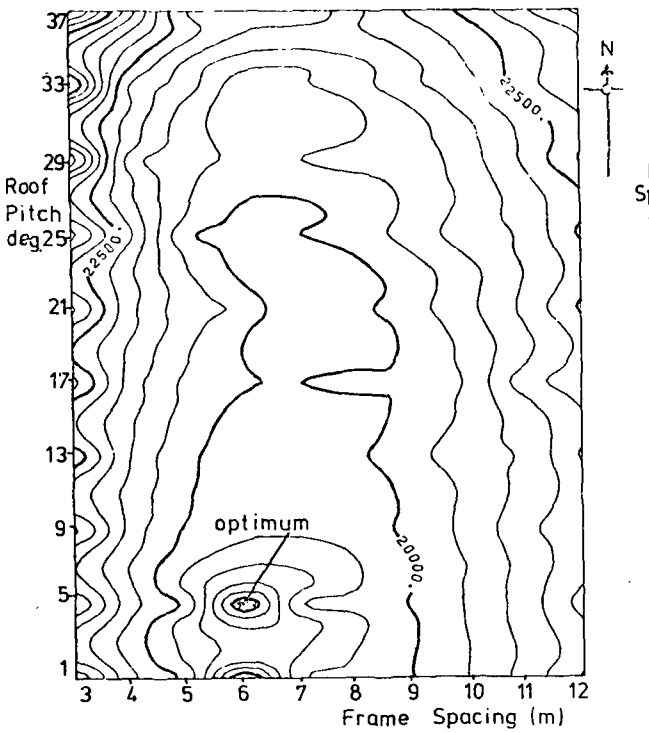


Figure 17. OPTIMAL RESPONSE FOR 1000 M² BUILDINGS

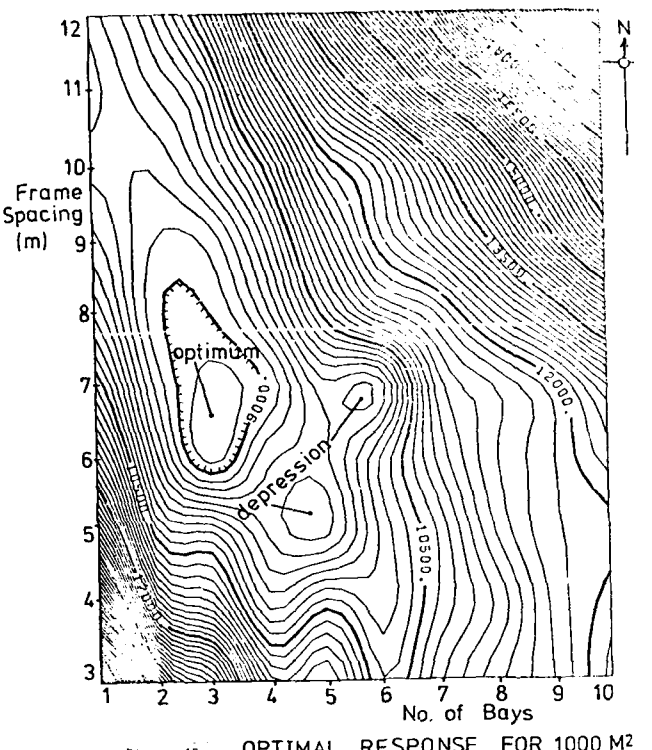


Figure 19. OPTIMAL RESPONSE FOR 1000 M² BUILDINGS

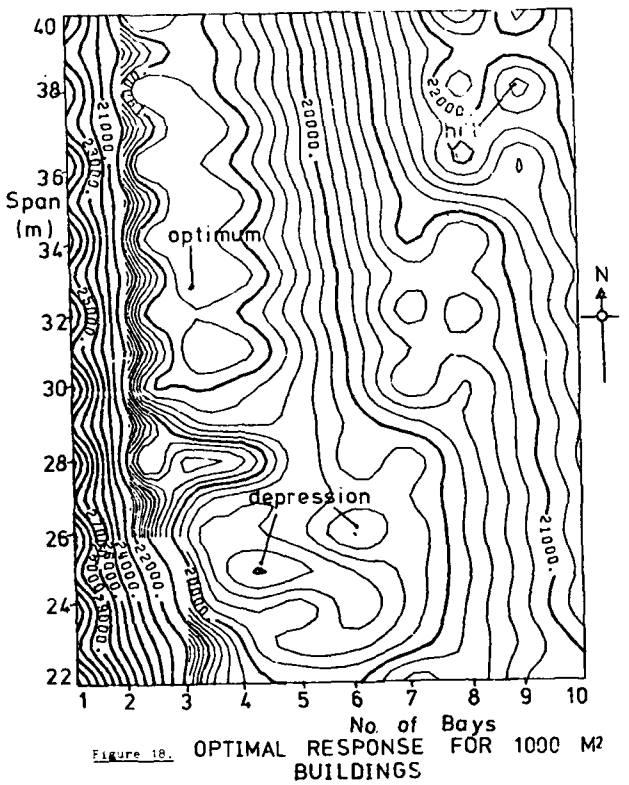
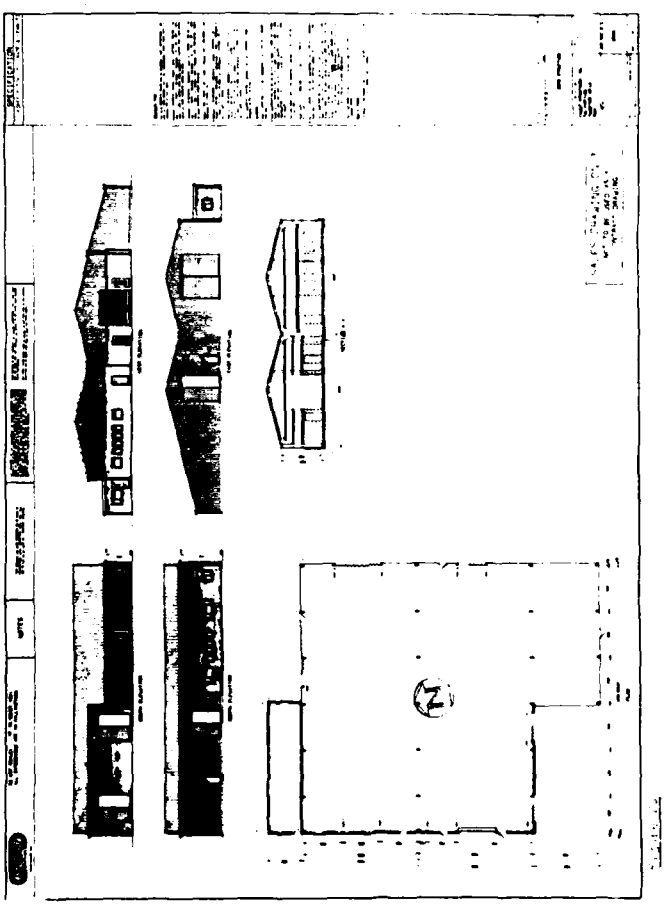
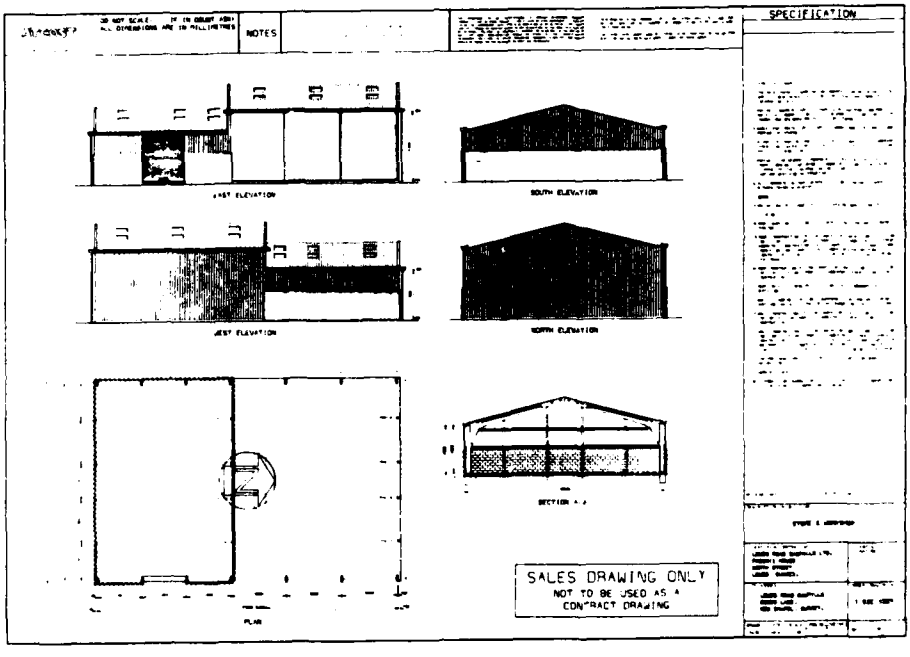
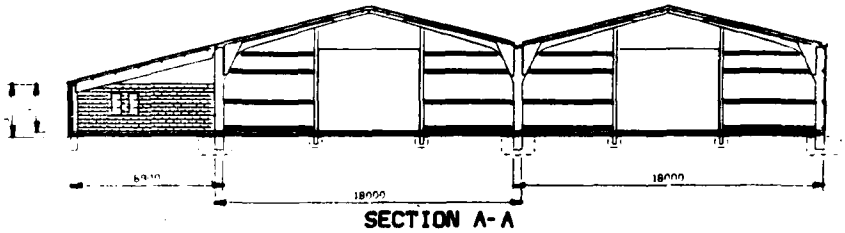


Figure 18. OPTIMAL RESPONSE FOR 1000 M² BUILDINGS





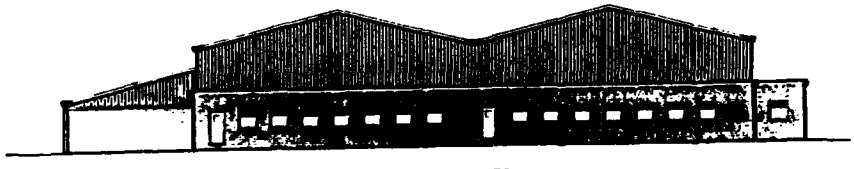


SECTION A-A

Figure 22.



WEST ELEVATION



EAST ELEVATION

Figure 23.

AD-P000 083

REINFORCED CONCRETE MEMBERS OPTIMIZING RELATIONSHIPS

Louis M. Laushey
University of Cincinnati
Cincinnati, Ohio 45221

Summary

Beams, columns, and beam-columns of reinforced concrete are analyzed to determine the optimum designs that result in the least total cost of materials. The analysis and results are generalized to be adaptable to both elastic and ultimate design methods, including any shape of stress block in the concrete.

A typical linear programming objective function defines the variable part of the cost of the materials. A Lagrangian Multiplier specifies the design moments, axial loads, or combinations. The objective function is simply $(C_c A_c + C_s A_s)$; with A_c and A_s being the determined optimum areas of concrete and steel for loads per inch width, and C_c and C_s the costs of unit volumes of the concrete and steel.

The ratios C_c/f_c and $C_s f/_s$ and $\frac{C_c/f_c}{C_s/f_s}$ prove to be the clue to the selection of the grades and quantities of the concrete and reinforcing steel. The optimum percentage of reinforcing steel for balanced design was found to be C_c/C_s. For the optimized designs, for stress blocks in the concrete that are rectangular, parabolic, or triangular, the optimum percent of steel was found to be $\frac{C_c/C_s}{1 + \frac{2\beta}{\alpha}(\frac{C_c/f_c}{C_s/f_s})}$, being only slightly less than C_c/C_s.

Stresses in the equations are generalized. The concrete and steel maximum stresses f_c and f_s are adaptable to the yield strength for ultimate design, or to the usual specified working stresses for elastic design.

The resulting equations for least cost include only the variable part of the total cost. Fixed costs are set aside temporarily, since their derivatives in the optimization are zero. Fixed costs then can be added to the minimized variable costs when estimating the total cost.

The efficiency of the materials, defined by C_c/f_c and C_s/f_s, change over time as prices fluctuate with changing economic conditions. The percent of steel to be selected should then change also with the current relative costs of the materials. Designers might consider changing from a fixed percent of steel, for a selected combination of materials, to more or less steel as the relative cost of concrete to steel increases or decreases.

Comparisons are made between the percent of steel required for bending by the usual elastic balanced design method and the optimized comparable triangular stress block, and between the relative economies of optimized elastic and ultimate designs. For columns, the most economical grades of materials and percent of load carrying steel is suggested by the efficiency ratios C_c/f_c and C_s/f_s.

Introduction

The design theories and codes for reinforced concrete beams, columns, and beam-columns are based on methods that assume the design loads will produce stresses equal to or less than specified maximum allowable stresses in each material. Cost is presumed minimized because the materials would be stressed to their allowable limits.

The ratio of unit cost to stress capacity of each material is seldom considered in selecting the relative amounts of concrete and reinforcing steel, nor in the choices from among the materials with different ultimate and yield strengths. The cost of the member or structure is almost always estimated only after it has been designed.

This paper presents methods that define and include the relative cost effectiveness of the materials, and their cost, before the design is completed. The most economical quantity and grade of each material is suggested for beams, columns, and beam-columns. Both elastic and ultimate design methods are included.

Variable Costs Only Considered

The final cost of the member or structure is, of course, the sum of many costs, some fixed and some variable. Fixed costs are all those unchanged for alternate designs within the range of practicality. Fixed costs include administration, supervision of construction, probably most of the design costs, and perhaps the cost of formwork, placing and finishing. Variable costs are the costs of the two materials, their sum depending on the amounts of each and their unit costs. The designer can be flexible in the determination of the variable unit costs, including both current unit costs of materials and those from any other source. Most conveniently, an estimated multiplication factor could be applied to the unit costs of the materials to be delivered to the construction site.

Fixed costs will drop out in the optimization process, since their derivatives are zero. Fixed costs can be simply added later to the minimized variable cost for the estimate of the total cost.

Table 1 gives a convenient conversion to the ratio C_c/C_s. The dimensions of the quantities in the ratio are dollars per square inch, per unit length of member.

$$C_c/C_s = \frac{(0.15)(\$/cu.yd.)}{(\$/ton)}$$

Concrete	Steel $/ton			
$/cu.yd.	$600/ton	$800/ton	$1000/ton	$1200/ton
40	1.00%	0.75%	0.60%	0.50%
60	1.50%	1.11%	0.90%	0.75%
80	2.00%	1.50%	1.20%	1.00%
100	2.50%	1.87%	1.50%	1.25%

Table 1

Generalized Stresses:

The stresses f_c and f_s can be chosen by the designer to suit the design method and specifications. Using the ultimate design method, $f_c = 0.85\, f'_c$ usually; and using the elastic method, $f_c = 0.45\, f'_c$ usually. Similarly, for the ultimate design method, $f_s = f_y$, and for the elastic method f_s is some fraction of the yield stress, f_y.

Throughout, f_c and f_s are generalized, to be consistent with the design method and codes.

Cost/Stress Ratios

The ratios C_c/f_c and C_s/f_s are measures of the economic efficiencies of the materials. The dimensions are dollars per square inch divided by pounds per square inch, for equal lengths. The ratios are simply the cost in dollars per pound of load carried. Throughout, it is assumed that the length of the member has been prescribed. Minimized variable costs are therefore for a unit length of member.

Width of Beams

It is well-known that narrow, deep beams are most efficient of materials. If generally, $M \propto bd^2 \propto Ad$, then area A is proportional to d^{-1}. The optimization process proved this fact. Differentiation with respect to the width of the beam indicated a beam of zero width. Since practical considerations of ceiling height and steel placement demand a beam of reasonable width, the analysis is made throughout for a beam of selected width. More precisely, the moments and loads are those for a one-inch width of beam.

Design Of Bending Members

Balanced Design Method

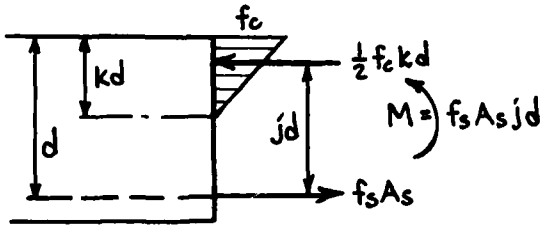


Fig. 1. Balanced Design Stress Block

The variable part of the cost that can be minimized is:

$$\text{Cost} = C_c d + C_s A_s + \lambda\, [M - f_s A_s jd]$$

The value of j in balanced design is $j = 1 - \frac{1}{3}\left(\frac{nfc}{f_s + nfc}\right)$, determined from the strengths and moduli of the materials selected. In the following differentiation of the objective function, j is then a constant.

$$\frac{\partial\, \text{Cost}}{\partial d} = 0 = C_c - \lambda\, f_s A_s j$$

$$\frac{\partial\, \text{Cost}}{\partial\, A_s} = 0 = C_s - \lambda\, f_s (\, jd\,)$$

$$\lambda = \left(\frac{C_c}{f_s A_s j}\right)\left(\frac{d}{d}\right) = \left(\frac{C_s}{f_s jd}\right)\left(\frac{A_s}{A_s}\right)$$

$$\frac{\text{Cost Concrete}}{M} = \frac{\text{Cost Steel}}{M} \qquad (1)$$

and

$$\frac{C_c}{C_s} = \frac{A_s}{d} = p \quad \text{(percent of steel)} \qquad (2)$$

Results show the percent of steel should be the ratio of the costs per unit volume of the concrete to steel, and the cost of the concrete should equal the cost of the steel.

The cost of both the concrete and steel should be λM, and the total cost of both, $2\,\lambda M = 2\,M\left(\frac{C_s}{f_s jd}\right)$

$$\text{Or Total Cost} = \frac{2M}{jd}\left(\frac{C_s}{f_s}\right) \qquad (3)$$

Further analysis discloses the interesting result that since

$$\frac{1}{2} f_c kd = f_s A_s$$

$$k = \left(\frac{2f_s}{f_c}\right)\left(\frac{A_s}{d}\right) = \left(\frac{2f_s}{f_c}\right) p$$

Defining $\bar{f}_c d = \frac{1}{2} f_c kd$, $\quad \frac{\bar{f}_c}{f_c} = \frac{k}{2} = \left(\frac{f_s}{f_c}\right)p = \frac{f_s C_c}{f_c C_s}$

Then

$$\frac{\bar{f}_c}{f_s} = \frac{C_c}{C_s} \qquad (4)$$

Thus, the ratios of unit cost to average stress should be the same for each material.

Alternative Stress Blocks

Fig. 2 shows three different stress blocks:

(a) Rectangular, for ultimate design: α=1, β=0.5
(b) Triangular, for elastic design: α=0.5, β=0.33
(c) Parabolic, as an option: α=0.67, β=0.375

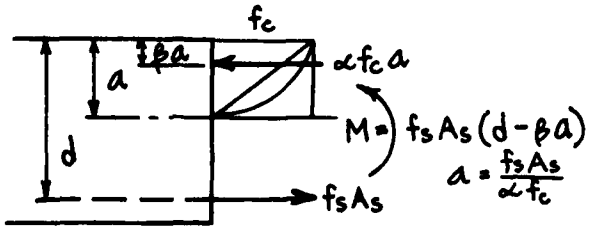


Fig. 2. Alternative Stress Blocks

The variable part of the materials cost is

$$\text{Cost} = C_c d + C_s A_s + \lambda[M - f_s A_s (d - \frac{\beta A_s f_s}{\alpha f_c})]$$

$$\frac{\partial \text{ Cost}}{\partial d} = 0 = C_c - \lambda[f_s A_s] = C_c - \lambda[f_s dp]$$

$$\frac{\partial \text{ Cost}}{\partial A_s} = 0 = C_s - \lambda[f_s d - \frac{2 f_s^2 A_s \beta / \alpha}{f_c}] = C_s - \lambda[f_s d(1 - \frac{2\beta f_s p}{\alpha f_c})]$$

Solving the λ equalities gives

$$p = \frac{C_c/C_s}{1 + \frac{2\beta}{\alpha}(\frac{C_c/f_c}{C_s/f_s})} \tag{5}$$

$$a/d = \frac{1}{2\beta + \alpha(\frac{C_s/f_s}{C_c/f_c})} \tag{6}$$

$$\text{Cost of Concrete} = \frac{\lambda M}{1 - \beta(a/d)} \tag{7a}$$

$$\text{Cost of Steel} = \frac{\lambda M (1 - 2\beta(a/d)}{1 - \beta(a/d)} \tag{7b}$$

$$\text{Cost Ratio Steel to Concrete} = 1 - 2\beta(a/d) \tag{7c}$$

$$\text{Total Cost} = 2\lambda M = (\frac{2M C_s}{d f_s})(1 + \frac{2\beta C_c/f_c}{\alpha C_s/f_s}) \tag{8}$$

Comparison of Eqns. 5-8 shows a similarity to Eqns. 1-3. The difference is that the balanced designs do not involve C_c and C_s in k or a, and j. In comparing the major results, for percent of steel and total costs:

(a) The percent of steel is C_c/C_s (Eqn. 2) for the optimized balanced design, and somewhat less in Eqn. 5 by the reduction amounting to the inverse of $(1 + \frac{2\beta}{\alpha}\frac{C_c/f_c}{C_s/f_s})$.

(b) The total cost is $\frac{2M}{d}(\frac{C_s}{f_s j})$ for the optimized balanced design, and somewhat less in Eqn. 8 by the amount that $1 + \frac{2\beta}{\alpha}\frac{C_c/f_c}{C_s/f_s}$ is less than $1/j$ in Eqn. 3.

Design Of Axially Loaded Members

A generalized approach that envelopes the choice of design method or code specifications is used here again. In all situations

$$F = A_s f_s + A_c f_c$$

and $$\text{Cost} = C_c A_c + C_s A_s + \lambda[F - f_s A_s - f_c A_c]$$

$$\frac{\partial \text{ Cost}}{\partial A_s} = 0 = C_s - \lambda f_s$$

$$\frac{\partial \text{ Cost}}{\partial A_c} = 0 = C_c - \lambda f_c$$

A requirement for the optimum is that

$$\lambda = C_s/f_s = C_c/f_c \tag{9}$$

Where the designer is given the option to select the amount of steel within a range, say 1% to 8%, he should consider choosing the minimum when $C_s/f_s > C_c/f_c$ and the maximum when $C_s/f_s < C_c/f_c$. More astutely, he might consider searching for different grades of steel and concrete that have nearly the same ratios of C/f. Then both materials would carry the same load per dollar expended, and the column design would be optimal.

It is recognized, however, that the steel has other functions than sharing the applied load. The importance of the steel in adding coherence to the column must definitely be a determining factor in selecting the grade and percent of steel to be used.

Eccentric Load

Referring to Fig. 3, where the concrete stress block is generalized again

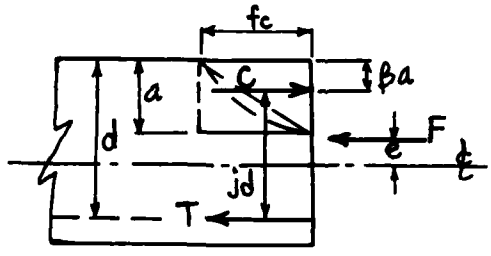


Fig. 3. Eccentric Load

$$(\alpha f_c a) = C = F + T \qquad \text{and } f_s A_s = T$$

$$a = \frac{F + T}{\alpha f_c}$$

$$M = Fe = C(d/2 - \beta a) + T(d/2)$$

$$= (F + T)(\frac{d}{2} - \frac{\beta(F + T)}{\alpha f_c}) + \frac{Td}{2}$$

$$= \frac{Fd}{2} + Td - \frac{\beta}{\alpha f_c}(F + T)^2$$

$$\text{Cost} = C_c d + C_s A_s + \lambda[M - \frac{Fd}{2} - f_s A_s d + \frac{\beta}{\alpha f_c}(F + f_s A_s)^2]$$

$$\frac{\partial \text{ Cost}}{\partial d} = 0 = C_c - \lambda[\frac{F}{2} + f_s A_s]$$

$$\frac{\partial \text{ Cost}}{\partial A_s} = 0 = C_s - \lambda[f_s d - \frac{2\beta}{\alpha f_c}(F+f_s A_s) f_s]$$

After some algebra

$$p = \frac{\frac{C_c}{C_s} - \frac{F}{f_c d}\left[\frac{2\beta\, C_c/C_s}{\alpha} + \frac{1}{2} f_c/f_s\right]}{1 + \frac{2\beta}{\alpha}\frac{C_c/f_c}{C_s/f_s}} \qquad (10)$$

$$\frac{a}{d} = \frac{pf_s}{\alpha f_c} + \frac{F}{\alpha f_c d} \qquad (11)$$

Eqns. 10 and 11 show the effect of the eccentric axial load F in reducing the required percentage of steel and increasing the area of the compressive stress block, compared to pure bending.

Comparison of Methods and Conclusions

Beams in Bending. The optimum total cost was found to be $2\lambda M$ for all design methods and all concrete stress blocks.

For the balanced design method, $\lambda = \frac{C_s}{f_s j d}$ and $p = C_c/C_s$. *For stress blocks that are rectangular*, triangular, or parabolic, where the designs using these blocks have been optimized, $\lambda = \frac{C_c}{f_s A_s} = \frac{C_c}{f_s p d}$, and $p = \frac{C_c/C_s}{1 + \frac{2\beta}{\alpha}\frac{C_c/f_c}{C_s/f_s}}$. Their cost, compared to the balanced design, is the amount $1 + (\frac{4}{3}\frac{C_c/f_c}{C_s/f_s})(j)$.

The size of $(4/3\,\frac{C_c/f_c}{C_s/f_s})$ is of the estimated approximate order of 0.1, since C_c/C_s is probably of the order of 0.01 (see Table 1) and f_s/f_c of the order of 10. For this approximation as an average of 0.1, the value of j would have to be at least $\frac{1}{1 + 4/3(0.1)} = 0.88$ in the balanced design to be as economical as the optimized elastic design. Further determination of competitive costs must be determined in each practical application using the more exact amount of $\frac{C_c/f_c}{C_s/f_s}$.

Elastic and Ultimate Designs. The comparison of these two optimized methods must consider the load factor LF applied to M for ultimate designs. Elastic or ultimate stresses must be used to conform with the elastic or ultimate moment.

For the triangular stress block using elastic loading limits

$$\text{Cost} = \frac{2M}{d}(\frac{C_s}{f_{se}})(\frac{1}{j})$$

where f_{se} is the maximum elastic working stress in the steel

For the rectangular ultimate stress block

$$\text{Cost} = \frac{2M(LF)}{d}\frac{C_s}{f_{sy}}[1 + \frac{2\beta}{\alpha}\frac{C_s f_s}{C_c f_c}] = \frac{2M(LF)C_s(1.1\pm)}{d\quad f_{sy}}$$

where f_{sy} is the yield stress of the steel.

The ratio of optimized materials costs for ultimate to elastic designs would be

$$\frac{\text{Cost Ultimate}}{\text{Cost Elastic}} = (LF)(\frac{f_{se}}{f_{sy}})(1.1j\pm)$$

Conclusions. The scope of this paper was not intended to include current prices and thus show more precisely the savings that could result from optimum designs. A comprehensive survey would be needed for different types of construction, under different conditions in different locations of the country.

Although optimum designs might prove to offer only small savings in the cost of construction, they are at least as easy to use as the present design methods. Of consideration in their usage is the opportunity for a better understanding and application of the economics involved in the mutual interaction of two materials working closely together.

Finally, optimum desig[illegible]ovide flexibility in choosing compatible grades of materials and their relative amounts for the most economical cost.

SESSION #11

OPTIMIZATION SOFTWARE I

AD-P000 084

ACCESS COMPUTER PROGRAM FOR THE SYNTHESIS OF LARGE STRUCTURAL SYSTEMS*

C. Fleury[1], R. K. Ramanathan[2], M. Salama[3], L. A. Schmit Jr.[4]

Summary

Recent extensions to ACCESS-3 computer program for structural synthesis are described herein. The original program was limited to the optimization of relatively small problems having truss, membrane and shear panel elements. The new extensions include: restructuring of the program to allow efficient out-of-core solution of the large matrices encountered during analysis, approximate problem generation and gradient evaluation, increasing the number of degrees-of-freedom per node from 3 to 6, and adding a triangular plate element which admits combined membrane and bending behavior.

Like its predecessor, the new version of the program combines the approximation concepts with primal or dual formulations to create a highly efficient optimization tool. However, to focus on the greater efficiency of the dual approach, extensions were implemented in the program to allow using the dual formulation for structures with pure or combined bending and membrane behavior, subject to constraints on frequencies, displacements and stresses. This resulted in two dual options; a simple dual and an extended dual. Examples are given to compare the relative computational efficiency of each of these schemes.

I. Introduction

In spite of the many recent developments of computer programs for the optimization of structural systems, there has not been a corresponding degree of their utilization by the civil, automotive and aerospace design community. Many of the design problems that can truly benefit from a formal optimization procedure typically involve relatively large number of degrees-of-freedom, design variables, and constraints. They also require the availability of various types of finite elements for structural modeling. While these requirements do not present significant difficulties from the point of view of achieving an optimum design, they place real limitations on the economic advantages of optimization methods as routine design tools.

A number of investigators (1, 2) have dealt with the difficulties cited above by coupling a user oriented general-purpose analysis program such as SPAR with an efficient general-purpose optimization program such as COMIN or SUMT. The resulting collection of programs have contributed notably to a wider acceptance of the formal optimization approaches as viable design tools.

An alternative approach to remedy the same difficulties is implemented in the capability described herein. The approach aims at developing an analysis-synthesis computer program which can handle the optimization of large structural systems with high efficiency. It is based on the premise that greater efficiency can be achieved by creating a dedicated special-purpose rather than a general-purpose analysis-synthesis program. Such special-purpose analysis-synthesis program is developed by introducing new capabilities and extensions to the existing ACCESS-3 computer program (3). The ACCESS-3 program was selected because it combined approximation concepts (design variable linking temporary deletion of uncritical constraints, and the generation of high quality explicit approximations for the retained constraints) with either a primal or a dual formulation to create an extremely efficient tool with several optimizers to choose from. However, being a research type program, the original ACCESS 3 was intentionally limited to the solution of relatively small problems having truss, membrane or shear panel elements.

In order to handle the optimization of structures with relatively large number of degrees-of-freedom, design variables and constraints, the program was restructured to revise the preprocessor, allow the use of six degrees-of-freedom per node, and permit out-of-core solution of the large matrix equations encountered during the analysis phase. Also, finite elements which admit pure bending or combined bending and membrane (axial) behavior were added to satisfy the need for a more comprehensive collection of elements. This required extensions that preserve the high efficiency of the dual formulation.

The following section gives the theoretical background with emphasis on the dual formulation and the reasons for requiring special finite element formulation depending on the element type. Sections 3, 4, and 5, respectively, describe the scope of the new capabilities, numerical examples and conclusions.

2. Theoretical Background

The structural optimization problem treated herein is one in which the total weight W is to be minimized by determining the member sizes a_i such that their behavior constraints (on deformations, stresses, and frequency) and side constraints are satisfied. This leads to the mathematical programming problem of the primal form:

Minimize $$W = \sum_{i=1}^{N} w_i \, a_i \qquad (1.1)$$

Subject to: behavior constraints

*This paper presents one phase of research carried out at the Applied Mechanics and Technology Section, Jet Propulsion Laboratory, California Institute of Technology, under contract NAS 7-100 sponsored by the National Aeronautics and Space Administration. The work was supported by Drs. S. Venneri and L. Harris, Materials and Structures Division, Office of Aeronautics and Space Technology, NASA. The programming support by C. Wong and J. McGregor of the Jet Propulsion Laboratory is gratefully acknowledged.

[1]Aerospace Laboratory, University of Liege, Belgium.

[2]Civil Engineering Dept., University of Southern Calif., Los Angeles.

[3]Applied Mechanics Technology Sec., Jet Propulsion Laboratory, California Institute of Technology, Pasadena.

[4]School of Engineering and Applied Science, University of California, Los Angeles.

$$h_j(\underline{a}) = \bar{U}_j - U_j(\underline{a}) \geq 0 \qquad j=1,2,\ldots M \qquad (1.2)$$

and side constraints on the ith design variable

$$\bar{a}_i \geq a_i \geq \underline{a}_i \qquad (1.3)$$

where

w_i is a coefficient that is constant for each of the N-groups of linked direct design variables a_i.

h_j denotes a typical behavior constraint having an upper bound $\bar{U}_j$ on the current value $U_j(\underline{a})$,

and $\bar{a}_i$, $\underline{a}_i$ are the upper and lower bounds on the direct design variables a_i.

Although the objective weight function (1.1) is linear in a_i, expression (1.2) for the behavior constraints h_j is nonlinear and implicit. This implicit nonlinearity is computationally burdensome, especially when dealing with large statically indeterminate structural systems. A complete finite element analysis is required for each numerical evaluation of the behavior constraints, and many iterations are usually required before achieving the optimum design.

1. Axial and Membrane Behavior

In the original ACCESS-3 code (3), the implicit nonlinearity is removed for the axial and membrane elements by replacing the direct design variables a_i by their reciprocal (intermediate variable), and by expanding the corresponding behavior constraints in a first order Taylor series. This results in the following convex, separable and explicit primal problem with linear constraints and nonlinear objective function:

$$\text{Minimize} \qquad W = \sum_{i=1}^{N} w_i / x_i \qquad (2.1)$$

Subject to

$$\tilde{h}_j(\underline{x}) = \bar{U}_j - \left[U_j^0 + \sum_{i=1}^{N} \left(U_{j,x_i}\right)^0 \left(x_i - x_i^0\right) \right] \geq 0$$

$$\bar{U}_j - \sum_{i=1}^{N} C_{ij}^A \, x_i \geq 0 \; ; \quad j \in m \qquad (2.2)$$

$$\text{and} \qquad \bar{x}_i \leq x_i \leq \underline{x}_i \qquad (2.3)$$

$$\text{where} \qquad x_i = 1/a_i \qquad (2.4)$$

The C_{ij}^A coefficients represent gradients of the response quantity of interest with respect to x_i. These coefficients are assumed constant within each design stage or iteration. Also, m is the set of retained behavior constraints for the current stage, and $\underline{x}_i$ and $\bar{x}_i$ are respectively, the lower and upper move limits for that stage.

While the primal problem in equations (2) may be partially solved as a sequence of unconstrained minimization subproblems (using an interior penalty function formulation) before resizing and performing a new analysis, it is more efficient to fully exploit the convex, separable and explicit form of equations (2). It was this view which led to the adoption in ACCESS-3 of the highly efficient dual formulation.

In the dual formulation the primal problem of equations (2) is replaced by maximization of the dual function $\ell(\underline{d})$, subject to non-negativity constraints on the dual variables d_j:

Maximize

$$\ell(\underline{d}) = \sum_{i=1}^{N} \left[\frac{w_i}{x_i(\underline{d})} + \sum_{j \in m} d_j \, C_{ij}^A \, x_i(\underline{d}) \right] - \sum_{j \in m} d_j \bar{U}_j \qquad (3.1)$$

$$\text{subject to} \qquad d_j \geq 0 \; ; \; j \in m \qquad (3.2)$$

$$\text{where} \qquad x_i = \underline{x}_i \quad \text{if} \quad \frac{w_i}{C_i^A} \leq \underline{x}_i^2 \qquad (3.3)$$

$$x_i = \bar{x}_i \quad \text{if} \quad \frac{w_i}{C_i^A} \geq \bar{x}_i^2 \qquad (3.4)$$

$$\text{otherwise } x_i = \sqrt{\frac{w_i}{C_i^A}} \quad , \quad \text{with } C_i^A = \sum_{j \in m} d_j \, C_{ij}^A \qquad (3.5)$$

The efficiency of the dual formulation of equations (3) is due to the fact that maximization is performed in the dual space whose dimension is low compared to its primal counterpart, and depends only on the number of critical constraints ($m_{cr} \in m$) in each stage. Also, the non-negativity constraint (3.2) is algebraically simple. Once the dual variables d_j are known, one can compute the values of the intermediate and hence the direct design variables x_i, a_i in closed form.

2. Combined Bending and Membrane (Axial) Behavior

The key to the high efficiency of the dual formulation of Eqs. (3) lies in starting with an explicit and separable form of the approximate primal problem that is demonstratably convex. This assures the equivalence of the primal and dual formulations (i.e. no duality gap). For axial and membrane elements, high quality explicit approximations were obtained by using the transformation (2.4) between the direct design variables a_i and the intermediate variables x_i.

a. Extended Dual. In the case of pure bending, since the bending rigidity of a plate element with thickness t_i is proportional to t_i^3, it is seen that the same transformation (2.4) may not yield high quality approximations for the displacement, frequency and stress behavioral constraints. In this regard, a number of possible transformations have been suggested (4). For example, in the pure bending of plate/shell elements, introducing intermediate design variables $y_i = 1/t_i^3$ assures separability and convexity of primal problems with displacement or frequency constraints. In combined membrane and bending, both transformations $x_i = 1/t_i$ for membrane and $y_i = 1/t_i^3$ for bending may be used simultaneously, depending on the type of behavior constraints.

With respect to the constraint type, it is possible to first decompose the total stiffness for elements in the i-linked group into a membrane component

k_i^A and a bending component k_i^B, so that

$$k_i = \frac{1}{x_i} k_i^A + \frac{1}{x_i^3} k_i^B \tag{4}$$

Superposing the reciprocal forms used successfully in the pure membrane and bending problems suggests an explicit approximation of the form:

$$\tilde{h}_j(\underline{x}) \quad \bar{U}_j - \sum_{i=1}^{N} \left(C_{ij}^A x_i + C_{ij}^B x_i^3 \right) \geq 0 \; ; \; j \in m \tag{5}$$

where C_{ij}^A and C_{ij}^B, respectively are matrix coefficients representing gradients of the displacement or frequency membrane component with respect to x_i, and bending component with respect to y_i. The corresponding dual formulation then takes the form:

Maximize

$$v(\underline{d}) \quad \sum_{i=1}^{N} \left[\frac{w_i}{x_i(\underline{d})} + \sum_{j \in m} d_j \left(C_{ij}^A x_i(\underline{d}) + C_{ij}^B x_i^3(\underline{d}) \right) \right] - \sum_{j \in m} d_j \bar{U}_j \tag{6.1}$$

subject to $$d_j \geq 0 \; ; \; j \in m \tag{6.2}$$

where $$x_i = \underline{x}_i \quad \text{if} \quad C_i^A \underline{x}_i^2 + C_i^B \underline{x}_i^4 \geq w_i \tag{6.3}$$

$$x_i = \bar{x}_i \quad \text{if} \quad C_i^A \bar{x}_i^{-2} + C_i^B \bar{x}_i^{-4} \leq w_i \tag{6.4}$$

Otherwise x_i is obtained from a closed form solution of the fourth order equation

$$-w_i + C_i^A x_i^2 + C_i^B x_i^4 = 0 \tag{6.5}$$

The following notation has been used above

$$C_i^A = \sum_{j \in m} d_j C_{ij}^A \quad \text{and} \quad C_i^B = \sum_{j \in m} 3 d_j C_{ij}^B \tag{6.6}$$

As for the stress constraints for combined plate membrane and bending behavior, they may be approximated by the explicit expression

$$\tilde{h}_j(\underline{x}) = \bar{U}_j - \sum_{i=1}^{N} \left(S_{ij}^A x_i + S_{ij}^B x_i^2 \right) \; ; \; j \in m \tag{7}$$

where the S_{ij}^A and S_{ij}^B matrix coefficients, respectively represent gradients of the stress membrane component with respect to x_i, and the stress bending component with respect to y_i.

Although it is still possible to employ equation (7) in constructing the dual problem, the resulting relationship between x_i and d_j does not lend itself to a closed form solution as was the case in equations (6.3, 4, 5). As such, a numerical solution must be invoked. For this reason, the extended dual scheme was not implemented for the stress constraints.

b. Simple Dual. It should be noted that having to compute two sets of gradients in the extended dual above (for combined membrane and bending), may or may not be computationally advantageous depending on the rate of convergence to the optimum design. This leads one to the view that adopting the x_i transformation of equation (2.4) may be computationally rewarding, even though it does not yield high quality approximations of the displacement, frequency, or stress constraints for combined bending and membrane behavior. In this case, an explicit approximation of any of these constraints may be written as follows:

$$\tilde{h}_j(\underline{x}) \equiv \bar{U}_j - \sum_{i=1}^{N} \bar{C}_{ij} x_i \geq 0 \quad ; \quad j \in m \tag{8}$$

in which $\bar{C}_{ij} = \left(\bar{C}_{ij}^A + \bar{C}_{ij}^B \right)$ with $\bar{C}_{ij}^A$ and $\bar{C}_{ij}^B$ respectively are matrix coefficients representing gradients with respect x_i for the membrane and the bending components of the response quantity in question. With equation (8) for the simplified dual, the combined membrane and bending behavior reverts to the original dual statement of equations (3), in which C_{ij}^A is now replaced by $\bar{C}_{ij}$.

From the above theory, it is clear that in order to take advantage of the powerful dual formulation, one must cast the element matrices (such as stiffness and mass and their gradients) as coefficients of the selected intermediate variables. This must be done during analysis, generation of the approximate problem, and gradient evaluation. The required form of these matrices depends on the element type. Since this is not usually needed in general-purpose analysis programs, these requirements seem to favor the development of special-purpose analysis-synthesis capability over modifying general-purpose analysis codes.

3. Scope of New Program Capabilities

The structural synthesis problem stated by equations (1), (2) and (3) for axial and membrane behavior was carried out in the original ACCESS-3 program using the approximation concepts approach along with various optimization algorithms; PRIMAL2, NEWSUMT, DUAL1 and DUAL2. The major limitations of the program were that during the analysis phase, the complete stiffness matrix of the structure for static analysis problems, and the complete stiffness and mass matrices for frequency analysis problems were required in core. Moreover, the preprocessing data for each element such as thickness, area, length, density, direction cosines, and unit stiffness and mass matrices were kept in core. These requirements severely limited the size of structural problems that could be analyzed and optimized using the ACCESS-3 code. The program was also limited to the solution of problems that could be modeled only by axial, membrane, and shear panel elements having a maximum of three degrees-of-freedom per node.

To overcome the above limitations and enhance the program capabilities the following extensions were implemented:

1. Each node in the structural model is now allowed to have as many as six degrees-of-freedom per node. This is a necessary step to permit the

inclusion of a larger variety of finite elements.

2. A triangular plate membrane-bending element (5,6) was added in order to broaden the class of problems that can be optimized by the program. The addition of a rectangular plate membrane-bending element as well as several beam elements with various cross section shapes are under development.

3. With regard to the ability to handle large size problems, the data management scheme was restructured and the original in-core solution algorithms were replaced by out-of-core solution schemes. The stiffness, mass, and connectivity matrices for each group of linked elements are now stored group by group on direct access files. After generation of all the group matrices is completed, they are recalled group by group during the assembly of the global matrices and the evaluation of the displacement and frequency gradients.

To compute the stresses during a given design stage, the element stress-displacement coefficient matrices along with the connectivity array are stored on a separate direct access file. These stress matrices are recalled element by element when forming the stress constraints. Subsequently, they are recalled selectively when forming the gradients for the retained potentially critical or critical constraints. This removes the necessity to save all element property data on the high speed core during the entire analysis and approximate problem generation phases.

The algorithm for solving the static and eigenvalue problems use the same out-of-core solution techniques of Ref. (5). The subspace iteration technique along with the Sturm-sequence check is used for finding the eigenvalues. It involves breaking of the global stiffness, mass, and displacement/load matrices into blocks. At any one time, only two blocks of either the stiffness or the mass matrix along with two blocks of the displacement/load matrix must be in high speed storage. The total number and size of each block are internally computed depending upon the number of unrestrained degrees-of-freedom and bandwidth of the entire problem, as well as on the size of available blank common storage. The decomposed stiffness matrix is computed two blocks at a time and saved on direct access files. These are subsequently recalled during back substitution, during eigenvalue solution and during evaluation of the displacement gradients.

4. In order to capitalize on the greater efficiency offered by the dual approach, both of the simple and extended dual formulations discussed in Section 2 were implemented in the program. The extended dual can be used only for displacement and frequency constraints. However, the simple dual formulation (DUAL2) as well as the previously available primal formulation (NEWSUMT) can be used for the displacement, frequency, and stress constraints in problems having membrane (axial) and bending behavior.

4. Numerical Examples

Example 1

Plate supported at four points. This example consists of a 10 x 12 in. rectangular steel plate for which similar results has been previously reported (1). The plate is subjected to line loads along the central and boundary lines as in Fig. 1. The finite element model and design variable linking scheme used are essentially those of Ref. (1), except that triangular plate elements were used instead of rectangular elements. Figure 1 also shows the symmetric model of one quarter of the plate, and Table 1 lists the applied loads. The plate material properties are: modulus of elasticity = 28×10^6 psi, Poisson's ratio = 0.3, and weight density = 0.248 lb/in^3. The imposed constraints include: minimum gage = 0.02 in., upper and lower bounds on the out-of-plane displacements = ±0.02 at the center (node 1) and at the corner (node 64), and maximum allowable Von Mises stress σ_v = 25,000 psi imposed on all finite elements in the model.

Instead of Von Mises criteria:

$$\sigma_v \geq \left[\sigma_x^2 + \sigma_y^2 + 3\,\sigma_{xy}^2 - \sigma_x\sigma_y\right]^{1/2},$$

Reference (1) employed Hill's criteria:

$$\sigma_H = \left[\left(\frac{\sigma_x}{\sigma_1}\right)^2 + \left(\frac{\sigma_y}{\sigma_2}\right)^2 + \left(\frac{\sigma_{xy}}{\sigma_{12}}\right)^2 - \frac{\sigma_x\sigma_y}{\sigma_1\sigma_2}\right]^{1/2} \leq 1$$

Table 1 Applied nodal forces for Example 1

Node number(s)	Applied nodal forces, in pounds
1	357.34
2-7	142.86
8	200
9, 17, 25, 33, 41, 49	171.43
57, 64	192.86
58-63	214.86
16, 24, 32, 40, 48, 56	257.14

The optimization starts with a feasible design having uniform thickness t_i = 0.71 for all 98 elements in the 32-linking groups. The corresponding total weight for the quarter plate is 5.2824 lb. After 12-stages, the design converged to 2.3859 lb when the simple dual approach was used. Figures 2 and 3 respectively show the optimum distribution of plate thickness and the total weight iteration history. At the optimum, the out-of-plane displacement at the corner (node 64) was near critical, and the stresses for most of the elements were either slightly critical or near critical. In Ref. (1), the same example was solved using a primal formulation with cubic extended interior penalty function. The differences in the thickness distribution and in the total weight between the present results and those of Ref. (1) may be attributed primarily to the employment of different stress criteria as mentioned above.

To illustrate the ability of the program in handling the optimization of larger problems, the same four-point supported plate was solved as half the plate, rather than one quarter. This more than doubled the number of unrestrained degrees-of-freedom, and doubled the number of elements as well as the number of linked design variables. The same stress, displacement, and minimum gage constraints were imposed as before. Here again, starting with 0.71 in. uniform thickness, the optimum was achieved after 12-stages, and the corresponding thickness distribution was symmetric to the third significant figure. The results were identical to Figs. (2) and (3).

Example 2

This example is intended to compare the computational advantages of the simple and the extended dual schemes discussed in Section 2. The problem selected

is the four point supported plate of Fig. 1. The constraints used here are those on minimum gage on all elements and on the out-of-plane displacements at nodes 1 and 64. However, no stress constraints are imposed. The optimum thickness distribution and the total weight iteration histories are shown in Figs. 4 and 5 for the two options. The move limits used were the same in both cases.

Contrary to what may be expected, Fig. 5 shows that the results of the extended dual seem to be consistently inferior to the simple dual. Although the first is based on more accurate approximation of the constraints than the latter. Furthermore, the extended dual required about 50% more computations per stage over the simple dual.

Example 3

To assess the results obtained in the previous example, further comparison between the two dual options was made for the cantilever plate problem in Fig. 6. The plate consists of 10 elements linked in 5 groups (underlined is the group number). The material properties are: elasticity modulus = 10×10^6 psi, Poisson's ratio = 0.3 and weight density = 0.3 lb/in.^{3}. A moment = 225.0 lb/in. is applied about the y-axis at the free end at each of node 1 and 2. The maximum allowed out-of-plane displacements at nodes 1 and 2 are ±0.5 in., and lower bounds are placed on the lowest three eigenvalues squares (2.8×10^5, 5.0×10^5, and 10.0×10^5).

Starting with a feasible design having 0.5 in. uniform thickness, the optimum thickness distribution was computed (see Table 2). At the optimum, both the simple and the extended dual produced near critical constraints on the first eigenvalue and the end displacements. Unlike the previous example, the interation histories shown in Fig. 7 for this example show that the extended dual was more efficient than the simple dual.

Table 2. Optimal thickness distribution, Example 3

Group No.	5	4	3	2	1
Simple Dual (6 stages)	0.4391	0.3732	0.3734	0.3167	0.3000
Extended Dual (4 stages)	0.4231	0.3975	0.3628	0.3149	0.3000

Example 4

The same cantilever plate problem of the previous example was used here to compare the performance of the primal approach of equations (2) using NEWSUMT, and the simple dual of equations (3), (8) using DUAL2. The imposed constraints for this problem consist of maximum out-of-plane displacements at nodes 1 and 2 of ±0.5 in., and maximum yield stress of ±100,000 psi (for all elements) based on Von Mises criterion.

In this case, the starting uniform thickness of 0.5 in. was infeasible for stresses. The minimum weight was achieved by both schemes; after 10 iterations using the primal approach, and after 5 iterations when the simple dual was used. The optimal distribution (Table 3) had near critical stresses which governed the design. The iteration histories in Fig. 8 clearly show the superiority of the simple dual over the primal approach.

Table 3 Optimal thickness distribution, Example 4

Group No.	5	4	3	2	1
Primal (10-stages)	0.5255	0.5212	0.5201	0.5200	0.5201
Simple dual (5-stages)	0.5252	0.5209	0. 197	0.5196	0.5196

5. Conclusions

A special-purpose analysis synthesis code was developed to handle the optimization of structural systems with relatively large number of degrees-of-freedom, design variables, and constraints with high degree of efficiency. The code is versatile in that it combines the widely-used approximation concepts with either primal or dual formulations. The primal approach is known to have the advantage of applicability to a wide class of problems with various constraint types. However, Examples (1) and (4) show that the simple dual approach is more efficient than the primal, in addition to its applicability to problems with constraints on frequencies, displacements and stresses, with or without bending behavior. It should, therefore, contribute to a wider acceptance of the formal optimization procedures as viable design tools.

On the other hand, although the extended dual is based on more accurate approximations of the displacement and frequency constraints over the simple dual scheme, Examples (2) and (3) seem to indicate that their relative efficiency is problem dependent. For this reason, further investigation and testing of the extended dual scheme will be carried out.

References

1. Prasad, B., and Haftka, R. T., "Optimal Structural Design with Plate Finite Elements," Proceeding of the ASCE, Journal of the Structural Div., ST11, Nov. 1979.

2. Sobieski, J. S., and Bhat, R. B., "Adaptable Structural Synthesis Using Advanced Analysis and Optimization Coupled by a Computer Operating System," Paper No. 79-0723 presented at the AIAA/ASME/ASCE/AHS 20th Conf., St. Louis, Missouri, April 1979.

3. Fleury, C., and Schmit, L. A., Jr., "Dual Methods and Approximation Concepts in Structural Synthesis," NASA-CR-3226, Dec. 1980.

4. Fleury, C., "Optimization of Large Flexural Finite Element Systems," presented at the NATO Advanced Study Institute on Optimization of Distributed Parameter Structures, Univ. of Iowa, April 1980.

5. Bathe, K. J., Wilson, E. L., and Peterson, F. E., "SAP-4 Structural Analysis Program for Static and Dynamic Response of Linear Systems," Report No. EERC 73-11 June 1973, Univ. of Calif., Berkeley.

6. Clough, R. W., and Felippa, C. A., "A Refined Quadralateral Element for the Analysis of Plate Bending," Proceedings of the Second Conf. on Matrix Methods in Structural Mechanics, Wright-Patterson Air Force Base, Ohio, Oct. 1968.

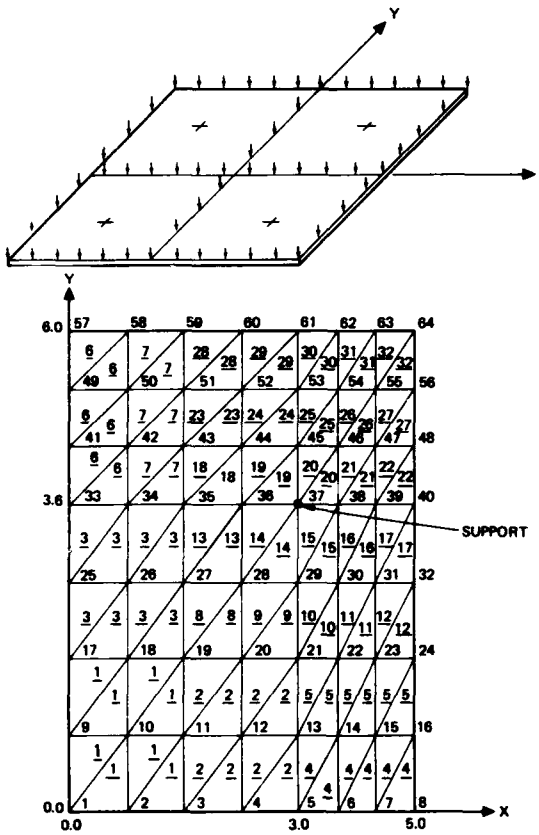


Fig. 1 Finite element model of rectangular plate supported on 4-points, Example 1. (Underlined are the linking group numbers)

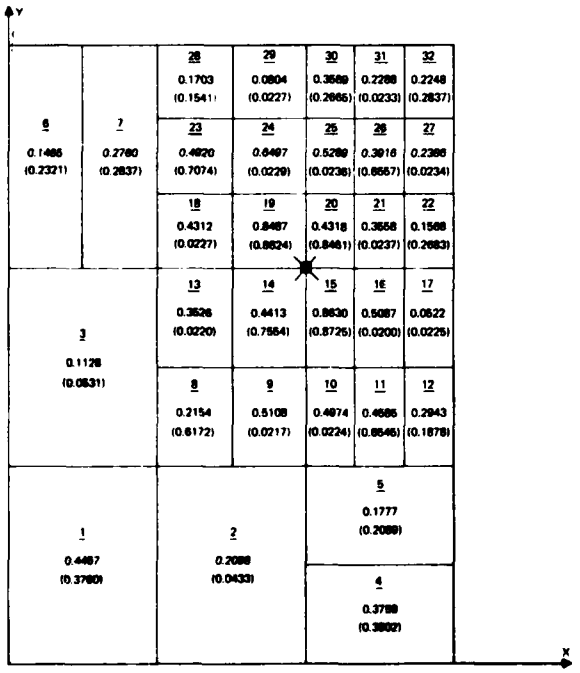


Fig. 2 Optimal thickness distribution for Example 1. Results of Ref. (1) shown in parentheses. The underlined are the linking group numbers.

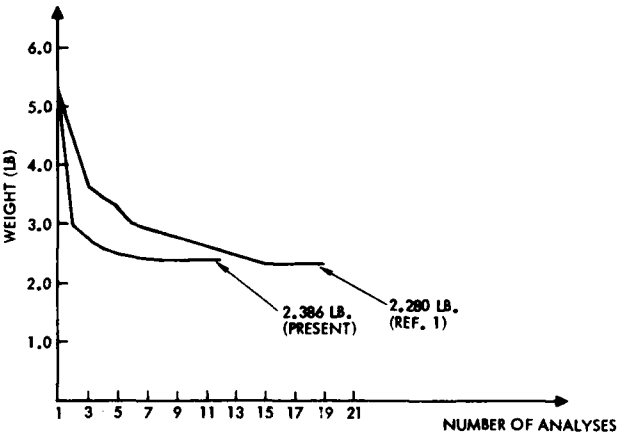


Fig. 3 Iteration history for Example 1.

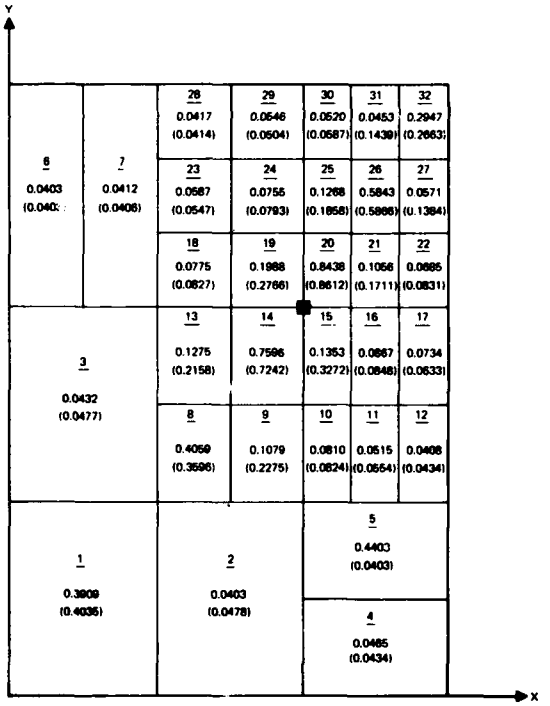


Fig. 4 Optimal thickness distribution, Example 2. Comparison of results for the simple dual and extended dual (shown in parentheses). Underlined are the linking group numbers.

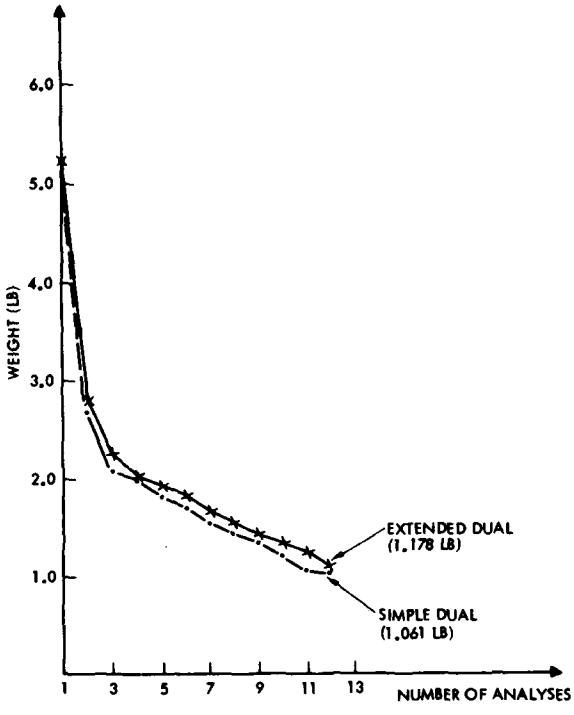


Fig. 5 Iteration history for Example 2.

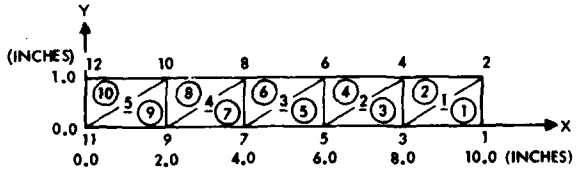


Fig. 6 Finite element model for Example 3.

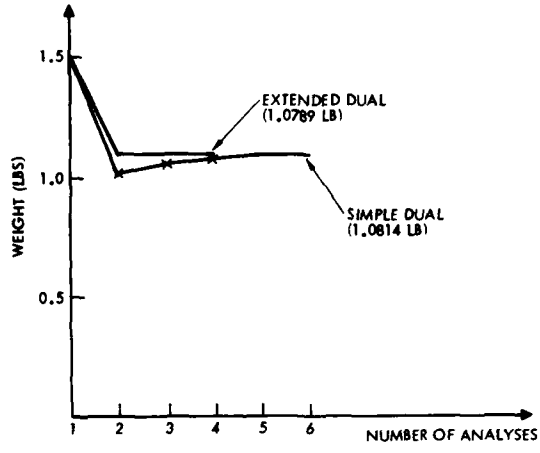


Fig. 7 Iteration history for Example 3.
("x" are infeasible design points)

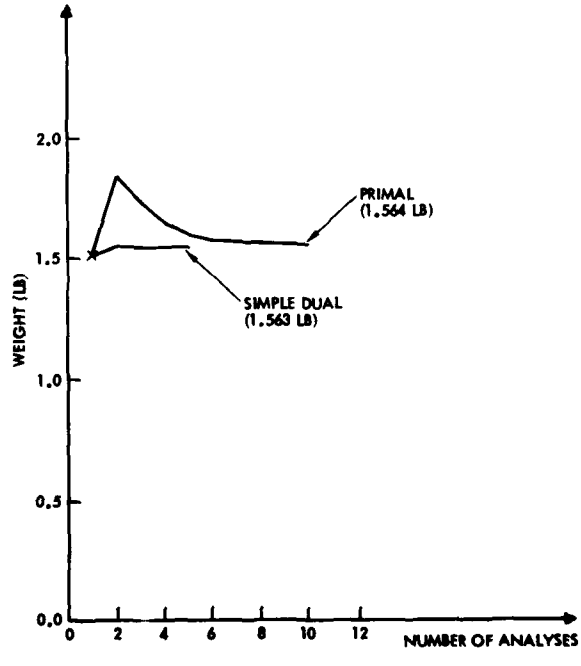


Fig. 8 Iteration history for Example 4.
("x" are infeasible design points)

AD-P000 085

A PROGRAMING SYSTEM FOR RESEARCH AND APPLICATIONS IN STRUCTURAL OPTIMIZATION

Jaroslaw Sobieszczanski-Sobieski* and James L. Rogers, Jr.**
NASA Langley Research Center
Hampton, VA 23665

Abstract

The paper describes a computer programing system designed to be used for methodology research as well as applications in structural optimization. The flexibility necessary for such diverse utilizations is achieved by combining, in a modular manner, a state-of-the-art optimization program, a production level structural analysis program, and user supplied and problem dependent interface programs. Standard utility capabilities existing in modern computer operating systems are used to integrate these programs. This approach results in flexibility of the optimization procedure organization and versatility in the formulation of constraints and design variables. Features shown in numerical examples include: (1) variability of structural layout and overall shape geometry, (2) static strength and stiffness constraints, (3) local buckling failure, and (4) vibration constraints. The paper concludes with a review of the further development trends of this programing system.

List of Symbols

F	- objective function
:	- function in general sense, denotes F or g
g	- constraint function
K	- stiffness matrix
L	- load
m	- number of constraint functions
n	- number of design variables
P	- load factor used as a variable
P_t	- magnitude of the target level for P
t	- thickness
u	- vector of displacements
v	- velocity
$\vec{x}$	- vector of design variables
x_i	- a design variable
z_i	- vertical displacements in a box beam
Ω	- cumulative constraint

Subscripts:

i	- design variable
j	- constraint function
o	- original value in extrapolation

Acronyms:

A-O Processor	- program converting the analysis program output to the optimization program input
CONMIN	- a particular optimization program used in PROSSS
O-A Processor	- program converting the optimization program output to the analysis program input
PROSSS	- Programing System for Structural Synthesis
SPAR	- a particular analysis program used in PROSSS

* Head, Multidisciplinary Analysis and Optimization Branch, LAD
** Computer Scientist

Introduction

The purpose of this paper is to describe a structural optimization program, called a Programing System for Structural Synthesis (PROSSS), which uniquely combines the almost unlimited flexibility required of a research tool for method development, with the reliability and simplicity of use expected from an application tool.

To provide a rationale for the implementation approach presented, the paper begins with a review of the requirements posed by the intended uses of the program in both research and applications. The implementation options are examined next, leading to a programing system alternative as a logical choice.

The principal components of the system, the way they are integrated, and the execution options are examined; and numerical examples are provided to illustrate the salient features pertinent to research and application. Included in the examples is a description of a version of the system operating in a distributed manner on a mainframe and a minicomputer.

The paper concludes with a brief review of the development trends stemming from the system capabilities and the current directions of the state-of-the-art evolution.

Structural Optimization Application and Research Requirements

In general, the function of the optimization procedure is to find a vector of design variables $\vec{x}$ that minimizes an objective function $F(\vec{x})$ while satisfying constraint equations $g(\vec{x})$. In a standard notation:

$$F(\vec{x}) \rightarrow \min \qquad (1)$$

subject to

$$g_j(\vec{x}) \leq 0 \quad 1 \leq j \leq m \qquad (2)$$

In various applications, the variables in eq. 1 and eq. 2 acquire different meanings, and solution of the equations with acceptable efficiency and accuracy may require a fairly elaborate numerical process. Therefore, building a computer program to support both the development and application of structural optimization methods poses a unique challenge of making the software flexible and adaptable, yet reliable and easy to use.

Diversity of Applications

The need for flexibility and adaptability stems, in part, from the need to be able to use the program to optimize structures of various types, e.g., an aircraft fuselage, a large space truss, or a nuclear reactor vessel. A single program general enough to answer all analysis needs for all the types of

PRECEDING PAGE

structures of interest, and efficient enough to perform well in an optimization loop at a reasonable cost, is not available. Consequently, an open-ended library of analysis programs has to be used.

In addition to the variety of types of structures, a variety of optimization problem formulations that differ by unique definitions of the design variables, constraints, and objective function will be of interest for each type of structure. Therefore, these portions of the code in which these formulations are embedded should be easy to replace.

Diversity of the Optimization Techniques and Procedures

A distinction between an optimization technique and an optimization procedure will be useful in this discussion. An optimization technique is a search algorithm whose function is to find a constrained minimum in a space defined by the design variables in which the objective function and constraint functions are computed by another algorithm--an analysis algorithm. A few examples of optimization techniques are: (1) a nonlinear mathematical programing using an interior or exterior penalty functions (Sequential Unconstrained Minimization Technique, SUMT, ref. 1), (2) a usable-feasible direction algorithm, ref. 2, (3) a linear programing algorithm (e.g., ref. 3), and (4) optimality criteria methods, such as the fully stressed design method. An optimization procedure is an entity of higher order and as such may command execution of several optimization techniques, analysis algorithms, and auxiliary housekeeping and user-interface algorithms. Two examples of optimization procedures are: (1) a simple arrangement in which the executions of a search algorithm (an optimization technique) and an analysis alternate until the search algorithms localize a constrained minimum, and (2) a more complex arrangement in which a linear programing algorithm is combined with the exact and approximate analyses to solve a nonlinear optimization problem as a series of linearized subproblems.

By its very nature, the optimization methodology development requires use of many existing techniques and procedures and a continual creation of new ones, hence, only a program of practically unrestricted flexibility in its organization will qualify as a test bed for such development. If the same test bed program is also to be used for solving quickly and efficiently the application problems as a routine support of ongoing design projects, then there is a need to reconcile the seemingly contradictory requirements of "researchy" flexibility on one hand, and the reliability and relative constancy expected from a production tool, on the other hand.

Hardware Adaptability

An additional consideration in development of an optimization program for research and applications is a need to capitalize on the opportunities periodically created by improvements in computer hardware. One such recent opportunity is distributed computing which, potentially at least, should improve computational efficiency by judiciously exploiting special features of the dissimilar computers in a network, and performing calculations in parallel whenever possible. It will be shown later that software flexible enough to meet the requirements pointed out in the previous two sections can also be adapted rather easily to distributed computing.

Considerations Leading to Programing System Approach

Regardless of the manner of implementation, the basic function of an optimization procedure is to carry out an iteration shown by a flowchart in figure 1 in which a search algorithm and an analysis algorithm are labeled Optimizer and Analyzer. The procedure can be implemented on the computer in a number of ways illustrated in figure 2 and reviewed in this section in order of increasing application flexibility.

The discussion begins with a "closed box" approach which is the least flexible, but potentially the most efficient in execution, the simplest to use, and progresses to the concept of a programing system of potentially complete generality. Between these two extremes, the concept of concentrating the search and analysis functions in separate subroutines is discussed.

Special Purpose "Closed Box"

By definition, the inner workings of a "closed box" program (fig. 2(a)) are set up for a predetermined scope of applications but not for easy access and modification by the users. This leaves the users with the input data as the only means for controlling the program functions within a range of options prescribed by the program developers. This adaptability limitation is an inevitable consequence of the "closed box" approach.

On the other hand, developers of a "closed box" program, being free of the user access and modification considerations, can gear the program organization for maximum computational efficiency, frequently by means of dispersing and intertwining the search and analysis functions with each other. Thus, in addition to being efficient, the program is practically impossible to "tinker" with and, therefore, maintains a permanent configuration and a repeatability of results. These are important features expected from a production tool in an engineering organization that might be concerned with a large number of applications of a limited variety and driven by stringent project deadlines.

Search and Analysis Algorithms as Subroutines

Under this approach, shown in figure 2(b), the user has available the two basic elements of an optimization procedure in the form of separate subroutines. It is up to the user to assemble these subroutines in a functional program and to include various convenience features such as stop and restart, intermediate result displays, and special termination criteria.

This implementation approach has the advantage of modularity, so that everything that depends on the physics of the program can be isolated in the analysis subroutine while the best available search algorithm can be selected and coded in the search subroutine. However, the obviously attractive option of using preexisting codes for these subroutines is restricted by the practical limitations the main program-subroutine organization imposes on the subroutine size.

Programing System

In comparison to the main program-subroutines arrangement, the concept of a programing system shown in figure 2(c) is the next logical step toward greater application flexibility. In a programing system (term

introduced in ref. 4), a user must furnish problem dependent code modules in addition to input data, in contrast to an ordinary program or system of programs which need only the input data to execute. A programing system allows the use of large stand-alone programs, or even systems of several large programs for the analysis and optimization functions, and isolates the definitions of the design variables, objective function, and constraints in separate problem dependent, user supplied programs executed between the Optimizer and the Analyzer. The system is controlled by an executive command language and other software utilities that constitute a connecting network, thus, in principle, any optimization procedure can be implemented, including optimization problems that in their analysis require many engineering disciplines in addition to structures. An example is a system for optimization of airframes including aerodynamic loads and aeroelastic effects, described in references 5 and 6. The concept of a programing system for optimization in general is a multifaceted subject for which literature references exist (e.g., refs. 4 and 7), therefore, the focus of the discussion which follows is on a particular programing system specialized for structural optimization.

Features of the PROSSS System

The particular system to which the attention is now turning is called PROSSS for Programing System for Structural Synthesis. Its principal components are, in general terms: optimizer, analyzer, processors interfacing optimizer to analyzer (O-A) and vice versa (A-O), and the connecting framework. Executions of these components can be sequenced in various ways as required by a particular optimization procedure. The components and the procedure execution options are reviewed in this section.

Analyzer

The function of the analyzer is to compute values of the behavior variables which characterize the physical object's response to the input quantities.

Overall characteristics. In PROSSS, the analyzer is the finite-element program SPAR documented in reference 8. SPAR was selected for the analyzer's function because of its computer efficiency, modularity, and data base capability. Input quantities consist of structural cross-section dimensions, material properties, element connectivity data, nodal point coordinates, and loads. Output quantities consist of displacements, internal forces, stresses, eigenvalues, and eigenmodes for vibration and buckling, etc. Another output quantity is the structural mass which is commonly used as the objective function. The library of finite elements in SPAR is adequate for analysis of skeletal and thin-walled structures.

SPAR is a collection of individual programs (processors that communicate with each other through a data base as indicated in fig. 3). The data base consists of one or more files which contain data sets output from the different processors. Each data set has a specific identifying name with which any processor can access it for input. Subroutines documented in reference 9 are available to store and retrieve the SPAR data sets by name from the SPAR data base. These subroutines can be executed by FORTRAN CALL statements and hence can be used to make the SPAR data storage accessible to non-SPAR FORTRAN programs.

SPAR executes on a processor-by-processor basis; each processor execution is commanded by a separate explicit command. A string of such commands interlaced with the input numerical data is written by the user for the problem at hand, and will be called a runstream in this paper. The data base facilitates an efficient and selective data transfer from SPAR to other programs, and the individual processor control allows the user to limit the number of processors executed repetitively in an optimization loop. For this purpose, the analyzer is divided into a nonrepeatable part executed once at the beginning of the procedure and a repeatable part executed many times in the optimization loop. Specifically, for invariant overall geometry, the nonrepeatable part generates nodal coordinates, material properties, constraint data and defines the loads. The repeatable part generates solutions of the load-deflection equations.

Computation of gradients. Most of the efficient mathematical optimization algorithms require not only the objective function and the constraint values but also their gradients to be evaluated for a given set of input values of the design variables x_i. The gradients can be computed by a finite-difference technique or by an analytical technique. An example of an analytical gradient is the differentiation of the matrix load-deflection equation, $Ku = L$, with respect to a design variable x_i. The result is a matrix equation

$$K \frac{\partial u}{\partial x_i} = \frac{\partial K}{\partial x_i} u + \frac{\partial L}{\partial x_i} \qquad (3)$$

from which $\partial u/\partial x_i$ can be obtained at a relatively small computational cost by reusing the previously decomposed stiffness matrix K, as shown in references 10 and 11. In SPAR, the analytical gradient computation is implemented by means of runstreams which are established specifically for this purpose and are a permanent part of PROSSS.

Optimizer

The function of the optmizer is to calculate a new vector of design variables $\vec{x}$ on the basis of the values of the objective function and the constraints, and, optionally, their gradients returned by the analyzer in response to a previously defined vector $\vec{x}$.

In PROSSS, the optimizer is the program CONMIN (ref. 12), which is based on the mathematical nonlinear programing technique of usable-feasible directions. In this report, CONMIN is viewed as a "black box" and attention is focused on the type of data it requires from the rest of the system, and on its execution options, since these features influence organization of the programing system.

The following execution modes are available in CONMIN:

(a) Execution that requires current values of the objective function and constraints.

(b) Execution that requires current values of the objective function, constraints and their gradients.

(c) Execution accelerated because of the linearity of either the objective function and/or the constraints.

In PROSSS, program CONMIN is embedded as a subroutine in a program which calls it, and saves intermediate data for restart.

Interface Processors

The optimizer provides input information to the repeatable part of the analyzer through an Optimizer-to-Analyzer (O-A) Processor and the analyzer supplies the information to the optimizer through an Analyzer-to-Optimizer (A-O) Processor. The O-A and A-O processors are user supplied and problem dependent. Capability of adding these two programs is the basis for the system's generality.

Optimizer-to-analyzer processor. The function of the O-A Processor is to convert the design variables to a set of input parameters written in a format required by the analyzer. In the case of structural optimization, these parameters are structural member sizes and nodal point coordinate data which are actual physical quantities and are seldom directly equivalent, one-to-one, to the design variables output by the optimizer. Thus, in a typical application, the conversions within the O-A Processor are not limited to formal changes only but also include such commonly used techniques as variable linking, scaling, and changing from direct to reciprocal variables (e.g., ref. 13). In PROSSS, the O-A Processor reads an output vector $\vec{x}$ from CONMIN, computes the structural parameters, and embeds them in a runstream written for the SPAR execution.

Analyzer-to-optimizer processor. The function of the A-O Processor is to compute the objective function, the constraints, and their gradients (if required) and to provide them in the format required by the optimizer. To do so, the A-O Processor extracts the pertinent behavior variables such as stresses, displacements, natural vibration frequencies, mode vectors, or buckling loads from the SPAR data base and combines them with the allowable values to form the constraint equations. Frequently, the allowable values are functions of $\vec{x}$ (instead of being constants) as, for example, in the case of local buckling constraints (e.g., ref. 14). Computation of such variable allowable values can be included among the functions of the A-O Processor. This processor may also be equipped with a logic to limit the set of constraints to those whose probability of remaining or becoming active is high, as proposed in reference 13. Organization of the A-O Processor, illustrated by the flow chart in figure 4, is problem independent, but the processor contains a section of code (box 4) which does depend on the problem at hand and must be tailored to it. In addition, the parameters in the call statements to the subroutines (box 3) (see ref. 9) that access the SPAR data base depend on the kind of data sets that need to be extracted as required by the particular constraints and objective function.

Connecting Network

A connecting network (executive software) is required to carry out a computational process such as shown in figure 1. It is also required to enable the user to monitor progress of the optimization process, and to stop and restart without loss of information generated before the interruption.

In PROSSS, the CDC-NOS (Network Operating System)[1] documented in reference 15 serves as the connecting network using the approach described in reference 5. The CDC-NOS furnishes the user with a repertory of commands (job control language, (JCL)) for executing programs in sequences, including if-test branching and transferring to a labeled statement, and for manipulation of permanent and temporary files. These capabilities are common in most current operating systems, consequently such systems as IBM's MVS or UNIVAC's Exec 8 could function as a connecting network instead of CDC-NOS.

Execution Flow Options

A variety of execution flow options can be set up using the components described previously. Organization of each flow option depends on how the optimizer is used, and on whether gradients are required as input to the optimizer and, if so, whether these gradients are generated analytically or by finite differences. The flow options currently available in PROSSS are the five shown in Table I.

Basic flow options. The two optimization procedures in Table I are: nonlinear mathematical programing (NLP) and piecewise linear approximations (PLA). Under the conventional NLP approach, the objective function and constraints are treated as nonlinear functions of the design variables. In the PLA procedure, which has been successfully used in a number of applications (e.g., refs. 13, 16, 17) the nonlinear optimization progresses as a sequence of linear optimization subproblems (stages). A linear approximation based on the Taylor series expansion, $f = f_o + \nabla f_o^T \Delta\vec{x}$, is used to compute the objective function and the constraint functions within each subproblem (stage). Side constraints on $\vec{x}$ control the linearization error.

Efficiency of PLA stems from replacing the full analysis of the physical problem with approximate analysis by linear extrapolation, which in structural applications requires a computer time of at least an order of magnitude smaller than the full analysis time. Additional time savings result at each stage because the optimizer executes faster when the problem is defined as linear (mode c in section "Optimizer"). The number of consecutive linear stages required for overall convergence depends on the degree of the problem nonlinearity.

The analysis capabilities with respect to calculation of gradients in Table I are: (1) computation of the behavior variables without gradients; (2) inclusion of gradients computed by finite differences; and (3) inclusion of gradients computed analytically.

Each of the five resulting options shown in Table I requires its own organization of the procedure flow. The organizationally simplest and most complex execution options, 1.1 and 2.3, respectively, are illustrated by flow charts in figures 5 and 6. The other options are described in detail in reference 18 and documented in reference 19. The flow chart in figure 5 is self-explanatory. In figure 6, the boxes 2, 3, and 4 may be regarded as functions of a single main program which calls the optimizer represented by box 1.

Auxiliary Option for Fully Stressed Design (FSD). If strength constraints are present in the problem, then convergence of all the foregoing optimization procedures can be improved by using a limited number (e.g. 3 to 5) of FSD iterations to generate initial cross-sectional dimensions of the structural members. Allowable stresses used in the FSD procedure can include material allowables (e.g., yield stress) and local buckling stresses which are

[1] Use of commercial products and names of manufacturers in this report does not constitute an official endorsement of such products or manufacturers, either expressed or implied, by the National Aeronautics and Space Administration.

functions of the cross-sectional dimensions as described in reference 20.

Two Basic Forms of the System

PROSSS exists in two basic forms: Skeleton Form and Specialized Form. The Skeleton Form consists of the following:

(1) The problem independent component programs such as SPAR, CONMIN, and the programs controlling execution of the linear stage optimization (figure 6) and FSD procedure.

(2) The SPAR runstream files for analytical gradients.

(3) The procedure files.

(4) The sets of JCL statements for each option.

To be used in a specific application, the Skeleton Form has to be turned into a Specialized Form. Problem dependent Interface Processors and the input data, including the SPAR runstreams, must be created and stored as files. In addition, standard names in the JCL statement file corresponding to the option chosen must be replaced with names selected for the problem dependent files.

Once the Specialized Form has been set up for a particular application, it can be protected from unauthorized alterations by using "software locks" (passwords) on all its files except the input data files. Several such Specialized Forms can be created from the common Skeleton Form for a variety of applications as illustrated in figure 7. Each such "frozen" Specialized Form can be used as a "black box" for a given class of problems that differ only by their input data. It is important to realize that although a Specialized Form is intended for use as a "black box" whose user is concerned only with the input and output data, it never becomes a previously defined "closed box" because it is always modular and accessible for modification.

In industrial organizations, preparation of the Specialized Forms would fall naturally into the domain of the staff specialist, while their application would be the task of the production oriented engineers. In research applications, the system modularity permits its major components SPAR and CONMIN to be replaced with other equivalent programs, and execution flows different than those described previously can also be constructed. Thus, PROSSS can be used as a test bed for development of new optimization procedures as well as an application tool.

Numerical Examples

Examples presented in this section illustrate PROSSS as an application tool and as a research test bed. The application examples have been selected from a larger sample (given in ref. 18) to show the variety of design variable formulations, types of constraints, and some of the execution options. The purpose of the research examples is to illustrate usefulness of PROSSS in trying out improvements in the ways of conducting the optimization, including the case of the system distributed between a mainframe and a minicomputer.

Application Examples

Example 1: Stiffened cylindrical shell. Several variants of a circular cylindrical shell reinforced by frames and longerons were studied. Finite-element model of the computationally largest variant (referred to as variant 1) is shown in figure 8. This variant is built up of membrane panels to represent skin, and beam elements (axial, bending and torsional stiffnesses) simulating transverse frames and longerons. Each frame and longeron may be regarded as a lumped representation (ref. 14) of several real frames and longerons. One end of the shell is clamped around the circumference, the other end is loaded by concentrated loads simulating distributed forces equivalent to a transverse force and torque. This variant has a large cut-out and a floor, and represents a simplified model of a transport aircraft fuselage segment.

This structure was expected to constitute a demanding test case for the following two reasons. First, the model contains 798 degrees of freedom, so it is a computationally large problem as far as optimization by mathematical programing is concerned. Secondly, the overall bending state of stress in a shell of this type depends on the in-plane stiffness of the frames; therefore, the design variables that govern the member cross-sectional dimensions become strongly coupled (e.g., ref. 14) and the optimization process is more difficult to converge.

Variant 1 was optimized by PLA using finite-difference gradients (Option 2.2) and the 10 design variables shown in figure 8. As indicated in the figure, many structural parameters are linked to a single design variable, so that 10 design variables govern the cross-sectional dimensions of all 356 elements in the finite-element model. Variables x_1 through x_6 govern the cross-sectional areas of the beam elements which have a channel cross-section whose proportions remain constant as its area changes. Thus, the cross-sectional area becomes a single variable that governs all the beam stiffness parameters. Variables x_7 through x_{10} govern the membrane panel thickness. The optimization constraints were on the beam element stresses and equivalent stresses (Huber-von Mises stress) in the panel elements. The iteration history of the design variables is shown in figure 9. Convergence is quite good considering the problem size and use of the piecewise linear approximations. As expected, the elements flanking the cutout have "grown" in the optimization process, as illustrated in figure 10.

To further demonstrate the adaptability of the procedure, a simplified variant 2 of the shell structure was formed by eliminating the floor and two end bays and substituting rods for longerons. Initially, the structure was optimized with stress constraints only. Subsequently, the resultant structure was optimized with an additional overall shell buckling constraint which required a 21 percent increase of the buckling load over and above the buckling load computed for the structure optimized with stress constraints only. Both optimizations were carried out by Option 1.1. A comparison of these two results showed that the structural mass increased by 9.6 percent because of the additional buckling constraint. Additional optimization of this variant (with two loading cases) was carried out with stress constraints using only analytical gradients (Option 2.3). Use of analytical gradients was found to reduce the execution time to approximately one-sixth of that required for Option 1.1. Three design variables, one for longerons, one for transverse-frames, and one for the skin were used in this case.

Locations of the node points in the finite-element model were considered as design variables in a further simplified variant 3 of the

shell structure. This variant has the cut-out eliminated, is subject to only one loading case (transverse force), and has the longerons restored to the beam form. Previously defined cross-sectional variables were retained. The three geometrical variables governed locations of the three intermediate frames. Optimization using Option 1.1 with stress and overall shell buckling constraints resulted in translation of the frames toward the loaded and unsupported end, as seen in figure 11.

Example 2: Portal framework shape optimization. A framework shown in figure 12 has been optimized with geometrical variables only to demonstrate the structural shape optimization. The variables defined in figure 12 are intended to allow the frame to transform into a truss. The constraints were imposed on stress and horizontal displacement as indicated in figure 12. Optimization, carried out by means of Option 1.1, has indeed produced the expected transformation of shape to an almost triangular truss. A side constraint on the length of the top horizontal member, necessary to preserve that member's nonzero length to avoid a matrix singularity, has kept the top of the frame from shrinking to a point.

Example 3: Torsion box vibration. This example demonstrates a "tuning" of the stiffness and mass distributions to achieve a prescribed change in an original structural vibration mode shapes. The structure is a torsion box shown in figure 13(a), built up of membrane panels, with thicknesses as the design variables indicated in the figure. Because concentrated nonstructural masses are affixed to one side of the box as shown in figure 13(a), the vibration modes for a structure that was initialized uniformly to a minimum gage exhibit a distinct torsion-bending coupling in the first four modes. This is illustrated in figure 13(b) by displacement of segment AB seen in view C. To reduce that coupling, the constraints of $(z_2 - z_1)/z_1 \leq 2$ are imposed on the free end vertical displacements z_1 (point A) and z_2 (point B) in modes 1 through 4. The result is a set of new modes shown in figure 13(b) which comply with the constraints. The thickness changes required to meet the constraints are indicated in figure 13(c). There are increases of thicknesses t_3 and t_5 in the SPAR beam directly supporting the concentrated masses, and t_4 in a panel that forms a counterbalance to the fixed masses.

Research Examples

Cumulative constraint. A direct search method such as usable-feasible directions method in the current PROSSS optimizer has a drawback--namely a large computer memory is required to keep track of each individual constraint in application to structures with numerous stress constraints, such as the stiffened cylindrical shell in the previous group of examples. To overcome this drawback, a cumulative constraint (ref. 7) was tried. The constraint is, in essence, the same as the well-known exterior penalty function and is formulated as:

$$\Omega = \sum_j (\langle g_j \rangle)^2 \qquad (4)$$

where

$$\langle g_j \rangle = \begin{cases} g_j, \text{ if } g_j > 0 \\ 0., \text{ if } g_j \leq 0 \end{cases}$$

The cumulative constraint Ω is a single measure of many constraint violations and its zero boundary is interpreted for purposes of usable-feasible directions algorithm as a hypersurface which is continuous through the first derivatives, providing the g_i functions are also continuous.

The stiffened cylindrical shell, variant 3 of example 1 above, optimized for minimum mass subject to individual strength constraints was taken as a reference case. The single cumulative constraint was introduced to replace 190 constraints by modifying the A-O processor. Relative to the reference case, the results indicated a slight (3 percent) reduction of the objective function, an increase of the total number of iterations from 6 to 8, and the optimizer memory requirement reduced by 99.7 percent.

Influence of the move limits. It is expected that the results of a piecewise linear optimization procedure such as Option 2.3 in PROSSS depend to some extent on the move limits allowed in each linear stage, but the extent of that dependence is not known. To shed some light on the dependence, the same stiffened cylindrical shell was optimized using PROSSS Option 2.3 by systematically changing the relative move limits. The result is shown in figure 14 as a plot of the objective function versus the relative move limit value imposed on all design variables and maintained constant from one linear stage to the next. The plot indicates that a wide interval of the move limit values exists where the optimal objective function is practically independent of these values, while the dependence is strong outside of the interval.

A leading variable technique. The same stiffened shell used in the two preceding examples was optimized for minimum mass subject to individual strength constraints using a somewhat unusual technique.

The two basic elements of the technique are: (1) adding the load magnitude P as another variable to the vector of design variables whose initial values were set large for the structural design variables but very small for the load variable, (2) restricting the load variable P by constraints, $g = 1 - P/P_t$ and $0 \leq P \leq P_t$, in order to make P grow to, and remain at, the desired level of fully-developed load P_t. Under this formulation, the load variable becomes a "leading" variable which grows to its target level "pulling" the entire design toward its final state.

The technique is of interest because of its implications for those cases where conventionally formulated optimization fails to find a feasible design. (The design feasibility per se was not an issue in the example case itself.) In such cases, it is usually easy to identify a physical quantity which is not a natural design variable but whose reduction in magnitude renders the initial design feasible. Such physical quantity may then be converted to a leading variable of a suitably low initial value, and therefore remove the difficulty of finding a feasible design.

A good example of this would be an optimization of a strength-sized wing structure for a required flutter speed and a minimum of a flutter structural mass penalty. In this case, the velocity v would be a candidate for a leading variable, analogous to P, and the required flutter speed would be analogous of P_t. A natural starting value for v would be the flutter velocity of the strength-sized structure.

Implementation of the technique required changes only to the O-A and A-O processors and produced a result illustrated in figure 15 by a plot of the objective function versus the consecutive iterations.

The final result is practically the same as in the reference case, and examination of the stress constraints as they were changing over the iterations illustrated in figure 16 for the constraints active at optimum, shows that they were never significantly violated. The only constraint that was ever strongly violated was the computationally trivial one imposed on the load variable (leading variable).

Distributing the system between a mainframe and a minicomputer. To test the system adaptability to different hardware configurations, a version of PROSSS was constructed placing the analyzer and the A-O processor on the CDC mainframe computer and the remainder of the system on the PRIME minicomputer as shown in figure 17. It was found that the modular organization of PROSSS was essential for expeditious development of the distributed version. The distributed version of PROSSS was verified (ref. 21) for correctness of its results as compared to the mainframe-only version and was used to explore systematically the relative efficiency of the five PROSSS options. Results of the efficiency results are plotted in figure 18 and show that Option 2.3, and PLA with analytical gradients as, by far, the most efficient one.

This distributed implementation, documented in detail in reference 21, has advantage of the optimal use of the best features of each type of computer--namely, the mainframe computer capability to perform a massive numerical analysis and the minicomputer flexibility and fast interactive response helping in the preparation of the problem, judgmental control of the execution, and review of the results. The main resulting benefit is improved productivity of the "man-machine system" manifested by a very significant reduction of the calendar time needed to complete optimization tasks. Various factors leading to that reduction are examined in reference 21.

Summary of the Examples

Summarizing the application examples, the following observations are noted. Transforming the system from one optimization option to another was simple to accomplish by changing the sequence in which components of the system were called for execution. Adaption from one variable and constraint combination to another was carried out by changes in the O-A and A-O processor codes. These adaptations as well as changes from one structure to another did not require any changes to the Connecting Network nor to the Analyser and Optimizer.

Similarly, the research examples demonstrated adaptability of a programing system to the algorithm procedural changes that reached deep into the problem formulation and yet required only minor and very localized modifications to the system modules.

It was a routine matter to monitor the status of the optimization process by means of displaying the intermediate data files. Stopping and restarting were facilitated by storing intermediate data.

This monitoring and interaction with the process was particularly easy and efficient in the distributed version owing to the quick response of the minicomputer in the interactive mode.

PROSSS Development Trends

Because of its test bed nature, PROSSS undergoes continual development; some possible future changes are summarized in this section.

Optimization Algorithms

Several improved optimization algorithms became available in recent years. Particularly, promising among these are: The augmented Lagrangian technique and the primal-dual methods (e.g., ref. 22). Programs based on those algorithms are logical candidates to convert the current single optimizer in PROSSS into a library of optimizers.

Optimum Sensitivity

It was shown in reference 23, that information about sensitivity of the optimum solution with respect to problem parameters can be generated at a relatively minor cost. An example of such sensitivity information might be a set of derivatives of the optimum cross-sectional areas and the structural mass with respect to the allowable stress value. It was also demonstrated in reference 23, that accuracy of extrapolation based on such derivatives is quite good for a fairly wide interval of the parameters. The modular organization of PROSSS should make insertion of the sensitivity analysis and the associated extrapolation capability a relatively straightforward task.

Multilevel Optimization

It is now widely recognized that a multilevel optimization scheme which breaks one large problem into a hierarchy of separately solved but coupled subproblems has a potential of making truly large structural optimization applications practical. One such scheme is proposed in reference 24. There is also a possibility to build a multilevel scheme on the basis of the optimum subproblem sensitivitiesto the parameters which themselves are the master problem design variables.

The fairly complex organization of the computational sequences and the associated data flow required by the multilevel schemes should be well supported by the flexible organization of PROSSS.

Distributed Computing

Starting from the two-computer version of PROSSS referred to in the research example section, a more ambitious undertaking may be initiated of a multicomputer network in which advantage would be taken of distributed processing. This concept fits well in a multilevel optimization scheme, because many subproblem optimizations could be performed simultaneously on many computers acting in parallel.

Shape Optimization

In comparison to the wealth of experience with cross-sectional optimization to structures, the experience with the optimization of the overall shape is very limited. The PROSSS capability to work with various types of design variables including those of overall geometry encourages exploration of the shape optimization. A development already initiated in this direction involved optimization of trusses using an analytical gradient technique in which the derivatives of the stiffness matrix with respect to the shape design variables were computed by means of finite difference.

Connecting Network and High-Level Language

The operating system and its command language (JCL) are an ultimate in flexibility and continue to support the PROSSS development. Their drawbacks are vulnerability to the operating system changes and the overhead penalty of the system operations. One means

available now for improvement in this regard is an Engineering Analysis Language (EAL) (ref. 25). The EAL is a system of programs and a data base which is a successor to the SPAR program and is operational on many different types of computers. It is enhanced by a command language that possesses a FORTRAN-like capability of loop, branch and jump. In addition to the standard structural analysis processors (the same ones as in SPAR), the EAL library of programs can be routinely augmented by user supplied codes. Thus, implementation of PROSSS in EAL may be done by adding to EAL the optimizer, the O-A and A-O processors for each application, and by translating the JCL procedures for the PROSSS options to the EAL command language (runstreams).

Still, the EAL is not the English-like language many users would like to have available to command a computer. Such language can, in principle at least, be provided so that an engineer could issue, for example, a command: "OPTIMIZE TRUSS FOR MINIMUM MASS AND STRENGTH CONSTRAINTS." For a command such as this to have the intended effect, a translator program standing between the user and the EAL would have to generate a corresponding sequence of the EAL instructions. However, the exact meaning of all the words used in the command would have to be coded first into the translator program, hence, the loss of flexibility.

A reasonable option appears to be to equip the specialized versions (see the previous discussion of the Skeleton and Specialized versions of PROSSS) with an English-like language for a production oriented user, while allowing a researcher to use the EAL command language directly.

Conclusions

A computer programing system is described which combines an optimization program, a structural analysis program, and user supplied problem dependent interface programs, for use in the structural optimization method development and applications. Standard utility capabilities existing in modern computer operating systems are used to integrate these programs. This approach results in flexibility of the optimization procedure organization and versatility of the formulation of constraints and design variables. Features of the programing system are illustrated by numerical examples, which include design variables of cross-sectional dimensions and overall shape and constraints on static and dynamic behavior. Included in the examples is a version of the system distributed between a mainframe and a minicomputer.

Five options are described for organizing the optimization procedures. The options comprise various combinations of nonlinear mathematical programing and piecewise linear approximations with analytical and finite-difference gradient techniques. Because of the system's inherent modularity, other software components could be substituted for the particular ones used herein to achieve a similar capability.

The system can be used in the following two basic ways:

(1) As a research test bed for development of optimization techniques and analysis oriented towards optimization applications. In this role, the system offers flexibility of execution and sequencing including restart and monitoring capabilities.

(2) As an application tool that can be adapted by a specialist to a very wide scope in types of problems and then used as a "black box" by production oriented engineers.

The system development trends are reviewed in the areas of the optimization algorithms, including multilevel schemes, optimum sensitivity analysis, distributed computing, overall structural shape optimization, and use of an improved connecting network and higher level command languages.

References

(1) Fiacco, A. V.; and McCormick, G. P.: Nonlinear Programing: Sequential Unconstrained Minimization Techniques. John Wiley and Sons, New York, 1968, Section 2.4.

(2) Zoutendijk, G.: Methods of Feasible Directions. Elsevier, Amsterdam, 1960.

(3) Garvin, W. W.: Introduction of Linear Programing. McGraw-Hill, New York, 1960.

(4) Schrem, E.: From Program Systems to Programing Systems for Finite-Element Analysis. Paper presented at U.S.-Germany Symposium: Formulations and Computational Methods in Finite-Element Analysis. MIT, Boston, MA, August 1976.

(5) Sobieszczanski, J.: Building a Computer Aided Design Capability Using a Standard Time Share Operation System. Proceedings of the ASME Winter Annual Meeting, Integrated Design and Analysis of Aerospace Structures, Houston, TX, November 30-December 5, 1975, pp. 93-112.

(6) Dovi, A. R.: ISSYS - An Integrated Synergistic Synthesis System. NASA Contractor Report 159221, Kentron International, Inc., Hampton Technical Center, Hampton, VA., February 1980.

(7) Sobieszczanski-Sobieski, Jaroslaw: From a "Black Box" to a Programing System: Remarks on Implementation and Application of Optimization Methods. Proceedings of a NATO Advanced Study Institute Session on Structural Optimization, University of Liege, Sart-Tilman, Belgium, August 4-15, 1980.

(8) Whetstone, W. D.: SPAR Structural Analysis System Reference Manual, System Level II, Volume I. NASA CR-145098-1, February 1977.

(9) Giles, G. L.; and Haftka, R. T.: SPAR Data Handling Utilities. NASA TM-78701, September 1978.

(10) Fox, Richard L.: Optimization Methods for Engineering Design. Addison-Wesley Publ. Co., Reading, Mass., 1971.

(11) Storaasli, O. O.; and Sobieszczanski, J.: On the Accuracy of the Taylor Approximation for Structure Resizing. AIAA J., Vol. 12, No. 2, February 1974, pp. 231-233.

(12) Vanderplaats, Garret N.: The Computer for Design and Optimization. Computing in Applied Mechanics, R. F. Hartung, ed., AMD - Vol. 18, American Soc. Mech. Eng., c. 1976, pp. 25-48.

(13) Schmit, L. A.; and Miura, H.: Approximation Concepts for Efficient Structural Synthesis. NASA CR-2552, March 1976.

(14) Sobieszczanski, Jaroslaw: Sizing of Complex Structures by the Integration of Several Different Optimal Design Algorithms. AGARD Lecture Series No. 70 on Structural Optimization, AGARD-LS-70, September 1974.

(15) Control Data Corporation; NOS Version 1 Reference Manual, NOS 1.3. CDC No. 60435400, September, 1979.

(16) Starnes, J. H.; and Haftka, R. T.: Preliminary Design of Composite Wings for Buckling, Strength and Displacement Constraints. A Collection of Technical Papers, AIAA/ASME 19th Structures, Structural Dynamics and Materials Conference, Bethesda, Md., April 3-5, 1978. AIAA Paper No. 78-466.

(17) Anderson, M. S.; and Stroud, W. J.: A General Panel Sizing Computer Code and Its Application to Composite Structural Panels. AIAA J., Vol. 17, No. 8, August 1979, pp 892, 897.

(18) Sobieszczanski-Sobieski, J.; and Bhat, R. B.: Adaptable Structural Synthesis Using Advanced Analysis and Optimization Coupled by a Computer Operating System. J. of Aircraft, Vol. 18, No. 2, February 1981, pp. 142-149.

(19) Rogers, J. L., Jr.; Sobieszczanski-Sobieski, J.; and Bhat, R. B.: An Implementation of the Programing Structural Synthesis System (PROSSS). NASA TM 83180, 1981.

(20) Giles, G. L.: Procedure for Automating Aircraft Wing Structural Design. J. of Str. Div. ASCE, Vol. 97, No. ST1, 1971, pp. 99-113.

(21) Rogers, J. L., Jr.; Dovi, A. R.; and Riley, K. M.: Distributing Structural Optimization Software Between a Mainframe and a Minicomputer. Proceedings of Engineering Software Second International Conference and Exhibition, London, England, March 24-26, 1981, pp. 400-415, editor, R. A. Adey, CML Publications.

(22) Fleury, Claude; and Schmit, Lucien A., Jr.: Dual Methods and Approximation Concepts in Structural Synthesis. NASA Contractor Report 3226, December 1980.

(23) Sobieszczanski-Sobieski, J.; Barthelemy, Jean-Francois; and Riley, Kathleen M.: Sensitivity of Optimum Solutions to Problem Parameters. Presented at AIAA/ASME/ASCE/AHS 22nd Structures, Structural Dynamics and Materials Conference, Atlanta, Ga., April 6-8, 1981. AIAA Paper No. 81-0548.

(24) Schmit, L. A.; and Ramanathan, R. K.: Multilevel Approach to Minimum Weight Design Including Buckling Constraints. AIAA Journal, Vol. 16, No. 2, February 1978, pp. 97-104.

(25) Whetstone, W. D.: EISI-EAL: Engineering Analysis Language. Presented at ASCE Conference on Computing and Civil Engineering, Baltimore, Md., June 1980.

Table I Optimization flow options

Procedure	No Gradients Supplied to Optimizer	Gradients Supplied to Optimizer	
		Finite Difference	Analytical
NLP	1.1	1.2	1.3
PLA	Not Applicable	2.2	2.3

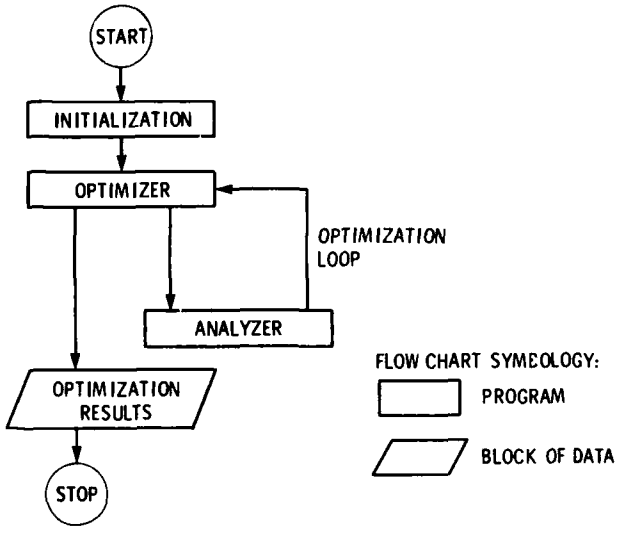


Fig. 1.- Generic components and a basic flow organization of an optimization procedure.

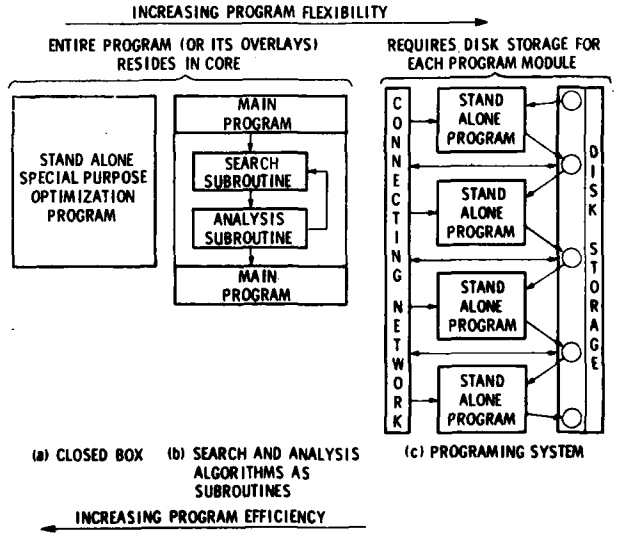


Fig. 2.- Approaches for implementing optimization methods.

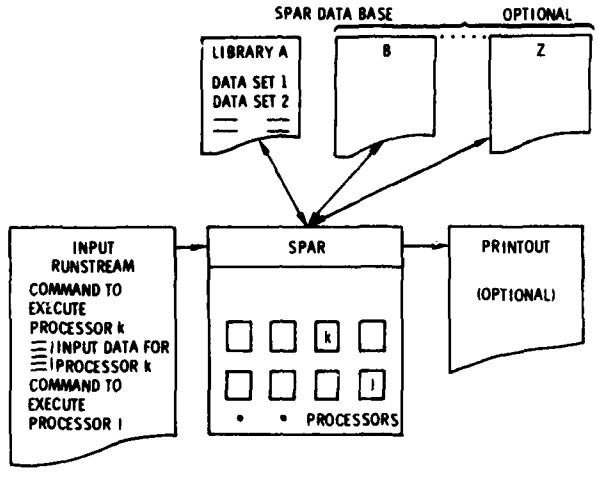


Fig. 3.- Finite-element program SPAR.

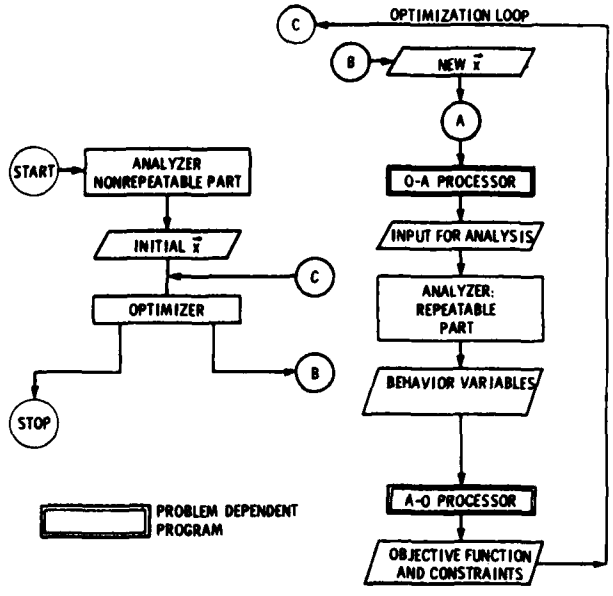


Fig. 5.- Flow chart for Option 1.1; the analyzer split into nonrepeatable and repeatable parts.

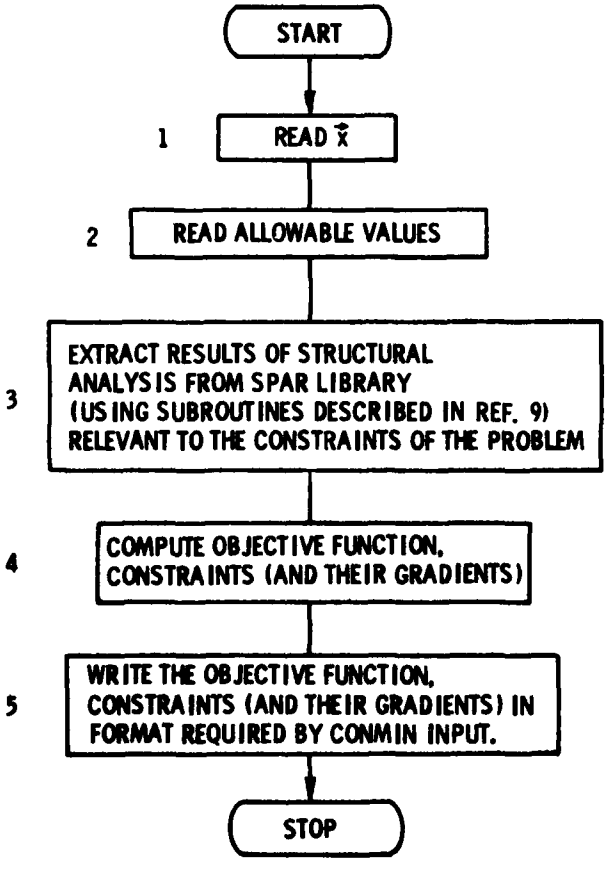


Fig. 4.- A-O Processor flow chart.

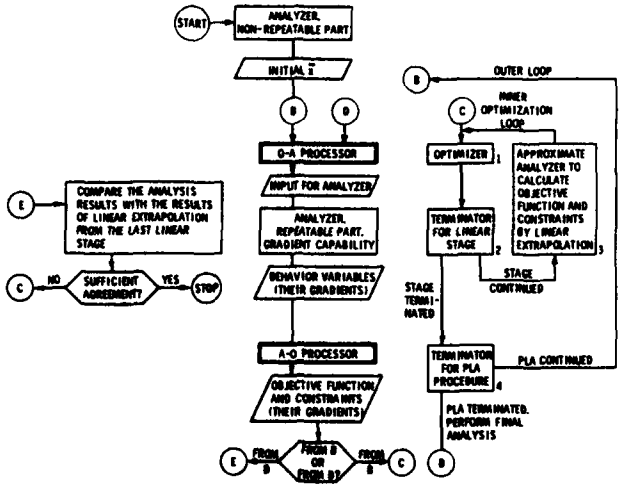


Fig. 6.- Flow chart for Option 2.3.

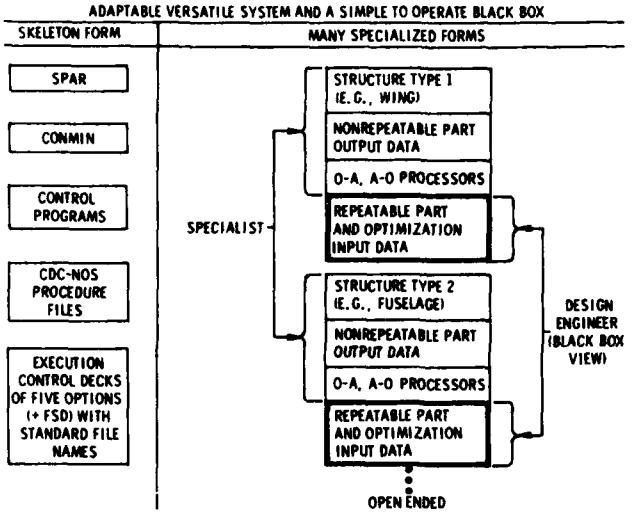


Fig. 7.- Skeleton and specialized forms of PROSSS.

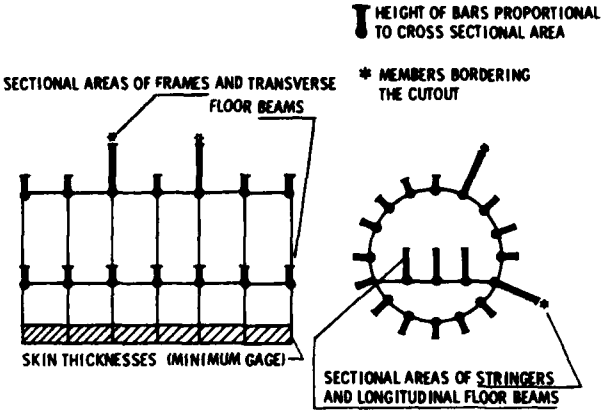


Fig. 10.- Relative member sizes obtained by optimization for Example 1, variant 1.

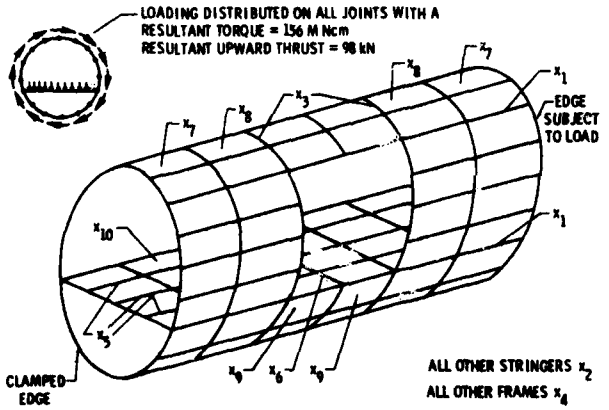


Fig. 8.- Example 1, stiffened cylindrical shell, variant 1.

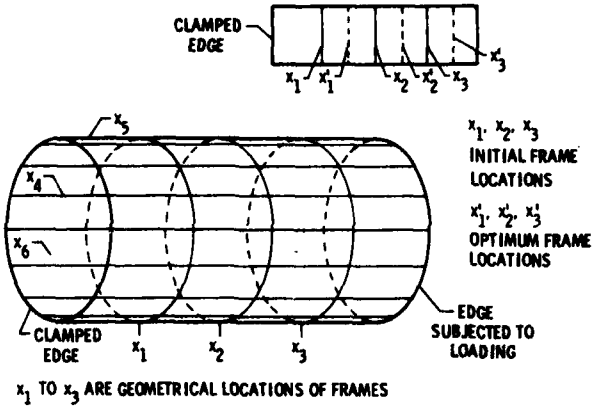


Fig. 11.- Initial and optimized positions of transverse frames in Example 1, variant 3.

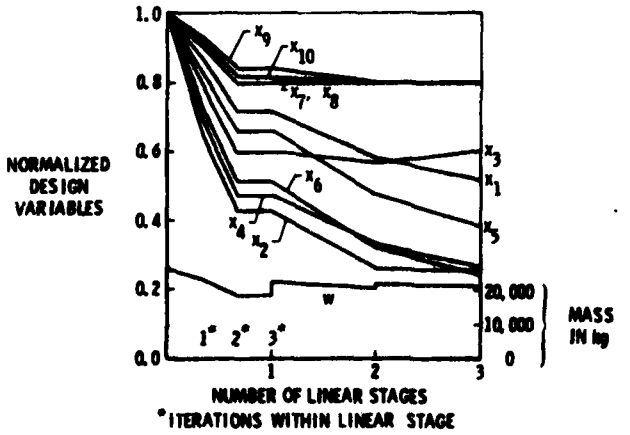


Fig. 9.- History of iterations for Example 1. Variant 1 using Option 2.2.

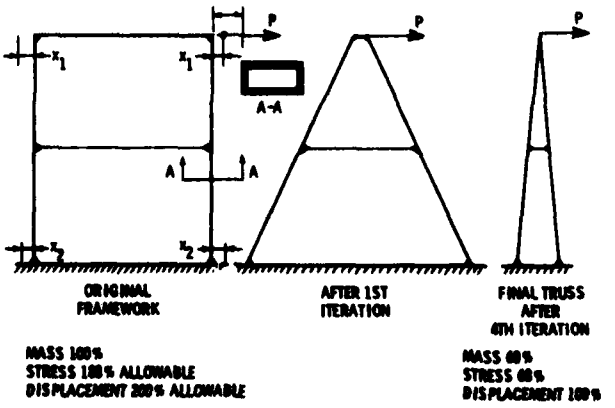
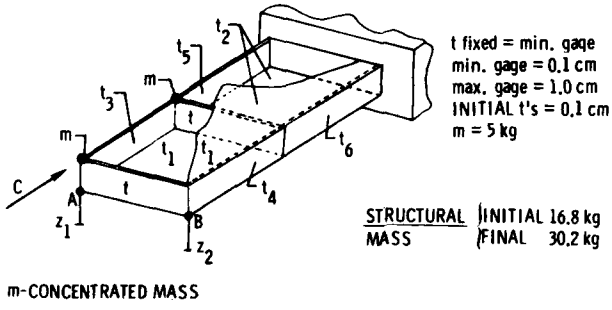
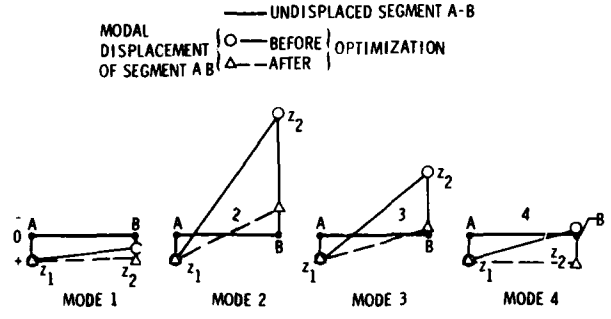


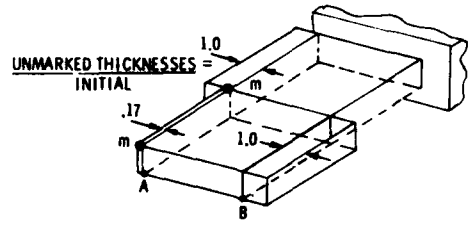
Fig. 12.- Transformation of a framework (Example 2) to a truss by optimization with geometrical variables.



(a) Thicknesses used as design variables.



(b) Modal displacements of segment AB (Fig. 13(a)), seen in view C.



(c) Dimensional arrows mark the spar beam web thicknesses increased in the optimization process; other thicknesses remained at the initial values.

Fig. 13.- Optimization of a torsion box (Example 3) to reduce torsion bending coupling in modes 1, 2, 3, and 4.

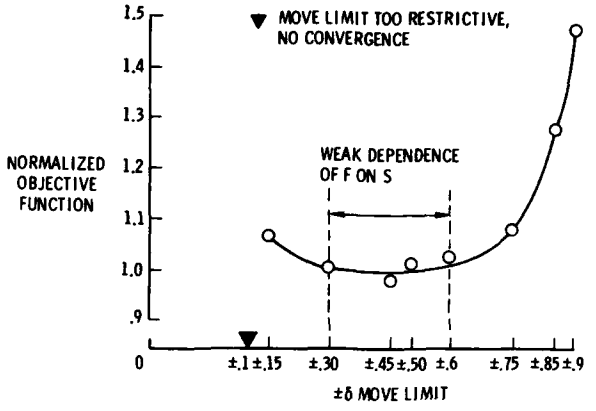


Fig. 14.- Normalized objective function (mass) vs. relative move limit.

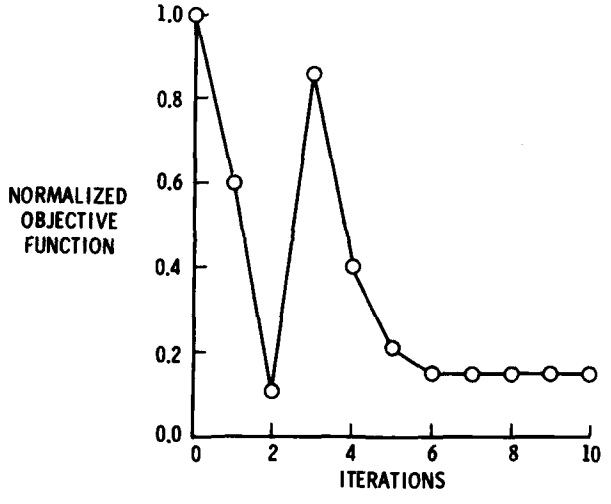


Fig. 15.- Objective function vs. the iteration number for a leading variable technique.

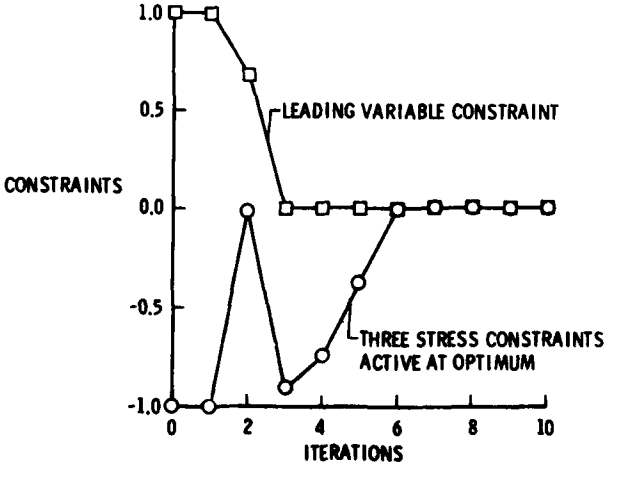


Fig. 16.- Constraints vs. the iteration number for a leading variable technique.

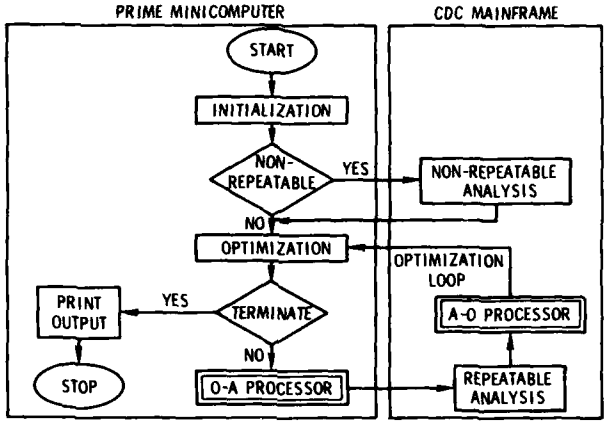


Fig. 17.- Flow chart of a distributed structural optimization software system.

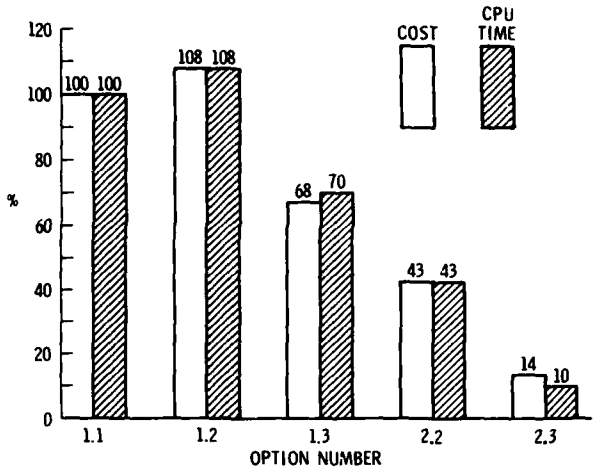


Fig. 18.- Option cost and time comparison.

AD-P000 086

LARGE SCALE STRUCTURAL OPTIMIZATION BY FINITE ELEMENTS

Claude Fleury
Senior Research Associate, NFSR
Aerospace Laboratory
University of Liège
Belgium

Abstract

The optimization code contained in the SAMCEF ("Système pour l'Analyse des Milieux Continus par Eléments Finis") is built to loop on the static and dynamic analysis modules. As a result all the possibilities offered by these modules are still applicable, as well as those of the auxiliary modules, like mesh generators, plotting capabilities, etc. It also implies that, given a finite element model, the user may ask for one or more optimization steps, without anything else to do than to define the design constraints. The design variables are taken as the transverse sizes of the finite elements, i.e., the cross-sectional areas of bars and beams or the thicknesses of membranes, shear panels and flat shells. The objective function to be minimized is defined as a linear function of the design variables and it corresponds, most often, to the structural weight. The constraints impose limitations on the design variables (side constraints and linking) and on quantities describing the structural response (behavior constraints), i.e., stresses and displacements under multiple static loading cases, natural frequencies and critical buckling loads. The optimization strategy converts the initial nonlinear programming problem into a sequence of explicit problems of algebraically simple separable form. Various primal and dual optimization schemes are available to solve the explicit subproblems. The approach presented can be viewed as a generalized optimality criteria technique as well as a linearization method in mathematical programming. Several examples of application to various structures will be offered to demonstrate the efficiency and generality of the SAMCEF optimization module.

Introduction

Because good designers consider structural optimization as a technique that should take into account all possible aspects of the design, they are often reluctant to the concept of structural synthesis methods developed in connection with finite element programs. However, when examining the design process, it is often possible to isolate a phase during which the shape of the structure is more or less frozen and the problem is limited to giving adequate dimensions to the various members. Such a situation is frequently encountered in the aerospace, naval or automobile industries, where the external shapes are, to a large extent, dictated by aero- or hydrodynamic considerations or by styling, while internal forms are often determined by various non-structural requirements. If the ultimate goal of the designer can be identified as corresponding to the minimization of an explicit function of the member sizes, and if the limitations on the design can be defined as, eventually implicit functions of the member sizes too, such as displacements, stresses, eigenfrequencies, etc., then the problem is tractable by automatic algorithms. They allow the designer to speed up significantly this part of the design process and to explore more systematically the various feasible designs.

The pure sizing optimization problems are especially crucial when complex structural forms are involved and when composite materials such as reinforced resins are employed. In these cases it becomes difficult, if not impossible, for the designer to have an intuitive understanding of the structural mechanics that is sufficient to lead to optimal sizing of the various members. Furthermore the designer is most of the time unable to take into account global constraints in the structure, like global flexibility, restrictions on displacements, frequencies of vibration, buckling modes, etc. It is only possible to verify a posteriori that such constraints are satisfied. Again these global constraints become more important in the context of highly complex, indeterminate structures. In the aerospace industry, the necessity of designing high performance structures has motivated significant research efforts to derive algorithms permitting a rapid and systematic exploration of the design space to determine the optimum material utilization.

It is worth pointing out that optimization methods should be considered as especially useful in the preliminary design phase. Using them when the design is practically frozen, with the hope of an ultimate improvement, is often disappointing. This is due to the fact that the optimization of a detailed design implies the formulation of a large number of constraints, some of which are not easily quantified. At the preliminary design stage, however, the constraints are usually more global and therefore more easily handled by the available formulations. It is also important that optimization methods be developed as auxiliary modules of the existing finite element program used by the designer. This avoids to duplicate the costly operation of establishing the finite element model and insures that all the facilities available in the general purpose program remain available, including computer graphics, data base systems and other computer aided design capabilities.

Problem Statement

The optimization module that has been developed for the SAMCEF (1) general purpose program is based on the following concepts. The design variables are taken as the transverse sizes of the structural members, namely, the cross-sectional areas of bar and beam elements and the thicknesses of shear panel, membrane, plate and flat shell elements. The objective function to be minimized is defined as a linear function of the member sizes a_i:

$$W = \sum_{i=1}^{n} \rho_i \ell_i a_i \qquad (1)$$

where ℓ_i is a geometrical factor such that the product $\ell_i a_i$ is the volume of the element (e.g. rib length or panel area) and ρ_i is a scalar quantity associated with the element. In most cases ρ_i is

PRECEDING PAGE

simply the material density, in which case W is the weight of the structure. The n design variables a_i represent the member sizes of either individual finite elements or, if design variable linking is used, of groups of finite elements corresponding each to the idealization of a given structural member. In this latter case the number of design variables, n, is smaller than the number of finite elements.

In addition to design variable linking, which can be viewed as assigning simple equality constraints, the design variables are subjected to the side constraints

$$\underline{a}_i \leq a_i \leq \bar{a}_i \qquad i = 1, n \tag{2}$$

where $\underline{a}_i$ and $\bar{a}_i$ are lower and upper limits that reflect fabrication and analysis validity considerations. The main constraints in the weight minimization problem are the behavior constraints, which impose limitations on quantities describing the structural response. The strength of the structure must primarily be considered in the design requirements, which results in stress limitations. For a specified set of external loads, the elastic limit of the materials may not be exceeded. In bar and shear panel elements the tensile stress limit is determined by the elastic properties of the material, while the compressive limit is generally reduced to take into consideration, in a simple manner, a safeguard against local buckling. In more general elements, like membranes, beams and plates, the stress limitation must be placed on some equivalent stress (e.g. Von Mises criterion). Becuase the stress constraints are usually considered with different loading conditions, they will be written in the form

$$\sigma_{k\ell} \leq \bar{\sigma}_k \qquad \begin{matrix} i = 1, n \\ \ell = 1, c \end{matrix} \tag{3}$$

where ℓ is the load index and $\bar{\sigma}_k$ is the allowable stress limits in the kth element. The displacement constraints considered in SAMCEF are defined as upper bounds on some linear combinations of the displacement degrees of freedom q used in the finite element model:

$$u_j = b_j^T q \qquad j = 1, f \tag{4}$$

where b_j is a vector of constants. The displacement constraints read thus as follows:

$$u_{j\ell} \leq \bar{u}_j \qquad \begin{matrix} j = 1, f \\ \ell = 1, c \end{matrix} \tag{5}$$

where $u_{j\ell}$ denotes the value of u_j under the ℓth loading condition and $\bar{u}_j$ is its upper limit. Note that this treatment includes the usual nodal displacement constraints, the relative displacement constraints, the slope constraints, etc.

The optimization strategy used in SAMCEF has been primarily developed for dealing with stress and displacement constraints, and extended later to the case of frequency and buckling constraints. Therefore, this paper will be initially focused on static response quantities, which are evaluated in SAMCEF by a displacement finite element method. The static structural analysis is thus performed by solving the systems of linear equations

$$Kq_\ell = g_\ell \tag{6}$$

where K is the structural stiffness matrix and g_ℓ represents the external forces acting in the ℓth loading condition. Once the displacement vectors q_ℓ are known, the stresses in the various members are evaluated from the equations

$$\sigma_{ke} = t_k^T q_\ell \tag{7}$$

where t_k denotes the appropriate row of the stress matrix for the kth element. Note that for a membrane element the stress matrix is made up of three rows, while is reduces to one row for a bar element.

Optimization Strategy

Initially the class of finite element models considered in this paper will be restricted to thin-walled structures (assembling of bars and membranes), for which the stress matrices are independent of the design variables and the stiffness matrix exhibits a linear form in the design variables:

$$K = \sum_{i=1}^{n} K_i = \sum_{i=1}^{n} a_i \bar{K}_i \tag{8}$$

where $\bar{K}_i$ is the stiffness matrix of the ith element when $a_i = 1$. In this case it is possible to generate first order explicit approximations of the stress and displacement constraints by introducing a certain number of additional loading cases in the structural analysis phase. The stress constraints can also be dealt with by stress-rationing, which corresponds to adotping zero order explicit approximations (fully stressed design concept). The optimization strategy is then to transform the primary problem into a sequence of explicit approximate problems which are easily tractable by mathematical programming algorithms.

Using first-order explicit approximations of the behavior constraints is equivalent to linearizing them with respect to the reciprocals of the design variables. This observation leads to the key idea for generalizing the optimization strategy to other types of constraints and to more sophisticated finite elements. It will be shown that constraints on natural frequencies and on critical buckling loads can be well approximated by expanding them in first order Taylor series in terms of the reciprocal variables. Also this rather general process will be extended to pure bending elements and flexion-extension elements.

First Order Explicit Approximation

The virtual load technique is used in SAMCEF to generate explicit approximations of the static response quantities. Considering a virtual load vector given numerically by b_j (Eq. 4), it follows that any displacement constraint (Eq.5) can be expressed as the sum of the contributions of each element:

$$u_{j\ell} = b_j^T q_\ell = q_\ell^T K q_\ell = \sum_{i=1}^{n} \frac{c_{ij}^{\ell}}{a_i} \leq \bar{u}_j \tag{9}$$

with

$$c_{ij\ell} = (q_j^T \bar{K}_i q_\ell)\, a_i^2 \qquad (10)$$

In these expressions q_j and q_ℓ are respectively the virtual and real displacement vectors and $\bar{K}_i$ is the element stiffness matrix appearing in Eq. 8. In a finite element model, the stresses are also linear combinations of the displacement degrees of freedom, just as the displacement constraints defined in Eq. 4. Therefore the above procedure can still be employed. By introducing a virtual load vector given numerically by the appropriate row t_k of the stress matrix (Eq. 7), each stress constraint (Eq. 3) can be explicitly approximated by

$$\sigma_{k\ell} = t_k^T q_\ell = q_k^T K q_\ell = \sum_{i=1}^{n} \frac{d_{ik\ell}}{a_i} \leq \bar{\sigma}_k \qquad (11)$$

with

$$d_{ik\ell} = (q_k^T \bar{K}_i q_\ell)\, a_i^2 \qquad (12)$$

Note that this technique is valid only for stress components. In a membrane element the constraint is usually placed on an equivalent stress whose square is a quadratic form of the displacements. An explicit expression of the form Eq. 11 can still be obtained by using special virtual load cases. For more complicated stress constraints, the general procedure given in the Reciprocal Design Variables section can be applied.

So the explicit expressions of the stress and displacement constraints exhibit the same form (Eqs. 9 and 11). We shall write them under the common notation:

$$\sum_{i=1}^{n} \frac{c_{ij}}{a_i} \leq \bar{u}_j \qquad j = 1, m \qquad (13)$$

where $\bar{u}_j$ donates an upper bound to a static response quantity u_j (stress, nodal displacement, relative displacement, etc.). The coefficients c_{ij} are constant in a statically determinate structure, so that Eq. 12 represents then the exact explicit form of the constraint. For a statically indeterminate structure, the c_{ij}'s depend implicitly on the design variables, because structural redundancy produces redistribution of the internal forces when the member sizes are modified. However it is essential to notice that the coefficients c_{ij} are not affected by a scaling of the design, that is by a multiplication of all the design variables by the same factor. In the design space such a scaling moves the design point along a line joining the origin to the current analysis point. Therefore the explicit expression (Eq. 13) yields the exact value of the constraint all along the scaling line. This means that the approximate restraint surface passes through the point of intersection of the corresponding exact restraint surface with the scaling line (Fig. 1). In addition, it can be proved that the explicit constraint (Eq. 13) furnishes also the exact derivatives of the response quantity u_j:

$$\frac{\partial u_j}{\partial a_i} = -\frac{c_{ij}}{a_i^2} = -q^T \frac{\partial K_i}{\partial a_i} q_j \qquad (14)$$

for any design point on the scaling line (2). It can therefore be concluded that the explicit forms (Eq. 13) represent first order approximations of the constraints on the scaling line. Geometrically, it means that each real restraint surface is replaced with a tangent surface at its point of intersection with the scaling line (Fig. 1).

Zero Order Explicit Approximations

The first order explicit approximation (Eq. 13) requires the application of an additional (virtual) loading case for each constraint. In many problems, the number of stress constraints is relatively important so that the number of additional loading cases leads to a significant increase in the analysis cost. This explains why lower order approximations are considered. For dealing with stress constraints, the most popular approach is based on the Fully Stressed Design (FSD) concept, which leads to transforming the constraints (Eq. 3) into simple side constraints

$$a_k \geq \tilde{a}_k \qquad k = 1, n \qquad (15)$$

The minimum values $\tilde{a}_k$ are given by the well known stress ratio formula

$$\tilde{a}_k = a_k^\circ \max_{\ell=1,\, c} \left\{ \frac{\sigma_{k\ell}^\circ}{\bar{\sigma}_k} \right\} \qquad (16)$$

where a_k° denotes the current design variables and $\sigma_{k\ell}^\circ$, the corresponding stresses. The FSD procedure can be interpreted as using zero order approximation of the constraints on the scaling line, because it relies on explicit expressions that preserve only the value of the stresses along that line, and not their derivatives. Geometrically, the real restraint surfaces are replaced by planes normal to the axes of the design space. Each plane passes by the point of intersection of the corresponding real restraint surface with the scaling line (Fig. 1).

The FSD criterion is clearly rigorous in the case of a statically determinate structure, for which the internal forces are constant. In the statically indeterminate case, however, the FSD criterion becomes approximate. It does not always converge to the true optimum and sometimes leads to instability or divergence of the optimization process. That is why SAMCEF offers the choice, for each stress constraint, between the rigorous first order approximation (Eq. 11) or the computationally inexpensive zero order approximation (Eq. 15). The selection of constraints requiring first order approximation can be made in advance on the basis of the physical judgement of the designer. It might also be performed automatically according to adequate selection criteria (2).

Reciprocal Design Variables

The virtual load procedure, yielding the explicit constraints (Eq. 13), is mainly used in optimality criteria approaches, which can be viewed as transforming the initial implicit problem into a sequence of explicit approximate problems. Each subproblem

results from replacing the behavior constraints $u_j \leq \bar{u}_j$ by their approximate forms (Eq. 13). On the other hand, the mathematical programming approach to structural optimization, after a period of inefficiency, has finally evolved into a powerful and now well established design procedure which is also based upon explicit approximation of the behavior constraints (3,4,5). The key idea is to linearize the response quantities with respect to the reciprocal design variables

$$x_i = \frac{1}{a_i} \tag{17}$$

which leads to the following explicit constraints:

$$u_j^\circ + \sum_{i=1}^{n} \left(\frac{\partial u_j}{\partial x_i} \right)^\circ (x_i - x_i^\circ) \leq \bar{u}_j \tag{18}$$

where the upperscript $^\circ$ denotes quantities evaluated at the current design point x°. The first partial derivatives of the response quantities are most often computed by using the pseudo-loads technique, which requires a number of additional loading cases equal to the number of design variables times the number of applied loading cases [see e.g. (5)]. In view of Eq. 14 , the virtual load procedure constitutes another (often less expensive) way of calculating the constraint derivatives. Indeed the coefficients c_{ij}, which are related to virtual strain energies in optimality criteria approaches, are also the gradients of the response quantities with respect to the reciprocal variables:

$$c_{ij} = \frac{\partial u_j}{\partial x_i} \tag{19}$$

Furthermore the definition (Eq. 10) of the c_{ij}'s clearly indicates that

$$u_j^\circ = \sum_{i=1}^{n} c_{ij}^\circ x_i^\circ \tag{20}$$

Therefore Eq. 18 can be rewritten

$$\sum_{i=1}^{n} c_{ij}^\circ c_i \leq \bar{u}_j \tag{21}$$

which is equivalent to Eq. 13 when recast in terms of the direct variables a_i.

From the foregoing developments, it is apparent that the explicit approximations of the behavior constraints used in both the optimality criteria and mathematical programming approaches (Eqs. 13 and 18, respectively) are identical. A unified approach to structural weight minimization of finite element systems has thus emerged, which consists in replacing the initial problem with a sequence of explicit approximate -- or linearized -- problems of the following form:

$$\text{minimize} \quad W = \sum_{i=1}^{n} \frac{\ell_i}{x_i} \tag{22}$$

subject to

$$\sum_{i=1}^{n} c_{ij} x_i \leq \bar{u}_j \tag{23}$$

$$\underline{x}_i \leq x_i \leq \bar{x}_i \tag{24}$$

where $\bar{x}_i = 1/\underline{a}_i$ and $\underline{x}_i = 1/\bar{a}_i$ are the new side constraints. The explicit constraints (Eq. 23) are represented in the space of the reciprocal variables by tangent planes to the real restraint surfaces (see Fig. 2).

This interpretation provides a clear understanding of the origin of the excellent performances of the optimality criteria approaches, as well as their divergence in certain cases. Their convergence properties depend upon the nonlinearity of the restraint surfaces in the space of the reciprocal variables, that is, on the structural redundancy. For a moderately statically indeterminate structure, these surfaces are close to planes and the convergence is fast and stable, independently of the number of design variables. However, in case of strong structural redundancy, the restraint surfaces are highly nonlinear and convergence instability can occur. Indeed the solution of the linearized problem lies far from the real restraint surfaces, so that after reanalysis and scaling of the design to obtain a feasible point, the weight might suddenly rise. As shown in Fig. 2, it may be desirable, in such a case, to limit the move of the design point along the linearized restraint surfaces, for example by adding move limits (i.e. artificially tightened side constraints). This is also the idea of the mixed method proposed in Ref. (6), where the linearized problem is solved only partially using a primal solution scheme. By modifying a convergence control parameter, the mixed method permits a gradual transition between a primal mathematical programming approach and an optimality criteria approach.

It is important to mention that this basic approach of transforming the initial problem into a sequence of explicit problems is now widely recognized and it is routinely employed for large scale industrial applications (7,8). Various solution schemes are available in SAMCEF to treat the explicit problem (Eq. 22-24). Depending upon their primal or dual character, the convergence properties of the whole optimization process are different (see Optimization Algorithms section).

Frequency Constraints

Constraints on natural frequencies usually consist in imposing lower limits

$$\omega_j^2 \geq \underline{\omega}_j^2 \qquad j = 1, m \tag{25}$$

They are directly written in terms of the squares of the frequencies, because these quantities naturally appear in the eigenproblem characterizing the structural modal analysis

$$K q_j - \omega_j^2 M q_j = 0 \tag{26}$$

In this equation, K and M represent the stiffness and mass matrices, and (q_j, j = 1, m) are the modal displacements, i.e., the eigenvectors solution of

Eq. 26 , associated with eigenvalues ω_j^2. The structural mass matrix has a linear form in terms of the design variables:

$$M = \sum_{i=1}^{n} M_i + M_c = \sum_{i=1}^{n} a_i \bar{M}_i + M_c \qquad (27)$$

where $\bar{M}_i$ and M_c are independent of the design variables. $\bar{M}_i$ denotes the mass matrix of the ith element when $a_i = 1$. M_c represents the contribution of the non-structural masses. It is well know that the first derivations of the frequencies with respect to the design variables are given by

$$\frac{\partial \omega_j^2}{\partial a_i} = \frac{1}{m_j} q_j^T \left(\frac{\partial K_i}{\partial a_i} - \omega_j^2 \frac{\partial M_i}{\partial a_i} \right) q_j = \frac{1}{a_i m_j} q_j^T \ldots$$

$$\ldots (K_i - \omega_j^2 M_i) q_j \qquad (28)$$

where m_j is the generalized mass of the jth mode:

$$m_j = q_j^T M q_j \qquad (29)$$

As explained in the Reciprocal Design Variables section, the optimization strategy employed in SAMCEF consists in linearizing the behavior constraints with respect to the reciprocal design variables, which gives

$$\omega_j^{o2} + \sum_{i=1}^{n} c_{ij}^{o} (x_i - x_i^{o}) \geq \underline{\omega}_j^2 \qquad (30)$$

In this expression, the c_{ij}'s denote the gradients of the eigenvalues with respect to the x_i's. From Eq. 17 and Eq. 28 , it comes

$$c_{ij} = \frac{\partial \omega_j^2}{\partial x_i} = - \frac{q_j^T K_i q_j - \omega_j^2 q_j^T M_i q_j}{m_j x_i} \qquad (31)$$

It can be observed that, in a general way:

$$\sum_{i=1}^{n} c_{ij} x_i = - \omega_j^2 + \frac{\omega_j^2}{m_j} (m_j - \bar{m}_j) = - \omega_j^2 \frac{\bar{m}_j}{m_j} \qquad (32)$$

where

$$\bar{m}_j = q_j^T M_c q_j = m_j \sum_{i=1}^{n} q_j^T M_i q_j \qquad (33)$$

represents the contribution of the fixed masses to the generalized mass. Therefore the explicit constraints (Eq. 30) reduce to the form:

$$\sum_{i=1}^{n} c_{ij}^{o} x_i \geq \underline{\omega}_j^2 - \omega_j^{o2} \left(1 + \frac{\bar{m}_j^{o}}{m_j} \right) \qquad (34)$$

In opposition with the case of stress and displacement constraints, the coefficient c_{ij} can now be affected by a scaling of the design. This means that the tangent plane (Eq. 34) does not necessarily pass through the point of intersection of the corresponding exact restraint surface with the scaling line. The effect of scaling depends upon the importance of the non structural masses. If there is no fixed mass, scaling does not modify the eigenvalues nor the associated eigenmodes. On the other hand, if the structural mass can be neglected, the eigenvalues increase in proportion to the scaling factor. In the intermediate case where structural and non structural masses contribute to the mass matrix with the same order of magnitude, the scaling process requires a new complete finite element analysis for determining the modified frequencies and eigen modes. It should be noted that numerical results tend to demonstrate that important non structural masses have a beneficial effect on the convergence stability in the overall optimization process. This is probably because the problem then behaves just as in the static case.

Buckling Constraints

Just as the natural frequencies, the critical load factors λ_j are defined through an eigenproblem

$$K q_j - \lambda_j S q_j = 0 \qquad (35)$$

where S represents the goemetric stiffness matrix and $(q_j, j=1, \ldots m)$ denote the eigenvectors solution of (Eq. 35), associated with eigenvalues λ_j. The physical meaning of q_j is that of displacements in the jth buckling mode, for a critical load factor λ_j. The buckling constraints consist in imposing lower limits on the buckling loads, however, they will be written in the form

$$\frac{1}{\lambda_j} \geq \frac{1}{\underline{\lambda}_j} \qquad j = 1, \ldots m \qquad (36)$$

because it has been found that better explicit approximations are generated when expanding the reciprocals of the buckling loads rather than the λ_j's themselves. The stiffness matrix K has the form in Eq. 8. The geometric stiffness matrix is related to the initial stress state in the elements and therefore it depends implicitly on all the design variables:

$$S = \sum_{i=1}^{n} S_i (a) \qquad (37)$$

It is worth recalling that the matrices S_i are independent of the design variables for a statically determinate structure. The first derivatives of the buckling loads are given by [see e.g. (9)]:

$$\frac{\partial \lambda_j}{\partial a_i} = \frac{1}{q_j^T S q_j} q_j^T \left(\frac{\partial K_i}{\partial a_i} - \lambda_j \frac{\partial S}{\partial a_i} \right) q_j \qquad (38)$$

In opposition with the static and dynamic cases previously discussed, the derivatives appearing in Eq. 38 are not directly available, because the elements of the geometrical stiffness matrix are functions of the stresses acting in the prebuckling state. However, by assuming that the terms $\frac{\partial S}{\partial a_i}$ are negligible, the gradients (Eq. 38) become easily computable. This assumption, which is typical of optimality criteria approaches for static constraints, amounts to not taking into account the effects of structural redundancy:

$$\frac{\partial S}{\partial a_i} = 0 \qquad i=1, \ldots n \tag{39}$$

Using the same basic approach as before, we linearize the behavior constraints (Eq. 36) with respect to the reciprocal design variables:

$$\frac{1}{\lambda_j^{\circ}} + \sum_{i=1}^{n} c_{ij}^{\circ} (x_i - x_i^{\circ}) \leq \frac{1}{\underline{\lambda}_j} \tag{40}$$

where, from Eqs. 8, 17, 38, and 39:

$$c_{ij} = \frac{\partial \left(\frac{1}{\lambda_j} \right)}{\partial x_i} = \frac{q_j^T K_i q_j}{s_j \lambda_j^2 x_i} \tag{41}$$

with

$$s_j = q_j^T S q_j \tag{42}$$

It is easily verified that

$$\sum_{i=1}^{n} c_{ij} x_i \equiv \frac{1}{\lambda_j} \tag{43}$$

so that the explicit constraints (Eq. 40) reduce to the simple form

$$\sum_{i=1}^{n} c_{ij}^{\circ} x_i \leq \frac{1}{\underline{\lambda}_j} \tag{44}$$

The reason for writing the buckling constraints in the reciprocal form (Eq. 36) is now apparent: the coefficients c_{ij} remain constant along the scaling line, just as in the case of stress and displacement constraints. Geometrically it means that each real restraint surface is replaced by its tangent plane at its point of intersection with the scaling line.

Bending Elements

The optimization strategy reviewed in the previous sections can be easily extended to the case of pure beam and plate elements subjected to flexural loads only. The way to deal with a beam element in uniaxial bending depends upon the relationship between the principal moment of inertia I and the cross-sectional area a. A wide variety of situations is taken into consideration by adopting the relation

$$I = ca^p \tag{45}$$

where c is a constant that depends only on the shape of the beam cross-section and p, a positive number. Most of the time p is taken as an integer number, equal to 1, 2, or 3. For example the case p=2 is that of beams whose cross-sectional shape is kept invariant during redesign (dilatation or contraction). The flexural regidity is proportional to the moment of inertia and therefore the structural stiffness matrix exhibits the following explicit form in terms of the cross sectional areas:

$$K = \sum_{i=1}^{n} K_i = \sum_{i=1}^{n} a_i^p \bar{K}_i \qquad p > 0 \tag{46}$$

where each matrix $\bar{K}_i$ is independent of the design variables a_i. Turning to solid plate elements subject to pure bending, since the stiffness is proportional to the cube of the thickness, it is apparent that Eq. 46 must be adopted with p=3. The optimization strategy can be derived just as in the case of thin-walled structures, by making a change of variables that tends to reduce the nonlinear character of the constraints,

$$x_i = \frac{1}{a_i^p} \tag{47}$$

and linearizing them with respect to the new variables x_i (Eqs. 18, 30, and 40). In the case of displacement constraints, it is easily shown that the first order Taylor series expansions (Eq. 18) reduce to the following form, when written in terms of the direct design variables a_i (9):

$$\sum_{i=1}^{n} \frac{c_{ij}}{a_i^p} \leq \bar{u}_j \tag{48}$$

The c_{ij} coefficients are the gradients of the response quantities u_j with respect to the intermediate variables x_i defined in Eq. 47, but they can also be interpreted as virtual strain energy densities in the structural members. In this connection, it should be noted that the virtual load procedure (First Order Explicit Approximations section) could directly be used to derive the explicit approximations (Eq. 48), instead of resorting to a linearization scheme.

When flexion and extension forces act simultaneously with comparable intensity at the element level, the definition (Eq. 46) of the stiffness matrix can no longer characterize the structural model with sufficient accuracy. For a rather general class of structural models, each element stiffness matrix can be assumed to have the following explicit form

$$K_i = \sum_{p=1}^{3} a_i^p K_i^{(p)} \tag{49}$$

where the matrices $K_i^{(p)}$ are independent of the design variables. For example, a flat shell element, made up of a membrane and a plate stacked together, is characterized by

$$K_i = a_i K_i^{(1)} + a_i^3 K_i^{(3)} \tag{50}$$

where the first term represents the stiffness in extension, and the second one, the stiffness in flexion. In Refs.(10) and (11), rather sophisticated first order explicit approximations were developed to take into account separately the effects of extension and flexion. It is however not at all certain that these complicated explicit constraints offer a definite advantage over simple first order Taylor series expansions with respect to the reciprocal design variables. More numerical investigation needs to be done before a final conclusion can be brought. In the meantime, the first order explicit approximations adopted in SAMCEF are obtained from a simple linearization process in terms of $1/a_i$. They exhibit the forms of Eq. 18 for stress/displacement constraints, Eq. 30 for frequency constraints, and Eq. 40 for buckling constraints. The gradients required in these expressions are respectively given by Eqs. 14, 28, and 38, in which, from Eq. 50 we must introduce

$$\frac{\partial K_i}{\partial a_i} = \sum_{p=1}^{3} p\, a_i^{p-1} K_i(p) \qquad (51)$$

Note that the derivatives of the mass and geometric stiffness matrices have the same form as for bar and membrane elements.

Optimization Algorithms

The explicit problem to be solved in each redesign stage exhibits the form of Eqs. 22-24. It is strictly convex and separable. Because of these properties, this problem can be solved efficiently by employing primal or dual algorithms. It should be emphasized that the primal algorithms can be used to solve only partially the approximate problem Eq. 22-24, while the dual algorithms cannot, because intermediate points in the dual space usually correspond to highly infeasible points in the primal space. Consequently the capability of controlling the convergence of the overall optimization process is available only if a primal optimizer is selected. On the other hand, it should be clearly recognized that using a dual algorithm yields results and convergence properties equivalent to those obtained using optimality criteria. The same is true for the primal algorithms if the approximate problems are solved completely.

Five distinct optimization algorithms are available in the SAMCEF program. The user can select any one of them depending upon the characteristics of each specific problem: the number of independent design variables, the number of behavior constraints, and the expected degree of non-linearity of the constraints.

PRIMAL 1 Optimizer

PRIMAL 1 is a first order projection algorithm based on the well known gradient projection method for linear constraints. It uses an orthogonal projection operator to generate a sequence of search directions that are constrained to reside in the subspace defined by the set of active constraint hyperplanes. The successive search directions are conjugated to each other as long as there is no change in the set of active constraints. The PRIMAL 1 optimizer operates in the space of the reciprocal design variables and it produces a sequence of steadily improving feasible designs with respect to the linearized problem. Hence PRIMAL 1 can be adequately used for seeking a partial solution to each explicit problem in such a way that the constraints of the primary problem remain almost satisfied. This is achieved by prescribing an upper limit on the number of one-dimensional minimizations performed before updating the approximate problem statement. PRIMAL 1 is thus the recommended option when the constraints of the primary problem are highly nonlinear in the reciprocal variables (strong structural redundancy). The algorithm is described in detail in the I-Beam section of Ref. (12).

PRIMAL 2 Optimizer

PRIMAL 2 is a second order projection algorithm especially well suited to the solution of problems with separable objective function and linear constraints. It uses a weighed projection operator to generate a sequence of Newton's search directions in the subspace formed by the intersections of the active constraint hyperplanes. Because the objective function (Eq. 22) is separable, its Hessian matrix is diagonal, which makes the second order algorithm no more complicated than the first order one. Consequently PRIMAL 2 exhibits the same features as PRIMAL 1, but it is far more efficient and it can be used to solve exactly each linearized problem (in which case it produces the same iteration history as the dual methods). PRIMAL 2 is thus a recommended option when the behavior constraints are very shallow in the space of the reciprocal variables (weak structural redundancy). Note however that the DUAL 2 option is usually more efficient. The PRIMAL 2 algorithm is described in the Composite Box Beam section of Ref. (12).

DUAL 2 Optimizer

For a convex problem, the Lagrangian multipliers associated with the constraints have the meaning of dual variables in terms of which an auxiliary and equivalent problem can be stated. This dual problem can be reduced to the maximization of the Lagrangian function subject to non-negativity constraints on the dual variables. Since, in addition, the explicit problem (Eq. 22-24) is of separable form, the dual formulation leads to a very efficient solution scheme. Each primal variable can be expressed in closed forms in terms of the dual variables by relations similar to those used in optimality criteria techniques (13). The dimensionality of the dual problem is equal to the number of linearized behavior constraints (Eq. 23), which is most often small when compared to the number of design variables. Therefore the dual problem exhibits a simpler form and a lower dimensionality than the primal problem.

DUAL 2 is a specially devised dual method which employs a second order Newton type of algorithm to find the maximum of the dual function when all the design variables are continuous. It operates in a sequence of dual subspaces with gradually increasing dimensions, so that the effective dimensionality of the dual problem does not exceed the number of active behavior constraints by more than one. Because this number is relatively low for many structural optimization problems of practical interest, the DUAL 2 optimizer is very efficient. It is thus the recommended option for pure continuous variable problems, unless the behavior constraints are expected to be highly nonlinear in the reciprocal variables. The algorithm is described in the DUAL 2 Optimizer section of Ref. (12), as well as in the Optimization Strategy section of Ref. (5).

DUAL 1 Optimizer

When some or all of the design variables, instead of varying continuously, can only take on available discrete values, the dual method formulation becomes particularly attractive (14). The discrete primal variables can still be explicitly expressed in terms of the continuous dual variables. The dual function remains continuous but it has discontinuous first derivatives. DUAL 1 is a dual method which employs a specially devised first order gradient projection type of algorithm to find the maximum of the dual function in the mixed discrete continuous case. The DUAL 1 algorithm incorporates special features for handling the dual function gradient discontinuities that arise from the primal discrete variables. These discontinuities occur on specific hyperplanes in the dual space. DUAL 1 determines usuable search directions by projecting the dual function gradient on the intersection of the successively encountered first order discontinuity planes. It should be noted that the DUAL 1 optimizer remains applicable to pure continous variable problems, in which case it reduces to a special form of the conjugate gradient method. However it is generally less efficient than the DUAL 2 optimizer. DUAL 1 was initially conceived for the ACCESS 3 program and it is described in detail in the Optimization Algorithms section of Ref. (5).

Envelope Method

When only one behavior constraint is active, the explicit problem can be solved analytically. Using the Lagrangian multiplier technique leads to a simple redesign formula. In the now classical envelope method (15), this approach is extended as follows: the redesign formula is first employed by treating each constraint separately, and then the largest value obtained for each design variable is selected to form an approximate solution. This intuitive procedure has the advantage of being very simple and not subject to ill-conditioning troubles (linearly dependent constraints, almost singular matrices, etc.) which can possibly arise in other methods. It should however be kept in mind that the envelope method is strictly valid only when a single behavior constraint is assigned. Otherwise it can produce results that differ substantially from the optimal solution.

Core Requirements

Because of their special implementation, which takes advantage from the simple form of the side constraints, the two projection algorithms PRIMAL 1 and PRIMAL 2 require a modest core size [see Ref. (9)]. The number of words necessary to solve a given explicit subproblem, with n independent design variables and m linearized behavior constraints, is approximately equal to

$$n\,(m + 10) + \frac{m\,(m + 1)}{2} + 3\,m \qquad (52)$$

This formula also applies to the DUAL 2 optimizer, however it should be modified for the DUAL 1 optimizer when discrete design variables are involved. Fig. 3 represents graphically the core requirement given by Eq. 52. It should be clearly recognized that, because design variable linking is most often employed in practical applications, the SAMCEF program is capable of dealing with structural optimization problems involving thousands of finite elements. For example, a problem with 500 design variables -- which might well correspond to 5000 elements -- and 20 linearized behavior constraints can fit in a core of less than 16,000 words (on IBM 370-158 the computer program requires then 256 K). Note that no core limitation is associated with the analysis modules of SAMCEF, because they are organized in such a way that they can solve very large problems using a modest size central core. They employ a frontal equation solver with substructuring and extensive peripheric storage.

It can be seen by examining Fig. 3 that the main limitation arises from the number m of behavior constraints retained in the linearized problem statement. If the number of constraints is raised up to 100 in the previous example (with 500 design variables), then the central core requirement increases to 60,000 words. In addition, it is obvious that linearizing the static behavior constraints demands a large computational effort, because this implies treating additional loading cases in the structural reanalyses (see Reciprocal Design Variables section). Finally the computer time expended in the optimizer itself can become prohibitively high when the number of linearized constraints is large. This is apparent in the case of dual algorithms, since the dimensionality of the dual problem is just equal to the number of linearized constraints. It is also true in the case of primal algorithms, because most of the computational effort quickly increases with the number of linear constraints (construction of the projection matrices, evaluation of the maximum allowable step length, selection of the set of active constraints, etc.).

Therefore it is important to reduce as much as possible the number of behavior constraints retained at each stage of the optimization process. This goal is achieved in SAMCEF in a rather crude way, by specifying a priori a reduced set of behavior constraints, on the basis of the designer insight and prior experience. A probably better technique would be to use automatic constraint deletion techniques, such as those proposed in Ref. (3). In this approach only the critical and potentially critical behavior constraints are included in the linearized problem statement at each redesign stage. Note that the static structural analysis must be decomposed in two parts: first the constraint values are computed for the real loading conditions, and then the gradients of the retained constraints are evaluated by adding virtual or pseudo-load cases. Finally, it should be emphasized that using zero order approximation for the stress constraints also permits a drastic reduction in the number of linearized constraints (see the Zero Order Explicit Approximations section).

Computer Program Implementation

In this section some indications are given about the way the previously developed concepts have been implemented in a computer program. The resulting optimization facilities are fully integrated in the general purpose finite element system SAMCEF (1), which is capable of solving large scale structural analysis problems (several thousands of degrees of freedom and finite elements). SAMCEF offers a fairly comprehensive finite element library and it is applicable to a wide variety of problems (linear, nonlinear, static, dynamic and thermal analyses, computer graphics, etc.). As indicated on the flow chart of Fig. 4, the optimization module of SAMCEF is built to loop on the general static, dynamic and stability analysis modules. This implies that all the possibilities offered by these modules are still available, as well as those of the auxiliary modules, like mesh generators, plotting modules for input and

output, etc. Given a finite element model, the user may ask for one or more optimization steps, without anything else to do than to define the constraints. In the current version of the SAMCEF program, three distinct optimization modules are provided to treat separately static constraints on stresses and displacements, dynamic constraints on natural frequencies and stability constraints on linear buckling loads. It is envisioned that the next version will include the possibility of taking simultaneously into account any combination of these three types of behavior constraints by using a data base system.

The program can evidently make use of the restart capabilities of the analysis modules, and it is also devised for an interactive use where the designer examines the solution after each optimization stage. After each structural analysis the program can be stopped, and then automatically restarted without repeating the analysis. It is indeed often desirable to allow for a human intervention in the redesign process. For example, very large structural models, because they are time consuming, cannot be treated in a single run and it is better executing the optimization program stage by stage with intermediate verification of the results. The control parameters can then be reset periodically to adequate values (change of the optimization algorithm, modification of move limits, selection of the linearized constraint, etc.). By storing in a data base the analysis results produced at each stage, it is moreover possible to restart the program at any previously generated design point. In this connection, it is expected that the concept of automatic redesign will be replaced in the future by that of interactive redesign on a graphic terminal, allowing therefore the design to easily monitor the optimization process. This will lead to a perspective where structural optimization methods are integrated into a Computer Aided Design system.

At the present time the elements whose dimensions are taken into account in the operational version of the program are limited to bar, membrane, pure beam (uniaxial bending), and flat shell elements. The next version will include more sophisticated beam elements. Nevertheless the structure may be idealized using any other type of element, but their dimensions remain unchanged by the optimization process. The stiffness and mass properties of such elements are not affected by redesign, however their contributions to the approximate constraints statement is taken into consideration in the form of fixed terms to be substracted from imposed limits. In particular the possibility of using super-elements exists and it is very useful for representing pre-optimized or fixed points in the structure. In absence of specification the thickness or cross-section of each finite element is taken as a design variable and is allowed to be independently resized. However the finite elements can be grouped in such a way that one design variable is assigned to each group. This design variable linking consists of equality constraints on the member sizes and it can thus be easily handled in the problem formulation, leading to a reduction in the number of independent design variables. The possibility exists in membrane elements to represent composite materials like fiber reinforced resins as the superposition of a number of layers with independent orthotropic properties. The thickness of each layer is then a separate design variable so that the superposition of results allows for the definition of the composite. Current research is diverted towards algorithms for selecting not only the number of flies in each layer, but also the type of material and the fiber orientation (16).

Numerical Examples

In this section a sample of numerical applications extracted from Ref (9) and (12) is presented to illustrate the power and the generality of the approach used in the SAMCEF program.

I-Beam

The first example is concerned with an I-beam structure subjected to frequency constraints (Fig. 5). The problem consists in minimizing the weight of the beam while imposing lower bounds on the frequencies of the three first eigenmodes: flange flexion, torsion and web flexion. Initially the problem was treated by using a pure membrane finite element model and including fictitious diaphragms in order to represent properly the torsional mode (9). Only five analyses are sufficient to generate an "optimum design" for this membrane model. However, when this final design was analyzed by using a more accurate model made up of flat shell elements, the torsional frequency limit (mode 2) was seen to be violated by 10%. Therfore the problem was run again with this new model, by resorting to sophisticated explicit approximations of the behavior constraints and employing a special purpose dual optimizer (10). In this paper, the problem was solved by using simple first order Taylor series (Eq. 30) and the standard dual algorithm (DUAL 2 optimizer), yielding surprisingly good results. The finite element model is made up of 25 flat shell elements characterized by a displacement field cubic in extension and quintic in flexion [hybrid quadrangular flat shell (1)]. The idealization involves 360 degrees of freedom. Results obtained for the two finite element models considered (membrane and flat shell) are given in Fig. 5 (iteration history data) and Table 1 (final designs). It can be seen that the use of flat shell elements, although yielding slower convergence than membrane elements, gives rise to satisfactory results. Also there is no penalty in employing linear explicit approximations rather than more complicated ones (10).

Composite Box Beam

The box beam illustrated in Fig. 6 has been proposed in Ref. (17) as an example of composite material design. The upper and lower skins are assumed to be made up of 0°, $\pm$ 45°, and 90° boron-epoxy laminates represented by stacking four constant strain orthotropic membrane elements in each rectangular region shown in Fig. 6. The transverse webs (shear panels) and the reinforcing bars are in aluminum. In the design of composite structures, a frequent requirement is to limit the deflections or to tailor the flexibilities according to given laws. Therefore no stress limitations have been introduced in this problem, which is governed entirely by a flexibility constraint. The loading is asymmetric and induces primarily bending deformations, but also a limited amount of torsion. The limitations in deflections are 14 in. at nodes 1 and 2, where the loads are 1000 lbs., and 15 in. at nodes 3 and 4, where the loads are 975 lbs. These limitations require evidently a non-symmetric design. Because only the tip deflections are limited, the shear webs keep the same thickness along the span. Therefore, using the double symmetry of the problem, the number of design variables can be reduced to 30. Results are presented in Tables 2 and 3, together with those obtained in Ref. (17). The convergence of the optimization process is monotonic and significantly faster than reported in Ref. (17). After the second analysis, the displacement at node 3 (15 in.) is already larger than the displacement at node 1 (13.8 in.), while in Ref. (17), 20 reanalyses are necessary to reverse the torsion in the box beam. The slight differences in the final designs (Table 3)

are due to the differences in the finite element models.

Euler Beam

Attention is now directed to the Euler sandwich column shown in Fig. 7. The beam has length ℓ and is hinged at both ends. The problem consists in minimizing its weight for a given critical buckling load P. For a sandwich beam with rectangular cross-sections the specific weight and stiffness (per unit length) are linearly related so that the problem can be treated as in the case of thin-walled structures. The analytical solution, obtained in Ref. (18) stipulates that at the optimum, the specific stiffness s (x) (and so the sheet thickness) and the lateral displacement u(x) that characterizes the critical buckling mode have a parabolic form:

$$s(x) = \frac{P}{2} x (\ell - x)$$

$$u(x) = \frac{4}{\ell^2} x (\ell - x) \qquad (53)$$

Using a finite element model involving 10 equal length segments, the discretized solution is generated by SAMCEF in six iterations. Table 4 reproduces the iteration history data. Note that by symmetry only five beam elements are necessary to describe the problem. The final design weighs 265.7 kg while the analytical solution (Eq. 53) leads to 260 kg. The continuous and discretized solutions are compared in Fig. 7 and Table 4. It can be seen that the numerical results are very close to the analytical ones, although the finite element model involves only 10 degrees of freedom.

As mentioned in the Bending Elements section, the optimum design of beam structures depends upon the relation between the moment of inertia and the cross-sectional area of the beam members. In order to illustrate the various possibilities permitted by Eq. 45, the Euler column problem is again considered, by assuming now a rectangular cross-section with height h and width b. It is apparent that the case where b is variable and h is constant reduces to the previously examined problem, because the bending stiffness for each member is linear with respect to the cross-sectional area. If b is kept constant and h is variable, then the expression (Eq. 46) of the stiffness matrix holds with p=3. Finally if the cross-section shape is kept invariant (i.e. fixed h/b ratio), p=2 must be adopted. In each of the three cases considered the finite element model involves five beam members (symmetry). In the initial design the width and the height of the rectangular cross-section are taken as 10 and 1, respectively, which leads to a weight equal to 10 (arbitrary unit system; see Fig. 8). After scaling of the design variables, the weight of the strictly critical, feasible design takes on different values in the three cases considered, because the scaling factor multiplies the moment of inertia of each beam element, rather than its cross-sectional area. Table 5 contains the iteration history data and the final designs for each three situations p=1, p=2, and p=3. Only 4 to 6 structural analyses are required to achieve convergence. The least weight design is obtained when the width of the cross-section is varied (p=1). The heaviest design is obtained by choosing the height of the cross-section as the variable quantity (p=3). The variations of the moment of inertia and of the cross-sectional area are displayed in Fig. 8 for the three cases considered.

Aircraft Spoiler

The spoiler represented in Fig. 9 is classically designed in light aluminum alloy sheet. The front spar and the secondary spar are joined by twelve ribs and covered by two skins reinforced by stringers. The spoiler is hinged at three points and actuated at one, in the midspan. The loads consist in pressure distribution on both faces, corresponding to two flight configurations. In one of them a flexibility constraint is imposed, which stipulates that the trailing edge has to remain straight within a tolerance ε = 0.5 mm, in order to eliminate contact with the flap. In the initial design, this requirement was achieved by precambering the spoiler (Fig. 9). This costly procedure has to be avoided in the final optimized design. So differential flexibility constraints are introduced, which assign an upper limit ε = 0.5 mm to the absolute value of the difference between any two deflections along the trailing edge (Fig. 11). In addition, maximum allowable stresses and minimum thicknesses are imposed, which differ from place to place depending on the material used and manufacturing considerations.

Several finite element models of the structure were investigated, made up of 27, 64, 125, and 627 elements (12). The final model is illustrated in Fig. 10. It involves 627 second degree displacement elements and 2300 degrees of freedom. Based upon experience accumulated from the study of the simpler models, it was concluded that the mixed method (Reciprocal Design Variables section) had to be used for solving the spoiler problem. So the PRIMAL 1 optimizer (PRIMAL 1 Optimizer section) was employed and it was necessary to limit the number of optimization steps to avoid divergence of the process. This means that any method based on optimality criteria (including dual algorithms) would probably not succeed in solving this problem. Results are presented in Fig. 11. As expected from the experience gained with the simplified problems, a good convergence was obtained with the mixed method by setting the number of minimization steps to $\bar{k}$ = 500, that is slightly below the number of design variables. Note that the initial increase in weight is due to the fact that the original design of the spoiler did not satisfy the differential flexibility constraints when precambering was suppressed. Hence after scaling up the member sizes to obtain a feasible design, the weight jumps from 10 to 40 kg. After 13 structural reanalyses, the original weight of 10 kg is recovered, but it corresponds of course to a very different design. After each iteration, the deflection is increased, however, the trailing edge keeps about the same shape and remains straight within the specified tolerance.

References

(1) SAMCEF, Système d'Analyse des Milieux Continus par Eléments Finis, LTAS, University of Liége, Belgium.

(2) Fleury, C., "An Efficient Optimality Criteria Approach to the Minimum Weight Design of Elastic Structures," Journal of Computers and Structures, Vol. 11, 1980, pp. 163-173.

(3) Schmit, L. A. and Miura, H., "Approximation Concepts for Efficient Structural Synthesis," NASA CR-2552, 1976.

(4) Fleury, C., "A Unified Approach to Structural Weight Minimization," Comp. Meth. Appl. Mech. Eng., Vol. 20, No. 1, 1979, pp. 17-38.

(5) Fleury, C. and Schmit, L. A., "Dual Methods and Approximation Concepts in Structural Synthesis," NASA CR-3226, 1980.

(6) Sander, G. and Fleury, C., "A Mixed Method in Structural Optimization," International Journal Num. Meth. Engrg., Vol. 13, No. 2, 1978, pp. 385-404.

(7) Petiau, C. and Lecina, G., "Eléments Finis et Optimization des Structures," AGARD CP-280, 1980, Paper 23.

(8) Morris, A. J., Bartholomew, P., and Dennis, J., "A Computer Based System for Structural Design, Analysis, and Optimization," AGARD CP-280, 1980, Paper 20.

(9) Fleury, C. and Sander, G., "Generalized Optimality Criteria for Frequency Constraints, Buckling Constraints, and Bending Elements," AFOSR TR-80-0107, 1979.

(10) Fleury, C., "On the Derivation of First Order Explicit Approximations to the Behavior Constraints in Structural Optimization," submitted for publication to the AIAA Journal, 1981.

(11) Fleury, C., Ramanathan, R. K., Salama, M., and Schmit, L. A., "ACCESS Computer Program for the Synthesis of Large Structural Problems," 1st Symp. Optim. Struct. Des., Tucson, AZ, Oct. 19-22, 1981.

(12) Fleury, C. and Sander, G., "Structural Optimization by Finite Elements," LTAS Report SA-58, University of Liege, Belgium, Grant AFOSR-77-3118, 1978.

(13) Fleury, C., "Structural Weight Optimization by Dual Methods of Convex Programming," International Journal Num. Meth. Engrg., Vol. 14, No. 12, 1979, pp. 1761-1783.

(14) Schmit, L. A. and Fleury, C., "Discrete-Continuous Variable Structural Synthesis Using Dual Methods," AIAA Journal, Vol. 18, No. 12, 1980, pp. 1515-1524.

(15) Gellatly, R. A. and Berke, L., "Optimal Structural Design," AFFDL TR-70-165, 1971

(16) Fleury, C., Braibant, V., and Sander, G., "A Dual Method Approach to Structural Synthesis Problems with Optimal Selection of Materials," 1st Symp. Optim. Struct. Des., Tucson, AZ, Oct. 19-22, 1981.

(17) Khot, N. S., Venkayya, V. B., and Berke, L., "Optimum Design of Composite Structures with Stress and Displacement Constraints," AIAA Paper 75-141, AIAA 13th Aerospace Sciences Meeting, Pasadena, California, 1975.

(18) Prager, W. and Taylor, J. E., "Problems of Optimal Structural Design," Journal Appl. Mech., ASME, Vol. 35, 1968, pp. 102-106.

Table 1 Final Designs for I-Beam Structure

thickness (mm) { membrane model / flat shell model

upper flange

15.80	17.30	11.67	6.143	1.815
15.97	14.96	10.00	5.049	1.349

web

5.101	3.602	3.329	3.294	1.997	free
2.711	4.168	3.938	3.910	2.294	end

lower flange

15.40	17.01	11.55	6.074	1.792
20.38	17.97	12.31	6.551	1.939

Table 2 Composite Box Beam. Iteration History Data

Analysis No.	SAMCEF (dual method)			Ref. (17)		
	weight (lbs)	deflections(in) nodes 1,2	deflections(in) nodes 3,4	weight (lbs)	deflections(in) nodes 1,2	deflections(in) nodes 3,4
1	42.74	14.00	13.03	59.57	14.00	13.38
2	18.31	13.85	15.00	22.05	14.00	13.38
3	16.62	13.93	15.00			
4	15.90	13.97	15.00			
5	15.34	13.97	15.00	14.70	14.00	13.54
6	14.88	13.98	15.00			
7	14.51	13.99	15.00			
8	14.24	13.99	15.00			
9	14.05	13.99	15.00			
10	13.94	14.00	15.00	14.76	14.00	13.83
20				14.66	14.00	14.30
30				14.62	14.00	14.63
40				14.60	14.00	14.82
50				14.59	14.00	14.91
60				14.58	14.00	14.96
70				14.58	14.00	14.98
80				14.58	14.00	14.99
90				14.58	14.00	14.99
100				14.58	14.00	14.99

Table 3 Composite Box Beam. Final Designs

member Nr.	SAMCEF (dual methods)				Reference (17)			
	thickness (in)				thickness (in)			
	total	0°	90°	±45°	total	0°	90°	±45°
1,2	0.01994	0.0050	0.0050	0.0100	0.01950	0.0049	0.0049	0.0098
3,4	0.02933	0.0144	0.0050	0.0100	0.03177	0.0166	0.0050	0.0100
5,6	0.04268	0.0277	0.0050	0.0100	0.04508	0.0298	0.0051	0.0102
7,8	0.05604	0.0411	0.0050	0.0100	0.05836	0.0430	0.0051	0.0102
9,10	0.06932	0.0544	0.0050	0.0100	0.07165	0.0563	0.0051	0.0103
11,12	0.08215	0.0672	0.0050	0.0100	0.08493	0.0695	0.0051	0.0103
13,14	0.09445	0.0795	0.0050	0.0100	0.09820	0.0828	0.0051	0.0103
15,16	0.1067	0.0918	0.0050	0.0112	0.1116	0.0961	0.0051	0.0103
17,18	0.1191	0.1041	0.0050	0.0125	0.1243	0.1088	0.0051	0.0103
19,21,... ...,35	0.02080				0.02056			
20,22,... ...,36	0.00684				0.00694			
37-54	0.00498				0.00500			
weight (lbs)	13.94				14.58			
number of analyses	10				100			

Table 4 Iteration History for Sandwich Beam

iteration	weight (kg)	critical load	face sheets thickness (cm)					model displacement			
			a_1	a_2	a_3	a_4	a_5	u_2	u_3	u_4	u_5
1	390.0	1.2337	1.0000	1.0000	1.0000	1.0000	1.0000	0.3090	0.5878	0.8090	0.9511
2	261.9	0.9826	0.1874	0.4792	0.7378	0.9268	1.0264	0.3722	0.6520	0.8469	0.9620
3	265.6	0.9993	0.2212	0.5257	0.7586	0.9118	0.9877	0.3591	0.6390	0.8393	0.9598
4	265.7	0.9999	0.2151	0.5181	0.7571	0.9179	0.9987	0.3615	0.6414	0.8408	0.9602
5	265.7	1.0000	0.2162	0.5196	0.7575	0.9169	0.9967	0.3610	0.6410	0.8405	0.9601
6	265.7	1.0000	0.2160	0.5193	0.7574	0.9171	0.9971	0.3611	0.6410	0.8406	0.9601
analytical solution	260.0	1.0000	0.1900	0.5100	0.7500	0.9100	0.9900	0.3600	0.6400	0.8400	0.9600

Table 5 Euler Column with Rectangular Cross-Section

a. Iteration History

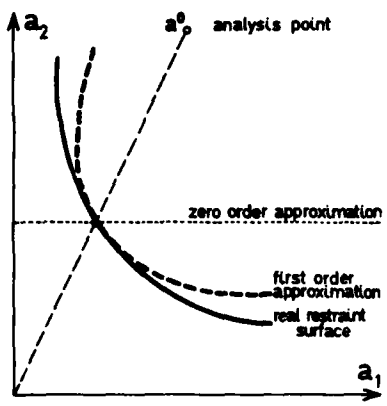
iteration	h constant		h/b constant		b constant	
	weight	scaling factor	weight	scaling factor	weight	scaling factor
1	9.7267	0.9727	9.8624	0.9727	9.9080	0.9727
2	8.2008	1.0177	8.7805	1.0439	9.0838	1.0662
3	8.1775	1.0007	8.7376	1.0046	9.0343	1.0104
4	8.1766	1.0000	8.7335	1.0004	9.0274	1.0012
5			8.7332	1.0000	9.0266	1.0002
6			8.7331	1.0000	9.0264	1.0000

b. Final Designs

element	I + a (h constant)				I + a^2 (h/b constant)				I + a^3 (b constant)			
	I	a	b	h	I	a	b	h	I	a	b	h
1	0.2160	2.592	2.592	1.0	0.1550	4.313	0.6567	6.567	0.1343	5.442	10.0	0.5442
2	0.5194	6.233	6.233	1.0	0.4785	7.578	0.8705	8.705	0.4651	8.233	10.0	0.8233
3	0.7574	9.089	9.089	1.0	0.7673	9.596	0.9796	9.796	0.7770	9.769	10.0	0.9769
4	9.9171	11.005	11.005	1.0	0.9727	10.804	1.0394	10.394	1.0044	10.642	10.0	1.0642
5	0.9970	11.964	11.964	1.0	1.0784	11.376	1.0666	10.666	1.1229	11.045	10.0	1.1045

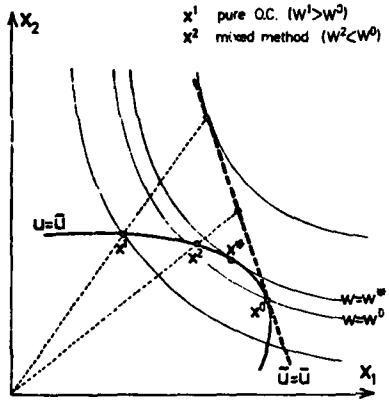
I : moment of inertia b : width

a : cross-sectional area h : height



EXPLICIT APPROXIMATIONS IN O.C. APPROACHES

FIG. 1



CONVERGENCE OF O.C. AND MIXED METHOD

FIG. 2

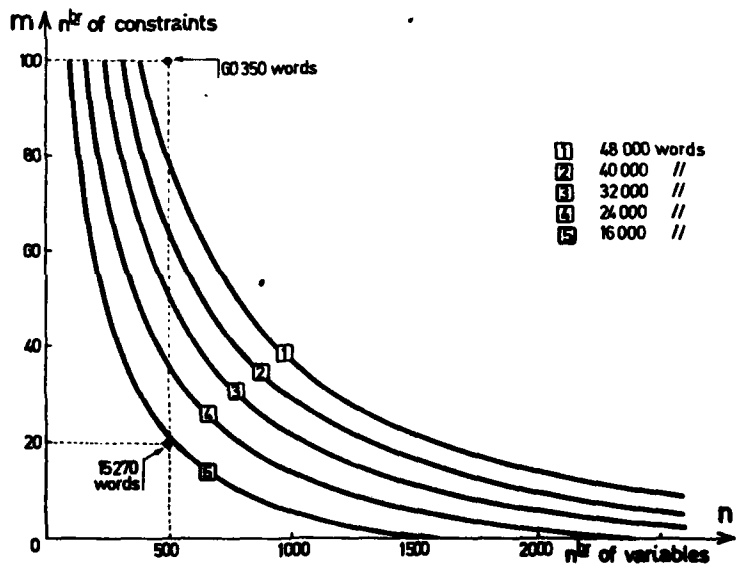


FIG. 3 CORE REQUIREMENT FOR OPTIMIZATION ALGORITHMS

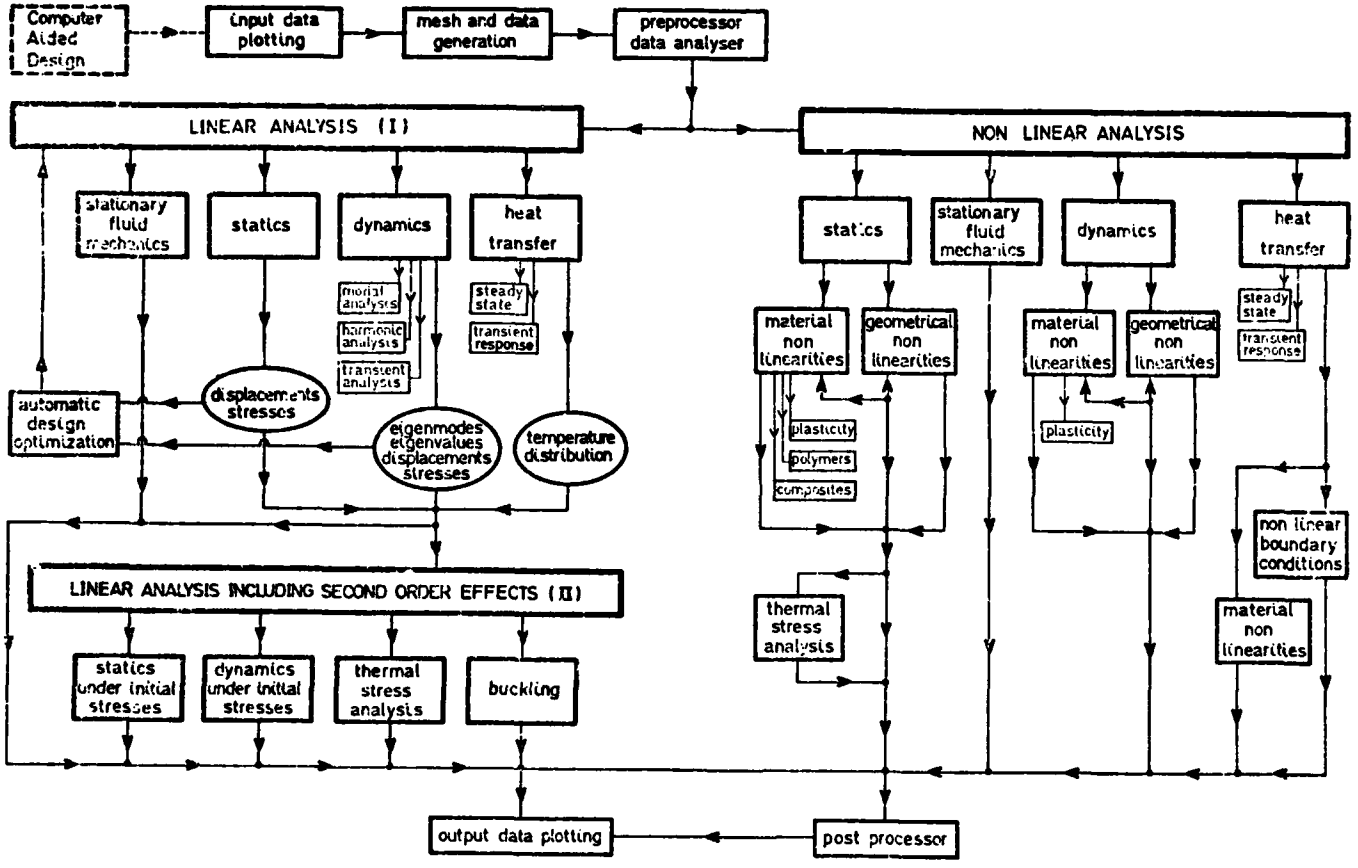


FIG. 4 THE SAMCEF SYSTEM

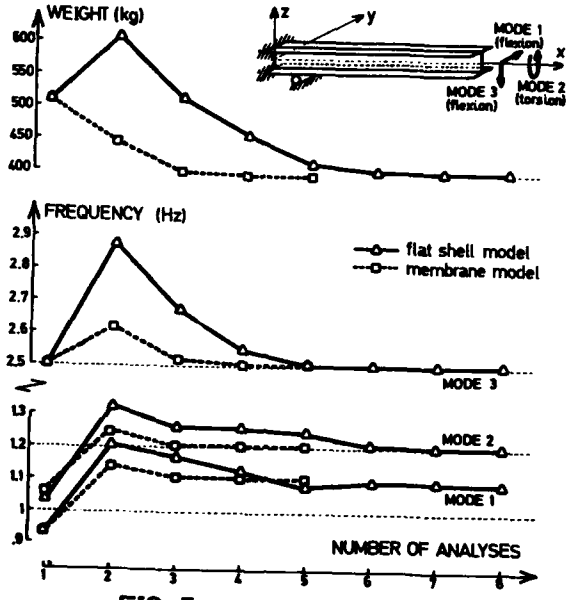


FIG. 5 I-BEAM STRUCTURE

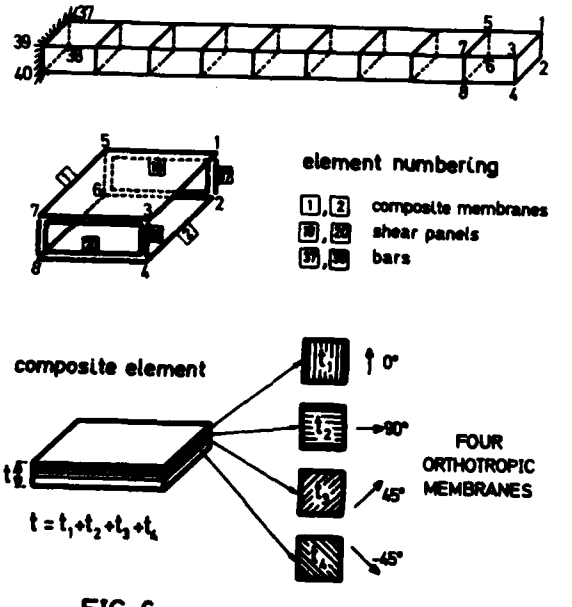
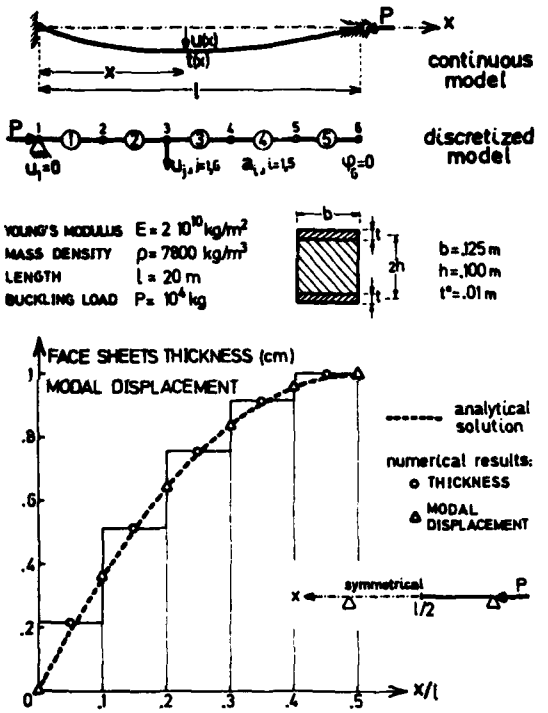
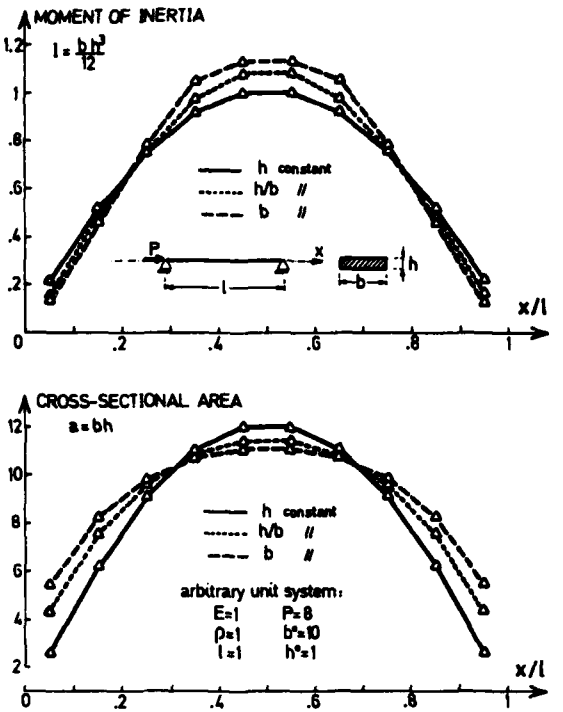


FIG. 6 COMPOSITE BOX BEAM



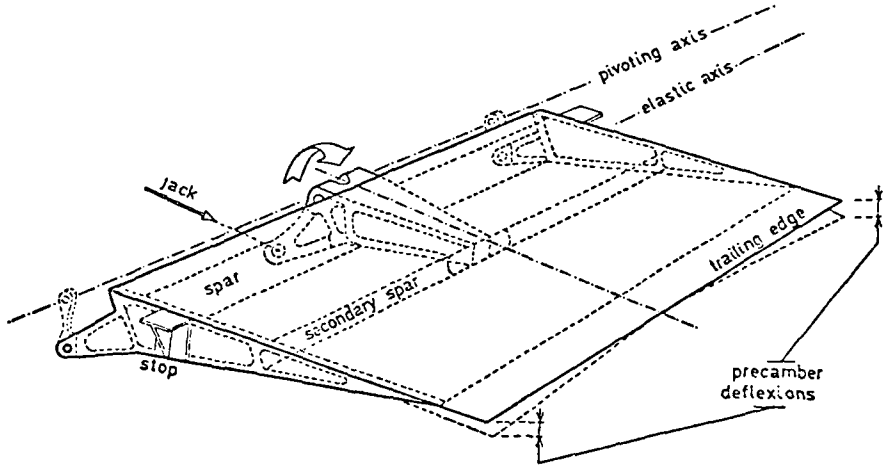
SANDWICH BEAM WITH EULER BUCKLING CONSTRAINT

FIG. 7



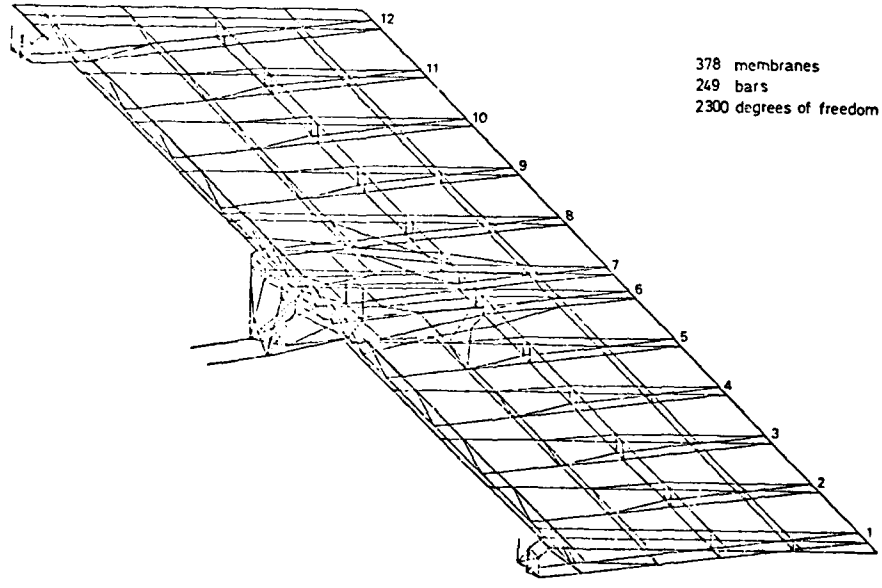
EULER COLUMN WITH RECTANGULAR CROSS-SECTION

FIG. 8



AIRCRAFT SPOILER

FIG. 9



AIRCRAFT SPOILER - FINITE ELEMENT MODEL

FIG. 10

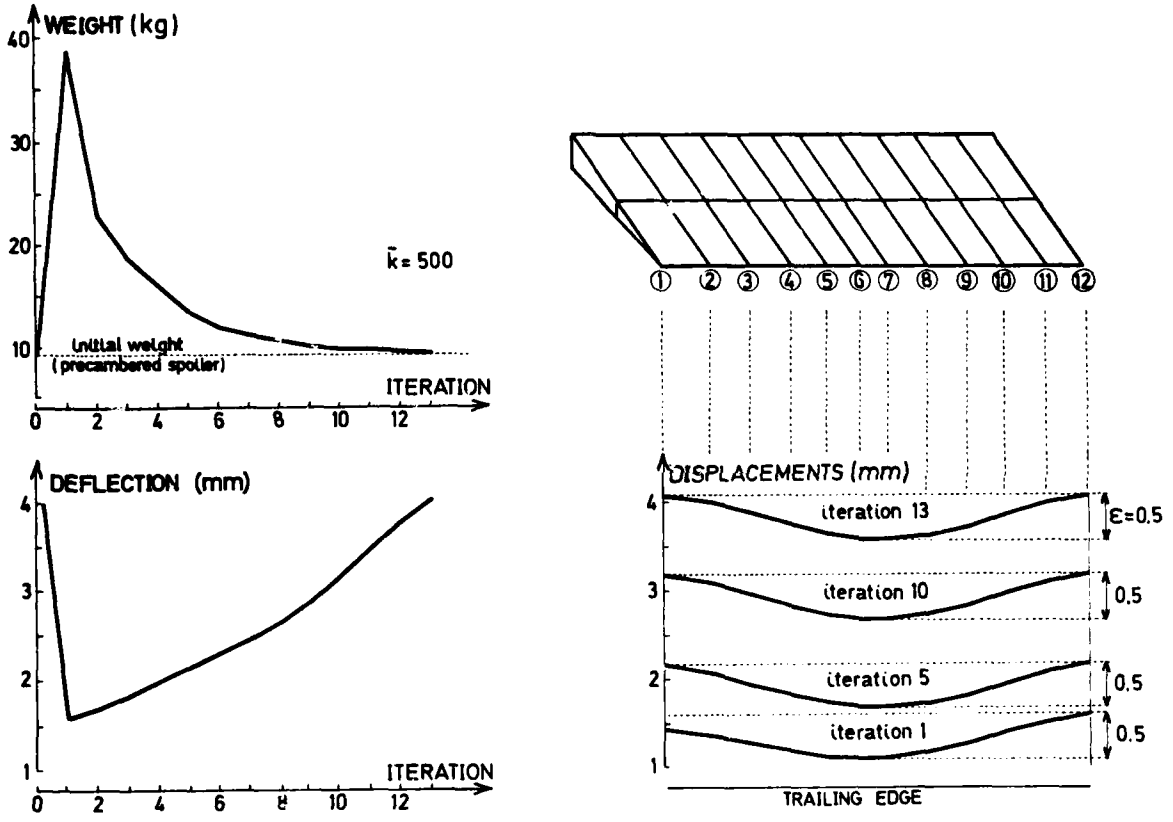


FIG. 11 AIRCRAFT SPOILER – ITERATION HISTORY

SESSION #12

OPTIMIZATION SOFTWARE II

AD-P000 087

AN INTERACTIVE SOFTWARE SYSTEM FOR OPTIMAL DESIGN OF STATICALLY AND DYNAMICALLY LOADED STRUCTURES WITH NONLINEAR RESPONSE

M. A. Bhatti†, V. Ciampi, K. S. Pister and E. Polak
Earthquake Engineering Research Center
and the Electronics Research Laboratory
University of California, Berkeley, California 94720

Summary

The definition of a design problem in terms of an optimization problem involves identifying an objective function and suitable constraint functions. Historically, since optimization techniques were first used in the aerospace industry, weight of the structure has been considered as the objective function. For design of structures subjected to dynamic loads, such as earthquake excitation, other objective functions such as life-time cost better reflect appropriate performance objectives. For some special types of structures, such as braced frames, maximizing energy absorption in the bracing system could be an objective. Thus, depending upon the application, many different functions of design parameters and/or structural response are possible candidates for consideration. The computer programs developed for optimal structural design, so far, have been specialized either for a particular objective function, such as minimum weight, or for particular structures, e.g., trusses or shear frames. In order to look at different problem formulations, a more flexible programming structure is needed, in which users can define their own objective and constraint functions in order to widen the range of applicability to practical problems.

The optimization algorithms used up to now to solve design problem have often been too primitive for the task at hand. For example, they have not been capable of solving non-convex problems and problems with dynamic constraints. Even in simple cases, the cost-benefit ratio has frequently been unfavorable because the algorithms failed to converge to a solution in a reasonable amount of computer time.

Recently, new algorithms have been developed, for general non-convex problems involving dynamic constraints, which have better convergence properties. At the same time, methods for early detection of ill-conditioning in mathematical programming problems are emerging. Since, in general, the transcription of a design problem into a mathematical programming problem is not unique, heuristics are currently being developed which suggest ways of changing the transcription to eliminate the ill-conditioning. However, these algorithms are still sensitive to the choice of internal parameters as well as initial values of design parameters.

In order to deal with these difficulties, an interactive software system for optimal design is indispensable. Interactive computing permits one to stop, restart or modify any of the parameters as the computation progresses. This results in substantial savings, not only in computing time, but also in overall time needed to carry out a design.

An additional advantage of an interactive system using computer graphics is that it can be used as a tool to familiarize designers with optimization techniques. They can change parameters of the algorithm and execute a few iterations while monitoring the computation closely through graphical information displays. This will give them a "feel" for these parameters and the algorithm itself, removing some of the "black box" character of the process.

This paper describes an interactive software system, OPTNSR, for optimal design of structures, in which the above attributes are incorporated.

Introduction

The common practice in design of structures is to use a trial and error design procedure. First, an initial design is chosen, which may then be analyzed using a computer program which simulates the behavior of the physical system. By looking at the results of computer simulation, the designer adjusts the initial design in an attempt to satisfy a set of given specifications which are usually not met by the initial design or to obtain a better design in terms of performances criteria. After the adjustment, a new simulation is performed and the process is repeated until a satisfactory design is obtained. The success of this procedure depends critically on the experience of the designer and may involve a considerable amount of professional-level effort.

Since the early 1950's, research in computer simulation of structural systems has made considerable progress, resulting in a number of excellent general purpose structural analysis programs (1-2). At the same time, several attempts have been made to automate the above design process using optimization techniques. A summary of this work is contained in the survey papers (3-6). Despite this considerable research activity, optimization techniques are not as widely used as might be expected. In the authors' opinion, the main reasons for this lack of interest are:

(i) Lack of a proper definition of design problems in terms of an optimization problem.

(ii) Lack of robust optimization algorithms applicable to general design problems involving dynamic constraints.

(iii) Lack of familiarity with optimization techniques.

The definition of a design problem in terms of an optimization problem involves identifying an objective function and suitable constraint functions. Historically, since optimization techniques were first used in the aerospace industry, weight of the structure has been considered as the objective function. For design of structures subjected to dynamic loads, such as earthquake excitation, other objective functions such as life-time cost better reflect appropriate performance objectives, (7). For some special types of structures, such as braced frames, maximizing energy absorption by the bracing system could be an objective. Thus, depending upon a particular application, any function of design parameters and/or structural response functions is a candidate for consideration as an objective. Obviously, along with different objective functions, one must define appropriate constraint functions in order that the problem is well-posed. The computer programs developed for optimal structural design, so far, have

†Currently at the University of Iowa, Iowa City, Iowa.

been specialized either for a particular objective function, such as minimum weight, (8,9), or for particular structures, e.g., trusses or shear frames. Hence, their application has been very limited. Thus, in order to look at different problem formulations, a more flexible programming structure is needed, in which users can define their own objective and constraint functions in order to widen the range of applicability to practical problems.

The optimization algorithms used up to now to solve the design problem have been too primitive for the task at hand. For example, they have not been capable of solving non-convex problems and problems with dynamic constraints. Even in simple cases, the cost-benefit ratio has frequently been unfavorable because the algorithm failed to converge to a solution in a reasonable amount of computer time. This situation may arise because of several factors, such as: ill-conditioning of the mathematical programming problem into which the design problem is translated; weak convergence properties of the algorithms used (e.g., penalty function method with conjugate gradient method for line search); poor choice of internal parameters of algorithm; or poor initial design. Since optimization algorithms may require several structural analyses per iteration, it is clear that very slow convergence or worse, no convergence at all, may be considered as a very expensive accident!

Recently, new algorithms have been developed, for general non-convex problems involving dynamic constraints (10-11), which have better convergence properties. At the same time, methods for early detection of ill-conditioning in mathematical programming problems are emerging. Since, in general, the transcription of a design problem into a mathematical programming problem is not unique, heuristics are currently being developed which suggest ways of changing the transcription to eliminate the ill-conditioning. However, these algorithms are still sensitive to the choice of internal parameters as well as initial values of design parameters.

In order to deal with these difficulties, an interactive software system for optimal design is indispensable. Interactive computing permits one to stop, restart or modify any of the parameters as the computation progresses. This results in substantial savings, not only in computing time, but also in overall time needed to carry out a design.

An additional advantage of an interactive system using computer graphics is that it can be used as a tool to familiarize designers with optimization techniques. They can change parameters of the algorithm and execute a few iterations while monitoring the computation closely through graphical information displays. This will give them a "feel" for these parameters and the algorithms itself, removing some of the "black box" character of the process.

In the following sections there is described an interactive software system, OPTSNR, for optimal design of structures, in which the above attributes are incorporated. The design criteria for the system are described first, followed by some of its important features. In a companion paper typical applications of the system to design of nonlinear structures subjected to dynamic loadings are presented (12).

System Design Criteria

In the authors' opinion, a general purpose software system for interactive optimal design of structures should be based on the following criteria:

Flexibility

As pointed out in the Introduction, since definition of a design problem in terms of an optimization problem is not unique, the software system should be flexible enough to permit incorporation of new objective functions and constraint functions.

Modularity

A system for optimal design brings together several areas of research, e.g., optimization algorithm development, finite element analysis, numerical analysis, computer hardware, etc. This necessitates that the system be modular so that new developments in any of the related fields can be easily incorporated.

Computational Efficiency

Since optimal design typically involves substantial number crunching, algorithms should be computationally efficient. Moreover, the programming should avoid unnecessary calculations and duplications of computations. However, computational efficiency should not be achieved at the cost of losing modularity.

Computer Graphics

It is generally easier to process large amounts of information when it is presented graphically. Therefore, the system should incorporate extensive graphics facilities to make interaction with the computer easier for creative problem solving.

Ease of Use

The system should be understandable and accessible to different types of users. That is, it should permit a new user to start, knowing only a few commands and learning more advanced concepts "on-line". The command structure should therefore have different levels so that routine design problems require the use of only a few higher level commands, whereas for nonconventional design problems an experienced designer can retain closer control of the design process by using basic lower level commands.

OPTNSR System Components

OPTNSR is an interactive software package for OPTimal design of statically and dynamically loaded structures with Nonlinear Structural Response. The system is currently operating on a DEC VAX 11/780 computer obtained through a grant from the National Science Foundation. The operating system is a virtual memory version of UNIX (a Bell System trademark) developed, at the University of California, Berkeley. The system was developed with design criteria described earlier in mind. System modularity and flexibility are emphasized by the fact that the whole system was based on existing software modules, each performing a specific task. Only the interfacing software was written and implemented. Thus, it is relatively easy to bring in new modules. The modules used in creating the OPTNSR system are:

OPTDYN (13)

This is a general purpose program which is capable of solving design problems which can be expressed in the format:

$$\min_{\underline{z}} f(\underline{z})$$

Subject to

$$\begin{aligned} \max_{\omega} \phi^j(z,\omega) &\le 0 \quad j = 1,\ldots,m \\ &\omega \in [\omega_o,\omega_c] \\ g^j(\underline{z}) &\le 0 \quad j = 1,\ldots,\ell \end{aligned} \tag{1}$$

where

$z \in R^p$ = vector of design variables

f = objective or cost function

ϕ^j = functional or dynamic constraints

g^j = conventional inequality constraints which depend on design variables only.

The program is based on a method of feasible directions, organized as a base program and a user-supplied section. The user-supplied section defines objective and constraint functions for a particular design problem and includes the following routines:

(a) PARSYM: Called once at the beginning of the program to specify fixed system parameters.

(b) FUNCF: To evaluate cost function.

(c) GRADF: To evaluate cost gradient.

(d) FUNCG: To evaluate simple inequality constraints.

(e) GRADG: To evaluate gradients of simple inequality constraints.

(f) FUNCPH: To evaluate functional inequality constraints.

(g) GRADPH: To evaluate gradients of functional inequality constraints.

This structure allows the flexibility needed in defining a design problem. More details about the functions of these routines can be found in (13,14).

INTRAC (15)

INTRAC is a general purpose, communication module for interactive systems. It is a command-oriented system and syntax of its commands is similar to the BASIC language. A summary of commands is included in Appendix A. A very important feature of INTRAC is that it allows use of "macros". A macro is a text file containing a sequence of commands stored on mass storage. A macro can be used as a new command causing the sequence of commands to be executed. Macros are instrumental in creating different levels of interaction. For example, for new users, simpler "commands" can be created which are actually macros which execute a sequence of lower level commands.

MINI-ANSR

This is a modified version of ANSR-I (2). It is modified for minicomputers with virtual memory operating systems. It is capable of analyzing linear and nonlinear structural systems subjected to static and dynamic loads. Some of the important features of the program are described below. For more details readers are referred to (2,14).

Structural Idealization.

The structure is idealized as an assemblage of discrete finite elements connected at nodes. Each node may possess up to six displacement degrees of freedom. Provision is made for degrees of freedom to be deleted or combined. This feature provides the user with ample flexibility in the idealization of the structure, and may permit the size of the problem to be substantially reduced.

The mass of the structure is assumed to be lumped at the nodes, so that the mass matrix is diagonal.

Loading.

Loads are assumed to be applied only at the nodes. Static and/or dynamic loads may be specified; however, static loads, if any, must be applied prior to the dynamic loads.

For static analysis, a number of static force patterns must be specified. Static loads are then applied in a series of load increments, each load increment being specified as a linear combination of static force patterns. This feature permits nonproportional loads to be applied. Each load increment can be specified to be applied in a number of equal steps.

The dynamic loading may consist of earthquake ground accelerations, time dependent nodal loads, and prescribed initial values of the nodal velocities and accelerations. These dynamic loadings can be specified to act singly or in combination.

Solution Techniques.

The program incorporates a solution strategy defined in terms of a number of control parameters. By assigning appropriate values to these parameters, a wide variety of solution schemes including step-by-step, iterative and mixed schemes, may be implemented.

For static analysis, a different solution scheme may be employed for each load increment. The use of this feature can reduce the solution time for structures in which the response must be computed more precisely for certain ranges of loading than for others. In such cases, a sophisticated solution scheme with equilibrium iteration might be used for the critical ranges of loading, whereas a simplier step-by-step scheme without iteration might suffice for other loading ranges.

The dynamic response is computed by step-by-step integration of incremental equations of motion using Newmark's method. A variety of integration operators may be obtained by assigning appropriate values to the parameters β and γ.

Programming Considerations.

The program is organized into a base program and an element library. New elements can easily be added without knowing anything about the base program, merely following clearly defined instructions (see (14) for details.)

Nonlinearities are introduced at the element level only, and may be due to large displacements, large strains and/or nonlinear materials. The programmer adding a new element may include any type or degree of nonlinearity in the behavior of the element.

The stiffness matrix is modified, rather than completely reformed, as the tangent stiffness changes. During solution, the decomposition is carried out only on that part of the updated stiffness matrix which follows the first modified coefficient. Significant savings in solution time can sometimes be obtained by numbering the nodes connecting nonlinear elements to be last, so that the decomposition operations are limited to the end of the matrix.

Finite Element Library.

At present, the following finite elements are included in the program. New finite elements may be added to the library with relative ease by following the instructions given in (14).

(i) Three dimensional elastic truss element which can be located arbitrarily in an X, Y, Z cartesian coordinate system. It can transmit axial forces only.

(ii) Three dimensinoal nonlinear truss element which may yield in tension and yield or buckle elastically in compression. Large displacement effects may be included. See (2) for theoretical details of this element.

(iii) Two-dimensional elastic beam elements, located arbitrarily in an X, Y cartesian coordinate system. Shear deformations are ignored.

(iv) Two dimensinoal nonlinear beam element, arbitrarily oriented in the global X, Y, Z reference frame. Each element must be assigned an axial stiffness plus a

major axis flexural stiffness. Torsional and minor axis flexural stiffnesses may also be specified if necessary. Flexural shear deformations and the effects of eccentric end connections can be taken into account. Yielding may take place only at concentrated plastic hinges at the element ends. Hinge formation is affected by the axial force and major axis bending moment only. Strain hardening and large displacement effects can be approximated. See (17) for theoretical details of this element

(v) Three dimensional nonlinear beam element, arbitrarily oriented in a global X, Y, Z reference frame. Each element must be assigned flexural stiffness and axial stiffness. Plastic hinges can form at the element ends. Interaction among the bending moments, torsional moment and axial force is taken into consideration. Displacements are assumed to be small, although the P-delta effect may be considered. Theoretical details are given in (17).

(vi) Energy absorbing element, arbitrarily oriented in a global X, Y, Z reference frame. This element transmits axial forces only and its hysteretic behavior is governed by a rate-type constitutive equation (16).

Interactive Use of OPTNSR System

Computational experience with batch use of the program OPTDYN revealed the following difficulties:

(i) The choice of parameters best suited for the problem at hand was not obvious and required several adjustments before reaching a set of parameters which gave good computational behavior.

(ii) Sometimes the problem was badly scaled with respect to the algorithm, requiring several adjustments before a solvable problem was obtained.

In order to cope with these difficulties the program was made interactive through the general purpose interactive language interpreter INTRAC. The interaction allows the designer:

(i) to interrupt the computing process, change parameter values and restart the process;

(ii) to control the flow of the algorithm by single-stepping through its loops (This feature is most useful in diagnosing reasons for poor computational behavior.);

(iii) to display quantities computed by the optimization and simulation algorithms;

(iv) to use the computer as a "scratch pad" for side computations on variables, vectors and matrices used in the algorithm. This feature is useful to perform tests not originally foreseen in the program and to check, for example, condition of key matrices, their eigenvalues, etc.

The first step in implementing interaction is to decide where the interaction should take place and what quantitites need to be changed and/or otherwise manipulated. According to the above considerations, interaction should be implemented at each step of the main loop of the algorithm as well as at each step of every internal loop. Thus breakpoints have been inserted after the corresponding statement of OPTDYN. At each breakpoint a subroutine INTCAL is called, which checks the condition associated with the breakpoint. The condition may be NEVER, ALWAYS or an IF clause. If it is NEVER, no action is taken and the control is returned to OPTDYN. If it is ALWAYS, INTCAL is called and an interaction phase takes place. The quantities which need to be changed or displayed are declared in a symbol table (data base). During the interaction phase (marked by a prompt '>'), the user has access to all these quantities and can modify them using the SET command. A number of quantities from OPTDYN which are needed during interaction have already been declared into the symbol table. A complete list is given in (14). The quantities which are related to a particular problem or simulation package can also be declared into the symbol table from subroutine PARSYM by simply calling a subroutine DECLAR with proper arguments. Again, see (14) for the programming details.

In OPTNSR interaction is handled through a set of commands. These commands are divided into the following categories:

(i) commands for flow control

(ii) commands to handle the symbol table

(iii) commands for graphics

(iv) commands for scratch pad

(v) miscellaneous commands

For the sake of brevity, only a summary of these commands is included as Appendix B; for details see (14).

These commands in combination with INTRAC commands (Appendix A), are used as basic building blocks to write macros that perform specified tasks. These macros provide the following features:

(a) Simple problems, or problems with which considerable experience has been acquired, require very little interaction since most of the parameters can be pre-set. In this case, a macro, called RUN, can be used to perform a specified number of iterations just as in batch mode.

(b) Complicated problems sometimes require that the computational behavior be monitored in more detail. A series of macros is available so that a user can essentially single step through the algorithm and change any of the parameters as desired.

(c) Special macros make the use of graphics and scratch pad easier.

In addition to these ready-made macros, users can write their own macros to perform specified tasks. Some of the more commonly used macros will be described here.

(i) RUN - Performs a specified number of iterations of the overall algorithm.

Syntax: RUN ⟨nitn⟩ ⟨option⟩

nitn : = number of iterations of the algorithm to be performed. The program will stop for further action, if the number of iterations exceeds 'nitn' and the optimum has not yet been achieved. The program can be restarted by using RUN macro again, if desired.

option : = {STORE|PRTALL}

If PRTALL option is specified, then the program prints iteration number, cost function (f), constraint violation function (ψ), optimality function (θ) and tolerance parameter (ε) on the terminal as the computation is progressing. With the 'STORE' option, functions f, ψ and design variables are stored in scratch pad, in arrays 'FG', 'PSIG' and 'ZG'. These arrays can be later used to plot, for example, the decrease in the cost versus iteration number, history of a particular variable over several iteration, etc. If no option is specified, only the iteration number is printed.

(ii) STEP2 - Computes objective and constraint functions. Syntax: STEP2.

This macro performs Step 2 of the algorithm, i.e., it computes the objective function f, simple inequality constraints g and functional constraints ϕ.

(iii) STEP3 - Computes a usable feasible direction Syntax: STEP3

This macro performs calculations in the step 3 of the algorithm to find a usable feasible direction. Angles between the direction vector and function gradients can be displayed by using macro PRTANG. If these angles are not satisfactory, some parameters can be changed and a new direction computed.

(iv) ARMIJO - Performs step length calculations using Armijo's rule. Syntax: ARMIJO ⟨nitn⟩ ⟨display⟩

nitn : = maximum number of iterations to be performed

display : = display option.

This macro performs iterations until either, the Armijo rule is satisfied or the number of iterations exceeds the maximum specified. For the display option, macros 'GRAPHO' or 'GRAPHOS' can be used. Both of these macros plot Armijo step and simple constraints as bar charts and functional constraints at each iteration within the loop. The only difference between the two is that GRAPHOS stores values of f, ψ and z in arrays FG, PSIG and ZG created by using RUN macro with STORE option. A typical plot generated by GRAPHO is shown in Figure 1. The graphics screen is divided into three windows. In the top window, a line corresponding to the current step length tried, is drawn. The line is below the diagonal line if the cost reduction is satisfactory, but is above the diagonal otherwise. In the middle window bars are drawn corresponding to g constraints and the maximum value of ϕ constraints. Bars at successive iterations are drawn a little to the right of the previous bars. The ε line is also shown. The bottom window is divided equally into several portions to accomodate all the functional constraints. The functional constraints are plotted at each iteration in their respective portions of the window.

These graphs gives a clear picture of what is going on within the Armijo loop. It is easy to identify a particular constraint that is causing difficulties in satisfying the Armijo rule. To correct this situation, a new direction can be computed with that particular constraint in the ε-active set or the problem may be rescaled.

(v) RARMIJO - Performs iterations of the overall algorithm with Armijo display

Syntax: RARMIJO ⟨nitn⟩

This macro combines RUN macro with the Armijo display GRAPHO. One iteration of the overall algorithm will be performed with the GRAPHO display in the step length loop. RESUME command is given to start the next iteration, as long as the number of iterations is less than nitn .

Note: A parallel macro, 'RARMIJOS', combines RUN with GRAPHOS for storing values in global arrays, as explained in 'ARMIJO'.

(vi) GRAPHF - Plots cost function versus iteration number

Syntax: GRAPHF ⟨yesno⟩

yesno : = {Y|N}

Plots cost function versus iteration number from the values of f stored in array FG. If yesno is 'Y', the curve will be marked to signify a new iteration.

A plot created by GRAPHF is shown in Figure 2(a).

(vii) GRAPHPSI - Plots ψ function versus iteration number

Syntax: GRAPHPSI ⟨yesno⟩

yesno : = {Y|N}

Plots ψ function versus iteration number from the values stored in PSIG. yesno has the same meaning as in GRAPHF. A plot created by this macro is shown in Figure 2(b).

(viii) GRAPHZ - Plots history of design variables

Syntax: GRAPHZ ⟨number⟩ ⟨yesno⟩

Plots a particular design variable, specified by number versus the iteration number from the array ZG. 'yesno' has the usual meaning.

Concluding Remarks

A software system for interactive optimal design of statically and dynamically loaded structures is presented. Typical applications of this software system are presented in a companion paper (12). Here, the software system is critically examined with reference to stated design criteria for a general purpose, interactive software system for optimal design.

Flexibility. A new design problem in the OPTNSR system is formulated by supplying routines for objective and constraint functions and their gradients. Thus the system is very flexible in this regard. However, for new design problems, it has been our experience that few revisions of the problem formulation are needed before arriving at a suitable formulation. Each change in objective or constraint function necessitates going to the FORTRAN level, making changes, compiling, linking and loading the whole system. This process is quite time consuming. Thus, it is highly desirable to have a higher level language for defining constraint and objective functions so that a minor change in objective or constraint functions does not necessitate linking and loading of the whole system.

Modularity. The OPTNSR system was constructed from several independently written software modules, thus, it is highly modular. New structural analysis packages or new interaction handling systems can easily be incorporated. The system does suffer from one drawback which stems from the fact that it is based on OPTDYN, which is a batch mode, one algorithm (feasible directions) program. It is a well known fact that different optimization algorithms perform differently on different classes of problems, some being more efficient than others for a particular problem. In a general purpose software system, it is desirable to have more than one algorithm (perhaps a library of algorithms) so that the user can choose the particular algorithm most suited to the problem at hand.

Computational Efficiency. The OPTNSR systems' basic computational modules use computer resources very efficiently. However, the macros are implemented in an inefficient manner. Each time a macro is executed, it is read from disc, its commands interpreted and then executed. This means that macros which are part of a loop will take unnecessarily long to execute. An effort was made to reduce disc I/O by keeping some of the commonly used macros in core , in an internal buffer, but this proved not to be enough. The system should be modified so that macros are read and interpreted only once when they are called for the first time.

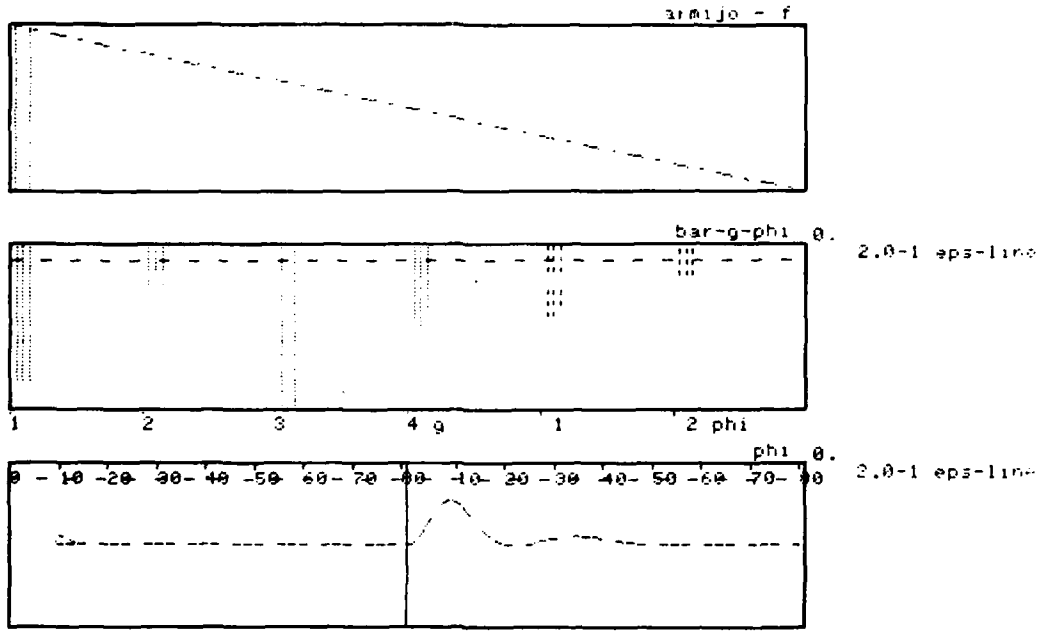


Fig. 1. A typical plot obtained by using the macro GRAPHO

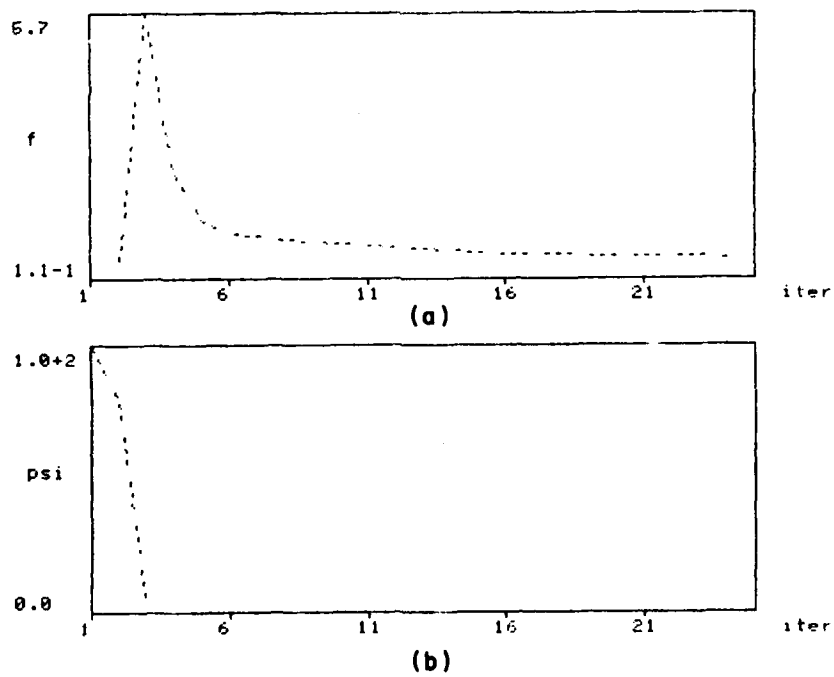


Fig. 2. A typical plot created by macros GRAPHF and GRAPHPSI

Computer Graphics. Most of the applications' graphics is implemented by writing macros which use lower level graphics primitives. Thus, some of the graphics is slower because of the way macros are implemented. Better implementation of macros would take care of this problem also.

Ease of Use. The system is relatively easy to become familiar with and use. However, some of the commands and breakpoint structure require detailed knowledge of the algorithm and its implementation. Moreover, the system in its present form is more suitable for research applications as opposed to industrial application.

From the above discussion it is seen that the OPTNSR system provides researchers with a very powerful and versatile tool for studies in the area of optimal design of nonlinear structural systems. However, it requires improvement to make it useful for broader research applications and ultimately industrial applications. Work is currently underway to overcome some of the limitations mentioned above.

Acknowledgement

Research sponsored by the National Science Foundation Grants ECS-79-13148, PFR-7908261 and ENG-7810442.

References

(1) Bathe, K. J., Wilson, E. L. and Peterson, F. E., "SAP IV - A Structural Analysis Program for Static and Dynamic Response of Linear Systems," Report No. EERC 73-11, Earthquake Engineering Research Center, University of California, Berkeley, June 1973.

(2) Mondkar, D. P. and Powell, G. H., "ANSR-I A General Purpose Program for Analysis of Nonlinear Structural Response," Report No. EERC 75-37, Earthquake Engineering Research Center, University of California, Berkeley, December 1975.

(3) Prager, W. and Sheu, C., "Recent Developments in Optimal Structural Design," Applied Mechanics Reviews, October 1968.

(4) Venkayya, V. B., "Structural Optimization: A Review and Some Recommendations," Intl. J. Numer. Methods Engr., Vol. 13, pp. 203-228 (1978).

(5) Pierson, B. L., "A Survey of Optimal Structural Design Under Dynamic Constraints," Int. J. Numer. Methods Engr., Vol. 4, pp. 491-499 (1972).

(6) Rangacharyulu, M. A. V. and Done, G. T. S., "A Survey of Structural Optimization Under Dynamic Constraints," Shock Vib. Dig., Vol. 11, No. 12, December 1979.

(7) Pister, K. S., "Optimal Design of Structures Under Dynamic Loading," NATO - NSF Advanced Study Institute on Optimization of Distributed Parameter Structures, University of Iowa, Iowa City, Iowa, May 21 - June 4, 1980.

(8) Miura, H. and Schmit, L. A., Jr., "ACCESS-1, Approximation Concepts for Efficient Structural Synthesis - Program Documentation and User's Guide," NASA CR-144905, National Aeronautics and Space Administration, May 1976.

(9) Arora, J. S., Nguyen, D. T., Belegundu, A. D. and Rajan, S. D., "Design Optimization Codes for Structures-DOCS," Technical Report No. 71, Division of Materials Engineering, The University of Iowa, Iowa City, Iowa, August 1980.

(10) Polak, E., "Algorithm for Optimal Design," NATO-NSF Advanced Study Institute on Optimization of Distributed Parameter Structures, The University of Iowa, Iowa City, Iowa, May 21 - June 4, 1980.

(11) Gonzaga, C., Polak, E. and Trahan, R., "An Improved Algorithm for a Class of Optimization Problems with Functional Inequality Constraints," Electronics Research Laboratory, Memo No. UCB/ERL - M78/56, University of California, Berkeley, 1978.

(12) Balling, R., Bhatti, M. A., Ciampi, V. and Pister, K. S., "Interactive Optimal Design of Dynamically Loaded Structures Using the OPTNSR Software System," These proceedings.

(13) Bhatti, M. A., Polak, E. and Pister, K. S., "OPTDYN - A General Purpose Optimization Program for Problems with or without Dynamic Constraints," Report No. UCB/EERC-79/16, Earthquake Engineering Research Center, University of California, Berkeley, July 1979.

(14) Bhatti, M. A., Ciampi, V., Pister, K. S. and Polak, E., "OPTNSR - An Interactive Software System for Optimal Design of Statically and Dynamically Loaded Structures with Nonlinear Response," Report No. UCB/EERC - 81/02, Earthquake Engineering Research Center, University of California, Berkeley, January 1981.

(15) Weislander, J. and Elmqvist, H., "INTRAC - A Communication Module for Interactive Programs," Department of Automatic Control, memo LUTFD2/(TFRT-3149)/1-060/(1978), Lund Institute of Technology, Lund, Sweden, August, 1978.

(16) Bhatti, M. A., "Optimal Design of Localized Nonlinear Systems with Dual Performance Criteria Under Earthquake Excitations," Report No. UCB/ERL - 79/15, Earthquake Engineering Research Center, University of California, Berkeley, July 1979.

(17) Riahi, A., Row, D. G., and Powell, G. H., "Three Dimensional Inelastic Frame Elements for the ANSR-I Program," Report No. UCB/EERC-78/06, Earthquake Engineering Research Center, University of California, Berkeley, CA, August 1978.

Appendix A - Summary of INTRAC Commands

1. MACRO - Begins a macro definition and creates a macro
2. FORMAL - Declares formal arguments in a macro definition. It can be used to extend the list of formal arguments anywhere in a macro
3. END - Ends a macro. Deactivates suspended macros.
4. SUSPEND - Suspends the execution of a macro
5. RESUME - Resumes the execution of a macro
6. LET - Assigns (allocates) variables
7. DEFAULT - Assigns a variable if it is unassigned or does not exist previously.
8. LABEL - Defines a label
9. GOTO - Makes unconditional jump
10. IF - Makes conditional jump
11. FOR - Starts a loop
12. NEXT - Ends a loop
13. WRITE - Writes variables and text strings.
14. READ - Reads values for variables from the terminal.

15. FREE - Re-initializes global variables.
16. SWITCH - Modifies switches in INTRAC
17. STOP - Stops the execution of the program.

Appendix B - Summary of Basic Commands

(A) Commands for Control Flow

1. BREAKS - Displays a list of breakpoints in the algorithm
2. WHERE - Displays the name of the current breakpoint
3. HALT - Sets up halt condition at specified breakpoints
4. GO - Starts execution from one breakpoint to another

(B) Commands to Handle Symbol Table

1. SYMBOL - Displays the symbol table
2. PRINT - Displays a variable from the symbol table
3. SET - Changes value of a variable in the symbol table
4. CHECK - Checks if a variable has been changed by SET command.
5. CLEAR - Clears flags used for CHECK
6. SETDIM - Changes dimensions of an array in the symbol table
7. TRANS - Transfers value of symbol table variable to INTRAC.

(C) Commands for Graphics

1. GRINIT - Initializes graphics mode
2. DEFINE - Defines rectangular windows on the screen by a user-specified name.
3. WINDOW - Enters a specified window
4. ERASE - Erases a specified window
5. COLOR - Sets color for subsequent graphics output
6. VECTOR - Draws a vector between specified starting and ending coordinates
7. MOVE - Moves cursor to specified coordinate
8. DRAW - Draws a vector
9. CURSOR - Moves cursor in preparation for text output
10. CURSOREL - Positions cursor a specified number of character size units away from (x,y) coordinate
11. TEXT - Outputs text at the posit of the graphics cursor.

(D) Commands for Scratchpad

1. GETDIM - Returns actual array dimension from the symbol table
2. PDIM - Creates a variable in scratchpad
3. PREM - Removes a variable from the scratchpad
4. PTAB - Displays scratchpad symbol table
5. PSCAL - Scalar operations in the scratchpad
6. PMAT - Matrix operations in the scratchpad

(E) Miscellaneous Commands

1. ALGO - Displays the solution algorithm
2. ED - Calls a text editor to write and modify macros
3. LIST - Lists a macro file
4. COPY - Copies a macro file
5. DELETE - Deletes a macro file
6. CSH - Calls shell to execute a UNIX command
7. HELP - Explains usage of the commands
8. HLPGR - Gives a list and syntax of macros for graphics
9. HLPPAD - Gives a list and syntax of macros which facilitate use of scratchpad

AD-P000 088

INTERACTIVE OPTIMAL DESIGN OF DYNAMICALLY LOADED STRUCTURES USING THE OPTNSR SOFTWARE SYSTEM

R. Balling, M. A. Bhatti,* V. Ciampi and K. S. Pister
Department of Civil Engineering
University of California
Berkeley, CA 94720

Summary

Some typical applications of optimization techniques to the design of nonlinear structures subjected to dynamic loadings are presented. The applications are based on the use of the interactive software system OPTNSR, described in a companion paper.

Introduction

The definition of a design problem in terms of an optimization problem involves identifying an objective function and suitable constraint functions. Historically, since optimization techniques were first used in the aerospace industry, weight of the structure has been considered as the objective function. For design of structures subjected to dynamic loads, such as earthquake excitation, other objective functions such as life-time cost better reflect appropriate performance objectives, (1). For some special types of structures, such as braced frames, maximizing energy absorption by the bracing system could be an objective. Thus, depending upon a particular application, any function of design parameters and/or structural response functions is a candidate for consideration as an objective. Obviously, along with different objective functions, one must define appropriate constraint functions in order that the problem is well-posed. Computer programs developed for optimal structural design, so far, typically have been specialized either for a particular objective function, such as minimum weight, (2,3), or for particular structures, e.g., trusses or shear frames. Hence, their application has been very limited. In order to look at different problem formulations for a wider class of design situations, an interactive software system OPTNSR (4) has been developed. Important features of the system are described in a companion paper (5). Here formulation is given and results are presented for two problems belonging to different categories:

(i) Minimum weight Design: A two story shear-type braced frame, subjected to an impulsive base motion is designed for minimum weight. Material nonlinearities are allowed in the braces. Time-dependent (or functional) constraints are imposed on maximum story drifts and maximum stresses in columns. Conventional inequality constraints, limiting minimum member sizes and the ratio between weight of the bracing and total weight of the structure are also imposed.

(ii) Design for Minimum Structural Response: Design of an earthquake isolation systems for a steam generator in a nuclear power plant is considered, such that rotations of the generator are minimized during an earthquake. In particular reference is made to a model structure which has been tested on the earthquake simulator at the Earthquake Engineering Research Center, University of California, Berkeley. The steam generator is supported at the base on rubber bearings with very low lateral stiffness, and is connected to an adjacent five-story steel frame through mild steel energy absorbing devices, at two different levels. Selection of mechanical properties of the two energy absorbing devices and their points of attachment to the steam generator constitutes the design problem.

*Currently at the University of Iowa, Iowa City, Iowa.

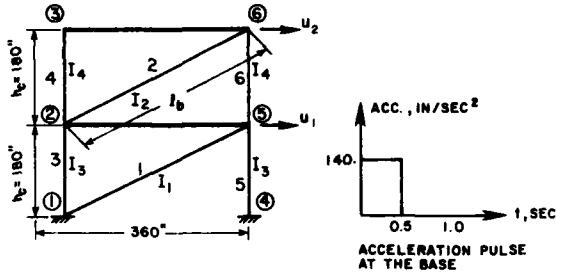


Fig. 1. Inelastic Braced Frame.

Minimum Weight Design of an Inelastic Frame Subjected to an Impulsive Base Motion

A two story shear-type braced frame (Fig. 1), subjected to an impulsive base motion, is designed for minimum weight under both conventional and functional constraints. Material nonlinearity is allowed in the diagonal bracing, which is modeled using a nonlinear truss element.

The ability of MINI-ANSR to accept specifications of both zero displacements and equal displacement components for different nodes, has been used to model the shear-type structure. Four design parameters appear naturally, the two areas of the diagonal bracing and the two moments of inertia of the columns, at the first and second floors, respectively. Area of cross section, A, and elastic section modulus, S, of columns are assumed to be related to moment of inertia I by the empirical relationships:

$$A = 0.8\, I^{1/2} \quad \text{(in inch units)} \tag{1}$$

$$S = 0.78\, I^{3/4} \tag{2}$$

For convenience of formulation of the problem, variables I_1 and I_2, having the dimensions of moments of inertia, are used as design variables instead of areas. For the bracing the same relationship, equation (1), is assumed to hold. The four design variables are then I_1, I_2 for the bracings, I_3 and I_4 for the columns. Constraints considered refer to story drifts, stresses in columns, minimum member sizes and ratio between weight of the bracing and total weight of the structure. The objective and constraint functions and their gradients are expressed as follows:

Objective Function

$$f(\underline{z}) = w_t = w_b + w_c = \text{total weight of the structure}$$
$$= \rho \ell_b (A_1 + A_2) + 2\rho h_c (A_3 + A_4)$$
$$= 0.8\, \rho \ell_b (I_1^{1/2} + I_2^{1/2}) + 1.6\, \rho h_c (I_3^{1/2} + I_4^{1/2})$$

Gradient of f

$$\nabla f = 0.4\rho [\ell_b I_1^{-1/2}, \ell_b I_2^{-1/2}, 2h_c I_3^{-1/2}, 2h_c I_4^{-1/2}]^T$$

Conventional Constraints

$$\left.\begin{array}{l} 1)\ g^1 = -I_1 + I^b_{min} \le 0 \\ 2)\ g^2 = -I_2 + I^b_{min} \le 0 \\ 3)\ g^3 = -I_3 + I^c_{min} \le 0 \\ 4)\ g^4 = -I_4 + I^c_{min} \le 0 \end{array}\right\} \text{Positiveness of the design variables } I^b_{min},\ I^c_{min} > 0$$

5) The weight of the bracing is desired to be less than a fixed fraction α of the total weight of the frame:

$$g^5 = \frac{w_b}{\alpha(w_b+w_c)} - 1 \le 0$$

Gradients of Conventional Constraints

$$\nabla g^1 = [-1,0,0,0]^T\ ,\quad \nabla g^2 = [0,-1,0,0]^T\ ,$$
$$\nabla g^3 = [0,0,-1,0]^T\ ,\quad \nabla g^4 = [0,0,0,-1]^T\ ,$$

$$\nabla g^5 = \frac{1}{\alpha(w_b+w_c)^2}\begin{Bmatrix} w_c & 0.4\,\ell_b\, I_1^{-1/2} \\ w_c & 0.4\,\ell_b\, I_2^{-1/2} \\ -w_b & 0.8\,h_c\, I_3^{-1/2} \\ -w_b & 0.8\,h_c\, I_4^{-1/2} \end{Bmatrix}$$

Functional Constraints

Maximum allowable story drift, a

$$1)\ |u_1| \le a \quad \text{or} \quad \phi^1 = \left(\frac{u_1}{a}\right)^2 - 1 \le 0 \qquad (*)$$

$$2)\ |u_2-u_1| \le a \quad \text{or} \quad \phi^2 = \left(\frac{u_2-u_1}{a}\right)^2 - 1 \le 0$$

Maximum allowable stress in columns, σ_a

$$3)\ \left|\frac{M_{1c}}{S_{1c}}\right| \le \sigma_a \quad \text{or} \quad \phi^3 = \frac{M_{1c}^2}{0.78^2 I_3^{3/2}\sigma_a^2} - 1 \le 0$$

$$4)\ \left|\frac{M_{2c}}{S_{2c}}\right| \le \sigma_a \quad \text{or} \quad \phi^4 = \frac{M_{2c}^2}{0.78^2 I_4^{3/2}\sigma_a^2} - 1 \le 0$$

Gradients of Functional Constraints

$$\nabla\phi^1 = \frac{2u_1}{a^2}\left[\frac{\partial u_1}{\partial I_1}, \frac{\partial u_1}{\partial I_2}, \frac{\partial u_1}{\partial I_3}, \frac{\partial u_1}{\partial I_4}\right]^T$$

$$\nabla\phi^2 = \frac{2(u_2-u_1)}{a^2}\left[\frac{\partial(u_2-u_1)}{\partial I_1}, \frac{\partial(u_2-u_1)}{\partial I_2}, \frac{\partial(u_2-u_1)}{\partial I_3}, \frac{\partial(u_2-u_1)}{\partial I_4}\right]^T$$

$$\nabla\phi^3 = \frac{2M_{1c}}{0.78^2\sigma_a^2 I_3^{3/2}}\left[\frac{\partial M_{1c}}{\partial I_1}, \frac{\partial M_{1c}}{\partial I_2}, \frac{\partial M_{1c}}{\partial I_3} - \frac{3}{4}\frac{M_{1c}}{I_3}, \frac{\partial M_{1c}}{\partial I_4}\right]^T$$

$$\nabla\phi^4 = \frac{2M_{2c}}{0.78^2\sigma_a^2 I_4^{3/2}}\left[\frac{\partial M_{2c}}{\partial I_1}, \frac{\partial M_{2c}}{\partial I_2}, \frac{\partial M_{2c}}{\partial I_3}, \frac{\partial M_{2c}}{\partial I_4} - \frac{3}{4}\frac{M_{2c}}{I_4}\right]^T$$

*Note that the constraint is divided by its upper limit resulting in a constraint function with values varying between 0 and -1, when feasible. This type of scaling improves computational behavior tremendously and should be used whenever possible.

Numerical Data

Material density, ρ = 0.1 lb/in^3

Young's Modulus, E = 30000. ksi

Maximum story drift, a = $\pm$ 0.45 in

Maximum stress in columns, σ_a = $\pm$ 24 ksi

Minimum value of the design variables,

I_{min} = 10. in^4 for the columns,

I_{min} = 0.1 in^4 for the bracing

Yield stress in the bracing, σ_y = $\pm$ 18 ksi

Masses at each floor, $m_1 = m_2$ = 208 lb x sec^2/inch

Base acceleration, a rectangular pulse of 140 in/sec^2, acting for 0.5 sec.

Duration of analysis, 1 sec in 100 steps.

Numerical Results

Numerical results for this example are presented in the form of an interactive dialogue with the computer (Appendix A). The name of the data file is "brace.data" which contains initial values of the optimization algorithm parameters, starting design vector and other data for the MINI-ANSR program.

Ten iterations of the optimization procedure are first performed using the macro "run" and the option "store". In this case the initial design is infeasible and seven iterations are needed to reach the feasible region.

At the end of ten iterations the results of the analysis corresponding to the new values of the design variables, now feasible, are displayed, using two new macros, specifically prepared for the problem, "gdisp" and "gmom". These macros display horizontal displacements of the two floors and end moments in the columns at the first and second level, as functions of the number of time steps.

Four more iterations are then requested, after which the decision is made to start monitoring very carefully what happens in the various stages of the procedure in order to make possible a rational adjustment of the parameters of the algorithm. Starting from iteration 15 macro "step3" is used, which stops the execution at the end of step 3, that is after the calculation of a direction has been completed. Command "prtang" gives at this point the angle between the direction vector and the cost function gradient and the angles between the direction vector and the ε-active constraint gradients. The first information that we have from "prtang" is that there is no active constraint at the start of this iteration. We can now use the macro "Armijo" in connection with the macro "graphos" to monitor what happens during the step length calculations up to the completion of iteration 15.

The information, which comes through the graphic representation, obtained using "graphos", is very rich and can be fully appreciated only if the forming of the lines on the screen rather than only the final picture is observed. For iteration 15 the information can be expressed in this way: the step length is reduced in Armijo and the constraint which causes this reduction is the constraint $\phi(2)$, which was not even active at the start of the iteration. As a consequence the iteration is a bad one, as can be verified looking at the very small reduction in the cost function f from the previous step ("prtall" command has been used at

the end of the iteration to print iteration number, cost function etc.).

In the subsequent iteration, as can be seen using "prtang" after "step3", constraint $\phi(2)$ is active and influences the choice of a direction. In "Armijo" the step length is increased until constraint g(5) is violated; at the same time constraint $\phi(2)$ ceases to be active.

Iteration 16 has been a good one, but the next is not. In fact in the direction finding stage constraint $\phi(2)$ is not active, while, during the Armijo phase, it is still $\phi(2)$ which gives trouble and forces reduction of the step length.

Finally, in iteration 18 both g(5) and $\phi(2)$ are active and influence the choice of a direction, as a consequence the iteration proves to be a good one.

Monitoring closely the algorithm's behavior during iterations 15 through 18 has given sufficient indication for an adjustment of the parameters. The slowing down of the solution process, connected with the alternation of a good step and a bad one, can be corrected by increasing the value of ε and forcing, consequently, both the constraints which are important at this stage, namely g(5) and $\phi(2)$, to be active at each iteration. However, increasing ε may not be sufficient, because ε may be automatically reset to the previously used smaller value in the ε-reduction stage of the algorithm and execution sent back to the direction finding stage. It is also important to reduce parameter δ at the same time. This is actually done in this example and in particular ε is set = 0.4 and $\delta = 10^{-7}$.

The solution process is then advanced for 5 more iterations, during which the effectiveness of the adjustment of parameters is observed.

Ten more iterations are performed, after which the cost function is plotted. Again the beneficial effect of the adjustment of parameters is clearly visible in the graph.

After 18 more iterations the termination criterion is satisfied and a message of congratulations appears on the screen.

Results of the analysis corresponding to the optimal values of the design variables are finally plotted before stopping.

Optimal Design of an Earthquake Isolation System for a Steam Generator in a Nuclear Power Plant

Analysis of the seismic response of large components in nuclear power plants is complicated by interaction between the component and the structure. For large components such as a steam generator, this interaction cannot be neglected in predicting the response. An experimental program was initiated at the Earthquake Engineering Research Center, University of California, Berkeley to investigate the feasibility of using rubber bearings at the base and energy-absorbing restrainers in connecting the component to the primary structure, to improve the structural integrity of the component with respect to seismic loadings (6). The experimental model used in the shaking-table tests is shown in Fig. 2. Details of the design and construction of the model and results of an extensive series of tests, where the mechanical properties of the energy-absorbing restrainers were varied, while keeping fixed their position, are given in (6).

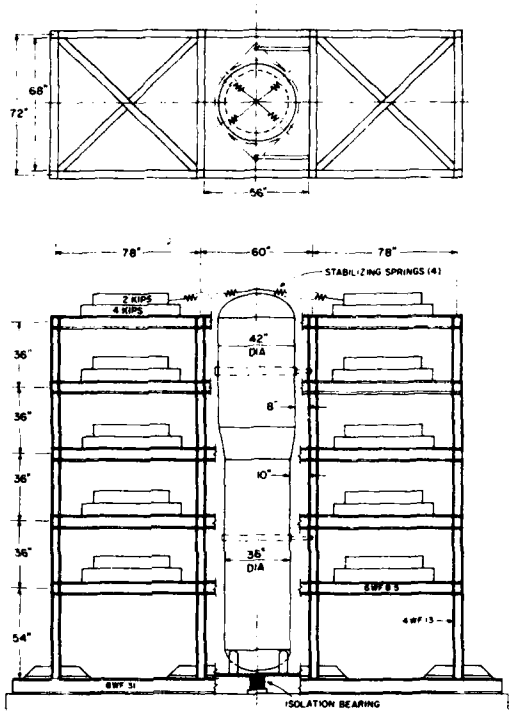


Fig. 2 Experimental Model for the Steel Frame with the Steam Generator

Observations from Test Results

To analyze test results it is convenient to refer specially to the following two extreme cases:

a) Steam generator rigidly connected to the table and elastically connected to the frame (conventional design)

b) Steam generator on rubber bearings, but not connected to the frame

Frame Response

The frame response was not very different in cases (a) and (b) and, in general, not significantly affected by the interaction with the steam generator.

Generator Response

In all the tests the steam generator responded essentially as a rigid body. All the other characteristics of the response were very significantly affected by the interaction with the frame.

In particular in case (a) accelerations were high and a rocking motion was predominant, due to some rotational flexibility of the "rigid" base connection.

In case (b) the accelerations were strongly cut down, due to base isolation, but the maximum displacements relative to the frame were almost doubled. Although the displacements were more uniformly distributed along the height than in case (a) there was still an important rocking motion of the generator.

Design Considerations for the Isolation System

From the observation of test results of these two extreme cases, it is clear that there are definite trade-offs between case (a) and case (b). The most

practical ("optimal") solution is probably somewhere in-between these two extreme cases. Major factors influencing response of the generator in these intermediate cases are location and mechanical properties of energy-absorbers. Since rocking motion is particularly undesirable for tall structures like the one in consideration, the most efficient isolation system is the one which minimizes rocking motion of the steam generator. At the same time lateral displacements and accelerations should be kept within reasonable limits. In subsequent sections an optimal design problem is formulated which is based upon the above considerations.

Mathematical Model of the Test Structure

From the test results, it is seen that there is very little influence of the generator on the frame response. Moreover, it was observed that the predominant response of the frame was in its first mode in the linear range. Thus, an equivalent elastic single degree of freedom system is used to represent the frame (Fig. 3). The displacements at the energy-absorbing device levels are computed based on first mode amplitudes. Based on the test results the generator is modelled as a rigid body with two degrees of freedom, lateral translation and rotation. The energy-absorbing devices are modelled using an axial stiffness element with the following constitutive equation (7)

$$\dot{F}(t) = \frac{F_0}{U_0}\left[\dot{u}(t) - |\dot{u}(t)|\left(\frac{F(t)}{F_0} - S(t)\right)^n\right] \tag{3}$$

$$S(t) = \alpha\left[\frac{u(t)}{U_0} - \frac{F(t)}{F_0}\right] \tag{4}$$

where F(t) is force in the device, U(t) is its displacement and $\dot{u}(t)$ the displacement rate. F_0, U_0, α and n are material property parameters. Physically, F_0 and U_0 are roughly yield force and yield displacement, α controls slope after yielding and n controls sharpness of transition from elastic to inelastic range. Note that, since this problem could not be modelled using the standard MINI-ANSR element library, special elements applicable only to this problem were developed for the analysis.

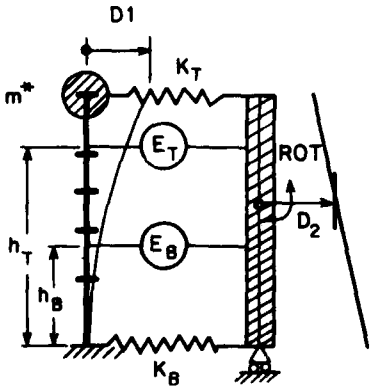


Fig. 3 Mathematical Model of the Test Structure

Design Problem Formulation

The isolation system design problem is formulated as a sequence of min-max problems. The objective is to minimize rotations of the steam generator subjected to constraints on relative displacements at the energy-absorber levels and accelerations of the steam generator. Conventional constraints are imposed to produce practical locations of energy-absorbers and positivity of design variables. Initially only the location of the energy-absorbers along the height of the steam generator is considered to vary, resulting in two design variables. Next, assuming that both devices have the same stiffness characteristics, four design variables, two locations and F_0 and U_0 are considered. Finally, the location and mechanical property parameters of both devices are allowed to vary, resulting in a design problem with six variables. In the first case, the starting values used were taken from the experimental program. In subsequent cases, starting values were the final values (improved, but not necessarily optimal) of the previous design case. The objective and constraint functions and their gradients are expressed as follows:

Objective function:

$$\min_{\underline{z}} \max_{t} [\theta(\underline{z},t)]^2 \tag{5}$$

$\underline{z}$ = Design variable vector

$\theta(\underline{z},t)$ = Rotation of the generator. Following (8), equation (5) can be expressed in nonlinear programming format by introducing an additional dummy cost variable as follows:

$$\min_{\underline{z}} z_d$$

such that $z_d \geq \max_t [\theta(\underline{z},t)]^2$

The design vector will now be written as:

$$\underline{z} = (z_d, z_1, z_2, \ldots, z_N)^T$$

Thus, the objective function is, $f(\underline{z}) = z_d$ and its gradient $\nabla f(z) = [1,0,\ldots,0]^T$.

Functional Constraints

(i) From objective function transformation:

$$\max_t [\theta(\underline{z},t)]^2 \leq z_d$$

$$\max_t \phi^1(\underline{z},t) = \frac{1}{z_d}[\theta(\underline{z},t)]^2 - 1.0 \leq 0$$

(ii) Constraint on relative displacement at top energy-absorbing device level

$$\max_t [U_1^R(\underline{z},t)]^2 \leq \delta^2$$

$U_1^R(\underline{z},t)$ = Relative displacement at top energy-absorber

δ = Allowable relative displacement

Thus, $\max_t \phi^2(\underline{z},t) = \frac{1}{\delta^2}[U_1^R(z,t)]^2 - 1.0 \leq 0$

(iii) Constraint on relative displacement at bottom energy-absorbing device level

$$\max_t [U_2^R(\underline{z},t)]^2 \leq \delta^2$$

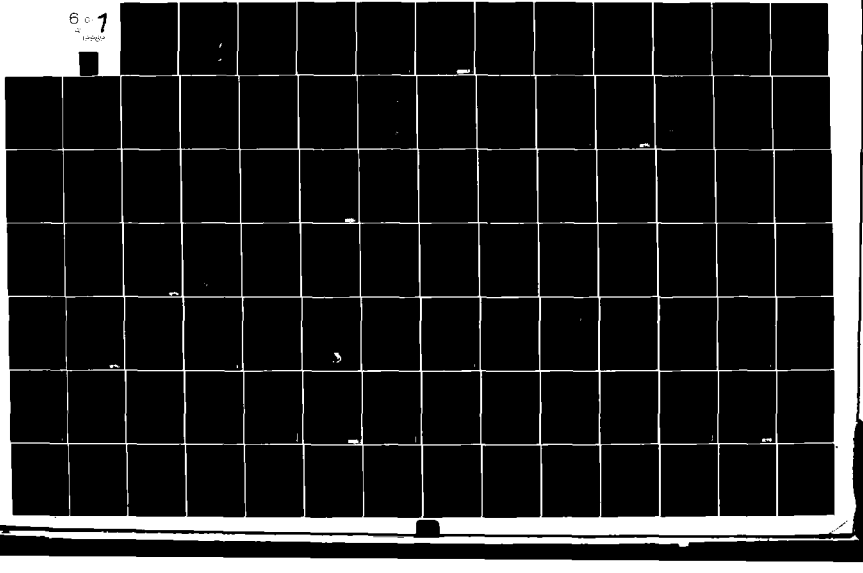
Thus, $\max_t \phi^3(\underline{z},t) = \frac{1}{\delta^2}[U_2^R(\underline{z},t)]^2 - 1.0 \leq 0$

(iv) Constraint on absolute acceleration of the generator

$$\max_t [\ddot{U}_G(\underline{z},t) + \ddot{U}_T(t)]^2 \leq \delta_a^2$$

AD-A119 989 ARIZONA UNIV TUCSON COLL OF ENGINEERING F/G 13/13
PROCEEDINGS OF THE INTERNATIONAL SYMPOSIUM ON OPTIMUM STRUCTURA--ETC(U)
1981 E ATREK, R H GALLAGHER N00014-80-G-0041
UNCLASSIFIED NL

6 of 7



$\ddot{U}_G(\underline{z},t)$ = Acceleration of the generator relative to the table.

$\ddot{U}_T(t)$ = Acceleration of the table

δ_a = Allowable value of the absolute acceleration.

Thus, $\max_t \phi^4(\underline{z},t) = \frac{1}{\delta_a^2}[\ddot{U}_G(\underline{z},t)+\ddot{U}_T(t)]^2 - 1.0 \leq 0$

Gradients of Functional Constraints

$$\nabla\phi^1(\underline{z},t) = \frac{2\theta(\underline{z},t)}{z_d}\left[-\frac{1}{2z_d}\theta(\underline{z},t), \frac{\partial\theta(\underline{z},t)}{\partial z_1},\ldots,\frac{\partial\theta(\underline{z},t)}{\partial z_N}\right]^T$$

$$\nabla\phi^2(\underline{z},t) = \frac{2U_1^R(\underline{z},t)}{\delta^2}\left[0, \frac{\partial u_2^R(\underline{z},t)}{\partial z_1},\ldots,\frac{\partial u_1^R(\underline{z},t)}{\partial z_N}\right]^T$$

$$\nabla\phi^3(\underline{z},t) = \frac{2U_2^R(\underline{z},t)}{\delta^2}\left[0, \frac{\partial U_2^R(\underline{z},t)}{\partial z_1},\ldots,\frac{\partial U_2^R(\underline{z},t)}{\partial z_N}\right]^T$$

$$\nabla\phi^4(\underline{z},t) = \frac{2[\ddot{U}_G(\underline{z},t)+\ddot{U}_T(t)]}{\delta_a^2}\left[0, \frac{\partial\ddot{U}_G(\underline{z},t)}{\partial z_1},\ldots,\frac{\partial\ddot{U}_G(\underline{z},t)}{\partial z_N}\right]^T$$

Conventional Constraints

(i) Constraints on maximum height of the devices

$h_T = z_1 \leq H$

$h_B = z_2 \leq H$

h_T = height of top device

h_B = height of bottom device

H = Total height of the generator

Thus, $g^1(\underline{z}) = \frac{z_1}{H} - 1.0 \leq 0$

$g^2(\underline{z}) = \frac{z_2}{H} - 1.0 \leq 0$

(ii) Constraints on minimum height of the devices.

$h_T = z_1 \geq H_{min}$

$h_B = z_2 \geq H_{min}$

H_{min} = minimum practical height

Thus, $g^3(\underline{z}) = -z_1 + H_{min} \leq 0$

$g^4(\underline{z}) = -z_2 + H_{min} \leq 0$

(iii) Positivity constraints

$g^5(\underline{z}) = -z_3 \leq 0$

$g^{N+2}(\underline{z}) = -z_N \leq 0$

Gradients of Conventional Constraints

$\nabla g^1(\underline{z}) = [0,\frac{1}{H},0,\ldots,0]^T$

$\nabla g^2(\underline{z}) = [0,0,\frac{1}{H},0,\ldots,0]^T$

$\nabla g^3(\underline{z}) = [0,-1,0,\ldots,0]^T$

$\nabla g^4(\underline{z}) = [0,0,-1,0,\ldots,0]^T$

$\nabla g^5(\underline{z}) = [0,0,0,-1,0,\ldots,0]^T$

$\nabla g^{N+2}(\underline{z}) = [0,\ldots,0,-1]^T$

Numerical Results of the Optimization Problem

Numerical results for the optimization problem previously formulated are presented in table 1 and in Fig. 5-12. The input acceleration used in the analyses was one of the records produced by the shaking-table during the tests (Fig. 4). It roughly corresponds to the El Centro NS 1940 record, with amplitudes multiplied by 0.75 and time scale divided by $\sqrt{3}$

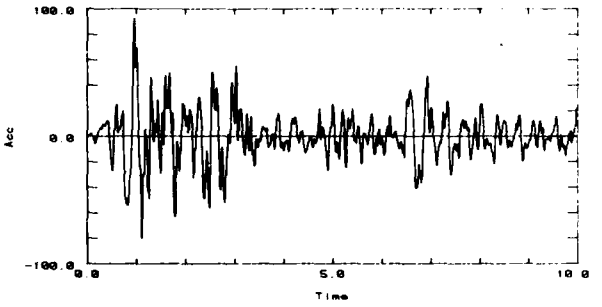


Fig. 4 Table Acceleration (in/sec^2) (Modified El Centro 1940 NS Component)

Table 1 shows:

a) Values of the optimization parameters corresponding to the initial design. They were chosen from the experimental tests as the ones giving the best results according to the enunciated design criteria.

b) Values of the parameters corresponding to an "improved" design after performing 15 iterations of the optimization procedures, where only two parameters, namely the locations h_T, h_B of the two energy-absorbers, were allowed to vary.

c) Values of the parameters corresponding to a new "improved" design after 30 iterations, where 4 parameters were allowed to vary.

d) as in (c) but with all 6 parameters varying.

As noted before values of the last iteration for one case were used as starting values for the subsequent case.

In Fig. 5, 6 and 7 the time history of rotation of the steam generator is presented for the three "improved" designs corresponding to the cases of 2, 4 and 6 design variables, respectively. The thin line shows, for comparison, the response corresponding to the initial design. The reduction of the maximum rotation and therefore the degree of improvement is apparent throughout. In particular for the final design, that is for the case with 6 variables, the maximum rotation in radiants is 0.0034, to be compared with a value of 0.006 for the initial design.

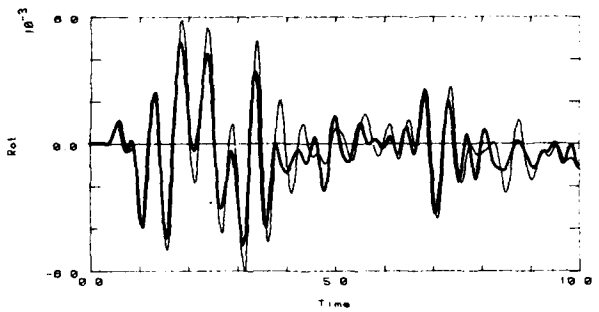


Fig. 5 Steam Generator Rotations (rad) (Case of 2 Design Variables)

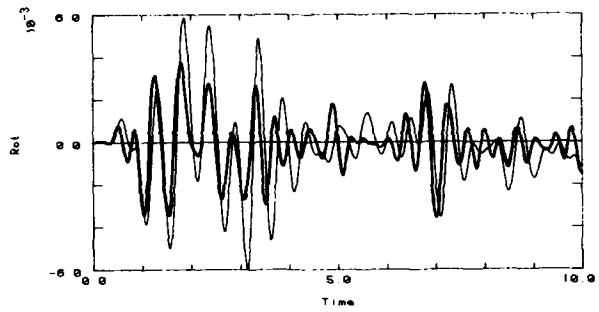


Fig. 6 Steam Generator Rotations (rad) (Case of 4 Design Variables)

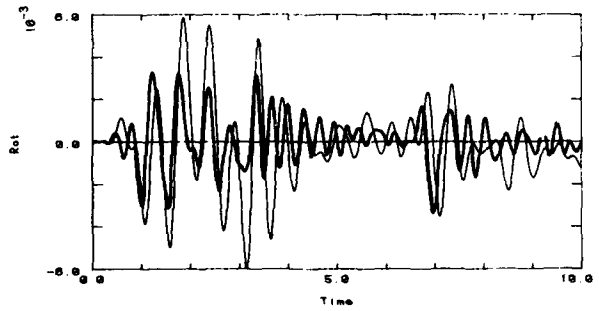


Fig. 7 Steam Generator Rotations (rad) (Case of 6 Design Variables)-Final Design

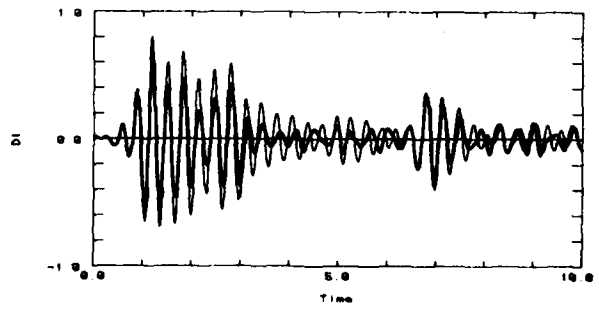


Fig. 8 Steel Frame Displacements at Top Floor (in)-Final Design

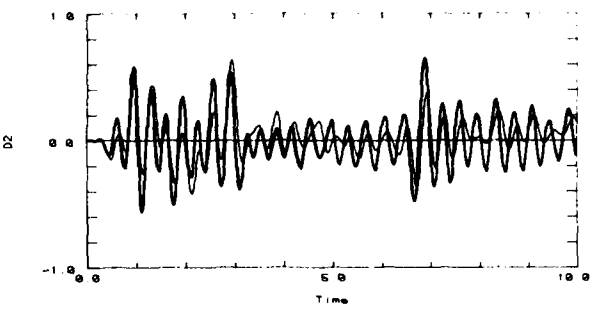


Fig. 9 Steam Generator Displacements (in)-Final Design

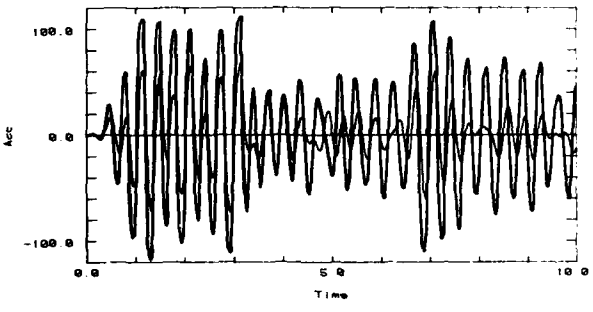


Fig. 10 Steam Generator Accelerations (in/sec^2)-Final Design

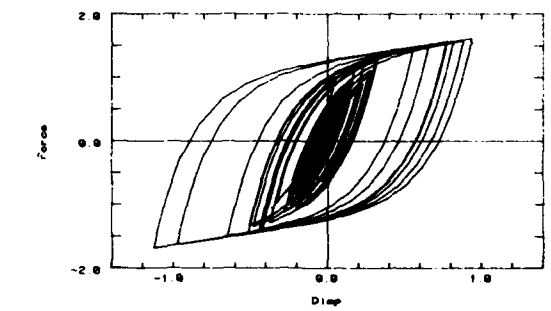


Fig. 11 Hysteresis Loops for Top Energy-Absorber (Force in Kips, Displacements in inches)-Final Design

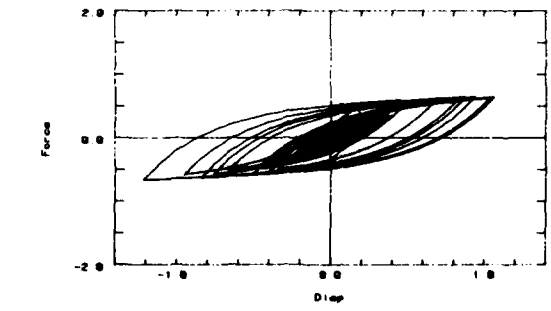


Fig. 12 Hysteresis Loops for Top Energy-Absorber (force in Kips, Displacements in inches)-Initial Design

Table 1

	F_{OT} (kips)	U_{OT} (inches)	F_{OB} (kips)	U_{OB} (inches)	h_T (inches)	h_B (inches)
Initial Design	0.65	0.45	0.65	0.45	160.	80.
2 variables (15 iter.)	0.65	0.45	0.65	0.45	179.	60.
4 variables (30 iter.)	1.12	0.42	1.12	0.42	176.	63.
6 variables (30 iter.)	1.46	0.25	1.25	0.31	173.	63.

Figures 8, 9 and 10 give, only for the final design, time histories of top floor displacement of the steel frame, lateral displacement and lateral total acceleration of the generator. Again the thin line gives corresponding time-histories for the initial design.

Note the slight reduction of the frame response and the growth of the generator acceleration in the final design. Finally Figs. 11 and 12 show the hysteretic response in the top energy-absorber, for the final and initial design respectively, and give an idea of the different energy dissipation involved in the two cases.

Concluding Remarks

Optimal design of two problems belonging to different categories is presented. These problems, even though somewhat academic in nature, serve the following important purposes:

(i) They clearly point out the need to have a flexible software system where new problem formulations can be easily incorporated.

(ii) The importance of user interaction and graphics is emphasized. In the braced frame example, graphics and interaction played a very important role in detecting and correcting poor computational behavior.

(iii) The isolation system design problem brings out an important feature which is related to scaling. The objective was to minimize rotation of the generator and the starting design gave a maximum rotation of roughly 6×10^{-3}. When this quantity is squared, it becomes even smaller, thereby increasing numerical difficulties because of round-off. A simple solution is to scale the rotations by a suitable factor (a factor of 1000 was used here). Since the magnitude of rotations may change drastically during the solution process, one scale may not be appropriate throughout and the system should allow the possibility of changing it interactively.

Acknowledgement

Research sponsored by the National Science Foundation Grant PFR-7908261. The support of Professor Ciampi by the Italian National Research Council during the course of the research is gratefully acknowledged.

References

(1) Pister, K. S., "Optimal Design of Structures Under Dynamic Loading," NATO-NSF Advanced Study Institute on Optimization of Distributed Parameter Structures, University of Iowa, Iowa City, Iowa, May 21 - June 4, 1980.

(2) Miura, H. and Schmit, L. A., Jr., "ACCESS-1, Approximation Concepts for Efficient Structural Synthesis - Program Documentation and User's Guide," NASA CR-144905, National Aeronautics and Space Administration, May 1976.

(3) Arora, J. S., Nguyen, D. T., Belegundu, A. D. and Rajan, S. D., "Design Optimization Codes for Structures-DOCS," Technical Report No. 71, Division of Materials Engineering, The University of Iowa, Iowa City, Iowa, August 1980.

(4) Bhatti, M. A., Ciampi, V., Pister, K. S. and Polak, E., "OPTNSR-An Interactive Software System for Optimal Design of Statically and Dynamically Loaded Structures with Nonlinear Response," Report No. UCB/EERC-81/02, Earthquake Engineering Research Center, University of California, Berkeley, January 1981.

(5) Bhatti, M. A., Ciampi, V., Pister, K. S. and Polak, E., "An Interactive Software System for Optimal Design of Statically and Dynamically Loaded Structures with Nonlinear Response," These proceedings.

(6) Kelly, J. M. "Shake Table Testing of Steam Generator Seismic Response," EPRI Report, in preparation.

(7) Bhatti, M. A. and K. S. Pister," Transient Response Analysis of Structural Systems with Nonlinear Behavior," Computers and Structures, Vol. 13, No. 1-3, pp. 181-188, June 1981.

(8) Bhatti, M. A., "Optimal Design of Localized Nonlinear Systems with Dual Performance Criteria Under Earthquake Excitations," Report No. UCB/EERC 79/15, Earthquake Engineering Research Center, University of California, Berkeley, CA, July 1979.

APPENDIX A

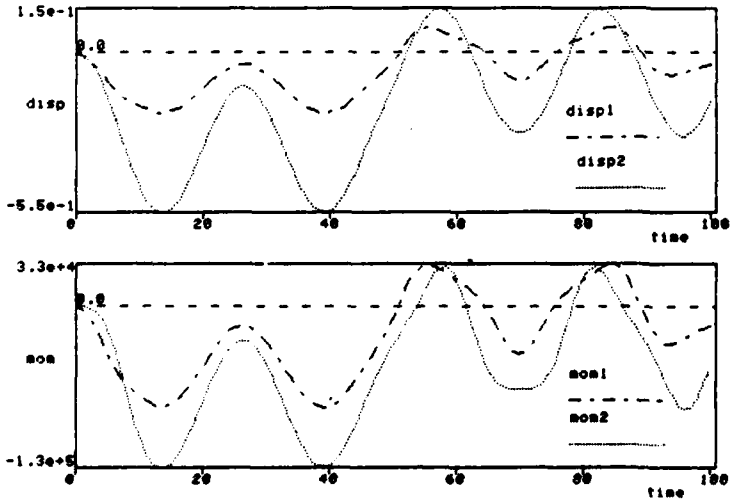
Dialogue for the Braced Frame Problem

```
Optimization Based Computer-Aided Design Group
      University of California
        Berkeley, California
            U. S. A.


          INTRAC-OPTDYN
An Interactive Optimization Program for
Design Problems Which can be Expressed as

                Minimize  f (z)
                   z
subject to
                  max  phi(z,t) (= 0
                   t
                      g(z)      (= 0

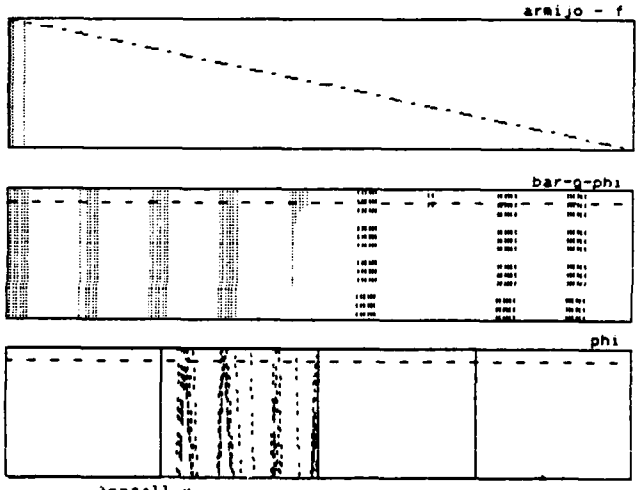
 Name of input data file:
( Default is "/usr/optcad/ciampi/optnsr.d/data" )
>brace.data
>print z
    20.0000
    20.0000
    20.0000
    20.0000
>run 10 store
The results of the entire computation will be stored
in the arrays FG PSIG and ZG(N:K)
Please state the total number of iterations you intend to
carry out: type in K = ?
    #100
I = 1  F = 0.545595  PSI = 29.7801
       THETA = 0.   E = 0.2
I = 2  F = 0.792752  PSI = 0.282556
       THETA = -0.504697  E = 0.2
I = 3  F = 0.815954  PSI = 0.19247
       THETA = -1.04588  E = 0.2
I = 4  F = 0.816696  PSI = 0.171042
       THETA = -1.30981  E = 0.2
I = 5  F = 0.81582  PSI = 0.152171
       THETA = -1.16204  E = 0.2
I = 6  F = 0.815235  PSI = 0.147019
       THETA = -0.995485  E = 0.2
I = 7  F = 0.994551  PSI = 0.0600003
       THETA = -0.121528  E = 0.2
I = 8  F = 0.979406  PSI = 0.
       THETA = -0.752086  E = 0.2
I = 9  F = 0.939237  PSI = 0.
       THETA = -3.69285E-4  E = 0.1
I = 10  F = 0.927019  PSI = 0.
       THETA = -3.32648E-4  E = 0.1
>print z
    93.3724
    17.8780
    70.7374
    68.0096
>grinit
enter terminal type (2=4027 3=RAMTEK 4=HP 5=4025):
4
>gdisp
>gmom
```




```
>run 4 store
I = 11  F = 0.914564  PSI = 0.
       THETA = -3.20792E-4  E = 0.1
I = 12  F = 0.901812  PSI = 0.
       THETA = -3.08574E-4  E = 0.1
I = 13  F = 0.900658  PSI = 0.
       THETA = -2.95997E-4  E = 0.025
I = 14  F = 0.859285  PSI = 0.
       THETA = -8.28777E-5  E = 0.025
>print z
    83.8015
    14.3257
    60.2608
    57.8666
>step3
Execution suspended at the end of STEP3
You may want to modify
 1. THETA parameters: PUSHF, PUSHG, PUSHPH, SCALE
 2. smear parameter: E
 3. test parameters: DELTA, MU1, MU2
Precomputation of the tests in STEP4 and STEP5
indicates that the program will branch to STEP6
>prtang
angles between search direction and cost
and e-active constraints gradients


function      angle          push-factors

F              180.             PUSHF =1
>armijo 20 graphos
rmijo test satisfied after 6  iterations
```




```
>prtall u
I = 15  F = 0.858089  PSI = 0.
       THETA = -3.11836E-4  E = 0.025
>step3
Execution suspended at the end of STEP3
You may want to modify
 1. THETA parameters: PUSHF, PUSHG, PUSHPH, SCALE,
 2. smear parameter: E
 3. test parameters: DELTA, MU1, MU2
Precomputation of the tests in STEP4 and STEP5
indicates that the program will branch to STEP6
>prtang
angles between search direction and cost
and e-active constraints gradients


function      angle          push-factors

F              123.722            PUSHF =1.
PHI(2,17)      91.3297         PUSHPH(2) = 1.
PHI(2,42)      90.7919         PUSHPH(2) = 1.
>armijo 20 graphos
Armijo test satisfied after 7. iterations

>prtall 0
I = 16  F = 0.810688  PSI = 0.
       THETA = -9.57191E-5  E = 0.025
>step3
Execution suspended at the end of STEP3
You may want to modify
 1. THETA parameters: PUSHF, PUSHG, PUSHPH, SCALE,
 2. smear parameter: E
 3. test parameters: DELTA, MU1, MU2
Precomputation of the tests in STEP4 and STEP5
indicates that the program will branch to STEP6
```

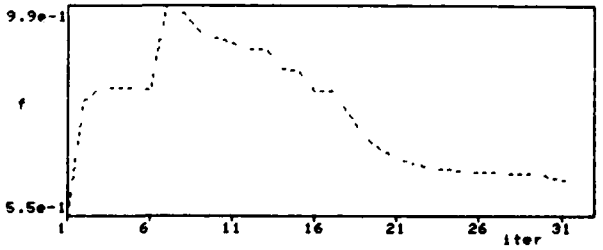
```
>prtang
angles between search direction and cost
and e-active constraints gradients


function      angle          push-factors

F               180.            PUSHF =1.
G(5)            115.447           PUSHG(5) = 1
>armijo 20 graphos
rmijo test satisfied after 6. iterations
>prtall 0
I = 17  F = 0.809427  PSI = 0
        THETA = -3.35419E-4  E = 0.025
>step3
Execution suspended at the end of STEP3
You may want to modify
 1. THETA parameters: PUSHF, PUSHG, PUSHPH, SCALE,
 2. smear parameter: E
 3. test parameters: DELTA, MU1, MU2
Precomputation of the tests in STEP4 and STEP5
indicates that the program will branch to STEP6
>prtang
angles between search direction and cost
and e-active constraints gradients


function      angle          push-factors

F               120.734           PUSHF =1.
G(5)            90.5866           PUSHG(5) = 1.
PHI(2,42)     90.7561           PUSHPH(2) = 1.
>armijo 20 graphos
Armijo test satisfied after 7. iterations
>prtall 0
I = 18  F = 0.767099  PSI = 0.
        THETA = -8.72311E-5  E = 0.025
>set e=0.4
>set delta=1.e-7
>run 5 store
RESTART STEP2
I = 18  F = 0.767099  PSI = 0.
        THETA = -4.169E-4  E = 0.4
I = 19  F = 0.714417  PSI = 0.
        THETA = -1.09364E-4  E = 0.4
I = 20  F = 0.686152  PSI = 0.
        THETA = -2.08688E-4  E = 0.4
I = 21  F = 0.669059  PSI = 0.
        THETA = -4.168E-4  E = 0.2
I = 22  F = 0.659096  PSI = 0.
        THETA = -2.30062E-4  E = 0.2
>run 10 store
I = 23  F = 0.648823  PSI = 0.
        THETA = -2.35104E-4  E = 0.2
I = 24  F = 0.645509  PSI = 0.
        THETA = -2.51892E-4  E = 0.1
I = 25  F = 0.642181  PSI = 0.
        THETA = -2.5219E-4  E = 0.1
I = 26  F = 0.640577  PSI = 0.
        THETA = -4.03809E-4  E = 0.05
I = 27  F = 0.638971  PSI = 0.
        THETA = -4.01688E-4  E = 0.05
I = 28  F = 0.635625  PSI = 0.
        THETA = -2.49178E-4  E = 0.05
I = 29  F = 0.634614  PSI = 0.
        THETA = -2.50443E-4  E = 0.05
I = 30  F = 0.633601  PSI = 0.
        THETA = -2.50826E-4  E = 0.025
I = 31  F = 0.625075  PSI = 0.
        THETA = -9.67802E-9  E = 0.025
I = 32  F = 0.624293  PSI = 0.
        THETA = -6.25456E-8  E = 0.025
>print z
    35.9056
    13.1914
    48.7632
    15.4738
>graphf n
```

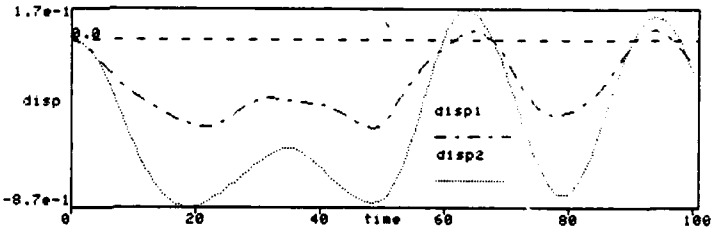


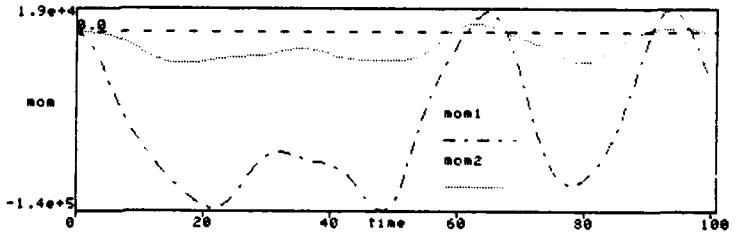

```
>run 30 prtall
I = 33  F = 0.623093  PSI = 0.
        THETA = -7.97265E-8  E = 0.025

I = 34  F = 0.622455  PSI = 0.
        THETA = -4.80294E-4  E = 0.025
I = 35  F = 0.621077  PSI = 0.
        THETA = -3.10373E-4  E = 0.025
I = 36  F = 0.6208  PSI = 0.
        THETA = -1.05315E-7  E = 0.025
I = 37  F = 0.620499  PSI = 0.
        THETA = -1.13584E-7  E = 0.025
I = 38  F = 0.620174  PSI = 0.
        THETA = -1.22273E-7  E = 0.025
I = 39  F = 0.620168  PSI = 0.
        THETA = -1.2572E-7  E = 0.025
I = 40  F = 0.619781  PSI = 0.
        THETA = -2.82831E-4  E = 0.0125
I = 41  F = 0.619569  PSI = 0.
        THETA = -1.55934E-4  E = 0.0125
I = 42  F = 0.619526  PSI = 0.
        THETA = -3.4879E-4  E = 0.00625
I = 43  F = 0.619483  PSI = 0.
        THETA = -3.48728E-4  E = 0.00625
I = 44  F = 0.61927  PSI = 0.
        THETA = -1.5601E-4  E = 0.00625
I = 45  F = 0.618031  PSI = 0.
        THETA = -2.43822E-5  E = 0.00625
I = 46  F = 0.618029  PSI = 0.
        THETA = -1.24928E-7  E = 0.00625
I = 47  F = 0.617913  PSI = 0.
        THETA = -2.8418E-4  E = 0.003125
I = 48  F = 0.617699  PSI = 0.
        THETA = -1.56505E-4  E = 0.003125
I = 49  F = 0.616444  PSI = 0.
        THETA = -2.47142E-5  E = 0.003125
I = 50  F = 0.616442  PSI = 0.
        THETA = -1.2364E-7  E = 0.003125

**************************************************
**********
   congratulations, here is the optimal solution

   objective function value=  0.616442d+00
>gdisp
>gmom
```






```
>print z
    35.1873
    13.1253
    57.1415
    10.0012

>stop
%
```

AD-P000 089

SWAY FRAMES OPTIMIZATION BY MEANS OF MINI COMPUTERS

P. Stojanovski, Assistant Professor
University "Kiril & Metodij" in Skopje
Faculty of Civil Engineering
91000 SKOPJE, Rade Končar - 16, YUGOSLAVIA

Summary

This paper deals with optimization of steel sway frames subject to stress, displacement and buckling constraints. The basic objective of the work is to develop an efficient method for sway frames optimization, which could be easily used on mini computers. The problem is formulated as a mathematical programming one, although some ideas and results from the optimality criteria based methods are employed.

The algorithm consists of a series of analysis and optimization steps. Sequential Linear Programming (SLP) in connection with adaptive move limits is used as mathematical model. The only design variables are the cross sectional properties of the structural members. They are assumed to be continuous. The objective function is formulated with non-negative coefficients, so that the dual simplex method could be used.

It is assumed that in the optimum solution only a limited number of the displacement constraints is active. Therefore only few displacement constraints should be formulated, the choice of which depends on the engineering experience and estimation of the designer.

Another assumption is that dominant portion of normal stresses is due to bending moments. By suitable transformations and simplifications, the stress constraints are stated as lower bounds of the design variables.

Buckling constraints are incorporated into the stress constraints. Only buckling of the elements is considered.

The method was checked with the results obtained by other workers. In all the cases fair results were obtained with less iterations. This gives hope that the method proposed could be efficiently used in civil engineering practice.

Introduction

Sway frames are frequently used in civil engineering practice. They withstand large wind and seismic loads without lateral bracing or any other safeguard, and resist deflections in their own plane by their flexural stiffness. It has been found out that the lateral sway often governs the choice of sections for their members (1). It is also evident that exact design of these frames is quite complicated problem. This is even emphasized when one tries to optimize this class of structures. In such a case a realistic objective could be the design which satisfies all the design requirements, while minimizing the weight or cost of the structure. In spite of the problem complexity, many authors have been working on frame optimisation by means of different approaches and some very good results have been achieved.

Brown and Ang (2) used the Rosen's "gradient projection method" for minimum weight elastic design of steel rigidly jointed frames. As they suggest, the method is rational and suitable for large digital computers.

Romstad and Wang (3) employed an SLP technique to get minimum weight design of trusses, continuous beams and rigid frames subject to stress and displacement constraints.

Arora, Haug and Rim (4) used state space optimal control technique to optimize plane frames. In addition to AISC Code requirements they also imposed displacement, natural frequency and design variables constraints on the frames considered.

Calafell and Willmert (5) proposed an SLP method for planar frames, which avoids formal analyses of the structure. The solution scheme employs some pivoting techniques to bypass Phase I of the simplex method, which speeds up the iteration process.

Majid (6) elaborated a general approach to linear structural optimization. Cross sectional properties of the elements together with the joint displacements are assumed as design variables.

Saka (7) presented a method, based on the same assumptions as in reference (6), for minimum weight design of rigidly jointed frames. Stress and displacement constraints according to B.S.449 were taken into consideration. The feature of the method is that no analysis of the structure is carried out during the iteration procedure.

Majid, Stojanovski and Saka (8) gave a method for minimum cost topological design of steel multistorey frames in which economic and some architectural requirements determine their final shape. They showed that this problem could be formulated as mixed variable integer programming problem, The examples presented showed that a minimum weight design, on its own, is not a sound philosophy to be taken as a substitute for a minimum cost design.

Levey and Fu (9) formulated the minimum weight design of frames as a discrete optimization problem. They used the complex-simplex method as a solution method, while the problem was formulated by means of the plastic collapse theory.

Miller and Moll (10) considered gabled frames with tapered members only and developed a computer program for their minimum weight design. The modified interior penalty function approach was used. The results obtained are of fair practical value. This work shows a possible way to make practising civil engineers familiar with structural optimisation.

PRECEDING PAGE

This paper is an attempt to produce an algorythm for sway frames minimum weight design, which will be able to reflect the real structural behaviour, while being relatively simple and easy for realization by means of mini computers. The following presentation of the method should reveal its advantages and limitations.

The design problem

This paper treats minimum weight design of steel sway frames subject to stress, displacement and local buckling constraints. The shape and topology of the frame are assumed to be constant. The structural elements are taken to be prismatic. The problem constraints are formulated according to Yugoslav Standards (11), although with no difficulty any other standards may be employed.

The design variables

The cross sectional areas of the structural members are taken as design variables. They are assumed to be continuous. All the relevant geometric properties of the cross sections are uniquely expressed in terms of the member areas, as shown in Fig.1. and equations (1).

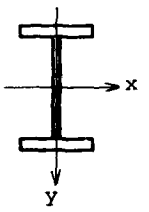


Fig.1. Cross section of a tipical structural element

$$I_x=a.A^b \qquad i_x=(I_x/A)^{0,5}=p.A^q$$
$$W_x=c.A^d \qquad i_y=r.A^s \qquad (1)$$

Here, I_x is the second moment of area about the x-axis, W_x is the appropriate section modulus, A is the area of the cross section, i_x is the radius of gyration about the x-axis, i_y is the radius of gyration about the y-axis, while a,b,c,d,p,q,r and s are constans dependent on the type of sections used. These could be obtained similarly as in reference (12). In such a manner the designer is able to use any table of available sections. Indeed, the real structures are composed out of discrete sections, but these assumptions considerably simplifie the problem formulation and solution.

The objective function

Since, only the minimun weight design of steel frames is considered, all coefficients of the objective function are non-negative. This means that a dual solution to the linearized problem is readily available. Therefore, the dual simplex method is used, which speeds up the iteration process.

The solution method

The structures considered are subject to stress, displacement and buckling constraints, which are formulated for selected set of joints and members only. It is well known that displacements and stresses in a structure are nonlinear functions of the design variables $\underline{A}(A_1,A_2,\ldots,A_{NG})$. This means that the problem is a nonlinear one.However, it could be solved in an iterative manner by successive linearization of the problem functions and application of some linear programming method.In spite of some drawbacks, the SLP techniques have some very useful features: robustness, reliability and simplicity.

The linearization of the constraints is carried out by means of their linear Taylor approximations. In such a way in the ν-th iteration the linear programming problem (the LP problem) could be cast in following form:

$$\text{Minimize} \quad \sum_{i=1}^{NG} l_i.A_i,$$

subject to (2)

$$S_j(\underline{A})=S_j(\underline{A}^\nu)+\nabla S_j(\underline{A}^\nu).(\underline{A}-\underline{A}^\nu) \leq S_{j,p}$$
$$j=1,2,\ldots..NC$$

The meaning of the symbols used is as follows:

NG - number of different groups of elements

NC - number of constraints

l_i - total length of all elements with cross sectional area A_i

A_i - cross sectional area of group i

$S_j(\underline{A})$ - j-th constraint of the design problem

$S_j(\underline{A}^\nu)$ - value of the constraint function S_j at a given point $\underline{A}^\nu(A_1,\ldots,A_{NG})$

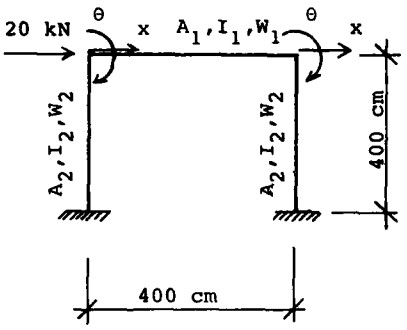
$\nabla S_j(\underline{A}^\nu)$ - gradient vector of S_j evaluated at $\underline{A}^\nu$

$\underline{A}$ - vector of unknown design variables

$\underline{A}^\nu$ - vector of the current values of the design variables

Note that appropriate adaptive move limits are added to the constraints in equations (2) in order to get and mantain convergence.

It is quite obvious that the accuracy of the linear approximations governs the accuracy of the whole iterative procedure. A very important question is how large move limits could be allowed and still to have good enough approximations of the constraints. A problem similar to this one has been treated by Storaasli and Sobieszczanski (13). They concluded that for the highly idealized finite element representation of their sample structure, the approximation's error is less than 16% over a range of -50% to 50% for simultaneous multielement modifications. Because in the advanced stages of the iteration the move limits are pretty tight the linear approximations in equations (2) are fully acceptable. Steel sway frames show similar behaviour, although for some types of loading the approximation's error could be higher then reported in reference (13). For example, consider the portal frame shown in Fig.2. This frame was analyzed for A_1=60 cm^2 and A_2=80 cm^2. Then A_1 and A_2 were gradualy varied (one at a time) from -100% to +100%. The response of the structure was computed by means of Taylor approximations and by means of an exact analysis. The outcome of this consideration was that sway frames could be more sensitive to the changes of some design



$I=0.995 \cdot A^{2.176}$

$W=1.007 \cdot A^{1.524}$

$E=21000\ kN/cm^2$

Fig.2. A portal frame

variables. For example, the dimensionless curves showing the accuracy of the joint displacements x and θ in terms of the change in A_2 are plotted in Fig.3.

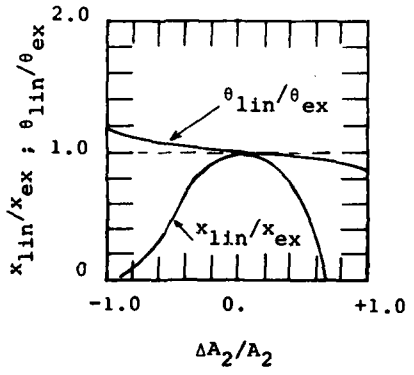


Fig.3. Accuracy of joint displacements for the portal frame

A brief inspection of these diagrams shows that for an engineering acceptable error of ±15%, the appropriate change in A_2 should not be greater then approximately 28%. Similar diagrams for other response quantities could be easily obtained.

On the basis of these considerations the following strategy for the move limits size was adopted:

The iteration starts with relatively large move limits (not more than ±50%). During the iteration process they are gradualy reduced till the convergence of the solution is obtained. The convergence criterion is the relative change of the volume in two subsequent iterative steps, which should be less then a specified tolerance ε. The value of 0.01 for ε was found to be satisfactory.

The design constraints

The displacement constraints

The joint displacements of the frame are functions of the cross sectional areas, because all geometric characteristics of the cross sections are uniquely related to them through equations (1).So it could be writen:

$$\underline{U}=\underline{U}(\underline{A}) \qquad (3)$$

Here,
$\underline{U}=(U_1,U_2,\ldots,U_{DF})$ is the vector of joint displacements, DF is the number of degrees of freedom of the frame and $\underline{A}$ is the vector of design variables.

If $\underline{A}^\nu=(A_1^\nu,\ldots,A_{NG}^\nu)$ denotes the current design in the ν-th iteration, U_j one of the joint displacements and δ_j its permissible value, the representative displacement constraint takes the following form:

$$|U_j| \leq \delta_j \text{ , or}$$

$$-\delta_j \leq U_j \leq \delta_j \qquad (4)$$

The function U_j could be linearized in the neghbourhood of the current design $\underline{A}^\nu$,taking the first order terms in its Taylor expansion:

$$U_j=U_j^\nu+\nabla U_j(\underline{A}^\nu).(\underline{A}-\underline{A}^\nu) \qquad (5)$$

Separation of the terms in equation (5) gives:

$$U_j=(U_j^\nu-\nabla U_j(\underline{A}^\nu).\underline{A}^\nu) + \nabla U_j(\underline{A}^\nu).\underline{A} \qquad (6)$$

If c_j denotes the expression in parentheses, the final linearized form of the displacement U_j is:

$$U_j= c_j^\nu + \nabla U_j(\underline{A}^\nu).\underline{A} \qquad (7)$$

, where c_j is a constant defined in each iterative step as

$$c_j^\nu= U_j^\nu - \nabla U_j(\underline{A}^\nu).\underline{A}^\nu \ ;$$

U_j^ν is the value of the displacement U_j in the ν-th iteration and $\nabla U_j(\underline{A}^\nu)$ is the gradient of U_j evaluated at $\underline{A}^\nu$.

Replacing equation (7) in (4) it is possible to write:

$$\nabla U_j(\underline{A}^\nu).\underline{A} \leq \delta_j - c_j \qquad (8a)$$

$$-\nabla U_j(\underline{A}^\nu).\underline{A} \leq \delta_j + c_j \qquad (8b)$$

From these relations it could be seen that for each restricted joint displacement, two constraints should be formulated. However, it is possible to take only one of equations (8) into consideration:

When $U_j^\nu > 0$ equation (8a) holds, and

when $U_j^\nu < 0$ equation (8b) is valid.

The key question in the previous consideration is the evaluation of the gradient components in a given design point $\underline{A}^\nu$. In other words the question is how to calculate the partial derivatives of the specified displacements for each current design $\underline{A}^\nu$. A very exact method for these calculations is given in reference (14)in the following form:

$$\partial\underline{U}/\partial A_i = -\underline{K}^{-1}.(\partial\underline{K}/\partial A_i).\underline{U} \qquad (9)$$

, where $\underline{K}$ is the overall stiffness matrix of the structure. Note, that use of equation (9) gives the derivatives of all displacements with respect to only one design variable A_i. This might be impractical in cases when only few joint displacements are restricted.

Another way of obtaining the derivatives of a given joint displacement, with respect to all design variables, is to use the dummy load approach due to Gellatly and Berke (15). The outcome of this approach is:

$$\partial U_l/\partial A_i = -\underline{U}^T.(\partial \underline{K}/\partial A_i).\underline{U}_l \qquad (10)$$

In equation (10) U_l is the l-th joint displacement, $\underline{U}^T$ is the transpose of the joint displacements vector due to external loads, while $\underline{U}_l$ is the vector of joint displacements due to a unit dummy load $\bar{P}_l=1$ in the direction of U_l. It should be pointed out that equation (10) could be expressed in terms of element displacements. In such a manner only elements with size characteristic A_i will contribute to $\partial U_l/\partial A_i$. The implementation of equation (10) requires a unit dummy load to be added, as a separate loading case, for each restricted joint displacement. The main feature of this method is that it is relatively easy to get the derivatives of any joint displacement with respect to any design variable. More details on this topic could be found elswere (15). In this paper equation (10) was used to obtain the joint displacement derivatives.

The stress constraints

Exact formulation. The influence of normal stresses is dominant for steel sway frames, although in some cases shear stresses could influence the design of some structural elements. However, in this paper only normal stresses are taken into consideration. Shear stresses could be easily incorporated into the problem formulation on the expence of some increase of the problem size.

The stress constraints could be defined for different groups of elements, one constraint per group with same cross sectional properties. This means that it is sufficient to find the representative element for each group. Then for the group j (j=1,2,....,NG) the stress constraint could be stated as:

$$|\sigma_j| \leq \sigma_{j,p} \qquad (11)$$

,where σ_j is the actual stress in the representative member and $\sigma_{j,p}$ is the permissible stress for group j.

Following the same reasoning as for the displacement constraints, the stress constraint for group j takes form:

$$\nabla\sigma_j(\underline{A}^\nu).\underline{A} \leq \sigma_{j,p} - \gamma_j^\nu \qquad (12a)$$

$$-\nabla\sigma_j(\underline{A}^\nu).\underline{A} \leq \sigma_{j,p} + \gamma_j^\nu \qquad (12b)$$

Here, $\nabla\sigma_j(\underline{A}^\nu)$ is the gradient vector of the stress σ_j at the current design point $\underline{A}^\nu$, and γ_j^ν is a constant defined in the ν-th iterative step as $\gamma_j^\nu = \sigma_j^\nu - \nabla\sigma_j(\underline{A}^\nu).\underline{A}^\nu$.

The normal stress in a frame element consists of two parts: one due to the normal force and another due to the bending moment:

$$\sigma_j = \sigma_j^N \pm \sigma_j^M \qquad (13)$$

Assuming that the influence of the bending moments is dominant, only one of equations (12) should be used, as shown in the next few lines.

1. When $N_j^\nu \geq 0$ and $M_j^\nu \geq 0$, then
   $|\sigma_j| = \sigma_j^N + \sigma_j^M \leq \sigma_{j,p}$; i.e. equation (12a) holds
2. When $N_j^\nu \geq 0$ and $M_j^\nu < 0$, then
   $-\sigma_{j,p} \leq |\sigma_j| = -\sigma_j^N + \sigma_j^M$; i.e. equation (12b) holds
3. When $N_j^\nu < 0$ and $M_j^\nu \geq 0$, then
   $|\sigma_j| = -\sigma_j^N + \sigma_j^M \leq \sigma_{j,p}$; i.e. equation (12a) holds
4. When $N_j^\nu < 0$ and $M_j^\nu < 0$, then
   $-\sigma_{j,p} \leq |\sigma_j| = \sigma_j^N + \sigma_j^M$; i.e. equation (12b) holds.

On the basis of this discussion it is easy to see that only one stress constraint per group of elements should be formulated. This constraint is set up for that element of the group j, which has the highest absolute value of the bending moment in the ν-th iteration. Note, that the combination of the biggest normal force and the appropriate bending moment is not taken into consideration. This case will be treated for compression members only, in the paragraph considering the buckling constraints. Futhermore, this load combination is important for column design only.

The gradient of the function σ_j at a given design point $\underline{A}^\nu$could be found by differentiating the equation (13) with respect to the design variables A_i (i=1,.,NG):

$$\partial\sigma_j/\partial A_i = \partial\sigma_j^N/\partial A_i \pm \partial\sigma_j^M/\partial A_i \qquad (14)$$

The two terms on the right hand side of the equation (14) could be defined as follows:

Since, $\sigma_j^N = N_j/A_j$

it is possible to differentiate this expression and get

$$\partial\sigma_j^N/\partial A_i = \frac{(\partial N_j/\partial A_i).A_j - N_j.(\partial A_j/\partial A_i)}{A_j^2} \qquad (15)$$

Similarly, $\sigma_j^M = M_j/W_j$ gives

$$\partial\sigma_j^M/\partial A_i = \frac{(\partial M_j/\partial A_i).W_j - M_j.(\partial W_j/\partial A_i)}{W_j^2} \qquad (16)$$

If use is made of equations (1) it could be concluded that:

$$\partial A_j/\partial A_i = \begin{cases} 0 \text{ for } i\neq j \\ 1 \text{ for } i=j \end{cases}$$

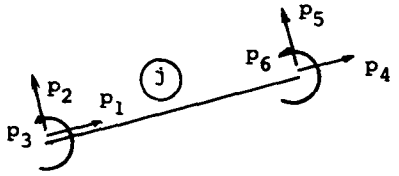
and

$$\partial W_j/\partial A_i = \begin{cases} 0 \text{ for } i \neq j \\ c.d.A_i^{d-1} \text{ for } i=j \end{cases}$$

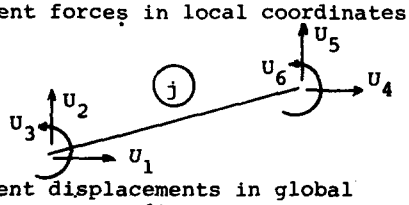
A brief analysis of equations (15) and (16) shows that the stress change in an element, when one design variable is varied, consists of two parts:

- one due to force redistribution in the elements, caused by the change of the design variable;
- and another due to the direct influence of the variable change on the stress considered.

The terms $\partial N_j/\partial A_i$ and $\partial M_j/\partial A_i$ in equations (15) and (16) could be evaluated similarly as in reference (16). The idea is that N_j and M_j are components of the vector of element forces of the representative element, as shown in Fig.4.



a) Element forces in local coordinates



b) Element displacements in global coordinates

Fig.4. Element forces and displacements

Futhermore, this vector could be easily related to the system joint displacements by means of the well known relation:

$$\underline{p}_j = \underline{k}_j.\underline{R}_j.\underline{U}_j + \underline{p}_j^* \qquad (17)$$

Here,

$\underline{p}_j$ is the vector of the element forces,

$\underline{U}_j$ is the vector of global end displacements of the representative element,

$\underline{p}_j^*$ is the vector of fixed ends forces,

$\underline{k}_j$ is the element stiffness matrix, and

$\underline{R}_j$ is the transformation matrix relating the end displacements of the element in the local and global coordinate system.

The components of the vectors $\underline{p}_j$ and $\underline{U}_j$ are shown in Fig.4.

Equation (17) could be differentiated with respect to A_i, which gives

$$\partial \underline{p}_j/\partial A_i = (\partial \underline{k}_j/\partial A_i).\underline{R}_j.\underline{U}_j + \underline{k}_j.\underline{R}_j.(\partial \underline{U}_j/\partial A_i) \qquad (18)$$

By means of equation (18) it is easy to calculate the derivatives of all element forces. Note, that the vector $\partial \underline{p}_j/\partial A_i$ contains all the relevant derivatives in equations (15) and (16).

From all these considerations it could be concluded that the exact stress constraints formulation is more complicated and time consuming then the formulation of the displacement constraints. It is also obvious that for their formulation at a given design point it is necessary to compute the derivatives of all joint displacements with respect to all design variables, as shown in Table 1.

JOINT DISPLACEMENTS	DESIGN VARIABLES 1		DESIGN VARIABLES i		DESIGN VARIABLES NG
1	$\partial U_1/\partial A_1$	.	$\partial U_1/\partial A_i$	.	$\partial U_1/\partial A_{NG}$
	.	.	.	.	.
1	$\partial U_1/\partial A_1$	.	$\partial U_1/\partial A_i$	.	$\partial U_1/\partial A_{NG}$
	.	.	.	.	.
DF	$\partial U_{DF}/\partial A_1$	.	$\partial U_{DF}/\partial A_i$	.	$\partial U_{DF}/\partial A_{NG}$

Table 1. The joint displacements derivatives

It should be pointed out that the stress constraint, when the maximum bending moment is in the span of the element, could be easily formulated, as shown in reference (16).

Approximate formulation. This formulation of the stress constraints is derived on the basis of two assumptions. The first one is that in two subsequent iterative steps the difference *in member forces* is relatively small. The other one is that stresses in an element depend on its cross sectional properties only, neglecting the influence of other elements on the redistribution of element forces and stresses. It is eveident that these assumptions are not always fulfiled strongly enough. However, for steel sway frames, the sway frequently governs the design, so that stresses are not active at the optimal design (8). Then, this formulation should preserve the permissible stress level in the structural elements.

Let M_j^ν and N_j^ν denote the maximum absolute values of the bending moment and the appropriate normal force for group j in the ν-th iteration. In such a manner the stress constraint for group j could be stated as:

$$N_j^\nu/A_j + M_j^\nu/W_j \leq \bar{\sigma}_{j,p} \qquad (19)$$

After some rearrangement and substituting equation (1) into (19) it is possible to write:

$$A_j \geq \left[\frac{c.N_j^\nu.A_j^{d-1} + M_j^\nu}{c.\sigma_{j,p}}\right]^{1/d} \qquad (20)$$

This expression could be considerably simplified if on the right hand side A_j^ν (the current value of the design variable A_j) is introduced instead of A_j. Thus, the final expression of the stress constraint for the group j is:

$$A_j \geq \left[\frac{c.N_j^{\nu}.(A_j^{\nu})^{d-1} + M_j^{\nu}}{c.\sigma_{j,p}} \right]^{1/d} \qquad (21)$$

The expression in brackets is constant for each iterative step, so that the stress constraints are defined as lower bounds of the design variables.

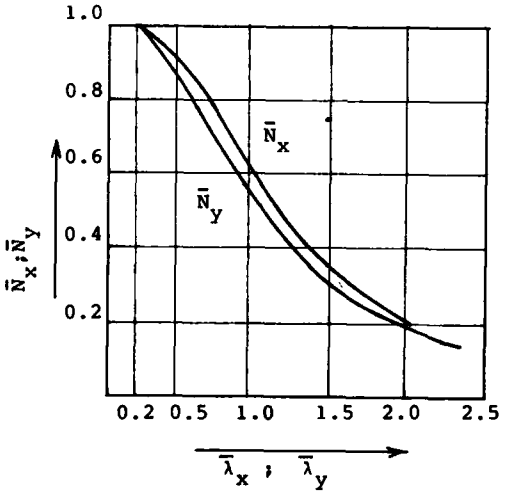
The buckling constraints

These constraints are set up for the columns only. Their formulation is based on reference (11) and takes into consideration the local buckling of the columns. The frames are assumed to be braced against "out of plane" buckling on each floor level, and that no bending moments act about the y-axis of the cross section (Fig.1). Few quantities, as specified in reference (11), are defined before the buckling constraints are set up.

a) Critical buckling stresses

$$\sigma_{cr,x}=\bar{N}_x.\sigma_y \qquad \sigma_{cr,y}=\bar{N}_y.\sigma_y \qquad (22)$$

Here, $\sigma_{cr,x}$ and $\sigma_{cr,y}$ are the critical buckling stresses about the x and y-axes, $\bar{N}_x$ and $\bar{N}_y$ are dimensionless coefficients defined in the standards and σ_y is the yielding stress of the material. The coefficients $\bar{N}_x$ and $\bar{N}_y$ are functions of the dimensionless coefficients λ_x and λ_y, as stated in the Yugoslav standards, and shown in Fig.5.



$$\lambda_E = \pi(E/\sigma_y)^2$$

$$\lambda_x=l_{ix}/i_x \qquad \lambda_y=l_{iy}/i_y$$

$$\bar{\lambda}_x=\lambda_x/\lambda_E \qquad \bar{\lambda}_y=\lambda_y/\lambda_E$$

Fig.5. Buckling curves according to JUS E7-081

In Fig.5. λ_E, λ_x, and λ_y are the the slenderness ratios of the section, E is the Young's modulus, i_x and i_y are the radii of gyration about the x and y-axis, while l_{ix} and l_{iy} are the effective buckling lengths about the two axes of the cross section.

b) Euler stresses, defined as

$$\sigma_{E,x}=\pi^2E/\lambda_x^2 \qquad \sigma_{E,y}=\pi^2E/\lambda_y^2 \qquad (23)$$

According to reference (11) to prevent local buckling of the elements the following conditions should be satisfied:

$$\frac{N}{A} + \frac{\mu}{\mu-1}.\frac{\beta M + Nf_0}{W} \leq \sigma_p \qquad (24)$$

$$N/A \leq \sigma_{cr,y}/\nu \qquad (25)$$

Here, N is the normal force in the element, M is the bending moment, A is the cross sectional area, W is the section modulus, μ is a coefficient defined as $\mu=A\sigma_{E,x}/N$, β is a coefficient dependent on the bending moments at the ends of the column - given with

$$\beta = 0.4 + 0.4\, M_1/M_2 \geq 0.4$$

$$|M_1| \leq |M_2|$$

$$M = |M_2|$$

In equation (25) ν denotes the safety factor, which ranges from 1,5 to 1.2 . The coefficient f_0 includes the effects of the initial imperfections of the structural element. It is described as

$$f_0 = (\sigma_y/\sigma_{cr,x} - 1).(1 - \sigma_{cr,x}/\sigma_{E,x}).\frac{W}{A} \qquad (26)$$

Denoting $s=(\sigma_y/\sigma_{cr,x} -1).(1 -\sigma_{cr,x}/\sigma_{E,x})$ and replacing the equation (1) into (26), the expression for f_0 becomes

$$f_0 = s.c.A^{d-1} \qquad (27)$$

The equation (24) could be simplified by replacing

$t = \mu/(\mu-1)$, and

substituting the equation (27) into it:

$$\frac{N}{A} + t\frac{\beta M + N.s.c.A^{d-1}}{c.A^d} \leq \sigma_p \qquad (28)$$

This expression could be rearranged in the following form:

$$A \geq \left[\frac{A^{d-1}.c.(1+t.s).N + t.\beta.M}{c.\sigma_p} \right]^{1/d} \qquad (29)$$

Similarly the equation (25) could be given as:

$$A \geq N.\nu/\sigma_{cr,y} \qquad (30)$$

On the basis of equations (29) and (30) it is possible to state the buckling constraints as lower bounds of the design variables A. To do this the same logic as for the displacement constraints applies. In such a manner the buckling constraints are formulated as:

$$A_j \geq N_j^{\nu}.\nu/\sigma_{cr,y} \qquad (31)$$

$$A_j \geq \left[\frac{c.(1+t.s).N_j^{\nu}.(A_j^{\nu})^{d-1} + t.\beta.M_j^{\nu}}{c.\sigma_{j,p}} \right]^{1/d} \quad (32)$$

Here, N_j^{ν} and M_j^{ν} are the maximum compression axial force and the appropriate bending moment for group j in the ν-th iteration. The other terms in the equations (31) and (32) have been defined previously.

The evaluated form of the buckling constraints shows that only one of the equations (31) and (32) should be used; the one which gives higher lower bound for the design variable A_j.

The design procedure

The proposed design procedure is based on the assumption that for steel sway frames, the horizontal joint displacements (or at least some of them) are active in the optimal design. The stress constraints are eventualy active in few sections, and they are formulated by means of the aproximate formulation given in the preceding paragraph. In other words the stress constraints are treated similarly as in some optimality criteria based methods. This formulation of the stress constraints preserves the stress level in the structural elements not to exceed its permissible value. The buckling constraints are given in similar form. In the cases when no significant horizontal joint displacements occur, the stress constraints should be formulated by means of the time and size consuming exact formulation, also given in the preceding paragraph. However, in such a case it is discussible whether such a frame could be considered as a sway frame.

The design procedure consists of the following steps:

1. Set up a table of available sections. All structural elements will be designed using this table. The table could be defined in any chosen manner, although some standardized table of sections is preffered.
2. Evaluate the coefficients a,b,c,d,p,q,r and s in equations (1).
3. Select the vector of initial design variables $\underline{A}^{\nu}$. Here, the superscript ν has the value 1 for the initial design. Prefferably the initial design should be feasible.
4. Analyze the structure for the external loads and the cross sectional properties defined with the current design $\underline{A}^{\nu}$.
5. Set up the coefficients of the objective function.
6. Arrange the move limits. Start the iterations with large move limits (±50%), and gradually reduce them to ±5%.
7. Calculate the derivatives of the restricted joint displacements by means of equation (10).
8. Using the results obtained in step 7 set up the displacement constraints.
9. Calculate the lower bounds of the design variables to meet the stress requirements, by means of equation (21).
10. Calculate the lower bounds of the design variables to satisfy the buckling constraints, by means of equs. (31) and (32).
11. Rearrange the move limits set up in step 6, if necessary. For some of the design variables the lower bounds might be defined by the stress or buckling requirements (step 9 and step 10).
12. Solve the LP problem, the objective function of which is set up in step 5. The constraints of the problem are defined in step 8. The lower bounds of the variables are stated in step 11, while the upper bounds are defined in step 6. Note, that the LP problem is solved by the standard dual simplex method, as given in reference (17). Also the lower bounds algorythm has been employed. In this manner a new solution $\underline{A}^{\nu+1}$ is available.
13. Check up the convergence. The experience obtained so far, shows that the objective function converges much better and faster then the design variables. The convergence criterion is that the relative change of the objective function in two subsequent iterative steps should be less then a spesified tolerance ε. If the convergence criterion is not satisfied set ν=ν+1 and proceed to step 3. If the convergence criterion is satisfied go to the next step.
14. Analyze the structure for the last set of design variables and print out all the relevant results.

The design examples

The design examples presented have also been solved elswere (4),(7).

The value of Young's modulus was taken as 20700 kN/cm^2.

Example 1. A two storey frame

This example has also been solved in reference (4). The frame geometry, acting loads and the cross sectional characteristics are shown in Fig.6.

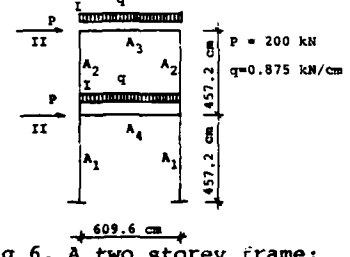
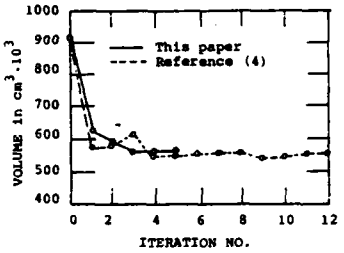


Fig.6. A two storey frame: geometry and loads

The permissible normal stress was taken as 16,5 kN/cm^2, while the yield sress is 25 kN/cm^2. The constans a,b,c,d,p,q,r and s have the values 1.724, 2.0, 0.87, 1.5, 1.313, 0,5, 0.768 and 0.5 respectively. The horizontal deflection of the second storey is restricted to 4.38 cm, while the horizontal displacement of the first storey is limited to 2,54 cm. The vertical displacements of the joints are limited to 2.54 cm. Two loading

conditions are applied to the structure, in Fig.6 denoted by symbols I and II.

The iterations were initiated from the same feasible design point as in reference (4): $A_1=A_2=A_3=A_4=$ 300 cm^2. The convergence criterion was satisfied after 5 iterative steps, the optimal values of the design variables being: A_1=250, A_2=132, A_3=124 and A_4=226 cm^2. The value of the objective function was reduced to 562661 cm^3, as opposed to 561789 cm^3 in reference (4), which is approximately 0,16% higher. Maximum stress violation was recorded in the first storey beam in amount of 1,08%, for the loading case II. The horizontal displacement of the first storey is at its upper bound. The iteration history of this structure is shown in Fig.7.



Fig,7. Iteration history of the two storey frame

Example 2. A four storey frame

This example has been solved in reference (7), as well. The geometry of the frame, acting loads and the cross sectional properties of the members are shown in Fig.8.

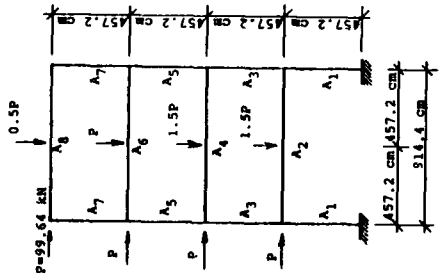


Fig.8. A four storey frame: geometry and loads

The structure is subject to stress and displacement constraints only. The values of a,b,c and d in equation (1) are taken as 3.2, 2.0, 1.452, and 1.5 respectively. The limits on the horizontal deflections of each storey are given as 1.41, 2.81, 4.22 and 5.63 cm respectively. The midspan vertical deflections of the beams are limited to 2.54 cm. The normal stresses are restricted to 16.5 kN/cm^2. The iterations were initiated from a feasible design point: $A_1=.....=A_8=280$ cm^2.

Convergence was obtained after 8 redesign steps, with optimal solution being:

A_1=231, A_2=230, A_3=184, A_4=262, A_5=145, A_6=186, A_7=148 and A_8=122 cm^2. The volume of the optimal frame is 135150 cm^3, as opposed to 134500 cm^3 in reference (7). The iteration history of this structure is shown in Fig.9. Note, that the problem formulation in reference (7) required 214 constraints and 36 design variables, while the method presented needed 24 constraints and 8 variables only.

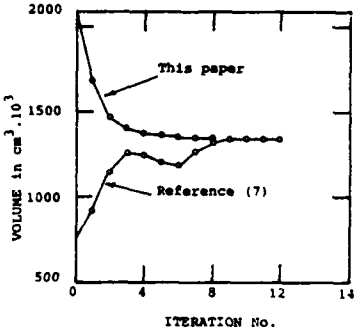


Fig.9. Iteration history of the four storey frame

References

(1) Majid,K.I.,Anderson,D., Elastic-Plastic Design of Sway Frames by Computer. Proc. ICE,41. UK, Dec. 1968.

(2) Brown,D.M.,Ang,A.H.-S., Structural Optimization by Nonlinear Programming. Jour.Struct.Div.,ASCE,ST6, Dec. 1966.

(3) Romstad,K.M.,Wang,C.K., Optimum Design of Framed Structures.Jour.Struct.Div., ASCE,ST12, Dec. 1966.

(4) Arora,J.S.,Haug,E.J.-Jr.,Rim,K., Optimal Design of Plane Frames. Journal of the Structural Division,ASCE,ST10, Oct. 1975.

(5) Calafell,D.O.,Willmert,K.D., Automated Resizing Optimization of Generally Loaded Frames via Linear Programming Techniques. Proc.Symp.Appls.Comp.Meths.in Engrg., Univ. S. Calif.,USA, August 1977.

(6) Majid,K.I., Optimum Design of Structures, Newnes-Butterworths,London,1974.

(7) Saka,M.P., Optimum Design of Rigidly Jointed Frames.Comps.Structs.,Vol.11,1980.

(8) Majid,K.I.,Stojanovski,P.,Saka,M.P., Minimum Cost Topological Design of Steel Sway Frames.The Struct.Engr.,V.58B, 1980.

(9) Levey,G.E.,Fu,K-C., A method in discrete frame optimization and its outlook. Comps.&Structs,Vol.10,1979.

(10) Miller,C.J.,Moll,T.G.-Jr.,Automated Design of Tapered Member Gabled Frames. Comps.&Structs.,Vol.10,1979.

(11) Yugoslav Standards for Steel Structures: JUS-U.E7.081,JUS-U.E7.096,JUS-U.E7.111.

(12) Templeman,A.B.,Structural Design for Minimum Cost Using the Method of Geometric Programming.Proc.ICE,46, 1971.

(13) Storaasli,O.O.,Sobieszczanski,J.,On the Accuracy of the Taylor Approximations for Structure Resizing.AIAA Jour.,Feb. 1974.

(14) Gallagher,R.H.,Zienkiewicz,O.C., Optimum Structural Design,J.Wiley,N.Y.,1977.

(15) Kiusalaas,J.,Minimum Weight Design via Optimality Criteria.NASA. D-7113,Dec.1972.

(16) Moses,F.,Onoda,S.,Min. Weight Dsgn. of Strs. with Appl. to El. Grillages. Int. J,Num.Meths.Engrg.,Vol 1,1969.

(17) Kunzi,H.P. et al: Num. Meths. of Mathl. Optimization, Accademic Press,N.Y. 1971.

AD-P000 090

EFFICIENT OPTIMUM DESIGN OF STRUCTURES--PROGRAM PODU

Qian Lingxi, Zhong Wanxie, Sui Yunkang, Zhang Jintong
Research Institute of Engineering Mechanics
Dalian Institute of Technology, Dalian, China

Abstract

An efficient optimization algorithm is developed for the engineering structures subject to multiple constraints. The highly non-linear and implicit problem is reduced to a sequence of quasi-linear constraints and explicit problems of the statically determinated structures. The method is based on the Kuhn-Tucker necessary conditions for optimality associated with a simple quadratic programming to determine the lagrange multipliers and to delete non-active constraints simultaneously. A number of examples including trusses and wing structures show that the method is efficient when compared with other competing techniques.

I. Introduction

With the development in computer science, great progress has been achieved in many areas in structural mechanics. Of particular importance is the emergence of the finite element method which provides an unprecedented computational capability to analyze most complex structures. At the same time, it is natural that the desire of structural optimization arises in the field of structural mechanics research. In 1960, it was first suggested by Schmit (1) that the coupling of finite element method and non-linear mathematical programming would generate automated structural design capabilities. Since 1968, another approach, namely optimality criterion method was introduced by Venkayya, Berke, Gellatly and others (2), and has appeared to be more practical for the automated design of large scale systems. At the end of the last decade, considerable efficient gains had been achieved in the mathematical programming approach by using approximation concepts. The programs, ACCESS 1, 2 3, developed by Schmit and his colleagues (3,4,5) usually generates optimum design after only 5 to 10 structural analyses. The two approaches are now comparable not only in their efficiency but also in their basic concepts as pointed out by Sander and Fleury (6) who deduced a mixed method from these two approaches.

This paper takes advantage of success of the past works and presents a new algorithm which appears to be simple in basic idea and rather efficient in computational aspect. The highly non-linear and implicit problem is reduced to a sequence of quasi-linear constraints and explicit problems. The algorithm incorporates a redesign procedure based on the Kuhn-Tucker necessary conditions for optimality associated with a simple quadratic programming to determine the active constraints and corresponding lagrange multipliers. A modular program is coded in Structured FORTRAN language and automatically translated into FORTRAN IV by a S.F. translator made by ourself. Example problems are presented to illustrate its efficiencies.

II. Basic Concepts

Consider a class of structures with preassigned topology, geometrical configuration and material of construction. They can be idealized as two or three dimensional systems composed of 3 types of elements: truss bars, isotropic or orthotropic constant strain triangle elements (CST) and symmetric shear panel elements (SSP). The design variables are understood to be the cross section of the bar, the thickness of CST and SSP. Let A_i denote all these variables and α_i its reciprocals, the primal problem of optimum design can be stated as:

$$\text{"PO"} \quad \begin{cases} \text{Find } A_i \text{ such that the weight of structure:} \\ W = \sum_i \bar{w}_i A_i \longrightarrow \min. & (1) \\ \text{with: } \sigma_{il} \le \bar{\sigma}_i, \quad u_{jl} \le \bar{u}_j, & (2) \end{cases}$$

$$\underline{A}_i \le A_i \le \bar{A}_i. \qquad (3)$$

where

$\bar{w}_i$ -- the weight of element i when $A_i = 1$,

σ_{il} -- the stress in the ith element under the lth load condition,

u_{jl} -- the displacement in the jth constrained degree of freedom under the lth load condition,

$\bar{\sigma}_i, \bar{u}_j$ -- the allowable upper limits of σ_{il} and u_{jl},

$\underline{A}_i, \bar{A}_i$ -- the lower and upper bounds of the design variable A_i.

This non-linear mathematical programming problem "PO" is very complicated because:

1. There is a large number of design variables, and necessity to identify active/passive variables in the process of redesign.
2. There is a large number of inequalities constraints, many of which are implicit functions of design variables, and necessity to identify critical/non-critical constraints in the process of redesign.

A practicable algorithm should be efficient so that the number of reanalysis is no more than about 10; its convergence should be stable and preferably very fast in the first few steps.

To make this difficult problem tractable, we have to replace it by a sequence of relatively simple and explicit problems. This can be accomplished through the coordinated use of the following devices:

1. Design variable linking -- each independent variable A_k controls a linking group of dependent variables F_i or t_i:

   for bar: $F_i = A_{k(i)} F_i^\circ$ (4)

   for CST and SSP: $t_i = A_{k(i)} t_i^\circ$ (5)

   in which

   $A_{k(i)}$ -- dimensionless independent variable of the linking group k,

   F_i, t_i -- dimensional dependent design variables of element i,

F_i, t_i° -- relative cross section of bar or thickness of plate when $A_k = 1$.

2. Making the constraint functions explicit -- assuming no redistribution of internal forces as in a statically determinated structure temporarily in deriving the redesign formulas.

3. Making the constraint functions linear or nearly linear -- using of reciprocal design variable $\alpha_k = \frac{1}{A_k}$.

4. Unification of constraint form -- the stress and size constraints are reduced to the same form as displacement's by the virtual work conception.

5. Bringing the design point to the boundary of feasible region by scaling step.

6. Selection of active (critical) constraints -- crude selection firstly, then automated and precise selection by quadratic programming.

7. Approximate reanalysis techniques.

Through devices 1 to 4, the primal problem "PO" can be reduced to the following problem "P1":

$$\text{"P1"} \quad \begin{cases} \text{Find } \alpha_k \text{ so that:} \\ W(\alpha_k) = \sum_k L_k/\alpha_k \longrightarrow \min. & (6) \\ \text{with: } G_r(\alpha_k) = \sum \tau_{rk}\, \alpha_k - \bar{\Delta}_r \le 0 & (7) \end{cases}$$

$$(k = 1, 2, \ldots, m; \quad r = 1, 2, \ldots, n)$$

where

$\alpha_k (= \frac{1}{A_k})$ -- reciprocal independent design variable of linking group k,

L_k -- total weight of linking group k,

$$L_k = \sum_{i \in k} W_i \text{ when } A_k = 1,$$

$G_r(\alpha_k)$ -- unified expression of constraints including stress, displacement and size constraints (see section III).

τ_{rk} -- parameters which are constants in statically determinated structures so that the constraint function $G_r(\alpha_k)$ is linear of α_k (see section III),

$W(\alpha_k)$ -- objective function, non-linear with α_k.

The problem "P1" will be subject to further transformation in applying Taylor's second order expansion to the objective function and in taking $\delta\alpha_k$ instead of α_k as variables. It gives problem "P2":

$$\text{"P2"} \quad \begin{cases} \text{Find } \delta\alpha_k \text{ so that:} \\ W(\delta\alpha_k) = W^\circ + \sum_k \left(\frac{-L_k}{(\alpha_k^\circ)^2}\, \delta\alpha_k + \frac{L_k}{(\alpha_k^\circ)^3}\, (\delta\alpha_k)^2 \right) \longrightarrow \min. & (8) \\ \text{with } G_r(\delta\alpha_k) = G_r^\circ + \sum_k \tau_{rk}^\circ\, \delta\alpha_k \le 0 & (9) \end{cases}$$

$$(k = 1, 2, \ldots, m; \quad r = 1, 2, \ldots, n)$$

where

$\delta\alpha_k$ -- independent variables which are the changes of current design α_k°,

$W(\delta\alpha_k)$ -- quadratic objective function,

$W^\circ = \sum_k L_k/\alpha_k^\circ$ -- value of objective function of current design α_k°,

$G_r(\delta\alpha_k)$ -- constraint functions, linear with $\delta\alpha_k$,

$G_r^\circ = \sum_k \tau_{rk}^\circ\, \alpha_k^\circ - \bar{\Delta}_r$ -- value of constraint functions of the current design α_k°.

This problem "P2" is a quadratic programming. A sequence of them can replace the primal problem "PO" for statically determinated structures. It also can be used for statically indeterminated structures providing the parameters τ_{rk} updated after each iteration. But we proceed as in the following to seek further simplification.

The lagrangian of the problem "P2" is

$$\Phi(\delta\alpha_k, \mu_r) = W(\delta\alpha_k) + \sum_r \mu_r\, G_r(\delta\alpha_k) \qquad (10)$$

Hence the Kuhn-Tucker conditions of optimality give:

$$\frac{\partial\Phi}{\partial(\delta\alpha_k)} = 0, \quad \mu_r\, G_r = 0, \quad G_r \le 0, \quad \mu_r \ge 0 \qquad (11)$$

$$(k = 1, 2, \ldots, m; \quad r = 1, 2, \ldots, n)$$

which can be reduced to:

$$\delta\alpha_k = \frac{\alpha_k^\circ}{2} \left[1 - \frac{(\alpha_k^\circ)^2}{L_k} \sum_r \mu_r\, \tau_{rk}^\circ \right] \qquad (12)$$

$$G_r^\circ + \sum_k \tau_{rk}^\circ\, \delta\alpha_k \begin{cases} = 0 \text{ if } \mu_r > 0 \\ \quad \text{(critical)} \\ < 0 \text{ if } \mu_r = 0 \\ \quad \text{(non-critical)} \end{cases} \qquad (13)$$

The formula (12) gives $\delta\alpha_k$, the change of the current design α_k° provided that the lagrange multipliers μ_r are all known. But the determination of μ_r is correlated to the identification of critical constraints and has been a difficult task. The traditional trial and error procedure is practical only if a few of constraints are imposed, and is exceedingly expansive for most practical problems. Recently Schmit and Fleury (5) presented a sound method based on the dual programming. We shall do as follows. Substituting (12) into (13) gives:

$$-\sum_{\rho=1}^{n} t_{r\rho}\, \mu_\rho + br \begin{cases} = 0 \text{ if } \mu_r > 0 \\ \quad (r = 1, 2, \ldots, n), \\ < 0 \text{ if } \mu_r = 0 \end{cases} \qquad (14)$$

where

$$t_{r\rho} = \sum_k \frac{(\alpha_k^\circ)^3}{2L_k}\, \tau_{rk}^\circ\, \tau_{\rho k}^\circ \qquad (15)$$

$$(r, \rho = 1, 2, \ldots, n).$$

$$br = \sum_k \frac{\alpha_k^\circ}{2}\, \tau_{rk}^\circ + G_r^\circ \qquad (16)$$

We observe that the vector of lagrange multiplier $\{\mu_r\}$ satisfying (12) and (13) must be the optimum solution of the following quadratic programming:

$$\text{"P}\mu\text{"} \begin{cases} \text{Find } \{\mu\} \text{ so that:} \\ Q(\mu) = \frac{1}{2}\{\mu\}^t [T] \{\mu\} - \{b\}^t \{\mu\} \longrightarrow \min. & (17) \\ \text{with } \{\mu\} \geq 0. & (18) \end{cases}$$

where

$\{\mu\}$ -- a $(n \times 1)$ vector of lagrange multiplier with components μ_r,

$[T]$ -- a $(n \times n)$ matrix with components $t_{r\rho}$ given by (15),

$\{b\}$ -- a $(n \times 1)$ vector with components b_r given by (16). This can be proved since the Kuhn-Tucker conditions of problem "Pμ", is none other than (14). The matrix [T] must be positive definite, this can be ascertained since for any $(n \times 1)$ vector $\{y\}$, we have

$$\{y\}^t [T] \{y\} = \sum_{\rho=1}^{n} \sum_{r=1}^{n} y_\rho \{\sum_{k=1}^{m} \frac{(\alpha_k^\circ)^3}{2L_k} \tau_{rk}^\circ \tau_{\rho k}^\circ\} y_r =$$

$$= \sum_{k=1}^{m} \frac{(\alpha_k^\circ)^3}{2L_k} (\sum_{\rho=1}^{n} y_\rho \tau_{\rho k}^\circ \sum_{r=1}^{n} y_r \tau_{rk}^\circ) =$$

$$= \sum_{k=1}^{m} \frac{(\alpha_k^\circ)^3}{2L_k} (\sum_{r=1}^{n} y_r \tau_{rk}^\circ)^2 > 0 \qquad (19)$$

The quadratic programming "P_μ" is much simpler than "P2". The number of variables is n and equal to that of constraints. But it may be greatly reduced by a preliminary deletion of the probable non-critical constraints. At the beginning of each iteration we can throw away a part of constraints which satisfy

$$G_r = \sum_k \tau_{rk} \alpha_k - \bar{\Delta}_r \leq -\beta|\bar{\Delta}_r| \qquad (20)$$

where β is a slack coefficient 0.2~0.4. The lagrange multipliers corresponding to these deleted constraints are assumed to be zero. A point must not be overlooked: the remaining constraints must be linearly independent.

In summary, with a current design α_k°, we formulate the quadratic programming "P_μ" which will determine the lagrange multipliers μ_r, then substitute them into (10) we obtain $\delta\alpha_k$ and a new design $\alpha_k = \alpha_k^\circ + \delta\alpha_k$ which will be the start point of the next iteration.

III. Formulation of Constraint Functions

The unified expression of different constraint functions is

$$G_r = \sum_{k=1}^{m} \tau_{rk} \alpha_k - \bar{\Delta}_r \leq 0, \qquad (21)$$

where r(=1,2,...,n) is No. of constraint, k(=1,2,...,m) is No. of independe t variable, $\bar{\Delta}_r$ and τ_{rk} will be described in the following for different constraints.

1. For displacement constraint $U_j - \bar{U}_j \leq 0$, in (20):

$$\bar{\Delta}_r = \bar{U}_j \qquad (22)$$

$$\sum_{k=1}^{m} \tau_{rk} \alpha_k = \sum_{k=1}^{m} \alpha_k \sum_{i \in k} \tau_{ji} = U_j \qquad (23)$$

where $\alpha_k = \frac{1}{A_k}$, the reciprocal independent design variable controlling the size of element i, τ_{ji} is the contribution of element i to the displacement u when $\alpha_k = 1$ and

$$\tau_{rk} = \sum_{i \in k} \tau_{ji} \qquad (24)$$

When element i is a bar (fig. 1a),

$$\tau_{ji} = (\frac{N_x N_x^j \ell}{EF^\circ})_i. \qquad (25)$$

When element i is a CST element (fig. 1b)

$$\tau_{ji} = [\lambda_1 N_x N_y^j + \lambda_2 (N_x N_y^j + N_y N_x^j) + \lambda_3 N_y N_y^j + \lambda_4 N_{xy} N_{xy}^j]_i. \qquad (26)$$

When element i is a SSP element (fig. 1c)

$$\tau_{ji} = [\lambda_1 N_x N_x^j + \lambda_4 N_{xy} N_{xy}^j]_i. \qquad (27)$$

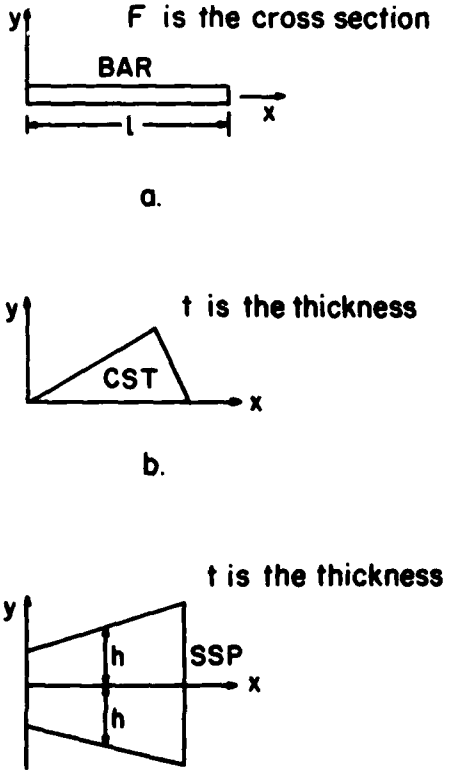


Fig. 1 elements

In formulas (25) (26) (27):

$(N_x, N_y, N_{xy})_i$ -- internal forces in element i due to real external loads which produce u_j,

$(N_x^j, N_y^j, N_{xy}^j)_i$ -- internal forces in element i due to virtual loads corresponding to u_j.

$$\lambda_1 = \frac{aD_3}{D_1D_3 - D_2^2}\ ,\ \lambda_2 = -\frac{aD_2}{D_1D_3 - D_2^2}\ ,$$
$$\lambda_3 = \frac{aD_1}{D_1D_3 - D_2^2}\ ,\ \lambda_4 = \frac{a}{D_4}\ , \tag{28}$$

where:

a -- surface area of CST and SSP element,

D_1, D_2, D_3, D_4 -- physical modulus for the orthotropic material in the Hook's law:

$$\begin{Bmatrix} N_x \\ N_y \\ N_{xy} \end{Bmatrix} = \begin{bmatrix} D_1 & D_2 & 0 \\ D_2 & D_3 & 0 \\ 0 & 0 & D_4 \end{bmatrix} \begin{Bmatrix} \varepsilon_x \\ \varepsilon_y \\ \varepsilon_{xy} \end{Bmatrix}. \tag{29}$$

2. For stress constraint $\sigma_j - \bar{\sigma}_j \le 0$, in (21):

$$\begin{cases} \bar{A}_r = \bar{\sigma}_j \\ \sum_{k=1}^{m} \tau_{rk}\,\alpha_k = \sum_{k=1}^{m} \alpha_k \sum_{i \in k} \tau_{ji} \end{cases} \tag{30}$$

$$\begin{cases} = (\sigma_x)_j & \text{for bar} \\ = (\sigma_x^2 + \sigma_y^2 - \sigma_x\sigma_y + 3\tau_{xy}^2)_j^{1/2} \end{cases} \tag{31}$$

for CST or SSP.

Since the stress in an element is correlated to the displacements of element nodes, the τ_{rk} in (31) may be computed by the same formulas (23) (27) as in the case of displacement constraints provided that the virtual internal forces N_x^j, N_y^j, N_{xy}^j are produced by adequate virtual loads. Let $\{P^v\}$ be the vector of virtual load, it is given explicitly without derivation for brevity:

a. for bar's stress

$$\{P^v\} = \frac{[S]^t}{F^\circ}\ , \tag{32}$$

b. for CST element's stress

$$\{P^v\} = \frac{[S]^t}{t^\circ\,(N_x^2 + N_y^2 + 3N_{xy}^2 - N_xN_y)^{1/2}} \begin{Bmatrix} N_x - \frac{N_y}{2} \\ N_y - \frac{N_x}{2} \\ 3N_{xy} \end{Bmatrix} \tag{33}$$

c. for SSP element's stress

$$\{P^v\} = \frac{[S]^t}{t^\circ\,(3N_x^2 + 3N_{xy}^2)^{1/2}} \begin{Bmatrix} 3N_x \\ 3N_{xy} \end{Bmatrix} \tag{34}$$

in which F° and t° are the relative cross section and thickness of element when $A_k = 1$ (see (4) and (5)), [S] is the matrix of transformation of the element displacement vector $\{D_\rho\}$ to the internal force vector $\{N\}$:

$$\{N\} = \frac{1}{\alpha}\,[S]\ \{D_\rho\}$$

3. For lower size constraints $A_k \ge \underline{A}_k$, in (21):

$$\begin{cases} \bar{A}_r = +\frac{1}{\underline{A}_k} = +\underline{\alpha}_k\ , \\ \sum_{k=1}^{n} \tau_{rk}\,\alpha_k = \alpha_k,\ \tau_{rk} = \begin{cases} 1 \text{ when } k = m(r) \\ 0 \text{ when } k \ne m(r) \end{cases} \end{cases} \tag{35, 36}$$

where m(r) is the No. of the design variable corresponding to r-th lower size constraint.

4. For upper size constraints $A_k \le \bar{A}_k$, in (21):

$$\begin{cases} \bar{A}_r = \frac{-1}{\bar{A}_k} = -\bar{\alpha}_k\ , \\ \sum_{k=1}^{n} \tau_{rk}\,\alpha_k = -\alpha_k,\ \tau_{rk} = \begin{cases} -1 \text{ when } k = m(r) \\ 0 \text{ when } k \ne m(r) \end{cases} \end{cases} \tag{37, 38}$$

where m(r) is the No. of the design variable corresponding to r-th upper size constraint.

IV. Program DDU

The basic steps in an iteration of optimization in the reciprocal design variable's space are illustrated in Fig. 2.

1. Do structure analysis at start point 1.
2. Do scaling step from point 1 to 2.
3. Do redesign step by Kuhn-Tucker necessary condition from point 2 to 3.
4. Do linear search associated with scaling step from point 3 to 5 through 4.

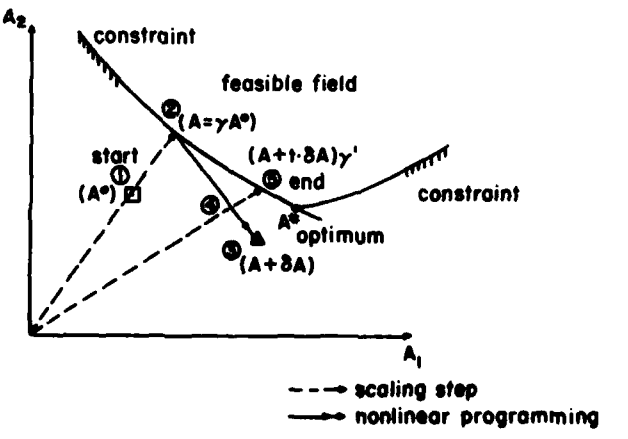


Fig. 2 An iteration of optimization

The last step requires some explanation. According to the algorithm described in Section II, an iteration is ended at point 3. To improve the convergence, we make an additional step to search a better end point 5. It consists of making an approximate analysis by perturbation at point 3, then the structural behavior of any point on line 2-3 can be estimated by interpolation or extrapolation. A one dimensional search along the line 2-3 associated with scaling step will give the point 5 nearer optimum.

DDDU is a structured modular program. The module of optimization is written in so called "meta-language" as follows:

IPASS = 0; (IPASS keeps the No. of reanalysis)

"LOOP"

IPASS=IPASS+1:

{Call GLOASM -- build the global stiffness matrix with the current design A°}

{Call LDLT1 -- make the global stiffness matrix triangularized}

{Call ANAL1 -- analysis under external loads}

{Call SCALGT -- scaling step to get point 2 in fig. 2: $A = \gamma A^{\circ}$}

{Call SELCON -- rude selection of concerned constraints}

{Call ANAL2 -- analysis with virtual loads corresponding concerned constraints}

{Call TAORK -- compute τ_{rk} which is the contribution of elements controlled by de- $A_k = 1$ to the constraint r}

{Call TMATRX -- build the matrix [T] and vector {b} for the quadratic programming "P_μ"}

{Call MUGRTO -- solve "P_μ" to get $\{\mu\}$ }

{Call DELTAA -- compute δA to get point 3 in fig. 2: $A + \delta A$}

{Call ONESCH -- linear search associated with scaling step}

{Call AREUPD -- get new design point 5: $(A + t\,\delta A)\ y'$}

{Call CONVER -- get convergency error EP}

"TEST"(EP.LT.TOLERA)"EXIT"

"ENDLOOP"

where, for the solution of quadratic programming "P_μ" with non-negative constraints, some well-known algorithms are available (7).

V. Sample Applications of DDDU

The results for five examples will be presented below in brief summary form and compared with other existing results. The efficiency of DDDU seems to be satisfactory. The program often provides near optimum results after a few of first iterations and gets refinement in the subsequent iterations. This should be an expectant property of the optimum design program since the designer could obtain a better design early and stop the optimization process if too expensive.

Problem 1: 3 bars truss (fig. 3)

Two load conditions:

i) $P_1 = 20$;

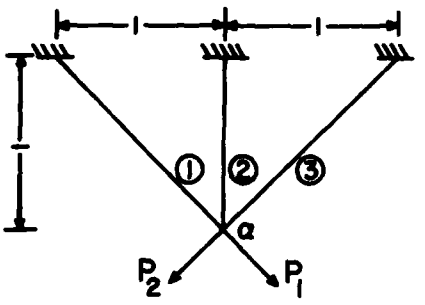


Fig. 3 3 bars truss

ii) $P_2 = 20$,

allowable stress:

$\bar{\sigma}_+ = 20$;

$\bar{\sigma}_- = 15$,

allowable vertical displacement of node a: 10/E,
Specific gravity: $\rho = 1$.

The results of optimization are given in Table 1 which shows that only one iteration is practically sufficient.

TABLE 1

	A_1	A_2	W
Initial	2.0	2.0	
1st iteration	0.6665	0.9442	2.8292
2nd iteration	0.6667	0.9428	2.8284
Theoretical	0.6667	0.943	2.8284

Problem 2: 10 bar truss (fig. 4)

One load condition: see fig. 4,

Material: $E = 10^7$; $\rho = 0.1$; min cross Section $\underline{A} = 0.1$,

allowable stress: $\bar{\sigma} = 25000$ (tension, compression),

allowable vertical displacement of node 1,2,3,4: $\pm$ 2 in.

The results of optimization and the comparison with other methods are given in Table 2 and the convergent history is shown in Table 3 and fig. 5.

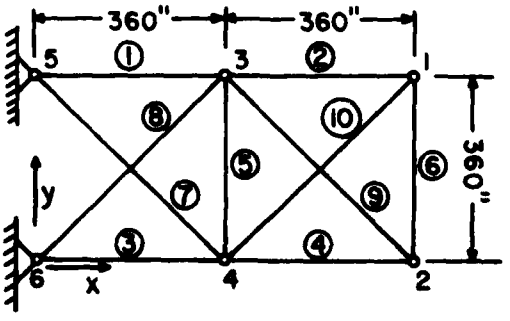


Fig. 4 10 bar truss

TABLE 2

Number of bar	Final designs (in^2)				
	ACCESS1	Schmit	Venkayya	Gellatly	DDDU
1	30.67	33.432	30.416	31.35	30.902
2	0.100	0.100	0.128	0.100	0.100
3	23.76	24.260	23.408	20.03	23.545
4	14.59	14.26	14.904	15.60	14.960
5	0.100	0.100	0.101	0.140	0.100
6	0.100	0.100	0.101	0.240	0.297
7	8.578	8.338	8.696	8.35	7.611
8	21.07	20.740	21.084	22.21	21.275
9	20.96	19.69	21.077	22.06	21.156
10	0.100	0.100	0.186	0.100	0.100
Weight	5076.85	5089.0	5084.9	5112	5069.4
Iterations	13	24	26	19	11

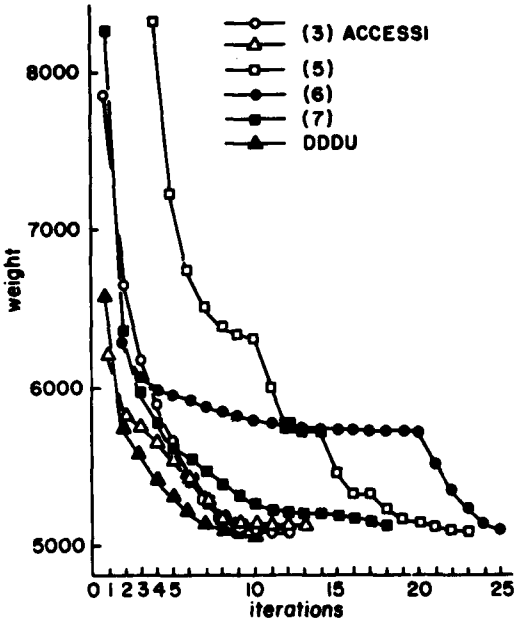


Fig. 5 Convergent history of pb. 2

TABLE 3

Iterations	ACCESS1	Schmit	Venkayya	Gellatly	DDDU
1	7852.9	12846.7	8266.1	8266	6575.0
2	6650.8	8733.4	6281.7	6356	5750.8
3	6161.4	9144.6	6065.7	5980	5603.9
4	5892.6	8332.5	5984.5	5779	5469.1
5	5656.3	7243.0	5963.1	5625	5323.9
6	5426.8	6749.6	5920.1	5547	5218.1
7	5790.8	6507.9	5881.6	5470	5101.8
8	5153.8	6384.3	5848.1	5392	5079.8
9	5110.3	6339.8	5819.7	5323	5077.6
10	5087.2	6314.9	5795.9	5266	5069.4
11	5081.1	5998.7	5776.4	5225	
12	5076.9	5750.1	5760.7	5200	
13		5734.6	5748.2	5195	
14		5705.6	5738.3	5206	
15		5468.8	5730.7	5195	
16		5315.8	5724.7	5169	
17		5306.2	5720.2	5147	
18		5215.8	5716.7	5112	
19		5162.9	5713.7		
20		5135.8	5712.2		
21		5107.0	5502.9		
22		5094.1	5343.8		
23		5089.0	5221.5		
24			5127.0		
25			5084.9		

Problem 3: 72 bars spatial truss (fig. 6)

Two load conditions:

i) $P_x = P_y = 5000$, $P_z = -5000$ at node 1;

ii) $P_z = -5000$ at node 1,2,3,4,

material: $E = 10^7$; $\rho = 0.1$; min cross section $\underline{A} = 0.1$,

allowable stress: $\bar{\sigma} = 25000$ (tension or compression),

allowable displacement: ± 0.25 in x, y, z direction at every node.

By design variable linking, number of independent variables = 16. In Table 4 and 5 are given the results, convergent history and comparisons.

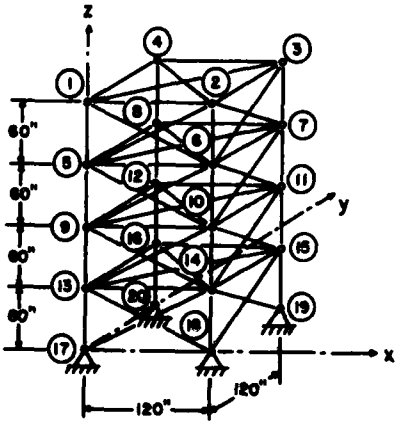


Fig. 6 72 bars spatial truss

TABLE 4

No. of design variable	FINAL DESIGNS						
	ACCESS NEWSUMT	ACCESS1 CONMIN	MIH	VENKAYYA	GELLATLY et al.	BERKE et al.	DDDU
1	0.1565	0.1558	0.1585	0.161	0.1492	0.1571	0.1564
2	0.5458	0.5484	0.5936	0.557	0.7733	0.5385	0.5457
3	0.4105	0.4105	0.3414	0.377	0.4534	0.4156	0.4106
4	0.5699	0.5614	0.6076	0.506	0.3417	0.5510	0.5692
5	0.5233	0.5228	0.2643	0.611	0.5521	0.5082	0.5237
6	0.5173	0.5161	0.5480	0.532	0.6084	0.5196	0.5171
7	0.1000	0.1000	0.1000	0.100	0.1000	0.1000	0.1000
8	0.1000	0.1133	0.1509	0.100	0.1000	0.1000	0.1001
9	1.267	1.268	1.1067	1.246	1.0235	1.2793	1.2683
10	0.5118	0.5111	0.5792	0.524	0.5421	0.5196	0.5116
11	0.1000	0.1000	0.1000	0.100	0.1000	0.1000	0.1000
12	0.1000	0.1000	0.1000	0.100	0.1000	0.1000	0.1000
13	1.885	1.885	2.0784	1.818	1.4636	1.8931	1.8862
14	0.5125	0.5118	0.5034	0.524	0.5207	0.5171	0.5123
15	0.1000	0.1000	0.1000	0.100	0.1000	0.1000	0.1000
16	0.1000	0.1000	0.1000	0.100	0.1000	0.1000	0.1000
Weight	379.640	379.792	388.63	381.2	395.97	379.67	379.62
Iterations	9	9	22	12	9	5	8

TABLE 5

Iterations	ACCESS1 NEWSUMT	ACCESS1 CONMIN	SCHMIT et al.	VENKAYYA	GELLATLY et al.	BERKE et al.	DDDU
1	731.15	415.15	809.12	656.8	656.77	656.77	449.67
2	477.95	383.79	838.09	478.6	416.07	387.01	403.38
3	397.43	380.63	796.16	455.0	406.21	379.67	387.38
4	383.27	380.42	763.61	446.9	399.06	379.87	379.95
5	380.47	379.91	736.69	445.5	396.82		379.69
6	379.86	379.79	716.63	445.4	396.02		379.63
7	379.68	379.79	708.77	401.7	395.97		379.62
8	379.64		645.07	391.5			
9			616.97	383.6			
10			525.29	381.6			
11			491.96	381.2			
12			468.69				
13			450.22				
14			433.77				
15			423.94				
16			413.65				
17			404.08				
18			397.43				
19			393.88				
20			388.14				
21			388.63				

Problem 4: 18 elements wing structure (fig. 7)

The structure consists of 5 bars, 5 CST and 8 SSP elements. Number of independent variables is 16.

Two load conditions:

i) $P_z = 5000$ at node 7;

ii) $P_z = 10000$ at node 5,

material: $E = 10^7$; $\nu = 0.3$; $\rho = 0.1$;
min cross section and thickness $\underline{A} = 0.1$; $\underline{t} = 0.02$,
allowable stress: $\sigma = 10000$ (tension or compression)

allowable displacements: ±2 at node 3,4,5,6,7 in x, y, z directions.

The results, convergent history and comparisons are shown in Tables 6 and 7.

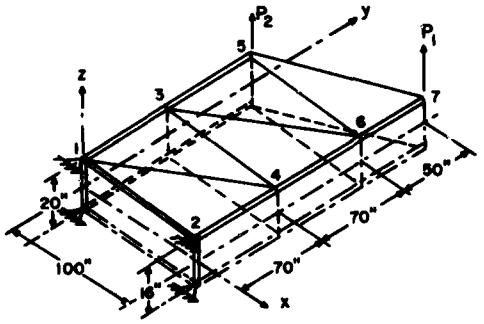


Fig. 7 18 elements wing structure

Problem 5: 133 elements Delta wing structure (fig. 8)

The structure consists of 63 CST elements and 70 SSP elements, the number of independent variables is reduced to 28 through variable linking.

One load condition: $P_z = 8075$ at node 10 to 44,

material: $E = 16.4 \times 10^6$, $\nu = 0.3$, $\rho = 0.16$,

allowable stress: $\bar{\sigma} = 125000$,

allowable displacements in z direction:

Nodes	10-17	18-24	25-29	30	31-35	36-39	40-42	43-44
$\bar{u}$	±14.0	±28.0	±42.0	±30.0	±56.0	±70.0	±84.0	±100.8

In Tables 8 and 9 are given the results of DDDU and comparisons with others.

TABLE 6

Type	No. of element	ACCESS1	DDDU
BAR	1	4.045	3.2349
	2	0.1001	0.1006
	3	0.1001	0.1006
	4	0.1330	0.2198
	5	0.1002	0.1006
CST	1, 2	0.08286	0.08922
	3, 4	0.05363	0.05118
	5	0.03786	0.03728
SSP	1	0.3636	0.4106
	2	0.2236	0.2282
	3	0.1310	0.1237
	4	0.1156	0.1297
	5	0.09166	0.09412
	6	0.02000	0.02012
	7	0.02000	0.02012
	8	0.03096	0.03018
Weight		402.97	407.571
Iterations		9	10

TABLE 7

Iterations	ACCESS1	DDDU
1	585.066	597.738
2	466.410	542.923
3	422.799	473.745
4	408.848	437.569
5	404.744	440.138
6	403.516	416.804
7	403.118	413.896
8	402.966	410.655
9		407.571

TABLE 8

Type	No. of variable	ACCESS1	DDDU
CST	1	0.0200	0.02001
	2	0.0200	0.02001
	3	0.1498	0.1522
	4	0.1450	0.1425
	5	0.0200	0.02001
	6	0.1164	0.1183
	7	0.1289	0.1270
	8	0.0200	0.02001
	9	0.09088	0.09236
	10	0.1223	0.1211
	11	0.06518	0.06616
	12	0.1172	0.1168
	13	0.03628	0.03669
	14	0.1074	0.1075
	15	0.08406	0.08418
	16	0.05036	0.05032
SSP	1	0.0200	0.02001
	2	0.0200	0.02001
	3	0.02172	0.02215
	4	0.02001	0.02001
	5	0.02001	0.02001
	6	0.02001	0.02001
	7	0.0200	0.02001
	8	0.05958	0.05960
	9	0.07531	0.07556
	10	0.07247	0.07240
	11	0.05702	0.05721
	12	0.0200	0.02001
Weight		10742.24	10781.92
Iterations		9	9

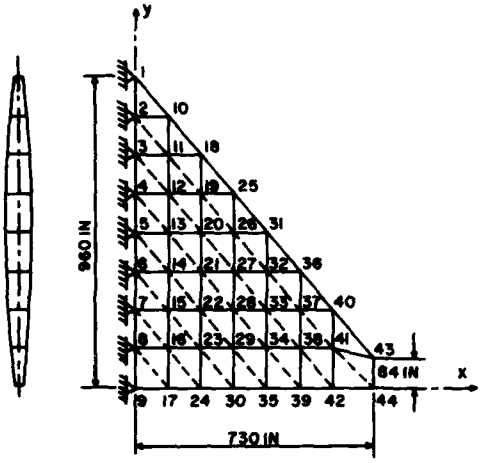


Fig. 8 133 elements Delta wing structure

TABLE 9

Iterations	ACCESS1	DDDU
1	14871.40	11875.34
2	12061.76	11199.21
3	11169.82	10865.03
4	10848.26	10814.00
5	10774.66	10799.37
6	10754.16	10792.16
7	10747.34	10785.96
8	10742.24	10781.92

VI Concluding Remarks

The present work and its program DDDU make full use of a series of experiences of structural optimization by the mathematical program method and as well as by the optimality criteria method. In addition, the automated deletion of non-active constraints is accomplished by a simple quadratic program, and the selection of active/passive variables is avoided by the unification of constraint treatment. All these seem to be rather effective to improve the convergence behavior, the numbers of iterations are less than 10 in all the five simple applications. Hence the DDDU could be used as a practical and efficient capability for minimum weight design of structural systems.

References

(1) Schmit, L. A., Structural Design by Systematic Synthesis. Proc. 2nd Conf. on Electronic Computation, ASCE (1960), pp. 105-132.

(2) Venkayya, V. B., Khot, N. S. and Reddy, V. S., Optimization of Structures Based on the Study of Strain Energy Distribution. Proc. 2nd Conf. on Matrix Methods in Structural Mechanics, WPAFB, AFFDL-TR-68-150, (1968), pp. 111-153.

(3) Schmit, L. A. and Miura, H., A New Structural Analysis/Synthesis Capability-ACCESS1. AIAA Paper No. 75-763, 1975, and Approximation Concepts for Efficient Structural Synthesis. NASA CR-2552, 1976.

(4) Schmit, L. A. and Miura, H., An Advanced Structural Analysis/Synthesis Capability-ACCESS2. AIAA/ASME/SAE 17TH Structures, Structural Dynamics and Material Conf. (1976), pp. 432-447.

(5) Schmit, L. A. and Fleury, C., An Improved Capability Based on Dual Methods-ACCESS3. AIAA/ASME 20th Structures, Structural Dynamics and Material Conf. (1979), pp. 23-50.

(6) Sander, G. and Fleury, C., A Mixed Method in Structural Optimization, International Journal for Numerical Methods in Engineering 13 (1978) pp. 385-404.

(7) Dantzig, G. B., Linear Programming and Extension, Princeton Univ. Press, 1963.

(8) Qian, L. X. and Zhong, W. X., A Method of Structural Optimization Program DDU-2. Journal of Dalian Institute of Technology 1, (1979), pp.1-21.

(9) Schmit, L. A. and Farshi, B., Some Approximation Concepts for Structural Synthesis. AIAA J., 12 (1974), 5, pp. 692-699.

(10) Venkayya, V. B., Design of Optimum Structures, J. Computers and Structures, 1. (1971) 1-2 pp. 265-309.

(11) Gellatly, R. A. and Berke, L., Optimal Structural Design, AFFDL-TR-70-165, 1971.

AD-P000 091

A COMPUTER PROGRAM SYSTEM FOR DESIGN OF POWER TRANSMISSON TOWERS

Lars Hanssen
SINTEF div of Structural Engineering
N 7034 Trondheim - NTH Norway

Summary

A computer program system for practical design of power transmission towers is presented. The system comprises modules of interactive graphical tower spotting, structural analysis and member sizing of towers in a transmission line, geometry optimization of single towers and a module for optimal adaptation of member sizes to production requirements.

The program system was developed to enable reduction of material costs related to tower manufacturing and to make the design process less laborious and tedious. The principles which the system is based upon reflect a compromise between flexibility and reliability on one side and simplicity and efficiency on the other.

The tower spotting module is an independent program with the objective of generating best possible tower locations and heights along a user supplied terrain profile. This module is developed in interactive graphical mode and allows for convenient control of the tower spotting process. Capabilities for automatic optimization of tower positions and heights are included in the module.

The analysis and sizing module can handle various types of towers idealized as truss structures. Efficiency is emphasized by using the finite element displacement method with a one level substructuring technique for the analysis and a stress-ratio procedure for the detailed sizing of individual towers. Reliability of the results is accomplished by considering non-linear effects in the response behaviour.

A module for optimization of tower geometry of single towers is also available in the system. Node coordinates are considered as design variables, whereas the tower topology, i e number of bar members and member connectivity has to be fixed.

To comply with production constraints regarding limitation of number of different tower designs in one and the same transmission line, a capability for optimal selection of tower strength levels is included. This part of the design process lies in a postprocessor unit and is separated from the design of each individual tower.

Introduction

A computer program system for practical design of power transmission towers (1), (2), (3), (4) has been developed by SINTEF* division of Structural Engineering on request from the Norwegian Water Resources and Electricity Board State Power System, which will be referred to as NVE** in the following.

The towers in question are of a truss type and are idealized by a set of bar members. NVE has been designing power transmission towers of this type for several years, but computerized procedures have been used to a limited extent. The routines adopted in the design work are well established and substantial experience and insight into the field has been gained.

When adressing SINTEF in this matter it was thus not to bring a revolution into the way of designing power transmission towers, but rather to find a convenient tool which would help reducing some of the time-consuming manual work involved in the design process. Also, the possibility of saving material expenses by adopting structural optimization to some degree was a desirable objective.

From the very start of the project it was realized that a development based on existing systems (5),(6) would not be feasible. It was judged as very difficult, if at all possible, to find a system which could cope with the design concepts well established by NVE without heavy modifications. It was therefore decided to develop a new system which could be more or less taylored to the design procedures used by NVE.

A treatment of the various concepts which this program system is based upon will be presented in the following. Some emphasis will be put on problem characteristics, solution strategy and program organization to illustrate how a structural design problem of this kind can be approached.

Purpose and capabilities

In the planning phase of the program system some main guidelines for the program development were established, guidelines which to some extent were decisive for the approaches and principles chosen.

The major objective was to develop a system which could be used to reduce material costs in the tower manufacturing process. The background for this objective was that some 8000 tons of steel representing a value of $ 9 mill are spent each year by NVE in tower production. Clearly a program for reducing this amount would be advantageous.

Another important objective was to reduce manual work needed in the transmission line design. Also, to computerize the process was belived to reduce the frequency of errors beeing made and to increase the accuracy of the structural analysis and design procedures.

It was emphasized that the system should be easy to use. This requirement was due to the fact that it should be possible to operate the program by persons with little or no experience in data processing.

Efficiency of the program system modules was another important aspect which was considered in the planning phase. A substantial number of towers were to be designed every year, and expenses related to computer usage had to be as low as possible.

The system should be flexible in that handling of various tower geometries should be possible. In effect, this requirement implied a system which could be used in design of towers of any configuration.

The above considerations led to a system based on a design process consisting of three separate stages:

Stage I. Tower spotting - A tower spotting module is available for determination of tower locations in a user defined terrain profile. In addition to tower locations, tower height for each individual tower is also determined. This module operates independently from the rest of the program system and no detailed analysis and sizing of the towers are carried out. Capabilities for optimization of locations and heights based on empirical formulaes for tower costs are included, and the tower spotting process is conveniently controlled by the user.

---

* The Foundation of Scientific and Industrial Research at the Norwegian Institute of Technology

** Norges Vassdrags- og Elektrisitetsvesen

PRECEDING PAGE

Stage II. Tower geometry optimization - This stage is only relevant when new tower types and configurations are to be investigated, and will not be part of the routines usually adopted in the tower design process. A representative set of loading conditions has to be supplied for this module since it is neither practically nor economically feasible to perform an optimization of the geometry for all towers in a line.

Stage III. Member sizing of towers in a line - All towers in a transmission line are analysed and member cross-sections are picked from a table of available profiles. Tower heights and loadings have already been determined by stage I and these results are used directly by stage III. Efficiency is emphasized in this module by using the finite element method with substructuring in the analysis of each tower and the stress-ratio concept for member sizing. Reliability of the results is accomplished by accounting for non-linear response effects in the analysis.

Stage IV. Selection of tower strength levels - When all towers in a line are analysed and members are sized according to the design criteria inherent in the program the towers are divided into strength levels. The background for this operation is that only a limited number of different tower designs can appear in a transmission line. All towers (actually part of the tower) within a strength level have identical strengths (i.e. their designs are identical in all respects, and the problem is to find these strength levels and how many and which towers should belong to each level. A procedure for solving this problem in a best possible way is available in the program system.

Problem characteristics

Fig. 1 shows a typical 420 kV suspension tower very commonly used for power transmission purposes in Norway. It consists of two vertical panels which are connected by a horizontal crossarm at the tower top and several horizontal panels at different height levels. There is also a system of guys between the two vertical panels which are prestressed in order to reduce displacements and to avoid undesirable dynamic effects. The load effects which are primarely caused by wind, ice and cooling of the conductors are transferred to the tower through a set of crossarm conductors and one wire on each earth-wire peak (top of vertical panel). The height if these towers range from 15 to 50 metres and the length of the horizontal crossarm is approximately 25 metres.

Other types of towers are also used by the NVE, both different kinds of suspension towers and stronger types for termination points and angle points. These towers will to a large extent have a structural behaviour similar to the suspension tower shown.

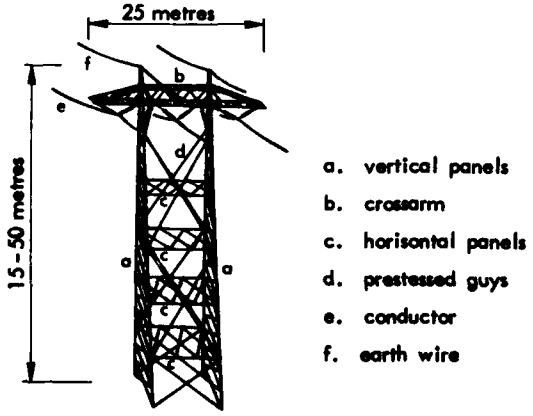


Fig 1 Typical 420 kV suspension tower

Several characteristics for the towers in question were decisive for the choice of design procedures.

First of all, it is realized that the towers are typical truss structures with only minor bending effects permitting analyses without rotational degrees of freedom. Even so, the analysis problem is of substantial magnitude in a structural optimization context in that towers with as many as 1000 bar members will be treated. To cope with local bending caused by iceload and self-weight of each member the user is given the possibility to supply member bending moments which are accounted for in the sizing process.

The tower structure is composed of plane panels and spatial sections with a high degree of repetition in geometry. This fact is utilized in that a one-level substructuring approach is adopted yielding an efficient analysis capability and leading to convenient handling of user data.

The towers to be analysed are usually weakly statically indeterminate. This means that only a small redistribution of member forces takes place as the tower stiffness changes. A stress-ratio type of procedure for member resizing is therefore appropriate in the design process.

Dynamic calculations are not included. However, suitable load factors on the wind loading are considered and prestressing of the guy system is favourable with respect to dynamic effects.

Member profiles can only be picked from a limited selection. This means that procedures based on continuous sizing variables are not well suited since it would be a difficult task to relate the variables to the profiles available. This problem is avoided when a profile table with all necessary information about the cross-sections is made available in the computer program.

To include deflection constraints has not been found necessary. It is assumed that deflections are kept on an acceptable level through prestressing of the tower guys. Neither is overall instability of the total tower structure considered. This failure mode is assumed not to occur for the towers designed. These assumptions simplify the design procedure considerably and lead to a substantial reduction of computer time.

Program organization

Fig. 2 is intended to give a survey of the program system organization. The PINTOS part of the system (Program for INteractive TOwer Spotting) is an independent program consisting of 3 separate processors; a preprocessor for terrain data input, a design processor for the tower spotting process and a postprocessor for output of final results. The preprocessor and the postprocessor are batch mode programs whereas the design module operates in interactive graphical mode. The results from the tower spotting program (tower heights and loadings) are used both as input for the MAST part of the system and as information about tower sites in the terrain.

The MAST part of the system which performs the detailed analysis and design of each tower in the line is divided into 3 programs, MAST1, MAST2 and MAST3 which are all batch mode programs.

MAST1 is a stand-alone program for analysis and design of a single tower structure with given geometry and loading. It consists of three separate processors, a preprocessor for data input, a design processor for analysis and member sizing and a postprocessor for printout of results.

MAST2 is used for analysis and design of all towers in a transmission line and can only be used together with MAST1 which initiates the calculation by analysing tower

parts which are identical for all towers. MAST2 consists of a series of processors for several tower types. The processors are divided into groups where each group corresponds to one tower type and consists of one preprocessor, one analysis processor and one postprocessor analogous to MAST1. The preprocessor reads data for the line, i e tower heights and tower loading (from PINTOS) and data for tower geometry generation. The design processor prepares data to define the towers and performs analysis and sizing of each individual tower one by one. The task of the postprocessor is to select in a best possible way a limited number of tower strength levels to conform with production requirements.

MAST3 optimizes tower geometry for a single tower with given topology and loading. The program can also be used to find the optimal prestressing level for towers with prestressed guys. MAST3 is also divided into 3 processors similar to MAST1 and MAST2, and can only operate together with MAST1 which is used to initiate the process through a first analysis and sizing of the initial tower geometry.

All 3 programs in MAST are attached to plotting capabilities, a mesh plotter MEPLOT and a production drawing plotter PRPLOT. The MAST programs are built up around 3 basic program units; TOG - a tower generator, ASI - an analysis and sizing unit and RAD - a result administrator.

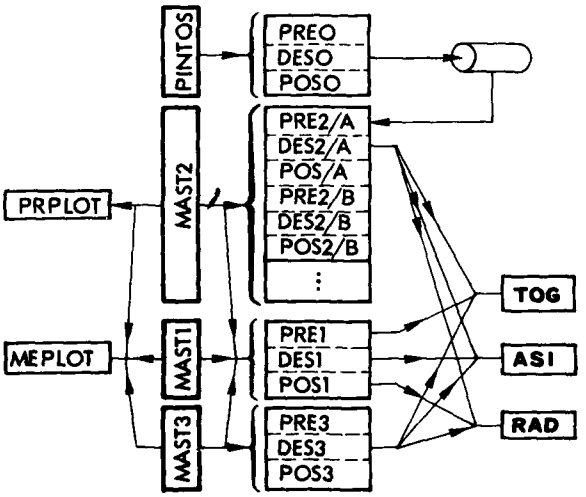


Fig 2 Program organization

Interactive tower spotting

General

The tower spotting process is concerned with how to determine tower locations and heights in a best possible way along a given terrain profile between two fixed predetermined points. This problem has traditionally been solved manually with the aid of a terrain profile drawing and templates to simulate catenaries in an approximate way. Also, several computer programs have been developed (7), (8) based on different types of procedures to search for optimum locations and heights.

There are obvious drawbacks in the manual approach; the process is very laborious, it requires a substantial amount of training and the final result will be encumbered with a certain degree of inaccuracy.

The computer programs developed in this field are batch mode programs leaving all decisions to the computer during the tower spotting process. Results from such programs are not always satisfactory because fully automation of all possible situations occuring in the tower spotting process is very difficult.

In the present effort the tower spotting process can be considered as a semi-automatic procedure where the user has extensive control over all decisions which are made.

The program which is developed in interactive graphical mode, is assumed to work on a cathode-ray screen equipped with a cursor capability. The program can display any portion of the terrain profile on the screen in several alternative ways. The terrain is displayed together with alphanumeric and graphical information about terrain conditions such as tower site availability, buildings, roads etc. Zooming capabilities are also available.

Towers can be introduced into the terrain, positioned and removed 'manually' by the user by operating the screen cursor. Catenaries for critical loading conditions are plotted automatically by the program. Catenary parameters are calculated approximately for single spans by an interpolation technique or 'exact' for several spans simultaneously by equilibrium iterations. Tower heights and positions can be optimized by the program. It is assumed that the total tower cost function is proportional to the tower heigths and proportional to a soil valuation factor which varies arbitrarily along the terrain profile. The optimization capabilities of the program can only be utilized when reasonable initial values regarding number of towers and tower locations have been given by the user. Also, only a limited number of towers should be considered simultaneously when optimizing tower heights and positions.

Terrain profile

Prior to the tower spotting is initiated, the terrain profile has to be defined between two fixed locations.

A substantial amount of data is needed to completely define the entire terrain profile. The program module to take care of the terrain data input is thus a crucial factor for convenient use of the program. Photographic and ordinary land surveying is used to generate coordinates for the terrain profile surface, buildings, roads etc along the transmission line. In areas where photographs of the terrain are not able to reproduce details with sufficient accuracy (heavy vegetation, difficult light conditions etc) ordinary land surveying is resorted to. Also, soil conditions for fundamentation have to be registered by inspection of the ground.

The terrain profile is idealized by a number of terrain locations defined by an x-coordinate from start of profile and several y-coordinates to define the profile perpendicular to the line direction. The terrain surface is linearized between these terrain locations.

'Exact' catenary calculation

When all towers in a section are located (Section = all spans between two angle points/termination point) catenaries can be calculated for these spans. A catenary is conveniently defined by the parameter c = H/q where H is the horizontal tension force in the catenary and q is the transverse loading per unit length. H depends on the loading q, the temperature level and the stiffness of the two end supports of the wire, as illustrated in Fig. 3.

The horizontal force H is found from the equation

$$f(H) = [h^2 + (2\frac{H}{Aq}\sinh\frac{aqA}{2H})^2][1 - \ell_0(1+\varepsilon(T-T_0)\frac{H}{EAa}]^2 - K^2 = 0$$

where A is the wire cross-section and ℓ_0 is the initial

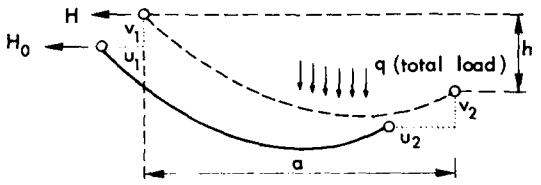


Fig 3 Catenary definition

length of the catenary. ε is the thermal expansion coefficient, $T-T_0$ is the temperature change, E is Young's modulus of elasticity and K is a constant independent of H. The remaining quantities are defined in Fig. 3. Assuming all parameters in the above equation to be known, H can be found by Newton-Raphson iteration of the relation $f(H) = 0$. When H is computed for all spans in the section, new values for the displacements u and v can be found for all towers, see Fig. 4. H is recalculated until convergence. Exact catenaries are found by a separate program, (9).

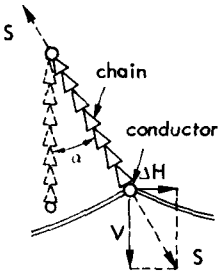


Fig 4 Support reactions

Approximate catenary calculation

During the build-up of a section (introduction, removal and positioning of towers) catenaries cannot be calculated according to the 'exact' procedure described because a complete section is needed. Also, the 'exact' procedure will be too time-consuming in an interactive program mode. The following approximate scheme is therefore used for incomplete sections.

Prior to the tower spotting process is started, 'exact' catenary parameters are computed for a set of actual span lengths a, equivalent span lengths b, loading values p (vertical load per unit length) and temperature values t. All parameters a, b, p and t are defined between appropriate lower and upper limits and the range between these limits is divided into equal increments. The catenary parameter is now considered as function of the 3 variables a, b and p (or t) and can be found for any combination of these by interpolation between the values for which exact parameters are available. The interpolation is carried out similar to an eight-node solid finite element as illustrated in Fig. 5, where the total a, b, p (or t)-space is divided into a given number of elements. The catenary parameter is found by

$$c = [\bar{\xi}\bar{\eta}\bar{\zeta}, \xi\bar{\eta}\bar{\zeta}, \bar{\xi}\eta\bar{\zeta}, \xi\eta\bar{\zeta}, \bar{\xi}\bar{\eta}\zeta, \xi\bar{\eta}\zeta, \bar{\xi}\eta\zeta, \xi\eta\zeta] \cdot C_0$$

where $\bar{\xi}=1-\xi$, $\xi=(a-a_{min})/\Delta a-i+1$
$\bar{\eta}=1-\eta$, $\eta=(b-b_{min})/\Delta b-j+1$
$\bar{\zeta}=1-\zeta$, $\zeta=(p-p_{min})/\Delta p-k+1$
see Fig. 5,

C_0 is a vector containing the exact parameter values for the eight 'node' corners of 'element' ijk.

For a given span, a and p (or t) are readily available while the equivalent span length b is computed from

$$b = \sqrt{\frac{\Sigma s_i^3}{\Sigma s_i}}$$ where s_i are the span lengths for a certain number of spans on each side of the span considered.

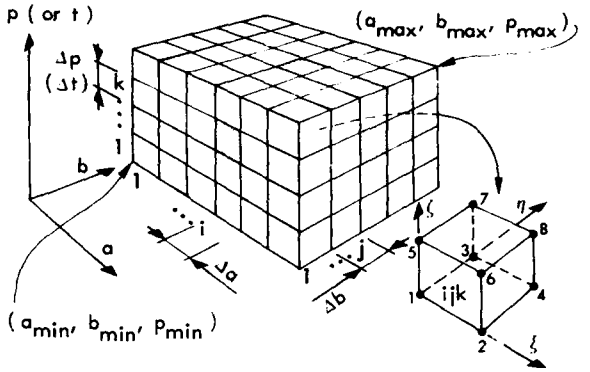


Fig 5 Catenary parameters by interpolation

Optimization of tower heights

The total cost of a tower section is expressed by

$$S = \sum_m (Ah+Bf(x)+C) + L\gamma$$

where h is tower height, m is number of towers in the section, f(x) is a soil valuation factor which depends on the tower location chosen and A, B and C are tower constants. L is the section length and γ is a cost parameter connected to transportation expenses.

Constraints to be satisfied for each tower and each span are

1. Ground clearance requirements
2. Transversal insulator swing limitations
3. Max and min allowable tower heights

The ground clearance requirement is expressed by (see Fig. 6)

$$-h_i b - h_j a \leq -kab\ell + y_{Ti} b + y_{Tj} a - (y_{Tc}+\delta)\ell$$

where k is the constant for a parabola approximating the exact catenary and δ is the minimum allowable ground clearance. The transversal insulator swing limitation is introduced because a minimum distance between conductor and tower side panel is required and is expressed by $T/V \leq tg\alpha$ (see Fig. 7) which yields

$$h_i c_a + h_j (c_a+c_b) + h_k c_b \leq R(\ell_a, \ell_b, k_a, k_b, \alpha, q_v, q_T, y_{Ti}, y_{Tj} y_{Tk})$$

where $c_a = q_{va}/k_a\ell_a$ and $c_b = q_{vb}/k_b\ell_b$, k_a and k_b are the parabola constants for span a and b, respectively.

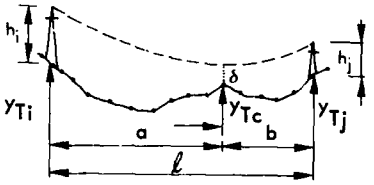


Fig 6 Ground clearance requirement

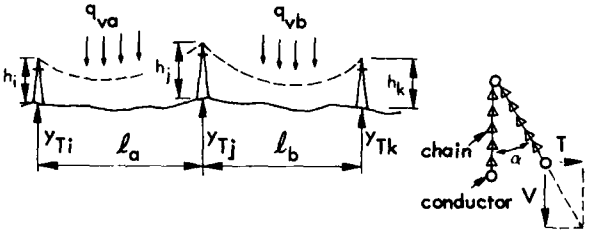


Fig 7 Transverse swing limitation

Evidently, both cost and constraints are linear functions of tower heights and the problem can be solved by linear programming (LP). To solve this problem in one single step is not an advisable approach because a substantial amount of storage and computer-time would be needed (500-1000 constraints in a problem with 20 towers). A simple strategy for reducing number of constraints has therefore been adopted. Initially, only one terrain location in each span is assumed to be critical with respect to the ground clearance requirement. Constraints on maximum and minimum tower heights and the transverse swing limitations are initially included only for towers where allowable values are exceeded. The LP-problem based on these assumptions is established and solved, and all constraints are recalculated from the resulting tower heights. If new constraints have become critical, these are added to the LP-tableau (coefficient matrix for LP-problem) and a new LP-solution is found. The process is continued until no new constraints are added. To avoid oscillations in the iteration process, constraints are never deleted from the LP-tableau. Good initial assumptions regarding the tower heights are thus advantageous for an efficient solution.

Optimization of tower positions

Before starting the optimization process it is assumed that all towers to be optimized are given reasonable initial positions. The reason is that the optimization procedure is not capable of handling local minima and separated feasible domains. As a guide for the user when giving initial tower positions the program has the possibility to put a marking on the screen representing the total cost of the tower line. By successive positioning of each tower a cost curve can be displayed giving a rough indication of usable initial tower positions.

The optimization process is based on a separation of position variables and height variables. Tower positions are optimized tower by tower until no improvement of the cost function is obtained. For each tower position to be optimized, optimal heights are found for the tower in question and a limited number of towers on each side. Thus a set of one-dimensional minimizations is carried out where the variables are tower positions and the merit function is the total cost of all towers. Since all design constraints are considered when heights are optimized only maximum and minimum limitation on tower position change need to be imposed. A macro flow diagram of the process is shown in Fig. 8.

The total cost of all towers will be a continuous but non-differentiable function and the one-dimensional minimizations are carried out using the golden section iteration procedure.

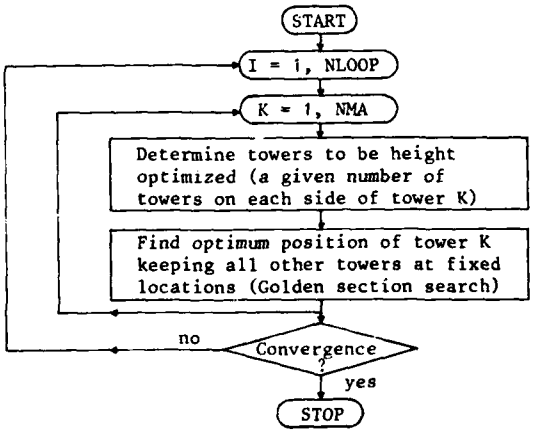


Fig 8 Optimization of tower positions

Use of tower spotting program

A set of commands is available in the design processor of the tower spotting program. A survey of the most important commands are shown in Table 1.

Table 1 - Survey of main commands

No	Command	Description
1	I	Introduce new tower in cursor position
2	P	Position tower closest to cursor until tower top coincides with cursor
3	D	Remove tower closest to cursor
4	B	Redisplay current picture with all corrections removed
5	N	Display next picture starting from cursor position
6	F	Display picture ahead of cursor position
7	X	Compute exact catenaries for current tower section
8	S	Set optimum configuration for current tower section
9	M	'Manual' optimum tower positioning, i e 1) move tower closest to cursor 2) optimize tower heights 3) mark total tower cost on screen
10	U	Optimize tower position for tower closest to cursor
11	A	Optimize tower position for all towers specified
12	O	Retrieve optimal configuration alternative

The terrain profile is usually extending over several kms and has to be divided into small portions to fit into the graphical screen with a reasonable scaling. The terrain is conveniently scaled to comprise 15-20 towers in one picture. The lay-out is determined by a set of parameters which can be chosen by the user. An example of picture lay-out is shown in Fig.9. The screen cursor is automatically displayed on the screen and its position is adjusted by two steering wheels on the screen console. Display of new terrain portions is controlled by means of the cursor and the commands B, N and F, see Table 1.

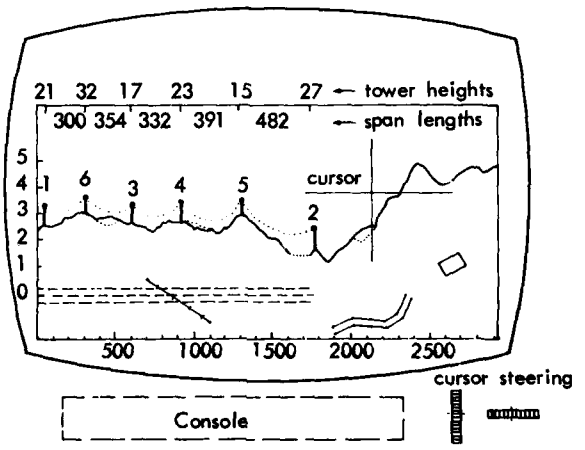


Fig 9 Screen picture lay - out

New transmission line towers are added from left to right in the terrain profile, and one tower section is introduced at a time. A reasonable initial configuration of the towers is generated by commands I, P and D. During this process approximate catenaries are displayed, enabling the user to satisfy the ground clearance requirements. When all towers in a section are included, exact catenaries for all spans can be computed using command X. Height optimization

of the towers within the section is then carried out by command M.

The configuration generated is now considered as an initial suggestion for an optimum configuration for the current tower section. This solution must be stored before further refinement of the section is started, which is done by calling the command S (Set optimum solution). Optimum tower positions are determined for all towers in the section one by one. Height optimization is carried out for a small number of towers (3-5) on each side of the tower for which the location is to be optimized. Sufficient accuracy is thereby obtained and the optimization process is fast enough in an interactive design context. Optimum tower positions are found by commands M, U and A. When optimum positions for all towers in the section are found, towers can be added to and/or deleted from the section to investigate alternative configurations. New catenaries are determined (command X) and all positions are optimized again. As many configurations as desired can be investigated for each tower section. The optimum configuration is retrieved by calling command O. When the current tower section is considered satisfactory, a next section is initiated by adding a suitable number of towers to the next angle point.

Member sizing of transmission line

General

A transmission line in this context consists of a given number of towers with given geometry and loading resulting from the tower spotting program. Design variables are thus member cross-sections for each of the towers in the line.

A sizing has to be carried out for each individual tower, the efficiency of the design procedure for one such tower is therefore of vital importance. Several approaches were considered before the program was developed; both dynamic programming, mathematical programming and optimality criteria methods.

A well known optimality criteria method is the fully stressed design concept which is based on the hypothesis that all members should be fully stressed in at least one loading condition. This leads to the very simple stress ratio iteration which is well suited for the present problem since no deflection constraints are to be considered and overall structure stability is known a priory to be non-critical. Also, the towers in question are very often weakly statically indeterminate requiring a small number og iterations in the stress ratio procedure. In the present case a fully stressed design cannot generally be expected since design variable linking caused by fabrication and symmetry requirements will be utilized.

The design procedure is illustrated in Fig. 10 which shows that a sequence of cycles consisting of an analysis phase and a sizing phase follows after the initial design is chosen. In each cycle all members

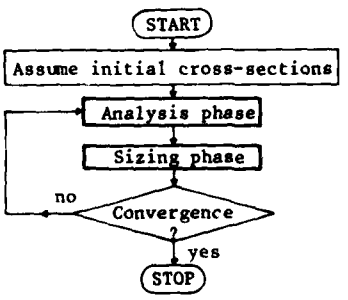


Fig 10 Analysis / sizing iteration

are resized according to the member forces found in the analysis. Experience has shown that the iteration converges fairly rapidly, usually after 2-3 cycles.

Substructuring

The structural analysis is based on a displacement formulation of the finite element method combined with a one level substructuring technique. This approach is well suited in the present case since a high degree of repetition in geometry is observed for the towers to be designed. Firstly, the data handling becomes convenient for the user who can work on independent planar substructures to a large extent. Secondly, the substructuring technique is efficient in that reduction of the finite element equations is carried out for different substructures only. Thirdly, the substructuring technique is suitable for reanalysis when parts of the structure are changed. This is indeed the situation when several towers in a line are analysed.

An example showing how a suspension tower can be divided into substructures is presented in Fig. 11. Here the vertical and horizontal panels are considered as two-dimensional substructures, whereas the top crossarm is divided into three-dimensional substructures. Alternative ways of substructure division can also be imagined.

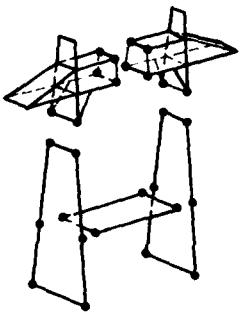


Fig 11 Substructuring of suspension tower

Prestressing

The effect of self-weight and prestressing of guys is considered as one loading condition. Guys are connected to supernodes only (nodes connecting the substructures) and prestressing forces are prescribed by the user. An initial analysis for the selfweight and these prestressing forces results in new guy forces which are deviating from the prescribed ones, and an iteration process is necessary to account for this unbalance. Total number of iterations needed for this loading condition is usually in the range of 4-8, and depends on the stiffness of the guys compared to the overall stiffness of the structure.

Loading

When the prestressing phase is completed, the structure is subjected to an arbitrary number of loading conditions caused by wind, ice and temperature. Each loading condition is treated individually and two kinds of non-linear effects can be accounted for; a) large transverse deflections of guys caused by ice loads and b) slips in bolts connecting different bar members. The first effect is illustrated in Fig.12a where also the behaviour of a simple no-compression bar is shown. The second effect is illustrated in Fig.12b where the reduction in member stiffness depends on the difference between hole- and bolt diameter Δd.

An iteration is carried out for all loading conditions. A constant stiffness procedure is adopted where the same stiffness matrix is used throughout the entire iteration, see Fig. 12c.

Sizing phase

When member- and guy forces have been determined by the analysis phase, members and guys are resized to resist these forces. Symmetry requirements and fabrication constraints are handled by member profile linking, i e members are divided into groups such that

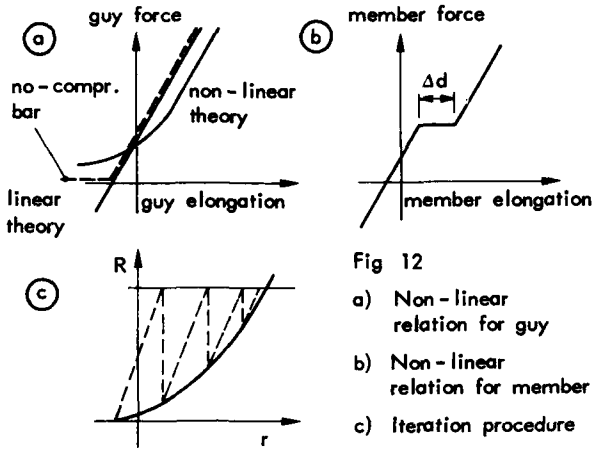


Fig 12
a) Non - linear relation for guy
b) Non - linear relation for member
c) Iteration procedure

all members in a group have identical cross-sections.

Member profiles are chosen from a profile table containing cross-sectional data for a limited number of profiles which are arranged in a sequence corresponding to increasing cost per unit length.

All members are sized against material failure and buckling. Sizing against buckling is also performed for member subsets ('long bars'). The bolt connection capacity is considered in the sizing process. Design criteria conform with the European recommendations for steel constructions (ECCS 1978) which are concentrated to a few subroutines and can easily be replaced by other criteria.

Transmission line approximations

A substantial number of towers with given heights and loading has to be analysed and sized during the design process of a transmission line. To achieve reasonable efficiency it was necessary to make several shortcuts and assumptions regarding the design procedure. The most important of these will be mentioned and commented upon in the following.

a. The tower loading is independent of tower stiffness. This implies that the loading is computed on the basis that all towers are infinitely stiff. Several loading conditions (15-20) are applied representing different combinations of wind, ice and temperature loads.

b. The horizontal crossarm is assumed to have the same stiffness for all towers in the line. This implies that all substructures in this part of the tower need be reduced only once and can be used in the analysis of all towers.

c. Each tower is analysed and sized separately. The member grouping is however, the same for all towers (short towers may miss some member groups) while the final profile assigned to each group varies from one tower to the next.

d. The geometry near the tower base is generated from a small amount of user data to facilitate data input.

e. Number of sizing cycles is set equal to one (one analysis followed by a resizing). Approximately 5% error in member forces is introduced through this assumption.

Optimal selection of tower strength

As all towers in a line are designed independently the tower strength (represented by the cross-sectional profiles for all member groups in the tower) will generally be different for all towers. This is not a feasible result in a production context where only a small number (5-10) of different tower strength levels can be tolerated. The problem is therefore to determine these strength levels (assuming that the number of levels is given) and to find the most favourable strength level for each tower. The following simple example shown in Fig. 13 is intended to illustrate the situation.

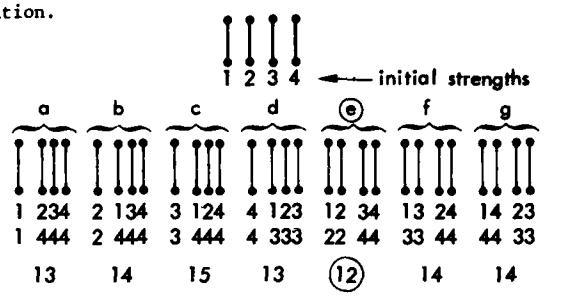


Fig 13 Example of strength level selection

Four towers containing only one member each are designed, yielding four different tower strengths. For simplicity, the tower number is also representing the tower strength and cost. If the production process requires only two different strength levels, there will be 7 different alternative ways a-g to achieve this, as shown in Fig. 13. The total cost of each alternative is computed remembering that all towers within a strength level will have the same strength (and cost) as the tower with highest strength. Clearly, alternative e is the most favourable one yielding the lowest total cost.

In a realistic problem the tower strength is represented, not by a single number, but by as many as 50 different profile groups for each tower. In a transmission line comprising 300-400 towers the optimal strength level selection is actually an enormous operation.

A graphical representation of a problem with 11 towers is given in Fig. 14. For simplicity, it is assumed that the number of member groups is the same for all towers. The individual design of each tower is represented by a graph yielding a profile strength for each member group. Three possible strength levels are indicated as full curves in the same diagram. Since no strength reduction is possible for any of the towers, the strengths for tower no. 1, 2, 3 and 11 are increased to coincide with level no. 1, strengths for tower no. 6, 7 and 9 to coincide with level no. 2 and strengths for tower no. 4, 5, 8 and 10 to coincide with level no. 3. If the strength level graphs should happen to cross each other, the strengths for each tower should be increased to coincide with a level

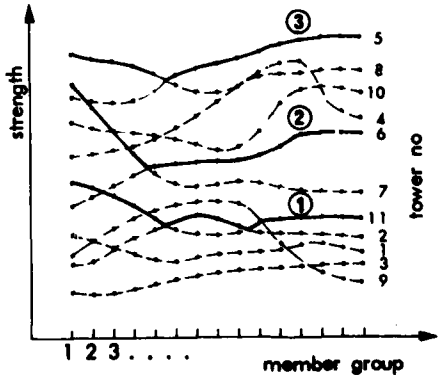


Fig 14 Tower strength representation

yielding the least tower cost increase. Ideally, all possible shapes and positions of the strength level graphs should be investigated to find the absolute best solution. In practice, such an attempt is not feasible and an approximate 3-step procedure is resorted to.

The first step is concerned with proper selection of NSL towers, the strength of which are used as an initial set of strength levels (NSL = number of strength levels). These towers can be chosen by the user. They can also be determined by the program based on the assumption that the initial strength level graphs (Fig. 14) should be as far apart from each other as possible.

The second step is to increase the strength for each of the remaining towers in turn to coincide with the most favourable strength level. During this operation each strength level is not assumed to be fixed but is also increased along with the strength of those towers which are already included in the level. Fig. 15 is intended to illustrate the effect of increasing the strength of tower no. k to strength level ℓ.

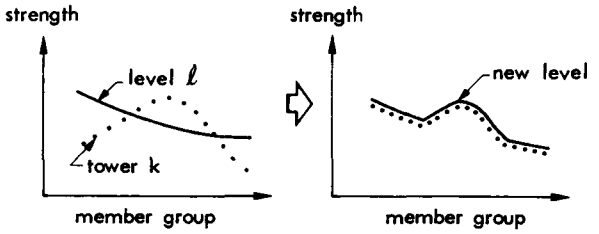


Fig 15 Strength level correction

When the second step is completed a first solution is available. This solution can be used directly or it can be improved further through a third step which implies that each tower in turn is shifted from one strength level to the next until no improvement in total cost is achieved. The process can be considered as a minimization problem where each tower represents one variable which can have as many values as number of strength levels. Since several minimum points will be present for this problem, an absolute minimum cannot be guaranteed. Experience has shown, however, that good solutions are obtained.

Optimization of tower geometry

The geometry optimization part of the program system is actually a by-product from the member sizing program. The efficiency of the geometry optimization is not of crucial importance because geometry is optimized only when new tower types are put into production, which is a relatively rare occation.

A set of geometry variables is used to define all node coordinates through relations of the form $\mathbf{x}=\mathbf{x}_0+\mathbf{A}\mathbf{c}$, where $\mathbf{x}$ is a vector of node x-coordinates, $\mathbf{x}_0$ is a constant contribution to this vector, $\mathbf{A}$ is a coefficient matrix and $\mathbf{c}$ is the vector of geometry variables. Similar expressions are established for y- and z-coordinates, and the tower geometry is constrained by linear explicit inequalities. The tower cost which can be found after a set of analysis and sizing cycles can now be considered as a function of the geometry variables, $\mathbf{c}$. Since member profiles are selected from a profile table, this cost function will be discontinuous and the problem will hence be to minimize an implicit, discontinuous objective function with continuous variables and linear, explicit constraints.

Two algorithms for function minimization are made available in the program; the combined random and direct search 'complex' method by Box (10) and the well known Powell's direct search method (11) modified to handle explicit linear constraints. The complex method is best suited in an initial stage to eliminate possible local minima. Powell's method is used as a final stage and should not be initiated too far from the minimum. One-dimensional searches are carried out using the golden section ratio iteration or by quadratic interpolation.

A simple console-type truss shown in Fig. 16 has been optimized with respect to two geometry variables using Powell's method. The cost function has been plotted as a two-dimensional contour map and shows that several local minima and maxima are present in the interesting variable range. The global minimum was found with sufficient accuracy after 13 function evaluations where each evaluation contained one analysis and one sizing phase.

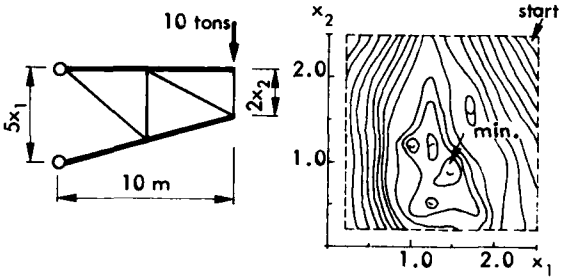


Fig 16 Console-type truss

Conclusions

A computer program system for design of power transmission towers has been presented. Emphasis has been put on approximations and assupmtions which are necessary to obtain a system which can be used in practical tower design work.

The program system presented is suited for towers which can be idealized as truss structures. Parts of the system may be of general interest, for instance the tower spotting module and the modules for analysis, member sizing and geometry optimization of single towers. The modules for member sizing of all towers in a line and the postprocessor for optimal selection of strength levels may be of less general interest unless a certain amount of modification is made.

The program system is not yet available to the public, but will probably be released in the near future.

References

(1) Hanssen, L., "PINTOS - A Program System for Interactive Tower Spotting", Preliminary User's Manual, SINTEF div. of Structural Engineering, N 7034 Trondheim-NTH, Norway, 1981 (not released per Oct 1981).

(2) Hanssen, L. and Holthe, K., "MAST1 - A Computer Program for Design of Power Transmission Towers", User's Manual, SINTEF div. of Structural Engineering, N 7034 Trondheim-NTH, Norway, 1977 (not released per Oct 1981).

(3) Hanssen, L., "MAST2 - A Computer Program for Design of Power Transmission Lines", User's Manual, SINTEF division of Structural Engineering, N 7034 Trondheim-NTH, Norway, 1978 (not released per Oct 1981).

(4) Hanssen, L., "MAST3 - A Computer Program for Tower Geometry Optimization", User's Manual, SINTEF div. of Structural Engineering, N 7034 Trondheim-NTH, Norway 1979 (not released per Oct 1981).

(5) Ahlborg, F. and Palm, Y., "Optimum Tower Spotting on Transmission Lines by Means of Electronic Computer", Swedish State Power Board, Blue-White Series No. 33, 1962.

(6) Ranyard, J.C. and Wren, A., The Optimum Arrangement of Towers in an Electric Power Transmission Line. *Computer Journal*, vol 10, no 2, pp 157-161, 1967.

(7) Pandapas, G., Optimization of Overhead Wire Systems by Linear and Non-linear Programming Techniques. *IEEE Power Engineering Society*, PES Winter Meeting, NY Feb 1979.

(8) Mitra, G. and Wolfenden, K., A computer Technique for optimizing the Sites and Heights of Transmission Line Towers - a Dynamic Programming Approach. *Computer Journal*, vol 10, no 4, pp 347-351, 1968.

(9) Landsend, K., "CECAR3 - A Computer Program for General Conductor Calculations", User's Manual, NVE - Norwegian Water Resources and Electricity Board (Confidential).

(10) Box, M.J., A New Method of Constrained Optimization and Comparison with other Methods. *Computer Journal*, Vol. 8, 1965.

(11) Fox, R.L., *Optimization Methods for Engineering Design*, Addision-Wesley Publishing Company, 1971.



CURRENT RESEARCH ON SHEAR BUCKLING AND THERMAL LOADS WITH PASCO: PANEL ANALYSIS AND SIZING CODE

AD-P000 092

W. Jefferson Stroud
William H. Greene
Melvin S. Anderson

NASA Langley Research Center
Hampton, VA 23665

Summary

A computer program PASCO for obtaining the detailed dimensions of optimum (least mass) stiffened composite structural panels is described. Design requirements in terms of inequality constraints can be placed on buckling loads or vibration frequencies, lamina stresses and strains, and overall panel stiffness for each of many load conditions. General panel cross sections can be treated. In an earlier paper, PASCO was described and studies were presented which showed the importance of accounting for an overall bow-type imperfection when designing a panel--a capability available in PASCO. Since that paper, detailed studies have shown that the buckling analysis VIPASA in PASCO can be overly conservative for long-wavelength buckling when the loading involves shear. To alleviate that deficiency, an analysis procedure involving a smeared orthotropic solution was investigated. Studies are presented that illustrate the conservatism in the VIPASA solution and the danger in a smeared orthotropic solution. PASCO's capability to design for thermal loadings is also described. Design studies illustrate the importance of the multiple load condition capability when thermal loads are present.

Symbols

A	planform area of stiffened panel
B	panel width (see fig. 6)
E	Young's modulus
e	overall bow in panel, measured at midlength (see fig. 1)
G_{12}	shear modulus of composite material in coordinate system defined by fiber direction
I	moment of inertia
L	panel length (see fig. 1)
M_x	applied bending moment per unit width of panel (see fig. 1)
N_x, N_y, N_{xy}	applied longitudinal compression, transverse compression, and shear loading, respectively, per unit width of panel (see fig. 1)
N_{x_E}	Euler buckling of panel - buckling load for $\lambda = L$
P	lateral pressure
S	area of panel cross section
u,v,w	buckling displacements
W	mass of stiffened panel
$\frac{W/A}{L}$	mass index
X,Y,Z	coordinate axes
x,y,z	coordinates
α	coefficient of thermal expansion
γ	N_x/N_{x_E}
ΔT	change in temperature
λ	buckling half-wavelength
μ_1, μ_2	Poisson's ratios of composite material in coordinate system defined by fiber direction, $\mu_2 = \mu_1 E_2/E_1$
ρ	density
σ	stress

Subscripts

1	fiber direction
2	normal to fiber direction
i	integer associated with plate element i

Introduction

The introduction of composite materials has greatly expanded the options for obtaining efficient structural designs. Because of the large number of design options, the task of finding the optimum configuration for a composite structure is more difficult than for the corresponding metal structure. This opportunity to obtain superior designs together with the difficulty of selecting among many options is making automated structural sizing an increasingly attractive design tool. Not only do composite materials provide an increase in the number of design variables, they can also cause an increase in the complexity of the failure modes. Rules of thumb that prevent undesirable proportions for metal structures are often inadequate for the corresponding composite structure. For that reason, the automated structural sizing procedure must incorporate accurate structural analysis methods. For stiffened composite structural panels, a computer program denoted PASCO (Panel Analysis and Sizing COde) has been developed and described in references 1-4. PASCO includes both the generality necessary to exploit the added design flexibility afforded by composite materials and an accurate buckling analysis--VIPASA[5] (Vibration and Instability of Plate Assemblies including Shear and Anisotropy)--to detect and account for complex buckling modes. PASCO can design for buckling, frequency, material strength and panel stiffness requirements. An important limitation of PASCO is that VIPASA underestimates the buckling load for long wavelength buckling when the

PRECEDING PAGE

loading involves shear.

This paper is divided roughly into three parts. In the first part, the capabilities of and approach used in PASCO are described briefly. In the second part, the conservatism in VIPASA for long-wavelength shear buckling is explained and illustrated. To alleviate that deficiency, an alternate analysis procedure based on a smeared orthotropic solution was investigated. Calculations are presented which show the danger in using that solution. In the third part, PASCO's capability to design for thermal loadings is described. Design studies illustrate the importance of the multiple load condition capability when thermal loads are present.

Description of PASCO

PASCO is described in detail in references 1-4; therefore, the description presented here is a summary.

Capabilities

PASCO has been designed to have sufficient generality in terms of panel configuration, loading, and practical constraints so that it can be used for sizing of panels in a realistic design application. The panel may have an arbitrary cross section composed of an assembly of plate elements with each plate element consisting of a balanced symmetric laminate of any number of layers. The panel cross section, material properties, loading, and temperature change are assumed to be uniform in the X direction (fig. 1). Any group of dimensions, including ply angles, may be selected as design variables; the remaining dimensions can be held fixed or related linearly to the design variables.

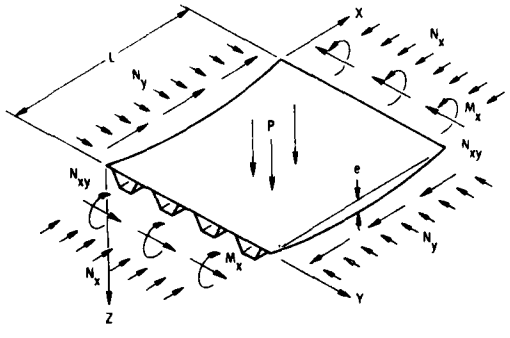


Figure 1.- Stiffened panel with initial bow, applied loading, and coordinate system.

The panel may be loaded by any combination of in-plane loadings (tension, compression, and shear) and lateral pressure as indicated in figure 1. Multiple load conditions can be treated. Thermal stresses resulting from temperature changes are calculated. The material properties corresponding to the temperature of each plate element may be changed for differert load cases. The effect of an overall panel imperfection e, shown in figure 1, can also be taken into account. One of the improvements that has been made to the code since reference 1 is that an overall bending moment M_X, shown in figure 1, can be accounted for in an approximate manner.

Realistic design constraints such as minimum ply thickness, fixed stiffener spacing, upper and/or lower bounds on extensional and shear stiffness may be prescribed. The vibration frequency of the panel (including the effect of prestress) may be specified to exceed a given value. Buckling loads and vibration frequencies are calculated by the VIPASA computer program.[5] Stresses and strains in each layer of each plate element are calculated and margins against material failure are calculated based on an assumed material strength failure criterion.

Optimization Approach

A nonlinear mathematical programming approach with inequality constraints is used to perform the optimization. The optimizer is CONMIN.[6,7]

Sizing variables.- The sizing variables (design variables) are the widths of the plate elements that make up the panel cross section, the ply thicknesses, and the ply orientation angles. Any set of widths, thicknesses and orientation angles can be selected as the active sizing variables. The remaining widths, thicknesses, and orientation angles can be held fixed or linked linearly to the active sizing variables. Upper and lower bounds can be specified.

Objective function.- The objective function is the panel mass index $\frac{W/A}{L}$, the panel mass per unit area divided by the panel length. The panel length is fixed; therefore, the quantity that is minimized is the panel mass per unit width.

Constraints.- Inequality constraints can be placed on buckling loads or vibration frequencies (loaded or unloaded), lamina stresses or strains (material strength constraints), and panel stiffness. These constraints can be applied for each of many load conditions.

For the buckling and vibration constraints, separate constraints are applied for each wavelength. With this approach, panels can be designed with a different margin of safety for each wavelength. Constraints can also be placed on several eigenvalues at the same wavelength.

For the material strength constraints, three strength criteria are available in PASCO: maximum lamina stress, maximum lamina mechanical strain, and the Tsai-Wu criterion[8]. For the maximum stress criterion, tension and compression limits are placed on lamina stresses in the fiber direction and transverse to the fiber direction. Limits are also placed on the shear stress. The maximum lamina mechanical strain criterion is defined similarly, except that the thermal strain is subtracted from the total strain to provide the mechanical strain. The Tsai-Wu criterion involves a quadratic function of the stresses. Failure is assumed to occur when the stress state in any lamina exceeds the failure criterion.

For the stiffness constraints, upper or lower bounds can be placed on the extensional stiffness, the shear stiffness, and the bending stiffness. These stiffnesses are "smeared" orthotropic stiffnesses for the overall panel, not individual plate element stiffnesses. The extensional stiffness is associatd with the N_x load, the shear stiffness with the N_{xy} load, and the bending stiffness with the M_x load. These loads are shown in figure 1.

Constraint Approximation.- A constraint approximation approach[9] is used in PASCO to increase the computational efficiency when the program is used for sizing. That approach is depicted schematically in

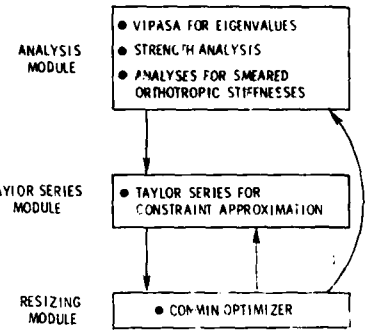


Figure 2.- General sizing approach used in PASCO.

figure 2. In the analysis module, all constraints are calculated with VIPASA and supporting subroutines. The program identifies the critical constraints and, using finite difference approximations, calculates derivatives of the critical constraints with respect to the sizing variables. These derivatives are then passed to the Taylor series module which generates a first order Taylor series expansion of each constraint. These expansions provide the approximate constraints for CONMIN. CONMIN interacts only with these approximate explicit functions that represent the contraints, not with VIPASA.

The design strategy consists of a series of sizing cycles in which CONMIN adjusts the values of the sizing variables based on approximate values of the constraints. An upper limit is imposed on the change of each sizing variable during each sizing cycle. The end point of one sizing cycle becomes the initial point of the next sizing cycle. Accurate values of the constraints and derivatives of the constraints are then recalculated, and new Taylor series expansions are generated. Ten sizing cycles are usually adequate to obtain convergence if the initial design is reasonably well chosen.

Shear Buckling Problem

As is pointed out earlier in this paper, an important limitation of PASCO is that VIPASA underestimates the buckling load when the loading involves shear and the buckle mode is a general or overall mode in which a single half wave extends from one end of the panel to the other. That shortcoming is explored in this section.

VIPASA Buckling Analysis

VIPASA, the buckling analysis program incorporated in PASCO, treats an arbitrary assemblage of plate elements with each plate element i loaded by N_{x_i}, N_{y_i}, and N_{xy_i}. The buckling analysis connects the individual plate elements and maintains continuity of the buckle pattern across the intersection of neighboring plate elements. The buckling displacement w assumed in VIPASA for each plate element is of the form

$$w = f_1(y)\cos\frac{\pi x}{\lambda} - f_2(y)\sin\frac{\pi x}{\lambda} \qquad (1)$$

Similar expressions are assumed for the inplane displacements u and v. The functions $f_1(y)$ and $f_2(y)$ allow various boundary conditions to be prescribed on the lateral edges of the panel. Boundary conditions cannot be prescribed on the ends of the panel.

For orthotropic plate elements with no shear loading, $f_2(y)$ is zero. The solution $f_1(y)\cos\frac{\pi x}{\lambda}$ gives a series of node lines that are straight, perpendicular to the longitudinal panel axis, and spaced λ apart as shown in figure 3. Along each of these node lines, the buckling displacements satisfy simple support boundary conditions. For values of λ given by $\lambda = L, L/2, L/3, \ldots L/m$, where m is an integer, the nodal pattern shown in figure 3 satisfies simple support boundary conditions at the ends of a finite, rectangular, stiffened panel of length L.

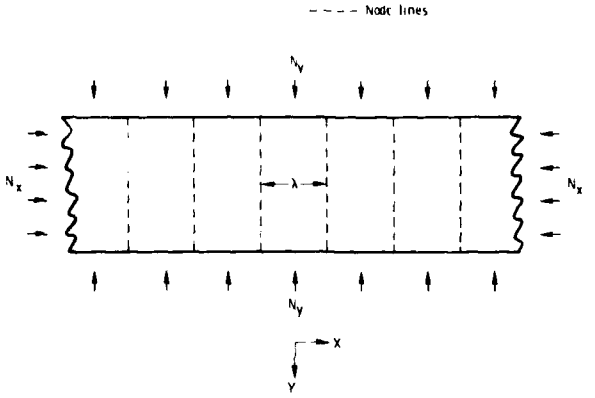


Figure 3.- Node lines produced by $w = f_1(y)\cos\frac{\pi x}{\lambda}$

For anisotropic plate elements and/or plate elements with a shear loading, $f_2(y)$ is not zero. (Because anisotropy generally has negligible effect for long wavelength buckling modes and because it is these long wavelength modes that are troublesome, reference to anisotropy is dropped in the following discussion). Node lines are skewed and not straight, but the node lines are still spaced λ apart as shown in figure 4. Since node lines cannot coincide with

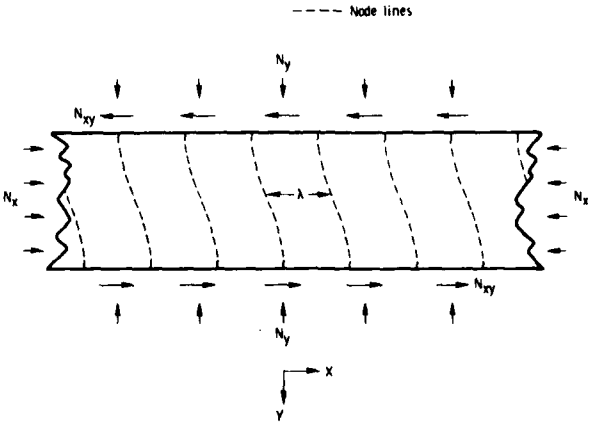


Figure 4.- Node lines produced by $w = f_1(y)\cos\frac{\pi x}{\lambda} - f_2(y)\sin\frac{\pi x}{\lambda}$

the ends of the rectangular panel, the VIPASA solution for loadings involving shear is accurate only when many buckles form along the panel length, in which case boundary conditions at the ends are not important. An example in which $\lambda = L/4$ is shown in figure 5.

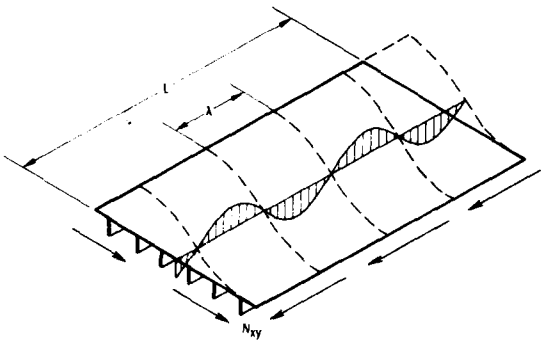


Figure 5.- Buckling of panel under shear loading. Mode shown is $\lambda = L/4$.

As λ approaches L, the VIPASA buckling anaylsis for a panel loaded by N_{xy} may underestimate the buckling load substantially. One explanation is as follows: As seen in figure 5, the skewed nodal lines given by VIPASA in the case of shear do not coincide with the end edges. Forcing node lines (and, therefore, simple support boundary conditions) to coincide with the end edges produces long-wavelength buckling loads that are, in many cases, appreciably higher than those determined by VIPASA.

In summary, for stiffened panels composed of orthotropic plate elements with no shear loading, the VIPASA solution is exact in the sense that it is the exact solution of the plate equations satisfying the Kirchoff-Love hypothesis. However, for stiffened panels having a shear loading the VIPASA solution can be very conservative for the case $\lambda = L$.

Because VIPASA is overly conservative in the case of long-wavelength buckling if a shear load is present, other easily-adaptable analysis procedures based on smeared orthotropic stiffnesses have been explored for the case $\lambda = L$.

Smeared Stiffener Solution

The objective of the analysis is to solve the shear buckling problem for the finite panel illustrated in figure 6. For buckling half-wavelength λ equal to panel length L, the mathematical model solved by VIPASA and the resulting node lines are similar to those illustrated in figure 7. The panel in figure 7 is infinitely long in the X direction.

It is assumed that a better approximation to the solution for the finite panel would be obtained with the infinitely wide panel shown in figure 8. Unfortunately, the mathematical model illustrated in figure 8 cannot be analyzed with VIPASA because VIPASA requires that the panel be uniform in the direction of the infinite dimension. However, the mathematical model obtained by smearing the stiffnesses of the stiffened panel of figure 8 can be analyzed with VIPASA. That solution is referred to as the smeared stiffener solution. It is obtained by interchanging the x and y loading and stiffnesses. The eigenvalue used is the lowest of the set for $\lambda = B, B/2, B/3, \ldots$ where B is the panel width. (The attempt to improve on the VIPASA solution for long-wavelength shear buckling is more involved than the discussion presented here. However,

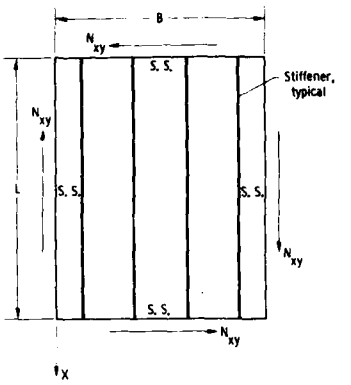


Figure 6.- Finite stiffened panel of length L and width B, simply supported on all four edges, and subjected to shear load N_{xy}.

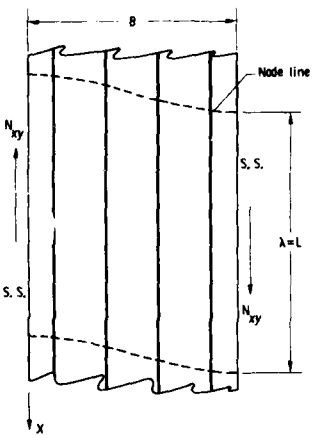


Figure 7.- Node lines given by VIPASA for shear buckling with $\lambda = L$.

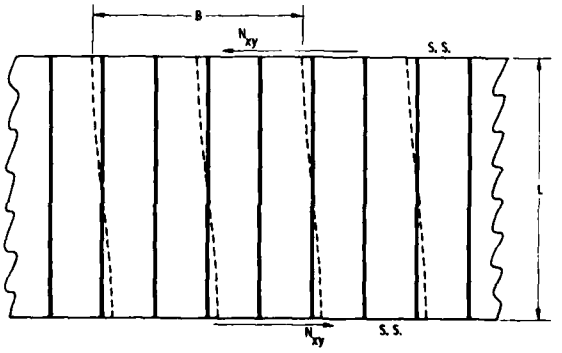
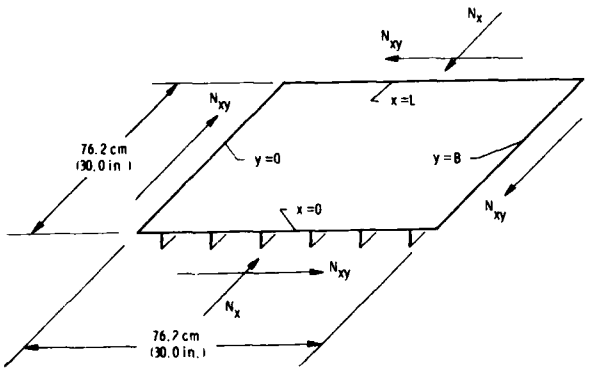


Figure 8.- Node lines for buckling of infinitely-wide stiffened panel.

the basic feature--smeared stiffener solution--of that solution approach and the conclusions regarding its suitability are the same as those presented here. A more complete discussion is presented in references 2 and 4).

Examples

Two stiffened panels were analyzed with PASCO and with the general finite element structural analysis code EAL (refs. 10, 11) to assess the validity of the VIPASA analysis for long wavelength shear buckling and the smeared stiffener solution. Both panels had six equally-spaced blade stiffeners, were 76.2 cm (30 in.) square, and were made of a graphite-epoxy composite material having the material properties given in table I. The loadings were combinations of longitudinal compression (N_x) and shear (N_{xy}). A schematic drawing showing the loading and overall dimensions for the example cases is shown in figure 9. The manner in which the applied loads were distributed over the cross section--the prebuckling stress state--is discussed in reference 2. In particular, the N_x load was distributed assuming uniform strain ϵ_x of the panel cross section with free transverse expansion of each plate element, so that N_{y_i} was zero. Buckling boundary conditions were simple support on all four edges. These boundary conditions are defined in figure 9. The panel cross sections were treated as collections of lines with no offsets to account for thicknesses. (Offsets are available in PASCO). The first example is discussed in greater detail than the second example.



Buckling boundary conditions are simple support on all four edges:
x = 0, L: u and $\frac{\partial w}{\partial x}$ are unrestrained, v = w = 0
y = 0, B: v and $\frac{\partial w}{\partial y}$ are unrestrained, u = w = 0

Figure 9.- Loading, dimensions, and boundary conditions for stiffened panel examples.

Example 1.- A repeating element of the composite blade-stiffened panel is shown in figure 10. Element widths are also shown. The wall construction for each plate element is given in table II. Only half the laminate is defined for each plate element because all laminates are symmetric. Plate element numbers are indicated by the circled numbers in figure 10. Fiber orientation angles are measured with respect to the X axis, which is parallel to the stiffener direction.

The single finite element type used in the EAL model for this and the other example is a four-node, quadrilateral, combined membrane and bending element. Both the membrane and bending stiffness matrices for the element are based on the assumed stress, hybrid

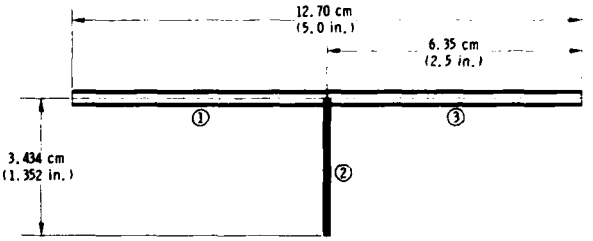


Figure 10.- Repeating element for example 1, composite blade-stiffened panel.

formulation of the Pian type.[10,12] The buckling or geometric stiffness matrix for the element is based on a conventional displacement formulation that includes terms allowing inplane (u and v displacements) as well as out-of-plane (w displacements) buckling modes. The Pian membrane formulation allows a single element across the depth of a blade stiffener to accurately represent its overall inplane bending behavior. The EAL designation for this element is E43. The finite element grid chosen for the EAL model is shown in figure 11. Two elements are used along the depth of the blade, four elements are used between blades, and 36 elements are used along the length, making a total of 1296 elements, and 1369 nodes. Based on convergence studies and other comparisons, it is believed that the finite element calculations presented in this paper differ from the exact solution by no more than approximately one percent and, therefore, provide benchmark calculations.

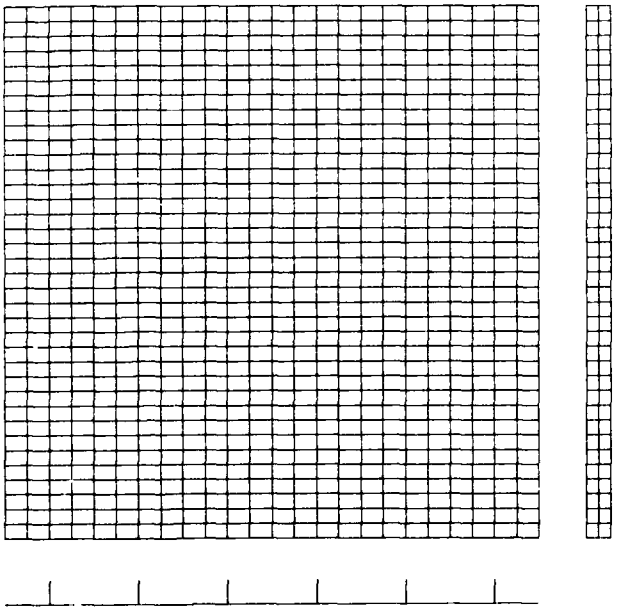


Figure 11.- EAL finite element model for example 1, composite blade-stiffened panel.

Buckling results are shown in figure 12. The curves indicate VIPASA and smeared stiffener solutions, and the circular symbols indicate EAL solutions. The solid curve represents the VIPASA solution for buckling half-wavelength λ equal to L. The dotted line at

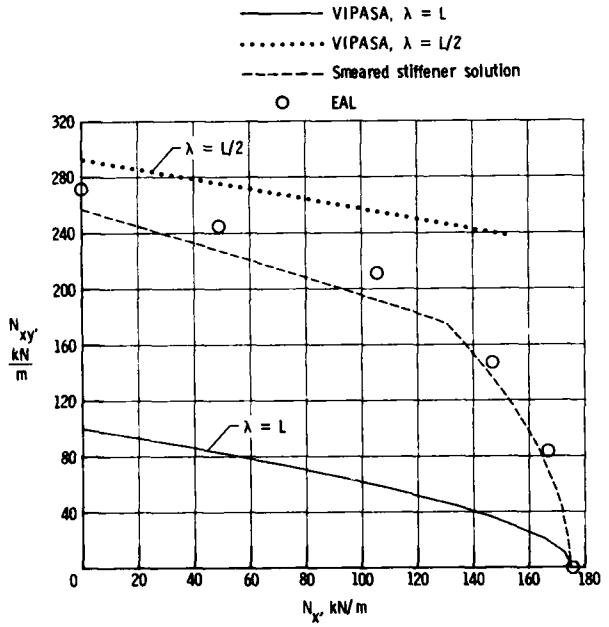


Figure 12.- Buckling load interaction for example 1, composite blade-stiffened panel.

the top of the figure represents the VIPASA solution for λ equal to L/2. The dashed curve represents the smeared stiffener solution and indicates solutions for the lowest buckling load of the set λ = B, B/2, B/3,.... where B is the panel width. The corner in the dashed curve that occurs at N_x equal to approximately 130 kN/m (750 lb/in) indicates a change in mode shape for the smeared stiffener solution. For N_x less than 130 kN/m, the buckling half-wavelength transverse to the stiffeners is equal to 38 cm (15 in.) which is three times the stiffener spacing. For N_x greater than 130 kN/m, the buckling half-wavelength transverse to the stiffeners is equal to 76 cm (30 in.) which is six times the stiffener spacing.

For this example, the smeared stiffener solution gives reasonably accurate estimates of the solution for all combinations of N_x and N_{xy}. For the loading N_x = 0, the smeared stiffener solution is about five percent lower than the EAL solution. For this same loading, the VIPASA solution for λ = L is about 63 percent lower than the EAL solution. For the loading N_{xy} = 0, the VIPASA solution for λ = L and the EAL solution agree to within 0.3 percent.

Detailed comparisons and benchmark calculations for six loadings are presented in table III. In this table, the quantity denoted FACTOR is the solution in terms of a scale factor for the specified loading. For example, for the loading N_x = 350.3 kN/m, N_{xy} = 175.1 kN/m (N_x = 2000 lb/in, N_{xy} = 1000 lb/in) the EAL solution of FACTOR = 0.4764 means that the solution is N_x = 0.4764 x 350.3 = 166.9 kN/m (952.8 lb/in) N_{xy} = 0.4764 x 175.1 = 83.37 kN/m (476.4 lb/in).

Finally, the buckling mode shape obtained with EAL for the case N_x = 0 is shown in figure 13. This contour plot of the buckling displacement w shows that the buckling half-wavelength transverse to stiffeners is approximately equal to three times the stiffener spacing, which was predicted by the smeared stiffener solution.

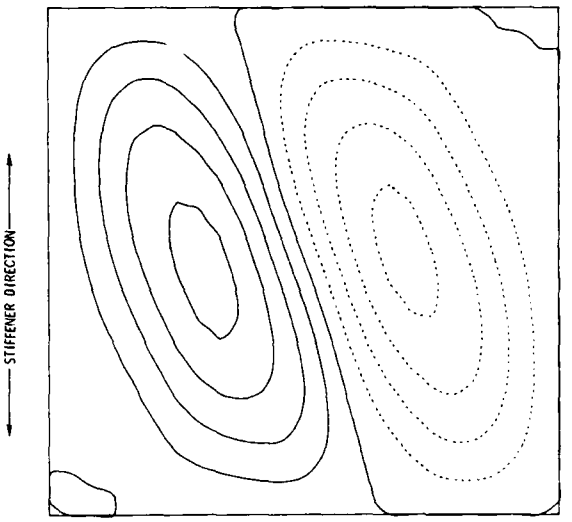


Figure 13.- Shear buckling mode shape obtained with EAL for example 1, composite blade-stiffened panel.

Example 2.- A repeating element of a heavily-loaded composite blade-stiffened panel is shown in figure 14. The wall construction for each plate element is given in table IV.

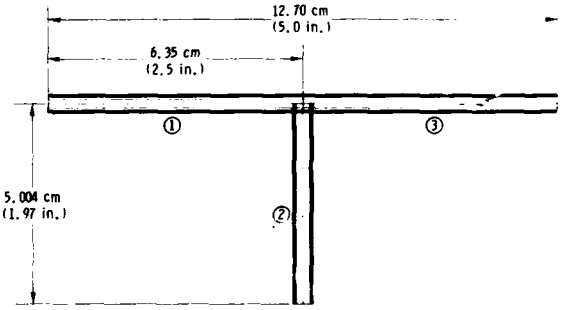


Figure 14.- Repeating element for example 2, heavily loaded, composite blade-stiffened panel.

Buckling solutions for example 2 are shown in figure 15. The solid curve indicates the VIPASA solution for λ = L. The dotted curves indicate VIPASA solutions for λ = L/2, L/4, and L/5. The dashed curve represents the smeared stiffener solution. As in the first example, the corners in the dashed curve indicate changes in mode shape. For N_x less than about 700 kN/m (4000 lb/in) the buckling half-wavelength transverse to the stiffeners is 1.5 times the stiffener spacing. For N_x greater than about 700 kN/m but less than about 1600 kN/m (9000 lb/in) the buckling half-wavelength transverse to the stiffeners is 2.0 times the stiffener spacing. For N_x greater than about 1600 kN/m but less than about 1800 kN/m, the buckling half-wavelength transverse to the stiffeners is 3.0 times the stiffener spacing.

For this example, the EAL results fall below both the smeared stiffener solution and the λ = L/2, L/4, and L/5 curves. For the N_x = 0 case, an examination of the EAL buckling mode shape presented in figure 16 shows that the lowest buckling load is an overall mode (λ = L) rather than a λ = L/2 mode, which might

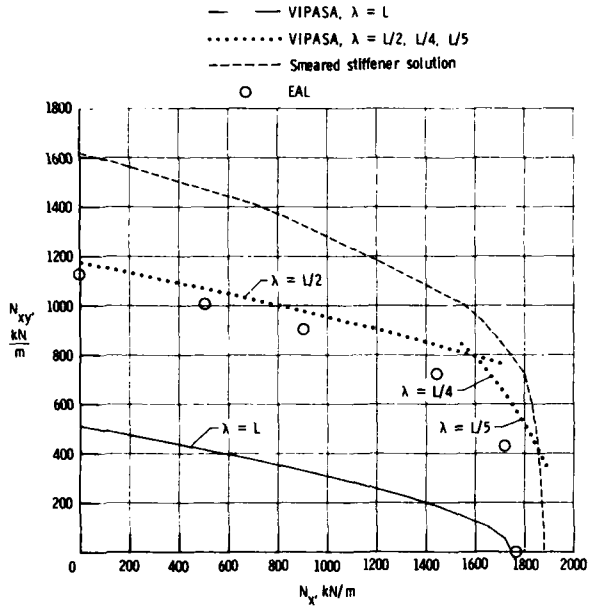


Figure 15.- Buckling load interaction for example 2, heavily-loaded, composite blade-stiffened panel.

have been assumed since the λ = L/2 solution is near the EAL solution. Detailed comparisons of solutions for six loadings are presented in table V.

Discussion of results.- The basic conclusion that can be drawn from these calculations and from similar results presented in reference 4 is that a buckling solution based on smearing the overall stiffnesses of a stiffened panel should be used only with caution.

In the first example, the smeared stiffener solution underestimated the overall buckling load slightly. In the second example, it greatly overestimated the overall buckling load. One factor that appeared to contribute to the error in the second example was that the buckle half-wavelength transverse to the stiffeners was only 1.5 times the stiffener spacing. Usually, that short a wavelength invalidates the stiffness smearing approach. In PASCO, the smeared stiffener solution should not be accepted if the buckle half-wavelength transverse to the stiffeners is less than 2.5 times the stiffener spacing.

Because an automated design procedure generally exploits a defect in an analysis, it is recommended that the smeared stiffener approach not be used in sizing applications. The panels designed using the standard VIPASA analysis will be light-weight and conservatively designed.

In all cases, the finite element solution for overall buckling falls between the VIPASA solutions for λ = L and λ = L/2. A solution approach for overall shear buckling that assumes the buckling mode to be a combination of the first few VIPASA modes is being studied. A special procedure is needed to combine these modes in such a way that the boundary conditions at the panel ends are satisfied.

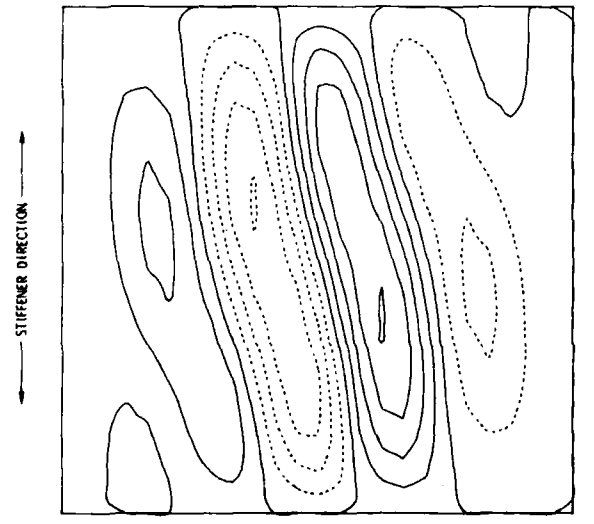


Figure 16.- Shear buckling mode shape obtained with EAL for example 2, heavily-loaded, composite blade-stiffened panel.

Thermal Loads In Panel Design

The PASCO program can perform a simplified thermal stress analysis, add the stress resultants due to the temperature effects to those obtained from other loadings and then determine the buckling load of the panel. A brief summary of this analysis will be given followed by design studies that illustrate how temperature and thermal stress can be treated in PASCO.

Thermal Stress Anaysis

In PASCO, a basic assumption in the buckling analysis is that all structural quantities and loadings are constant along the length. Therefore, temperatures must be assumed constant along the length, and any stress distribution determined as being representative of the stress distribution in the center of the panel is also assumed constant along the length. Temperature may vary along the width and depth direction of the panel but is constant through the thickness of a given wall cross-section. The temperature distribution is prescribed; it does not change as the sizing variables are changed.

The classical equation for thermal stress in a beam is the basis of the analysis

$$\sigma = \alpha E \Delta T - \frac{1}{S}\int_S \alpha E \Delta T \, dS - \frac{z}{I}\int_S \alpha E \Delta T z \, dS \qquad (2)$$

This equation suitably modified to account for orthotropic laminate properties (as shown in detail in ref. 2) is used in two different ways in PASCO. Consider a panel over many supports as illustrated in figure 17. The behavior of an individual bay would depend on its location. In the end bay, the stress distribution predicted by equation (2) would develop. The end bay would also have a bow produced by the bending moment generated by the underlined term. If there were an axial load N_x as well, this bow and the bending stresses produced by the bow would be increased by the

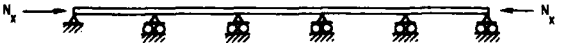


Figure 17.- Panel over many supports.

ratio $1/(1-\gamma)$, the beam-column effect. All these effects are included in PASCO when a parameter ITHERM is set equal to 1.

In the center of the panel, any tendency to bow would be restrained by adjacent bays and the stress distribution would be given by equation (2) with the underlined term omitted. In this case, there would be no bow due to thermal stress. This stress analysis is performed when the parameter ITHERM is set to zero.

When designing a panel subject to temperature, it is customary to require that the load also be sustained without temperature. In addition, if the panel spans many supports and if the same detailed dimensions are to be used for both end bays and interior bays, then the panel must be designed to carry the load with and without the thermal bow. The result is a multiple load condition problem. Such design problems are illustrated in the following examples.

Examples

Design requirements.- Several example studies were carried out to determine the effect on panel mass of design requirements involving temperature change. All studies used the overall dimensions, basic configuration, and stacking sequence of the blade-stiffened panels used in the shear buckling studies. Three types of studies are presented. In the first study, panels were made of a graphite-epoxy material having the properties given in table I. Sizing variables were the depth of the blade and the thicknesses of the plies; ply angles were fixed. The second study was similar to the first, except that ply angles were added to the sizing variables. In the third study, panels were made of aluminum. The importance of the thermal bow and the importance of the multiple load condition capability are demonstrated.

To provide for the bending loads that occur when the panel is allowed to take on a thermal bow, the blade portion of the stiffened panel was divided into seven sections as shown in figure 18. (The load N_{x_i} in each plate element i is uniform). The tip element of the blade was made very small so that prebuckling strains could be calculated accurately near the tip of the blade. These strains were monitored and used in the material strength criterion that is based on maximum mechanical strain. The normal strains were required to be less than 0.004, and the shear strain less than 0.01.

The following five load conditions were used:

Load Condition	N_x, kN/m (Compression)	Thermal Bow	Temperature Change, ΔT, ^{o}K
1	175.1	No	-111.1
2	175.1	No	Variable
3	175.1	No	0
4	175.1	Yes	Variable
5	175.1	Yes	-111.1

The loading 175.1 kN/m corresponds to 1000 lb/in, and the temperature change $-111.1^{o}K$ corresponds to $-200^{o}F$. Temperature changes are measured with respect to the temperature for a zero residual stress state in the composite material. Normally, this reference temperature is higher than room temperature. The three design temperature changes then correspond to a uniform cold condition ($\Delta T = -111.1^{o}K$), a transition condition in which the skin is hot and the tip of the blade is cold (variable), and a uniform hot condition ($\Delta T = 0^{o}$). In the transition condition (variable), the temperature change in each element is as follows: skin, $0^{o}K$; first element in blade (adjacent to skin), $-36.1^{o}K$; second element, $-66.7^{o}K$; third to seventh elements are $-86.1^{o}K$, $-97.2^{o}K$, $-105.5^{o}K$, $-108.3^{o}K$, $-111.1^{o}K$.

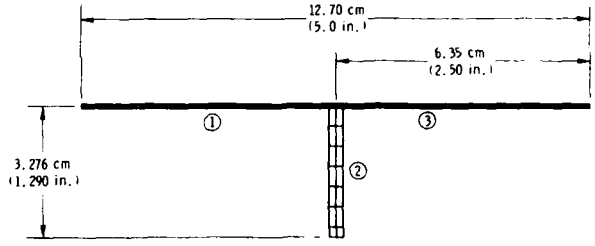


Figure 18.- Repeating element for graphite-epoxy panel designed for load conditions 1 to 5.

Graphite-epoxy panels, fixed ply angle.- Results of the design study for the graphite-epoxy blade-stiffened panel with fixed ply angles are presented in table VI. The first column (far left) indicates the load conditions used to obtain a design. For example, the third entry in that column indicates load conditions 1, 2, and 3. The second column is the mass index $\frac{W/A}{L}$ of the minimum mass panel that supports that combination of load conditions. The final five columns are the ratios of the lowest buckling load to the design loading for each of the five loading conditions. The ratios are applied to both the compressive load and the change in temperature.

The data in the first row shows that a panel designed for a temperature change (load condition 1) need not carry the load when the temperature is removed (load condition 3). The panel designed for load conditions 3, 4, and 5 is the same as the panel designed for all five load conditions. The dimensions of the repeating element for that panel are shown in figure 18. Thicknesses are given in table VII. The skin consists of $+45^{o}$ plies only; the blade consists of 0° and $\pm 45^{o}$ plies only.

Graphite-epoxy panels, variable ply angle.- In two panels, ply angles were allowed to vary. Each panel was designed to carry load conditions 1 to 5. In the first panel, only the angles in the skin were varied. The result was that the skin of the final design consisted only of $+58.2^{o}$ plys and the mass index was reduced 6% to 4.052 kg/m^3. In the second panel, the angles of the plys originally at $+45^{o}$ in both the skin and the blade and the angles of the plys originally at 0° in the blade were varied. The additional mass reduction was negligible.

Aluminum panels.- Design studies similar to those presented in table VI for graphite-epoxy panels were also carried out for aluminum panels having the material properties given in table VIII. Results are presented in table IX. Since uniform temperature changes produce no thermal stress for these panels, the original five loading conditions reduce to three: 1, 2, and 4. The repeating element for the panel that supports all three loads is shown in figure 19.

Discussion of results.- Three conclusions can be drawn from these calculations. First, when design requirements involve thermal loads it is advisable to use a multiple load condition approach with various temperature distributions and end support conditions. For the examples presented in this paper, the increase in

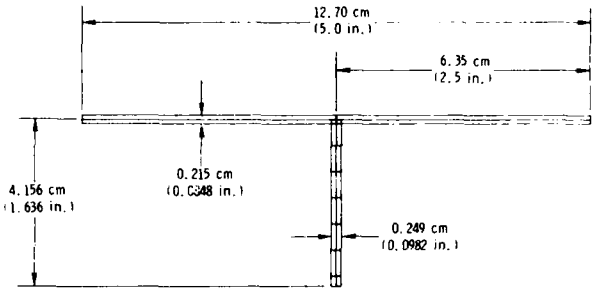


Figure 19.- Repeating element for aluminum panel designed for load conditions 1, 2, and 4.

panel mass caused by using this approach is small compared to the increase in load carrying ability for off-design load conditions that may be encountered in service. This is true whether the panel is graphite-epoxy or aluminum.

The second conclusion is that it is more important to use the multiple load condition capability for composite panels than for metal panels. The increase in the number of design variables provided by composite materials allows a composite structure to be tailored very well to a specific load condition. However, this highly tailored structure may have very little load carrying ability for off-design conditions. This point is illustrated in reference 13 for the case of damage tolerance in wing structures.

The third conclusion is that ply angle variation can provide a moderate (6%) reduction in mass even in a five-load-condition-design.

Concluding Remarks

A computer program denoted PASCO for obtaining the dimensions of optimum (least mass) stiffened composite structural panels is described. The capabilities of and approach used in PASCO are discussed briefly.

PASCO's buckling analysis (VIPASA) is reviewed, and an important shortcoming of that analysis--underestimation of long wavelength shear buckling loads--is explained. Studies involving combined longitudinal compression and shear loadings are presented to demonstrate VIPASA's conservatism for long-wavelength shear buckling. It is shown that an easily adaptable smeared orthotropic solution may be unconservative for predicting long-wavelength shear buckling. Therefore, it is recommended that the smeared solution not be used for sizing applications.

Studies also demonstrate the capability in PASCO to design for thermal stresses, to account for multiple loading conditions, and to use ply angles as sizing variables. The importance of using the multiple load condition capability for thermal loadings is illustrated for both graphite-epoxy and aluminum panels. Ply angle variation provided a 6% mass reduction for a multiple load condition case.

References

1. Anderson, Melvin S.; and Stroud, W. Jefferson: A General Panel Sizing Computer Code and Its Application to Composite Structural Panels. AIAA J., Vol. 17, No. 8, August 1979, pp. 892-897.

2. Stroud, W. Jefferson; and Anderson, Melvin S.: PASCO: Structural Panel Analysis and Sizing Code, Capabilty and Analytical Foundations. NASA TM 80181, 1980.

3. Anderson, Melvin S.; Stroud, W. Jefferson; Durling, Barbara J.; and Hennessy, Katherine W.: PASCO: Structural Panel Analysis and Sizing Code, Users Manual. NASA TM 80182, 1980.

4. Stroud, W. Jefferson; Greene, William H.; and Anderson, Melvin S.: Buckling Loads for Stiffened Panels Subjected to Combined Longitudinal Compression and Shear Loadings: Results Obtained with PASCO, EAL, and STAGS Computer Programs. NASA TM 83194, 1981.

5. Wittrick, W. H.; and Williams, F. W.: Buckling and Vibration of Anisotropic or Isotropic Plate Assemblies Under Combined Loadings, Int. J. of Mech. Sci., Vol. 16, 1974, pp. 209-239.

6. Vanderplaats, Garret N.: CONMIN - A Fortran Program for Constrained Function Minimization. User's Manual. NASA TM X-62,282, 1973.

7. Vanderplaats, G. N.; and Moses, F.: Structural Optimization by Methods of Feasible Directions. National Symposium on Computerized Structural Analysis and Design, Washington, DC, March 1972.

8. Jones, Robert M.: Mechanics of Composite Materials. Scripta Book Co., 1975.

9. Schmit, Lucien A., Jr.; and Miura, Hirokazu: Approximation Concepts for Efficient Structural Synthesis. NASA CR-2552, 1976.

10. EISI/SPAR Reference Manual, System Level 103, Engineering Information Systems Inc., San Jose, CA, January 1979.

11. Whetstone, W. D.: Engineering Data Management and Structure of Program Functions in New Techniques in Structural Analysis by Computer (Compiled by R. J. Melosh and M. Salana) ASCE Preprint 3601, ASCE Convention and Exposition, Boston, Massachusetts, 1979.

12. Gallagher, Richard H.: Finite Element Analysis, Fundamentals. Prentice-Hall, 1975.

13. Starnes, James H., Jr.; and Haftka, Raphael T.: Preliminary Design of Composite Wing Box Structures For Global Damage Tolerance. Proceedings of AIAA/ASME/ASCE/AHS 21st Structures, Structural Dynamics, and Materials Conference, Seattle, WA, May 12-14, 1980, pp. 529-538.

TABLE I.- LAMINA PROPERTIES OF GRAPHITE-EPOXY MATERIAL USED IN CALCULATIONS

Symbol	Value in SI Units	Value in US Customary Units
E_1	131.0 GPa	19.0×10^6 psi
E_2	13.0 GPa	1.89×10^6 psi
G_{12}	6.41 GPa	$.93 \times 10^6$ psi
μ_1	.38	.38
α_1	$-.378 \times 10^{-6}$ 1/°K	$-.21 \times 10^{-6}$ 1/°F
α_2	28.8×10^{-6} 1/°K	16×10^{-6} 1/°F
ρ	1581 kg/m^3	0.0571 lbm/in^3

TABLE II.- WALL CONSTRUCTION FOR EACH PLATE ELEMENT IN EXAMPLE 1

Layer number starting with outside layer	Thickness		Fiber orientation, deg
	cm	in.	
Plate elements 1 and 3			
1	0.01397	0.00550	45
2	.01397	.00550	-45
3	.01397	.00550	-45
4	.01397	.00550	45
5	.01397	.00550	0
6	.12573	.04950	90
Plate element 2			
1	0.01397	0.00550	45
2	.01397	.00550	-45
3	.01397	.00550	-45
4	.01397	.00550	45
5	.02794	.01100	0

TABLE III.- BUCKLING LOADS FOR EXAMPLE 1

Loading, kN/m		Factor			
		VIPASA		Ortho. plate	EAL
N_x	N_{xy}	$\lambda = L$	$\lambda = L/2$		
0	175.1	0.5721	1.6641	1.4683	1.5525
35.0	175.1	.5353	1.5614	1.3098	1.3985
87.6	175.1	.4862	1.4248	1.1222	1.2060
175.1	175.1	.4182	1.2357	.8222	.8397
350.3	175.1	.3200		.4690	.4764
175.1	0	1.0005		.9970	1.0030

TABLE IV.- WALL CONSTRUCTION FOR EACH PLATE ELEMENT IN EXAMPLE 2

Layer number starting with outside layer	Thickness		Fiber orientation, deg
	cm	in.	
Plate elements 1 and 3			
1	0.01618	0.00637	45
2	.01618	.00637	-45
3	.01618	.00637	-45
4	.01618	.00637	45
5	.06325	.02490	0
6	.10566	.04160	90
Plate element 2			
1	0.02090	0.00823	45
2	.02090	.00823	-45
3	.02090	.00823	-45
4	.02090	.00823	45
5	.17145	.06750	0

TABLE V.- BUCKLING LOADS FOR EXAMPLE 2

Loading, kN/m		Factor			
		VIPASA		Ortho. plate	EAL
N_x	N_{xy}	$\lambda = L$	$\lambda = L/2$		
0	175.1	2.9225	6.6998	9.2435	6.4424
87.6	175.1	2.6742	6.0385	8.0628	5.753
175.1	175.1	2.4574	5.4654	6.7945	5.1630
350.3	175.1	2.0997	4.5367	4.8627	4.124
700.5	175.1	1.5964		2.6424	2.4543
175.1	0	9.9724		10.7300	10.076

TABLE VI.- MASS INDEX AND RATIO OF BUCKLING LOAD TO DESIGN LOAD FOR FIVE GRAPHITE-EPOXY PANELS DESIGNED FOR SEVERAL COMBINATIONS OF LOAD CONDITIONS

Design load conditions	$\frac{W/A}{L}$, kg/m^3	Ratio of lowest buckling load to design load for the following load conditions				
		1	2	3	4	5
1	2.610	1.00	0.05	0.05	0.05	0.13
1,2	4.132	1.00	1.00	.98	.87	.77
1-3	4.158	1.00	1.00	1.00	.88	.77
1-4	4.297	1.07	1.00	1.00	1.00	.95
1-5	4.325	1.04	1.00	1.00	1.00	1.00

TABLE VII.- WALL CONSTRUCTION FOR EACH PLATE ELEMENT IN GRAPHITE-EPOXY PANEL DESIGNED FOR LOAD CONDITIONS 1 TO 5

Layer number starting with outside layer	Thickness		Fiber orientation, deg
	cm	in.	
Plate elements 1 and 3			
1	0.01411	0.005555	45
2	.01411	.005555	-45
3	.01411	.005555	-45
4	.01411	.005555	45
Plate element 2			
1	0.00214	0.000842	45
2	.00214	.000842	-45
3	.00214	.000842	-45
4	.00214	.000842	45
5	.17679	.069604	0

TABLE VIII.- PROPERTIES OF ALUMINUM USED IN EXAMPLE CALCULATIONS

Symbol	Value in SI Units	Value in US Customary Units
E	68.9 GPa	10×10^6 psi
G	26.2 GPa	3.8×10^6 psi
μ	.33	.33
α	23.4×10^{-6} 1/°K	13×10^{-6} 1/°F
ρ	2712 kg/m^3	0.098 lbm/in^3

TABLE IX.- MASS INDEX AND RATIO OF BUCKLING LOAD TO DESIGN LOAD FOR THREE ALUMINUM PANELS DESIGNED FOR SEVERAL COMBINATIONS OF LOAD CONDITIONS

Design load conditions	$\frac{W/A}{L}$, kg/m^3	Ratio of lowest buckling load to design load for the following load conditions		
		1	2	4
1	8.866	1.00	0.86	0.27
1,2	9.158	1.00	1.00	.20
1,2,4	10.569	1.42	1.00	1.00

AD-P000 093

PANDA--INTERACTIVE COMPUTER PROGRAM FOR PRELIMINARY MINIMUM WEIGHT DESIGN OF COMPOSITE OR ELASTIC-PLASTIC, STIFFENED CYLINDRICAL PANELS AND SHELLS UNDER COMBINED IN-PLANE LOADS

David Bushnell
Lockheed Palo Alto Research Laboratory
3251 Hanover Street, Palo Alto, California 94304

Summary

An analysis and an interactive computer program are described through which minimum weight designs of composite, stiffened, cylindrical panels can be obtained subject to general and local buckling constraints and stress and strain constraints. The panels are subjected to arbitrary combinations of in-plane axial, circumferential, and shear resultants. Nonlinear material effects are included if the material is isotropic or has stiffness in only one direction (as does a discrete or a smeared stiffener). Several types of general and local buckling modes are included as constraints in the optimization process, including general instability, panel instability with either stringers or rings smeared out, local skin buckling, local crippling of stiffener segments, and general, panel, and local skin buckling including the effects of stiffener rolling. Certain stiffener rolling modes in which the panel skin does not deform but the cross section of the stiffener does deform are also accounted for. The interactive PANDA system consists of three independently executed modules that share the same data base. In the first module an initial design concept with rough (not necessarily feasible or accurate) dimensions are provided by the user in a conversational mode. In the second module the user decides which of the design parameters of the concept are to be treated by PANDA as decision variables in the optimization phase. In the third module the optimization calculations are carried out. Results are presented of a parameter study on optimization of hydrostatically compressed, ring stiffened, elastic- plastic cylindrical shells designed for pressures from about 700 psi to 5000 psi. The feasibility of the optimum designs obtained by PANDA are verified by applications of BOSOR5.

Introduction

Objective

The objective of the development of PANDA has been to create an interactive computer program for engineers which derives minimum weight designs of stiffened cylindrical panels under combined in-plane loads, N_x , N_y , and N_{xy} . The loading of the stiffened panel is assumed in most cases to result in uniform membrane strain components e_x and e_y in both skin and stiffeners and uniform shear strain e_{xy} in the skin. Meridional bending between rings in the prebuckling phase is included for shells without axial stiffeners. Nonlinear material behavior is included in the prebuckling analysis if the material is isotropic or has strength only in one direction (smeared or discrete stiffeners).

Buckling loads are calculated by use of simple assumed displacement functions. For example, general instability of panels with balanced laminates and no shear loading is assumed to occur in the familiar $w(x,y) = C\sin(ny)\sin(mx)$ mode. In the presence of in-plane shear and/or unbalanced laminates, both local and general buckling patterns are assumed to have the form

$$w(x,y) = C\{\cos[(n+mc)y-(m+nd)x] - \cos[(n-mc)y+(m-nd)x]\}$$

in which either c or d are zero, depending on the geometry and the stiffness of the entire panel or whatever portion of the panel is under consideration.

The skin is cylindrical with radius R and the stiffeners are composed of assemblages of flat plate segments the lengths of which are large compared to the widths and the widths of which are large compared to the thicknesses. These flat plate segments are oriented either normal or parallel to the plane of the panel skin.

Figure 1 shows an example of the panel geometry. The overall dimensions of the panel are (a,b) and the spacings of the stiffeners are (a_o , b_o).

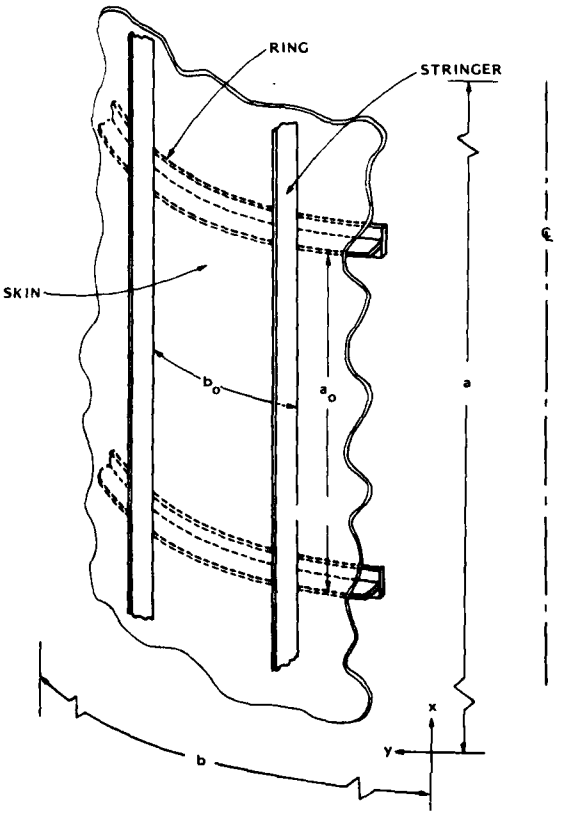


Fig. 1 Stiffened cylindrical panel with overall dimensions (a,b), ring spacing a_o , and stringer spacing b_o

PRECEDING PAGE

Material Properties

If the material is orthotropic or anisotropic, buckling is assumed to occur at stress levels for which this material remains elastic. Feasible designs are constrained by maximum stress or strain criteria. Plasticity with arbitrary strain hardening is permitted if the material is isotropic or if it has stiffness in one coordinate direction only, as does the continuum representation of each segment of a smeared stiffener. The cylindrical skin and stiffener segments can be composed of multiple layers of isotropic or orthotropic material, as depicted in Fig. 2. Each layer has a unique angle of orthotropy relative in the case of the panel skin to the direction of the generator (x- direction) and in the case of a stiffener segment to the stiffener axis. In the buckling analysis the segments of the stiffeners are assumed to be monocoque and isotropic or orthotropic, not layered anisotropic. Therefore, equivalent orthotropic properties for stiffener segments are calculated from input data for the stiffener segment laminates provided by the program user.

Types of Buckling

Optimum designs with respect to weight are obtained in the presence of constraints due to local and general buckling, maximum tensile and compressive stress or strain, maximum shear strain, and lower and upper bounds on skin layer thicknesses, stiffener cross section dimensions, and stiffener spacings. Design parameters allowed to vary during the optimization phase include panel skin laminae thickness and winding angles, spacings of stiffeners, and thicknesses and widths of the segments of ring and stringer cross sections.

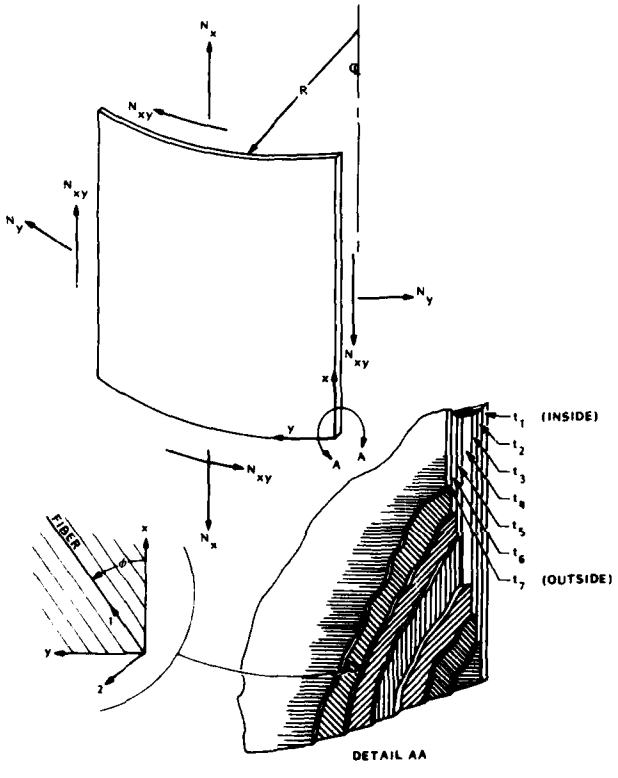


Fig. 2 Coordinates, loading and wall construction

The buckling formulas are derived from Donnell's equations (Reference [1]) with a posteriori application of a reduction factor $*(n_c^2 - 1)/n_c^2$ for panels in which the axial half wavelength of the buckling pattern is longer than the panel radius of curvature, R. The circumferential wave index, n_c, equals $n\pi R/b$ or $n\pi R/b_o$, with n being the number of half waves in the circumferential direction over the span b or b_o, respectively.

The many types of buckling included in the PANDA analysis are summarized in Table 1 and are briefly described next.

Skin Buckling. For the case of balanced laminates and no in-plane shear, local buckling of the skin is assumed to have the form

$$w_{skin} = C_{skin} \sin\left(\frac{\bar{n}_{skin}\pi y}{b_o}\right)\sin\left(\frac{\bar{m}_{skin}\pi x}{a_o}\right) \qquad (1)$$

in which $\bar{n}_{skin}$ and $\bar{m}_{skin}$ are the numbers of half-waves between stringers with spacing b_o and rings with spacing a_o, respectively. Equation (1) implies simple support boundary conditions at stiffener lines of attachment. With shear present and/or unbalanced laminates the skin buckling pattern has the form given in the second paragraph under Objective.

General Instability. General instability buckling modes of panels with balanced laminates and no shear also have the form given in Eq.(1) with a_o, b_o, $\bar{n}_{skin}$, and $\bar{m}_{skin}$ replaced by quantities appropriate to the overall dimensions (a,b) of the panel. PANDA also calculates values for "semi-general" instability, that is buckling between rings with smeared stringers and buckling between stringers with smeared rings.

Buckling of Stiffeners. Local buckling of the ith stiffener segment implies

$$w^i_{stiff} = C^i_{stiff} \sin\left(\frac{\pi \bar{y}_i}{b_i}\right)\sin\left(\frac{\bar{m}^i_{stiff}\pi\bar{x}}{\ell}\right) \qquad (2)$$

for each stiffener segment with both long edges supported (called "internal" segments in Fig. 3). As shown in Fig. 3 the quantity $\bar{x}$ is the coordinate along the stiffener axis, $\bar{y}_i$ is the coordinate perpendicular to $\bar{x}$ in the plane of the ith stiffener segment, b_i is the width of the stiffener segment, and ℓ is the length of the stiffener segment. ($\ell = a_o$ for stringers and $\ell = b_o$ for rings). For stiffener segments with only one long edge supported, (called "end" segments), the local buckling modal displacement is assumed to be in the form

$$w^i_{stiff} = C^i_{stiff}\, \bar{y}_i \sin\left(\frac{\bar{m}^j_{stiff}\pi\bar{x}}{\ell}\right) \qquad (3)$$

The stiffener segment buckling analysis is carried out with the assumption that each "internal" segment buckles with its own $\bar{m}^i$. This assumption implies that rotational incompatibility exists at junctions between segments with differing critical values of $\bar{m}^i$. "End" segments are assumed to buckle at the critical $\bar{m}^j$ of the segment to which they are joined. The buckling modes (2) and (3) are shown in Fig. 4.

Rolling Modes. Additional types of panel and stiffener buckling are considered here. These are called "rolling" modes. The first kind of rolling mode involves both skin and stiffeners and is local or "semi-general", the characteristic half-wave-length being integer fractions of the lengths (a_o , b_o), or (a,b_o) or (a_o , b). In these rolling modes the stiffener cross sections rotate about their lines of attachment to the panel skin as shown in Fig. 5a. The cross sections do not deform in the plane of the paper. They do warp, however. The other types of rolling instability do not involve the skin at all. Only the stiffener web deforms, the rest of the stiffener cross section displacing and rotating as a rigid body, as displayed in Fig. 5b. One of these rolling modes (Fig. 5b) occurs in both rings and stringers and in both curved and flat panels. In this mode the buckling deformations are nonuniform (sinusoidal) along the axis of the stiffener.

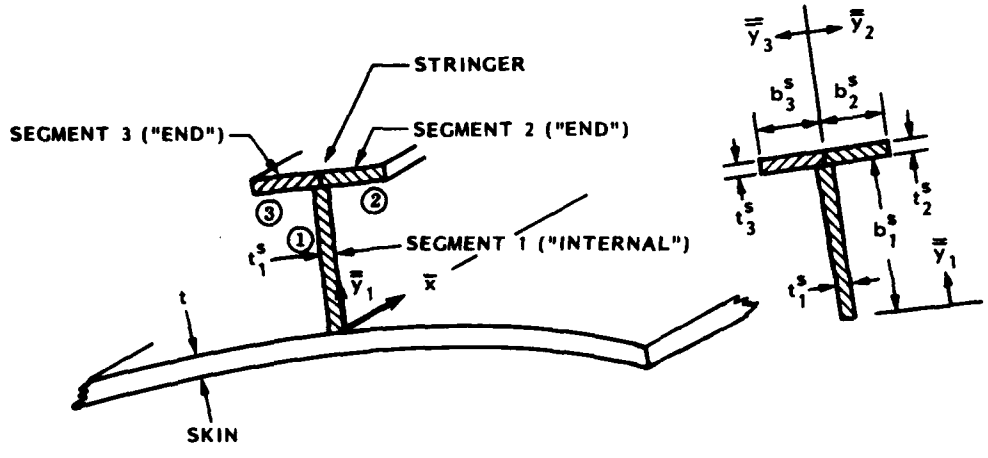
Table 1 Buckling Modes Included in the PANDA Analysis

TYPE OF BUCKLING	MODEL USED FOR ESTIMATE
1. General instability	Buckling of skin and stiffeners together with smeared rings and stringers. Panel is simply supported along the edges x = 0, y = 0, x = a, and y = b.
2. Local instability	Buckling of skin between adjacent rings and adjacent stringers. Portion of panel bounded by adjacent stiffeners is simply supported. Stiffeners take their share of the load in the prebuckling analysis but are disregarded in the stability analysis.
3. Panel instability	
(a) between rings with smeared stringers	Buckling of skin and stringers between adjacent rings. Portion of panel bounded by adjacent rings is simply supported. Stringers are smeared. Simple support conditions imposed at y = 0 and y = b. Rings take their share of the load in the prebuckling analysis, but are disregarded in the stability analysis.
(b) between stringers with smeared rings	Buckling of skin and rings between adjacent stringers. Portion of panel between adjacent stringers is simply supported. Rings are smeared. Simple support conditions imposed at x = 0 and x = a. Stringers take their share of the load in the prebuckling analysis, but are disregarded in the stability analysis.
4. Local crippling of stiffener segments	
(a) "internal" segments (Figs. 3, 4)	Individual stiffener segment buckles as if it were a long flat strip simply supported along its two long edges. Loading is compression along the stiffener axis. Curvature of ring segments is ignored.
(b) "end" segments (Figs. 3, 4)	Individual stiffener segment buckles as if it were a long flat strip simply supported along the long edge at which it is attached to its neighboring segment or to the panel skin, and free along the opposite edge. Loading is compression along the stiffener axis. Number of half waves along the stiffener axis is the same as that of the part of the structure to which the "end" is attached. Curvature of ring segments is ignored.
5. Local rolling with skin buckling between stiffeners (Fig. 5a)	Same as 2. "Local instability" except that the strain energy in the stiffeners and the work done by the prebuckling compression in the stiffeners are included in the buckling formula. Stiffener cross sections do not deform as the stiffeners twist about their lines of attachment to the panel skin.
6. Rolling instability	
(a) with smeared stringers (Fig. 5a)	Same as 3. "Panel instability", Type (a), except that the strain energy of rings and work done by prebuckling compression along the ring centroidal axis are included in the buckling formula. Ring cross section does not deform as the ring twists about its line of attachment to the panel skin.
(b) with smeared rings (Fig. 5a)	Same as 3. "Panel instability", Type (b), except that the strain energy of stringers and work done by prebuckling compression along the stringer centroidal axis are included in the buckling formula. Stringer cross section does not deform as it twists about its line of attachment to the panel skin.
7. Rolling of stringers no buckling of skin (Fig. 5b)	Stringer web cross section deforms but the flange cross section does not. Buckling mode has waves along the stringer axis.
8. Rolling of rings, no buckling of skin (Fig. 5b)	Ring web cross section deforms but the flange cross section does not. The buckling mode has waves along the ring axis. This mode is sometimes called "frame tripping" by those interested in submarine structures.
9. Axisymmetric rolling of rings, no buckling of skin (Fig. 5c)	Same as "Rolling of rings", except that the buckling mode has zero waves around the circumference of the panel.

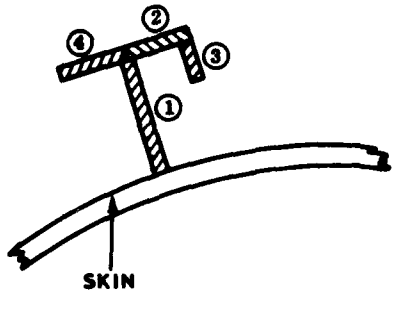
The other rolling mode (Fig. 5c) occurs only in the cases of internal rings on cylindrical panels under external pressure and external rings on cylindrical panels under internal pressure. In this mode buckling deformations are uniform along the axis of the ring. Stiffener rolling in the more general mode (Fig. 5b) is due to compression along the stiffener axis and is only weakly dependent on the curvature ot this axis. On the other hand, the local ring buckling depicted in Fig. 5c is axisymmetric and arises because of the circumferential curvature of the stiffener axis and prestress in the stiffener segments. It is interesting to note that axisymmetric rolling can occur even if there are no compressive stresses anywhere in the structure, as is the case for internally pressurized cylindrical shells with external rings.

Optimization

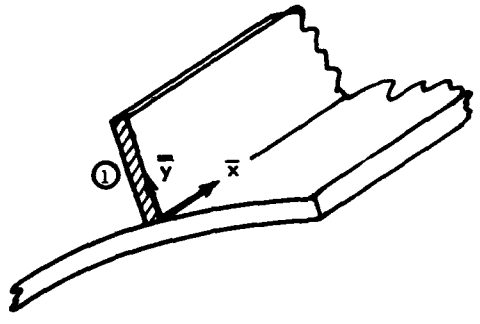
The subroutine CONMIN [2,3] is used in PANDA for finding minimum weight designs. This subroutine, written by Vanderplaats in the early 1970's, is based on a nonlinear constrained search algorithm due to Zoutendijk [4]. Briefly, the analytic technique used in CONMIN is to minimize an objective function (panel weight, for example) until one or more constraints, in this case buckling loads, maximum stress or strain, and upper and lower bounds on decision variables, become active. The minimization process then continues by following the constraint boundaries in decision variable space in a direction such that the value of the objective function continues to decrease. When a point is reached where no further decrease in the objective function is obtained, the process is terminated.



(a) A "T"-shaped stiffener must be treated as if it consists of three segments, one "internal" and two "ends".



(b) Segments ① and ② are "internal"; ③ and ④ are "ends".

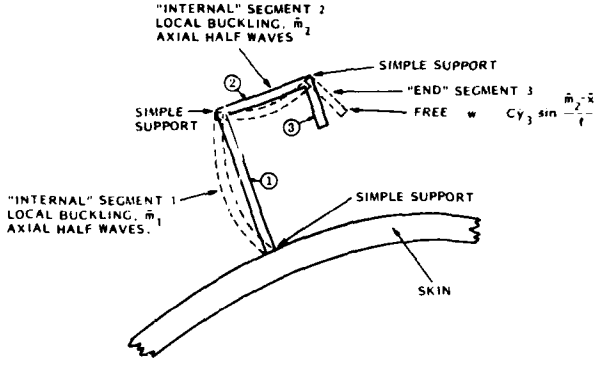


(c) Segment ① is an "end".

Fig. 3 Stiffener nomenclature and local coordinates $\bar{x}$ and $\bar{y}_1$

Review of the Literature and Evaluation of PANDA

A brief review of previous work on optimization of stiffened shells and panels under destabilizing loads is given in Ref. [5]. In addition, Ref. [5] contains results of many test cases for buckling and optimization in which comparisons with the literature are given.



EACH "INTERNAL" STIFFENER SEGMENT IS ASSUMED TO BE SIMPLY-SUPPORTED AT ITS EDGES. THE "END" SEGMENT REMAINS STRAIGHT IN THE WIDTH COORDINATE AS SEGMENTS 2 AND 3 BUCKLE TOGETHER WITH THE SAME $\bar{m}$ $\bar{m}_2$.

Fig. 4 Local buckling of stiffener segments

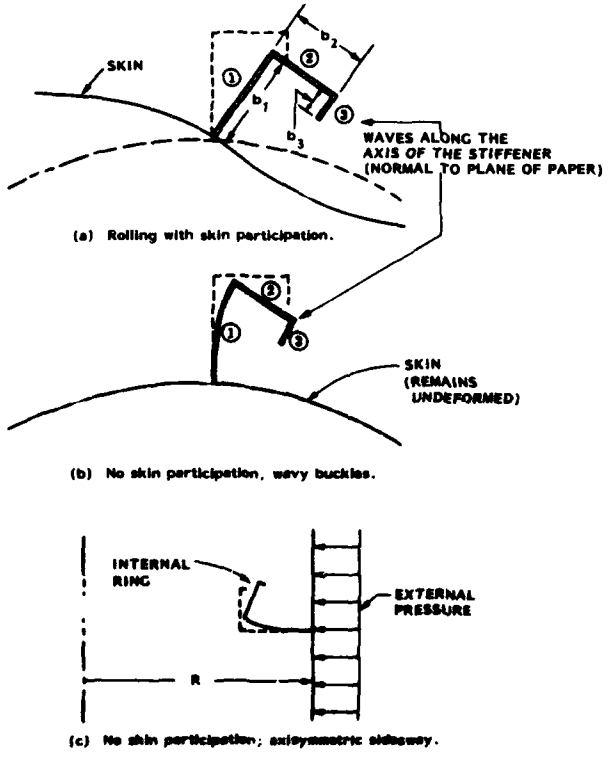


Fig. 5 Three types of "rolling" of a stiffener

Imperfection Sensitivity

It should be emphasized that PANDA does not account explicitly for initial structural imperfections. As the code is now written, the user should design a panel to higher loads than those actually to be seen in service; the deleterious effects of initial imperfections can be accounted for in this way.

Flow of Calculations in PANDA

Figures 6 and 7 show the flow of calculations in PANDA. Each of the top two boxes in Figure 6 represents a separate interactive computer program. In the first program (called BEGIN) the user, with a specific concept in mind (e.g. knowing in advance that he wants to find the minimum weight design of a composite cylindrical shell of 7 layers stiffened by T-shaped composite internal rings and I-shaped aluminum external stringers) provides the material properties, loads, and starting design in a "conversational" mode.

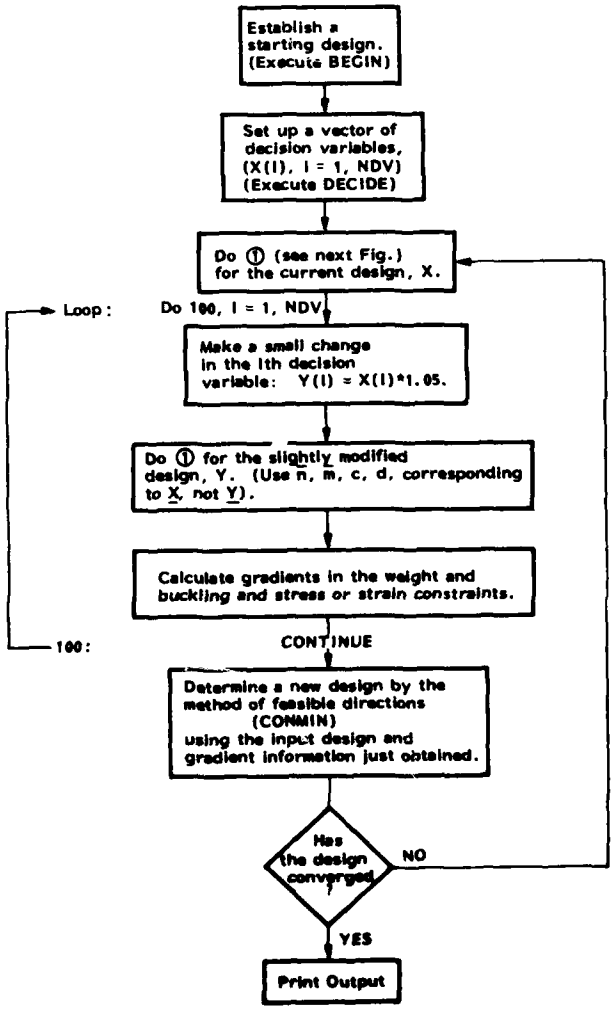


Fig. 6 Flow of calculations in PANDA for an optimization analysis

In the second program (called DECIDE) the user decides whether he wants to do simply a buckling analysis of the starting design or whether he wants to do an optimization analysis. If he wants to do an optimization analysis, the user is then asked, also in this second program, to identify which of the design parameters are to be allowed to vary during the optimization process, that is which of the design parameters are to be "decision variables" and what are the lower and upper bounds of these decision variables. The user can also specify at this time that certain of the design parameters be "linked" to (to vary in proportion with) certain of the decision variables. For example, in laminated composite wall construction the thicknesses of layers with plus winding angles are usually taken to be equal to those with minus the same winding angles; the width of Segment 3 of a T-shaped stiffener is equal to that of Segment 2 (Fig.3a).

When the first two programs have been executed (through commands "RUN BEGIN" and "RUN DECIDE", respectively), the user next executes the main analysis module through the command "RUN PANCON", which performs, with some on-line interaction with the user, the rest of the calculations indicated in Figures 6 and 7.

Prebuckling Analysis

If the materials of the skin and stiffeners remain elastic at the load level specified by the designer, then the prebuckling analysis consists of:

1. an approximate determination of the circumferential strain midway between rings and circumferential strain at ring centroids for panels stiffened by rings only;

2. an approximate determination of the axial bending midway between rings; and

3. a computation from the known strain field and known material properties of how much of the total load is carried by the skin and how much is carried by the stiffeners. (The in-plane shear load is carried only by the skin.)

In the case of panels or complete cylindrical shells stiffened by rings and subjected to uniform laterial pressure, the stress in the skin midway between rings can be rather sensitive to the ring cross section area and spacing for configurations with rather closely spaced rings. Such configurations represent optimum designs of submarine pressure hulls, for example. The buckling pressure corresponding to local instability depends directly on the midbay circumferential stress. When the material behavior is nonlinear, the buckling pressure corresponding to general instability also depends on the state of strain at midbay because the reduced moduli of the skin there naturally act to decrease the coefficients C_{ij} of the integrated constitutive law, which appear in the buckling equations.

Inclusion of Plasticity. The flow of calculations in the prebuckling phase is displayed in Fig. 8. As can be seen from this flow, the process is iterative. In the presence of plastic flow, the objectives of the prebuckling computations, in addition to the three just listed for the elastic case, are:

1. to compute instantaneous values for the reduced moduli of each layer of the panel skin, which are used to calculate the integrated constitutive law governing stability; and

2. to compute instantaneous moduli of the segments of the rings and stringers.

These objectives are summarized in the two boxes in the lower left-hand corner of Fig. 8. Iterations at a given design state continue until the prebuckling strain components change no more than .01 % from their values as of the previous iteration. Figure 9 shows the results of several prebuckling iterations for a given design and load for a ring stiffened cylindrical shell subjected to uniform hydrostatic compression. Quadratic extrapolation of the strain components is used every four iterations.

Bifurcation Buckling

It is easy to see from Fig. 6 that if there are a large number, NDV, of decision variables (NDV > 6, say) many, many buckling load factors must be computed, especially if the case is complicated so that many different kinds of buckling modes must be considered. For example, in the case displayed in Fig. 10, for which 11 different types of buckling are investigated, as listed in Table 1, there might be as many as 7 decision variables: t, a_o, b_o, t^s, b^s, t^r, and b^r (identified in Figure 10). Thus, each execution of the loop, (I = 1, NDV), in Figure 6 requires calculation of NDV * 11 = 77 critical buckling load factors. Each of the 77 critical buckling load factors represents the results of minimization of the potential energy with respect to the wave indices $\bar{m}$ and $\bar{n}$ and the buckling nodal line slopes c or d. In order to save computer time in PANDA the buckling modal parameters, $\bar{m}(i)$, $\bar{n}(i)$, c(i), and d(i), i = 1, 2 .. 11 corresponding to the 11 critical modes for the current "baseline" design (X(J), J = 1, NDV) are held constant for the slightly perturbed designs Y investigated in the loop over NDV. These perturbed designs must be evaluated with regard to stress and buckling in order to generate gradients of weight and constraint conditions needed by the optimiser CONMIN [2,3].

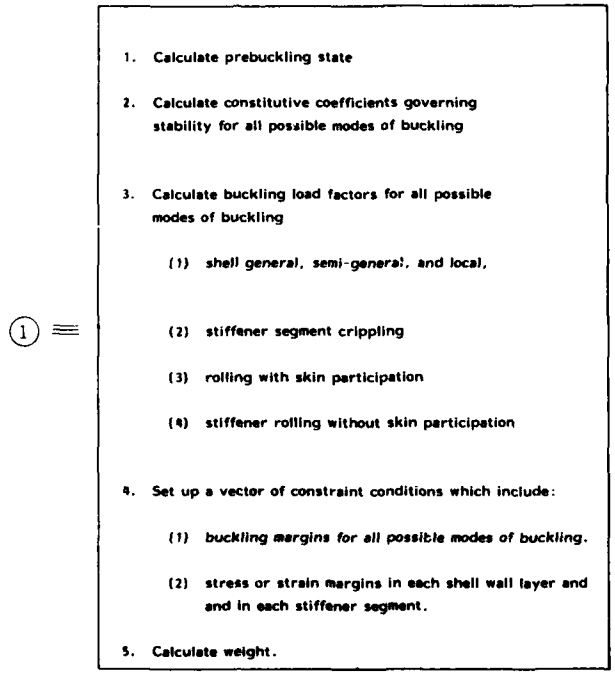


Fig. 7 The structural analysis module of PANDA. This module is embedded in the executable processor PANCON.

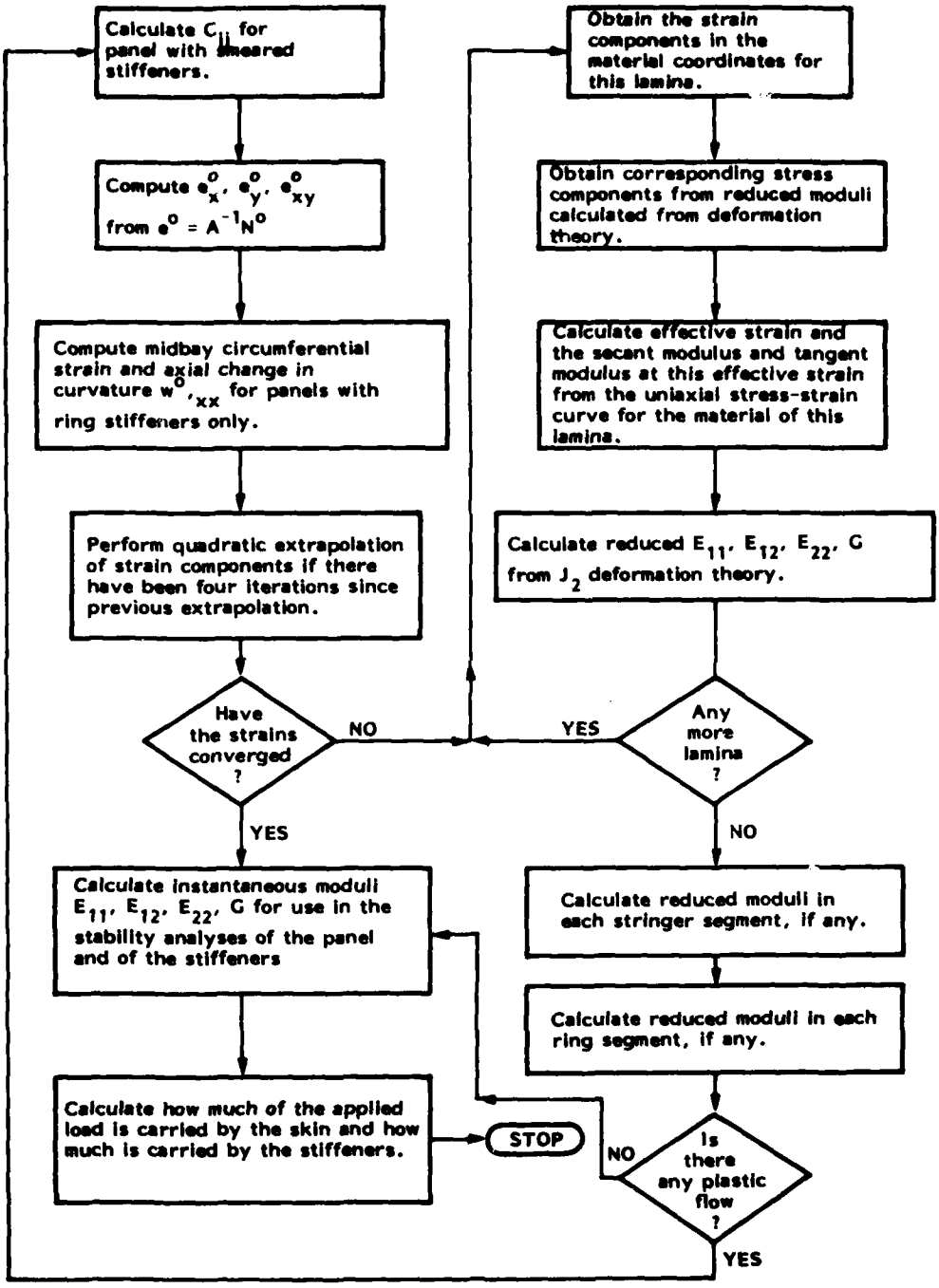


Fig. 8 Flow of calculations for elastic-plastic prebuckling analysis in PANDA

Parameter Study: Optimum Design of Elastic-Plastic, Ring-Stiffened Cylinders under Hydrostatic Compression

Tables 2 and 3 and Figures 11-16 pertain to this investigation. The main purpose of the study is to compare PANDA buckling predictions for optimum designs and BOSOR5 [6] predictions for the same designs for a range of loading over which the amount of prebuckling plastic flow varies. BOSOR5 is an appropriate standard of comparison for ring stiffened cylindrical shells stressed under hydrostatic compression beyond the material proportional limit; there exist numerous comparisons with test results [7].

PANDA Results

The optimum designs and buckling pressure factors and modes from PANDA are listed in Tables 2 and 3. A typical configuration is shown in Fig. 11(a). The decision variables in the optimization process are the six dimensions listed as headings in columns 3-8 of Table 2. The results for each design pressure in Table 2 were obtained by first optimizing such that the ring spacing was included as a decision variable. The ring spacing was then set to a new value as near the optimum value as possible consistent with the condition that there be an integral number of rings within the cylinder length of 172 inches. A new optimum was calculated corresponding to this new value of ring spacing, which was not allowed to vary during this second optimization process. It is seen from Table 3 that for a wide range of design pressures the optimum design is characterized by many nearly simultaneous buckling modes.

BOSOR5 Results

Figures 11 and 12 show the BOSOR5 models. Half the length of the shell is modeled, with symmetry and antisymmetry conditions as indicated in Fig. 11. (The mid length of the cylinder is at the top of the figure.) The reference surface of the cylindrical shell is taken to be the inner surface. The web of each ring, treated as a flexible shell branch, is assumed to penetrate the flange to the middle surface of the flange. The material of the ring at the structural plane of symmetry at the bottom in Fig. 11 has half the stiffness of the other rings. All flanges except the two nearest the midlength of the shell are modeled as discrete rings; the top two flanges are modeled as flexible shell branches. The stress-strain curve for the material is given in Table 19 of Ref. [5].

Figure 12 shows the nodal points in the discretized BOSOR5 models of the optimum designs corresponding to each of the design pressures p_o listed in Tables 2 and 3. Nodal points are concentrated in the portion of the structure nearest the plane of symmetry at the top of Fig. 11 in order

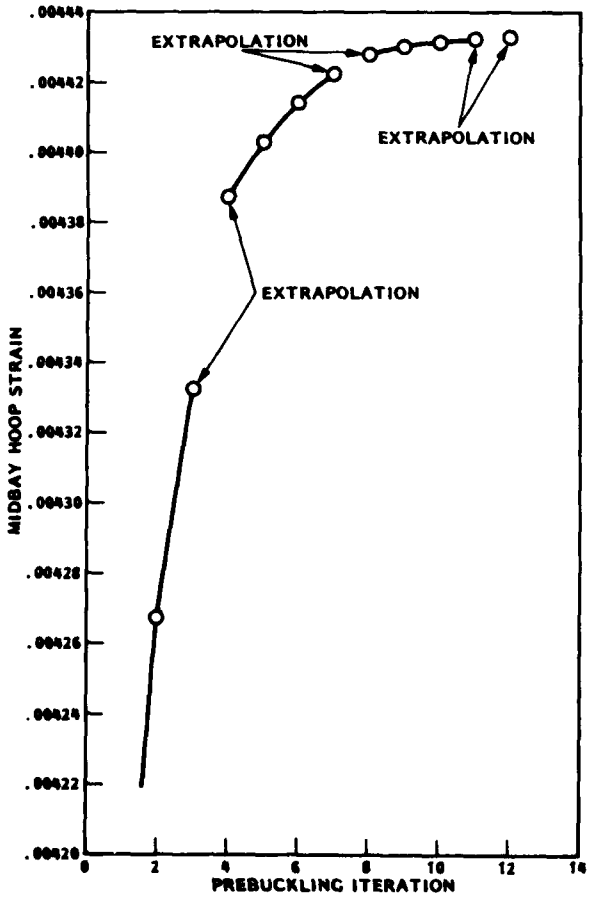


Fig. 9 Typical convergence of the prebuckling strain in the plastic region. This case corresponds to a hydrostatically compressed, ring stiffened cylindrical shell.

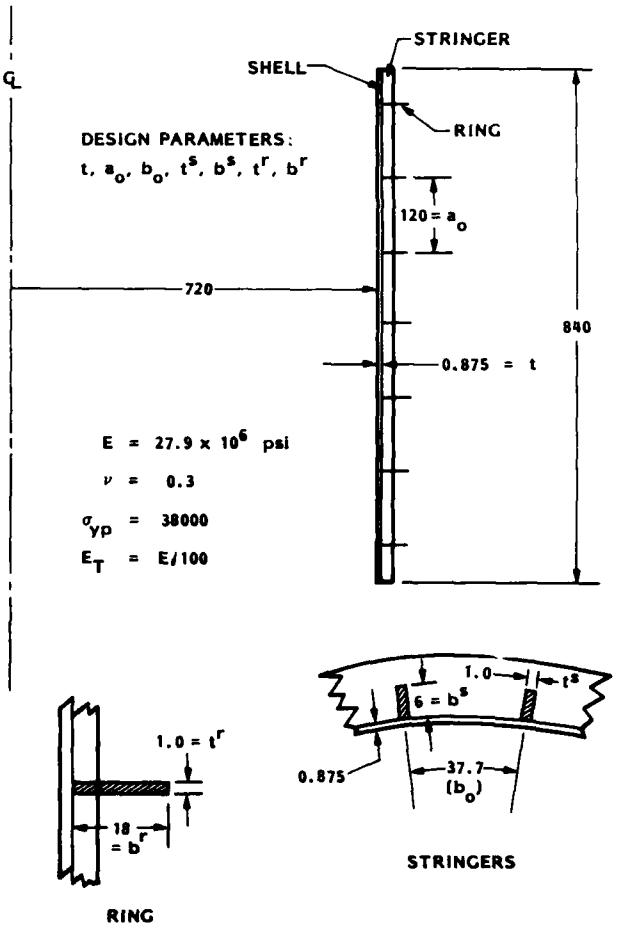


Fig. 10 Ring and stringer stiffened cylindrical shell with dimensions typical of a large containment vessel for a nuclear reactor.

Table 2 Optimum Designs of Hydrostatically-Compressed, Ring-Stiffened Cylinders Derived by PANDA. Radius to Shell Middle Surface = 44.625 in.; Length = 172 in.; T-Shaped Internal Rings.

Pressure P_o (psi)	Weight (lbs)	Thickness of Shell (inches)	Ring Spacing (inches)	WEB		FLANGE	
				Thickness (inches)	Height (inches)	Thickness (inches)	Height (inches)
677	2898	0.289	5.93	0.112	3.44	0.077	1.65
1355	4951	0.493	9.05	0.202	5.03	0.131	2.51
2032	6835	0.688	11.47	0.276	6.21	0.177	3.17
2710	8662	0.807	11.47	0.351	6.95	0.262	4.51
2710*	8724	0.822	11.47	0.346	6.85	0.261	4.46
3388	10694	0.998	13.23	0.460	7.82	0.310	4.97
4066	12682	1.244	15.65	0.560	7.96	0.377	4.75
4743	14667	1.519	19.11	0.651	8.42	0.394	4.60

* Model in which the shell wall is treated as if it consists of five identical layers, in order to account for the variation of midbay prebuckling axial strain through the wall thickness.

Table 3 Buckling Pressure Factors and Modes for Various Types of Instability Predicted by PANDA

Design Pressure, P_o (psi)	General Instability	Local Skin Buckling	Buckling of Web	Buckling of Flange	Rolling with Skin Buckling	Rolling, No Skin Buckling	Axisymmetric Rolling
677	1.0011(1,2)[a]	1.0003(1,16)	1.0(40)	1.0(40)	1.0(1,10)	1.11(4)	1.21(0)
1355	1.0(1,2)	1.0(1,13)	1.0(29)	1.0(29)	1.0(1,9)	1.05(3)	1.10(0)
2032	1.0(1,2)	1.0(1,12)	1.0(24)	1.0(24)	1.0(1,8)	1.01(2)	1.03(0)
2710	1.0(1,2)	1.0(1,11)	1.0(22)	1.0(22)	1.01(1,6)	1.00(1)	1.00(0)
2710[b]	1.0(1,2)	1.0(1,10)	1.0(22)	1.0(22)	0.999(1,5)	1.01(2)	1.02(0)
3388	1.02(1,2)	1.03(1,10)	1.06(19)	1.04(19)	1.03(1,6)	1.03(2)	1.04(0)
4066	1.0(1,2)	1.07(1,9)	1.10(19)	1.11(19)	1.06(1,7)	1.07(2)	1.08(0)
4743	1.0(1,2)	1.07(1,8)			1.06(1,7)	1.07(3)	1.08(0)

[a] Numbers in parentheses are (axial, circumferential) waves in buckling pattern (axial halfwaves, circ. full waves). For local skin buckling and rolling with skin buckling the axial half-wave-index refers to the number of half-waves between adjacent rings. Where only one number is given, it refers to the number of full circumferential waves.

[b] 5-layered model.

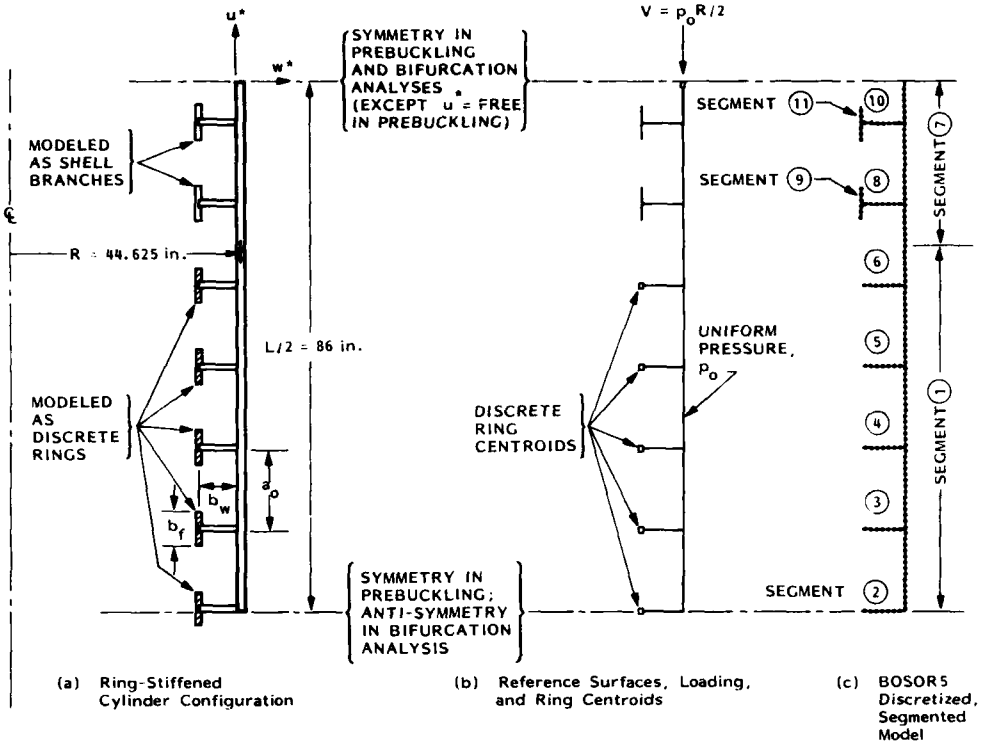


Fig. 11 Hydrostatically compressed, internally ring stiffened cylindrical shells: Modeling strategy for BOSOR5 analyses of the minimum weight designs obtained by PANDA for design pressures p_o ranging from p_o = 677 psi to p_o = 4743 psi. (See Table 2 for dimensions.)

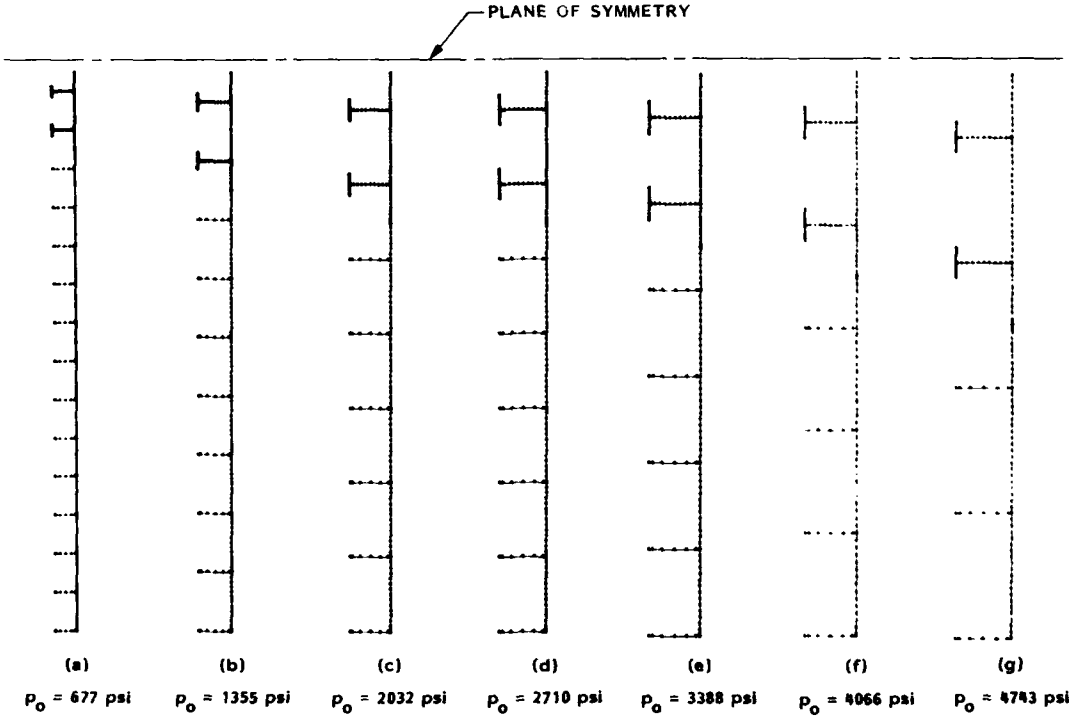


Fig. 12 Hydrostatically compressed, internally ring stiffened cylindrical shells: BOSOR5 discretized models corresponding to minimum weight designs obtained by PANDA for design pressures ranging from 677 psi to 4743 psi. (See Table 2)

to obtain converged buckling pressures for local shell, web, and flange buckling modes.

Figure 13 demonstrates that all of the optimum designs are stressed beyond the material proportional limit at design pressures p_o from 677 to 4743 psi. It is interesting that for optimum designs with p_o from 2710 to 4743 psi the effective plastic strains at the midsurface halfway between rings are close to the 0.2 per cent yield strain, a result obtained from a rather rigorous analysis that confirms the appropriateness of earlier engineering design practice.

Comparison of PANDA and BOSOR5 Buckling Pressures

Figure 14 represents (indirectly) a comparison between PANDA and BOSOR5 buckling predictions because the lowest buckling load factor for each optimum design predicted by PANDA is very close to unity (p_{cr} = design pressure, p_o). Typical buckling modes from BOSOR5 are plotted in Fig. 15.

Figure 14 indicates that PANDA yields slightly unconservative local skin buckling loads and web buckling loads for optimum designs for pressures p_o in the range from 677 to 3388 psi. This slight unconservativeness is an effect of nonlinear material behavior. It is caused in large part by the neglect in the one-layer PANDA models of the variation of axial strain through the shell wall thickness half way between rings. One can see from the pre-bifurcation deflected shape shown in Fig. 15(a), for example, that there is more axial compression and hence greater effective strain at the outer fiber of the shell wall than at the middle fiber, to which the solid points on the stress-strain curve in Fig. 13 correspond. This bending effect is not included in the results shown in Fig. 14 because the shell wall in the PANDA models from which Fig. 14 was generated was assumed to consist of only one layer. The instantaneous (tangent) stiffness coefficients C_{ij} for the stability analysis are calculated only at the middle surface of each layer, so that in the case of a one-layered model axial bending is not accounted for.

Figure 16 demonstrates the effect of modeling the shell wall in the PANDA analysis as if it consisted of 5 layers of equal thickness rather than just one layer. In Fig. 16 comparisons between results from BOSOR5 and PANDA are given for the case p_o = 2710 psi, with buckling pressures plotted as functions of the number of circumferential waves $\bar{n}$. Figure 16(a) displays this comparison for the optimum design corresponding to use of a one-layer PANDA model (Table 2, fourth row), and Fig. 16(b) gives comparisons for the slightly different optimum design (Table 2, fifth row) obtained by PANDA with use of a five-layer model. In the five-layer model the degree of unconservativeness of the PANDA predictions corresponding to local skin buckling has been reduced by about half and the PANDA prediction of the pressure at which local web buckling occurs is no longer greater than the BOSOR5 prediction for this mode.

The five-layer model in PANDA is more accurate than the one-layer model because of the contribution

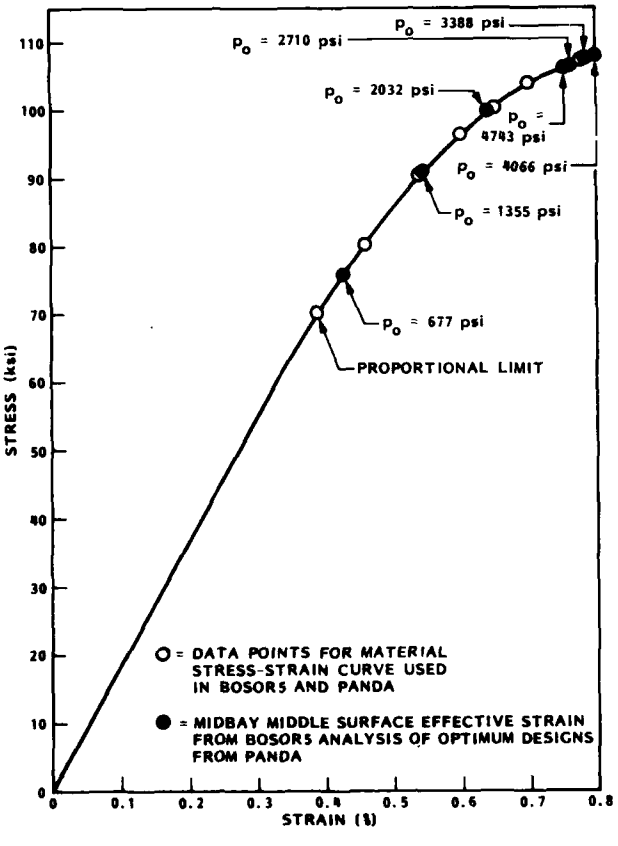


Fig. 13 Hydrostatically compressed, internally ring stiffened cylindrical shells: Midbay effective membrane strains at the design pressures for the optimized configurations shown in Figure 12.

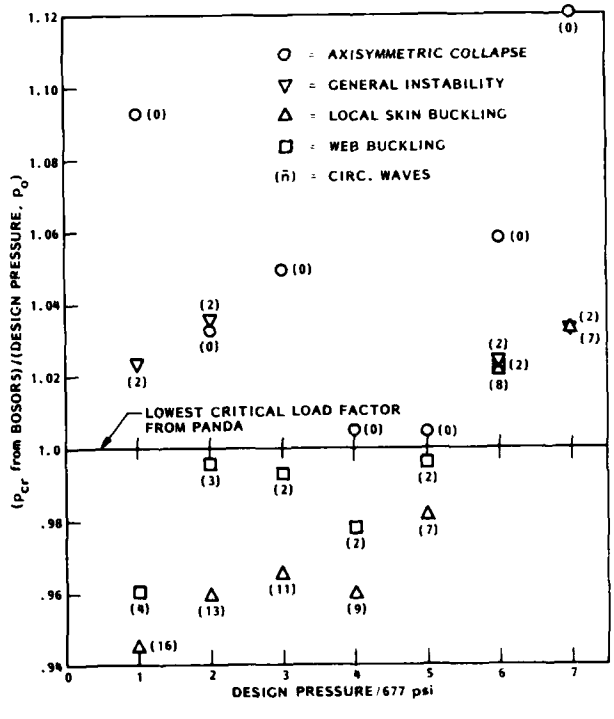


Fig. 14 Hydrostatically compressed, internally ring stiffened cylindrical shells: Comparison of buckling loads obtained from PANDA and from BOSOR5. This is a comparison because the critical loads from PANDA are all very near unity, as seen from Table 3.

to the prebuckling meridional strain $e_1^k(z)$ of the term due to prebuckling change in meridional curvature, $(-zw,^o_{xx})$, in which z is the coordinate normal to the shell middle surface (positive outward): In the one-layer model z is zero at the layer middle surface, so there is no contribution to e_1 due to axial bending. In the five-layer model, however, the two layers, 4 and 5, lying outside the shell middle surface have positive z, so that $e_1^{(4)}$ and $e_1^{(5)}$ are larger (in absolute value) than $e_1^{(1)}$, $e_1^{(2)}$, or $e_1^{(3)}$. For shells that are stressed only a small amount beyond the material proportional limit, particularly if an elastic-plastic interface exists within the shell wall thickness that is oriented parallel to the middle surface, the absolute increases in $e_1^{(4)}$ and $e_1^{(5)}$ above the absolute value of middle surface strain $e_1^{(3)}$, cause a greater decrease in the instantaneous integrated stiffness coefficients C_{ij} governing stability than the increase of C_{ij} caused by the decrease in $e_1^{(1)}$, and $e_1^{(2)}$ below the absolute value of $e_1^{(3)}$.

How PANDA Performs on the VAX Computer

PANDA operates at a reasonable speed for interactive computing on a minicomputer such as the VAX. For example, the optimum design of the ring and stringer-stiffened cylindrical shell shown in Fig. 36(d), to which the results in Fig. 16 correspond, is obtained in four sets of five iterations each, the first set requiring 22 seconds at the terminal, the second 18 seconds, the third 15 seconds, and the fourth 12 seconds. This means that every two to four seconds a new design is generated as iterations progress toward the optimum, a reasonable speed at which to obtain optimum designs in a conversationally interactive mode.

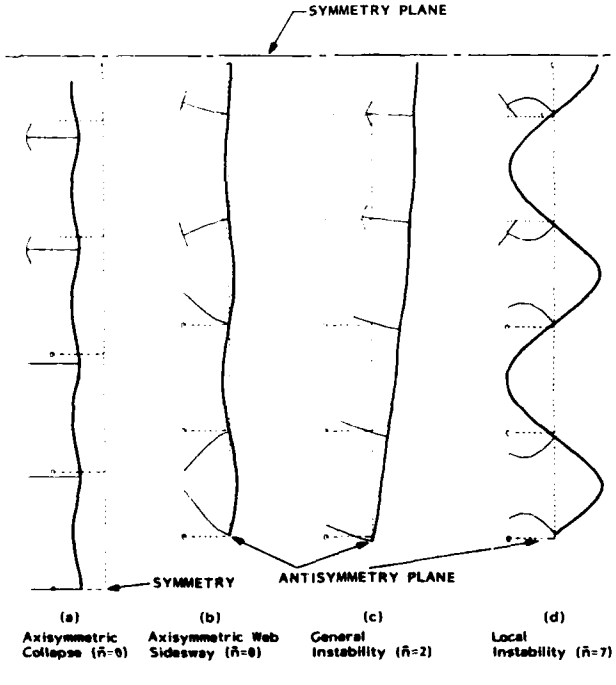


Fig. 15 Buckling modes predicted by BOSOR5 for the optimum design corresponding to p_o = 4743 psi.

Acknowledgments

Part of the effort to develop PANDA was sponsored by the U.S. Air Force, Aeronautical Systems Division, Wright Patterson AFB, Ohio, under Contract AFFDL F33615-76-C-3105. Dr. Narendra S. Khot (AFWAL/FIBRA) was project engineer.

Much of the support for the development of PANDA came from the 1980 and 1981 Lockheed Independent Development Programs. For this support the author is greatly endebted to Bill Sable. Some of the support for production of this report was provided by the 1981 Lockheed Independent Research Program.

References

[1] L. H. Donnell, "A new theory for the buckling of a thin cylinder under axial compression and bending", Trans. ASME Vol. 56, No. 11, 795-806 (1934)

[2] G. N. Vanderplaats, "CONMIN--a FORTRAN program for con- strained function minimization," NASA TM X-62-282, version updated in March 1975, Ames Research Center, Moffett Field, CA (Aug. 1973)

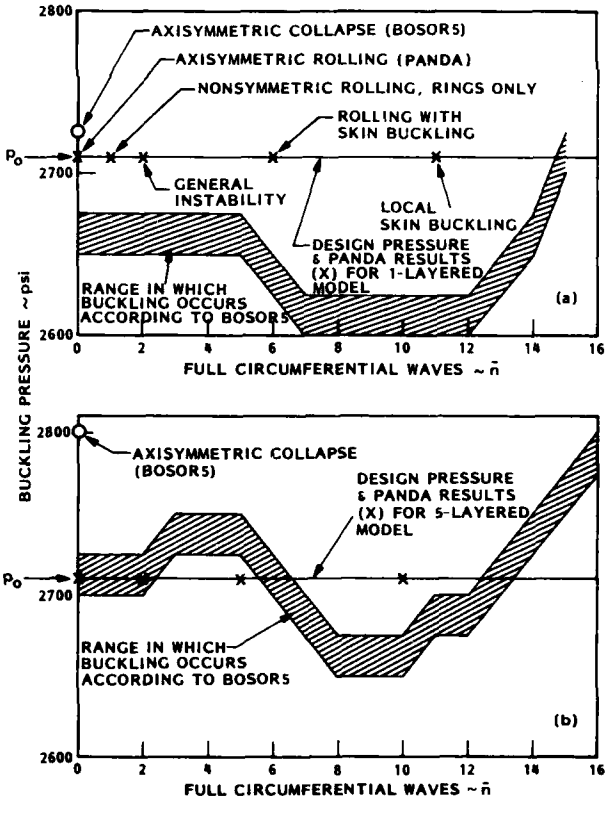


Fig. 16 Hydrostatically compressed, internally ring-stiffened cylindrical shells optimized by PANDA for a design pressure of 2710 psi. Comparisons of buckling predictions from BOSOR5 and PANDA: (a) minimum weight design corresponding to a one-layered model in PANDA; (b) minimum weight design corresponding to a 5-layered model in PANDA.

[3] G. N. Vanderplaats and F. Moses, " Structural optimization by methods of feasible directions," Computers and Structures, Vol. 3, pp 739-755 (1973)

[4] Zoutendijk, G., Methods of feasible directions, Elsevier Publishing Company, Amsterdam, 1960.

[5] D. Bushnell, "Panel optimization with integrated software (POIS)", Volume 1: "PANDA--Interactive program for preliminary minimum weight design", Report No. AFWAL-TR-81-3073, Flight Dynamics Laboratory, Air Force Wright Aeronautical Laboratories, Wright Patterson AFB, Ohio (July 1981)

[6] D. Bushnell, "BOSOR5--program for buckling of elastic-plastic complex shells of revolution including large deflections and creep," Computers & Structures, Vol. 6, pp. 221-239 (1976)

[7] D. Bushnell, "Buckling of elastic-plastic shells of revolution with discrete elastic-plastic ring stiffeners," International Journal of Solids and Structures, Vol. 12, pp. 51-66 (1976)

AD-P000 094

INTERACTIVE OPTIMUM DESIGN SYSTEM

T. Altuzarra, C. Knopf-Lenoir, C. Sayettat and G. Touzot
Université de Technologie
BP 233, 60206 Compiègne, France

This work is concerned with the development of an interactive system for the definition, analysis and optimization of two-dimensional elastic structures. At any time during the optimization process, the user can, with the help of his personal experience, either continue iterations, if the shape evolution of the structure seems to be interesting, or interact, if he considers that the search direction of the algorithm will not yield to a correct solution. All the information is stored in a logical and relational data base, which contains, besides the current state of the structure, the "history" of its evolution. Thus, several previously obtained configurations can be easily merged and compared.

1. - Introduction

This paper deals with the elaboration of an interactive system combining computer aided design, finite elements and mathematical optimization technics, for the optimum shape design of two-dimensional structures.

First, methods have been developped to represent the admissible variations of unknown boundaries and several optimization methods have been implemented and tested [1], [2].

Then the resulting finite elements and optimization programs have been integrated into an interactive graphic package (PREMEF) leading to the "S.I.C." design system.

The purpose of this system is to provide the possibility to interact with the optimization process, to examine intermediate results, to modify the shape obtained by the algorithm, to add or remove design parameters or constraints during the computations.

2. - Optimization problem

2.1. - Definition of the design parameters.

We consider a plane elastic structure V subjected to high stress concentrations. A part S_0 of the boundary of V is supposed to be known. Another part S is to be determined in order to reduce the maximum stresses which exist on a part s of the boundary of V.

The shape of S is defined by boundary nodes positions and is constrained by several requirements which depend on the particular structure considered : boundary variations limited by internal and external limits S_i and S_e, curvature sign or regularity, parts of S supposed to be straight lines,.... Some of these shape restrictions are explicitly taken into account by selecting convenient design variables ; the others are added as optimization constraints.

The design variables are to be selected to :

- lead to complex enough boundary shapes
- minimize the computer time related to the number of variables and constraints
- avoid unadmissible shapes of boundary and elements.

A particular mesh is defined near the unknown boundary S ; it will be updated during the optimization process. The nodes of this "moving mesh" are located on straight lines called "meridians" (Figure 1)

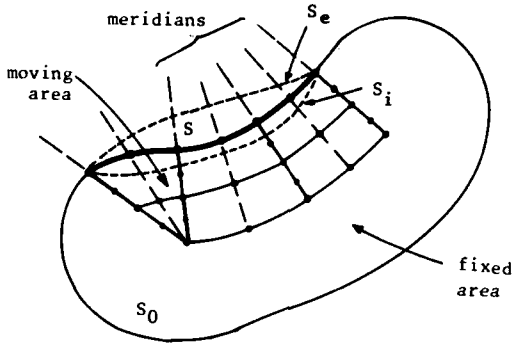
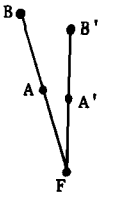


Figure 1

The coordinates of the nodes located on the boundary S are computed using the optimization program or are given by the user. The coordinates of the nodes in the moving area are modified in order to maintain a regular mesh : each node remains on its meridian defined by a fixed node and a boundary node ; moreover the node is "homotheticaly" translated along the meridian (Figure 2).



F : fixed node
B, B' : boundary node before and after updating
A, A' : node located on the meridian before and after updating

$$\frac{AF}{BF} = \frac{A'F}{B'F}$$

Figure 2

The parameters definition procedure consists in defining for each meridian :

- the corresponding design parameters, if any.
- the relationship between the coordinates of the boundary node of the meridian and its design parameters or those related to other meridians.

This information constitutes the "meridian type". In order to allow various kinds of boundary deformation, the following meridian types are defined (negative type means no design parameter associated to this type of meridian) :

a) type 1 (meridian (I) on Figure 3)

- the parameter is the distance $I\text{-}I_0$
- the slope of the meridian is fixed ; the boundary node can move along a segment of meridian limited by S_i and S_e.

b) type 2 (meridian (J))

- the parameters are the coordinates of the boundary node
- the slope of the meridian is variable ; the boundary node is restricted to move inside a given rectangle.

PRECEDING PAGE

c) type -1 (or -2) (meridian (K))

- no parameter
- the boundary node K remains on a straight segment AB. The coordinates of the node K are computed from the parameters of the meridians (A) and (B). The type of both end meridians (A) and (B) is 1 (or 2). The node K is a slave node. The nodes A and B are master nodes.

d) type -3 (meridian (C))

- no parameter
- the boundary node C belongs to a straight boundary segment CB which remains parallel to its original direction. The coordinates of C are computed from the parameters of the type 1 meridian (B).

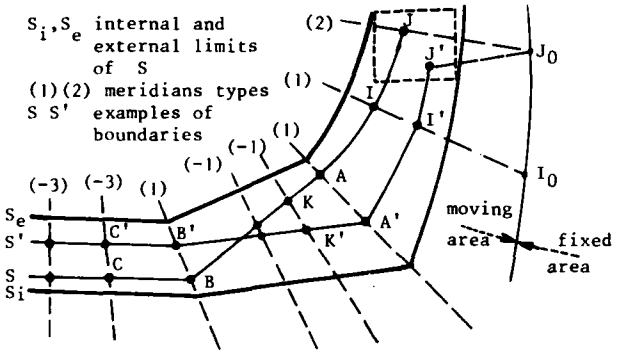


Figure 3

e) type 4 (or -4) (meridians (E) and (F) on Figure 4)

This type is used to represent slider contact between two solids V_1 and V_2. If the meridian types are 2 (or -2) in the solid V_1, the corresponding meridian types should be 4(or -4) in the solid V_2. The coordinates of the boundary nodes of V_2 are computed from the parameters related to the meridians of V_1.

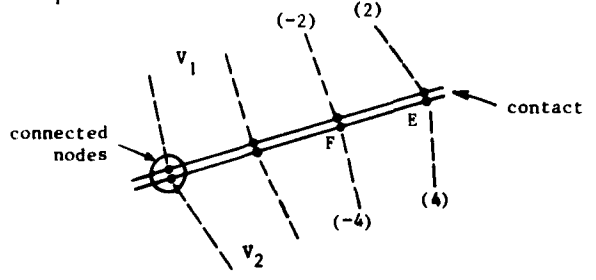


Figure 4

When each meridian type is defined, the global set of design parameters

$$p = (p_1 \dots p_P)$$

defines the shape of S.

Some remarks can be made about this parameter definition procedure :

- the use of design parameters that are more restrictive than the coordinates of each boundary node is very suitable because it reduces both the number of parameters and the number of constraints.
- other types of meridians can be defined in order to represent particular geometrical shapes such as circles. The only condition requested is that the coordinates of the moving nodes can be derived with respect to the parameters.
- a good choice of the meridians (initial moving mesh) preserves good shapes for moving elements.
- the finite element connectivity is not changed during the optimization process ; this simplifies the programs, saves computer time and avoids numerical instabilities due to remeshing.
- the procedure can be extended to three-dimensional problems.

The technological restrictions imposed to the solid shape can be taken into account by a convenient choice of meridians, by putting limits on the parameters and by adding constraints to the optimization problem. For instance, the curvature of S between 3 nodes can be controlled by a non linear constraint :

$$C(p) \leqslant 0$$

2.2. - Formulation of the optimization problem.

The risk of crack initiation is related to the stress σ_T in the direction tangent to the boundary. Thus we minimize the maximum value of σ_T on a given part s of the boundary :

$$\underset{S}{\text{Minimize}} \max_{s} \sigma_T \qquad (1)$$

It would be possible to minimize any other function of stresses, strains and displacements.

After discretization this is expressed as :

$$\underset{S}{\text{Minimize}} \left(\max_{k} \sigma_k\right) \qquad (2)$$

with respect to the design parameters p

where σ_k $k = 1,\dots, L$ are the values of σ_T calculated at discrete points of s. Let U be the nodal displacements vector, K the structural stiffness matrix and F the vector of equivalent nodal loads. We have :

$$K(p)\ U = F(p)$$

$$\sigma_k(p) = R_k^T(p)\ U$$

We can note that vector R_k depends only upon the design parameters required to define the discretization point k ; on the other hand, U depends on all the design parameters.

As stated in (2), the problem cannot be solved by a gradient method, because the "maximum" function cannot be derived. We transforme it as :

Minimize μ with respect to the variables (μ, p) subject to the constraints (3)

$$\mu - \sigma_k \geqslant 0 \qquad k = 1,\dots, L$$

where μ is an additional variable introduced to take the "maximum" function into account.

With the design parameter set previously defined, σ_k can be derived with respect to p ; gradient calculations are carried out by using an adjoint state vector, P_k ; this involves the solution of :

$$K P_k = R_k$$

for each σ_k, but it avoids approximate and expensive numerical derivations. Finally, gradients are expressed as :

$$\frac{\partial \sigma_k}{\partial p_i} = \frac{\partial R_k}{\partial p_i} U - P_k^T \left(\frac{\partial K}{\partial p_i} U - \frac{\partial F}{p_i} \right)$$

The problem stated in (3) can be solved by any classical minimization algorithm admitting non linear constraints. Different methods have been tested : linearized centers method, penalization methods ; we finally adopted a Powell's algorithm [3], [4] : it is a variable metric method where the search direction is calculated by solving a quadratic programming problem ; each iteration may require more than one criterion and constraints calculations, but the algorithm is very efficient and convergence is generally fast (less than 10 iterations).

2.3. - Problems related to batch processing.

Several problems are related to the use of shape optimization programs in a batch processing environment :

- any automatic convergence criterion cannot stop the computations if a boundary shape becomes "strange" in a human sense.
- often, it is only necessary to compute the first improvements of the shape and to submit it to the users's judgment.
- a minimum number of constraints should be used in the first iterations. Additional constraints should only be added if they appear to be necessary.
- the data preparation is longer than in standard F.E.M. analysis.

These problems can be simplified using interactive technics.

3. - The S.I.C. interactive optimum shape design system

3.1. - General organization.:

The main functions of the system are :

- creation, display, and updating of finite elements data (mesh, boundary conditions, loading), and data related to optimization (meridians, constraints, criterion). These functions are provided by the PREMEF finite element pre-processor.
- management of a large amount of data related to several configurations of the solid, to F.E. computations and to optimization. The data are stored in the ETAMINE data base management system.
- management of computation modules to allow dynamic changes of
  - * design parameters
  - * constraints
  - * criterion
  - * F.E. data

This is controlled by an overall control processor which avoids unuseful calculations, and updates the data as required.

3.2. - ETAMINE data base management system.

The SIC system manipulates several kinds of data, the number of which is increasing during the system development :

- data related to the geometric definition of the structure : points, lines, circles, polygons, surfaces, objects and sub-objects which are collections of previous entities.
- data related to finite elements : nodes and elements computed by automatic mesh generation programs, loadings and boundary conditions, mechanical properties, solutions (displacements and stresses).
- data related to optimization : meridian types, design variables, constraints, configurations (all the data defining the structure and its shape at a given level of optimization).

Numerous relationships exist between the previous data : for instance a node should be linked to its meridian, to its elements, to boundary conditions....

ETAMINE allows the creation, deletion and updating of any kind of data and data link . It is a data base system build on entity-relation principle with a hierarchical data structure. The data organisation can be dynamically modified. ETAMINE is written in ANSI FORTRAN and exists in 16 and 32 bits versions.

For instance the access to the coordinates of the first node on a meridian is written as :

```
CALL BASE('I COOR OF NODE 1 OF LINK N OF MERI 7')
```

3.3. - PREMEF finite element pre-processor :

PREMEF is an interactive finite element data preparation system. It is based on a hierarchical structure of points, lines, surfaces, solids. It includes the following set of functions :

- creation or modification of entities from keyboard, digitizer
- selective display and erasing of entities on color raster screen
- mesh generation on lines, surfaces, volumes
- several geometric operations such as surface intersection,
- display of analysis results : deformed shapes, stress level contours...
- interface with analysis and optimization programs.

Some examples of PREMEF commands are :

```
SHOW /POIN  Displays all points in the data base

ERASE /ELEM 7 10   Erases elements 7 to 10
```

SURF S1 P1 P2 P3 P4 /CYL creates a cylinder defined by points P1, P2, P3, P4.

MESH S1 meshes the surface S1

OPTI 2 executes 2 iterations of optimization.

3.4. - Computation control processor.

From the user's point of view the optimization procedure appears as successive structural computations. After each analysis, it is possible to modify any kind of data. The overall process is illustrated by Figure 5 :

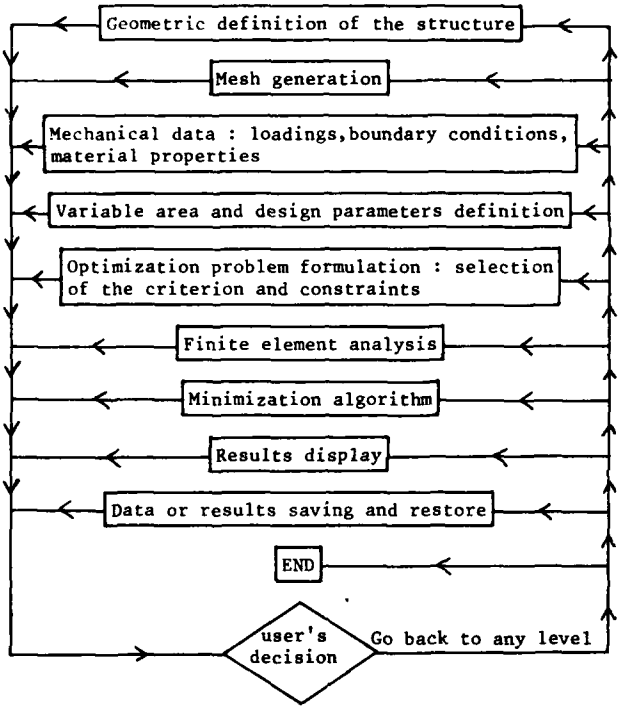


Figure 5

In such a procedure a number of checks must be performed to verify the data consistency at any time and to select the next module to execute.

Any inconsistent information provided by the user is detected and pointed out by the system. A first check is done at the data definition level. A second check is performed just before activating F.E. modules in order to detect any data omission. The data base is explored and all necessary information is extracted to create the equivalent of the data set required by a batch run.

Another problem is the determination and optimization of the sequence of module executions. When successive computations and updatings are done some results remain valid and others should be updated : for instance, it is not usefull to recompute the stiffness matrix corresponding to the fixed elements as long as the fixed area is not modified. This management is performed with the help of a table driven control processor ; two flags are associated with each execution module :

- the first flag is set on or off during the problem formulation and then is never modified. It indicates if the module is to be executed or not for the problem considered. Moreover the table is organized in such a way to provide the sequence of module executions.
- The second flag is set off when the results of the module are no more available because some of its input have been modified. The flag is set on after the module execution.

4. - Examples

4.1. - Square plate with a hole.

In the first example (Figure 6) the problem is to determine the shape S of a hole located at the center of a square plate ; uniform normal tensions are applied on the edges BC and CD of the plate. The shape optimization reduces the maximum stress on the boundary of the hole.

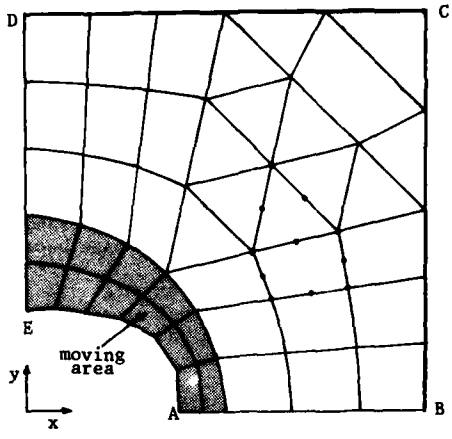


Figure 6

The mesh uses 6 or 8 nodes isoparametric elements; 12 elements are included in the variable area. The boundary S is defined by alternating type 1 and type -1 meridians, so that the middle node of an element is linked to the corner nodes. The shape is then defined by 7 nodes which move along fixed meridians. There are 7 design variables, and 5 constraints to maintain the convexity of S.

The computer time required for one analysis (including criterion, constraints and gradient computation) is about 16 seconds on VAX 780.

Two types of loading are considered :

- uniform tensions : $F_x = 1$ on BC, $F_y = 1$ on CD. The optimization process has been initialized with two different initial shapes (a) and (b)(Figure 7a,b). The solution, which is obviously a circle and a uniform stress distribution, is obtained in both cases.

  The initial shape (a) requires 5 analysis and the stress reduction is 40 %. The initial shape (b) requires 12 analysis. In this case, after 4 analysis, the optimization procedure is interrupted (shape b'), then the search direction algorithm is reinitialized. The next iteration is very efficient and gives the

optimum circular shape.

- uniform tensions : $F_x = 1$ on BC, $F_y = 3$ on CD. In that case, the bounds are reached by some parameters so the stress distribution is not completely uniform. The maximum stress reduction is 60 % ; it required 12 analysis (200 seconds of VAX 780 computer time) (see Figures 7c).

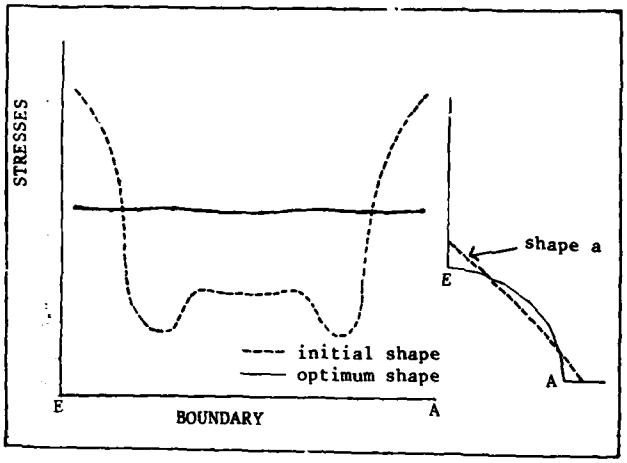


Figure 7a

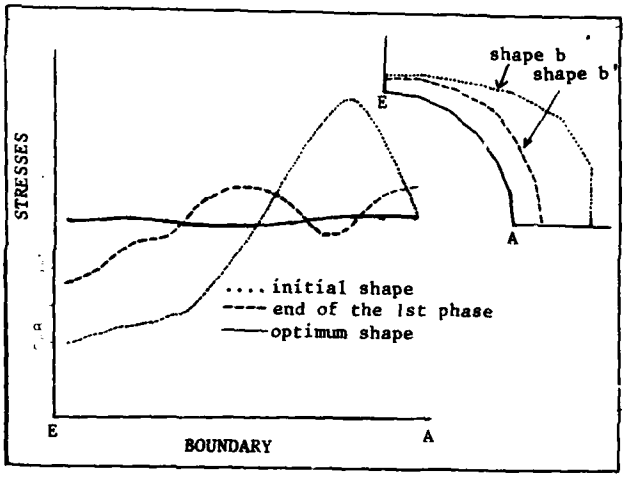


Figure 7b

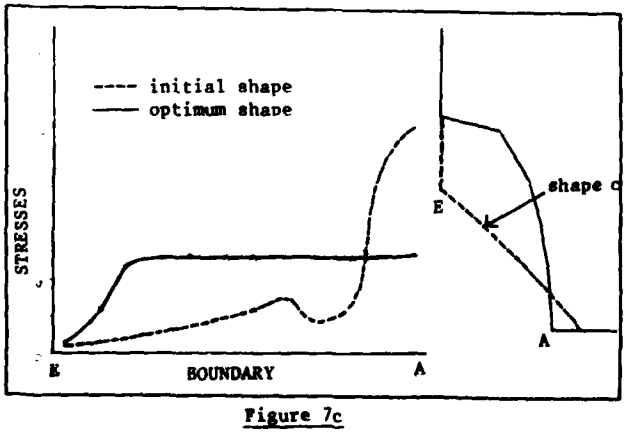


Figure 7c

4.2. - Disk of aircraft engine :

In the second example a aircraft engine disk is considered (Figure 8). The shapes of two boundaries of this structure are to be determined : the parts G'K' of the blade (on Figure 9) and BE of the disk. The stresses are calculated along AB.

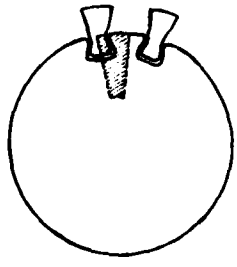
The centrifugal force of the blade is represented by a uniform tension applied on the segment H'G'. The problem is discretized with 134 quadratic elements (58 in the variable area), 26 parameters of different types, and 20 constraints to maintain the regularity of the curvature of S. (Figure 9).

The optimization is carried out in two phases :

- 16 discretization points are used to compute the stresses to be minimized. The first iteration (2 analysis) gives the boundary (p'). The maximum stress decreasing is 34 %. (Figure 10)

- to improve this result the number of discretisation points is increased : the next iteration (2 analysis) uses 32 points to compute the stresses. It gives the boundary (p''). It can be noted that the stress distribution is then uniform on a large part of the boundary.

The computer time required by one analysis (as previously defined) is about 2mn with 16 stress points and 2mn 30'' with 32 stress points (VAX 780).



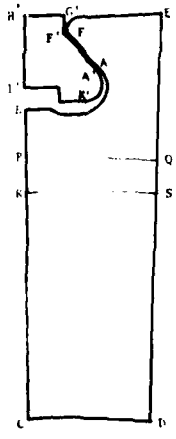


Figure 8

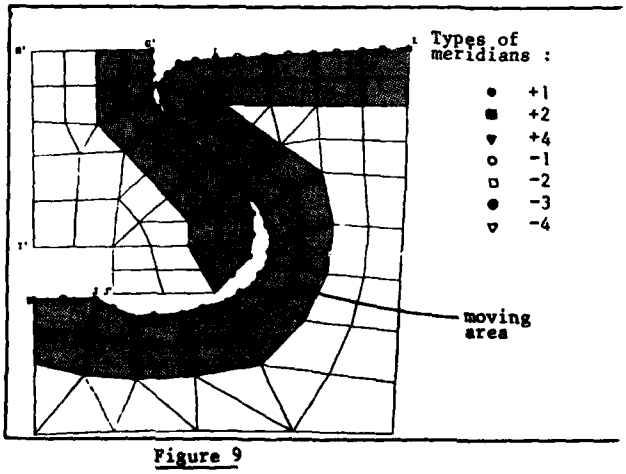
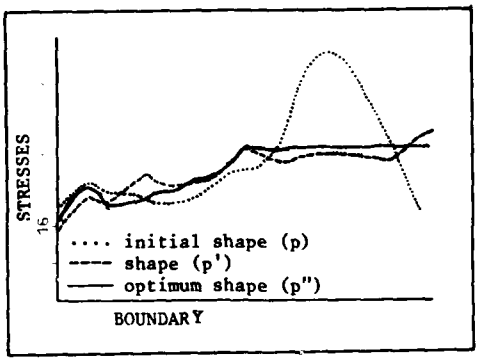


Figure 9



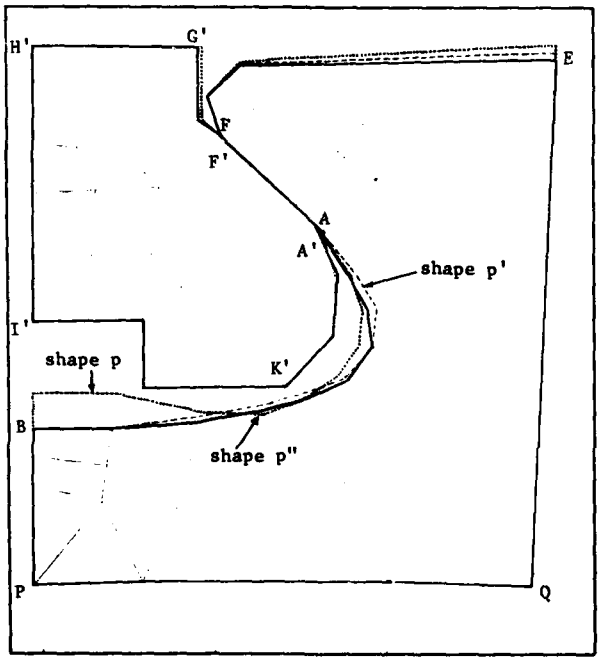


Figure 10

5.- Concluding remarks

The two examples have been presented to show the efficiency of the optimization procedure. The advantage of interactive design system appears when it is used to solve complex or uncompletely defined problems. It is then possible to solve successive approximate small problems or to test successive design hypothesis. The next developments will be directed towards an extension of the types of design variables (thickness, mechanical properties), of the criterion and the constraints (different functions of stresses and displacements, weights,...). Then a tri-dimensional extension should be considered.

References

[1] Knopf-Lenoir, C., Touzot, G., et Yvon, J.P., Optimisation de la forme d'une pièce plane élastique (attache aube-disque) pour minimiser les contraintes, rapport final du contrat 76 / 452, DRET, Paris, 1978.

[2] Knopf-Lenoir, C., Touzot, G., et Yvon, J.P., Optimisation d'attache aube-disque de turbomachine, rapport final du contrat 78/224, DRET, Paris, 1980.

[3] Powell, M.J.D., A fast algorithm for nonlinearly constrained optimization calculations, presented at the 1977 Dundee conference on Numerical Analysis.

[4] Powell, M.J.D., Variable metric methods for constrained optimization, presented at the Third International Symposium on Computing Methods in Applied Sciences and Engineering (IRIA, France)

[5] Sayettat, C., Gestion des données pour la Conception Assistée par Ordinateur, rapport UTC, Compiègne, France, 1980.

SESSION #13

NEW METHODS AND SPECIAL APPLICATIONS

AD-P000 095

OPTIMAL PRINCIPLES FOR DESIGN OF INDETERMINATE TRUSSES

Louis M. Laushey
University of Cincinnati
Cincinnati, Ohio 45221

Summary

The methods suggested for the design of indeterminate trusses resemble the straightforward steps in the design of determinate trusses. Stresses of the highest amount are selected first to satisfy continuity. Then optimum reactions are chosen, followed by the determination of the member forces to satisfy static equilibrium. Finally, the member areas are obtained by dividing the forces by the stresses.

The calculations usually required to design a redundant truss are greatly simplified and reduced. Simultaneous equations are avoided for multiply-redundant structures. No iterative trials are needed for a convergence to an indefinite optimum.

Two principles are introduced to achieve an optimized design directly.

1. The Transmissible Potential Energy of the loads and reactions.

2. The Conservation of Volume of the structure under loads.

The Transmissible Potential Energy of the external loads and reactions is equal to the sum of each member force multiplied by the length of the member. This principle applies to both real and virtual loads. The total volume required of all of the members is proportional to this product, $\Sigma|F|L$, since $\Sigma AL = \Sigma FL/S$. Modified shear and moment diagrams are used to determine $\Sigma|F|L$.

The Conservation of Volume leads to a range of statically correct reactions that require the same volume (or weight) of truss to carry the same loads.

Maximum allowable design stresses are found applicable for all those indeterminate trusses where $\Sigma\ SUL = 0$ over both the tension and the compression members separately. Specifically, since ΣSUL must be zero, if $\Sigma^t UL = \Sigma^c UL = 0$, then $S_t\Sigma^t UL + S_c\Sigma^c UL = S_t(0) + S_c(0) = 0$.

The weights of indeterminate trusses are compared to the weights required of alternative determinate trusses. Conditions for identical weights are described, and found to exist in practical situations.

Emphasis is placed on the important conclusion that some indeterminate trusses cannot be optimized to the extent of the maximum allowed stresses in all members. Reasons why are shown, and easy methods are given to arrive quickly at near-optimum designs.

The classic three-bar truss is shown to be analyzed easily, and designed directly, by the direct-design method.

Introduction

The design of an indeterminate truss is presently a cut-and-try process. The stresses can be determined only for a trial structure that is fully proportioned. After trial areas are assumed, the redundants can be calculated, the bar forces found by statics, and the trial stresses determined by dividing these bar forces by the trial areas. The member areas are then resized on the basis of the stresses from the trial, and the process is repeated. There should be a convergence with each iteration.

There is no knowledge or guarantee that any convergence will lead to members sized so that each will be stressed to some specified maximum amount. There is sometimes no guarantee that the final structure will be of minimum weight.

A well-designed indeterminate structure requires calculations blended with judgment of the efficiency of the proposed geometrical arrangement of the members. An optimum design must provide for:

1. Compatible Strains. - Member strains that satisfy the continuity of the structure; no misfits or gaps at the joints, and no displacements at the reactions.

2. Predetermined Stresses. - Member stresses equal to the maximum allowable design specifications, or as near as can be to satisfy compatible strains.

3. Optimum Reactions. - Redundant forces, and other forces that follow by statics, that require areas of the members that sum to the minimum total weight.

The Direct-Design Method

The Direct-Design Method reverses the usual design process for an indeterminate structure.

The method first satisfies the continuity of strains with the assignment of the highest possible allowable stresses; then selects optimum redundant forces; and finally determines the optimum member areas that yield the least total volume of the members

Continuity and Stresses

When a virtual load is applied at each redundant

$$1\# \times \Delta'' = 0 = \Sigma\frac{FUL}{AE} = \frac{1}{E}\Sigma S(UL) = 0$$

For the most optimal structures, $\Sigma(UL)$ will be equal to zero; proof to be given later. Further, the $\Sigma(UL)$ over both the tension and compression members separately will be zero, ideally. Then with the modulus of elasticity (E) constant,

$$S_t\Sigma^t UL = 0 \quad \text{and} \quad S_c\Sigma^c UL = 0$$

For these situations, the tension and compression stresses, S_t and S_c, can be the maximum allowable design stresses. Fortunately, S_c does not need to equal S_t, thus allowing for smaller stresses in the compression members.

Redundant Reactions

Forces can be assigned to the redundants and the remaining forces determined by statics. The member areas are calculated from these forces and the assigned stresses. Several redundant forces can be tried to result in the most practical distribution of member sizes throughout the structure.

Minimum Weight

The same minimum total weight of structure will result from any selected redundant force; proof to be given later.

Other Considerations

Only well-configured indeterminate structures can be designed to the maximum of optimality. A haphazard addition of redundancies can result in an awkward structure where the members are literally loading each other, instead of sharing the external loads. The art and intuition of the designer is all-important in the delineation of the conformation and dimensions of the line diagram of the structure for which member sizes will be sought. The early recognition of the members that will be in tension, and those in compression, will be helpful in conceiving a well-configured structure that can be optimized easily for least weight.

Illustrative Example

Fig. 1a shows a one-degree indeterminate truss for which areas are required to minimize the weight of the structure.

Fig. 1b contains the listing of the virtual bar forces U, and UL, when the center reaction is chosen as the redundant. The summation of UL is shown to be zero over the whole truss, over the diagonals (all in compression), and over the chords (all in tension).

Fig. 1c shows arbitrary design stresses that can be assigned to achieve the requirement of $\Sigma S(UL) = 0$. Fig. 1d shows that the $\Sigma S(UL)$, like ΣUL, is zero over both the tension and compression members.

Fig. 1e and 1f involve two arbitrary sets of reactions that satisfy statics. For the top chord to be in tension, the right reaction must be less than 40, and the left less than 60. The top chord must be in tension to agree with the sign of the stress assigned in Fig. 1c.

The ΣAL, the volume of truss material required, is exactly the same, 187.5 cu. units. All other statically-consistent reactions, within the limiting range, would require exactly the same volume of material.

Transmissible Potential Energy

This principle of the transmissible potential energy of the loads and reactions is basic to the development of direct, optimum-design method.

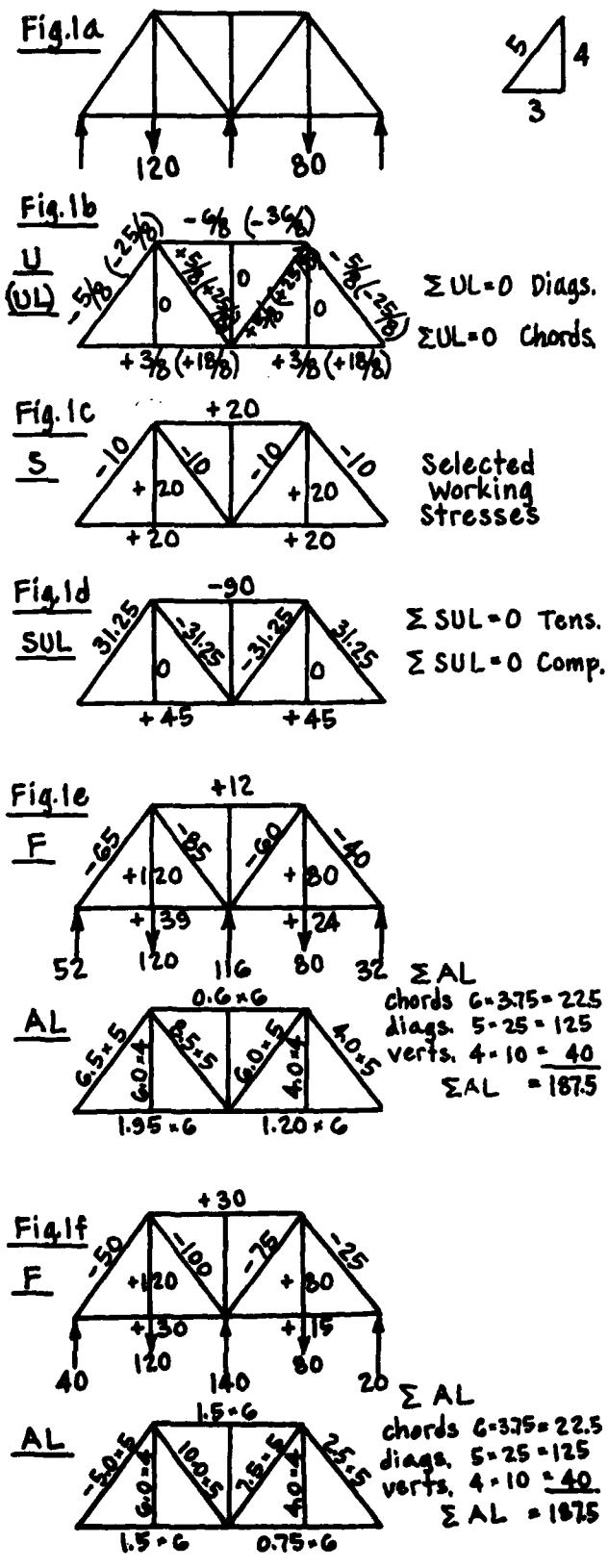
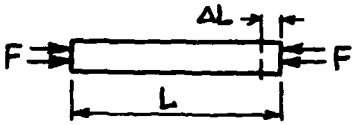


Fig. 1. Illustrative Example

Fig. 2 illustrates the concept.



$$\Delta L = \frac{FL}{AE}$$

$$FL = EA\Delta L$$

$$FL = E(\Delta Vol.)$$

The usual assumption is made that the area and specific weight of the bar is unchanged for the calculation of the stress from the load F, but the length changes by an amount ΔL. The equation $\Delta L = \frac{FL}{AE}$, to be used frequently, is based on this assumption. Hereafter, the change in volume will be A ΔL.

Well-known in mechanics is the principle of the transmissibility of a force, allowed for certain purposes. However, the potential energy of a force is changed when it is translated along its line of action. In Fig. 2, the work done is FL if one or both vector arrowheads (the points of application) were translated to touch each other. As an aside, the modulus of elasticity might be viewed as $E = \frac{FL}{\Delta\ Vol.}$, the transmissible potential energy required for a unit volume change.

Application

In a network of members, the sum of the transmissible potential energy (TPE) in all of the members will be found equal to the TPE of the loads and reactions. Plus and minus signs must be attached to each FL to distinguish between arrowheads that would move forward along their lines of application (for compression), and in the reverse sense (for tension).

If all loads and reactions act at a common level, there is no TPE. The sum of FL over the members is zero. If the loads and reactions are not applied at a common level, the sum of FL over the bars can be calculated easily.

Fig. 2a shows load Pa acting at the same level line of action as the reactions. There is zero TPE because the vector heads of the resultant of the reactions and the load touch each other. If Pa were raised to the position shown by Pa', the TPE would be minus $P_a'y$ Fig. 2b shows the amount of the TPE for a group of loads.

Fig. 2c demonstrates that the TPE need not be calculated in only a vertical direction in the manner of true potential energy being able to do work because of an elevated vertical position. Fig. 2d shows that the TPE is independent of the internal arrangement of members, and independent of determinacy or indeterminacy.

Fig. 2e indicates the importance of the location of the arrowheads, and how movement must be made to alignment to calculate the TPE.

Fig. 2f shows that a couple, or couples, have no PTE, for they inherently can be translated or rotated without affecting the statics of the reactions.

Fig. 2g provides the transition to further usefulness, indicating that a virtual load has touching arrowheads when a bar is cut. Redundants then conveniently produce $\Sigma UL = 0$.

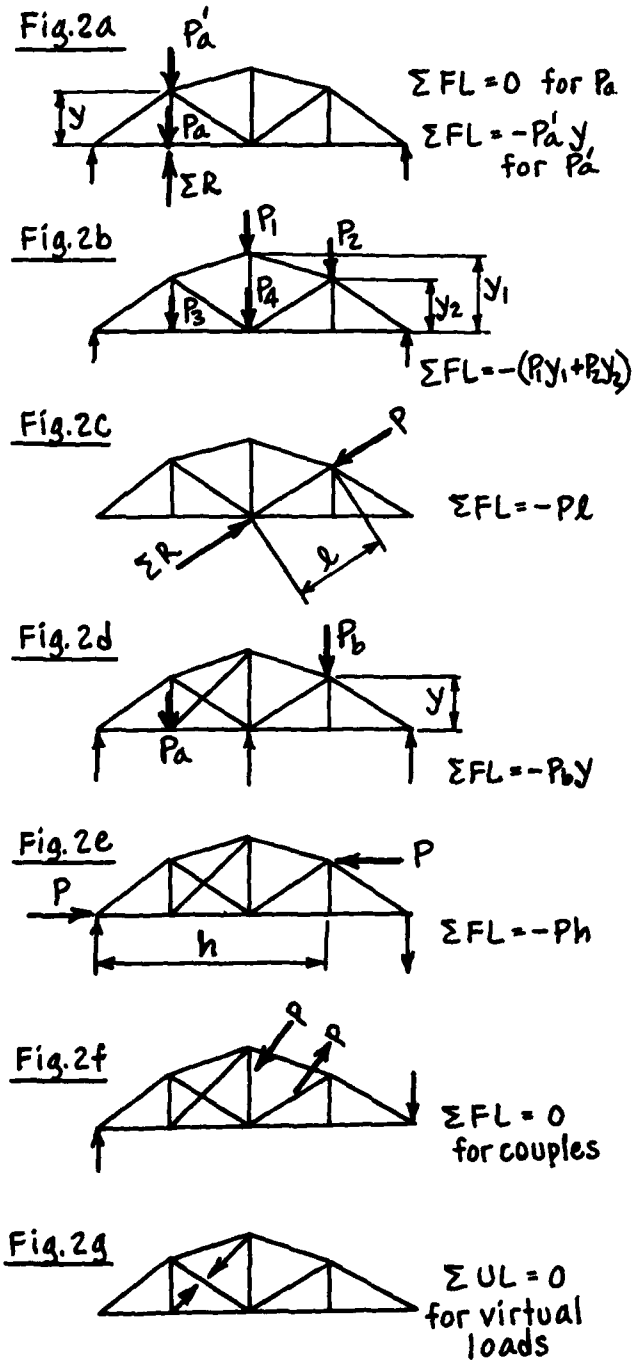


Fig. 2. Transmissible Potential Energy

Conservation of Volume

Assuming no change in volume of the assemblage of members when loaded, $\Sigma A\,\Delta L = 0$.

Then $\Sigma A\,\Delta L = \Sigma A(\frac{FL}{AE}) = \Sigma\frac{FL}{E} = \frac{1}{E}\Sigma FL = 0$

It is proved then that there is no change in volume when there is zero external transmissible potential energy. More generally, the internal volume change is equal to the transmissible potential energy of the external loads and reactions, divided by the modulus of elasticity.

Minimum Weight

To minimize the total weight of a truss, $\Sigma\gamma AL$ must be minimized, or to minimize the volume, ΣAL must be minimized.

The magnitude of the redundants in an indeterminate truss that minimize the volume are disclosed by differentiation.

$$\frac{d}{dR}\Sigma AL = \frac{d}{dR}\Sigma\frac{FL}{S} = 0$$

If the stresses have been set previously to satisfy $\Sigma SUL = 0$, the stresses can be considered constants. Then

$$\frac{d}{dR}\Sigma FL = 0 = \Sigma\frac{dF}{dR}L = \Sigma UL = 0$$

Any redundant then will yield the same minimum total volume if ΣUL has already been made zero. The only limitation is that the selected redundant forces must be within the range that will produce signs of the stresses that were assigned to the members in setting $\Sigma SUL = 0$.

The Importance of $\Sigma|F|L$

The concept of ΣFL for real applied loads was found useful because it permitted extension to the application of a 1-lb. virtual load, giving $\Sigma UL = 0$. Incidentally, students find the ΣFL useful as a check on the probable validity of their calculation of member forces.

Volume Proportional to $\Sigma|F|L$

Since volume = $\Sigma AL = \Sigma\frac{FL}{S}$, and F and S have the same sign, all members contribute positive amounts in the summation. Again, if the stresses have already been selected to satisfy continuity, the minimum $\Sigma|F|L$ will correspond to the minimum volume.

Magnitude of $\Sigma|F|L$

Anologous shear and moment diagrams, modified slightly from those for beams, can be constructed and used to determine $\Sigma|F|L$. The modified shear and moment diagrams can be best explained by examples. The goal will be to relate the ordinates of these diagrams to the member forces and the volume needed for the truss.

Shear Diagram. Consider first an uncomplicated truss shown by Fig. 3a. The shear is restricted to the diagonals. Fig. 3b shows the shear in each panel. Since the force in each diagonal is the vertical

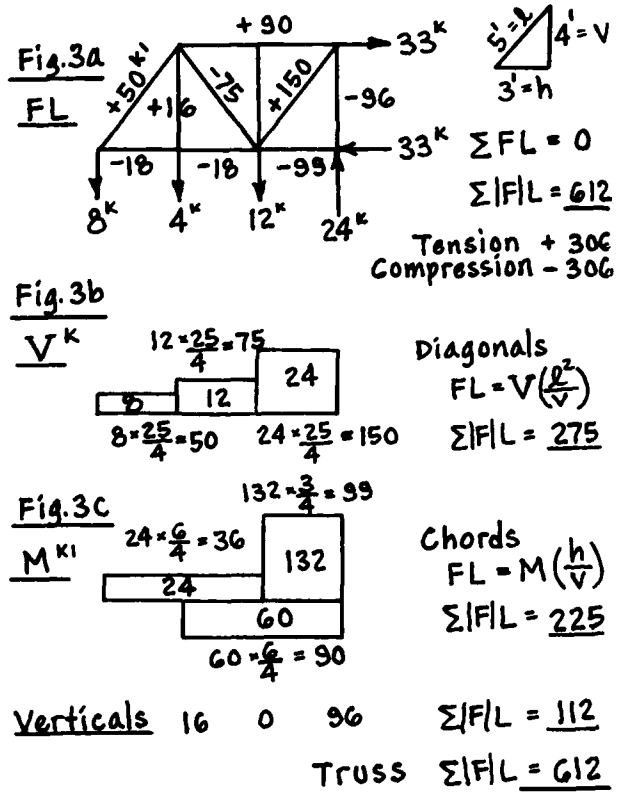


Fig. 3. Shears and Moments

shear multiplied by ℓ/V, the FL for each diagonal is

$$FL = (\text{Shear})(\frac{\ell^2}{V})$$

Moment Diagram. Fig. 3c shows the moments at all upper and lower chord panel points. The moment is shown constant over a panel length because the force in the bars of the opposite chord are constant over the length of the panel. The force in any chord is the moment in the appropriate opposite chord divided by the spacing of the chords. The FL for each chord is then

$$FL = (\text{Moment})(\frac{h}{V})$$

Vertical Members. The ΣFL in the verticals must be added to the summations for the chords and diagonals to complete the total summation.

Total Volume

The truss that is perfectly optimized to minimum volume will have the same $\Sigma|F|L$ over both the tension and the compression members. The stresses in each will have been set to the maximum design amounts. Then

$$\text{Vol} = \Sigma AL = \frac{1}{S_t}\overset{t}{\Sigma}|F|L + \frac{1}{S_c}\overset{c}{\Sigma}|F|L$$

These requirements are shown to be met in the example, Fig. 3.

Alternative Structures

The advantages and disadvantages of indeterminate structures are well-known, and will not be discussed here. The relative weights of indeterminate and determinate trusses, to carry the same loads, does need to be given some attention. The following example will disclose the weights required for different types of trusses.

Fig. 4a shows the amounts of F and (FL) for two determinate trusses. The summation of |F|L over both the tension and compression members is the same, 1500. This result only illustrates that the design stresses can always be used to determine the areas in a determinate truss.

Fig. 4b shows the addition of a tie rod between the trusses, making the truss indeterminate. The values of UL are seen to sum to zero over both the tension and the compression members. Thus, $\Sigma SUL = 0$ is satisfied by $\frac{1}{S_c^c}\Sigma UL = 0$ and $\frac{1}{S_t^t}\Sigma UL = 0$. The design stresses for tension and compression can be equal to those used for the determinate truss.

Figs. 4c and d show the amounts of F and FL for two arbitrary sets of reactions that satisiy statics. Again, as for the determinate truss, the ΣFL is 1500 over both the tension and compression members. The required weight would be identical to that for the determinate trusses. Any end reactions between 0 and 60 would yield the same total weight.

Fig. 4e assumes the end reactions to be zero. This truss also requires the same total weight as all of the others.

Discussion of Results. The shear and moment diagrams explain the previous results of the same required weight for all trusses.

The shear ordinates in each of the panels for the alternative trusses are:

	Panel				
	1	2	3	4	Σ
Fig. 4a	60	60	60	60	240
Fig. 4c	40	80	80	40	240
Fig. 4d	20	100	100	20	240
Fig. 4e	0	120	120	0	240

The moment ordinates over the panel length, calculated at the appropriate panel point are:

	Panel Point				
	1	2	3	4	Σ
Fig. 4a	180	180	180	180	
		0	0		720
Fig. 4c	120	120	120	120	
		120	120		720
Fig. 4d	60	60	60	60	
		240	240		720
Fig. 4e		360	360		720

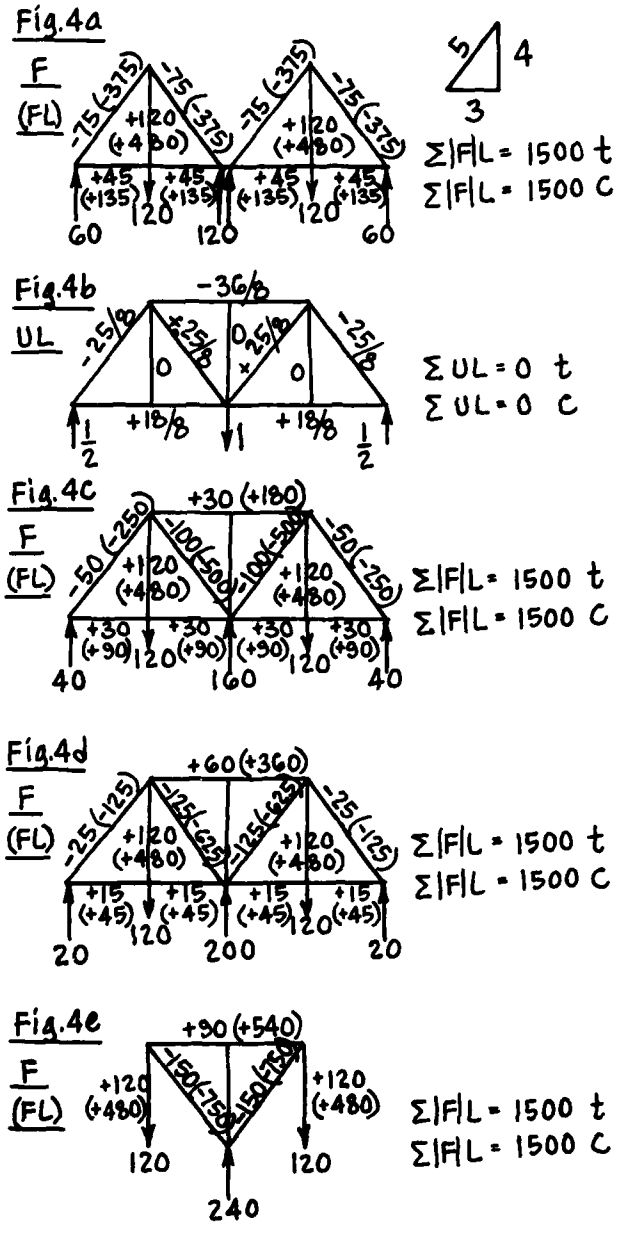


Fig. 4. Alternative Structures

The shear and moment diagrams for the different trusses are not identical, but their areas are equal if the real values of the areas are summed. Equal weights then result for all these alternative trusses.

Summary. The real values of the ordinates and areas of the shear and moment diagrams determine the member forces and the areas required in the chords and diagonals.

Internal Redundants

It would be a gross mistake to conclude that all indeterminate trusses can be ideally optimal.

Cross-Bracing. Consider Figs. 5a and 5b.

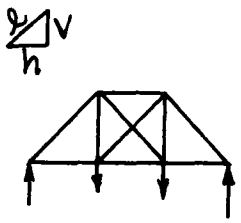


Fig. 5a

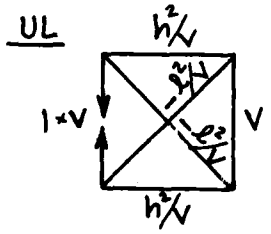


Fig. 5b

There is a dilemma in the assignment of working stresses to make ΣS(UL) = 0. Inspection of Fig. 5b shows there should be tension in one vertical, one horizontal, and one diagonal for ΣSUL = 0 over the tension and compression members separately. This arrangement would be awkward for the loads shown in Fig. 5a. Both diagonals and both verticals should share in supporting the loads instead of one member loading another.

The common usage of two crossed diagonal tension rods, with negligible compression capability, is a statically determinate arrangement that is, however, appropriate for moving or variable loads.

The Three-Bar Truss

Following the many previous investigators of this classic problem, the author can't resist applying the direct-design method to the three-bar truss.

In Fig. 6a, the problem is to minimize the total weight required to support the loads P and H. The following steps will illustrate and summarize the direct-design method.

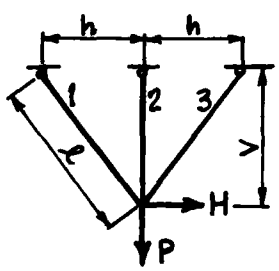


Fig. 6a

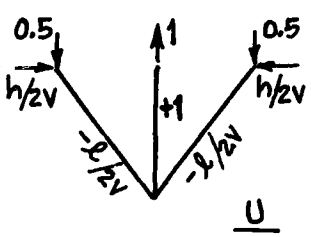


Fig. 6b

1. Apply a 1-lb. virtual load at the center reaction and get the U-forces, Fig. 6b. Then

$$\Sigma UL = 1 \times v - 2\left(\frac{\ell^2}{2v}\right) = \frac{1}{v}[v^2 - v^2 - h^2] = -\frac{h^2}{v}$$

$$PTE = -\left(\frac{h}{2v}\right)(2h) = -\frac{h^2}{v}$$

and as a check, $\Sigma UL = PTE$

2. Conceive stress patterns, two alternatives shown on Figs. 6c and 6d.

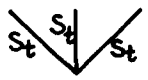


Fig. 6c



Fig. 6d

3. Calculate ΣSUL, required to be zero.

For Fig. 6c, $0 = S_t\left[-2\left(\frac{\ell^2}{2v}\right)+v\right] = S_t v\left[1-\frac{\ell^2}{v^2}\right] = 0$

The required geometry would be one vertical bar, $\ell = v$, a trivial solution.

For Fig. 6d, $0 = S_t\left(-\frac{\ell^2}{2v} + v\right) + S_c\left(-\frac{\ell^2}{2v}\right)$

giving $$\frac{S_c}{S_t} = \frac{v^2 - h^2}{\ell^2}$$

Results show that the compression bar should be omitted if $v = h$; otherwise the third bar should be in compression or tension, depending on $v \lesssim h$.

4. Determine the volume required for Fig. 6d.

$$\Sigma AL = \frac{(F_1+F_2)\ell}{S_t} + \frac{F_3\ell}{S_3} = \frac{1}{S_t}\left[(F_1+F_2)\ell + (F_3\ell)\frac{(\ell^2)}{(v^2-h^2)}\right]$$

Inspection again shows that Bar 3 should be omitted because of (v^2-h^2) in the denominator.

Then $$\Sigma AL = \frac{F_1\ell + F_2\ell}{S_t} = \frac{PTE}{S_t} = \frac{Hh + Pv}{S_t}$$

5. Determine the reactions and bar forces by statics, Fig. 6e, and the areas using S_t as the allowed working stress.

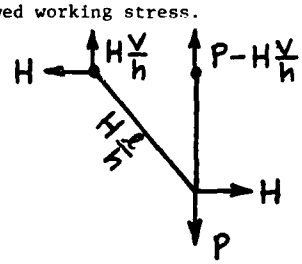


Fig. 6e
Optimized Bar Forces

As a check,

$$\Sigma AL = \frac{1}{S_t}\left[H\frac{\ell^2}{h} + (P - H\frac{v}{h})v\right] = \frac{1}{S_t}[Hh + Pv]$$

6. Summary:

$$PTE = S\Sigma Vol = E\varepsilon\Sigma Vol = E\Sigma\Delta Vol.$$

Previous Work

The ideas and methods presented here are those published by the Author in 1958.* Any repetition is for the information of those who did not see the more extensive original publication that includes theorems and corrollaries for minimum weight, and many optimized designs for multiple external and internal redundants using a method of superposing a group of statically determinate sub-trusses.

*"Direct Design of Optimum Indeterminate Trusses." Louis M. Laushey. Dec., 1958. Paper 1867, ST 8, Jour. Struct. Div., ASCE.

AD-P000 096

A NEW METHOD FOR OPTIMAL DESIGN OF STRUCTURES

Renwei Xia[a], P. T. Hsu[b], M. M. Chen[c]
College of Engineering
Boston University
Boston, MA 02215

Abstract

A new method for optimal design of structures is presented. The structure is subjected to multiple loading conditions and behavioral constraints on nodal displacements, element stresses and constraints on member sizes. This new method is based on the Kuhn-Tucker conditions, in which the gradients of active constraints are expressed through Taylor series expansion in terms of design variable so that a new design point can be generated. Recursion formulas for the iteration determination of the design variables are thus derived.

The related tasks of computing the first and second derivatives of nodal displacements and stresses with respect to design variables are also formulated. These formulations are simple and powerful. A typical three-bar truss structure has been optimized to illustrate the application of this method. Since the direction of the optimization process is directly derived from the Kuhn-Tucker conditions, it has been shown that this new method is considerably more efficient.

I. Introduction

As the finite element methods are progressed along with the development of large scale digital computers, the computational methods of structural optimization have been one of the most important research subjects in the field of structural mechanics in the last twenty years. Numerous significant work on structural optimization have been done by L. A. Schmit[1-3], R. H. Gallagher[4-5], R. A. Gellatly[5-8], V. B. Venkayya[9-10], E. J. Haug[11-12] and many others (13-15).

The mathematical formulation of structural optimization can be stated simply as follows:

Find $A = \{A_1, A_2, \ldots, A_N\}^T$, (design variable vector) (1)

such that $g_j(A) \leq 0$, $(j=1,2,\ldots,J)$, (inequality constraints) (2)

$h_e(A) = 0$, $(e=1,2,\ldots,E)$, (equality constraints) (3)

and $f(A) \rightarrow \text{Min}$ (objective function) (4)

In the truss design, if the structural configuration is given the design variable vector A will consist of the cross-sectional areas of the bars. The objective function f(A) is generally taken to be the weight of the truss. With ρ_i and L_i being the density and the length of the member i, respectively, the objective function can be expressed as,

$$f(A) = \sum_{i=1}^{N} \rho_i L_i A_i \tag{5}$$

The inequality constraints $g_j(A) \leq 0$, $(j=1,2,\ldots,J)$ here may, according to design requirements, be displacement constraints, stress constraints, geometry constraints and others. The equality constraint equations $h_e(A) = 0$, $(e=1,2,\ldots,E)$, may be equilibrium equations and compatibility equations of the structure under the action of external loads. In general, the equality constraint equations are dealt with in structural analysis, so that the optimization problems include only the inequality constraint equations, which may be highly nonlinear in most cases. Therefore, the minimization problems discussed here are generally very complicated, which can only be handled through various numerical techniques.

The N design variables may form a N-dimensional Euclidean space E^N. Any point or vector $A = \{A_1, A_2, \ldots, A_N\}^T$ in the space represents a design program. The set of points

$$R = \{A \mid g_j(A) \leq 0,\ j=1,2,\ldots,J\}$$

is defined as the feasible region. Any point $A \in R$ represents a feasible design program, which is called the feasible solution. If $A \in R$ and there are some i's such that $g_i(A) = 0$, with $i \in I(A)$, where $I(A) = \{i \mid g_i(A) = 0,\ 1 \leq i \leq J\} = (1,2,\ldots,m)$, then the point A is at the boundary surface of the feasible region R, and the corresponding constraints $g_i(A) = 0$, $i \in I(A)$, are called active constraints. Because of the linearity of the objective function (5), the optimal point certainly lies at the boundary surface.

It is well known that two approaches of optimization are most used in structural design; the mathematical-programming approach and the optimality criteria method. In the former approach the iterative design formula can be written as

$$A^{(k+1)} = A^{(k)} + \alpha^{(k)} \cdot S^{(k)}, \quad (k=1,2,\ldots) \tag{6}$$

where $\alpha^{(k)}$ and $S^{(k)}$ are the step size and the direction vector in the kth iteration, respectively. The differences among various mathematical programming approaches lie only in different ways to decide $\alpha^{(k)}$ and $S^{(k)}$. It is worth noting that most of the methods used at present to define the direction vectors are based on simply reducing the values of the objective functions, and they do not have any direct relationships with convergent conditions or the Kuhn-Tucker conditions, which can be expressed as

$$\sum_{i=1}^{m} \lambda_i \cdot \nabla g_i(A) + \nabla f(A) = 0 \tag{7}$$
$$\lambda_i \geq 0$$

where $\nabla g_i(A)$'s are active constraint gradients, $\nabla g_i(A) = \left\{\frac{\partial g_i(A)}{\partial A_1}, \ldots, \frac{\partial g_i(A)}{\partial A_N}\right\}^T$ and λ_i's are the Lagrangian multipliers: $\nabla f(A)$ is the gradient of the objective function $\nabla f(A) = \left\{\frac{\partial f(A)}{\partial A_1}, \ldots, \frac{\partial f(A)}{\partial A_N}\right\}^T$.

When the optimality criteria methods are used to solve optimization problems, a Lagrangian function is generally written as

$$\phi(A) = f(A) + \sum_{j=1}^{J} \lambda_j \cdot g_j(A) \tag{8}$$

The conditions for the optimum value of the objective function f(A) with the constraint functions $g_j(A)$'s can then be obtained,

---

[a] Visiting Research Professor from Peking Institute of Aeronautics and Astronautics

[b] Associate Professor of Systems Engineering, deceased

[c] Professor of Aerospace and Mechanical Engineering

$$\frac{\partial \phi}{\partial A_i} = \frac{\partial f(A)}{\partial A_i} + \sum_{j=1}^{J} \lambda_j \cdot \frac{\partial g_j(A)}{\partial A_i} = 0 \qquad (9)$$

$$\lambda_j \cdot g_j(A) = 0 \qquad (i=1,2,\cdots,N)$$

$$\lambda_j \geq 0, \qquad (j=1,2,\cdots,J)$$

From equations (9) a simplified form of optimality criteria can be written as follows:

$$\sum_{j=1}^{J} \lambda_j \cdot e_{ij} = 1 \qquad (i=1,2,\cdots,N), \qquad (10)$$

where $$e_{ij} = -\left(\frac{\partial g_j(A)}{\partial A_i} \Big/ \frac{\partial f(A)}{\partial A_i}\right) \qquad (11)$$

It has the physical meaning as the energy density in the structure.

Generally speaking, equation (9) or (10) can not always be satisfied unless the design point A happens to be an optimum. Therefore it is necessary to form an iterative formula.

$$A_i^{(k+1)} = A_i^{(k)} \cdot \left(\sum_{j=1}^{J} \lambda_j \cdot e_{ij}\right)^{\frac{1}{2}}, \quad (i=1,2,\cdots,N) \qquad (12)$$

It is obvious that equations (12) are associated with convergent condition (9) or (10), and they have been used successfully in some optimal designs. But there is still no guarantee that they will always be convergent.

The method to be presented in the following is based on the Kuhn-Tucker conditions, in which the **active** constraint gradients are expressed through Taylor series expansion in terms of design variables. So that a new design point, at which the Kuhn-Tucker conditions would be satisfied, can be generated directly. Naturally, because of the approximations of Taylor series expansion, the design procedure developed in this manner still requires some steps of iteration.

In addition to the constraint gradients, the Hessian matrix of the second derivatives of the constraint functions is also included in the method presented here. It seems that the computations of the first and second derivatives of the displacements and, especially, the stresses of trusses are quite extensive and complicated. However, it is possible to derive simple formula for computing them as we will present them in the following.

II. Design Theory

In mathematical-programming approaches, the Kuhn-Tucker conditions is given by equation (7) or,

$$\nabla G(A) \cdot \lambda + \nabla f(A) = 0 \qquad (13)$$

where

$$\nabla G(A) = \left[\nabla g_1(A), \nabla g_2(A), \cdots, \nabla g_m(A)\right]$$

$$\lambda = \{\lambda_1, \lambda_2, \cdots, \lambda_m\}^T$$

The Lagrangian multipliers can be determined from the following equation[17]

$$\lambda = -\left[\nabla G(A)^T \cdot \nabla G(A)\right]^{-1} \cdot \nabla G(A)^T \cdot \nabla f(A) \qquad (14)$$

Obviously, equation (7) or (13) in general does not hold except when A is an optimal point. A new design point should then be generated to satisfy equation (7) or (13). The constraint functions $g_i(A)$, $(i=1, 2,\cdots,m)$, at the new point A should be expressed through the Taylor series expansion at the current point A.

$$g_i(A) = g_i(A_\cdot) + \nabla g_i(A_\cdot)^T \cdot (A - A_\cdot) + \tfrac{1}{2}(A - A_\cdot)^T \cdot H_i(A_\cdot) \cdot (A - A_\cdot) \qquad (15)$$

where $H_i(A_\cdot)$ is the Hessian matrix

$$H_i(A_\cdot) = \begin{Bmatrix} \frac{\partial^2 g_i(A)}{\partial A_1^2} & \cdots & \frac{\partial^2 g_i(A)}{\partial A_1 \partial A_N} \\ \vdots & & \vdots \\ \frac{\partial^2 g_i(A)}{\partial A_1 \partial A_N} & \cdots & \frac{\partial^2 g_i(A)}{\partial A_N^2} \end{Bmatrix} \qquad (A_\cdot)$$

and then the constraint gradients at the new point A should be

$$\nabla g_i(A) = \nabla g_i(A_\cdot) + H_i(A_\cdot) \cdot (A - A_\cdot) \qquad (16)$$

By substituting equation (16) into equation (7) or (13), a new design point can be obtained as

$$A = A_\cdot - H(A_\cdot)^{-1} \cdot \left(\nabla G(A_\cdot) \cdot \lambda + \nabla f(A_\cdot)\right) \qquad (17)$$

where $$H(A_\cdot) = \left[\lambda_1 H_1(A_\cdot) + \cdots + \lambda_m \cdot H_m(A_\cdot)\right]$$

$$= \sum_{i=1}^{m} \lambda_i \cdot H_i(A_\cdot) \qquad (18)$$

and $$\lambda = -\left[\nabla G(A_\cdot)^T \cdot \nabla G(A_\cdot)\right]^{-1} \cdot \nabla G(A_\cdot)^T \cdot \nabla f(A_\cdot)$$

Because of the approximations of the Taylor series expansion, a recursive expression for the determination of design variables is necessary:

$$A^{(k+1)} = A^{(k)} - H(A^{(k)})^{-1} \cdot \left(\nabla G(A^{(k)}) \cdot \lambda^{(k)} + \nabla f(A^{(k)})\right), \quad (k=0,1,\cdots) \qquad (19)$$

The convergent condition of equation (19) is naturally the Kuhn-Tucker conditions at point $A^{(k)}$, that is

$$\nabla G(A^{(k)}) \cdot \lambda^{(k)} + \nabla f(A^{(k)}) = 0$$

so that $$A^{(k+1)} = A^{(k)}$$

III. The Derivatives of Structural Behaviors

From the statement mentioned above, it is quite evident that computing the derivatives of structural node displacements and element stresses with respect to design variables is an important task in not only the approach presented here but also the other methods of structural optimization. During the last few years some work on the computational methods of the first derivatives of structural behaviors with respect to design variables have been developed[18-22]. But it seems that the computational formulas of the second derivatives of structural behaviors, which are necessary in the method presented here and some other mathematical-programming approaches, have not yet been achieved. Obviously, the computations of the second derivatives of displacements and stresses are quite extensive and complicated, especially for the case where the number of design variables becomes too

large. However, it is possible to derive simple formulas for computing the second derivatives for single force elements, such as axial force bars and shearing panels.

3.1 The First Derivatives

For a truss structure the displacement U_r at some node point of the structure can be calculated by the virtual load method as[21]

$$U_r = \sum_{i=1}^{N} \frac{S_i^V \cdot S_i^R \cdot L_i}{E_i A_i} \qquad (20)$$

Where S_i^V is the internal force in the ith bar element due to a unit virtual force applied in the direction Ur.

S_i^R is the internal force in the ith bar element induced by the external loading system acted on the structure.

L_i, A_i and E_i are the length, the cross-sectional area and Young's modulus of the ith bar, respectively.

N is the numbers of bars of the structure.

By taking the derivative of Ur with respect to design variable A_j, the following equation is obtained.

$$\frac{\partial Ur}{\partial A_j} = -\frac{S_j^V \cdot S_j^R \cdot L_j}{E_j A_j^2} + \sum_{i=1}^{N} \left(\frac{\partial S_i^R}{\partial A_j} S_i^V + \frac{\partial S_i^V}{\partial A_j} S_i^R\right) \frac{L_i}{E_i A_i} \qquad (21)$$

The summation of the term on the RHS should actually be zero, because it represents the virtual work done of the self-equilibrium internal force systems and displacements. Equation (21) then becomes

$$\frac{\partial Ur}{\partial A_j} = -\frac{S_j^V \cdot S_j^R \cdot L_j}{E_j A_j^2}, \quad (j=1,2,\cdots,N), \qquad (22)$$

or

$$\frac{\partial Ur}{\partial A_j} = -\frac{\sigma_j^V \cdot \sigma_j^R \cdot L_j}{E_j}, \quad (j=1,2,\cdots,N) \qquad (23)$$

Where σ_j^V and σ_j^R are stresses corresponding to S_j^V and S_j^R, respectively.

From the matrix methods of structural analysis, it is well known that the stress in a bar element g of the structure in common coordinate system (Fig. 1) can be expressed as

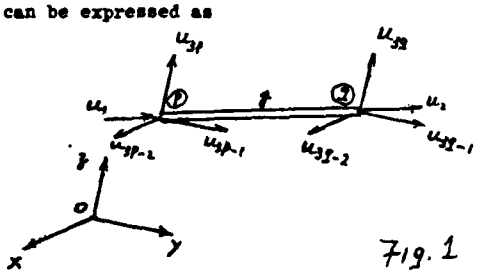


Fig. 1

$$\sigma_g = \frac{E_g}{L_g}\{-l_{pq},-m_{pq},-n_{pq},l_{pq},m_{pq},n_{pq},\}_g \begin{bmatrix} U_{3p-2} \\ U_{3p-1} \\ U_{3p} \\ U_{3q-2} \\ U_{3q-1} \\ U_{3q} \end{bmatrix}_g \qquad (24)$$

Where l_{pq}, m_{pq}, n_{pq} are direction cosines of the angles between the line pq and the three coordinate axes: OX, OY and OZ, respectively.

For simplicity, the equation (24) can be re-written as

$$\sigma_g = C_g^T \cdot U_g \qquad (25)$$

Where

$$C_g^T = \frac{E_g}{L_g}\{-l_{pq},-m_{pq},-n_{pq},l_{pq},m_{pq},n_{pq}\}_g$$

$$U_g = \{U_{3p-2},U_{3p-1},U_{3p},U_{3q-2},U_{3q-1},U_{3q}\}^T$$

From equation (25), the value of the stress σ_g in element g of the structure can be viewed as the virtual work done by the generalized virtual force C_g along the generalized actual displacement U_g, so that it can be derived as

$$\sigma_g = \sum_{i=1}^{N} \frac{S_i^{Vg} \cdot S_i^R \cdot L_i}{E_i A_i} \qquad (26)$$

Where S_i^{Vg} is the internal force in element i induced by the generalized virtual force C_g, which is applied in the directions corresponding to the displacement vector U_g of the element g. Other symbols in equation (26) have the same meanings as those described in equation (20).

Referring to equations (20) to (23), it is evident that the derivative of the stress σ_g, is

$$\frac{\partial \sigma_g}{\partial A_j} = -\frac{\sigma_j^{Vg} \cdot \sigma_j^R \cdot L_j}{E_j}, \quad (j=1,2,\cdots,N) \qquad (27)$$

It is important to point out that the computation of the derivative of stress is just as simple as that of displacement, and both can be calculated for only one virtual loading case.

From equation (27) it is clear that the derivatives of stress with respect to design variables are zero except $\frac{\partial \sigma_g}{\partial A_g}$ for determinate structures, because the generalized virtual force C_g expressed in equation (25) is a set of self-equilibrium forces.

3.2 The Second Derivatives

The computational formulas for second derivatives of displacements and stresses can be derived by means of the equations (23) and (27).

By differentiating equation (23), the following equation is obtained

$$\frac{\partial^2 Ur}{\partial A_j \partial A_k} = -\left(\frac{\partial \sigma_j^V}{\partial A_k} \cdot \sigma_j^R + \frac{\partial \sigma_j^R}{\partial A_k} \cdot \sigma_j^V\right) \cdot \frac{L_j}{E_j} \qquad (28)$$

By applying equation (27) and from the definition of all the parameters, the following expressions can be given

$$\frac{\partial \sigma_j^R}{\partial A_k} = - \frac{\sigma_k^{Vj} \cdot \sigma_k^R \cdot L_k}{E_k} \qquad (29)$$

and $$\frac{\partial \sigma_j^V}{\partial A_k} = - \frac{\sigma_k^{Vj} \cdot \sigma_k^V \cdot L_k}{E_k} \qquad (30)$$

Where σ_k^{Vj} represents the stress in element k due to the generalized virtual force C_j, which is applied in the directions corresponding to the displacement vector U_j of the element j.

σ_k^V is the stress in element k induced by a unit virtual force applied in the direction U_r.

σ_k^R is the stress in element k due to the external forces acted on the structure.

By substituting equations (29) and (30) into equation (28), the second derivative of displacement U_r with respect to design variables can finally be derived as

$$\frac{\partial^2 U_r}{\partial A_j \partial A_k} = (\sigma_j^R \cdot \sigma_k^V + \sigma_k^R \cdot \sigma_j^V) \frac{\sigma_k^{Vj} \cdot L_j \cdot L_k}{E_j E_k} \qquad (31)$$

$$(j=1,2,\cdots,N)$$

$$(k=1,2,\cdots,N)$$

The number of structural analyses for computing the Hessian Matrix of the second derivatives of node displacement from equation (31) is thus as high as (N+2). However, it should be pointed out that the (N+1) structural analyses for virtual force conditions expressed by the superscripts V_j, $(j=1,2,\cdots,N)$, and V in equation (31) can simultaneously be completed when Gaussan elimination technique is used to solve the matrix equation of equilibrium which has (N+1) virtual force vectors. Thus the evaluation of the second derivatives does not really add too much extra effort in computation.

The second derivative of stress σ_g with respect to design variables can similarly derived by differentiating equation (27)

$$\frac{\partial^2 \sigma_g}{\partial A_j \partial A_k} = - \left(\frac{\partial \sigma_j^{Vg}}{\partial A_k} \cdot \sigma_j^R + \frac{\partial \sigma_j^R}{\partial A_k} \cdot \sigma_j^{Vg} \right) \frac{L_j}{E_j} \qquad (32)$$

Where $$\frac{\partial \sigma_j^{Vg}}{\partial A_k} = - \frac{\sigma_k^{Vj} \cdot \sigma_k^{Vg} \cdot L_k}{E_k} \qquad (33)$$

Substituting equations (33) and (29) into equation (32), the second derivative of stress σ_g then is

$$\frac{\partial^2 \sigma_g}{\partial A_j \partial A_k} = (\sigma_j^R \cdot \sigma_k^{Vg} + \sigma_k^R \cdot \sigma_j^{Vg}) \frac{\sigma_k^{Vj} \cdot L_j \cdot L_k}{E_j \cdot E_k} \qquad (34)$$

$$(j=1,2,\cdots,N)$$

$$(k=1,2,\cdots,N)$$

From equation (34), it can be seen that if only stress constraints are considered, no matter how many active stress constraints are there, the computations of the Hessian matrices of stresses can be completed by only one structural analysis when Gaussan elimination technique is used to solve the matrix equation of equilibrium which has (N+1) force vectors, one of which is corresponding to the loading condition, the others correspond to virtual force systems.

4. Illustrative Example

A consideration of a three-bar truss example shown in Fig. 2, has been commonly used to demonstrate various optimal design approaches. The truss is subjected to two loading conditions. Because of the symmetry of loading and geometry the number of design variables and constraints can be reduced. In this case, design variables A_1 and A_3 must be identical, and only one loading condition should be considered. The allowable stresses and $\sigma^{(+)}$=20,000 psi for positive stress and $\sigma^{(-)}$=-15,000 psi for negative stress. Only stress constraints are taken into consideration here.

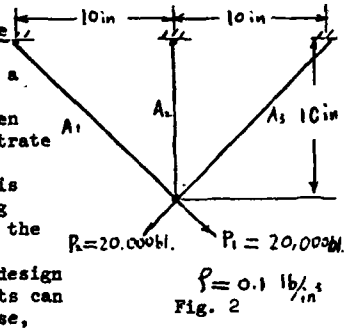


Fig. 2

Two kinds of design steps are alternatively taken in design procedure. One is the scaling step which moves a design point to the boundary surface along a line joining the origin of the N-dimensional coordinate system to the current design point in design space. The other is to modify the design at the boundary surface according to equation (17). The results of the computations are shown in Table 1. The optimal design is quickly achieved in just four iteration cycles.

Table 1

Iteration Cycle	Design Variables		Weight
(k)	$A_1(in^2)$	$A_2(in^2)$	W(lbs)
0	0.707	0.707	2.707
1	0.870	0.313	2.774
2	0.757	0.507	2.648
3	0.792	0.400	2.640
4	0.789	0.408	2.639

5. Conclusions

A new mathematical-programming approach has been developed for otpiaml truss design. The approach is based on the Kuhn-Tucker conditions. The active constraint gradients involved in the Kuhn-Tucker conditions are expressed by Taylor series expansion in terms of design variables, so that a new design point can be generated.

The computational formulas for the first and second derivatives of node displacements and element stresses for truss structures have also been derived. These formulas can be used not only in the method presented here, they also can be applied to other methods of structural optimisation and approximating

structural analysis.

Currently, the method present in this paper is being tried to generalize to the optimal design of large scale structures. It is expected that the computational efforts of the Hessian matrix can be significantly simplified by using the principle of Saint Venant to large scale structures.

Acknowledgment

We are indebted to many colleagues for their help during the course of this work. In particular, we want to thank Professor Lucien A. Schmit of UCLA, Dr. R.A. Gellatly of Bell Aerospace, and Professor T.H.H. Pian of M.I.T. for their valuable comments regarding to our work.

References

1. L.A. Schmit, "Structural Design by Systematic Synthesis", Proceedings of the Second Conference on Electronic Computation, ASCE, September 1960.

2. L.A. Schmit, Farshi, B., "Some Approximation Concepts for Structural Synthesis" AIAA/ASME/SAE 14th Structures, Structural Dynamics and Materials Conference, Williamsburgh, March 1973.

3. L.A. Schmit, H. Miura, "Approximation Concepts for Efficient Structural Synthesis", NASACR-2552 (1976).

4. Gallagher, R.H., "Fully-Stressed Design" Optimum Structural Design, Theory and Applications, edited by R.H. Gallagher and O.C. Zienkiewic, John Wiley and Sons, 1973.

5. R.A. Gellatly, R.H. Gallagher, "A Procedure for Automated Minimum Weight Structural Design; Part I: Theoretical Basis" Aeron. Quart., 17, 1966.

6. R.A. Gellatly, "Development of Procedures for Large Scale Automated Minimum Weight Structural Design" AFFDL-TR-66-180, December 1966.

7. R.A. Gellatly, L. Berke, "Optimum Structural Design", AFFDL-TR-70-165.

8. R.A. Gellatly, R.D. Thom, "Force Method Optimization" AFWAL-TR-80-3006.

9. V.B. Venkayya, N.S. Khot, and V.S. Reddy, "Energy Distribution in an Optimum Structural Design" AFFDL-TR-68-150.

10. V.B. Venkayya, N.S. Khot and L. Berke, "Application of Optimality Criteria Approaches to Automated Design of Large Practical Structures" AGARD Second Symposium on Structural Optimization, April 1973, Milan, Italy.

11. A.K. Govil, J.S. Arora and E.J. Haug, "Optimal Design of Wing Structures with Substructuring" Comput. Structures 10(6), 1979.

12. A.K. Govil, J.S. Arora and E.J. Haug "Optimal Design of Frames with Substructuring" Comput. Structures 12, 1980.

13. R. Rasani, "The Behavior of the Fully-Stressed Design of Structures and its Relationship to Minimum Weight Design", AIAA Journal Vol. 3, No. 12., Dec. 1965.

14. W. Dwyer, R. Emerton and I. Ojalvo, "An Automated Procedure for the Optimization of Practical Aerospace Structures". AFFDL-TR-70-118.

15. G. Zoutendijk, "Methods of Feasible Directions" Elsevier, 1960.

16. J.B. Rosen, "The Gradient Projection Method for Nonlinear Programmings Part I: Linear Constraints" SIAM J., 8, 1960; "Part II: Nonlinear Constraints", SIAM J., 9, 1961.

17. Zhang Chenxu, Renwei Xia, "On Some Problems of Feasible Direction Methods" Journal of the Aeronautical Society of China, March 1979 and Proceedings of the 4th International Conference and Exhibition on Computers in Engineering and Building Design at Brighton Metropole, Sussex, UK, April, 1980.

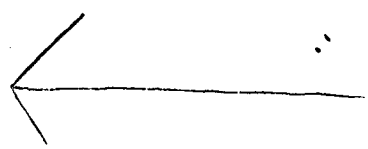
18. Berk, L. and Khot, N.S., "A Simple Virtual Strain Energy Method to Fully Stress Design Structures With Dissimilar Stress Allowables and Material Properties", AFFDL-TM-77-28-FBR, December 1977.

19. Renwei Xia, H.O. Linsu, "Several Techniques about Structural Optimization" (In Chinese) BH-B399 PIAA, Peking, 1978.

20. J.S. Arora, E.J. Haug, "Methods of Design Sensitivity Analysis in Structural Optimization" AIAA. J. Vol. 17, No. 9, September 1979.

21. D. Johnson "The Derivation of Design Sensitivities by the Flexibility Method" AIAA Paper 80-0721.

22. L. Berke, "Convergence Behavior of Iterative Resizing Procedures Based on Optimality Criteria", AFFDL-TM-72-1-FBR.



AD-P000 097

OPTIMAL FINITE ELEMENT DISCRETIZATION A DYNAMIC PROGRAMMING APPROACH

Y.Seguchi, M.Tanaka* and Y.Tomita**

Department of Systems Engineering, Kobe University
Rokkodai, Nada, Kobe 657, Japan
* Division of Systems Science, Kobe University
Rokkodai, Nada, Kobe 657, Japan
**Department of Mechanical Engineering, Kobe University
Rokkodai, Nada, Kobe 657, Japan

SUMMARY An investigation from the topological aspect of the optimal finite element idealization is carried out for the linear elastic system. The criterion for the topological optimization is based on the minimization of the total potential energy, the Rayleigh quotient, and the energy quotient for the static equilibrium, free vibration, and Euler buckling problems, respectively. Firstly, in order to clarify the relation between the functional to be minimized and the discretization topology, the dynamic programming approach proposed by Distefano et al. is extended to the two kind of eigenvalue problems, that is, the free vibration and the Euler buckling analysis.

For the discretization optimization, the structure of the multistage decision process is easily seen in static equilibrium problem and the usual dynamic programming procedure works well. The optimization problem for the free vibration is similarly formulated in the multistage form, but this is more complicated than the above case and the approximate solution procedure using upper-bound property of the eigenfrequency is also proposed. In the case of Euler buckling, the usual decomposition procedure to the multistage form does not work, since the static equilibrium field in stable mode is coupled with the optimization of the discretization in unstable mode. To overcome this difficulty, the inverse transformation technique is introduced and the state reduction technique gives the optimal discretization topology, approximately. Some numerical examples show the remarkable improvement of the accuracy by the topological optimization and the importance of the topological aspect of the finite element idealization.

INTRODUCTION

The finite element method becomes tremendously popular in applied science. It is so broadly known that the accuracy of the finite element solution largely depend upon the discretization scheme used such as element model, element number, discretization geometry and topology that the user of this method usually select a discretization model at the beginning of their work.

Although a simple approach to the more accurate solution is to increase the discretization number or to employ the higher order elements, it leads to the increase of its computational cost. One of the rational method to conquer this is to improve the finite element discretization pattern under the restriction of discretization number. This problem is referred as the optimal discretization problem. The rational approach to this is taken the initiatives by McNeice and Marcal[1], Prager[2]and the related authours, who minimize the total potential energy under the fixed discretization topology with respect to the nodal coordinate specifying the present discretization geometry. Carroll and Baker[3] investigated the existence of the optimal solution and Carroll[4] treated not only the elastostatic problem but also the eigenvalue problem. Furthermore, Seguchi et al.[5] generalized this technique to cover not only the discretization error but also the computational error by introducing the two factor decision criterion of the total potential energy and the condition number.

On the other hand, many of the recent investigations discuss this problem from the practical point of view. they are intended to obtain the nearly optimal discretization scheme by interactive application working with the finite element solutions. The outline of the investigation is found in the review paper by Shephard[6]. The techniques are useful to improve the initial estimate of the pattern in the practical computer works under the current state of art in the computer performance but there might be ambiguity in the discretization optimality as in any heuristic approach.

The purpose of this paper is to obtain the optimal discretization topology by incorporating the variables of the topology into the finite element formulation restricting the element attribute and discretization number. The topological optimization procedure is formulated in the context of the dynamic programming, minimizing the functional for static equilibrium problem, free vibration problem, and Euler buckling problem of linear elastic systems. Firstly, in order to clarify the relation between the functional and discretization topology, finite element analysis procedure based on dynamic programming is presented and, secondly, topological optimization process is revealed. Some numerical examples also presented.

DYNAMIC PROGRAMMING APPROACH TO FINITE ELEMENT ANALYSIS

The dynamic programming formulation of the finite element method proposed by Distefano and Samartine[7] for static equilibrium problem is introduced and extended to the optimization process of the finite element discretization topology to be discussed in what follows. Here, its outline is briefly reviewed and its extention for free vibration and Euler buckling analysis is presented.

PRECEDING PAGE

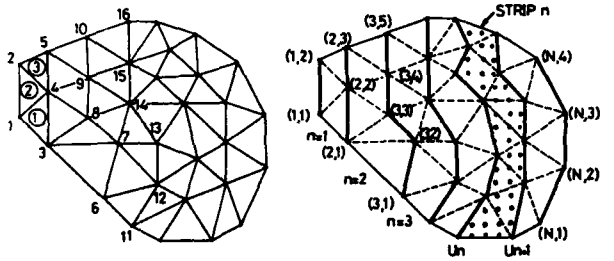
STATIC EQUILIBRIUM PROBLEM[7]

Without loosing the generality, it is possible to group the whole finite elements into (N-1) strips as shown in Fig.1. Denoting the strip column displacement vector for nodes which are on the column n, u_n, the strain energy and the work done by external force of the strip n are expressed as

$$U_n(u_n,u_{n+1})=(1/2)[u_n\ u_{n+1}]\begin{bmatrix}K_{11}(n) & K_{12}(n)\\ K_{21}(n) & K_{22}(n)\end{bmatrix}\begin{bmatrix}u_n\\ u_{n+1}\end{bmatrix} \quad (1a)$$

$$V_n(u_n,u_{n+1})=[u_n\ u_{n+1}]\begin{bmatrix}P_1(n)\\ P_2(n)\end{bmatrix} \quad (1b)$$

respectively, where $P_1(n)$ and $P_2(n)$ are the column force vector corresponding to the n and n+1 side of the strip n.



Finite Element Discretization

Grouping Elements to Strips

Fig.1 Discretization and Strips

Since the total potential energy of the system, J, can be obtained by the sum of the potential energy of each strip n, J_n, as

$$J(u_1,..,u_N)=\sum_{n=1}^{N-1}J_n(u_n,u_{n+1})=\sum_{n=1}^{N-1}(U_n-V_n) \quad (2)$$

According to the principle of minimum potential energy, the minimization problem

$$\min_{u_j(j=1,..,N)}[J_{N-1}+J_{N-2}+ \cdots +J_1] \quad (3)$$

must be solved to obtain the nodal displacements. To accomplish this minimization by dynamic programming, the following functional $f_n(u_n)$ is introduced.

$$f_n(u_n)=\min_{u_j(j=n+1,..,N)}\sum_{i=n}^{N-1}J_i(u_i,u_{i+1}) \quad (4)$$

From the definition of f_n, the recurrsive formulation for the minimization problem (3) is obtained as

$$f_n(u_n)=\min_{u_{n+1}}[J_n(u_n,u_{n+1})+f_{n+1}(u_{n+1})] \quad (5)$$

and the necessary condition of minimization can be written as

$$\partial J_n/\partial u_{n+1}+df_{n+1}/du_{n+1}=0 \quad (6)$$

As far as linear elastic systems are concerned, the functional f_n should be expressed as a quadratic form of u_n as follows:

$$f_n(u_n)=(1/2)u_nR_n^ou_n+u_nr_n^o+(1/2)s_n^o \quad (7)$$

where the matrices R_n^o, vectors r_n^o, and scalars s_n^o are to be determined later. Using (1) and (7), the necessary condition (6) is expressed explicitely as

$$u_{n+1}=-[K_{22}(n)+R_{n+1}^o]^{-1}[K_{21}(n)u_n+r_{n+1}^o-P_2(n)] \quad (8)$$

Substitution of (7) and (8) into (5) gives the recurrence relations for R_n^o, r_n^o, and s_n^o:

$$R_n^o=K_{11}(n)-K_{12}(n)[K_{22}(n)+R_{n+1}^o]^{-1}K_{21}(n) \quad (9a)$$

$$r_n^o=-P_1(n)+K_{12}(n)[K_{22}(n)+R_{n+1}^o]^{-1}[P_2(n)-r_{n+1}^o] \quad (9b)$$

$$s_n^o=-[P_2(n)-r_{n+1}^o]\ [K_{22}(n)+R_{n+1}^o]^{-1}[P_2(n)-r_{n+1}^o]+s_{n+1}^o \quad (9c)$$

The initial conditions of the recurrence formula (8) and (9) are

$$R_1^ou_1+r_1^o=0 \quad (10)$$

$$R_n^o=0\ ,\ r_N^o=0\ ,\ s_N^o=0 \quad (11)$$

FREE VIBRATION PROBLEM

A leading principle for free vibration problem of undamped system is of the harmonic version of Hamilton's principle. According to the usual finite element procedure, this principle states the stationality of the functional L;

$$L(u)=\omega^2T(u)-U(u) \longrightarrow \text{stationary} \quad (12)$$

where U is strain energy and T is the kinetic energy. This stationary condition is attained in the dynamic programming approach here. Total functional L is expressed as the sum of one of each strips as follows:

$$L(u_1,..,u_N)=\sum_{n=1}^{N-1}L_n(u_n,u_{n+1})=\sum_{n=1}^{N-1}(\omega^2T_n-U_n+V_n) \quad (13)$$

where U_n and V_n are defined by (1a,b) and

$$T_n=(1/2)[u_n\ u_{n+1}]\begin{bmatrix}M_{11}(n) & M_{12}(n)\\ M_{21}(n) & M_{22}(n)\end{bmatrix}\begin{bmatrix}u_n\\ u_{n+1}\end{bmatrix} \quad (14)$$

In this case, force vectors $P_1(n)$ and $P_2(n)$ in V_n satisfy the self-equilibrium condition;

$$V_1+V_2+ \cdots +V_{N-1}=0 \quad \text{or} \quad P_1(n)+P_2(n-1)=0 \quad (15)$$

Introduction of new functional defined by

$$g_n(u_n)=\text{stationary}_{u_j(j=n+1,..,N)}\sum_{i=n}^{N-1}L_i(u_i,u_{i+1}) \quad (16)$$

gives the recurrsive formulation for stationary problem of functional L,

$$g_n(u_n)=\text{stationary}_{u_{n+1}}[L_n(u_n,u_{n+1})+g_{n+1}(u_{n+1})] \quad (17)$$

and then the stationary condition for these subproblems are

$$\partial L_n/\partial u_{n+1}+dg_{n+1}/du_{n+1}=0 \quad (18)$$

For the linear elastic systems, a following quadratic form can be suitably employed for g_n:

$$g_n(u_n)=(1/2)u_n[\omega^2S_n-R_n]u_n-u_n[\omega^2s_n-r_n]+(1/2)t_n \quad (19)$$

Thus the stationary condition (17) becomes

$$[\{K_{22}(n)+R_{n+1}\}-\omega^2\{M_{22}(n)+S_{n+1}\}]u_{n+1}$$
$$+[K_{21}(n)-\omega^2M_{21}(n)]u_n-[P_2(n)+r_{n+1}-\omega^2s_{n+1}]=0 \quad (20)$$

Substituting (19) and (20) into (17) and comparing the corresponding coefficients, the final form of governing equations are obtained as

$$[\{K_{22}(n)+R_{n+1}\}-\omega^2\{M_{22}(n)+S_{n+1}\}]u_{n+1} +[K_{21}(n)-\omega^2 M_{21}(n)]u_n = 0 \quad (21)$$

$$R_n=K_{11}(n)-2K_{12}(n)B_nC_n+C_nB_n[K_{22}(n)+R_{n+1}]B_nC_n$$
$$S_n=M_{11}(n)-2M_{12}(n)B_nC_n+C_nB_n[M_{22}(n)+S_{n+1}]B_nC_n$$
$$r_n=0 \ , \ s_n=0 \ , \ t_n=0 \ , \ R_N=0 \ , \ S_N=0 \quad (22)$$
$$B_n=[\{K_{22}(n)+R_{n+1}\}-\omega^2\{M_{22}(n)+S_{n+1}\}]^{-1}$$
$$C_n=K_{21}(n)-\omega^2 M_{21}(n) \qquad n=1,2,..,N-1$$

The non-trivial conditions for (21)

$$\det[\{K_{22}(n)+R_{n+1}\}-\omega^2\{M_{22}(n)+S_{n+1}\}]=0 \qquad n=1,2,..,N-1 \quad (23)$$

are the characteristic equations for free vibration problem.

EULER BUCKLING PROBLEM

Let the incremental potential energy referred to a certain equilibrium configuration with initial stress be

$$\Pi=\sum_{n=1}^{N-1}\Pi_n(u_n,u_{n+1})=\sum_{n=1}^{N-1}(U_n-\lambda W_n) \quad (24)$$

where u_n is the incremental displacement. The incremental strain energy U_n has the same form as (1a) and the work done by the initial stress is written as follows:

$$W_n=(1/2)[u_n \ u_{n+1}]\begin{bmatrix}K^G_{11}(n) & K^G_{12}(n)\\ K^G_{21}(n) & K^G_{22}(n)\end{bmatrix}\begin{bmatrix}u_n\\ u_{n+1}\end{bmatrix} \quad (25)$$

The newly introduced functional h_n and its recurrence expression, that is,

$$h_n(u_n)=\min_{u_j(j=n+1,..,N)}\sum_{i=n}^{N-1}\Pi_i(u_i,u_{i+1}) \quad (26)$$

$$h_n(u_n)=\min_{u_{n+1}}[\Pi_n(u_n,u_{n+1})+h_{n+1}(u_{n+1})] \quad (27)$$

give the dynamic programming formulation of the problem. The necessary condition of the minimization is written by

$$\partial\Pi_n/\partial u_{n+1}+dh_{n+1}/du_{n+1}=0 \quad (28)$$

Since the problem is concerned with the linear elastic system subject to small displacement, we can assume a quadratic form for h_n:

$$h_n(u_n)=(1/2)u_n[\bar{R}_n-\lambda\bar{S}_n]u_n+u_n[\bar{r}_n-\lambda\bar{s}_n]+(1/2)\bar{t}_n \quad (29)$$

Thus the necessary condition (28) becomes

$$[\{K_{22}(n)+\bar{R}_{n+1}\}-\lambda\{K^G_{22}(n)+\bar{S}_{n+1}\}]u_{n+1} +[K_{21}(n)-\lambda K^G_{21}(n)]u_n+[\bar{r}_{n+1}-\lambda\bar{s}_{n+1}]=0 \quad (30)$$

Substitution (29) and (30) into (27) and comparison of the coefficients lead the following governing equations:

$$[\{K_{22}(n)+\bar{R}_{n+1}\}-\lambda\{K^G_{22}(n)+\bar{S}_{n+1}\}]u_{n+1} +[K_{21}(n)-\lambda K^G_{21}(n)]u_n=0 \quad (31)$$

$$\bar{R}_n=K_{11}(n)-2K_{12}(n)A(n)K^{ef}_{21}(n) +K^{ef}_{12}(n)A(n)[K_{22}(n)+\bar{R}_{n+1}]A(n)K^{ef}_{21}(n)$$
$$\bar{S}_n=K^G_{11}(n)-2K^G_{12}(n)A(n)K^{ef}_{21}(n) +K^{ef}_{12}(n)A(n)[K^G_{22}(n)+\bar{S}_{n+1}]A(n)K^{ef}_{21}(n) \quad (32)$$
$$\bar{r}_n=0 \ , \ \bar{s}_n=0 \ , \ \bar{t}_n=0 \ , \ \bar{R}_N=0 \ , \ \bar{S}_N=0$$

where

$$A(n)=[\{K_{22}(n)+\bar{R}_{n+1}\}-\lambda\{K^G_{22}(n)+\bar{S}_{n+1}\}]^{-1}$$
$$K^{ef}_{ij}(n)=K_{ij}(n)-\lambda K^G_{ij}(n) \qquad i,j=1,2$$

The non-trivial condition of (31) is the characteristic equation as

$$\det[\{K_{22}(n)+R_{n+1}\}-\lambda\{K^G_{22}(n)+S_{n+1}\}]=0 \quad (33)$$

The minimum value of λ which satisfies (33) is the load multiplier corresponding to the initial stress field.

OPTIMIZATION OF DISCRETIZATION TOPOLOGY

The accuracy of the finite element solution and the value of the functional obtained deeply depend upon the discretization used. Since the solution obtained by the finite element procedure of Ritz type has the bounding property of the real solution, the improvement of the accuracy of the solution is achieved by improving the value of the functional obtained with respect to the discretization topology. In this section, the multistage structure of the topological optimization problem of the finite element discretization is revealed.

STATIC EQUILIBRIUM PROBLEM

According to the principle of minimum potential energy, the solution of finite element displacement method gives the upper-bound of the exact one. Then, the improvement of the solution is done by minimizing the total potential energy, J with respect to the discretization topology, d, that is,

$$J \xrightarrow[d]{} \min. \quad (34)$$

Noting that the external force vector at the column n, P_n, and the internal force vector transferred to the strip n-1, $P_2(n-1)$ are related by

$$P_2(n-1)=P_n-P_1(n) =P_n+K_{12}(n)[K_{22}(n)+R^o_{n+1}]^{-1}[r^o_{n+1}-P_2(n)]+r^o_n \quad (35)$$

and the stiffness matrices of the strip n, $K_{ij}(n)$ $i,j=1,2$ are assumed to depend upon the finite element discretization topology d_n, then (35) may be formally described as

$$P_2(n-1)=P_2(n-1)(d_n,P_2(n)) \quad (36)$$

Similarly, the potential energy for the strip n, J_n is written as

$$J_n=J_n(d_n,P_2(n)) \quad (37)$$

In order to formulate the optimization process as

multistage process, the following functional is introduced:

$$F_n(P_2(n))=\min_{d_j(j=1,..,n)}\sum_{i=1}^{n}J_i(d_i,P_2(i)) \tag{38}$$

which can be rewritten in the recurrence form,

$$F_n(P_2(n))=\min_{d_n}[J_n(d_n,P_2(n))+F_{n-1}(P_2(n-1))] \tag{39}$$

The initial condition of the subproblems (39) is

$$F_1(P_2(1))=\min_{d_1} J_1(d_1,P_2(1)) \tag{40a}$$

and the initial condition of the transformation (36) is

$$P_2(N)=P_N \tag{40b}$$

The mathematical structure expressed by (36) to (40) is a serial multistage decision process so that the dynamic programming procedure can be easily applied.

FREE VIBRATION PROBLEM

Though the functional L is regarded as a functional for the free vibration analysis, an alternative functional referred as Rayleigh quotient is suitable for the optimization problem[8]. The value of minimized Rayleigh quotient gives the square of fundamental circular frequency and its approximated version obtained by finite element procedure ensures the upper-bound of the exact one. It is reasonable in this context that the further Rayleigh quotient is minimized, the more accurate solution is obtained. The principle for the Rayleigh quotient is written as follows:

$$R_\omega = U \,/\, T \xrightarrow[d]{} \min \tag{41}$$

where

$$U=\sum_{n=1}^{N-1}U_n \ , \ T=\sum_{n=1}^{N-1}T_n$$

Since the matrix $K_{ij}(n)$ is the function of the discretization topology of the strip n, d_n, and the strain energy U is decomposed as

$$U=\sum_{i=1}^{n}U_i+\sum_{i=n+1}^{N-1}U_i \tag{42}$$

The second term of (42) can be assumed to be the quadratic form of R_{n+1}:

$$U=\sum_{i=1}^{n}U_i(d_i)+\tilde{U}_{n+1} \ , \ \tilde{U}_{n+1}=u_{n+1}R_{n+1}u_{n+1} \tag{43}$$

Similarly, the kinetic energy can be expressed as

$$T=\sum_{i=1}^{n}T_i(d_i)+\tilde{T}_{n+1} \ , \ \tilde{T}_{n+1}=u_{n+1}S_{n+1}u_{n+1} \tag{44}$$

Then, the Rayleigh quotient has the form

$$R_\omega=R_\omega(d_1,..,d_n,R_{n+1},S_{n+1}) =[\sum_{i=1}^{n}U_i+\tilde{U}_{n+1}] \,/\, [\sum_{i=1}^{n}T_i+\tilde{T}_{n+1}] \tag{45}$$

where matrices R_{n+1}, S_{n+1} are dependent on the discretization topologies d_{n+1}, ... ,d_{N-1} implicitely. The minimization problem of the functional (45) is easily transformed into two-stage decision process as

$$\tilde{R}_\omega(R_{n+1},S_{n+1})=\min_{d_1,..,d_n}R_\omega(d_1,..,d_n,R_{n+1},S_{n+1})$$
$$\min_{d_i(i=1,..,N-1)}R_\omega=\min_{d_j(j=n+1,..,N-1)}\tilde{R}_\omega(R_{n+1},S_{n+1}) \tag{46}$$

Applying this decomposition to each step successively, the multistage decision process which minimizes the Rayleigh quotient with respect to discretization topology is written as

$$d_1^*(R_2,S_2)=\operatorname{argmin}_{d_1}R_\omega(d_1,R_2,S_2)$$
$$....$$
$$d_n^*(R_{n+1},S_{n+1})=\operatorname{argmin}_{d_n}R_\omega(d_1^*,..,d_{n-1}^*,d_n,R_{n+1},S_{n+1}) \tag{47}$$
$$....$$
$$d_{N-1}^*(R_N,S_N)=\operatorname{argmin}_{d_{N-1}}R_\omega(d_1^*,...,d_{N-2}^*,d_{N-1},R_N,S_N)$$

s.t.

$$R_n=R_n(R_{n+1},S_{n+1},d_n) \ , \ R_N=0$$
$$S_n=S_n(R_{n+1},S_{n+1},d_n) \ , \ S_N=0 \tag{48}$$

The precise expressions of (48) are the first and the second equations of (32). This problem has the multistage structure of serial type and is easily solved by the dynamic programming procedure.

This multistage decision problem (47) and (48) has state variables R_{n+1} , S_{n+1} and the growth of their dimension pulls up the computational effort of the dynamic programming procedure rapidly. To overcome this trouble, a tactical simplification technique is proposed. Consider the modified two-stage decision process which puts the additional constraint $u_{n+1}=0$ onto the original problem (46). Denoting the eigenvalue of the original problem ω and of modified problem $\bar{\omega}$, then it is known that the following relations exists[9]:

$$\bar{\omega} \geq \omega \tag{49}$$

This additional constraint is equivalent to the restriction of the state variables into $R_{n+1}=0$, $S_{n+1}=0$ and the original problem is modified into the simpler problem.

$$\bar{d}_1^*,..,\bar{d}_n^*=\operatorname{argmin}_{d_1,..,d_n}R_\omega(d_1,..,d_n,0,0)$$
$$\bar{d}_{n+1}^*,..,\bar{d}_{N-1}^*=\operatorname{argmin}_{d_j(j=n+1,..,N-1)}R_\omega(\bar{d}_1^*,..,\bar{d}_n^*,R_{n+1},S_{n+1}) \tag{50}$$

Applying this technique successively, the simplified multistage decision process is given.

$$\bar{d}_n^*=\operatorname{argmin}_{d_n}R_\omega(\bar{d}_1^*,..,\bar{d}_{n-1}^*,d_n,0,0) \tag{51}$$

EULER BUCKLING PROBLEM

The minimum load multiplier can be expressed as the minimum value of the energy quotient R_λ

$$R_\lambda = U \,/\, W \tag{52}$$

with respect to the displacement vector. It is reasonable that the minimum load multiplier, that is, eigenvalue should be as low as possible, since the eigenvalue due to the approximate eigenvector is proved to be always an upper-bound to the true one in the displacement method.

From the viewpoint of finite element analysis, Euler buckling problem has formally the same mathematical structure as to the free vibration problem when replacing the mass matrix with the geometrical

stiffness matrix. But it is easily shown that the relation between the geometrical stiffness matrix and the discretization topology is more complicated than that of mass matrix. While the mass matrices $M_{ij}(n)$ depend only on the discretization topology of the strip n, d_n, the geometrical stiffness matrices $K^G_{ij}(n)$ depend not only on the topology d_n but also on the initial stress field in the strip n corresponding to the stable equilibrium configuration $\mathring{\sigma}_n$. This stress field is calculated from the stable displacement vectors of the strip n, u^o_n, u^o_{n+1} which are governed by (8) so that the geometrical stiffness matrices may be expressed formally as follows:

$$K^G_{ij}(n)=K^G_{ij}(n)(d_n,u^o_n,R^o_{n+1},r^o_{n+1}) \qquad i,j=1,2 \tag{53}$$

The incremental strain energy U_n and the work W_n may be described by

$$\begin{aligned} U_n&=U_n(d_n)\\ W_n&=W_n(d_n,u^o_n,R^o_{n+1},r^o_{n+1}) \end{aligned} \tag{54}$$

Eqs.(8) and (9) are also rewritten as follows:

$$u^o_{n+1}=u^o_{n+1}(d_n,u^o_n,R^o_{n+1},r^o_{n+1}) \tag{55a}$$

$$R^o_n=R^o_n(d_n,R^o_{n+1}) \tag{55b}$$

$$r^o_n=r^o_n(d_n,R^o_{n+1},r^o_{n+1}) \tag{55c}$$

According to the decomposition used in the free vibration problem, U and W are modified into

$$\begin{aligned} U&=\sum_{i=1}^{n}U_i(d_i)+\sum_{j=n+1}^{N-1}U_j(d_j)\\ W&=\sum_{i=1}^{n}W_i(d_i,u^o_i,R^o_{i+1},r^o_{i+1})+\sum_{j=n+1}^{N-1}W_j(d_j,u^o_j,R^o_{j+1},r^o_{j+1}) \end{aligned} \tag{56}$$

Although the strain energy U is decomposed into two parts, one part which includes $d_1, \dots, d_n$ and the other part which does not, the work W is not decomposed in such manner. Then, the energy quotient R_λ can not have the same form as the Rayleigh quotient R_ω in (45). Thus, it is clarified that the Euler buckling problem has not the same structure as the free vibration problem in the optimal discretization problem.

The reason why the Euler buckling problem has the more complicated mathematical structure is in the existence of the two kind of the state transition; one is the direction from n to n+1 and the another is the opposite direction. To conquer this difficulty, the inverse transformation of state variables u^o_n is introduced:

$$u^o_n=u^o_n(d_n,u^o_{n+1},R^o_{n+1},r^o_{n+1}) \tag{55a'}$$

This is a formal presentation of inverse transformation of (55a) and the more details is found in Ref.[10]. The state transition rules (55a',b,c) modify the expression of work W_i and energy quotient R_λ.

$$W_i=W_i(d_i,..,d_n,u^o_{n+1},R^o_{n+1},r^o_{n+1}) \tag{56}$$

$$R_\lambda=\frac{\sum_{i=1}^{n}U_i(d_i)+\bar{U}_{n+1}(\bar{R}_{n+1})}{\sum_{i=1}^{n}W_i(d_i,..,d_n,u^o_{n+1},R^o_{n+1},r^o_{n+1})+\bar{W}_{n+1}(\bar{S}_{n+1})} \tag{57}$$

where
$$\begin{aligned} \bar{U}_{n+1}&=u_{n+1}\bar{R}_{n+1}u_{n+1}\\ \bar{W}_{n+1}&=u_{n+1}\bar{S}_{n+1}u_{n+1} \end{aligned} \tag{58}$$

Since u^o_{n+1}, R^o_{n+1}, r^o_{n+1} do not include $d_1, \dots, d_n$, the minimization problem of energy quotient can be decomposed into two-stage decision process;

$$\begin{aligned} &\bar{R}_\lambda(u^o_{n+1},R^o_{n+1},r^o_{n+1},\bar{R}_{n+1},\bar{S}_{n+1})\\ &\quad=\min_{d_1,..,d_n}R_\lambda(d_1,..,d_n,u^o_{n+1},R^o_{n+1},r^o_{n+1},\bar{R}_{n+1},\bar{S}_{n+1})\\ &\min_{d_i(i=1,..,N-1)}R_\lambda\\ &\quad=\min_{d_j(j=n+1,..,N-1)}\bar{R}_\lambda(u^o_{n+1}R^o_{n+1}r^o_{n+1}\bar{R}_{n+1},\bar{S}_{n+1}) \end{aligned} \tag{59}$$

The successive application of this decomposition gives the multistage expression of the optimal discretization problem;

$$\begin{aligned} &d^*_n(u^o_{n+1},R^o_{n+1},r^o_{n+1},\bar{R}_{n+1},\bar{S}_{n+1})\\ &\quad=\operatorname{argmin}_{d_n}R_\lambda(d^*_1,..,d^*_{n-1},d_n,u^o_{n+1},R^o_{n+1},r^o_{n+1},\bar{R}_{n+1},\bar{S}_{n+1}) \end{aligned} \tag{60}$$

s.t.

$$\begin{aligned} \bar{R}_n&=\bar{R}_n(d_n,u^o_{n+1},\bar{R}_{n+1},\bar{S}_{n+1}) \ , \ \bar{R}_N=0\\ \bar{S}_n&=\bar{S}_n(d_n,u^o_{n+1},\bar{R}_{n+1},\bar{S}_{n+1}) \ , \ \bar{S}_N=0 \end{aligned} \tag{61}$$

and the equations (55a',b,c).

This multistage decision process has too many state variables to be solved directly and, similar to the free vibration problem, we employ the state variables reduction strategy[11]. The topologies which are implicitely included in the state variables u^o_{n+1}, R^o_{n+1}, r^o_{n+1}, $\bar{R}_{n+1}$, $\bar{S}_{n+1}$ are replaced by the initial estimate $d^{(1)}_{n+1}, \dots, d^{(1)}_{N-1}$ and the second estimate is derived from the simplified multistage decision process;

$$\begin{aligned} d^{*(2)}_n=\operatorname{argmin}_{d_n}&R_\lambda(d^{*(2)}_1,..,d^{*(2)}_{n-1},d_n,\\ &u^{o(1)}_{n+1},R^{o(1)}_{n+1},r^{o(1)}_{n+1},\bar{R}^{(1)}_{n+1},\bar{S}^{(1)}_{n+1}) \end{aligned} \tag{62}$$

The simplified problem is solved iteratively by replacing the previous estimate with current one. As the solution obtained by the simplified problem depends upon the initial estimate, it is required to start this process from the several initials and pick up the best one.

NUMERICAL EXAMPLES

In order to demonstrate the improvement of the accuracy of the solution by the topological optimization, simple numerical examples of two-dimensional system are presented.

STATIC EQUILIBRIUM PROBLEM

Consider the cantilever beam shown in Fig.2. The discretization shown in Fig.3 (A) is the regular topology and (B) is the symmetric topology with respect to the neutral axis. Fig.3 (C) and (D) show the discretization topologies attained the maximum and minimum potential energy levels, respectively. The discretization with optimal topology (D) gives the 16.7% lower potential energy level than that of (C), though the popular discretizations (A) and (B) give the potential level fairly close to that of (C). To illustrate the improvement of the solution, Fig.4 and 5 show the deflection curve at the neutral axis and the bending stress on the surface obtained with the discretization (A), (D), and the finer discretization which has twice the number of the elements (E). These results show that the topological optimization leads the remarkable improvement of the accuracy in the coarse discretization.

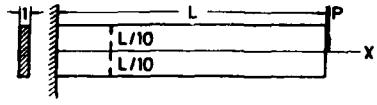


Fig. 2 Cantilever Beam Under End Load

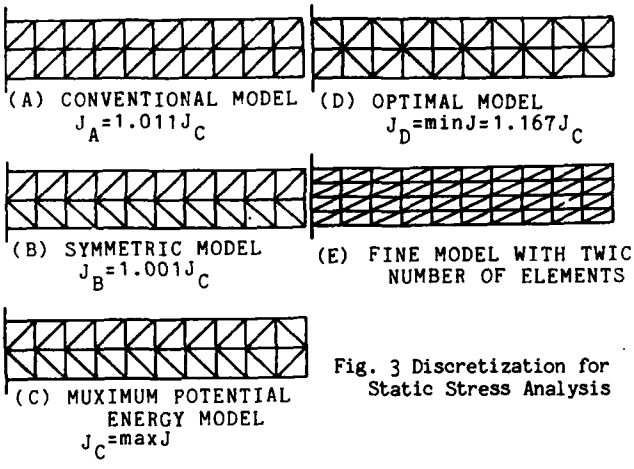


Fig. 3 Discretization for Static Stress Analysis

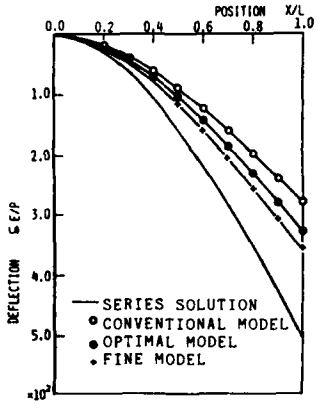


Fig. 4 Deflection Curve of the Neutral Axis

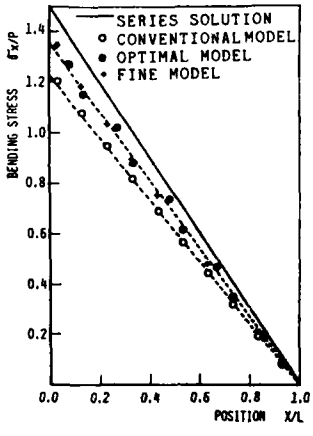


Fig. 5 Bending Stress on the Surface

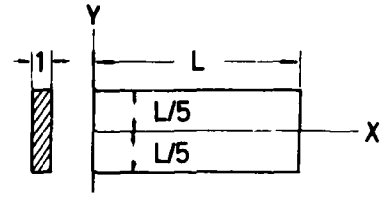


Fig. 6 Clamped-Free Uniform Structure

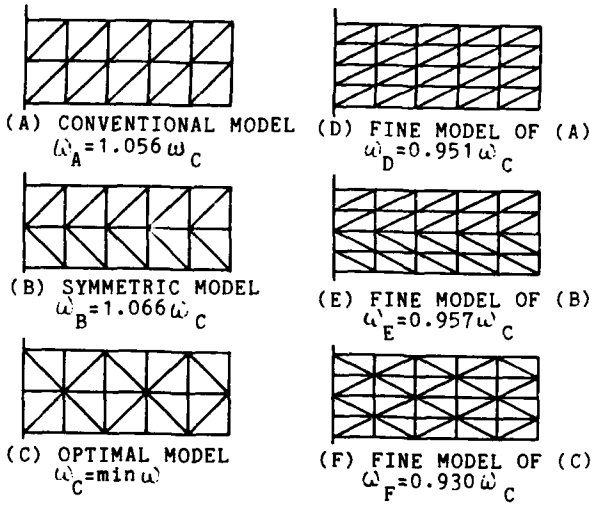


Fig. 7 Discretization for Free Vibration Analysis

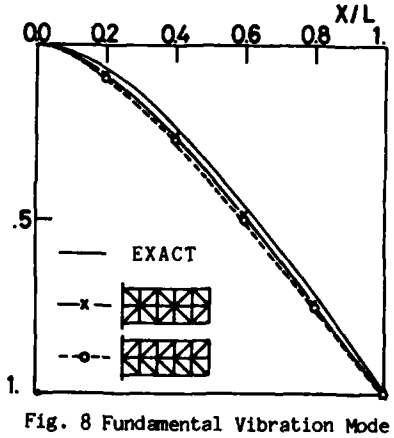


Fig. 8 Fundamental Vibration Mode

FREE VIBRATION PROBLEM

Consider the in-plane vibration of two-dimensional model shown in Fig.6. The discretization shown in Fig.7 (A), (B), and (C) are the coarse models with 18 nodes and 20 elements. Fig.7 (A) is the regular topology and (B) is the symmetric topology. Fig.7 (C) is the optimal topology of the coarse model. The discretizations Fig.7 (A) and (B) give the 5.6% and 6.6% higher eigenfrequencies than the optimal one of (C), respectively. The discretization Fig.7 (D), (E), and (F) are the finer models with twice the number of the elements and the discretization (F) which has the similar topology to the optimal one of the coarse model gives the most accurate solution among the three. The results by these models are summarized in the Table 1, where ω_{EXACT} is calculated by the beam theory. Fig.8 shows the fundamental vibration mode of the discretizations (B), (C) and the exact solution.

Table 1 Natural Frequency Ratio of Clamped-Free Uniform Structure

Discretization	(A)	(B)	(C)	(D)	(E)	(F)	Exact
Number of Elements	20	20	20	40	40	40	-
Number of Nodes	18	18	18	30	30	30	-
Frequency ω	1.390	1.403	1.316	1.251	1.260	1.224	1.176
ω/ω_C	1.056	1.066	1.	.951	.957	.930	-
ω/ω_{EXACT}	1.182	1.193	1.119	1.064	1.071	1.041	1.

EULER BUCKLING PROBLEM

An in-plane buckling for the same structure as the previous example subjected to the uniform load at the free end as shown in Fig.9 is discussed. The discretization Fig.10 (A), (B), (C), and (D) are coarse models with the 18 nodes and 20 elements. Fig.10 (A) is the regular topology and (B), (C) are the symmetric regular topologies. Fig.10 (D) is the optimal topology for the coarse model. The regular and symmetric regular discretization (A), (B), and (C) give the 11.4%, 12.3%, and 8.8% higher buckling load than that of the optimal topology (D). It is interesting that one of the symmetric regular topology (B) is more discouraging than the regular one (A) and (C) is more encouraging than (A). The discretization (E), (F), (G), and (H) are the fine models with 30 nodes and 40 elements and these models have the topologies similar to the coarse models (A), (B), (C), and (D), respectively. In this case, the fine model similar to the optimal one in the coarse model is also the optimal topology in the fine model. The results by these models are summarized in the Table 2, where P^E_{Theory} is elementary solution.

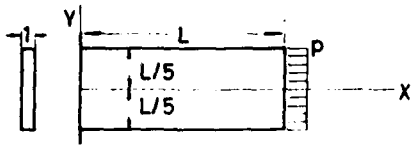


Fig. 9 Uniform Structure Under Uniform Axial Load

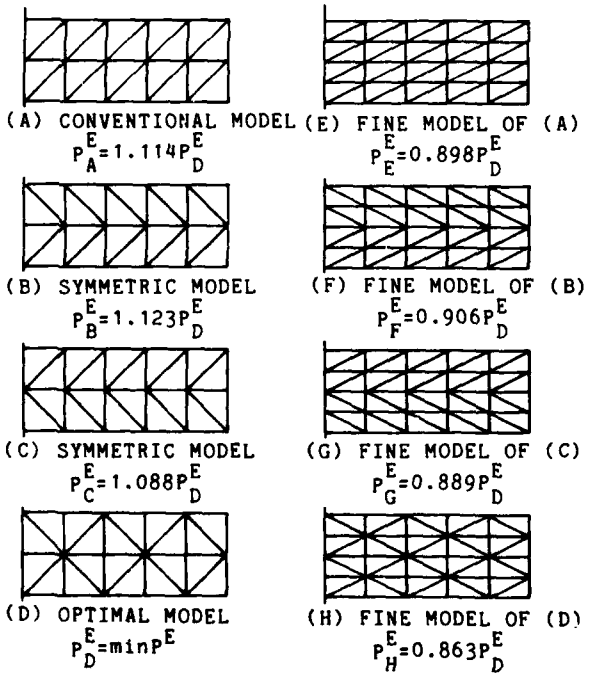


Fig. 10 Discretization for Euler Buckling Analysis

Table 2 Buckling Load Ratio of Uniform Structure

Discretization	A	B	C	D	E	F	G	H	Theory
	20 elements, 18 nodes				40 elements, 30 nodes				
$P^E \times 10^{-5}$	.2104	.2134	.2066	.1900	.1707	.1722	.1689	.1639	.1382
P^E/P^E_D	1.114	1.123	1.088	1.	.898	.906	.889	.863	--
P^E/P^E_H	1.284	1.302	1.261	1.159	1.041	1.051	1.031	1.	--
P^E/P^E_{Theory}	1.522	1.544	1.495	1.375	1.235	1.246	1.222	1.186	1.

CONCLUSIONS

This paper presents the basic investigation concerning the relation between the accuracy of the finite element solution and the discretization topology which has not discussed enough in the past. In order to clarify the relation between the functional to be minimized and the discretization topology, the dynamic programming procedure for the finite element analysis proposed by Distefano et al. is extended to the free vibration analysis and the Euler buckling analysis. It is revealed that the optimal discretization problem for the static stress analysis has the structure of simple serial multistage decision process and the problem for the free vibration and the Euler buckling problem have also the structure of multistage decision process which are not so simple as the statical stress analysis. Though these eigenvalue problems have the same form for the finite element analysis problem, they are essentially different in mathematical structures for the optimal discretization problem. Some numerical examples illustrate the remarkable improvement of the accuracy of the solution by the topological optimization showing that the importance of the topology in the finite element modeling.

REFERENCES

[1] McNeice,G.M. & Marcal,P.V.,'Optimization of Finite Element Grid Based on Minimum Potential Energy', Trans. ASME, Ser.B, 95(1973)186-190.
[2] Prager,W.,'A Note on the Optimal Choice of Finite Element Grids', Computer Methods in Applied Mechanics & Engineering, 6(1975)363-366.
[3] Carroll,W.E. & Barker,R.M.,'A Theorem for Optimal Finite Element Idealization', International Journal of Solids & Structures, 9(1973)883-895.
[4] Carroll,W.E.,'Recent Developments Dealing with Optimum Finite Element Analysis Techniques', Finite Element Grid Optimization, ASME,1979.
[5] Seguchi,Y. et al.,'Optimal Finite Element Discretization Based on Two-Factor Decision Criterion of Potential Energy and Condition Number', Proc. Symposium on Applications of Computer Methods in Engineering, Vol.I, Los Angels, California, 1977.
[6] Shephard,M.S.,'Finite Element Grid Optimization - A Review', Finite Element Grid Optimization, ASME, 1979.
[7] Distefano,N. & Samartin,A.,'A Dynamic Programming Approach to the Formulation and Solution of Finite Element Equations',Computer Methods in Applied Mechanics and Engineering, 5(1975)37-52.
[8] Washizu,K., Variational Methods in Elasticity and Plasticity, 2nd ed., Pergamon Press, 1975.
[9] Courant,R. & Hilbert,D., Methods of Mathematical Physics, Vol.I, John Wiley, 1965.
[10] Nemhauser,G.L., Introduction to Dynamic Programming, John Wiley, 1966.
[11] Norman,J.M., Heuristic Procedures in Dynamic Programming, Manchester Univ. Press, 1972.

AD-P000 098

OPTIMIZATION PROCEDURE FOR MATERIAL COMPOSITION OF COMPOSITE MATERIAL STRUCTURES

Juhachi Oda

Department of Mechanical Engineering,
Kanazawa University,
Kodatsuno, Kanazawa, 920, Japan

Summary

This study deals with the problem optimising grain dispersed and fiber reinforced material structures. The optimization procedure is presented for the cases of the minimum weight and the maximum stiffness designs of structures. In these cases the design variables are volume percents of grain or fiber in several parts of structure and it is subjected to strength or volume constraint. The relations between the design variables and the mechanical properties of composite materials are very important to formulate the design problems. To obtain the relations, a new simulation technique applying the Monte Carlo method is introduced to the grain dispersed materials and the well-known law of mixture used for the fiber reinforced materials.

The procedure is applied to triangular and cantilever beams made of SAP (Sintered Aluminum Powder) or GFRP (Glass Fiber Reinforced Plastic). The finite element method is used to obtain the stress distributions and the strain energies of these structures, and furthermore several non-linear programming techniques are used to search a numerical optimum value of volume percent. It is shown that the results obtained for the grain dispersed mateial are very similar to those of the fiber reinforced materials for the same design problem.

Introduction

In recent years, considerable attention has been focused on the use of composite materials in several structures as airplane or automobile. Therefore, if effective design procedures are applied for these composite structures, the weights will be saved due to their high strength to weight ratio.

Kicher and Chao (1) developed an optimum design method for the fiber reinforced composite cylindrical shells, that are designed to satisfy the limiting stress and instability constraints. Cairo and Hadcock (2), and Cairo (3) have presented a procedure to select an optimum layup of preselected orientations of boron epoxy laminates for a single element. The technique was applied by Lansing *et al.* (4) to design wing and empennage structures. Khot *et al.* (5) presented an optimization method for the minimum weight design of structures made from fiber reinforced composite materials. McKeown (6) developed a technique optimising multilaminar fiber-reinforced continua with object of maximum stiffness. In these techniques, however, the analysed structures are only made of fiber reinforced materials and furthermore the load conditions or the shapes are specified for the special cases.

In this paper, an effective optimization method is presented for the minimum weight or the maximum stiffness design problem of structures, which are made of grain dispersed or fiber reinforced composite material and the shapes are optional but excepted from the design variables. The design variables are the contents of second phase materials and the optimization technique is based on the finite element method and several non-linear programming methods. By using the presented technique, the material compositions in triangular and cantilever beams are optimized and the results presented.

Optimization Problems and Design Variables

For the composite material structures, we can take into account the following design problems :

(i) Minimum weight design problem.

(ii) Maximum stiffness design problem.

On the other hand, many factors as illustrated in Table 1 influence to the weight or stiffness of the composite material structures. That is, all the factors in Table 1 will be considered as the design variables in the above mentioned problems.

On the design constraint conditions, we can consider the following conditions :

(1) Constraint condition of strength : This means that an equivalent stress σ at an optional point in structure must be smaller than a given stress limit σ_c :

$$\sigma \leqq \sigma_c$$

(2) Constraint condition of stiffness : this means that a displacement δ at an optional point in structure must be smaller than a displacement limit δ_c :

$$\delta \leqq \delta_c$$

(3) Constraint condition of weight : This means that a total weight W of structure must be smaller than a given weight limit W_c :

$$W \leqq W_c$$

(4) Other constraint conditions, e.g. limitations on cost of structure or volume percent and orientation of second phase in composite material.

Thus, the design problems optimising the composite material structures are to optimise the previously presented problems (i) and (ii), of which the design variables must be chosen from one shown in Table 1, subjected to the constraint conditions (1) to (4). We can, however, consider a large number of cases for such problems. Then, in this paper, though a procedure optimising structure is considered for the design problems (i) and (ii), the structure is made of only the grain dispersed or the continuous fiber reinforced material. Furthermore, the second phase content or fiber orientation is considered as the design variables. In the following chapters, the formulation for such problems will be presented in detail for the structures of grain dispersed and fiber reinforced composite materials, respectively.

Structure of Grain Dispersed Composite Material

Formulation of Design Problems

As shown in Fig. 1, a structure is divided into many finite elements and each of them is made of the grain dispersed material of grain content V_{gi}. For this structure, if the shape and the load condition are fixed, the previously presented design problems (i) and (ii) will be formulated concrelely as follows :

(i) Minimum weight design problem

$$\min \quad W = \sum_{i=1}^{n} v_i \{ \gamma_g V_{gi} + \gamma_m (1 - V_{gi}) \} \tag{1}$$

$$\text{subject to} \quad \sigma_i \leqq \sigma_{Bi} \tag{2}$$

(ii) Maximum stiffness design problem

$$\min \quad U = \sum_{i=1}^{n} \frac{1}{2} v_i \{\sigma_i\}^T \{\varepsilon_i\} \tag{3}$$

$$\text{subject to} \quad \sigma_i \leqq \sigma_{Bi} \quad \text{or} \quad W \leqq W_c \tag{4}$$

where, W and U are total weight and strain energy of structure, respectively. Eq.(3) is due to the fact (7) that the maximum stiffness design problem is equal to

PRECEDING PAGE

Table 1. Factors Influencing mechanical properties of composite materials

(1) Mechanical Properties of matrix and second phase : Young's modulus, Poisson's ratio, Tensile strength, etc.
(2) Shapes of second phase : Micro-balloon, Grain, Fiber, Flake, etc.
(3) Construction types of second phase in matrix : Uniform or unidirectional distribution, Random distribution, Laminate type, etc.
(4) Volume percent of second phase
(5) Others : Boundary conditions between matrix and second phase, Effect of void and crack, etc.

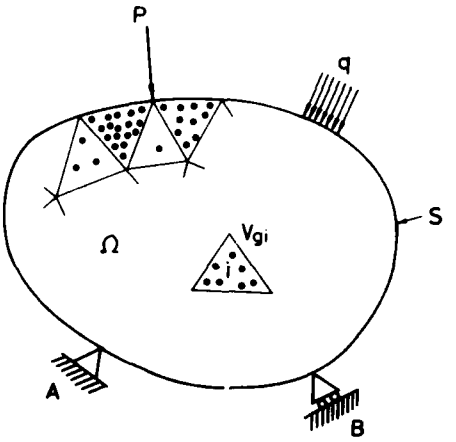


Fig. 1 Grain dispersed composite material

minimize the total strain energy of structure. γ_m and γ_g are specific weights of matrix and grain. σ_i, σ_{Bi} $\{\sigma_i\}$ and $\{\varepsilon_i\}$ indicate equivalent stress, critical strength, stress and strain vectors in element i, respectively. v_i is volume of element i.

Furthermore, the constraint condition of weight in Eq.(4) can be rewritten to the following form by using grain volume percent :

$$\sum_{i=1}^{n} v_i V_{gi} / \sum_{i=1}^{n} v_i \leq V_{gc} \tag{5}$$

$$1 > V_{gi} \geq 0 \tag{6}$$

Where, V_{gc} is the volume limit of grain corresponding to W_c. On the other hand, the constraint condition of strength in Eq. (2) or (4) is given by using the von Mises criterion and the equation is

$$\sigma_{1i}^2 + \sigma_{2i}^2 - \sigma_{1i}\sigma_{2i} \leq \sigma_{Bi} \tag{7}$$

Where, σ_{1i} and σ_{2i} are two principal stresses in element i.

Formulation of Material Properties

In order to analyse the design problems (i) and (ii) presented in the previous section, the two-dimensional finite element method is used, and in the formulas the well-known stress-strain matrix, which contains the material properties, is introduced. Therefore, the mechanical properties as Young's modulus E, Poisson's ratio ν and critical strength σ_B of composite material must be determined in the closed form of grain volume percent V_g. That is, the following equations must be formulated concretely :

$$E = f_1(V_g)\ ,\quad \nu = f_2(V_g)\ ,\quad \sigma_B = f_3(V_g) \tag{8),(9),(10)}$$

But, to determine theoretically these equations for the several composite materials is very difficult for the present. Then, a model simulating grain dispersed material is used here (8). The Monte Carlo method and the finite element method are applied to the model. From the analytical result the above mentioned elastic properties E and ν are estimated numerically. Figure 2 shows the simulation model, in which matrix and grain are corresponding to the small square elements. These locations in the model are determined by using the random numbers generated by computer and the number of grain elements is limited by V_{gc}. If this model is loaded uniformly as shown in Fig.2 and the corresponding displacements in y and x directions are calculated, E and ν of the model will be obtained easily from these values. Thus, from the many estimated values f_1 and f_2 can be determined. On the other hand, the equation f_3 for σ_B can be estimated by using the repeated experimental data of σ_B for the grain dispersed composite materials.

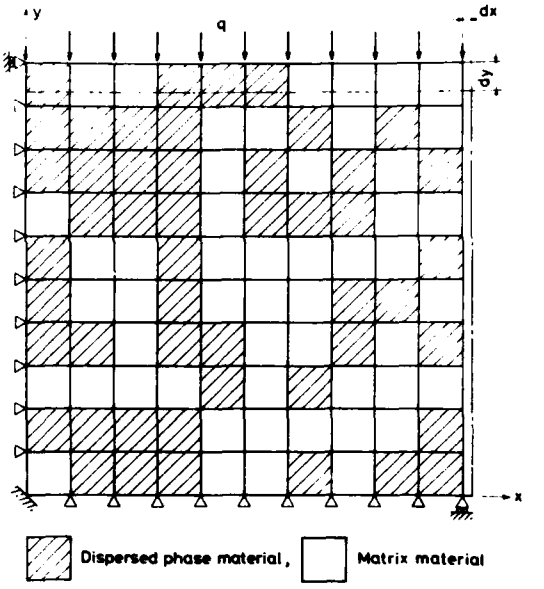


Fig. 2 Simulation model of grain dispersed composite materials

Optimization Techniques

Previously presented problems (i) and (ii) are non-linear optimization problems with constraint conditions on the design variables V_{gi}. For such problems, many useful non-linear optimization methods (9) are studied. In this paper, the sequential linear programming (SLP), the reduced gradient method (R G method) and the Rosenbrock method using the sequential unconstrained minimization technique are used. From the results obtained by these methods, the effectiveness will be compared each other.

Numerical Examples

By using the above mentioned technique, the composite material structures made from SAP (Sinted Alu-

Table 2. Mechanical properties of aluminium grain and alumina constructing SAP

	Young's modulus GPa (Kgf/mm²)	Poisson's ratio	Specific weight N/mm³ (Kgf/mm³)
Aluminium	70.61 (7200)	0.33	2.6×10^{-5} (2.7×10^{-6})
Alumina (Al_2O_3)	393.25 (40100)	0.20	3.9×10^{-5} (4.0×10^{-6})

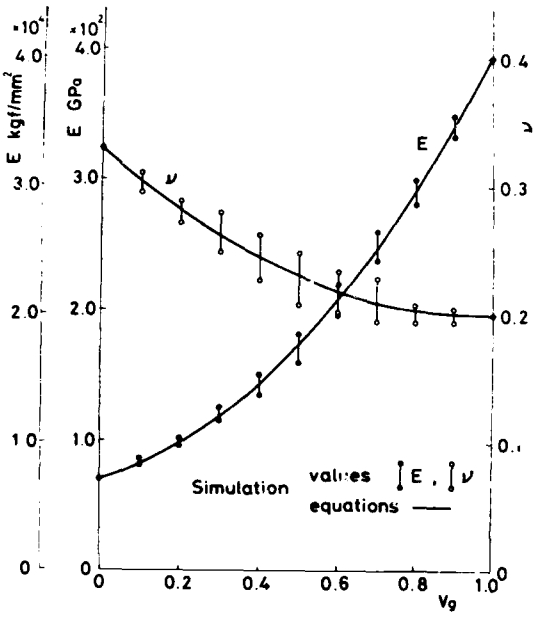


Fig. 3 Estimated E , ν and these equation

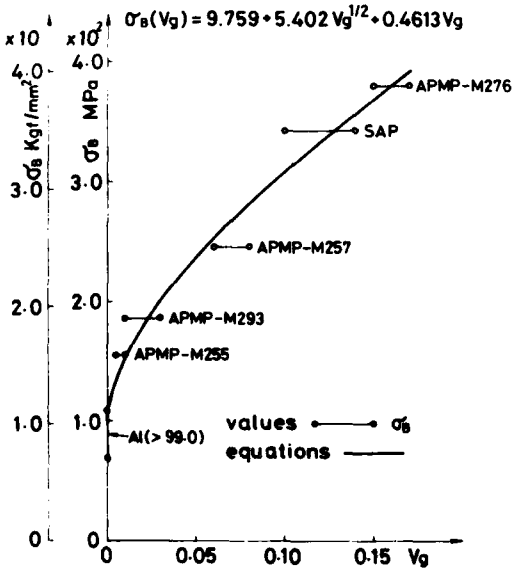


Fig. 4 Reported data of σ_B and the equation

minium Powder Product) are optimized. The grain and the matrix composing SAP have the mechanical properties as shown in Table 2. These values are used for the simulation model in Fig.2 and the mechanical properties E and ν of SAP are estimated. Figure 3 shows the results. In this figure, continuous lines are the curves approximated by using the least square method for the estimated values and given as

$$f_1(V_g) = 7200 + 89.95\,V_g + 2.391\,V_g^2 \quad (11)$$

$$f_2(V_g) = 0.33 - 2.675\times10^{-2}V_g + 1.357\times10^{-5}V_g^2 \quad (12)$$

Similarly, f_3 is determined from the reported data as shown in Fig.4 and expressed in the form :

$$f_3(V_g) = 9.759 + 5.402\,V_g^{\frac{1}{2}} + 0.4613\,V_g \quad (13)$$

Example 1 As the first example, a triangular beam as shown in Fig. 5, that is subdivided to two elements and loaded by a load P at the end, is considered. Figures 6 and 7 show the results for the minimum weight design problem. The former figure is correspond to the

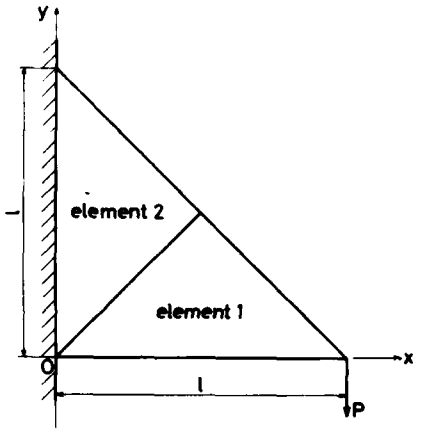


Fig. 5 Triangular beam subjected to load P

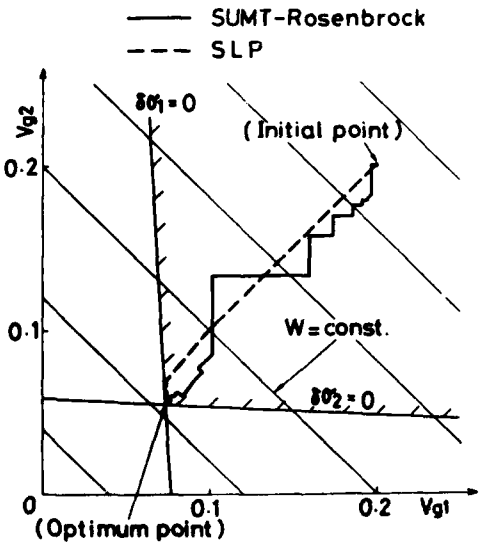


Fig. 6 Design plane, constraints and solutions for . minimum weight design problem

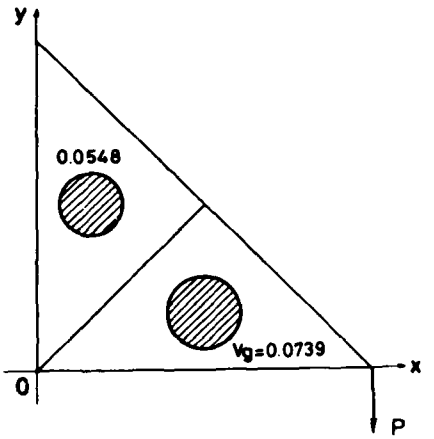


Fig.7 Grain contents for minimum weight design problem

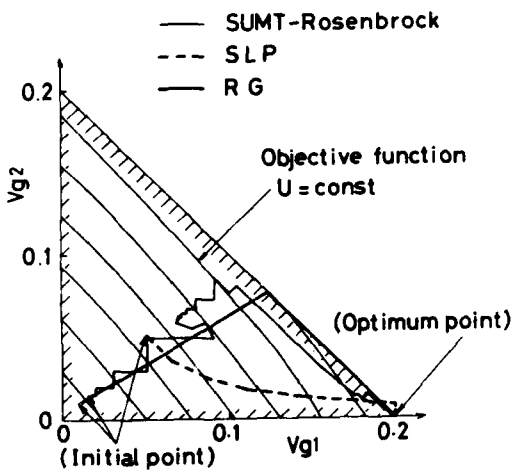


Fig. 8 Design plane, constraints and solutions for maximum stiffness design problem

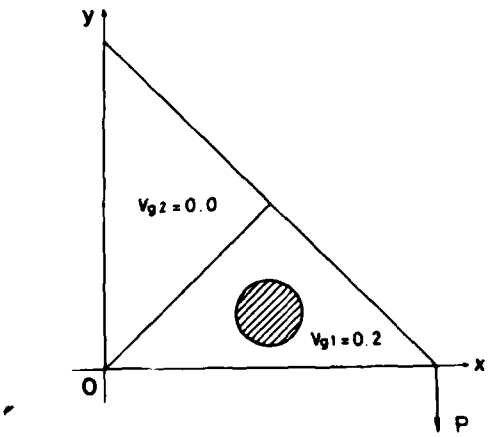


Fig.9 Grain contents for maximum stiffness design problem

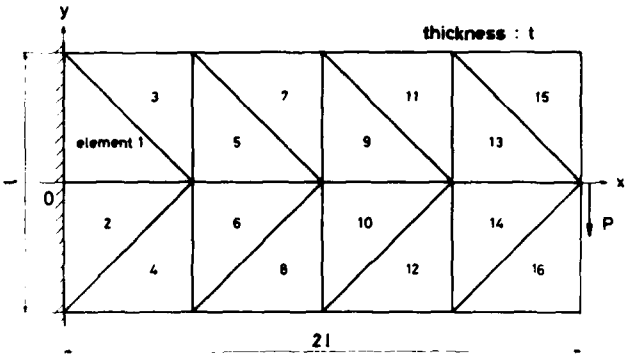


Fig. 10 Cantilever beam subjected to load P

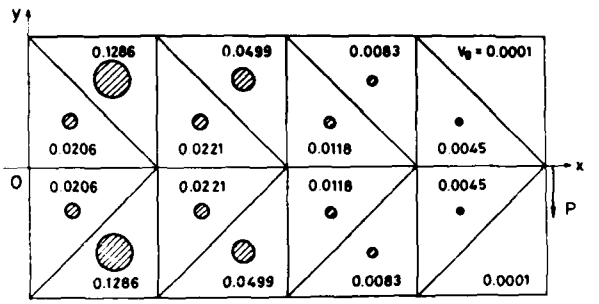


Fig. 11 Grain contents for minimum weight design problem

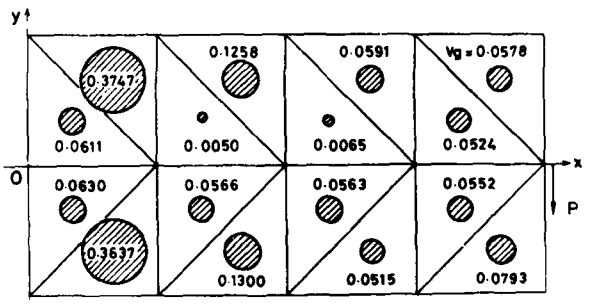


Fig. 12 Grain contents for maximum stiffness design problem

process seeking an optimum solution and the latter is the graphically presented result of the solution. Similarly, figures 8 and 9 show the seeking process of solution and the result for the maximum stiffness design problem. In this problem, V_{gc} is limited as 0.2. From Figs.6 and 8, it is recognized that all the seeking techniques (SLP, RG and Rosenbrock methods) seek exactly the optimum solution, but the number of seeking steps are very different among these techniques. Furthermore, it is obvious from Figs. 7 and 9 that the grains distribute in high density in the element subjected to high stress. This tendensy is remarkable for the solution of maximum stiffness design.

Example 2 The second example is a cantilever beam as shown in Fig.10, that is subdivided to 16 elements. All the conditions to calculate this example are equal to those of the first example. Figures 11 and 12 show graphically the optimum solutions for the minimum weight and the maximum stiffness designs, respectively. From these results, we can also recognized the tendency presented previously for the grain distribution of the first example.

Structure of Fiber Reinforced Composite Materials

Formulation of Design Problems

Consider a two-dimensional structure reinforced by fibers as shown in Fig. 13. If the shape and the load condition of the structure are fixed, the previously mentioned minimum weight and the maximum stiffness design problems will be formulated as follows :

(i) Minimum weight design problem

$$\min \quad W = \sum_{i=1}^{n} v_i \{\gamma_f V_{fi} + \gamma_m (1 - V_{fi})\} \tag{14}$$

$$\text{subject to} \quad \sigma_i \leqq \sigma_{Bi} \tag{15}$$

(ii) Maximum stiffness design problem

$$\min \quad U = \sum_{i=1}^{n} \frac{1}{2} v_i \{\sigma_i\}^T \{\varepsilon_i\} \tag{16}$$

$$\text{subject to } \sigma_i \leqq \sigma_{Bi} \quad \text{or} \quad W \leqq W_c \tag{17}$$

where, γ_f is specific weight of fiber and V_{fi} is fiber content in element i. On the constraint condition of weight in Eq. (17), the following formulas will be given by using V_{fi} :

$$\sum_{i=1}^{n} v_i V_{fi} / \sum_{i=1}^{n} v_i \leqq V_{fc} \tag{18}$$

$$1 > V_{fi} \geqq 0 \tag{19}$$

where, V_{fc} is the volume limit of fiber corresponding to W_c. On the other hand, the constraint condition of strength in Eq.(15) or (17) will be given as follow :

$$H_i (V_{fi}, \theta_i) \leqq 0 \tag{20}$$

$$H_i (V_{fi}, \theta_i) = \left(\frac{\sigma_{Li}}{F_{Li}}\right)^2 - \left(\frac{F_{Ti}}{F_{Li}}\right)\left(\frac{\sigma_{Li}}{F_{Li}}\right)\left(\frac{\sigma_{Ti}}{F_{Ti}}\right) + \left(\frac{\sigma_{Ti}}{F_{Ti}}\right)^2 + \left(\frac{\tau_{LTi}}{F_{LTi}}\right)^2 - 1$$

This is an application form of the Hill's yield criterion for anisotropic material. In the form, $\{\sigma_{LT}\}_i^T = [\sigma_{Li}, \sigma_{Ti}, \tau_{LTi}]$. σ_{Li}, σ_{Ti} and τ_{LTi} are the normal and shearing stresses in the principal directions L and T in element i, respectively. These stresses can be presented as the following form by using the x-y coordinate stresses $\{\sigma_{xy}\}_i$:

$$\{\sigma_{LT}\}_i = [M]\{\sigma_{xy}\}_i \tag{21}$$

where

$$[M] = \begin{bmatrix} l_i^2 & m_i^2 & -2l_i m_i \\ m_i^2 & l_i^2 & 2l_i m_i \\ l_i m_i & -l_i m_i & (l_i^2 - m_i^2) \end{bmatrix}, \quad l_i = \cos\theta_i, \; m_i = \sin\theta_i$$

Furthermore, F_{Li} and F_{Ti} are the tensile strengths in the directions L and T in element i. F_{LTi} indicates the shearing strength between matrix and fiber. All the values depend on the fiber volume percent V_{fi} and will be formulated in detail at the next section.

Formulation of Material Properties

Let's consider to formulate the material properties as young's modulus, Poisson's ratio and breaking strength of the fiber reinforced composite materials. These properties depend not only the material properties of matrix and fiber but also V_f. On the elastic properties, the following formulas are known, that were considered by Yamawaki (10) :

$$\begin{aligned} E_L &= E_f V_f + E_m (1 - V_f) \\ E_T &= (1 - c) \frac{E_f E_m}{E_m V_f + E_f (1 - V_f)} + c \{E_f V_f + E_m (1 - V_f)\} \\ \nu_{LT} &= (1 - c)\{\nu_f V_f + \nu_m (1 - V_f)\} + c \frac{\nu_f E_f V_f + \nu_m E_m (1 - V_f)}{E_f V_f + E_m (1 - V_f)} \\ G_{LT} &= (1 - c) \frac{G_f G_m}{G_m V_f + G_f (1 - V_f)} + c \{G_f V_f + G_m (1 - V_f)\} \end{aligned} \tag{22}$$

where, E_f, E_m, ν_f, ν_m, G_f and G_m are the longitudinal elastic moduli, Poisson's ratio and transverse elastic moduli of fiber and matrix, respectively. Moreover, c is the coefficient depending on the distance between fibers. For example, the value for the composite material of glass and epoxy resin is given as

$$c = 0.4 V_f - 0.025 \tag{23}$$

On the other hand, the breaking strength F_{Li}, F_{Ti} and F_{LTi} in Eq. (20) are not formulated theoretically up to the present. Then, the following equations are assumed here :

$$\begin{aligned} F_L &= \sigma_{ft} V_f + \sigma_m (1 - V_f), \\ F_T &= \sigma_m, \quad F_{LT} = \tau_m \end{aligned} \tag{24}$$

where, the first equation is an application form of the well-known law of mixture for the strength of composite material. σ_{ft} and σ_m are the tensile strength of fiber and the yielding point of matrix, respectively. τ_m is the shearing strength at the boundary between fiber and matrix.

Optimization Techniques

All the problems formulated in Eqs. (14) to (17) are non-linear optimum problems with the constraint conditions. Therefore, the optimization techniques discribed previously for the grain dispersed composite materials can be used also for these problems. But the number of design variables, which indicate the fiber volume percent V_{fi} and the orientation θ_i, are twice

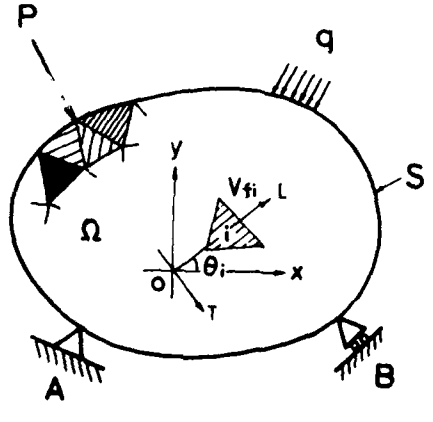


Fig. 13 Fiber reinforced composite material

of those of the grain dispersed composite material. Then, consider the following assumption to decrease the design variables :

Reinforceing fiber alway distributes in the direction of maximum stress in the element.

Up to the present, this has been verified nearly from the phenomenal fact (11) for the fiber distributions in the biomaterials as bone or wood. If this assumption is applied to the design problem, the number of design variables will be decreased because θ_i is decided only by the stress distributions. Figure 14 shows the computational process for the design problems by using the assumption.

Numerical Examples

Example 1 The first example is the same triangular beam as shown in Fig. 5. The beam is composed of epoxy resin and glass fiber with the composition in Table 3. Figures 15 and 16 show the seeking process, in which the Rosenbrock method only is used, to obtain the solution for the minimum weight design and the result. On the other hand, figures 17 and 18 show those of the maximum stiffness design, where V_{fc} is given as 0.4. From Figs. 16 and 18, it is recognized that the fiber distributions are very similar each other. The results also are similar to those of grain dispersed composite material as shown in Figs. 7 and 9.

Example 2 As the second example, the cantilever beam as shown in Fig.10 is considered. All the conditions to calculate this example are equal to those of the first example. Figures 19 and 20 show graphically the optimum solutions for the minimum weight and the maximum stiffness designs, respectively. From these results, it is obvious that the fibers distribute in high density in the elements subjected to high stresses. This tendency is seen for all the examples presented previously. Therefore, it will be concluded that the solution for the minimum weight design is nearly equal to one of the maximum stiffness design.

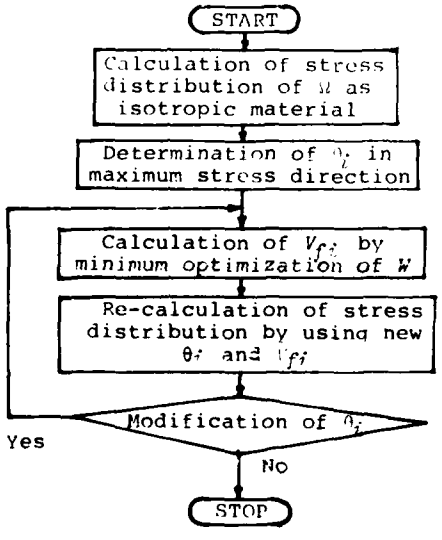
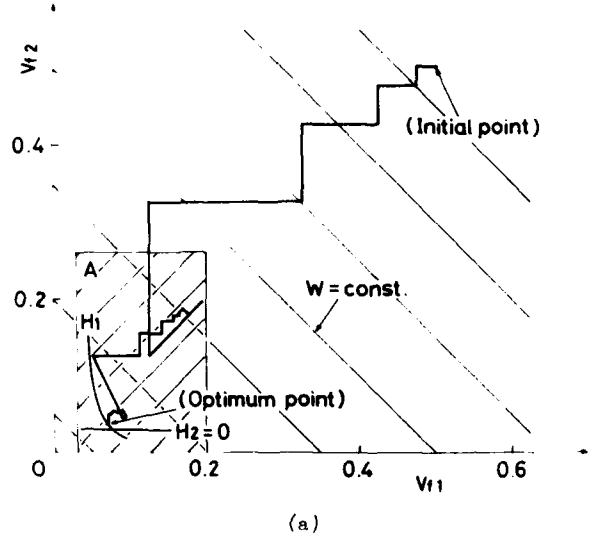


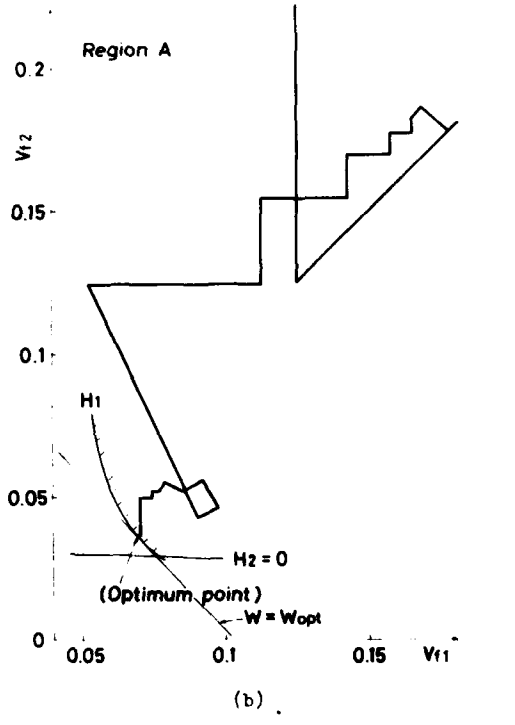
Fig. 14 Computational process for fiber reinforced composite material structure

Table 3. Mechanical properties of glass fiber and epoxy resin constructing GFRP

	Young's modulus GPa (kgf/mm²)	Poisson's ratio	Yield stress and tensile strength MPa (kgf/mm²)	Specific weight N/mm³ (kgf/mm³)
Matrix (Epoxy resin)	E_m = 3.43 (350)	ν_m = 0.35	σ_{mY} = 78 (8.0) : τ_{mY} = 20 (2.0)	γ_m = 1.13 x10⁻⁵ : 1.15 x10⁻⁶
Fiber (Grass)	E_f = 72.75 (7400)	ν_f = 0.22	σ_{fY} = 1961 (200.0)	γ_f = 255x10⁻⁵ : 260x10⁻⁶



(a)



(b)

Fig.15 Design plane, constraints and solutions for minimum weight design problem

Conclusion

It has been demonstrated in this paper that a optimization procedure based on the finite element method and numerical search techniques can be used successfully to optimize practical structures with composite materials. The optimization procedure is pre-

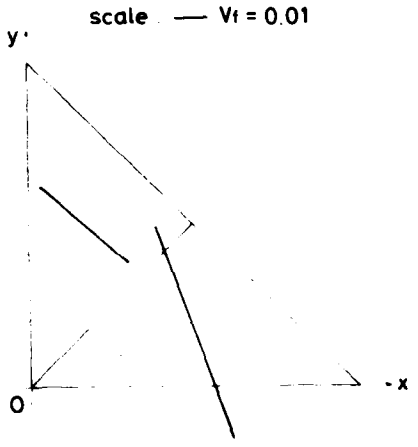


Fig.16 Fiber contents for minimum weight design problem

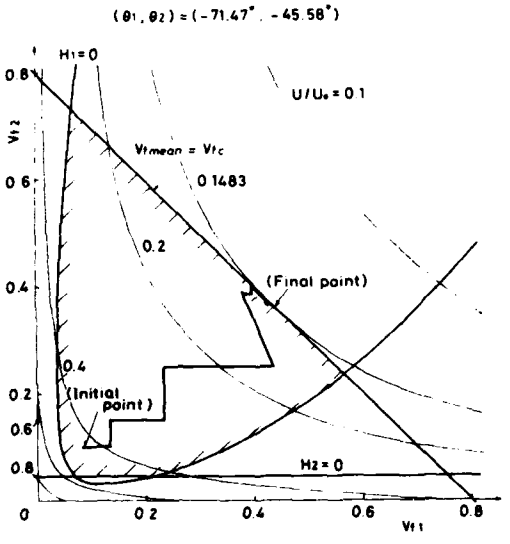


Fig. 17 Design plane, constraints and solutions for maximum stiffness design problem

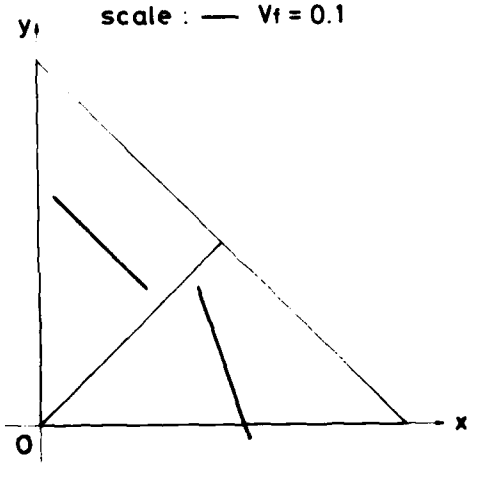


Fig. 18 Fiber contents for maximum stiffness design problem

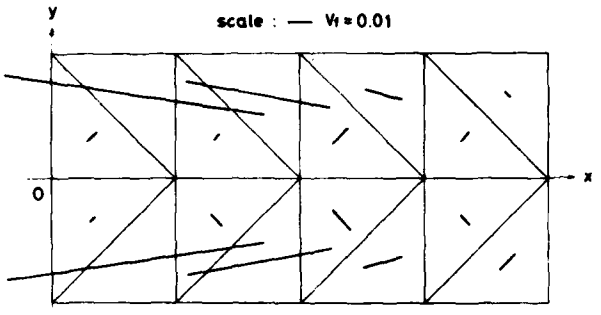


Fig. 19 Fiber contents for minimum weight design problem

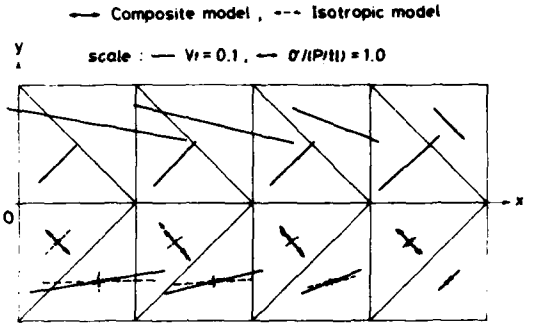


Fig. 20 Fiber contents for maximum stiffness design problem

sented for the cases of minimum weight and maximum stiffness design of structures, which are made of grain dispersed and fiber reinforced materials. In these cases the design variables are the volume percent of grain or fiber and the structures are subjected to the strength or the weight constraints.

The presented procedure is applied to triangular and cantilever beams made from SAP (Sintered Aluminum Powder) or GFRP (Glass Fiber Reinforced Plastic). From these results, it is shown that the solutions obtained for the grain dispersed material are very similar to those of fiber reinforced materials for the same design problems, and also the solution of minimum weight design is nearly equal to one of the maximum stiffness design.

Acknowledgement

The numerical examples presented in this paper are performed by the help of Y. Kido and T. Nayuki. The writer wishes to thank for their help.

Reference

(1) Kicher, T. P. and Chao, T., Minimum Weight Design of Stiffened Fiber Composite Cylinders. J. Aircraft 8, 562, 1971.

(2) Cairo, R. P. and Hadcock, R. N., "Optimum Design and Strength Analysis of Boron Epoxy Laminates," TR AC-SM-8084, Grumman Aircraft Engineering Corporation, Bethpage, New York, 1968.

(3) Cairo, R. P., "Optimum Design of Boron Epoxy Laminares," TR AC-SM-8089, Grumman Aircraft Engineering Corporation, Bethpage, New York, 1970.

(4) Lansing, W., Dwyer, W., Emerton, R. and Rannalli, E., Application of Fully Stressed Design Procedures to Wing and Empennage Structures. J. Aircraft 8, 683, 1971.
(5) Khot, N. S., Venkayya, V. B., Johnson, C. D. and Tischler, V. A., Application of Optimality Criterion to Fiber Reinforced Composites, AFFDL-TR-73-6.
(6) McKeown, J. J., Optimal Composite Structures by Deflection-Variable Programming, Comp. Meth. Appl. Mech. Engng. 12, 155, 1977.
(7) Hemp, W. S., Optimum Structures, Oxford University Press, Oxford, 1973.
(8) Miyamoto, H., Oda, J. and Sakata, S., Simulation of Young's modulus and Poisson's Ratio of Spheroidal Graphite Cast Iron. Jour. Japan Soc. Mech. Engrs. (in Japanese), 77, 146, 1974.
(9) Gallagher, R. H. and Zienkiewicz, O. C., Optimum Structural Design, John Wiley & Sons, London, 1973.
(10) Yamawaki, K. and Uemura, M., "An Analysis for Elastic Moduli of Unidirectional Fiber-Reinforced and Multilayered Composite Materials," Rep. Inst. Space and Aeronautical Sci. Univ. Tokyo, 7, 315, 1971.
(11) Liebowitz, H., Fracture, VII, Academic Press, New York, 1968.

SOME SMEAR-OUT MODELS FOR INTEGRALLY STIFFENED PLATES WITH APPLICATIONS TO OPTIMAL DESIGN*)

AD-P000 099

Martin Philip Bendsøe**)

Mathematical Institute
The Technical University of Denmark
DK-2800 Lyngby
Denmark

Summary

It has been recognized for some time that in many cases rib stiffened plates are more efficient than unstiffened ones. We consider a plate optimization problem where the plate thickness and the direction and concentration of two mutually orthogonal fields of integral stiffeners are used as design variables. In order to perform a structural analysis for the elastic case, a smear-out process is carried out, and the rigidity tensor for an anisotropic plate is obtained. Optimality conditions for minimum compliance under fixed total plate volume are derived by variational analysis. Necessary conditions for different types of local designs are also developed and compared to very recent results obtained for plastic design. Finally, numerical results for the special case of axisymmetric plates are discussed.

Introduction

In the recent papers [1] and [2] integrally stiffened plates have been considered for solving the problem of minimum compliance for thin, elastic plates with given material volume and constraints on the thickness variation. The papers are concerning axisymmetric plates equipped with a field of infinitely many, infinitely thin circumferential stiffeners of rectangular cross-section, and the density of stiffeners (and the thickness of the solid plate) is (are) used as design variable(s). The results obtained clearly show the superiority of this new model, as compared to the traditionally continuous model where only thickness is considered as a design variable. The paper [1] also shows that for practical purposes a lumping of the infinitely many, infinitely thin stiffeners will not significantly alter the performance index obtained from this idealized model. Of other recent papers concerned with stiffened plates [3] and the survey [4] shall be mentioned.

The present paper deals with a generalization of the model described above to an arbitrary plate without symmetry properties. The model considered consists of an integrally stiffened plate of variable thickness. It is stiffened by two orthogonal fields of infinitely many, infinitely thin integral stiffeners of rectangular section and of fixed maximum height. The structural analysis is based on Kirchhoff plate theory and a smear-out bending rigidity tensor is obtained by using the methods of [3]. The minimum compliance design problem for the plate has four design variables: two densities of stiffeners, an angle describing the direction of the stiffeners and the thickness of the solid plate. Each of the independent design variable depend on two spatial variables. Necessary conditions for optimality are obtained in Section 2.3, using variational analysis, see for example [5]. These equations provide the basis for a (future) numerical analysis, and are used in this paper to obtain necessary conditions for the existence of solid subregions of intermediate thickness in the optimal plate. Since the plate model described in this paper contains the axisymmetric models of the papers [1], [2] and [3] as special cases, the superiority of the model is already established.

It should be noted that a model similar to that considered in this paper has been used by Rozvany *et al.* [6] to study the problem of optimal design of plastic plates, and that K.A. Lurie *et al.* [7,8,9] have also used the model with one field of stiffeners for finding the G-closure for optimization problems in torsion, plate bending and conductivity.

As this paper is concerned with shell-theory usual tensor-notation is used throughout; the Einstein-conventions apply where indices appear but a coordinate-free notation is also used to some extent (see e.g. [10] or [11]).

2. The Optimization Problem

We consider the problem of finding a plate model which can provide an appropriate basis for optimal design of thin, elastic, solid plates, whose thickness h is variable and identifies the distance between the upper and lower plate surface, which are assumed to be disposed symmetrically with respect to the plate midplane. The total plate volume is assumed to be specified, as well as material properties, the plate domain Ω and thickness constraint values h_{min} and h_{max}:

$$h_{min} \leq h \leq h_{max}$$

For exemplification the design objective is taken to be minimum compliance, i.e. maximum integral stiffness, for a given static load distribution p.

We shall use Kirchhoff plate theory as the basis for the structural analysis, and since it is our conjecture that the optimal plate will be equipped with many thin ribs, a smear-out process is necessary in order to obtain a continuous effective plate bending rigidity tensor $D_{\alpha\beta\kappa\gamma}$.

2.1. The Model

The generalized plate model proposed here consists of a solid part of variable thickness h, $0 < h_{min} \leq h \leq h_{max}$ that is equipped with two systems of infinitely thin integral stiffeners of variable concentrations μ, γ and directions $\underline{t}, \underline{n}$, where $\underline{t}$ and $\underline{n}$ are orthogonal unit vectors, see Fig. 1.

The concentrations are defined by

$$\mu = \lim_{\Delta x \to 0} \frac{\sum_i \Delta c_i}{\Delta x}$$

where Δx is the extent of an element in the direction of $\underline{n}$ and Δc_i is the width of the i'th stiffener directed along $\underline{t}$ in the element. Each stiffener has a rectangular cross-section of height $h_{max} - h$.

*) Work supported by the Danish Council for Scientific and Industrial Research, grant no. 16-0189, and suggested by N. Olhoff, Dept. of Solid Mechanics, The Technical University of Denmark.

**) Presently with The Division of Applied Mathematics, Brown University, Providence, R.I. 02912, USA.

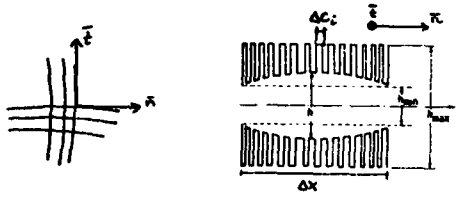


Fig. 1.

Note that the plate model for $\mu \equiv 0$ and $\gamma \equiv 0$ reduces to the solid plate of variable thickness h used traditionally for plate optimization, and for $\mu \equiv 0$ or $\gamma \equiv 0$ the model comprises that used in Refs. [1,2,3] to obtain numerical results for optimization of axisymmetric plates.

The new plate model has four design variables: the thickness h, the concentrations μ, γ and the direction of the stiffeners given by an angle θ, so that

$$\bar{n} = (\cos\theta, \sin\theta) \qquad \bar{t} = (-\sin\theta, \cos\theta)$$

in a fixed Cartesian coordinate system. The plate is geometrically anisotropic, so it is necessary to consider the plate bending rigidity as a tensor in the moment-curvature relationships (Hooke's law). This tensor $D_{\alpha\beta\kappa\gamma}$ will depend on the design variables h, μ, γ, θ, which in turn are functions of the two independent spatial variables for the plate.

2.2. Formulation of the Problem

If we denote the plate deflection function by w the plate optimization problem can be formulated as follows:

With h, μ, γ, θ as design variables, *minimize*

$$\pi = \int_\Omega pw\,d\Omega \tag{1}$$

subject to the constraints

$$\text{Volume} = \int_\Omega \Big(\lambda h + (1-\lambda)h_{max}\Big)d\Omega = V\,,$$

$$h_{min} \le h \le h_{max} \quad \text{in} \quad \Omega\,, \tag{2}$$

$$0 \le \mu \le 1\,, \quad 0 \le \gamma \le 1, \quad \text{in} \quad \Omega\,,$$

where $\lambda = (1-\mu)(1-\gamma)$ is the area-density of plate of intermediate thickness h, $h_{min} \le h < h_{max}$.

The load p and the deflection w are connected through the plate equation, Hooke's law and the definition of curvatures, i.e.,

$$\text{divdiv}\,\hat{M} = p \tag{3}$$

$$\hat{M} = M^{\alpha\beta} = D^{\alpha\beta\kappa\gamma}\, e_{\kappa\gamma} \tag{4}$$

$$e = e_{\alpha\beta} = d(dw) \tag{5}$$

where $\hat{M}$ is the contravariant moment tensor and e is the covariant curvature tensor. dT denotes the covariant derivative of a tensor T. Note that $D_{\alpha\beta\kappa\gamma}$ is a function $D_{\alpha\beta\kappa\gamma}(h, \mu, \gamma, \theta)$.

2.3. Necessary Conditions for Optimality

Following the path of Refs. [1], [2], [3], we find the governing optimality equations for the design problem (1), (2), by variational analysis. In this analysis the plate equations (3)-(5) can be included in two different ways, both leading to the same stationarity equations.

The compliance π in (1) can be rewritten as

$$\pi = \int_\Omega D^{\alpha\beta\kappa\gamma}\, e_{\alpha\beta} e_{\kappa\gamma}\, d\Omega \tag{6}$$

using the plate equations (3)-(5) and appropriate homogeneous boundary conditions, see Refs. [2] or [13]. Using this form of the compliance, we can construct an augmented functional π^* defined by

$$\begin{aligned}\pi^* = &\int_\Omega D^{\alpha\beta\kappa\gamma}\, e_{\alpha\beta} e_{\kappa\gamma}\, d\Omega \\ &- \Lambda\Big[\int_\Omega \Big(\lambda h + (1-\lambda)h_{max}\Big)d\Omega - V\Big] \\ &- \int_\Omega \eta_1[h - h_{max} + \sigma_1^2]d\Omega - \int_\Omega \eta_2[h_{min} - h + \sigma_2^2]d\Omega \\ &- \int_\Omega \alpha_1[\mu - 1 + \zeta_1^2]d\Omega - \int_\Omega \alpha_2[\zeta_2^2 - \mu]d\Omega \\ &- \int_\Omega \beta_1[\gamma - 1 + \xi_1^2]d\Omega - \int_\Omega \beta_2[\xi_2^2 - \gamma]d\Omega \end{aligned} \tag{7}$$

where the constraints (2) are adjoined to the functional π in (6) by the Lagrangian multipliers $\Lambda, \eta_1, \eta_2, \alpha_1, \alpha_2, \beta_1, \beta_2$, and where the real slack-variables $\sigma_1, \sigma_2, \zeta_1, \zeta_2, \xi_1, \xi_2$ converts the inequality constraints on h, μ and γ into equality constraints.

Alternatively, an augmented functional, say $\hat{\pi}$, can be constructed from the original form (1) of the compliance π, but then the plate equation (3) has to be adjoined. Stationarity requirements for $\hat{\pi}$ lead to the same Euler-Lagrange equations as those following from stationarity of π^* in Eq. (7). The variational analysis of $\hat{\pi}$ can be found in the Appendix of Ref. [12], where the plate boundary conditions are used during the calculation; the calculations are based on the assumption that the plate is isotropic, but a careful investigation of the calculations shows that the result applies to any linearly elastic plate problem.

The stationarity conditions for π^* with respect to the design variables h, μ, γ and θ, respectively, are found to be

$$\frac{\partial D^{\alpha\beta\kappa\gamma}}{\partial h}\, e_{\alpha\beta} e_{\kappa\gamma} = \Lambda(1-\mu)(1-\gamma) + \eta_1 - \eta_2 \tag{8}$$

$$\frac{\partial D^{\alpha\beta\kappa\gamma}}{\partial \mu}\, e_{\alpha\beta} e_{\kappa\gamma} = \Lambda(1-\gamma)(h_{max} - h) + \alpha_1 - \alpha_2 \tag{9}$$

$$\frac{\partial D^{\alpha\beta\kappa\gamma}}{\partial \gamma}\, e_{\alpha\beta} e_{\kappa\gamma} = \Lambda(1-\mu)(h_{max} - h) + \beta_1 - \beta_2 \tag{10}$$

$$\frac{\partial D^{\alpha\beta\kappa\gamma}}{\partial \theta}\, e_{\alpha\beta} e_{\kappa\gamma} = 0 \tag{11}$$

These equations constitute the four optimality conditions in our problem.

Stationarity of π^* with respect to the slack variables leads to switching conditions which when combined with Eqs. (8)-(11) and the appropriate Kuhn-Tucker equations, lead to

$$\begin{aligned} &\alpha_1 = 0\,, \quad \alpha_2 \ge 0 \quad \text{if} \quad \mu = 0 \\ &\alpha_1 = 0\,, \quad \alpha_2 = 0 \quad \text{if} \quad 0 < \mu < 1 \\ &\alpha_1 \ge 0\,, \quad \alpha_2 = 0 \quad \text{if} \quad \mu = 1 \end{aligned} \tag{12}$$

$$\begin{aligned} &\beta_1 = 0\,, \quad \beta_2 \ge 0 \quad \text{if} \quad \gamma = 0 \\ &\beta_1 = 0\,, \quad \beta_2 = 0 \quad \text{if} \quad 0 < \gamma < 1 \\ &\beta_1 \ge 0\,, \quad \beta_2 = 0 \quad \text{if} \quad \gamma = 1 \end{aligned} \tag{13}$$

$$\eta_1 = 0 \ , \ \eta_2 \geq 0 \quad \text{if} \quad h = h_{min}$$
$$\eta_1 = 0 \ , \ \eta_2 = 0 \quad \text{if} \quad h_{min} < h < h_{max} \qquad (14)$$
$$\eta_1 \geq 0 \ , \ \eta_2 = 0 \quad \text{if} \quad h = h_{max}$$

Stationarity of π^* with respect to the Lagrangian multipliers leads to the corresponding constraint equations.

The equations (8) to (14) will be used in Section 3.1 for derivation of specific conditions for purely solid sub-regions of intermediate thickness occurring in the optimal plate. But first we need to establish the tensor $D_{\alpha\beta\kappa\gamma}$ for our plate model.

3. The Smear-out Process

3.1. Continuity Considerations

Let two subdomains A and B of a plate have a common boundary curve ψ.

Let e^A respectively e^B and M^A respectively M^B denote the homogeneous curvatures (bending tensors) and bending moments (tensors) in A respectively B. Along the curve ψ we define a unit tangential vector $\bar{t}$ and a unit normal vector $\bar{n}$, so that $(\bar{n}, \bar{t})$ is positively oriented. The continuity conditions across ψ must express continuity of the normal component of the bending moment and the tangential components of the curvatures, and can, with reference to the coordinate system $(\bar{n}, \bar{t})$, be written as (see [3], [7], [2]):

$$M^A_{\alpha\beta} n_\alpha n_\beta = M^B_{\alpha\beta} n_\alpha n_\beta \quad \text{or} \quad p(M^A) = p(M^B) \qquad (15)$$
$$e^A_{\alpha\beta} n_\alpha t_\beta = e^B_{\alpha\beta} n_\alpha t_\beta \quad \text{or} \quad q(e^A) = q(e^B) \qquad (16)$$
$$e^A_{\alpha\beta} t_\alpha t_\beta = e^B_{\alpha\beta} t_\alpha t_\beta \quad \text{or} \quad r(e^A) = r(e^B) \qquad (17)$$

along ψ.

(Here only subscripts are used as we work in an orthogonal frame; repeated indices still imply summation).

3.2. One Field of Stiffeners

Consider the model described in Section 2.1 with just one field of stiffeners, such that, e.g., $\gamma = 0$. We shall now describe in brief how we obtain an average bending tensor $D_{\alpha\beta\kappa\gamma}$ that describes the properties of this plate:

$$M_{\alpha\beta} = D_{\alpha\beta\kappa\gamma} e_{\kappa\gamma} \qquad (18)$$

where M and e are the average bending moment tensor and the average curvature tensor, respectively, for the (anisotropic) plate. The basic infinitesimal element of the plate has the form shown in fig. 2, where A is plate of height h and B the stiffener of height h_{max} and width $\mu\Delta$. We consider the tensors e^A, M^A and e, M to be constant and defined everywhere in

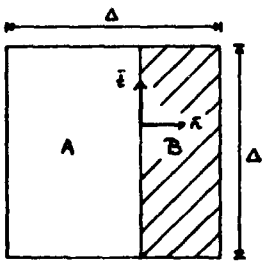


Fig. 2.

this small element. Using the continuity equations (15), we have (see [3])

$$e = (1-\mu)e^A + \mu e^B$$
$$M = (1-\mu)M^A + \mu M^B$$
$$e^A = e + An_\alpha n_\beta$$
$$e^B = e + Bn_\alpha n_\beta$$
$$M^A_{\alpha\beta} = D^-_{\alpha\beta\kappa\gamma} e^A_{\kappa\gamma} \ , \ M^B = D^+_{\alpha\beta\kappa\gamma} e^B_{\kappa\gamma}$$
$$p(M^A) = p(M^B)$$

where D^+ and D^- are the (isotropic) bending rigidity tensors for plate of heights h_{max} and h, respectively.

Combining these equations, we obtain

$$D_{\alpha\beta\kappa\gamma} = (1-\mu)D^-_{\alpha\beta\kappa\gamma} + \mu D^+_{\alpha\beta\kappa\gamma} - \frac{\mu(1-\mu)}{\tilde{D}} (D^-_{\alpha\beta\varepsilon\theta} - D^+_{\alpha\beta\varepsilon\theta})(D^-_{\zeta\eta\kappa\gamma} - D^+_{\zeta\eta\kappa\gamma}) n_\zeta n_\eta n_\varepsilon n_\theta \qquad (19)$$

with

$$\tilde{D} = \left((1-\mu)D^+_{\alpha\beta\kappa\gamma} + \mu D^-_{\alpha\beta\kappa\gamma}\right) n_\alpha n_\beta n_\kappa n_\gamma \qquad (20)$$

(For an alternative calculation, see [2]).

3.3. The General Case

In the general case the basic small element of the plate has the form as illustrated in Fig. 3, where C

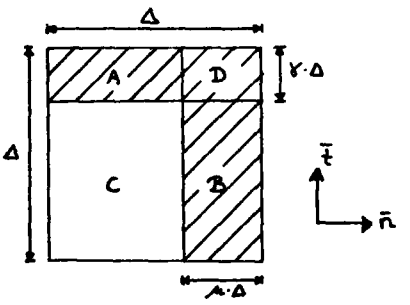


Fig. 3.

is plate of intermediate thickness h and A, B, D indicate stiffeners of height h_{max}. In the regions A, B, C, D we have bending tensors e^A, e^B, e^C, e^D and bending moment tensors M^A, M^B, M^C, M^D, and the average curvature tensor e and average bending moment tensor M are defined by

$$e = \gamma(1-\mu)e^A + \mu(1-\gamma)e^B + (1-\mu)(1-\gamma)e^C + \mu\gamma e^D \qquad (21)$$

$$M = \gamma(1-\mu)M^A + \mu(1-\gamma)M^B + (1-\mu)(1-\gamma)M^C + \mu\gamma M^D \qquad (22)$$

M and e are connected via the smear-out bending tensor $D_{\alpha\beta\kappa\gamma}$ (cf. (18)). As for the case with just one field of stiffeners we will consider all the tensors as being constant within the small standard element. This puts severe constraints on the number of continuity conditions of the form (15)-(17) one can require to be satisfied, as one is very likely to end up with conditions for isotropy. In the following we will require the conditions (15)-(17) to be satisfied between A and C and between B and C, while we will only require (16) and (17) to be satisfied between the regions A and D and between the regions B and D.

As the curvature tensors are symmetric, the condition (16) for these tensors together with the relation (21) imply that the curvatures can be written in the form

$$\begin{aligned} e^A_{\alpha\beta} &= e_{\alpha\beta} + A_1 n_\alpha n_\beta + A_2 t_\alpha t_\beta \\ e^B_{\alpha\beta} &= e_{\alpha\beta} + B_1 n_\alpha n_\beta + B_2 t_\alpha t_\beta \\ e^C_{\alpha\beta} &= e_{\alpha\beta} + C_1 n_\alpha n_\beta + C_2 t_\alpha t_\beta \\ e^D_{\alpha\beta} &= e_{\alpha\beta} + D_1 n_\alpha n_\beta + D_2 t_\alpha t_\beta \end{aligned} \tag{23}$$

The condition (17) and the formula (21) now gives that the constants A_i , B_i , C_i , D_i , $i=1,2$ are connected as follows:

$$\begin{aligned} &A_1 = C_1 \;\; ; \;\; B_1 = D_1 \;\; ; \;\; A_2 = D_2 \;\; ; \;\; B_2 = C_2 \\ \text{and} \quad &(1-\mu)A_1 + \mu B_1 = 0 \;\; ; \;\; \gamma A_2 + (1-\gamma)B_2 = 0 \end{aligned} \tag{24}$$

Finally the condition (15) for the regions A and C and B and C gives

$$p(M^B) = p(M^C) \quad \text{and} \quad r(M^A) = r(M^C) \tag{25}$$

Using the fact that the pairs (M^A, e^A) , (M^B, e^B) and (M^D, e^D) are connected via the tensor D^+ , and that M^C and e^C are connected via D^- , the equations (23), (24), (25) can be reduced to two equations in the two unknowns A_1 and A_2 . Solving for A_1 , A_2 and rewriting (22) using tensors $e^A, \ldots e^D$ and D^+, D^- , one gets an expression

$$M_{\alpha\beta} = D_{\alpha\beta\kappa\gamma}\, e_{\kappa\gamma} \tag{26}$$

where

$$\begin{aligned} D_{\alpha\beta\kappa\gamma} &= (1-\lambda)D^+_{\alpha\beta\kappa\gamma} + \lambda D^-_{\alpha\beta\kappa\gamma} \\ &+ \mu(1-\mu)(1-\gamma)\frac{E_1}{\bar{D}}(D^+ - D^-)_{\alpha\beta\varepsilon\theta}\, n_\varepsilon n_\theta (D^+ - D^-)_{\zeta\eta\kappa\gamma}\, n_\zeta n_\eta \\ &+ \gamma(1-\gamma)(1-\mu)\frac{E_2}{\bar{D}}(D^+ - D^-)_{\alpha\beta\varepsilon\theta}\, t_\varepsilon t_\theta (D^+ - D^-)_{\zeta\eta\kappa\gamma}\, t_\zeta t_\eta \\ &- \mu(1-\mu)(1-\gamma)\gamma\frac{E_3}{\bar{D}}(D^+ - D^-)_{\alpha\beta\varepsilon\theta}\, n_\varepsilon n_\theta (D^+ - D^-)_{\zeta\eta\kappa\gamma}\, t_\zeta t_\eta \\ &- \mu(1-\mu)(1-\gamma)\gamma\frac{E_3}{\bar{D}}(D^+ - D^-)_{\alpha\beta\varepsilon\theta}\, t_\varepsilon t_\theta (D^+ - D^-)_{\zeta\eta\kappa\gamma}\, n_\zeta n_\eta \end{aligned} \tag{27}$$

with

$$\lambda = (1-\mu)(1-\gamma) \tag{28}$$

$$E_1 = [(1-\gamma)D^+ + \gamma D^-]_{\alpha\beta\kappa\gamma}\, t_\alpha t_\beta t_\kappa t_\gamma \tag{29}$$

$$E_2 = [(1-\mu)D^+ + \mu D^-]_{\alpha\beta\kappa\gamma}\, n_\alpha n_\beta n_\kappa n_\gamma \tag{30}$$

$$E_3 = [D^- - D^+]_{\alpha\beta\kappa\gamma}\, n_\alpha n_\beta t_\kappa t_\gamma \tag{31}$$

$$\bar{D} = -E_1 E_2 + \mu\gamma E_3^2 \tag{32}$$

It should be noted that in this calculation it has been used that

$$D^\pm_{\alpha\beta\kappa\gamma}\, n_\alpha n_\beta t_\kappa t_\gamma = D^\pm_{\alpha\beta\kappa\gamma}\, t_\alpha t_\beta n_\kappa n_\gamma$$

for the plate regions A to D .

Comparing with the result in Section 3.2 for one field of stiffeners, one notes that the equation (27) for $\gamma = 0$ or $\mu = 0$ reduces exactly to the smear-out tensor given by (19) for one field of stiffeners. For $(\gamma, \mu) = (0, 0)$ the formula (27) reduces to $D = D^-$, i.e. D is the tensor for an isotropic plate of thickness h , and for $\gamma = 1$ or $\mu = 1$ (27) reduces to $D = D^+$, i.e. D is the bending rigidity tensor for a plate of constant thickness h_{max} . So the tensor given by (27) reduces to the correct, known rigidity tensors in the limits of no stiffeners, one field of stiffeners and solid plate of maximum allowable thickness. Finally one should note that the formula is symmetric in the sence that if $(\mu, \bar{t})$ and $(\gamma, \bar{n})$ are formally interchanged in the formula one ends up with the same formula, so the modeling does not introduce any unique direction.

For practical applications we have to rewrite the formula (27) applying the well-known expressions for D^+ and D^- (see e.g. [3]), and using that

$$\bar{n} = (\cos\theta, \sin\theta) \quad , \quad \bar{t} = (-\sin\theta, \cos\theta)$$

in a given orthogonal frame of reference. For reasons of brevity the resulting large and messy formulas will not be stated here.

If the assumption of mutually orthogonal stiffeners is dropped a similar smear-out process can still be performed by imposing the same conditions of continuity, but the calculations become very messy.

The authors of Refs. [7], [8], [9] have used a model as described in Section 3.2 to obtain a solution to the G-closure problem for torsional bars [7], for conducting media [8] and for some special cases of thin plates [9]. They call this model for a mixing of the first order, and introduce a mixing of the second order as a mixing of the first order of two materials obtained themselves as mixing of the first order. An averaged bending rigidity tensor for the mixing of the second order is of the form (19) where the tensor D^+ and D^- now denote the bending rigidity tensors for the two components of the first order; D^+ and D^- are then also of the form (19). If, for example, $\gamma \ll \mu$ and γ is very small in the model described in Section 3.3, one could regard this as being composed of a mixing of the second order with a density μ of material with bending rigidity tensor D^+ and a density $(1-\mu)$ of a first order mixing of a plate stiffened with stiffeners of density γ . Calculating the resulting average bending rigidity tensor using the method of [7], one obtains a formula that in the given limit (γ small, $\gamma \ll \mu$) is identical to the formula (27).

4. Some Results

Combining the results of Section 2.3 and Section 3.3 one has a basis for a numerical analysis, as well as it is possible to derive certain analytic expressions of necessary conditions for special types of subregions.

4.1. Necessary Condition for Purely Solid Sub-Regions of Intermediate Thickness

A purely solid sub-region of intermediate thickness is characterized by

$$\mu = 0 \quad , \quad \gamma = 0 \quad , \quad h_{min} < h < h_{max} \tag{33}$$

Equations (8) - (11) then reduce to

$$\frac{\partial D^{\alpha\beta\kappa\gamma}}{\partial h}\, e_{\alpha\beta} e_{\kappa\gamma} = \Lambda \tag{34}$$

$$\frac{\partial D^{\alpha\beta\kappa\gamma}}{\partial \mu}\, e_{\alpha\beta} e_{\kappa\gamma} \leq \Lambda(h_{max} - h) \tag{35}$$

$$\frac{\partial D^{\alpha\beta\kappa\gamma}}{\partial \gamma}\, e_{\alpha\beta} e_{\kappa\gamma} \leq \Lambda(h_{max} - h) \tag{36}$$

$$\frac{\partial D^{\alpha\beta\kappa\gamma}}{\partial \theta}\, e_{\alpha\beta} e_{\kappa\gamma} = 0 \tag{37}$$

where the conditions (33) have been introduced via Eqs. (12) - (14).

It is noted that for $\mu \equiv 0$ and $\gamma \equiv 0$ we have $D = D^{-}$, i.e. it is independent of the angle θ. This implies that (37) is trivially satisfied and that (34) can be reduced to (see Section 3.2 in [1]):

$$3h^2\left[e_{11}^2 + e_{22}^2 + 2(1-\nu)e_{12}^2 + 2\nu e_{11}e_{22}\right] = \Lambda \qquad (38)$$

where ν is Poisson's ratio for the isotropic, linearly elastic plate material.

As the tensor $D_{\alpha\beta\kappa\gamma}$ reduces to the form of (19) for $\mu \equiv 0$ or $\gamma \equiv 0$, it is again possible to apply the results of [1]. Using the coordinate system $(\bar{n}, \bar{t})$ Eqs. (35) and (36) reduce to

$$\frac{(D_{max} - D)}{h_{max} - h}\left[(1-\nu^2)e_{22}^2 + 2(1-\nu)e_{12}^2 + \frac{D}{D_{max}}(e_{11} + \nu e_{22})^2\right] \leq \Lambda \qquad (39)$$

$$\frac{(D_{max} - D)}{h_{max} - h}\left[(1-\nu^2)e_{11}^2 + 2(1-\nu)e_{12}^2 + \frac{D}{D_{max}}(e_{22} + \nu e_{11})^2\right] \leq \Lambda \qquad (40)$$

where $D = h^3$ and $D_{max} = h_{max}^3$ (to be exact $D = Eh^3/12(1-\nu^2)$ where E is Young's modulus, but for convenience we use just $D = h^3$).

Equation (38) can be rewritten as

$$3h^2\left[(1-\nu^2)e_{22}^2 + 2(1-\nu)e_{12}^2 + (e_{11} + \nu e_{22})^2\right] = \Lambda \qquad (41)$$

or

$$3h^2\left[(1-\nu^2)e_{11}^2 + 2(1-\nu)e_{12}^2 + (e_{22} + \nu e_{11})^2\right] = \Lambda \qquad (42)$$

Combining (39) and (41) and (40) and (42) we obtain the inequalities

$$(2h + h_{max})\left[(1-\nu^2)e_{22}^2 + 2(1-\nu)e_{12}^2\right] \leq \frac{h^2}{h_{max}^3}(h^2 + 2h\,h_{max} + 3h_{max}^2)(e_{11} + \nu e_{22})^2 \qquad (43)$$

and

$$(2h + h_{max})\left[(1-\nu^2)e_{11}^2 + 2(1-\nu)e_{12}^2\right] \leq \frac{h^2}{h_{max}^3}(h^2 + 2h\,h_{max} + 3h_{max}^2)(e_{22} + \nu e_{11})^2 \qquad (44)$$

which constitute the necessary conditions for a purely solid sub-region of intermediate thickness in the optimal plate.

Equations (43) and (44) are valid in any orthogonal frame of reference, as $(\bar{n}, \bar{t})$ was fixed but arbitrarily chosen. We can thus extend the results of [1] on the configuration of the optimal plate at its edge by using a coordinate-system $(\bar{n}, \bar{t})$ with $\bar{n}$ (or $\bar{t}$) directed along the plate edge. We are then able to conclude that a purely solid sub-region of intermediate thickness will never appear at a simply supported or free edge of an optimally designed plate.

Following [1] once more one can by using coordinates where the bending moment tensor is represented by a diagonal matrix (i.e. the principal directions of the moment tensor) rewrite (43) and (44) to

$$\frac{1}{1 - 2\nu\lambda + \lambda^2} \geq \frac{1 + 2\alpha}{(1-\nu^2)(1 + \alpha + \alpha^2)^2} \qquad (45)$$

$$\frac{1}{1 - 2\nu(1/\lambda) + (1/\lambda)^2} \geq \frac{1 + 2\alpha}{(1-\nu^2)(1 + \alpha + \alpha^2)^2} \qquad (46)$$

where

$$\alpha = \frac{h}{h_{max}} \quad \text{and} \quad \lambda = m_{22}/m_{11} \qquad (47)$$

(m_{11}, m_{22} are the values of the principal moments).

The inequalities (45), (46) divide the (λ, α)-plane into two separate regions, see Fig. 4. Combinations of λ and α calculated for the thickness and moments at points in an intermediate, purely solid subregion in an optimal design must be within the unhatched region of Fig. 4. For further discussion the reader is referred to Ref. [1].

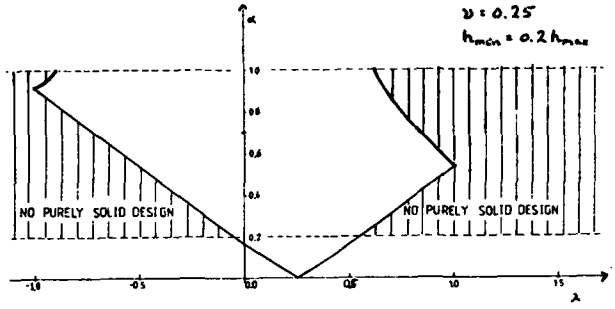


Fig. 4.

It should be noted that the unhatched region of Fig. 4 is found from necessary conditions where stationarity with respect to the direction of the stiffeners is trivially satisfied. If this is taken into consideration one should expect a much larger hatched region, see Ref. [2].

3.2. Numerical Results

Numerical results have been obtained by the authors of Ref. [1] for the model discussed in this paper for the special case of an axisymmetric plate, which means that there is just one (circumferential) field of stiffeners. These results clearly show the superiority of the new model.

For practical purposes the designs under discussion must be considered as limiting designs, resulting from a idealized mathematical formulation. In practice an optimal design obtained from the model described in this paper can be used if the systems of the infinitely many, infinitely thin stiffeners are lumped into a finite number of stiffeners of finite width (to meet buckling requirements etc.). This will of course move the performance index from its optimal value, but the calculations of [1] show that the optimal designs are rather insensitive to reasonable modifications of the type described.

3.3. Plastic Design

A plate model with the same geometry as that considered here has recently been used (see Ref. [6]) as the basis for obtaining minimum weight designs for solid plastic plates. The static determinancy of plastic plates implies that exhaustive analytic developments are possible. It is of special interest for our paper that it is shown in [6] that two fields of stiffeners will be orthogonal in an optimal, plastically designed plate. This has been assumed a priori for elastic plates in this paper, but the author has encountered great difficulty in establishing a proof of this conjecture. It is however fairly easy,

using a min-min formulation as in Ref. [2], Section 2(e), to show that stiffeners directed along the principal directions of the moment tensor (and thus orthogonal stiffeners) is a stationary situation.

Acknowledgement: The author wishes to thank Prof., dr. K.A. Lurie and Prof., dr.techn. Niels Olhoff for valuable discussions.

References:

[1] K.-T. Cheng and N. Olhoff: Regularized Formulation for Optimal Design of Axisymmetric Plates. Int. J. Solids Struct. (to appear)

[2] K.-T. Cheng: On Non-Smoothness in Optimal Design of Solid, Elastic Plates. Int. J. Solids Struct., Vol. 17 (1981), pp. 795-810.

[3] N. Olhoff, K.A. Lurie, A.V. Cherkaev and A.V. Fedorov: Sliding Regimes and Anisotropy in Optimal Design of Vibrating Axisymmetric Plates. Int. J. Solids Struct., Vol. 17 (1981), pp. 931-948.

[4] R.T. Haftka and B. Prasad: Optimum Structural Design with Plate Bending Elements - A Survey. AIAA Journal, Vol. 19 (1981), pp. 517-522.

[5] N. Olhoff: Structural Optimization by Variational Methods. CISM notes, Udine 1981.

[6] G.I.N. Rozvany, N. Olhoff, K.-T. Cheng and J.E. Taylor: On the Solid Plate Paradox in Structural Optimization. J. Struct. Mech. (to appear)

[7] K.A. Lurie, A.V. Cherkaev and A.V. Fedorov: Regularization of Optimal Design Problems for Bars and Plates. Part I, II and III. JOTA (to appear)

[8] K.A. Lurie and A.V. Cherkaev: G-Closure of a Set of Anisotropically Conducting Media in the Two-Dimensional Case. DCAMM Report No. 213, The Technical University of Denmark, Lyngby, Denmark 1981.

[9] K.A. Lurie and A.V. Cherkaev: G-Closure of Some Particular Sets of Admissible Material Characteristics for the Problem of Bending of Thin Plates. DCAMM Report No. 214, The Technical University of Denmark, Lyngby, Denmark 1981.

[10] R. Valid: Mechanics of Continuous Media and Analysis of Structures, Volume 26 in the North-Holland Series in Applied Mathematics and Mechanics, North-Holland, Amsterdam 1981.

[11] M. Bendsøe: Shell Theory for Mathematicians (in Danish), MAT-Report No. 69, Mathematical Institute, The Technical University of Denmark, Lyngby, Denmark 1981.

[12] K.-T. Cheng and N. Olhoff: An Investigation Concerning Optimal Design of Solid Elastic Plates. Int. J. Solids Struct., Vol. 17 (1981), pp. 305-323.

[13] N. Olhoff and K.-T. Cheng: Optimal Design of Solid Elastic Plates, in Optimization of Distributed Parameter Structures (Eds. E.J. Haug and J. Cea), Sijthoff and Nordhoff, Alphen aan den Rijn, Netherlands, 1981.



AD-P000 100

ELASTIC SYNTHESIS FOR LARGE DISPLACEMENTS

J.A. Teixeira de Freitas, Associate Professor
J.P.B. Moitinho de Almeida, Monitor

Departamento de Engenharia Civil
Instituto Superior Técnico
Universidade Técnica de Lisboa
Av Rovisco Pais
1096 Lisboa Codex
Portugal

Summary

A mathematical programming formulation is presented for the elastic synthesis of truss structures with specified topographic and mechanical properties, undergoing finite displacements.

The description for Statics and Kinematics, valid for arbitrarily large displacements and deformations, is expressed in either mesh or nodal formats, according to the connectivity properties of the fundamental substructures selected to describe the assembled structure.

The non-linear elastic constitutive relations, accounting for member instability and initial imperfection effects, are expressed in the alternative flexibility and stiffness formats.

Four alternative formulations, generated through an automatic solution procedure, are obtained to describe the minimization of a design objective subject to the fundamental conditions of equilibrium, compatibility and elastic causality within the domain of allowable stresses and/or displacements.

Reference is made to a perturbation technique based gradient method, designed to guarantee a monotonical improvement of the design object of the resulting non-linear mathematical programming problem.

1. Introduction

The problem of minimizing a (not necessarily linear) cost function W on the cross-sectional areas $\underline{A}$ of an elastic space truss manifesting a non-linear behaviour at the working load level $\underline{\lambda}$, can be stated in the form

$$\text{Min } W(\underline{A}): \underline{A} \in A \tag{1.1}$$

The feasible region A in the above non-linear mathematical program represents the domain of the A-space wherein the design constraints on stresses, displacements and cross-sectional areas

$$\underline{\sigma}^{-}_{*} \leq \underline{\sigma} \leq \underline{\sigma}^{+}_{*} \tag{1.2a}$$

$$\underline{\delta}^{-}_{*} \leq \underline{\delta} \leq \underline{\delta}^{+}_{*} \tag{1.2b}$$

$$\underline{A}^{-}_{*} \leq \underline{A} \leq \underline{A}^{+}_{*} \tag{1.2c}$$

and the state conditions on equilibrium, compatibility and elastic causality are simultaneously satisfied.

2. Statics and Kinematics

Let α {β} represent the static (kinematic) indeterminacy of the structure and

$$B = \alpha + \beta \tag{2.1}$$

the number of independent stress- and corresponding strain-resultants $\underline{X}$ and $\underline{u}$.

The lagrangian description of equilibrium (2.2a) and compatibility (2.2b)

$$\begin{bmatrix} \cdot & \underline{E} \\ \underline{C} & \cdot \end{bmatrix} \begin{bmatrix} \underline{k}_1 \\ \underline{s}_2 \end{bmatrix} = \begin{bmatrix} \underline{s}_1 \\ \underline{k}_2 \end{bmatrix} \tag{2.2a}$$

$$\tag{2.2b}$$

valid for arbitrarily large displacements and deformations can be expressed in dual form

$$\underline{E} = \underline{C}^{T} \tag{2.3}$$

if additional, self-equilibrating forces $\underline{\pi}$ are applied to each member and the strain-resultant field $\underline{u}$ is corrected by additional deformations $\underline{u}_{\pi}$.

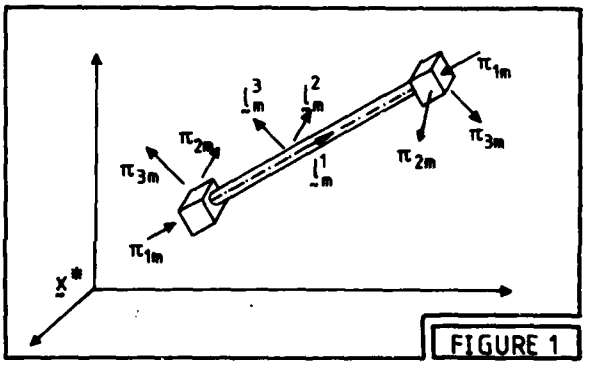


FIGURE 1

The use of additional or ficticious forces in linear formulations to simulate non-linear structural behaviour can be traced back to Denke (1). The same concept was adopted by Smith (2) to preserve Static-Kinematic Duality (3,4) in first-order non-linear elastoplastic frame analysis and later extended (5) to model the response of elastic, elastoplastic and rigid-plastic planar skeletal structures undergoing arbitrarily large displacements; the definition of the additional forces and deformations in the context of space trusses (6) is given in the Appendix.

Summarized in Table 1 are the variables $\underline{s}$ and $\underline{k}$ selected to describe the static and kinematic fields, depending on whether the structure, idealized as a connected graph, is interpreted as an assemblage of mesh or nodal substructures; $\underline{p}$ {$\underline{q}$} collects the α {β} indeterminate forces { displacements } and $\underline{v}$ {$\underline{Q}$} the corresponding displacements {forces}, $\underline{\delta}$ grouping the displacements associated with the loading $\underline{\lambda}$, and $\underline{\delta}_{\pi}$ those with the additional forces $\underline{\pi}$.

Table 1	Description	
Operator	Mesh	Nodal
$\underset{\sim}{s}_1$	$\underset{\sim}{X}$	$\underset{\sim}{Q} = \underset{\sim}{0}$
$\underset{\sim}{k}_1$	$\underset{\sim}{u}+\underset{\sim}{u}_\pi$	$\underset{\sim}{q}$
$\underset{\sim}{s}_2$	$\{ \underset{\sim}{p},\ \underset{\sim}{\pi},\ \underset{\sim}{\lambda} \}$	$\{ \underset{\sim}{X},\ -\underset{\sim}{\pi},\ -\underset{\sim}{\lambda} \}$
$\underset{\sim}{k}_2$	$\{ \underset{\sim}{v}=\underset{\sim}{0},\ \underset{\sim}{\delta}_\pi, \underset{\sim}{\delta} \}$	$\{ \underset{\sim}{u}+\underset{\sim}{u}_\pi, \underset{\sim}{\delta}_\pi, \underset{\sim}{\delta} \}$
$\underset{\sim}{E}=\underset{\sim}{C}$	$\left[\underset{\sim}{B} \mid \underset{\sim}{B}_\pi \mid \underset{\sim}{B}_0\right]$	$\left[\underset{\sim}{A} \mid \underset{\sim}{A}_\pi \mid \underset{\sim}{A}_0\right]$

The state operators (2.3), the entries of which are constant as they are solely dependent on the initial topography of the structure, can be assembled manually or by implementation of automatic assemblage procedures, as indicated in the Appendix.

The linear description for Statics and Kinematics, valid for infinitesimal displacements and deformations, is recovered by setting $\underset{\sim}{\pi}$ and $\underset{\sim}{u}_\pi$ to zero and removing from (2.2b) the definition for $\underset{\sim}{\delta}_\pi$, thus rendered irrelevant.

3. Elastic Constitutive Relations

The relationship of causality associating stress- and strain-resultants, in both flexibility (3.1a) and stiffness (3.1b) formats

$$\underset{\sim}{u} = \underset{\sim}{F}\,\underset{\sim}{X}\ , \quad \underset{\sim}{X} = \underset{\sim}{K}\,\underset{\sim}{u} \qquad (3.1a,b)$$

wherein $\underset{\sim}{F}\,\underset{\sim}{K} = \underset{\sim}{I} = \underset{\sim}{K}\,\underset{\sim}{F}$

is obtained by quantifying the behaviour of the finite-elements embodying the geometric and mechanical properties of the structural members, the simply supported bar loaded by the member stress-resultant X_m.

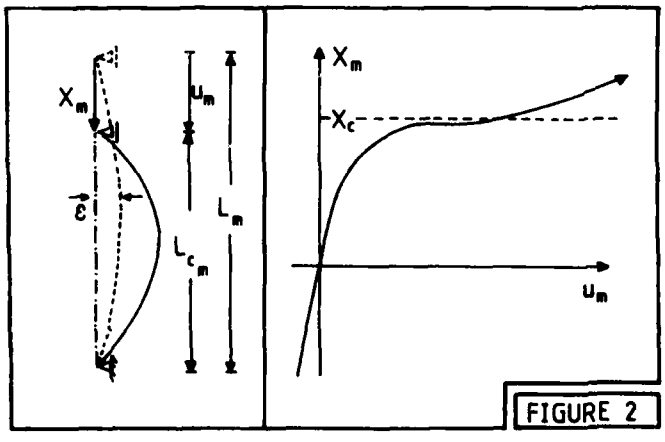


FIGURE 2

Initial deflections ε and residual end-moments can be incorporated in the non-linear definition of the member flexibility and stiffness functions

$$F_m = \left(\frac{L}{EA}\right)_m f_m(X,u,\gamma), \quad K_m = \left(\frac{EA}{L}\right)_m k_m(X,u,\gamma) \qquad (3.2a,b)$$

to simulate the effect of manufacture imperfections; in the above, E_m represents the m-th member modulus of elasticity and γ_m its slenderness ratio.

4. Iterative Solution Programs

Depending on the description adopted for the state equations, the optimization program (1.1)

$$\text{Min } W(\underset{\sim}{A}):\ \{(1.2),(2.2),(3.1)\} \qquad (4.1)$$

can be expressed in four alternative formats, namely, nodal-stiffness, nodal-flexibility, mesh-stiffness and mesh-flexibility, the former and latter of which correspond to the displacement and force methods formulations.

Non-linearity is inherent in programs (4.1) even when infinitesimal displacements ($\underset{\sim}{\pi}=\underset{\sim}{u}_\pi=\underset{\sim}{0}$) and deformations ($f_m=k_m=1$) are assumed, and it is aggravated when equilibrium is performed on the displaced structure ($\underset{\sim}{\pi} \neq \underset{\sim}{0}$), large displacements are accounted for in the compatibility equations ($\underset{\sim}{u}_\pi \neq \underset{\sim}{0}$) and finite deformations are accepted in the elastic constitutive relations.

The qualitatively identical structure presented by the optimization programs (4.1) for both linear and non-linear structural behaviour, suggests the utilization of a solution procedure consisting in coupling an iterative routine on the additional forces and deformations to any of the currently used algorithms to solve structural optimization under linear response.

5. Incremental Formulations

The incremental description of equilibrium (5.1a) and compatibility (5.1b)

$$\left[\begin{array}{c|c} -\underset{\sim}{K}_G & \underset{\sim}{E}_* \\ \hline \underset{\sim}{C}_* & \underset{\sim}{F}_G \end{array}\right] \left[\begin{array}{c} \Delta\underset{\sim}{s}_1 \\ \hline \Delta\underset{\sim}{s}_2 \end{array}\right] = \left[\begin{array}{c} \Delta\underset{\sim}{s}_1 \\ \hline \Delta\underset{\sim}{k}_2 \end{array}\right] + \left[\begin{array}{c} \underset{\sim}{R}_s \\ \hline \underset{\sim}{R}_k \end{array}\right] \qquad (5.1a)$$

$$(5.1b)$$

wherein Static-Kinematic Duality

$$\underset{\sim}{E}_* = \underset{\sim}{C}_* \qquad (5.2)$$

is preserved, is obtained (6,7) by taking finite increments on every variable

$$\underset{\sim}{s} = \underset{\sim}{s} + \Delta\underset{\sim}{s}\ , \quad \underset{\sim}{k} = \underset{\sim}{k} + \Delta\underset{\sim}{k} \qquad (5.3a.b)$$

describing the static and kinematic fields, as indicated in the Appendix, the intervening operators being summarized in Table 2.

Table 2	Description	
Operator	Mesh	Nodal
$\Delta\underset{\sim}{s}_1$	$\Delta\underset{\sim}{X}$	$\underset{\sim}{0}$
$\Delta\underset{\sim}{k}_1$	$\Delta\underset{\sim}{u}$	$\Delta\underset{\sim}{q}$
$\Delta\underset{\sim}{s}_2$	$\{\Delta\underset{\sim}{p},\ \Delta\underset{\sim}{\pi},\ \Delta\underset{\sim}{\lambda}\}$	$\{\Delta\underset{\sim}{X},\ -\Delta\underset{\sim}{\lambda}\}$
$\Delta\underset{\sim}{k}_2$	$\{\underset{\sim}{0},\ \underset{\sim}{0},\ \Delta\underset{\sim}{\delta}\}$	$\{\Delta\underset{\sim}{u},\ \Delta\underset{\sim}{\delta}\}$
$\underset{\sim}{E}_* = \underset{\sim}{C}_*$	$\underset{\sim}{E}$	$\left[\underset{\sim}{A} - \underset{\sim}{A}_\pi\underset{\sim}{Q} \mid \underset{\sim}{A}_0\right]$
$\underset{\sim}{F}_G$	$\underset{\sim}{D}\,\underset{\sim}{P}\,\underset{\sim}{D}$	$\underset{\sim}{0}$
$\underset{\sim}{K}_G$	$\underset{\sim}{0}$	$\underset{\sim}{A}_\pi\,\underset{\sim}{P}\,\underset{\sim}{A}_\pi$
$\underset{\sim}{R}_s$	$\underset{\sim}{0}$	$\underset{\sim}{A}_\pi\,\underset{\sim}{R}_\pi$
$\underset{\sim}{R}_k$	$\underset{\sim}{D}\,\underset{\sim}{R}_\pi + \underset{\sim}{E}\,\underset{\sim}{R}_{u\pi}$	$\{-\underset{\sim}{R}_{u\pi},\ \underset{\sim}{0}\}$

AD-A119 989 ARIZONA UNIV TUCSON COLL OF ENGINEERING F/G 13/13
PROCEEDINGS OF THE INTERNATIONAL SYMPOSIUM ON OPTIMUM STRUCTURA--ETC(U)
1981 E ATREK, R H GALLAGHER N00014-80-G-0041
UNCLASSIFIED NL



Matrices $\underline{P}$ and $\underline{Q}$ are block-diagonal with entries defined by (A.15) and (A.9), respectively, and

$$\underline{D} = \underline{P}^{-1} \left[\underline{Q}\,\underline{B} \mid \underline{Q}\,\underline{B}_{\pi} - \underline{I} \mid \underline{Q}\,\underline{B}_{o} \right] \tag{5.4}$$

Taking in (3.1.2) finite increments (5.3), while letting

$$A_i = A_i\,(1-\Delta a_i) \qquad 1 \leq i \leq B \tag{5.5}$$

for the cross-sectional area variations, the incremental version of the flexibility and stiffness descriptions of the elastic constitutive relations become

$$\Delta \underset{\sim}{u} = \underline{F}\,\Delta \underset{\sim}{X} + \underline{G}\,\Delta \underset{\sim}{a} + \underset{\sim}{R}_u \tag{5.6a}$$

and

$$\Delta \underset{\sim}{X} = \underline{K}\,\Delta \underset{\sim}{u} + \underline{H}\,\Delta \underset{\sim}{a} + \underset{\sim}{R}_x \tag{5.6b}$$

respectively.

The design constraints (1.2) can be treated similarly to yield

$$\underset{\sim}{\sigma}^{-} \leq \underline{\Omega}^{-1}\,\Delta \underset{\sim}{X} + \underline{\Sigma}\Delta \underset{\sim}{a} + \underset{\sim}{R}\sigma \leq \underset{\sim}{\sigma}^{+} \tag{5.7a}$$

$$\underset{\sim}{\delta}^{-} \leq \Delta \underset{\sim}{\delta} \leq \underset{\sim}{\delta}^{+}\,, \quad \underset{\sim}{a}^{-} \leq \Delta \underset{\sim}{a} \leq \underset{\sim}{a}^{+} \tag{5.7b,c}$$

the superscripted quantities representing the current potentials for the variables in question; $\underline{\Omega}$ and $\underline{\Sigma}$ are diagonal matrices the entries of which are the current cross-sectional areas and stresses, respectively, and $\underset{\sim}{R}_{\sigma}$ a non-linear residual vector of the form

$$\underset{\sim}{R}_{\sigma} = \{\Delta\sigma_i\ \Delta a_i\}, \quad 1 \leq i \leq B \tag{5.8}$$

Similarly, $\underset{\sim}{R}_u$, $\underset{\sim}{R}_x$, $\underset{\sim}{R}_{u\pi}$ and $\underset{\sim}{R}_{\pi}$, the latter being defined in (A.16) and (A.17), respectively, collect all non-linear terms present in the incremental state equations (5.1,6).

The definition of $\underline{F}$, $\underline{K} = \underline{F}^{-1}$, $\underline{G}$, $\underline{H} = -\underline{K}\,\underline{G}$, $\underset{\sim}{R}_u$ and $\underset{\sim}{R}_x = -\underline{K}\,\underset{\sim}{R}_u$ depends on the adopted member stability functions, several definitions of which are presented in the literature.

6. Incremental Solution Programs

Let $\underset{\sim}{v}$ represent a generic program variable satisfying the state equations (2.2) and (3.1) at the design load level λ.

Problem (1.1) can now be restated as to find a finite variation $\Delta \underset{\sim}{v}$ so that $\underset{\sim}{v} + \Delta \underset{\sim}{v}$ is an optimal solution for the required load carrying capacity ($\Delta\lambda = \underline{0}$) and expressed as

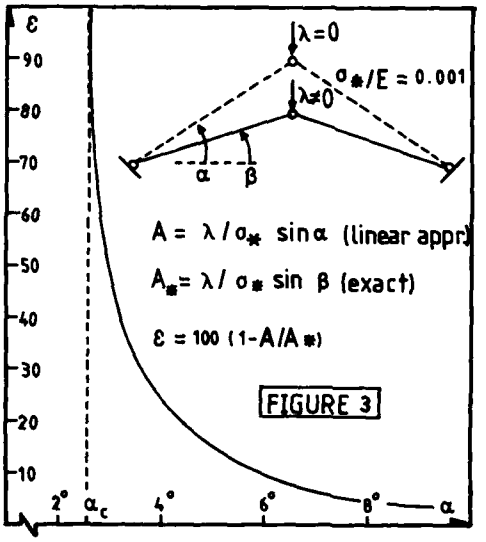
$$\text{Max } \Delta Z = \underset{\sim}{d}\,\Delta \underset{\sim}{a} + R_z : \{(5.1,5,6)\} \tag{6.1}$$

wherein R_z collects the non-linear terms present in the objective function, if any.

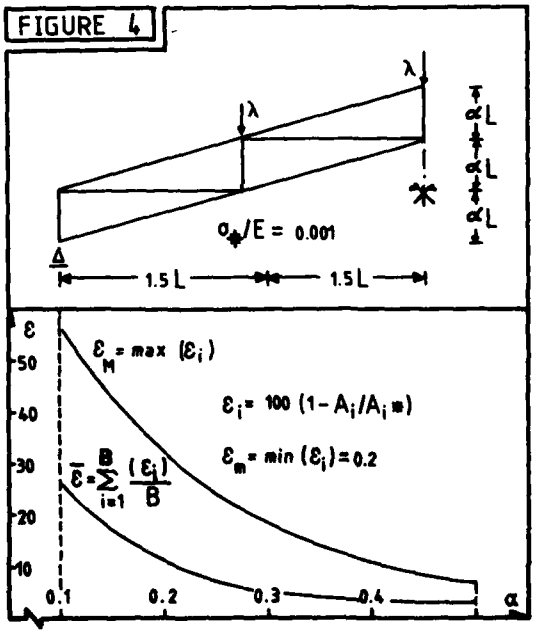
As all non-linear terms present in the constraint set of problem (6.1) are collected in the residuals $\underset{\sim}{R}$ the analitical expressions of which are known at the onset, programs (6.1) can be generated automatically and numerically processed using a non-linear programming algorithm; in particular, just by treating the residual terms as constants, the solution of program (6.1) can be reduced to a sequential linear programming problem.

7. Numerical Applications

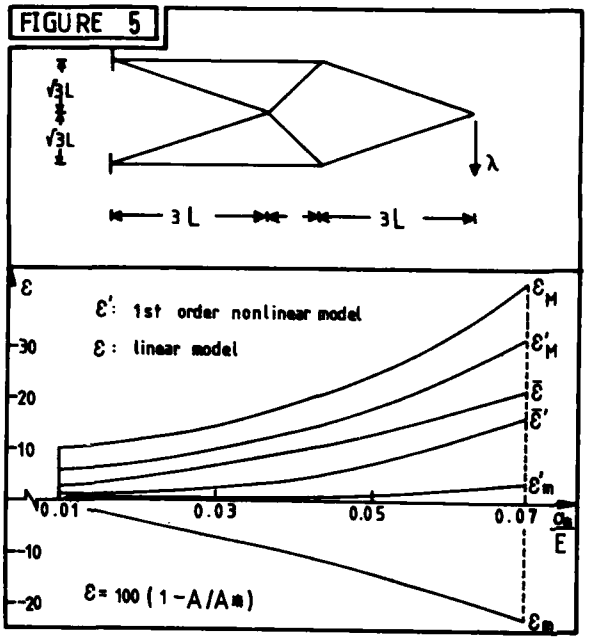
A comparative analysis of the optimal solutions provided by the linear and "exact" formulations, as non-linear structural behaviour sets in, is presented in the following.



The structures shown in Figs 3 and 4 were selected to illustrate the effect of non-linear behaviour in the stress-constrained weight optimization of shallow arches; the graphs shown represent the variation in the error ε relating the optimal cross-sectional areas predicted by the linear and non-linear models, A and A_*, respectively.



The cantilever shown in Fig. 5 was used to illustrate the effect of non-linear behaviour caused by the development of large displacements; point load displacements of the order of half of the basis span were induced by accepting very high σ_*/E ratios.



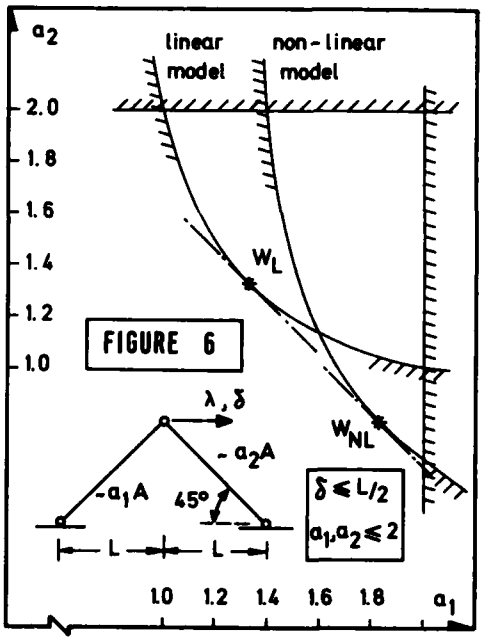
According to our experience, the essential role of the non-linear model consists in redistributing the structural member weights provided by the linear model optimization procedure; despite the significant errors that could be found in the allocation of the members cross-sectional areas, the difference in the estimate for the total weight of the structure, provided by the linear and non-linear models, would seldom exceed 10%.

The redistribution of weight is particularly evident in the displacement-constrained weight optimization problem shown in Fig. 6, wherein an error of about 2% is found in the optimal structural weight, despite differences exceeding 25 and 65% in the optimum cross-sectional area estimates.

The numerical results presented below were obtained using Schwefel evolution strategies algorithm (7) and the perturbation technique based gradient method (8) briefly described in the Appendix.

The results obtained using Schwefel's algorithm proved to be significantly dependent on the initial estimates provided for the design variables; however, as it is extremely simple to encode and requires very little computer core, it is thought that this algorithm is particularly well suited to perform the shake-down of the provided initial solution, thus stabilizing the solution sequence.

The perturbation technique based algorithm generates stable solution sequences by guaranteeing a monotonical improvement of the objective function. The rules to detect the activation and releasing of constraints and to determine the optimum step length at each iteration, are accurate and of simple implementation. The core it requires is significant due to the necessity of saving n+1 allocations for each variable, n representing the number of terms taken in the series expansion (n=3, in general); execution time and core requirements are strongly interdependent as the step length is dictated, for a given truncation error, by the number of terms taken in the series expansion, the higher order terms of which become increasingly significant as the degree of non-linearity in the objective and constraint functions increases.



The displacement method (incremental) formulation was adopted since it is associated with the most compact of the alternative descriptions for the system governing equations.

In what concerns the numerical implementation efficiency, the advantage that the force method enjoys over the displacement method, when a linear approximation in the state equations is adopted, can only be regained under non-linear behaviour if the topography of the structure is such and the members numbering sequence so devised as to induce a quasi-diagonal format for the geometric flexibility sub-matrix associated with the additional forces. The force method reassumes its competitiveness when a first-order non-linear approximation

$$u_\pi = \pi_1 = 0 \ , \ \pi_i = \frac{\delta_{\pi i}}{L} \ , \quad i = 2,3$$

to the exact description of Statics and Kinematics is admissible, as it usually happens in practical applications.

Acknowledgements

This research has been sponsored by the National (Portuguese) Institute of Scientific Research (INIC) through the Mechanics and Structural Engineering Centre (CMEST), Technical University of Lisbon.

References

(1) Denke, P.H., "Non-linear and Thermal Effects on Elastic Vibrations", Tech. Rept. SM-30426, Douglas Aircraft Company, 1960.

(2) Smith, D.L., First-Order Large Displacement Elastoplastic Analysis of Frames Using the Generalized Force Concept, Engineering Plasticity by Mathematical Programming, Pergamon Press, 1977.

(3) Munro, J., "The Stress Analysis and Topology of Skeletal Structures", Rept CSTR 14, Imperial College London, 1965.

(4) Munro, J. and D.L. Smith, Linear Programming in Plastic Limit Analysis and Synthesis, Int. Symp. Computer Aided Structural Design, 1972.

(5) Teixeira de Freitas, J.A., The Elastoplastic Analysis of Planar Frames for Large Displacements by Mathematical Programming, Ph.D. Thesis, Univ. of London, 1979.

(6) Teixeira de Freitas, J.A., "Analise Elastica de Estruturas Articuladas Espaciais Sujeitas a Grandes Deslocamentos", Rept. CMEST 5-2, Univ. Tecnica de Lisboa, 1980.

(7) Schwefel, H.P., Numerische Optimierung von Computer-Modellen mittels der Evolutionsstrategie, ISR26, Birkhauser Verlag, Easle und Stuttgart, 1977.

(8) Teixeira de Freitas, J.A., "A Perturbation Technique Based Nonlinear Programming Algorithm", Rept CMEST 5-7, Univ. Tecnica de Lisboa, 1981.

APPENDIX

A1. Nodal Description of Statics and Kinematics

Assume that a nodal sub-structure, a (not necessarily straight) prismatic bar m limited by end nodes i and j, is dissected from a discretized space truss just prior and immediately after the loading is applied.

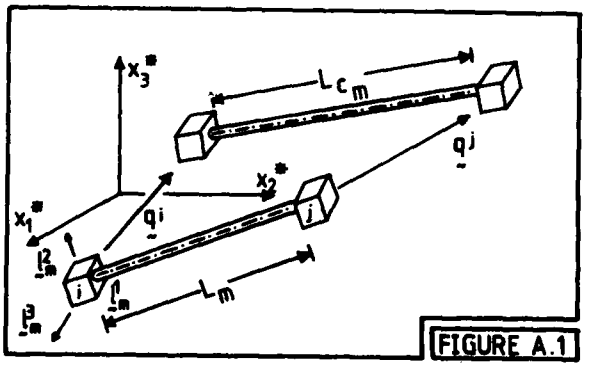


FIGURE A.1

Let the displacement field be defined by vector

$$\underset{\sim}{q}_m = \{\underset{\sim}{q}^i \ , \ \underset{\sim}{q}^j\} \qquad (A.1)$$

which collects the displacements suffered by nodes i and j, measured in the global system of reference $\underset{\sim}{x}^*$, and let the deformation field be characterized by the difference

$$u_m = L_m - L_{c_m} \qquad (A.2)$$

between the initial and final member chord lengths. If ficticious deformations

$$u_{\pi_m} = \delta_{\pi 1_m} - u_m \qquad (A.3)$$

are added to the stress-resultants field, the exact description for the nodal substructure compatibility condition can be expressed in the explicitly linear form

$$\begin{bmatrix} u+u_\pi \\ \hline \delta_\pi \end{bmatrix}_m = \begin{bmatrix} \underline{A} \\ \hline \underline{A}_\pi \end{bmatrix}_m \underset{\sim}{q}_m \qquad (A.4a)$$

$$(A.4b)$$

wherein

$$\underline{A}_m = \left[\underset{\sim}{\ell}^1 \,|\, -\underset{\sim}{\ell}^1\right]_m \ , \ \underline{A}_{\pi m} = \left[\underline{\tilde{L}} \,|\, -\underline{\tilde{L}}\right]_m \ , \qquad (A.5a,b)$$

the m-th member inital position direction cosines being collected in

$$\underline{L}_m = \left[\underset{\sim}{\ell}^1 \,|\, \underset{\sim}{\ell}^2 \,|\, \underset{\sim}{\ell}^3\right]_m \qquad (A.5)$$

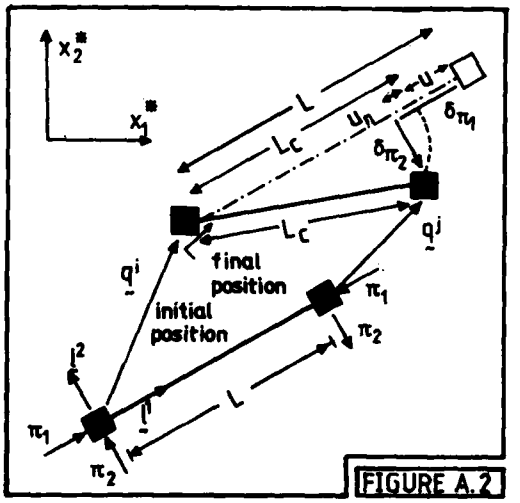


FIGURE A.2

The additional force displacements $\underline{\delta}_{\pi m}$, illustrated in Fig. A.2 for the planar case, are related with the member deformations u_m through the following compatibility condition

$$L_{c_m} = (L-\delta_{1\pi})^2_m + \delta^2_{2\pi_m} + \delta^2_{3\pi_m} \qquad (A.7)$$

Collecting the nodal forces in vector

$$\underline{Q}_m = \{\underline{Q}^i, \underline{Q}^j\} \qquad (A.8)$$

and defining the stress field by the member end-forces X_m, the exact description for the nodal substructure equilibrium condition can be expressed in an explicitly linear form, preserving Static-Kinematic Duality,

$$\underline{Q}_m = \left[\underline{\bar{A}} \,|\, \underline{\bar{A}}_\pi\right]_m \begin{bmatrix} -\underline{X} \\ \hline \underline{\pi} \end{bmatrix}_m \qquad (A.9)$$

if use is made of ficticious or additional forces

$$\underline{\pi}_m = \underline{Q}_m \, X_m \qquad (A.10)$$

wherein

$$\underset{\sim}{Q}_m = \left[1 - \frac{L-\delta_{\pi 1}}{L_c}, \frac{\delta_{\pi 2}}{L_c}, \frac{\delta_{\pi 3}}{L_c}\right]_m \qquad (A.11)$$

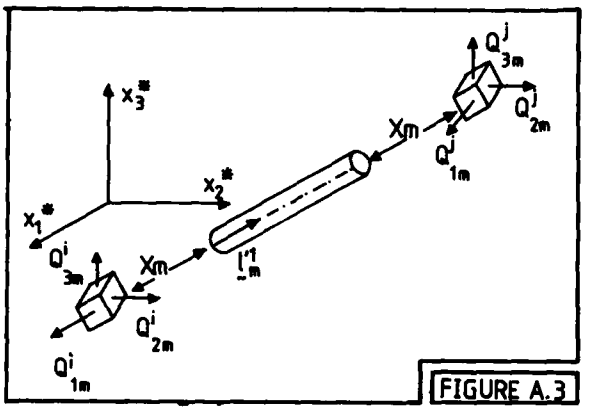


FIGURE A.3

Let the B nodal substructure displacement vectors (A.1) be collected in $\underset{\sim}{q}_*$ and $\underset{\sim}{q}$ group the β indeterminate structure displacements.

Nodal connectivity and the structure kinematic boundary conditions are implemented by defining the incidence

$$\underset{\sim}{q}_* = \underset{\sim}{J}\,\underset{\sim}{q}$$

which substituted into system (A.4), extended to embrace all B nodal sub-structures compatibility conditions, yields definition (2.2b) for the structure nodal description of Kinematics, wherein

$$\underset{\sim}{A} = \underset{\sim}{A}_*\,\underset{\sim}{J}\ ,\ \underset{\sim}{A}_\pi = \underset{\sim}{A}_{\pi *}\,\underset{\sim}{J}\ ,$$

$\underset{\sim}{A}_*$ and $\underset{\sim}{A}_{\pi *}$ being the block-diagonal matrices

$$\underset{\sim}{A}_* = \left[\underset{\sim}{A}_m\right]\ ,\ \underset{\sim}{A}_{\pi *} = \left[\underset{\sim}{A}_{\pi m}\right]$$

and $\underset{\sim}{A}_o$ an incidence matrix relating the applied load displacements $\underset{\sim}{\delta}$ with the independent nodal displacements $\underset{\sim}{q}$.

The nodal description of Statics (2.2a), requiring nodal equilibrium along the indeterminate displacement directions, is obtained by implementing a similar assemblage procedure on the nodal substructure equilibrium conditions (A.9):

$$\underset{\sim}{Q} = \underset{\sim}{0} = \underset{\sim}{J}\,\underset{\sim}{Q}_* + \underset{\sim}{A}_o\,\underset{\sim}{\lambda}$$

A2. Mesh Description of Statics and Kinematics

The fundamental mesh substructure , particularly well suited for framed structures, is by definition a ring of arbitrary topography; more appropriate to planar (space) truss structures are however statically indeterminate assemblages of triangular (tethaedrical) pin-jointed substructures.

Statics and Kinematics of the mesh substructure can be set up through a similar procedure (5) and assembled automatically to obtain the structure equilibrium and compatibility conditions (2.2), using either cut-cycle bases or regional cycle bases.

An alternative procedure consists in obtaining the mesh description by transforming the nodal description: let $\underset{\sim}{X}'$ and $\underset{\sim}{X}''$ collect β and α of the B = α+β elements of $\underset{\sim}{X}$, respectively, so that the nodal equilibrium equation (2.2a) can be written in the equivalent, partitioned, form

$$\underset{\sim}{A}'\,\underset{\sim}{X}' = -\underset{\sim}{A}''\,\underset{\sim}{X}'' + \underset{o\sim}{A}\,\lambda + \underset{\sim}{A}_\pi\,\underset{\sim}{\pi} \qquad (A.12)$$

The mesh state operators

$$\underset{\sim}{B} = \left[\begin{array}{c} -\underset{\sim}{C}^{-1}\,\underset{\sim}{A}'' \\ \hline \underset{\sim}{I} \end{array}\right]\ ,\ \underset{\sim}{B}_o = \left[\begin{array}{c} \underset{\sim}{C}^{-1}\,\underset{\sim}{A}_o \\ \hline \underset{\sim}{0} \end{array}\right]\ ,\ \underset{\sim}{B}_\pi = \left[\begin{array}{c} \underset{\sim}{C}^{-1}\,\underset{\sim}{A}_\pi \\ \hline \underset{\sim}{0} \end{array}\right]$$

wherein $\underset{\sim}{C} = \underset{\sim}{A}'$ (or $\underset{\sim}{C}' = \underset{\sim}{A}'\,\underset{\sim}{A}'$ to guarantee positive definiteness), are obtained by identifying $\underset{\sim}{X}''$ with the indeterminate forces $\underset{\sim}{p}$ and solving (A.12) for $\underset{\sim}{X}'$.

A3. Incremental Additional Forces and Deformations

Taking finite increments (5.3) in (A.3) and (A.10,11) and eliminating in the resulting equation the incremental member deformation resulting from the incremental version of (A.7), the following definitions are found for the incremental additional forces

$$\Delta\underset{\sim}{\pi}_m = \underset{\sim}{P}_m\,\Delta\underset{\sim}{\delta}_{\pi_m} + \underset{\sim}{Q}_m\,X_m + \underset{\sim}{R}_{\pi_m} \qquad (A.13)$$

and deformations

$$\Delta u_{\pi_m} = \underset{\sim}{Q}_m\,\Delta\underset{\sim}{\delta}_{\pi_m} + R_{u\pi_m} \qquad (A.14)$$

wherein

$$\underset{\sim}{P}_m = \frac{X_m}{L_{c_m}}\left[\begin{array}{c|c|c} Q_1^2 & (1-Q_1)Q_2 & (1-Q_1)Q_3 \\ \hline (1-Q_1)Q_2 & 1-Q_2^2 & -Q_2\,Q_3 \\ \hline (1-Q_1)Q_3 & -Q_2\,Q_3 & 1-Q_3^2 \end{array}\right]_m \qquad (A.15)$$

$$R_{u\pi_m} = \frac{1}{2L_{c_m}}\left(\sum_{i=1}^{3}\Delta\delta^2_{\pi_i} - \Delta u^2\right)_m \qquad (A.16)$$

and

$$\underset{\sim}{R}_{\pi_m} = \frac{1}{L_{c_m}}\left(\Delta\underset{\sim}{\pi}\,\Delta u + \Delta\underset{\sim}{\delta}_\pi\,\Delta X - \underset{\sim}{\pi}\,R_{u\pi}\right)_m +$$

$$+ \frac{1}{L_{c_m}}\left[\begin{array}{c} X\,R_{u\pi} - \Delta u\,\Delta X \\ \hline 0 \\ \hline 0 \end{array}\right]_m \qquad (A.17)$$

A4. A Perturbation Technique Base Solution Procedure

Assuming that at the current solution point ($\underset{\sim}{v}$, $\underset{\sim}{\lambda}$) the structure is stable, all but the design variables $\Delta\underset{\sim}{a}$ can be eliminated from program (6.1) by simple pivoting on the non-singular state operators present in the equality constraint set (5.1,6) thus reducing the optimization problem to form

$$\text{Max } \Delta w \qquad \text{(A.18a)}$$

subject to:-

$$\Delta w = \tilde{c}\ \Delta a + R_w \qquad \text{(A.18b)}$$

$$\Delta y = C\ \Delta a + R \qquad \text{(A.18c)}$$

$$\Delta y + c_o \geq 0 \qquad \text{(A.18d)}$$

wherein R_w {R} collects the non-linear residuals present in the objective-function {constraint set}; it is assumed that, after a suitable transformation, the gradients present in constraints (A.18b,c) are unit modulus vectors.

Expanding all variables, say Δx, in a power series on a perturbation parameter ε

$$\Delta x = x^{(n)}\ \varepsilon^n/n! \qquad \text{(A.19)}$$

and equating the same order terms, system (A.18b,c) is replaced by the equivalent infinite set of equations

$$w^{(n)} = c\ a^{(n)} + \delta_{1n}\ R_{wn} \qquad \text{(A.20a)}$$

$$y^{(n)} = C\ a^{(n)} + \delta_{1n}\ R_n \qquad \text{(A.20b)}$$

(δ_{mn}, $m=1$, representing the kronecker symbol), which are linear and recursive as the n-th order residual terms are functions of lower than the n-th order design variable coefficients, eg

$$R_n = R_n(\dot{a},\ \ddot{a},\ \ldots,\ a^{(n-1)})$$

Identification of the perturbation parameter with the objective function, $\varepsilon = \Delta w$, implying, according to (A.20a), that

$$w^{(n)} = \delta_{1n} \qquad \text{(A.21)}$$

enhances the substitution of the non-linear programming problem (A.18) by an equivalent problem , consisting in finding feasible directions Δa satisfying the linear system

$$\tilde{c}\ a^{(n)} + \delta_{1n}\ R_{wn} = \delta_{1n} \qquad 1 \leq n \leq \infty \qquad \text{(A.22)}$$

and non-negative step lengths ε (thus guaranteeing the monotonical improvement of the objective function w) which are determined either by bounding the series (A.19) truncation error e

$$\varepsilon_{max} = \min_i \{|en!/a_i^{(n)}|^{1/n}\} \qquad \text{(A.23a)}$$

or by the activation of the i-th constraint

$$c_{oi} + y_i^{(n)}\ \varepsilon_{max}^n/n! = 0$$

yielding

$$\varepsilon_{max} = \min \{\psi_n(-c_{oi}/\dot{y}_i)^n\} \qquad \text{(A.23b)}$$

wherein

$$\psi_1 = 1,\ \psi_2 = -\ddot{y}_i/2\dot{y}_i,\ \psi_3 = 2\psi_2^2 - \dddot{y}_i/b\dot{y}_i,\ \ldots$$

The general expression for the feasible direction is

$$\dot{x} = c\ ,\quad x^{(n)} = -R_{wn}\ \dot{x}\ ,\quad (n \geq 2) \qquad \text{(A.24a,b)}$$

when all constraints are inactive and

$$\dot{x} = (c + \tilde{C}'\ \beta)\ \alpha \qquad \text{(A.25a)}$$

$$x^{(n)} = R_n - (\tilde{c}\ R_n' + R_{zn})\ \dot{x} \qquad (n \geq 2) \qquad \text{(A.25b)}$$

when a subset of constraints are active, $c_o' = 0$ in (A.18d); C' and R_n' represent the structural matrix and the residual terms associated with such constraints. Vector β represents the deviation from the steepest ascent direction c and is evaluated by solving the following linear programming problem

$$\text{Min } \tilde{b}\ \beta:\ B\ \beta \geq b \qquad \text{(A.26)}$$

wherein $b = -C'\ c$ and $B = C'\ \tilde{C}'$

requiring the maximization of the objective gradient in form $\dot{w} = \alpha v$, where, according to (A.20a) and (A.25a) $v = 1 - \tilde{b}\ \beta$ and $\alpha > 0$, while satisfying the currently potentially active constraints

$$\dot{y}' = C'\ \dot{x} \geq 0$$

Self-duality in programs (A.26) enables its direct resolution, from which are derived the tests on unboundedness ($\beta_i \to \infty$) and optimality (unique if $v<0$, multiple if $v=0$); if neither of these situations arise, $v>0$, α is set to $\alpha = 1/v$ to regain an objective function controlling procedure (A.21).

AD-P000 101

DERIVATION AND CONVERGENCE OF POWER SERIES IN STRUCTURAL DESIGN

Joseph Whitesell
Department of Mechanical Engineering
and Applied Mechanics
Ann Arbor, MI 48109

Abstract

Design sensitivity analysis plays an important role in the optimal design of structures but usually only first order derivatives are computed. When high order derivatives are used substantial reductions in computational effort can result but a question of convergence of the resulting power series in the design variable arises. If the change in the design parameter is smaller than the radius of convergence of the series then the model's response can be approximated to arbitrary accuracy by the series without reanalysis. If the design change is larger then the series is less useful. In this paper the computation and convergence properties of power series for static responses and eigensystems are discussed. A technique for enlarging the region of convergence is presented along with several example problems.

I. The Efficiency of Power Series

The effort required to compute a function's higher order derivatives often discourages their use in numerical analysis. There are important cases however, where high order information can be determined at an operating point of a single independent variable with considerably less effort than that required to carry out a function evaluation at a different operating point.

To illustrate this, suppose

$$\begin{aligned} k &= k_0 + k_1 x + k_2 x^2 + \cdots \\ u &= u_0 + u_1 x + u_2 x^2 + \cdots \\ f &= f_0 + f_1 x + f_2 x^2 + \cdots \end{aligned} \tag{1}$$

are formal power series [1] and we wish to solve the problem

$$ku = f \tag{2}$$

for the coefficients u_i. This problem can be solved using matrix notation by representing each of the series in (1) by a matrix of special structure called a semicirculant matrix [1].

We re-write (2) in terms of semicirculant matrices as

$$\begin{bmatrix} k_0 & k_1 & k_2 & k_3 & \cdots \\ & k_0 & k_1 & k_2 & \cdots \\ & & k_0 & k_1 & \cdots \\ & & & k_0 & \cdots \\ & & & & \ddots \end{bmatrix} \begin{bmatrix} u_0 & u_1 & u_2 & u_3 & \cdots \\ & u_0 & u_1 & u_2 & \cdots \\ & & u_0 & u_1 & \cdots \\ & & & u_0 & \cdots \\ & & & & \ddots \end{bmatrix} = \begin{bmatrix} f_0 & f_1 & f_2 & f_3 & \cdots \\ & f_0 & f_1 & f_2 & \cdots \\ & & f_0 & f_1 & \cdots \\ & & & f_0 & \cdots \\ & & & & \ddots \end{bmatrix} \tag{3}$$

or

$$K\,U = F \tag{4}$$

and determine the coefficients u_i by solving the finite dimensional triangular system constructed from the first i rows and columns of the matrices K, U and F.

The coefficients u_i may be written as

$$u_i = k_0^{-1} \left[f_i - \sum_{j=0}^{i-1} k_{i-j}\, u_j \right] \tag{5}$$

In applications, it is important to consider the relative computational effort involved in determining k_0^{-1} as compared with the operation of multiplication implied in (5). If computing k_0^{-1} and the multiplication operation require comparable effort, then computing each u_i will require a significant effort relative to the inversion of k_0. However, if a relatively large effort is required to find k_0^{-1} then determining u_0 could cost significantly more than the additional cost required to determine its successors u_i. In other words, computing higher order coefficients u_i becomes relatively less expensive when division (inversion) is more costly than multiplication. Such is the case when the objects k_i are matrices in R^{nxn} and the objects u_i and f_i are vectors in R^n. (When the coefficients k_i must also be computed, then the cost of determining the coefficients u is increased accordingly.)

Convergence rate is also important in numerical work. We shall see that it is not necessarily sensitive to system size. It depends instead on the sizes of certain eigenvalues related to the system. So the number of terms need not be large even if the model is large. This makes using power series an attractive alternative to directly re-solving the structural model.

Unfortunately, sometimes the convergence radius is not large enough. To remedy this, a method which can effectively enlarge the radius of convergence is presented in the next section.

II. Power Series for Static Response

This section begins with a simple example.

Example 1

Suppose that structure AB is composed of two components A and B each with stiffness matrices K_A and K_B and let the stiffness matrix [2] of structure AB be given by

$$K_{AB} = K_A + K_B \tag{6}$$

Then the matrix-valued function $K(x) = K_A + x\,K_B$ satisfies $K(0) = K_A$ and $K(1) = K_{AB}$. Now consider the problem

$$K(x)u(x) = f \tag{7}$$

where f is a known constant force and $x \in [0,1]$. A power series for the vector-valued function u(x) can be obtained from (5) as

$$u_0 = K_A^{-1} f$$

and

PRECEDING PAGE

$$u_i = -K_A^{-1} K_B u_{i-1} \tag{8}$$

If the power series representing u(x) converges for x=1 then the effect of adding component B to component A on the displacement u can be evaluated without inverting the matrix K_{AB}. To evaluate the radius of convergence of the series we make use of a theorem from complex variable theory [1] which states that the radius of convergence of the power series representing a function f near some point x_0 is equal to the radius of the largest disk in the complex plane centered at x_0 inside of which f or an analytic continuation of f is analytic. For problem (7) the points for which the function u(x) is not analytic are the points p which satisfy

$$\det(K(p)) = 0 \tag{9}$$

or

$$(K_A + pK_B)v = 0 \tag{10}$$

Equation (10) amounts to a generalized eigenvalue problem whose roots are negative since K_A may be assumed to be positive definite (K>0) and K_B positive (semi) definite ($K \geq 0$). The eigenvalue p of smallest absolute value then is the radius of convergence for the series representing u(x). We extend these ideas to more general problems through the following theorem

Theorem 1.

Let $K(x): C \to C^{nxn}$ be an analytic matrix-valued function with power series

$$K(x) = K_0 + K_1 x + K_2 x^2 + \ldots \tag{11}$$

and let $f(x): C \to C^n$ be an analytic vector-valued function with power series

$$f(x) = f_0 + f_1 x + f_2 x^2 + \ldots \tag{12}$$

Then u(x) in

$$K(x)u(x) = f(x) \tag{13}$$

may be represented by the power series

$$u(x) = u_0 + u_1 x + u_2 x^2 + \ldots \tag{14}$$

where the coefficients u_i are given by

$$u_i = K_0^{-1} \left[f_i - \sum_{j=0}^{i-1} K_{i-j} u_j \right]. \tag{15}$$

Series (14) is convergent within a disk centered at the origin with radius equal to the modulus of the smallest (in modulus) p satisfying the nonlinear eigenvalue problem

$$(K_0 + p K_1 + p^2 K_2 + \ldots)v = 0 \tag{16}$$

Example 2

Let

$$K_A = \begin{bmatrix} 1 & -1 \\ -1 & 2 \end{bmatrix} \quad K_B = \begin{bmatrix} 1 & 0 \\ 0 & 0 \end{bmatrix} \text{ and } f = \begin{bmatrix} 1 \\ 0 \end{bmatrix} \tag{17}$$

and consider the problem

$$[K_A + x K_B] u(x) = f \tag{18}$$

Using (15) we determine a power series for u(x)

$$u(x) = \begin{bmatrix} 2 \\ 1 \end{bmatrix} - x \begin{bmatrix} 4 \\ 2 \end{bmatrix} + x^2 \begin{bmatrix} 8 \\ 4 \end{bmatrix} - x^3 \begin{bmatrix} 16 \\ 8 \end{bmatrix} + \ldots \tag{19}$$

The radius of convergence for (19) is found from

$$\det (K_A + p K_B) = 0 \tag{20}$$

as $r = |p| = 1/2$.

The effective convergence radius can be greatly improved in this case by considering the following modification of (18)

$$2 [(1-x/2)K_A + x/2 K_B] u(x) = f \tag{21}$$

Now the radius of convergence is found by solving

$$\det[K_A + 1/2(K_B - K_A)q] = 0 \tag{22}$$

for q of smallest modulus and we find that r = 2.

The eigenvalues p of (20) and q of (22) can be directly compared if both problems are converted to standard form [3]. We arrive at

$$[K_A^{-1} K_B - (1 - 2/q) I]v = 0 \tag{23}$$

$$[K_A^{-1} K_B + 1/p I]v = 0 \tag{24}$$

showing that

$$1 - 2/q = -1/p \tag{25}$$

or

$$q = 2p/(p+1) \tag{26}$$

from which we find that

$$q \geq 1 \quad \text{for} \quad p \leq -1/3. \tag{27}$$

We conclude this discussion by deriving bounds for (27). Again we assume $K_A > 0$ and $K_B \geq 0$. Let λ_A be the smallest eigenvalue of K_A and let λ_B be the largest eigenvalue of K_B. Then if

$$\lambda_A \geq \lambda_B/3 \tag{28}$$

then

$$-p \leq 1/3, \tag{29}$$

This follows since the eigenvalues of K_A can be shifted by no more than $\frac{1}{3}\lambda_B$ by the addition of

pK_B to K_A [3]. Now

$$\lambda_A \geq ||K_A^{-1}||^{-1} \tag{30}$$

and

$$\lambda_B \leq ||K_B|| \tag{31}$$

where $||\cdot||$ is a suitable matrix norm. So if

$$||K_A^{-1}||^{-1} \geq 1/3\ ||K_B|| \tag{32}$$

then (28) and therefore (29) hold and (27) is guaranteed for values of x as large as $|x| = 1$. (Failure of (32) does not necessarily imply failure of convergence for $x = 1$).

Example 3

Let K_A, K_B and f be defined as in example 2. From (15) and (21) we have

$$u_0 = 1/2\ K_A^{-1}\ f \tag{33}$$

$$u_i = 1/2\ [I - K_A^{-1}\ K_B]\ u_{i-1} \tag{34}$$

$$u(x) = \begin{bmatrix} 1 \\ 1/2 \end{bmatrix} - x \begin{bmatrix} 1/2 \\ 1/4 \end{bmatrix} + x^2 \begin{bmatrix} 1/4 \\ 1/8 \end{bmatrix} - x^3 \begin{bmatrix} 1/8 \\ 1/16 \end{bmatrix} + x^4 \begin{bmatrix} 1/16 \\ 1/32 \end{bmatrix} - x^5 \begin{bmatrix} 1/32 \\ 1/64 \end{bmatrix} + \ldots -$$

This series converges at $x = 1$ to

$$u(1) = \begin{bmatrix} 2/3 \\ 1/3 \end{bmatrix}$$

which is the exact solution of the problem $(K_A + K_B)\ u = f$ of example 2.

III. Power Series for Eigensystems

The derivation of power series for eigenvalues and eigenvectors is similar to the above but the details are more complicated. Since the problem is treated elsewhere [4,5], we will only quote the following result.

Theorem 2.

Let K(x) be an analytic matrix-valued function of $x \in C$ which is real symmetric for $x \in R$ and let K(x) have power series

$$K(x) = K_0 + K_1 x + K_2 x^2 + \ldots \tag{35}$$

Then $\lambda(x)$ and u(x) in

$$K(x)u(x) = \lambda(x)u(x) \tag{36}$$

may be represented by the power series

$$u(x) = u_0 + u_1 x + u_2 x^2 + \ldots \tag{37}$$

and

$$\lambda(x) = \lambda_0 + \lambda_1 x + \lambda_2 x^2 + \ldots \tag{38}$$

where λ_0 is a non-repeated eigenvalue of K_0 and u_0 is the corresponding eigenvector satisfying $u_0^T u_0 = 1$ and where the coefficients λ_i and u_i are given by

$$u_i = -K_\lambda^+ \sum_{j=0}^{i-1} [K_{i-j} - \lambda_{i-j} I] u_j \tag{39}$$

and

$$\lambda_i = u_0^T \sum_{j=0}^{i-1} K_{i-j}\ u_j \tag{40}$$

The matrix K_λ^+ is a generalized inverse [6] of the matrix $(K_0 - \lambda_0 I)$ satisfying

$$K_\lambda^+\ u = 0. \tag{41}$$

Furthermore [5] if $K_i = 0$, $i \geq 2$ then the series are convergent within a disk centered at the origin with radius greater than or equal to

$$d/(2||K_1||) \tag{42}$$

where d is the distance between λ_0 and the nearest eigenvalue of K_0.

Remark: Note that the bound (42) is attainable in

$$K(x) = \begin{bmatrix} \varepsilon & x \\ x & -\varepsilon \end{bmatrix} \text{ but in } K(x) = \begin{bmatrix} x & 0 \\ 0 & x+\varepsilon \end{bmatrix}$$

it is a severe underestimate.

III. Summary and Conclusions

The simple properties of power series have made them fundamental to mathematical analysis. Their actual use in numerical work however has often been discouraged due to the difficulty of computing high order derivatives. This objection does not apply to work involving linear systems where algorithms for computing power series are simple and efficient.

This paper has presented methods for computing power series for linear system responses and for estimating convergence rate. At this time, these methods have not been applied to large structural models but their use for line searches in structural optimization and for other design sensitivity applications appears promising.

References

(1) Henrici, P., Applied and Computational Complex Analysis, Vol. I, Wiley Insterscience, New York, 1974.

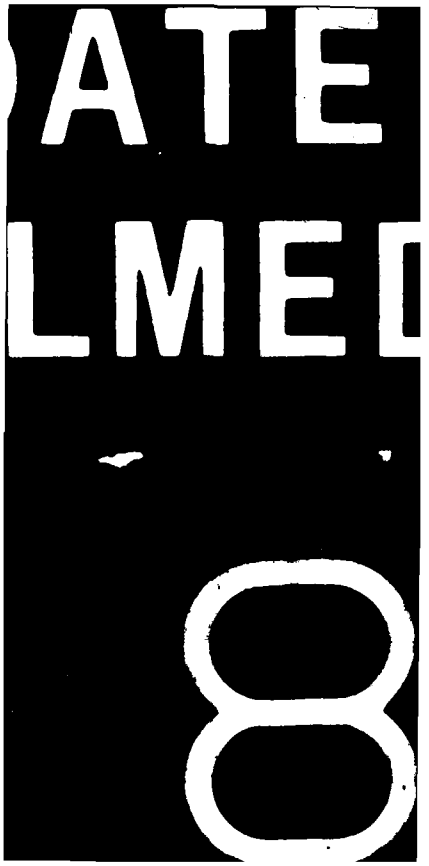
(2) Zienkiewicz, O.C., The Finite Element Method, McGraw-Hill, New York, 1978.

(3) Wilkinson, J.H., The Algebraic Eigenvalue Problem, Clarendon Press, London, 1965.

(4) Whitesell, Joseph E., Design Sensitivity in Dynamical Systems, Ph.D. Thesis, Michigan State University, 1980.

(5) Kato, T., Perturbation Theory for Linear Operators, Springer-Verlag, New York, 1976, 2nd Ed.

(6) Ben-Israel, A. and Greville, T.N.E., Generalized Inverses: Theory and Applications, John Wiley & Sons, New York, 1974.


ATE
LME
8